REPORT 195

THE COOLING AND EXHUMATION OF THE ALBANY–FRASER OROGEN, WESTERN AUSTRALIA, CONSTRAINED BY $^{40}Ar/^{39}Ar$, Rb/Sr AND U/Pb THERMOCHRONOLOGY

by E Scibiorski
The University of Western Australia

THE UNIVERSITY OF WESTERN AUSTRALIA

Government of Western Australia
Department of Mines, Industry Regulation and Safety

Geological Survey of Western Australia

Government of **Western Australia**
Department of **Mines, Industry Regulation and Safety**

REPORT 195

THE COOLING AND EXHUMATION OF THE ALBANY–FRASER OROGEN, WESTERN AUSTRALIA, CONSTRAINED BY $^{40}Ar/^{39}Ar$, Rb/Sr AND U/Pb THERMOCHRONOLOGY

by
E Scibiorski
The University of Western Australia

PERTH 2019

Geological Survey of Western Australia

REFERENCE
The recommended reference for this publication is:
Scibiorski, E 2019, The cooling and exhumation of the Albany–Fraser Orogen, Western Australia, constrained by $^{40}Ar/^{39}Ar$, Rb/Sr and U/Pb thermochronology: Geological Survey of Western Australia, Report 195, 675p.

ISBN 978-1-74168-859-7
ISSN 1834-2280

A catalogue record for this book is available from the National Library of Australia

Grid references in this publication refer to the Geocentric Datum of Australia 1994 (GDA94). Locations mentioned in the text are referenced using Map Grid Australia (MGA) coordinates, Zones 50 and 51. All locations are quoted to at least the nearest 100 m.

About this publication

This Report is a PhD thesis researched, written and compiled as part of a collaborative project between the Geological Survey of Western Australia (GSWA) and The University of Western Australia. Although GSWA has provided field and in-kind support for this project, the scientific content of the Report, and the drafting of figures, was the responsibility of the author. No editing has been undertaken by GSWA.

Published 2019 by the Geological Survey of Western Australia
This Report is published in digital format (PDF) and is available online at <www.dmp.wa.gov.au/GSWApublications>.

Further details of geoscience publications are available from:
Information Centre
Department of Mines, Industry Regulation and Safety
100 Plain Street
EAST PERTH WESTERN AUSTRALIA 6004
Telephone: +61 8 9222 3459 Facsimile: +61 8 9222 3444
www.dmp.wa.gov.au/GSWApublications

Cover photograph: S–C fabric in orthogneiss associated with sinistral shearing at Munglinup Beach, west of Esperance. Head of hammer is about 20 cm long

The cooling and exhumation of the Albany-Fraser Orogen, Western Australia, constrained by $^{40}Ar/^{39}Ar$, Rb/Sr and U/Pb thermochronology

Elisabeth Scibiorski

BSc (Hons)

This thesis is presented for the degree of Doctor of Philosophy

at

The University of Western Australia

School of Earth Sciences

April 2017

Thesis Declaration

I, Elisabeth Scibiorski, certify that:

This thesis has been substantially accomplished during enrolment in the degree.

This thesis does not contain material which has been accepted for the award of any other degree or diploma in my name, in any university or other tertiary institution, except where acknowledgement has been made in the text.

No part of this work will, in the future, be used in a submission in my name, for any other degree or diploma in any university or other tertiary institution without the prior approval of The University of Western Australia.

This thesis contains published work and/or work prepared for publication, some of which has been co-authored, as outlined in the Author Declaration on page xx.

No part of this work is in any way a violation or infringement of any copyright, trademark, patent, or other rights whatsoever of any person.

The work described in this thesis was funded by the Australian Research Council grant LP0991834.

Signature: 

Date: 11 April 2017

Abstract

The Albany-Fraser Orogen is a Neoarchean to Mesoproterozoic orogen that wraps around the southern and south-eastern margins of the Archean Yilgarn craton. Following a long Neoarchean to early Mesoproterozoic history of basin formation and sediment deposition, magmatism, and deformation, the orogen was deformed at high grades during the two-stage Mesoproterozoic Albany-Fraser Orogeny (Stage I: 1330 – 1260 Ma; Stage II: 1225 – 1140 Ma). However, few existing data constrain the cooling and exhumation of the orogen following Stage II of orogeny.

The purpose of this project was to describe the cooling history of the Albany-Fraser Orogen, with temperature-time (T-t) pairs derived from $^{40}Ar/^{39}Ar$, Rb/Sr and U/Pb thermochronology.

In the west Albany-Fraser Orogen, $^{40}Ar/^{39}Ar$ thermochronology of hornblende, muscovite and biotite reveals cooling at c. 22 – 33 °C/Ma between c. 1169 - 1159 Ma, following c. 1180 Ma amphibolite to granulite facies metamorphism. This fast cooling requires a fast exhumation mechanism consistent with the initiation of cooling in an actively deforming tectonic setting. Therefore, the widespread transpressional deformation in the west Albany-Fraser Orogen is interpreted as the driver of fast cooling and exhumation.

In the Biranup Zone of the east Albany-Fraser Orogen, $^{40}Ar/^{39}Ar$ thermochronology of hornblende, muscovite and biotite yields unrealistically old cooling ages (e.g. older than U/Pb zircon ages of metamorphism), despite producing statistically robust $^{40}Ar/^{39}Ar$ plateaus. In contrast, Rb/Sr biotite thermochronology yields consistent c. 1133 Ma cooling ages, 31 – 394 Ma younger than $^{40}Ar/^{39}Ar$ biotite ages in the same samples. Because Sr and Ar have similar closure temperatures for diffusion in biotite, the two chronometers should yield similar ages. Therefore, the old $^{40}Ar/^{39}Ar$ ages reflect the widespread presence of cryptic excess argon in the eastern Biranup Zone, possibly introduced by a flux of Ar-rich fluids derived from the underlying Archean Yilgarn craton.

In the Fraser Zone of the east Albany-Fraser Orogen, cooling was heterogenous. To the southwest, hornblende and biotite $^{40}Ar/^{39}Ar$ thermochronology dates cooling

at c. 1217 – 1205 Ma, supporting earlier interpretations that the southwestern Fraser Zone remained dry and cool during Stage II orogenesis. However, c. 100 km to the northeast, a single sample yields a $^{40}Ar/^{39}Ar$ biotite cooling age at c. 1157 Ma, providing some of the first evidence that the Fraser Zone was affected by thermal metamorphism during Stage II, although the effect of this event was heterogenous within the domain.

Finally, U/Pb titanite thermochronology of five samples in the east Albany-Fraser Orogen provides new T-t constraints on metamorphism and the initiation of cooling. Chondrite-normalised rare earth element (REE) patterns are used to characterise and map multiple titanite populations within each sample, and contribute to understanding the factors controlling the distribution of U and Pb in titanite. In addition, the heavy-REE pattern of titanite is identified as a geochemical indicator to link titanite growth with garnet growth.

Titanite U/Pb ages date magmatism in the Fraser Zone at c. 1303 Ma, amphibolite facies metamorphism and garnet growth in the eastern Biranup Zone at c. 1190 Ma, and cooling through the closure temperature for Pb diffusion in titanite (c. 650 °C) at c. 1162 Ma. These data allow calculation of c. 7 – 10 °C/Ma cooling rates for the eastern Biranup Zone, between the U/Pb titanite ages and the c. 1133 Ma Rb/Sr biotite cooling ages. A final titanite U/Pb age in the south-eastern Biranup Zone dates amphibolite facies metamorphism at c. 1172 Ma.

Together, the $^{40}Ar/^{39}Ar$, Rb/Sr and U/Pb thermochronology describe a cooling history for the Albany-Fraser Orogen with two key features. First, cooling following Stage II orogeny was significantly faster in the west than in the east. This is a product of the consistent northwest-southeast direction of compression acting on a curved orogen: the significant transpression in the west Albany-Fraser Orogen leads to fast exhumation and cooling, whereas the less transpressional and more directly compressional setting of the east Albany-Fraser Orogen leads to slower exhumation and cooling, possibly driven by processes such as post-orogenic extensional collapse. Second, the preservation of early-Stage II $^{40}Ar/^{39}Ar$ cooling ages in the southwestern Fraser Zone suggests it remained cool and dry during Stage II, and occupied a

shallow crustal level during orogenesis. Therefore, it is proposed that the southwestern Fraser Zone acted as an orogenic lid in the east Albany-Fraser Orogen, and is comparable with the Orogenic Lid of the North American Grenville Province.

Acknowledgements

Many people have helped, directly or indirectly, to shape this thesis, and I would like to thank them here.

First and foremost, this thesis could not have happened without the guidance, support and advice of Eric Tohver. Eric has been a wonderful mentor and teacher, who encouraged me to follow my interests, gain experience in a wide range of areas, and pursue several fruitful collaborations. When I first knocked on his door as an undergraduate to ask about potential Honours projects, I had no idea that I would still be here several years later. I would do it all over again.

My other supervisors, Tony Kemp and Fred Jourdan, have also been instrumental in guiding the thesis, and navigating the many unknowns and difficulties. Beyond sharing their analytical skills and expert knowledge, I've learnt much from Tony's meticulous, thorough approach both in and out of the lab, and from Fred's scepticism and no-nonsense attitude to research.

Many thanks go to Chris Kirkland, who has been a patient source of advice for all things titanite and Albany-Fraser related. Chris first suggested the titanite study, and provided essential guidance and feedback on the data interpretations. I would also like to thank Catherine Spaggiari for sharing her expert knowledge of the Albany-Fraser Orogen, and thank the Geological Survey of Western Australia for supporting and providing a vehicle for two field trips to the east Albany-Fraser Orogen (despite almost irredeemably bogging a vehicle in mud at the end of the first trip).

In 2016, I was lucky enough to spend an enjoyable two months at the University of Bern to collect the Rb/Sr data, which would not have been possible without the generosity of Klaus Mezger. It was an honour to meet and work with such an esteemed scientist, and I learnt much from him.

Much of the data acquired during this project relied on the expertise and enthusiastic support of a myriad of people from various institutions. I would particularly like to thank Malcolm Roberts, Janet Muhling, and Alexandra Suvorova at the Centre for Microscopy Characterisation and Analysis at UWA; Adam Frew and

Celia Mayers at the Western Australian Argon Isotope Facility at Curtin University; Noreen Evans at the GeoHistory Facility at Curtin University; and Hauke Vollstaedt and Igor Villa for their assistance in the lab at the University of Bern.

I would like to thank UWA for a Robert and Maude Gledden Postgraduate Scholarship that provided financial support during my candidature, and thank ANSTO and the WA division of the Geological Society of Australia for funding that allowed me to travel to multiple conferences. This research was also supported by an Australian Government Research Training Program (RTP) scholarship.

I've found that postgraduate students are generally a welcoming and friendly bunch, both here at UWA and during my short stay in Bern. Someone clever once wrote, "There are some things you can't share without ending up liking each other," and writing a PhD thesis is certainly one of them. The many coffee breaks, dinners, weekend hiking trips, and conversations with friends like Linda, Vik, Matt, Jeroen, Mariana, Alannah, and Edel have been a source of inspiration, encouragement, and entertainment.

Finally, and most importantly, I would like to thank my family, both the one I was born into and the one I've chosen. I could not have started this thesis without my parents, who have always supported me through every endeavour. It is because of the foundation they have given me that I am able to dream big and pursue ambitious goals. I could not have finished this thesis without Andrew's unwavering love and support – his bad jokes, his excellent taste in movies, his patience and encouragement, his practical help and emotional support, and his love have all been important in keeping me sane, letting me focus on finishing, and giving me the perspective to remember what is truly important in life.

Table of Contents

List of Figures

List of Tables

List of Appendices

Authorship Declaration: Co-Authored Publications

This thesis contains the results of research that I, Elisabeth Scibiorski (ES), conducted within the School of Earth and Environment at The University of Western Australia. Except where indicated below, all work and writing is my own. Chapters 3 - 6 of this thesis consist of two published journal articles, and two unpublished manuscripts prepared for submission. This section clearly identifies the contributions of each co-author.

Chapter 3

This chapter has been published as:

Scibiorski, E., Tohver, E., and Jourdan, F., 2015, Rapid cooling and exhumation in the western part of the Mesoproterozoic Albany-Fraser Orogen, Western Australia: Precambrian Research, v. 265, p. 232-248.

ES was the principal author of the article. ES undertook all sample preparation and $^{40}Ar/^{39}Ar$ analyses, developed the Monte Carlo simulation, compiled the summary of global orogenic cooling rates, and wrote the manuscript, together with fundamental advice and discussion with E. Tohver (ET) and F. Jourdan (FJ). ET collected the samples, and FJ supervised the $^{40}Ar/^{39}Ar$ analyses and performed the initial data reduction. Both ET and FJ provided editorial comments and revisions of the manuscript.

The $^{40}Ar/^{39}Ar$ data reported in this chapter were collected for ES's Bachelor of Science (Honours) thesis in 2012. However, a substantial portion of this chapter was completed during the PhD candidacy: the Monte Carlo simulation, integration of the new data with a global compilation of orogenic cooling rates, and the writing of the manuscript (the text of the Honours thesis was completely rewritten for publication).

Chapter 4

This chapter has been published as:

Scibiorski, E., Tohver, E., Jourdan, F., Kirkland, C. L., and Spaggiari, C. V., 2016, Cooling and exhumation along the curved Albany-Fraser orogen, Western Australia: Lithosphere, v. 8, no. 5, p. 551-563.

ES was the principal author of the article. ES undertook all sample preparation, performed the Monte Carlo simulation, led the data interpretation, and wrote the manuscript, together with advice and discussion with all co-authors. ET assisted ES with sample collection. FJ performed the $^{40}Ar/^{39}Ar$ analyses and performed the initial data reduction. ET, FJ, C. L. Kirkland (CK) and C. V. Spaggiari (CS) provided editorial comments and revisions of the manuscript.

Chapter 5

This chapter is an unpublished manuscript, prepared for submission to a peer-reviewed journal as:

Scibiorski, E., Tohver, E., Mezger, K., Jourdan, F., and Vollstaedt, H., Cryptic excess argon in biotite: $^{40}Ar/^{39}Ar$ plateau ages tested with Rb/Sr geochronology.

ES was the principal author of the article. ES undertook all sample preparation, performed the SEM imaging, EMP and Rb MC-ICPMS analyses, led the data interpretation, and wrote the manuscript, together with advice and discussion with all co-authors. ET assisted ES with sample collection. K. Mezger (KM) assisted with sample preparation for Rb/Sr analyses, age calculation, and data interpretation. H. Vollstaedt (HV) performed the Sr TIMS analyses and data reduction, and assisted with calculation of error propagation. ET and FJ provided editorial comments and revisions of the manuscript.

Additional assistance was provided by Dr M. Roberts for the biotite EMP analyses, and Dr I. M. Villa for the Rb MC-ICPMS analyses.

Chapter 6

This chapter is an unpublished manuscript, prepared for submission to a peer-reviewed journal as:

Scibiorski, E., Kirkland, C. L., Kemp, A. I. S., Tohver, E., and Evans, N. J., Using the trace element signature to constrain polygenetic titanite growth, garnet growth and U/Pb geochronology.

ES was the principal author of this manuscript. ES selected the samples, performed the SEM imaging, led the data interpretation, and wrote the manuscript, with crucial advice and discussion from CK, A. I. S. Kemp (AK), and ET. ET assisted ES with sample collection. N. J. Evans (NE) performed the titanite LA-ICPMS analyses and initial data processing. CK performed an additional correction on the U/Pb data. AK provided assistance for the garnet LA-ICPMS analyses and data reduction. CK, AK and ET provided editorial comments and revisions of the manuscript.

Additional assistance was provided by Dr M. Roberts for the garnet EMP analyses, and Dr A. Suvorova for the FEI Varios SEM imaging.

I, Eric Tohver, certify that the student's statements regarding their contribution to each of the works listed above are correct.

Coordinating supervisor signature: 

Date: 17/3/17

Chapter 1

Introduction

1 Introduction

1.1 Thermochronology and orogenic cooling

The exposure of deeply buried orogenic roots at the surface of the Earth provides a valuable window into mid- to lower-crustal processes during orogenesis. These high-grade terranes are often exhumed long after the end of crustal thickening, driven by slow processes such as orogenic collapse and isostatic rebound, although deep crustal rocks may also be exhumed quickly within an actively deforming tectonic setting (e.g. Busch et al., 1997; Petitgirard et al., 2009; Little et al., 2011; Pownall et al., 2014).

A key approach to uncovering the orogenic processes leading to exhumation is through characterising the thermal history of the rock. The influence of exhumation rates and processes on cooling is well established (Ring et al., 1999; Reiners and Brandon, 2006). For example, periods of slow, uniform cooling suggest coeval slow, uniform exhumation (e.g. Möller et al., 2000), whereas rocks that are exhumed rapidly from depth will experience isothermal decompression, followed by fast cooling until thermal equilibrium is attained (Ring et al., 1999; Whitney et al., 2004).

The primary technique for determining cooling histories is thermochronology. Thermochronology is based on the temperature-dependent retention of the daughter product of a radioactive decay scheme, where the age given by a thermochronometer is interpreted to date the time that the mineral passes through its closure temperature (Dodson, 1973). The closure temperature of a mineral is the temperature below which the mobile radiogenic daughter product begins to accumulate, and is no longer able to diffuse in or out of the mineral (e.g. McDougall and Harrison, 1988; Cosca et al., 1991).

Whilst an ideal thermochronological age may be interpreted to date cooling through the closure temperature, in reality, determining the geological significance of an apparent age may be more difficult. As with all geochronology, thermochronology rests upon several key assumptions that may not always be justified, and must therefore be constantly re-evaluated. For example, to record a true

cooling age, a mineral must grow above its closure temperature; a mineral that grows below its closure temperature will instead record a growth age (e.g. Gray and Foster, 2004; Challandes et al., 2008).

Although diffusive closure in natural systems occurs over a temperature interval, it is normally modelled as a single point, where accumulation of the radiogenic daughter product above the closure temperature is balanced by later diffusive loss (McDougall and Harrison, 1988). The closure temperature model assumes no excess retention of the radiogenic daughter product above the closure temperature; i.e. the rate of diffusive loss is faster than the rate of radioactive decay. However, if diffusive loss of the daughter product is inhibited, the mineral will yield an age that is older than the true age of cooling. Fluids often play an important role in the removal of radiogenic decay products (Kelley, 2002); consequently, in dry, high-temperature terranes, diffusive loss may be inhibited (Baxter, 2007) and the primary control on ages may be mineral (re)crystallization (e.g. Glodny et al., 2008; Walker et al., 2016). Alternatively, a high concentration of the daughter product may result in its diffusion into, rather than out of, the mineral of interest (e.g. excess Ar is ubiquitous in many ultra-high pressure terranes; Scaillet, 1996; Ruffet et al., 1997). Finally, a mineral thermochronometer may also be perturbed by partial or complete recrystallization as a product of fluid flow, deformation, or alteration (Villa, 2016).

The diffusive closure temperature varies for different decay schemes and in different minerals; for example, Ar diffusion has a closure temperature between 490 – 580 °C in hornblende, and 280 – 350 °C in biotite (Harrison, 1981; Harrison et al., 1985). In contrast, Pb in titanite has a wide range of possible closure temperatures, from 650 – 1030 °C (depending on temperature of growth and lattice damage; Cherniak, 2010). Accordingly, the lower closure temperatures of the $^{40}Ar/^{39}Ar$ thermochronometer mean it is typically interpreted to date cooling in orogenic terranes (e.g. Cosca et al., 1991; Busch et al., 1997), whereas the wide range of Pb closure temperatures in titanite mean a U/Pb age may date metamorphic titanite growth, magmatic titanite growth, or less commonly, cooling through the closure temperature (e.g. Mezger et al., 1991; Smith et al., 2009; Gao et al., 2012).

The use of multiple thermochronometers in multiple minerals will result in several temperature-time (T-t) pairs that describe the thermal evolution of a rock through time. This cooling history may then be linked to specific orogenic and exhumation processes, by integrating thermochronology with structural and metamorphic data (e.g. Willigers et al., 2002; Jessup et al., 2006)

1.2 The Albany-Fraser Orogen

The Albany-Fraser Orogen is a Neoarchean to Mesoproterozoic orogen that curves around the southern and south-eastern margins of the Archean Yilgarn Craton (Figure 1.1). From the Neoarchean to the Paleoproterozoic, the orogen records several episodes of basin formation, sediment deposition, magmatism, and deformation (Spaggiari et al., 2011; Spaggiari et al., 2014a; Smithies et al., 2015). These were followed and overprinted by the Mesoproterozoic Albany-Fraser Orogeny, divided into Stage I (1330 – 1260 Ma) and Stage II (1225 – 1140 Ma) on the basis of U/Pb zircon geochronology (Clark et al., 2000; Spaggiari et al., 2011). The Albany-Fraser Orogeny was a high-grade metamorphic and deformational event accompanied by extensive mafic and felsic magmatism, and is responsible for most of the crustal architecture, structural fabrics, mineralogy, and geochronology preserved throughout the orogen (Spaggiari et al., 2011). Stage I and Stage II have been traditionally interpreted to record continental collision and suturing between the West Australian and Mawson cratons during the assembly of Rodinia (Myers, 1995; Clark et al., 2000; Cawood and Korsch, 2008), although this interpretation has been challenged more recently (Spaggiari et al., 2014a; Spaggiari et al., 2016).

Most early research in the Albany-Fraser Orogen focused on describing and dating the deformation, metamorphism, and magmatism during Mesoproterozoic orogeny (e.g. Beeson et al., 1988; Pidgeon, 1990; Nelson et al., 1995; Clark et al., 2000; Bodorkos and Clark, 2004). More recently, two major greenfields gold and nickel discoveries in the east Albany-Fraser Orogen (Tropicana, AngloGold Ashanti, 2005; Nova, Sirius Resources, 2012) highlighted how little was known about the orogen, and resulted in an ongoing research campaign by the Geological Survey of Western Australia (GSWA) to map and describe the orogen (Spaggiari et al., 2011). The

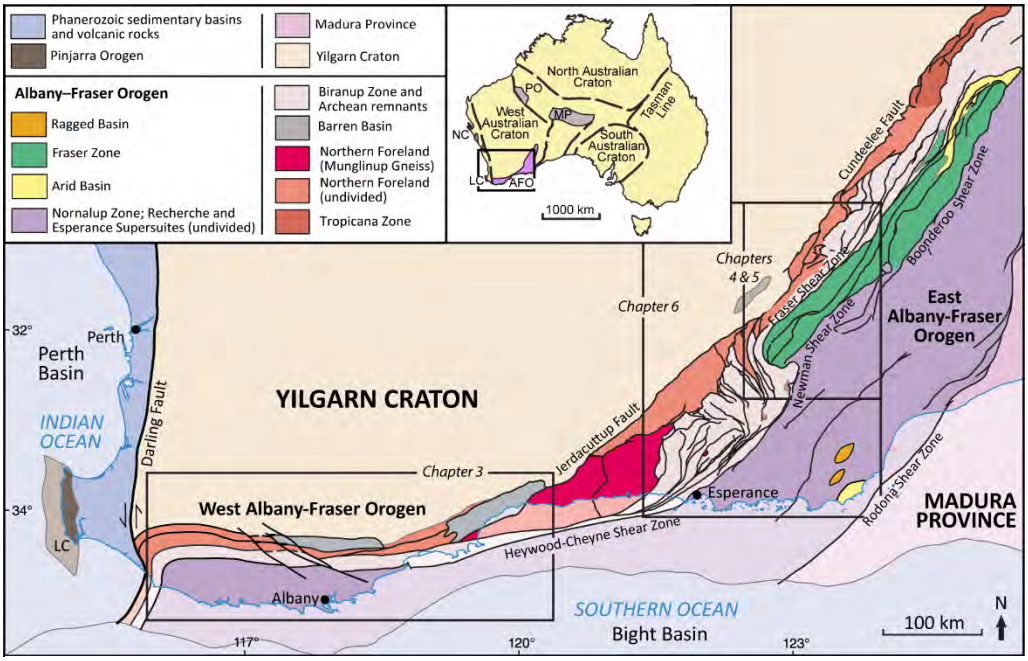

Figure 1.1 Interpreted bedrock geology map of the Albany-Fraser Orogen, showing the relative areas covered by each chapter. The inset next to the legend shows the location of Mesoproterozoic tectonic units within Australia, including the Albany-Fraser Orogen. Abbreviations: AFO, Albany-Fraser Orogen; LC, Leeuwin Complex; MP, Musgrave Province; NC, Northampton Complex; PO, Paterson Orogen. Inset after Kirkland et al. (2011); bedrock geology map after Spaggiari et al. (2014a).

primary focus of GSWA has been the collection of regional-scale datasets, including geochronology (mainly U/Pb in zircon), geophysics (seismic, aeromagnetic and gravity) and geochemistry (e.g. Spaggiari et al., 2014b; Smithies et al., 2015; Geological Survey of Western Australia, 2016).

However, the cooling and exhumation history of the orogen has been largely unexplored. Previously published thermochronology is limited to seven hornblende K/Ar ages and several poorly constrained biotite Rb/Sr ages in the west Albany-Fraser Orogen (Stephenson et al., 1977; Black et al., 1992; Libby and De Laeter, 1998), and one biotite Rb/Sr age and one hornblende $^{40}Ar/^{39}Ar$ age from the east Albany-Fraser Orogen (Baksi and Wilson, 1980; Fletcher et al., 1991). This thesis targets this knowledge gap by using thermochronology to uncover the thermal history of the Albany-Fraser Orogen at the end of Mesoproterozoic orogeny.

1.3 Research objectives

The primary objective of this thesis is to describe the cooling history of the Albany-Fraser Orogen after the end of Mesoproterozoic orogeny, from amphibolite to granulite facies metamorphism at ≥ 700 °C to ~ 300 °C. Specifically, to achieve this goal, I seek to:

1. Produce temperature-time pairs that describe the thermal evolution of the orogen, using: (a) U/Pb titanite thermochronology to narrow the gap between metamorphism and magmatism, and the high-temperature end of the cooling path, and; (b) $^{40}Ar/^{39}Ar$ and Rb/Sr thermochronology to span cooling through the c. 550 – 300 °C temperature interval.
2. Test the robustness of the $^{40}Ar/^{39}Ar$ thermochronology in the east Albany-Fraser Orogen with Rb/Sr thermochronology.
3. To aid in determining the geological significance of the titanite U/Pb data, explore the use of trace element chemistry in titanite as a geochemical indicator.

1.4 Thesis structure

This thesis is presented as a series of published papers and manuscripts prepared for submission to peer-reviewed journals (Chapters 3 – 6). The chapters are presented in chronological order of completion, because Chapters 3 and 4 were accepted for publication before the work in Chapters 5 and 6 was complete. The text and figures of the two published papers are reproduced as published, but have been reformatted for consistency in the thesis (i.e. font changes, and re-numbering of figures, tables and appendices). Because the geological background and methods are reproduced in full, there is some unavoidable repetition of these components between chapters.

Chapter Two provides a detailed review of the current understanding of the geology of the Albany-Fraser Orogen, and all previously published thermochronology.

Chapter Three presents the results of $^{40}Ar/^{39}Ar$ thermochronology in the west Albany-Fraser Orogen, and integrates these data with the global record of orogenic cooling. This chapter is published as:

Scibiorski, E., Tohver, E., and Jourdan, F., 2015, Rapid cooling and exhumation in the western part of the Mesoproterozoic Albany-Fraser Orogen, Western Australia: Precambrian Research, v. 265, p. 232-248.

Chapter Four presents the results of $^{40}Ar/^{39}Ar$ thermochronology in the east Albany-Fraser Orogen, and compares these data with the cooling record in the west Albany-Fraser Orogen established in Chapter Three. This chapter is published as:

Scibiorski, E., Tohver, E., Jourdan, F., Kirkland, C. L., and Spaggiari, C. V., 2016, Cooling and exhumation along the curved Albany-Fraser orogen, Western Australia: Lithosphere, v. 8, no. 5, p. 551-563.

Chapter Five uses Rb/Sr biotite thermochronology to test for the presence of excess argon in the $^{40}Ar/^{39}Ar$ data reported in Chapter Four, despite nearly ubiquitous $^{40}Ar/^{39}Ar$ degassing plateaus. Cryptic excess argon produces anomalously old $^{40}Ar/^{39}Ar$ ages that are difficult to recognise because, in isolation, the data are statistically acceptable. This manuscript has been prepared for submission to *Chemical Geology*.

Chapter Six reports five U/Pb titanite ages from the east Albany-Fraser Orogen, and explores the use of trace element chemistry as a geochemical indicator in titanite. The heavy rare earth element pattern is used to link titanite crystallisation to metamorphic garnet growth. This manuscript has been prepared for submission to *Earth and Planetary Science Letters*.

Chapter Seven summarises and discusses the results of the thesis. The thermochronology data are integrated to produce an overall cooling and exhumation history for the Albany-Fraser Orogen.

1.5 References

Baksi, A. K., and Wilson, A. F., 1980, An attempt at Argon dating of two granulite-facies terranes: Chemical Geology, v. 30, p. 109-120.

Baxter, E. F., 2007, Grain boundary partitioning of Ar and He: Geochimica et Cosmochimica Acta, v. 71, p. 434-451.

Beeson, J., Delor, C. P., and Harris, L. B., 1988, A structural and metamorphic traverse across the Albany Mobile Belt, Western Australia: Precambrian Research, v. 40/41, p. 117-136.

Black, L. P., Harris, L. B., and Delor, C. P., 1992, Reworking of Archaean and Early Proterozoic components during a progressive, Middle Proterozoic tectonothermal event in the Albany Mobile Belt, Western Australia: Precambrian Research, v. 59, p. 95-123.

Bodorkos, S., and Clark, D., 2004, Evolution of a crustal-scale transpressive shear zone in the Albany-Fraser Orogen, SW Australia: 2. Tectonic history of the Coramup Gneiss and a kinematic framework for Mesoproterozoic collision of the West Australian and Mawson cratons: Journal of Metamorphic Geology, v. 22, p. 713-731.

Busch, J. P., Mezger, K., and van der Pluijm, B., 1997, Suturing and extensional reactivation in the Grenville orogen, Canada: Geology, v. 25, no. 6, p. 507-510.

Cawood, P. A., and Korsch, R. J., 2008, Assembling Australia: Proterozoic building of a continent: Precambrian Research, v. 166, p. 1-38.

Challandes, N., Marquer, D., and Villa, I. M., 2008, P-T-t modelling, fluid circulation, and ^{39}Ar-^{40}Ar and Rb-Sr mica ages in the Aar Massif shear zones (Swiss Alps): Swiss Journal of Geosciences, DOI: 10.1007/s00015-008-1260-6.

Cherniak, D. J., 2010, Diffusion in accessory minerals: zircon, titanite, apatite, monazite and xenotime: Reviews in Mineralogy and Geochemistry, v. 72, p. 827-869.

Clark, D., Hensen, B., and Kinny, P., 2000, Geochronological constraints for a two-stage history of the Albany-Fraser Orogen, Western Australia: Precambrian Research, v. 102, p. 155-183.

Cosca, M. A., Sutter, J. F., and Essene, E. J., 1991, Cooling and inferred uplift/erosion history of the Grenville Orogen, Ontario: Constraints from $^{40}Ar/^{39}Ar$ thermochronology: Tectonics, v. 10, no. 5, p. 959-977.

Dodson, M. H., 1973, Closure temperature in cooling geochronological and petrological systems: Contributions in Mineralogy and Petrology, v. 40, p. 259-274.

Fletcher, I. R., Myers, J. S., and Ahmat, A. L., 1991, Isotopic evidence on the age and origin of the Fraser Complex, Western Australia: a sample of Mid-Proterozoic lower crust: Chemical Geology (Isotope Geoscience Section), v. 87, p. 197-216.

Gao, X.-Y., Zheng, Y.-F., Chen, Y.-X., and Guo, J., 2012, Geochemical and U-Pb age constraints on the occurrence of polygenetic titanites in UHP metagranite in the Dabie orogen: Lithos, v. 136-139, p. 93-108.

Geological Survey of Western Australia, 2016, Compilation of geochronology information 2016: Government of Western Australia, ISBN: 9781741686876.

Glodny, J., Kühn, A., and Austrheim, H., 2008, Geochronology of fluid-induced eclogite and amphibolite facies metamorphic reactions in a subduction-collision system, Bergen Arcs, Norway: Contributions in Mineralogy and Petrology, v. 156, p. 27-48.

Gray, D. R., and Foster, D. A., 2004, $^{40}Ar/^{39}Ar$ thermochronologic constraints on deformation, metamorphism and cooling/exhumation of a Mesozoic accretionary wedge, Otago Schist, New Zealand: Tectonophysics, v. 385, p. 181-210.

Harrison, T. M., 1981, Diffusion of ^{40}Ar in hornblende: Contributions in Mineralogy and Petrology, v. 78, p. 324 - 331.

Harrison, T. M., Duncan, I., and McDougall, I., 1985, Diffusion of ^{40}Ar in biotite: Temperature, pressure and compositional effects: Geochimica et Cosmochimica Acta, v. 49, p. 2461 - 2468.

Jessup, M. J., Jones, J. V. I., Karlstrom, K. E., Williams, M. L., Connelly, J. N., and Heizler, M. T., 2006, Three Proterozoic orogenic episodes and an intervening exhumation event in the Black Canyon of the Gunnison Region, Colorado: The Journal of Geology, v. 114, p. 555-576.

Kelley, S. P., 2002, Excess argon in K-Ar and Ar-Ar geochronology: Chemical Geology, v. 188, no. 1-2, p. 1-22.

Kirkland, C. L., Spaggiari, C. V., Pawley, M. J., Wingate, M. T. D., Smithies, R. H., Howard, H. M., Tyler, I. M., Belousova, E. A., and Poujol, M., 2011, On the edge: U–Pb, Lu–Hf, and Sm–Nd data suggests reworking of the Yilgarn craton margin during formation of the Albany-Fraser Orogen: Precambrian Research, v. 187, no. 3–4, p. 223-247.

Libby, W. G., and De Laeter, J. R., 1998, Biotite Rb-Sr age evidence for Early Palaeozoic tectonism along the cratonic margin in southwestern Australia: Australian Journal of Earth Sciences, v. 45, no. 623-632.

Little, T. A., Hacker, B. R., Gordon, S. M., Baldwin, S. L., Fitzgerald, P. G., Ellis, S., and Korchinski, M., 2011, Diapiric exhumation of Earth's youngest (UHP) eclogites in the gneiss domes of the D'Entrecasteaux Islands, Papua New Guinea: Tectonophysics, v. 510, p. 39-68.

McDougall, I., and Harrison, T. M., 1988, Geochronology and thermochronology by the $^{40}Ar/^{39}Ar$ method, New York, Oxford University Press, Oxford Monographs on Geology and Geophysics.

Mezger, K., van der Pluijm, B., Essene, E. J., and Halliday, A. N., 1991, Synorogenic collapse: A perspective from the middle crust, the Proterozoic Grenville Orogen: Science, v. 254, no. 5032, p. 695-698.

Möller, A., Mezger, K., and Schenk, V., 2000, U-Pb dating of metamorphic minerals: Pan-African metamorphism and prolonged slow cooling of high pressure granulites in Tanzania, East Africa: Precambrian Research, v. 104, p. 123-146.

Myers, J. S., 1995, Geology of the Esperance 1:1 000 000 sheet: Geological Survey of Western Australia, 1:1 000 000 Geological Series Explanatory Notes, p. 10.

Nelson, D. R., Myers, J. S., and Nutman, A. P., 1995, Chronology and evolution of the Middle Proterozoic Albany-Fraser Orogen, Western Australia: Australian Journal of Earth Sciences, v. 42, no. 5, p. 481 - 495.

Petitgirard, S., Vauchez, A., Egydio-Silva, M., Bruguier, O., Camps, P., Monié, P., Babinski, M., and Mondou, M., 2009, Conflicting structural and geochronological data from the Ibituruna quartz-syenite (SE Brazil): Effect of protracted "hot" orogeny and slow cooling rate?: Tectonophysics, v. 477, p. 174-196.

Pidgeon, R. T., 1990, Timing of plutonism in the Proterozoic Albany Mobile Belt, southwestern Australia: Precambrian Research, v. 47, p. 157-167.

Pownall, J. M., Hall, R., Armstrong, R. A., and Forster, M. A., 2014, Earth's youngest known ultrahigh-temperature granulites discovered on Seram, eastern Indonesia: Geology, v. 42, no. 4, p. 279-282.

Reiners, P. W., and Brandon, M. T., 2006, Using thermochronology to understand orogenic erosion: Annual Review of Earth and Planetary Sciences, v. 34, p. 419-466.

Ring, U., Brandon, M. T., Willett, S. D., and Lister, G. S., 1999, Exhumation processes: Geological Society of London Special Publications, v. 154, p. 1-27.

Ruffet, G., Gruau, G., Ballèvre, M., Féraud, G., and Philippot, P., 1997, Rb-Sr and ^{40}Ar-^{39}Ar laser probe dating of high-pressure phengites from the Sesia zone (Western Alps): underscoring of excess argon and new age constraints on the high-pressure metamorphism: Chemical Geology, v. 141, p. 1-18.

Scaillet, S., 1996, Excess ^{40}Ar transport scale and mechanism in high-pressure phengites: A case study from an eclogitized metabasite of the Dora-Maira nappe, western Alps: Geochimica et Cosmochimica Acta, v. 60, no. 6, p. 1075-1090.

Smith, M. P., Storey, C. D., Jeffries, T. E., and Ryan, C. G., 2009, *In situ* U-Pb and trace element analysis of accessory minerals in the Kiruna District, Norrbotten, Sweden: New constraints on the timing and origin of mineralization: Journal of Petrology, v. 50, no. 11, p. 2063-2094.

Smithies, R. H., Spaggiari, C. V., and Kirkland, C. L., 2015, Building the crust of the Albany-Fraser Orogen: constraints from granite geochemistry: Geological Survey of Western Australia, Report 150, p. 49p.

Spaggiari, C. V., Kirkland, C. L., Pawley, M. J., Smithies, R. H., Wingate, M. T. D., Doyle, M. G., Blenkinsop, T. G., Clark, C., Oorschot, C. W., Fox, L. J., and Savage, J., 2011, The geology of the east Albany-Fraser Orogen - a field guide: Geological Survey of Western Australia, Record 2011/23, p. 92.

Spaggiari, C. V., Kirkland, C. L., Smithies, R. H., and Wingate, M. T. D., 2014a, Tectonic links between Proterozoic sedimentary cycles, basin formation and magmatism in the Albany-Fraser Orogen, Western Australia: Geological Survey of Western Australia, Report 133.

Spaggiari, C. V., Occhipinti, S. A., Korsch, R. J., Doublier, M. P., Clark, D. J., Dentith, M. C., Gessner, K., Doyle, M. G., Tyler, I. M., Kennett, B. L. N., Costelloe, R. D., Fomin, T., and Holzschuh, J., 2014b, Interpretation of Albany-Fraser seismic lines 12GA-AF1, 12GA-AF2 and 12GA-AF3: implications for crustal architecture, *in* Spaggiari, C. V., and Tyler, I. M., eds., Albany-Fraser Orogen seismic and magnetotelluric (MT) workshop 2014: extended abstracts, Record 2014/6, Geological Survey of Western Australia, p. 28 - 51.

Spaggiari, C. V., Smithies, R. H., Wingate, M. T. D., Kirkland, C. L., and England, R. N., 2016, Exposing the Eucla basement: what separates the Albany-Fraser Orogen and the Gawler Craton?, GSWA 2016 extended abstracts: promoting the prospectivity of Western Australia, Geological Survey of Western Australia, Record 2016/2, p. 36-41.

Stephenson, N. C. N., Russell, T. G., Stubbs, D., and Kalocsai, G. I. Z., 1977, Potassium-argon ages of hornblendes from Precambrian gneisses from the south coast of

Western Australia: Journal of the Royal Society of Western Australia, v. 59, no. 4, p. 105-109.

Villa, I. M., 2016, Diffusion in mineral geochronometers: Present and absent: Chemical Geology, v. 420, p. 1-10.

Walker, S., Thirlwall, M. F., Strachan, R. A., and Bird, A. F., 2016, Evidence from Rb-Sr mineral ages for multiple orogenic events in the Caledonides of Shetland, Scotland: Journal of the Geological Society, v. 173, p. 489-503.

Whitney, D. L., Teyssier, C., and Fayon, A. K., 2004, Isothermal decompression, partial melting and exhumation of deep continental crust, *in* Grocott, J., McCaffrey, K. J. W., Taylor, G., and Tikoff, B., eds., Vertical Coupling and Decoupling in the Lithosphere, Volume 227, Geological Society of London, Special Publications, p. 313-326.

Willigers, B. J. A., van Gool, J. A. M., Wijbrans, J. R., Krogstad, E. J., and Mezger, K., 2002, Posttectonic cooling of the Nagssugtoqidian Orogen and a comparison of contrasting cooling histories in Precambrian and Phanerozoic orogens: The Journal of Geology, v. 110, p. 503-517.

Chapter 2

The Albany-Fraser Orogen

2 The Albany-Fraser Orogen

The Albany-Fraser Orogen is located in southwestern Australia, and extends for at least 1200 km along the southern and south-eastern margins of the Archean Yilgarn Craton (Figure 2.1). The orogen is bordered by the Musgrave Province to the northeast, is juxtaposed against the Madura Province to the east along the Rodona Shear Zone, and is overprinted by the Pinjarra Orogen to the west. Exposure is severely limited; much of the orogen is under cover of vegetation with little outcrop, and in the east the orogen is overlain by Phanerozoic sediments of the Eucla Basin. To the south, the orogen is truncated by the Australian continental margin, although the Albany-Fraser Orogen continues in Antarctica as part of the larger Albany-Fraser-Wilkes Orogen (Fitzsimons, 2000; Aitken et al., 2014).

The Albany-Fraser Orogen consists of Neoarchean to Paleoproterozoic rocks that were deformed and metamorphosed by the Mesoproterozoic Albany-Fraser Orogeny (Stage I, 1330 – 1260 Ma; Stage II, 1225 – 1140 Ma) (Clark et al., 2000; Spaggiari et al., 2015). The high-grade Mesoproterozoic deformation is responsible for most of the structural fabrics and mineral assemblages preserved throughout the orogen, and for the present tectonic architecture (Spaggiari et al., 2011; Korsch et al., 2014).

The orogen is subdivided into two major tectonic components: the Archean Northern Foreland, and the Paleo to Mesoproterozoic Kepa Kurl Booya Province (Spaggiari et al., 2009). The Northern Foreland consists of those Yilgarn Craton rocks that were deformed and metamorphosed during the Albany-Fraser Orogeny. The Kepa Kurl Booya Province is the igneous and metamorphic basement of the Albany-Fraser Orogen and is, in turn, subdivided into the shear zone-bound Biranup, Nornalup, Fraser and Tropicana Zones (Spaggiari et al., 2009). Deep seismic reflection lines across the central, east and northeast Albany-Fraser Orogen suggest that these shear zones (both domain-bounding structures, and internal structures) are dominantly listric and dip to the southeast, away from the margin of the Yilgarn Craton (Spaggiari et al., 2014c).

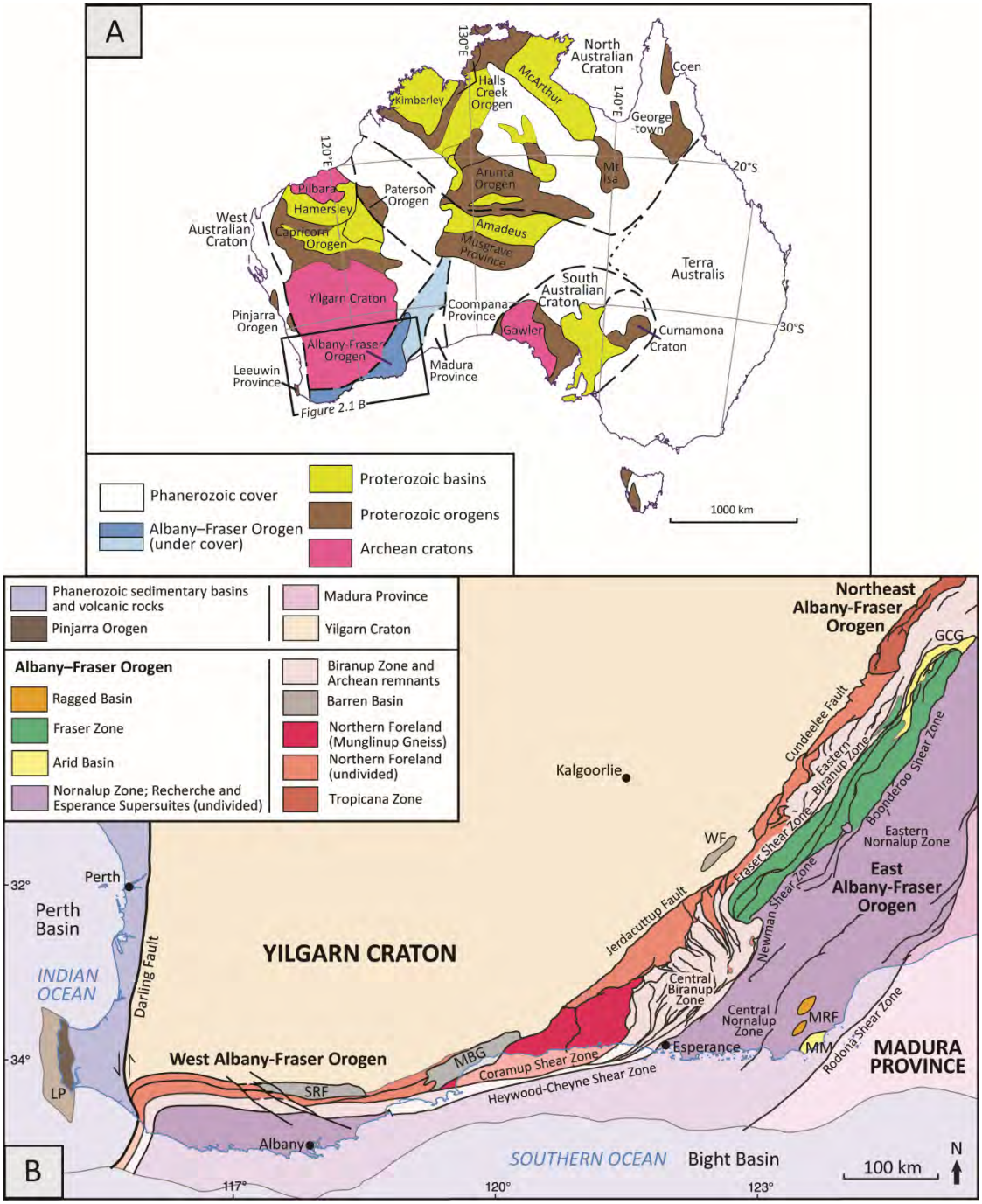

Figure 2.1 (A) Simplified tectonic map of Australia showing the distribution of Archean and Proterozoic tectonic units within Australia. The light blue area indicates the inferred extent of the Albany-Fraser Orogen underneath the Phanerozoic Eucla Basin. Map after Spaggiari et al. (2011). **(B)** Interpreted bedrock geology map of the Albany-Fraser Orogen, showing the location of the major tectonic units, and the regions designated 'west', 'central', 'east' and 'northeast'. Abbreviations: GCG, Gwynne Creek Gneiss; MBG, Mount Barren Group; MM, Malcolm Metamorphics; MRF, Mount Ragged Formation; SRF, Stirling Range Formation; WF, Woodline Formation. Map after Spaggiari et al. (2014b).

2.1 Northern Foreland

The Northern Foreland consists of the southern and south-eastern margins of the Yilgarn Craton, dominated by c. 2720 – 2620 Ma orthogneisses and deformed by the Mesoproterozoic Albany-Fraser Orogeny (Spaggiari et al., 2009). Deformation intensity and metamorphic grade increases to the south and southeast (i.e. towards the Kepa Kurl Booya Province), from greenschist facies to amphibolite facies (Beeson et al., 1988). The granulite-facies Munglinup Gneiss is a higher-grade component of the Northern Foreland, contained within thrust sheets and exhumed from a deeper level (Spaggiari et al., 2009). Despite high-grade Mesoproterozoic deformation, the dominance of c. 2660 Ma granitic orthogneisses, the presence of remnant greenstone belts, and zircon Hf signatures yielding c. 3200 Ma model ages suggest a Yilgarn Craton source for the Munglinup Gneiss (Spaggiari et al., 2009; Kirkland et al., 2011b).

2.2 Tropicana Zone

The Tropicana Zone consists mainly of c. 2720 Ma Archean orthogneisses, overprinted by prolonged 2718 – 2554 Ma granulite facies metamorphism (Kirkland et al., 2014). The prolonged metamorphism is interpreted to suggest that the Tropicana Zone represents a slice of deep Archean crust, which was exhumed to shallow crustal levels by c. 2515 Ma, based on U/Pb rutile and $^{40}Ar/^{39}Ar$ biotite thermochronology (Occhipinti et al., 2014). The Tropicana Zone was thrust onto the Yamarna Terrane of the Yilgarn Craton before 1783 Ma (Kirkland et al., 2014), and was heterogeneously deformed by Paleoproterozoic and Mesoproterozoic tectonothermal events; it retains some Archean gneissic fabrics, but is also locally intruded by Paleoproterozoic granites of the adjacent Biranup Zone (Occhipinti et al., 2014).

The Tropicana Zone has a distinctly different age history to the adjacent Yilgarn Craton, and cannot be correlated with any known component of the Yilgarn Craton (e.g. the Yamarna Terrane). Because the Tropicana Zone was thrust over the margin of the Yilgarn Craton, and is intruded by Paleoproterozoic rocks of the Biranup Zone, it is considered part of the Kepa Kurl Booya Province and not the Northern Foreland (Spaggiari et al., 2014a).

2.3 Paleoproterozoic Biranup and Nornalup Zones

The orogen-parallel Biranup Zone extends the entire length of the Albany-Fraser Orogen (Figure 2.1); it is thrust over the Northern Foreland, and is tectonically interleaved with Northern Foreland rocks in the central Biranup Zone (Spaggiari et al., 2014a). The Nornalup Zone is the southernmost and easternmost unit of the orogen, and like the Biranup Zone, spans the full length of the orogen.

The Biranup Zone is dominated by c. 1815 – 1625 Ma orthogneiss, paragneiss and metagabbro (Spaggiari et al., 2014a). The lack of any corresponding Paleoproterozoic overprinting of the Yilgarn Craton led to previous suggestions that the Biranup Zone was an exotic, accreted terrane (Nelson et al., 1995; Clark et al., 2000; Spaggiari et al., 2009). However, zircon Hf isotope signatures suggest the Paleoproterozoic magmatic rocks of the Biranup Zone consist of reworked Archean Yilgarn Craton material (εHf values as low as -12.2), with some input of new, juvenile material leading to increasingly juvenile signatures in younger rocks (εHf up to 2.2); and that therefore, the Biranup Zone formed as a magmatic arc on the Yilgarn Craton margin (Kirkland et al., 2011a).

The Paleoproterozoic component of the Nornalup Zone is c. 1810 – 1760 Ma in age, although few Paleoproterozoic rocks have been described due to the volumetric dominance of Mesoproterozoic granitic intrusions (Spaggiari et al., 2014a). Similarities in their Paleoproterozoic age components suggest the Nornalup Zone may be an outboard continuation of the Biranup Zone, rather than an exotic accreted terrane (Spaggiari et al., 2015).

Several distinct magmatic events are recognised within the Paleoproterozoic record. The oldest Paleoproterozoic rocks in the Biranup and Nornalup Zones are the granitic orthogneisses of the Salmon Gums Event (c. 1815 – 1800 Ma), followed by magmatism of the Ngadju Event (c. 1780 – 1760 Ma) in the Biranup, Nornalup and Tropicana Zones. The Biranup Orogeny (c. 1710 – 1650 Ma) comprises mainly granitic magmatism in the eastern Biranup Zone, and includes the Zanthus Event, a c. 1680 Ma amphibolite- to granulite-facies compressional event, and intrusion of the c. 1665 - 1660 Ma Eddy Suite, consisting of isotopically juvenile metagranodiorite and

metagabbro (Kirkland et al., 2011a). Rocks of the Eddy Suite were heterogeneously deformed during the Mesoproterozoic, and some primary magmatic fabrics and magma mingling textures are preserved (Kirkland et al., 2011a).

2.4 Barren Basin (1815 – 1600 Ma)

The Paleoproterozoic sedimentary rocks of the Albany-Fraser Orogen are interpreted as the remnants of an extensive sedimentary basin, the Barren Basin, which encompassed at least 1000 km along the southern and south-eastern margins of the Yilgarn Craton (Spaggiari et al., 2014b). Sedimentary units of the Barren Basin include the Stirling Range Formation, Mount Barren Group, Lindsay Hill Formation, Woodline Formation, Fly Dam Formation, and other unnamed paragneisses and schists; these rocks overlie and are variously derived from the Yilgarn Craton, Northern Foreland, and Biranup and Nornalup Zones (Figure 2.1; Spaggiari et al., 2014b).

Based on the dominantly quartz-rich lithologies, the Barren Basin is interpreted as a shallow basin system, with sediment deposition in a moderate to high energy, fluvial to marine environment (Spaggiari et al., 2015). Most Barren Basin rocks were deformed at low grades during the Mesoproterozoic, and relict sedimentary structures such as bedding or ripples are preserved (e.g. Rasmussen et al., 2004; Hall et al., 2008). The exception is the amphibolite- to granulite facies metapelitic Fly Dam Formation, which is interpreted to represent a mudstone and siltstone-dominated succession deposited in a deep marine environment (Spaggiari et al., 2015).

Depositional ages within the Barren Basin are constrained to 1815 – 1600 Ma (Spaggiari et al., 2014b). Two major sediment sources are inferred from detrital zircon geochronology: the adjacent Yilgarn Craton (2800 – 2600 Ma), and magmatic rocks of the Biranup Zone (1900 – 1600 Ma, with a peak at 1700 – 1650 Ma) (Spaggiari et al., 2014b). No local source is recognised for a minor component of detrital zircons with 2550 – 1900 Ma ages, suggesting some input of exotic material into the Barren Basin (Spaggiari et al., 2015).

Spaggiari et al. (2015) suggest a continental rift or back-arc setting for the Barren Basin due to the abundance of mature sediment, the dominance of locally-derived

material, and the lack of evidence for nearby subduction, accretion, or a magmatic arc. This is supported by dominantly felsic magmatism in the Biranup and Nornalup Zones that persisted for much of the duration of the Barren Basin. The lack of detrital zircons with 1600 – 1455 Ma ages throughout the Albany-Fraser Orogen is interpreted as a result of the transition to a tectonically quiescent passive margin by c. 1600 Ma (Spaggiari et al., 2015).

2.5 Arid Basin (1600 – 1300 Ma)

Like the Barren Basin, the sedimentary rocks of the Arid Basin are interpreted as the remnants of a formerly extensive basin system. The Arid Basin contains sedimentary units deposited after 1600 Ma (i.e. the end of Paleoproterozoic magmatism in the Biranup Zone) but deformed by Stage I of the Albany-Fraser Orogeny (1330 – 1260 Ma), and includes the Malcolm Metamorphics, Gwynne Creek Gneiss, Snowys Dam Formation, and unnamed paragneisses in the western Nornalup Zone (Figure 2.1; Love, 1999; Spaggiari et al., 2015).

The sedimentary sequences of the Arid Basin are composed primarily of sandstones and mudstones with minor calcareous and iron-rich rocks, although the Malcolm Metamorphics also contain mafic volcanic or volcaniclastic sequences (Spaggiari et al., 2015). Two detrital zircon populations have been correlated with local sediment sources: the magmatic rocks of the Biranup Zone (1700 – 1650 Ma), and magmatic and metamorphic rocks in the Tropicana, Nornalup and Biranup Zones (1825 – 1725 Ma) (Spaggiari et al., 2015). A third detrital zircon population at 1425 – 1375 Ma cannot be correlated with any known rocks in the Yilgarn Craton, or the Tropicana, Biranup, or Nornalup Zones (Spaggiari et al., 2015). Although these zircons are exotic to the Yilgarn Craton and Albany-Fraser Orogen, a nearby source is inferred due to the relative abundance of this age population; therefore, Spaggiari et al. (2015) suggest the c. 1410 Ma Loongana Arc, an oceanic arc located in the Madura Province immediately to the east of the Albany-Fraser Orogen, was a significant sediment source for the Arid Basin. These interpretations are supported by the similarity of Hf isotope signatures of detrital zircons with their inferred magmatic or metamorphic sources: εHf values of +12 to -2 for zircons in sedimentary

rock derived from the Loongana Arc, and εHf values of +8 to -10 for detrital zircons derived from magmatic rocks of the Biranup Zone (Spaggiari et al., 2015).

As previously discussed, sediment deposition in the Barren Basin ceased by c. 1600 Ma as it transitioned to a passive margin environment; therefore, the Arid Basin is interpreted to have commenced as a passive margin basin, with sediment deposition onto Biranup and Nornalup Zone substrates (Spaggiari et al., 2015). Minimal sedimentary input from the Yilgarn Craton implies that the Yilgarn Craton was not exposed at this time. Sedimentary input from the c. 1410 Ma oceanic Loongana Arc suggests that, by this time, convergence was occurring to the east of the Albany-Fraser Orogen; east-dipping subduction is inferred (Spaggiari et al., 2015). The eventual closure of this shrinking oceanic basin, the accretion of the Loongana Arc onto the eastern edge of the orogen, and accompanying slab detachment are interpreted as the tectonic causes of Stage I of the Albany-Fraser Orogeny; however, regardless of tectonic interpretation, sedimentation in the Arid Basin ceased by c. 1300 Ma (Spaggiari et al., 2015).

2.6 The Mesoproterozoic Albany-Fraser Orogeny

2.6.1 Recherche Supersuite (1330 – 1280 Ma)

The oldest evidence of Stage I activity in the orogen is the intrusion of the dominantly felsic Recherche Supersuite, which commenced at 1330 Ma and continued until 1280 Ma (Pidgeon, 1990; Nelson et al., 1995; Clark et al., 1999; Love, 1999; Clark et al., 2000; Spaggiari et al., 2011; Smithies et al., 2015). In the east Albany-Fraser Orogen, the Recherche Supersuite is subdivided by geochemistry into the Southern Hills Suite (1320 – 1287 Ma) and the Gora Hill Suite (1330 – 1283 Ma) (Smithies et al., 2015). The Southern Hills Suite has been identified throughout the east Albany-Fraser Orogen, and consists of highly evolved, small degree anatectic melts from felsic or quartzofeldspathic sources (Smithies et al., 2015). The Gora Hill Suite is more spatially restricted (central and eastern Nornalup Zone and Fraser Zone only) and varies spatially and temporally: the oldest intrusions are in the south-eastern Nornalup Zone, near the Rodona Shear Zone, and are relatively evolved, tending to syenogranitic compositions. Towards the northwest, magmatism

progressively decreases in age, compositions are less evolved (towards granodiorite), and whole-rock Nd isotopes record the mixing of crustal melts with increasing proportions of juvenile (mantle-derived) magmas (εNd isotopes form an array from -3.5 to -9.5; Smithies et al., 2015). The evolution of the Gora Hill Suite is interpreted to reflect a tectonic process such as northwest-progressing extensional orogenic collapse, and either a progressively shallower magma source, or the exposure of deeper crustal levels to the northwest (Smithies et al., 2015).

Spaggiari et al. (2011) note that Recherche Supersuite magmatism is less common in the west Albany-Fraser Orogen than in the east, although this may reflect a lack of geochronological data rather than a real spatial trend. Evidence of Stage I magmatism in the west Albany-Fraser Orogen is limited to three U/Pb zircon ages between c. 1290 – 1300 Ma from outcrops near Albany (Pidgeon, 1990; Love, 1999).

2.6.2 Fraser Zone (1305 – 1290 Ma)

The Fraser Zone is a c. 400 km long, 50 km wide, shear zone-bound domain within the east Albany-Fraser Orogen (Figure 2.1). It is lithologically distinct within the orogen, and is composed of c. 1305 – 1290 Ma coeval gabbroic and granitic intrusions into sedimentary rocks of the Snowys Dam Formation of the Arid Basin (Maier et al., 2016). Geochemical and whole-rock Nd isotopic analysis (εNd from -0.0 to -3.7) suggests the magmatic rocks are derived from mixing between juvenile, mantle-derived magmas and felsic crustal rocks with a Biranup Zone-like composition (Kirkland et al., 2011a; Smithies et al., 2015; Maier et al., 2016). Maier et al. (2016) suggest that the mafic and felsic lithologies are simply the endmembers of the same mixing process.

Due to the coeval timing, the voluminous mafic magmatism is interpreted as the driver of high temperature, medium to low pressure metamorphism throughout the Fraser Zone (Clark et al., 2014). Peak c. 850 °C and 7 – 9 kbar metamorphism in the Fraser Zone occurred at c. 1290 Ma, although metamorphic zircon growth as old as c. 1305 Ma has also been reported (Spaggiari et al., 2011; Clark et al., 2014). U/Pb monazite ages in the southwestern Fraser Zone range from 1285 – 1268 Ma (Clark et al., 2014).

The lack of Stage II U/Pb ages in the Fraser Zone, together with a 1285 ± 15 Ma $^{40}Ar/^{39}Ar$ hornblende age (Baksi and Wilson, 1980) and a 1268 ± 20 Ma Rb/Sr biotite age (Fletcher et al., 1991), has led most studies to interpret significant cooling and exhumation of the Fraser Zone to a shallow structural level following granulite metamorphism (Fletcher et al., 1991; Clark et al., 2000; Spaggiari et al., 2011; Clark et al., 2014). Exhumation of the Fraser Zone by along-strike extrusion to the southwest is supported by kinematic indicators along the Fraser and Newman Shear Zones (the north-western and south-eastern boundaries of the Fraser Zone, respectively), and the localised pattern of Biranup Zone deformation around the southwestern end of the Fraser Zone (Figure 2.1; Spaggiari et al., 2011).

Previous interpretations have suggested that the Fraser Zone represents a slice of the lower crust tectonically emplaced at a high crustal level (Fletcher et al., 1991); that the Fraser Zone comprises the remnants of accreted oceanic arcs (Condie and Myers, 1999); or that the Fraser Zone was a lower-crustal hot zone emplaced during extension, such as slab rollback in a back-arc setting (Kirkland et al., 2011a; Spaggiari et al., 2014b; Smithies et al., 2015). More recently, Maier et al. (2016) suggest that the Fraser Zone was emplaced in a dominantly extensional setting, possibly related to orogenic collapse. This interpretation is based on a lack of evidence for continued subduction after the accretion of the Loongana Arc, as well as the interpretation of extensional collapse as the driver of Recherche Supersuite magmatism (Smithies et al., 2015; Maier et al., 2016).

2.6.3 Deformation and metamorphism during Stage I (1330 – 1260 Ma)

In addition to the Recherche Supersuite magmatism and the emplacement of the Fraser Zone, Stage I orogeny resulted in high-grade metamorphism and northwest-directed compression throughout the Albany-Fraser Orogen. However, few well-defined pressure-temperature (P-T) constraints exist for Stage I metamorphism.

As described above, Stage I commenced with c. 1330 Ma intrusion of the Recherche Supersuite in the south-eastern Nornalup Zone, near the Rodona Shear Zone. Further to the east, Clark et al. (2000) describe northwest-directed Stage I folding in the central Nornalup Zone and in the Malcolm Metamorphics of the Arid

Basin. Early Stage I metamorphism in the Malcolm Metamorphics reached c. 750 °C and 4 – 5 kbar at or before c. 1330 Ma, and was followed by horizontal northwest-southeast shortening at a lower temperature before c. 1313 Ma (Clark et al., 2000).

Granulite facies metamorphism in the Fraser Zone, as described above, was coeval with mafic magmatism and reached c. 850 °C and 7 – 9 kbar at c. 1290 Ma, and was followed by isothermal decompression at c. 9 kbar (Clark et al., 2014).

To the south, the Coramup Gneiss is a belt of high-strain rocks in the central Albany-Fraser Orogen. Bodorkos and Clark (2004b, 2004a) report a Stage I history of c. 1300 Ma granulite facies metamorphism during extension (800-850°C, 5-7kbar) followed by c. 1290 Ma burial and recrystallization at high pressures during northwest-directed thrusting and folding (800-850°C; c 10kbar). A final phase of high temperature decompression (700-800°C, 7-8kbar) is accompanied by the intrusion of 1290 – 1280 Ma sills of the Recherche Supersuite (Bodorkos and Clark, 2004a).

In the west Albany-Fraser Orogen, evidence of Stage I is limited to three U/Pb zircon ages of Recherche Supersuite magmatism (Pidgeon, 1990; Love, 1999). Structural studies by Beeson et al. (1988) and Duebendorfer (2002) identify dextral transpression and northwest-southeast shortening in the west Albany-Fraser Orogen; however, the deformational events described by these authors have not been directly dated, and could correlate to either Stage I or Stage II of orogeny.

2.6.4 Ragged Basin (c. 1315 - 1175 Ma)

The Ragged Basin consists of metasedimentary rocks deposited after the end of Stage I orogeny, although the only known unit is the Mount Ragged Formation, located in the central Nornalup Zone (Figure 2.1). Sediment maturity and the quartz-rich succession of the Mount Ragged Formation are interpreted as the product of deposition in a shallow, intracontinental, extensional basin dominated by a large fluvial system with shifting braided channels (Waddell et al., 2015).

Most detrital zircons with ages of 1815 – 1320 Ma can be correlated with sediment input from the erosion of local Albany-Fraser Orogen crystalline basement rocks (Waddell et al., 2015). However, detrital zircon age components at 1560 Ma and 2490 Ma are exotic to the Albany-Fraser Orogen; these were either derived directly from

the exotic source, or were recycled through erosion of the nearby Malcolm Metasediments (Waddell et al., 2015).

The conservative estimate of a c. 1315 Ma maximum depositional age for the Mount Ragged Formation suggests that, following Stage I orogeny, the central Nornalup Zone was uplifted and eroded (Clark et al., 2000; Waddell et al., 2015). A minimum depositional age constraint of 1175 ± 12 Ma is provided by a cross-cutting, undeformed monzogranite, although this also post-dates amphibolite facies metamorphism and deformation during Stage II orogeny (Waddell et al., 2015).

2.6.5 Gnowangerup and Fraser dyke swarms (1215 – 1200 Ma)

The c. 1215 – 1200 Ma Gnowangerup and Fraser dyke swarms are orogen-parallel, tholeiitic dolerite dykes that intrude both the Yilgarn Craton and the Albany-Fraser Orogen, and were metamorphosed during Stage II (Figure 2.1; Evans, 1999; Clark et al., 2000; Wingate et al., 2000). In the west Albany-Fraser Orogen, the Gnowangerup dykes have been interpreted as the heat source for 1215 ± 20 Ma greenschist facies metamorphism in the Stirling Range Formation (Rasmussen et al., 2004).

2.6.6 Esperance Supersuite (1200 – 1140 Ma)

Stage II was accompanied by c. 1200 – 1140 Ma syn- to late-tectonic magmatism, with the intrusion of the voluminous granitic Esperance Supersuite into the Biranup and Nornalup Zones (Pidgeon, 1990; Black et al., 1992; Nelson et al., 1995; Smithies et al., 2015; Geological Survey of Western Australia, 2016).

In the Nornalup Zone of the west Albany-Fraser Orogen, U/Pb zircon ages of the Esperance Supersuite (formerly named the 'Burnside Batholith') are restricted to a narrow 1190 – 1170 Ma age range (Pidgeon, 1990; Black et al., 1992). The oldest Esperance Supersuite granites are foliated (Black et al., 1992), and are cross-cut by younger, undeformed granites that Pidgeon (1990) interpreted as post-tectonic. In the east Albany-Fraser Orogen, Esperance Supersuite granites range from c. 1200 – 1135 Ma (Nelson et al., 1995; Geological Survey of Western Australia, 2016). However,

most U/Pb zircon ages are between c. 1200 – 1160 Ma; the ages of two younger outliers are poorly constrained, at 1138 ± 38 Ma and 1135 ± 56 Ma (Nelson et al., 1995).

Smithies et al. (2015) divide the Esperance Supersuite into the Truslove Suite and the Booanya Suite according to geochemistry. Granites of the Truslove Suite have been identified in the central Biranup Zone and the central and eastern Nornalup Zone; field relationships, granite geochemistry, and a low εHf value of -15 for zircon from one sample suggest the Truslove Suite is generally derived from the partial melting of local source rocks (e.g. the felsic Paleoproterozoic orthogneisses of the Biranup Zone) (Kirkland et al., 2014; Smithies et al., 2015). The Booanya Suite has only been identified in the central and eastern Nornalup Zone, and its geochemistry suggests it is derived from the high-temperature melting of anhydrous lower crust, with possible juvenile (mantle-derived) input. Similarities in whole-rock Nd isotopic composition between the Booanya Suite (εNd from -4.9 to -7.3), Truslove Suite (εNd of one sample is -6.9), and Gora Hill Suite (of the Stage I Recherche Supersuite; εNd from -3.5 to -9.4) suggest a similar crustal residence age for the source of these granites (Smithies et al., 2015). Therefore, Smithies et al. (2015) suggest that the characteristic geochemistry of the Booanya Suite must derive from distinctly different melting conditions, such as higher source temperatures associated with crustal extension.

2.6.7 Deformation and metamorphism during Stage II (1225 – 1140 Ma)

Throughout most of the orogen, the oldest known Stage II event is the intrusion of the Gnowangerup and Fraser dyke swarms, although early Stage II metamorphism may have commenced at c. 1225 Ma in the central Biranup Zone (Spaggiari et al., 2009). Regardless, by c. 1200 Ma, Stage II was an orogen-wide, high-grade metamorphic event accompanied by northwest-directed shortening and extensive granitic magmatism (i.e. Esperance Supersuite).

There are few discernible spatial or temporal trends in Stage II deformation and metamorphism; the main exception is the Northern Foreland, where deformation intensity increases from greenschist to amphibolite facies towards the south and southeast (Beeson et al., 1988). Similarly, metamorphism in the Mount Barren Group, which overlies the Northern Foreland, grades from sub-greenschist facies in the north

to upper amphibolite facies in the south (Wetherley, 1998; Dawson et al., 2003). Garnet-biotite geothermometry and geothermobarometry of Mount Barren Group metapelites in the KFMASH system yielded metamorphic pressures and temperatures of 6 – 11 kbar and 625 – 650 °C (garnet-staurolite-kyanite-biotite-muscovite-quartz assemblages; Wetherley, 1998). Peak metamorphism, dated at 1205 ± 10 Ma, was interpreted to be coeval with the folding and thrusting of the Mount Barren Group onto the Northern Foreland during northwest-southeast compression (Wetherley, 1998; Dawson et al., 2003).

The Biranup Zone was deformed at upper amphibolite to granulite facies during Stage II. In the eastern Biranup Zone, upper amphibolite facies metamorphism (6.5 – 8.5 kbar, 675 – 725 °C) is constrained by c. 1190 – 1155 Ma U/Pb ages of zircon and titanite (Geological Survey of Western Australia, 2016; Kirkland et al., 2016). Within the Coramup Gneiss to the south, granulite facies metamorphism (5 – 6 kbar, 780 – 800 °C) coincided with northwest-vergent folding and dextral transpression, dated at 1168 ± 12 Ma by a syn-kinematic pegmatite in a shear zone (Bodorkos and Clark, 2004b, a). These ages overlap with primarily 1190 – 1170 Ma U/Pb zircon ages in the western Biranup Zone, dating granulite facies metamorphism and migmatisation during multiple episodes of northwest-southeast shortening (Black et al., 1992; Nelson et al., 1995; Spaggiari et al., 2009; Barquero-Molina, 2010).

Although Stage II deformation in the Nornalup Zone is not well constrained, existing U/Pb data suggest a shorter duration for metamorphism in the west than in the east. In the western Nornalup Zone, Black et al. (1992) dated granulite facies metamorphism at c. 1200 Ma, followed by dextral transpression and thrusting at c. 1190 Ma. Deformation presumably ceased within 10 – 20 Ma, as younger 1180 – 1170 Ma Esperance Supersuite intrusions are undeformed (Pidgeon, 1990; Black et al., 1992).

In the central Nornalup Zone, the greenschist to amphibolite facies (c. 4 – 5 kbar, 550 °C) Mount Ragged Formation was deformed by northwest-vergent folding and thrusting with a minimum age of 1175 ± 12 Ma, and shearing in the Malcolm Metamorphics pre-date an undeformed pegmatite at 1165 ± 5 Ma (Clark et al., 2000;

Waddell et al., 2015). The end of Stage II orogeny is defined by the intrusion of two undeformed Esperance Supersuite plutons in the central Nornalup Zone, with poorly constrained ages of 1138 ± 38 Ma and 1135 ± 56 Ma (Nelson et al., 1995).

Beeson et al. (1988) described two amphibolite- to granulite-facies tectonothermal events involving dextral transpression and northwest-directed thrusting in the west Albany-Fraser Orogen. Similarly, Duebendorfer (2002) describes three high grade deformational events, driven by northwest-directed compression. None of these events have been directly dated, but the second stage of Beeson et al. (1988) is interpreted to correlate with Stage II of orogeny.

2.6.8 The Fraser Zone during Stage II

Much of the current understanding of Stage I and Stage II in the Albany-Fraser Orogen depends on U/Pb zircon geochronology (e.g. Geological Survey of Western Australia, 2016). However, zircons in the Fraser Zone yield only Stage I ages for metamorphism and magmatism, despite its position between the Biranup and Nornalup Zones, both of which record high grade Stage II metamorphism (Figure 2.1). Recrystallised rims on a single monazite sample also yield a Stage II age of 1234 ±17 Ma at Gnamma Hill in the southwestern Fraser Zone (Clark et al., 2014). This may either be interpreted as geochronological evidence of Stage II, or alternatively, may represent monazite dissolution and reprecipitation due to the infiltration of a hydrothermal fluid (Clark et al., 2014).

A 1285 ± 15 Ma $^{40}Ar/^{39}Ar$ hornblende age and a 1268 ± 20 Ma Rb/Sr biotite age suggest the Fraser Zone was exhumed to shallow crustal levels after Stage I, and largely escaped thermal metamorphism during Stage II (Baksi and Wilson, 1980; Fletcher et al., 1991). Cooling following Stage I is supported by the brittle fracture of c. 1270 Ma zircon rims from a sample in the Gwynne Creek Gneiss (located between the north-eastern Biranup and Fraser Zones; Figure 2.1), which are filled by c. 1193 Ma hydrothermal zircon growth, requiring uplift and brittle deformation between 1270 – 1193 Ma (Kirkland et al., 2016). Clark et al. (2014) suggested that the absence of Stage II U/Pb zircon ages is a product of the cooling and strengthening of the Fraser

Zone after Stage I, rendering it less susceptible to later metamorphism or deformation.

More recently, Kirkland et al. (2016) reported a Stage I, c. 1299 Ma U/Pb titanite age from the Fraser Shear Zone, the north-western boundary of the Fraser Zone. However, small titanite grains in this sample record a Stage II age of 1205 ± 16 Ma, requiring metamorphism at temperatures of 695 – 725 °C. Kirkland et al. (2016) note that the U/Pb system is more susceptible to resetting in titanite than in zircon, and based on this sample, suggest the Fraser Zone was deformed at upper amphibolite facies during Stage II.

2.6.9 Tectonic setting of Stage I and Stage II

Traditionally, Stage I of the Albany-Fraser Orogeny was interpreted as a collisional orogen, recording the suturing of the West Australian Craton (including the Yilgarn Craton) to the Mawson Craton (encompassing present-day South Australia and East Antarctica) during the assembly of Rodinia (e.g. Clark et al., 2000; Bodorkos and Clark, 2004b; Spaggiari et al., 2009). This interpretation was based on similar c. 1300 Ma ages for deformation in the adjacent terranes, including the Bunger Hills of East Antarctica, the Musgrave Province to the northeast, and the Coompana Block to the east (Black et al., 1992; Myers, 1995; Clark et al., 2000). Following on from Stage I continental collision, Stage II was traditionally interpreted as a period of 'intracontinental reactivation', although no cause for this reactivation was proposed (e.g. Clark et al., 2000; Bodorkos and Clark, 2004b; Spaggiari et al., 2011).

However, this interpretation has been recently challenged (Kirkland et al., 2015; Smithies et al., 2015; Spaggiari et al., 2015; Maier et al., 2016; Spaggiari et al., 2016). In the Madura Province to the east of the Nornalup Zone, c. 1410 Ma rocks with juvenile, oceanic affinities have been interpreted as a relic oceanic arc above an east-dipping subduction zone (the Loongana Arc; Spaggiari et al., 2014b; Kirkland et al., 2017). Subduction of the intervening ocean basin and accretion of the arc onto the eastern Albany-Fraser Orogen at c. 1330 Ma is suggested as the initial driver of Stage I, with subsequent orogenic collapse resulting in felsic magmatism of the Recherche Supersuite (Spaggiari et al., 2014b; Smithies et al., 2015; Maier et al., 2016).

This interpretation places the orogen into a continental margin setting for Stage II, rather than the previously assumed intracontinental setting. However, the tectonic driver of Stage II orogeny remains unclear.

The intraplate geochemical signature of the Booanya Suite granites led Smithies et al. (2015) to suggest that Esperance Supersuite magmatism was driven by extension. Based on new geochemistry and geochronology from the Madura and Coompana Provinces, Spaggiari et al. (2016) note that granitic magmatism at c. 1200 – 1140 Ma is not confined to the Albany-Fraser Orogen. The recently identified Moodini Supersuite in the Madura and Coompana Provinces, and the Pitjantjatjara Supersuite of the Musgrave Province to the northeast, are coeval with and compositionally equivalent to the Esperance Supersuite (Spaggiari et al., 2016; Kirkland et al., 2017). This widespread high temperature magmatic event has been named the Maralinga Event, and is interpreted to result from high temperature, low pressure melting of the relatively thin oceanic crust separating the Yilgarn and Mawson Cratons (Spaggiari et al., 2016).

However, all structural studies in the Albany-Fraser Orogen support significant northwest-directed compression during Stage II, in some places synchronous with or overprinting Esperance Supersuite magmatism (Beeson et al., 1988; Black et al., 1992; Myers, 1995; Clark et al., 2000; Duebendorfer, 2002; Bodorkos and Clark, 2004b; Barquero-Molina, 2010; Waddell et al., 2015). Of these, only one study identified significant extension during Stage II: Barquero-Molina (2010) describes several phases of northwest-vergent folding alternating with phases of 'bidirectional extension' (i.e. flattening) in the western Biranup Zone.

One important point suggested by this study is that multiple tectonic processes may have been active at different times, or even simultaneously, within the orogen. This is especially likely considering the long, 85-million-year duration of Stage II (i.e. longer than the time that has elapsed since the Indian plate collided with the Eurasian plate). Regardless, the specific tectonic processes driving Stage II orogeny remain unclear.

The importance of geological constraints from adjacent terrains for understanding the tectonic setting of the Albany-Fraser Orogen is highlighted by new geochemical and isotopic data from the poorly understood Madura and Coompana Provinces (Spaggiari et al., 2016; Kirkland et al., 2017). These domains are interpreted to consist of reworked oceanic crust, stabilised and cratonised during the Maralinga Event. Crucially, the preservation of unsubducted oceanic crust between the West Australian and South Australian Cratons suggests that the two cratons may never have actually collided (Kirkland et al., 2017).

The new interpretations of Spaggiari et al. (2016) and Kirkland et al. (2017) raise important questions about the nature and location of the boundary between the West Australian Craton and the West Mawson Craton (the East Antarctic component of the Mawson Craton), i.e. the role and extent of the west Albany-Fraser Orogen. Former models interpreted the orogen as a single, long collisional orogen, with the west Albany-Fraser Orogen marking the implied suture zone between the southern Yilgarn Craton and the West Mawson Craton (Clark et al., 2000; Bodorkos and Clark,

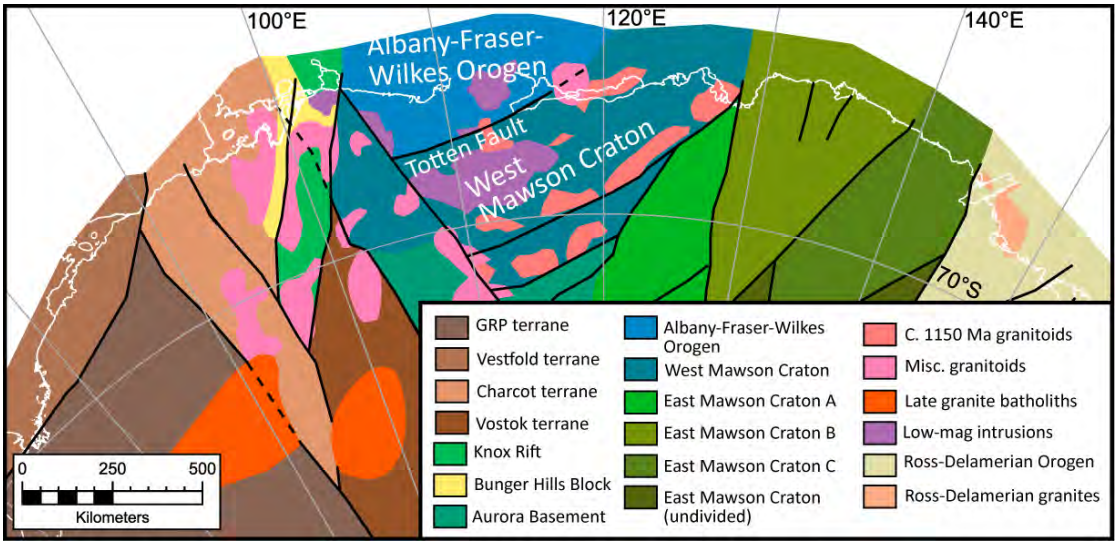

Figure 2.2 Interpreted bedrock geology map of Wilkes Land, East Antarctica, showing the major tectonic units and overprinting magmatic suites. The Antarctic component of the Albany-Fraser Orogen extends for up to 250 km under cover of the ice sheet, and very little geological information is available for the West Mawson Craton. The Totten Fault is the Antarctic equivalent of the Rodona Shear Zone. GRP terrane: Gamburtsev-Ruker-Princess Elizabeth Land. Modified from Aitken et al. (2014).

2004b; Spaggiari et al., 2009). Geophysical data allow possible correlation of major structures and units of the Albany-Fraser Orogen across to Wilkes Land; for example, the subglacial geology interpreted by Aitken et al. (2014) suggests that the orogen may extend for up to 250 km under cover of ice in Antarctica (Figure 2.2). Given the lack of evidence for collisional orogenesis in the east of the orogen (Spaggiari et al., 2016), it is possible that collision only occurred with the West Mawson Craton, or that no part of the orogen was affected by continental collision. However, the composition and origin of the West Mawson Craton south of the Totten Fault (the Antarctic continuation of the Rodona Shear Zone, defining the boundary of the Albany-Fraser Orogen) is unknown, as is the nature of the boundary between the Albany-Fraser Orogen and the West Mawson Craton (Figure 2.2; Payne et al., 2009; Aitken et al., 2014).

2.7 Previous Thermochronology

The current understanding of the geological history of the Albany-Fraser Orogen depends primarily on age constraints from U/Pb zircon geochronology (e.g. Clark et al., 2000; Spaggiari et al., 2014b; Geological Survey of Western Australia, 2016). The few existing thermochronological data, primarily Rb/Sr, K/Ar and $^{40}Ar/^{39}Ar$ mineral ages, are summarised in Figure 2.3 and discussed here.

Early K/Ar and Rb/Sr dating of muscovite and biotite in the Fraser Zone yielded 1210 – 1280 Ma mineral ages (Aldrich et al., 1959; Wilson et al., 1959), which were recalculated to 1240 – 1280 Ma by Wilson and Baksi (1984). However, these three reports include very little additional information about the samples: the analytical data are not included, and the sample locality is described only as 'Fraser Range'.

Additional thermochronology in the east Albany-Fraser Orogen is restricted to a hornblende $^{40}Ar/^{39}Ar$ age of 1285 ± 15 Ma from the southwestern Fraser Zone (Baksi and Wilson, 1980; sample locality given in Wilson and Baksi, 1984) and a two-point biotite-whole rock Rb/Sr age of 1264 ± 20 Ma from the eastern margin of the Fraser Zone (Fletcher et al., 1991). As discussed in section 2.3.4 above, these data are used as evidence for the cooling of the Fraser Zone below c. 350 °C following Stage I orogeny (e.g. Spaggiari et al., 2011; Clark et al., 2014).

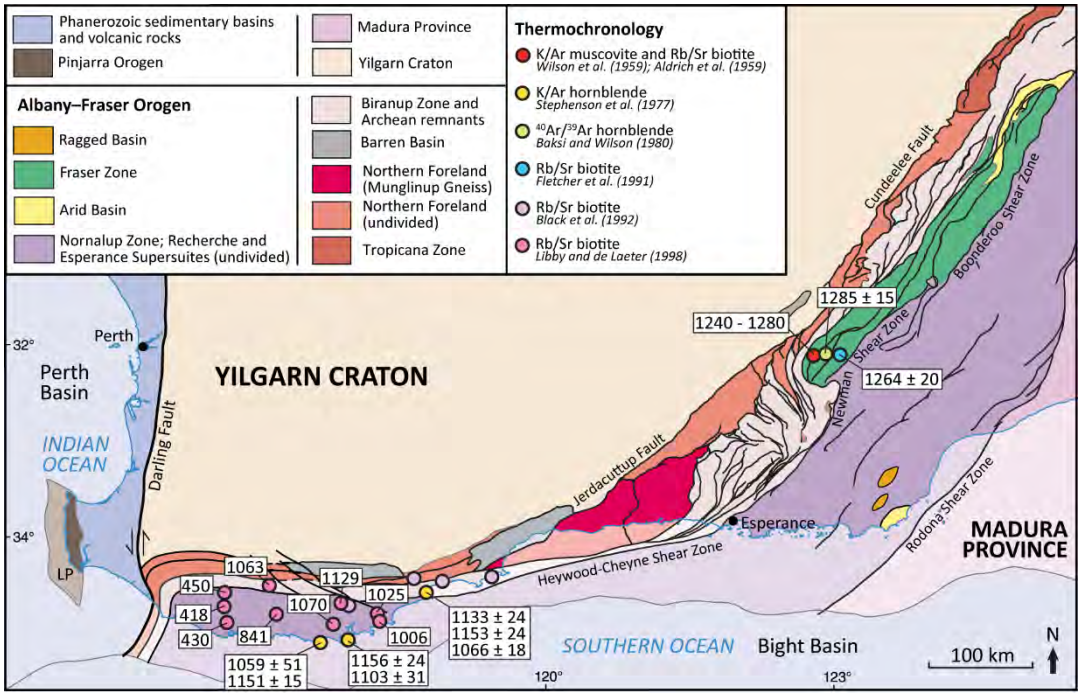

Figure 2.3 Interpreted bedrock geology map of the Albany-Fraser Orogen, showing published K/Ar, Rb/Sr and $^{40}Ar/^{39}Ar$ thermochronology ages in Ma. Map after Spaggiari et al. (2014b).

In the Biranup and Nornalup Zones of the west Albany-Fraser Orogen, Stephenson et al. (1977) report seven hornblende K/Ar ages between 1059 – 1156, interpreted to date either the emplacement of undeformed granite plutons (i.e. the Esperance Supersuite), or to date uplift and cooling following regional metamorphism. However, unlike the $^{40}Ar/^{39}Ar$ step-heating technique, K/Ar dating does not allow for the recognition of radiogenic argon loss, mineral alteration, or the presence of excess $^{40}Ar^*$. Therefore, the hornblende K/Ar ages provide only semi-quantitative constraints, and are most likely to be minimum ages given that minor diffusive argon loss is commonly recognised in $^{40}Ar/^{39}Ar$ thermochronology. This interpretation of variable amounts of unrecognised radiogenic argon loss is further supported by the fact that the 1156 Ma maximum age of Stephenson et al. (1977) approaches the c. 1169 Ma $^{40}Ar/^{39}Ar$ hornblende ages reported in Chapter 3, and that many of the $^{40}Ar/^{39}Ar$ degassing spectra yielded total fusion ages that were younger than the plateau ages.

Black et al. (1992) report ten Rb/Sr ages from the west Albany-Fraser Orogen, four of which are multi-mineral isochrons rather than whole-rock isochrons (i.e.

thermochronometers rather than geochronometers). However, the analysed phases are notably in disequilibrium and do not yield statistically significant isochron ages unless biotite or feldspar are excluded from the calculation, suggesting open-system behaviour for one or more minerals within these samples (Black et al., 1992).

Libby and De Laeter (1998) report several biotite Rb/Sr ages from across southwestern Australia, including nine ages for the west Albany-Fraser Orogen (Figure 2.3). Three of these ages are calculated as two-point biotite-whole rock isochrons; the remaining six are calculated with an assumed initial $^{87}Sr/^{86}Sr$ of 0.70. Biotite Rb/Sr ages decrease from c. 1130 Ma near Albany to c. 420 Ma near Walpole, due to overprinting of the Albany-Fraser Orogen by inferred Pan-African tectonism along the western margin of the Yilgarn Craton (Libby and De Laeter, 1998).

Libby and De Laeter (1998) use the ^{87}Rb decay constant recommended by Steiger and Jäger (1977). Recalculating their oldest Rb/Sr biotite age with the ^{87}Rb decay constant recommended by Villa et al. (2015) results in a c. 1.6% increase in age, i.e. from c. 1130 Ma to c. 1148 Ma for the Rb/Sr biotite age near Albany. The recalculated age is comparable with the $^{40}Ar/^{39}Ar$ biotite ages reported in Chapter 3.

2.8 References

Aitken, A. R. A., Young, D. A., Ferraccioli, F., Betts, P. G., Greenbaum, J. S., Richter, T. G., Roberts, J. L., Blankenship, D. D., and Siegert, M. J., 2014, The subglacial geology of Wilkes Land, East Antarctica: Geophysical Research Letters, v. 41, p. 2390-2400.

Aldrich, L. T., Wetherill, G. W., Bass, M. N., Compston, W., Davis, G. L., and Tilton, G. R., 1959, Mineral age measurements: Carnegie Institute of Washington Yearbook, v. 58, p. 237-250.

Baksi, A. K., and Wilson, A. F., 1980, An attempt at Argon dating of two granulite-facies terranes: Chemical Geology, v. 30, p. 109-120.

Barquero-Molina, M., 2010, Kinematics of bidirectional extension and coeval NW-directed contraction in orthogneisses of the Biranup Complex, Albany Fraser Orogen, Southwestern Australia: Geological Survey of Western Australia, Report 109, p. 205.

Beeson, J., Delor, C. P., and Harris, L. B., 1988, A structural and metamorphic traverse across the Albany Mobile Belt, Western Australia: Precambrian Research, v. 40/41, p. 117-136.

Black, L. P., Harris, L. B., and Delor, C. P., 1992, Reworking of Archaean and Early Proterozoic components during a progressive, Middle Proterozoic tectonothermal event in the Albany Mobile Belt, Western Australia: Precambrian Research, v. 59, p. 95-123.

Bodorkos, S., and Clark, D., 2004a, Evolution of a crustal-scale transpressive shear zone in the Albany-Fraser Orogen, SW Australia: 1. P-T conditions of Mesoproterozoic metamorphism in the Coramup Gneiss: Journal of Metamorphic Geology, v. 22, p. 691 - 711.

-, 2004b, Evolution of a crustal-scale transpressive shear zone in the Albany-Fraser Orogen, SW Australia: 2. Tectonic history of the Coramup Gneiss and a kinematic framework for Mesoproterozoic collision of the West Australian and Mawson cratons: Journal of Metamorphic Geology, v. 22, p. 713-731.

Clark, C., Kirkland, C. L., Spaggiari, C. V., Oorschot, C. W., Wingate, M. T. D., and Taylor, B., 2014, Proterozoic granulite formation driven by mafic magmatism: An example from the Fraser Range Metamorphics, Western Australia: Precambrian Research, v. 240, p. 1-21.

Clark, D., Hensen, B., and Kinny, P., 2000, Geochronological constraints for a two-stage history of the Albany-Fraser Orogen, Western Australia: Precambrian Research, v. 102, p. 155-183.

Clark, D. J., Kinny, P. D., Post, N. J., and Hensen, B. J., 1999, Relationships between magmatism, metamorphism and deformation in the Fraser Complex, Western Australia: constraints from new SHRIMP U-Pb zircon geochronology: Australian Journal of Earth Sciences, v. 46, p. 923-932.

Condie, K. C., and Myers, J. S., 1999, Mesoproterozoic Fraser Complex: geochemical evidence for multiple subduction-related sources of lower crustal rocks in the Albany-Fraser Orogen, Western Australia: Australian Journal of Earth Sciences, v. 46, p. 875-882.

Dawson, G. C., Krapez, B., Fletcher, I. R., McNaughton, N. J., and Rasmussen, B., 2003, 1.2 Ga thermal metamorphism in the Albany-Fraser orogen of Western Australia: consequence of collision or regional heating by dyke swarms?: Journal of the Geological Society, London, v. 160, p. 29-37.

Duebendorfer, E. M., 2002, Regional correlation of Mesoproterozoic structures and deformational events in the Albany-Fraser orogen, Western Australia: Precambrian Research, v. 116, p. 129 - 154.

Evans, T., 1999, Extent and nature of the 1200 Ma Wheatbelt dyke swarm, south-western Australia: University of Western Australia, BSc (Honours) thesis (unpublished).

Fitzsimons, I., 2000, Grenville-age basement provinces in East Antarctica: Evidence for three separate collisional orogens: Geology, v. 28, no. 10, p. 879-882.

Fletcher, I. R., Myers, J. S., and Ahmat, A. L., 1991, Isotopic evidence on the age and origin of the Fraser Complex, Western Australia: a sample of Mid-Proterozoic lower crust: Chemical Geology (Isotope Geoscience Section), v. 87, p. 197-216.

Geological Survey of Western Australia, 2016, Compilation of geochronology information 2016: Government of Western Australia, ISBN: 9781741686876.

Hall, C. E., Jones, S. A., and Bodorkos, S., 2008, Sedimentology, structure and SHRIMP zircon provenance of the Woodline Formation, Western Australia: Implications for the tectonic setting of the West Australian Craton during the Paleoproterozoic: Precambrian Research, v. 162, p. 577-598.

Kirkland, C. L., Smithies, R. H., and Spaggiari, C. V., 2015, Foreign contemporaries - Unravelling disparate isotopic signatures from Mesoproterozoic Central and Western Australia: Precambrian Research, v. 265, p. 218-231.

Kirkland, C. L., Smithies, R. H., Spaggiari, C. V., Wingate, M. T. D., Quentin de Gromard, R., Clark, C., Gardiner, N. J., and Belousova, E. A., 2017, Proterozoic crustal evolution of the Eucla basement, Australia: Implications for destruction of oceanic crust during emergence of Nuna: Lithos, DOI: 10.1016/j.lithos.2017.01.029.

Kirkland, C. L., Spaggiari, C. V., Johnson, T. E., Smithies, R. H., Danišík, M., Evans, N., Wingate, M. T. D., Clark, C., Spencer, C., Mikucki, E., and McDonald, B. J., 2016, Grain size matters: Implications for element and isotopic mobility in titanite: Precambrian Research, v. 278, p. 283-302.

Kirkland, C. L., Spaggiari, C. V., Pawley, M. J., Wingate, M. T. D., Smithies, R. H., Howard, H. M., Tyler, I. M., Belousova, E. A., and Poujol, M., 2011a, On the edge: U–Pb, Lu–Hf, and Sm–Nd data suggests reworking of the Yilgarn craton margin during formation of the Albany-Fraser Orogen: Precambrian Research, v. 187, no. 3–4, p. 223-247.

Kirkland, C. L., Spaggiari, C. V., Smithies, R. H., and Wingate, M. T. D., 2014, Cryptic pyrogeny of craton margins: geochronology and isotope geology of the Albany-Fraser Orogen, with implications for evolution of the Tropicana Zone, *in*

Spaggiari, C. V., and Tyler, I. M., eds., Albany-Fraser Orogen seismic and magnetotelluric (MT) workshop 2014: extended abstracts, Geological Survey of Western Australia, Record 2014/6, p. 89-101.

Kirkland, C. L., Spaggiari, C. V., Wingate, M. T. D., Smithies, R. H., Belousova, E., and Murphy, R., 2011b, Inferences on crust-mantle interaction from Lu-Hf isotopes: a case study from the Albany-Fraser Orogen: Geological Survey of Western Australia, Record 2011/12, p. 25.

Korsch, R. J., Spaggiari, C. V., Occhipinti, S. A., Doublier, M. P., Clark, D. J., Dentith, M. C., Doyle, M. G., Kennett, B. L. N., Gessner, K., Neumann, N. L., Belousova, E., Tyler, I. M., Costelloe, R. D., Fomin, T., and Holzschuh, J., 2014, Geodynamic implications of the 2012 Albany-Fraser deep seismic reflection survey: a transect from the Yilgarn Craton across the Albany-Fraser Orogen to the Madura Province, *in* Spaggiari, C. V., and Tyler, I. M., eds., Albany-Fraser Orogen seismic and magnetotelluric (MT) workshop 2014: extended abstracts, Record 2014/6, Geological Survey of Western Australia, p. 142-173.

Libby, W. G., and De Laeter, J. R., 1998, Biotite Rb-Sr age evidence for Early Palaeozoic tectonism along the cratonic margin in southwestern Australia: Australian Journal of Earth Sciences, v. 45, no. 623-632.

Love, G. J., 1999, A study of wall-rock contamination in a tonalitic gneiss from King Point, near Albany, Western Australia: Curtin University of Technology, BSc (Honours) thesis (unpublished).

Maier, W. D., Smithies, R. H., Spaggiari, C. V., Barnes, S. J., Kirkland, C. L., Kiddie, O., and Roberts, M. P., 2016, The evolution of mafic and ultramafic rocks of the Mesoproterozoic Fraser Zone, Albany-Fraser Orogen, and implications for Ni-Cu sulfide potential of the region: Geological Survey of Western Australia, Record 2016/8, p. 49.

Myers, J. S., 1995, Geology of the Esperance 1:1 000 000 sheet: Geological Survey of Western Australia, 1:1 000 000 Geological Series Explanatory Notes, p. 10.

Nelson, D. R., Myers, J. S., and Nutman, A. P., 1995, Chronology and evolution of the Middle Proterozoic Albany-Fraser Orogen, Western Australia: Australian Journal of Earth Sciences, v. 42, no. 5, p. 481 - 495.

Occhipinti, S. A., Doyle, M. G., Spaggiari, C. V., Korsch, R. J., Cant, G., Martin, K., Kirkland, C. L., Savage, J., Less, T., Bergin, L., and Fox, L. J., 2014, Interpretation of the deep seismic reflection line 12GA-T1: northeastern Albany-Fraser Orogen, *in* Spaggiari, C. V., and Tyler, I. M., eds., Albany-Fraser Orogen seismic and magnetotelluric (MT) workshop 2014: extended abstracts, Geological Survey of Western Australia, Record 2014/6, p. 52-68.

Payne, J. L., Hand, M., Barovich, K. M., Reid, A., and Evans, D. A. D., 2009, Correlations and reconstruction models for the 2500-1500 Ma evolution of the Mawson Continent: Geological Society of London Special Publications, DOI: 10.1144/SP323.16.

Pidgeon, R. T., 1990, Timing of plutonism in the Proterozoic Albany Mobile Belt, southwestern Australia: Precambrian Research, v. 47, p. 157-167.

Rasmussen, B., Fletcher, I. R., Bengtson, S., and McNaughton, N. J., 2004, SHRIMP U-Pb dating of diagenetic xenotime in the Stirling Range Formation, Western Australia: 1.8 billion year minimum age for the Stirling biota: Precambrian Research, v. 133, p. 329 - 337.

Smithies, R. H., Spaggiari, C. V., and Kirkland, C. L., 2015, Building the crust of the Albany-Fraser Orogen: constraints from granite geochemistry: Geological Survey of Western Australia, v. Report 150, p. 49p.

Spaggiari, C., Bodorkos, S., Barquero-Molina, M., Tyler, I., and Wingate, M. T. D., 2009, Interpreted bedrock geology of the southern Yilgarn and central Albany-Fraser Orogen, Western Australia: Geological Survey of Western Australia, Record 2009/10, p. 84.

Spaggiari, C. V., Kirkland, C. L., Pawley, M. J., Smithies, R. H., Wingate, M. T. D., Doyle, M. G., Blenkinsop, T. G., Clark, C., Oorschot, C. W., Fox, L. J., and Savage,

J., 2011, The geology of the east Albany-Fraser Orogen - a field guide: Geological Survey of Western Australia, Record 2011/23, p. 92.

Spaggiari, C. V., Kirkland, C. L., Smithies, R. H., Occhipinti, S. A., and Wingate, M. T. D., 2014a, Geological framework of the Albany-Fraser Orogen, *in* Spaggiari, C. V., and Tyler, I. M., eds., Albany-Fraser Orogen seismic and magnetotelluric (MT) workshop 2014: extended abstracts, Record 2014/6, Geological Survey of Western Australia, p. 12-27.

Spaggiari, C. V., Kirkland, C. L., Smithies, R. H., and Wingate, M. T. D., 2014b, Tectonic links between Proterozoic sedimentary cycles, basin formation and magmatism in the Albany-Fraser Orogen, Western Australia: Geological Survey of Western Australia, Report 133.

Spaggiari, C. V., Kirkland, C. L., Smithies, R. H., Wingate, M. T. D., and Belousova, E., 2015, Transformation of an Archean craton margin during Proterozoic basin formation and magmatism: The Albany-Fraser Orogen, Western Australia: Precambrian Research, v. 266, p. 440-466.

Spaggiari, C. V., Occhipinti, S. A., Korsch, R. J., Doublier, M. P., Clark, D. J., Dentith, M. C., Gessner, K., Doyle, M. G., Tyler, I. M., Kennett, B. L. N., Costelloe, R. D., Fomin, T., and Holzschuh, J., 2014c, Interpretation of Albany-Fraser seismic lines 12GA-AF1, 12GA-AF2 and 12GA-AF3: implications for crustal architecture, *in* Spaggiari, C. V., and Tyler, I. M., eds., Albany-Fraser Orogen seismic and magnetotelluric (MT) workshop 2014: extended abstracts, Record 2014/6, Geological Survey of Western Australia, p. 28 - 51.

Spaggiari, C. V., Smithies, R. H., Wingate, M. T. D., Kirkland, C. L., and England, R. N., 2016, Exposing the Eucla basement: what separates the Albany-Fraser Orogen and the Gawler Craton?, GSWA 2016 extended abstracts: promoting the prospectivity of Western Australia, Geological Survey of Western Australia, Record 2016/2, p. 36-41.

Steiger, R. H., and Jäger, E., 1977, Subcommision on geochronology: Convention on the use of decay constants in geo- and cosmochronology: Earth and Planetary Science Letters, v. 36, p. 359-362.

Stephenson, N. C. N., Russell, T. G., Stubbs, D., and Kalocsai, G. I. Z., 1977, Potassium-argon ages of hornblendes from Precambrian gneisses from the south coast of Western Australia: Journal of the Royal Society of Western Australia, v. 59, no. 4, p. 105-109.

Villa, I. M., De Bièvre, P., Holden, N. E., and Renne, P. R., 2015, IUPAC-IUGS recommendation on the half life of ^{87}Rb: Geochimica et Cosmochimica Acta, v. 164, p. 382-385.

Waddell, P. J., Timms, N. E., Spaggiari, C. V., Kirkland, C. L., and Wingate, M. T. D., 2015, Analysis of the Ragged Basin, Western Australia: Insights into syn-orogenic basin evolution within the Albany-Fraser Orogen: Precambrian Research, v. 261, p. 166-187.

Wetherley, S., 1998, Tectonometamorphic evolution of the Mount Barren Group, Albany-Fraser Province, Western Australia: PhD thesis, University of Western Australia.

Wilson, A. F., and Baksi, A. K., 1984, Oxygen isotope fractionation and disequilibrium displayed by some granulite facies rocks from the Fraser Range, Western Australia: Geochimica et Cosmochimica Acta, v. 48, no. 3, p. 423-432.

Wilson, A. F., Compston, W., Jeffery, P. M., and Riley, G. H., 1959, Radiactive ages from the Precambrian rocks in Australia: Journal of the Geological Society of Australia, v. 6, no. 2, p. 179-195.

Wingate, M. T. D., Campbell, I. H., and Harris, L. B., 2000, SHRIMP baddeleyite age for the Fraser Dyke Swarm, southeast Yilgarn Craton, Western Australia: Australian Journal of Earth Sciences, v. 47, p. 309-313.

Chapter 3

Rapid cooling and exhumation in the western part of the Mesoproterozoic Albany-Fraser Orogen, Western Australia

3 Rapid cooling and exhumation in the western part of the Mesoproterozoic Albany-Fraser Orogen, Western Australia

Elisabeth Scibiorski[a,*], Eric Tohver[a], Fred Jourdan[b]

[a]School of Earth and Environment, University of Western Australia, Perth, Western Australia

[b]Western Australian Argon Isotope Facility, John de Laeter Centre, Department of Applied Geology, Curtin University, Perth, Western Australia

Abstract

The Albany-Fraser Orogen of southwestern Australia is an understudied orogenic belt, which is interpreted to record the Mesoproterozoic suturing of the Yilgarn Craton of Western Australia to the Mawson Craton of East Antarctica during Rodinia assembly. Previous U-Pb geochronology has dated peak amphibolite to granulite-facies metamorphism in the orogen at ca 1180 Ma. Here, we report the first $^{40}Ar/^{39}Ar$ thermochronology of hornblende, biotite and muscovite grains from a 360 km transect across the western Albany-Fraser Orogen, and uncover a record of strikingly fast syn-orogenic cooling and exhumation.

To the north, muscovites from the Northern Foreland record cooling at ca 1159 Ma. In the central and southern domains of the orogen, the Biranup and Nornalup Zones, hornblende yields ca 1169 Ma cooling ages, and biotite yields ca 1172 – 1144 Ma cooling ages. The new cooling ages imply that the three domains were exhumed rapidly following peak metamorphism at ca 1180 Ma, attained a similar structural level by ca 1159 Ma, and have experienced a uniform exhumation history since that time. To constrain mineral closure temperatures and post-peak metamorphic cooling rates, we conducted a Monte Carlo simulation, which fully propagates uncertainty and minimises error correlations. Modelling of cooling from hornblende to biotite closure temperatures (ca 585 °C and 365 °C respectively) in the Nornalup and Biranup Zones yields fast cooling rates of 33^{+17}_{-9} °C/Ma and 22^{+7}_{-5} °C/Ma respectively. These fast

cooling rates imply rapid exhumation in an active tectonic setting undergoing peak metamorphism. Although the structural evolution of the Albany-Fraser Orogen remains poorly constrained, the transpressional tectonic activity associated with deformation in the western part of the Albany-Fraser Orogen may have been an active driver of this fast exhumation. This is distinctly different from exhumation models for granulite-facies domains in other Mesoproterozoic orogens, which typically experience post-orogenic, slow 1 – 5 °C/Ma cooling, driven by mechanisms such as orogenic collapse and erosion. We consider that the observed differences reflect the interpreted syn-tectonic transpressional exhumation history of the Albany-Fraser Orogen, which is an underrepresented tectonic regime in the Mesoproterozoic cooling record.

3.1 Introduction

Exhumation processes can be difficult to ascertain, especially in ancient orogenic belts. Thermochronology can be used to determine the distribution of cooling ages and rates across an orogen, providing an important tool in resolving orogenic exhumation histories. Orogenic cooling rates may be highly variable, and when taken in isolation are not diagnostic of a particular exhumation mechanism (Ring et al., 1999). However, when integrated with other datasets such as structural and metamorphic histories, cooling rates may be correlated with tectonic setting and with exhumation mechanism. For example, in collisional settings, large hot orogens (LHO), which are characterised by a plateau in the hinterland, typically experience slow exhumation driven by orogenic collapse. In contrast, small cold orogens (SCO) are rheologically stronger and do not undergo orogenic collapse, but are exhumed more quickly by erosion (Jamieson and Beaumont, 2013).

A compounding factor in comparing cooling histories from different orogens is the empirical correlation between decreasing cooling rate and increasing orogenic age. Dunlap (2000) showed that cooling rates in ancient Proterozoic collisional orogens are slower than those in Phanerozoic orogens (Dunlap, 2000). Empirical estimates of cooling rates in Proterozoic orogens are between 0.5 and 5 °C/Ma, whereas those for Phanerozoic orogens range from 5 to 50 °C/Ma (Dunlap, 2000; Willigers et al., 2002) and up to 150 - 350 °C/Ma in young, tectonically active orogens (e.g. Zeck et al., 1992; Arnaud et al., 1993). Dunlap (2000) suggested that the difference in cooling rates reflects the decreasing preservation potential of the thermochronological record with age, as Proterozoic orogens are more vulnerable to isotopic resetting than Phanerozoic orogens. Additionally, the present-day surface exposures of many Proterozoic orogens consist of the deeply eroded orogenic cores, which were at deep crustal levels during orogeny and were not exhumed until well after the orogenic cycle was complete (Willigers et al., 2002). Consequently, the Proterozoic thermochronological record is therefore biased towards slow post-orogenic cooling, rather than the faster, syn-orogenic processes recorded in the upper-crustal rocks typically exposed in Phanerozoic orogens (Willigers et al., 2002).

The cooling records of global Mesoproterozoic orogens vary in their degree of preservation, as thermal histories are vulnerable to overprinting by later heating events. For example, both the Natal Metamorphic Province of South Africa and the Eastern Ghats Belt of India were active in the Mesoproterozoic assembly of Rodinia, but yield few data about post-orogenic cooling due to overprinting by ca 500 Ma Pan-African tectonism (Jacobs et al., 1997; Mezger and Cosca, 1999). In contrast, records of cooling and exhumation from the Grenville Orogen of North America, its inferred counterpart in the South American Amazon Craton and the Sveconorwegian Orogen of Scandinavia have not been overprinted, and are comparatively well understood due to several thermochronological studies (e.g. Page et al., 1996; Busch et al., 1997; Bingen et al., 1998; Cosca et al., 1998; Tohver et al., 2004; Bingen et al., 2008; Rivers, 2008). Although less extensively studied, cooling histories have also been determined for the intracontinental Reynolds Range, Mt. Isa Province and Mount Woods Inlier in central and northern Australia (McLaren et al., 1999; Spikings et al., 2002; Vry and Baker, 2006; Forbes et al., 2012).

In this article, we introduce the Albany-Fraser Orogen of Western Australia (Figure 3.1) as an example of a Mesoproterozoic orogen that preserves a strikingly fast cooling history, that appears to defy the trend of decreasing cooling rate with increasing orogenic age. Although the tectonic setting of the Albany-Fraser Orogen is not well understood, it is thought to record the Mesoproterozoic suturing of the Yilgarn Craton to the combined Mawson and Gawler cratons during the assembly of Rodinia (Clark et al., 2000). The orogen curves around the margin of the Yilgarn Craton, such that it strikes east-west in the western region, and strikes northeast-southwest in the north-eastern region (Figure 3.1). The direction of convergence during orogeny is interpreted to be northwest-southeast, and consequently the western part of the orogen experienced a significant component of transpressive deformation, whereas the eastern part of the orogen was deformed in a more directly compressive stress regime (Bodorkos and Clark, 2004b).

In this article, we report the first $^{40}Ar/^{39}Ar$ thermochronology from the western part of the Albany-Fraser Orogen. We use these results in combination with previously published data relating to the inferred bulk stress regime of collisional

orogeny to constrain the post-peak metamorphic cooling and exhumation history of the orogen. The cooling of the western Albany-Fraser Orogen is shown to be much faster than that in other Mesoproterozoic orogens, and is interpreted to represent fast cooling in a transpressional setting.

3.2 Regional geology

3.2.1 Tectonic setting of the Albany-Fraser Orogen

The Albany-Fraser Orogen extends ca 1200 km along the southern and south-eastern margins of the Yilgarn Craton of Western Australia (Figure 3.1). The orogen

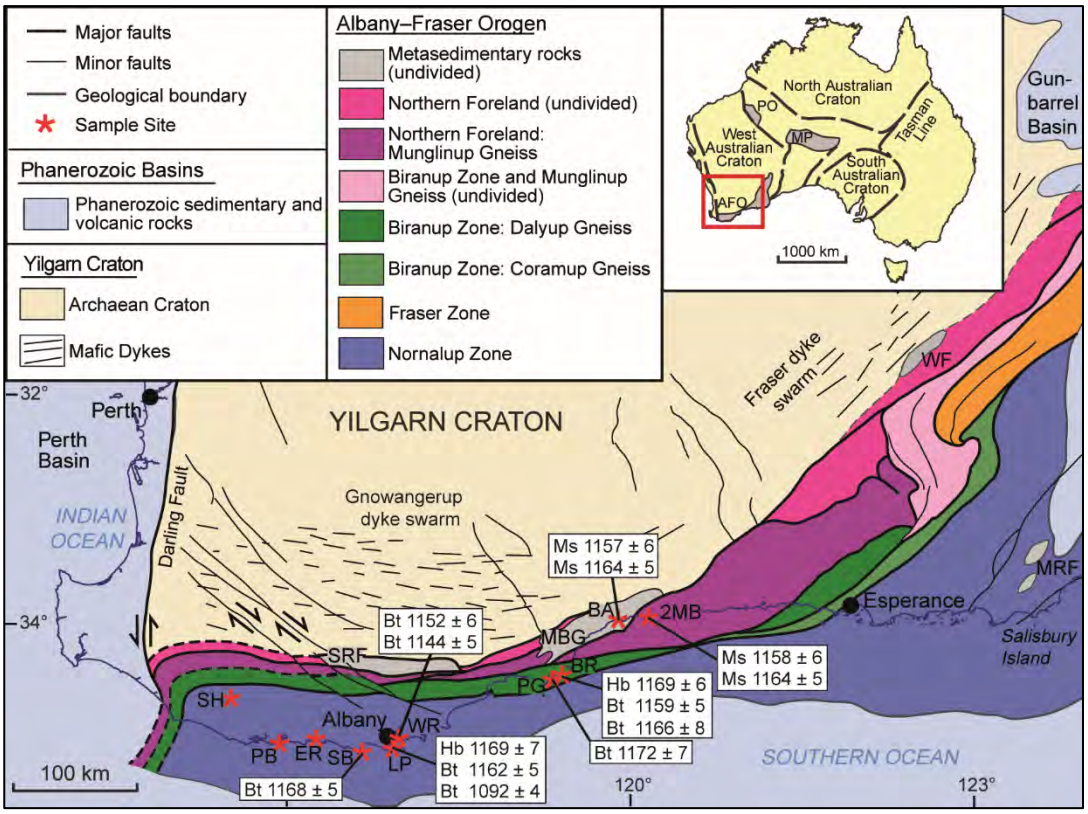

Figure 3.1 Map of the Albany-Fraser Orogen showing sample sites and results of $^{40}Ar/^{39}Ar$ thermochronology. Inset at top right shows location of the Albany-Fraser Orogen within Australia. Abbreviations: Barrens Beach (BA); Bremer Bay (BR); Elephant Rocks (ER); Ledge Point (LP); Mount Barren Group (MBG); Mount Ragged Formation (MRF); Peaceful Bay (PB); Point Gordon (PG); Shelley Beach (SB); Shannon (SH); Stirling Range Formation (SRF); Woodline Formation (WF); Whalehead Rock (WR); Two-Mile Beach (2MB). Modified after Kirkland et al. (2011a) and Spaggiari et al. (2009).

consists of mostly Paleo- to Mesoproterozoic rocks formed on or close to the margin of the Yilgarn Craton, which were subsequently deformed to high metamorphic grades during the late Mesoproterozoic Albany-Fraser Orogeny (Kirkland et al., 2011a; Spaggiari et al., 2011). The tectonic setting of the Albany-Fraser Orogeny is not well constrained; however, it has been subdivided into two stages on the basis of U-Pb geochronology. Stage I (1350 – 1260 Ma) was originally interpreted as the product of collision between the Yilgarn and Mawson Cratons (Clark et al., 2000). However, due to the lack of evidence for any magmatic arcs or exotic accreted terranes, Stage I has recently been suggested to have occurred in a continental rift or back-arc setting (Spaggiari et al., 2014). Stage II (1210 – 1140 Ma) is generally attributed to 'intracontinental reactivation', although a more explicit cause for orogenesis in this initial model (e.g. far-field response to a distant collisional event) is never stated (Clark et al., 2000; Kirkland et al., 2011a; Spaggiari et al., 2014). Both Stage I and Stage II involved a component of northwest-directed shortening, transpressive deformation at amphibolite to granulite facies conditions, and were associated with granitic magmatism (Myers, 1993; Clark et al., 2000; Bodorkos and Clark, 2004b; Kirkland et al., 2011a).

The Albany-Fraser Orogen is divided into several tectonic domains on the basis of lithological and geochronological differences. At the northern margin of the orogen is the Northern Foreland, composed of 3.0 – 2.6 Ga Archaean gneisses and granites of the Yilgarn Craton (Spaggiari et al., 2011). The Northern Foreland was reworked during the Albany-Fraser Orogeny (the naming convention for this domain follows that established by Clark et al., 2000 and subsequent authors) (Fitzsimons and Buchan, 2005). To the south and south-east are the orogen-parallel, fault-bound Biranup, Nornalup and Fraser Zones (Spaggiari et al., 2011) (Figure 3.1). The Paleoproterozoic Biranup Zone is dominated by ca 1815 – 1625 Ma orthogneisses; the Nornalup Zone also contains a less voluminous, poorly exposed Paleoproterozoic basement component of similar composition and age, but is largely composed of syn-orogenic, granitic intrusions (Spaggiari et al., 2014). The Biranup and Nornalup Zones are allochthonous to the Yilgarn Craton, and are considered to have formed along its southern and south-eastern margin during the Paleoproterozoic, possibly in an arc to

back-arc setting (Kirkland et al., 2011b; Spaggiari et al., 2011). The Fraser Zone is composed of voluminous granitic and mafic magmatic intrusions emplaced at mid- to lower-crustal levels during Stage I of the Albany-Fraser Orogeny (Kirkland et al., 2011a; Kirkland et al., 2011b; Clark et al., 2014).

Three basins are inferred from the sedimentary record of the Albany-Fraser Orogen: the ca 1815 – 1600 Ma Barren Basin, the ca 1600 – 1305 Ma Arid Basin, and the ca 1280 – 1200 Ma Ragged Basin (Spaggiari et al., 2014). In the western part of the Albany-Fraser Orogen, the Stirling Range Formation and Mount Barren Group are part of the Barren Basin, and were deposited onto a Northern Foreland substrate (Spaggiari et al., 2014) (Figure 3.1).

3.2.2 The Albany-Fraser Orogeny

Stage I of the Albany-Fraser Orogeny (1350 – 1260 Ma) was marked by northwest-directed shortening and deformation at amphibolite to granulite facies conditions, accompanied by the emplacement of the granitic Recherche Supersuite. This was followed by a period of tectonic quiescence, during which sediments of the ca 1280 – 1200 Ma Ragged Basin were deposited onto exhumed granite of the Recherche Supersuite in the eastern part of the Nornalup Zone (Spaggiari et al., 2014).

Stage II orogenesis (1210 – 1140 Ma) resulted in high-grade metamorphism across the Albany-Fraser Orogen. In the Northern Foreland, the intensity of deformation increases towards the southern and south-eastern margins (Beeson et al., 1988) and the eastern Munglinup Gneiss was metamorphosed at upper amphibolite to granulite facies at ca 1190 Ma (Spaggiari et al., 2011). The Mount Barren Group, deposited onto Northern Foreland basement and adjacent to the contact with the Biranup Zone, records peak metamorphism at 560 – 675 °C and 7 – 12 kbar at ca 1205 Ma (Wetherley, 1998; Dawson et al., 2003). Granulite facies deformation in the Biranup Zone (700 – 900 °C, 5 – 10 kbar) was continuous throughout Stage II, with U-Pb zircon ages recording ca 1225 – 1150 Ma metamorphic zircon growth and pegmatite crystallisation (Black et al., 1992; Nelson, 1995a, b; Bodorkos and Clark, 2004a, b; Spaggiari et al., 2009; Barquero-Molina, 2010). U-Pb ages of metamorphic zircon growth in the Nornalup Zone record ca 1215 – 1155 Ma

metamorphism, migmatisation and shearing at amphibolite to granulite facies (Clark, 1995; Clark et al., 2000; Adams, 2012). Metamorphic conditions are constrained to 500 – 600 °C, 4 – 5 kbar in the Mount Ragged Formation (Clark et al., 2000). These data suggest that high grade metamorphism in the Albany-Fraser Orogen lasted ca 75 Ma (e.g. Clark et al., 2000; Bodorkos and Clark, 2004b; Barquero-Molina, 2010).

Regional high-temperature Stage II metamorphism was accompanied by a complex sequence of folding, ductile shearing and thrusting throughout the Albany-Fraser Orogen, summarised briefly here. In the Northern Foreland, both the Stirling Range Formation and the Mount Barren Group experienced significant northwards-directed thrusting during Stage II, although these events have not been directly dated (Wetherley, 1998; Dawson et al., 2003; Kirkland et al., 2011a). Ductile shearing related to oblique compression occurred at ca 1168 Ma and 1187 – 1150 Ma in the eastern and western Biranup Zone respectively, as recorded by the U-Pb zircon crystallisation ages of synkinematic pegmatites and anatectic melts (Bodorkos and Clark, 2004b; Spaggiari et al., 2009). In the Nornalup Zone, Stage II deformation was accompanied by voluminous granitic magmatism, although the lack of geochemical data means that the tectonic setting of this magmatism is unconstrained. The Burnside Batholith was emplaced from 1190 – 1170 Ma in the western Nornalup Zone (Pidgeon, 1990; Black et al., 1992; Fitzsimons and Buchan, 2005), and the Esperance Supersuite was emplaced from 1200 – 1140 Ma in the east (Nelson et al., 1995; Spaggiari et al., 2011). The end of Stage II orogeny is defined by the cessation of Esperance Supersuite magmatism (Clark et al., 2000).

3.2.3 Previous thermochronology

The cooling and exhumation of the Albany-Fraser Orogen have not previously been studied in detail. Fletcher et al. (1991) calculated a biotite whole-rock Rb-Sr isochron of 1268 ± 20 Ma from the Fraser Zone. This suggests the Fraser Zone was exhumed from peak metamorphic conditions (ca 850 °C, 7 – 9 kbar at ca 1290 Ma) to the Rb-Sr biotite closure temperature of ca 400 °C at the end of Stage I (Clark et al., 2014). This thermal history contrasts with the adjacent Nornalup and Biranup Zones, which were deformed during both Stage I and Stage II (Oorschot, 2011). The reason

for this is not well understood, although a tectonic model has been proposed for the exhumation of the Fraser Zone by extrusion to the southwest (Spaggiari et al., 2011). Stephenson et al. (1977) obtained hornblende K-Ar cooling ages between 1160 – 1060 Ma from amphibolites and low-grade granulites in the western Albany-Fraser Orogen, which they interpreted as prograde mineral growth recording the age of late-orogenic uplift and cooling. These data were collected prior to routine use of the $^{40}Ar/^{39}Ar$ step-heating technique, which allows for the recognition of radiogenic argon loss, the effect of alteration, or the presence of excess $^{40}Ar^*$ in a mineral, and as a result are considered as semi-quantitative constraints for cooling ages only. The $^{40}Ar/^{39}Ar$ thermochronology reported in this paper therefore represents the first modern study of orogenic cooling and exhumation in the western Albany-Fraser Orogen.

3.3 Research methods

3.3.1 Sample collection

The primary aim during sample collection was to ensure representative lithologies and geographical spread across the different domains of the western Albany-Fraser Orogen. Nineteen samples were collected from a 360km transect across the Northern Foreland, Nornalup and Biranup Zones (Figure 3.1). From these samples, 22 individual crystals (16 biotite, 4 muscovite and 2 hornblende) were analysed using $^{40}Ar/^{39}Ar$ thermochronology. Sample lithologies are summarised in Table 3.1, and sample locations and detailed petrography are described in Appendix 3.1.

3.3.2 Analytical methods

Samples were crushed and sieved to separate the 125 – 250 μm fraction, which was washed in acetone and deionised water to remove dust. Optically unaltered 125 – 250 μm grains of biotite (16 samples), muscovite (4 samples) and hornblende (2 samples) were separated by hand-picking under a binocular microscope.

Table 3.1 Summary of $^{40}Ar/^{39}Ar$ thermochronology results from the western Albany-Fraser Orogen. Abbreviations are: MSWD, mean square weighted deviation; P, P-value; n, number of steps used in the plateau.

Sample	Lithology	Field site	Mineral	Plateau characteristics				
				Age (Ma, ± 2σ)	^{39}Ar (%)	MSWD	P	n
Nornalup Zone								
AF02-1	Enderbitic orthogneiss	Ledge Point	Hb	1169 ± 7	100	0.76	0.52	4
AF01	Bt metagranite	Ledge Point	Bt	1092 ± 4	84	1.34	0.19	13
AF02-1	Enderbitic orthogneiss	Ledge Point	Bt	1162 ± 5	70	0.67	0.64	6
AF02-2	Enderbitic orthogneiss	Whalehead Rock	Bt	1152 ± 6	90	0.74	0.71	12
AF03	Tonalitic orthogneiss	Whalehead Rock	Bt	1144 ± 5	98	1.40	0.16	13
AF04-1	Metagranite	Shannon	Bt					
AF04-2	Bt orthogneiss	Shannon	Bt					
AF05	Bt metagranite	Elephant Rocks	Bt	>970[a]				
AF06	Bt Hb metagranite	Shelley Beach	Bt	1168 ± 5	91	1.02	0.43	15
AF08A	Bt augen gneiss	Peaceful Bay	Bt					
AF08B	Grt paragneiss	Peaceful Bay	Bt					
AF08C	Amphibolite	Peaceful Bay	Bt	>1140[a]				
AF08D	Bt Grt orthogneiss	Peaceful Bay	Bt	>980[a]				
Biranup Zone								
BREM-6	Intermediate granulite	Fishery Beach	Hb	1169 ± 6	100	1.32	0.20	13
BREM-2	Intermediate granulite	Point Gordon	Bt	1172 ± 7	100	0.49	0.79	6
BREM-6	Intermediate granulite	Fishery Beach	Bt	1159 ± 5	88	0.40	0.94	10
BREM-10	Felsic granulite	Fishery Bay headland	Bt	1166 ± 8	90	0.77	0.38	2
Northern Foreland								
AF01-SCH	Grt St schist	SW of Barrens Beach	Bt	*1191 ± 6*[b]	*54*	*1.41*	*0.21*	*10*
AF01-SCH	Grt St schist	SW of Barrens Beach	Ms	1157 ± 6	100	0.53	0.86	10
BREM-SA	Bt St Ky schist	Barrens Beach	Ms	1164 ± 5	96	0.80	0.67	15
2MB-01	Qz orthogneiss	Two Mile Beach	Ms	1159 ± 5	98	0.87	0.58	14
2MB-02	Pl orthogneiss	Two Mile Beach	Ms	1157 ± 5	90	1.40	0.17	12

[a] Minimum age (sample did not form an age plateau).

[b] Mini-plateau (weighted mean age includes 50 – 70% of total ^{39}Ar)

Samples were loaded into 22 large wells of an aluminium disc measuring 1.9 cm in diameter and 0.3 cm in depth. These wells were bracketed by small wells containing Fish Canyon sanidine (FCs), used as a neutron flux monitor. The FCs has an age of 28.294 ± 0.037 Ma (1σ) (Renne et al., 2010). The mean J-value (irradiation parameter) computed from the standard FCs grains within the small pits is 0.00903 ± 0.00002 (0.22%), calculated as the average and standard deviation of J-values of the standard FCs grains within each irradiation disc. An automated air pipette was used to monitor mass discrimination, which had a mean value of 1.00 ± 0.34 per Dalton (atomic mass unit) relative to an air ratio of 298.56 ± 0.31 (Lee et al., 2006). The correction factors for interfering isotopes were: $(^{39}Ar/^{37}Ar)_{Ca}$ = 7.60x10^{-4} (± 7%); $(^{36}Ar/^{37}Ar)_{Ca}$ = 2.81x10^{-4} (± 3%); and $(^{40}Ar/^{39}Ar)_{K}$ = 6.76x10^{-4} (± 10%).

The $^{40}Ar/^{39}Ar$ analyses were performed at the Western Australian Argon Isotope Facility at Curtin University. The methodology for these analyses is outlined in detail in Appendix 3.2. Appendix 3.3 contains Ar isotope data corrected for blank, mass discrimination and radioactive decay, with individual errors given at the 2σ level.

In this study, the criteria for the determination of an age plateau are as follows: plateaus must include at least 70% of the total measured ^{39}Ar, and they should be distributed over at least three consecutive steps that agree at a 95% confidence level and satisfy a probability of fit (P) of at least 0.05. Plateau ages are given at the 2σ level, and are calculated using the mean of all plateau steps, weighted by the inverse variance of their individual analytical error. Mini-plateaus are defined similarly, but include 50% - 70% of the total ^{39}Ar. Mini-plateau ages are less robust than plateau ages. All sources of uncertainty are included in the calculations.

3.4 $^{40}Ar/^{39}Ar$ thermochronology results

3.4.1 Nornalup Zone

One hornblende and five biotite grains from the Nornalup Zone produced robust $^{40}Ar/^{39}Ar$ cooling ages (Table 3.1). The hornblende from orthogneiss AF02-1 produced a flat step-heating spectrum with a cooling age of 1169 ± 7 Ma (Figure 3.2). Four biotite

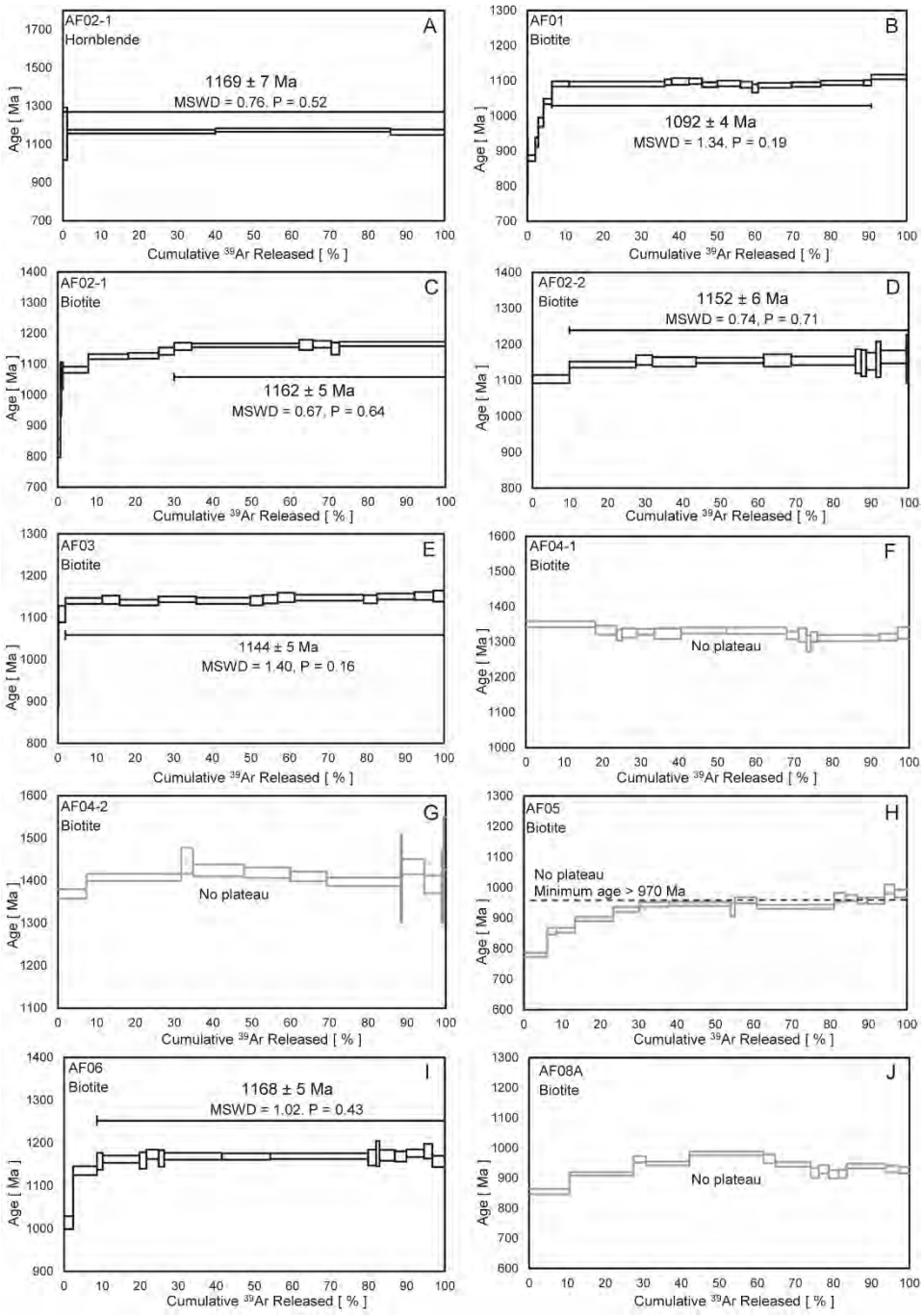

Figure 3.2 $^{40}Ar/^{39}Ar$ apparent age spectra, where individual steps are graphed against cumulative percentage of ^{39}Ar released. Uncertainties are given at 2σ for plateau (>70% ^{39}Ar released) ages. The MSWD and probability (P) are given for plateau and mini-plateau ages. Two hornblende grains **(A, N)**, eight biotite grains **(B, C, D, E, I, O, P, Q)** and four muscovite grains **(S, T, U, V)** yielded statistically robust age plateaus (>70% of ^{39}Ar released). **(R)** One biotite from the Northern Foreland yielded a mini-plateau (>50% of ^{39}Ar released). **(F, G, H, J, K, L, M)** Seven biotite samples from the Nornalup Zone yielded no age plateau. Thermochronological data tables are available in Appendix 3.3.

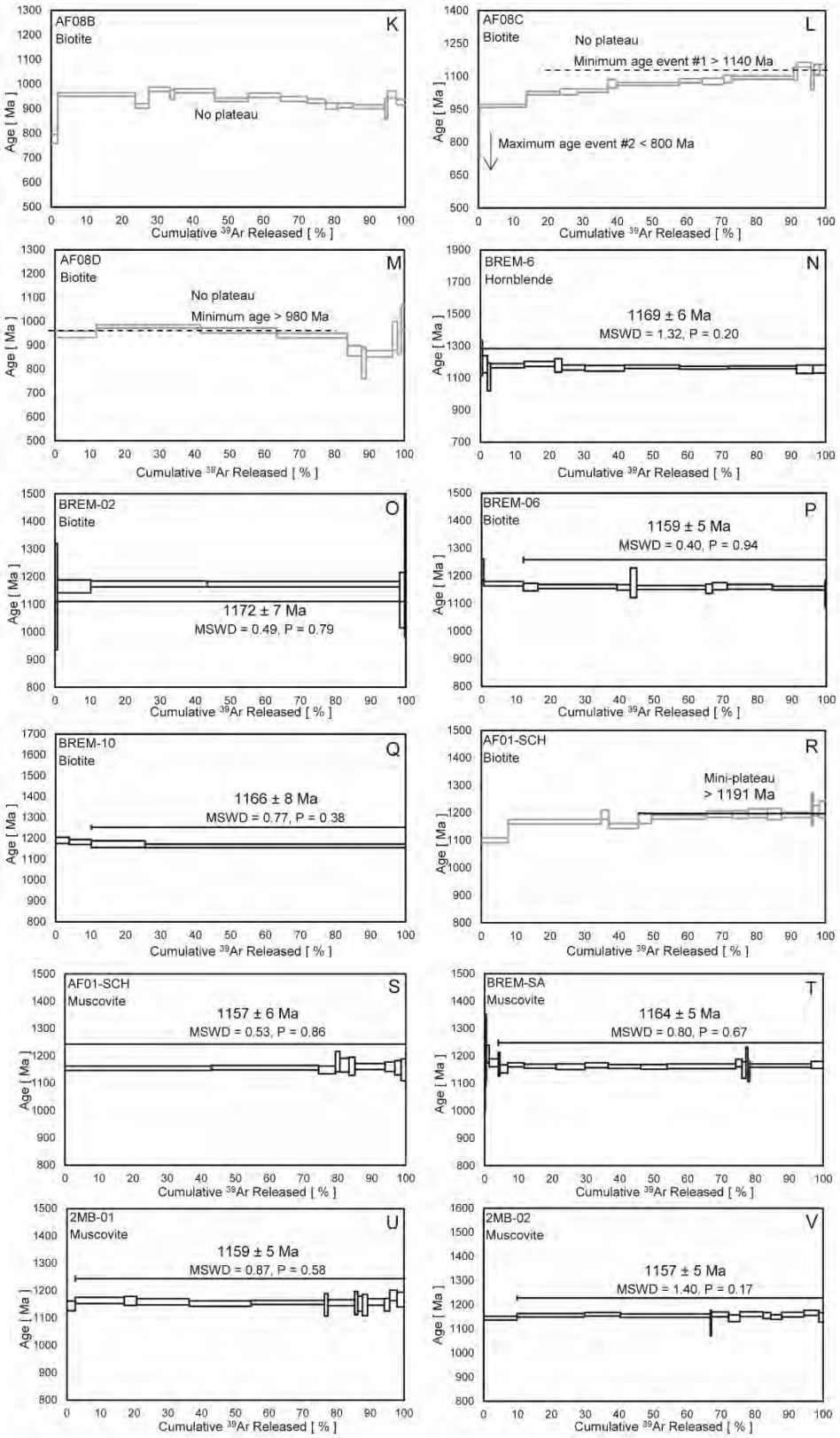

Figure 3.2 (Continued)

grains (orthogneisses AF02-1, AF02-2 and AF03, and metagranite AF06) produced weighted plateau ages ranging from 1168 ± 5 Ma to 1144 ± 5 Ma, with no apparent geographical trend in cooling ages (Figures 3.1 and 3.2). Biotite from metagranite AF01 records a much younger plateau age of 1092 ± 4 Ma (Table 3.1).

The remaining seven biotite grains analysed from the Nornalup Zone (AF04-1, AF04-2, AF05, AF08A – D) did not produce statistically robust plateau ages (Table 3.1). Samples AF05 (Elephant Rocks), AF08C and AF08D (Peaceful Bay) provide minimum cooling ages of ≥970 Ma, ≥1140 Ma and ≥980 Ma respectively (Figure 3.2). These minimum cooling ages are significantly younger than the statistically robust biotite cooling ages from the Nornalup Zone, excluding metagranite AF01. The spatial proximity of Elephant Rocks and Peaceful Bay suggests a local thermal event may have caused a loss of radiogenic ^{40}Ar, resulting in the absence of a plateau age in the five samples collected at these sites (Figure 3.1).

3.4.2 Biranup Zone

The hornblende and three biotite grains from the Biranup Zone all produced simple, flat step-heating spectra and yielded statistically robust plateau ages (Table 3.1; Figure 3.2). The hornblende from granulite BREM-6 yielded a cooling age of 1169 ± 6 Ma, and the biotite cooling age from the same sample is 1159 ± 5 Ma. Sample BREM-10, located 0.2 km to the SE, records a biotite cooling age of 1166 ± 8 Ma, and sample BREM-2 records a similar biotite cooling age of 1172 ± 7. These ages are similar to the hornblende and biotite cooling ages from the Nornalup Zone (Table 3.1).

3.4.3 Northern Foreland

The four muscovite grains analysed from the Northern Foreland (schists AF01-SCH and BREM-SA, and orthogneisses 2MB-01 and 2MB-02) give statistically indistinguishable cooling ages ranging from 1164 ± 5 Ma to 1157 ± 6 Ma, with a weighted mean age of 1159 ± 6 Ma (P = 0.10) (Table 3.1, Figure 3.2).

A biotite grain from schist AF01-SCH produced a mini-plateau (54% of ^{39}Ar), giving a minimum age of ≥1191 Ma (Table 3.1, Figure 3.2). As the conditions defining a mini-plateau are barely met (50 – 70% of the ^{39}Ar released), and considering that

mini-plateau ages can be inaccurate (as opposed to plateau ages), this age is not as robust as the other biotite ages. Additionally, the age of this biotite is ca 35 Ma older than muscovite from the same sample, despite the lower closure temperature of biotite (Harrison et al., 1985; Harrison et al., 2009). Therefore, the preferred explanation is ^{40}Ar enrichment in the biotite grain, and no geological significance is attached to its apparent age.

3.4.4 Calculation of closure temperatures and cooling rates

^{40}Ar/^{39}Ar analyses record the last time a rock cooled through the mineral-specific closure temperature for argon diffusion, and may be calculated by iterating Equation 1 (Dodson, 1973).

$$\frac{E}{R \times T_c} = ln\left(-\frac{A \times R \times T_{c0}^2 \times D_0}{E \times \frac{dT}{dt} \times a^2}\right) \qquad \textit{Equation (1)}$$

In Equation 1, E is the activation energy, R is the gas constant, T_c is the closure temperature, A is the volume constant, T_{c0} is the initial estimate of closure temperature, D_0 is the diffusion coefficient, $\frac{dT}{dt}$ is the cooling rate and a is the grainsize. Equation 1 was used to calculate closure temperatures (T_c) for those hornblende, muscovite and biotite grains that produced statistically robust ^{40}Ar/^{39}Ar age plateaus. Three iterations of the equation were sufficient to calculate the closure temperature (results in Table 3.2; see Table A3.4-1 in Appendix 3.4 for the input values). Initial closure temperature estimates (T_{c0}) were 300 °C for biotite (Harrison et al., 1985), 425 °C for muscovite (Harrison et al., 2009) and 550 °C for hornblende (Harrison, 1981). Grainsize (a) was measured at the time of ^{40}Ar/^{39}Ar analysis. Values for the activation energy (E), diffusion coefficient (D_0) and volume constant (A) for biotite were taken from Grove and Harrison (1996), as biotites analysed in this study have similar Fe/Mg ratios (X_{annite} = 0.6 – 0.8 for this study, compared to X_{annite} = 0.54 – 0.71). Values for the activation energy (E), diffusion coefficient (D_0) and volume constant (A) were taken from Harrison (1981) for hornblende and Harrison et al. (2009) for muscovite. Individual cooling rates (dT/dt) were mostly calculated using peak Stage II metamorphic conditions (see Table A3.4-2 in Appendix 3.4). The ages of metamorphism are taken from U-Pb ages of zircon and monazite growth; although

Table 3.2 Peak metamorphic conditions, closure temperatures and cooling rates for samples recording post-Stage II cooling of the Albany Mobile Belt. Peak metamorphic conditions were established using published temperature and age data for these sample sites (see Table 3.4-2 in Appendix 3.4 for more detail). Closure temperatures and cooling rates were calculated using a Monte Carlo simulation (Section 3.4.4).

Sample	Mineral	Peak Stage II age (Ma)	Peak Stage II temperature (°C)	$^{40}Ar/^{39}Ar$ cooling age (Ma)	Closure temperature (°C ± 2σ)	Cooling rate (°C/Ma, $^{+Q3}_{-Q1}$)
Nornalup Zone						
AF02-1	Hb	1169 ± 8	800 ± 100	1169 ± 7	594 ± 58	57^{+55}_{-23}
AF02-1	Bt	1169 ± 7[a]	594 ± 29[a]	1162 ± 5	367 ± 36	33^{+17}_{-9}
AF02-2	Bt	1174 ± 12	650 ± 50	1152 ± 6	352 ± 28	$13.5^{+3.5}_{-2.3}$
AF03	Bt	1174 ± 12	650 ± 50	1144 ± 5	354 ± 26	$9.9^{+1.8}_{-1.4}$
AF06	Bt	1169 ± 8	600 ± 100	1168 ± 5	389 ± 46	57^{+52}_{-23}
Biranup Zone						
BREM-6	Hb	1178 ± 3	800 ± 75	1169 ± 6	576 ± 48	44^{+30}_{-14}
BREM-2	Bt	1177 ± 11	800 ± 100	1172 ± 7	382 ± 42	69^{+59}_{-24}
BREM-6	Bt	1169 ± 6[b]	576 ± 24[b]	1159 ± 5	363 ± 30	22^{+7}_{-5}
BREM-10	Bt	1169 ± 6[b]	576 ± 24[b]	1166 ± 8	377 ± 44	43^{+36}_{-15}
Northern Foreland						
AF01-SCH	Ms	1205 ± 10	620 ± 50	1157 ± 6	414 ± 66	$4.2^{+0.8}_{-0.7}$
BREM-SA	Ms	1205 ± 10	620 ± 50	1164 ± 5	425 ± 68	$4.7^{+0.9}_{-0.9}$
2MB-01	Ms	1195 ± 15	700 ± 100	1159 ± 5	424 ± 68	$7.7^{+1.8}_{-1.5}$
2MB-02	Ms	1195 ± 15	700 ± 100	1157 ± 5	430 ± 68	$7.1^{+1.7}_{-1.4}$

[a]Peak metamorphic conditions here are the cooling age and closure temperature of hornblende AF02-1, from the same sample site/same unit.

[b]Peak metamorphic conditions here are the cooling age and closure temperature of hornblende BREM-6, from the same sample site/same unit.

mineral growth ages may not truly represent the duration of metamorphism, they are the only available constraints at present. The exceptions are biotite grains AF01, AF02-1, BREM-6 and BREM-10, as these four biotites are from field sites also containing a hornblende cooling age (Table 3.1). The temperature-time (T-t) pair provided by the hornblende cooling age and closure temperature is used to calculate the mineral-to-mineral cooling path, i.e. for cooling between hornblende and biotite closure temperatures.

The precise values of E, D_0 and dT/dt are uncertain; E and D_0 are experimentally determined parameters, and dT/dt is calculated from SHRIMP U/Pb and $^{40}Ar/^{39}Ar$ ages which are typically reported with an associated error of ±1σ – 2σ. A further source of uncertainty comes from the co-dependence of closure temperature and cooling rate (Equation 1): a mineral's T_c depends on dT/dt, but calculation of dT/dt is dependent on T_c. Upon repeated iterations of Equation 1, T_c and dT/dt converge to a mean, although the geological significance of the result depends on the initial estimates of these two variables. In order to include all sources of uncertainty in the calculation of closure temperatures and cooling rates, but also minimise error correlations in the results and obtain a realistic final uncertainty, we carried out a Monte Carlo simulation. A Monte Carlo simulation performs a calculation by assigning a random number for uncertain variables, with random numbers set between boundaries given by the known uncertainty distribution of the variable. By repeating the calculation many times, a probability distribution of the most likely results is generated (Figure 3.3). The Monte Carlo simulation was performed using 20,000 trials, using the Microsoft Excel add-on program Analytic Solver Platform (Frontline Systems Inc., 2013). A more detailed description of the Monte Carlo simulation methodology, inputs and outputs is available in Appendix 3.4.

Histograms of the distribution of biotite closure temperatures from AF02-1 and BREM-6 are shown in Figure 3.3. The population is evenly distributed around a mean; this is typical of the results from all 14 Monte Carlo simulations (see Figure A3.4-1 in Appendix 3.4). The mean closure temperature of each population of 20,000 trials is reported in Table 3.2, with ±2σ error. The closure temperature for hornblende

is ca 585 ± 50 °C, for biotite is ca 365 ± 35 °C and for muscovite is ca 425 ± 70 °C. These closure temperatures are up to 65 °C higher than the average values usually calculated or measured by other authors, typically ca 550 °C for hornblende, ca 300 °C for biotite and ca 425 °C for muscovite (e.g. Harrison, 1981; Grove and Harrison, 1996; Harrison et al., 2009; Forbes et al., 2012; Ueda et al., 2012). However, the values calculated here take into account the range of possible values and distribution of each parameter, rather than simply taking the average of each of these values; therefore, these are considered good estimates of the true closure temperatures for these particular samples, within error.

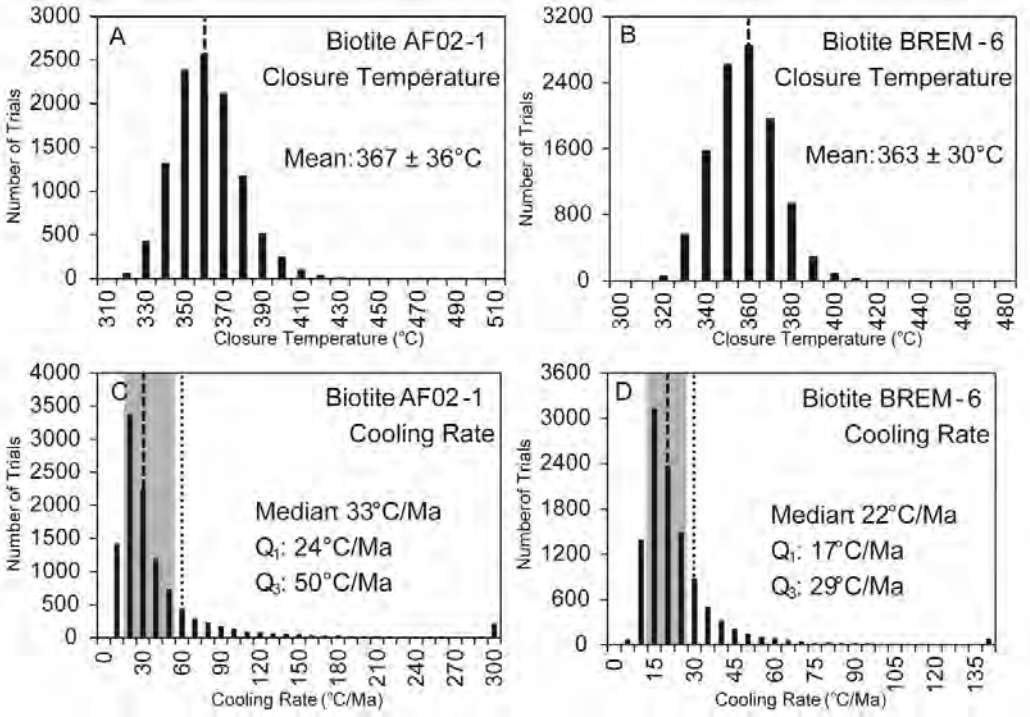

Figure 3.3 Histograms showing the distribution of the results of Monte Carlo simulations for biotites AF02-1 and BREM-6. The shapes of these distributions are also representative of the results from all other grains. Appendix 3.4 contains relevant calculation details and results from all other grains. **(A, B)** Argon closure temperatures are distributed evenly around the mean. The dashed line shows the approximate location of the mean, reported with ± 2σ. **(C, D)** Histogram of modelled cooling rates between Stage II metamorphic conditions and argon closure temperature. The dashed line shows the approximate location of the population median, reported with the lower (Q1) and upper (Q3) quartiles; the shaded area is the interquartile range. The dotted line is the mean. Due to the strongly right-tailed skew of the histogram, caused by the large range in mathematically calculated cooling rates, the mean of the whole population is skewed to unrealistically high values. Therefore, the median is considered a better measure of the central tendency of this population.

Histograms showing the distribution of cooling rates from the Monte Carlo simulations for biotites AF02-1 and BREM-6 are shown in Figure 3.3. The strongly right-tailed skew of the histogram is due to the large range of mathematically calculated cooling rates, and is typical of the results from all Monte Carlo simulations (see Figure A3.4-2 in Appendix 3.4). The outliers with extremely high values greatly increase the mean and the standard deviation of the distribution to unrealistically high values. The median is a better measure of the central tendency of a skewed population, and the lower and upper quartiles (Q_1 and Q_3) are a more robust measure of scale than the standard deviation. The median cooling rate of each population is reported in Table 3.2, with lower and upper quartiles ($^{+Q3}_{-Q1}$).

3.5 Discussion

3.5.1 Cooling and exhumation of the western Albany-Fraser Orogen

Two hornblende, eight biotite and four muscovite grains yielded statistically robust age plateaus (>70% of ^{39}Ar released); plateaus are generally flat and low in complexity (Figure 3.2). One biotite from the Northern Foreland yielded a mini-plateau (50 – 70% of ^{39}Ar released), and seven biotite samples from the Nornalup Zone yielded no age plateaus (Figure 3.2). Results are summarised in Table 3.1, with all ages reported at the 2σ uncertainty level.

One biotite grain from the Nornalup Zone (AF01) yielded a plateau age that is a significant outlier to the main population of biotite cooling ages (Table 3.1). ^{40}Ar loss and age resetting due to a local heating event is considered unlikely, as sample AF02-1 was collected at the same field site and records an older biotite cooling age compatible with the other results. Two possible explanations are considered: (a) sample AF01 may belong to a currently undescribed granitic intrusion which post-dates the cooling of the Nornalup Zone, or (b) the two samples from Ledge Beach are separated by a later structure which was not identified at the outcrop. In the absence of supporting evidence or similar results, this outlier is treated as such, and is excluded from further discussion.

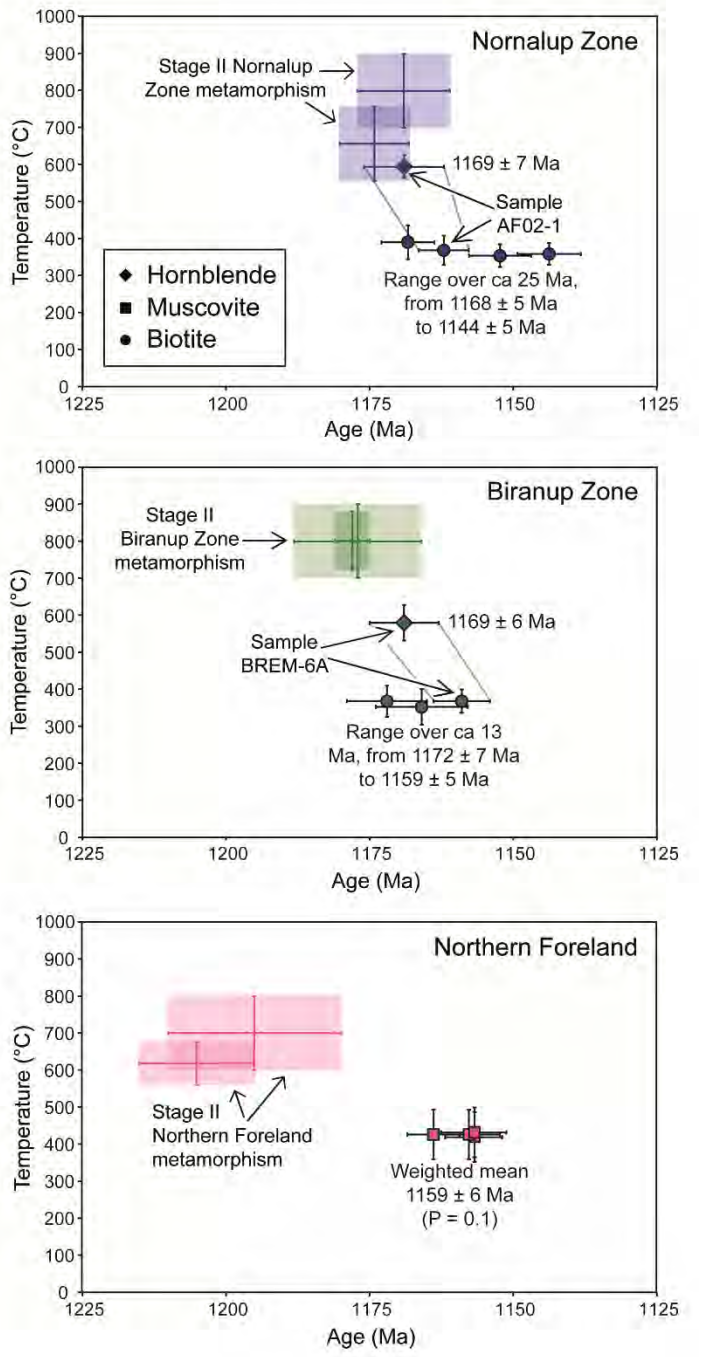

Figure 3.4 Temperature-time graphs for cooling following Stage II orogeny in the western Albany-Fraser Orogen, based on the $^{40}Ar/^{39}Ar$ cooling ages. The shaded boxes represent the conditions of peak Stage II metamorphism in each domain, using a combination of published metamorphic data and mineral crystallisation ages (see Table 3.4-2 in Appendix 3.4). Only the youngest syn-metamorphic mineral crystal-lisation ages are plotted, as the cooling rate is calculated from the youngest time of peak meta-morphism. Data from samples AF02-1 in the Nornalup Zone and BREM-6 in the Biranup Zone is labelled; these samples produced both hornblende and biotite cooling ages, and therefore provide the best-constrained post-peak cooling paths.

3.5.2 Cooling of the Nornalup and Biranup Zones

The short gap between the time of peak Stage II metamorphism (amphibolite to granulite facies at ca 1225 – 1150 Ma, from metamorphic zircon growth) and the cooling ages obtained by $^{40}Ar/^{39}Ar$ thermo-chronology is evidence for fast cooling in the Nornalup and Biranup Zones over this temperature interval (Figure 3.4). Specifically, the available data suggest that the Nornalup Zone was at upper amphibolite facies conditions at ca 1169 Ma, and the Biranup Zone was at granulite facies conditions at ca 1178 Ma (Spaggiari et al., 2009; Spaggiari et al., 2011). The hornblende $^{40}Ar/^{39}Ar$ cooling ages from the Nornalup and Biranup Zones are indistinguishable, recording cooling through the closure temperature of ca 585 ± 50 °C at ca 1169 Ma (Figure 3.4). Similarly, the main population of biotite $^{40}Ar/^{39}Ar$ cooling ages from the Nornalup Zone overlaps (within uncertainty) with the biotite cooling ages from the Biranup Zone, and records cooling through the closure temperature of ca 365 ± 35 °C at 1172 – 1144 Ma (Figure 3.4). The similarity in both hornblende and biotite cooling ages in the Nornalup and Biranup Zones implies that despite their different high-temperature metamorphic histories, these two domains were structurally juxtaposed by ca 1169 Ma, and shared a common cooling history after this time.

Both the Nornalup and Biranup Zones exhibit a large range in cooling rates, calculated for cooling from peak metamorphism at amphibolite to granulite facies to biotite closure temperatures at ca 365 ± 35 °C. Cooling rates vary between 10 – 60 °C/Ma in the Nornalup Zone (Table 3.2). These results imply fast cooling across the Nornalup Zone, and the apparent lack of a geographical trend in cooling rates suggests it acted as a largely coherent block during exhumation. In the Biranup Zone, calculated cooling rates show a similar spread over 20 – 70 °C/Ma (Table 3.2). Samples AF02-1 (Nornalup Zone) and BREM-6 (Biranup Zone) each yielded two well-defined temperature-time (T-t) pairs, from hornblende and biotite thermochronology. As there can be no doubt that the samples in question passed through both sets of T-t conditions, these data provide the best constraints in the present data set for cooling rates in these two domains. In the Nornalup Zone, sample AF02-1 records cooling between hornblende closure (594 ± 58 °C) and biotite closure (367 ± 36 °C) at a median

rate of 33^{+17}_{-9} °C/Ma (Table 3.2, Figure 3.3). In the Biranup Zone, sample BREM-6 records cooling between hornblende closure (576 ± 48 °C) and biotite closure (363 ± 30 °C) at a median rate of 22^{+7}_{-5} °C/Ma (Table 3.2, Figure 3.3). The overall similarity of the timing and rate of cooling in the two domains, when uncertainties are considered, suggests they may have been exhumed by similar mechanisms.

3.5.3 Cooling of the Northern Foreland

The Northern Foreland was metamorphosed to high grades during early Stage II of the Albany-Fraser Orogeny, with the overlying Mount Barren Group attaining Barrovian staurolite zone conditions at ca 1205 Ma and the Munglinup Gneiss undergoing migmatisation at upper amphibolite facies at ca 1195 Ma (Wetherley, 1998; Dawson et al., 2003; Spaggiari et al., 2011). The four muscovite $^{40}Ar/^{39}Ar$ cooling ages from the Northern Foreland are statistically indistinguishable, with a weighted mean of 1159 ± 6 Ma, and record cooling from peak amphibolite facies conditions through the muscovite closure temperature of ca 425 ± 70 °C (Figure 3.4). Median cooling rates in the Northern Foreland are ca 4.5 °C/Ma in the Mount Barren Group and ca 7.4 °C/Ma in the Munglinup Gneiss, only 16km to the east (Figure 3.1; Table 3.2). It should be noted that the assumed T-t of peak metamorphism in the Munglinup Gneiss is based upon zircon growth ages from Quagi Beach and Powell Point, ca 115 km to the east of the samples analysed here; unfortunately, there are currently no U-Pb data from closer to our Munglinup Gneiss samples (Table 3.4-2 in Appendix 3.4; Spaggiari et al., 2011). It is uncertain how applicable these metamorphic data are to the Munglinup Gneiss samples analysed here, due to the lateral extent of the region classified as Munglinup Gneiss; however, no other T-t data exist for this unit. Therefore, we interpret the Munglinup Gneiss cooling rates calculated here as approximations. In any case, the variation in cooling rates between the two units suggests that the boundary between them, the Jerdacuttup Fault, played a role in their differential exhumation histories. However, there is no difference in muscovite cooling ages between the Munglinup Gneiss and the Mount Barren Group, suggesting that movement across the Jerdacuttup Fault had ceased by ca 1159 Ma.

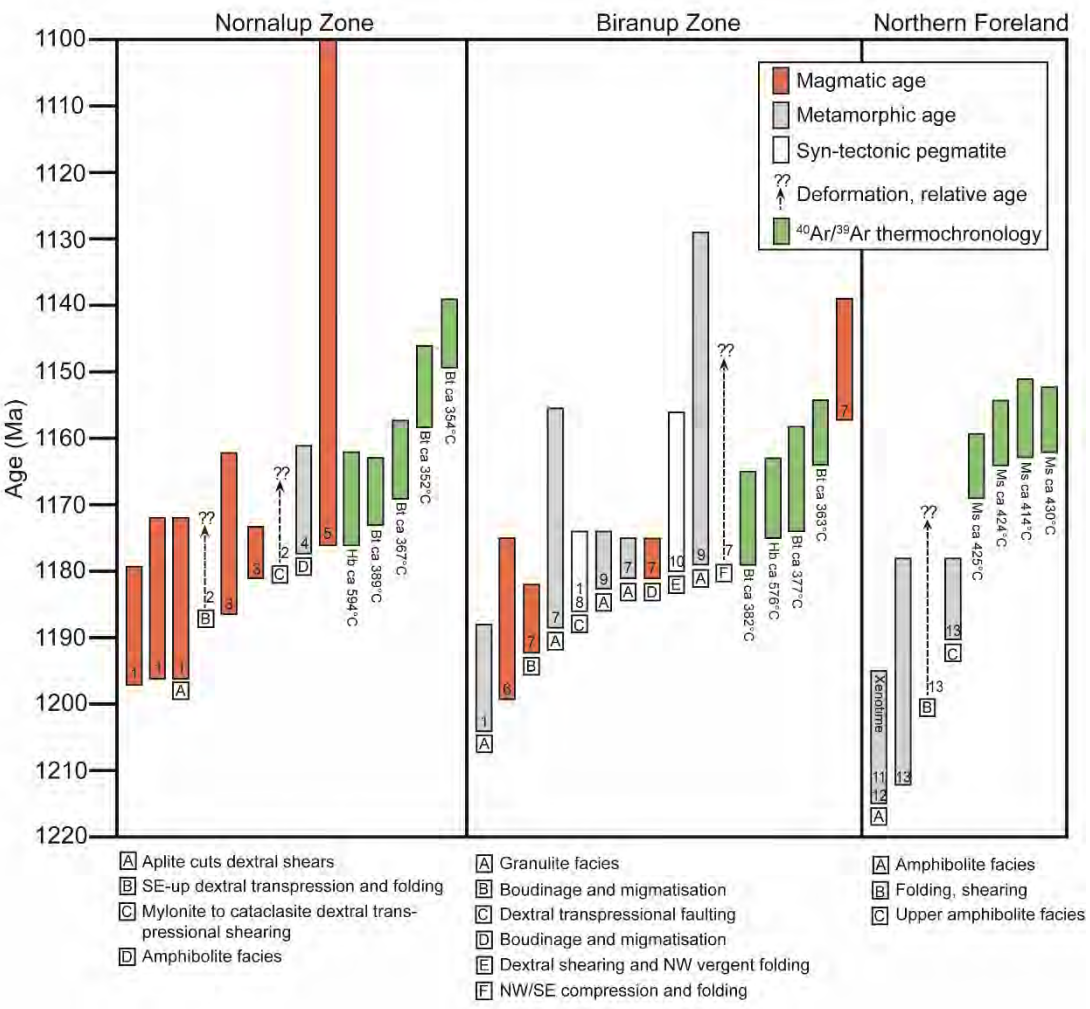

Figure 3.5 Summary of Stage II geochronological data from the western and central Albany-Fraser Orogen. Data are plotted by age at the 2σ level of uncertainty. Red bars are magmatic ages, grey bars are metamorphic ages and white bars are syn-tectonic pegmatite ages. All are SHRIMP U/Pb zircon ages unless otherwise specified. Dashed arrows represent regional deformational events where the relative timing has been established, but there is no absolute dating. The interpreted structural context of a sample or the metamorphic grade is indicated where possible. Green bars are $^{40}Ar/^{39}Ar$ thermochronology data from this study. Cooling to ca 350°C in the Nornalup and Biranup Zones was synchronous with late-Stage II metamorphism, magmatism and dextral transpression, but post-dates peak deformation in the Northern Foreland. Numbers inside the bars refer to the source of the data as follows: 1. Black et al. (1992); 2. Duebendorfer (2002); 3. Pidgeon (1990); 4. Clark (1995); 5. Clark et al. (2000); 6. Nelson et al. (1995); 7. Barquero-Molina (2010); 8. Beeson et al. (1988); 9. Spaggiari et al. (2009); 10. Bodorkos and Clark (2004); 11. Dawson et al. (2003); 12. Wetherley (1998); 13. Spaggiari et al. (2011).

3.5.4 Exhumation of the western Albany-Fraser Orogen

The Nornalup and Biranup Zones were cooled from peak Stage II metamorphic conditions (ca 600 – 800 °C) to ca 365 ± 35 °C between ca 1175 Ma and 1159 Ma, at median rates of ca 33 $^{+17}_{-9}$ °C/Ma and 22 $^{+7}_{-5}$ °C/Ma respectively; the Northern Foreland was cooled from ca 620 – 700 °C to ca 425 ± 70 °C between ca 1200 Ma and 1159 Ma, at rates of 4.5 – 7.4 °C/Ma. These ages fall within the commonly reported duration of Stage II of the Albany-Fraser Orogeny, 1215 – 1140 Ma (e.g. Clark et al., 2000; Kirkland et al., 2011a; Spaggiari et al., 2011).

Figure 3.5 is a compilation of published Stage II geochronological data from the western and central Albany-Fraser Orogen. The data include both magmatic and metamorphic ages, and where dated, the ages of specific deformational events. In the Nornalup and Biranup Zones, magmatism, metamorphism and dextral transpression related to NW-SE compression were widespread in the period ca 1190 – 1170 Ma. The $^{40}Ar/^{39}Ar$ cooling ages from this study are synchronous (within uncertainties) to the peak deformation ages from these domains (Figure 3.5), indicating extensive syn- to late-orogenic cooling and exhumation in an actively deforming tectonic environment.

This fast cooling in an actively deforming tectonic setting requires a similarly fast, syn-tectonic exhumation mechanism. Evidence for shearing, faulting and folding associated with transpressional deformation is widespread in the Nornalup and Biranup Zones during this period (Figure 3.5). Transpression plays an important role in the deformation of the western Albany-Fraser Orogen, due to the manner in which compressional stresses are interpreted to have been resolved along the curved orogen (Bodorkos and Clark, 2004b). The extensive transpressional history of the western Albany-Fraser Orogen has been described in several structural studies (e.g. Beeson et al., 1988; Black et al., 1992; Wetherley, 1998; Duebendorfer, 2002; Bodorkos and Clark, 2004b; Barquero-Molina, 2010), and many of the available geochronological data fall within the period ca 1190 – 1170 Ma (Figure 3.5). Therefore, we suggest that the fast, syn-orogenic exhumation of the Nornalup and Biranup Zones may have been driven by widespread transpressional deformation.

Numerical modelling suggests that transpressional zones between two colliding blocks may experience very fast exhumation rates of lower-crustal rocks, as transpressional structures are often nearly vertical and are interpreted to extend to deep crustal levels (Fossen and Tikoff, 1998). The compressional component of the transpressional forces is then inferred to use these structures as conduits to exhume rocks from deep to shallow settings (Fossen and Tikoff, 1998). An example is the Southern Alps of New Zealand, which record the ongoing oblique collision of the Pacific and Australian plates. Cretaceous high-pressure granulites were exhumed by Late Tertiary transpressional structures in the Fiordland Terrane of the Southern Alps (Claypool et al., 2002), and Cenozoic exhumation rates as high as 95 °C/Ma have been recorded along the transpressive Alpine Fault (Batt et al., 2000). Another transpressional structure recording fast uplift is the King Range, a restraining bend in the San Andreas Fault, which records Quaternary exhumation rates of ca 90 °C/Ma (Dumitru, 1991). Granulite facies rocks in the Musgrave Province of central Australia were exhumed in a positive flower structure, with Cambrian cooling rates of ca 10 – 12 °C/Ma (Camacho and McDougall, 2000). These examples of fast transpressional exhumation of lower crustal rocks support the inferred transpressional setting of the western Albany-Fraser Orogen.

Regardless of the exhumation mechanism, the uniformity of hornblende and biotite cooling ages suggests that relative motion between the Nornalup and Biranup Zones had ceased by ca 1169 Ma. This implies a decline in the role of tectonically-driven exhumation processes (i.e. thrusting or shearing, which offset adjacent terranes), and the increasing role of passive isostasy-driven exhumation processes such as erosion after 1169 Ma. This model of initial exhumation driven first by transpression, then the erosion of the uplifted region and associated quick cooling, is presented as a schematic tectonic model in Figure 3.6.

In the Northern Foreland, peak deformation is recorded by metamorphic zircon growth and is post-dated by the $^{40}Ar/^{39}Ar$ muscovite cooling ages (Figure 3.5). The paucity of geochronological and structural data from the Northern Foreland hinders interpretation of an exhumation mechanism for this domain. However, muscovite cooling ages of ca 1159 ± 6 Ma in the Northern Foreland overlap with biotite cooling

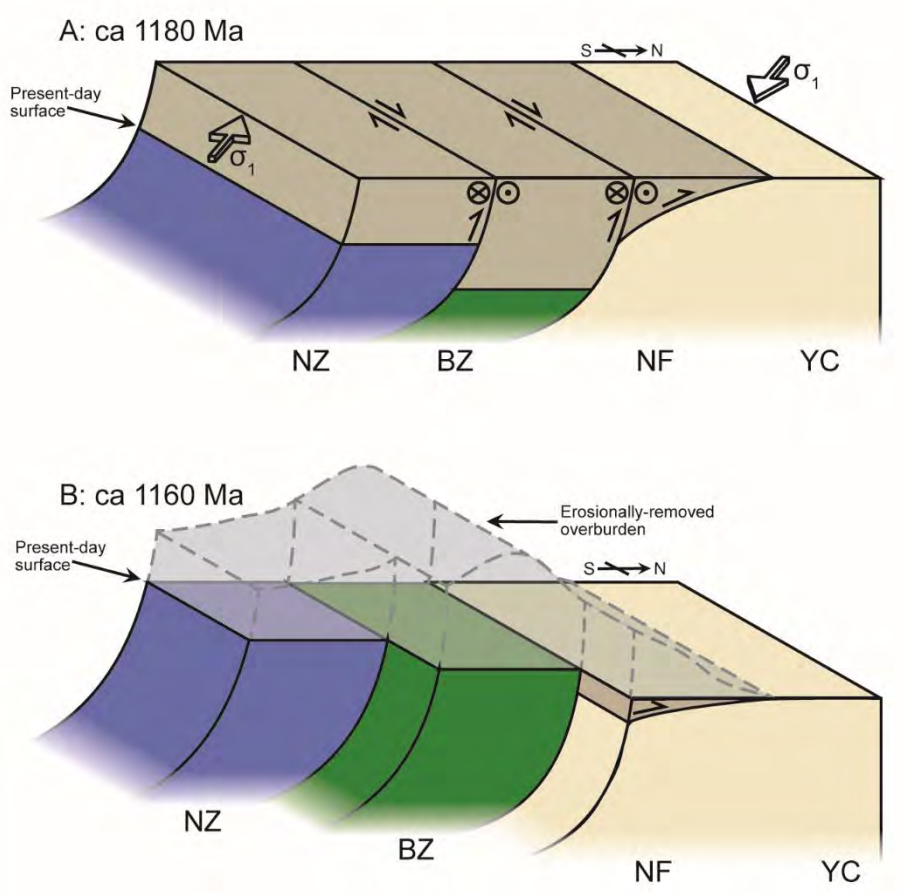

Figure 3.6 Schematic tectonic model for the exhumation of the western Albany-Fraser Orogen during Stage II transpression. Data for this figure is summarised in Table A3.5-1 in Appendix 3.5. **(A)** At 1180 Ma, the Biranup and Nornalup Zones were undergoing peak Stage II metamorphism and deformation at granulite and amphibolite facies respectively. Transpressional deformation was widespread throughout the orogen at this time (see Figure 3.5). **(B)** By ca 1160 Ma, transpression had juxtaposed domains at similar crustal levels, and present-day surfaces had been quickly cooled to the closure temperatures of argon in biotite and muscovite. After ca 1160 Ma, tectonic activity in the western Albany-Fraser Orogen appears to have largely ceased, although emplacement of the granitic Burnside Batholith continued for up to 20 Myr.

ages of ca 1175 – 1144 Ma in the Nornalup and Biranup Zones. Based on calculated muscovite closure temperatures of ca 425 ± 70 °C and biotite closure temperatures of ca 365 ± 35 °C, differential cooling and exhumation of domains in the western Albany-Fraser Orogen after ca 1159 Ma was restricted to less than ca 110 °C cooling of the Northern Foreland relative to the Nornalup and Biranup Zones. This inferred small temperature difference, together with the similarity of muscovite cooling ages in the

Northern Foreland to biotite cooling ages in the Nornalup and Biranup Zones, suggests that all three domains attained similar crustal levels at similar times. Therefore, we interpret that the same tectonically-driven processes responsible for the fast exhumation of the Nornalup and Biranup Zones close to the centre of the orogen, also contributed to the exhumation of the Northern Foreland along the margin of the Yilgarn Craton (Figure 3.6).

The relatively slower cooling rates in the Northern Foreland reflect the older ages for Stage II deformation in this domain, leading to a larger gap between metamorphic ages and cooling ages. Slower cooling may also reflect slower exhumation rates, due to a diminished magnitude of tectonically-driven exhumation processes at the northern margin of the orogen; i.e. a diminished magnitude of exhumation starting at shallower crustal levels than in the Nornalup and Biranup Zones. The Northern Foreland was exhumed comparatively slowly along the margin of the Yilgarn Craton, whilst the Nornalup and Biranup Zones, closer to the centre of the orogen, were exhumed more quickly (Figure 3.6).

Although the cooling and exhumation of the western Albany-Fraser Orogen is synchronous with widespread Stage II tectonic activity in this part of the orogen, the data discussed here are insufficient to extrapolate the syn- to late-orogenic cooling and exhumation history to the eastern part of the orogen. The eastern Albany-Fraser Orogen is likely to have experienced a more complex cooling and exhumation history; crucially, the role of the Fraser Zone during Stage II is poorly understood, as it was exhumed to shallow crustal levels following Stage I tectonic activity (Fletcher et al., 1991; Oorschot, 2011; Kirkland et al., 2011a).

3.5.5 Comparison with the global record of orogenic cooling

The new results presented in this paper show that the western Albany-Fraser Orogen preserves a history of fast cooling. To better understand this cooling history, we integrate it with the existing global record of orogenic cooling. A compilation of published cooling rates from orogens ranging in age from the Paleoproterozoic to the present is listed in Table 3.3, and graphed in Figure 3.7.

Table 3.3 Compilation of orogenic cooling rates through geological history. Orogens are categorised by tectonic style. This data is also presented in Figure 3.7.

Orogen	Cooling age (Ma)	Cooling rate (°C/Ma)	Exhumation mechanism	Source
Albany-Fraser Orogen, SW Australia				
Nornalup Zone	1169	57	Transpressional thrusting	This article
	1169	33		
	1174	13.5		
	1174	9.9		
	1169	57		
Biranup Zone	1178	44		
	1177	69		
	1169	22		
	1169	43		
Northern Foreland	1205	4.2		
	1205	4.7		
	1195	7.7		
	1195	7.1		
Metamorphic Core Complexes				
Eastern Mojave Desert, California/Arizona,	20	45	Extensional tectonics	Foster et al. (1990)
USA	48	6	Erosion during tectonic quiescence	
Northern Snake Range, Nevada, USA	45	32.5	Extensional denudation	Lee (1995)
Shuswap Metamorphic Core Complex, Canadian Cordillera	52	50	Extensional tectonics and ductile thinning	Vanderhaeghe et al. (2003)
Old Woman Mountains, California, USA	72	100	Cooling following magmatic intrusion	Foster et al. (1990); Foster et al. (1992)
Fosdick Mountains, Marie Byrd Land, West Antarctica	100	70	Cooling following intrusion; extensional uplift	Richard et al. (1994)
Liaonan Metamorphic Core Complex, North China Craton	117	30	Extensional shearing	Yang et al. (2007)
Intracontinental Orogens				
Mount Painter Inlier, South Australia	315	6	Uplift driven by thrusting	McLaren et al. (2002)
Arltunga Nappe Complex, Central Australia	345	3.25	Imbricate thrusting	Dunlap and Teyssier (1995)

Orogen	Cooling age (Ma)	Cooling rate (°C/Ma)	Exhumation mechanism	Source
Mt. Isa Province, Northeast Australia	1130	4	Thermal relaxation and erosion	Spikings et al. (2002)
	1315	4		
	1466	1.5	Erosion	McLaren et al. (1999)
Mount Woods Inlier, northeast Gawler Craton, South Australia	1530	4	Thrusting along Southern Overthrust	Forbes et al. (2012)
	1560	6		
Reynolds Range, Central Australia	1564	2.5	Slow exhumation during tectonic quiescence	Vry and Baker (2006)
Transpressional Orogens				
King Range, San Andreas Fault	1.2	90	Transpression a result of restraining bend in the San Andreas fault	Dumitru (1991)
Southern Alps, New Zealand	1.68	95	Transpressional faulting associated with the Alpine Fault	Batt et al. (2000)
	4.9	60		
	7	40		Batt et al. (2004)
	10	10		
Fiordland, New Zealand	115	5.5	Extensional tectonic activity	Flowers et al. (2005)
Musgrave Province, central Australia	495	12	Transpressional faulting (positive flower structure)	Camacho and McDougall (2000)
	500	1.3		
	503	11		
	510	10		
Mzumbe Terrane, Natal Metamorphic Province	1050	5	Cooling following oblique collision	Jacobs and Thomas (2001); Jacobs et al. (1997)
Nova Brasilândia Metasedimentary Belt	1090	2.5	Cooling following oblique collision	Tohver et al. (2004); Tohver et al. (2006)
Accretionary Orogens and Magmatic Arcs				
Central Range, Taiwan	2	120	Erosion	Liu et al. (2000)
Sierra San Pedro Martin Pluton, Baja California, Mexico	95	40	Cooling of an intrusive pluton	Ortega-Rivera et al. (1997)
Northeast Tanzania, Pan-African Granulites	515	3.5	Cooling following cessation of magmatic activity	Möller et al. (2000)
Bamble Terrane, Sveconorwegian Orogen	1085	3	Erosion following thrusting	Bingen et al. (2008); Cosca et al. (1998); Slagstad et al. (2013)
	1123	5.5		

Orogen	Cooling age (Ma)	Cooling rate (°C/Ma)	Exhumation mechanism	Source
Pikwitonei Granulite Domain, Superior Province	2410	1.5	Erosion caused by uplift due to unspecified tectonic processes	Mezger et al. (1990)
Collisional Orogens: Small, Cold				
Western Tauern Window, Eastern Alps, Austria	14	34	Uplift due to thrusting	Von Blanckenburg et al. (1989)
Pennine Nappes, Western European Alps	38	50	Contractional or extensional tectonic activity	Barnicoat et al. (1995)
Black Hills, South Dakota	1715	2.3	Not stated; post-orogenic?	Dahl et al. (1999); Krogstad and Walker (1994)
	1730	0.6		Dahl et al. (1999); rate calculated from hornblende and biotite $^{40}Ar/^{39}Ar$ plateau ages
Collisional Orogens: Transitional				
Betic Cordilleras, Spain	19	250	Extension following delamination	Zeck et al. (1992)
Bohemian Massif, Variscan Belt, Central Europe	332	8.2	Compressionally-driven extrusion	Tajčmanová et al. (2006)
Monts Du Lyonnais Complex, Massif Central, Variscan Belt, France	320	10	Post-exhumation recovery to a steady-state geotherm	Costa et al. (1993)
	345	50	Tectonically-driven exhumation, mechanism unclear	
Collisional Orogens: Large, Hot				
Kongur Shan, Eastern Pamir, China	2	150	Extrusion through combined normal and thrust faulting	Arnaud et al. (1993)
Liachar Thrust, Chogo Lungma Area, NE Pakistan	2	240	Hanging wall of thrust	Whittington (1996)
Southern Himalayan Front, Tibet and India	3	45	Erosion driven by extrusion	Thiede et al. (2004)
Nanga Parbat-Haramosh Massif, Himalaya	6	55	Erosion	George et al. (1995)
Karakoram Mountains, Himalaya	9	30	Erosion driven by normal faulting, possible gravitational collapse due to overthickening	Krol et al. (1996)
Western margin of Nanga Parbat-Haramosh Massif, Himalaya	14	6	Transpressional faulting	Zeitler (1985)
Ribiera-Aracuai Belt, SE Brazil	480	5	Slow post-orogenic exhumation	Petitgirard et al. (2009)
	535	3		

Orogen	Cooling age (Ma)	Cooling rate (°C/Ma)	Exhumation mechanism	Source
Mazinaw Domain, Grenville Orogen, Canada	920	4.5	Orogenic collapse	Busch et al. (1996)
Muskoka Domain, Grenville Orogen, Canada	995	2.1	Orogenic collapse	Rivers (2008)
	1020	4		
Natashquan Domain, Grenville Orogen, Canada	1020	1.5	Orogenic collapse	Rivers (2008)
Collisional Orogens: Unknown Temperature-Magnitude Classification				
Ouachita Orogen, USA	250	2.25	Erosion	Corrigan et al. (1998)
South Norwegian Caledonides	405	10	Extensional collapse following delamination of the lower crust	Andersen et al. (1991)
Borborema Province, Brazil	520	3.5	Shearing	Monie et al. (1997)
	568	20		
Dahomeyide Orogen, West African Craton	598	17.5	Thrusting	Attoh et al. (1997)
Sharbot Lake Domain, Grenville Orogen, Canada	780	1	Post-orogenic cooling following Shawinigan metamorphism	Busch et al. (1996)
Mylonite Zone, Sveconorwegian Orogen	915	10.5	Extensional shearing driven by gravitational collapse	Bingen et al. (2008); Page et al. (1996); Slagstad et al. (2013)
Southern Rogaland-Vest Agder in the Telemarkia Terrane, Sveconorwegian Orogen	920	15	Cooling following magmatic intrusion and post-orogenic extension	Bingen et al. (2008); Slagstad et al. (2013)
Eastern Ghats Belt	950	1	No mechanism proposed	Crowe et al. (2001)
Grenville Front Tectonic Zone, Grenville Orogen, Canada	960	2.5	Thrusting during late Rigolet metamorphism	Rivers (2008)
Grenville Front Tectonic Zone, Grenville Orogen, Canada	980	11	Thrusting during late Rigolet metamorphism	Rivers (2008)
Adirondack Lowlands, New York (Grenville Orogen)	1148	1.5	Post-orogenic cooling following Shawinigan metamorphism	Dahl et al. (2004); Mezger et al. (1991)
Halls Creek Orogen, Western Australia	1695	1.5	Heat dissipation and erosion	Bodorkos and Reddy (2004)
Nagssugtoqidian Orogen	1400	2	Erosion driven by post-orogenic isostatic reequilibration	Willigers et al. (2002)
	1740	6		
	1762	3		

Any discussion of cooling rates must examine the role of controlling variables such as exhumation mechanism and tectonic setting. Cooling rates vary between tectonic settings (Figure 3.7) and may also vary within an orogen; for example, cooling in intracontinental orogens is typically slow and regionally uniform (e.g. 4 °C/Ma, Mt. Isa Province, northeast Australia; Spikings et al., 2002). Fast cooling in actively deforming terranes is often linked to uplift driven by faulting or shearing, which may occur in compressional (e.g. 150 °C/Ma, Kongur Shan, Eastern Pamir, China; Arnaud et al., 1993), transpressional (e.g. 95 °C/Ma, Southern Alps, New Zealand; Batt et al., 2000) or extensional settings (e.g. 50 °C/Ma, Shuswap Metamorphic Core Complex, Canadian Cordillera; Vanderhaeghe et al., 2003).

As the Albany-Fraser Orogen is interpreted as a product of continental collision, we will focus on exhumation and cooling in collisional tectonic settings. Collisional orogens are subdivided into small cold orogens (SCO), transitional orogens (TO) or large hot orogens (LHO) according to the temperature-magnitude classification scheme of Beaumont et al. (2006) (Figure 3.7, Table 3.3). This classification scheme proposes that orogens evolve along a continuum between the endmember SCOs and LHOs. SCOs are characterised by limited crustal thickening and heating, and little to no ductile deformation; as the orogen continues to grow in magnitude through terrane accretion or crustal thickening, it may eventually transition into an LHO, where prolonged crustal heating results in the development of a central elevated plateau above a weak lower crust (Jamieson and Beaumont, 2013). LHOs commonly undergo syn- to post-orogenic collapse, which is a slow process driven by the gravitational instability of the hot, thickened, melt-weakened lower crust underneath the plateau (Jamieson and Beaumont, 2013). As SCOs are colder and rheologically stronger, the do not undergo orogenic collapse; instead, erosion is the dominant exhumation mechanism (Jamieson and Beaumont, 2013). A common feature of SCOs is the exhumation of deep crustal material along shear zones; bringing this hot material to the surface results in rapid, late-stage cooling.

Cooling rates may vary even within the same tectonic setting, as is evident when comparing cooling histories amongst Mesoproterozoic collisional orogens (Figure 3.7). The Mazinaw, Muskoka and Natashquan Domains of the Grenville Orogen (an

LHO) were exhumed following orogenic collapse, and typically experienced cooling from peak metamorphic temperatures at rates of 1 – 5 °C/Ma (Figure 3.7 and Table 3.3). Faster 11 °C/Ma cooling in the Grenville Front Tectonic Zone is a result of thrusting at the orogenic margin during late Rigolet metamorphism, rather than orogenic collapse of the plateau, reflecting the heterogeneity of exhumation processes across the orogen (Rivers, 2008). In the Sveconorwegian Orogen (traditionally a collisional orogen, but recently suggested as accretionary; Slagstad et al., 2013), fast 15 °C/Ma cooling in Southern Rogaland-Vest Agder follows magmatic intrusion and post-orogenic extension, and 6 – 15 °C/Ma cooling from 500 – 350 °C in the Mylonite Zone is driven by extensional shearing (Page et al., 1996; Bingen et al., 1998). The Bamble Terrane of the Sveconorwegian Orogen also records a period of slightly faster 3 – 8 °C/Ma cooling from ca 725 – 550 °C following accretionary orogenesis (Bingen et al., 2008).

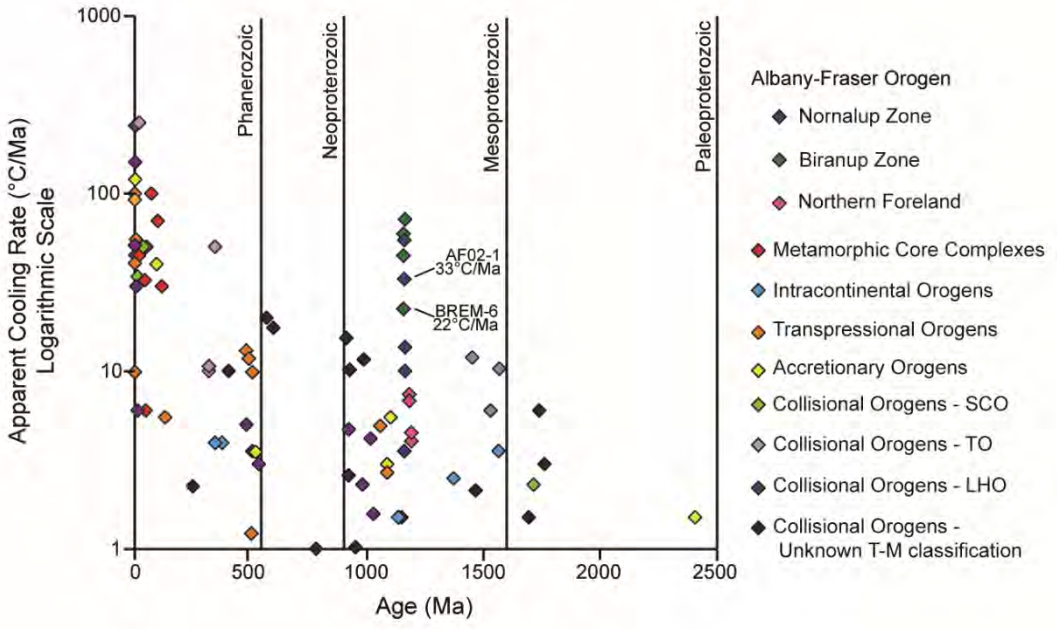

Figure 3.7 Cooling rates from several orogens around the world are plotted against the age of orogeny. Cooling rates are plotted on a logarithmic axis. The age value is the midpoint of the cooling event. Cooling rates are categorised by tectonic setting; the Albany-Fraser Orogen cooled much more quickly than is typical for a Mesoproterozoic orogen. Cooling rates are sourced from references listed in Table 3.3.

In contrast, after high-grade Stage II metamorphism, the Nornalup and Biranup Zones cooled at rates of ca 33^{+17}_{-9} °C/Ma and 22^{+7}_{-5} °C/Ma respectively, significantly faster than in any other Mesoproterozoic orogen (Figure 3.7). The Northern Foreland cooled more slowly at 4.5 – 7.4 °C/Ma, although this is still faster than cooling in many domains of other Mesoproterozoic orogens (Figure 3.7). Exhumation in the western part of the Albany-Fraser Orogen was driven by syn- to late-orogenic transpressional processes, rather than post-orogenic extension or erosion. This exhumation and cooling history fits with an inferred SCO or TO classification for the western part of the orogen. However, regardless of any considerations of tectonic setting, the western Albany-Fraser Orogen preserves an unusually fast cooling history when compared to other Mesoproterozoic orogens.

The cooling history of the Albany-Fraser Orogen stands in contrast to the correlation between increasing cooling rate and decreasing orogenic age. Independent of tectonic setting, cooling in Proterozoic orogens is mostly between 0.5 and 5 °C/Ma, but may be an order of magnitude faster in Phanerozoic orogens (Figure 3.7; Willigers et al., 2002). Several factors are considered to contribute to the apparent increase in cooling rates in more recent time. Deep erosion in older orogens may contribute to a form of sample bias, as many Proterozoic orogens expose rocks that were at a deep crustal level during orogeny (Willigers et al., 2002). These terranes do not reach isotopic closure until the post-orogenic phase, by which time exhumation is controlled by slow, post-orogenic processes (Willigers et al., 2002). These long isothermal periods, common in Proterozoic orogens, also lead to partial isotopic resetting of thermochronometers once below their closure temperatures (Dunlap, 2000). However, these explanations rely on an assumption of fundamentally unchanged orogenic processes (Willigers et al., 2002). This assumption needs to be re-evaluated in light of evidence suggesting a secular change in orogenic processes through time, related to the cooling of the Earth (Brown, 2007). For example, many Precambrian orogens were anomalously hot when compared to modern Phanerozoic orogens (Chardon et al., 2009). There is considerable recent evidence that orogeny and deformation in a hot lithosphere is fundamentally different to that in a cold lithosphere (e.g. Collins, 2002; McLaren et al., 2005; Cagnard et al., 2006; Chardon et

al., 2009). If colder orogens are more likely to preserve fast cooling rates (e.g. Jamieson and Beaumont, 2013), the abundance of different orogenic styles at different times may also contribute to the apparent decrease of cooling rate with increasing orogenic age.

Cooling in the western Albany-Fraser Orogen is unusually fast compared to other Mesoproterozoic orogens, but is not unusual when compared to Phanerozoic orogens. This suggests that the Albany-Fraser Orogeny may belong to a tectonic regime that is underrepresented in the Mesoproterozoic cooling record, but common in the Phanerozoic. This explanation is supported by a transpressional exhumation mechanism for the western part of the Albany-Fraser Orogen. Following Mesoproterozoic cooling and exhumation, the thermochronological record of the Albany-Fraser Orogen was protected by the tectonic quiescence of the orogen, resulting in the preservation of this unusually fast Mesoproterozoic cooling history.

3.6 Conclusion

This article reports the first $^{40}Ar/^{39}Ar$ thermochronology from the western part of the Albany-Fraser Orogen of Western Australia. The Nornalup and Biranup Zones share a similar cooling history, with hornblende cooling ages at ca 1169 Ma, and biotite cooling ages clustered around ca 1159 Ma. These ages correspond to cooling rates of ca 33 $^{+17}_{-9}$ °C/Ma in the Nornalup Zone and ca 22 $^{+7}_{-5}$ °C/Ma in the Biranup Zone, for cooling between ca 585 – 365 °C. The Northern Foreland records muscovite cooling ages at ca 1159 Ma, which constrains cooling to 4.5 – 7.4 °C/Ma between ca 620 – 425 °C. All cooling ages from the Albany-Fraser Orogen fall within the duration of Stage II of orogeny (1210 – 1140 Ma) and are interpreted to record syn- to late-orogenic exhumation as a result of orogen-wide tectonic activity. The transpressional tectonic activity commonly associated with deformation in the western Albany-Fraser Orogen may have been an active driver of this fast exhumation.

The fast cooling and syn-orogenic exhumation history of the western Albany-Fraser Orogen sets it apart from other Mesoproterozoic orogens, which typically experienced slow cooling driven by exhumation mechanisms such as orogenic collapse and isostatically-driven erosion. The western Albany-Fraser Orogen is

unique for its preservation of the syn- to late-orogenic transpressional exhumation processes occurring in an actively deforming orogen. This is supported by evidence of fast exhumation in other transpressional tectonic settings. The record of syn-orogenic exhumation is eroded or overprinted in other Mesoproterozoic orogens; therefore, the thermochronological record in those orogens only preserves the slower post-orogenic cooling history.

3.7 Acknowledgements

We thank Dr. Dave Moecher for assistance with fieldwork, and Dr. Tony Kemp, whose review of an earlier draft greatly improved this article. Thoughtful reviews by Toby Rivers and an anonymous reviewer helped to focus the writing. We also gratefully acknowledge Celia Mayers and Adam Frew for their help in the Western Australian Argon Isotope Facility at Curtin University, and the staff at the UWA Centre for Microscopy and Microanalysis for their assistance. This research was sponsored by the Australian Research Council (LP0991834) and a University of Western Australia Research Fellowship to E. Tohver. E. Scibiorski gratefully acknowledges an Apache Energy Geosciences Scholarship.

3.8 References

Adams, M., 2012, Structural and geochronological evolution of the Malcolm Gneiss, Nornalup Zone, Albany-Fraser Orogen, Western Australia: Geological Survey of Western Australia, Record 2012/4, p. 105.

Andersen, T.B., Jamtveit, B., Dewey, J.F., and Swensson, E., 1991, Subduction and eduction of continental crust: major mechanisms during continent- continent collision and orogen extensional collapse, a model based on the south Norwegian Caledonides: Terra Nova, v. 3, p. 303-310.

Arnaud, N.O., Brunel, M., Cantagrel, J.M., and Tapponnier, P., 1993, High cooling and denudation rates at Kongur Shan, Eastern Pamir (Xinjiang, China) revealed by $^{40}Ar/^{39}Ar$ alkali feldspar thermochronology: Tectonics, v. 12, p. 1335 - 1346.

Attoh, K., Dallmeyer, R., and Affaton, P., 1997, Chronology of nappe assembly in the Pan-African Dahomeyide orogen, West Africa: evidence from $^{40}Ar/^{39}Ar$ mineral ages: Precambrian Research, v. 82, p. 153-171.

Barnicoat, A.C., Rex, D.C., Guise, P.G., and Cliff, R.A., 1995, The timing of and nature of greenschist facies deformation and metamorphism in the upper Pennine Alps: Tectonics, v. 14, p. 279-293.

Barquero-Molina, M., 2010, Kinematics of bidirectional extension and coeval NW-directed contraction in orthogneisses of the Biranup Complex, Albany Fraser Orogen, Southwestern Australia: Geological Survey of Western Australia Report, v. 109, p. 205.

Batt, G.E., Baldwin, S.L., Cottam, M.A., Fitzgerald, P.G., Brandon, M.T., and Spell, T.L., 2004, Cenozoic plate boundary evolution in the South Island of New Zealand: New thermochronological constraints: Tectonics, v. 23, p. 17.

Batt, G.E., Braun, J., Kohn, B.P., and McDougall, I., 2000, Thermochronological analysis of the dynamics of the Southern Alps, New Zealand: GSA Bulletin, v. 112, p. 250-266.

Beaumont, C., Nguyen, M.H., Jamieson, R.A., and Ellis, D.J., 2006, Crustal flow modes in large hot orogens, in: Law, R.D., Searle, M.P., and Godin, L. (Eds.), Channel

Flow, Ductile Extrusion and Exhumation in Continental Collision Zones: Geological Society, London, Special Publications, p. 91-145.

Beeson, J., Claude, P., and Lyal, B., 1988, A structural and metamorphic traverse across the Albany Mobile Belt, Western Australia: Precambrian Research, v. 40/41, p. 117-136.

Bingen, B., Boven, A., Punzalan, L., Wijbrans, J.R., and Demaiffe, D., 1998, Hornblende $^{40}Ar/^{39}Ar$ geochronology across terrane boundaries in the Sveconorwegian Province of S. Norway: Precambrian Research, v. 90, p. 159-185.

Bingen, B., Nordgulen, Ø., and Viola, G., 2008, A four-phase model for the Sveconorwegian orogeny, SW Scandinavia: Norwegian Journal of Geology, v. 88, p. 43-72.

Black, L.P., Harris, L.B., and Claude, P., 1992, Reworking of Archaean and Early Proterozoic components during a progressive, Middle Proterozoic tectonothermal event in the Albany Mobile Belt, Western Australia: Precambrian Research, v. 59, p. 95-123.

Bodorkos, S., and Reddy, S. M., 2004, Proterozoic cooling and exhumation of the northern central Halls Creek Orogen, Western Australia: constraints from a reconnaissance $^{40}Ar/^{39}Ar$ study: Australian Journal of Earth Sciences, v. 51, p. 591 - 609.

Bodorkos, S., and Clark, D., 2004a, Evolution of a crustal-scale transpressive shear zone in the Albany-Fraser Orogen, SW Australia: 1. P-T conditions of Mesoproterozoic metamorphism in the Coramup Gneiss: Journal of Metamorphic Geology, v. 22, p. 691 - 711.

Bodorkos, S., and Clark, D., 2004b,, Evolution of a crustal-scale transpressive shear zone in the Albany-Fraser Orogen, SW Australia: 2. Tectonic history of the Coramup Gneiss and a kinematic framework for Mesoproterozoic collision of the West Australian and Mawson cratons: Journal of Metamorphic Geology, v. 22, p. 713-731.

Brown, M., 2007, Metamorphic conditions in orogenic belts: a record of secular change: International Geology Review, v. 49, p. 193-234.

Busch, J. P., Essene, E. J., and van der Pluijm, B., 1996, Evolution of deep-crustal normal faults: constraints from thermobarometry in the Grenville Orogen, Ontario, Canada: Tectonophysics, v. 265, p. 83-100.

Busch, J.P., Mezger, K., and van der Pluijm, B., 1997, Suturing and extensional reactivation in the Grenville orogen, Canada: Geology, v. 25, p. 507-510.

Cagnard, F., Durrieu, N., Gapais, D., Brun, J.-P., and Ehlers, C., 2006, Crustal thickening and lateral flow during compression of hot lithospheres, with particular reference to Precambrian times: Terra Nova, v. 18, p. 72-78.

Camacho, A., and McDougall, I., 2000, Intracratonic, strike-slip partitioned transpression and the formation and exhumation of eclogite facies rocks: An example from the Musgrave Block, central Australia: Tectonics, v. 19, p. 978-996.

Chardon, D., Gapais, D., and Cagnard, F., 2009, Flow of ultra-hot orogens: A view from the Precambrian, clues for the Phanerozoic: Tectonophysics, v. 477, p. 105-118.

Clark, C., Kirkland, C.L., Spaggiari, C.V., Oorschot, C.W., Wingate, M.T.D., and Taylor, B., 2014, Proterozoic granulite formation driven by mafic magmatism: An example from the Fraser Range Metamorphics, Western Australia: Precambrian Research, v. 240, p. 1-21.

Clark, D., Hensen, B., and Kinny, P., 2000, Geochronological constraints for a two-stage history of the Albany-Fraser Orogen, Western Australia: Precambrian Research, v. 102, p. 155-183.

Clark, W.C., 1995, Granite petrogenesis, metamorphism and geochronology of the western Albany-Fraser Orogen, Albany, Western Australia. Curtin University of Technology, BSc (Honours) thesis (unpublished).

Claypool, A.L., Klepeis, K.A., Dockrill, B., Clarke, G.L., Zwingmann, H., and Tulloch, A.J., 2002, Structure and kinematics of oblique continental convergence in northern Fiordland, New Zealand: Tectonophysics, v. 359, p. 329-358.

Collins, W.J., 2002, Hot orogens, tectonic switching, and creation of continental crust: Geology, v. 30, p. 535-538.

Corrigan, J., Cervany, P.F., Donelick, R.A., and Bergman, S.C., 1998, Postorogenic denudation along the late Paleozoic Ouachita trend, south central United States of America: Magnitude and timing constraints from apatite fission track data: Tectonics, v. 17, p. 587-603.

Cosca, M.A., Mezger, K., and Essene, E.J., 1998, The Baltica-Laurentia connection: Sveconorwegian (Grenvillian) metamorphism, cooling, and unroofing in the Bamble Sector, Norway: The Journal of Geology, v. 106, p. 539-552.

Costa, S., Maluski, H., and Lardeaux, J.-M., 1993, ^{40}Ar-^{39}Ar chronology of Variscan tectono-metamorphic events in an exhumed crustal nappe: the Monts du Lyonnais complex (Massif Central, France): Chemical Geology (Isotope Geoscience Section), v. 105, p. 339-359.

Crowe, W.A., Cosca, M.A., and Harris, L.B., 2001, ^{40}Ar/^{39}Ar geochronology and Neoproterozoic tectonics along the northern margin of the Eastern Ghats Belt in north Orissa, India: Precambrian Research, v. 108, p. 237 - 266.

Dahl, P.S., Holm, D.K., Gardner, E.T., Hubacher, F.A., and Foland, K.A., 1999, New constraints on the timing of Early Proterozoic tectonism in the Black Hills (South Dakota), with implications for docking of the Wyoming province with Laurentia: GSA Bulletin, v. 111, p. 1335 - 1349.

Dahl, P.S., Pomfrey, M.E., and Foland, K.A., 2004, Slow cooling and apparent tilting of the Adirondack Lowlands, Grenville Province, New York, based on ^{40}Ar/^{39}Ar ages: GSA Memoirs, v. 197, p. 299-323.

Dawson, G.C., Krapez, B., Fletcher, I.R., McNaughton, N.J., and Rasmussen, B., 2003, 1.2 Ga thermal metamorphism in the Albany-Fraser orogen of Western Australia: consequence of collision or regional heating by dyke swarms?: Journal of the Geological Society, London, v. 160, p. 29-37.

Dodson, M.H., 1973, Closure temperature in cooling geochronological and petrological systems: Contributions in Mineralogy and Petrology, v. 40, p. 259-274.

Duebendorfer, E.M., 2002, Regional correlation of Mesoproterozoic structures and deformational events in the Albany-Fraser orogen, Western Australia: Precambrian Research, v. 116, p. 129 - 154.

Dumitru, T., 1991, Major Quaternary uplift along the northernmost San Andreas fault, King Range, northwestern California: Geology, v. 19, p. 526-529.

Dunlap, W.J., 2000, Nature's diffusion experiment: The cooling-rate cooling-age correlation: Geology, v. 28, p. 139-142.

Dunlap, W.J., and Teyssier, C., 1995, Paleozoic deformation and isotopic disturbance in the southeastern Arunta block, central Australia: Precambrian Research, v. 71.

Fitzsimons, I., and Buchan, C., 2005, Geology of the Western Albany-Fraser Orogen, Western Australia - a field guide: Western Australian Geological Survey, Record 2005/11, p. 32.

Fletcher, I.R., Myers, J.S., and Ahmat, A.L., 1991, Isotopic evidence on the age and origin of the Fraser Complex, Western Australia: a sample of Mid-Proterozoic lower crust: Chemical Geology (Isotope Geoscience Section), v. 87, p. 197-216.

Flowers, R.M., Bowring, S.A., Tulloch, A.J., and Klepeis, K.A., 2005, Tempo of burial and exhumation within the deep roots of a magmatic arc, Fiordland, New Zealand: Geology, v. 33, p. 17-20.

Forbes, C.J., Giles, D., Jourdan, F., Sato, K., Omori, S., and Bunch, M., 2012, Cooling and exhumation history of the northeastern Gawler Craton, South Australia: Precambrian Research, v. 200-203, p. 209-238.

Fossen, H., and Tikoff, B., 1998, Extended models of transpression and transtension, and application to tectonic settings, in: Holdsworth, R.E., Strachan, R.A., Dewey, J.F. (Eds.), Continental transpressional and transtensional tectonics: Geological Society, London, Special Publications, p. 15-33.

Foster, D., Harrison, T.M., Miller, C.F., and Howard, K.A., 1990, The $^{40}Ar/^{39}Ar$ thermochronology of the eastern Mojave Desert, California, and adjacent western Arizona with implications for the evolution of metamorphic core complexes: Journal of Geophysical Research, v. 95, p. 20005-20024.

Foster, D., Miller, C.F., Harrison, T.M., and Hoisch, T.D., 1992, $^{40}Ar/^{39}Ar$ thermochronology and thermobarometry of metamorphism, plutonism, and tectonic denudation in the Old Woman Mountains area, California: Geological Society of America Bulletin, v. 104, p. 176-191.

George, M., Reddy, S.M., and Harris, N., 1995, Isotopic constraints on the cooling history of the Nanga Parbat-Haramosh Massif and Kohistan arc, western Himalaya: Tectonics, v. 14, p. 237-252.

Grove, M., and Harrison, T.M., 1996, $^{40}Ar^*$ diffusion in Fe-rich biotite: American Mineralogist, v. 81, p. 940-951.

Harrison, T.M., 1981, Diffusion of ^{40}Ar in hornblende: Contributions in Mineralogy and Petrology, v. 78, p. 324 - 331.

Harrison, T.M., Célérier, J., Aikman, A.B., Hermann, J., and Heizler, M.T., 2009, Diffusion of ^{40}Ar in muscovite: Geochimica et Cosmochimica Acta, v. 73, p. 1039-1051.

Harrison, T.M., Duncan, I., and McDougall, I., 1985, Diffusion of ^{40}Ar in biotite: Temperature, pressure and compositional effects: Geochimica et Cosmochimica Acta, v. 49, p. 2461 - 2468.

Jacobs, J., Falter, M., Thomas, R.J., Kunz, J., and Jeßberger, E.K., 1997, $^{40}Ar/^{39}Ar$ thermochronological constraints on the structural evolution of the Mesoproterozoic Natal Metamorphic Province, SE Africa: Precambrian Research, v. 86, p. 71 - 92.

Jacobs, J., and Thomas, R.J., 2001, A titanite fission track profile across the southeastern Archaean Kaapvaal Craton and the Mesoproterozoic Natal Metamorphic Province, South Africa: evidence for differential cryptic Meso- to Neoproterozoic tectonism: Journal of African Earth Sciences, v. 33, p. 323 - 333.

Jamieson, R.A., and Beaumont, C., 2013, On the origin of orogens: GSA Bulletin 125, p. 1671 - 1702.

Kirkland, C.L., Spaggiari, C.V., Pawley, M.J., Wingate, M.T.D., Smithies, R.H., Howard, H.M., Tyler, I.M., Belousova, E.A., and Poujol, M., 2011a, On the edge: U–Pb, Lu–Hf, and Sm–Nd data suggests reworking of the Yilgarn craton margin during formation of the Albany-Fraser Orogen: Precambrian Research, v. 187, p. 223-247.

Kirkland, C.L., Spaggiari, C.V., Wingate, M.T.D., Smithies, R.H., Belousova, E., and Murphy, R., 2011b, Inferences on crust-mantle interaction from Lu-Hf isotopes: a case study from the Albany-Fraser Orogen: Geological Survey of Western Australia, Record 2011/12, p. 25.

Krogstad, E.J., and Walker, R.J., 1994, High closure temperatures of the U-Pb system in large apatites from the Tin Mountain pegmatite, Black Hills, South Dakota, USA: Geochimica et Cosmochimica Acta, v. 58, p. 3845-3853.

Krol, M., Zeitler, P.K., Poupeau, G., and Pecher, A., 1996, Temporal variations in the cooling and denudation history of the Hunza plutonic complex, Karakoram Batholith, revealed by $^{40}Ar/^{39}Ar$ thermochronology: Tectonics, v. 15.

Lee, J.B., 1995, Rapid uplift and rotation of mylonitic rocks from beneath a detachment fault: Insights from potassium feldspar $^{40}Ar/^{39}Ar$ thermochronology, northern Snake Range, Nevada: Tectonics, v. 14, p. 54-77.

Lee, J.Y., Marti, K., Severinghaus, J.P., Kawamura, K., Yoo, H.S., Lee, J.B., and Kim, J.S., 2006, A redetermination of the isotopic abundance of atmospheric Ar: Geochimica et Cosmochimica Acta, v. 70, p. 4507-4512.

Liu, T.-K., Chen, Y.-G., Chen, W.-S., and Jiang, S.-H., 2000, Rates of cooling and denudation of the Early Penglai Orogeny, Taiwan, as assessed by fission-track constraints: Tectonophysics, v. 320, p. 69-82.

McLaren, S., Dunlap, W.J., Sandiford, M., and McDougall, I., 2002, Thermochronology of high heat-producing crust at Mount Painter, South

Australia: implications for tectonic reactivation of continental interiors: Tectonics, v. 21, p. 1-17.

McLaren, S., Sandiford, M., and Hand, M., 1999, High radiogenic heat-producing granites and metamorphism - An example from the western Mount Isa inlier, Australia: Geology, v. 27, p. 679-684.

McLaren, S., Sandiford, M., and Powell, R., 2005, Contrasting styles of Proterozoic crustal evolution: A hot-plate tectonic model for Australian terranes: Geology, v. 33, p. 673-676.

Mezger, K., Bohlen, S.R., and Hanson, G.N., 1990, Metamorphic history of the Archean Pikwitonei granulite domain and the Cross Lake subprovince, Superior Province, Manitoba, Canada: Journal of Petrology, v. 31, p. 483-517.

Mezger, K., and Cosca, M.A., 1999, The thermal history of the Eastern Ghats Belt (India) as revealed by U-Pb and $^{40}Ar/^{39}Ar$ dating of metamorphic and magmatic minerals: implications for the SWEAT correlation: Precambrian Research, v. 94, p. 251-271.

Mezger, K., Rawnsley, C.M., Bohlen, S.R., and Hanson, G.N., 1991, U-Pb garnet, sphene, monazite, and rutile ages: implications for the duration of high-grade metamorphism and cooling histories, Adirondack Mts., New York: The Journal of Geology, v. 99, p. 415-428.

Moecher, D.P., McDowell, S.M., Samson, S., and Miller, C.F., 2014, Ti-in-zircon thermometry and crystallization modeling support hot Grenville granite hypothesis: Geology, v. 42, p. 267-270.

Möller, A., Mezger, K., and Schenk, V., 2000, U-Pb dating of metamorphic minerals: Pan-African metamorphism and prolonged slow cooling of high pressure granulites in Tanzania, East Africa: Precambrian Research, v. 104, p. 123-146.

Monie, P., Caby, R., and Arthaud, M.H., 1997, The Neoproterozoic Brasiliano orogeny in northeast Brazil: $^{40}Ar/^{39}Ar$ and petrostructural data from Ceara: Precambrian Research, v. 81, p. 241-264.

Myers, J.S., 1993, Precambrian history of the West Australian Craton and adjacent orogens: Annual Review of Earth and Planetary Sciences, v. 21, p. 453 - 485.

Nelson, D.R., 1995a, 83649: granite pegmatite, Lake Gidong Headland, in: Nelson, D.R. (Ed.), Compilation of SHRIMP U-Pb zircon geochronology data, 1994: Geological Survey of Western Australia, Record 1995/3, Perth, Western Australia, p. 33-36.

Nelson, D.R., 1995b, 83676A: hornblende syenogranite gneiss, Mount Andrew, in: Nelson, D.R. (Ed.), Compilation of SHRIMP U-Pb zircon geochronology data, 1994: Geological Survey of Western Australia, Record 1995/3, Perth, Western Australia, p. 49-52.

Nelson, D.R., Myers, J.S., and Nutman, A.P., 1995, Chronology and evolution of the Middle Proterozoic Albany-Fraser Orogen, Western Australia: Australian Journal of Earth Sciences, v. 42, p. 481 - 495.

Oorschot, C.W., 2011, P-T-t evolution of the Fraser Zone, Albany-Fraser Orogen, Western Australia: Geological Survey of Western Australia, Record 2011/18, p. 101.

Ortega-Rivera, A., Farrar, E., Hanes, J.A., Archibald, D.A., Gastil, R.G., Kimbrough, D.L., Zentilli, M., López-Martínez, M., Féraud, G., and Ruffet, G., 1997, Chronological constraints on the thermal and tilting history of the Sierra San Pedro Mártir pluton, Baja California, México, from U/Pb, $^{40}Ar/^{39}Ar$, and fission-track geochronology: GSA Bulletin, v. 109, p. 728-745.

Page, L.M., Möller, C., Johansson, L., 1996, $^{40}Ar/^{39}Ar$ geochronology across the Mylonite Zone and the Southwestern Granulite Province in the Sveconorwegian Orogen of S Sweden: Precambrian Research, v. 79, p. 239-259.

Petitgirard, S., Vauchez, A., Egydio-Silva, M., Bruguier, O., Camps, P., Monié, P., Babinski, M., and Mondou, M., 2009, Conflicting structural and geochronological data from the Ibituruna quartz-syenite (SE Brazil): Effect of protracted "hot" orogeny and slow cooling rate?: Tectonophysics, v. 477, p. 174-196.

Pidgeon, R.T., 1990, Timing of plutonism in the Proterozoic Albany Mobile Belt, southwestern Australia: Precambrian Research, v. 47, p. 157-167.

Renne, P.R., Mundil, R., Balco, G., Min, K., and Ludwig, K.R., 2010, Joint determination of ^{40}K decay constants and $^{40}Ar^*/^{40}K$ for the Fish Canyon sanidine standard, and improved accuracy for $^{40}Ar/^{39}Ar$ geochronology: Geochimica et Cosmochimica Acta, v. 74, p. 5349 - 5367.

Richard, S.M., Smith, C.H., Kimbrough, D.L., Fitzgerald, P.G., Luyendyk, B.P., and McWilliams, M.O., 1994, Cooling history of the northern Ford Ranges, Marie Byrd Land, West Antarctica: Tectonics, v. 13, p. 837-857.

Ring, U., Brandon, M.T., Willett, S.D., and Lister, G.S., 1999, Exhumation processes: Geological Society of London Special Publications, v. 154, p. 1-27.

Rivers, T., 2008, Assembly and preservation of lower, mid, and upper orogenic crust in the Grenville Province - Implications for the evolution of large hot long-duration orogens: Precambrian Research, v. 167, p. 237-259.

Slagstad, T., Roberts, N.M.W., Marker, M., Røhr, T.S., and Schiellerup, H., 2013, A non-collisional, accretionary Sveconorwegian orogen: Terra Nova, v. 25, p. 30-37.

Spaggiari, C., Bodorkos, S., Barquero-Molina, M., Tyler, I., and Wingate, M.T.D., 2009, Interpreted bedrock geology of the southern Yilgarn and central Albany-Fraser Orogen, Western Australia: Geological Survey of Western Australia, Record 2009/10, p. 84.

Spaggiari, C., Kirkland, C.L., Pawley, M.J., Smithies, R.H., Wingate, M.T.D., Doyle, M.G., Blenkinsop, T.G., Clark, C., Oorschot, C.W., Fox, L.J., and Savage, J., 2011, The geology of the east Albany-Fraser Orogen - a field guide: Geological Survey of Western Australia, Record 2011/23, p. 92.

Spaggiari, C.V., Kirkland, C.L., Smithies, R.H., and Wingate, M.T.D., 2014, Tectonic links between Proterozoic sedimentary cycles, basin formation and magmatism in the Albany-Fraser Orogen, Western Australia: Geological Survey of Western Australia, Report 133.

Spikings, R.A., Foster, D., Kohn, B.P., and Lister, G.S., 2002, Post-orogenic (<1500 Ma) thermal history of the Palaeo-Mesoproterozoic, Mt. Isa province, NE Australia: Tectonophysics, v. 349, p. 327 - 365.

Stephenson, N.C.N., Russell, T.G., Stubbs, D., and Kalocsai, G.I.Z., 1977, Potassium-argon ages of hornblendes from Precambrian gneisses from the south coast of Western Australia: Journal of the Royal Society of Western Australia, v. 59, p. 105-109.

Tajčmanová, L., Konopásek, J., and Schulmann, K., 2006, Thermal evolution of the orogenic lower crust during exhumation within a thickened Moldanubian root of the Variscan belt of Central Europe: Journal of Metamorphic Geology, v. 24, p. 119-134.

Thiede, R., Bookhagen, B., Arrowsmith, J.R., Sobel, E.R., and Strecker, M.R., 2004, Climatic control on rapid exhumation along the Southern Himalayan Front: Earth and Planetary Science Letters, v. 222, p. 791-806.

Tohver, E., Teixeira, W., van der Pluijm, B., Geraldes, M.C., Bettencourt, J.S., and Rizzotto, G., 2006, Restored transect across the exhumed Grenville orogen of Laurentia and Amazonia, with implications for crustal architecture: Geology, v. 34, p. 669-672.

Tohver, E., van der Pluijm, B., Mezger, K., Essene, E.J., Scandolara, J.E., and Rizzotto, G., 2004, Significance of the Nova Brasilândia metasedimentary belt in western Brazil: Redefining the Mesoproterozoic boundary of the Amazon craton: Tectonics, v. 23, TC6004, doi: 6010.1029/2003TC001563.

Ueda, K., Jacobs, J., Thomas, R.J., Kosler, J., Horstwood, M.S., Wartho, J.A., Jourdan, F., Emmel, B., and Matola, R., 2012, Postcollisional high-grade metamorphism, orogenic collapse, and differential cooling of the East African Orogen of Northeast Mozambique: The Journal of Geology, v. 120, p. 507-530.

Vanderhaeghe, O., Teyssier, C., McDougall, I., and Dunlap, W.J., 2003, Cooling and exhumation of the Shuswap Metamorphic Core Complex constrained by $^{40}Ar/^{39}Ar$ thermochronology: GSA Bulletin, v. 115, p. 200-216.

Von Blanckenburg, F., Villa, I.M., Baur, H., Morteani, G., and Steiger, R.H., 1989, Time calibration of a PT-path from the Western Tauern Window, Eastern Alps: the problem of closure temperatures: Contributions in Mineralogy and Petrology, v. 101, p. 1-11.

Vry, J.K., and Baker, J.A., 2006, LA-MC-ICPMS Pb-Pb dating of rutile from slowly cooled granulites: Confirmation of the high closure temperature for Pb diffusion in rutile: Geochimica et Cosmochimica Acta, v. 70, p. 1807-1820.

Wetherley, S., 1998, Tectonometamorphic evolution of the Mount Barren Group, Albany-Fraser Province, Western Australia. PhD thesis, University of Western Australia.

Whittington, A.G., 1996, Exhumation overrated at Nanga Parbat, northern Pakistan: Tectonophysics, v. 260, p. 215-226.

Willigers, B.J.A., van Gool, J.A.M., Wijbrans, J.R., Krogstad, E.J., and Mezger, K., 2002, Posttectonic cooling of the Nagssugtoqidian Orogen and a comparison of contrasting cooling histories in Precambrian and Phanerozoic orogens: The Journal of Geology, v. 110, p. 503-517.

Yang, J.-H., W, F.-Y., Chung, S.-L., Lo, C.-H., Wilde, S.A., and Davis, G.A., 2007, Rapid exhumation and cooling of the Liaonan metamorphic core complex: inferences from $^{40}Ar/^{39}Ar$ thermochronology and implications for Late Mesozoic extension in the eastern North China Craton: GSA Bulletin, v. 119, p. 1405-1414.

Zeck, H.P., Monié, P., Villa, I.M., and Hansen, B.T., 1992, Very high rates of cooling and uplift in the Alpine belt of the Betic Cordilleras, southern Spain. Geology, v. 20, p. 79-82.

Zeitler, P.K., 1985, Cooling history of the NW Himalaya, Pakistan: Tectonics, v. 4, p. 127-151.

Chapter 4

Cooling and exhumation along the curved Albany-Fraser Orogen, Western Australia

4 Cooling and exhumation along the curved Albany-Fraser Orogen, Western Australia

Elisabeth Scibiorski[1], Eric Tohver[1], Fred Jourdan[2], Christopher L. Kirkland[3], Catherine Spaggiari[4]

[1]School of Earth and Environment, University of Western Australia, M006 35 Stirling Highway, Crawley, WA 6009, Australia

[2]Western Australian Argon Isotope Facility, Department of Applied Geology, Curtin University, Bentley, WA 6102, Australia

[3]Centre for Exploration Targeting, Department of Applied Geology, Curtin University, Bentley, WA 6102, Australia

[4]Geological Survey of Western Australia, 100 Plain Street, East Perth, WA 6004, Australia

Abstract

The Albany-Fraser Orogen of Western Australia exhibits a distinct 45° primary (pre-orogenic) curvature. Consequently, northwest-southeast compression during Mesoproterozoic orogeny was orthogonal to orogenic strike in the east of the orogen, but was oblique in the west. This produced different structural settings in the east and west of the orogen, with a greater component of dextral transpression in the west. We report new $^{40}Ar/^{39}Ar$ thermochronology from the east Albany-Fraser Orogen, and compare these results to the cooling history of the west to examine how cooling varies between the differently-striking domains of a curved orogen.

The $^{40}Ar/^{39}Ar$ analyses of hornblende, muscovite and biotite grains encompass a range of metaigneous and metasedimentary lithologies from two lithotectonic domains. The eastern Biranup Zone yields five hornblende cooling ages at ca. 1190 Ma and seven muscovite and biotite cooling ages between ca. 1171 and 1158 Ma. Hornblende and biotite in the southwestern Fraser Zone record cooling between ca.

1217 and 1205 Ma, and the central Fraser Zone reached $^{40}Ar/^{39}Ar$ biotite closure temperature at ca. 1157 Ma.

Slow 8.2 – 9.5 °C/m.y. cooling in the eastern Biranup Zone commenced 20 m.y. earlier than 22 – 33 °C/m.y. cooling in the west Albany-Fraser Orogen. The differences in cooling rate are a result of the different structural settings in the east and west. However, similar mica $^{40}Ar/^{39}Ar$ cooling ages in the east and west record a convergence in cooling history. This suggests that exhumation had become increasingly decoupled from compressional tectonics, instead driven by more passive processes related to isostatic rebound and erosion.

4.1 Introduction

Exhumation controls when, where, and how rocks are exposed on the Earth's surface. The cooling history of an orogen is strongly correlated with its exhumation history; i.e. rocks which are exhumed quickly from depth will also undergo fast cooling. Consequently, cooling rates provide a mechanism to understand the movement paths of lithotectonic packages. Cooling rates commonly vary within an orogen, and are not uniquely diagnostic of a specific exhumation mechanism (Ring et al., 1999). Nevertheless, knowledge of a region's cooling history may aid in determining the drivers of exhumation when considered together with other information, such as structure or metamorphism (Moore and England, 2001).

The structural setting within an orogen will affect which exhumation mechanisms operate and will consequently affect cooling rates, but previous studies have focused on comparisons between different orogens (e.g. Ring et al., 1999; Willigers et al., 2002; Forbes et al., 2012). However, no two orogens are identical, and the differing features may be those that most affect exhumation and cooling. These variables include upper or lower plate geometry (e.g. Ratschbacher et al., 1993), rheology (e.g. Gerya and Stöckhert, 2002), rock age (Mouthereau et al., 2013), and radiogenic heat production, all of which will determine the thermomechanical state of the lithosphere, and thereby influence structural development and exhumation (McLaren et al., 2005; Chardon et al., 2009; Jamieson and Beaumont, 2013). Climatic factors such as orographic rainfall-driven erosion or glaciation will also influence the

tectonic evolution and exhumation of an orogen (e.g. Koons et al., 2003; Enkelmann et al., 2009), but are extremely difficult to ascertain in ancient orogens. In addition, there is a well-established correlation between orogenic age and apparent cooling rate that requires the secular evolution of the Earth to be incorporated into comparisons of cooling histories from different geological periods (Dunlap, 2000; Willigers et al., 2002; Scibiorski et al., 2015).

The Albany-Fraser Orogen (AFO) of Western Australia is a Neoarchean to Mesoproterozoic orogen. It is characterised by a 45° change in strike from east to west as it curves around the margin of the Yilgarn Craton, although the principal direction of convergence during Mesoproterozoic orogeny is consistently northwest-southeast (Bodorkos and Clark, 2004b; Spaggiari et al., 2011). Consequently, the dominant deformation style varies, from craton-vergent thrusting in the east where convergence is at a high angle to the orogen, to dextral transpression in the west where convergence is more oblique (Beeson et al., 1988; Bodorkos and Clark, 2004b). Therefore, the significant curvature of the belt provides a rare opportunity to examine the effect of changing structural setting on the exhumation of rocks of comparable lithology and metamorphic grade.

In the west AFO, recent $^{40}Ar/^{39}Ar$ thermochronology established a history of extremely fast (22 – 33 °C/m.y.) and synorogenic cooling, inferred to be driven by the transpressional setting (Scibiorski et al., 2015). In the east AFO, numerous high-temperature mineral age constraints are available (primarily U-Pb crystallisation ages of zircon; Geological Survey of Western Australia, 2015) but published work on the cooling history is restricted to four ca. 1280 – 1220 Ma mineral ages from the Fraser Zone (muscovite K-Ar and Rb-Sr, Wilson et al., 1959; biotite 40Ar/39Ar, Baksi and Wilson, 1980; biotite-whole rock Rb-Sr, Fletcher et al., 1991) and four ca. 1225 – 1140 Ma U-Pb titanite cooling ages from the Biranup and Fraser Zones (Kirkland et al., 2016). We use $^{40}Ar/^{39}Ar$ thermochronology to study cooling in the eastern part of the orogen, and compare these results to the cooling history of the west AFO. Differences in the timing and rate of cooling are discussed in the context of different structural settings.

4.2 Geological background

4.2.1 Tectonic setting of the Albany-Fraser Orogen

The AFO extends for more than 1200 km along the southern and south-eastern margins of the Yilgarn Craton of Western Australia (Figure 4.1). During the two-stage Mesoproterozoic Albany-Fraser Orogeny, the Neoarchean to Paleoproterozoic igneous and sedimentary rocks of the orogen were deformed and metamorphosed at high grades (Stage I: 1330 – 1260 Ma; Stage II: 1225 – 1140 Ma) (Clark et al., 2000; Spaggiari et al., 2011). Previous interpretations attributed Stage I to the Mesoproterozoic suturing of the Yilgarn Craton to the Mawson and Gawler cratons of East Antarctica and South Australia, with Stage II a result of later intracratonic reactivation (Clark et al., 2000; Bodorkos and Clark, 2004b). More recent evidence has suggested a continental rift or distal backarc setting for Stage I, and support for the intracontinental setting of Stage II, although the cause of this reactivation remains enigmatic (Smithies et al., 2015). However, regardless of tectonic setting, Stage II is responsible for the crustal architecture preserved throughout the orogen and its dominant metamorphic and structural fabrics; most earlier fabrics and mineral assemblages were replaced, or are preserved only as vestiges (Spaggiari et al., 2009).

The curvature of the AFO results in a 45° change in strike from east to west (Figure 4.1). Most curved orogens are oroclines: orogens which undergo bending during orogeny (Carey, 1955; Weil and Sussman, 2004). However, the curvature of the AFO is primary, reflecting the margin of the Yilgarn Craton (Spaggiari et al., 2009). There is no structural evidence for the spatial accommodation of oroclinal bending, such as buckling or radial folding in the central hinge zone, or stretching in the eastern or western limbs (e.g. Weil, 2006). Additionally, isotopic evidence suggests that the AFO formed in situ at the margin of the Yilgarn Craton (Kirkland et al., 2011), yet the Yilgarn Craton preserves no evidence of having been folded into its present-day configuration.

Structural studies in both the east and west AFO have independently concluded that deformation during Stage II was driven by northwest-directed compression (Beeson et al., 1988; Myers, 1995; Clark et al., 2000; Duebendorfer, 2002; Bodorkos and

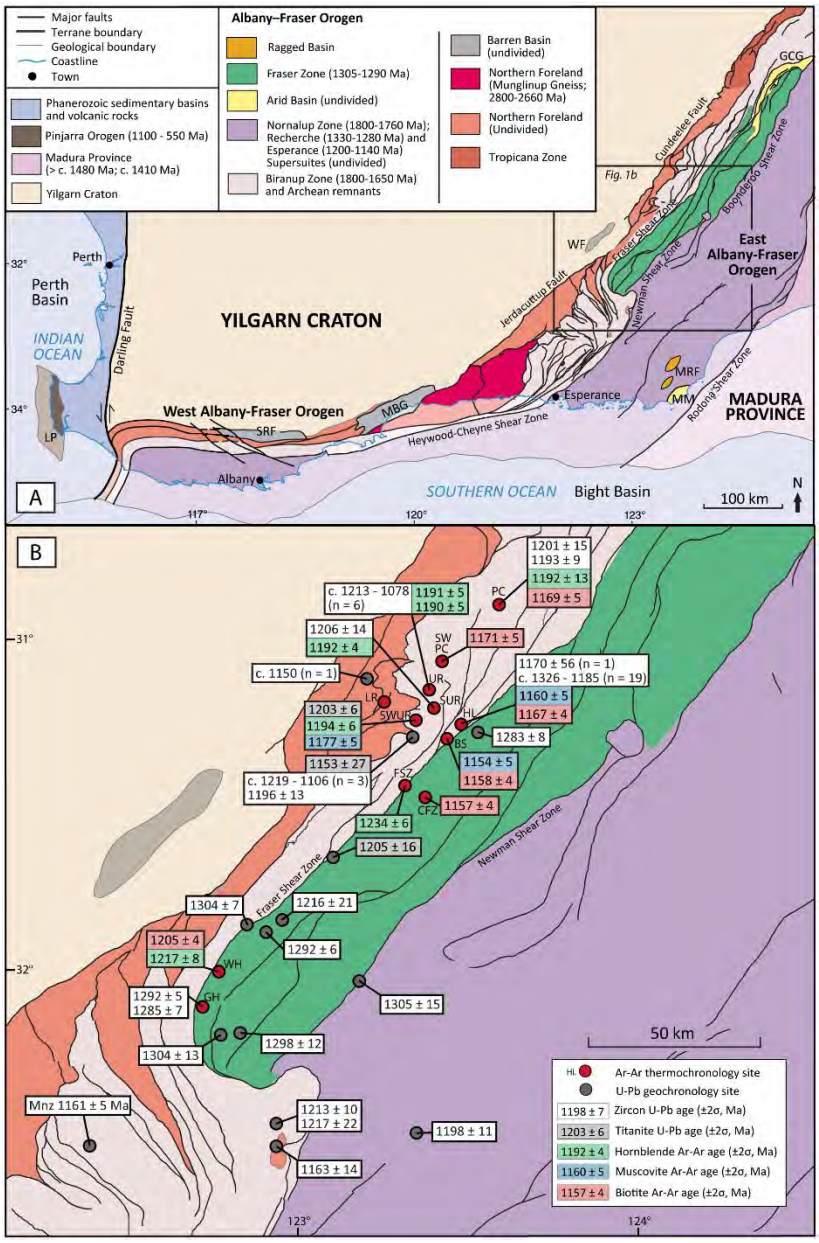

Figure 4.1 (A) Simplified interpreted bedrock geology of the Albany-Fraser Orogen with tectonic subdivisions. **(B)** Interpreted bedrock geology map of the eastern Albany-Fraser Orogen, showing sample sites, new $^{40}Ar/^{39}Ar$ thermochronology and existing Stage II (1225 – 1140 Ma) U-Pb zircon, monazite, and titanite geochronology. U-Pb zircon geochronology older than Stage II is not shown for clarity, except in the Fraser Zone where Stage I geochronology is shown. Abbreviations: BS - Buningonia Soak; CFZ - Central Fraser Zone; FSZ - Fraser Shear Zone; GCG - Gwynne Creek Gneiss; GH - Gnamma Hill; HL - Harris Lake; LP - Leeuwin Province; LR - Lake Rivers; MBG - Mount Barren Group; MM - Malcolm Metamorphics; MRF - Mount Ragged Formation; PC - Ponton Creek; SF - Stirling Range Formation; SUR - S of Uraryie Rock; SWPC - SW of Ponton Creek; SWUR - SW of Uraryie Rock; UR - Uraryie Rock; WF - Woodline Formation; WH - Wyralinu Hill. Modified from Spaggiari et al. (2014a). Geochronology data are from Geological Survey of Western Australia (2015) and Kirkland et al. (2016).

Clark, 2004b; Spaggiari et al., 2014b). In the east, shortening was at a high angle to the orogen, and Stage II deformation resulted in craton-vergent thrusting, shearing, and folding, generally with a minor component of dextral transpression (Myers, 1995; Clark et al., 2000; Bodorkos and Clark, 2004b; Spaggiari et al., 2014b; Waddell et al., 2015).

4.2.2 Lithotectonic subdivisions and geochronology

The AFO is divided into two main tectonic components: the Archean Northern Foreland, and the dominantly Paleo- to Mesoproterozoic Kepa Kurl Booya Province, which in turn is subdivided into the Tropicana, Biranup, Fraser and Nornalup Zones (Figure 4.1; Spaggiari et al., 2014a). The Northern Foreland is the part of the Archean Yilgarn Craton intruded by Paleoproterozoic magmas and subsequently reworked by the Albany-Fraser Orogeny (Spaggiari et al., 2015). Metamorphic grade and deformation intensity increase toward the south and southeast away from the cratonic margin, from greenschist to amphibolite facies (Beeson et al., 1988; Spaggiari et al., 2015). The Biranup and Nornalup Zones are composed of ca. 1815 – 1630 Ma Paleoproterozoic ortho- and paragneisses, and were deformed at upper amphibolite to granulite facies during the Albany-Fraser Orogeny, recorded by widespread metamorphic zircon growth (Beeson et al., 1988; Clark et al., 2000; Spaggiari et al., 2011). Phase equilibrium models suggest Stage I pressure-temperature (P-T) conditions in the south-eastern Biranup Zone were 700 – 850 °C and 5 – 7 kbar, increasing to 10 kbar; this was followed by Stage II metamorphism at 750 – 800 °C and 5 – 6 kbar (Bodorkos and Clark, 2004a). In the north-eastern Biranup Zone, Stage II metamorphism reached 675 – 725 °C and 6.5 – 8.5 kbar (Kirkland et al., 2016). Granitic rocks of the ca. 1330 – 1280 Ma Recherche Supersuite and ca. 1200 – 1140 Ma Esperance Supersuite intrude the Biranup and Nornalup Zones; these magmatic events are coeval with Stage I and Stage II of orogeny, respectively (Pidgeon, 1990; Nelson et al., 1995; Spaggiari et al., 2014a).

In the east AFO, the Biranup and Nornalup Zones are separated by the Fraser Zone (Figure 4.1). The Fraser Zone is bound by shear zones on all sides, and is composed of paragneisses with depositional ages between ca. 1335 and 1295 Ma,

interlayered with ca. 1290 Ma sheets of metagabbro and felsic orthogneisses (Spaggiari et al., 2011; Clark et al., 2014). Magmatism was coeval with granulite-facies metamorphism at ~ 850 °C and 7 – 9 kbar, during Stage I of orogeny (Clark et al., 2014). The effect of Stage II orogeny within the Fraser Zone is not well understood, due to the lack of any Stage II ages in the existing U-Pb geochronology data set despite its location between the high-grade Stage II deformed Biranup and Nornalup Zones (Spaggiari et al., 2011). However, a single U-Pb titanite age suggests the Fraser Zone may have experienced temperatures as high as 695 – 725 °C during Stage II, suggesting a mid-crustal position alongside the Biranup Zone (Kirkland et al., 2016).

4.3 Methods

We collected 25 samples across 170 km in the east AFO from the Northern Foreland, the Fraser Zone, and the Biranup Zone (Figure 4.1). Sample descriptions and locations are summarised in Table 4.1; metamorphic assemblages show no evidence of any retrograde overprint. From these 25 samples, 13 hornblende, 3 muscovite and 22 biotite grains were analysed using $^{40}Ar/^{39}Ar$ thermochronology. Single grains were step-heated by rastering a continuous laser over the sample, and Ar isotopes in the released gas were measured in static mode with a MAP 215-50 mass spectrometer. The $^{40}Ar/^{39}Ar$ analyses were performed at the Western Australian Argon Isotope Facility at Curtin University. Sample preparation and analytical methods are described in Appendix 4.1. Appendix 4.2 contains Ar isotope data corrected for blanks, mass discrimination, and radioactive decay, with individual errors given at 1σ.

The criteria used to determine an age plateau follow Jourdan et al. (2009): plateaus must contain more than 70% of the total measured ^{39}Ar; plateaus must contain at least 3 consecutive steps; and plateaus must satisfy a probability of fit (P) >0.05. Plateau ages are calculated from the mean of all plateau steps, weighted by the inverse variance of the analytical error of each step, and are reported with an uncertainty of 2σ. Mini-plateaus are defined similarly, but contain 50 – 70% of the measured ^{39}Ar, and are less robust than plateau ages. All sources of analytical error are included in the calculations.

Table 4.1 Summary of sample locations, lithology, and analysed minerals.

Field site	Sample	Lithology	Latitude	Longitude	Minerals		
					Hb	Ms	Bt
Northern Foreland							
Lake Rivers	EAF011	amphibolite	-31.248134	123.259641	2		
Fraser Zone							
Central Fraser Zone	EAF046	metagranite	-31.43926403	123.538424			1
Wyralinu Hill	EAF054	metadolerite	-32.0467930	122.795057	1		1
Wyralinu Hill	EAF055B	metagranite	-32.0467930	122.795057	1		
Gnamma Hill	EAF060	mafic granulite	-32.18092198	122.697752	2		
Gnamma Hill	EAF061	pelitic gneiss	-32.18092198	122.697752			2
Fraser Fault Zone							
Fraser Fault Zone	EAF051	granitic mylonite	-31.58328398	123.267036	1		
Fraser Fault Zone	EAF052	granitic mylonite	-31.58328398	123.267036	1		
Biranup Zone							
Harris Lake	EAF021	metanorite	-31.31733198	123.484967			2
Harris Lake	EAF022	muscovite schist	-31.31624803	123.482687		1	
Harris Lake	EAF018	metagranite	-31.30901302	123.483607			1
Harris Lake	EAF020-2	quartzofeldspathic gneiss	-31.30959196	123.483091			1
Buningonia Soak	EAF027	muscovite schist	-31.35488701	123.433094		1	
Buningonia Soak	EAF029	quartzofeldspathic gneiss	-31.35488701	123.433094			1
Buningonia Soak	EAF030	gneissose amphibolite	-31.35273898	123.434121	1		
Uraryie Rock	EAF035	metagranite	-31.18497301	123.421842	2		1
Uraryie Rock	EAF036	granitic gneiss	-31.17295001	123.413636	2		3
South of UR	EAF017	granitic gneiss	-31.25792398	123.431605	3		3
Southwest of UR	EAF015	muscovite schist	-31.27957201	123.369269		1	
Southwest of UR	EAF012	metagranite	-31.28334001	123.360023	2		1
Ponton Creek	EAF038	amphibolite	-30.90960000	123.642918	1		
Ponton Creek	EAF039B	biotite schist	-30.91110203	123.644351			1
Ponton Creek	EAF041	migmatitic gneiss	-30.91160696	123.645413			1
Ponton Creek	EAF042	metagranodiorite	-30.91338602	123.643762			3
Southwest of PC	EAF037	quartzofeldspathic gneiss	-31.04851998	123.454971			1

Note: Hb – hornblende; Ms – muscovite; Bt – biotite; UR – Uraryie Rock; PC – Ponton Creek

4.4 Results

The results for the $^{40}Ar/^{39}Ar$ analyses are listed in Table 4.2. In total, 38 grains were analysed; 16 grains from 15 samples returned geologically significant plateau ages. Plateau graphs for these 16 grains are in Figure 4.2; the degassing spectra are generally flat and low in complexity. The remaining degassing spectra are in Appendix 4.2; samples either did not produce a plateau (6 grains) or contained excess argon (16 grains). Inverse isochrons could not be calculated due to the highly radiogenic composition of the trapped Ar component.

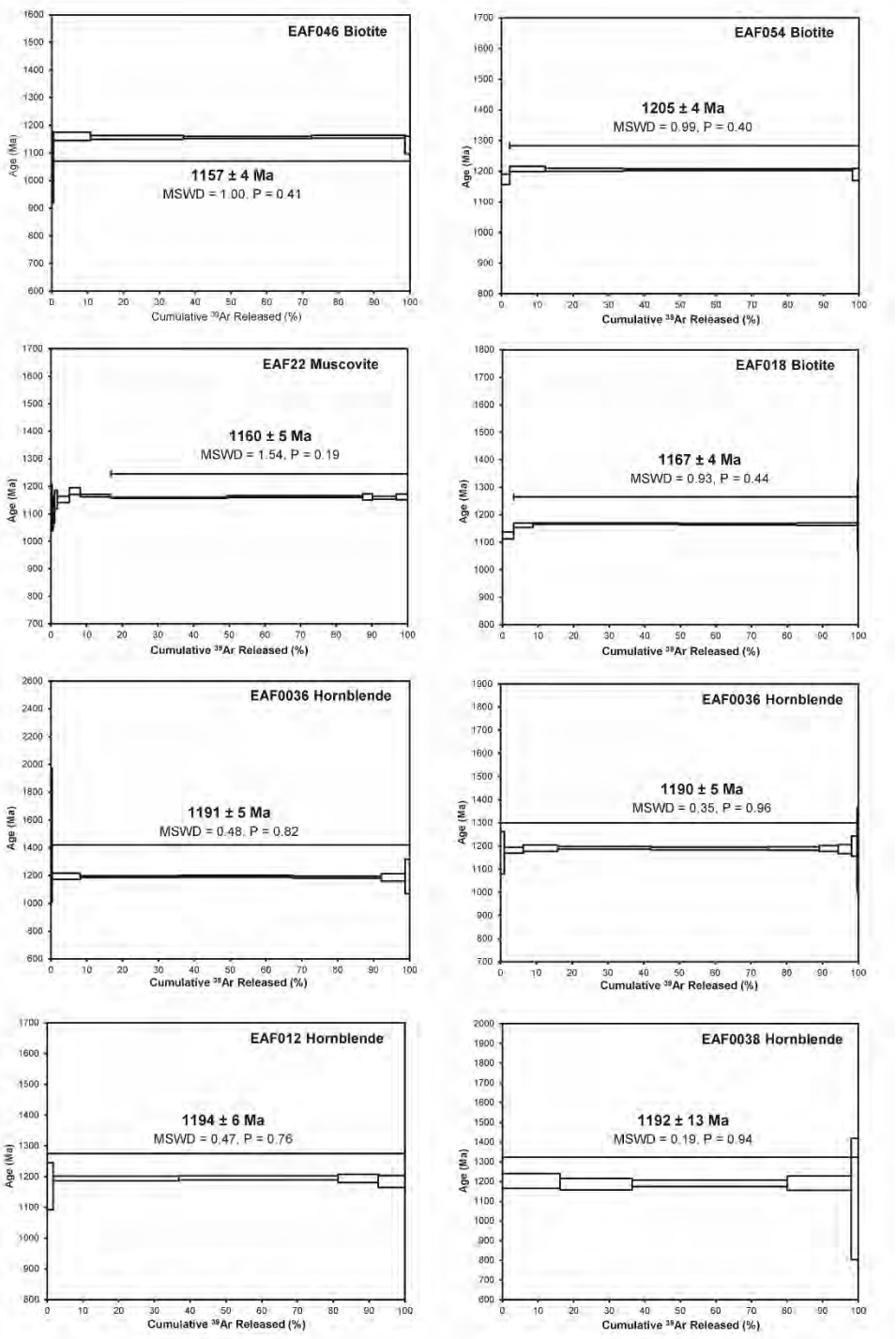

Figure 4.2 The $^{40}Ar/^{39}Ar$ apparent age spectra of all analyses producing geologically significant plateau ages, with individual steps graphed against cumulative percentage of ^{39}Ar released. Plateau age uncertainties are 2σ and are reported with the mean square of weighted deviates (MSWD) and probability (P). Thermochronological data tables and the remaining $^{40}Ar/^{39}Ar$ apparent age spectra are in Appendix 4.2.

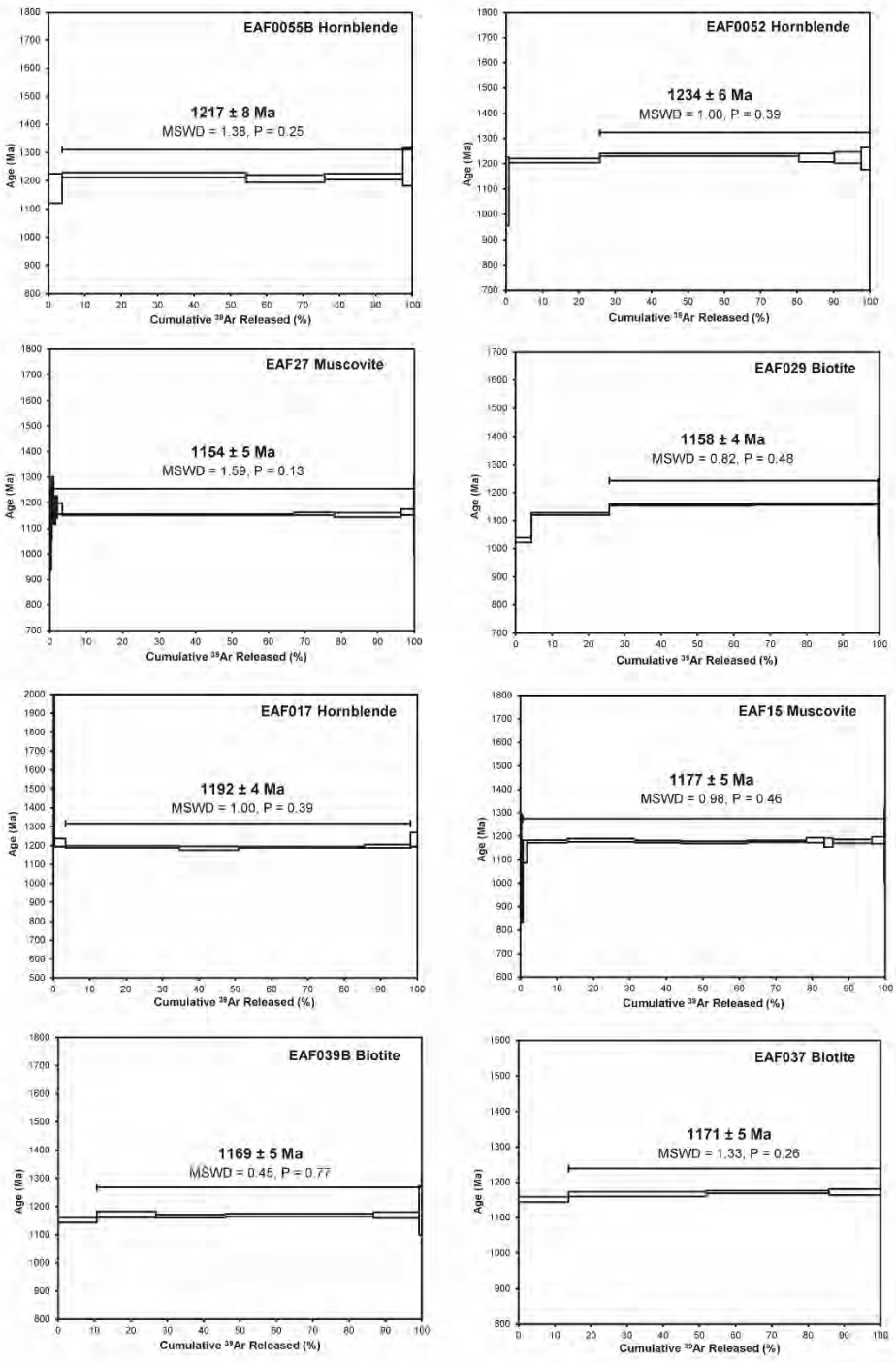

Figure 4.2 (Continued)

4.4.1 $^{40}Ar/^{39}Ar$ plateau ages by domain

At the southern end of the Fraser Zone, two samples, EAF055B and EAF054, yielded hornblende and biotite plateau ages of 1217 ± 8 Ma and 1205 ± 4 Ma, respectively. A single sample 100 km to the northeast produced a younger biotite plateau age of 1157 ± 4 Ma (EAF046). Hornblende EAF052 from the Fraser Shear Zone produced a plateau age of 1234 ± 6 Ma.

In the Biranup Zone, five hornblendes from four samples give remarkably consistent plateau ages ranging from 1194 ± 6 Ma to 1190 ± 5 Ma, with a weighted mean of 1192 ± 2 Ma (samples EAF012, EAF017, EAF038, and EAF036). Muscovites from samples EAF015, EAF022 and EAF027 give plateau ages ranging from 1177 ± 5 Ma to 1154 ± 5 Ma, younging over a distance of 12 km to the east. Four biotites produced plateau ages from 1171 ± 5 Ma to 1158 ± 4 Ma, with no apparent geographical trend (samples EAF018, EAF029, EAF037 and EAF039B).

Hornblende from sample EAF011 in the Northern Foreland contained excess argon, and did not return a geologically significant age.

4.4.2 Excess argon

Excess argon is ^{40}Ar that does not come from the in situ decay of ^{40}K, or from the presence of atmospheric argon, and violates the assumption that all ^{40}Ar in a sample is from one of these two sources (McDougall and Harrison, 1988). Excess argon is a common occurrence in argon thermochronology, particularly in metamorphic terranes, and is important to identify because it produces anomalously old mineral ages that do not represent the true cooling history of the sample (Lanphere and Dalrymple, 1976; Harrison and McDougall, 1981; Kelley, 2002). The typical explanation for excess argon is a high ambient partial pressure of ^{40}Ar (e.g. Foland, 1983) although inherited argon has also been suggested (McDougall and Harrison, 1988).

In most cases, excess ^{40}Ar is easily identifiable due to its distribution in the mineral, which typically produces degassing spectra with a saddle-shaped pattern, and a convergence toward supra-atmospheric values ($^{40}Ar/^{36}Ar > 298$) in the inverse

Table 4.2 Summary of $^{40}Ar/^{39}Ar$ thermochronology results from the eastern Albany-Fraser Orogen, Western Australia.

Locality	Sample	Lithology	Mineral	Plateau characteristics					Excess argon	Zircon or titanite age (Ma, ± 2σ)	Zircon or titanite sample number
				Age (Ma, ± 2σ)	^{39}Ar (%)	n	MSWD	P			
Northern Foreland											
LR	EAF011	amphibolite	*Hb*	*1642 ± 13*	*100*	*5*	*0.53*	*0.71*	*1, 3*	*1287 ± 21*	*194791; zircon*
Fraser Zone											
CFZ	EAF046	metagranite	Bt	1157 ± 4	99	5	1.00	0.41			
WH	EAF054	metadolerite	Bt	1205 ± 4	98	4	0.99	0.40			
WH	EAF055B	metagranite	Hb	1217 ± 8	96	4	1.38	0.25			
GH	EAF060	mafic granulite	*Hb*	*np*							
GH	EAF061	garnet gneiss	*Bt*	*np*							
			Bt	*np*							
Fraser Shear Zone											
FSZ	EAF051	granitic mylonite	*Hb*	*np*							
FSZ	EAF052	granitic mylonite	Hb	1234 ± 6	74	4	1.00	0.39			
Biranup Zone											
HL	EAF021	metanorite	*Bt*	*1557 ± 5*	*92*	*3*	*0.62*	*0.54*	*1, 3*	*c. 1185*	*194722; zircon*
			Bt	*1304 ± 4*	*86*	*7*	*0.96*	*0.45*	*1, 3*	*c. 1185*	*194722; zircon*
HL	EAF022	muscovite schist	Ms	1160 ± 5	83	5	1.54	0.19			
HL	EAF018	metagranite	Bt	1167 ± 4	97	5	0.93	0.44			
HL	EAF020-2	quartzofeldspathic gneiss	*Bt*	*1182 ± 4*	*81*	*4*	*0.86*	*0.46*	*1*		
BS	EAF027	muscovite schist	Ms	1154 ± 5	99	8	1.59	0.13			
BS	EAF029	quartzofeldspathic gneiss	Bt	1158 ± 4	74	4	0.82	0.48			
BS	EAF030	gneissose amphibolite	*Hb*	*1270 ± 7*	*82*	*5*	*0.24*	*0.91*	*3*	*c. 1185*	*194722; zircon*
UR	EAF035	metagranite	*Bt*	*1210 ± 6*	*92*	*4*	*1.75*	*0.15*	*3*	*1162 ± 39*	*194726; zircon*
			Hb	*1245 ± 5*	*93*	*6*	*1.64*	*0.14*	*3*	*1162 ± 39*	*194726; zircon*
UR	EAF036	granitic gneiss	Hb	1191 ± 5	100	7	0.48	0.82			
			Hb	1190 ± 5	100	10	0.35	0.96			

Locality	Sample	Lithology	Mineral	Plateau characteristics					Excess argon	Zircon or titanite age (Ma, ± 2σ)	Zircon or titanite sample number
				Age (Ma, ± 2σ)	^{39}Ar (%)	n	MSWD	P			
			Bt	*1231 ± 5*	*61*	*4*	*0.43*	*0.73*	*2*		
			Bt	*np*							
SUR	EAF017	granitic gneiss	Hb	1192 ± 4	95	4	1.00	0.39			
			Hb	*1206 ± 4*	*100*	*6*	*0.35*	*0.89*	*1, 2, 3*	*1206 ± 14*	*194725; zircon*
			Bt	*1243 ± 5*	*96*	*7*	*1.93*	*0.07*	*1, 2, 3*	*1206 ± 14*	*194725; zircon*
			Bt	*1372 ± 4*	*68*	*3*	*1.19*	*0.31*	*1, 2, 3*	*1206 ± 14*	*194725; zircon*
			Bt	*1333 ± 5*	*76*	*4*	*1.10*	*0.35*	*1, 2, 3*	*1206 ± 14*	*194725; zircon*
SWUR	EAF015	muscovite schist	Ms	1177 ± 5	99	11	0.98	0.46			
SWUR	EAF012	metagranite	Hb	1194 ± 6	100	5	0.47	0.76			
			Bt	*1212 ± 4*	*89*	*4*	*1.60*	*0.19*	*1, 2, 3*	*1203 ± 6*	*184387; titanite*
PC	EAF038	amphibolite	Hb	1192 ± 13	100	5	0.19	0.94			
PC	EAF039B	biotite schist	Bt	1169 ± 5	89	5	0.45	0.77			
PC	EAF041	migmatitic gneiss	*Bt*	*1233 ± 6*	*100*	*4*	*2.06*	*0.10*	*2, 3*	*1193 ± 9*	*194734; zircon*
PC	EAF042	metagranodiorite	*Bt*	*1281 ± 4*	*95*	*10*	*1.40*	*0.18*	*2, 3*	*1193 ± 9*	*194734; zircon*
			Bt	*1281 ± 4*	*77*	*6*	*1.92*	*0.09*	*2, 3*	*1193 ± 9*	*194734; zircon*
			Bt	*np*							
SWPC	EAF037	quartzofeldspathic gneiss	Bt	1171 ± 5	86	3	1.33	0.26			

Note: The rationales for identifying excess argon are: (1) inconsistent results from the same mineral at the same site; (2) biotite age is greater than hornblende or muscovite from the same site; (3) biotite or hornblende age is greater than published U-Pb zircon or titanite age from the same site. Hb - hornblende; Ms - muscovite; Bt - biotite; np - no plateau age; MSWD - mean square weighted deviation; P - P-value; n - number of steps used in the plateau. Locality names correspond with those in Figure 4.1b: BS - Buningonia Soak; CFZ - Central Fraser Zone; FSZ - Fraser Fault Zone; GH - Gnamma Hill; HL - Harris Lake; LR - Lake Rivers; PC - Ponton Creek; SUR - S of Uraryie Rock; SWPC - SW of Ponton Creek; SWUR - SW of Uraryie Rock; UR - Uraryie Rock; WH - Wyralinu Hill. U-Pb zircon data are from Geological Survey of Western Australia (2015) and U-Pb titanite data are from Kirkland et al. (2016). Italics indicate samples that have been excluded on the basis of either not producing a valid plateau age or containing excess argon.

isochron plot ($^{36}Ar/^{40}Ar$ versus $^{39}Ar/^{40}Ar$) (McDougall and Harrison, 1988). A more cryptic form of excess argon, in which the sample produces a geologically unrealistically old plateau age, was previously documented in metamorphic terranes (e.g. Foland, 1983; Batt et al., 2000; Willigers et al., 2004; Rolland et al., 2009).

Several of the analysed samples contain excess argon (Table 4.2). Anomalously old plateau ages were readily identified in samples where a mineral with a low closure temperature (e.g., biotite at ~350 °C) produced an apparent plateau age significantly older than a higher temperature event (e.g., U-Pb zircon age). Excess argon may also be identified by a lack of reproducibility of plateau ages from replicate analyses of a given sample. To this end, minerals were re-analysed from several samples to check for the reproducibility of plateau ages. For example, sample EAF021 produced $^{40}Ar/^{39}Ar$ biotite plateau ages at 1557 ± 5 Ma and 1304 ± 4 Ma, both of which are significantly older than the U-Pb age of metamorphic zircon growth, ca. 1185 Ma (Table 4.2).

Using these criteria, 16 grains from 11 samples yielding plateau ages contain excess argon. Table 4.2 presents the data used to detect excess argon in each sample. Despite excess argon contamination, some authors are able to extract geologically useful information from the inverse isochron plot (e.g. Roddick et al., 1980; Rolland et al., 2009). However, due to the large quantity of radiogenic argon in our samples, there is no spread of data points along the mixing line, and excess $^{40}Ar^*$ is not visible on the inverse isochron (Appendix 4.2). The data from these samples are not geologically significant, and are not discussed further.

4.4.3 Mineral closure temperatures and cooling rates

The $^{40}Ar/^{39}Ar$ analyses may record mineral crystallisation ages, the last time a rock cooled through its mineral-specific closure temperature for argon diffusion, or hydrous recrystallization ages (McDougall and Harrison, 1988; Villa, 2016). Typical estimates of argon closure temperatures are ~550 °C for hornblende, ~425 °C for muscovite, and ~350 °C for biotite (Harrison, 1981; Harrison et al., 1985; Harrison et al., 2009), although a given crystal closure temperature also depends on variables such as cooling rate, grain size, composition, activation energy, and diffusion

coefficient (Dodson, 1973). As all samples were metamorphosed at conditions above their closure temperature, and there is no petrological evidence for hydrous recrystallization, we interpret all mineral plateau ages as cooling ages.

A pair of hornblende and mica cooling ages from the same sample or the same site allows the calculation of cooling rates between the mineral closure temperatures. We obtained three such suitable hornblende-mica pairs, and calculated mica closure temperatures and cooling rates using a Monte Carlo simulation that iterates Dodson's equation for closure temperature (Dodson, 1973). A Monte Carlo simulation is a statistical technique that performs a calculation many times, and thereby includes all sources of uncertainty in the calculation, but also minimises error correlations and gives a realistic final uncertainty. Inputs to the simulation and histograms of the results are in Appendix 4.3; the procedure was described in detail in Scibiorski et al. (2015).

The calculated cooling rates and mica closure temperatures are presented in Table 4.3. Hornblende closure temperatures were not calculated, as this would require better constraints on the age and temperature of metamorphism at the sample sites than are currently available. To the southwest of Uraryie Rock, the Biranup Zone records cooling of $8.2\ ^{+1.9}/_{-1.5}$ °C/m.y. between ~550 °C and 410 ± 58 °C (assumed and calculated closure temperatures of hornblende EAF012 and muscovite EAF015, respectively). At Ponton Creek, 50 km to the northeast, the Biranup Zone records cooling of $9.5\ ^{+2.4}/_{-1.5}$ °C/m.y. between ~550 °C and 331 ± 24 °C (closure temperatures of hornblende EAF038 and biotite EAF039B). Both cooling intervals occur over a similar period of ca. 1190 – 1170 Ma. At Wyralinu Hill in the southwestern Fraser Zone, cooling from ~550 °C to 340 ± 26 °C (closure temperatures of hornblende EAF055B and biotite EAF054) occurred at a rate of $17.5\ ^{+5.5}/_{-3.3}$ °C/m.y., although it took place over an earlier period, ca. 1217 – 1205 Ma.

In the following discussion we assume mineral closure temperatures of ~550 °C for hornblende, ~425 °C for muscovite, and ~350 °C for biotite, except for those 3 mica samples where closure temperatures could be calculated (Table 4.3). The calculated closure temperatures are identical, within error, to the assumed closure temperatures.

Table 4.3 Cooling rates for hornblende and mica cooling age pairs from the same locality in the eastern Albany-Fraser Orogen.

Locality	Hornblende cooling age		Mica cooling age			Monte Carlo Simulation	
	Sample	Cooling age (Ma, ± 2σ)	Sample	Mineral	Cooling age (Ma, ± 2σ)	Mica closure temperature (°C, ± 2σ)	Cooling rate (°C/m.y., +Q3/-Q1)
Biranup Zone							
SW of Uraryie Rock	EAF012	1194 ± 6	EAF015	Ms	1177 ± 5	410 ± 58	8.2, +1.9/-1.5
Ponton Creek	EAF038	1192 ± 13	EAF039B	Bt	1169 ± 5	331 ± 24	9.5, +2.4/-1.5
Fraser Zone							
Wyralinu Hill	EAF055B	1217 ± 8	EAF054	Bt	1205 ± 4	340 ± 26	17.5, +5.5/-3.3

Note: Cooling rates and closure temperatures were calculated using a Monte Carlo simulation with 20,000 trials, in order to include all sources of uncertainty, minimise error correlations, and give a realistic final uncertainty. The distribution of cooling rates is strongly positively skewed, and is reported as a median with error defined by the lower and upper quartiles. The median is a better measure of the central tendency of a skewed population than the mean, and the lower and upper quartiles are a more robust measure of scale than the standard deviation. Inputs to the simulation and histograms of the results are in Appendix 4.2. Ms – muscovite; Bt – biotite.

4.5 Discussion

4.5.1 Cooling and exhumation in the east Albany-Fraser Orogen

Fraser Zone

The new $^{40}Ar/^{39}Ar$ thermochronology reported here provides evidence that the Fraser Zone was affected by metamorphism associated with Stage II (1225 – 1140 Ma) of the Albany-Fraser Orogeny. The southwestern part of the Fraser Zone was at ~550 °C ($^{40}Ar/^{39}Ar$ hornblende closure temperature) at ca. 1217 Ma and cooled to 340 ± 26 °C (calculated $^{40}Ar/^{39}Ar$ biotite closure temperature) by ca. 1205 Ma; the central Fraser Zone passed through ~350 °C ($^{40}Ar/^{39}Ar$ biotite closure temperature) at ca. 1157 Ma; and the Fraser Shear Zone records a hornblende cooling age of ca. 1234 Ma (Table 4.2). These results complement recent U-Pb titanite geochronology which suggests that the Fraser Shear Zone underwent temperatures as high as 695 – 725 °C at 1205 ± 16 Ma, placing it into the mid-crust alongside the Biranup Zone (Kirkland et al., 2016). The agreement between the $^{40}Ar/^{39}Ar$ and U-Pb data contributes towards resolving a long-standing problem in the AFO: the effects of Stage II in the Fraser Zone had previously been unrecognised, due to the complete absence of Stage II ages in the U-Pb zircon geochronological record, despite the Fraser Zone juxtaposition between high-grade Stage II deformed rocks of the Biranup and Nornalup Zones (Spaggiari et al., 2011).

Cooling of the 200-km-long Fraser Zone was not homogenous. By ca. 1205 Ma, the southwestern Fraser Zone had cooled at a rate of $17.5\ ^{+5.5}/_{-3.3}$ °C/m.y. to ~340 °C. In contrast, the 1157 Ma biotite cooling age 100 km to the northeast (sample EAF046) suggests that the central Fraser Zone did not cool to ~350 °C for another 50 m.y. (Figure 4.1). Faulting within the Fraser Zone itself may have resulted in this varying timing for exhumation, a common feature of orogenic exhumation (e.g. Cosca et al., 1992; Fügenschuh and Schmid, 2005). Alternatively, in Spaggiari et al. (2011) it was proposed that exhumation was driven by the lateral extrusion of the Fraser Zone to the southwest during early Stage II. The extrusion model is based on kinematic indicators for dextral movement in the Fraser Shear Zone and sinistral movement in

the Newman Shear Zone, which form the northwest and southeast boundaries, respectively, of the Fraser Zone (Spaggiari et al., 2011).

The extrusive exhumation model requires that the Fraser and Newman Shear Zones were active simultaneously, either synchronous with or preceding the Fraser Zone cooling ages reported here. Although the deformation fabrics in the Fraser and Newman Shear Zones have not been directly dated, the 1234 ± 6 Ma $^{40}Ar/^{39}Ar$ hornblende cooling age and the younger 1205 ± 16 Ma U-Pb titanite age (22 km southwest) indicate a heterogenous thermal history along the Fraser Shear Zone (Kirkland et al., 2016). In addition, it is difficult to reconcile the extrusion model with current thermal models of Stage II, where the Fraser Zone was cooler and rheologically stronger than the surrounding, hotter Biranup and Nornalup Zones.

Eastern Biranup Zone

Hornblende cooling ages across the sampled area of the eastern Biranup Zone are remarkably consistent. The region passed through ~550 °C ($^{40}Ar/^{39}Ar$ hornblende closure temperature) at ca. 1190 Ma, followed by cooling to ~425 – 350 °C ($^{40}Ar/^{39}Ar$ muscovite and biotite closure temperatures) between ca. 1175 – 1155 Ma (Table 4.2). Two cooling rates were calculated for the eastern Biranup Zone: ~8.2 $^{+1.9}/_{-1.5}$ °C/m.y. southwest of Uraryie Rock, and ~9.5 $^{+2.4}/_{-1.5}$ °C/m.y. at Ponton Creek, 50 km to the northeast along strike.

The timing of cooling is in the middle of Stage II of orogeny (1225 – 1140 Ma), which implies that the mid-crustal migmatised rocks of the Biranup Zone were already cooling from peak metamorphic conditions by ca. 1190 Ma. This is supported by the ca. 1206 – 1190 Ma zircon and titanite U-Pb ages recording Stage II metamorphic mineral growth in the eastern Biranup Zone (Figure 4.1; Geological Survey of Western Australia, 2015; Kirkland et al., 2016). Some of the zircon U-Pb geochronology from this region records ages younger than ca. 1185 Ma, but these data are not precise and may also be inaccurate, due to discordance (driven by common Pb content or by minor radiogenic Pb loss), small population sizes ($n \leq 3$; due to insufficient overgrowths of datable size), and/or analyses forming no coherent age, potentially indicating prolonged metamorphic zircon growth. In Figure 4.1,

these complex zircon populations are reported as a range defined by the individual analyses. Therefore, it is clear that the high-grade Stage II metamorphism (675 – 725 °C and 6.5 - 8.5 kbar in the Fly Dam Formation; Kirkland et al., 2016) that caused extensive metamorphic zircon growth within the Biranup Zone ceased by ca. 1190 Ma, and was followed by initially fast cooling to ~550 °C. The region then cooled to ~425 – 350 °C by ca. 1175 – 1155 Ma, at rates of 8.2 – 9.5 °C/m.y.

Cooling in the sampled area of the eastern Biranup Zone was contemporaneous with metamorphism and magmatism elsewhere in the orogen (Spaggiari et al., 2011). Widespread metamorphic zircon growth continued until at least ca. 1160 Ma throughout the orogen, and until ca. 1154 Ma in the central and south-eastern Biranup Zone; Esperance Supersuite magmatism in the south-eastern Biranup Zone and in the Nornalup Zone continued until ca. 1140 Ma (Geological Survey of Western Australia, 2015; Smithies et al., 2015). Cooling in the north-eastern Biranup Zone, therefore, preceded the end of Stage II of orogeny.

4.5.2 Comparison to the west Albany-Fraser Orogen

The comparison of cooling histories between the east and west AFO reveals a 20 m.y. difference in the timing of cooling through the $^{40}Ar/^{39}Ar$ hornblende closure temperature, but this difference disappears by the time the limbs of the orogen pass through the biotite $^{40}Ar/^{39}Ar$ closure temperature (Figure 4.3). In the eastern Biranup Zone, hornblende cooling ages are ca. 1190 Ma; the western Biranup Zone and Nornalup Zone cooled through hornblende closure temperatures 20 m.y. later, ca. 1170 Ma (Scibiorski et al., 2015). However, muscovite and biotite cooling ages share a similar range and distribution: in the east, muscovite cooling ages range from 1175 to 1155 Ma and biotite cooling ages range from 1170 to 1160 Ma; in the west, muscovite cooling ages are ca. 1160 Ma and biotite cooling ages range from ca. 1170 to 1150 Ma (Figure 4.3; Scibiorski et al., 2015). The exceptions are the samples from the Fraser Shear Zone and from the southwestern end of the Fraser Zone, which record hornblende and biotite cooling ages 30 – 50 m.y. older than in the eastern Biranup Zone (Figure 4.3). Comparing cooling rates in the east and the west tells a similar story: cooling at ~8.2 – 9.5 °C/m.y. in the eastern Biranup Zone and ~17.5

°C/m.y. in the Fraser Zone is 2 – 4 times slower than the fast 22 – 33 °C/m.y. cooling of the western Biranup and Nornalup Zones (inset in Figure 4.3).

We consider the differences in the timing and rate of cooling along the orogen to be caused by differences in structural setting. The principal northwest-southeast convergence direction is oblique to the east-west oriented west AFO, but is orthogonal to the east AFO; this geometry results in a greater component of transpressional deformation to the west than in the east (Figure 4.4). The northwest-southeast direction of convergence has been established from several structural studies in both the east AFO (Myers, 1995; Clark et al., 2000; Bodorkos and Clark, 2004b; Spaggiari et al., 2014b; Waddell et al., 2015) and the west AFO (Beeson et al., 1988; Wetherley, 1998; Duebendorfer, 2002; Barquero-Molina, 2010). Structural

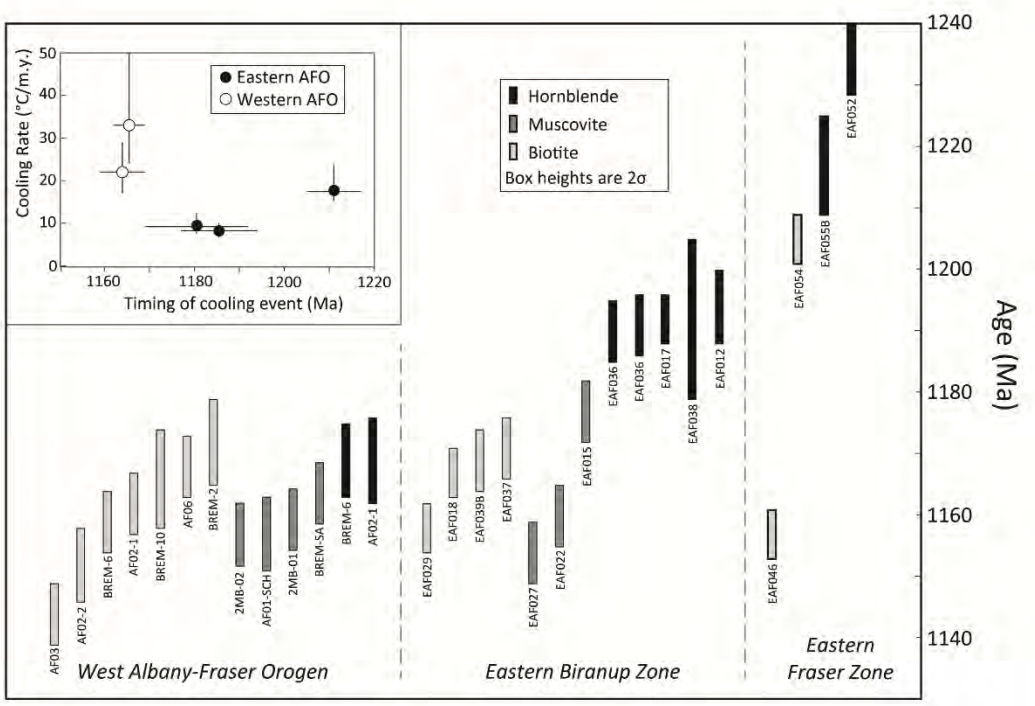

Figure 4.3 Comparison of $^{40}Ar/^{39}Ar$ cooling ages and cooling rates in the east and west Albany-Fraser Orogen. Cooling ages are labelled with the relevant sample name; data for the west Albany-Fraser Orogen is from Scibiorski et al. (2015). Hornblende cooling ages in the east are ~20 m.y. older than in the west, but muscovite and biotite cooling ages have a similar range and distribution. Inset shows cooling rates calculated between $^{40}Ar/^{39}Ar$ hornblende and mica (muscovite or biotite) cooling ages. The timing of the cooling event is the midpoint between the hornblende and the mica cooling age.

evidence includes the following: a pervasive northeast-southwest-striking foliation in the east AFO that strikes increasingly west-southwest–east-southeast towards the west (all listed studies); northeast-southwest-striking thrust and shear zones (all listed studies); kinematic indicators in these thrust and shear zones suggesting a combination of northwest thrusting, dextral shear, and southeast-up transport (Beeson et al., 1988; Myers, 1995; Wetherley, 1998; Duebendorfer, 2002); northwest-vergent folding (Wetherley, 1998; Duebendorfer, 2002; Bodorkos and Clark, 2004b; Barquero-Molina, 2010; Spaggiari et al., 2014b; Waddell et al., 2015); in the west AFO, conjugate shear sets suggesting dextral shearing (Beeson et al., 1988; Duebendorfer, 2002); and in the east AFO, duplexes and folded thrust sheets recording transport to the west-northwest over the margin of the Yilgarn Craton (Myers, 1995; Spaggiari et al., 2014b; Waddell et al., 2015).

Difference in the timing of cooling

Two possible explanations are considered for the 20 m.y. difference in $^{40}Ar/^{39}Ar$ hornblende cooling ages between the east (ca. 1190 Ma) and west AFO (ca. 1170 Ma). In the first hypothesis, whilst the east AFO is slowly exhuming at 1190 Ma, exhumation in the west AFO is negligible for 20 m.y. until a tipping point is reached that results in sudden fast exhumation. Possible reasons for this delay in cooling and the trigger for subsequent exhumation include a change in the dominant stress direction (e.g. Bodorkos and Clark, 2004b); the development of structures that facilitated exhumation; or crustal anatexis or melt intrusion, resulting in weakening of the crust and assisting shearing (e.g. Hollister, 1993). An alternative hypothesis is that the west AFO was already undergoing fast exhumation at 1190 Ma, but the top of the exhumed section is missing, so the cooling ages exposed at the surface are 20 m.y. younger. A consequence of and test for this second hypothesis is that the rocks exposed in the west AFO should have originated deeper within the crust than those in the east AFO. The three existing Stage II P-T models are insufficient to test this theory. Granulite facies pressure constraints of 6.5 – 8.5 kbar in the north-eastern Biranup Zone and ~10 kbar in the south-eastern Biranup Zone are from sites located 50-100 km from the margin of the Yilgarn Craton (Bodorkos and Clark, 2004a; Kirkland et al., 2016). These cannot be meaningfully compared with ~8 kbar in the

amphibolite-facies Mount Barren Group of the western Northern Foreland, which overlies the Yilgarn Craton (Wetherley, 1998).

Difference in the rate of cooling

In the east AFO, where deformation is dominated by craton-vergent thrusting and folding, relatively slow ~8.2 – 9.5 °C/m.y. cooling in the Biranup Zone fits with similar cooling records from other compressional orogens (e.g. McLaren et al., 2002; Tohver et al., 2006; Bingen et al., 2008; Rivers, 2008). The significance of the earlier initiation of ~17.5 °C/m.y. cooling in the Fraser Zone is as yet unresolved. Although the new $^{40}Ar/^{39}Ar$ thermochronology provides evidence that the Fraser Zone was thermally affected by Stage II orogeny, the extent of associated Stage II deformation is unknown and the Fraser Zone has no structural or lithological equivalents in the western part of the orogen (unlike the Northern Foreland, Biranup, and Nornalup Zones, which span the length of the orogen).

The significantly faster exhumation of the west AFO is interpreted as a consequence of transpressional deformation in an obliquely compressional setting (Scibiorski et al., 2015). Although anomalously fast for Mesoproterozoic cooling, this may simply be due to the paucity of preserved cooling records from transpressional settings in the geological record (Scibiorski et al., 2015). Cooling rates of 22 – 33 °C/m.y. are not unusual when compared to other transpressional orogens (e.g. Camacho and McDougall, 2000; Batt et al., 2004).

Numerical models of exhumation in transpressional orogens by Koons et al. (2003) showed that strain is initially partitioned into simple shear- and pure shear-dominated structures (e.g. the exhumation of granulites in southern Madagascar; Martelat et al., 1999), but may form a single oblique structure after thermal weakening of the upper crust. Due to the strike-slip component, faults and shear zones in transpressional settings may be steeper and extend to deeper crustal levels than in purely extensional or compressional settings (Fossen and Tikoff, 1998). These deep and steeply dipping fault and shear zones provide a conduit for the rapid uplift and exhumation of lower crustal rocks (Fossen and Tikoff, 1998). The contractional component of movement then allows a large amount of vertical transport to occur in

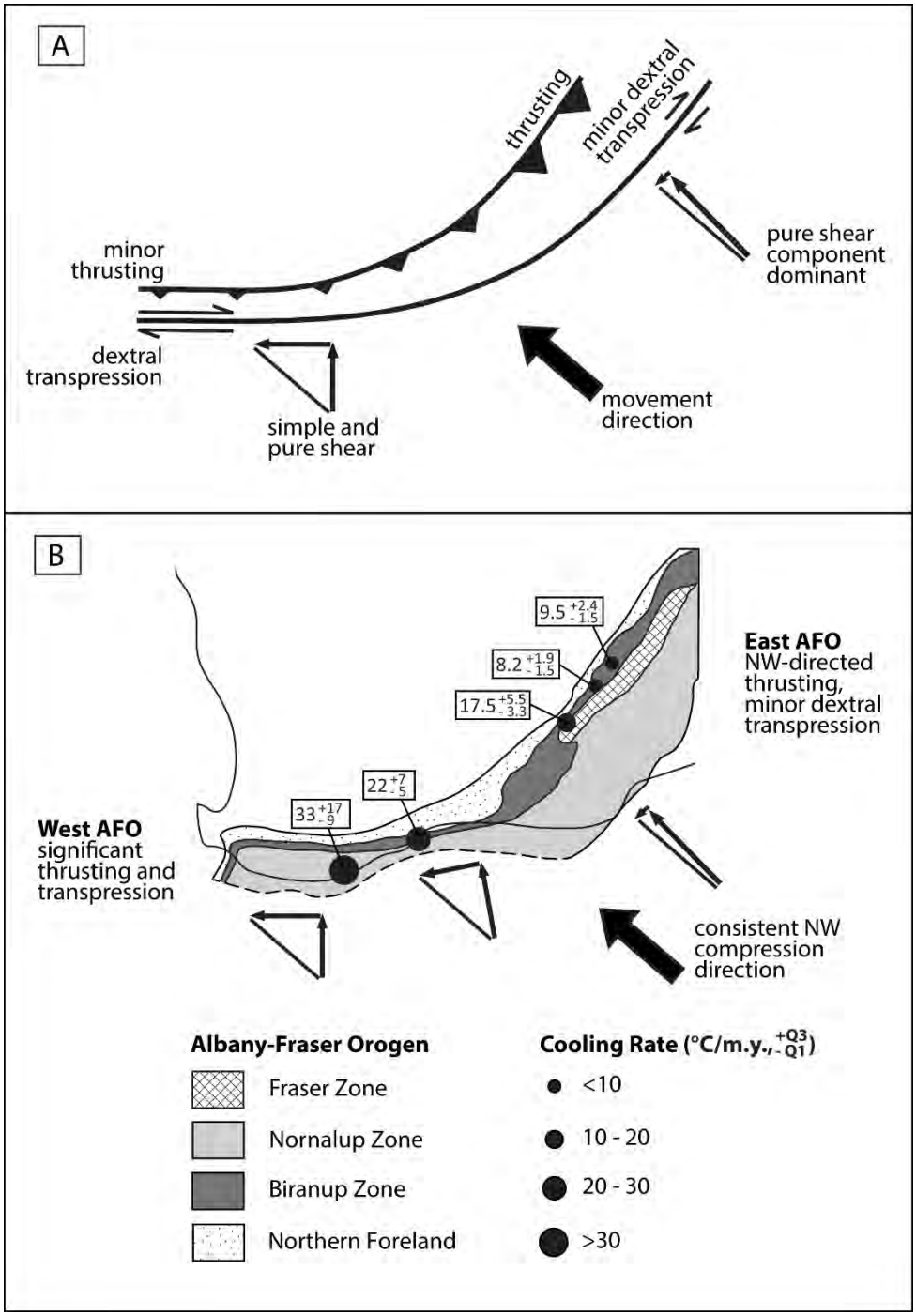

Figure 4.4 (A) Schematic diagram of a curved shear zone showing how kinematics will vary as a result of the changing magnitudes of the simple and pure shear components. Simple and pure shear may be accommodated on separate structures (as shown, for clarity), or a single structure may accommodate both components (i.e., oblique movement). **(B)** During Stage II of the Albany-Fraser Orogeny, stress directions reconstructed from structural geology are consistently oriented northwest-southeast. The 45° curvature of the orogen means this stress is accommodated differently in the west and the east; the differently-striking parts of the orogen also record unique cooling histories.

a short space of time, resulting in rapid uplift and when combined with erosion, rapid exhumation.

Just as kinematics and strain vary along different segments of curved shear zones (Lin and Jiang, 2001), the different deformation styles along the AFO are a larger scale example of this variation (Figure 4.4; Tikoff and Teyssier, 1994; Fossen and Tikoff, 1998). This coupled variance of deformation and cooling within a single orogen demonstrates the influence of the structural setting, controlled in the AFO by the curvature of the cratonic margin, on orogenic exhumation and cooling.

Convergence of mica cooling ages

Successive periods in an orogen's cooling history may reveal changes in exhumation mechanism (e.g. Favaro et al., 2015). By the time the eastern and western limbs of the AFO passed through muscovite $^{40}Ar/^{39}Ar$ closure temperature, differences in the timing of cooling had strongly decreased; by the time biotite closure temperature was reached, these differences had disappeared. In other words, with the exception of a biotite cooling age in the Fraser Zone and a muscovite cooling age in the eastern Biranup Zone, the range of mica $^{40}Ar/^{39}Ar$ cooling ages is uniform across the orogen (Figure 4.3). The convergence in cooling history between east and west suggests that exhumation was increasingly decoupled from compressional tectonics. The most likely candidates are simple isostatic uplift and erosion, processes that operate in all orogens (e.g. Gilchrist et al., 1994). Alternatively, prolonged residence of the orogen in the partial retention zone of biotite (~200 – 300 °C) could also have resulted in the smoothing of cooling ages across the orogen due to partial resetting of the thermochronometer (e.g. Dunlap, 2000). This explanation requires nearly isothermal conditions over a long period of time, and therefore also requires that the orogen is tectonically quiescent, placing a lower age limit on the end of compressional tectonic activity. The convergence of muscovite and biotite cooling ages therefore marks the decreasing role of exhumation associated with compressional processes, and a transition to the more passive processes of isostatic uplift and erosion.

4.6 Conclusions

The 45° change in strike from east to west along the 1200 km Albany-Fraser Orogen provides a rare opportunity to examine the effect of changing structural setting in a single orogen, on the cooling of rocks with comparable lithology and similar prograde metamorphic history. Cooling at 8.2 – 9.5 °C/m.y. in the eastern Biranup Zone, where deformation is dominated by northwest-southeast-directed thrusting and folding, is relatively slow. In contrast, fast 22 – 33 °C/m.y. cooling commenced 20 m.y. earlier in the transpressional west Albany-Fraser Orogen. This difference is a result of the accommodation of the consistent northwest-southeast stress direction along the curved orogen. The convergence of cooling histories in the east and west is recorded by similar mica cooling ages across the orogen; this distribution suggests a decrease in exhumation driven by compression, and an increase in the role of more passive processes such as isostatic uplift and erosion.

4.7 Acknowledgements

We thank the convenors of the illuminating and enjoyable session at the 2015 annual meeting of the Geological Society of America for the opportunity to be a part of this special issue. We are grateful to the Geological Survey of Western Australia for logistical and financial support with fieldwork, and Celia Mayers and Adam Frew for their help in the Western Australian Argon Isotope Facility at Curtin University. C. Spaggiari publishes with the permission of the executive director of the Geological Survey of Western Australia. This research was sponsored by the Australian Research Council (LP0991834) and a Robert and Maude Gledden Postgraduate Scholarship to E. Scibiorski. Reviews by S. McLaren and B. Bingen helped to improve this paper.

4.8 References

Baksi, A. K., and Wilson, A. F., 1980, An attempt at Argon dating of two granulite-facies terranes: Chemical Geology, v. 30, p. 109-120.

Barquero-Molina, M., 2010, Kinematics of bidirectional extension and coeval NW-directed contraction in orthogneisses of the Biranup Complex, Albany Fraser Orogen, Southwestern Australia: Geological Survey of Western Australia, Report 109, p. 205.

Batt, G. E., Baldwin, S. L., Cottam, M. A., Fitzgerald, P. G., Brandon, M. T., and Spell, T. L., 2004, Cenozoic plate boundary evolution in the South Island of New Zealand: New thermochronological constraints: Tectonics, v. 23, no. 4, p. 17.

Batt, G. E., Braun, J., Kohn, B. P., and McDougall, I., 2000, Thermochronological analysis of the dynamics of the Southern Alps, New Zealand: GSA Bulletin, v. 112, no. 2, p. 250-266.

Beeson, J., Delor, C. P., and Harris, L. B., 1988, A structural and metamorphic traverse across the Albany Mobile Belt, Western Australia: Precambrian Research, v. 40/41, p. 117-136.

Bingen, B., Nordgulen, Ø., and Viola, G., 2008, A four-phase model for the Sveconorwegian orogeny, SW Scandinavia: Norwegian Journal of Geology, v. 88, p. 43-72.

Bodorkos, S., and Clark, D., 2004a, Evolution of a crustal-scale transpressive shear zone in the Albany-Fraser Orogen, SW Australia: 1. P-T conditions of Mesoproterozoic metamorphism in the Coramup Gneiss: Journal of Metamorphic Geology, v. 22, p. 691 - 711.

-, 2004b, Evolution of a crustal-scale transpressive shear zone in the Albany-Fraser Orogen, SW Australia: 2. Tectonic history of the Coramup Gneiss and a kinematic framework for Mesoproterozoic collision of the West Australian and Mawson cratons: Journal of Metamorphic Geology, v. 22, p. 713-731.

Camacho, A., and McDougall, I., 2000, Intracratonic, strike-slip partitioned transpression and the formation and exhumation of eclogite facies rocks: An

example from the Musgrave Block, central Australia: Tectonics, v. 19, no. 5, p. 978-996.

Carey, S. W., 1955, The orocline concept in geotectonics: Papers and Proceedings of the Royal Society of Tasmania, v. 89, p. 255-288.

Chardon, D., Gapais, D., and Cagnard, F., 2009, Flow of ultra-hot orogens: A view from the Precambrian, clues for the Phanerozoic: Tectonophysics, v. 477, p. 105-118.

Clark, C., Kirkland, C. L., Spaggiari, C. V., Oorschot, C. W., Wingate, M. T. D., and Taylor, B., 2014, Proterozoic granulite formation driven by mafic magmatism: An example from the Fraser Range Metamorphics, Western Australia: Precambrian Research, v. 240, p. 1-21.

Clark, D., Hensen, B., and Kinny, P., 2000, Geochronological constraints for a two-stage history of the Albany-Fraser Orogen, Western Australia: Precambrian Research, v. 102, p. 155-183.

Cosca, M. A., Essene, E. J., Kunk, M. J., and Sutter, J. F., 1992, Differential unroofing within the Central Metasedimentary Belt of the Grenville Orogen: constraints from $^{40}Ar/^{39}Ar$ thermochronology: Contributions in Mineralogy and Petrology, v. 110, p. 211-225.

Dodson, M. H., 1973, Closure temperature in cooling geochronological and petrological systems: Contributions in Mineralogy and Petrology, v. 40, p. 259-274.

Duebendorfer, E. M., 2002, Regional correlation of Mesoproterozoic structures and deformational events in the Albany-Fraser orogen, Western Australia: Precambrian Research, v. 116, p. 129 - 154.

Dunlap, W. J., 2000, Nature's diffusion experiment: The cooling-rate cooling-age correlation: Geology, v. 28, no. 2, p. 139-142.

Enkelmann, E., Zeitler, P. K., Pavlis, T. L., Garver, J. I., and Ridgway, K. D., 2009, Intense localized rock uplift and erosion in the St Elias orogen of Alaska: Nature Geoscience, v. 2, p. 360-363.

Favaro, S., Schuster, R., Handy, M. R., Scharf, A., and Pestal, G., 2015, Transition from orogen-perpendicular to orogen-parallel exhumation and cooling during crustal indentation - key constraints from $^{147}Sm/^{144}Nd$ and $^{87}Rb/^{87}Sr$ geochronology (Tauern Window, Alps): Tectonophysics, v. 665, p. 1-16.

Fletcher, I. R., Myers, J. S., and Ahmat, A. L., 1991, Isotopic evidence on the age and origin of the Fraser Complex, Western Australia: a sample of Mid-Proterozoic lower crust: Chemical Geology (Isotope Geoscience Section), v. 87, p. 197-216.

Foland, K. A., 1983, $^{40}Ar/^{39}Ar$ incremental heating plateaus for biotites with excess argon: Isotope Geoscience, v. 1, p. 3-21.

Forbes, C. J., Giles, D., Jourdan, F., Sato, K., Omori, S., and Bunch, M., 2012, Cooling and exhumation history of the northeastern Gawler Craton, South Australia: Precambrian Research, v. 200-203, p. 209-238.

Fossen, H., and Tikoff, B., 1998, Extended models of transpression and transtension, and application to tectonic settings, *in* Holdsworth, R. E., Strachan, R. A., and Dewey, J. F., eds., Continental transpressional and transtensional tectonics, Volume 135, Geological Society, London, Special Publications, p. 15-33.

Fügenschuh, B., and Schmid, S. M., 2005, Age and significance of core complex formation in a very curved orogen: Evidence from fission track studies in the South Carpathians (Romania): Tectonophysics, v. 404, p. 33-53.

Geological Survey of Western Australia, 2015, Compilation of geochronology information 2015: Government of Western Australia, ISBN: 9781741686234.

Gerya, T. V., and Stöckhert, B., 2002, Exhumation rates of high pressure metamorphic rocks in subduction channels: The effect of rheology: Geophysical Research Letters, v. 29, no. 8, p. 102-1 – 102-4.

Gilchrist, A. R., Summerfield, M. A., and Cockburn, H. A. P., 1994, Landscape dissection, isostatic uplift, and the morphologic development of orogens: Geology, v. 22, p. 963-966.

Harrison, T. M., 1981, Diffusion of ^{40}Ar in hornblende: Contributions in Mineralogy and Petrology, v. 78, p. 324 - 331.

Harrison, T. M., Célérier, J., Aikman, A. B., Hermann, J., and Heizler, M. T., 2009, Diffusion of ^{40}Ar in muscovite: Geochimica et Cosmochimica Acta, v. 73, p. 1039-1051.

Harrison, T. M., Duncan, I., and McDougall, I., 1985, Diffusion of ^{40}Ar in biotite: Temperature, pressure and compositional effects: Geochimica et Cosmochimica Acta, v. 49, p. 2461 - 2468.

Harrison, T. M., and McDougall, I., 1981, Excess ^{40}Ar in metamorphic rocks from Broken Hill, New South Wales: implications for ^{40}Ar/^{39}Ar age spectra and the thermal history of the region Earth and Planetary Science Letters, v. 55, p. 123-149.

Hollister, L. S., 1993, The role of melt in the uplift and exhumation of orogenic belts: Chemical Geology, v. 108, p. 31-48.

Jamieson, R. A., and Beaumont, C., 2013, On the origin of orogens: GSA Bulletin, v. 125, no. 11/12, p. 1671 - 1702.

Jourdan, F., Marzoli, A., Bertrand, H., Cirilli, S., Tanner, L. H., Kontak, D., McHone, G., Renne, P. R., and Bellieni, G., 2009, 40Ar/39Ar ages of CAMP in North America: implications for the Triassic-Jurassic boundary and the 40K decay constant bias: Lithos, v. 110, p. 167-180.

Kelley, S. P., 2002, Excess argon in K-Ar and Ar-Ar geochronology: Chemical Geology, v. 188, no. 1-2, p. 1-22.

Kirkland, C. L., Spaggiari, C. V., Johnson, T. E., Smithies, R. H., Danišík, M., Evans, N., Wingate, M. T. D., Clark, C., Spencer, C., Mikucki, E., and McDonald, B. J., 2016, Grain size matters: Implications for element and isotopic mobility in titanite: Precambrian Research, v. 278, p. 283-302.

Kirkland, C. L., Spaggiari, C. V., Pawley, M. J., Wingate, M. T. D., Smithies, R. H., Howard, H. M., Tyler, I. M., Belousova, E. A., and Poujol, M., 2011, On the edge: U–Pb, Lu–Hf, and Sm–Nd data suggests reworking of the Yilgarn craton margin during formation of the Albany-Fraser Orogen: Precambrian Research, v. 187, no. 3–4, p. 223-247.

Koons, P. O., Norris, R. J., Craw, D., and Cooper, A. F., 2003, Influence of exhumation on the structural evolution of transpressional plate boundaries: an example from the Southern Alps, New Zealand: Geology, v. 31, no. 1, p. 3-6.

Lanphere, M. A., and Dalrymple, G. B., 1976, Identification of excess ^{40}Ar by the $^{40}Ar/^{39}Ar$ age spectrum technique: Earth and Planetary Science Letters, v. 32, p. 141-148.

Lin, S., and Jiang, D., 2001, Using along-strike variation in strain and kinematics to define the movement direction of curved transpressional shear zones: an example from northwestern Superior Province, Manitoba: Geology, v. 29, no. 9, p. 767-770.

Martelat, J. E., Lardeaux, J.-M., Nicollet, C., and Rakotondrazafy, R., 1999, Exhumation of granulites within a transpressive regime: an example from southern Madagascar: Gondwana Research, v. 2, no. 3, p. 363-367.

McDougall, I., and Harrison, T. M., 1988, Geochronology and thermochronology by the $^{40}Ar/^{39}Ar$ method, New York, Oxford University Press, Oxford Monographs on Geology and Geophysics.

McLaren, S., Dunlap, W. J., Sandiford, M., and McDougall, I., 2002, Thermochronology of high heat-producing crust at Mount Painter, South Australia: implications for tectonic reactivation of continental interiors: Tectonics, v. 21, no. 2, p. 1-17.

McLaren, S., Sandiford, M., and Powell, R., 2005, Contrasting styles of Proterozoic crustal evolution: A hot-plate tectonic model for Australian terranes: Geology, v. 33, no. 8, p. 673-676.

Moore, M. A., and England, P. C., 2001, On the inference of denudation rates from cooling ages of minerals: Earth and Planetary Science Letters, v. 185, p. 265-284.

Mouthereau, F., Watts, A. B., and Burov, E., 2013, Structure of orogenic belts controlled by lithosphere age: Nature Geoscience, DOI: 10.1038/NGEO1902.

Myers, J. S., 1995, Geology of the Esperance 1:1 000 000 sheet: Geological Survey of Western Australia, 1:1 000 000 Geological Series Explanatory Notes, p. 10.

Nelson, D. R., Myers, J. S., and Nutman, A. P., 1995, Chronology and evolution of the Middle Proterozoic Albany-Fraser Orogen, Western Australia: Australian Journal of Earth Sciences, v. 42, no. 5, p. 481 - 495.

Pidgeon, R. T., 1990, Timing of plutonism in the Proterozoic Albany Mobile Belt, southwestern Australia: Precambrian Research, v. 47, p. 157-167.

Ratschbacher, L., Linzer, H.-G., and Moser, F., 1993, Cretaceous to Miocene thrusting and wrenching along the central South Carpathians due to a corner effect during collision and orocline formation: Tectonics, v. 12, no. 4, p. 855-873.

Ring, U., Brandon, M. T., Willett, S. D., and Lister, G. S., 1999, Exhumation processes: Geological Society of London Special Publications, v. 154, p. 1-27.

Rivers, T., 2008, Assembly and preservation of lower, mid, and upper orogenic crust in the Grenville Province - Implications for the evolution of large hot long-duration orogens: Precambrian Research, v. 167, p. 237-259.

Roddick, J. C., Cliff, R. A., and Rex, D. C., 1980, The evolution of excess argon in Alpine biotites - a ^{40}Ar-^{39}Ar analysis: Earth and Planetary Science Letters, v. 48, p. 185-208.

Rolland, Y., Cox, S. F., and Corsini, M., 2009, Constraining deformation stages in brittle-ductile shear zones from combined field mapping and $^{40}Ar/^{39}Ar$ dating: The structural evolution of the Grimsel Pass area (Aar Massif, Swiss Alps): Journal of Structural Geology, v. 31, no. 11, p. 1377-1394.

Scibiorski, E., Tohver, E., and Jourdan, F., 2015, Rapid cooling and exhumation in the western part of the Mesoproterozoic Albany-Fraser Orogen, Western Australia: Precambrian Research, v. 265, p. 232-248.

Smithies, R. H., Spaggiari, C. V., and Kirkland, C. L., 2015, Building the crust of the Albany-Fraser Orogen: constraints from granite geochemistry: Geological Survey of Western Australia, Report 150, p. 49p.

Spaggiari, C., Bodorkos, S., Barquero-Molina, M., Tyler, I., and Wingate, M. T. D., 2009, Interpreted bedrock geology of the southern Yilgarn and central Albany-

Fraser Orogen, Western Australia: Geological Survey of Western Australia, Record 2009/10, p. 84.

Spaggiari, C. V., Kirkland, C. L., Pawley, M. J., Smithies, R. H., Wingate, M. T. D., Doyle, M. G., Blenkinsop, T. G., Clark, C., Oorschot, C. W., Fox, L. J., and Savage, J., 2011, The geology of the east Albany-Fraser Orogen - a field guide: Geological Survey of Western Australia, Record 2011/23, p. 92.

Spaggiari, C. V., Kirkland, C. L., Smithies, R. H., Occhipinti, S. A., and Wingate, M. T. D., 2014a, Geological framework of the Albany-Fraser Orogen, *in* Spaggiari, C. V., and Tyler, I. M., eds., Albany-Fraser Orogen seismic and magnetotelluric (MT) workshop 2014: extended abstracts, Record 2014/6, Geological Survey of Western Australia, p. 12-27.

Spaggiari, C. V., Kirkland, C. L., Smithies, R. H., Wingate, M. T. D., and Belousova, E., 2015, Transformation of an Archean craton margin during Proterozoic basin formation and magmatism: The Albany-Fraser Orogen, Western Australia: Precambrian Research, v. 266, p. 440-466.

Spaggiari, C. V., Occhipinti, S. A., Korsch, R. J., Doublier, M. P., Clark, D. J., Dentith, M. C., Gessner, K., Doyle, M. G., Tyler, I. M., Kennett, B. L. N., Costelloe, R. D., Fomin, T., and Holzschuh, J., 2014b, Interpretation of Albany-Fraser seismic lines 12GA-AF1, 12GA-AF2 and 12GA-AF3: implications for crustal architecture, *in* Spaggiari, C. V., and Tyler, I. M., eds., Albany-Fraser Orogen seismic and magnetotelluric (MT) workshop 2014: extended abstracts, Record 2014/6, Geological Survey of Western Australia, p. 28 - 51.

Tikoff, B., and Teyssier, C., 1994, Strain modeling of displacement-field partitioning in transpressional orogens: Journal of Structural Geology, v. 16, no. 11, p. 1575-1588.

Tohver, E., Teixeira, W., van der Pluijm, B., Geraldes, M. C., Bettencourt, J. S., and Rizzotto, G., 2006, Restored transect across the exhumed Grenville orogen of Laurentia and Amazonia, with implications for crustal architecture: Geology, v. 34, no. 8, p. 669-672.

Villa, I. M., 2016, Diffusion in mineral geochronometers: Present and absent: Chemical Geology, v. 420, p. 1-10.

Waddell, P. J., Timms, N. E., Spaggiari, C. V., Kirkland, C. L., and Wingate, M. T. D., 2015, Analysis of the Ragged Basin, Western Australia: Insights into syn-orogenic basin evolution within the Albany-Fraser Orogen: Precambrian Research, v. 261, p. 166-187.

Weil, A. B., 2006, Kinematics of orocline tightening in the core of an arc: Paleomagnetic analysis of the Ponga Unit, Cantabrian Arc, northern Spain: Tectonics, v. 25, no. 3, DOI: 10.1029/2005TC001861.

Weil, A. B., and Sussman, A. J., 2004, Classifying curved orogens based on timing relationships between structural development and vertical-axis rotations: Geological Society of America Special Papers, v. 383, p. 1-15.

Wetherley, S., 1998, Tectonometamorphic evolution of the Mount Barren Group, Albany-Fraser Province, Western Australia: PhD thesis, University of Western Australia.

Willigers, B. J. A., Mezger, K., and Baker, J. A., 2004, Development of high precision Rb-Sr phlogopite and biotite geochronology; an alternative to $^{40}Ar/^{39}Ar$ tri-octahedral mica dating: Chemical Geology, v. 213, p. 339-358.

Willigers, B. J. A., van Gool, J. A. M., Wijbrans, J. R., Krogstad, E. J., and Mezger, K., 2002, Posttectonic cooling of the Nagssugtoqidian Orogen and a comparison of contrasting cooling histories in Precambrian and Phanerozoic orogens: The Journal of Geology, v. 110, p. 503-517.

Wilson, A. F., Compston, W., Jeffery, P. M., and Riley, G. H., 1959, Radiactive ages from the Precambrian rocks in Australia: Journal of the Geological Society of Australia, v. 6, no. 2, p. 179-195.

Chapter 5

Cryptic excess argon in biotite: $^{40}Ar/^{39}Ar$ plateau ages tested with Rb/Sr geochronology

5 Cryptic excess argon in biotite: $^{40}Ar/^{39}Ar$ plateau ages tested with Rb/Sr geochronology

Scibiorski, E[1]; Tohver, E[1]; Mezger, K[2]; Jourdan, F[3]; Vollstaedt, H[2,4]

[1]School of Earth Sciences, University of Western Australia, 35 Stirling Highway, Crawley, WA 6009, Australia

[2]Institut für Geologie, Universität Bern, Baltzerstrasse 1+3, 3012 Bern, Switzerland

[3]Western Australian Argon Isotope Facility, Department of Applied Geology, Curtin University, Bentley, WA 6102, Australia

[4]Thermo Fisher Scientific, Bremen, Germany

Abstract

In $^{40}Ar/^{39}Ar$ thermochronology, excess argon is ^{40}Ar that does not derive from the *in situ* radioactive decay of ^{40}K, or from the measurable input of atmospheric argon, and results in unrealistically high daughter-parent ratios and anomalously old apparent ages. Excess argon is typically identified by a saddle-shaped $^{40}Ar/^{39}Ar$ degassing spectrum. However, biotite in some samples from the Albany-Fraser Orogen of Western Australia is interpreted to contain excess argon despite a well-defined $^{40}Ar/^{39}Ar$ plateau. This "cryptic excess argon" is suspected where plateau ages (1) are older than existing constraints on cooling, such as U/Pb zircon ages of amphibolite to granulite facies metamorphism, and (2) are not reproducible upon replicate analysis of the same sample. In this contribution, we use Rb/Sr geochronology to test the interpretation of cryptic excess argon in biotite from the Biranup Zone of the east Albany-Fraser Orogen.

The nine samples analysed by Rb/Sr date cooling at c. 1133 Ma, and are 31 – 394 Ma younger than the $^{40}Ar/^{39}Ar$ ages from the same samples. Given that the closure temperature of Sr in biotite is similar to that of Ar in biotite, this distribution of ages cannot be explained by simple monotonic cooling, by biotite growth or recrystallisation below the closure temperature, or by K loss during alteration of

biotite. We propose that these samples contain cryptic excess argon, possibly incorporated from a flux of Ar-rich fluids derived from the underlying Archean Yilgarn Craton.

Due to the presence of the $^{40}Ar/^{39}Ar$ plateau age, cryptic excess argon is difficult to identify *a priori*, without comparison to additional geochronological constraints. We suggest several guidelines for the recognition of cryptic excess argon. Cryptic excess argon may be present if $^{40}Ar/^{39}Ar$ ages contradict additional geochronological constraints on cooling; if ages are not reproducible from the same sample or same site; or if cooling ages vary between sites without a plausible geologic or tectonic explanation. Where a regional problem with cryptic excess argon has been identified, the youngest $^{40}Ar/^{39}Ar$ ages can only provide maximum age constraints. In regions affected by excess argon, Rb/Sr geochronology may provide a more robust alternative to date orogenic cooling.

5.1 Introduction

One of the key assumptions in K/Ar geochronology is that all ^{40}Ar present in a sample is either a product of the *in situ* decay of ^{40}K, or marks the presence of atmospheric argon (McDougall and Harrison, 1988). Because argon is highly incompatible in minerals under normal circumstances, this assumption is commonly valid, and most geochronology using the K/Ar decay scheme yields geologically reasonable ages that fit with independent geochronological constraints (Kelley, 2002).

However, excess argon – ^{40}Ar from a source other than the *in situ* decay of ^{40}K or atmospheric argon – has long been reported in all minerals commonly dated with the K/Ar decay scheme, including amphibole, muscovite, biotite, and feldspar (e.g. Brewer, 1969; Roddick et al., 1980; Harrison and McDougall, 1981). If not accounted for, the presence of excess radiogenic daughter product increases the apparent age of the mineral; often, these old ages are geologically unreasonable (e.g. a biotite $^{40}Ar/^{39}Ar$ age in a granite that is older than the zircon U/Pb age of crystallisation; Lanphere and Dalrymple, 1976). Excess argon is more common in metamorphic than in igneous rocks, and is particularly common in high pressure terranes (e.g. eclogites, blueschists and UHP rocks; Li et al., 1994; Scaillet, 1996; Ruffet et al., 1997; Kelley, 2002).

In many cases, the usage of the inverse isochron approach may help to identify the presence of excess (or inherited) ^{40}Ar and, if only one reservoir of excess Ar is present in the sample, to calculate a geologically meaningful age without relying on any assumption for the composition of the trapped ^{40}Ar (e.g. McDougall and Harrison, 1988). This is common practice for igneous rocks associated with hot spots (e.g. Sharp and Renne, 2005) and melt rock associated with impact structures (e.g. Jourdan et al., 2009). However, the inverse isochron approach is seldom applicable in the case of old metamorphic rocks, as the data points tend to cluster near the radiogenic axis in an inverse isochron plot. The absence of measurable atmospheric argon in some samples that produce unrealistically old apparent ages (e.g. Scibiorski et al., 2016) suggests that an alternative reservoir of excess argon must be present.

Samples containing excess argon often produce a saddle-shaped $^{40}Ar/^{39}Ar$ degassing spectrum, where the apparent age of the gas released during the first and

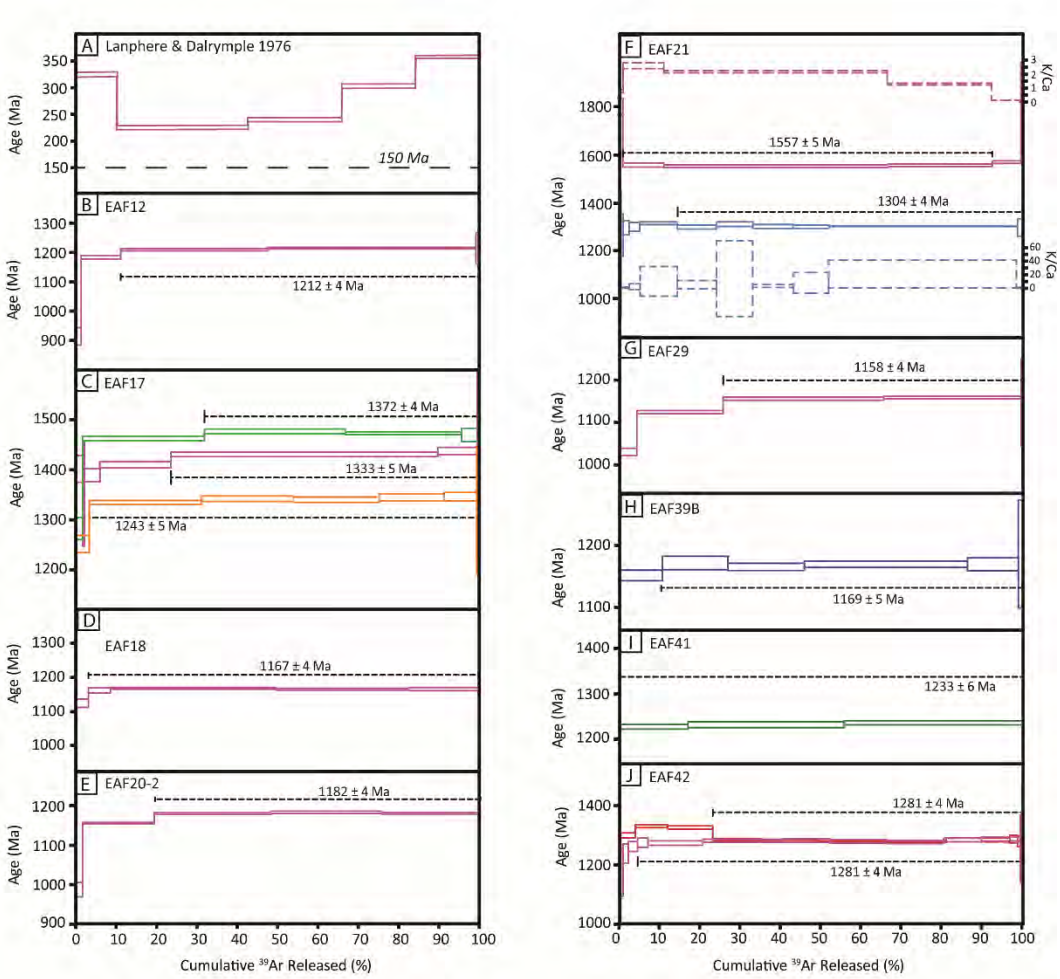

Figure 5.1 $^{40}Ar/^{39}Ar$ degassing spectra of biotites containing excess argon, with individual steps graphed against cumulative percentage of ^{39}Ar released. **(A)** Sample at top left is from Lanphere and Dalrymple (1976), and displays the saddle-shaped degassing spectrum typical for biotite containing excess argon. **(B – J)** The remaining samples are from the Biranup Zone of the east Albany-Fraser Orogen, and display ubiquitous plateaus (dashed lines) despite the presence of cryptic excess argon. Plateau age uncertainties are 2σ. K/Ca ratio is shown for sample EAF21, where biotite is intergrown with hornblende. Data from Scibiorski et al. (2016).

last steps is significantly older than steps in the middle (e.g. Figure 5.1a; Lanphere and Dalrymple, 1976). These saddle-shaped spectra are considered diagnostic for excess argon (e.g. Harrison and McDougall, 1981; Kelley, 2002). However, several authors have also reported excess argon in samples that yielded well-defined plateaus but anomalously old $^{40}Ar/^{39}Ar$ ages (Figure 5.1b – j; Scibiorski et al., 2016). Because the affected samples yield acceptable plateau statistics, the excess argon,

hereafter labelled *cryptic excess argon,* is difficult to identify. Cryptic excess argon has been identified in a range of minerals including hornblende (Pankhurst et al., 1973; Adams and Gabites, 1985), muscovite (Ruffet et al., 1995; Batt et al., 2000), and biotite (Foland, 1983; Baxter et al., 2002; Willigers et al., 2004; Stübner et al., 2017). It is only in comparison with conflicting data from other geochronometers (or even additional $^{40}Ar/^{39}Ar$ data from the same sample) that the $^{40}Ar/^{39}Ar$ ages are shown to be geologically unreasonable.

In this article, we use Rb/Sr biotite geochronology to test for the presence of cryptic excess argon in biotites of the Albany-Fraser Orogen of Western Australia. Because Ar and Sr have similar closure temperatures in biotite, the $^{40}Ar/^{39}Ar$ and Rb/Sr geochronometers should yield similar ages; if the $^{40}Ar/^{39}Ar$ ages are significantly older than the Rb/Sr ages, cryptic excess argon may be reasonably suspected (e.g. Ruffet et al., 1997; Batt et al., 2000; Willigers et al., 2004).

The new Rb/Sr biotite ages are significantly younger than previously published $^{40}Ar/^{39}Ar$ biotite ages that are based on step-heating plateaus containing up to 100% of the released ^{39}Ar (Scibiorski et al., 2016). We use these results to discuss the source and retention of cryptic excess argon, and suggest a series of guidelines for its recognition in $^{40}Ar/^{39}Ar$ geochronology.

5.2 Previous $^{40}Ar/^{39}Ar$ thermochronology in the Albany-Fraser Orogen

The Albany-Fraser Orogen of southwestern Australia extends for c. 1200 km along the southern and south-eastern margins of the Archean Yilgarn Craton, and is separated into several fault-bound domains on the basis of lithology and tectonic history (Figure 5.2). The primary division is between the Archean Northern Foreland and the Mesoproterozoic Kepa Kurl Booya Province, which is in turn subdivided into the Tropicana, Biranup, Fraser and Nornalup Zones (Spaggiari et al., 2009). Although the orogen preserves a long history of magmatism, basin formation, and deformation from the Neoarchean to the Mesoproterozoic, the geological record is dominated by high-grade deformation during the two-stage Mesoproterozoic Albany-Fraser Orogeny (Stage I, 1330 – 1260 Ma; Stage II, 1225 – 1140 Ma) (Clark et al., 2000;

Spaggiari et al., 2011; Spaggiari et al., 2014a). The cooling and exhumation of the orogen following Mesoproterozoic orogeny is known primarily from $^{40}Ar/^{39}Ar$ thermochronology (Baksi and Wilson, 1980; Scibiorski et al., 2015; Scibiorski et al., 2016) and one Rb/Sr biotite-whole rock age (Fletcher et al., 1991).

In the west Albany-Fraser Orogen, $^{40}Ar/^{39}Ar$ thermochronology in the Biranup and Nornalup Zones yielded c. 1170 Ma hornblende and c. 1170 – 1150 Ma biotite cooling ages, indicative of fast 22 – 33 °C/Ma cooling, and consistent with known U/Pb zircon constraints (Scibiorski et al., 2015). In the east Albany-Fraser Orogen, 8.2 – 9.5 °C/Ma cooling rates for the Biranup Zone were calculated from c. 1190 Ma hornblende and 1170 – 1160 Ma biotite $^{40}Ar/^{39}Ar$ cooling ages (Scibiorski et al., 2016). The Fraser Zone produced a range of cooling ages: two $^{40}Ar/^{39}Ar$ hornblende ages of c. 1285 Ma

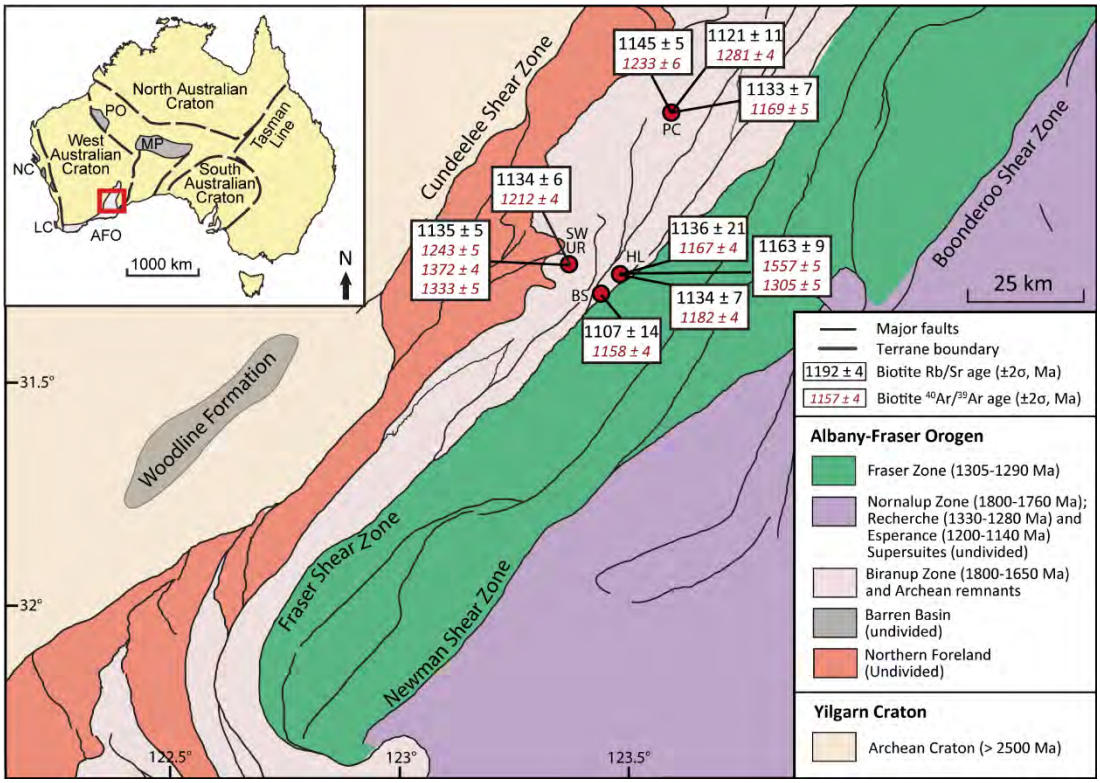

Figure 5.2 Interpreted bedrock geology map of the east Albany-Fraser Orogen, showing sample sites and results of Rb/Sr and $^{40}Ar/^{39}Ar$ geochronology. Inset at top left shows location of the Albany-Fraser Orogen within Australia. Abbreviations for sample sites are: BS, Buningonia Soak; HL, Harris Lake; PC, Ponton Creek; SW UR, Southwest of Uraryie Rock. Inset after Kirkland et al. (2011); bedrock geology map after Spaggiari et al. (2014a).

and c. 1217 Ma; one c. 1268 Ma Rb/Sr biotite age; and two biotite $^{40}Ar/^{39}Ar$ ages of 1205 Ma and 1157 Ma (Baksi and Wilson, 1980; Fletcher et al., 1991; Scibiorski et al., 2016).

However, of the 27 hornblende, muscovite and biotite $^{40}Ar/^{39}Ar$ *plateau* ages yielded by samples in the Biranup Zone of the east Albany-Fraser Orogen, 15 were excluded due to the suspected presence of excess argon in these samples (Scibiorski et al., 2016). Excess argon was interpreted where apparent $^{40}Ar/^{39}Ar$ ages were unrealistically old, either because hornblende and biotite $^{40}Ar/^{39}Ar$ ages were older than U/Pb zircon ages of metamorphism or magmatism, or biotite $^{40}Ar/^{39}Ar$ ages were older than muscovite or hornblende $^{40}Ar/^{39}Ar$ ages. Excess argon was also inferred for samples that yielded $^{40}Ar/^{39}Ar$ ages that were not reproducible within error upon replicate analysis (e.g. sample EAF17 in Figure 5.1c). Due to the highly radiogenic composition of the trapped Ar component, inverse isochrons could not be used to confirm the presence of excess argon. The remaining $^{40}Ar/^{39}Ar$ ages fit with the established sequence of U/Pb and $^{40}Ar/^{39}Ar$ mineral closure temperatures; these 12 samples were interpreted as free of excess argon.

Here, we use Rb/Sr biotite geochronology to test these interpretations. The samples selected for Rb/Sr analysis include a mixture of Biranup Zone samples interpreted to contain excess argon, and 'control' samples with no interpreted excess argon.

5.3 Methods

5.3.1 Sample selection

Nine samples from the east Albany-Fraser Orogen were selected for Rb/Sr analysis based on their $^{40}Ar/^{39}Ar$ results (Scibiorski et al., 2016). Sample locations and brief descriptions of lithologies and mineral assemblages are presented in Table 5.1, and are shown on a map of the orogen in Figure 5.2.

These samples come from four localities within the Biranup Zone: Uraryie Rock, Harris Lake, Buningonia Soak, and Ponton Creek. They were chosen to include a mixture of samples where excess argon was already suspected (biotite $^{40}Ar/^{39}Ar$ plateau ages were older than $^{40}Ar/^{39}Ar$ hornblende ages and/or U/Pb zircon ages), and

Table 5.1 Sample localities, petrography, and biotite $^{40}Ar/^{39}Ar$ thermochronology results. Abbreviations: np, no plateau age; MSWD, mean square weighted deviation; P, P-value; n, number of steps used in the plateau. $^{40}Ar/^{39}Ar$ data from Scibiorski et al. (2016).

Sample	Locality	Lithology	Assemblage	Latitude	Longitude	Plateau characteristics				
						Age (Ma, ± 2σ)	^{39}Ar (%)	n	MSWD	P
EAF012	SW of Uraryie Rock	Paragneiss	Qz-Grt-Pl-Bt-Kfs-Hb-Tt-Rt-Ilm	-31.28334	123.360023	1212 ± 4	89	4	1.60	0.19
EAF017	SW of Uraryie Rock	Gneiss	Qz-Kfs-Pl-Hb-Grt-Bt-Tt	-31.257924	123.431605	1243 ± 5	96	7	1.93	0.07
						1372 ± 4	68	3	1.19	0.31
						1333 ± 5	76	4	1.10	0.35
EAF018	Harris Lake	Metagranite	Kfs-Qz-Bt-Grt	-31.309013	123.483607	1167 ± 4	97	5	0.93	0.44
EAF020-2	Harris Lake	Augen gneiss	Kfs-Qz-Bt-Grt-Hb-Cpx	-31.309592	123.483091	1182 ± 4	81	4	0.86	0.46
EAF021	Harris Lake	Metagabbronorite	Pl-Cpx-Opx-Bt-Ilm-Hb	-31.317332	123.484967	1557 ± 5	92	3	0.62	0.54
						1304 ± 4	86	7	0.96	0.45
EAF029	Buningonia Soak	Augen gneiss	Qz-Kfs-Bt-Pl-Grt	-31.354887	123.433094	1158 ± 4	74	4	0.82	0.48
EAF039B	Ponton Creek	Biotite schist	Qz-Kfs-Pl-Bt-Grt-Ilm	-30.911102	123.644351	1169 ± 5	89	5	0.45	0.77
EAF041	Ponton Creek	Migmatitic gneiss	Qz-Pl-Bt-Grt-Ilm-Tt	-30.911607	123.645413	1233 ± 6	100	4	2.06	0.10
EAF042	Ponton Creek	Metagranodiorite	Qz-Kfs-Pl-Bt-Grt-Hb-Ilm	-30.913386	123.643762	1281 ± 4	95	10	1.40	0.18
						1281 ± 4	77	6	1.92	0.09

'control' samples where no excess argon was suspected (biotite $^{40}Ar/^{39}Ar$ plateau ages fit with the thermal history established from other minerals).

Petrographically, samples appear fresh and unaltered, and biotite is in equilibrium with the high-grade mineral assemblage (Figure 5.3). The only exception is sample EAF21, where some biotite is rimmed by amphibole.

5.3.2 Biotite compositions and quantifying alteration

Backscatter electron (BSE) imaging was used to identify any biotite alteration not visible by optical microscopy, and representative biotite grains were analysed by wavelength dispersive spectroscopy at the Centre for Microscopy, Characterisation and Analysis (University of Western Australia, Perth, Australia). Compositional analyses of biotite were acquired on a JEOL JXA8530F electron microprobe equipped with 5 tuneable wavelength dispersive spectrometers, and with operating conditions of a 40° take-off angle, and beam energy of 15 keV. The beam current was 15 nA, and the beam diameter was defocussed to 5 μm.

Elements were acquired using analyzing crystals LiF for Ti kα, Fe kα and Mn kα; PETJ for Ca kα and K kα; PETH for Cl kα and Rb lα; TAP for Mg kα, Si kα, Al kα and Na kα; and LDE1 for F kα. The standards were Fluorite for F kα, Magnetite for Fe kα, Periclase for Mg kα, Rutile for Ti kα, Tugtupite for Cl kα, Wollastonite for Ca kα, Si kα, Rb-Zn Glass for Rb lα, Jadeite for Na kα, Mn for Mn kα, Orthoclase for K kα, and Kakanui Pyrope for Al kα. Counting time was 10 seconds for Si kα and Al kα; 20 seconds for Na kα, Mg kα, Ti kα, Ca kα, K kα, Fe kα, Mn kα, Cl kα and Rb lα; and 60 seconds for F kα.

The intensity data was corrected for Time Dependent Intensity (TDI) loss (or gain) using a self-calibrated correction for Si kα, K kα, Fe kα, F kα and Rb lα. MAN background intensity data was used throughout (Donovan and Tingle, 1996). Interference corrections were applied to Fe for interference by Mn (Donovan et al., 1993).

Detection limits were 0.007 wt% for Cl kα, 0.011 wt% for Ca kα, 0.013 wt% for Al kα, 0.038 wt% for Mn kα, and 0.063 wt% for Ti kα. Analytical sensitivity (at the 99% confidence level) ranged from 0.425 % relative for Si kα, to 0.787 % relative for K kα,

to 2.555 % relative for F kα, to 20.111 % relative for Ca kα, to 27.058 % relative for Rb lα.

Oxygen was calculated by cation stoichiometry and included in the matrix correction. Oxygen equivalent from halogens (F/Cl/Br/I) was not subtracted in the matrix correction. Element H was calculated by stoichiometry to oxygen, at 0.167 atoms H relative to 1.0 atom of O. The ZAF algorithm utilised was the Armstrong-Love/Scott correction (Armstrong, 1988).

Biotite compositions were calculated on a 20(O) + 4(OH, F, Cl) basis, assuming all Fe is present as Fe^{2+}. The relative areas of altered and unaltered biotite were quantified using the program ImageJ (Schneider et al., 2012) to threshold the BSE images. Total loss of K as a result of alteration was calculated from the measured K contents of altered and unaltered biotite (Table 5.2).

5.3.3 Rb/Sr thermochronology

Rock samples were coarsely crushed between tungsten carbide plates. The 250 – 500 μm fraction was separated by sieving, and washed in deionised water and acetone. Biotite grains were separated by picking under a microscope, then ground under ethanol in an agate mortar, and sieved with 150 μm mesh to remove high-Sr inclusions such as apatite and feldspar. A portion of the coarsely crushed material was powdered in a tungsten carbide disc mill to produce the whole-rock (WR) powder.

Biotite (0.01 – 0.015 g; > c. 100 crystals, depending on grainsize) and WR (0.1 g) samples were weighed into Teflon PFA vials and spiked with a mixed ^{87}Rb-^{84}Sr spike. Samples were dissolved in 1 ml HF-HNO_3 on a hotplate for 4 days, then loaded on AG50W-X8 cation exchange resin (Bio-Rad) in 5 cm columns using 2.5 M HCl for the initial separation of Rb and Sr.

The Rb fraction was dissolved in 1.5 ml HF to precipitate SrF_2 and centrifuged at 5000 rpm for 10 minutes. Rubidium was then separated by carefully pipetting the solution from the top, leaving the solid SrF2 at the bottom of the vial. Rubidium was further purified from any remaining Sr by ion chromatography performed with 0.5

ml Teflon columns filled with Sr resin (100-150 μm particle size; TRISKEM International).

The Sr fraction obtained from the AG50W-X8 cation exchange resin was also purified from Rb by ion chromatography using 0.5 ml Teflon columns filled with Sr resin. Strontium was then treated in a mixture of 50 μl 30 % H_2O_2 and 200 μl 7 M HNO_3 in a closed beaker at 80°C to oxidise any residual resin.

Rubidium was dissolved in 1 M HNO_3 and analysed on a Neptune Plus™ High Resolution Multicollector ICP-MS (Thermo Fisher Scientific, Bremen, Germany) at the University of Bern, Switzerland. Data was acquired at a typical ^{87}Rb signal intensity of 1V. Instrumental mass fractionation was monitored by standard-bracketing using a common Rb solution, and then applying a natural $^{87}Rb/^{85}Rb$ ratio of 0.385617 and an exponential mass fractionation correction.

Strontium was dissolved in 2 μl 6.4 M HCl, loaded on single Re filaments with 1.5 μl of a Ta_2O_5-activator, and analysed on a Triton Plus™ Multicollector Thermal Ionization Mass Spectrometer (Thermo Fisher Scientific, Bremen, Germany). Measurement commenced when the signal intensity on mass 88 reached 3 V. A total of 150 cycles were measured, each with 8.4 seconds' integration time. A Rb interference correction was applied using the $^{87}Rb/^{85}Rb$ ratio determined with the MC-ICP-MS and an exponential mass fractionation correction. The 2σ analytical uncertainty for all $^{87}Sr/^{86}Sr$ measurements was determined by repeated analysis of the standard SRM987, and is 0.710348 ± 0.000024. This value is within the range of the certified value of 0.710140 ± 0.000260 for this standard (Moore et al., 1973). Accordingly, no offset correction was performed for any sample.

Ages and uncertainties on the two-point isochrons were calculated using the Rb/Sr decay constant recommended by Villa et al. (2015). This decay constant produces Rb/Sr ages that are ~1.6% older than Rb/Sr ages calculated using the decay constant recommended by Steiger and Jäger (1977), which was widely used in the last 40 years.

Table 5.2 Effect of alteration and summary of Rb/Sr and $^{40}Ar/^{39}Ar$ age data. Abbreviations: Hb, hornblende; alt., alteration.

Sample	Locality	Lithology	Alteration	% K loss	Rb/Sr age (Ma)	Significance of Rb/Sr age	$^{40}Ar/^{39}Ar$ age (Ma)	Significance of $^{40}Ar/^{39}Ar$ ages
EAF012	SW of Uraryie Rock	Paragneiss	None		1134 ± 6	Cooling	1212 ± 4	Excess Ar
EAF017	SW of Uraryie Rock	Gneiss	Minor	0.5	1135 ± 5	Cooling	1243 ± 5	Excess Ar
							1372 ± 4	Excess Ar
							1333 ± 5	Excess Ar
EAF018	Harris Lake	Metagranite	Minor	0.6	1136 ± 21	Cooling	1167 ± 4	Excess Ar
EAF020-2	Harris Lake	Augen gneiss	None		1134 ± 7	Cooling	1182 ± 4	Excess Ar
EAF021	Harris Lake	Metagabbronorite	None		1163 ± 9	Sr gain from Hb	1557 ± 5	Excess Ar + mixing with Hb
							1304 ± 4	Excess Ar + mixing with Hb
EAF029	Buningonia Soak	Augen gneiss	None		1107 ± 14	Cooling or minor Sr loss	1158 ± 4	Excess Ar + late minor Ar loss
EAF039B	Ponton Creek	Biotite schist	Minor	0.2	1133 ± 7	Cooling	1169 ± 5	Excess Ar
EAF041	Ponton Creek	Migmatitic gneiss	Significant	5	1145 ± 5	Rb loss during alt.	1233 ± 6	Excess Ar + K loss during alt.
EAF042	Ponton Creek	Metagranodiorite	None		1121 ± 11	Cooling	1281 ± 4	Excess Ar
							1281 ± 4	Excess Ar

5.4 Results

5.4.1 Biotite compositions and quantifying alteration

In eight samples, conventional petrographic microscopy shows that biotites are fresh and unaltered, and are in equilibrium with the high-grade mineral assemblages (Figure 5.3). The only exception is metagabbronorite EAF21, where some biotites are rimmed by amphibole. No chlorite was identified in any sample.

Despite petrographically unaltered appearances, BSE imaging of biotite shows minor alteration in four samples. Alteration is visible as very narrow (< 5 μm) darker zones around grain edges or along cleavage planes. Biotite in the remaining five samples appears homogenous and unaltered. BSE images of four samples are shown in Figure 5.3, and the remainder are in Appendix 5.1.

EMP analyses of representative unaltered and altered zones of biotite are in Table 5.3. Altered zones have lower oxide totals than unaltered zones, due both to the compositional changes associated with alteration, and due to the difficulty of analysing the uneven surfaces produced by alteration. Because of the low totals, these analyses are considered approximations, and are used only as evidence that altered zones have lost potassium relative to unaltered zones.

Unaltered biotites are mostly Fe-rich, with $X_{Mg} < 0.5$ in all pelitic and granitic lithologies; metagabbronorite EAF21 has biotite $X_{Mg} = 0.52$. The generally high Ti content of unaltered biotite is consistent with biotite equilibration at high temperatures, i.e. amphibolite- to granulite-facies (Patiño Douce, 1993).

Analyses of unaltered zones of biotite contain 9.62 – 9.95 wt% K_2O. Whilst all biotite alteration resulted in net K loss, the relative magnitude of alteration varied in each sample; altered zones of biotite contain 2.34 – 7.60 wt% K_2O (Table 5.3). The Rb content of unaltered biotite ranges from 0.0 – 0.24 wt% Rb_2O, and 0.0 – 0.14 in altered zones of biotite; however, the lower end of these ranges may reflect a Rb content below the analytical detection limit (c. 0.05 wt % Rb_2O) rather than the absence of Rb.

The relative content of K_2O in altered and unaltered biotite was used to approximate the total K loss in each biotite (Table 5.2). For three biotites with visible

alteration in BSE, the altered part of the grain constitutes < 3% of its area, corresponding with a total K loss of < 0.6%; biotite in sample EAF41 was subject to 5% K loss.

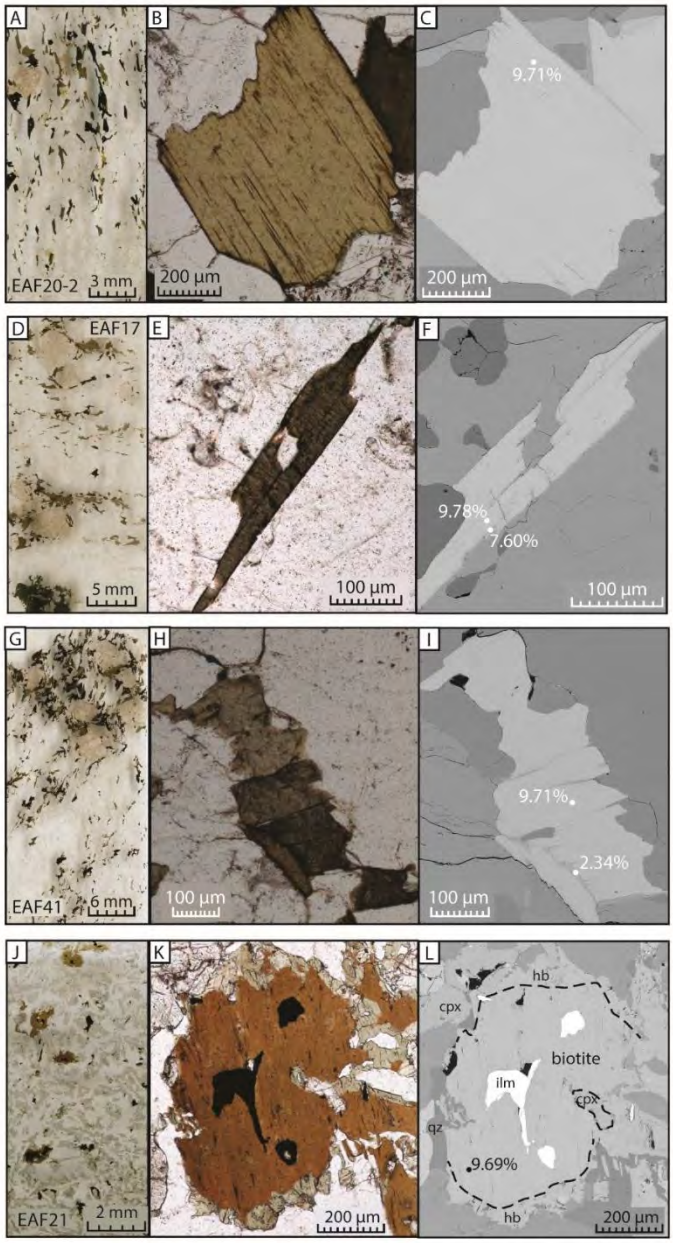

Figure 5.3 Plain polarised light (PPL) and backscatter electron (BSE) images of sample textures and representative biotites from four samples. (A – C) In sample EAF20-2, biotite is unaltered and is in equilibrium with the amphibolite-grade fabric. (D – F) Biotite in EAF17 is in equilibrium with the metamorphic assemblage, but slight alteration is visible in BSE imaging. (G – I) In sample EAF41, biotite is in equilibrium with the metamorphic assemblage, but alteration is visible in BSE imaging along grain boundaries. (J – L) Biotite in sample EAF21 is rimmed and partially replaced by hornblende.

Table 5.3 Representative biotite compositions from electron microprobe analysis.

	EAF12	EAF17		EAF18		EAF20-2	EAF21	EAF29	EAF39B		EAF41		EAF42
		unalt.	altered	unalt.	altered				unalt.	altered	unalt.	altered	
SiO_2	35.42	35.45	33.23	34.55	35.37	34.88	35.65	35.40	35.56	37.69	34.91	27.87	34.75
TiO_2	3.98	3.32	2.62	2.31	4.28	2.41	5.82	2.66	4.33	2.49	4.45	4.24	3.89
Al_2O_3	14.49	15.06	14.89	15.09	15.46	15.53	13.95	16.25	15.02	16.71	15.22	14.02	14.68
FeO	21.83	21.88	22.75	27.88	15.13	26.91	18.46	26.73	23.49	17.05	23.27	24.22	25.97
MnO	0.10	0.09	0.08	0.33	0.22	0.18	-	0.24	0.00	0.06	0.13	0.15	0.18
MgO	8.87	9.19	9.59	4.93	4.90	5.39	11.10	5.20	7.42	6.74	7.37	7.45	6.53
CaO	0.02	0.02	0.06	-	1.07	0.03	0.03	0.02	0.00	1.25	0.03	1.96	0.04
Na_2O	0.07	0.03	0.07	0.05	0.19	0.04	0.06	0.04	0.07	0.06	0.05	-	0.13
K_2O	9.87	9.78	7.60	9.67	5.89	9.71	9.69	9.62	9.95	6.71	9.71	2.34	9.67
Rb_2O	-	0.08	-	0.24	0.09	0.13	0.08	0.09	0.05	0.10	0.07	0.14	0.18
Cl	0.15	0.20	0.16	0.19	0.22	0.20	0.07	0.15	0.07	0.02	0.20	0.18	0.22
F	0.39	0.65	0.60	1.20	1.05	0.84	0.33	1.14	0.80	0.28	0.58	0.67	0.65
H_2O	3.62	3.51	3.38	3.16	3.04	3.35	3.74	3.29	3.49	3.66	3.52	3.00	3.47
O=F	- 0.20	- 0.32	- 0.29	- 0.55	- 0.49	- 0.40	- 0.16	- 0.51	- 0.35	- 0.12	- 0.29	- 0.32	- 0.32
Total	98.62	98.93	94.75	99.05	86.40	99.20	98.82	100.33	99.92	92.70	99.24	85.92	100.05
						Biotite formula based on 20 O + 4 (OH, F)							
Si	5.521	5.488	5.368	5.486	5.912	5.508	5.462	5.484	5.484	5.956	5.432	4.976	5.439
Al	2.479	2.512	2.632	2.514	2.088	2.492	2.520	2.516	2.516	2.044	2.568	2.949	2.561
T site	*8.00*	*8.00*	*8.00*	*8.00*	*8.00*	*8.00*	*7.99*	*8.00*	*8.00*	*8.00*	*8.00*	*7.93*	*8.00*
Al	0.183	0.237	0.203	0.311	0.958	0.398	0.000	0.452	0.213	1.069	0.223	0.000	0.148
Ti	0.467	0.387	0.318	0.276	0.538	0.286	0.671	0.309	0.503	0.296	0.521	0.569	0.458
Fe^{2+}	2.846	2.832	3.074	3.703	2.115	3.553	2.366	3.463	3.029	2.253	3.029	3.616	3.400
Mn	0.013	0.012	0.011	0.044	0.031	0.024	0.000	0.032	0.000	0.009	0.017	0.023	0.024
Mg	2.061	2.120	2.309	1.166	1.221	1.269	2.536	1.202	1.707	1.589	1.711	1.981	1.525
M site	*5.57*	*5.59*	*5.92*	*5.50*	*4.86*	*5.53*	*5.57*	*5.46*	*5.45*	*5.22*	*5.50*	*6.19*	*5.56*
Ca	0.004	0.003	0.011	0.000	0.192	0.004	0.004	0.004	0.000	0.211	0.005	0.375	0.007
Na	0.000	0.008	0.000	0.025	0.009	0.013	0.008	0.009	0.005	0.011	0.007	0.000	0.019
K	1.961	1.931	1.566	1.959	1.255	1.956	1.893	1.901	1.958	1.354	1.928	0.532	1.931
Rb	0.022	0.010	0.021	0.015	0.061	0.011	0.019	0.013	0.020	0.020	0.016	0.017	0.039
I site	*1.99*	*1.95*	*1.60*	*2.00*	*1.54*	*1.98*	*1.92*	*1.93*	*1.98*	*1.60*	*1.96*	*0.92*	*2.00*
Cl	0.040	0.052	0.045	0.050	0.063	0.053	0.019	0.039	0.018	0.005	0.054	0.054	0.059
F	0.193	0.320	0.308	0.602	0.553	0.418	0.159	0.559	0.392	0.141	0.288	0.378	0.323
OH	3.767	3.628	3.647	3.348	3.385	3.529	3.822	3.402	3.590	3.854	3.658	3.567	3.618
Anion	*4.00*	*4.00*	*4.00*	*4.00*	*4.00*	*4.00*	*4.00*	*4.00*	*4.00*	*4.00*	*4.00*	*4.00*	*4.00*
XMg	0.42	0.43	0.43	0.24	0.37	0.26	0.52	0.26	0.36	0.41	0.36	0.35	0.31

5.4.2 Rb/Sr thermochronology

The Rb/Sr data are summarised in Table 5.4. Rb/Sr ages are calculated from two-point biotite-whole rock isochrons, and are depicted in Figure 5.4, in comparison with U/Pb and $^{40}Ar/^{39}Ar$ geochronology at these sites. The nine Rb/Sr biotite ages range from 1107 – 1163 Ma; five of these samples produced statistically indistinguishable Rb/Sr biotite ages of 1133 – 1136 Ma (Table 5.4).

Comment on two-point isochrons

Any isochron used for the purpose of geochronology makes the assumption that all points along the line are in equilibrium with each other. When isochrons are based on several data points, the assumption of equilibrium is statistically tested by calculating a MSWD, which is a measure of the goodness of fit of the isochron line to the data points. As any two points make a line, this test is not available for two-point isochrons. However, provided the equilibrium assumption is valid, then the isochron derived from two data points is meaningful. For example, Walker et al. (2016) showed that using multi-point isochrons made no changes to the results already derived from two-point isochrons on different samples.

The 11 new Rb/Sr ages we report are calculated from two-point biotite-whole rock isochrons. Petrographically, the biotites in these samples are in equilibrium with the upper amphibolite- to granulite-facies metamorphic assemblages, and samples are fresh and unaltered, unless specified otherwise (Figure 5.3). Because the slope of the isochron is largely controlled by the high $^{87}Sr/^{86}Sr$ ratios of biotite, the age is insensitive to uncertainty in the Sr_0 or Sr* content of the whole rock (e.g. Tohver et al., 2005). For example, for sample EAF17, a 10% increase in Sr_0 (from 0.7242 to 0.7966) results in a 0.7% decrease in the age (from 1135 Ma to 1126 Ma). In addition, five of the nine ages from the Biranup Zone are identical, within error (Table 5.4). We consider it is extremely unlikely that samples from a wide geographical area could produce such consistent results if equilibrium had not been attained, or if the samples were compromised by alteration.

Table 5.4 Rb/Sr analytical results and ages of 2-point biotite-WR isochrons. Abbreviations: WR, whole rock; SE, standard error.

Sample	Locality	Lithology		Rb (ppm)	Sr (ppm)	$^{87}Rb/^{86}Sr$	2 SE	$^{87}Sr/^{86}Sr$	2 SE	$^{87}Sr/^{86}Sr$ initial	Age (Ma)	2σ (Ma)
EAF12	SW of Uraryie Rock	Paragneiss	Biotite	430.7	4.691	454.4	2.4	7.971112	0.000012	0.7162	1134	6
			WR	162.5	230.6	2.047	0.012	0.748890	0.000010			
EAF17	SW of Uraryie Rock	Gneiss	Biotite	472.8	4.423	599.8	2.8	10.307848	0.000015	0.7242	1135	5
			WR	187.0	372.7	1.458	0.016	0.747479	0.000008			
EAF18	Harris Lake	Metagranite	Biotite	1006	11.93	397.6	7.4	7.155021	0.000007	0.7955	1136	21
			WR	401.9	134.1	8.865	0.095	0.9373	0.000010			
EAF20-2	Harris Lake	Augen gneiss	Biotite	663.2	3.829	2320	15	37.8159	0.0010	0.7605	1134	7
			WR	264.9	109.0	7.14	0.10	0.874631	0.000009			
EAF21	Harris Lake	Metagabbronorite	Biotite	331.5	3.085	619.8	4.6	10.862644	0.000023	0.7071	1163	9
			WR	26.66	157.6	0.4898	0.0047	0.715155	0.000009			
EAF29	Buningonia Soak	Augen gneiss	Biotite	812.3	8.537	477.3	5.8	8.209698	0.000010	0.7688	1107	14
			WR	358.5	177.9	5.917	0.091	0.861045	0.000010			
EAF39B	Ponton Creek	Biotite schist	Biotite	564.3	4.795	729.4	4.4	12.380071	0.000026	0.7414	1133	7
			WR	223.9	154.9	4.224	0.019	0.808831	0.000035			
EAF41	Ponton Creek	Migmatitic gneiss	Biotite	521.2	3.852	1025.6	4.8	17.270955	0.000054	0.7374	1145	5
			WR	233.0	131.4	5.186	0.043	0.821045	0.000009			
EAF42	Ponton Creek	Metagranodiorite	Biotite	542.8	6.195	417.9	3.9	7.336799	0.000010	0.7397	1121	11
			WR	247.0	167.0	4.246	0.063	0.806712	0.000009			

5.5 The interpretation of Rb/Sr and $^{40}Ar/^{39}Ar$ ages

The new Rb/Sr data were collected to test for the presence of cryptic excess argon in nine biotite samples. Using Rb/Sr to test the validity of $^{40}Ar/^{39}Ar$ ages requires that the Rb/Sr chronometer records a cooling age, i.e. the age at which the biotite cools below the closure temperature for Sr diffusion. This also assumes that the diffusive loss of Sr and Ar is minimal below the closure temperature, i.e. that biotite is a closed system (in addition to the whole-rock, in the case of Rb/Sr).

However, Rb/Sr and $^{40}Ar/^{39}Ar$ biotite ages may reflect a combination of several processes that affect the distribution of Rb, Sr, K and Ar, including: the diffusion of Sr and Ar above their closure temperatures in biotite; the timing of biotite growth or recrystallisation relative to the closure temperature; K and Rb loss during alteration; or the incorporation of excess argon. These processes are discussed in the context of assumptions about the open or closed system behaviour of a thermochronometer.

5.5.1 Thermally activated diffusion of Sr and Ar in metamorphic rocks

The closure temperature of a chronometer is the temperature at which the mobile radiogenic daughter product becomes fixed, and is no longer able to diffuse in or out of the mineral (McDougall and Harrison, 1988). Above the closure temperature, open-system behaviour is assumed; i.e. the rate of diffusive loss from the mineral is faster than the rate of radioactive decay, and there is no excess retention of the radiogenic daughter product. Below the closure temperature, closed-system behaviour is assumed: the loss of the radiogenic daughter product is inhibited.

Therefore, a mineral that crystallises above its closure temperature and then experiences monotonic cooling is expected to date the time at which it cools below its closure temperature, whereas a mineral that crystallises or recrystallises below its closure temperature will record a growth age. For any individual grain, the closure temperature may vary within a mineral-specific range, depending on a number of variables such as grainsize, cooling rate, and composition (Dodson, 1973).

The range of possible closure temperatures for Ar diffusion in biotite is relatively well established. Laboratory diffusion experiments yield closure temperatures of c.

310 ± 50 °C for a cooling rate of 10 °C/Ma, corresponding to a typical activation energy (E_a) = 47 ± 2 kcal/mol and diffusivity (D_0) = 0.077 $^{+0.21}/_{-0.06}$ cm^2/s for a biotite with X_{annite} ~ 0.5 (Harrison et al., 1985; Grove and Harrison, 1996). Field calibrations based on borehole temperature measurements and metamorphic mineral isograds yield a wider range of closure temperatures (c. 300 °C, Purdy and Jäger, 1976; > 400 °C, Verschure et al., 1980; > 400 °C, Del Moro et al., 1982).

The only published laboratory diffusion data for Sr in biotite are preliminary results measured between 800 – 900 °C (Giletti, 1991), which yield a closure temperature of c. 200 °C for a cooling rate of 10 °C/Ma (Jenkin, 1997). However, this closure temperature is significantly lower than empirically-determined values of c. 320 – 435 °C, based on borehole temperature measurements, metamorphic mineral isograds, and interpolation between other thermochronometers (Purdy and Jäger, 1976; Verschure et al., 1980; Del Moro et al., 1982; Willigers et al., 2004). To model Sr diffusion in biotite with a more realistic closure temperature of c. 350 °C, Jenkin (1997) uses E_a = 25 kcal/mol (from Giletti, 1991) and $D_0 = 2 \times 10^{-9}$ cm^2/s (150x slower than Giletti, 1991). These parameters suggest the diffusivity of Sr is significantly slower than Ar in biotite, as might be expected for the diffusion of a cation compared with a noble gas; however, the activation energy for Sr diffusion measured by Giletti (1991) is significantly lower than that of Ar.

Although the range of possible closure temperatures for Sr and Ar diffusion are similar, insufficient empirical evidence is available to determine whether Sr or Ar diffusive closure normally occurs at a higher temperature. Early studies comparing biotite Rb/Sr and K/Ar ages in the thermal halo around igneous intrusions suggested a slightly higher closure temperature for Sr than Ar (Hart, 1964; Hanson and Gast, 1967). However, other studies comparing Rb/Sr and K/Ar ages do not provide conclusive evidence; in some samples, the Rb/Sr age is older, and in others, it is younger (e.g. Verschure et al., 1980; Del Moro et al., 1982). This remains true even if mineral ages are recalculated using the most recent recommended decay constants (Renne et al., 2011; Villa et al., 2015). In addition, the accuracy of these K/Ar ages is uncertain; due to the inability to recognise minor radiogenic Ar loss, K/Ar ages are often slightly younger than $^{40}Ar/^{39}Ar$ step-heating plateau ages.

More recent empirical evidence from biotite is limited, as very few studies report both Rb/Sr and $^{40}Ar/^{39}Ar$ ages from the same samples, except to demonstrate that one isotope system has been disturbed and does not yield geologically meaningful ages (e.g. Ruffet et al., 1997; Willigers et al., 2004; Challandes et al., 2008). Regional geochronology compilations including Rb/Sr, K/Ar and $^{40}Ar/^{39}Ar$ biotite ages also do not systematically yield older ages for one isotope system, although these comparisons are further complicated by the effect of composition, lithology or grainsize on closure temperature, which may vary between samples (e.g. Tohver et al., 2006; Luth and Willingshofer, 2008)

In summary, the available data suggest that Sr and Ar diffusion in biotite have similar closure temperatures within the range c. 300 – 400 °C, and are probably within c. 50 °C in most cases due to the lack of a systematic sequence of ages from the two chronometers. Therefore, a sample that crystallised above its closure temperature and then experienced monotonic cooling should yield similar Rb/Sr and $^{40}Ar/^{39}Ar$ cooling ages, with a difference proportional to the precise difference in closure temperatures in that sample, as well as the cooling rate.

In contrast, a mineral that crystallises or recrystallises below the closure temperature (e.g. deformation and fluid flow may assist dissolution and precipitation processes) will record a growth age, or a mixed age if only partially recrystallised (Gray and Foster, 2004; Villa, 2016). For a biotite that crystallises at a low temperature, both the Rb/Sr and $^{40}Ar/^{39}Ar$ chronometers will record the same growth age (e.g. Kirschner et al., 2003).

5.5.2 Anomalous closed or open system behaviour – inherited or excess daughter product, and alteration

Interpreting mineral ages as cooling or growth ages assumes that thermally-activated volume diffusion is efficient at removing the radiogenic daughter product from the mineral above the closure temperature (open system behaviour), and that diffusive loss is inhibited below the closure temperature (closed system behaviour). However, if either of these assumptions is violated, the apparent age of the mineral will not date cooling or growth.

Diffusion rates are generally assumed to be solely dependent on the temperature of the system. However, closed-system behaviour above the closure temperature, typically due to fluid-absent metamorphism, may lead to the accumulation of inherited excess radiogenic daughter product, therefore yielding mineral ages older than the age of cooling through the closure temperature. For example, the Western Gneiss Region of Norway preserves examples of dry granulite rocks that were subjected to eclogitic conditions without phase re-equilibration (Glodny et al., 2008b; McDonald et al., 2016). Glodny et al. (2008a, 2008b) show that Sr diffusion in both muscovite and biotite was slow or absent in these dry granulite relics, despite reaching high temperatures (> 700 °C) during eclogitisation and amphibolite facies retrogression. Similarly, McDonald et al. (2016) report biotite $^{40}Ar/^{39}Ar$ age populations that span the entire metamorphic cycle, despite long, 10 – 15 Ma intervals spent at amphibolite facies conditions during retrogression. For these rocks, the resetting of the K/Ar and Rb/Sr chronometers is controlled by mica recrystallisation rather than by diffusive loss of Ar or Sr, despite long-term heating above the closure temperature.

Rather than closed-system behaviour inhibiting the loss of the radiogenic daughter product, in some cases open-system behaviour above the closure temperature may lead to a mineral incorporating an excess of the radiogenic daughter product from an external source. Typically, this leads to a decoupling of the two decay systems, with apparently old ages affecting only the K/Ar system and not Rb/Sr. This is primarily because the diffusion of Sr^{2+} (a cation) and Ar (a noble gas) are inherently different; because argon is non-reactive, its incorporation into crustal minerals is through solubility processes rather than chemical substitution (Rutter, 1983). The incorporation of excess argon, e.g. due to a high partial pressure of argon in the rock (rather than simply inherited argon retained in a dry system), will yield a significantly older $^{40}Ar/^{39}Ar$ apparent age, but the Rb/Sr age will be unaffected (e.g. Ruffet et al., 1997; Batt et al., 2000; Willigers et al., 2004).

Below the closure temperature, open-system behaviour is typically a result of biotite alteration or fluid-assisted recrystallisation, and results in mineral ages that are younger than the cooling or growth age. Biotite alteration will affect the Rb/Sr

and $^{40}Ar/^{39}Ar$ chronometers differently. Potassium is a major constituent of biotite, and is bound as K^+ at the interlayer I-site, along with Na and minor Ca; Rb^+ also substitutes for K^+. Because the I-site does not normally contain vacancies, an unaltered biotite should contain c. 10 wt% K_2O (Cesare et al., 2008).

An early indicator of biotite alteration is the loss of K at the I-site, accompanied by processes such as radiogenic ^{40}Ar loss, $^{39}Ar_K$ recoil into K-depleted biotite, and $^{39}Ar_K$ recoil out of the altered biotite (Ferrow et al., 1999; Smith et al., 2008). The effect of these processes on the $^{40}Ar/^{39}Ar$ age will depend on the relative proportions and timing of K and Ar loss. Both increases and decreases in ages have been reported in altered samples; however, beyond c. 20% K loss, apparent ages sharply decrease due to massive Ar loss (Mitchell and Taka, 1984; Roberts et al., 2001; Smith et al., 2008).

Like the K/Ar chronometer, the effect of Rb and Sr loss during biotite alteration will depend on the relative proportions and timing of Rb and Sr loss. Jeong et al. (2006) report an increase in Rb/Sr ages as a result of alteration, and suggest that K is preferentially removed (i.e. a biotite with 3% Rb loss will have >3% K loss), such that the effect on $^{40}Ar/^{39}Ar$ ages will be greater than on Rb/Sr ages.

We calculate an upper limit for potential increases in $^{40}Ar/^{39}Ar$ (and Rb/Sr) ages due to K and Rb loss during alteration by assuming no Ar or Sr loss (using Equation 2.8 in McDougall and Harrison, 1988; Table 5.2). 3% K loss produces a 2.3% overestimation in the $^{40}Ar/^{39}Ar$ age. For a true age of 1135 Ma, this corresponds to an apparent $^{40}Ar/^{39}Ar$ age of 1161 Ma, or an age overestimation of 26 Ma. The apparent age obtained from such an altered biotite does not correspond to any event of geological significance. For a biotite with only 0.5% K loss, however, the age will be overestimated by 0.37 % (i.e. 1139 Ma rather than 1135 Ma), which is comparable to the 2σ analytical errors on $^{40}Ar/^{39}Ar$ and Rb/Sr ages and is considered a reasonable approximation of the true cooling age.

Because the amount and timing of alteration may vary between individual biotite grains in a sample, $^{40}Ar/^{39}Ar$ analyses of several altered biotite grains in the same sample may yield a range of apparent ages with little to no reproducibility (e.g. Roberts et al., 2001). Rb/Sr dating of altered samples may yield more reproducible,

but still meaningless, ages, because multiple biotite grains are dissolved and analysed in each aliquot, which will average the effect of heterogenous alteration throughout the sample. In addition, a two-point biotite-whole rock Rb/Sr age may be immune to the alteration of metamorphic phases besides biotite, although this requires that the whole-rock remains a closed system. For example, Challandes et al. (2008) report late fluid circulation in a shear zone that reset the Rb/Sr and not the $^{40}Ar/^{39}Ar$ chronometer. This was interpreted as a product of open-system behaviour that affected the composition of the whole-rock system, although biotite remained unaltered. Therefore, K/Ar ages were preserved, but Rb/Sr ages decreased, and the assumption of equilibrium between the biotite and whole-rock (necessary for obtaining meaningful Rb/Sr ages) was violated.

5.5.3 Geological significance of Biranup Zone ages

Excess argon was previously suspected in several Biranup Zone samples because $^{40}Ar/^{39}Ar$ biotite ages were older than $^{40}Ar/^{39}Ar$ hornblende ages or U/Pb zircon ages, or because the $^{40}Ar/^{39}Ar$ biotite ages were not reproducible (Table 5.1).

In the Biranup Zone, the new Rb/Sr biotite ages are significantly younger than the $^{40}Ar/^{39}Ar$ biotite ages from these samples (Figure 5.4). This is true both for samples where excess argon was suspected, as well as the three 'control' samples that agreed with previously established thermochronological evidence. The $^{40}Ar/^{39}Ar$ biotite ages vary between 1158 – 1557 Ma (Table 5.2). In contrast, the Rb/Sr biotite ages range from 1107 – 1163 Ma, and are at least 31 Ma younger than the $^{40}Ar/^{39}Ar$ ages in the same samples. Several explanations are considered for the Rb/Sr and $^{40}Ar/^{39}Ar$ ages: (1) biotite (re)crystallisation below the closure temperature; (2) monotonic cooling through the Sr and Ar closure temperatures in biotite; (3) K loss during alteration resulting in older $^{40}Ar/^{39}Ar$ ages; (4) fluid circulation resulting in younger Rb/Sr ages; (5) the incorporation of excess argon in biotite.

Biotite crystallisation or recrystallisation below the closure temperature is considered unlikely, as sample petrography and the high Ti and F content of biotite suggest equilibration with the high-grade regional metamorphism, rather than biotite growth at low temperatures (Figure 5.3). In addition, low-temperature mineral

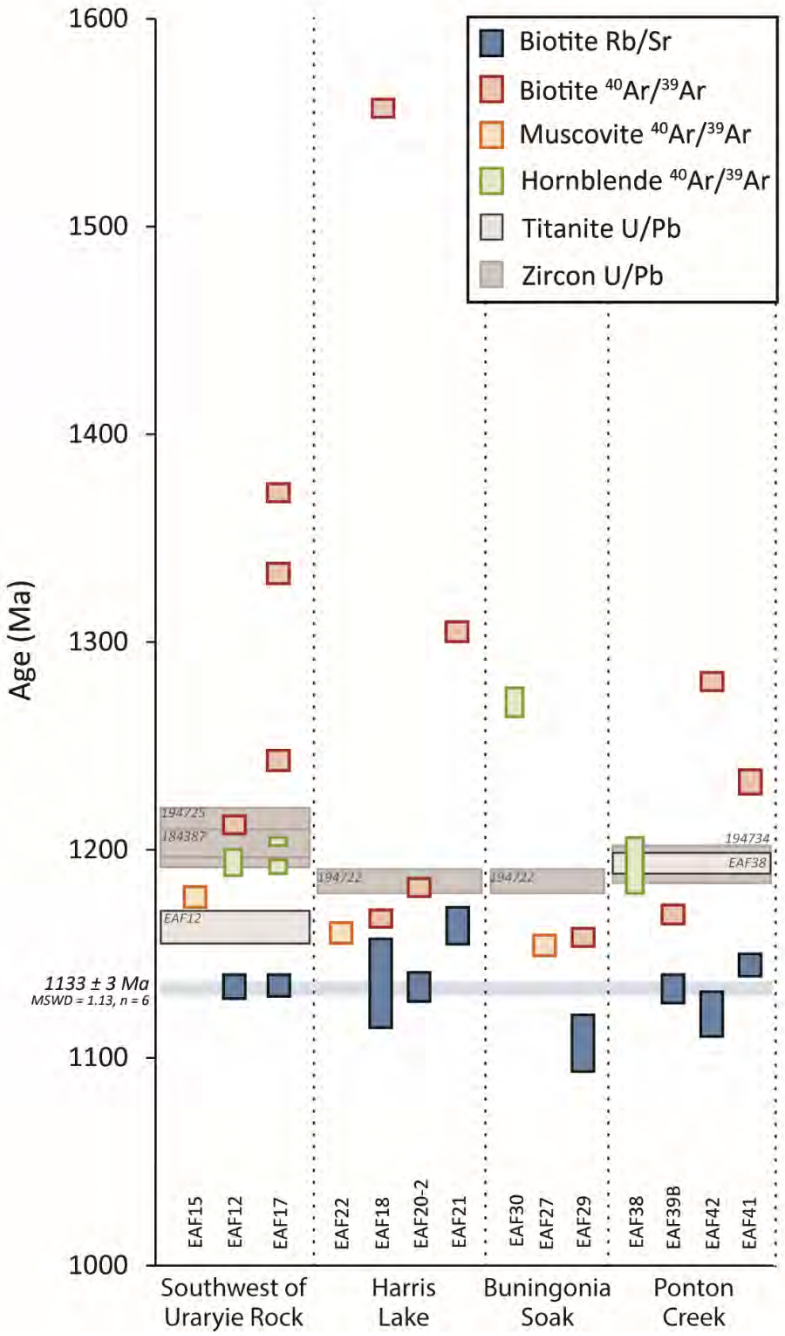

Figure 5.4 Summary of Rb/Sr and $^{40}Ar/^{39}Ar$ geochronology from sample sites in the east Albany-Fraser Orogen. Six of the Rb/Sr ages date cooling at a weighted mean age of 1133 ± 3 Ma (light blue horizontal bar; two older and one younger sample are discussed in the text). In contrast, the $^{40}Ar/^{39}Ar$ ages of hornblende, biotite and muscovite are affected by excess argon and are not geologically significant. The grey bars show the closest U/Pb titanite and zircon ages of metamorphism and/or magmatism; data are labelled with sample number, and are taken from Geological Survey of Western Australia (2016) and Chapter 6.

growth is expected to produce similar Rb/Sr and $^{40}Ar/^{39}Ar$ biotite ages, but this is not observed.

Six of the nine Rb/Sr biotite ages are similar, with a weighted mean age of 1133 ± 3 Ma (MSWD = 1.13) across 50 km and three sample localities. This suggests that the c. 1133 Ma Rb/Sr ages are geologically significant, and are interpreted to record cooling through the Sr closure temperature in biotite. Although separated by shear zones, these localities also shared a common high-grade geological history, recorded by similar c. 1190 Ma U/Pb zircon and titanite ages for amphibolite facies metamorphism (Figure 5.4). An alternative interpretation in which the Rb/Sr ages date fluid circulation rather than cooling (due to perturbation of the Rb/Sr system in the whole-rock; e.g. Challandes et al., 2008) is considered unlikely because of the preservation of pristine, unaltered, amphibolite-facies assemblages with no petrographic evidence of late deformation or fluid infiltration on the retrograde path (Figure 5.3a, d).

The $^{40}Ar/^{39}Ar$ ages are unlikely to date cooling, based on comparison with other thermochronological evidence. Scibiorski et al. (2016) interpret the youngest $^{40}Ar/^{39}Ar$ ages of 1158 – 1169 Ma as dating cooling through the closure temperature, as these are the only $^{40}Ar/^{39}Ar$ data younger than widespread c. 1190 Ma U/Pb zircon ages of amphibolite facies metamorphism (> 700 °C; Geological Survey of Western Australia, 2016; Kirkland et al., 2016). However, a new U/Pb titanite age from sample EAF12 dates cooling through c. 650 °C at 1163 ± 8 Ma (Chapter 6; Figure 5.4). Although this age does not necessarily contradict the 1158 – 1169 Ma $^{40}Ar/^{39}Ar$ ages (as they are within error), near-instantaneous cooling from 650 °C would be required to reach the Ar closure temperature within this short space of time.

In addition, as discussed above, the available data suggest that Sr and Ar diffusion in biotite have similar closure temperatures within the range c. 300 – 400 °C, probably within c. 50 °C. Assuming a 50 °C difference in Rb and Sr closure temperatures, together with the minimum 31 Ma gap between Rb/Sr and $^{40}Ar/^{39}Ar$ ages from the same samples, a maximum cooling rate of ~1.6 °C/Ma can be calculated between the Sr and Ar closure temperatures. This would, unrealistically, require that

slow 1.6 °C/Ma cooling rates developed (and were then stabilised for at least 31 Ma) after extremely fast cooling from high-grade metamorphism; and with no effect on biotite ages despite subsequent slow cooling through the partial retention zone for argon in biotite (e.g. Little et al., 1999; Dunlap, 2000).

Finally, we note that all localities with multiple samples produced a wide range of biotite $^{40}Ar/^{39}Ar$ ages, despite widely consistent Rb/Sr ages (Figure 5.4). For the youngest $^{40}Ar/^{39}Ar$ ages to be interpreted as cooling ages, a plausible explanation is required for why some samples from the same localities contain excess argon (i.e. $^{40}Ar/^{39}Ar$ ages are older than the U/Pb zircon and titanite constraints on metamorphism), and others do not (i.e. $^{40}Ar/^{39}Ar$ ages are younger than the U/Pb in zircon and titanite). Therefore, the $^{40}Ar/^{39}Ar$ ages are interpreted not to date cooling.

K (and/or Rb) loss during biotite alteration also does not sufficiently explain the difference in Rb/Sr and $^{40}Ar/^{39}Ar$ ages. BSE imaging shows that biotite in four samples is unaltered, minor alteration is visible in three samples, and two samples are more substantially altered (Figure 5.3; Appendix 5.1).

For the seven unaltered (EAF12, EAF20-2, EAF29 and EAF42) or slightly altered (EAF17, EAF18, and EAF39B) samples, the old $^{40}Ar/^{39}Ar$ apparent ages cannot be explained by K loss during alteration. In the three slightly altered samples, alteration is visible as very narrow (<5 μm) rims around grain edges (Figure 5.3f). Quantification of K loss based on EMP biotite compositions and image analysis shows that despite the minor alteration, these biotites are < 0.6% K deficient (Table 5.2). This is insufficient to explain the old $^{40}Ar/^{39}Ar$ ages as a product of K deficiency in altered biotites; for example, to produce an apparent $^{40}Ar/^{39}Ar$ age of 1243 Ma, 108 Ma older than the Rb/Sr age (as with EAF17), requires 11.7% K loss. Therefore, the only remaining explanation for the old $^{40}Ar/^{39}Ar$ ages from these unaltered and slightly altered biotites is the incorporation of excess argon.

Six of the Rb/Sr biotite ages from these unaltered and slightly altered samples are similar, with a weighted mean age of 1133 ± 3 Ma (MSWD = 1.13) across 50 km and three sample localities. As previously stated, this suggests that despite some minor alteration, the Rb/Sr ages are geologically significant. The negligible effect of the

alteration on Rb/Sr ages is consistent with the preferential loss of K rather than Rb from biotite during alteration (Jeong et al., 2006). The 1107 ± 14 Ma Rb/Sr biotite age for sample EAF29 is significantly younger than this main population; as biotite in this sample is unaltered, it is possible that this age dates a younger cooling history for the most southerly sample. However, this sample also produced the youngest $^{40}Ar/^{39}Ar$ age (1158 ± 4 Ma), and the $^{40}Ar/^{39}Ar$ age spectrum suggests minor diffusive Ar loss from biotite, possibly driven by thermal or hydrothermal activity (Figure 5.1g). If Ar loss was accompanied by Sr loss, this could explain the younger Rb/Sr age of this outlier.

Sample EAF41 is significantly altered, with an estimated total 5 % K loss (Table 5.2). As is expected for biotite affected by Rb loss during alteration, the Rb/Sr age of EAF41 is older than other Rb/Sr ages at the same site (Table 5.2). However, producing the 1233 ± 6 Ma $^{40}Ar/^{39}Ar$ biotite age requires c. 10% K loss, and more than 10% if K loss was accompanied by any Ar loss during alteration. Therefore, although Rb loss during alteration may be sufficient to explain the slightly older Rb/Sr age, a significant contribution of excess argon is still required to explain the $^{40}Ar/^{39}Ar$ age.

Although biotite in sample EAF21 is homogenous in BSE imaging and EMP analysis shows no measurable K loss (Table 5.3), it is rimmed by symplectitic hornblende and quartz (Figure 5.3k, l). Biotite in this sample was not at equilibrium, but undergoing breakdown and partial replacement by hornblende, an upper amphibolite facies reaction (Gardien et al., 2000). Despite careful preparation of biotite separates, due to the difficulty of separating intergrown hornblende and biotite, some mixing of hornblende and biotite may have occurred. The presence of hornblende in the older of the two biotite grains selected for $^{40}Ar/^{39}Ar$ analysis is supported by the low K/Ca ratios in this sample (Figure 5.1f).

Mixing of hornblende and biotite will significantly increase both the apparent Rb/Sr and $^{40}Ar/^{39}Ar$ ages. Rb/Sr ages increase because hornblende typically incorporates very little Rb but can be Sr-rich (> 100 ppm; in contrast, biotite typically has < 10 ppm; Griffin and Murthy, 1969); $^{40}Ar/^{39}Ar$ ages increase because Ar diffusion in hornblende has a higher closure temperature than in biotite (c. 550 °C; Harrison,

1981). Mixing of biotite and hornblende may explain why the Rb/Sr age for this sample is c. 28 Ma older than other Rb/Sr ages at this site. However, even a mixed $^{40}Ar/^{39}Ar$ age should still fall in between the endmember ages of the two minerals, yet both $^{40}Ar/^{39}Ar$ ages (1304 Ma and 1557 Ma) are significantly older than U/Pb zircon growth during high-grade metamorphism at c. 1185 Ma at this site (Kirkland et al., 2010). To explain these old ages, both biotite and hornblende in EAF21 must contain excess argon. The presence of excess argon in the hornblende is supported by the previous interpretation of cryptic excess argon in several additional Biranup Zone hornblende samples, which also produced anomalously old Ar/Ar hornblende ages (Scibiorski et al., 2016).

In summary, the new Rb/Sr cooling ages show that excess argon is present in all biotite samples in the Biranup Zone, and that even the youngest $^{40}Ar/^{39}Ar$ ages do not date cooling through the Ar closure temperature.

5.6 Discussion of cryptic excess argon

Excess argon in $^{40}Ar/^{39}Ar$ geochronology is often identified by a saddle-shaped step-heating spectrum (Figure 5.1a; Lanphere and Dalrymple, 1976; Harrison and McDougall, 1981). This characteristic degassing spectrum has been interpreted as evidence that the excess argon is hosted in fluid, melt or mineral inclusions, because inclusions may contain high concentrations of excess argon, and release argon during step-heating both at very low and at very high temperatures (Kelley, 2002).

Two explanations are typically proposed for the occurrence of a plateau age for minerals containing cryptic excess argon. First, excess and radiogenic ^{40}Ar may have been homogenized in the sample during analysis, such that the apparent plateau is an artefact of laser rastering during the step-heating method (e.g. Renne, 1995). Alternatively, a plateau age may be interpreted to suggest that the excess argon must be homogenously distributed within the mineral lattice itself (e.g. Willigers et al., 2004). Regardless, because argon is non-reactive, it is not structurally bound into any mineral; its incorporation into crustal minerals is through solubility processes rather than chemical substitution. Grove and Harrison (1996) suggest that argon in biotite primarily occupies vacant interlayer sites between the 2:1 layers, as well as crystalline

defects and phase boundaries. Other studies have shown that unoccupied ring structures, such as the hexagonal rings formed by $(Si,Al)O_4$ tetrahedral units in mica, are also favourable locations for noble gases (e.g. Damon and Kulp, 1958; Jackson et al., 2015).

5.6.1 Source of cryptic excess argon

The most common explanations for the source of cryptic excess argon are inherited argon (i.e. retained in the mineral despite prolonged heating above the closure temperature), or a high partial pressure of argon in the rock leading to its partitioning into the mineral (e.g. Kelley, 2002; McDonald et al., 2016).

Reports of minerals retaining inherited argon well above their theoretical closure temperatures occur in dry, fluid-absent rocks, where transport of Ar or other elements is limited (Scaillet, 1996; Kelley and Wartho, 2000; Baxter, 2007; McDonald et al., 2016). However, the Biranup Zone was not dry during Stage II metamorphism. Migmatisation is observed throughout the domain, suggesting metamorphism in fluid-present conditions, and both migmatised and un-migmatised samples contain excess argon (Table 5.2). In addition, many of the biotite $^{40}Ar/^{39}Ar$ ages are older than earlier high-temperature events, and cannot be fully explained by inherited argon; an additional source of excess argon is required.

The alternative explanation, a high partial pressure of argon, requires a mechanism to produce and sustain large quantities of Ar in the rock (Baxter, 2003). Typically, this is either a low rate of Ar migration in a K-rich lithology leading to the buildup of locally derived excess Ar (e.g. Scaillet, 1996), possibly assisted by the breakdown of another K-rich phase containing radiogenic Ar (e.g. white mica; McDonald et al., 2016), or a flux of Ar-rich fluids (Kelley, 2002).

Almost all Biranup Zone samples are K-rich granitic or pelitic gneisses (Table 5.2), and this may have contributed to a high rate of local radiogenic Ar generation. However, metagabbronorite EAF21 contains the oldest $^{40}Ar/^{39}Ar$ ages of any sample, and the presence of excess argon in K-poor lithologies suggests that K-rich lithologies are not the only source of excess Ar in the Biranup Zone.

Although hydrous fluids are a sink for Ar in most systems (Ar is more soluble in hydrous fluids than in minerals by several orders of magnitude), fluids may act as an Ar source, particularly if they are sourced from ancient basement rocks (Kelley, 2002). Because the fluids present during Biranup Zone metamorphism did not remove radiogenic Ar from the system, we suggest a flux of Ar-rich fluids may have been a major source of excess argon. These Ar-rich fluids could easily have been sourced from the Archean Yilgarn Craton rocks that underlie the Biranup Zone in this part of the orogen (Spaggiari et al., 2014b).

5.6.2 Retention of cryptic excess argon

A key assumption in $^{40}Ar/^{39}Ar$ thermochronology is that Ar equilibrates with an infinite reservoir, which allows all radiogenic Ar produced above the closure temperature of the mineral to be removed from the mineral, and from the rock.

Because Ar is significantly more soluble in hydrous fluids than in minerals, fluids play an important role in the accumulation or removal of excess argon. In fluid-poor systems (e.g. a dry granulite), Ar transport is minimised, and excess Ar may accumulate at grain boundaries and eventually be partitioned into minerals (e.g. Scaillet, 1996; Kelley, 2002; Baxter, 2007). In many fluid- (or melt-) present systems, Ar is partitioned into fluids rather than into minerals, and fluids effectively behave as infinite reservoirs (Kelley, 2002; Baxter, 2003). The importance of fluids in controlling the distribution of Ar is supported by studies such as McDonald et al. (2016), where the re-hydration of previously dry assemblages leads to a reduction in apparent $^{40}Ar/^{39}Ar$ ages. However, fluids saturated in Ar cannot act as infinite reservoirs, and a flux of Ar-rich fluids – as we propose for the Biranup Zone – will introduce, rather than remove, excess Ar (Kelley, 2002).

The retention of excess argon in biotite may also depend on the mineralogy in the surrounding rock volume. Ar solubility depends on factors such as crystal structure and lattice defects, and is therefore heterogeneously distributed between different minerals in a rock (e.g. Damon and Kulp, 1958; Thomas et al., 2008; Jackson et al., 2015). Because other minerals may act as net argon sinks, lithology and mineral distribution coefficients are critical to understanding the distribution of excess argon,

both at the sample and mineral scale (e.g. Baxter et al., 2002; Baxter, 2003). However, at the regional scale of our Biranup Zone samples, we observe no clear lithological or mineralogical correlation with excess argon content (Table 5.2). The partial pressure of argon was high enough for it to be diffused into the biotite crystal lattice, regardless of the ability of other minerals to accommodate significant quantities of argon. Nevertheless, the incorporation of excess argon in several minerals rather than just biotite is supported by the presence of excess argon in hornblendes in the Biranup Zone samples, which also yield old apparent $^{40}Ar/^{39}Ar$ ages (Scibiorski et al., 2016).

Despite significant excess argon in the eastern Biranup Zone, $^{40}Ar/^{39}Ar$ thermochronology of hornblende, muscovite and biotite from the west Albany-Fraser Orogen (c. 700 km along strike) shows none of the observed indicators for cryptic excess argon: ages are reproducible, are consistent with mineral closure temperatures, and are consistent with U/Pb age constraints (Scibiorski et al., 2015). This suggests that the movement of Ar-rich fluids, as well as any locally-derived radiogenic argon, was restricted to the east Albany-Fraser Orogen.

5.6.3 Identification of cryptic excess argon

The data we report here support previous studies that show the $^{40}Ar/^{39}Ar$ system in mica is susceptible to the incorporation of cryptic excess argon (e.g. Foland, 1983; Batt et al., 2000; Baxter et al., 2002; Willigers et al., 2004; Stübner et al., 2017). Because the degassing spectra form plateaus, cryptic excess argon is difficult to identify without prior knowledge of the 'true' age. To this end, the following guidelines may assist in the identification of cryptic excess argon.

1. Cryptic excess argon is likely to be present if minerals with lower closure temperatures yield $^{40}Ar/^{39}Ar$ ages that are older than minerals with higher closure temperatures. This includes $^{40}Ar/^{39}Ar$ biotite ages older than U/Pb ages of metamorphic zircon or titanite growth, $^{40}Ar/^{39}Ar$ biotite ages that are older than $^{40}Ar/^{39}Ar$ hornblende ages, and $^{40}Ar/^{39}Ar$ biotite ages significantly older than Rb/Sr biotite ages (e.g. Figure 5.4).
2. Cryptic excess argon may be present if $^{40}Ar/^{39}Ar$ plateau ages from the same mineral in the same sample or same site are inconsistent (beyond

what may be expected from variations in analytical uncertainties or variations in closure temperature due to slight differences in grainsize). All minerals in one sample have experienced the same thermal history, so repeat analyses should produce consistent cooling ages. Samples affected by excess argon typically show poor reproducibility (e.g. Figure 5.4; Scaillet, 1996).

3. If cooling ages vary between sample localities, there should be a plausible tectonic or regional explanation for the different cooling histories (e.g. Busch et al., 1997).
4. Because cryptic excess argon is only identifiable in comparison with other samples, the interpretation of $^{40}Ar/^{39}Ar$ thermochronology should proceed with caution if there are no additional data available to provide an independent constraint on the timing of cooling. In this case, we advise the systematic step-heating $^{40}Ar/^{39}Ar$ analysis of duplicate and triplicate samples to test for any inconsistencies.
5. If there is an identified regional problem with cryptic excess argon, interpretation should also proceed with caution. Whilst the youngest sample in an area will contain the least excess argon, and may approach the true cooling history, any $^{40}Ar/^{39}Ar$ age can only be considered a maximum age constraint. In some cases, it may be possible to determine regional trends in cooling from biotites containing cryptic excess argon (e.g. Batt et al., 2000). However, this may not always be possible; the new Rb/Sr data reported here suggest that even the youngest $^{40}Ar/^{39}Ar$ ages are significantly older than the cooling of the Biranup Zone (e.g. Figure 5.4).

We note that the existing criteria commonly used to assess the quality of $^{40}Ar/^{39}Ar$ thermochronology remain necessary (i.e. plateau statistics, inverse isochron, K/Cl ratio, K/Ca ratio, the analysis of unaltered samples). Whilst this study shows that a plateau age does not guarantee a geologically significant $^{40}Ar/^{39}Ar$ age, it is nevertheless crucial for the confident interpretation of $^{40}Ar/^{39}Ar$ data in metamorphic terranes.

5.7 Conclusion

We used Rb/Sr biotite geochronology to test for the presence of excess argon in the Biranup Zone of the east Albany-Fraser Orogen. All nine samples yield Rb/Sr ages that are 31 – 394 Ma younger than the $^{40}Ar/^{39}Ar$ plateau ages from the same samples. These ages contradict the similarity of Sr and Ar closure temperatures in biotite, and cannot be explained as a product of K loss during alteration, as samples are generally fresh and unaltered; instead, all nine Biranup Zone samples contain cryptic excess argon.

We propose that excess argon was introduced to the Biranup Zone by a flux of Ar-rich fluids sourced from the underlying Archean Yilgarn Craton basement. Combined with a high rate of local radiogenic Ar production in the dominantly K-rich lithologies, a high partial pressure of argon was generated, and excess argon was diffused into minerals including biotite and hornblende.

Cryptic excess argon is so named because it is homogenously distributed within the biotite crystal lattice, and produces statistically robust $^{40}Ar/^{39}Ar$ step-heating plateaus with old apparent ages. It is difficult to identify based only on the Ar data (i.e. it is not visible on the inverse isochron), especially if there are no additional geochronology data available to provide an independent constraint on the timing of cooling. Where there is an identified regional problem with cryptic excess argon, the youngest $^{40}Ar/^{39}Ar$ biotite ages can only be interpreted as maximum ages. In these terranes, provided samples are fresh and unaltered, Rb/Sr thermochronology may provide a robust alternative to $^{40}Ar/^{39}Ar$ thermochronology, because it is unaffected by the presence of excess argon.

5.8 References

Adams, C. J., and Gabites, J. E., 1985, Age of metamorphism and uplift in the Haast Schist Group at Haast Pass, Lake Wanaka and Lake Hawea, South Island, New Zealand: New Zealand Journal of Geology and Geophysics, v. 28, no. 1, p. 85-96.

Armstrong, J., 1988, Quantitative analysis of silicate and oxide minerals: comparison of Monte Carlo, ZAF and phi-rho-z procedures: Microbeam analysis, v. 23, p. 239-246.

Baksi, A. K., and Wilson, A. F., 1980, An attempt at Argon dating of two granulite-facies terranes: Chemical Geology, v. 30, p. 109-120.

Batt, G. E., Braun, J., Kohn, B. P., and McDougall, I., 2000, Thermochronological analysis of the dynamics of the Southern Alps, New Zealand: GSA Bulletin, v. 112, no. 2, p. 250-266.

Baxter, E. F., 2003, Quantification of the factors controlling the presence of excess ^{40}Ar or ^{4}He: Earth and Planetary Science Letters, v. 216, p. 619-634.

-, 2007, Grain boundary partitioning of Ar and He: Geochimica et Cosmochimica Acta, v. 71, p. 434-451.

Baxter, E. F., DePaolo, D. J., and Renne, P. R., 2002, Spatially correlated anomalous $^{40}Ar/^{39}Ar$ "age" variations in biotites about a lithological contact near Simplon Pass, Switzerland: A mechanistic explanation for excess Ar: Geochimica et Cosmochimica Acta, v. 66, no. 6, p. 1067-1083.

Brewer, M. S., 1969, Excess radiogenic argon in metamorphic micas from the eastern Alps, Austria: Earth and Planetary Science Letters, v. 6, p. 321-331.

Busch, J. P., Mezger, K., and van der Pluijm, B., 1997, Suturing and extensional reactivation in the Grenville orogen, Canada: Geology, v. 25, no. 6, p. 507-510.

Cesare, B., Satish-Kumar, M., Cruciani, G., Pocker, S., and Nodari, L., 2008, Mineral chemistry of Ti-rich biotite from pegmatite and metapelitic granulites of the Kerala Khondalite Belt (southeast India): Petrology and further insight into titanium substitutions: American Mineralogist, v. 93, p. 327-338.

Challandes, N., Marquer, D., and Villa, I. M., 2008, P-T-t modelling, fluid circulation, and ^{39}Ar-^{40}Ar and Rb-Sr mica ages in the Aar Massif shear zones (Swiss Alps): Swiss Journal of Geosciences, DOI: 10.1007/s00015-008-1260-6.

Clark, D., Hensen, B., and Kinny, P., 2000, Geochronological constraints for a two-stage history of the Albany-Fraser Orogen, Western Australia: Precambrian Research, v. 102, p. 155-183.

Damon, P. E., and Kulp, J. L., 1958, Excess helium and argon in beryl and other minerals: American Mineralogist, v. 43, p. 433-459.

Del Moro, A., Puxeddu, M., Radicati di Brozolo, F., and Villa, I. M., 1982, Rb-Sr and K-Ar ages on minerals at temperatures of 300°-400° C from deep wells in the Larderello geothermal field (Italy): Contributions in Mineralogy and Petrology, v. 81, p. 340-349.

Dodson, M. H., 1973, Closure temperature in cooling geochronological and petrological systems: Contributions in Mineralogy and Petrology, v. 40, p. 259-274.

Donovan, J. J., Snyder, D. A., and Rivers, M. L., 1993, An improved interference correction for trace element analysis: Microbeam Analysis, v. 2, p. 23-28.

Donovan, J. J., and Tingle, T. N., 1996, An improved mean atomic number background correction for quantitative microanalysis: Journal of Microscopy and Microanalysis, v. 2, no. 1, p. 1-7.

Dunlap, W. J., 2000, Nature's diffusion experiment: The cooling-rate cooling-age correlation: Geology, v. 28, no. 2, p. 139-142.

Ferrow, E. A., Kalinowski, B. E., Veblen, D. R., and Schweda, P., 1999, Alteration products of experimentally weathered biotite studied by high-resolution TEM and Mössbauer spectroscopy: European Journal of Mineralogy, v. 11, p. 999-1010.

Fletcher, I. R., Myers, J. S., and Ahmat, A. L., 1991, Isotopic evidence on the age and origin of the Fraser Complex, Western Australia: a sample of Mid-Proterozoic lower crust: Chemical Geology (Isotope Geoscience Section), v. 87, p. 197-216.

Foland, K. A., 1983, $^{40}Ar/^{39}Ar$ incremental heating plateaus for biotites with excess argon: Isotope Geoscience, v. 1, p. 3-21.

Gardien, V., Thompson, A. B., and Ulmer, P., 2000, Melting of biotite + plagioclase + quartz gneisses: the role of H_2O in the stability of amphibole: Journal of Petrology, v. 41, no. 5, p. 651-666.

Geological Survey of Western Australia, 2016, Compilation of geochronology information 2016: Government of Western Australia, ISBN: 9781741686876.

Giletti, B. J., 1991, Rb and Sr diffusion in alkali feldspars, with implications for cooling histories of rocks: Geochimica et Cosmochimica Acta, v. 55, p. 1331-1343.

Glodny, J., Kühn, A., and Austrheim, H., 2008a, Diffusion versus recrystallization processes in Rb-Sr geochronology: Isotopic relics in eclogite facies rocks, Western Gneiss Region, Norway: Geochimica et Cosmochimica Acta, v. 72, p. 506-525.

-, 2008b, Geochronology of fluid-induced eclogite and amphibolite facies metamorphic reactions in a subduction-collision system, Bergen Arcs, Norway: Contributions in Mineralogy and Petrology, v. 156, p. 27-48.

Gray, D. R., and Foster, D. A., 2004, $^{40}Ar/^{39}Ar$ thermochronologic constraints on deformation, metamorphism and cooling/exhumation of a Mesozoic accretionary wedge, Otago Schist, New Zealand: Tectonophysics, v. 385, p. 181-210.

Griffin, W. L., and Murthy, V. R., 1969, Distribution of K, Rb, Sr and Ba in some minerals relevant to basalt genesis: Geochimica et Cosmochimica Acta, v. 33, no. 11, p. 1389-1414.

Grove, M., and Harrison, T. M., 1996, $^{40}Ar^*$ diffusion in Fe-rich biotite: American Mineralogist, v. 81, p. 940-951.

Hanson, G. N., and Gast, P. W., 1967, Kinetic studies in contact metamorphic zones: Geochimica et Cosmochimica Acta, v. 31, p. 1119-1153.

Harrison, T. M., 1981, Diffusion of ^{40}Ar in hornblende: Contributions in Mineralogy and Petrology, v. 78, p. 324 - 331.

Harrison, T. M., Duncan, I., and McDougall, I., 1985, Diffusion of ^{40}Ar in biotite: Temperature, pressure and compositional effects: Geochimica et Cosmochimica Acta, v. 49, p. 2461 - 2468.

Harrison, T. M., and McDougall, I., 1981, Excess ^{40}Ar in metamorphic rocks from Broken Hill, New South Wales: implications for $^{40}Ar/^{39}Ar$ age spectra and the thermal history of the region Earth and Planetary Science Letters, v. 55, p. 123-149.

Hart, S. R., 1964, The petrology and isotopic-mineral age relations of a contact zone in the Front Range, Colorado: The Journal of Geology, v. 72, no. 5, p. 493-525.

Jackson, C. R. M., Parman, S. W., Kelley, S. P., and Cooper, R. F., 2015, Light noble gas dissolution into ring structure-bearing materials and lattice influences on noble gas recycling: Geochimica et Cosmochimica Acta, v. 159, p. 1-15.

Jenkin, G. R. T., 1997, Do cooling paths derived from mica Rb-Sr data reflect true cooling paths?: Geology, v. 25, no. 10, p. 907-910.

Jeong, G. Y., Cheong, C. S., and Kim, J., 2006, Rb-Sr and K-Ar systems of biotite in surface environments regulated by weathering processes with implications for isotopic dating and hydrological cycles of Sr isotopes: Geochimica et Cosmochimica Acta, v. 70, p. 4734-4749.

Jourdan, F., Renne, P. R., and Reimold, W. U., 2009, An appraisal of the ages of terrestrial impact structures: Earth and Planetary Science Letters, v. 286, no. 1-2, p. 1-13.

Kelley, S. P., 2002, Excess argon in K-Ar and Ar-Ar geochronology: Chemical Geology, v. 188, no. 1-2, p. 1-22.

Kelley, S. P., and Wartho, J. A., 2000, Rapid kimberlite ascent and the significance of Ar-Ar ages in xenolith phlogopites: Science, v. 289, p. 609-611.

Kirkland, C. L., Spaggiari, C. V., Johnson, T. E., Smithies, R. H., Danišík, M., Evans, N., Wingate, M. T. D., Clark, C., Spencer, C., Mikucki, E., and McDonald, B. J., 2016, Grain size matters: Implications for element and isotopic mobility in titanite: Precambrian Research, v. 278, p. 283-302.

Kirkland, C. L., Spaggiari, C. V., Pawley, M. J., Wingate, M. T. D., Smithies, R. H., Howard, H. M., Tyler, I. M., Belousova, E. A., and Poujol, M., 2011, On the edge: U–Pb, Lu–Hf, and Sm–Nd data suggests reworking of the Yilgarn craton margin during formation of the Albany-Fraser Orogen: Precambrian Research, v. 187, no. 3–4, p. 223-247.

Kirkland, C. L., Wingate, M. T. D., Spaggiari, C. V., and Pawley, M. J., 2010, 194722: siliciclastic schist, Harris Lake; Geochronology Record 850: Geological Survey of Western Australia, p. 6p.

Kirschner, D. L., Masson, H., and Cosca, M. A., 2003, An $^{40}Ar/^{39}Ar$, Rb/Sr, and stable isotope study of micas in low-grade fold-and-thrust belt: an example from the Swiss Helvetic Alps: Contributions in Mineralogy and Petrology, v. 145, p. 460-480.

Lanphere, M. A., and Dalrymple, G. B., 1976, Identification of excess ^{40}Ar by the $^{40}Ar/^{39}Ar$ age spectrum technique: Earth and Planetary Science Letters, v. 32, p. 141-148.

Li, S., Wang, S., Chen, Y., Liu, D., Qiu, J., Zhou, H., and Zhang, Z., 1994, Excess argon in phengite from eclogite: Evidence from dating of eclogite minerals by Sm-Nd, Rb-Sr and $^{40}Ar/^{39}Ar$ methods: Chemical Geology, v. 112, p. 343-350.

Little, T. A., Mortimer, N., and McWilliams, M. O., 1999, An episodic Cretaceous cooling model for the Otago-Marlborough Schist, New Zealand, based on $^{40}Ar/^{39}Ar$ white mica ages: New Zealand Journal of Geology and Geophysics, v. 42, no. 3, p. 305-325.

Luth, S. W., and Willingshofer, E., 2008, Mapping of the post-collisional cooling history of the Eastern Alps: Swiss Journal of Geosciences, v. 101, p. S207-S223.

McDonald, C. S., Warren, C. J., Mark, D. F., Halton, A. M., Kelley, S. P., and Sherlock, S. C., 2016, Argon redistribution during a metamorphic cycle: Consequences for determining cooling rates: Chemical Geology, v. 443, p. 182-197.

McDougall, I., and Harrison, T. M., 1988, Geochronology and thermochronology by the $^{40}Ar/^{39}Ar$ method, New York, Oxford University Press, Oxford Monographs on Geology and Geophysics.

Mitchell, J. G., and Taka, A. S., 1984, Potassium and argon loss patterns in weathered micas: Implications for detrital mineral studies, with particular reference to the Triassic palaeogeography of the British Isles: Sedimentary Geology, v. 39, p. 27-52.

Moore, L. J., Moody, J. R., Barnes, I. L., Gramlich, J. W., Murphy, T. J., Paulsen, P. J., and Shields, W. R., 1973, Trace determination of rubidium and strontium in silicate glass standard reference materials: Analytical Chemistry, v. 45, no. 14, p. 2384-2387.

Pankhurst, R. J., Moorbath, S., Rex, D. C., and Turner, G., 1973, Mineral age patterns in ca. 3700 My old rocks from West Greenland: Earth and Planetary Science Letters, v. 20, p. 157-170.

Patiño Douce, A. E., 1993, Titanium substitution in biotite: an empirical model with applications to thermometry, O_2 and H_2O barometries, and consequences for biotite stability: Chemical Geology, v. 108, p. 133-162.

Purdy, J. W., and Jäger, E., 1976, K-Ar ages on rock forming minerals from the Central Alps, Mem. 1st: Geol. Petrol. Univ. Padova, v. 30, p. 1-321.

Renne, P. R., 1995, Excess ^{40}Ar in biotite and hornblende from the Noril'sk 1 intrusion, Siberia: implications for the age of the Siberian Traps: Earth and Planetary Science Letters, v. 131, p. 165 – 176.

Renne, P. R., Balco, G., Ludwig, K. R., Mundil, R., and Min, K., 2011, Response to the comment by W.H. Schwarz et al. on "Joint determination of ^{40}K decay constants and $^{40}Ar^*/^{40}K$ for the Fish Canyon sanidine standard, and improved accuracy for $^{40}Ar/^{39}Ar$ geochronology" by P.R. Renne et al. (2010): Geochimica et Cosmochimica Acta, v. 75, p. 5097-5100.

Roberts, H. J., Kelley, S. P., and Dahl, P. S., 2001, Obtaining geologically meaningful ^{40}Ar-^{39}Ar ages from altered biotite: Chemical Geology, v. 172, p. 277-290.

Roddick, J. C., Cliff, R. A., and Rex, D. C., 1980, The evolution of excess argon in Alpine biotites - a ^{40}Ar-^{39}Ar analysis: Earth and Planetary Science Letters, v. 48, p. 185-208.

Ruffet, G., Féraud, G., Balèvre, M., and Kiénast, J. R., 1995, Plateau ages and excess argon in phengites: an ^{40}Ar-^{39}Ar laser probe study of Alpine micas (Sesia Zone, Western Alps, northern Italy): Chemical Geology, v. 121, p. 327-343.

Ruffet, G., Gruau, G., Ballèvre, M., Féraud, G., and Philippot, P., 1997, Rb-Sr and ^{40}Ar-^{39}Ar laser probe dating of high-pressure phengites from the Sesia zone (Western Alps): underscoring of excess argon and new age constraints on the high-pressure metamorphism: Chemical Geology, v. 141, p. 1-18.

Rutter, E. H., 1983, Pressure solution in nature, theory and experiment: Journal of the Geological Society of London, v. 140, p. 725-740.

Scaillet, S., 1996, Excess ^{40}Ar transport scale and mechanism in high-pressure phengites: A case study from an eclogitized metabasite of the Dora-Maira nappe, western Alps: Geochimica et Cosmochimica Acta, v. 60, no. 6, p. 1075-1090.

Schneider, C. A., Rasband, W. S., and Eliceiri, K. W., 2012, NIH Image to ImageJ: 25 years of image analysis: Nature Methods, v. 9, no. 7, p. 671 - 675.

Scibiorski, E., Tohver, E., and Jourdan, F., 2015, Rapid cooling and exhumation in the western part of the Mesoproterozoic Albany-Fraser Orogen, Western Australia: Precambrian Research, v. 265, p. 232-248.

Scibiorski, E., Tohver, E., Jourdan, F., Kirkland, C. L., and Spaggiari, C. V., 2016, Cooling and exhumation along the curved Albany-Fraser orogen, Western Australia: Lithosphere, v. 8, no. 5, p. 551-563.

Sharp, W. D., and Renne, P. R., 2005, The $^{40}Ar/^{39}Ar$ dating of core recovered by the Hawaii Scientific Drilling Project (phase 2), Hilo, Hawaii: Geochemistry, Geophysics, Geosystems, v. 6, no. 4.

Smith, M. E., Singer, B. S., Carroll, A. R., and Fournelle, J. H., 2008, Precise dating of biotite in distal volcanic ash: Isolating subtle alteration using $^{40}Ar/^{39}Ar$ laser

incremental heating and electron microprobe techniques: American Mineralogist, v. 93, p. 784-795.

Spaggiari, C., Bodorkos, S., Barquero-Molina, M., Tyler, I., and Wingate, M. T. D., 2009, Interpreted bedrock geology of the southern Yilgarn and central Albany-Fraser Orogen, Western Australia: Geological Survey of Western Australia, Record 2009/10, p. 84.

Spaggiari, C. V., Kirkland, C. L., Pawley, M. J., Smithies, R. H., Wingate, M. T. D., Doyle, M. G., Blenkinsop, T. G., Clark, C., Oorschot, C. W., Fox, L. J., and Savage, J., 2011, The geology of the east Albany-Fraser Orogen - a field guide: Geological Survey of Western Australia, Record 2011/23, p. 92.

Spaggiari, C. V., Kirkland, C. L., Smithies, R. H., and Wingate, M. T. D., 2014a, Tectonic links between Proterozoic sedimentary cycles, basin formation and magmatism in the Albany-Fraser Orogen, Western Australia: Geological Survey of Western Australia, Report 133.

Spaggiari, C. V., Occhipinti, S. A., Korsch, R. J., Doublier, M. P., Clark, D. J., Dentith, M. C., Gessner, K., Doyle, M. G., Tyler, I. M., Kennett, B. L. N., Costelloe, R. D., Fomin, T., and Holzschuh, J., 2014b, Interpretation of Albany-Fraser seismic lines 12GA-AF1, 12GA-AF2 and 12GA-AF3: implications for crustal architecture, *in* Spaggiari, C. V., and Tyler, I. M., eds., Albany-Fraser Orogen seismic and magnetotelluric (MT) workshop 2014: extended abstracts, Record 2014/6, Geological Survey of Western Australia, p. 28 - 51.

Steiger, R. H., and Jäger, E., 1977, Subcommision on geochronology: Convention on the use of decay constants in geo- and cosmochronology: Earth and Planetary Science Letters, v. 36, p. 359-362.

Stübner, K., Warren, C. J., Ratschbacher, L., Sperner, B., Kleeberg, R., Pfänder, J., and Grujic, D., 2017, Anomalously old biotite $^{40}Ar/^{39}Ar$ ages in the NW Himalaya: Lithosphere, DOI: 10.1130/L586.1.

Thomas, J. B., Cherniak, D. J., and Watson, E. B., 2008, Lattice diffusion and solubility of argon in forsterite, enstatite, quartz and corundum: Chemical Geology, v. 253, p. 1-22.

Tohver, E., Teixeira, W., van der Pluijm, B., Geraldes, M. C., Bettencourt, J. S., and Rizzotto, G., 2006, Restored transect across the exhumed Grenville orogen of Laurentia and Amazonia, with implications for crustal architecture: Geology, v. 34, no. 8, p. 669-672.

Tohver, E., van der Pluijm, B., Mezger, K., Scandolara, J. E., and Essene, E. J., 2005, Two stage tectonic history of the SW Amazon craton in the late Mesoproterozoic: identifying a cryptic suture zone: Precambrian Research, v. 137, p. 35-59.

Verschure, R. H., Andriessen, P. A. M., Boelrijk, N. A. I. M., Hebeda, E. H., Maijer, C., Priem, H. N. A., and Verdurmen, E. A. T., 1980, On the thermal stability of Rb-Sr and K-Ar biotite systems: Evidence from coexisting Sveconorwegian (ca 870 Ma) and Caledonian (ca 400 Ma) biotites in SW Norway: Contributions in Mineralogy and Petrology, v. 74, p. 245-252.

Villa, I. M., 2016, Diffusion in mineral geochronometers: Present and absent: Chemical Geology, v. 420, p. 1-10.

Villa, I. M., De Bièvre, P., Holden, N. E., and Renne, P. R., 2015, IUPAC-IUGS recommendation on the half life of ^{87}Rb: Geochimica et Cosmochimica Acta, v. 164, p. 382-385.

Walker, S., Thirlwall, M. F., Strachan, R. A., and Bird, A. F., 2016, Evidence from Rb-Sr mineral ages for multiple orogenic events in the Caledonides of Shetland, Scotland: Journal of the Geological Society, v. 173, p. 489-503.

Willigers, B. J. A., Mezger, K., and Baker, J. A., 2004, Development of high precision Rb-Sr phlogopite and biotite geochronology; an alternative to ^{40}Ar/^{39}Ar tri-octahedral mica dating: Chemical Geology, v. 213, p. 339-358.

Chapter 6

Using the trace element signature of titanite to constrain polygenetic titanite growth, garnet growth and U/Pb geochronology

6 Using the trace element signature of titanite to constrain polygenetic titanite growth, garnet growth and U/Pb geochronology

Scibiorski, E[1]; Kirkland, C. L.[2]; Kemp, A. I. S.[1]; Tohver, E[1]; Evans, N. J.[3]

[1] School of Earth Sciences, The University of Western Australia, Crawley, Australia

[2] Centre for Exploration Targeting – Curtin Node, Department of Applied Geology, Curtin University, Bentley, Australia

[3] John de Laeter Centre, The Institute for Geoscience Research, Department of Applied Geology, Curtin University, Bentley, Australia

Abstract

The petrological information preserved in the trace element signature of titanite is a valuable complement to *in situ* U/Pb geochronology. We used laser ablation-inductively coupled plasma mass spectrometry (LA-ICPMS) to analyse trace element and U/Pb compositions of titanite in five amphibolite- to granulite-facies samples from the east Albany-Fraser Orogen of Western Australia. Chondrite-normalised rare earth element (REE) abundance patterns are used to identify and discriminate between populations of titanite with distinct trace element signatures. These REE populations correlate with zoning of titanite visible in backscatter electron (BSE) images.

Unzoned titanite grains that show compositional variation in REE content at the thin-section scale allow the spatial controls on titanite composition to be identified. In two samples, titanite composition correlates with proximity to garnet, and in one sample titanite composition correlates with gneissic compositional banding.

The Dy/Yb ratio (a measure of heavy-REE enrichment) can be used as a geochemical indicator to link titanite growth to garnet growth. Titanite that crystallised in equilibrium with garnet is HREE-depleted with Dy/Yb > 2, whereas titanite that crystallised in the absence of garnet typically has flat HREE patterns with

Dy/Yb < 2. The titanite grains investigated in this study have a wide range of Eu and LREE signatures, with no obvious correlation to mineralogy, lithology, or growth environment. In addition, the Th/U ratio is not uniquely diagnostic of metamorphic or magmatic titanite. For the five samples reported here, these trace elements are useful only to discriminate between titanite populations, but not as geochemical indicators.

By integrating the REE signatures with U/Pb data, the five new titanite U/Pb ages can be linked to a range of processes: magmatic titanite crystallisation, metamorphic titanite growth, garnet growth, and/or cooling through the closure temperature for Pb diffusion in titanite.

6.1 Introduction

Titanite ($CaTiSiO_5$) is a common accessory mineral in a wide range of lithologies, and the U/Pb geochronometer in titanite provides a valuable window into magmatic and metamorphic processes. The wide range of reported closure temperatures for Pb diffusion in titanite (650 - 1030 °C; Cherniak, 2010) means that individual U/Pb ages may date regional cooling, or titanite crystallisation, either from a magma, during solid-state metamorphism, or during fluid-rock interaction (e.g. Gao et al., 2012; Kirkland et al., 2016). Because of the range of possible interpretations for each titanite U/Pb age, identifying the processes controlling the distribution of U and Pb is crucial (i.e. volume diffusion or recrystallisation).

As only one of many minerals that can contain Ti and Ca, titanite is reactive and susceptible to metamorphic recrystallisation at high temperature, which contributes to the complexity of interpreting U/Pb data from this mineral (Frost et al., 2000). However, recrystallisation or new titanite growth commonly produces compositional zoning, and is accompanied by variations in trace element content that may provide valuable petrological information (e.g. Storey et al., 2007; Lucassen et al., 2011; Bruand et al., 2014; Papapavlou et al., 2017).

With laser ablation-inductively coupled plasma mass spectrometry (LA-ICPMS), extensive trace element datasets can be collected to complement the U/Pb data. This approach is common for minerals such as zircon and monazite, where trace element indicators are used to link U/Pb data to specific geological events (Kylander-Clark et al., 2013). For example, the Th/U ratio in zircon can be used to discriminate between metamorphic and magmatic growth in some circumstances (Rubatto, 2002; c.f. Kirkland et al., 2015), and the Y + heavy rare earth element (HREE) content of monazite is strongly related to the growth or consumption of xenotime and garnet (Spear and Pyle, 2002, 2010).

However, the potential for using the trace element content of titanite as a geochemical indicator is yet to be fully explored. Whilst the Hayden et al. (2008) calibration of the Zr-in-Tt thermometer is widely used to determine the temperature

of titanite crystallisation, trace elements other than Zr are not routinely investigated (e.g. Spencer et al., 2013; Schwartz et al., 2016).

Several studies demonstrate that titanite trace element chemistry can provide useful petrologic insights, particularly when combined with detailed backscatter electron (BSE) imaging. For example, Lucassen et al. (2011) examined the relationships between fluid-mobile (Sr, U), moderately fluid-mobile (rare earth elements; REE) and fluid-immobile (high field strength elements; HFSE) elements and connected this chemical information with detailed titanite petrography to understand spatial and temporal variability in fluid composition. Similarly, Stearns et al. (2015) used the occurrence of spatial variability in Sr, Zr and Y to identify recrystallisation events in titanite. A small number of studies use chondrite-normalised REE patterns to discriminate between older titanite cores and younger metamorphic rims (Storey et al., 2007; Smith et al., 2009; Gao et al., 2012; Bruand et al., 2014). In these studies, the REE patterns are linked to magma composition, crystal fractionation, and fluid composition during titanite recrystallisation. More recently, Papapavlou et al. (2017) suggest that the light-REE (LREE) composition of titanite may reflect the co-crystallisation of LREE-enriched phases such as allanite or monazite.

Here, we explore various paths to link the trace element content of titanite to specific petrological events and to the U/Pb geochronology. We use chondrite-normalised REE patterns to identify different populations of titanite within five samples of garnet-bearing and garnet-free metamorphic rocks from the Albany-Fraser Orogen of Western Australia, and then examine the relationships between titanite composition, metamorphic (re)crystallisation, garnet growth, and U/Pb geochronology.

6.2 Background

6.2.1 Trace elements in titanite

Titanite typically contains less than 0.02 wt% REE, although up to 4 wt% REE has been reported from titanite in pegmatites (Frost et al., 2000). The REEs substitute for

Ca^{2+} in the seven-coordinated site, along with other large ions such as U, Th, Mn, Na, Mg and Pb. On the octahedral site, Fe^{3+} and Al^{3+} substitute for Ti, although Zr, Ta and Nb are also common (Frost et al., 2000).

Experimental measurements of titanite/melt partition coefficients show that titanite has a preference for the MREE (Nd – Dy) over the LREE and HREE at a range of silicate melt compositions (Tiepolo et al., 2002; Prowatke and Klemme, 2005). However, the trace element content in natural titanite strongly depends on element availability during crystallisation (Lucassen et al., 2011). Element availability is controlled by factors such as bulk sample composition, fluid composition, and mineral growth or breakdown (in turn controlled by pressure and temperature). The importance of element availability is supported by the wide range in reported chondrite-normalised REE patterns: titanite may display a combination of LREE depletion or enrichment, negative or positive Eu anomaly, and depleted or enriched HREE (Storey et al., 2007; Smith et al., 2009; Gao et al., 2012; Bruand et al., 2014; Papapavlou et al., 2017).

Experimental measurements of trace element diffusivity in titanite show that REE diffusion is more than four orders of magnitude slower than Pb diffusion, with closure temperatures for Nd diffusion in the range 920 – 1170°C (Cherniak, 1993). This means that the REE composition of titanite is effectively permanent at most crustal temperatures, unless titanite is completely recrystallised during metamorphism.

6.2.2 Pb closure temperature in titanite

Diffusion experiments in titanite show that Pb diffusion is strongly dependent on grainsize and crystal damage (Cherniak, 1993). Diffusion experiments at temperatures below 850°C revealed significantly faster Pb diffusion than expected by extrapolating the results of diffusion experiments carried out above c. 850°C. Cherniak (1993, 2010) attributed these two apparently contradictory trends to the influence of radiation damage in the titanite crystal: at low temperatures, Pb diffusivity is significantly enhanced by radiation damage, but at high temperatures, a damaged crystal lattice is quickly annealed. Based on these data, Cherniak (2010)

suggest a wide range of possible closure temperatures for Pb diffusion in titanite of 650 – 1030 °C.

Accordingly, titanite U/Pb ages have been linked to a wide range of processes, typically a mixture of inheritance, metamorphic recrystallisation, or cooling through the closure temperature for Pb diffusion (e.g. Mezger et al., 1993; Scott and St-Onge, 1995; Corfu, 1996; Zhang and Schärer, 1996). More recently, Gao et al. (2012) and Spencer et al. (2013) both reported inherited U/Pb ages in titanite that was subjected to HP-UHP metamorphism at temperatures above 800°C and 750 °C, respectively. Spencer et al. (2013) suggested that titanite ages were controlled by (re)crystallisation, rather than thermal diffusion. Stearns et al. (2015) and Schwartz et al. (2016) similarly assumed titanite ages are (re)crystallisation ages, as U/Pb signatures survived mid- to upper amphibolite facies conditions (c. 700°C). However, Kirkland et al. (2016) report the partial resetting of U/Pb in magmatic titanite by volume diffusion of Pb at c. 700°C, with the degree of age resetting correlated with titanite grainsize.

These studies show that the geological significance of a U/Pb titanite age may vary with each sample, depending on factors such as lattice damage, grainsize, fluid activity, and history of metamorphic (re)crystallisation.

6.2.3 Geology of the Albany-Fraser Orogen

The Albany-Fraser Orogen of southwestern Australia extends for c. 1200 km along the southern and south-eastern margins of the Archean Yilgarn Craton (Figure 6.1). The orogen records a long Neoarchean to Paleoproterozoic history of magmatism, basin formation, and deformation, overprinted by the two-stage, high grade Mesoproterozoic Albany-Fraser Orogeny (Stage I, 1330 – 1260 Ma; Stage II, 1225 – 1140 Ma) (Clark et al., 2000; Spaggiari et al., 2011; Spaggiari et al., 2014).

The Albany-Fraser Orogen is separated into the Northern Foreland and the Kepa Kurl Booya Province, which is in turn subdivided into the Tropicana, Biranup, Fraser and Nornalup Zones (Spaggiari et al., 2009; Spaggiari et al., 2014). Here, we focus on the effects of Mesoproterozoic orogeny on the Fraser and Biranup Zones, where our samples were collected.

The Biranup Zone consists of c. 1815 – 1630 Ma orthogneisses and paragneisses (Spaggiari et al., 2011). It was deformed and metamorphosed at amphibolite to granulite facies during the Albany-Fraser Orogeny, and intruded by the granitic Recherche and Esperance Supersuites, coeval with Stage I and Stage II of orogeny, respectively (Spaggiari et al., 2009; Smithies et al., 2015).

The Fraser Zone is a shear zone-bound domain in the east Albany-Fraser Orogen, located between the Biranup and Nornalup Zones (Figure 6.1). In the Fraser Zone, 1335 – 1295 Ma sedimentary rocks were deformed to paragneiss by c. 1290 Ma granulite facies metamorphism, coeval with the c. 1300 – 1290 Ma intrusion of extensive metagabbro and felsic orthogneisses (Clark et al., 2014; Maier et al., 2016).

Mesoproterozoic orogeny and previous U/Pb titanite geochronology

The current understanding of the timing and distribution of metamorphism during the two stages of the Albany-Fraser Orogeny relies primarily on U/Pb zircon geochronology (Geological Survey of Western Australia, 2016). Individual U/Pb zircon ages are typically interpreted to date magmatism and/or peak metamorphism. The U/Pb zircon data are complemented by a small number of studies using thermobarometric modelling (Bodorkos and Clark, 2004a; Clark et al., 2014; Kirkland et al., 2016), U/Pb titanite geochronology (Kirkland et al., 2016), and $^{40}Ar/^{39}Ar$ thermochronology (Scibiorski et al., 2015; Scibiorski et al., 2016).

Stage I of orogeny (1330 – 1260 Ma) was a high temperature, moderate to high pressure metamorphic event, accompanied by extensive coeval mafic and felsic magmatism (Bodorkos and Clark, 2004a; Spaggiari et al., 2011; Smithies et al., 2015). Peak Stage I metamorphism in the Fraser Zone at c. 1290 Ma reached 850 °C and 7 – 9 GPa (Clark et al., 2014). In the south-eastern Biranup Zone, c. 1300 Ma granulite facies metamorphism was followed by high pressure burial and recrystallisation at 800 – 850 °C and 10 GPa, followed by decompression to 7 – 8 GPa at 700 – 800 °C by 1290 Ma (Bodorkos and Clark, 2004a, b).

Stage II (1225 – 1140 Ma) was a widespread, pervasive event driven by northwest-directed compression, and is responsible for the dominant craton-vergent architecture of the orogen (Bodorkos and Clark, 2004b; Spaggiari et al., 2011; Korsch

et al., 2014). Deformation was accompanied by high temperature and moderate pressure metamorphism, and extensive felsic magmatism (Spaggiari et al., 2011; Smithies et al., 2015).

In the north-eastern Biranup Zone, most U/Pb zircon ages for Stage II metamorphism and magmatism are between 1205 – 1190 Ma, with c. 1190 Ma peak metamorphism at one locality reaching 675 – 725 °C and 6.5 – 8.5 GPa (Geological Survey of Western Australia, 2016; Kirkland et al., 2016). U/Pb titanite geochronology

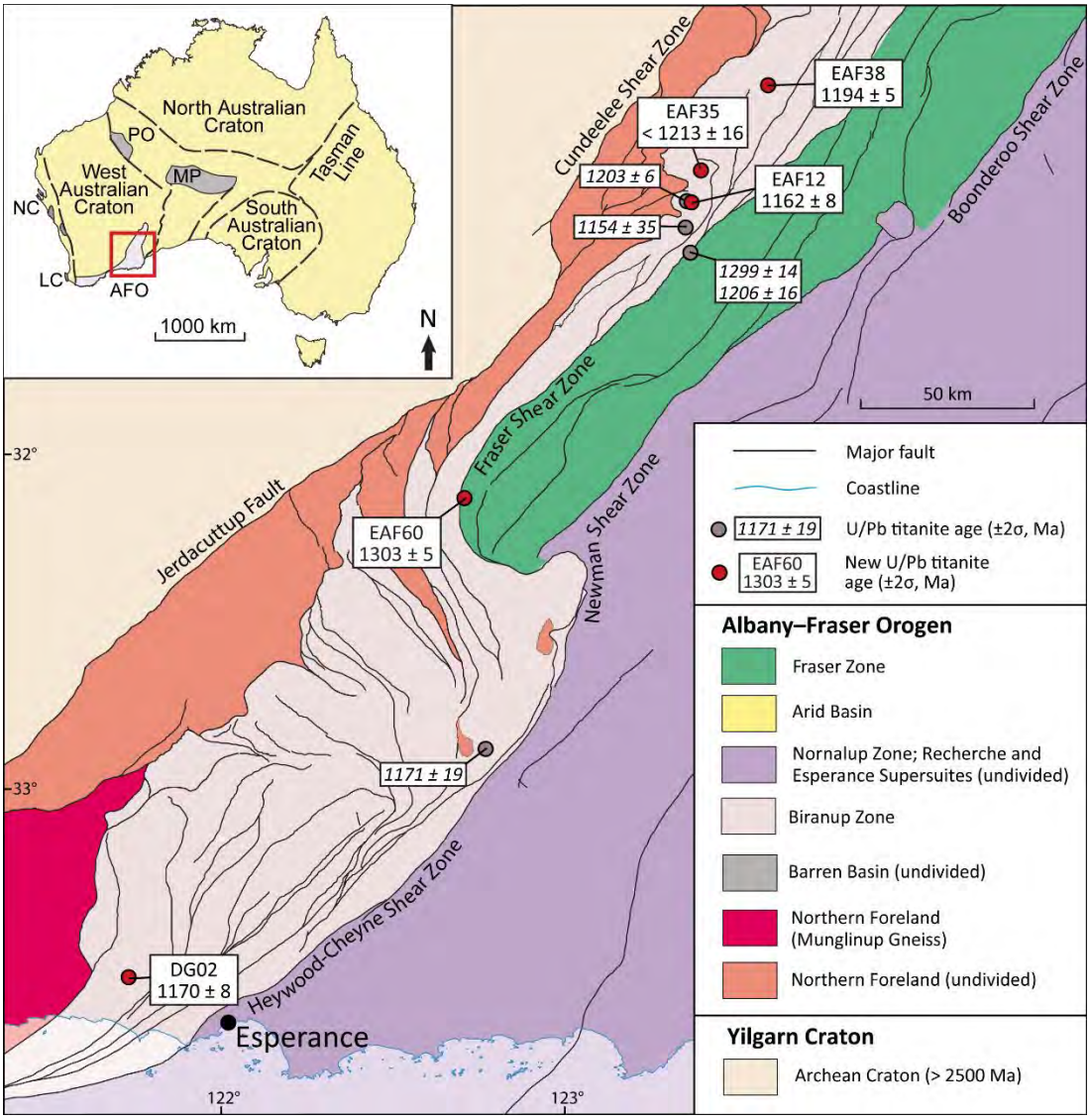

Figure 6.1 Interpreted bedrock geology of the eastern Albany-Fraser Orogen, showing sample sites and both new and existing U/Pb titanite geochronology. Inset at top left shows location of the Albany-Fraser Orogen within Australia. Geological map modified from Spaggiari et al. (2014); inset after Kirkland et al. (2011). Geochronology data from Kirkland et al. (2016).

in this region produced a metamorphic titanite crystallisation age of 1203 ± 6 Ma, and a titanite age of 1153 ± 27 Ma interpreted as the age of closure to radiogenic Pb diffusion (i.e. cooling; Kirkland et al., 2016).

A wider range of U/Pb zircon ages are reported in the south-eastern Biranup and Nornalup Zones, with ages of magmatism and metamorphism between 1225 – 1155 Ma. Stage II metamorphism in the south-eastern Biranup Zone at c. 1170 Ma reached 750 – 800 °C and 5 – 6 GPa (Bodorkos and Clark, 2004a, b). The only U/Pb titanite age from the south-eastern Biranup Zone is interpreted to date metamorphic titanite crystallisation at 1171 ± 19 Ma (Kirkland et al., 2016).

Unlike the neighbouring Biranup and Nornalup Zones, the Fraser Zone records only Stage I U/Pb zircon geochronology (Geological Survey of Western Australia, 2016; Maier et al., 2016). Clark et al. (2014) suggested that cooling and strengthening of the Fraser Zone after Stage I rendered it less susceptible to later deformation. However, Kirkland et al. (2016) report an early Stage II U/Pb titanite age of 1206 ± 15 Ma from the Fraser Shear Zone, which forms the north-western boundary of the Fraser Zone. A minimum temperature of 675 – 725 °C is calculated for this Stage II resetting of the U/Pb titanite geochronometer (Kirkland et al., 2016). In addition, $^{40}Ar/^{39}Ar$ hornblende and biotite thermochronology in the Fraser Zone also yields ages that range from c. 1217 – 1157 Ma (Scibiorski et al., 2016). These observations indicate heterogenous Stage II resetting in the Fraser Zone, and suggest that the interior of the Fraser Zone did not reach the same granulite facies conditions as the adjacent Biranup and Nornalup Zones.

6.3 Methods

6.3.1 Sample petrography

Five samples were collected from the Fraser and Biranup Zones of the eastern Albany-Fraser Orogen, encompassing a range of lithologies (Figure 6.1; Table 6.1). The selected samples contain titanite in a variety of textural associations: in the groundmass as anhedral to subhedral grains (EAF60, EAF35, DG02) or as wedge-

Table 6.1 Sample localities and petrography.

Sample	Site, Domain	Lithology	Assemblage	Lat	Long	Population	Titanite textures	Compositional zoning
EAF60	Gnamma Hill, Fraser Zone	Mafic gneiss	Cpx-Opx-Pl-Qz-Grt-Ilm-Tt-Hb-Rt-Ap-Zrc	-32.180922	122.697752	60A	Large anhedral to subhedral grains	Narrow <10 μm rims on some grains
						60B	Large subhedral grains; adjacent to garnet	Strongly zoned
EAF12	Fly Dam Formation, Biranup Zone	Pelitic garnet gneiss	Qz-Grt-Pl-Or-Bt-Hb-Tt-Ilm-Ap-Rt-Zrc-All	-31.283340	123.360023	12A	Subhedral to anhedral inclusions in garnet porphyroblasts	Zoned along subgrain boundaries
						12B, 12C	Large wedge-shaped grains in the matrix	Core-rim zoning common Rims typically <20 μm
EAF35	Uraryie Rock, Biranup Zone	Granitic gneiss	Qz-Mc-Pl-Hb-Bt-Tt-Grt-Ilm-Ap-Rt-Zrc-All	-31.184973	123.421842	All	Large subhedral grains; some cores and rims separated by a halo of rutile inclusions	Core-rim zoning common; rims up to 100 μm Patchy zoning in some cores
EAF38	Ponton Creek, Biranup Zone	Garnet amphibolite	Pl-Hb-Qz-Grt-Tt-Rt-Ilm-Ap-Zrc	-30.909600	123.642918	38A	Titanite rims rutile and/or ilmenite	None
						38B	Subhedral grain; distant from garnet	Irregular, patchy zoning
DG02	Daly Downs, Biranup Zone	Tonalitic orthogneiss	Pl-Qz-Or-Bt-Hb-Mt-Ilm-Tt-Rt-Ap-Zrc	-33.689631	121.609178	All	Small subhedral grains in the matrix; thin (10 μm) rims around magnetite	None

shaped crystals (EAF12); as anhedral inclusions in garnet (EAF12); and as rims around rutile, ilmenite and/or magnetite (EAF38, DG02).

Samples were imaged with a FEI Varios XHR scanning electron microscope (SEM) using an in-column concentric back scatter (CBS) detector at the Centre for Microscopy and Characterisation at The University of Western Australia (Perth, Australia). Brief sample descriptions are in Table 6.1; Appendix 6.1 contains detailed petrography and descriptions of the structural context and existing geochronology at sample sites.

6.3.2 Titanite LA-ICPMS analyses

LA-ICPMS data were collected at the GeoHistory Facility in the John de Laeter Centre, Curtin University, Perth, Australia. Titanite grains were analysed *in situ* in polished thin sections, during two analytical sessions. The Resonetics RESOlution M-50A-LR system used for ablation incorporates a Compex 102 193 nm excimer UV laser; analysis was performed at a 4 Hz laser repetition rate with a laser energy of 1 – 2 J/cm^2 (measured at the sample surface). During ablation, the sample cell was flushed with ultrahigh purity He (350 mL/min) and N (3.8 mL/min). Isotopic abundances were measured using an Agilent 7700s quadrupole ICPMS, with high purity Ar as the plasma gas (1 L/min). During both analytical sessions, 50 μm diameter spots were ablated for 40 s between two 15 s periods of background analysis.

For samples EAF12, DG02, EAF60 and EAF38, the following elements were monitored for 0.03 s each: ^{23}Na, ^{27}Al, ^{29}Si, ^{44}Ca, ^{49}Ti, ^{51}V, ^{52}Cr, ^{55}Mn, ^{57}Fe, ^{89}Y, ^{90}Zr, ^{93}Nb, ^{139}La, ^{140}Ce, ^{141}Pr, ^{146}Nd, ^{147}Sm, ^{153}Eu, ^{157}Gd, ^{159}Tb, ^{163}Dy, ^{165}Ho, ^{166}Er, ^{169}Tm, ^{172}Yb, ^{175}Lu, ^{178}Hf, ^{181}Ta, ^{182}W, ^{204}Pb, ^{206}Pb, ^{207}Pb, ^{208}Pb, ^{232}Th, ^{238}U. For sample EAF35, the same elements were monitored for 0.03 s each, with the following changes: ^{43}Ca instead of ^{44}Ca; ^{56}Fe instead of ^{57}Fe; additional measurement of ^{47}Ti; ^{182}W was not measured.

REE data for titanite unknowns were reduced using the trace elements data reduction scheme in Iolite (Paton et al., 2011). International glass standard NIST 610 was used as the primary standard to calculate elemental concentrations (using ^{29}Si as the internal standard element) and to correct for instrument drift. 14.2% Si was assumed for titanite unknowns.

Mass spectra were reduced using the VizualAge_UcomPbine data reduction scheme in Iolite and in-house Excel macros (Paton et al., 2011; Chew et al., 2014). The primary age standard was titanite OLT (1015 ± 2 Ma; Kennedy et al., 2010). To verify the ages, titanite BLR (1047 ± 0.4 Ma; Aleinikoff et al., 2007) was employed as a secondary reference material. The age of BLR was determined by regression from contemporaneous common Pb through the uncorrected data, yielding an age of 1047 ± 5 Ma (MSWD = 1.3), within analytical uncertainty of the accepted value (1047 ± 0.4 Ma).

6.3.3 Garnet LA-ICPMS analyses

Garnet LA-ICPMS analyses were carried out at the Advanced Analytical Centre at James Cook University in Townsville, Australia, with a Geolas 193 nm ArF excimer laser coupled to a Varian ICP-MS 820. Garnet was analysed *in situ* in the same polished thin sections as the titanite. Following c. 30 s of background acquisition (laser firing with closed shutter), 44 μm diameter spots were ablated for 30 s at a 10 Hz laser repetition rate and laser energy of 4 J/cm^2. Ablation was conducted in ultrahigh purity He (0.35 L/min), which was combined with Ar (1 L/min) prior to transport into the ICP. The following elements were monitored: ^{29}Si, ^{43}Ca, ^{44}Ca, ^{51}V, ^{52}Cr, ^{85}Rb, ^{88}Sr, ^{89}Y, ^{91}Zr, ^{181}Ta (0.01 s each); ^{49}Ti, ^{93}Nb, ^{140}Ce, ^{143}Nd, ^{147}Sm, ^{151}Eu, ^{157}Gd, ^{159}Tb, ^{163}Dy, ^{165}Ho, ^{169}Tm, ^{171}Yb, ^{175}Lu, ^{179}Hf, ^{208}Pb, ^{232}Th, ^{238}U (0.02 s each); ^{139}La, ^{141}Pr, ^{167}Er (0.03 s each).

Data were reduced using the Glitter software package (Van Achterbergh et al., 1999). International glass standard NIST 610 was used as the primary standard to calculate elemental concentrations (using ^{29}Si as the internal standard element) and to correct for instrument drift. The garnet Si abundances used for calibration of elemental concentrations were 18.1 wt% for EAF60, 17.0 wt% for EAF12 and 17.4 wt% for EAF38. These garnet compositions were analysed by wavelength dispersive spectroscopy, using a JEOL JXA8530F electron microprobe at the Centre for Microscopy, Characterisation and Analysis (University of Western Australia, Perth, Australia). A detailed methodology for the microprobe analyses is in Appendix 6.2.

6.3.4 Common lead correction and titanite U/Pb ages

In U/Pb geochronology, common lead (Pb_C) is Pb incorporated into the mineral during crystallisation, recrystallisation, or as a laboratory contaminant; i.e., not from the *in situ* decay of U. Titanite commonly incorporates significant amounts of Pb_C, and so every measurement can be considered to contain a mixture of radiogenic lead (Pb*) and Pb_C. This is illustrated schematically on a Tera-Wasserburg concordia plot in Figure 6.2. To determine meaningful titanite U/Pb ages, a correction for the presence of Pb_C is essential, especially where the ratio of Pb* to Pb_C is small.

Although widely used in U/Pb SHRIMP and TIMS geochronology, the ^{204}Pb correction is not always suitable for U/Pb titanite data collected by LA-ICPMS. This is because the Ar gas used in the mass spectrometer also contains Hg, and, unless steps are taken to eliminate this (e.g. Storey et al., 2006), ^{204}Hg interferes isobarically with the measurement of ^{204}Pb. The most abundant isotope of mercury, ^{202}Hg, is present in such low concentrations that precise measurement on a quadrupole mass spectrometer is difficult, and the propagation of errors associated with this measurement will introduce large uncertainties into the ^{204}Pb-corrected U/Pb data (e.g. 2σ errors greater than 10%; Storey et al., 2006).

For titanite, the most commonly used alternative is the ^{207}Pb-correction (e.g. Spencer et al., 2013; Kirkland et al., 2016; Schwartz et al., 2016). This method assumes that every measured data point lies on a mixing line between radiogenic lead (0% Pb_C) and common lead (100% Pb_C). A line is drawn from the $^{207}Pb/^{206}Pb$ composition of the common lead component (the upper intercept of the mixing line) through the data point, and then regressed back onto the concordia to determine the ^{207}Pb-corrected $^{238}U/^{206}Pb$ age (Figure 6.2).

The most important assumption in the ^{207}Pb correction is choosing an appropriate $^{207}Pb/^{206}Pb$ composition for common lead. One approach is to assume a Pb_C composition based on a global lead evolution model, such as Stacey and Kramers (1975); however, regional deviations in Pb_C composition from this model have been demonstrated (e.g. Zartman and Doe, 1981). An alternative approach is to regress the uncorrected data, and then use the upper intercept as the common lead composition (e.g. sample EAF12; Figure 6.3b). An advantage of this approach is that the data itself

defines the Pbc composition, which in many cases is preferable to a model-based correction. However, in some samples the U/Pb analyses are not sufficiently spread along the Pbc-Pb* mixing line to allow clear definition of the common lead composition (i.e. there is a restricted range of $^{207}Pb/^{206}Pb$ ratios). Nonetheless, plotting our data on a single Tera-Wasserburg plot shows that all five samples appear to have a similar common lead composition, and we use this average $^{207}Pb/^{206}Pb$ ratio of 0.738 ± 0.026 to calculate the ^{207}Pb-corrected ages (Appendix 6.3).

The Tera-Wasserburg plot is also useful for evaluating whether analyses have been affected by Pb and/or U mobility. Assuming all titanite crystallised at the same time, titanite that has been subject to Pb loss (or U gain) will have a higher $^{238}U/^{206}Pb$ ratio but unchanged $^{207}Pb/^{206}Pb$ ratio, resulting in data points plotting to the right of the Pbc-Pb* mixing line (Figure 6.2). Conversely, Pb gain (or U loss) will shift data to the left of the mixing line.

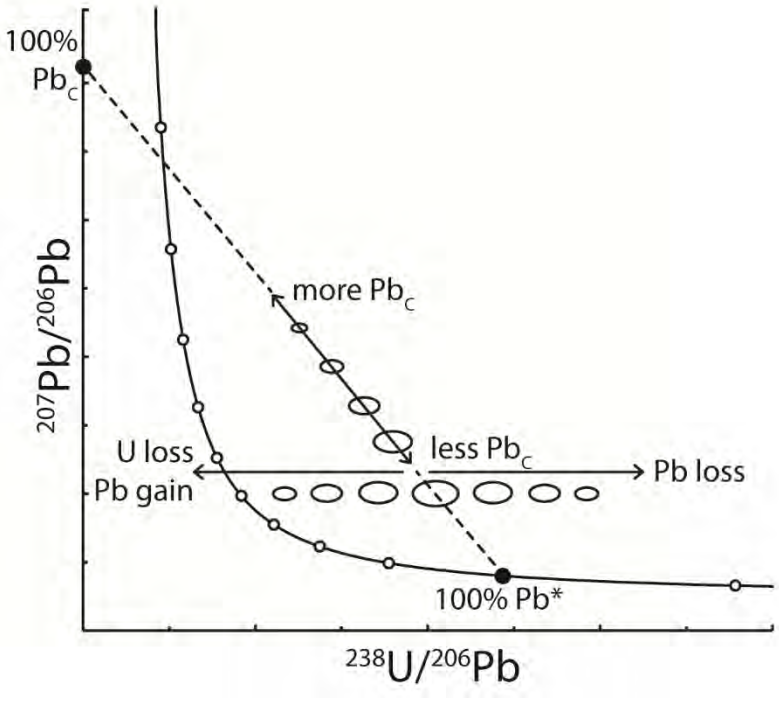

Figure 6.2 Schematic Tera-Wasserburg concordia plot illustrating the main processes affecting the distribution of U/Pb data in titanite. A data point containing 100% radiogenic Pb (Pb*) will be concordant. The incorporation of progressively larger amounts of common Pb (Pbc) will shift data along a mixing line from Pb* towards Pbc. Data points may be shifted to the right and left of the mixing line due to Pb loss, and U loss or Pb gain, respectively.

Age inheritance (the preservation of multiple age components in a single sample) will add further complexity to the distribution of U/Pb data. Incomplete resetting of the U/Pb age (e.g. by Pb diffusion during metamorphism) will shift data points to the right according to the degree of Pb loss, producing a horizontal array of data. In addition, if recrystallised or partially recrystallised titanite contains multiple populations of Pb_C with different compositions, the presence of U/Pb data points that fall on different Pb_C-Pb* mixing lines with different slopes may produce an apparently curved data array.

Titanite U/Pb ages were determined as follows. First, analyses subject to significant Pb and/or U mobility, based on displacement relative to a well defined Pb_C-Pb* mixing line, were excluded from age determination. Next, where statistically appropriate, the age was taken as the lower intercept of a regression of the U/Pb data calculated using Isoplot 4 (Ludwig, 2012). This bypasses any uncertainty introduced by the assumption of a Pb_C composition, as the data themselves define Pb_C. For samples where the data were too clustered to calculate a meaningful lower intercept, the regression was anchored at a $^{207}Pb/^{206}Pb$ common lead composition of 0.738.

We note that the two samples for which the ^{207}Pb-correction was necessary (EAF60 and EAF38) are also those samples which are least sensitive to the choice of common lead composition. The U/Pb analyses for these samples plot close to the concordia (due to high Pb^*/Pb_C ratios), and hence the lower intercept is insensitive to changes in the assumed common lead composition (Figures 6.3a, d).

6.3.5 Zirconium thermometry

We use the zirconium-in-titanite (Zr-in-Tt) thermometer as calibrated by Hayden et al. (2008) to calculate average titanite crystallisation temperatures for each sample (Table 6.2). The thermometer is based on a mineral assemblage that contains quartz, rutile and zircon, and the three minerals are present and in equilibrium with each other in all samples.

The Zr-in-Tt temperature calculation requires an assumption of the pressure at which the titanite crystallised. Recent thermobarometry by Clark et al. (2014) and

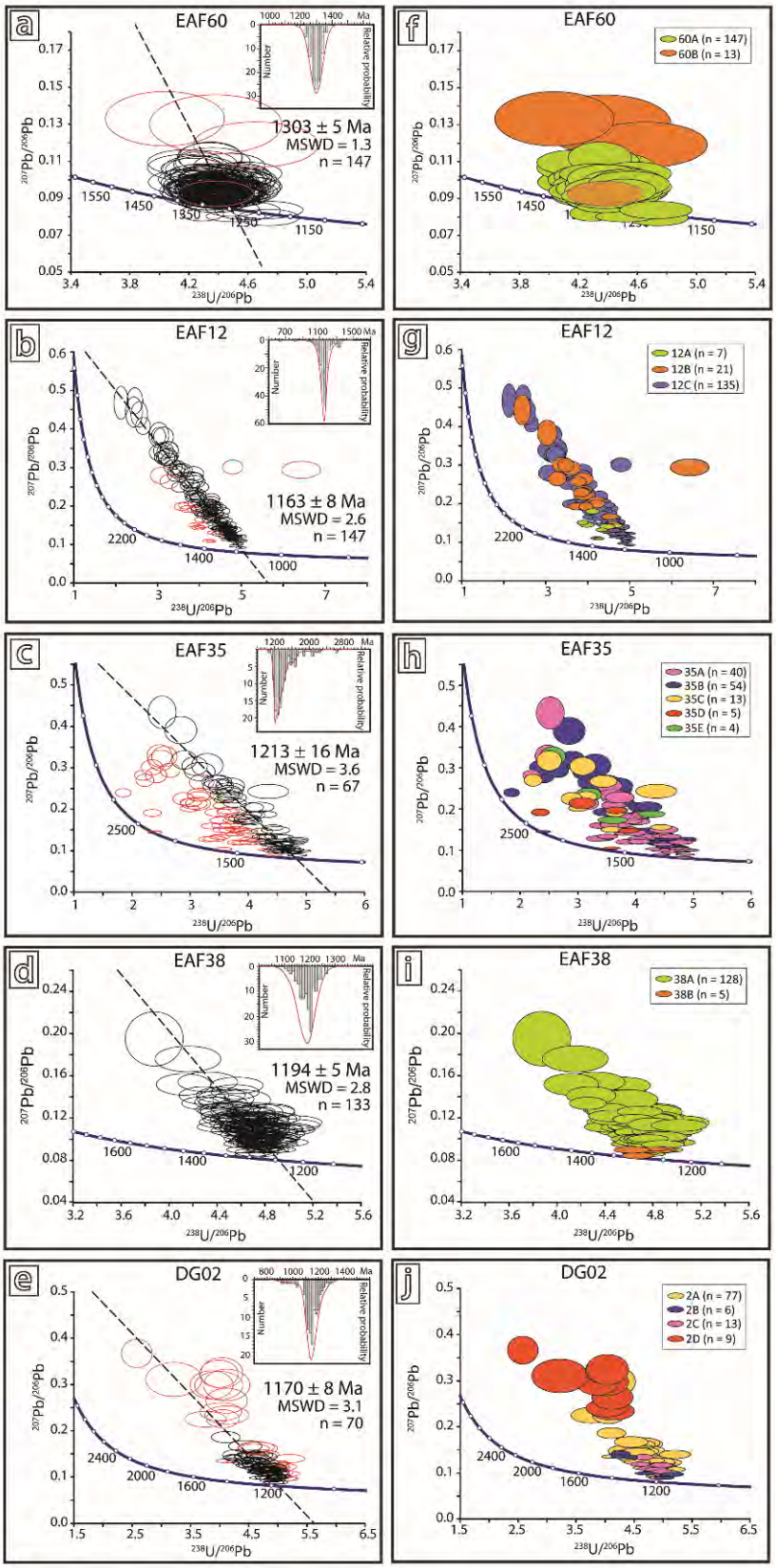

Figure 6.3 Tera-Wasserburg concordia plots showing U/Pb analyses. Error ellipses are plotted at 2σ. **(A – E)** Black analyses were used for the age calculation, and red analyses were excluded. Insets show histograms of ^{207}Pb-corrected ^{238}U/^{206}Pb ages. **(F – J)** U/Pb data are coloured according to titanite REE population.

Table 6.2 Summary of titanite populations and U/Pb age of each sample. T refers to the zirconium-in-titanite thermometer, calculated according to Hayden et al. (2008). Population averages are given for Th/U, U, Pb, REE, Zr and T.

Sample	Site, Domain	Lithology	U/Pb age (Ma)	Age significance	Population	n	Th/U	U (ppm)	Pb (ppm)	REE (ppm)	Zr (ppm)	T ± 2σ (°C)	Range (°C)
EAF60	Gnamma Hill, Fraser Zone	Mafic gneiss	1303 ± 5	Magmatism	60A	147	4.71	27	40	4404	2242	909 ± 10	886 – 922
					60B	13	0.49	4	5	927	347	789 ± 10	783 – 801
EAF12	Fly Dam Formation, Biranup Zone	Pelitic garnet gneiss	1163 ± 8	Cooling age	12A	7	0.39	55	60	5390	173	738 ± 24	726 - 762
					12B	21	0.14	24	32	887	105	712 ± 24	677 – 730
					12C	135	0.07	53	57	1376	148	730 ± 14	711 - 752
EAF35	Uraryie Rock, Biranup Zone	Granitic gneiss	1213 ± 16	Metamorphism (maximum age)	35A	40	0.54	50	61	1556	99	709 ± 26	682 - 736
					35B	54	0.17	37	47	1025	114	714 ± 32	701 - 728
					35C	12	0.24	16	32	660	100	709 ± 28	693 - 748
					35D	5	0.37	35	66	880	94	705 ± 34	691 - 734
					35E	4	0.31	27	46	1344	102	711 ± 12	704 - 717
EAF38	Ponton Creek, Biranup Zone	Garnet amphibolite	1194 ± 5	Metamorphism	38A	128	3.83	51	51	6111	256	760 ± 14	740 - 778
					38B	5	1.29	106	104	7843	273	763 ± 12	755 -771
DG02	Daly Downs, Biranup Zone	Tonalitic orthogneiss	1170 ± 8	Metamorphism	2A	77	3.53	38	51	6235	299	750 ± 24	706 - 767
					2B	6	2.42	79	101	10415	341	758 ± 8	752 - 763
					2C	13	2.90	60	76	9975	348	759 ± 10	753 - 766
					2D	9	8.50	5.5	13	1488	245	738 ± 32	698 - 750

Kirkland et al. (2016) constrains metamorphic pressures in the Fraser Zone (0.9 GPa) and in the Fly Dam Formation of the northern Biranup Zone (0.7 GPa), respectively; these pressures are used for samples EAF60, EAF12, EAF35 and EAF38. For sample DG02, we used the Stage II metamorphic pressure (0.55 GPa) derived by Bodorkos and Clark (2004a) in the Coramup Gneiss of the southern Biranup Zone. The spread in Zr content for titanite from each sample results in a range in Zr-in-Tt temperatures, which are reported as a population mean ± 2σ.

6.4 Results

The major, trace element and U/Pb data from the titanite LA-ICPMS analyses are given in Appendix 6.4. Figure 6.3 shows titanite U/Pb data from each sample, Figures 6.4 – 6.8 show representative titanite BSE images, and Figure 6.9 shows chondrite-normalised titanite REE patterns (chondrite composition from Palme and O'Neill, 2003).

For each sample, titanite analyses are separated into populations based on trace element composition, summarised in Table 6.2. Titanite populations are named with the sample number and an arbitrary letter; e.g. the two populations in sample EAF60 are '60A' and '60B'.

6.4.1 EAF60: Gnamma Hill, Fraser Zone

Titanite in mafic gneiss EAF60 occurs as large anhedral to subhedral grains and is mostly unzoned in BSE images, although some grains display narrow (<10 μm) rims and two grains are more complexly zoned (Figure 6.4b, c). The 160 analyses on 41 titanite grains are divided into two populations based on trace element and U/Pb composition.

The main population (60A) of 147 analyses produced a chondrite-normalised REE pattern with decreasing LREE, a slightly negative Eu anomaly (average Eu/Eu* = 0.79), and decreasing HREE (Figure 6.9a). These 39 grains have an average Zr-in-Tt crystallisation temperature of 909 ± 10 °C (± 2σ). Population 60B contains the remaining 13 analyses, which are mixed analyses of the light and dark zones on the two complexly zoned titanite grains (Figure 6.4c). These titanite REE patterns are

generally steeper, especially from Gd to Yb, have a positive Eu anomaly (average Eu/Eu* = 1.60), and contain less total REE than population 60A. The Zr-in-Tt crystallisation temperature for this population is 789 ± 10 °C (± 2σ).

The U/Pb analyses from population 60A form a single cluster just above concordia (Figure 6.3a), interpreted to reflect a single-age Pb* component mixed with minor amounts of Pb_C (up to 4%). An anchored regression from Pb_C produces a lower intercept age of 1303 ± 5 Ma (MSWD = 1.3, n = 147).

The twelve analyses in population 60B were excluded from the age calculation due to low U and Pb content. Eight analyses contained too little U and Pb to calculate an age (U < 2 ppm). The remaining four analyses did yield apparent ages but also had low U and Pb contents (6 – 18.5 ppm U and 7 – 18.5 ppm Pb, compared to 20 – 35 ppm U and 24 – 53 ppm Pb for population 60A; Table 6.2), and higher Pb_C/Pb* ratios than analyses in 60A (up to 7% Pb_C for 60B, compared to < 4% for 60A).

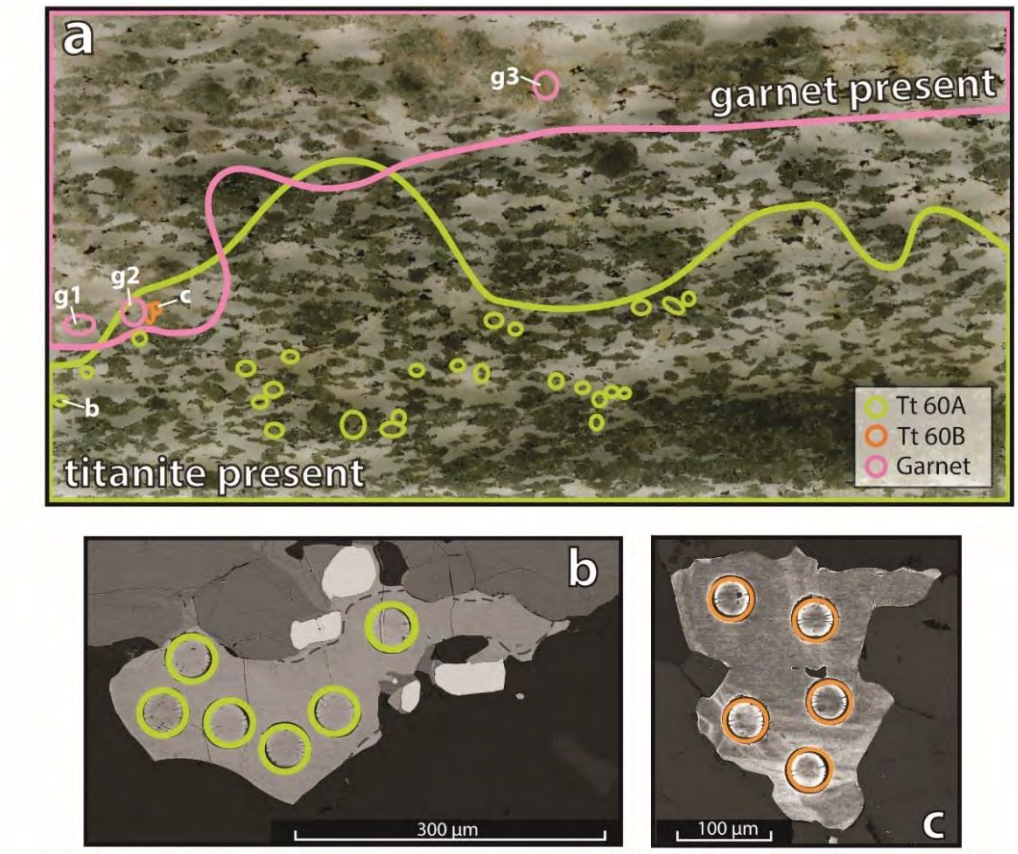

Figure 6.4 (A) Image of thin section EAF60 showing locations of analysed titanite (green and orange) and garnet (pink), and outlining the distribution of titanite and garnet in thin section. **(B)** Representative BSE image of titanite in population 60A. Faint, narrow titanite rims are outlined by dark grey dashed lines. **(C)** Representative BSE image of titanite in population 60B.

6.4.2 EAF12: Fly Dam Formation, Biranup Zone

Titanite in pelitic garnet gneiss EAF12 occurs in two textural relationships: as large wedge-shaped grains in the matrix, and as subhedral to anhedral inclusions in garnet porphyroblasts (Figure 6.5). Titanite in the matrix displays core-rim zoning in BSE images; rims are typically <20 μm in width, and in some grains the boundary between core and rim is gradational. For titanite inclusions in garnet, zoning correlates with subgrain boundaries and fractures. The 163 analyses of 40 titanite grains are divided into three populations on the basis of their REE patterns: 12A, 7 analyses of titanite inclusions in garnet enriched in LREE and with flat HREE patterns; 12B, 21 analyses of titanite cores in the matrix with positive LREE slopes and flat HREE patterns; and 12C, the main population of 135 analyses with overall

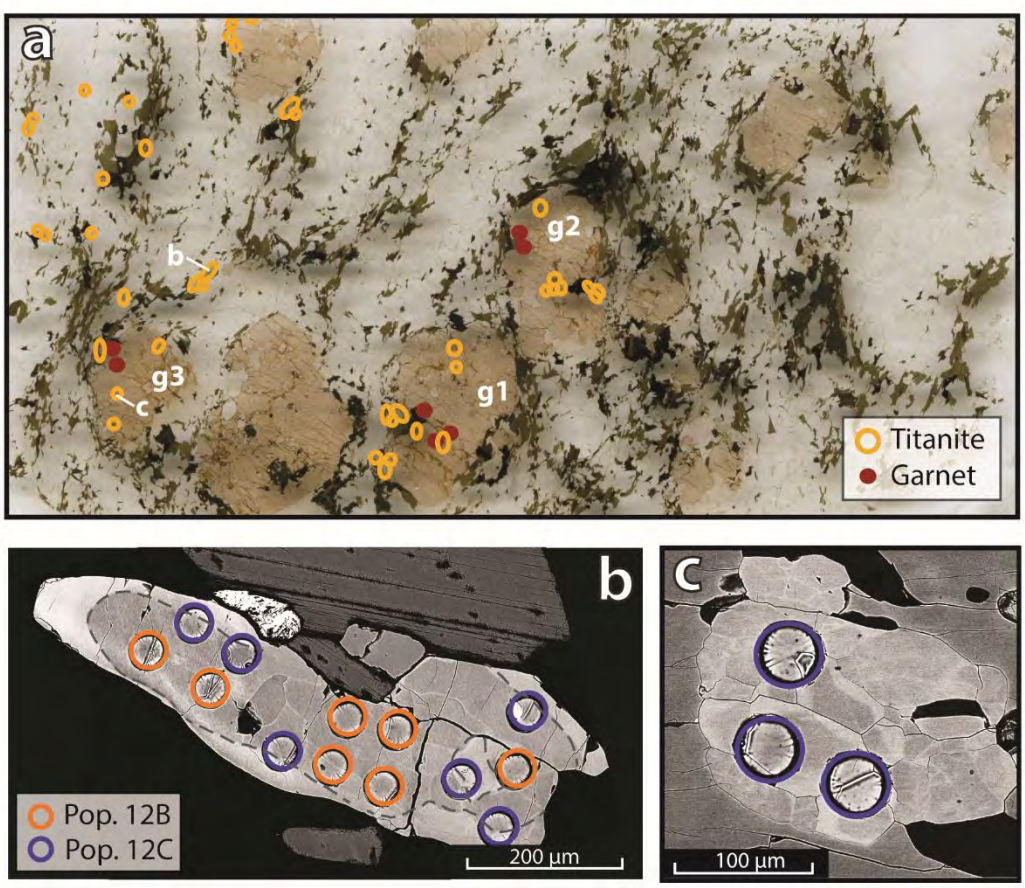

Figure 6.5 (A) Image of thin section EAF12 showing locations of analysed titanite grains (yellow) and garnet (red). **(B)** Representative BSE image of titanite in matrix, showing core-rim zoning. Zoning is gradational in places and is traced out with a dashed line. Analyses are coloured by titanite population. **(C)** Representative BSE image of a titanite inclusion in garnet, showing patchy zoning along internal grain boundaries.

convex-up REE patterns and small negative Eu anomalies (average Eu/Eu* = 0.83). Although the REE patterns correlate with the zoning visible in BSE images, the distinction between populations 12B and 12C (cores and rims of matrix titanite) is gradational, in agreement with the gradational core-rim zoning in some grains (Figure 6.5b). There is no difference in Zr-in-Tt crystallisation temperature between the three populations, and the average temperature is 728 ± 20°C (± 2σ).

The U/Pb analyses define a discordant array that is interpreted to reflect mixing between Pb_C and a single Pb* component (Figure 6.3b). Titanite in the matrix (12B and 12C) defines the Pb_C – Pb* mixing line, and contains up to 61% Pb_C. In contrast, titanite inclusions in garnet (12A) contain only up to 32% Pb_C, and plot slightly to the left of the Pb_C – Pb* mixing line.

Although a Pb_C – Pb* mixing line is well defined, a single regression through all 163 analyses is not favoured due to 14 analyses scattering to the left of the mixing line. These 14 outliers are interpreted to represent an older, partially reset generation of titanite, and are excluded from the age calculation (see further discussion in section 6.5.3 below). A further two outliers plot significantly to the right of the Pb_C – Pb* mixing line, and are excluded as they are interpreted to be affected by Pb loss. A regression through the remaining 147 titanite U/Pb analyses produces a lower intercept age of 1163 ± 8 Ma (MSWD = 2.6).

6.4.3 EAF35: Uraryie Rock, Biranup Zone

Titanite in granitic gneiss EAF35 occurs as large subhedral grains. Most titanites display strong core-rim zoning in BSE images with a halo of rutile inclusions separating core and rim; some cores also have irregular, patchy zoning (Figure 6.6b). The 116 analyses on 37 titanite grains are separated into five populations on the basis of their REE patterns. Most titanite has a positively-sloped LREE pattern with either a flat HREE pattern (population 35A; n = 40) or a negatively-sloped HREE pattern (35B; n = 54). The populations correspond to the compositional zoning visible in BSE images. There is no difference in titanite crystallisation temperature between the five populations, with an average Zr-in-Tt temperature of 711 ± 30 °C.

The U/Pb analyses show a complex distribution on the Tera-Wasserburg concordia (Figure 6.3c), with a significant spread of analyses both to the left and right of the inferred mixing line between Pb_C and Pb*. Analyses contain up to 54% Pb_C. Insufficient analyses of clearly recognizable titanite rims (n = 3) does not allow for clear assessment of any age relationship between core and rim domains. There is no correlation between U/Pb isotopic composition and the five REE groups, or the rutile content of the titanite grain.

The horizontal spread to the left and right of the inferred Pb_C – Pb* mixing line is an indicator of significant Pb and/or U mobility, either as a result of partial resetting of the geochronometer during metamorphism, and/or Pb loss, and/or the presence of

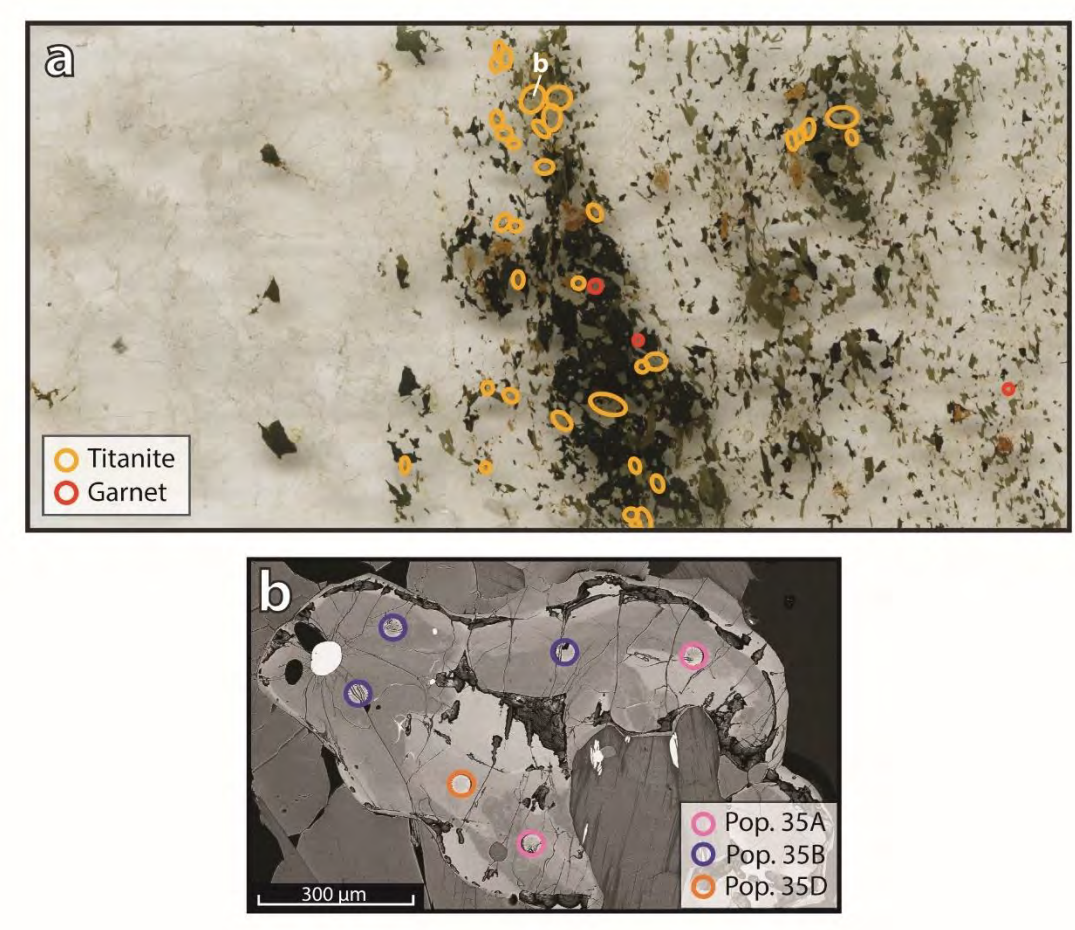

Figure 6.6 (A) Image of thin section EAF35 showing locations of analysed titanite grains (yellow) and location of all garnet grains in the thin section (red). **(B)** Representative BSE image of titanite with patchy zoning in the core, and core and rim titanite separated by a halo of rutile inclusions. Analyses are coloured by titanite population.

an older titanite component. A histogram of ^{207}Pb-corrected ^{238}U/^{206}Pb ages shows a probability maximum at c. 1210 Ma with a long tail to older ages (Figure 6.3c). The simplest explanation for these older analyses is that they represent an earlier generation of titanite with partially reset U/Pb ages. An unanchored regression through the analyses with the 67 youngest ^{207}Pb-corrected ^{238}U/^{206}Pb ages produces a lower intercept age of 1213 ± 16 Ma (MSWD = 3.6). The same 67 analyses yield a weighted mean ^{207}Pb-corrected ^{238}U/^{206}Pb age of 1214 ± 10 Ma (MSWD = 3.6).

6.4.4 EAF38: Ponton Creek, Biranup Zone

Titanite in garnet amphibolite EAF38 occurs as rims around rutile and ilmenite, and with the exception of a single grain, is unzoned in BSE images (Figure 6.7b, c).

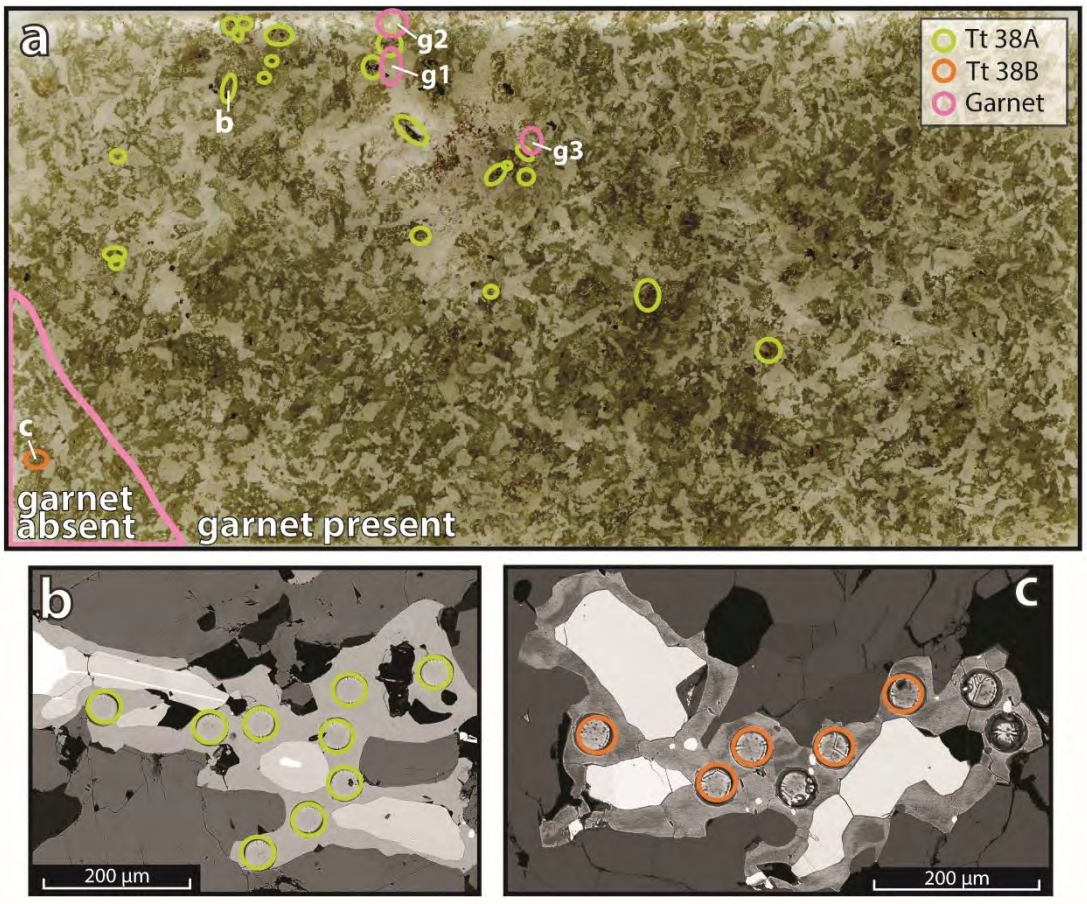

Figure 6.7 (A) Image of thin section EAF38 showing locations of analysed titanite (green and orange) and garnet (pink), and outlining the distribution of garnet in the thin section. **(B)** Representative BSE image of titanite in population 38A. **(C)** Representative BSE image of titanite in population 38B, showing patchy zoning. Although eight spots were analysed on the grain, three analyses are excluded due to ablating small zircon inclusions.

The 133 analyses of 24 grains are separated into two populations on the basis of REE chemistry (Figure 6.9e). The main population, 38A, consists of 128 analyses on unzoned grains with steeply negative sloping REE patterns (average Ce/Yb = 145). Population 38B contains 5 analyses on the only zoned titanite grain; the LREE trend is similar to 38A, but HREE are less depleted (average Ce/Yb = 32). Notably, this grain is located in the part of the thin section that lacked garnet (Figure 6.7a). There is no difference in titanite crystallisation temperatures between the two populations, with an average Zr-in-Tt temperature of 760 ± 14 °C.

When plotted on a Tera-Wasserburg concordia, the U/Pb analyses cluster at the lower end of a well-defined mixing line between Pb_C and Pb*, with up to 17% Pb_C (Figure 6.3d). There is some horizontal spread of analyses to higher $^{238}U/^{206}Pb$ ratios, interpreted as a result of minor Pb and/or U mobility. There is no correlation between U/Pb isotopic composition and trace element content, or rutile inclusions in the titanite grains.

A histogram of ^{207}Pb-corrected $^{238}U/^{206}Pb$ ages shows a nearly symmetrical distribution around a probability maximum at c. 1198 Ma, suggesting most titanite in the sample either grew or cooled at this time (Figure 6.3d). An anchored regression on all 133 analyses produces a lower intercept age of 1194 ± 5 Ma (MSWD = 2.8).

6.4.5 DG02: Daly Downs, Biranup Zone

Titanite in tonalitic orthogneiss DG02 occurs in two textural positions: as small, subhedral grains in the matrix, and as thin rims around large magnetite crystals. All titanite is unzoned in BSE images (Figure 6.8b - e). The 105 analyses are separated into four populations, which do not correlate with textural association. These are: 2A, 77 analyses with negatively-sloped LREE, positive Eu anomalies (average Eu/Eu* = 1.90) and flat to slightly enriched HREE; 2B, six analyses with similar REE pattern to 2A but higher total REE, Pb and U content; 2C, 13 analyses with a smooth REE pattern with a slight negative slope (average Ce/Yb = 12); and 2D, nine analyses with negatively-sloped LREE, large positive Eu anomalies (average Eu/Eu* = 12.1) and flat to slightly enriched HREE (Figure 6.9f). Populations 2A, 2B and 2C have significantly higher REE abundances than population 2D, with averages of 6235, 10415, 9975 and

1488 ppm respectively. The average Zr-in-Tt crystallisation temperature is 753 ± 18 °C for populations 2A, 2B and 2C, and 738 ± 32 °C for population 2D.

Most U/Pb analyses cluster close to concordia and contain less than 16% Pb_C (Figure 6.3e). Twelve analyses contain significantly more Pb_C (22 - 43%) and appear to define an array between Pb* and Pb_C. Of the four populations, 2A, 2B and 2C do not differ in Tera-Wasserburg concordia space; however, all nine analyses in population 2D plot in the high-Pb_C group (Figure 6.3j). There is no correlation between U or Pb content and whether titanite rims magnetite or occurs in the matrix.

The 12 analyses with high Pb_C contain significantly less total Pb and U (Pb = 6.5 – 22 ppm; U = 2.5 – 12 ppm) than the analyses with low Pb_C (Pb = 18 – 173 ppm; U = 12 – 103 ppm). Due to the high Pb_C/Pb^* ratios and low total Pb content, Pb_C has a

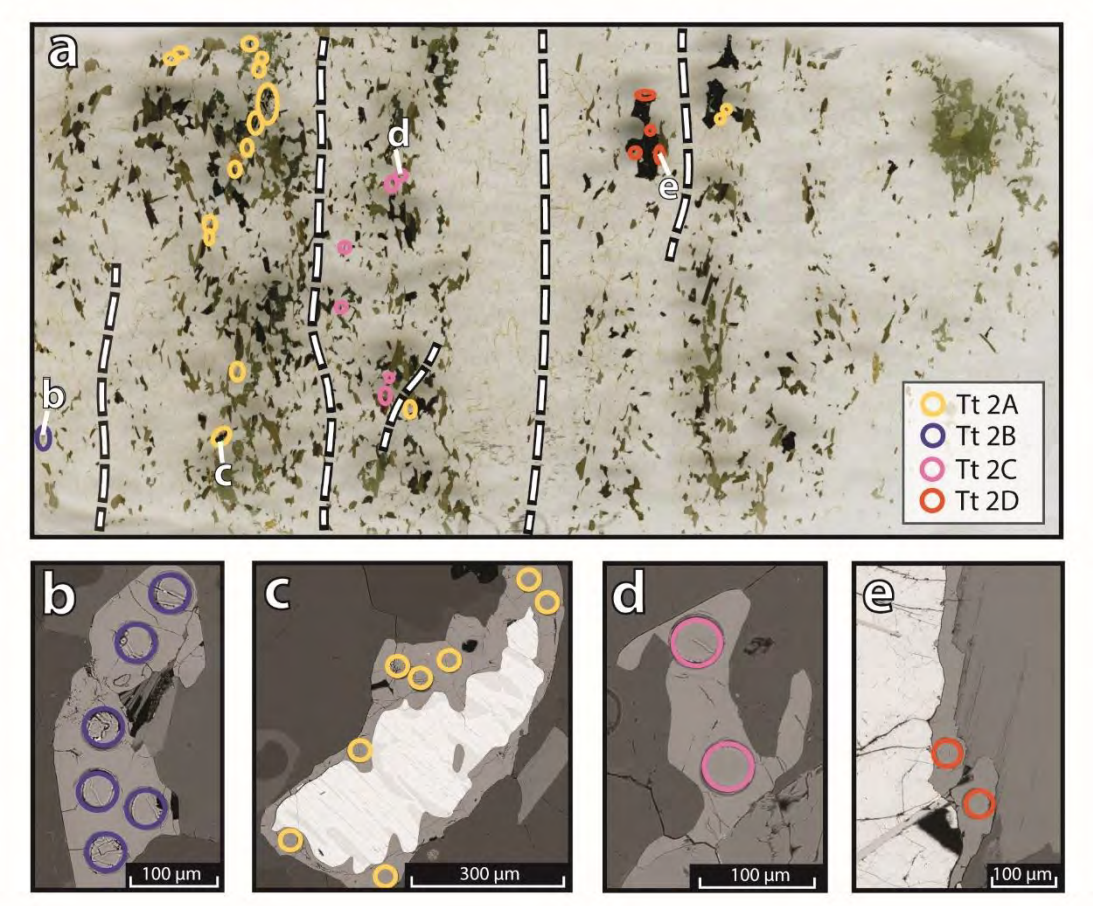

Figure 6.8 (A) Image of thin section DG02 showing locations of analysed titanite grains, coloured according to REE population. **(B - E)** Representative BSE image of titanite in each population.

disproportionate effect on these 12 analyses; therefore, they are excluded from the age calculation.

Minor Pb and/or U mobility in this sample is evidenced by the spread in $^{238}U/^{206}Pb$ ratios for a given $^{207}Pb/^{206}Pb$ ratio. A histogram of ^{207}Pb-corrected $^{238}U/^{206}Pb$ ages shows a wide range from 1030 to 1309 Ma, with a probability maximum at 1148 Ma; the spread to younger ages is interpreted as a result of Pb loss. An anchored regression of the 72 analyses with the oldest ^{207}Pb-corrected $^{238}U/^{206}Pb$ ages produces a lower intercept age of 1175 ± 9 Ma (MSWD = 4.4); excluding two outliers, the lower intercept age is 1170 ± 8 Ma (MSWD = 3.1).

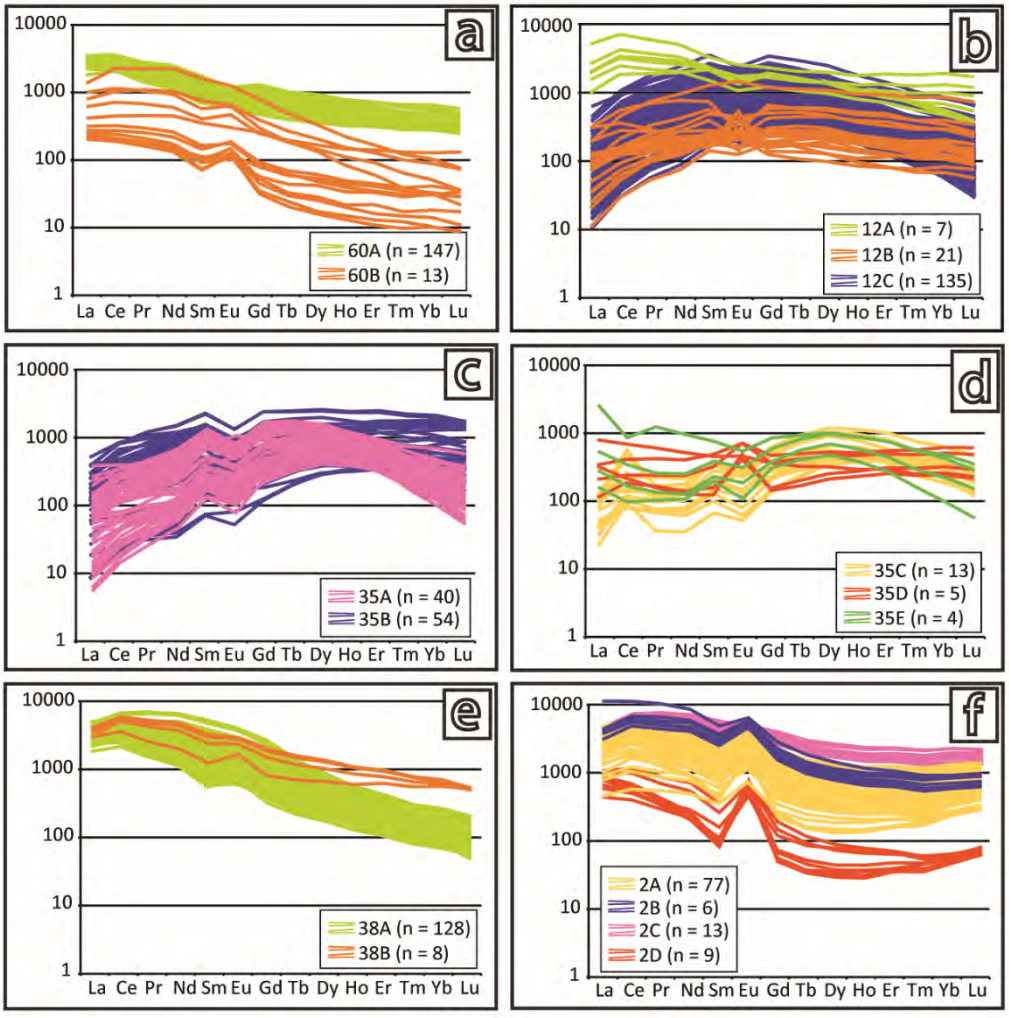

Figure 6.9 Chondrite-normalised REE patterns of titanite in each sample. Patterns are coloured according to population. **(A)** Sample EAF60; **(B)** sample EAF12; **(C – D)** sample EAF35, shown on two plots for legibility; **(E)** sample EAF38; **(F)** sample DG02.

6.4.6 Garnet compositions and REE patterns

The major and trace element composition of garnet in samples EAF60, EAF12 and EAF38 was analysed by WDS and by LA-ICPMS. The full results of these analyses are in Appendix 6.2, and chondrite-normalised REE patterns are in Figure 6.10 (chondrite composition from Palme and O'Neill, 2003).

In EAF60, small anhedral garnet grains are spatially associated with pyroxene, hornblende and ilmenite. Garnet is almandine-rich with a typical composition of $Alm_{55}Gro_{35}Py_{7}Sp_{2}$, and is not compositionally zoned for major elements. Garnet REE patterns are LREE depleted with flat, but somewhat variable, trends from Eu to Lu; one garnet rim is slightly HREE depleted (Figure 6.10a).

Sample EAF12 contains numerous large (4 – 10 mm) rounded garnets with average composition $Alm_{48}Gro_{39}Py_{8}And_{3}Sp_{2}$, and with slightly Fe-enriched rims and Mg-enriched cores. HREE patterns are flat to slightly enriched, with no difference between cores or rims (Figure 6.10b).

Garnet in sample EAF38 is small-grained (0.2 – 1 mm), euhedral and poikilitic with an average composition of $Alm_{54}Gro_{22}Py_{21}$-$And_{2}Sp_{2}$, and with Fe-rich rims and Mg-rich cores. There is significant variability in the slope of the HREE pattern, which correlates with analyses on garnet cores and rims: garnet cores are HREE-enriched or flat, whereas garnet rims are HREE-depleted (Figure 6.10c).

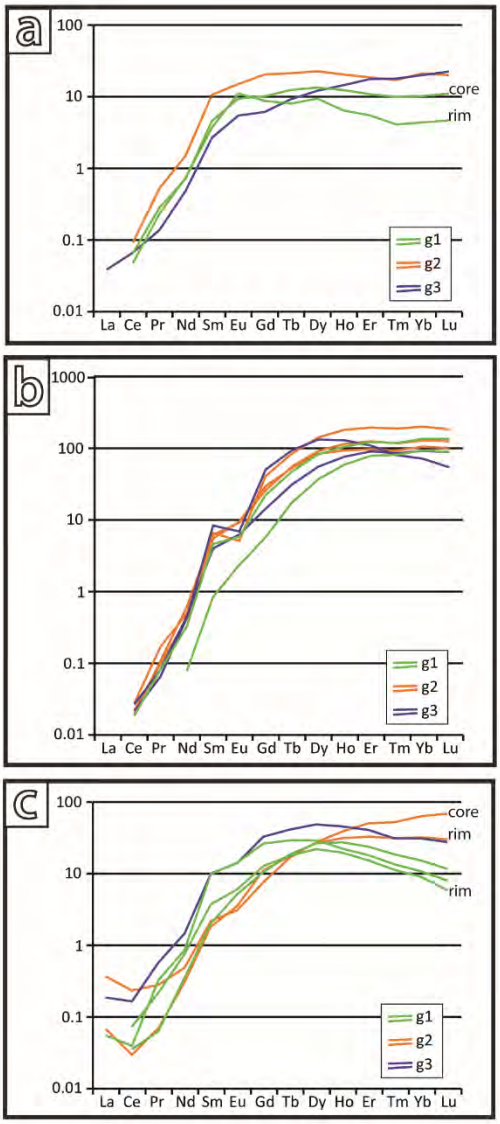

Figure 6.10 Chondrite-normalised REE patterns of garnet in **(A)** sample EAF60; **(B)** sample EAF12; **(C)** sample EAF38. Labels g1, g2 and g3 correspond to the garnets labelled in Figures 4a, 5a and 7a. Where analyses are clearly on garnet core or rim, these are labelled as such; the remaining analyses are intermediate between core and rim.

6.5 Discussion

6.5.1 Identifying titanite populations

BSE images of zoning in titanite can be used to identify (re)crystallisation processes, which may then be correlated with changes in the concentration of major and trace elements (e.g. Lucassen et al., 2011; Gao et al., 2012). The REE signature provides one simple way to identify and discriminate between multiple populations for large numbers of titanite analyses (e.g. Storey et al., 2007; Gao et al., 2012; Bruand et al., 2014).

We use chondrite-normalised REE patterns, together with BSE images, to identify 2 - 5 titanite populations in all five samples. Some of these populations would not have been recognised using only BSE images, because of the low signal contrast between different compositions of titanite, particularly when comparing two non-adjacent, individually unzoned titanite grains. In addition, we note that the zoning in most samples was not visible during initial imaging with an older generation, less sensitive SEM, but required the more sensitive, in-column BSE detector on a FEI Varios XHR SEM. This highlights the potential for using REE patterns to identify titanite compositional populations not visible with standard imaging techniques.

In the following discussion, 'population' refers only to a group of titanite analyses with a distinct composition, whereas 'generation' is used to describe a titanite population that crystallised at a specific time. Several conclusions about titanite crystallisation can be drawn from the relationships between titanite trace element content, the zoning visible in BSE images, and spatial and textural characteristics.

Titanite zoning in BSE images

Compositional zoning in titanite can be linked to crystallisation processes, just as in other minerals such as zircon (e.g. Connelly, 2000; Corfu et al., 2003; Taylor et al., 2016). For example, changes in pressure, temperature or fluid composition may result in core-rim zoning; zoning may be sharp or smooth depending on whether titanite growth is continuous (Lucassen et al., 2011). Solid state diffusion may smooth formerly sharp boundaries over time, whereas titanite recrystallisation due to fluid

infiltration will produce irregular zoning following fractures, grain and subgrain boundaries (e.g. Papapavlou et al., 2017). Conversely, a uniform titanite composition, both at the single-grain and sample scale, may suggest either rapid crystallisation during a single event, or equilibration of compositions over long periods of time by intracrystalline diffusion (Smith et al., 2009; Lucassen et al., 2011).

All samples except DG02 contain at least one titanite grain that is visibly zoned in BSE images, and in which the different zones correspond to different REE populations. This is an important observation, because the presence of titanite with different compositions within a single grain suggests either that there are multiple generations of titanite growth, or that titanite crystallised under changing conditions.

Core-rim zoning is observed in samples EAF60, EAF12, and EAF35. Titanite rims are narrow (<10 μm) and sharp in sample EAF60, suggesting minimal overgrowth on an older titanite generation (Figure 6.4b). In contrast, the gradational boundaries between zones in some grains in sample EAF12 may be a result of continuous titanite growth during changing P-T conditions, or of solid-state diffusion re-equilibrating compositions across formerly sharp boundaries (Figure 6.5b). In sample EAF35, the separation of titanite cores and rims by a ring of rutile inclusions provides strong evidence that changing P-T conditions drove the core-rim zoning (Figure 6.6b). This texture suggests the prograde breakdown of titanite to form rutile, later followed by additional titanite growth and possible retrogression of rutile to titanite.

Irregular zoning following fractures and subgrain boundaries is visible in sample EAF12, both in the cores of large titanite grains, and in titanite inclusions in garnet. This is interpreted as evidence for fluid-assisted titanite recrystallisation (Figure 6.5c).

Although no sample contained a single, uniform titanite population, the main population of titanite in sample EAF60 (population 60A) is remarkably homogenous in REE content and U/Pb age, and is unzoned, with the exception of sharp, narrow rims (Figure 6.4b). Together with the high Zr-in-Tt temperature (909 ± 10 °C), and a U/Pb age that predates metamorphic zircon growth at this locality by c. 10 Ma (Clark et al., 2014), this suggests that titanite population 60A is magmatic, and records igneous crystallisation.

Spatial trace element variability

Titanite in samples EAF60, EAF38 and DG02 produced multiple REE populations, but titanite composition varies between grains, not within grains (Figures 6.4a, 6.7a, 6.8a). Examining the spatial relationship between titanite location and trace element composition in these samples shows that trace element availability at the cm to mm-scale during titanite (re)crystallisation was an important control on composition.

In EAF60 and EAF38, titanite REE composition correlates with proximity to garnet (Figure 6.4a, 6a). Of the 41 titanite grains in mafic gneiss EAF60, only two grains are directly adjacent to garnet, and it is the analyses on these two grains that deviate from the homogenous, dominant main titanite population. Conversely, of the 24 grains analysed in sample EAF38, only one grain is not adjacent to garnet, and the analyses on this grain form a unique REE population (38B). The two grains in sample EAF60 and one grain in sample EAF38 are also the only irregularly zoned titanite grains in each sample, and are interpreted as recording the partial recrystallisation of older titanite during metamorphism.

The spatial distribution of the four titanite generations in sample DG02 is illustrated in Figure 6.8a, demonstrating the clear variation of titanite composition between biotite-rich schlieren in the gneiss. Within each of the schlieren, titanite in both textural positions (small, subhedral grains in the matrix, and thin rims around large magnetite crystals) has the same composition, and the same REE pattern. This suggests that the primary control on titanite composition in sample DG02 is the availability of trace elements during crystallisation. Within each schlieren, titanite grew in a single, short period of time, producing grains with uniform compositions.

6.5.2 REE and Th/U as geochemical indicators in titanite

The major and trace element composition of titanite is controlled by element availability and compatibility at the time of crystallisation (e.g. Smith et al., 2009; Gao et al., 2012). Two titanite grains that crystallise under different conditions (e.g. igneous crystallisation from a magma vs. later metamorphic growth) and in equilibrium with different minerals are expected to differ in composition. Variations

in trace element signatures can, therefore, provide important information about the crystallisation processes of the titanite (Lucassen et al., 2011).

A small number of existing studies report chondrite-normalised REE patterns (Storey et al., 2007; Smith et al., 2009; Gao et al., 2012; Bruand et al., 2014; Papapavlou et al., 2017). These studies divide titanite into populations according to microstructure (rim or core), and in each case, the populations are distinct with respect to REE composition.

Gao et al. (2012) analysed a single sample in which magmatic titanite cores are overgrown by metamorphic titanite rims. They report high REE content, strongly negative Eu anomalies, and flat MREE-HREE (heavy-REE) patterns in the cores, and also suggest the high Th/U ratios in titanite cores are diagnostic of magmatic titanite. The metamorphic rims, in contrast, have low REE content, slightly negative Eu anomalies, are HREE depleted, and have low Th/U ratios.

Storey et al. (2007) interpret a flat middle-REE (MREE) pattern in titanite cores as an indicator of equilibrium crystallisation during metamorphism, due to the preferential incorporation of MREE into the titanite lattice (Tiepolo et al., 2002; Prowatke and Klemme, 2005). Light-REE (LREE) enrichment in titanite rims is interpreted as a result of either closed-system REE fractionation during titanite growth, or titanite crystallisation in the presence of a LREE-rich fluid. In either case, the REE patterns in titanite rims are interpreted to reflect regional trends in trace element enrichment during metasomatism (Storey et al., 2007). Similarly, Smith et al. (2009) attribute changes in titanite REE content to the composition of circulating hydrothermal fluids, and Bruand et al. (2014) attribute small changes in titanite REE content to equilibrium crystal fractionation, and the changing chemistry of the whole-rock as a result of magma mixing. More recently, Papapavlou et al. (2017) report LREE-depletion in titanite as a product of the co-crystallisation of a LREE-sequestering mineral such as allanite.

To build on these studies, below, we explore the use of the REE pattern and Th/U ratio in titanite as geochemical indicators.

Titanite HREE content and garnet growth

Garnet is one of the most useful thermobarometric minerals, and so characterising the crystallisation history of titanite relative to this bellwether mineral would provide valuable thermal constraints on the U/Pb age data. Titanite preferentially incorporates the MREE over the LREE and the HREE (Tiepolo et al., 2002; Prowatke and Klemme, 2005), whereas garnet strongly prefers the HREE. Therefore, titanite that crystallises in equilibrium with garnet is expected to be significantly HREE depleted, as any available HREE are preferentially partitioned into garnet.

To investigate the relationship between titanite and garnet HREE content, we examine three garnet-bearing samples (EAF60, EAF12, EAF38) and one sample without garnet (DG02). In the following discussion, the Dy/Yb ratio is used as a measure of the slope of the heavy rare earth patterns (HREE), where a high Dy/Yb ratio means titanite is depleted in HREE relative to the MREE.

The REE patterns of titanite and of coexisting garnet are summarised in Figures 6.9 and 6.10 respectively. Titanite HREE patterns range from flat to depleted, with average Dy/Yb ratios of 1.3 – 13. Garnet displays flat to enriched HREE patterns (Dy/Yb = 0.6 – 1.6), although some garnets are slightly HREE depleted at the rims (Dy/Yb = 2.0 – 4.2; particularly in EAF38).

As can be seen in Figure 6.11, titanite that crystallised in the presence of garnet is significantly more HREE depleted (lower Dy/Yb ratios) than titanite that crystallised in the absence of garnet.

For example, sample DG02 contains no garnet, and all titanite in the sample has a low average Dy/Yb = 1.6.

Sample EAF60 contains two titanite populations. Titanite in the main population, 60A, is located away from the garnet in the thin section, and is interpreted as relict magmatic titanite; this population also has a low average Dy/Yb of 2.7. In contrast, the two strongly zoned titanite grains in population 60B are adjacent to garnet (Figure 6.4a). Analyses of titanite cores in these two grains have low Dy/Yb ratios of ~ 2.4, but those analyses that ablated the lighter zoned rims are HREE depleted, with higher

Dy/Yb ratios of 3.6 – 6.5, proportional to mixing between the light and dark zoned titanite (Figure 6.11). The garnet adjacent to these two grains is HREE-enriched with a Dy/Yb ratio of 0.93 (garnet g2 in Figure 6.10a), suggesting the HREE were preferentially incorporated into garnet rather than titanite during the metamorphic recrystallisation of igneous titanite.

Conversely, most titanite in garnet amphibolite EAF38 is spatially associated with abundant garnet, and titanite Dy/Yb ratios in this main population (38A) are high, with an average Dy/Yb = 6.2 and up to 13.2 in one grain. Titanite in this sample occurs as coronas around intergrown rutile and ilmenite, suggesting it is a product of the retrograde breakdown of rutile to form titanite. Garnet Dy/Yb ratios in EAF38

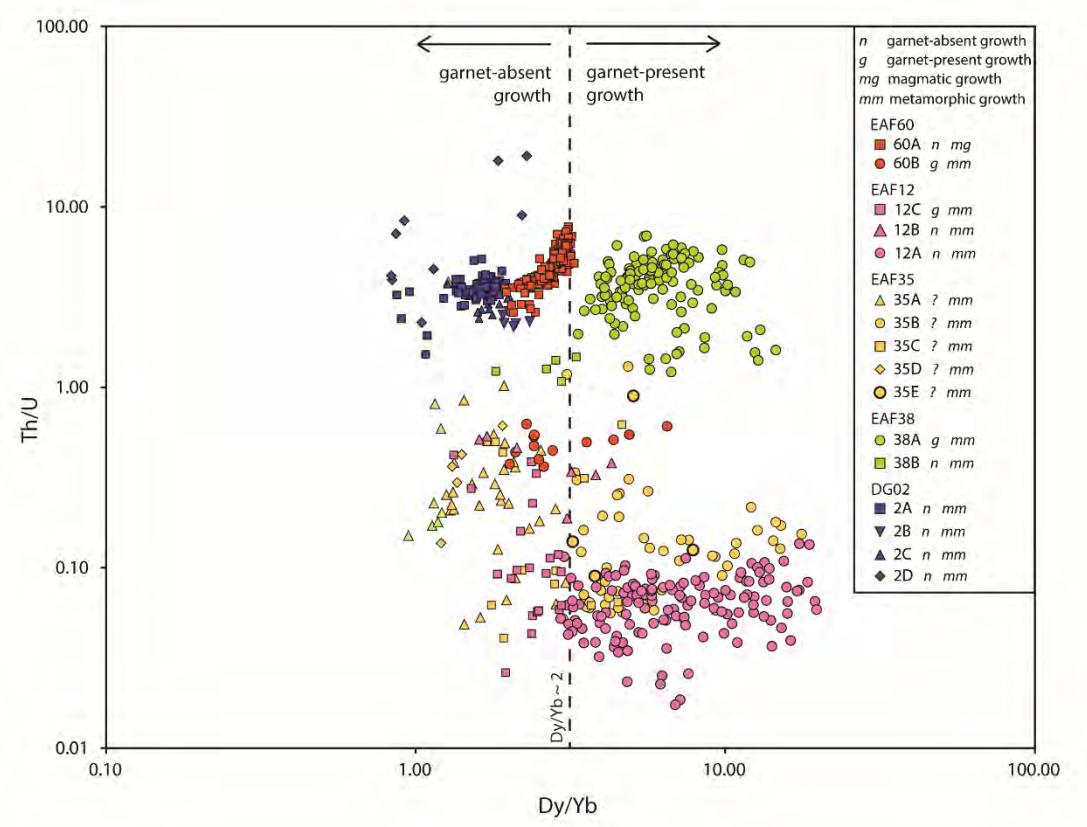

Figure 6.11 Dy/Yb ratio plotted against Th/U ratio of all analyses, subdivided by titanite REE population. Dy/Yb (a measure of HREE fractionation) is > 2 for titanite that crystallised in the presence of significant garnet (*g*), but is < 2 for titanite that did not crystallise in equilibrium with garnet (*n*). The exception is titanite from EAF35, which has a complex, polygenetic growth history. The Th/U ratio cannot be used as a diagnostic tool to discriminate between magmatic (*mg*) and metamorphic (*mm*) titanite.

range from 0.6 in one garnet core (HREE enriched), to 4.2 in one garnet rim (HREE depleted). HREE depletion in garnet rims suggests that garnet crystallised in a closed system with finite REE content, in which early garnet growth reduces the amount of HREE available for later growth (e.g. Whitehouse and Platt, 2003). In addition, although the total HREE content of titanite is higher than that of garnet, the modal abundance of garnet in sample EAF38 is significantly greater. Therefore, garnet growth must have been an important control on the availability of HREE during metamorphism, and consequently during titanite growth.

This conclusion is further supported by the fact that the titanite grain with the most enriched HREE signature is the grain furthest from garnet in the thin section (average Dy/Yb = 2.7; Figure 6.7a). Notably, this is also the only grain in this sample to exhibit zoning in BSE images. The irregular zoning suggests the partial recrystallisation of an older titanite generation, possibly fluid-assisted and during metamorphism. Because this titanite grain rims rutile, a retrograde reaction texture suggesting rutile breakdown, both titanite generations probably post-date significant garnet growth. Therefore, the low Dy/Yb ratio of this titanite grain (population 38B) may reflect a small equilibration volume for HREE, such that the availability of HREE during titanite growth (and/or recrystallisation) was not strongly affected by garnet growth elsewhere in the sample.

The main population of titanite in sample EAF12 (12C), occurring as single grains or as rims on larger zoned titanite grains, has a high average Dy/Yb = 8.0. In contrast, the titanite cores that constitute populations 12A (inclusions in garnet) and 12B (in the matrix) have lower average Dy/Yb ratios of 2.8 and 2.3 respectively. The flat to HREE-enriched garnet patterns in this sample (Dy/Yb = 0.6 – 1.25; one garnet rim with Dy/Yb = 2.9) suggest HREE were preferentially incorporated into garnet. While the actual HREE content of some titanites is higher than that of garnet, the modal abundance of garnet is significantly greater (Figure 6.5a), and therefore the HREE-depletion of population 12C is a product of metamorphic titanite growth in the presence of garnet. The low Dy/Yb ratios of titanite cores (12A and 12B) are a record of early titanite growth, prior to the crystallisation of garnet.

Although garnet crystallisation will strongly influence the HREE available for subsequent titanite crystallisation, we note that titanite HREE content also depends on factors such as bulk-rock composition, or the growth of another HREE-sequestering mineral. For example, 58 of 116 titanite analyses in sample EAF35 are depleted in HREE (average Dy/Yb = 6.5; Figure 6.9c-d). However, the thin section contains only three small (< 0.4 mm diameter) garnet grains, with no observable relationship between garnet and titanite HREE content (with the caveat that the 3D distribution of garnet cannot be determined from thin section). Therefore, the high titanite Dy/Yb ratios cannot obviously be attributed to garnet growth. Instead, we note that EAF35 contains at least two titanite generations: textural characteristics suggest prograde breakdown of early titanite to form rutile, and later retrograde breakdown of rutile to form new titanite. A polygenetic growth history is also supported by the complex distribution of U/Pb data from sample EAF35 (Figure 6.3c). The different titanite generations may have crystallised under significantly different conditions, possibly in equilibrium with different mineral assemblages.

Regardless, the samples analysed in this study provide strong evidence that garnet crystallisation contributes to depleted HREE patterns in titanite. Titanite that crystallised in the absence of garnet typically has flat HREE patterns with Dy/Yb ratios < 2 (e.g. samples DG02 and EAF60), whereas titanite that crystallised in equilibrium with sufficient garnet is HREE depleted, with Dy/Yb > 2 (e.g. samples EAF38 and EAF12; Figure 6.11). The spatial relationship of garnet and titanite in samples EAF38 and EAF60 suggests a millimetre-scale control on REE equilibration between these two phases. Alternatively, if a sample contains titanite with both flat and depleted HREE patterns, titanite growth may have occurred both prior to and during (or after) the appearance of garnet, respectively (if supported by textural information; e.g. EAF12). The HREE content of complexly zoned titanite that potentially crystallised at different times and under a range of conditions is more difficult to interpret (e.g. EAF35).

Titanite Eu anomaly and LREE content

The factors affecting Eu and LREE in the analysed samples are difficult to untangle. As with other accessory minerals, the REE budget depends both on the

whole-rock composition, and the timing of titanite crystallisation relative to other minerals (Bruand et al., 2014). For example, Papapavlou et al. (2017) show that titanite will be LREE-depleted if it crystallises after minerals that preferentially incorporate the LREE (e.g. monazite, allanite and apatite); conversely, titanite may be LREE-enriched if it crystallises after minerals that preferentially incorporate the HREE (e.g. garnet and zircon). In zircon, Eu anomalies are typically linked to co-crystallisation with plagioclase, although a negative Eu anomaly may also reflect an inherited signature from the protolith (Rubatto, 2002); these same factors are also expected to influence the Eu content of titanite. In addition, Eu is redox sensitive, and partitioning will be strongly influenced by the oxidation state (e.g. Philpotts, 1970), although Eu^{3+} is most likely during titanite crystallisation because the presence of titanite implies high fO_2.

To add to this complexity, the trace element content of titanite strongly depends on local element availability during crystallisation (Lucassen et al., 2011). For example, we have already identified cm- to mm-scale controls on titanite composition relative to the spatial distribution of garnet in samples EAF60 and EAF38, and relative to the gneissic compositional banding in DG02.

In our five samples, titanite Eu anomalies range from negative (e.g. EAF12) to positive (e.g. DG02), and LREE patterns range from enriched (e.g. EAF38) to depleted (e.g. EAF35) (Figure 6.9). There is no obvious correlation of Eu or LREE with mineralogy (e.g. plagioclase, pyroxene, amphibole, apatite), lithology, or whether titanite crystallised during metamorphism or magmatism.

In these five samples, the usefulness of the Eu anomaly and LREE pattern appears limited to providing evidence for titanite recrystallisation and/or elemental mobility; i.e. as an aid in discriminating between populations of titanite.

The Th/U ratio

On the basis of a single sample, Gao et al. (2012) suggest that high Th/U ratios (> 1.5) may be diagnostic of magmatic titanite, whereas metamorphic titanite yields low Th/U ratios (< 1.5). We test this conclusion by calculating average Th/U ratios for each titanite population across our five samples (Figure 6.11).

In samples EAF12 and EAF35, the titanite textures unambiguously indicate that titanite grew during metamorphism, in equilibrium with the metamorphic mineral assemblage and fabric. The Th/U ratio in these samples is low, ranging from 0.06 – 0.54. The two titanite grains in sample EAF60 that were recrystallised in the presence of garnet during metamorphism also have low average Th/U ratios of 0.49, whereas the main population of magmatic titanite has a high average Th/U ratio of 4.71.

However, titanite in sample EAF38 also grew during metamorphism, yet the main population (38A; spatially associated with garnet) has a high average Th/U ratio of 3.8. The one titanite grain that was partially recrystallised during metamorphism has a lower average Th/U ratio of 1.29.

In sample DG02, titanite REE composition varies between gneissic compositional bands, which suggests that titanite crystallisation was associated with the development of the metamorphic fabric. Most titanite in this sample has average Th/U ratios of 2.4 – 3.5.

Therefore, although the highest and lowest Th/U ratios do appear to correspond with magmatic and metamorphic titanite respectively, the high Th/U ratios of metamorphic titanite in EAF38 and DG02 contradict this association (Figure 6.11). These data suggest that the conclusion of Gao et al. (2012) with regards to metamorphic titanite and low Th/U is not ubiquitous across all growth environments, and is of limited use as a diagnostic tool.

6.5.3 REE patterns and the geological significance of titanite U-Pb ages

An important application of the titanite REE patterns is their ability to link the U/Pb data to specific titanite populations and geologic processes. Given the wide range in possible closure temperatures for Pb diffusion in titanite (650 – 1030 °C; Cherniak, 2010), and the possibility for U/Pb ages in titanite to record magmatic crystallisation, solid-state metamorphic growth, or cooling, identifying the processes controlling the distribution of the U/Pb data is crucial for understanding the geological significance of a U/Pb age.

The U/Pb data for each sample are plotted by titanite REE population on a Tera-Wasserburg concordia in Figure 6.3f – j. The relationships between titanite

composition, Pb_C and $^{238}U/^{206}Pb$ contribute to deciphering the geological significance of the U/Pb age. The five new titanite U/Pb ages record a combination of magmatic inheritance (EAF60), metamorphic growth ages (EAF35, EAF38 and DG02), and cooling (EAF12).

Sample EAF60: Magmatic crystallisation age; metamorphic rims

Sample EAF60 contains two populations of titanite: the compositionally homogenous magmatic main population (60A), and two zoned titanite grains depleted in HREE and adjacent to garnet (60B) (Figure 6.4). The analyses in 60B contain more Pb_C and less total U and Pb than analyses in population 60A, interpreted as a result of the partial recrystallisation of these two titanite grains during metamorphism and garnet growth.

Titanite in sample EAF60, therefore, preserves evidence of two events: igneous titanite crystallisation at 1303 ± 5 Ma (60A), and metamorphic titanite recrystallisation (60B). The high Zr-in-Tt crystallisation temperature of 909 ± 10 °C for population 60A is consistent with the emplacement temperatures of a mafic magma (e.g. Huppert and Sparks, 1988). Although no age could be calculated for the metamorphic recrystallisation of 60B, the Zr-in-Tt crystallisation temperatures for these two titanite grains are 789 ± 10 °C. The sharp, narrow rims visible in BSE images of some titanite in population 60A may also be a product of this metamorphic event (Figure 6.4b).

Sample EAF35: Maximum age for metamorphism

Titanite in sample EAF35 has a wide range of compositions, and is separated into five populations on the basis of REE chemistry (Figure 6.9d-e). The sample is texturally complex; irregularly zoned titanite cores are surrounded by a halo of rutile inclusions, which are in turn overgrown by more titanite. The multiple generations of titanite may have crystallised under significantly different conditions, possibly in equilibrium with different mineral assemblages.

The U/Pb data are also complex, with significant dispersion on the Tera-Wasserburg concordia. Titanite populations do not correlate with position on the concordia, and Pb and/or U mobility (responsible for the horizontal spread of analyses on the concordia) has affected all populations of titanite (Figure 6.3h). The

lack of any correlation between titanite population and age suggests that volume diffusion of Pb and/or U is the primary control on age in this sample (i.e. rather than the recrystallisation of titanite, which would homogenise compositions).

It is difficult to attach geological significance to the complex data in this sample, especially given the presence of multiple generations of titanite and evidence for significant U/Pb mobility. The simplest explanation is that older titanite generations are partially reset by volume diffusion of Pb during later metamorphism. However, the oldest six individual titanite analyses have ^{207}Pb-corrected ^{238}U/^{206}Pb ages between 1680 – 2470 Ma. These are older than the 1668 ± 11 Ma U/Pb zircon age for the magmatic crystallisation of another sample of granodiorite gneiss at this locality (Kirkland et al., 2012), suggesting that Pb gain and/or U loss may have affected some titanite grains.

The sample of granodiorite gneiss analysed by Kirkland et al. (2012) also yielded a poorly constrained U/Pb zircon age for metamorphism at 1162 ± 39 Ma (1σ, n = 6). Conservatively, the U/Pb titanite age of 1213 ± 16 Ma age for the 67 youngest ^{207}Pb-corrected analyses is interpreted as a maximum age for overprinting metamorphism. Textural and compositional information suggests that EAF35 may have crystallised a significant proportion of its titanite prior to this event, but due to significant (and incomplete) resetting of the U/Pb geochronometer, geologically meaningful ages are not preserved for these older generations.

Because U/Pb of titanite in sample EAF35 was partially reset during metamorphism, the Zr-in-Tt crystallisation temperature of 711 ± 30 °C may be based on one or more of these older titanite generations, and is not a reliable thermal constraint for 1213 ± 16 Ma metamorphism.

Sample EAF38: Metamorphic growth age

As discussed above, the main population of titanite in sample EAF38 (38A) is unzoned in BSE images, and crystallised with (or after) garnet, forming HREE-depleted titanite coronas around intergrown rutile and ilmenite (Figure 6.7b). The irregularly zoned, partially recrystallised titanite grain in population 38B also rims rutile, but spatial considerations and the lower Dy/Yb ratio suggest this grain did not

(re)crystallise in equilibrium with garnet (possibly due to a small equilibration volume).

Notably, the two titanite populations incorporated different amounts of Pb_C (Figure 6.3i). Titanite in population 38B (partially recrystallised during metamorphism) contains up to 1.6% Pb_C. In contrast, titanite in population 38A (completely (re)crystallised during metamorphism) contains up to 17% Pb_C. However, all titanite in sample EAF38 records the same U/Pb age (Figure 6.3d). The unzoned, homogenous appearance and composition of population 38A suggests it crystallised in a single, short event. Population 38B contains older, partially recrystallised titanite, but to record the same age as population 38A, the U/Pb chronometer must have been completely reset during metamorphism.

The titanite U/Pb age of 1194 ± 5 Ma is within error of a nearby zircon U/Pb age dating high-grade metamorphism (1193 ± 9 Ma; Kirkland et al., 2010). Therefore, the titanite age is interpreted to date metamorphic titanite (re)crystallisation during or following garnet growth, at a Zr-in-Tt crystallisation temperature of 760 ± 14 °C (Table 6.2).

Sample DG02: Metamorphic growth age

In sample DG02, titanite composition varies spatially with the gneissic compositional banding (Figure 6.8a). As in sample EAF38, the four titanite populations in DG02 incorporated different amounts of Pb_C, yet titanite in all populations is interpreted to record the same U/Pb age, as demonstrated by all analyses falling on a single Pb_C – Pb* mixing line (analyses that plot significantly to the right are interpreted as affected by Pb loss) (Figure 6.3e, j).

The single age population supports the interpretation of a schlieren-scale spatial control on titanite composition. Because titanite crystallised coevally throughout the sample, the differences in Pb_C content are simply a result of local elemental availability during titanite crystallisation.

Although no additional U/Pb zircon geochronology exists at this locality, Bodorkos and Clark (2004b, 2004a) report a U/Pb zircon age of 1168 ± 12 Ma from a syn-kinematic pegmatite dyke 25 km to the southwest, interpreted to date 750 – 800

°C, 5 – 6 GPa metamorphism. Therefore, the 1170 ± 8 Ma titanite U/Pb age for sample DG02 is interpreted as the age of titanite growth during metamorphism throughout the sample, with a Zr-in-Tt crystallisation temperature of 753 ± 18 °C.

Sample EAF12: Cooling age

Titanite in sample EAF12 occurs as inclusions in garnet and in the matrix; both types of titanite display core-rim zoning in BSE images. Populations 12A and 12B consist of the cores of zoned titanite grains, and pre-date garnet growth; the main population (12C) is composed of analyses of unzoned grains and rims of zoned grains, and grew in equilibrium with garnet. Although not unambiguous, due to the small number of analyses (n = 7), population 12A appears to plot slightly to the left of the Pb_C – Pb* mixing line (Figure 6.3g). In contrast, populations 12B and 12C have the same range of U/Pb compositions.

This correlation of titanite population 12A with older ^{207}Pb-corrected $^{238}U/^{206}Pb$ ages suggests that the U/Pb system in this population was not fully reset by metamorphism. Population 12A is therefore interpreted as an older generation of titanite, overprinted by metamorphic rims and partially reset during metamorphism. The apparent age of this relic titanite population is poorly defined at 1260 ± 74 Ma (MSWD = 20), and is not considered geologically significant. In addition, as this age reflects incomplete U/Pb resetting, the original titanite growth event for population 12A must have been > 1260 ± 74 Ma.

In contrast, populations 12B and 12C yield a single, well-defined U/Pb age of 1163 ± 8 Ma, even though REE patterns suggest that the two populations crystallised at different times relative to garnet. This 1163 ± 8 Ma titanite age is interpreted as a cooling age, based on two key points.

First, the preservation of titanite with different REE compositions means that EAF12 was not subject to U/Pb resetting by pervasive metamorphic recrystallisation, which would be expected to produce a single population of homogenous composition. Rather, volume diffusion of Pb above the closure temperature must have been the major driver of U/Pb resetting in sample EAF12.

Second, although the U/Pb age of titanite in EAF12 is well-defined (Figure 6.3b), it is significantly younger than the age of metamorphism at this locality. A different sample from this locality yielded an 1196 ± 11 Ma U/Pb age for metamorphic zircon rims, interpreted as the age of high-grade metamorphism and migmatisation (garnet gneiss 194789; Kirkland et al., 2016). Assuming titanite in EAF12 crystallised during this metamorphic event, the Zr-in-Tt titanite crystallisation temperature of 728 ± 30 °C provides a constraint on the temperature of this metamorphism.

Another titanite sample from this locality produced a median ^{207}Pb-corrected ^{238}U/^{206}Pb titanite age of 1203 ± 6 Ma, interpreted as approximating the age of metamorphism (sample 184386; Kirkland et al., 2016). Nonetheless, the youngest 45% of titanite analyses in sample 184386 yield a weighted average ^{207}Pb-corrected ^{238}U/^{206}Pb age of 1164 ± 5 Ma, within error of the inferred 1163 ± 8 Ma cooling age for titanite in sample EAF12. This suggests that titanite in sample 184386 has undergone a degree of partial resetting of the U/Pb system, with the ages of individual analyses spread between metamorphism at c. 1203 Ma, and cooling through the Pb closure temperature 40 Ma later. In contrast, the titanite U/Pb chronometer in EAF12 appears to have been more pervasively reset, and preserves dominantly cooling ages.

6.6 Conclusion

In this study, we explore the use of the trace element composition of titanite as a geochemical indicator in five titanite samples from the east Albany-Fraser Orogen, Western Australia.

Chondrite-normalised REE patterns are used to group titanite analyses into several populations, which correspond with the compositional zoning visible in BSE images and have distinct major and trace element compositions. The REE patterns are useful for mapping the spatial distribution of titanite populations in each sample, and for identifying the dominant processes controlling the U/Pb systematics.

Analyses of titanite cores and rims in samples EAF12 and EAF35 show that earlier generations of titanite are partially recrystallised and rimmed by later titanite with a different composition. In contrast, differences in titanite composition at the single-grain scale is a product of cm- to mm-scale differences in trace element

availability during titanite crystallisation, either due to proximity to garnet during metamorphic recrystallisation (samples EAF60 and EAF38), or due to differences in trace element availability between schlieren in a gneiss (sample DG02).

The HREE content of titanite can be used to link titanite and garnet crystallisation. Titanite that crystallises in equilibrium with abundant garnet is HREE depleted, with high Dy/Yb ratios > 2 (samples EAF38 and EAF12), whereas titanite crystallising in the absence of sufficient garnet typically has flat HREE patterns with low Dy/Yb ratios < 2 (DG02 and EAF60). However, the factors affecting the LREE content and Eu anomaly in titanite are complex, and these trace elements are mainly useful for discriminating between titanite populations with different compositions.

Although the Th/U ratio is highest in inferred magmatic titanite (sample EAF60) and lowest in metamorphic titanite (sample EAF12), this ratio is not a uniquely diagnostic tool; metamorphic titanite in samples EAF38 and DG02 also yields high Th/U ratios.

Finally, we integrate the textural, spatial and petrological interpretations with the U/Pb data to evaluate the geological significance of each titanite age. The five U/Pb ages record a combination of magmatic inheritance (EAF60), metamorphic crystallisation ages (EAF35, EAF38 and DG02), and titanite cooling ages (EAF12).

6.7 References

Aleinikoff, J. N., Wintsch, R. P., Tollo, R. P., Unruh, D. M., Fanning, C. M., and Schmitz, M. D., 2007, Ages and origins of rocks of the Killingworth dome, south-central Connecticut: implications for the tectonic evolution of southern New England: American Journal of Science, v. 307, p. 63-118.

Bodorkos, S., and Clark, D., 2004a, Evolution of a crustal-scale transpressive shear zone in the Albany-Fraser Orogen, SW Australia: 1. P-T conditions of Mesoproterozoic metamorphism in the Coramup Gneiss: Journal of Metamorphic Geology, v. 22, p. 691 - 711.

-, 2004b, Evolution of a crustal-scale transpressive shear zone in the Albany-Fraser Orogen, SW Australia: 2. Tectonic history of the Coramup Gneiss and a kinematic framework for Mesoproterozoic collision of the West Australian and Mawson cratons: Journal of Metamorphic Geology, v. 22, p. 713-731.

Bruand, E., Storey, C. D., and Fowler, M., 2014, Accessory mineral chemistry of high Ba-Sr granites from Northern Scotland: Constraints on petrogenesis and records of whole-rock signature: Journal of Petrology, v. 55, no. 8, p. 1619-1651.

Cherniak, D. J., 1993, Lead diffusion in titanite and preliminary results on the effects of radiation damage on Pb transport: Chemical Geology, v. 110, p. 177-194.

-, 2010, Diffusion in accessory minerals: zircon, titanite, apatite, monazite and xenotime: Reviews in Mineralogy and Geochemistry, v. 72, p. 827-869.

Chew, D. M., Petrus, J. A., and Kamber, B. S., 2014, U-Pb LA-ICPMS dating using accessory mineral standards with variable common Pb: Chemical Geology, v. 363, p. 185-199.

Clark, C., Kirkland, C. L., Spaggiari, C. V., Oorschot, C. W., Wingate, M. T. D., and Taylor, B., 2014, Proterozoic granulite formation driven by mafic magmatism: An example from the Fraser Range Metamorphics, Western Australia: Precambrian Research, v. 240, p. 1-21.

Clark, D., Hensen, B., and Kinny, P., 2000, Geochronological constraints for a two-stage history of the Albany-Fraser Orogen, Western Australia: Precambrian Research, v. 102, p. 155-183.

Connelly, J. N., 2000, Degree of preservation of igneous zonation in zircon as a signpost for concordancy in U/Pb geochronology: Chemical Geology, v. 172, p. 25-39.

Corfu, F., 1996, Multistage zircon and titanite growth and inheritance in an Archean gneiss complex, Winnipeg River Subprovince, Ontario: Earth and Planetary Science Letters, v. 141, p. 175-186.

Corfu, F., Hanchar, J. M., Hoskin, P. W. O., and Kinny, P. D., 2003, Atlas of zircon textures: Reviews in Mineralogy and Geochemistry, v. 53, no. 1, p. 469-500.

Frost, B. R., Chamberlain, K. R., and Schumacher, J. C., 2000, Sphene (titanite): phase relations and role as a geochronometer: Chemical Geology, v. 172, p. 131-148.

Gao, X.-Y., Zheng, Y.-F., Chen, Y.-X., and Guo, J., 2012, Geochemical and U-Pb age constraints on the occurrence of polygenetic titanites in UHP metagranite in the Dabie orogen: Lithos, v. 136-139, p. 93-108.

Geological Survey of Western Australia, 2016, Compilation of geochronology information 2016: Government of Western Australia, ISBN: 9781741686876.

Hayden, L. A., Watson, E. B., and Wark, D. A., 2008, A thermobarometer for sphene (titanite): Contributions in Mineralogy and Petrology, v. 155, p. 529-540.

Huppert, H. E., and Sparks, R. S. J., 1988, The generation of granitic magmas by intrusion of basalt into continental crust: Journal of Petrology, v. 29, no. 3, p. 599-624.

Kennedy, A. K., Kamo, S. L., Nasdala, L., and Timms, N. E., 2010, Grenville skarn titanite: potential reference material for SIMS U-Th-Pb analysis: Canadian Mineralogist, v. 48, p. 1423-1443.

Kirkland, C. L., Smithies, R. H., Taylor, R. J. M., Evans, N., and McDonald, B. J., 2015, Zircon Th/U ratios in magmatic environs: Lithos, v. 212-215, p. 397-414.

Kirkland, C. L., Spaggiari, C. V., Johnson, T. E., Smithies, R. H., Danišík, M., Evans, N., Wingate, M. T. D., Clark, C., Spencer, C., Mikucki, E., and McDonald, B. J., 2016, Grain size matters: Implications for element and isotopic mobility in titanite: Precambrian Research, v. 278, p. 283-302.

Kirkland, C. L., Spaggiari, C. V., Wingate, M. T. D., Smithies, R. H., Belousova, E., and Murphy, R., 2011, Inferences on crust-mantle interaction from Lu-Hf isotopes: a case study from the Albany-Fraser Orogen: Geological Survey of Western Australia, Record 2011/12, p. 25.

Kirkland, C. L., Wingate, M. T. D., Spaggiari, C. V., and Pawley, M. J., 2010, 194734: migmatitic granitic gneiss, Ponton Creek: Geological Survey of Western Australia, Geochronology Record 857.

-, 2012, 194726: granodioritic gneiss, Uraryie Rock; Geochronology Record 1020: Geological Survey of Western Australia, 4p.

Korsch, R. J., Spaggiari, C. V., Occhipinti, S. A., Doublier, M. P., Clark, D. J., Dentith, M. C., Doyle, M. G., Kennett, B. L. N., Gessner, K., Neumann, N. L., Belousova, E., Tyler, I. M., Costelloe, R. D., Fomin, T., and Holzschuh, J., 2014, Geodynamic implications of the 2012 Albany-Fraser deep seismic reflection survey: a transect from the Yilgarn Craton across the Albany-Fraser Orogen to the Madura Province, *in* Spaggiari, C. V., and Tyler, I. M., eds., Albany-Fraser Orogen seismic and magnetotelluric (MT) workshop 2014: extended abstracts, Record 2014/6, Geological Survey of Western Australia, p. 142-173.

Kylander-Clark, A. R. C., Hacker, B. R., and Cottle, J. M., 2013, Laser-ablation split-stream ICP petrochronology: Chemical Geology, v. 345, p. 99-112.

Lucassen, F., Franz, G., Dulski, P., Romer, R. L., and Rhede, D., 2011, Element and Sr isotope signatures of titanite as indicator of variable fluid composition in hydrated eclogite: Lithos, v. 121, p. 12-24.

Ludwig, K. R., 2012, User's manual for Isoplot 3.75, a geochronological tooklit for Microsoft Excel, Berkeley, CA, USA, Berkeley Geochronology Center Special Publication.

Maier, W. D., Smithies, R. H., Spaggiari, C. V., Barnes, S. J., Kirkland, C. L., Kiddie, O., and Roberts, M. P., 2016, The evolution of mafic and ultramafic rocks of the Mesoproterozoic Fraser Zone, Albany-Fraser Orogen, and implications for Ni-Cu sulfide potential of the region: Geological Survey of Western Australia, Record 2016/8, p. 49.

Mezger, K., Essene, E. J., van der Pluijm, B., and Halliday, A. N., 1993, U-Pb geochronology of the Grenville Orogen of Ontario and New York: constraints on ancient crustal tectonics: Contributions in Mineralogy and Petrology, v. 114, p. 13-26.

Palme, H., and O'Neill, H. S. C., 2003, Cosmochemical estimates of mantle composition, *in* Carlson, R. W., ed., Mantle and core. Treatise on Geochemistry, Volume 2: Amsterdam, Elsevier.

Papapavlou, K., Darling, J. R., Storey, C. D., Lightfoot, P. C., Moser, D. E., and Lasalle, S., 2017, Dating shear zones with plastically deformed titanite: New insights into the orogenic evolution of the Sudbury impact structure (Ontario, Canada): Precambrian Research, v. 291, p. 220-235.

Paton, C., Hellstrom, J., Paul, B., Woodhead, J., and Hergt, J., 2011, Iolite: Freeware for the visualisation and processing of mass spectrometric data: Journal of Analytical Atomic Spectrometry, v. 26, no. 12, p. 2508-2518.

Philpotts, J. A., 1970, Redox estimation from a calculation of Eu^{2+} and Eu^{3+} concentrations in natural phases: Earth and Planetary Science Letters, v. 9, p. 257-268.

Prowatke, S., and Klemme, S., 2005, Effect of melt composition on the partitioning of trace elements between titanite and silicate melt: Geochimica et Cosmochimica Acta, v. 69, no. 3, p. 695-709.

Rubatto, D., 2002, Zircon trace element geochemistry: partitioning with garnet and the link between U-Pb ages and metamorphism: Chemical Geology, v. 184, p. 123-138.

Schwartz, J. J., Stowell, H. H., Klepeis, K. A., Tulloch, A. J., Kylander-Clark, A. R. C., Hacker, B. R., and Coble, M. A., 2016, Thermochronology of extensional orogenic collapse in the deep crust of Zealandia: Geosphere, v. 12, no. 3, p. 31pp.

Scibiorski, E., Tohver, E., and Jourdan, F., 2015, Rapid cooling and exhumation in the western part of the Mesoproterozoic Albany-Fraser Orogen, Western Australia: Precambrian Research, v. 265, p. 232-248.

Scibiorski, E., Tohver, E., Jourdan, F., Kirkland, C. L., and Spaggiari, C. V., 2016, Cooling and exhumation along the curved Albany-Fraser orogen, Western Australia: Lithosphere, v. 8, no. 5, p. 551-563.

Scott, D. J., and St-Onge, M. R., 1995, Constraints on Pb closure temperature in titanite based on rocks from the Ungava orogen, Canada: Implications for U-Pb geochronology and P-T-t path determinations: Geology, v. 23, no. 12, p. 1123-1126.

Smith, M. P., Storey, C. D., Jeffries, T. E., and Ryan, C. G., 2009, *In situ* U-Pb and trace element analysis of accessory minerals in the Kiruna District, Norrbotten, Sweden: New constraints on the timing and origin of mineralization: Journal of Petrology, v. 50, no. 11, p. 2063-2094.

Smithies, R. H., Spaggiari, C. V., and Kirkland, C. L., 2015, Building the crust of the Albany-Fraser Orogen: constraints from granite geochemistry: Geological Survey of Western Australia, Report 150, p. 49p.

Spaggiari, C., Bodorkos, S., Barquero-Molina, M., Tyler, I., and Wingate, M. T. D., 2009, Interpreted bedrock geology of the southern Yilgarn and central Albany-Fraser Orogen, Western Australia: Geological Survey of Western Australia, Record 2009/10, p. 84.

Spaggiari, C. V., Kirkland, C. L., Pawley, M. J., Smithies, R. H., Wingate, M. T. D., Doyle, M. G., Blenkinsop, T. G., Clark, C., Oorschot, C. W., Fox, L. J., and Savage, J., 2011, The geology of the east Albany-Fraser Orogen - a field guide: Geological Survey of Western Australia, Record 2011/23, p. 92.

Spaggiari, C. V., Kirkland, C. L., Smithies, R. H., and Wingate, M. T. D., 2014, Tectonic links between Proterozoic sedimentary cycles, basin formation and magmatism in the Albany-Fraser Orogen, Western Australia: Geological Survey of Western Australia, Report 133.

Spear, F. S., and Pyle, J. M., 2002, Apatite, monazite, and xenotime in metamorphic rocks: Reviews in Mineralogy and Geochemistry, v. 48, no. 1, p. 293-335.

-, 2010, Theoretical modeling of monazite growth in a low-Ca metapelite: Chemical Geology, v. 273, p. 111-119.

Spencer, K. J., Hacker, B. R., Kylander-Clark, A. R. C., Andersen, T. B., Cottle, J. M., Stearns, M. A., Poletti, J. E., and Seward, G. G. E., 2013, Campaign-style titanite U-Pb dating by laser-ablation ICP: Implications for crustal flow, phase transformations and titanite closure: Chemical Geology, v. 341, p. 84-101.

Stacey, J. S., and Kramers, J. D., 1975, Approximation of terrestrial lead isotope evolution by a two-stage model: Earth and Planetary Science Letters, v. 26, p. 207-221.

Stearns, M. A., Hacker, B. R., Ratschbacher, L., Rutte, D., and Kylander-Clark, A. R. C., 2015, Titanite petrochronology of the Pamir gneiss domes: Implications for middle to deep crust exhumation and titanite closure to Pb and Zr diffusion: Tectonics, v. 34, no. 4, p. 784-802.

Storey, C. D., Jeffries, T. E., and Smith, M. P., 2006, Common lead-corrected laser ablation ICP-MS U-Pb systematics and geochronology of titanite: Chemical Geology, v. 227, p. 37-52.

Storey, C. D., Smith, M. P., and Jeffries, T. E., 2007, In situ LA-ICP-MS U-Pb dating of metavolcanics of Norrbotten, Sweden: Records of extended geological histories in complex titanite grains: Chemical Geology, v. 240, p. 163-181.

Taylor, R. J. M., Kirkland, C. L., and Clark, C., 2016, Accessories after the facts: Constraining the timing, duration and conditions of high-temperature metamorphic processes: Lithos, v. 264, p. 239-257.

Tiepolo, M., Oberti, R., and Vannucci, R., 2002, Trace-element incorporation in titanite: constraints from experimentally determined solid/liquid partition coefficients: Chemical Geology, v. 191, p. 105-119.

Van Achterbergh, E., Ryan, C. G., and Griffin, W. L., 1999, Glitter: on line intensity reduction for the laser ablation inductively coupled plasma mass spectrometry: 9th Goldschmidt Conf.

Whitehouse, M. J., and Platt, J. P., 2003, Dating high-grade metamorphism - constraints from rare-earth elements in zircon and garnet: Contributions in Mineralogy and Petrology, v. 145, p. 61-74.

Zartman, R. E., and Doe, B. R., 1981, Plumbotectonics - the model: Tectonophysics, v. 75, p. 135-162.

Zhang, L.-S., and Schärer, U., 1996, Inherited Pb components in magmatic titanite and their consequence for the interpretation of U-Pb ages: Earth and Planetary Science Letters, v. 138, p. 57-65.

Chapter 7

Discussion

7 Discussion

The aim of this thesis was to determine the thermal history of the Albany-Fraser Orogen following Mesoproterozoic orogeny. Although some studies had previously investigated the cooling of the orogen, the existing data were few, spatially limited (primarily in the west of the orogen), poorly constrained, and/or used analytical techniques that have since been superseded (e.g. K/Ar dating rather than $^{40}Ar/^{39}Ar$ step-heating) (Stephenson et al., 1977; Baksi and Wilson, 1980; Fletcher et al., 1991; Black et al., 1992; Libby and De Laeter, 1998). The $^{40}Ar/^{39}Ar$, Rb/Sr and U/Pb thermochronology reported in the preceding chapters provide several new constraints on cooling across the length of the orogen. In addition, the discussion of cryptic excess argon in biotite contributes to an improved understanding of the limitations of $^{40}Ar/^{39}Ar$ thermochronology, and the investigation of trace elements in titanite contributes to improving the utility and application of titanite U/Pb thermochronology. The following discussion summarises the major findings of the thesis, examines their significance for the Albany-Fraser Orogen, and highlights the broader implications of these results.

7.1 Summary of cooling in the Albany-Fraser Orogen

In the west Albany-Fraser Orogen, $^{40}Ar/^{39}Ar$ cooling ages in the Biranup and Nornalup Zones are c. 1170 Ma for hornblende and c. 1170 – 1150 Ma for biotite; the Northern Foreland yields muscovite $^{40}Ar/^{39}Ar$ ages at c. 1159 Ma (Figure 7.1; Chapter 3). A Monte Carlo simulation of cooling rates from hornblende to biotite closure temperatures in the Biranup and Nornalup Zones yields fast cooling rates of c. 33 °C/Ma and 22 °C/Ma respectively. The Northern Foreland may have cooled more slowly, based on U/Pb zircon ages of metamorphism and $^{40}Ar/^{39}Ar$ muscovite ages (c. 4 – 8 °C/Ma). However, this cooling is poorly constrained, because the temperature at which the zircon grew is unknown.

In the east Albany-Fraser Orogen, 8.2 – 9.5 °C/Ma cooling rates for the Biranup Zone were initially calculated from c. 1190 Ma hornblende and 1170 – 1160 Ma biotite $^{40}Ar/^{39}Ar$ cooling ages (Chapter 4). The Fraser Zone produced two different $^{40}Ar/^{39}Ar$ cooling ages: 1205 Ma in the southwest, and 1157 Ma at a site 100 km to the northeast

(Figure 7.1). However, the Rb/Sr biotite thermochronology reported in Chapter 5 showed that the $^{40}Ar/^{39}Ar$ ages from the eastern Biranup Zone are affected by cryptic excess argon, and do not date cooling. Instead, the Rb/Sr ages date the cooling of the eastern Biranup Zone through c. 350°C (the closure temperature for Sr diffusion in biotite) at c. 1135 Ma (Figure 7.1).

The U/Pb titanite ages discussed in Chapter 6 provide additional constraints on the temperature of magmatism, metamorphism and zircon growth in the east Albany-Fraser Orogen. In the Fraser Zone, c. 1305 Ma magmatic titanite growth at > 900 °C was partially overprinted by metamorphic titanite recrystallization at c. 790 °C, in the presence of garnet. No U/Pb titanite age could be determined for the overprinting event, but a likely candidate is the regional granulite facies metamorphism at c. 1290 Ma (Clark et al., 2014).

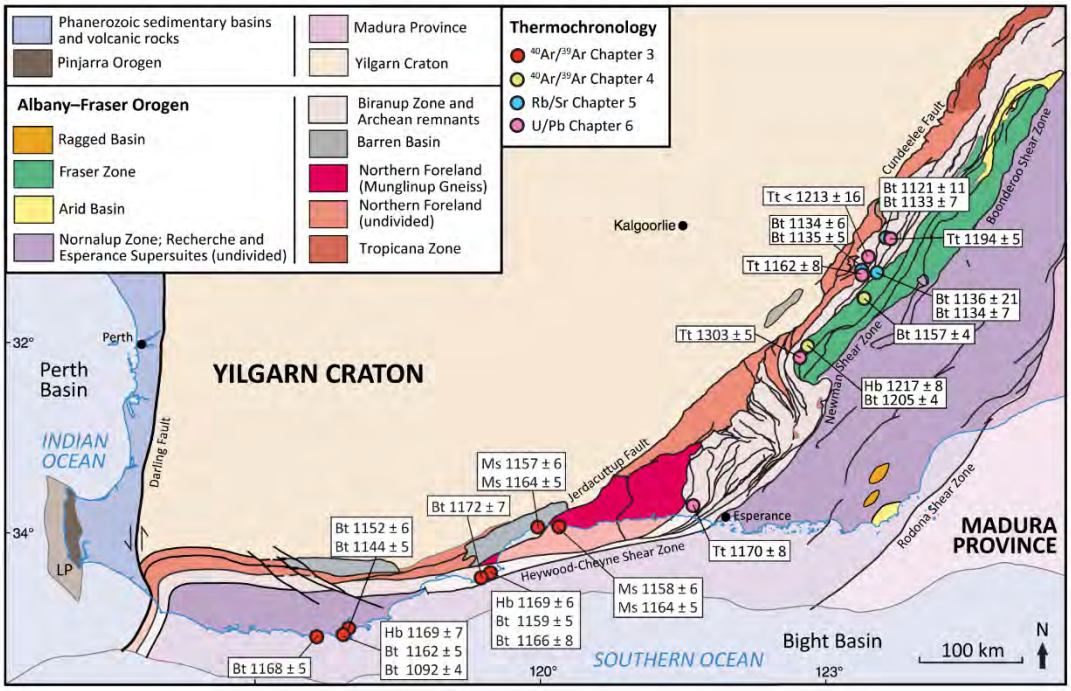

Figure 7.1 Interpreted bedrock geology map of the Albany-Fraser Orogen, summarising the new thermochronology reported in previous chapters of this thesis. Only geologically significant ages are shown (i.e. excluding $^{40}Ar/^{39}Ar$ thermochronology contaminated by excess argon). All ages in Ma, with ± 2σ uncertainty; map after Spaggiari et al. (2014c).

In the eastern Biranup Zone, titanite growth at c. 1195 Ma and c. 760 °C was synchronous with garnet growth during amphibolite facies metamorphism; titanite in another sample recorded cooling through the Pb closure temperature (c. 650 °C) at c. 1162 Ma. These data fit well with previous U/Pb titanite geochronology and P-T constraints on metamorphism in the eastern Biranup Zone (Kirkland et al., 2016), and provide useful T-t constraints on the initiation of orogenic cooling. A cooling rate of 7 °C/Ma is calculated for cooling from the 1195 Ma U/Pb titanite growth age to a Rb/Sr biotite cooling age of 1133 Ma (from 760 to 350 °C); cooling from the 1162 Ma titanite cooling age (650 to 350 °C) requires a slightly faster rate of 10 °C/Ma.

In the southern Biranup Zone, 1170 ± 8 Ma titanite growth at c. 750 °C provides the first T-t constraint on Biranup Zone metamorphism to the west of the Coramup Shear Zone. This new data point is in good agreement with the 1168 ± 12 Ma U/Pb zircon age of a syn-kinematic pegmatite dyke in the Coramup Gneiss (25 km to the southeast) interpreted to date 750 – 800 °C, 5 – 6 GPa metamorphism (Bodorkos and Clark, 2004b).

The Mesoproterozoic cooling history of the Albany-Fraser Orogen is summarised in Figure 7.2. The thermochronological data are plotted on temperature-time graphs (excluding $^{40}Ar/^{39}Ar$ ages affected by excess argon). The existing U/Pb zircon and titanite ages from closest to the sample sites are also shown (Geological Survey of Western Australia, 2016; Kirkland et al., 2016). Figure 7.2 illustrates two important characteristics of the cooling history of the Albany-Fraser Orogen: (1) the difference in the rate of cooling between east and west; and (2) the distinct record of the Fraser Zone.

7.1.1 Cooling was fast in the west, but slow in the east.

As first discussed in Chapter 4, the curvature of the Albany-Fraser Orogen around the southern and south-eastern margins of the Yilgarn Craton resulted in important differences in structural setting along the orogen. Stage II deformation in both the west and east Albany-Fraser Orogen occurred within a tectonic regime of northwest-directed compression. In the eastern Biranup Zone, this was primarily resolved as craton-vergent folding and thrusting, with a minor component of dextral

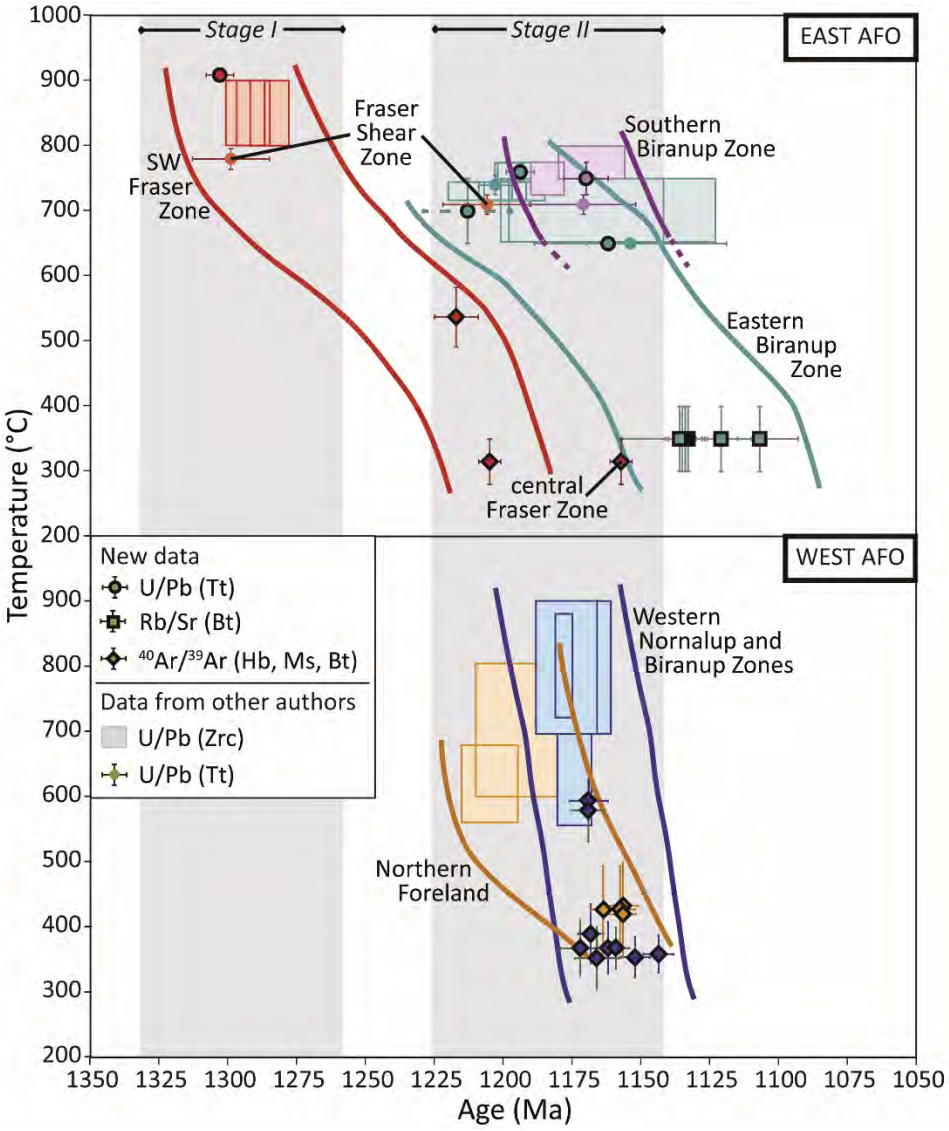

Figure 7.2 Temperature-time plot summarising the cooling history of the Albany-Fraser Orogen (AFO). All new thermochronology discussed in previous chapters is shown, except for $^{40}Ar/^{39}Ar$ thermochronology that is interpreted to be contaminated by excess argon. Published U/Pb zircon and titanite ages from closest to the sample sites are also shown: zircon samples 194714, 194715, 194789, 184387, 194725, 194726, 194722, 194724, 194734, 194790, and 184334 (from Geological Survey of Western Australia, 2016), and titanite samples 184393, 194386, 184387, and 194826 (from Kirkland et al., 2016). $^{40}Ar/^{39}Ar$ ages in the west AFO are plotted at the closure temperatures calculated in Chapter 3. The $^{40}Ar/^{39}Ar$ age in the east AFO is plotted at a closure temperature of 315 ± 35 °C (Harrison et al., 1985). Rb/Sr biotite ages are plotted at a closure temperature of 350 ± 50 °C. U/Pb titanite growth ages are plotted at their Zr-in-Tt temperatures (Chapter 6; Kirkland et al., 2016). U/Pb titanite cooling ages are plotted at a Pb closure temperature of 650 °C. U/Pb zircon ages are plotted at temperatures either from nearby thermobarometry (Clark et al., 2014; Kirkland et al., 2016; Bodorkos and Clark, 2004b), from nearby Zr-in-Tt thermometry, or at an estimated amphibolite facies temperature of 700 ± 50 °C. All ages are given with ± 2σ uncertainty.

transpression (Myers, 1995; Clark et al., 2000; Bodorkos and Clark, 2004b; Spaggiari et al., 2014a; Waddell et al., 2015). However, in the western Biranup and Nornalup Zones, transpressional deformation dominated (Beeson et al., 1988; Duebendorfer, 2002; Bodorkos and Clark, 2004b; Barquero-Molina, 2010).

Regardless, the thermochronology summarised in Figure 7.2 shows that the rate of cooling was significantly faster in the west than in the east of the orogen: c. 22 – 33 °C/Ma in the western Biranup and Nornalup Zones, compared to c. 7 – 10 °C/Ma in the eastern Biranup Zone. The timing of cooling with respect to Stage II orogeny (1225 -1140 Ma) also differs between the west and the east.

In the western Biranup and Nornalup Zones, magmatism, metamorphism and deformation related to dextral transpression is widespread in the period c. 1190 – 1170 Ma (see Figure 3.5 of Chapter 3; Beeson et al., 1988; Pidgeon, 1990; Black et al., 1992; Duebendorfer, 2002; Bodorkos and Clark, 2004b; Barquero-Molina, 2010). Because the fast cooling, dated between c. 1175 to 1159 Ma (hornblende to biotite $^{40}Ar/^{39}Ar$ cooling ages), commenced within this actively deforming tectonic setting, the transpressional deformation is interpreted as the driver of exhumation. As discussed in Chapter 4, the combination of contractional movement and deep, steeply dipping structures in transpressional settings may lead to the rapid uplift and exhumation of lower crustal rocks (Fossen and Tikoff, 1998).

In the eastern Biranup Zone, the new c. 1195 Ma U/Pb titanite age for metamorphism (Chapter 6) is consistent with the predominantly c. 1206 - 1190 Ma U/Pb zircon ages of magmatism, metamorphism, and deformation (Figure 7.2; see section 4.2.6, 'Eastern Biranup Zone'). The c. 1162 Ma titanite U/Pb cooling age and c. 1133 Ma biotite Rb/Sr cooling ages show that cooling significantly post-dates peak metamorphism in the eastern Biranup Zone.

The exhumation of the eastern Biranup Zone is syn-orogenic in comparison with the duration of Stage II of orogeny, as defined by Spaggiari et al. (2014a) (1225 – 1140 Ma). However, the interpreted continuation of metamorphism, magmatism and deformation until c. 1140 Ma is based on U/Pb zircon data from the southern Biranup and Nornalup Zones (Spaggiari et al., 2011; Smithies et al., 2015; Geological Survey

of Western Australia, 2016). The 1170 ± 8 Ma U/Pb titanite growth age in the southern Biranup Zone fits with this long duration of high-grade metamorphism. In contrast, in the eastern Biranup Zone, U/Pb zircon and titanite ages of magmatism and metamorphism are mostly older than c. 1190 Ma (all younger zircon ages are poorly constrained and within error of 1190 Ma, e.g. 1170 ± 28 Ma; see discussion in section 4.2.6, 'Eastern Biranup Zone'), and the new U/Pb titanite thermochronology suggests cooling had commenced by c. 1162 Ma. However, the age of the end of northwest-directed compression in the eastern Biranup Zone is not well constrained. For this reason, the driver of cooling in the eastern Biranup Zone can be interpreted as either: (1) syn-orogenic folding and thrusting leading to uplift, erosion and exhumation, or (2) extensional exhumation due to gravitational collapse (e.g. Mezger et al., 1991; Reddy et al., 2003; Maino et al., 2012).

Regardless, linking the difference in cooling rates along the Albany-Fraser Orogen to changes in structural setting is supported by comparison with the global record of orogenic cooling (see Figure 3.7 in Chapter 3). Typical granulite cooling rates in Mesoproterozoic collisional orogens are 1 – 5 °C/Ma, driven by post-orogenic exhumation mechanisms such as orogenic collapse and erosion (Mezger et al., 1991; Willigers et al., 2002; Rivers, 2008). Some terranes within these orogens record slightly faster cooling rates of c. 6 – 15 °C/Ma, a result of tectonically-driven exhumation such as thrusting or extensional shearing (Page et al., 1996; Bingen et al., 2008; Rivers, 2008). Cooling in the eastern Biranup Zone at 7 – 10 °C/Ma agrees with this record of generally slow cooling in Mesoproterozoic convergent settings.

In contrast, cooling in the west Albany-Fraser Orogen is significantly faster than in other Mesoproterozoic orogens. This is interpreted to reflect the paucity of preserved cooling records from transpressional settings in the Mesoproterozoic, as the fast cooling rates of 22–33 °C/Ma are not unusual when compared to other transpressional orogens (e.g. Camacho and McDougall, 2000; Batt et al., 2004; Foster et al., 2009). This under-representation of ancient transpressional settings in the geological record is interpreted to reflect their lower preservation potential, as compared with terranes exhumed post-orogenically. Rocks exhumed syn-orogenically (e.g. by extrusion in an actively deforming transpressional setting) are

more likely to be removed by erosion, long before rocks exhumed by slow, post-orogenic processes are exposed at the surface (e.g. Willigers et al., 2002).

7.1.2 The role of the Fraser Zone

The intrusive gabbroic and granitic rocks of the Fraser Zone crystallised between c. 1305 – 1290 Ma, and were metamorphosed at granulite facies at c. 1290 Ma (Spaggiari et al., 2009; Clark et al., 2014). Based on their coeval timing, magmatism is interpreted as the driver of metamorphism (Clark et al., 2014). However, the effect of Stage II orogeny (1225 – 1140 Ma) on the Fraser Zone has long been contentious. The U/Pb zircon record of magmatism and metamorphism in the Fraser Zone does not record Stage II ages, despite its position between the Biranup and Nornalup Zones, which were deformed at amphibolite to granulite facies during Stage II. This record, together with a 1285 ± 15 Ma $^{40}Ar/^{39}Ar$ hornblende age and a 1268 ± 20 Ma Rb/Sr biotite age from the southwestern Fraser Zone (Baksi and Wilson, 1980; Fletcher et al., 1991), led Clark et al. (2014) to suggest that the cooling and strengthening of the Fraser Zone after Stage I granulite metamorphism rendered it less susceptible to deformation during subsequent tectonic events.

However, Kirkland et al. (2016) reported a U/Pb age of 1205 ± 16 Ma for partially recrystallised titanite from the Fraser Shear Zone, the western boundary of the Fraser Zone. This was interpreted as evidence that the Fraser Zone was, after all, subjected to metamorphism at c. 700 °C during Stage II. Kirkland et al. (2016) noted that Pb in titanite was more susceptible to age resetting than Pb in zircon, and agreed with earlier suggestions that new zircon growth was inhibited in the dehydrated, refractory Fraser Zone that had already been subjected to one granulite facies event.

The new thermochronology reported in Chapters 4 and 6 provides additional constraints on the evolution of the Fraser Zone (Figure 7.1). The new data include a 1305 Ma U/Pb magmatic titanite growth age at Gnamma Hill, 1217 – 1205 Ma $^{40}Ar/^{39}Ar$ hornblende and biotite ages recording early Stage II cooling at Wyralinu Hill, and a 1157 Ma $^{40}Ar/^{39}Ar$ biotite age from the central Fraser Zone, c. 100 km to the northeast.

The new data from the southwest Fraser Zone (Wyralinu and Gnamma Hill) do not support temperatures of c. 700°C during Stage II. These samples are from a similar latitude as the Fletcher et al. (1991) and Baksi and Wilson (1980) samples; together, they span the width of the Fraser Zone, and support cooling of the southwest Fraser Zone below c. 350 °C (Ar closure temperature in biotite) either before or early in Stage II (Figure 7.1).

The apparent contradiction with the 1205 ± 16 Ma U/Pb titanite age of Kirkland et al. (2016) is resolved by considering the relative location of samples. The Kirkland et al. (2016) titanite sample is located within the Fraser Shear Zone; Wyralinu Hill and Gnamma Hill are a further 90 km to the southwest, and are 1 – 2 km east of the Fraser Shear Zone, within the Fraser Zone itself. Shear zones commonly act as fluid pathways (Oliver, 1996), and titanite within the shear zone will be more vulnerable to deformation- and fluid-assisted recrystallization than titanite at Gnamma Hill. This is supported by a 1234 Ma $^{40}Ar/^{39}Ar$ hornblende age from the Fraser Shear Zone, which is older than the Kirkland et al. (2016) U/Pb titanite age; the old hornblende age is interpreted to reflect excess argon introduced along the shear zone by the same Ar-rich fluids that infiltrated the adjacent Biranup Zone.

The geological significance of the 1157 Ma $^{40}Ar/^{39}Ar$ biotite age from the central Fraser Zone is ambiguous, as it is a single data point with no additional nearby geochronological constraints. This sample is from a locality 100 km to the northeast of Wyralinu Hill (although is close to the Fraser Shear Zone titanite sample), and in Chapter 4 was interpreted to date exhumation and cooling c. 50 Ma later than in the southwest, possibly as a product of internal faulting within the domain leading to dissimilar cooling histories (Figure 7.2, 7.3). Regardless, this suggests that the thermal effects of Stage II were heterogenous within the Fraser Zone, and does not contradict the interpretation that much of the Fraser Zone (i.e. the southwest, where the most geochronological constraints are available) remained dry and cool during Stage II orogenesis.

Low temperatures for the southwest Fraser Zone suggest a relatively shallow crustal position during Stage II (Figure 7.3). Therefore, it is proposed that the

southwest Fraser Zone may have acted as an orogenic lid to the east Albany-Fraser Orogen, analogous to the Orogenic Lid in the Grenville Province (Rivers, 2008, 2012). The Orogenic Lid in the Grenville Province is a collective name for terranes that lack evidence for penetrative Grenvillian metamorphism, but are juxtaposed between largely amphibolite- to granulite-deformed domains. Rivers (2008) argues that the preservation of the Orogenic Lid is a result of gravitational collapse within the Grenville Province, supported by normal-sense shearing along the boundaries of the Orogenic Lid. Similarly, for the cool Fraser Zone to be juxtaposed between two domains that record significant high-grade Stage II deformation, bound by the east-dipping Fraser Shear Zone and west-dipping Newman Shear Zone, significant extensional movement along both shear zones is required (Figure 7.3). The timing of this movement is uncertain; at present, the only age constraint for either shear zone is the partial recrystallization of titanite at 1206 ± 15 Ma (Kirkland et al., 2016).

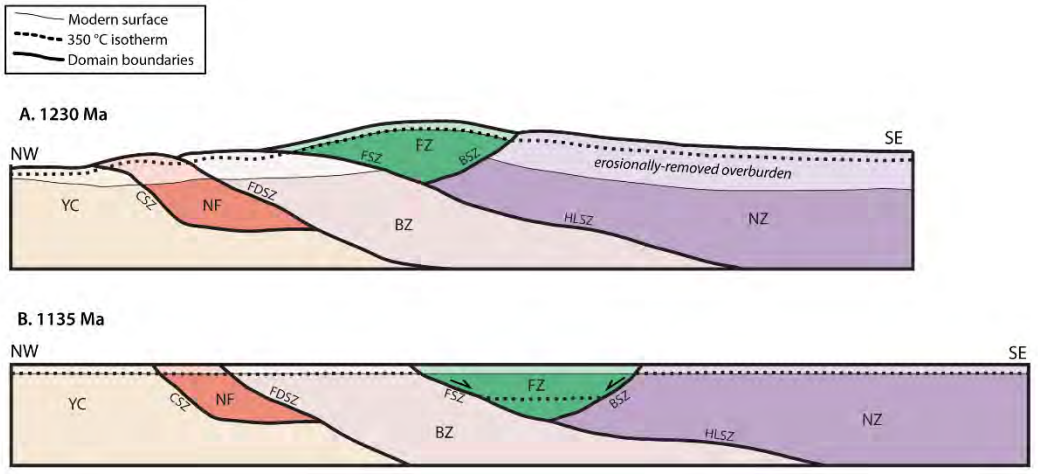

Figure 7.3 Schematic northwest-southeast cross sections of the east Albany-Fraser Orogen before and after Stage II orogeny, showing the relative positions of the Fraser, Biranup and Nornalup Zones. **(A)** The rocks currently exposed at the surface of the southwestern Fraser Zone cooled below c. 350 °C at c. 1205 Ma. The southwestern Fraser Zone occupied a shallow structural level during Stage II, and remained cool for the duration of orogeny (i.e. an 'orogenic lid'). **(B)** The Fraser Zone was juxtaposed against the Stage II-deformed Biranup and Nornalup Zones by extension. Cross section B is based on interpreted seismic profile 12GA-AF3 in Spaggiari et al. (2014b). Abbreviations: BSZ, Boonderoo Shear Zone; BZ, Biranup Zone; CSZ, Cundeelee Shear Zone; FDSZ, Frog Dam Shear Zone; FSZ, Fraser Shear Zone; FZ, Fraser Zone; HLSZ, Harris Lake Shear Zone; NF, Northern Foreland; NZ, Nornalup Zone; YC, Yilgarn Craton.

7.2 Cryptic excess argon in the eastern Biranup Zone

The suspected presence of cryptic excess argon in the eastern Biranup Zone was subsequently verified by testing $^{40}Ar/^{39}Ar$ biotite ages with Rb/Sr biotite ages (Chapter 4, Chapter 5). This discovery is important for future studies of cooling, both in the Albany-Fraser Orogen and more broadly. In the eastern Biranup Zone of the Albany-Fraser Orogen, $^{40}Ar/^{39}Ar$ thermochronology is not a suitable approach. Instead, Rb/Sr thermochronology of muscovite and biotite may yield cooling ages through a similar temperature interval.

Although the $^{40}Ar/^{39}Ar$ data in the Fraser Zone were not tested with Rb/Sr thermochronology, excess Ar is considered unlikely for the sample from the southwest Fraser Zone. Excess argon in the Biranup Zone was introduced by Ar-rich fluids, presumably during Stage II metamorphism, yet the absence of Stage II U/Pb zircon (and titanite; Chapter 6) ages has been interpreted as evidence that the Fraser Zone remained dry and cool during Stage II (i.e. not at the same structural level as the Biranup Zone, providing an additional barrier to the movement of fluids) (Clark et al., 2014). However, without further evidence, it is not possible to rule out the presence of excess argon c. 100 km to the northeast in the central Fraser Zone, as the Stage II $^{40}Ar/^{39}Ar$ age from the central Fraser Zone is similar to the youngest $^{40}Ar/^{39}Ar$ apparent ages from the adjacent Biranup Zone, and may record a similar geological (and hydrothermal) history.

Although the presence or absence of excess argon in the west Albany-Fraser Orogen has not been extensively tested by Rb/Sr thermochronology, the c. 1148 Ma Rb/Sr biotite ages of Libby and De Laeter (1998) near Albany (recalculated with the most recently recommended Rb/Sr decay constant; Villa et al., 2015) are comparable with the $^{40}Ar/^{39}Ar$ biotite ages reported in Chapter 3. In addition, the $^{40}Ar/^{39}Ar$ thermochronology from the west Albany-Fraser Orogen displayed none of the indicators of excess argon that were evident in the east: $^{40}Ar/^{39}Ar$ ages are reproducible, they are consistent with the expected sequence of closure temperatures, and they do not contradict existing constraints on the cooling history.

The extent of excess argon in the regions not sampled is unknown (e.g. in the eastern Northern Foreland and Nornalup Zone). As discussed in Chapter 5, the proposed source of the excess argon is a flux of Ar-rich fluids derived from the Archean Yilgarn Craton underlying the eastern Biranup Zone. Given this source, excess argon is also likely to be present in the Northern Foreland adjacent to the eastern Biranup Zone. This is supported by the single $^{40}Ar/^{39}Ar$ hornblende age reported for the Northern Foreland, which was interpreted to contain excess argon (Table 4.2, Chapter 4). The substrate to the eastern Nornalup Zone is unknown; however, based on deep reflection seismic data, Yilgarn Craton rocks are not interpreted to significantly extend underneath the Nornalup Zone, and in addition, are buried more deeply than underneath the Biranup Zone (Spaggiari et al., 2014b). In the absence of any data, this suggests that the Nornalup Zone is less likely to have been infiltrated by the same Ar-rich fluids.

The discussion of cryptic excess argon in Chapter 5 may also be useful to researchers working outside the Albany-Fraser Orogen. Cryptic excess argon is not widely discussed; most reports of $^{40}Ar/^{39}Ar$ thermochronology focus on the new, geologically significant age constraints, rather than on samples affected by excess argon (e.g. Batt et al., 2000; Reddy et al., 2003). In addition, cryptic excess argon is difficult to recognise without additional geochronological constraints. Chapter 5 describes several criteria for assessing the presence of cryptic excess argon in $^{40}Ar/^{39}Ar$ data, and for improving confidence in the data used to construct of orogenic thermal histories. Cryptic excess argon is likely to be present if (1) minerals with lower closure temperatures yield $^{40}Ar/^{39}Ar$ ages that are older than minerals with higher closure temperatures, and (2) $^{40}Ar/^{39}Ar$ plateau ages from the same mineral in the same sample or same site are inconsistent. Where there is no additional data available to provide an independent constraint on the timing of cooling, the interpretation of $^{40}Ar/^{39}Ar$ thermochronology should proceed with caution, and if there is an identified regional problem with cryptic excess argon, even the youngest $^{40}Ar/^{39}Ar$ ages can only be considered as maximum constraints.

7.3 Trace elements in titanite as a geochemical indicator for garnet growth and correlation with U/Pb ages

With the development of LA-ICPMS techniques and the ability to quickly generate large datasets, *in situ* U/Pb titanite geochronology has become increasingly popular. However, the closure temperature for Pb in titanite has a wide range, from 650 – 1030 °C, depending on processes such as crystallisation temperature and lattice damage (Cherniak, 2010). Accordingly, U/Pb titanite ages may date metamorphic growth, magmatic growth, cooling through the Pb diffusion closure temperature, or a mixture between these processes (Storey et al., 2007; Smith et al., 2009; Kirkland et al., 2016). To distinguish these scenarios, it is crucial to understand the processes controlling the distribution of radiogenic Pb in the titanite (i.e. recrystallization or volume diffusion). Several studies have been published detailing the interpretation of complex U/Pb titanite data (e.g. Storey et al., 2007; Smith et al., 2009; Lucassen et al., 2011; Gao et al., 2012; Papapavlou et al., 2017). However, although variations in trace element content are used to recognise titanite recrystallization, no diagnostic geochemical indicator has been identified.

In Chapter 6, detailed sample petrography coupled with variations in trace element composition (chondrite-normalised REE patterns) was used to distinguish multiple titanite generations and recrystallization processes within five samples from the east Albany-Fraser Orogen. The chapter demonstrates the suitability of the REE pattern to classify and describe compositional variability in titanite at a thin section scale, as well as at the individual grain scale (i.e. compositional variability within zoned titanite). The samples demonstrated mm- to cm-scale lithological controls on the trace element composition of titanite, which either reflect the proximity of titanite to garnet, or stem from the development of gneissic compositional banding.

The most important result from this chapter is the use of the Dy/Yb ratio (i.e. a measure of the slope of the HREE) as a geochemical indicator to determine whether titanite crystallised in equilibrium with garnet. The correlation between zircon HREE content and garnet growth has long been recognised, and is often useful in zircon geochronology (Rubatto, 2002; Taylor et al., 2016), but Chapter 6 is the first time this has been tested and applied to titanite. This means that in two samples, the U/Pb

titanite ages can be directly linked to both the temperature of titanite growth (Zr-in-Tt thermometry; Hayden et al., 2008), and to garnet growth during metamorphism. This allows the U/Pb titanite ages to be used as thermochronometers, by providing two well-constrained T-t points on the thermal path of the orogen, and also demonstrates the potential for U/Pb titanite thermochronology to contribute to understanding T-t histories in metamorphic rocks.

7.4 Limitations

This thesis describes the thermal history of the Albany-Fraser Orogen in two main transects: the west Albany-Fraser Orogen, and the east Albany-Fraser Orogen. In order to obtain an orogen-scale overview of orogenic cooling, there is a trade-off between sample coverage and sample density; the samples span a total along-strike distance of c. 800 km. Consequently, the interpretations based on these data are broad and regional in scale, and small-scale differences in cooling (e.g. at the sub-10 km scale) are not easily identified.

In addition, there are several gaps in the data coverage: for example, most of the Fraser Zone, the southern Albany-Fraser Orogen (Esperance and to the east), the far northeast Albany-Fraser Orogen (towards the Musgrave Province), and the eastern Nornalup Zone. In the absence of data, orogen-scale interpretations (i.e. fast cooling in the west, and slow in the east) are extrapolated to fill these gaps; however, a more detailed (and accurate) picture of cooling in the Albany-Fraser Orogen may emerge if these additional datasets are acquired.

The interpretation of cooling trajectories is also limited by the paucity of P-T-t information for Stage I and Stage II of orogeny. Only four studies have used thermobarometry to evaluate the P-T conditions of metamorphism during Stage I and/or Stage II: Bodorkos and Clark (2004a); Clark et al. (2014); Wetherley (1998); and Kirkland et al. (2016). At most sample sites, metamorphism is broadly described as 'amphibolite facies' or 'granulite facies', and the U/Pb zircon dates for metamorphism or magmatism (if present) are not constrained to a more precise temperature interval. To deal with this uncertainty in a quantitative manner, Chapters 3 and 4 use Monte Carlo modelling in the calculation of cooling rates. Whilst this is a robust method for

calculations involving uncertainty, the results would be further improved by using better T-t constraints for metamorphism. To this end, the original reason for carrying out the U/Pb titanite thermochronology (Chapter 6) was to improve the T-t constraints at the high-temperature end of the cooling path.

Similarly, the interpretation of exhumation processes based on cooling paths is limited by the paucity of detailed structural studies, particularly in the east of the orogen (Beeson et al., 1988; Clark et al., 2000; Duebendorfer, 2002; Bodorkos and Clark, 2004b; Barquero-Molina, 2010; Adams, 2012; Waddell et al., 2015). Although overall northwest-directed convergence during Stage I and Stage II is undisputed by these studies, the correlation of fast cooling with transpression in the west, and slow cooling with convergence in the east, is based only on the structural studies listed above. Whilst the thermochronological data are robust, further structural geology will provide an improved framework within which to interpret these data.

7.5 Further Work

As discussed in 'Limitations' above, further thermochronology is required to address the remaining gaps in sample coverage, primarily in the eastern Nornalup Zone and the southern and north-eastern Albany-Fraser Orogen. The sample coverage of the Fraser Zone could also be significantly improved. The Fraser Zone samples that produced geologically significant results in this thesis are from Wyralinu Hill and Gnamma Hill, both located at the southwestern end of the Fraser Zone and only 1 – 2 km east of the Fraser Shear Zone (Figure 7.1). Although outcrop of the Fraser Zone is severely limited (in the northeast, it is overlain by Phanerozoic rocks of the Eucla Basin), additional samples from across its 50 km width and > 400 km length would improve constraints on its thermal history, and test the suggestion that it acted as an orogenic lid during Stage II of orogeny.

Spaggiari et al. (2014b) interpreted the 3-D structure of the crust, based on deep reflection seismic data, in three main transects across the east Albany-Fraser Orogen. Integrating any new thermochronological data with crustal structure as revealed by these seismic cross-sections may allow for the specific structures controlling differential cooling and exhumation across strike to be identified. Alternatively,

targeted thermochronology across the large, crustal-scale shear zones identified in the seismic cross-sections could be used to determine the role of these structures in orogenic cooling. Interpretations of extensional collapse in the east Albany-Fraser Orogen during Stage II (Smithies et al., 2015) could be tested by using thermochronology to determine whether the last phase of movement on major shear zones was normal or reverse (e.g. Busch et al., 1997).

The fast cooling of the west Albany-Fraser Orogen is unusual within the Mesoproterozoic orogenic record, but is not unusual when compared to cooling in modern transpressional settings (e.g. Batt et al., 2000; Camacho and McDougall, 2000; Foster et al., 2009). As few cooling histories for Mesoproterozoic transpressional settings exist (e.g. Tohver et al., 2006), it would be interesting to study cooling in other Mesoproterozoic transpressional settings to see whether fast cooling is typical, and to determine the drivers of exhumation (e.g. the Natal Metamorphic Province; Spencer et al., 2015). To this end, a more detailed study of the west Albany-Fraser Orogen may uncover the specific structures (shear zones and faults) involved in the fast cooling.

In Chapter 6, the HREE content of titanite was identified as a geochemical indicator to link titanite growth with garnet growth. To confirm this discovery, the relationship could be tested with titanite from garnet-bearing and garnet-free samples from another orogen. An alternative test would be to directly date garnet interpreted to be in equilibrium with titanite, and compare the U/Pb titanite and Sm/Nd garnet ages (assuming both chronometers record growth ages, rather than cooling ages) to determine the relative timing of garnet and titanite growth.

Finally, the U/Pb ages of titanite are interpreted to record a mixture of titanite growth ages, and cooling ages through the closure temperature for Pb diffusion. However, the reason why most samples in Chapter 6 recorded growth ages rather than cooling ages is not understood. A detailed study of U/Pb in titanite that takes into account variables such as titanite composition, sample lithology, metamorphic grade, cooling path, and fluid history may address this question.

7.6 References

Adams, M., 2012, Structural and geochronological evolution of the Malcolm Gneiss, Nornalup Zone, Albany-Fraser Orogen, Western Australia: Geological Survey of Western Australia, Record 2012/4, p. 105.

Baksi, A. K., and Wilson, A. F., 1980, An attempt at Argon dating of two granulite-facies terranes: Chemical Geology, v. 30, p. 109-120.

Barquero-Molina, M., 2010, Kinematics of bidirectional extension and coeval NW-directed contraction in orthogneisses of the Biranup Complex, Albany Fraser Orogen, Southwestern Australia: Geological Survey of Western Australia, Report 109, p. 205.

Batt, G. E., Baldwin, S. L., Cottam, M. A., Fitzgerald, P. G., Brandon, M. T., and Spell, T. L., 2004, Cenozoic plate boundary evolution in the South Island of New Zealand: New thermochronological constraints: Tectonics, v. 23, no. 4, p. 17.

Batt, G. E., Braun, J., Kohn, B. P., and McDougall, I., 2000, Thermochronological analysis of the dynamics of the Southern Alps, New Zealand: GSA Bulletin, v. 112, no. 2, p. 250-266.

Beeson, J., Delor, C. P., and Harris, L. B., 1988, A structural and metamorphic traverse across the Albany Mobile Belt, Western Australia: Precambrian Research, v. 40/41, p. 117-136.

Bingen, B., Nordgulen, Ø., and Viola, G., 2008, A four-phase model for the Sveconorwegian orogeny, SW Scandinavia: Norwegian Journal of Geology, v. 88, p. 43-72.

Black, L. P., Harris, L. B., and Delor, C. P., 1992, Reworking of Archaean and Early Proterozoic components during a progressive, Middle Proterozoic tectonothermal event in the Albany Mobile Belt, Western Australia: Precambrian Research, v. 59, p. 95-123.

Bodorkos, S., and Clark, D., 2004a, Evolution of a crustal-scale transpressive shear zone in the Albany-Fraser Orogen, SW Australia: 1. P-T conditions of

Mesoproterozoic metamorphism in the Coramup Gneiss: Journal of Metamorphic Geology, v. 22, p. 691 - 711.

-, 2004b, Evolution of a crustal-scale transpressive shear zone in the Albany-Fraser Orogen, SW Australia: 2. Tectonic history of the Coramup Gneiss and a kinematic framework for Mesoproterozoic collision of the West Australian and Mawson cratons: Journal of Metamorphic Geology, v. 22, p. 713-731.

Busch, J. P., Mezger, K., and van der Pluijm, B., 1997, Suturing and extensional reactivation in the Grenville orogen, Canada: Geology, v. 25, no. 6, p. 507-510.

Camacho, A., and McDougall, I., 2000, Intracratonic, strike-slip partitioned transpression and the formation and exhumation of eclogite facies rocks: An example from the Musgrave Block, central Australia: Tectonics, v. 19, no. 5, p. 978-996.

Cherniak, D. J., 2010, Diffusion in accessory minerals: zircon, titanite, apatite, monazite and xenotime: Reviews in Mineralogy and Geochemistry, v. 72, p. 827-869.

Clark, C., Kirkland, C. L., Spaggiari, C. V., Oorschot, C. W., Wingate, M. T. D., and Taylor, B., 2014, Proterozoic granulite formation driven by mafic magmatism: An example from the Fraser Range Metamorphics, Western Australia: Precambrian Research, v. 240, p. 1-21.

Clark, D., Hensen, B., and Kinny, P., 2000, Geochronological constraints for a two-stage history of the Albany-Fraser Orogen, Western Australia: Precambrian Research, v. 102, p. 155-183.

Duebendorfer, E. M., 2002, Regional correlation of Mesoproterozoic structures and deformational events in the Albany-Fraser orogen, Western Australia: Precambrian Research, v. 116, p. 129 - 154.

Fletcher, I. R., Myers, J. S., and Ahmat, A. L., 1991, Isotopic evidence on the age and origin of the Fraser Complex, Western Australia: a sample of Mid-Proterozoic lower crust: Chemical Geology (Isotope Geoscience Section), v. 87, p. 197-216.

Fossen, H., and Tikoff, B., 1998, Extended models of transpression and transtension, and application to tectonic settings, *in* Holdsworth, R. E., Strachan, R. A., and Dewey, J. F., eds., Continental transpressional and transtensional tectonics, Volume 135, Geological Society, London, Special Publications, p. 15-33.

Foster, D. A., Goscombe, B. D., and Gray, D. R., 2009, Rapid exhumation of deep crust in an obliquely convergent orogen: The Kaoko Belt of the Damara Orogen: Tectonics, v. 28, DOI: 10.1029/2008TC002317.

Gao, X.-Y., Zheng, Y.-F., Chen, Y.-X., and Guo, J., 2012, Geochemical and U-Pb age constraints on the occurrence of polygenetic titanites in UHP metagranite in the Dabie orogen: Lithos, v. 136-139, p. 93-108.

Geological Survey of Western Australia, 2016, Compilation of geochronology information 2016: Government of Western Australia, ISBN: 9781741686876.

Harrison, T. M., Duncan, I., and McDougall, I., 1985, Diffusion of ^{40}Ar in biotite: Temperature, pressure and compositional effects: Geochimica et Cosmochimica Acta, v. 49, p. 2461 - 2468.

Hayden, L. A., Watson, E. B., and Wark, D. A., 2008, A thermobarometer for sphene (titanite): Contributions in Mineralogy and Petrology, v. 155, p. 529-540.

Kirkland, C. L., Spaggiari, C. V., Johnson, T. E., Smithies, R. H., Danišík, M., Evans, N., Wingate, M. T. D., Clark, C., Spencer, C., Mikucki, E., and McDonald, B. J., 2016, Grain size matters: Implications for element and isotopic mobility in titanite: Precambrian Research, v. 278, p. 283-302.

Libby, W. G., and De Laeter, J. R., 1998, Biotite Rb-Sr age evidence for Early Palaeozoic tectonism along the cratonic margin in southwestern Australia: Australian Journal of Earth Sciences, v. 45, no. 623-632.

Lucassen, F., Franz, G., Dulski, P., Romer, R. L., and Rhede, D., 2011, Element and Sr isotope signatures of titanite as indicator of variable fluid composition in hydrated eclogite: Lithos, v. 121, p. 12-24.

Maino, M., Dallagiovanna, G., Dobson, K. J., Gaggero, L., Persano, C., Seno, S., and Stuart, F., 2012, Testing models of orogen exhumation using zircon (U-Th)/He

thermochronology - insight from the Ligurian Alps, Northern Italy: Tectonophysics, v. 560-561, p. 84-93.

Mezger, K., van der Pluijm, B., Essene, E. J., and Halliday, A. N., 1991, Synorogenic collapse: A perspective from the middle crust, the Proterozoic Grenville Orogen: Science, v. 254, no. 5032, p. 695-698.

Myers, J. S., 1995, Geology of the Esperance 1:1 000 000 sheet: Geological Survey of Western Australia, 1:1 000 000 Geological Series Explanatory Notes, p. 10.

Oliver, N. H. S., 1996, Review and classification of structural controls on fluid flow during regional metamorphism: Journal of Metamorphic Geology, v. 14, p. 477-492.

Page, L. M., Möller, C., and Johansson, L., 1996, $^{40}Ar/^{39}Ar$ geochronology across the Mylonite Zone and the Southwestern Granulite Province in the Sveconorwegian Orogen of S Sweden: Precambrian Research, v. 79, p. 239-259.

Papapavlou, K., Darling, J. R., Storey, C. D., Lightfoot, P. C., Moser, D. E., and Lasalle, S., 2017, Dating shear zones with plastically deformed titanite: New insights into the orogenic evolution of the Sudbury impact structure (Ontario, Canada): Precambrian Research, v. 291, p. 220-235.

Pidgeon, R. T., 1990, Timing of plutonism in the Proterozoic Albany Mobile Belt, southwestern Australia: Precambrian Research, v. 47, p. 157-167.

Reddy, S. M., Wheeler, J., Butler, R. W. H., Cliff, R. A., Freeman, S., Inger, S., Pickles, C., and Kelley, S. P., 2003, Kinematic reworking and exhumation within the convergent Alpine Orogen: Tectonophysics, v. 365, p. 77-102.

Rivers, T., 2008, Assembly and preservation of lower, mid, and upper orogenic crust in the Grenville Province - Implications for the evolution of large hot long-duration orogens: Precambrian Research, v. 167, p. 237-259.

-, 2012, Upper-crustal orogenic lid and mid-crustal core complexes: signature of a collapsed orogenic plateau in the hinterland of the Grenville Province: Canadian Journal of Earth Sciences, v. 49, no. 1, p. 1-42.

Rubatto, D., 2002, Zircon trace element geochemistry: partitioning with garnet and the link between U-Pb ages and metamorphism: Chemical Geology, v. 184, p. 123-138.

Smith, M. P., Storey, C. D., Jeffries, T. E., and Ryan, C. G., 2009, *In situ* U-Pb and trace element analysis of accessory minerals in the Kiruna District, Norrbotten, Sweden: New constraints on the timing and origin of mineralization: Journal of Petrology, v. 50, no. 11, p. 2063-2094.

Smithies, R. H., Spaggiari, C. V., and Kirkland, C. L., 2015, Building the crust of the Albany-Fraser Orogen: constraints from granite geochemistry: Geological Survey of Western Australia, Report 150, p. 49p.

Spaggiari, C., Bodorkos, S., Barquero-Molina, M., Tyler, I., and Wingate, M. T. D., 2009, Interpreted bedrock geology of the southern Yilgarn and central Albany-Fraser Orogen, Western Australia: Geological Survey of Western Australia, Record 2009/10, p. 84.

Spaggiari, C. V., Kirkland, C. L., Pawley, M. J., Smithies, R. H., Wingate, M. T. D., Doyle, M. G., Blenkinsop, T. G., Clark, C., Oorschot, C. W., Fox, L. J., and Savage, J., 2011, The geology of the east Albany-Fraser Orogen - a field guide: Geological Survey of Western Australia, Record 2011/23, p. 92.

Spaggiari, C. V., Kirkland, C. L., Smithies, R. H., Occhipinti, S. A., and Wingate, M. T. D., 2014a, Geological framework of the Albany-Fraser Orogen, *in* Spaggiari, C. V., and Tyler, I. M., eds., Albany-Fraser Orogen seismic and magnetotelluric (MT) workshop 2014: extended abstracts, Record 2014/6, Geological Survey of Western Australia, p. 12-27.

Spaggiari, C. V., Occhipinti, S. A., Korsch, R. J., Doublier, M. P., Clark, D. J., Dentith, M. C., Gessner, K., Doyle, M. G., Tyler, I. M., Kennett, B. L. N., Costelloe, R. D., Fomin, T., and Holzschuh, J., 2014b, Interpretation of Albany-Fraser seismic lines 12GA-AF1, 12GA-AF2 and 12GA-AF3: implications for crustal architecture, *in* Spaggiari, C. V., and Tyler, I. M., eds., Albany-Fraser Orogen seismic and magnetotelluric (MT) workshop 2014: extended abstracts, Record 2014/6, Geological Survey of Western Australia, p. 28 - 51.

Spaggiari, C. V., Kirkland, C. L., Smithies, R. H., and Wingate, M. T. D., 2014c, Tectonic links between Proterozoic sedimentary cycles, basin formation and magmatism in the Albany-Fraser Orogen, Western Australia: Geological Survey of Western Australia, Report 133.

Spencer, C. J., Thomas, R. J., Roberts, N. M. W., Cawood, P. A., Millar, I., and Tapster, S., 2015, Crustal growth during island arc accretion and transcurrent deformation, Natal Metamorphic Province, South Africa: New isotopic constraints: Precambrian Research, v. 265, p. 203-217.

Stephenson, N. C. N., Russell, T. G., Stubbs, D., and Kalocsai, G. I. Z., 1977, Potassium-argon ages of hornblendes from Precambrian gneisses from the south coast of Western Australia: Journal of the Royal Society of Western Australia, v. 59, no. 4, p. 105-109.

Storey, C. D., Smith, M. P., and Jeffries, T. E., 2007, In situ LA-ICP-MS U-Pb dating of metavolcanics of Norrbotten, Sweden: Records of extended geological histories in complex titanite grains: Chemical Geology, v. 240, p. 163-181.

Taylor, R. J. M., Kirkland, C. L., and Clark, C., 2016, Accessories after the facts: Constraining the timing, duration and conditions of high-temperature metamorphic processes: Lithos, v. 264, p. 239-257.

Tohver, E., Teixeira, W., van der Pluijm, B., Geraldes, M. C., Bettencourt, J. S., and Rizzotto, G., 2006, Restored transect across the exhumed Grenville orogen of Laurentia and Amazonia, with implications for crustal architecture: Geology, v. 34, no. 8, p. 669-672.

Villa, I. M., De Bièvre, P., Holden, N. E., and Renne, P. R., 2015, IUPAC-IUGS recommendation on the half life of ^{87}Rb: Geochimica et Cosmochimica Acta, v. 164, p. 382-385.

Waddell, P. J., Timms, N. E., Spaggiari, C. V., Kirkland, C. L., and Wingate, M. T. D., 2015, Analysis of the Ragged Basin, Western Australia: Insights into syn-orogenic basin evolution within the Albany-Fraser Orogen: Precambrian Research, v. 261, p. 166-187.

Wetherley, S., 1998, Tectonometamorphic evolution of the Mount Barren Group, Albany-Fraser Province, Western Australia: PhD thesis, University of Western Australia.

Willigers, B. J. A., van Gool, J. A. M., Wijbrans, J. R., Krogstad, E. J., and Mezger, K., 2002, Posttectonic cooling of the Nagssugtoqidian Orogen and a comparison of contrasting cooling histories in Precambrian and Phanerozoic orogens: The Journal of Geology, v. 110, p. 503-517.

Appendices

Appendix 3.1: Sample descriptions

Ledge Point (Lat: 35° 01' 12.10" S, Lon: 118° 00' 15.02" E)

AF01: Biotite Metagranite

Mineralogy: Pl, Or, Qtz, Bt, Mc, Mt

Sample AF01 is a largely undeformed biotite metagranite dominated by the original igneous mineralogy and textures, although some recrystallization of plagioclase and quartz and the presence of minor amounts of chlorite and epidote suggest low-grade deformation. No foliation is present. Biotite is coarse-grained and contains poikilitic inclusions of plagioclase and orthoclase. The metagranite has been suggested to be part of the 1190 – 1170 Ma Burnside Batholith, although this has not been tested by geochronology (Fitzsimons and Buchan, 2005).

AF02-1: Enderbitic Orthogneiss

Mineralogy: Pl, Bt, Cpx, Mc; minor Hb, Mt, Opx

Sample AF02-1 is a compositionally banded and foliated enderbitic orthogneiss with porphyroblasts of clino- and orthopyroxene. The orthogneiss is cut by a tonalite vein (mineralogy Pl, Qz, Mc). The unit has not been dated and its relationship to metagranite AF01 (also sampled at Ledge Point) is unknown (Fitzsimons and Buchan, 2005).

Whalehead Rock (Lat: 35° 01' 54.36" S, Lon: 117° 55' 13.48" E)

AF02-2: Enderbitic Orthogneiss

Mineralogy: Pl, Qz, Hb, Opx, Ilm; minor Bt

Sample AF02-2 is a coarse-grained enderbitic orthogneiss, collected ca 9km to the west of enderbitic orthogneiss AF02-1. The orthogneiss is compositionally banded and foliated, with sutured grain boundaries and some recrystallization of plagioclase and quartz. The crystallisation age of the igneous protolith to the orthogneiss has

been dated at 1289 ± 10 Ma using SHRIMP U-Pb zircon geochronology (Pidgeon, 1990).

AF03: Tonalitic Orthogneiss

Mineralogy: Pl, Bt, Qz, Or, Hb

Sample AF03 is a coarse grained, plagioclase and biotite-rich orthogneiss. Hornblende overprints partly polygonally recrystallised plagioclase and biotite. No foliation is visible in thin section. From SHRIMP U/Pb zircon geochronology, the age of intrusion of the tonalite is ca 1300 Ma (Love, 1999).

Shannon (Lat: 34° 40' 19.34" S, Lon: 116° 23' 10.39" E)

AF04-1: Metagranite

Mineralogy: Qz, Kfs, Pl, Bt, Hb

Sample AF04-1 is an inequigranular, porphyritic metagranite consisting mainly of quartz and feldspar, with lesser biotite and hornblende. A foliation is defined by recrystallised quartz, and the alignment of biotite and some feldspar grains.

AF04-2: Biotite orthogneiss

Mineralogy: Qz, Mc, Bt, Pl, Or; minor Ep

Sample AF04-2 is a biotite orthogneiss, with a strong foliation defined by biotite and recrystallised quartz. Large, internally fractured and heavily sericitised feldspar porphyroclasts are surrounded by anastomosing bands of quartz and biotite, suggesting retrograde overprinting of peak metamorphic conditions.

Elephant Rocks (Lat: 35° 01' 33.63" S, Lon: 117° 14' 18.39" E)

AF05: Biotite metagranite

Mineralogy: Mc, Qz, Pl, Bt; minor Cpx

Sample AF05 is a coarse-grained biotite metagranite containing large 1 – 2 cm feldspar and quartz phenocrysts. No foliation is visible, although the recrystallization of some quartz grains, strong sericitisation of feldspars and presence of minor amounts of chlorite suggest low-grade deformation. This unit may be equivalent to the megacrystic granite described by Duebendorfer (2002) at Green's Pool, 500m NW of Elephant Rocks.

Shelley Beach (Lat: 35° 06' 38.51" S, Lon: 117° 37' 46.03" E)

AF06: Biotite hornblende metagranite

Mineralogy: Pl, Or, Qz, Bt, Hb; minor Cpx

Sample AF06 is a coarse-grained biotite hornblende metagranite containing large 2 – 5 cm feldspar and quartz phenocrysts. Clinopyroxene occurs as reaction rims around some biotite grains. No foliation is visible, although minor recrystallization of quartz has occurred, myrmekitic reaction rims are common and feldspars are sericitised along intragranular fractures, suggesting at least low-grade deformation or alteration has occurred.

Peaceful Bay (Lat: 35° 03' 40.11" S, Lon: 116° 55' 35.76" E)

AF08A: Biotite augen gneiss

Mineralogy: Qz, Pl, Bt, Or, Mcl; minor Chl, Il

Sample AF08A is a coarse-grained biotite orthogneiss containing 1 – 5 cm feldspar, biotite and quartz porphyroclasts. A foliation is defined by the orientation of biotite laths, and myrmekitic reaction rims are common at the boundaries between feldspar grains. Feldspars are strongly sericitised and grain boundaries are generally lobate to sutured. The lack of metamorphic indicator minerals makes the interpretation of deformation conditions difficult. This unit is equivalent to the augen gneiss described by Duebendorfer (2002) at Peaceful Bay, which contains three ductile fabrics including shear bands.

AF08B: Garnet paragneiss

Mineralogy: Qz, Grt, Py, Bt; minor Chl

Paragneiss AF08B is mainly composed of quartz, and contains 2 – 4 cm porphyroblasts of quartz and garnet. A strong foliation is defined by biotite, elongation of quartz grains and weak compositional banding. The foliation bends around garnet porphyroblasts. Chlorite occurs as inclusions within garnet, preserving an earlier lower temperature assemblage. Quartz deformation textures and the mineral assemblage suggest at least amphibolite facies conditions were attained. Quartz-garnet paragneiss AF08B is equivalent to the garnet ± biotite-bearing quartzite described by Duebendorfer (2002) at Peaceful Bay.

AF08C: Amphibolite

Mineralogy: Pl, Hb, Qz, Or, Bt, Mc; minor Cpx,Il

Sample AF08C is a granoblastic amphibolite containing plagioclase porphyroblasts. No foliation is present, although grain boundaries are sutured and the dominant mineral assemblage Pl-Hb suggests amphibolite facies deformation. This lithology is described as a biotite-hornblende diorite by Duebendorfer (2002).

AF08D: Biotite garnet orthogneiss

Mineralogy: Qz, Pl, Bt, Grt, Mc

Sample AF08D is a granoblastic orthogneiss composed mostly of quartz and plagioclase, containing some 0.5 cm garnet porphyroblasts. A foliation is defined by biotite and by the elongation of some quartz grains. Grain boundaries are sutured and myrmekitic textures are common. Feldspars are generally sericitised and minor amounts of chlorite occur as epitaxial overgrowths on biotite.

Point Gordon (Lat: 34° 27’ 28.50” S, Lon: 119° 24’ 24.54” E)

BREM-2: Intermediate granulitic orthogneiss

Mineralogy: Pl, Or, Qz, Hb, Cpx, Mt, Mc, Opx

Sample BREM-2 is a foliated orthogneiss composed mainly of 0.5 cm quartz, plagioclase and orthoclase grains. Hornblende, clinopyroxene and orthopyroxene are present as 0.3 mm grains with strong alteration along intragranular fractures and cleavage planes. Grain boundaries are sutured and some compositional banding is evident.

Fishery Beach (Lat: 34° 25' 32.88" S, Lon: 119° 24' 01.20" E)

BREM-6: Intermediate granulitic orthogneiss

Mineralogy: Pl, Qz, Or, Opx, Il, Cpx, Bt

Sample BREM-6 is a foliated orthogneiss consisting mainly of 1.5 mm elongate feldspar and quartz grains. Grain boundaries are sutured with some exsolution of quartz and feldspar. Pyroxene, ilmenite and biotite are present as 0.2 – 0.5 mm grains, with some larger orthopyroxene porphyroblasts. Ortho- and clinopyroxene grains are strongly altered along cleavage planes and fractures, and feldspars are moderately sericitised.

Fishery Bay Headland (Lat: 34° 25; 36.24" S, Lon: 119° 24' 8.64" E)

BREM-10: Felsic granulite

Mineralogy: Or, Pl, Bt, Grt, Mt, Il, Chl, Ms, Opx

Sample BREM-10 is a weakly compositionally banded felsic granulite composed largely of orthoclase, plagioclase, biotite and garnet. The thin section preserves peak metamorphic textures, unevenly overprinted by Chl and Ms associated with retrograde metamorphism. Less altered portions of the thin section preserve polygonally recrystallised grain boundaries, near-granoblastic textures and minor Opx. Where strongly overprinted, grain boundaries are sutured, little Grt is present and some feldspars are replaced by Chl and Ms pseudomorphs. The weak foliation and feldspar sericitisation throughout the thin section are interpreted as results of the retrograde alteration.

SW of Barrens Beach (Lat: 33° 57' 10.40" S, Lon: 119° 58' 31.47" E)

AF01-SCH: Garnet staurolite schist

Mineralogy: Qz, Ms, Bt, Grt, Chl, St, Tur

AF01-SCH is composed mainly of fine-grained polygonally recrystallised quartz. A strong foliation is defined by anastomosing mica shear bands, and the elongation of quartz and staurolite. Garnet and starolite porphyroblasts contain abundant poikiloblastic quartz inclusions. The foliation bends around garnet porphyroblasts, which display typical 'snowball' textures such as the rotated pattern of inclusions and curvature of the grain boundary. A second generation of chlorite and biotite growth is present as larger grains oriented at high angles to the dominant foliation direction.

Barrens Beach (Lat: 33° 55' 33.78" S, Lon: 120° 01' 55.35" E)

BREM-SA: Biotite staurolite kyanite schist

Mineralogy: Qz, Ms, Bt, St, Ky

BREM-SA is composed mainly of fine-grained polygonally recrystallised quartz, interspersed with anastomosing mica shear bands. Staurolite and kyanite porphyroblasts are spatially associated with the mica shear bands, and contain abundant poikiloblastic quartz inclusions. An asymmetrical crenulation cleavage is defined by folding of the shear bands, which also resulted in bending of some staurolite, kyanite and muscovite grains. Three generations of biotite growth are present, and minor amounts of chlorite occur as epitaxial overgrowths on biotite.

North Two Mile Beach (Lat: 33° 56'36.37" S, Lon: 120° 09'09.20" E)

2MB-01: Quartz orthogneiss

Mineralogy: Qz, Pl, Mc, Bt, Ms

2MB-01 is an equigranular orthogneiss composed mainly of quartz, with lesser amounts of feldspar and mica. Grain boundaries are sutured and some quartz grains

are polygonally recrystallised. A foliation is defined by mica alignment and quartz and plagioclase elongation. Feldspars show minor amounts of sericitisation.

South Two Mile Beach (Lat: 33° 56'37.97" S, Lon: 120° 09'07.75" E)

2MB-02: Plagioclase orthogneiss

Mineralogy: Pl, Qz, Or, Bt, Ms

2MB-02 is an equigranular orthogneiss composed mainly of plagioclase, with lesser amounts of quartz, alkali feldspar, biotite and muscovite. A foliation is defined by mica alignment. Feldspar and quartz grains show some polygonal recrystallisation, with some larger grains and sutured boundaries remaining. In areas where less recyrstallisation has occurred, feldspars are strongly sericitised and show disequilibrium exsolution textures at grain boundaries, and biotite appears to be breaking down to form muscovite.

References

Duebendorfer, E. M., 2002, Regional correlation of Mesoproterozoic structures and deformational events in the Albany-Fraser orogen, Western Australia: Precambrian Research, v. 116, p. 129 - 154.

Fitzsimons, I., and Buchan, C., 2005, Geology of the Western Albany-Fraser Orogen, Western Australia - a field guide: Western Australian Geological Survey, Record 2005/11, p. 32.

Love, G. J., 1999, A study of wall-rock contamination in a tonalitic gneiss from King Point, near Albany, Western Australia: Curtin University of Technology, BSc (Honours) thesis (unpublished).

Pidgeon, R. T., 1990, Timing of plutonism in the Proterozoic Albany Mobile Belt, southwestern Australia: Precambrian Research, v. 47, p. 157-167

Appendix 3.2: Detailed analytical methods for $^{40}Ar/^{39}Ar$ thermochronology

Samples were crushed and sieved to separate the 125 – 250 μm fraction, which was washed in acetone and deionised water to remove dust. Optically unaltered 125 – 250 μm grains of biotite (16 samples), muscovite (4 samples) and hornblende (2 samples) were separated by hand-picking under a binocular microscope.

Samples were loaded into 22 large wells of an aluminium disc measuring 1.9 cm in diameter and 0.3 cm in depth. These wells were bracketed by small wells containing Fish Canyon sanidine (FCs), used as a neutron flux monitor. The FCs has an age of 28.294 ± 0.037 Ma (1σ) (Renne et al., 2010). To minimise nuclear interference reactions, the disc was Cd-shieled, and irradiated for 40 hours in the USGS TRIGA nuclear reactor (Oregon, USA) in a central position.

The mean J-value computed from the standard FCs grains within the small pits is 0.00903 ± 0.00002 (0.22%), calculated as the average and standard deviation of J-values of the standard FCs grains within each irradiation disc. An automated air pipette was used to monitor mass discrimination, which had a mean value of 1.00 ± 0.34 per Dalton (atomic mass unit) relative to an air ratio of 298.56 ± 0.31 (Lee et al., 2006). The correction factors for interfering isotopes were: $(^{39}Ar/^{37}Ar)_{Ca} = 7.60x10^{-4}$ (± 7%); $(^{36}Ar/^{37}Ar)_{Ca} = 2.81x10^{-4}$ (± 3%); and $(^{40}Ar/^{39}Ar)_{K} = 6.76x10^{-4}$ (± 10%).

The $^{40}Ar/^{39}Ar$ analyses were performed at the Western Australian Argon Isotope Facility at Curtin University. Samples were step-heated in 12 – 18 steps using a 110 W Spectron Laser Systems, by rastering a continuous Nd-YAG (IR, 1064 nm) laser over the sample for one minute, to ensure homogenous heating. The gas released from the sample was purified in a stainless steel extraction line using two SAES AP10 getters and one GP50 getter. Ar isotopes were measured in static mode with a MAP 215-50 mass spectrometer (resolution ~450; sensitivity $4x10^{-14}$ mol/V) with a Balzers SEV 217 electron multiplier using 9 – 10 cycles of peak-hopping. Data acquisition was performed with the Argus program written by M.O. McWilliams, and run under a LabView environment. Raw data were processed using ArArCALC software

(Koppers, 2002), and ages were calculated using the decay constants recommended by (Renne et al., 2011). A blank was monitored after every 4 steps, with a typical ^{40}Ar range of $3x10^{-16}$ – $5x10^{-16}$ mol. Appendix 3.3 contains Ar isotope data corrected for blank, mass discrimination and radioactive decay, with individual errors given at the 2σ level.

In this study, the criteria for the determination of an age plateau are as follows: plateaus must include at least 70% of the total measured ^{39}Ar, and plateaus should be distributed over at least three consecutive steps that agree at a 95% confidence level and satisfy a probability of fit (P) of at least 0.05. Plateau ages in Table 3.1 and Figure 3.2 are given at the 2σ level, and are calculated using the mean of all plateau steps, weighted by the inverse variance of their individual analytical error. Mini-plateaus are defined similarly, but include 50% - 70% of the total ^{39}Ar. Mini-plateau ages are less robust than plateau ages. All sources of uncertainty are included in the calculations.

References

Koppers, A. A. P., 2002, ArArCALC-software for $^{40}Ar/^{39}Ar$ age calculations: Computers & Geosciences, v. 28, p. 605 - 619.

Lee, J. Y., Marti, K., Severinghaus, J. P., Kawamura, K., Yoo, H. S., Lee, J. B., and Kim, J. S., 2006, A redetermination of the isotopic abundance of atmospheric Ar: Geochimica et Cosmochimica Acta, v. 70, p. 4507-4512.

Renne, P. R., Balco, G., Ludwig, K. R., Mundil, R., and Min, K., 2011, Response to the comment by W.H. Schwarz et al. on "Joint determination of ^{40}K decay constants and $^{40}Ar^*/^{40}K$ for the Fish Canyon sanidine standard, and improved accuracy for $^{40}Ar/^{39}Ar$ geochronology" by P.R. Renne et al. (2010): Geochimica et Cosmochimica Acta, v. 75, p. 5097-5100.

Renne, P. R., Mundil, R., Balco, G., Min, K., and Ludwig, K. R., 2010, Joint determination of ^{40}K decay constants and $^{40}Ar^*/^{40}K$ for the Fish Canyon sanidine standard, and improved accuracy for $^{40}Ar/^{39}Ar$ geochronology: Geochimica et Cosmochimica Acta, v. 74, p. 5349 - 5367.

Appendix 3.3: $^{40}Ar/^{39}Ar$ thermochronology results

Table A3.3-1 Hb AF02-1 Incremental Heating

		^{36}Ar (a)	^{37}Ar (ca)	^{38}Ar (cl)	^{39}Ar (k)	^{40}Ar (r)	Age (Ma)	± 2σ (Ma)	^{40}Ar (r) (%)	^{39}Ar (k) (%)	K/Ca	± 2σ
3M25530D	**56.40 W**	**0.0000036**	**0.0008416**	**0.0000020**	**0.0002700**	**0.0268584**	**1154.41**	**± 137.52**	**96.13**	**1.11**	**0.166**	**± 0.719**
3M25531D	**56.70 W**	**0.0000101**	**0.0280959**	**0.0001124**	**0.0094204**	**0.9499072**	**1166.16**	**± 9.89**	**99.68**	**38.86**	**0.174**	**± 0.029**
3M25532D	**57.00 W**	**0.0000005**	**0.0364422**	**0.0001314**	**0.0111140**	**1.1308021**	**1173.89**	**± 9.41**	**100.01**	**45.84**	**0.158**	**± 0.023**
3M25534D	**57.20 W**	**0.0000025**	**0.0116020**	**0.0000431**	**0.0034383**	**0.3452042**	**1162.45**	**± 14.50**	**99.78**	**14.18**	**0.154**	**± 0.051**
	Σ	0.0000157	0.0769817	0.0002889	0.0242427	2.4527719						

Table A3.3-2 Hb AF02-1 Detailed Results

	^{40}Ar (r)/ ^{39}Ar (k)	± 2σ	Age (Ma)	± 2σ (Ma)	MSWD	^{39}Ar (k) (%, n)	K/Ca	± 2σ
Age Plateau	101.14148	± 0.72495 ± 0.72%	1168.76	± 7.23 ± 0.62%	0.76 52%	100.00 4	0.163	± 0.017
			Full External Error	± 9.09	2.63	2σ Confidence Limit		
			Analytical Error	± 6.16	1.0000	Error Magnification		
Total Fusion Age	101.17558	± 0.74302 ± 0.73%	1169.05	± 7.36 ± 0.63%		4	0.163	± 0.019
			Full External Error	± 9.20				
			Analytical Error	± 6.32				

Table A3.3-3 Bt AF01 Incremental Heating

		^{36}Ar (a)	^{37}Ar (ca)	^{38}Ar (cl)	^{39}Ar (k)	^{40}Ar (r)	Age (Ma)	± 2σ (Ma)	^{40}Ar (r) (%)	^{39}Ar (k) (%)	K/Ca	± 2σ
2A22613D	55.60 W	0.000013	0.000114	0.000002	0.000640	0.043170	856.71	± 79.19	91.91	0.09	2.4	± 1.9
2A22614D	55.80 W	0.000083	0.001162	0.000018	0.014222	0.991665	879.67	± 8.51	97.56	2.01	5.3	± 0.9
2A22615D	55.90 W	0.000025	0.000163	0.000000	0.005154	0.383098	925.01	± 14.51	98.07	0.73	13.6	± 9.7
2A22617D	56.00 W	0.000060	0.000330	0.000004	0.010024	0.804701	982.00	± 13.38	97.82	1.42	13.1	± 4.4
2A22618D	56.10 W	0.000041	0.000341	0.000021	0.015812	1.369700	1040.90	± 7.73	99.11	2.23	19.9	± 9.2
2A22691D	**56.20 W**	**0.000064**	**0.000540**	**0.000013**	**0.032078**	**2.957097**	**1090.94**	**± 7.26**	**99.36**	**4.53**	**25.5**	**± 13.4**
2A22692D	**56.30 W**	**0.000172**	**0.004974**	**0.000229**	**0.177995**	**16.402871**	**1090.67**	**± 6.83**	**99.69**	**25.14**	**15.4**	**± 1.2**
2A22694D	**56.30 W**	**0.000005**	**0.000073**	**0.000000**	**0.013032**	**1.208873**	**1096.09**	**± 8.18**	**99.87**	**1.84**	**76.7**	**± 260.9**
2A22695D	**56.40 W**	**0.000005**	**0.000473**	**0.000034**	**0.032515**	**3.023514**	**1098.07**	**± 9.29**	**99.95**	**4.59**	**29.5**	**± 16.4**
2A22696D	**56.50 W**	**0.000007**	**0.000337**	**0.000019**	**0.024517**	**2.282578**	**1099.07**	**± 8.09**	**99.91**	**3.46**	**31.3**	**± 23.7**
2A22697D	**56.60 W**	**0.000001**	**0.000429**	**0.000025**	**0.028726**	**2.640404**	**1088.58**	**± 6.67**	**100.01**	**4.06**	**28.8**	**± 17.6**
2A22699D	**56.70 W**	**0.000001**	**0.000692**	**0.000050**	**0.043216**	**3.990690**	**1092.35**	**± 8.41**	**100.01**	**6.10**	**26.9**	**± 10.4**
2A22700D	**56.80 W**	**0.000002**	**0.000458**	**0.000018**	**0.021608**	**1.986741**	**1088.83**	**± 8.68**	**100.02**	**3.05**	**20.3**	**± 11.5**
2A22701D	**56.90 W**	**0.000005**	**0.000152**	**0.000016**	**0.011079**	**1.005724**	**1078.45**	**± 11.77**	**99.86**	**1.56**	**31.4**	**± 51.4**
2A22702D	**57.20 W**	**0.000003**	**0.001130**	**0.000056**	**0.062178**	**5.706409**	**1087.31**	**± 7.20**	**99.98**	**8.78**	**23.7**	**± 5.8**
2A22707D	**57.50 W**	**0.000003**	**0.001443**	**0.000040**	**0.055041**	**5.063152**	**1089.21**	**± 6.13**	**100.02**	**7.77**	**16.4**	**± 3.4**
2A22708D	**58.00 W**	**0.000004**	**0.002602**	**0.000065**	**0.080000**	**7.405016**	**1094.30**	**± 6.28**	**99.98**	**11.30**	**13.2**	**± 0.8**
2A22721D	**58.50 W**	**0.000004**	**0.000525**	**0.000018**	**0.014104**	**1.304907**	**1093.94**	**± 7.85**	**100.08**	**1.99**	**11.5**	**± 5.1**
2A22722D	70.00 W	0.000005	0.013869	0.000047	0.066133	6.245576	1110.86	± 6.51	99.97	9.34	2.1	± 0.1
	Σ	0.000482	0.029808	0.000678	0.708073	64.815886						

Table A3.3-4 Bt AF01 Detailed Results

	^{40}Ar (r)/ ^{39}Ar (k)	± 2σ	Age (Ma)	± 2σ (Ma)	MSWD	^{39}Ar (k) (%, n)	K/Ca	± 2σ
Age Plateau	92.2538	± 0.2737 ± 0.30%	1091.56	± 4.34 ± 0.40%	1.34	84.18 13	14.2	± 1.2
			Full External Error	± 6.77	2.18	Statistical T Ratio		
			Analytical Error	± 2.43	1.1564	Error Magnification		
Total Fusion Age	91.5384	± 0.2605 ± 0.28%	1085.20	± 4.27 ± 0.39%		19	10.2	± 0.4
			Full External Error	± 6.70				
			Analytical Error	± 2.32				

Table A3.3-5 Bt AF02-1 Incremental Heating

		^{36}Ar (a)	^{37}Ar (ca)	^{38}Ar (cl)	^{39}Ar (k)	^{40}Ar (r)	Age (Ma)	± 2σ (Ma)	^{40}Ar (r) (%)	^{39}Ar (k) (%)	K/Ca	± 2σ
2A22394D	56.00 W	0.000015	0.000386	0.000000	0.001680	0.108554	827.71	± 30.99	96.06	0.70	1.87	± 0.57
2A22395D	55.50 W	0.000010	0.000030	0.000000	0.000469	0.039520	1018.65	± 87.66	92.70	0.19	6.67	± 21.54
2A22396D	55.70 W	0.000005	0.000053	0.000002	0.001038	0.092302	1061.84	± 43.53	98.48	0.43	8.37	± 16.43
2A22397D	56.00 W	0.000025	0.001574	0.000046	0.015742	1.435223	1081.92	± 10.25	99.47	6.53	4.30	± 0.40
2A22399D	56.10 W	0.000005	0.001690	0.000079	0.024941	2.393771	1124.30	± 8.24	99.94	10.35	6.35	± 0.56
2A22400D	56.20 W	0.000012	0.001238	0.000041	0.018903	1.820840	1127.33	± 9.27	99.81	7.84	6.57	± 0.53
2A22401D	56.30 W	0.000006	0.000690	0.000019	0.009567	0.937966	1142.21	± 12.30	99.81	3.97	5.96	± 1.12
2A22402D	**56.40 W**	**0.000001**	**0.000781**	**0.000019**	**0.011039**	**1.101920**	**1157.53**	**± 12.30**	**99.97**	**4.58**	**6.08**	**± 0.86**
2A22421D	**56.60 W**	**0.000010**	**0.003600**	**0.000153**	**0.066732**	**6.687238**	**1160.83**	**± 6.03**	**99.95**	**27.69**	**7.97**	**± 0.44**
2A22422D	**56.70 W**	**0.000010**	**0.000519**	**0.000034**	**0.008586**	**0.862207**	**1162.57**	**± 16.37**	**99.67**	**3.56**	**7.11**	**± 2.10**
2A22423D	**56.80 W**	**0.000009**	**0.000888**	**0.000030**	**0.011315**	**1.139034**	**1164.71**	**± 11.48**	**99.78**	**4.69**	**5.48**	**± 1.03**
2A22424D	**56.90 W**	**0.000005**	**0.000482**	**0.000007**	**0.005079**	**0.502944**	**1150.68**	**± 19.63**	**99.71**	**2.11**	**4.53**	**± 1.52**
2A22426D	**60.00 W**	**0.000005**	**0.005584**	**0.000165**	**0.065941**	**6.647083**	**1165.89**	**± 7.30**	**99.98**	**27.36**	**5.08**	**± 0.29**
	Σ	0.000118	0.017517	0.000596	0.241033	23.768601						

Table A3.3-6 Bt AF02-1 Detailed Results

	^{40}Ar (r)/ ^{39}Ar (k)	± 2σ	Age (Ma)	± 2σ (Ma)	MSWD	^{39}Ar (k) (%, n)	K/Ca	± 2σ
Age Plateau	100.3544	± 0.4534 ± 0.45%	1162.06	± 5.40 ± 0.46%	0.68	70.0 6	5.92	± 1.12
			Full External Error	± 7.70	2.57	Statistical T Ratio		
			Analytical Error	± 3.87	1.0000	Error Magnification		
Total Fusion Age	98.6115	± 0.3651 ± 0.37%	1147.12	± 4.88 ± 0.43%		13	5.92	± 0.19
			Full External Error	± 7.29				
			Analytical Error	± 3.14				

Table A3.3-7 Bt AF02-2 Incremental Heating

		^{36}Ar (a)	^{37}Ar (ca)	^{38}Ar (cl)	^{39}Ar (k)	^{40}Ar (r)	Age (Ma)	± 2σ (Ma)	^{40}Ar (r) (%)	^{39}Ar (k) (%)	K/Ca	± 2σ
2A22902D	55.90 W	0.000015	0.000425	0.000019	0.010349	0.968361	1103.22	± 11.18	99.55	9.82	10.5	± 3.9
2A22903D	**56.00 W**	**0.000009**	**0.000369**	**0.000028**	**0.018687**	**1.834875**	**1143.47**	**± 8.18**	**99.85**	**17.73**	**21.8**	**± 11.4**
2A22904D	**56.10 W**	**0.000009**	**0.000007**	**0.000004**	**0.004615**	**0.460019**	**1156.23**	**± 13.52**	**100.56**	**4.38**	**300.4**	**± 8161.2**
2A22906D	**56.20 W**	**0.000003**	**0.000532**	**0.000016**	**0.012184**	**1.207368**	**1151.27**	**± 12.96**	**99.93**	**11.56**	**9.8**	**± 3.5**
2A22907D	**56.30 W**	**0.000005**	**0.000379**	**0.000020**	**0.018925**	**1.884065**	**1155.21**	**± 7.74**	**99.92**	**17.95**	**21.5**	**± 10.9**
2A22908D	**56.40 W**	**0.000007**	**0.000050**	**0.000015**	**0.007730**	**0.769794**	**1155.44**	**± 17.45**	**99.74**	**7.33**	**67.0**	**± 240.4**
2A22909D	**56.50 W**	**0.000011**	**0.000504**	**0.000017**	**0.018003**	**1.790627**	**1154.43**	**± 11.93**	**99.82**	**17.08**	**15.4**	**± 5.6**
2A22911D	**56.60 W**	**0.000000**	**0.000011**	**0.000000**	**0.001587**	**0.157543**	**1152.86**	**± 33.74**	**99.91**	**1.51**	**59.4**	**± 874.8**
2A22912D	**56.80 W**	**0.000002**	**0.000008**	**0.000000**	**0.001382**	**0.136356**	**1147.51**	**± 36.69**	**100.49**	**1.31**	**75.9**	**± 1625.6**
2A22913D	**57.00 W**	**0.000001**	**0.000088**	**0.000000**	**0.002804**	**0.278336**	**1152.61**	**± 23.87**	**99.94**	**2.66**	**13.6**	**± 28.2**
2A22928D	**57.30 W**	**0.000006**	**0.000053**	**0.000006**	**0.001280**	**0.127904**	**1158.18**	**± 49.65**	**101.35**	**1.21**	**10.4**	**± 60.6**
2A22929D	**58.00 W**	**0.000012**	**0.000657**	**0.000017**	**0.007229**	**0.727964**	**1165.05**	**± 17.73**	**100.50**	**6.86**	**4.7**	**± 2.2**
2A22930D	**75.00 W**	**0.000008**	**0.000133**	**0.000005**	**0.000628**	**0.062778**	**1159.23**	**± 67.12**	**103.99**	**0.60**	**2.0**	**± 4.7**
	Σ	0.000013	0.003217	0.000146	0.105404	10.405990						

Table A3.3-8 Bt AF02-2 Detailed Results

	^{40}Ar (r)/ ^{39}Ar (k)	± 2σ	Age (Ma)	± 2σ (Ma)	MSWD	^{39}Ar (k) (%, n)	K/Ca	± 2σ
Age Plateau	99.2093	± 0.4735 ± 0.48%	1152.26	± 5.53 ± 0.48%	0.74	90.18 12	7.1	± 2.9
			Full External Error	± 7.76	2.20	Statistical T Ratio		
			Analytical Error	± 4.06	1.0000	Error Magnification		
Total Fusion Age	98.7246	± 0.4720 ± 0.48%	1148.09	± 5.52 ± 0.48%		13	14.1	± 3.4
			Full External Error	± 7.74				
			Analytical Error	± 4.06				

Table A3.3-9 Bt AF03 Incremental Heating

		^{36}Ar (a)	^{37}Ar (ca)	^{38}Ar (cl)	^{39}Ar (k)	^{40}Ar (r)	Age (Ma)	± 2σ (Ma)	^{40}Ar (r) (%)	^{39}Ar (k) (%)	K/Ca	± 2σ
2A22723D	55.60 W	0.000012	0.000017	0.000000	0.000479	0.038926	991.43	± 105.34	91.55	0.12	12	± 203
2A22724D	55.80 W	0.000034	0.000096	0.000013	0.007038	0.662739	1108.42	± 19.43	98.49	1.80	32	± 99
2A22726D	**56.00 W**	**0.000103**	**0.000270**	**0.000037**	**0.037270**	**3.643903**	**1139.87**	**± 7.15**	**99.17**	**9.54**	**59**	**± 68**
2A22727D	**56.10 W**	**0.000017**	**0.000149**	**0.000026**	**0.017716**	**1.737510**	**1142.52**	**± 9.94**	**99.71**	**4.53**	**51**	**± 106**
2A22728D	**56.20 W**	**0.000025**	**0.000292**	**0.000067**	**0.039321**	**3.826436**	**1135.91**	**± 6.90**	**99.80**	**10.06**	**58**	**± 61**
2A22729D	**56.30 W**	**0.000010**	**0.000224**	**0.000039**	**0.038226**	**3.753029**	**1143.41**	**± 6.85**	**99.92**	**9.78**	**73**	**± 99**
2A22731D	**56.40 W**	**0.000019**	**0.000222**	**0.000092**	**0.054732**	**5.352003**	**1140.00**	**± 7.30**	**99.90**	**14.00**	**106**	**± 150**
2A22732D	**56.50 W**	**0.000010**	**0.000075**	**0.000020**	**0.012840**	**1.255990**	**1140.31**	**± 11.19**	**99.75**	**3.28**	**74**	**± 298**
2A22733D	**56.60 W**	**0.000004**	**0.000029**	**0.000015**	**0.014698**	**1.443798**	**1143.82**	**± 9.97**	**99.91**	**3.76**	**215**	**± 2178**
2A22734D	**56.80 W**	**0.000004**	**0.000002**	**0.000029**	**0.017490**	**1.726451**	**1147.96**	**± 11.18**	**99.93**	**4.47**	**3165**	**± 397879**
2A22736D	**57.00 W**	**0.000017**	**0.000542**	**0.000083**	**0.069751**	**6.881433**	**1147.52**	**± 7.05**	**99.93**	**17.85**	**55**	**± 31**
2A22737D	**57.20 W**	**0.000006**	**0.000114**	**0.000013**	**0.013453**	**1.320973**	**1143.51**	**± 9.62**	**99.85**	**3.44**	**51**	**± 137**
2A22738D	**57.50 W**	**0.000014**	**0.000374**	**0.000043**	**0.037854**	**3.747062**	**1150.36**	**± 7.29**	**99.89**	**9.68**	**44**	**± 35**
2A22757D	**58.00 W**	**0.000008**	**0.000070**	**0.000031**	**0.019210**	**1.904101**	**1151.48**	**± 9.66**	**99.88**	**4.91**	**118**	**± 191**
2A22758D	**80.00 W**	**0.000001**	**0.000072**	**0.000022**	**0.010786**	**1.068691**	**1151.14**	**± 13.23**	**99.97**	**2.76**	**65**	**± 101**
	Σ	0.000283	0.002373	0.000529	0.390864	38.363046						

Table A3.3-10 Bt AF03 Detailed Results

	^{40}Ar (r)/ ^{39}Ar (k)	± 2σ	Age (Ma)	± 2σ (Ma)	MSWD	^{39}Ar (k) (%, n)	K/Ca	± 2σ
Age Plateau	98.2170	± 0.3195 ± 0.33%	1143.72	± 4.63 ± 0.41%	1.39	98.08 13	52	± 19
			Full External Error	± 7.12	2.18	Statistical T Ratio		
			Analytical Error	± 2.75	1.1783	Error Magnification		
Total Fusion Age	98.1493	± 0.2806 ± 0.29%	1143.14	± 4.44 ± 0.39%		15	71	± 33
			Full External Error	± 7.00				
			Analytical Error	± 2.42				

Table A3.3-11 Bt AF04-1 Incremental Heating

		^{36}Ar (a)	^{37}Ar (ca)	^{38}Ar (cl)	^{39}Ar (k)	^{40}Ar (r)	Age (Ma)	± 2σ (Ma)	^{40}Ar (r) (%)	^{39}Ar (k) (%)	K/Ca	± 2σ
2A22824D	55.70 W	0.000129	0.000015	0.000172	0.049409	6.105764	1350.08	± 8.56	99.37	18.22	1415	± 14713
2A22825D	55.80 W	0.000010	0.000018	0.000053	0.014787	1.795125	1333.28	± 12.52	99.84	5.45	347	± 2741
2A22826D	55.90 W	0.000012	0.000019	0.000023	0.003601	0.430754	1319.37	± 15.93	99.19	1.33	84	± 673
2A22827D	56.00 W	0.000001	0.000015	0.000029	0.010373	1.248607	1325.28	± 13.54	99.98	3.83	294	± 3277
2A22829D	56.10 W	0.000009	0.000087	0.000046	0.012975	1.567817	1328.87	± 7.94	99.83	4.79	64	± 118
2A22830D	56.20 W	0.000007	0.000005	0.000058	0.018574	2.231701	1323.54	± 15.17	99.91	6.85	1630	± 51847
2A22831D	56.30 W	0.000019	0.000092	0.000098	0.032309	3.920921	1332.92	± 7.84	99.86	11.92	151	± 226
2A22832D	56.40 W	0.000005	0.000237	0.000126	0.042271	5.124667	1331.98	± 9.13	99.97	15.59	77	± 50
2A22834D	56.50 W	0.000005	0.000012	0.000024	0.008779	1.048995	1318.41	± 11.36	99.87	3.24	312	± 4343
2A22846D	56.60 W	0.000007	0.000122	0.000015	0.005312	0.635745	1319.90	± 19.85	100.35	1.96	19	± 23
2A22847D	56.70 W	0.000002	0.000016	0.000007	0.003244	0.378177	1295.32	± 22.91	99.86	1.20	87	± 822
2A22848D	56.90 W	0.000006	0.000078	0.000008	0.004594	0.546681	1314.57	± 14.01	100.35	1.69	25	± 48
2A22849D	57.30 W	0.000011	0.000092	0.000155	0.043817	5.195141	1311.12	± 8.65	99.94	16.16	205	± 432
2A22851D	57.80 W	0.000003	0.000117	0.000033	0.012886	1.532774	1314.18	± 10.00	100.05	4.75	47	± 59
2A22852D	75.00 W	0.000005	0.000164	0.000012	0.008189	0.986814	1326.32	± 16.31	99.85	3.02	21	± 13
	Σ	0.000198	0.000806	0.000859	0.271119	32.749685						

Table A3.3-12 Bt AF04-1 Detailed Results

	^{40}Ar (r)/ ^{39}Ar (k)	± 2σ	Age (Ma)	± 2σ (Ma)	MSWD	^{39}Ar (k) (%, n)	K/Ca	± 2σ
Age Plateau	Cannot Calculate							
Total Fusion Age	120.7944	± 0.4096 ± 0.34%	1328.56	± 5.22 ± 0.39%		15	145	± 107
			Full External Error	± 8.07				
			Analytical Error	± 3.19				

Table A3.3-13 Bt AF04-2 Incremental Heating

		^{36}Ar (a)	^{37}Ar (ca)	^{38}Ar (cl)	^{39}Ar (k)	^{40}Ar (r)	Age (Ma)	± 2σ (Ma)	^{40}Ar (r) (%)	^{39}Ar (k) (%)	K/Ca	± 2σ
2A22853D	55.90 W	0.000079	0.000071	0.000031	0.008728	1.099918	1368.82	± 11.15	97.91	7.33	53	± 123
2A22854D	56.00 W	0.000015	0.000053	0.000164	0.029082	3.815070	1407.65	± 8.55	99.88	24.43	234	± 766
2A22856D	56.10 W	0.000007	0.000090	0.000020	0.003685	0.502997	1446.88	± 29.88	99.61	3.10	18	± 31
2A22857D	56.20 W	0.000015	0.000030	0.000068	0.015677	2.091077	1423.99	± 14.18	99.79	13.17	228	± 1315
2A22858D	56.30 W	0.000010	0.000078	0.000071	0.014091	1.869269	1418.56	± 12.51	99.84	11.84	77	± 176
2A22859D	56.40 W	0.000006	0.000054	0.000062	0.011287	1.484274	1410.02	± 11.42	99.88	9.48	89	± 322
2A22861D	56.50 W	0.000001	0.000119	0.000128	0.022631	2.938345	1397.59	± 9.93	100.01	19.01	82	± 128
2A22877D	56.70 W	0.000000	0.000071	0.000005	0.000369	0.048238	1404.44	± 102.91	100.10	0.31	2	± 8
2A22878D	56.90 W	0.000000	0.000064	0.000045	0.006900	0.928359	1432.56	± 18.03	99.99	5.80	46	± 153
2A22879D	57.20 W	0.000007	0.000262	0.000032	0.005369	0.692521	1391.25	± 21.04	99.69	4.51	9	± 8
2A22880D	57.80 W	0.000003	0.000003	0.000001	0.000525	0.067378	1386.21	± 85.29	98.88	0.44	82	± 6644
2A22882D	75.00 W	0.000004	0.000037	0.000006	0.000683	0.097123	1488.47	± 61.53	98.87	0.57	8	± 48
	Σ	0.000144	0.000439	0.000634	0.119024	15.634569						

Table A3.3-14 Bt AF04-2 Detailed Results

	^{40}Ar (r)/ ^{39}Ar (k)	± 2σ	Age (Ma)	± 2σ (Ma)	MSWD	^{39}Ar (k) (%, n)	K/Ca	± 2σ
Age Plateau	Cannot Calculate							
Total Fusion Age	131.3561	± 0.5799 ± 0.44%	1408.92	± 6.09 ± 0.43%		12	116	± 184
			Full External Error	± 8.89				
			Analytical Error	± 4.32				

Table A3.3-15 Bt AF05 Incremental Heating

		^{36}Ar (a)	^{37}Ar (ca)	^{38}Ar (cl)	^{39}Ar (k)	^{40}Ar (r)	Age (Ma)	± 2σ (Ma)	^{40}Ar (r) (%)	^{39}Ar (k) (%)	K/Ca	± 2σ
2A22579D	55.60 W	0.000180	0.000444	0.000026	0.018457	1.106094	779.09	± 6.83	95.36	6.07	17.9	± 5.7
2A22580D	55.80 W	0.000043	0.000122	0.000005	0.007344	0.495923	857.57	± 10.91	97.47	2.42	25.8	± 35.6
2A22581D	55.90 W	0.000048	0.000307	0.000015	0.014860	1.007896	860.61	± 8.02	98.60	4.89	20.8	± 9.6
2A22582D	56.00 W	0.000060	0.000407	0.000000	0.030128	2.151650	896.46	± 7.09	99.17	9.91	31.9	± 12.5
2A22584D	56.10 W	0.000017	0.000225	0.000015	0.021090	1.574320	928.11	± 8.14	99.68	6.94	40.4	± 26.7
2A22585D	56.20 W	0.000014	0.000234	0.000024	0.023321	1.781299	944.89	± 7.56	99.76	7.67	42.9	± 27.7
2A22586D	56.30 W	0.000025	0.000355	0.000047	0.048978	3.749341	946.53	± 6.51	99.80	16.11	59.3	± 26.8
2A22602D	56.40 W	0.000005	0.000031	0.000000	0.003431	0.255671	926.83	± 20.56	99.40	1.13	47.6	± 188.4
2A22603D	56.50 W	0.000006	0.000071	0.000025	0.017495	1.361574	958.75	± 9.73	99.87	5.75	106.3	± 179.3
2A22604D	56.60 W	0.000022	0.000653	0.000046	0.061330	4.634173	936.98	± 6.58	99.86	20.17	40.4	± 8.0
2A22605D	56.70 W	0.000003	0.000069	0.000001	0.008585	0.676413	967.89	± 14.82	100.13	2.82	53.4	± 88.1
2A22607D	56.90 W	0.000006	0.000068	0.000001	0.009566	0.750826	965.11	± 9.80	99.77	3.15	60.2	± 122.5
2A22608D	57.10 W	0.000009	0.000002	0.000003	0.008021	0.623079	957.38	± 9.97	99.56	2.64	2020.5	± 136684
2A22609D	57.50 W	0.000006	0.000143	0.000016	0.013697	1.063492	957.00	± 10.51	99.84	4.50	41.1	± 39.4
2A22610D	58.00 W	0.000005	0.000100	0.000015	0.008041	0.656296	994.62	± 14.42	99.75	2.64	34.5	± 38.9
2A22612D	70.00 W	0.000013	0.000064	0.000006	0.009751	0.780872	980.19	± 12.71	99.51	3.21	65.3	± 118.9
	Σ	0.000456	0.003234	0.000245	0.304094	22.668918						

Table A3.3-16 Bt AF05 Detailed Results

	^{40}Ar (r)/ ^{39}Ar (k)	± 2σ	Age (Ma)	± 2σ (Ma)	MSWD	^{39}Ar (k) (%, n)	K/Ca	± 2σ
Age Plateau	Cannot Calculate							
Total Fusion Age	74.5458	± 0.2433 ± 0.33%	927.13	± 3.97 ± 0.43%		16	40.4	± 6.9
			Full External Error	± 6.00				
			Analytical Error	± 2.37				

Table A3.3-17 Bt AF06 Incremental Heating

		^{36}Ar (a)	^{37}Ar (ca)	^{38}Ar (cl)	^{39}Ar (k)	^{40}Ar (r)	Age (Ma)	± 2σ (Ma)	^{40}Ar (r) (%)	^{39}Ar (k) (%)	K/Ca	± 2σ
2A22528D	55.60 W	0.000078	0.000506	0.000005	0.006851	0.573259	1013.76	± 15.05	96.10	2.36	5.8	± 1.7
2A22529D	55.70 W	0.000066	0.000391	0.000021	0.018342	1.783257	1135.12	± 10.33	98.90	6.31	20.2	± 6.6
2A22530D	**55.80 W**	**0.000006**	**0.000002**	**0.000011**	**0.004319**	**0.431001**	**1157.23**	**± 19.84**	**99.56**	**1.49**	**1064.8**	**± 87715**
2A22531D	**55.90 W**	**0.000054**	**0.000381**	**0.000021**	**0.028016**	**2.811909**	**1162.16**	**± 8.14**	**99.43**	**9.64**	**31.6**	**± 9.4**
2A22533D	**56.00 W**	**0.000001**	**0.000027**	**0.000009**	**0.005331**	**0.533031**	**1158.84**	**± 19.30**	**100.03**	**1.83**	**84.5**	**± 421.6**
2A22534D	**56.10 W**	**0.000001**	**0.000128**	**0.000009**	**0.009403**	**0.956311**	**1173.56**	**± 10.84**	**99.98**	**3.24**	**31.6**	**± 34.1**
2A22535D	**56.20 W**	**0.000001**	**0.000006**	**0.000009**	**0.004147**	**0.417028**	**1163.92**	**± 19.54**	**100.05**	**1.43**	**307.4**	**± 5886.8**
2A22536D	**56.30 W**	**0.000012**	**0.000505**	**0.000064**	**0.043972**	**4.447254**	**1168.74**	**± 8.01**	**99.92**	**15.13**	**37.5**	**± 9.6**
2A22538D	**56.40 W**	**0.000004**	**0.000305**	**0.000031**	**0.036999**	**3.739310**	**1168.10**	**± 7.58**	**99.97**	**12.73**	**52.1**	**± 16.6**
2A22569D	**56.50 W**	**0.000009**	**0.001258**	**0.000113**	**0.074698**	**7.557987**	**1169.10**	**± 6.65**	**99.96**	**25.70**	**25.5**	**± 4.3**
2A22570D	**56.60 W**	**0.000007**	**0.000004**	**0.000006**	**0.006196**	**0.624677**	**1166.08**	**± 18.62**	**99.65**	**2.13**	**596.3**	**± 24649**
2A22571D	**56.70 W**	**0.000000**	**0.000017**	**0.000007**	**0.002709**	**0.276078**	**1175.35**	**± 29.74**	**100.04**	**0.93**	**66.8**	**± 694.7**
2A22572D	**56.90 W**	**0.000006**	**0.000133**	**0.000019**	**0.011445**	**1.160581**	**1171.02**	**± 12.65**	**99.86**	**3.94**	**36.9**	**± 49.8**
2A22574D	**57.10 W**	**0.000002**	**0.000043**	**0.000006**	**0.008989**	**0.909005**	**1168.57**	**± 12.11**	**100.07**	**3.09**	**90.3**	**± 374.2**
2A22575D	**57.50 W**	**0.000001**	**0.000077**	**0.000026**	**0.013526**	**1.379765**	**1176.09**	**± 9.03**	**99.97**	**4.65**	**75.1**	**± 178.8**
2A22576D	**58.00 W**	**0.000003**	**0.000103**	**0.000011**	**0.006215**	**0.637487**	**1180.85**	**± 17.06**	**100.14**	**2.14**	**25.9**	**± 45.2**
2A22577D	**70.00 W**	**0.000024**	**0.000104**	**0.000016**	**0.009493**	**0.947228**	**1157.18**	**± 13.05**	**99.26**	**3.27**	**39.1**	**± 67.8**
	Σ	0.000262	0.003992	0.000383	0.290651	29.185168						

Table A3.3-18 Bt AF06 Detailed Results

	^{40}Ar (r)/ ^{39}Ar (k)	± 2σ	Age (Ma)	± 2σ (Ma)	MSWD	^{39}Ar (k) (%, n)	K/Ca	± 2σ
Age Plateau	101.0867	± 0.3343 ± 0.33%	1168.30	± 4.73 ± 0.41%	1.02	91.33 15	29.3	± 3.6
			Full External Error	± 7.26	2.14	Statistical T Ratio		
			Analytical Error	± 2.84	1.0077	Error Magnification		
Total Fusion Age	100.4129	± 0.3314 ± 0.33%	1162.56	± 4.71 ± 0.41%		17	31.3	± 5.1
			Full External Error	± 7.23				
			Analytical Error	± 2.83				

Table A3.3-19 Bt AF08A Incremental Heating

		^{36}Ar (a)	^{37}Ar (ca)	^{38}Ar (cl)	^{39}Ar (k)	^{40}Ar (r)	Age (Ma)	± 2σ (Ma)	^{40}Ar (r) (%)	^{39}Ar (k) (%)	K/Ca	± 2σ
2A22759D	55.70 W	0.000114	0.001038	0.000015	0.024381	1.638925	854.49	± 8.72	97.96	10.59	10.1	± 1.9
2A22760D	55.90 W	0.000015	0.001247	0.000050	0.038468	2.814150	913.57	± 5.92	99.84	16.71	13.3	± 2.0
2A22762D	56.00 W	0.000004	0.000013	0.000017	0.007736	0.605095	962.44	± 10.99	100.19	3.36	265.8	± 3724.4
2A22763D	56.10 W	0.000001	0.000750	0.000037	0.026533	2.036844	948.59	± 6.65	100.01	11.52	15.2	± 3.5
2A22764D	56.20 W	0.000012	0.001094	0.000045	0.044870	3.598406	981.25	± 6.65	99.90	19.49	17.6	± 3.6
2A22765D	56.30 W	0.000001	0.000123	0.000007	0.007079	0.555031	964.32	± 14.73	99.96	3.07	24.7	± 33.3
2A22767D	56.40 W	0.000011	0.001137	0.000016	0.021601	1.650381	945.09	± 7.38	99.79	9.38	8.2	± 1.4
2A22768D	56.50 W	0.000007	0.000191	0.000002	0.004742	0.348866	917.61	± 16.39	99.37	2.06	10.7	± 10.5
2A22769D	56.60 W	0.000002	0.000210	0.000000	0.006061	0.452805	928.75	± 13.94	100.12	2.63	12.4	± 11.7
2A22770D	56.80 W	0.000002	0.000210	0.000000	0.005800	0.423612	912.40	± 14.73	100.11	2.52	11.9	± 10.5
2A22772D	57.00 W	0.000003	0.000184	0.000000	0.004987	0.365502	914.90	± 13.59	100.27	2.17	11.7	± 11.0
2A22773D	57.50 W	0.000008	0.001828	0.000034	0.023204	1.759281	939.45	± 7.96	100.14	10.08	5.5	± 0.7
2A22791D	58.00 W	0.000005	0.000704	0.000012	0.008331	0.623523	930.01	± 11.04	99.78	3.62	5.1	± 1.3
2A22792D	75.00 W	0.000000	0.001490	0.000003	0.006457	0.480768	926.31	± 10.59	99.98	2.80	1.9	± 0.2
	Σ	0.000147	0.010219	0.000237	0.230249	17.353189						

Table A3.3-20 Bt AF08A Detailed Results

	^{40}Ar (r)/ ^{39}Ar (k)	± 2σ	Age (Ma)	± 2σ (Ma)	MSWD	^{39}Ar (k) (%, n)	K/Ca	± 2σ
Age Plateau	Cannot Calculate							
Total Fusion Age	75.3669	± 0.2590 ± 0.34%	935.10	± 4.07 ± 0.44%		14	9.7	± 0.7
			Full External Error	± 6.09				
			Analytical Error	± 2.51				

Table A3.3-21 Bt AF08B Incremental Heating

		^{36}Ar (a)	^{37}Ar (ca)	^{38}Ar (cl)	^{39}Ar (k)	^{40}Ar (r)	Age (Ma)	± 2σ (Ma)	^{40}Ar (r) (%)	^{39}Ar (k) (%)	K/Ca	± 2σ
2A22493D	55.60 W	0.000076	0.000132	0.000011	0.004758	0.284318	777.32	± 18.16	92.61	1.83	15.5	± 17.7
2A22494D	55.80 W	0.000060	0.000627	0.000057	0.057096	4.435927	957.47	± 7.71	99.59	21.94	39.2	± 9.0
2A22496D	55.90 W	0.000002	0.000093	0.000012	0.009936	0.723672	910.41	± 9.49	99.93	3.82	45.7	± 66.2
2A22497D	56.00 W	0.000002	0.000247	0.000014	0.015647	1.251647	979.32	± 8.77	99.96	6.01	27.2	± 12.7
2A22498D	56.10 W	0.000007	0.000026	0.000006	0.003026	0.234848	956.79	± 18.28	99.12	1.16	50.0	± 223.9
2A22499D	56.20 W	0.000017	0.000341	0.000036	0.029726	2.356007	972.38	± 8.16	99.78	11.42	37.5	± 13.3
2A22501D	56.30 W	0.000006	0.000618	0.000020	0.024582	1.855943	936.39	± 7.64	99.90	9.45	17.1	± 3.3
2A22502D	56.40 W	0.000004	0.000415	0.000026	0.023742	1.836796	954.35	± 8.87	99.94	9.12	24.6	± 8.4
2A22503D	56.50 W	0.000010	0.000342	0.000026	0.019797	1.500760	939.35	± 9.62	99.79	7.61	24.9	± 9.4
2A22504D	56.60 W	0.000002	0.000235	0.000018	0.013457	1.007223	930.06	± 8.71	99.93	5.17	24.7	± 11.2
2A22506D	56.70 W	0.000010	0.000223	0.000007	0.008636	0.629239	910.73	± 12.55	99.51	3.32	16.6	± 9.4
2A22507D	56.90 W	0.000005	0.000628	0.000030	0.011837	0.864906	912.68	± 9.12	99.83	4.55	8.1	± 1.6
2A22523D	57.00 W	0.000005	0.002429	0.000029	0.023040	1.671488	907.61	± 7.59	99.90	8.85	4.1	± 0.2
2A22524D	57.20 W	0.000005	0.000053	0.000000	0.001893	0.135458	897.84	± 42.42	99.01	0.73	15.2	± 36.6
2A22525D	58.00 W	0.000002	0.000191	0.000000	0.006676	0.518327	957.02	± 13.02	100.13	2.57	15.0	± 10.7
2A22526D	70.00 W	0.000003	0.000180	0.000000	0.006390	0.475665	926.09	± 12.44	99.82	2.46	15.2	± 10.3
	Σ	0.000212	0.006780	0.000291	0.260237	19.782222						

Table A3.3-22 Bt AF08B Detailed Results

	^{40}Ar (r)/ ^{39}Ar (k)	± 2σ	Age (Ma)	± 2σ (Ma)	MSWD	^{39}Ar (k) (%, n)	K/Ca	± 2σ
Age Plateau	Cannot Calculate							
Total Fusion Age	76.0162	± 0.2787 ± 0.37%	941.37	± 4.20 ± 0.45%		16	16.5	± 1.3
			Full External Error	± 6.20				
			Analytical Error	± 2.69				

Table A3.3-23 Bt AF08C Incremental Heating

		^{36}Ar (a)	^{37}Ar (ca)	^{38}Ar (cl)	^{39}Ar (k)	^{40}Ar (r)	Age (Ma)	± 2σ (Ma)	^{40}Ar (r) (%)	^{39}Ar (k) (%)	K/Ca	± 2σ
2A22428D	55.50 W	0.000021	0.000047	0.000007	0.000812	0.050335	800.94	± 73.94	88.90	0.33	7.4	± 28.1
2A22429D	55.80 W	0.000198	0.000856	0.000015	0.033515	2.633420	965.89	± 6.73	97.80	13.43	16.8	± 3.7
2A22431D	55.90 W	0.000054	0.000562	0.000047	0.024253	2.056521	1024.11	± 8.20	99.22	9.72	18.5	± 6.3
2A22432D	56.00 W	0.000035	0.000285	0.000013	0.012866	1.098373	1029.42	± 13.41	99.06	5.16	19.4	± 11.7
2A22433D	56.10 W	0.000028	0.000705	0.000034	0.021644	1.861589	1035.29	± 8.49	99.56	8.67	13.2	± 3.5
2A22434D	56.20 W	0.000003	0.000120	0.000013	0.005893	0.526788	1066.03	± 20.79	99.81	2.36	21.1	± 30.9
2A22436D	56.30 W	0.000021	0.000934	0.000076	0.045324	4.049966	1065.66	± 6.71	99.84	18.16	20.9	± 4.4
2A22437D	56.40 W	0.000014	0.000300	0.000015	0.016341	1.485748	1079.69	± 9.43	99.73	6.55	23.4	± 13.9
2A22438D	56.50 W	0.000009	0.000735	0.000012	0.015597	1.414975	1077.91	± 14.49	99.81	6.25	9.1	± 2.3
2A22439D	56.70 W	0.000006	0.000253	0.000012	0.006073	0.557779	1087.88	± 16.36	99.69	2.43	10.3	± 8.0
2A22459D	56.90 W	0.000027	0.001331	0.000054	0.044250	4.095944	1094.32	± 7.07	99.80	17.73	14.3	± 1.8
2A22460D	57.00 W	0.000001	0.000023	0.000011	0.002624	0.248172	1112.19	± 30.03	99.83	1.05	48.4	± 328.2
2A22461D	57.20 W	0.000001	0.000241	0.000005	0.009972	0.990079	1152.91	± 10.44	100.03	4.00	17.8	± 11.9
2A22462D	57.50 W	0.000003	0.000082	0.000009	0.002073	0.188570	1080.16	± 41.52	100.55	0.83	10.9	± 20.7
2A22464D	58.00 W	0.000009	0.000043	0.000008	0.003832	0.370772	1130.98	± 23.99	99.29	1.54	38.1	± 141.4
2A22465D	60.00 W	0.000012	0.000048	0.000003	0.004490	0.434226	1130.63	± 24.98	99.19	1.80	40.3	± 129.8
	Σ	0.000435	0.006374	0.000334	0.249558	22.063259						

Table A3.3-24 Bt AF08C Detailed Results

	^{40}Ar (r)/ ^{39}Ar (k)	± 2σ	Age (Ma)	± 2σ (Ma)	MSWD	^{39}Ar (k) (%, n)	K/Ca	± 2σ
Age Plateau	Cannot Calculate							
Total Fusion Age	88.4094	± 0.3112 ± 0.35%	1057.12	± 4.51 ± 0.43%		16	16.8	± 1.9
			Full External Error	± 6.77				
			Analytical Error	± 2.82				

Table A3.3-25 Bt AF08D Incremental Heating

		^{36}Ar (a)	^{37}Ar (ca)	^{38}Ar (cl)	^{39}Ar (k)	^{40}Ar (r)	Age (Ma)	± 2σ (Ma)	^{40}Ar (r) (%)	^{39}Ar (k) (%)	K/Ca	± 2σ
2A22466D	55.60 W	0.000059	0.000005	0.000000	0.010602	0.810811	945.82	± 13.60	97.89	11.77	875	± 27250
2A22467D	55.80 W	0.000019	0.000020	0.000011	0.026869	2.146588	978.37	± 6.77	99.73	29.83	579	± 4422
2A22469D	55.90 W	0.000010	0.000011	0.000017	0.019703	1.539705	961.78	± 10.81	99.80	21.88	761	± 10118
2A22470D	56.00 W	0.000001	0.000007	0.000008	0.018214	1.382630	940.36	± 10.09	100.03	20.22	1120	± 24634
2A22471D	56.10 W	0.000009	0.000030	0.000003	0.003742	0.259733	876.44	± 21.09	99.01	4.16	53	± 187
2A22472D	56.20 W	0.000001	0.000039	0.000000	0.001030	0.066372	825.84	± 66.68	99.61	1.14	11	± 28
2A22474D	56.40 W	0.000004	0.000110	0.000019	0.006898	0.469898	863.52	± 13.47	100.27	7.66	27	± 31
2A22475D	56.60 W	0.000003	0.000096	0.000012	0.001283	0.097236	939.30	± 60.18	100.99	1.42	6	± 8
2A22491D	57.30 W	0.000001	0.000151	0.000000	0.000909	0.066431	912.99	± 47.38	99.60	1.01	3	± 2
2A22492D	70.00 W	0.000000	0.000056	0.000010	0.000815	0.068310	1014.67	± 52.08	100.19	0.91	6	± 11
	Σ	0.000089	0.000525	0.000080	0.090066	6.907713						

Table A3.3-26 Bt AF08D Detailed Results

	^{40}Ar (r)/ ^{39}Ar (k)	± 2σ	Age (Ma)	± 2σ (Ma)	MSWD	^{39}Ar (k) (%, n)	K/Ca	± 2σ
Age Plateau	Cannot Calculate							
Total Fusion Age	76.6962	± 0.4624 ± 0.60%	947.92	± 5.50 ± 0.58%		10	74	± 58
			Full External Error	± 7.16				
			Analytical Error	± 4.44				

Table A3.3-27 Hb BREM-6 Incremental Heating

		^{36}Ar (a)	^{37}Ar (ca)	^{38}Ar (cl)	^{39}Ar (k)	^{40}Ar (r)	Age (Ma)	± 2σ (Ma)	^{40}Ar (r) (%)	^{39}Ar (k) (%)	K/Ca	± 2σ
3M25390D	**56.00 W**	**0.0000011**	**0.0001182**	**0.0000131**	**0.0002876**	**0.0310617**	**1226.12**	**± 110.93**	**101.08**	**0.64**	**1.261**	**± 27.830**
3M25392D	**57.00 W**	**0.0000020**	**0.0011972**	**0.0000157**	**0.0006419**	**0.0662821**	**1186.66**	**± 53.39**	**99.09**	**1.42**	**0.278**	**± 0.601**
3M25393D	**57.00 W**	**0.0000103**	**0.0010319**	**0.0000122**	**0.0004167**	**0.0391917**	**1107.55**	**± 86.50**	**92.69**	**0.92**	**0.209**	**± 0.504**
3M25395D	**57.00 W**	**0.0000114**	**0.0124507**	**0.0001157**	**0.0044155**	**0.4512427**	**1177.70**	**± 13.08**	**99.25**	**9.75**	**0.184**	**± 0.042**
3M25396D	**57.00 W**	**0.0000020**	**0.0116278**	**0.0001085**	**0.0040101**	**0.4151012**	**1188.83**	**± 15.77**	**99.86**	**8.86**	**0.179**	**± 0.043**
3M25397D	**57.00 W**	**0.0000001**	**0.0029499**	**0.0000283**	**0.0009090**	**0.0930644**	**1179.32**	**± 41.95**	**100.04**	**2.01**	**0.160**	**± 0.150**
3M25398D	**57.00 W**	**0.0000025**	**0.0084491**	**0.0000854**	**0.0030158**	**0.3039074**	**1165.61**	**± 15.81**	**99.75**	**6.66**	**0.185**	**± 0.058**
3M25400D	**57.00 W**	**0.0000108**	**0.0153625**	**0.0001264**	**0.0052057**	**0.5218383**	**1161.10**	**± 17.71**	**99.38**	**11.50**	**0.176**	**± 0.025**
3M25401D	**57.00 W**	**0.0000016**	**0.0190853**	**0.0001794**	**0.0072219**	**0.7319907**	**1170.60**	**± 10.57**	**100.06**	**15.95**	**0.196**	**± 0.029**
3M25402D	**57.00 W**	**0.0000111**	**0.0183787**	**0.0001560**	**0.0063292**	**0.6373717**	**1165.03**	**± 9.17**	**99.48**	**13.98**	**0.178**	**± 0.021**
3M25404D	**58.00 W**	**0.0000144**	**0.0234859**	**0.0002383**	**0.0090005**	**0.9086385**	**1167.17**	**± 8.95**	**99.53**	**19.88**	**0.199**	**± 0.024**
3M25405D	**58.00 W**	**0.0000097**	**0.0056437**	**0.0000543**	**0.0021625**	**0.2151933**	**1154.85**	**± 26.36**	**98.67**	**4.78**	**0.198**	**± 0.054**
3M25406D	**65.00 W**	**0.0000082**	**0.0040675**	**0.0000537**	**0.0016611**	**0.1657774**	**1157.32**	**± 24.71**	**98.55**	**3.67**	**0.212**	**± 0.089**
	Σ	0.0000797	0.1238485	0.0011868	0.0452774	4.5806612						

Table A3.3-28 Hb BREM-6 Detailed Results

	^{40}Ar (r)/ ^{39}Ar (k)	± 2σ	Age (Ma)	± 2σ (Ma)	MSWD	^{39}Ar (k) (%,n)	K/Ca	± 2σ
Age Plateau	101.17342	± 0.57873 ± 0.57%	1169.03	± 6.21 ± 0.53%	1.32 20%	100.00 13	0.186	± 0.011
			Full External Error	± 8.30	1.82	2σ Confidence Limit		
			Analytical Error	± 4.92	1.1496	Error Magnification		
Total Fusion Age	101.16877	± 0.54325 ± 0.54%	1168.99	± 5.97 ± 0.51%		13	0.189	± 0.015
			Full External Error	± 8.12				
			Analytical Error	± 4.62				

Table A3.3-29 Bt BREM-2 Incremental Heating

		^{36}Ar (a)	^{37}Ar (ca)	^{38}Ar (cl)	^{39}Ar (k)	^{40}Ar (r)	Age (Ma)	± 2σ (Ma)	^{40}Ar (r) (%)	^{39}Ar (k) (%)	K/Ca	± 2σ
3M31185D	**57.00 W**	**0.0000042**	**0.0000146**	**0.0000031**	**0.0002221**	**0.0234047**	**1127.44**	**± 192.37**	**94.97**	**0.61**	**6.5**	**± 375.7**
3M31186D	**57.00 W**	**0.0000125**	**0.0003973**	**0.0000049**	**0.0034758**	**0.3825387**	**1164.50**	**± 23.42**	**99.04**	**9.57**	**3.8**	**± 9.3**
3M31187D	**58.00 W**	**0.0000003**	**0.0002226**	**0.0000472**	**0.0120406**	**1.3390021**	**1173.44**	**± 10.38**	**100.01**	**33.16**	**23.3**	**± 106.2**
3M31189D	**58.00 W**	**0.0000059**	**0.0002849**	**0.0000919**	**0.0199538**	**2.2170868**	**1172.69**	**± 9.56**	**99.92**	**54.95**	**30.1**	**± 97.6**
3M31190D	**58.00 W**	**0.0000022**	**0.0002773**	**0.0000005**	**0.0004852**	**0.0503761**	**1115.20**	**± 100.17**	**98.69**	**1.34**	**0.8**	**± 2.8**
3M31191D	**65.00 W**	**0.0000065**	**0.0005152**	**0.0000000**	**0.0001379**	**0.0168780**	**1258.28**	**± 275.96**	**113.07**	**0.38**	**0.1**	**± 0.2**
	Σ	0.0000179	0.0006969	0.0001476	0.0363154	4.0292864						

Table A3.3-30 Bt BREM-2 Detailed Results

	^{40}Ar (r)/ ^{39}Ar (k)	± 2σ	Age (Ma)	± 2σ (Ma)	MSWD	^{39}Ar (k) (%,n)	K/Ca	± 2σ
Age Plateau	111.02797	± 0.86432 ± 0.78%	1172.04	± 7.47 ± 0.64%	0.49 79%	100.00 6	0.1	± 0.2
			Full External Error	± 10.56	2.26	2σ Confidence Limit		
			Analytical Error	± 6.71	1.0000	Error Magnification		
Total Fusion Age	110.95262	± 0.89800 ± 0.81%	1171.46	± 7.71 ± 0.66%		6	22.4	± 76.7
			Full External Error	± 10.73				
			Analytical Error	± 6.98				

Table A3.3-31 Bt BREM-6 Incremental Heating

		^{36}Ar (a)	^{37}Ar (ca)	^{38}Ar (cl)	^{39}Ar (k)	^{40}Ar (r)	Age (Ma)	± 2σ (Ma)	^{40}Ar (r) (%)	^{39}Ar (k) (%)	K/Ca	± 2σ
2A22794D	55.90 W	0.000060	0.000013	0.000006	0.001503	0.161882	1223.67	± 38.79	90.10	0.68	49	± 574
2A22796D	56.10 W	0.000023	0.000074	0.000102	0.025196	2.558536	1172.19	± 8.12	99.74	11.47	147	± 289
2A22797D	**56.20 W**	**0.000007**	**0.000013**	**0.000039**	**0.009178**	**0.918541**	**1159.77**	**± 13.63**	**99.77**	**4.18**	**298**	**± 3399**
2A22798D	**56.30 W**	**0.000017**	**0.000008**	**0.000223**	**0.050313**	**5.047889**	**1161.84**	**± 7.39**	**99.90**	**22.91**	**2764**	**± 55713**
2A22799D	**56.40 W**	**0.000008**	**0.000004**	**0.000026**	**0.008505**	**0.850410**	**1158.96**	**± 10.02**	**99.72**	**3.87**	**923**	**± 34072**
2A22801D	**56.50 W**	**0.000007**	**0.000007**	**0.000019**	**0.004059**	**0.413651**	**1175.37**	**± 53.46**	**99.47**	**1.85**	**246**	**± 5141**
2A22802D	**56.70 W**	**0.000008**	**0.000044**	**0.000163**	**0.044094**	**4.406336**	**1158.44**	**± 7.32**	**99.95**	**20.08**	**427**	**± 1494**
2A22803D	**56.90 W**	**0.000004**	**0.000027**	**0.000016**	**0.004131**	**0.410833**	**1154.25**	**± 17.28**	**99.72**	**1.88**	**65**	**± 432**
2A22804D	**57.20 W**	**0.000001**	**0.000088**	**0.000047**	**0.009510**	**0.955735**	**1163.25**	**± 12.78**	**99.98**	**4.33**	**46**	**± 75**
2A22806D	**57.50 W**	**0.000008**	**0.000031**	**0.000116**	**0.029001**	**2.906647**	**1160.95**	**± 8.60**	**99.91**	**13.21**	**396**	**± 1756**
2A22807D	**58.00 W**	**0.000009**	**0.000017**	**0.000157**	**0.033251**	**3.315040**	**1156.44**	**± 6.57**	**99.92**	**15.14**	**853**	**± 7539**
2A22808D	**75.00 W**	**0.000008**	**0.000046**	**0.000000**	**0.000847**	**0.082273**	**1134.58**	**± 47.75**	**97.24**	**0.39**	**8**	**± 26**
	Σ	0.000159	0.000061	0.000914	0.219588	22.027773						

Table A3.3-32 Bt BREM-6 Detailed Results

	^{40}Ar (r)/ ^{39}Ar (k)	± 2σ	Age (Ma)	± 2σ (Ma)	MSWD	^{39}Ar (k) (%, n)	K/Ca	± 2σ
Age Plateau	100.0164	± 0.3713 ± 0.37%	1159.17	± 4.92 ± 0.42%	0.40	87.84 10	12	± 24
			Full External Error	± 7.36	2.26	Statistical T Ratio		
			Analytical Error	± 3.17	1.0000	Error Magnification		
Total Fusion Age	100.3143	± 0.3729 ± 0.37%	1161.71	± 4.93 ± 0.42%		12	1545	± 13309
			Full External Error	± 7.37				
			Analytical Error	± 3.18				

Table A3.3-33 Bt BREM-10 Incremental Heating

		^{36}Ar (a)	^{37}Ar (ca)	^{38}Ar (cl)	^{39}Ar (k)	^{40}Ar (r)	Age (Ma)	± 2σ (Ma)	^{40}Ar (r) (%)	^{39}Ar (k) (%)	K/Ca	± 2σ
3M31196D	58.00 W	0.0000117	0.0002801	0.0000165	0.0063887	0.724714	1190.66	± 15.14	99.52	3.84	9.81	± 39.73
3M31198D	58.00 W	0.0000188	0.0006242	0.0000465	0.0104194	1.170532	1182.22	± 12.08	99.52	6.27	7.18	± 13.21
3M31199D	**58.00 W**	**0.0000254**	**0.0001732**	**0.0000792**	**0.0257583**	**2.860336**	**1172.18**	**± 15.73**	**99.74**	**15.49**	**63.94**	**± 463.26**
3M31200D~	**65.00 W**	**0.0000849**	**0.0179325**	**0.0004713**	**0.1237444**	**13.615224**	**1164.25**	**± 8.78**	**99.81**	**74.41**	**2.97**	**± 0.45**
	Σ	0.0001407	0.0181034	0.0006136	0.1663108	18.370806						

Table A3.3-34 Bt BREM-10 Detailed Results

	^{40}Ar (r)/ ^{39}Ar (k)	± 2σ	Age (Ma)	± 2σ (Ma)	MSWD	^{39}Ar (k) (%, n)	K/Ca	± 2σ
Age Plateau	110.26718	± 0.98357 ± 0.89%	1166.12	± 8.33 ± 0.71%	0.77 38%	89.89 2	2.97	± 0.45
			Full External Error	± 11.16	3.83	2σ Confidence Limit		
			Analytical Error	± 7.67	1.0000	Error Magnification		
Total Fusion Age	110.46071	± 0.90471 ± 0.82%	1167.63	± 7.77 ± 0.67%		4	3.95	± 0.74
			Full External Error	± 10.75				
			Analytical Error	± 7.05				

Table A3.3-35 Bt AF01-SCH Incremental Heating

		^{36}Ar (a)	^{37}Ar (ca)	^{38}Ar (cl)	^{39}Ar (k)	^{40}Ar (r)	Age (Ma)	± 2σ (Ma)	^{40}Ar (r) (%)	^{39}Ar (k) (%)	K/Ca	± 2σ
2A22883D	55.70 W	0.000036	0.000007	0.000013	0.013653	1.272122	1099.71	± 8.88	99.15	7.85	786	± 23342
2A22884D	55.90 W	0.000024	0.000075	0.000001	0.047081	4.754398	1167.42	± 8.02	99.85	27.08	269	± 786
2A22885D	56.00 W	0.000000	0.000010	0.000000	0.003662	0.381109	1193.45	± 17.18	100.01	2.11	156	± 3865
2A22887D	56.10 W	0.000002	0.000036	0.000000	0.014946	1.483912	1152.88	± 9.18	99.97	8.60	177	± 1061
2A22888D	**56.20 W**	**0.000005**	**0.000165**	**0.000012**	**0.006754**	**0.692745**	**1180.84**	**± 18.70**	**100.23**	**3.89**	**18**	**± 23**
2A22889D	**56.30 W**	**0.000005**	**0.000041**	**0.000011**	**0.027604**	**2.842895**	**1184.40**	**± 6.81**	**100.06**	**15.88**	**287**	**± 1638**
2A22890D	**56.40 W**	**0.000004**	**0.000022**	**0.000004**	**0.013262**	**1.384200**	**1196.02**	**± 11.52**	**99.92**	**7.63**	**257**	**± 2444**
2A22892D	**56.50 W**	**0.000003**	**0.000022**	**0.000003**	**0.008020**	**0.835095**	**1194.00**	**± 14.12**	**100.11**	**4.61**	**154**	**± 1511**
2A22893D	**56.60 W**	**0.000004**	**0.000021**	**0.000016**	**0.009397**	**0.983373**	**1198.32**	**± 15.19**	**100.12**	**5.41**	**188**	**± 1915**
2A22894D	**56.80 W**	**0.000007**	**0.000015**	**0.000008**	**0.007284**	**0.759705**	**1195.42**	**± 19.99**	**100.28**	**4.19**	**210**	**± 3159**
2A22897D	**57.00 W**	**0.000001**	**0.000056**	**0.000013**	**0.015199**	**1.579697**	**1192.38**	**± 8.92**	**100.01**	**8.74**	**116**	**± 445**
2A22898D	**57.20 W**	**0.000004**	**0.000019**	**0.000003**	**0.000858**	**0.091298**	**1213.43**	**± 58.50**	**101.29**	**0.49**	**20**	**± 204**
2A22899D	**57.80 W**	**0.000003**	**0.000062**	**0.000001**	**0.003101**	**0.328021**	**1207.81**	**± 18.71**	**100.27**	**1.78**	**21**	**± 73**
2A22900D	**75.00 W**	**0.000001**	**0.000016**	**0.000000**	**0.003027**	**0.321661**	**1211.74**	**± 30.47**	**100.05**	**1.74**	**81**	**± 1013**
	Σ	0.000032	0.000386	0.000086	0.173847	17.710232						

Table A3.3-36 Bt AF01-SCH Detailed Results

	^{40}Ar (r)/^{39}Ar (k)	± 2σ	Age (Ma)	± 2σ (Ma)	MSWD	^{39}Ar (k) (%, n)	K/Ca	± 2σ
Age Plateau	103.8047	± 0.5749 ± 0.55%	1191.26	± 6.17 ± 0.52%	1.41	54.36 10	18	± 22
			Full External Error	± 8.33	2.26	Statistical T Ratio		
			Analytical Error	± 4.83	1.1883	Error Magnification		
Total Fusion Age	101.8723	± 0.3970 ± 0.39%	1174.96	± 5.07 ± 0.43%		14	194	± 411
			Full External Error	± 7.51				
			Analytical Error	± 3.36				

Table A3.3-37 Ms AF01-SCH Incremental Heating

		^{36}Ar (a)	^{37}Ar (ca)	^{38}Ar (cl)	^{39}Ar (k)	^{40}Ar (r)	Age (Ma)	± 2σ (Ma)	^{40}Ar (r) (%)	^{39}Ar (k) (%)	K/Ca	± 2σ
2A22990D	**56.50 W**	**0.000025**	**0.000178**	**0.000007**	**0.055706**	**5.543267**	**1154.83**	**± 7.74**	**99.86**	**42.82**	**134**	**± 244**
2A22991D	**56.60 W**	**0.000004**	**0.000031**	**0.000035**	**0.041104**	**4.097871**	**1156.43**	**± 7.95**	**99.97**	**31.59**	**570**	**± 5804**
2A22992D	**56.70 W**	**0.000003**	**0.000085**	**0.000000**	**0.006368**	**0.628903**	**1148.34**	**± 14.00**	**100.16**	**4.90**	**32**	**± 121**
2A22993D	**56.90 W**	**0.000001**	**0.000156**	**0.000001**	**0.001728**	**0.176882**	**1179.08**	**± 37.19**	**100.19**	**1.33**	**5**	**± 10**
2A22995D	**57.20 W**	**0.000001**	**0.000075**	**0.000004**	**0.003416**	**0.344597**	**1166.43**	**± 25.10**	**99.91**	**2.63**	**20**	**± 88**
2A22996D	**57.60 W**	**0.000001**	**0.000130**	**0.000000**	**0.002278**	**0.228587**	**1162.15**	**± 32.95**	**100.14**	**1.75**	**8**	**± 19**
2A22997D	**58.00 W**	**0.000003**	**0.000024**	**0.000006**	**0.011554**	**1.158016**	**1160.99**	**± 11.18**	**99.93**	**8.88**	**203**	**± 2691**
2A22998D	**58.20 W**	**0.000009**	**0.000098**	**0.000001**	**0.003729**	**0.373457**	**1160.25**	**± 17.26**	**99.32**	**2.87**	**16**	**± 52**
2A23000D	**58.60 W**	**0.000001**	**0.000053**	**0.000007**	**0.002398**	**0.239032**	**1156.44**	**± 26.12**	**100.14**	**1.84**	**19**	**± 120**
2A23001D	**72.00 W**	**0.000005**	**0.000095**	**0.000000**	**0.001817**	**0.179570**	**1148.80**	**± 40.65**	**99.19**	**1.40**	**8**	**± 28**
	Σ	0.000040	0.000926	0.000060	0.130098	12.970184						

Table A3.3-38 Ms AF01-SCH Detailed Results

	^{40}Ar (r)/ ^{39}Ar (k)	± 2σ	Age (Ma)	± 2σ (Ma)	MSWD	^{39}Ar (k) (%, n)	K/Ca	± 2σ
Age Plateau	99.7245	± 0.5016 ± 0.50%	1156.67	± 5.70 ± 0.49%	0.52	100.00 10	6	± 8
			Full External Error	± 7.80	2.26	Statistical T Ratio		
			Analytical Error	± 4.29	1.0000	Error Magnification		
Total Fusion Age	99.6953	± 0.5299 ± 0.53%	1156.42	± 5.89 ± 0.51%		10	60	± 66
			Full External Error	± 7.93				
			Analytical Error	± 4.54				

Table A3.3-39 Ms BREM-SA Incremental Heating

		^{36}Ar (a)	^{37}Ar (ca)	^{38}Ar (cl)	^{39}Ar (k)	^{40}Ar (r)	Age (Ma)	± 2σ (Ma)	^{40}Ar (r) (%)	^{39}Ar (k) (%)	K/Ca	± 2σ
2A22934D	**56.60 W**	**0.000012**	**0.000041**	**0.000000**	**0.000474**	**0.045195**	**1118.71**	**± 119.56**	**92.51**	**0.18**	**4.9**	**± 27.5**
2A22935D	**56.80 W**	**0.000001**	**0.000004**	**0.000000**	**0.000442**	**0.045800**	**1190.17**	**± 101.68**	**99.26**	**0.17**	**51.1**	**± 2781.8**
2A22936D	**57.00 W**	**0.000002**	**0.000020**	**0.000000**	**0.000430**	**0.046727**	**1230.74**	**± 121.83**	**98.78**	**0.16**	**9.4**	**± 106.5**
2A22937D	**57.30 W**	**0.000003**	**0.000040**	**0.000000**	**0.002380**	**0.251814**	**1207.92**	**± 31.74**	**100.30**	**0.90**	**25.3**	**± 126.3**
2A22939D	**57.50 W**	**0.000004**	**0.000016**	**0.000005**	**0.006976**	**0.710820**	**1175.20**	**± 14.91**	**99.83**	**2.63**	**183.9**	**± 2517.1**
2A22940D	**57.60 W**	**0.000002**	**0.000099**	**0.000000**	**0.001270**	**0.128653**	**1170.12**	**± 43.17**	**100.51**	**0.48**	**5.5**	**± 12.0**
2A22941D	**57.80 W**	**0.000012**	**0.000034**	**0.000002**	**0.006302**	**0.625565**	**1152.72**	**± 14.97**	**99.42**	**2.38**	**79.8**	**± 458.2**
2A22942D	**58.00 W**	**0.000008**	**0.000016**	**0.000018**	**0.012746**	**1.288047**	**1168.04**	**± 7.04**	**100.20**	**4.81**	**333.1**	**± 4584.7**
2A22944D	**58.20 W**	**0.000000**	**0.000008**	**0.000009**	**0.024994**	**2.511021**	**1163.01**	**± 7.04**	**100.00**	**9.43**	**1313.7**	**± 33239**
2A22945D	**58.30 W**	**0.000004**	**0.000127**	**0.000006**	**0.022496**	**2.254245**	**1160.81**	**± 10.09**	**99.94**	**8.49**	**76.1**	**± 128.8**
2A22975D	**58.40 W**	**0.000004**	**0.000146**	**0.000004**	**0.018342**	**1.849579**	**1166.17**	**± 9.19**	**99.93**	**6.92**	**54.0**	**± 136.8**
2A22976D	**58.50 W**	**0.000009**	**0.000123**	**0.000011**	**0.025397**	**2.547779**	**1161.75**	**± 6.88**	**99.90**	**9.58**	**88.6**	**± 264.0**
2A22977D	**58.60 W**	**0.000000**	**0.000178**	**0.000015**	**0.020549**	**2.058191**	**1160.41**	**± 8.39**	**99.99**	**7.75**	**49.6**	**± 101.5**
2A22978D	**58.70 W**	**0.000009**	**0.000018**	**0.000006**	**0.054013**	**5.422773**	**1162.42**	**± 8.69**	**99.95**	**20.37**	**1292.8**	**± 27109**
2A22980D	**58.80 W**	**0.000021**	**0.000104**	**0.000004**	**0.004756**	**0.484180**	**1174.38**	**± 13.96**	**98.75**	**1.79**	**19.6**	**± 70.4**
2A22981D	**59.00 W**	**0.000010**	**0.000070**	**0.000002**	**0.003042**	**0.300446**	**1148.46**	**± 29.86**	**99.04**	**1.15**	**18.7**	**± 97.4**
2A22982D	**59.30 W**	**0.000001**	**0.000066**	**0.000000**	**0.001537**	**0.158202**	**1183.72**	**± 49.00**	**99.74**	**0.58**	**10.0**	**± 56.0**
2A22983D	**59.80 W**	**0.000007**	**0.000056**	**0.000000**	**0.001596**	**0.156833**	**1144.02**	**± 37.06**	**98.77**	**0.60**	**12.2**	**± 81.3**
2A22985D	**63.00 W**	**0.000012**	**0.003366**	**0.000024**	**0.047947**	**4.829051**	**1165.14**	**± 6.16**	**99.92**	**18.09**	**6.1**	**± 0.7**
2A22986D	**72.00 W**	**0.000002**	**0.000044**	**0.000007**	**0.009431**	**0.952569**	**1167.61**	**± 12.62**	**99.92**	**3.56**	**92.8**	**± 779.1**
	Σ	0.000097	0.003134	0.000113	0.265120	26.667489						

Table A3.3-40 BREM-SA Detailed Results

	^{40}Ar (r)/ ^{39}Ar (k)	± 2σ	Age (Ma)	± 2σ (Ma)	MSWD	^{39}Ar (k) (%, n)	K/Ca	± 2σ
Age Plateau	100.5591	± 0.2973 ± 0.30%	1163.80	± 4.55 ± 0.39%	0.80	95.96 15	6.1	± 0.7
			Full External Error	± 7.13	2.14	Statistical T Ratio		
			Analytical Error	± 2.54	1.0000	Error Magnification		
Total Fusion Age	100.5866	± 0.3310 ± 0.33%	1164.04	± 4.71 ± 0.40%		20	36.4	± 15.8
			Full External Error	± 7.23				
			Analytical Error	± 2.82				

Table A3.3-41 Ms 2MB-01 Incremental Heating

		^{36}Ar (a)	^{37}Ar (ca)	^{38}Ar (cl)	^{39}Ar (k)	^{40}Ar (r)	Age (Ma)	± 2σ (Ma)	^{40}Ar (r) (%)	^{39}Ar (k) (%)	K/Ca	± 2σ
2A23020D	**56.20 W**	**0.000062**	**0.000036**	**0.000004**	**0.003653**	**0.359153**	**1144.59**	**± 17.65**	**95.06**	**2.53**	**43**	**± 450**
2A23021D	**56.40 W**	**0.000059**	**0.000059**	**0.000014**	**0.020982**	**2.111363**	**1164.39**	**± 11.36**	**99.17**	**14.51**	**152**	**± 1000**
2A23022D	**56.50 W**	**0.000014**	**0.000013**	**0.000014**	**0.005273**	**0.529697**	**1162.84**	**± 16.53**	**99.23**	**3.65**	**175**	**± 5014**
2A23024D	**56.70 W**	**0.000002**	**0.000019**	**0.000003**	**0.022569**	**2.258753**	**1159.72**	**± 11.29**	**99.97**	**15.61**	**507**	**± 9844**
2A23025D	**56.80 W**	**0.000013**	**0.000049**	**0.000016**	**0.026536**	**2.635073**	**1153.06**	**± 9.86**	**99.85**	**18.35**	**234**	**± 1843**
2A23026D	**56.90 W**	**0.000016**	**0.000035**	**0.000020**	**0.031450**	**3.138430**	**1157.25**	**± 7.66**	**99.84**	**21.75**	**383**	**± 3960**
2A23029D	**57.00 W**	**0.000002**	**0.000140**	**0.000000**	**0.001503**	**0.148430**	**1148.58**	**± 40.90**	**99.67**	**1.04**	**5**	**± 6**
2A23030D	**57.10 W**	**0.000002**	**0.000103**	**0.000023**	**0.011508**	**1.147000**	**1156.21**	**± 10.99**	**100.04**	**7.96**	**48**	**± 89**
2A23031D	**57.20 W**	**0.000001**	**0.000064**	**0.000001**	**0.001363**	**0.135635**	**1154.84**	**± 42.46**	**99.79**	**0.94**	**9**	**± 27**
2A23032D	**57.40 W**	**0.000003**	**0.000085**	**0.000000**	**0.001959**	**0.194491**	**1153.03**	**± 27.36**	**100.45**	**1.35**	**10**	**± 21**
2A23034D	**57.70 W**	**0.000003**	**0.000071**	**0.000000**	**0.002198**	**0.217076**	**1148.23**	**± 38.62**	**100.36**	**1.52**	**13**	**± 34**
2A23035D	**58.20 W**	**0.000002**	**0.000028**	**0.000004**	**0.007187**	**0.719061**	**1159.44**	**± 11.64**	**100.10**	**4.97**	**111**	**± 653**
2A23036D	**58.70 W**	**0.000004**	**0.000007**	**0.000000**	**0.002244**	**0.221727**	**1148.97**	**± 23.24**	**100.48**	**1.55**	**145**	**± 4050**
2A23037D	**59.50 W**	**0.000001**	**0.000052**	**0.000004**	**0.003126**	**0.321353**	**1182.90**	**± 19.04**	**100.12**	**2.16**	**26**	**± 81**
2A23039D	**72.00 W**	**0.000007**	**0.000117**	**0.000002**	**0.003077**	**0.311020**	**1168.16**	**± 26.85**	**100.70**	**2.13**	**11**	**± 21**
	Σ	0.000148	0.000141	0.000106	0.144627	14.448260						

Table A3.3-42 Ms 2MB-01 Detailed Results

	^{40}Ar (r)/ ^{39}Ar (k)	± 2σ	Age (Ma)	± 2σ (Ma)	MSWD	^{39}Ar (k) (%, n)	K/Ca	± 2σ
Age Plateau	99.9716	± 0.4378 ± 0.44%	1158.79	± 5.31 ± 0.46%	0.87	97.47 14	3	± 5
			Full External Error	± 7.52	2.16	Statistical T Ratio		
			Analytical Error	± 3.74	1.0000	Error Magnification		
Total Fusion Age	99.9000	± 0.4526 ± 0.45%	1158.18	± 5.40 ± 0.47%		15	442	± 3374
			Full External Error	± 7.58				
			Analytical Error	± 3.87				

Table A3.3-43 Ms 2MB-02 Incremental Heating

		^{36}Ar (a)	^{37}Ar (ca)	^{38}Ar (cl)	^{39}Ar (k)	^{40}Ar (r)	Age (Ma)	± 2σ (Ma)	^{40}Ar (r) (%)	^{39}Ar (k) (%)	K/Ca	± 2σ
2A23002D	**56.40 W**	**0.000077**	**0.000065**	**0.000014**	**0.028996**	**2.851264**	**1144.72**	**± 7.82**	**99.20**	**9.85**	**193**	**± 499**
2A23003D	**56.50 W**	**0.000003**	**0.000029**	**0.000020**	**0.058464**	**5.829798**	**1156.60**	**± 6.68**	**99.99**	**19.87**	**860**	**± 5294**
2A23005D	**56.60 W**	**0.000011**	**0.000052**	**0.000038**	**0.031051**	**3.111045**	**1160.68**	**± 7.18**	**99.90**	**10.55**	**255**	**± 881**
2A23006D	**56.70 W**	**0.000009**	**0.000085**	**0.000046**	**0.078143**	**7.773701**	**1154.59**	**± 6.56**	**99.96**	**26.55**	**396**	**± 899**
2A23009D	**56.80 W**	**0.000002**	**0.000051**	**0.000000**	**0.000972**	**0.093160**	**1123.55**	**± 52.53**	**99.41**	**0.33**	**8**	**± 39**
2A23010D	**57.00 W**	**0.000003**	**0.000105**	**0.000018**	**0.014764**	**1.477693**	**1159.76**	**± 9.64**	**99.93**	**5.02**	**61**	**± 141**
2A23011D	**57.20 W**	**0.000003**	**0.000092**	**0.000000**	**0.009783**	**0.960986**	**1143.83**	**± 13.97**	**99.89**	**3.32**	**46**	**± 121**
2A23012D	**57.50 W**	**0.000007**	**0.000087**	**0.000012**	**0.020039**	**2.007880**	**1160.74**	**± 9.69**	**99.89**	**6.81**	**99**	**± 259**
2A23014D	**57.80 W**	**0.000003**	**0.000078**	**0.000000**	**0.006807**	**0.677767**	**1155.30**	**± 12.50**	**99.87**	**2.31**	**38**	**± 116**
2A23015D	**58.20 W**	**0.000001**	**0.000035**	**0.000000**	**0.009444**	**0.933336**	**1149.00**	**± 9.35**	**100.03**	**3.21**	**116**	**± 949**
2A23016D	**58.80 W**	**0.000003**	**0.000039**	**0.000006**	**0.019251**	**1.925061**	**1159.02**	**± 9.96**	**99.95**	**6.54**	**210**	**± 1326**
2A23017D	**59.50 W**	**0.000000**	**0.000177**	**0.000014**	**0.012929**	**1.304072**	**1166.40**	**± 10.37**	**100.00**	**4.39**	**31**	**± 43**
2A23019D	**72.00 W**	**0.000015**	**0.000077**	**0.000000**	**0.003645**	**0.359685**	**1147.73**	**± 19.60**	**98.78**	**1.24**	**20**	**± 65**
	Σ	0.000135	0.000430	0.000169	0.294286	29.305448						

Table A3.3-44 Ms 2MB-01 Detailed Results

	^{40}Ar (r)/ ^{39}Ar (k)	± 2σ	Age (Ma)	± 2σ (Ma)	MSWD	^{39}Ar (k) (%, n)	K/Ca	± 2σ
Age Plateau	99.7403	± 0.3769 ± 0.38%	1156.81	± 4.95 ± 0.43%	1.37	90.15 12	22	± 25
			Full External Error	± 7.26	2.20	Statistical T Ratio		
			Analytical Error	± 3.23	1.1711	Error Magnification		
Total Fusion Age	99.5814	± 0.3248 ± 0.33%	1155.45	± 4.67 ± 0.40%		13	294	± 563
			Full External Error	± 7.07				
			Analytical Error	± 2.78				

Appendix 3.4: Calculation of closure temperatures and cooling rates

Table A3.4-1 Initial inputs to Dodson's equation (main text, Equation 1), used to calculate mineral closure temperatures and cooling rates within those hornblende, biotite and muscovite grains that produced a statistically robust $^{40}Ar/^{39}Ar$ cooling age (Dodson, 1973). Grainsize (a) was measured at the time of $^{40}Ar/^{39}Ar$ analysis. Values for the activation energy (E), diffusion coefficient (D_0) and volume constant (A) for biotite were taken from Grove and Harrison (1996), as biotites analysed in this study have similar Fe/Mg ratios (X_{annite} = 0.6 – 0.8 for this study, compared to X_{annite} = 0.54 – 0.71). Values for the activation energy (E), diffusion coefficient (D_0) and volume constant (A) were taken from Harrison (1981) for hornblende and Harrison et al. (2009) for muscovite. Individual cooling rates (dT/dt) were mostly calculated using peak Stage II metamorphic conditions (Table A3.4-2). The exceptions are biotite grains AF01, AF02-1, BREM-6 and BREM-10, as these four biotites are from field sites also containing a hornblende cooling age (Table 3.1). The temperature-time (T-t) pair provided by the hornblende cooling age and closure temperature is used to calculate the mineral-to-mineral cooling path, i.e. for cooling between hornblende and biotite closure temperatures.

Sample	Mineral	T_{c0} (°C)	a (μm)	E (kcal/mol)	D_0 (cm²/s)	A	dT/dt (°C/Ma)
Nornalup Zone							
AF02-1	Hb	550	334	64.1 ± 1.7	$0.024\ ^{+0.053}_{-0.011}$	55	280
AF01	Bt	300	408	50.5 ± 2.2	$0.4\ ^{+0.96}_{-0.28}$	27	4
AF02-1	Bt	300	296	50.5 ± 2.2	$0.4\ ^{+0.96}_{-0.28}$	27	102
AF02-2	Bt	300	309	50.5 ± 2.2	$0.4\ ^{+0.96}_{-0.28}$	27	19
AF03	Bt	300	396	50.5 ± 2.2	$0.4\ ^{+0.96}_{-0.28}$	27	12
AF06	Bt	300	412	50.5 ± 2.2	$0.4\ ^{+0.96}_{-0.28}$	27	375
Biranup Zone							
BREM-6	Hb	550	268	64.1 ± 1.7	$0.024\ ^{+0.053}_{-0.011}$	55	179
BREM-2	Bt	300	335	50.5 ± 2.2	$0.4\ ^{+0.96}_{-0.28}$	27	250
BREM-6	Bt	300	333	50.5 ± 2.2	$0.4\ ^{+0.96}_{-0.28}$	27	42
BREM-10	Bt	300	330	50.5 ± 2.2	$0.4\ ^{+0.96}_{-0.28}$	27	219
Northern Foreland							
AF01-SCH	Ms	425	327	63 ± 7	$2.3\ ^{+70}_{-2.2}$	55	4
BREM-SA	Ms	425	441	63 ± 7	$2.3\ ^{+70}_{-2.2}$	55	5
2MB-01	Ms	425	331	63 ± 7	$2.3\ ^{+70}_{-2.2}$	55	11
2MB-02	Ms	425	415	63 ± 7	$2.3\ ^{+70}_{-2.2}$	55	5

Table A3.4-2 Age and temperature of peak Stage II metamorphism at each sample site, used to calculate cooling rates to $^{40}Ar/^{39}Ar$ mineral closure. To establish peak Stage II metamorphic conditions, published high temperature crystallisation ages from close to the sample location were used, and metamorphic ages (e.g. zircon rim growth) were preferenced over magmatic ages.

Location	Samples	Stage II meta-morphic age (Ma)	Source	Peak Stage II temperature (°C)	Source
Nornalup Zone					
Ledge Point	AF01 AF02-1	1169 ± 7	Metamorphic zircon growth at Ledge Beach (Clark, 1995)	800 ± 100	Granulite facies metamorphism (Fitzsimons and Buchan, 2005)
Whalehead Rock	AF02-2 AF03	1174 ± 12	Intrusion age of the Albany Adamellite, 5 km W of Whalehead Rock (Pidgeon, 1990)	650 ± 50	Regional mid-upper amphibolite facies conditions (Stephenson, 1974)
Shelley Beach	AF06	1169 ± 8	Metamorphic zircon growth at Ledge Beach, 35km E of Shelley Beach (Clark, 1995)	600 ± 100	Thin-section petrography suggests equilibration at amphibolite facies
Biranup Zone					
Point Gordon	BREM-2	1177 ± 11	Weighted mean of 5 metamorphic and magmatic U-Pb zircon ages at Point Henry and Short Beach (Spaggiari et al., 2009)	800 ± 100	Thin-section petrography suggests equilibration at granulite facies
Fishery Beach	BREM-6	1178 ± 3	Age of granodiorite crystallisation and high-grade metamorphism on the Fisheries Bay headland (Spaggiari et al., 2009)	800 ± 75	Geothermometry of syn-deformational pegmatite at Fishery Beach (Black et al., 1992)
Fishery Bay headland	BREM-10	1178 ± 3	Age of granodiorite crystallisation and high-grade metamorphism on the Fisheries Bay headland (Spaggiari et al., 2009)	800 ± 75	Geothermometry of syn-deformational pegmatite at Fishery Beach (Black et al., 1992)
Northern Foreland					
Barrens Beach	AF01-SCH BREM-SA	1205 ± 10	Metamorphic xenotime and monazite growth in the Mount Barren Group (Dawson et al., 2003)	620 ± 50	Peak metamorphic conditions of the Mount Barren Group (Wetherley, 1998)
Two Mile Beach	2MB-01 2MB-02	1195 ± 15	Average of metamorphic zircon growth ages in the Munglinup Gneiss (Spaggiari et al., 2011)	700 ± 100	Upper amphibolite to granulite facies metamorphism (Spaggiari et al., 2011)

Monte Carlo Simulation

The Monte Carlo simulation was performed in Excel, using the Excel add-on program Analytic Solver Platform (Frontline Systems Inc., 2013). The probability distribution of each uncertain variable is summarised in Table A3.4-3. The Monte Carlo simulation was performed using 20,000 trials. In each trial, Analytic Solver Platform randomly selects a value for uncertain variables, based on the user-defined probability distributions. These values are then used to calculate closure temperature and cooling rate by iterating Dodson's equation (Equation 1; Dodson, 1973). Three iterations of the equation were sufficient to calculate the closure temperature (further iterations change the output value by less than 0.1%; e.g. a closure temperature of 346°C as compared to 347°C). The cooling rate was recalculated after each iteration of the equation, based on the newly calculated closure temperature. For samples where peak metamorphic age and $^{40}Ar/^{39}Ar$ cooling age overlap (e.g. hornblende AF02-1; Table 3.2), some trials result in a negative cooling rate; for some samples, this was up to 13,808 of the initial 20,000 trials. As negative cooling rates cannot be recorded by minerals with well-defined closure temperatures, the results of these simulations are excluded from the Monte Carlo simulation. A minimum of 6,192 trials for each sample produced usable results.

After 20,000 trials, histograms of output values are generated, showing the distribution of calculated closure temperatures (Figure A3.4-1) and cooling rates (Figure A3.4-2). These histograms represent the probability distribution of the true value of the variables calculated during the Monte Carlo simulation.

Table A3.4-3 Probability distributions and values of variables used in the Monte Carlo simulation. The uncertainty of each random variable used in the Monte Carlo simulation was modelled using either a uniform, triangular or normal probability distribution. The values of all other variables used in Equation 1 are the same as those given in Table A3.4-1 above. The Monte Carlo simulation models the changes in output values (closure temperature and cooling rate) based on changing input values.

Variable	Input Probability Distribution	Value	Source
Hornblende			
E	Triangular (min, mode, max)	64.1 ± 1.7 kcal/mol	Harrison (1981)
D_0	Triangular (min, mode, max)	$0.024\ ^{+0.053}_{-0.011}$ cm²/s	
Biotite			
E	Triangular (min, mode, max)	50.5 ± 2.2 kcal/mol	Grove and Harrison (1996)
D_0	Triangular (min, mode, max)	$0.4\ ^{+0.96}_{-0.28}$ cm²/s	
Muscovite			
E	Triangular (min, mode, max)	63 ± 7 kcal/mol	Harrison et al. (2009)
D_0	Triangular (min, mode, max)	$22.3\ ^{+70}_{-2.2}$ cm²/s	
Metamorphic age (Ma)	Normal (mean, σ)	Varies for each mineral	Table A3.4-2
Metamorphic temperature (°C)	Uniform (min, max)	Varies for each mineral	Table A3.4-2
$^{40}Ar/^{39}Ar$ cooling age (°C)	Normal (mean, σ)	Varies for each mineral	Table 3.1
Closure temperature (°C)	Not modelled with a probability distribution	The value of the closure temperature is directly calculated by iterating Equation 1 as part of each trial	
Cooling rate (°C/Ma)	Not modelled with a probability distribution	Initially calculated based on metamorphic age, metamorphicm temperature, $^{40}Ar/^{39}Ar$ cooling age and the initial estimate of $^{40}Ar/^{39}Ar$ closure temperature T_{C0}. The cooling rate is recalculated after every iteration of Equation 1, using the new closure temperature directly calculated as part of each iteration	

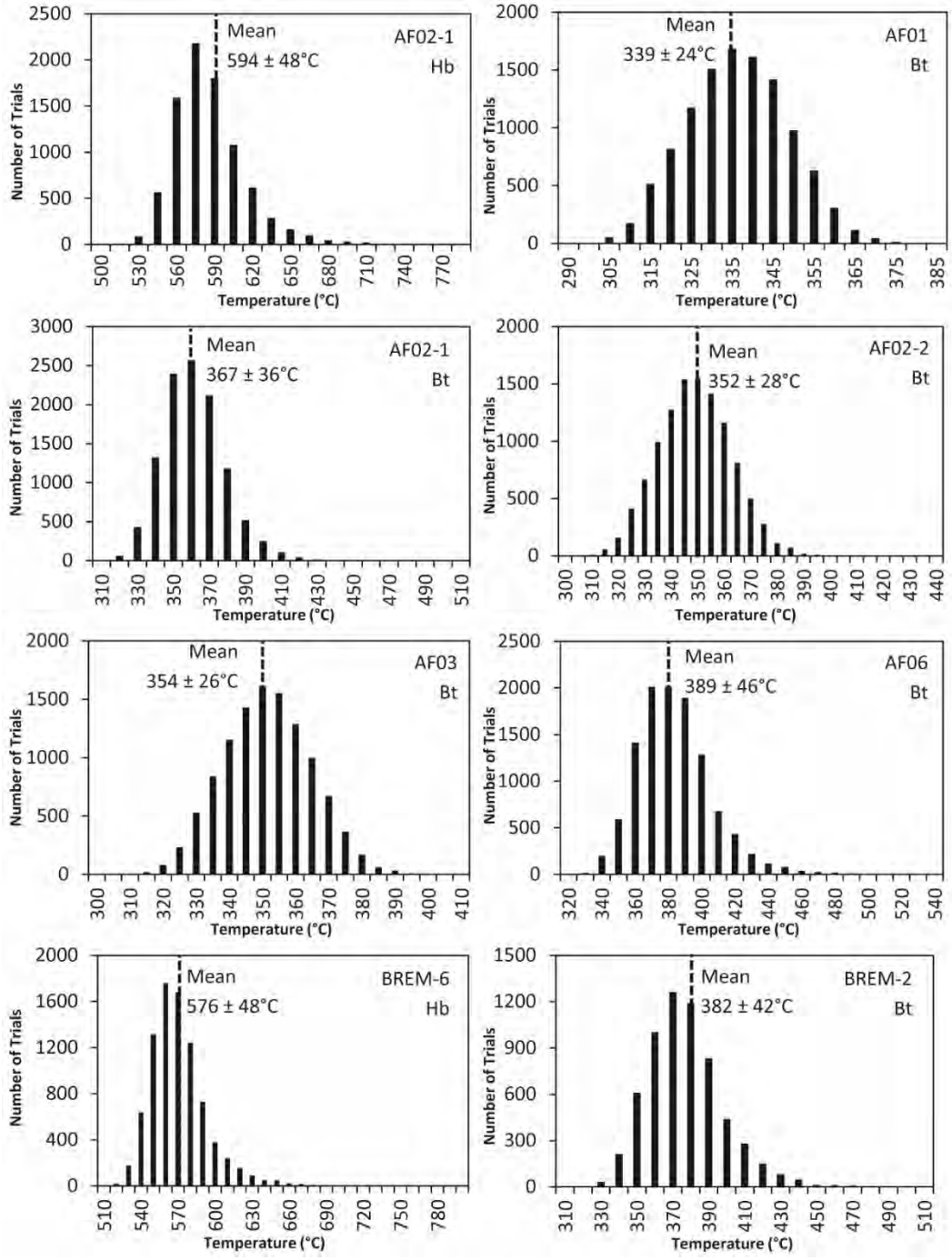

Figure A3.4-1 Histograms showing the distribution of the results of a 20,000-trial Monte Carlo simulation modelling the argon closure temperature in hornblende, biotite and muscovite grains. The dashed line shows the approximate location of the mean, reported with ± 2σ.

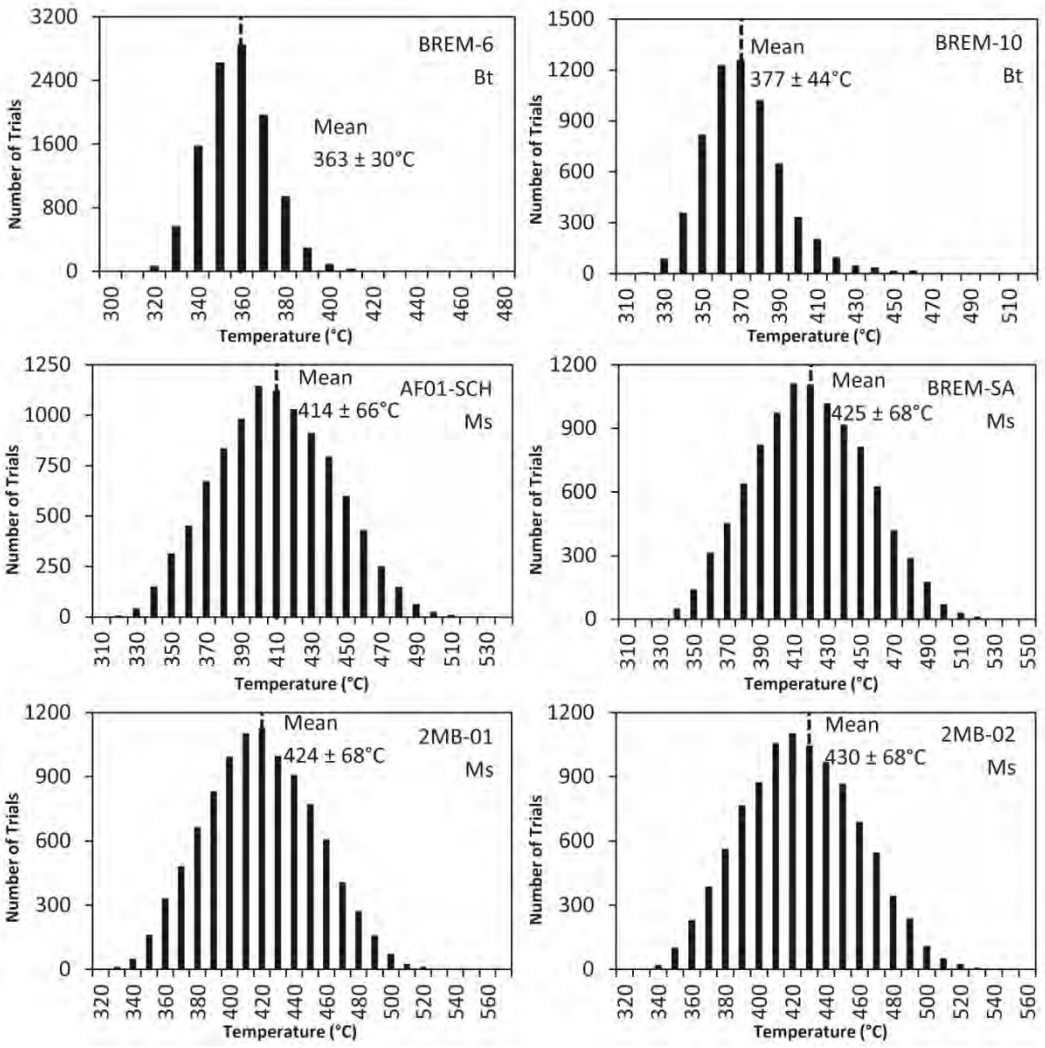

Figure A3.4-1 (Continued)

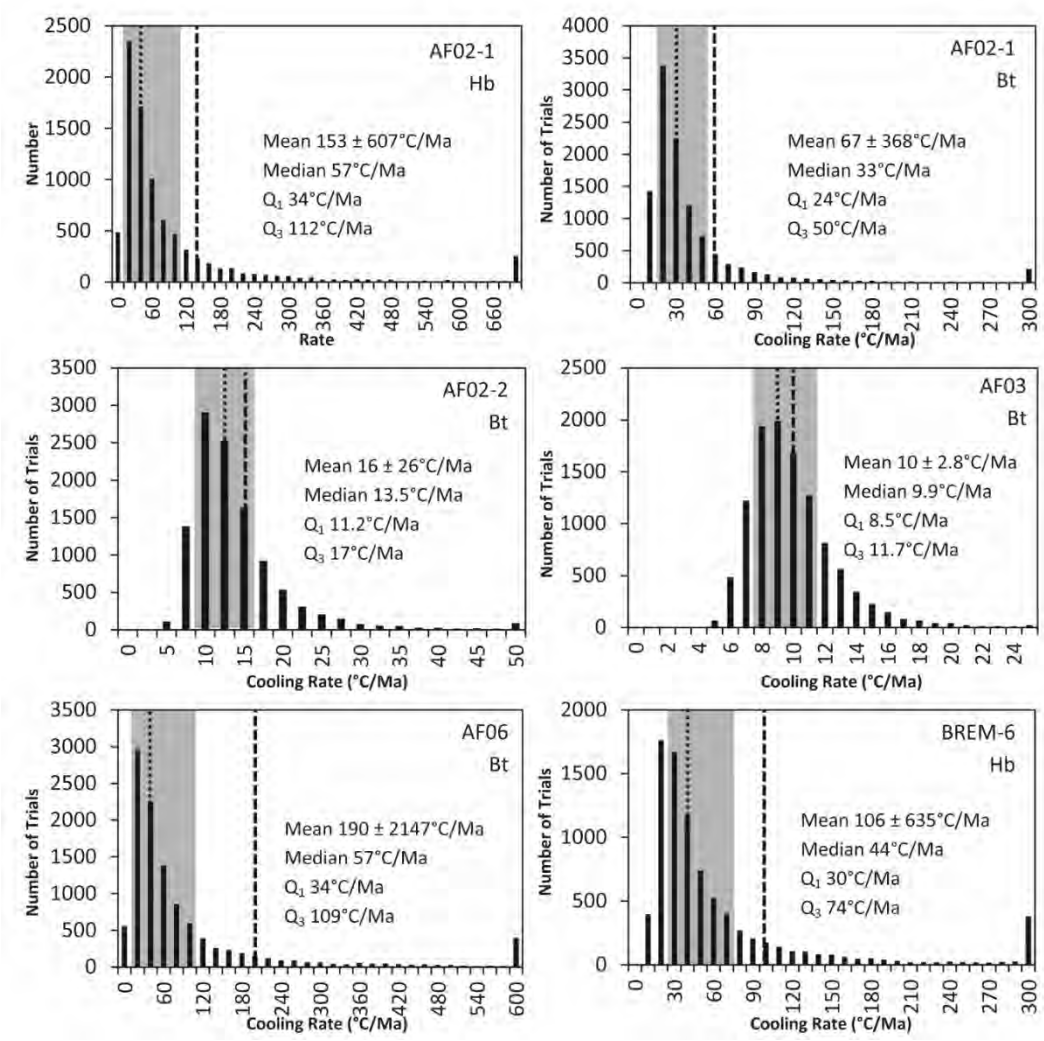

Figure A3.4-2 Histograms showing the distribution of the results of Monte Carlo simulations modelling the cooling rate between Stage II metamorphic conditions and argon closure temperature in hornblende, biotite and muscovite grains. The dashed line is the population mean (±σ), and the dotted line is the median. Q_1 and Q_3 are the lower and upper quartiles respectively. The shaded area is the inter-quartile range. The strongly right-tailed skew of the histograms is due to the large range in mathematically calculated cooling rates. This also skews the mean and standard deviation to unrealistically high values. For this reason, the median is a better measure of the central tendency of this population, and the inter-quartile range is a more robust measure of scale than the standard deviation. This is a conservative approach which reduces the reported cooling rates for each population of results.

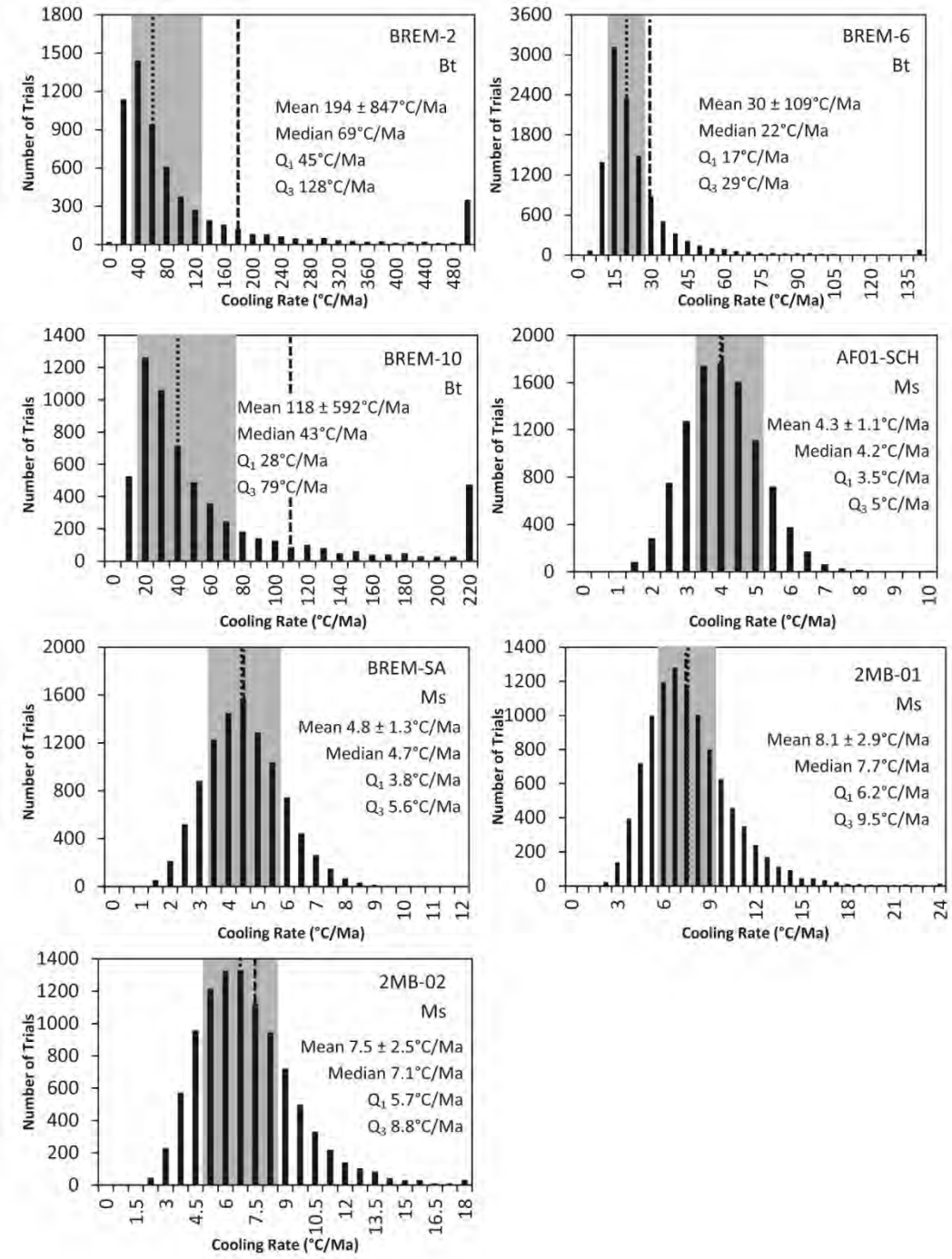

Figure A3.4-2 (Continued)

References

Black, L. P., Harris, L. B., and Delor, C. P., 1992, Reworking of Archaean and Early Proterozoic components during a progressive, Middle Proterozoic tectonothermal event in the Albany Mobile Belt, Western Australia: Precambrian Research, v. 59, p. 95-123.

Clark, W. C., 1995, Granite petrogenesis, metamorphism and geochronology of the western Albany-Fraser Orogen, Albany, Western Australia: Curtin University of Technology, BSc (Honours) thesis (unpublished).

Dawson, G. C., Krapez, B., Fletcher, I. R., McNaughton, N. J., and Rasmussen, B., 2003, 1.2 Ga thermal metamorphism in the Albany-Fraser orogen of Western Australia: consequence of collision or regional heating by dyke swarms?: Journal of the Geological Society, London, v. 160, p. 29-37.

Dodson, M. H., 1973, Closure temperature in cooling geochronological and petrological systems: Contributions in Mineralogy and Petrology, v. 40, p. 259-274.

Fitzsimons, I., and Buchan, C., 2005, Geology of the Western Albany-Fraser Orogen, Western Australia - a field guide: Western Australian Geological Survey, Record 2005/11, p. 32.

Grove, M., and Harrison, T. M., 1996, $^{40}Ar^*$ diffusion in Fe-rich biotite: American Mineralogist, v. 81, p. 940-951.

Harrison, T. M., 1981, Diffusion of ^{40}Ar in hornblende: Contributions in Mineralogy and Petrology, v. 78, p. 324 - 331.

Harrison, T. M., Célérier, J., Aikman, A. B., Hermann, J., and Heizler, M. T., 2009, Diffusion of ^{40}Ar in muscovite: Geochimica et Cosmochimica Acta, v. 73, p. 1039-1051.

Pidgeon, R. T., 1990, Timing of plutonism in the Proterozoic Albany Mobile Belt, southwestern Australia: Precambrian Research, v. 47, p. 157-167.

Spaggiari, C., Bodorkos, S., Barquero-Molina, M., Tyler, I., and Wingate, M. T. D., 2009, Interpreted bedrock geology of the southern Yilgarn and central Albany-

Fraser Orogen, Western Australia: Geological Survey of Western Australia, Record 2009/10, p. 84.

Spaggiari, C. V., Kirkland, C. L., Pawley, M. J., Smithies, R. H., Wingate, M. T. D., Doyle, M. G., Blenkinsop, T. G., Clark, C., Oorschot, C. W., Fox, L. J., and Savage, J., 2011, The geology of the east Albany-Fraser Orogen - a field guide: Geological Survey of Western Australia, Record 2011/23, p. 92.

Stephenson, N. C. N., 1974, Petrology of the Albany and Torbay adamellite plutons, near Albany, Western Australia: Journal of the Geological Society of Australia, v. 21, no. 3, p. 219-246.

Wetherley, S., 1998, Tectonometamorphic evolution of the Mount Barren Group, Albany-Fraser Province, Western Australia: PhD thesis, University of Western Australia.

Appendix 3.5: Stage II geochronology from the Albany-Fraser Orogen

Table A3.5-1 Compilation of published Stage II geochronology and structural data for the western and central Albany-Fraser Orogen.

Age (Ma)	Data type	Event	Location	Source
Nornalup Zone				
1188 ± 9	Zircon	"Late-tectonic" granite	Mount Franklin, 200km W of Albany	Black et al. (1992)
1184 ± 12	Zircon	Magmatic age of a deformed granite	Porongorups	Black et al. (1992)
1184 ± 12	Zircon	"Post-tectonic" aplite cutting dextral shear zones	Porongorups	Black et al. (1992)
Synchronous with D2 as described above	Relative age	D2: ENE striking foliation and NW vergent folding; SE-up transport + dextral component D3: Conjugate mylonite to cataclastite shear zones; dextral set dominant, sinistral set subordinate; overall suggests dextral transpression due to NW-SE shortening	Western Nornalup Zone, west of Albany	Duebendorfer (2002)
1177 ± 4	Zircon	Post-tectonic adamellite	Mt Chudalup (very western end of the orogen)	Pidgeon (1990)
1174 ± 12	Zircon	Post-tectonic adamellite	Mt Melville, Albany	Pidgeon (1990)
1169 ± 8	Zircon	Amphibolite facies metamorphism (2nd metamorphic zircon generation in the sample)	Ledge Beach	Clark (1995)
1138 ± 38	Zircon	Granite intrusion (Esperance Supersuite)	Esperance Harbour	Clark et al. (2000)
Biranup Zone				
1196 ± 8	Zircon	Granulite facies metamorhism	Groper Bluff	Black et al. (1992)
1187 ± 12	Zircon	Crystallisation age of folded pegmatite dyke	Lake Gidong	Nelson et al. (1995)
1187 ± 5	Zircon core	Migmatitic granite intrusion into a m-scale boudin neck during boudinage	Point Henry	Barquero-Molina (2010)

Age (Ma)	Data type	Event	Location	Source
1180 ± 6	Zircon age of syn-tectonic pegmatite	D2 oblique thrusting with a dextral transcurrent component due to NNW compression, followed by a change to NW compression and continued dextral transpression during amphibolite facies metamorphism	Pegmatite from Pallinup Estuary; D2 recorded throughout the Nornalup and Biranup Zones of the Western Albany-Fraser Orogen	Structure: Beeson et al. (1988) Age: Black et al. (1992)
1172 ± 16	Zircon rim	Granulite facies metamorphism, followed by or coeval with NW-SE compression producing folding	Point Henry	Barquero-Molina (2010)
1178 ± 4	Zircon	High-grade metamorphism	Point Henry	Spaggiari et al. (2009)
1178 ± 3	Zircon core and rim	Migmatitic granitic intrusion into a dm-scale boudin neck during boudinage and granulite facies metamorphism; followed by/coeval with further NW-SE compression producing folding	Fisheries Bay	Barquero-Molina (2010)
1168 ± 12	Zircon age of a synkinematic pegmatite	High T low P M2a metamorphism; D2 dextral shearing along SE dipping shear zones and NW vergent folding	Coramup Gneiss	Bodorkos and Clark (2004)
1154 ± 25	Zircon	High-grade metamorphism	Short Beach	Spaggiari et al. (2009)
1148 ± 9	Zircon	Granite intrusion	Short Beach headland	Barquero-Molina (2010)
Northern Foreland				
1205 ± 10	Xenotime	Amphibolite facies metamorphism, extensive folding and localised shearing suggesting NW-SE compression	Mount Barren Group	Age: Dawson et al. (2003) PT and structure: Wetherley (1998)
"during Stage II"	Relative dating	F3 tight folds and conjugate shear zones suggesting NW-SE compression	Eastern Munglinup Gneiss	Spaggiari et al. (2011)
1195 ± 17	Zircon rims	Metamorphism	Powell Point, eastern Munglinup Gneiss	Spaggiari et al. (2011)
1184 ± 6	Zircon rims	Upper amphibolite facies metamorphism	West of Quagi Beach, eastern Munglinup Gneiss	Spaggiari et al. (2011)

References

Barquero-Molina, M., 2010, Kinematics of bidirectional extension and coeval NW-directed contraction in orthogneisses of the Biranup Complex, Albany Fraser Orogen, Southwestern Australia: Geological Survey of Western Australia, Report 109, p. 205.

Beeson, J., Delor, C. P., and Harris, L. B., 1988, A structural and metamorphic traverse across the Albany Mobile Belt, Western Australia: Precambrian Research, v. 40/41, p. 117-136.

Black, L. P., Harris, L. B., and Delor, C. P., 1992, Reworking of Archaean and Early Proterozoic components during a progressive, Middle Proterozoic tectonothermal event in the Albany Mobile Belt, Western Australia: Precambrian Research, v. 59, p. 95-123.

Bodorkos, S., and Clark, D., 2004, Evolution of a crustal-scale transpressive shear zone in the Albany-Fraser Orogen, SW Australia: 2. Tectonic history of the Coramup Gneiss and a kinematic framework for Mesoproterozoic collision of the West Australian and Mawson cratons: Journal of Metamorphic Geology, v. 22, p. 713-731.

Clark, D., Hensen, B., and Kinny, P., 2000, Geochronological constraints for a two-stage history of the Albany-Fraser Orogen, Western Australia: Precambrian Research, v. 102, p. 155-183.

Clark, W. C., 1995, Granite petrogenesis, metamorphism and geochronology of the western Albany-Fraser Orogen, Albany, Western Australia: Curtin University of Technology, BSc (Honours) thesis (unpublished).

Dawson, G. C., Krapez, B., Fletcher, I. R., McNaughton, N. J., and Rasmussen, B., 2003, 1.2 Ga thermal metamorphism in the Albany-Fraser orogen of Western Australia: consequence of collision or regional heating by dyke swarms?: Journal of the Geological Society, London, v. 160, p. 29-37.

Duebendorfer, E. M., 2002, Regional correlation of Mesoproterozoic structures and deformational events in the Albany-Fraser orogen, Western Australia: Precambrian Research, v. 116, p. 129 - 154.

Nelson, D. R., Myers, J. S., and Nutman, A. P., 1995, Chronology and evolution of the Middle Proterozoic Albany-Fraser Orogen, Western Australia: Australian Journal of Earth Sciences, v. 42, no. 5, p. 481 - 495.

Pidgeon, R. T., 1990, Timing of plutonism in the Proterozoic Albany Mobile Belt, southwestern Australia: Precambrian Research, v. 47, p. 157-167.

Spaggiari, C., Bodorkos, S., Barquero-Molina, M., Tyler, I., and Wingate, M. T. D., 2009, Interpreted bedrock geology of the southern Yilgarn and central Albany-Fraser Orogen, Western Australia: Geological Survey of Western Australia, Record 2009/10, p. 84.

Spaggiari, C. V., Kirkland, C. L., Pawley, M. J., Smithies, R. H., Wingate, M. T. D., Doyle, M. G., Blenkinsop, T. G., Clark, C., Oorschot, C. W., Fox, L. J., and Savage, J., 2011, The geology of the east Albany-Fraser Orogen - a field guide: Geological Survey of Western Australia, Record 2011/23, p. 92.

Wetherley, S., 1998, Tectonometamorphic evolution of the Mount Barren Group, Albany-Fraser Province, Western Australia: PhD thesis, University of Western Australia.

Appendix 4.1: Detailed analytical methods for $^{40}Ar/^{39}Ar$ thermochronology

Samples were crushed and sieved to separate the 125 – 250 μm fraction, which was washed in acetone and deionised water to remove dust. Optically unaltered 125 – 250 μm grains of biotite (22 samples), muscovite (3 samples) and hornblende (13 samples) were separated by hand-picking under a binocular microscope.

Samples were loaded into 38 large wells of 3 aluminium discs measuring 1.9 cm in diameter and 0.3 cm in depth. These wells were bracketed by small wells containing either Fish Canyon sanidine (FCs), Hb3gr hornblende, or WA1ms muscovite, used as neutron flux monitors. The ages of these standards are: FCs, 28.294 Ma ± 0.13 % (1σ) (Renne et al., 2011); Hb3gr, 1081.0 Ma ± 0.11 % (1σ) (Renne et al., 2011); WA1ms, 2614.2 Ma ± 0.055 % (1σ) (Jourdan et al., 2014). To minimise nuclear interference reactions, the disc was Cd-shieled, and irradiated for 40 hours in the USGS TRIGA nuclear reactor (Oregon, USA) in a central position.

The mean J-values computed from the standard grains within the small pits are: FCs, 0.01074950 ± 0.00002096 (± 0.19%); Hb3gr, 0.01086400 ± 0.00002607 (± 0.24%); WA1ms, 0.01085500 ± 0.00002062 (± 0.19%). Mean J-values are calculated as the average and standard deviation of J-values of the standard grains within each irradiation disc. An automated air pipette was used to monitor mass discrimination, which had a mean value of 1.00 ± 0.34 per Dalton (atomic mass unit) relative to an air ratio of 298.56 ± 0.31 (Lee et al., 2006). The correction factors for interfering isotopes were: $(^{39}Ar/^{37}Ar)_{Ca} = 7.60x10^{-4}$ (± 7%); $(^{36}Ar/^{37}Ar)_{Ca} = 2.81x10^{-4}$ (± 3%); and $(^{40}Ar/^{39}Ar)_{K} = 6.76x10^{-4}$ (± 10%).

The $^{40}Ar/^{39}Ar$ analyses were performed at the Western Australian Argon Isotope Facility at Curtin University. Samples were step-heated in 4 – 14 steps using a 110 W Spectron Laser Systems, by rastering a continuous Nd-YAG (IR, 1064 nm) laser over the sample for one minute, to ensure homogenous heating. The gas released from the sample was purified in a stainless steel extraction line using two SAES AP10 getters and one GP50 getter. Ar isotopes were measured in static mode with a MAP 215-50

mass spectrometer (resolution ~450; sensitivity $4x10^{-14}$ mol/V) with a Balzers SEV 217 electron multiplier using 9 – 10 cycles of peak-hopping. Data acquisition was performed with the Argus program written by M.O. McWilliams, and run under a LabView environment. Raw data were processed using ArArCALC software (Koppers, 2002), and ages were calculated using the decay constants recommended by (Renne et al., 2011). A blank was monitored after every 4 steps, with a typical ^{40}Ar range of $3x10^{-16}$ – $5x10^{-16}$ mol. Appendix 4.2 contains Ar isotope data corrected for blank, mass discrimination and radioactive decay, with individual errors given at the 2σ level.

In this study, the criteria for the determination of an age plateau are as follows: plateaus must include at least 70% of the total measured ^{39}Ar, and plateaus should be distributed over at least three consecutive steps that agree at a 95% confidence level and satisfy a probability of fit (P) of at least 0.05. Plateau ages in Table 4.2 and Figure 4.2 are given at the 2σ level, and are calculated using the mean of all plateau steps, weighted by the inverse variance of their individual analytical error. Mini-plateaus are defined similarly, but include 50% - 70% of the total ^{39}Ar. Mini-plateau ages are less robust than plateau ages. All sources of uncertainty are included in the calculations.

References

Jourdan, F., Frew, A., Joly, A., Mayers, C., and Evans, N. J., 2014, WA1ms: A ~2.61 Ga muscovite standard for $^{40}Ar/^{39}Ar$ dating: Geochimica et Cosmochimica Acta, v. 141, p. 113-126.

Koppers, A. A. P., 2002, ArArCALC-software for $^{40}Ar/^{39}Ar$ age calculations: Computers & Geosciences, v. 28, p. 605 - 619.

Lee, J. Y., Marti, K., Severinghaus, J. P., Kawamura, K., Yoo, H. S., Lee, J. B., and Kim, J. S., 2006, A redetermination of the isotopic abundance of atmospheric Ar: Geochimica et Cosmochimica Acta, v. 70, p. 4507-4512.

Renne, P. R., Balco, G., Ludwig, K. R., Mundil, R., and Min, K., 2011, Response to the comment by W.H. Schwarz et al. on "Joint determination of ^{40}K decay constants

and $^{40}Ar^*/^{40}K$ for the Fish Canyon sanidine standard, and improved accuracy for $^{40}Ar/^{39}Ar$ geochronology" by P.R. Renne et al. (2010): Geochimica et Cosmochimica Acta, v. 75, p. 5097-5100.

Appendix 4.2: $^{40}Ar/^{39}Ar$ thermochronology results

Table A4.2-1 EAF011 Hornblende

Incremental Heating			36Ar(a) [V]	37Ar(ca) [V]	38Ar(cl) [V]	39Ar(k) [V]	40Ar(r) [V]	Age (Ma)	± 2σ	40Ar(r) (%)	39Ar(k) (%)	K/Ca	± 2σ
5M37251D	60 °C	4	0.0000201	0.0014605	0.0000082	0.0001120	0.0122163	1403.05	± 675.54	67.05	0.88	0.0330	± 0.0151
5M37252D	60 °C	4	0.0000008	0.0254381	0.0000105	0.0032323	0.4495568	1653.21	± 25.47	99.95	25.35	0.0546	± 0.0036
5M37253D	61 °C	4	0.0000073	0.0495096	0.0000236	0.0068556	0.9381676	1635.73	± 16.72	100.23	53.76	0.0595	± 0.0032
5M37254D	61 °C	4	0.0000106	0.0174001	0.0000045	0.0024032	0.3315755	1644.56	± 28.16	100.96	18.85	0.0594	± 0.0040
5M37257D	62 °C	4	0.0000036	0.0018950	0.0000030	0.0001484	0.0223535	1741.32	± 444.49	105.08	1.16	0.0337	± 0.0136

Information on Analysis	Results	40(r)/39(k)	± 2σ	Age (Ma)	± 2σ	MSWD (p)	39Ar(k) (%,n)	K/Ca	± 2σ
Sample = EAF0011HBL	**Age Plateau**	137.59885	± 1.59599	1641.63	± 13.20	0.53	100.00	0.0570	± 0.0053
Material = Hbl			± 1.16%		± 0.80%	71%	5		
Location = Laser			Full External Error		± 16.49	2.41	2σ Confidence Limit		
Analyst = Fred Jourdan			Analytical Error		± 12.51	1.0000	Error Magnification		
Project = ALBANYFRASER_ES12									
Mass Discrimination Law = POW	**Total Fusion Age**	137.54313	± 1.84066	1641.19	± 15.04		5	0.0573	± 0.0021
Irradiation = I19t40h			± 1.34%		± 0.92%				
J = 0.01074950 ± 0.00002096			Full External Error		± 17.99				
FCs = 28.294 ± 0.031 Ma			Analytical Error		± 14.43				
MDF = 1.003135 ± 0.06									

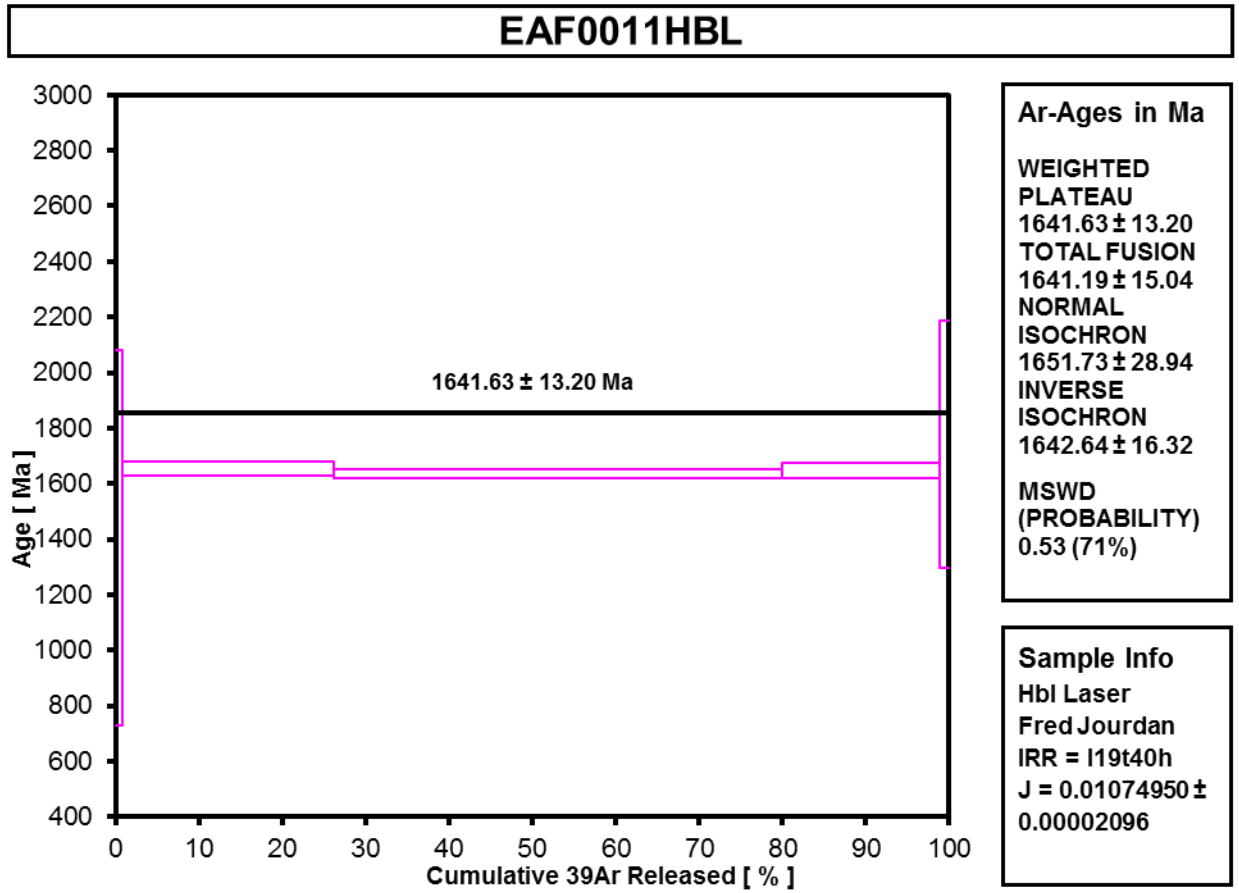

Figure A4.2-1 EAF011 Hornblende

Table A4.2-2 EAF046 Biotite

Incremental Heating			36Ar(a) [V]	37Ar(ca) [V]	38Ar(cl) [V]	39Ar(k) [V]	40Ar(r) [V]	Age ± 2σ (Ma)	40Ar(r) (%)	39Ar(k) (%)	K/Ca ± 2σ
5M36239D	58 °C		0.0000311	0.0000793	0.0000043	0.0007884	0.055956	1032.82 ± 114.15	85.77	0.48	4 ± 10
5M36240D	58 °C	4	0.0000329	0.0001012	0.0000256	0.0169148	1.401648	1160.10 ± 15.03	99.30	10.33	72 ± 114
5M36241D	59 °C	4	0.0000127	0.0000498	0.0000267	0.0424841	3.504346	1156.17 ± 6.68	99.89	25.95	366 ± 1198
5M36243D	59 °C	4	0.0000019	0.0001579	0.0000782	0.0586029	4.836331	1156.60 ± 4.03	99.99	35.80	160 ± 185
5M36244D	60 °C	4	0.0000075	0.0007628	0.0000363	0.0426073	3.526545	1159.10 ± 4.97	100.06	26.03	24 ± 8
5M36245D	61 °C	4	0.0000058	0.0001159	0.0000005	0.0023056	0.184142	1128.86 ± 32.50	99.07	1.41	9 ± 16

Information on Analysis	Results	40(r)/39(k) ± 2σ	Age ± 2σ (Ma)	MSWD	39Ar(k) (%,n)	K/Ca ± 2σ
Sample = EAF046BIO	**Age Plateau**	82.58669 ± 0.26830	1157.22 ± 4.27	1.00	99.52	21 ± 10
Material = bio		± 0.32%	± 0.37%	41%	5	
Location = Laser		Full External Error	± 10.98	2.41	2σ Confidence Limit	
Analyst = Fred Jourdan		Analytical Error	± 2.78	1.0003	Error Magnification	
Project = ALBANYFRASER_ES12						
Mass Discrimination Law = POW	**Total Fusion Age**	82.52121 ± 0.30024	1156.54 ± 4.49		6	73 ± 36
Irradiation = I19t40h		± 0.36%	± 0.39%			
J = 0.01085500 ± 0.00002062		Full External Error	± 11.06			
WA1ms = 2613.000 ± 2.352 Ma		Analytical Error	± 3.11			
MDF = 1.003122 ± 0.07						

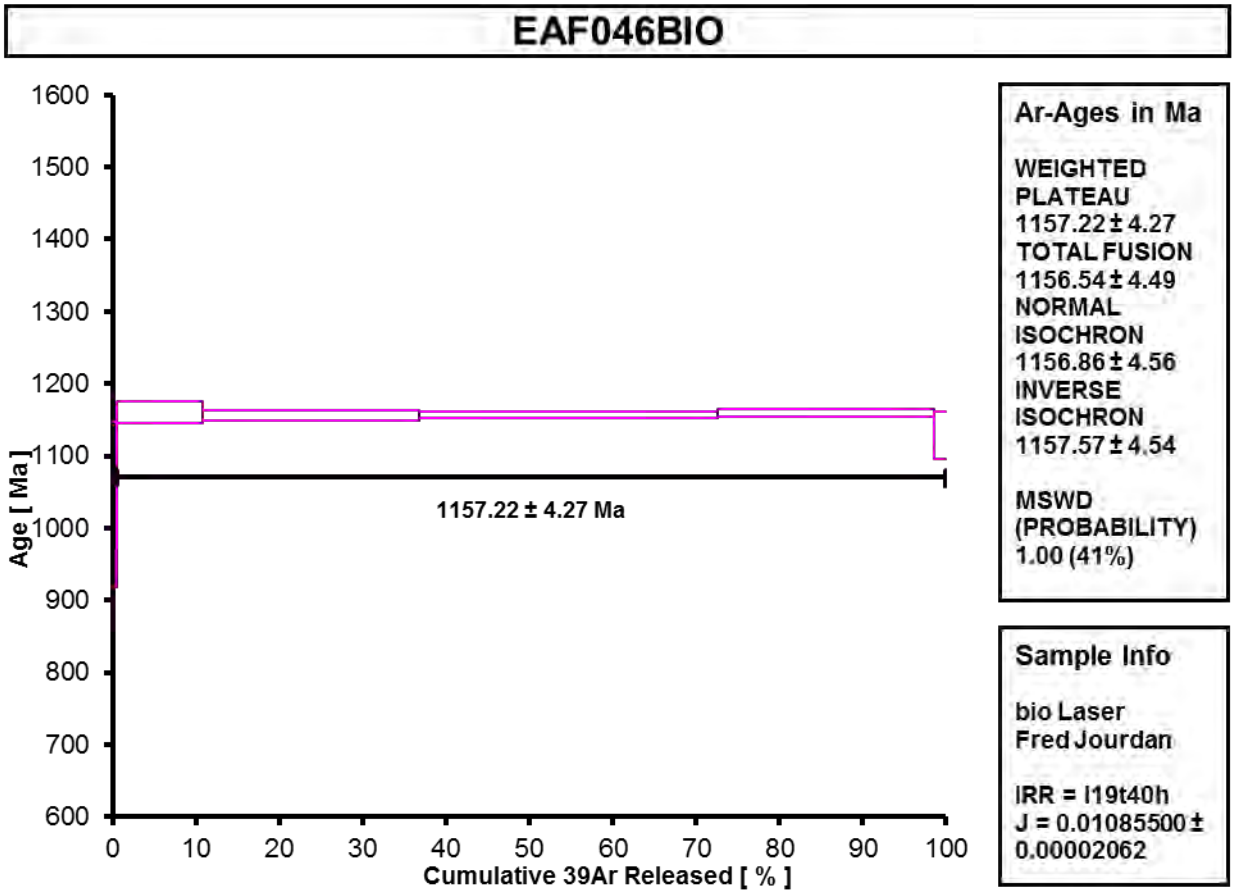

Figure A4.2-2 EAF046 Biotite

Table A4.2-3 EAF054 Biotite

Incremental Heating			36Ar(a) [V]	37Ar(ca) [V]	38Ar(cl) [V]	39Ar(k) [V]	40Ar(r) [V]	Age (Ma)	± 2σ	40Ar(r) (%)	39Ar(k) (%)	K/Ca	± 2σ
5M36222D	58 °C		0.0000196	0.0002388	0.0000000	0.0040648	0.342074	1173.38	± 16.72	98.32	2.30	7.3	± 7.9
5M36223D	59 °C	4	0.0000209	0.0005647	0.0000052	0.0174872	1.529991	1207.28	± 8.90	99.59	9.88	13.3	± 7.1
5M36225D	59 °C	4	0.0000135	0.0012599	0.0000231	0.0386466	3.370838	1204.57	± 4.88	99.88	21.83	13.2	± 2.8
5M36226D	60 °C	4	0.0000038	0.0017925	0.0000059	0.1136185	9.916337	1205.12	± 3.12	99.99	64.18	27.3	± 4.3
5M36227D	61 °C	4	0.0000077	0.0010319	0.0000040	0.0032198	0.275984	1189.32	± 19.23	99.17	1.82	1.3	± 0.3

Information on Analysis	Results	40(r)/39(k)	± 2σ	Age (Ma)	± 2σ	MSWD	39Ar(k) (%,n)	K/Ca	± 2σ
Sample = EAF054BIO	**Age Plateau**	87.25300	± 0.24793	1204.88	± 4.17	0.99	97.70	1.6	± 2.6
Material = bio			± 0.28%		± 0.35%	40%	4		
Location = Laser			Full External Error		± 11.25	2.63	2σ Confidence Limit		
Analyst = Fred Jourdan			Analytical Error		± 2.50	1.0000	Error Magnification		
Project = ALBANYFRASER_ES12									
Mass Discrimination Law = POW	**Total Fusion Age**	87.18652	± 0.24657	1204.21	± 4.16		5	15.6	± 1.9
Irradiation = I19t40h			± 0.28%		± 0.35%				
J = 0.01085500 ± 0.00002062			Full External Error		± 11.24				
WA1ms = 2613.000 ± 2.352 Ma			Analytical Error		± 2.49				
MDF = 1.003122 ± 0.07									

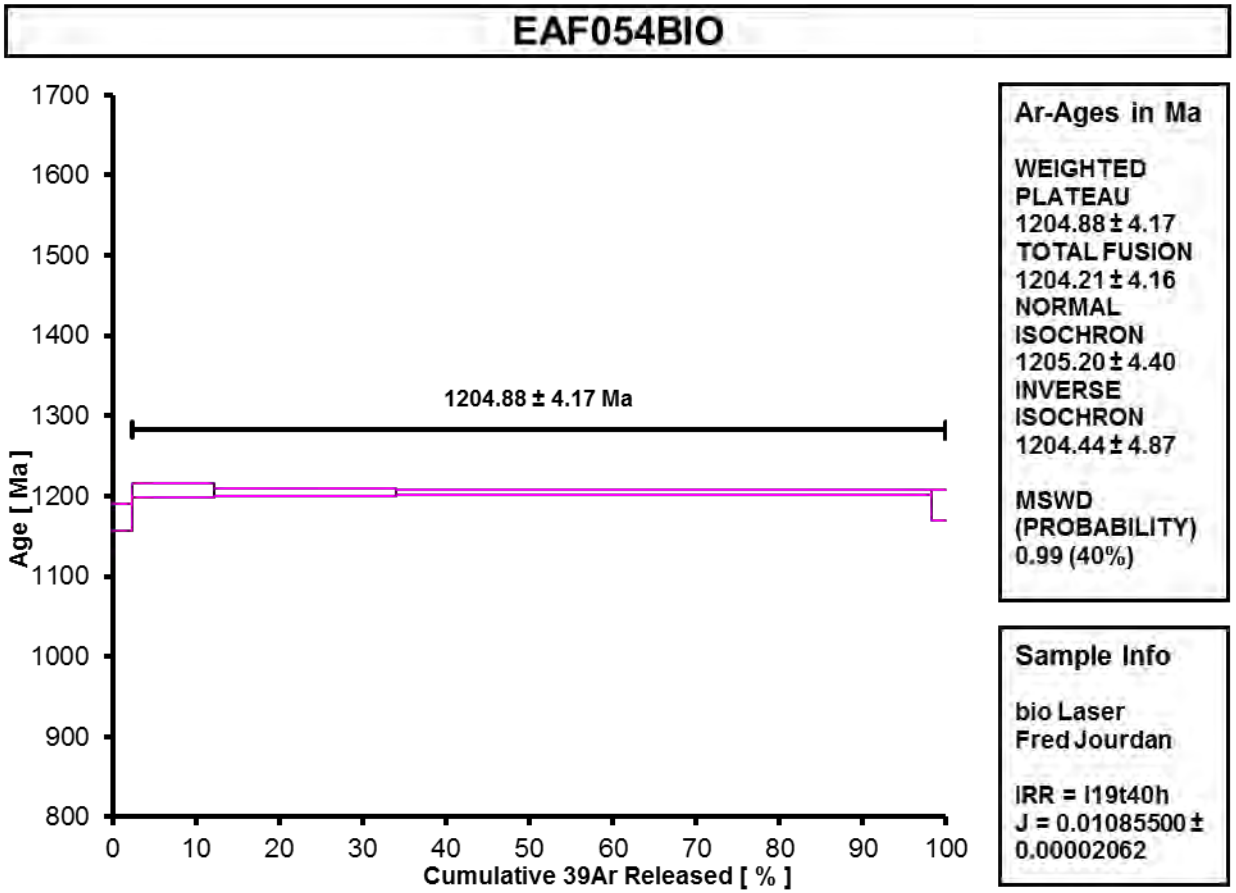

Figure A4.2-3 EAF054 Biotite

Table A4.2-4 EAF055B Hornblende

Incremental Heating			36Ar(a) [V]	37Ar(ca) [V]	38Ar(cl) [V]	39Ar(k) [V]	40Ar(r) [V]	Age ± 2σ (Ma)	40Ar(r) (%)	39Ar(k) (%)	K/Ca ± 2σ
5M37448D	60 °C		0.0000124	0.0023959	0.0000020	0.0008699	0.0738286	1173.00 ± 51.55	95.24	3.75	0.156 ± 0.053
5M37449D	60 °C	4	0.0000109	0.0354418	0.0000524	0.0117188	1.0510302	1221.38 ± 8.59	99.69	50.56	0.142 ± 0.009
5M37450D	61 °C	4	0.0000049	0.0138971	0.0000392	0.0050018	0.4416988	1207.67 ± 13.15	99.67	21.58	0.155 ± 0.014
5M37451D	61 °C	4	0.0000057	0.0140771	0.0000243	0.0049987	0.4450497	1214.88 ± 10.50	99.62	21.57	0.153 ± 0.014
5M37453D	62 °C	4	0.0000063	0.0013598	0.0000115	0.0005903	0.0546419	1249.61 ± 67.46	96.69	2.55	0.187 ± 0.109

Information on Analysis	Results	40(r)/39(k)	± 2σ	Age ± 2σ (Ma)		MSWD	39Ar(k) (%,n)	K/Ca ± 2σ
Sample = EAF0055BHBL	**Age Plateau**	89.21954	± 0.69894	1216.74	± 7.75	1.38	96.25	0.147 ± 0.007
Material = Hbl			± 0.78%		± 0.64%	25%	4	
Location = Laser			Full External Error		± 10.93	2.63	2σ Confidence Limit	
Analyst = Fred Jourdan			Analytical Error		± 6.94	1.1738	Error Magnification	
Project = ALBANYFRASER_ES12								
Mass Discrimination Law = POW	**Total Fusion Age**	89.14092	± 0.62592	1215.96	± 7.11		5	0.148 ± 0.007
Irradiation = I19t40h			± 0.70%		± 0.58%			
J = 0.01075940 ± 0.00002098			Full External Error		± 10.48			
FCs = 28.294 ± 0.037 Ma			Analytical Error		± 6.22			
MDF = 1.003236 ± 0.05								

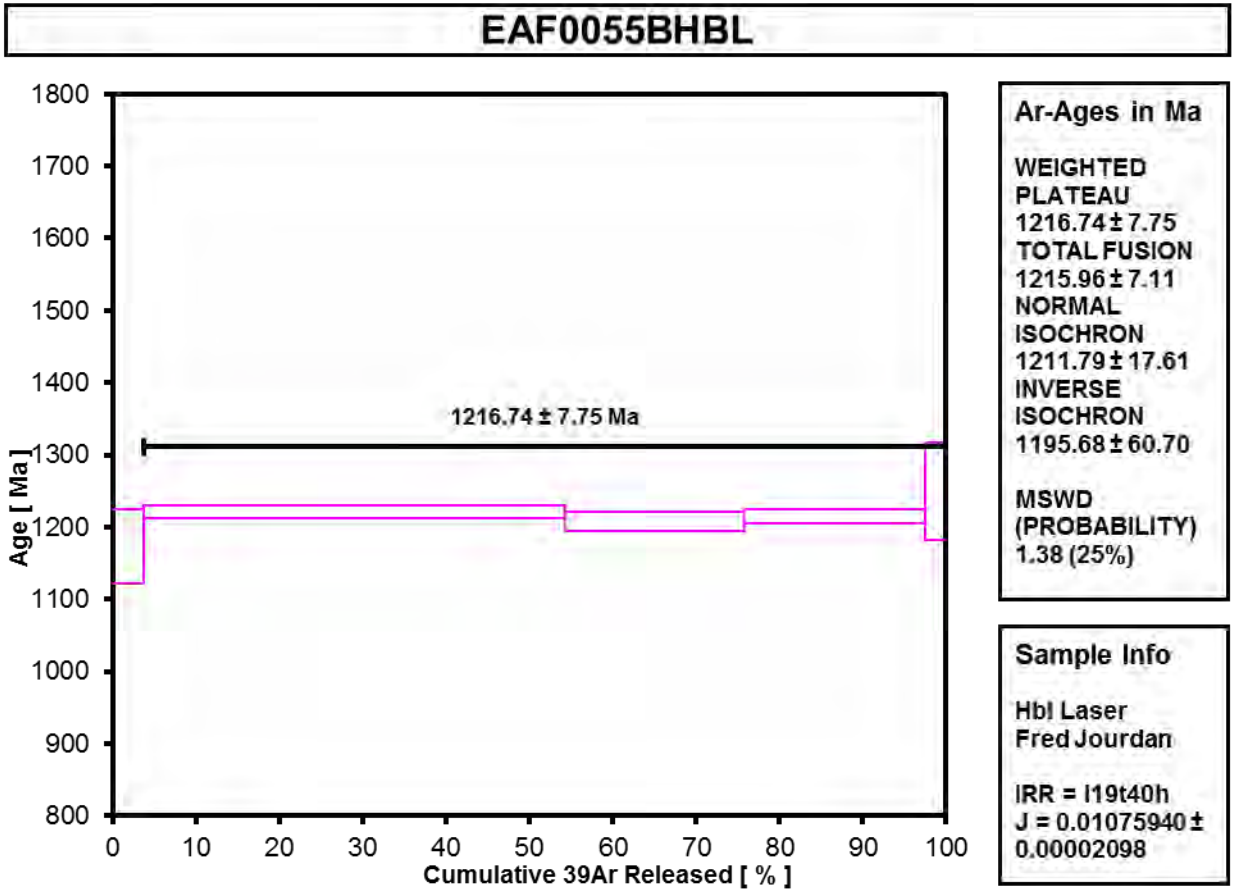

Figure A4.2-4 EAF055B Hornblende

Table A4.2-5 EAF060 Hornblende

Incremental Heating		36Ar(a) [V]	37Ar(ca) [V]	38Ar(cl) [V]	39Ar(k) [V]	40Ar(r) [V]	Age (Ma)	± 2σ	40Ar(r) (%)	39Ar(k) (%)	K/Ca	± 2σ
5M38073D	60 °C	0.0000058	0.0022344	0.0000011	0.0000081	0.0485413	7580.15	± 3278.14	96.55	3.28	0.0016	± 0.0031
5M38074D	60 °C	0.0000129	0.0027586	0.0000000	0.0000064	0.0107617	5341.78	± 3087.18	73.64	2.61	0.0010	± 0.0019
5M38075D	61 °C	0.0000057	0.0030615	0.0000000	0.0000460	0.0205830	3195.54	± 787.17	92.41	18.67	0.0065	± 0.0047
5M38077D	61 °C	0.0000014	0.0083999	0.0000000	0.0001860	0.0229257	1535.69	± 229.52	101.92	75.45	0.0095	± 0.0028

Information on Analysis	**Results**	40(r)/39(k)	± 2σ	Age (Ma)	± 2σ	MSWD	39Ar(k) (%,n)	K/Ca	± 2σ
Sample = EAF0060HBL Material = Hbl Location = Laser Analyst = Fred Jourdan Project = ALBANYFRASER_ES12 Mass Discrimination Law = POW Irradiation = I19t40h J = 0.01085500 ± 0.00002062 FCs = 28.294 ± 0.037 Ma MDF = 1.003286 ± 0.05	**Age Plateau Cannot Calculate**								
	Total Fusion Age	417.05961	± 71.22764 ± 17.08%	3091.36	± 253.00 ± 8.18% Full External Error ± 253.58 Analytical Error ± 252.94		4	0.0064	± 0.0018

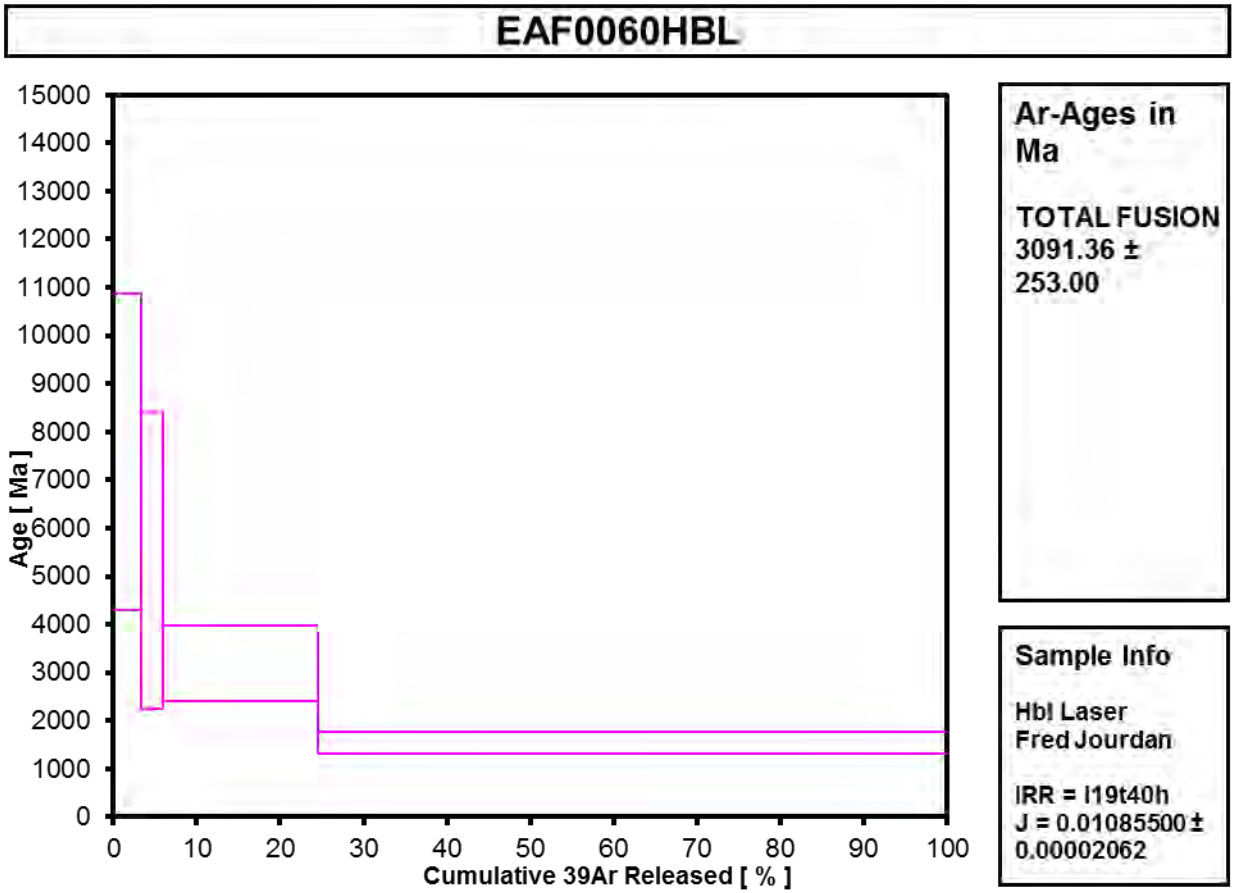

Figure A4.2-5 EAF060 Hornblende

Table A4.2-6 EAF061 Biotite 1

Incremental Heating		36Ar(a) [V]	37Ar(ca) [V]	38Ar(cl) [V]	39Ar(k) [V]	40Ar(r) [V]	Age ± 2σ (Ma)	40Ar(r) (%)	39Ar(k) (%)	K/Ca ± 2σ
5M36211D	58 °C	0.0000555	0.0000769	0.0000000	0.0131715	0.926084	1025.47 ± 5.53	98.24	7.05	73.7 ± 215.8
5M36212D~	59 °C	0.0001294	0.0018450	0.0000000	0.1096498	8.841234	1136.87 ± 3.81	99.56	58.67	25.6 ± 4.1
5M36215D	60 °C	0.0000185	0.0000560	0.0000000	0.0568526	4.836179	1182.69 ± 3.23	99.89	30.42	436.8 ± 1688.4
5M36216D	61 °C	0.0000052	0.0001208	0.0000090	0.0062406	0.519090	1163.34 ± 14.50	99.70	3.34	22.2 ± 38.6
5M36217D	63 °C	0.0000018	0.0000554	0.0000009	0.0009729	0.084160	1197.33 ± 69.55	100.65	0.52	7.6 ± 27.7

Information on Analysis	Results	40(r)/39(k) ± 2σ	Age ± 2σ (Ma)	MSWD	39Ar(k) (%,n)	K/Ca ± 2σ
Sample = EAF061BIO	**Age Plateau Cannot Calculate**					
Material = bio						
Location = Laser						
Analyst = Fred Jourdan						
Project = ALBANYFRASER_ES12						
Mass Discrimination Law = POW	**Total Fusion Age**	81.36849 ± 0.24397	1144.56 ± 4.10		5	45.2 ± 13.2
Irradiation = I19t40h		± 0.30%	± 0.36%			
J = 0.01085500 ± 0.00002062			Full External Error ± 10.83			
WA1ms = 2613.000 ± 2.352 Ma			Analytical Error ± 2.54			
MDF = 1.003122 ± 0.07						

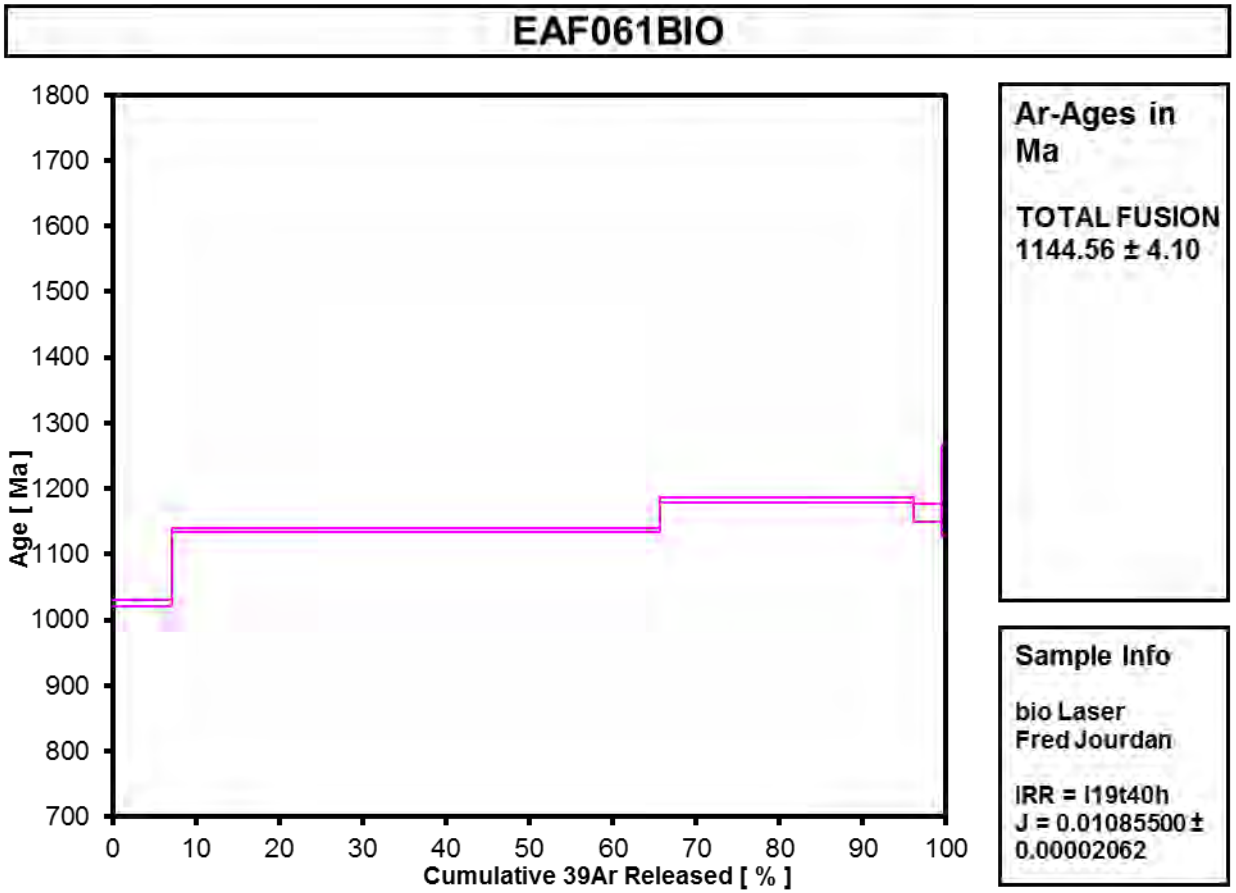

Figure A4.2-6 EAF061 Biotite 1

Table A4.2-7 EAF061 Biotite 2

Incremental Heating		36Ar(a) [V]	37Ar(ca) [V]	38Ar(cl) [V]	39Ar(k) [V]	40Ar(r) [V]	Age (Ma)	± 2σ	40Ar(r) (%)	39Ar(k) (%)	K/Ca	± 2σ
5M38055D	60 °C	0.0000104	0.0007572	0.0000000	0.0009685	0.073078	1081.88	± 54.55	104.42	0.35	0.5	± 1.3
5M38056D	60 °C	0.0000140	0.0001278	0.0000021	0.0026056	0.181242	1017.11	± 25.67	97.75	0.94	8.8	± 110.2
5M38058D	60 °C	0.0000363	0.0008388	0.0000103	0.0079128	0.586909	1067.96	± 11.09	98.19	2.86	4.1	± 8.7
5M38059D	60 °C	0.0000079	0.0007250	0.0000000	0.0123554	0.997002	1137.52	± 5.09	99.76	4.47	7.3	± 16.8
5M38060D	60 °C	0.0000552	0.0015536	0.0000000	0.0726366	5.954035	1150.83	± 3.58	99.72	26.26	20.1	± 25.7
5M38061D	60 °C	0.0000151	0.0019249	0.0000000	0.0582293	4.835443	1161.92	± 3.79	99.91	21.05	13.0	± 12.4
5M38063D	61 °C	0.0000009	0.0011907	0.0000000	0.0528012	4.455164	1175.64	± 1.94	99.99	19.09	19.1	± 29.3
5M38064D	61 °C	0.0000008	0.0020290	0.0000124	0.0265010	2.228885	1172.87	± 5.31	99.99	9.58	5.6	± 4.6
5M38065D	61 °C	0.0000013	0.0022609	0.0000000	0.0107752	0.904898	1171.58	± 8.82	100.04	3.90	2.0	± 1.6
5M38066D	61 °C	0.0000064	0.0017920	0.0000000	0.0089739	0.750115	1167.56	± 12.30	99.74	3.24	2.2	± 2.2
5M38068D	61 °C	0.0000118	0.0009072	0.0000000	0.0052414	0.436511	1164.39	± 13.80	99.20	1.89	2.5	± 4.7
5M38069D	62 °C	0.0000113	0.0000773	0.0000000	0.0154344	1.315578	1184.44	± 6.82	99.74	5.58	85.9	± 2037.5
5M38070D	63 °C	0.0000158	0.0007028	0.0000000	0.0017777	0.146435	1155.03	± 36.28	96.88	0.64	1.1	± 3.3
5M38071D	66 °C	0.0000029	0.0003484	0.0000000	0.0003935	0.031766	1137.91	± 138.58	97.32	0.14	0.5	± 2.5

Information on Analysis	Results	40(r)/39(k)	± 2σ	Age (Ma)	± 2σ	MSWD	39Ar(k) (%,n)	K/Ca	± 2σ
Sample = EAF0061BIO	**Age Plateau**								
Material = Bio	**Cannot Calculate**								
Location = Laser									
Analyst = Fred Jourdan									
Project = ALBANYFRASER_ES12									
Mass Discrimination Law = POW	**Total Fusion Age**	82.77849	± 0.16011	1159.20	± 3.65		14	8.0	± 3.7
Irradiation = I19t40h			± 0.19%		± 0.31%				
J = 0.01085500 ± 0.00002062				Full External Error	± 8.24				
FCs = 28.294 ± 0.037 Ma				Analytical Error	± 1.66				
MDF = 1.003286 ± 0.05									

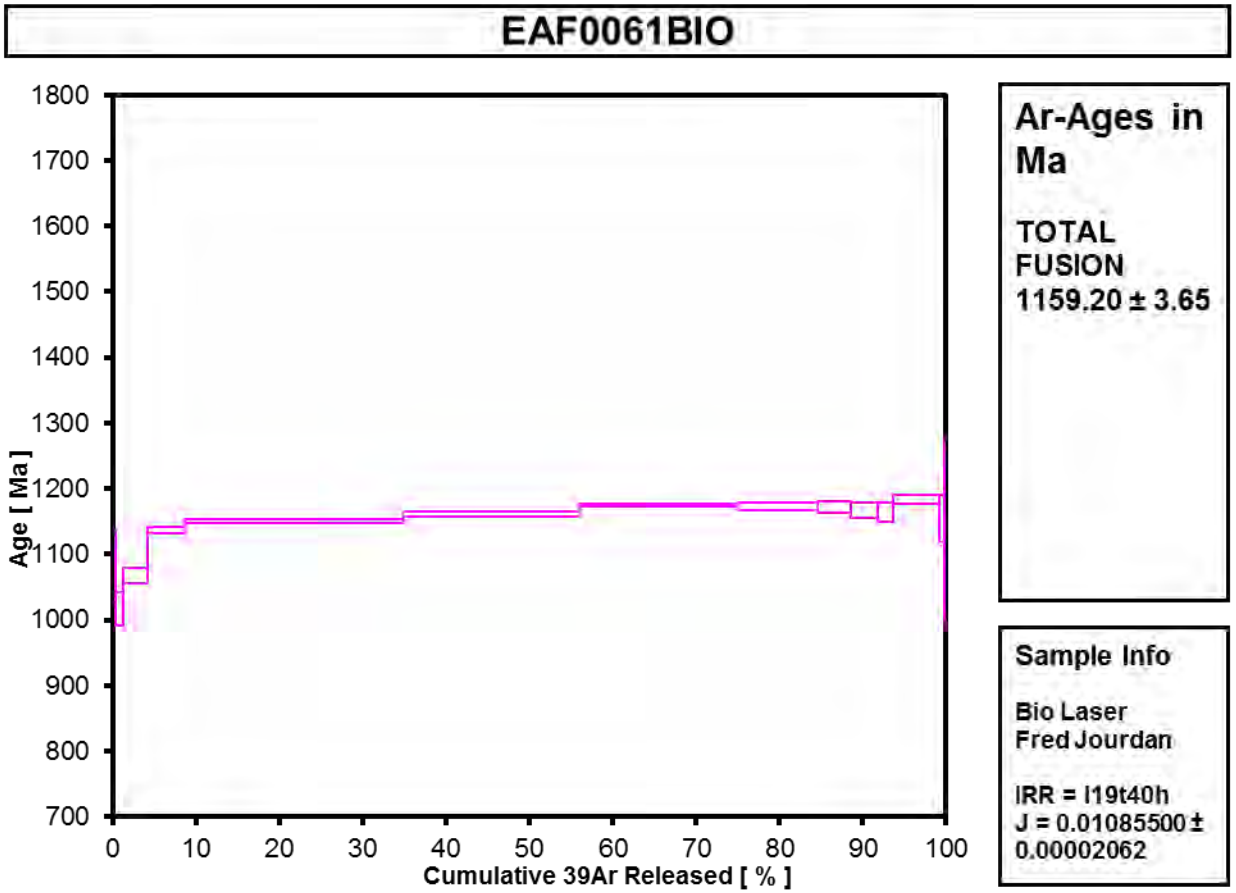

Figure A4.2-7 EAF061 Biotite 2

Table A4.2-8 EAF051 Hornblende

Incremental Heating			36Ar(a) [V]	37Ar(ca) [V]	38Ar(cl) [V]	39Ar(k) [V]	40Ar(r) [V]	Age (Ma)	± 2σ	40Ar(r) (%)	39Ar(k) (%)	K/Ca	± 2σ
5M36674D	65 °C	4	0.0000359	0.0128134	0.0000012	0.0042682	0.3318641	1099.18	± 18.39	96.87	100.00	0.143	± 0.009

Information on Analysis	Results	40(r)/39(k)	± 2σ	Age (Ma)	± 2σ	MSWD	39Ar(k) (%,n)	K/Ca	± 2σ
Sample = EAF0051	**Age Plateau Cannot Calculate**								
Material = Hbl									
Location = Laser									
Analyst = Fred Jourdan									
Project = ALBANYFRASER_ES12									
Mass Discrimination Law = POW	**Total Fusion Age**	77.75248	± 1.73573	1099.18	± 18.66		1	0.143	± 0.009
Irradiation = I19t40h			± 2.23%		± 1.70%				
J = 0.01075940 ± 0.00002098				Full External Error	± 19.92				
FCs = 28.294 ± 0.037 Ma				Analytical Error	± 18.39				
MDF = 1.003357 ± 0.06									

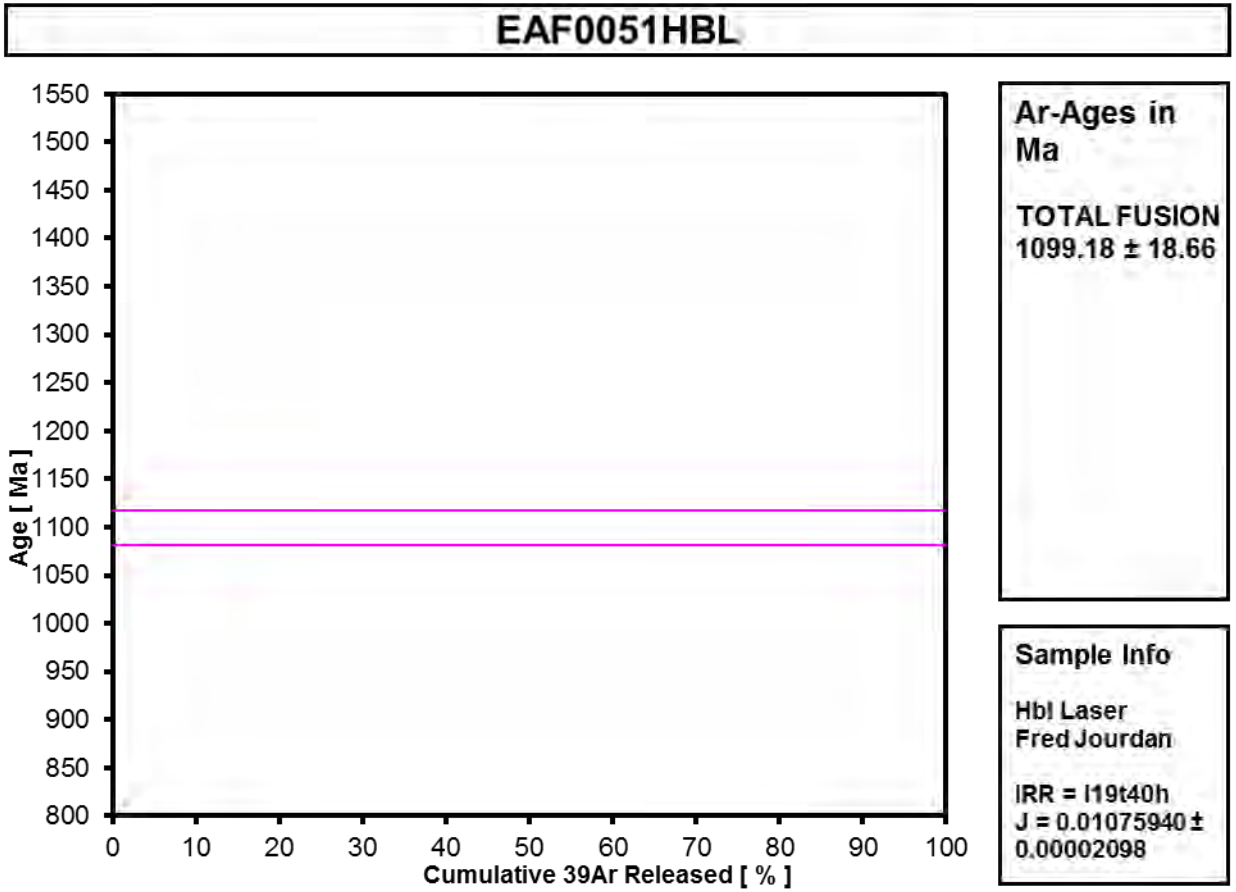

Figure A4.2-8 EAF051 Hornblende

Table A4.2-9 EAF52 Hornblende

Incremental Heating			36Ar(a) [V]	37Ar(ca) [V]	38Ar(cl) [V]	39Ar(k) [V]	40Ar(r) [V]	Age (Ma)	± 2σ	40Ar(r) (%)	39Ar(k) (%)	K/Ca	± 2σ
5M37315D	59.5 %		0.0000077	0.0007574	0.0000065	0.0003131	0.0241196	1091.61	± 135.14	91.31	0.79	0.178	± 0.186
5M37316D	60.0 %		0.0000111	0.0289093	0.0000207	0.0098662	0.8766028	1213.06	± 8.13	99.62	24.92	0.147	± 0.009
5M37317D	60.5 %	4	0.0000083	0.0678498	0.0000621	0.0216901	1.9764684	1235.54	± 4.92	100.12	54.78	0.137	± 0.007
5M37318D	61.0 %	4	0.0000037	0.0124422	0.0000036	0.0038755	0.3485017	1223.72	± 16.50	99.69	9.79	0.134	± 0.011
5M37320D	61.5 %	4	0.0000111	0.0089566	0.0000159	0.0028890	0.2601553	1224.95	± 22.02	98.74	7.30	0.139	± 0.019
5M37321D	62.0 %	4	0.0000125	0.0028336	0.0000047	0.0009602	0.0860691	1220.86	± 43.27	95.85	2.43	0.146	± 0.041

Information on Analysis	Results	40(r)/39(k)	± 2σ	Age (Ma)	± 2σ	MSWD	39Ar(k) (%,n)	K/Ca	± 2σ
Sample = EAF0052HBL	**Age Plateau**	90.96560	± 0.46645	1233.99	± 5.76	1.00	74.29	0.137	± 0.006
Material = Hbl			± 0.51%		± 0.47%	39%	4		
Location = Laser			Full External Error		± 9.62	2.63	2σ Confidence Limit		
Analyst = Fred Jourdan			Analytical Error		± 4.59	1.0008	Error Magnification		
Project = ALBANYFRASER_ES12									
Mass Discrimination Law = POW	**Total Fusion Age**	90.21326	± 0.43736	1226.58	± 5.54		6	0.140	± 0.005
Irradiation = I19t40h			± 0.48%		± 0.45%				
J = 0.01075940 ± 0.00002098			Full External Error		± 9.46				
FCs = 28.294 ± 0.031 Ma			Analytical Error		± 4.32				
MDF = 1.002943 ± 0.07									

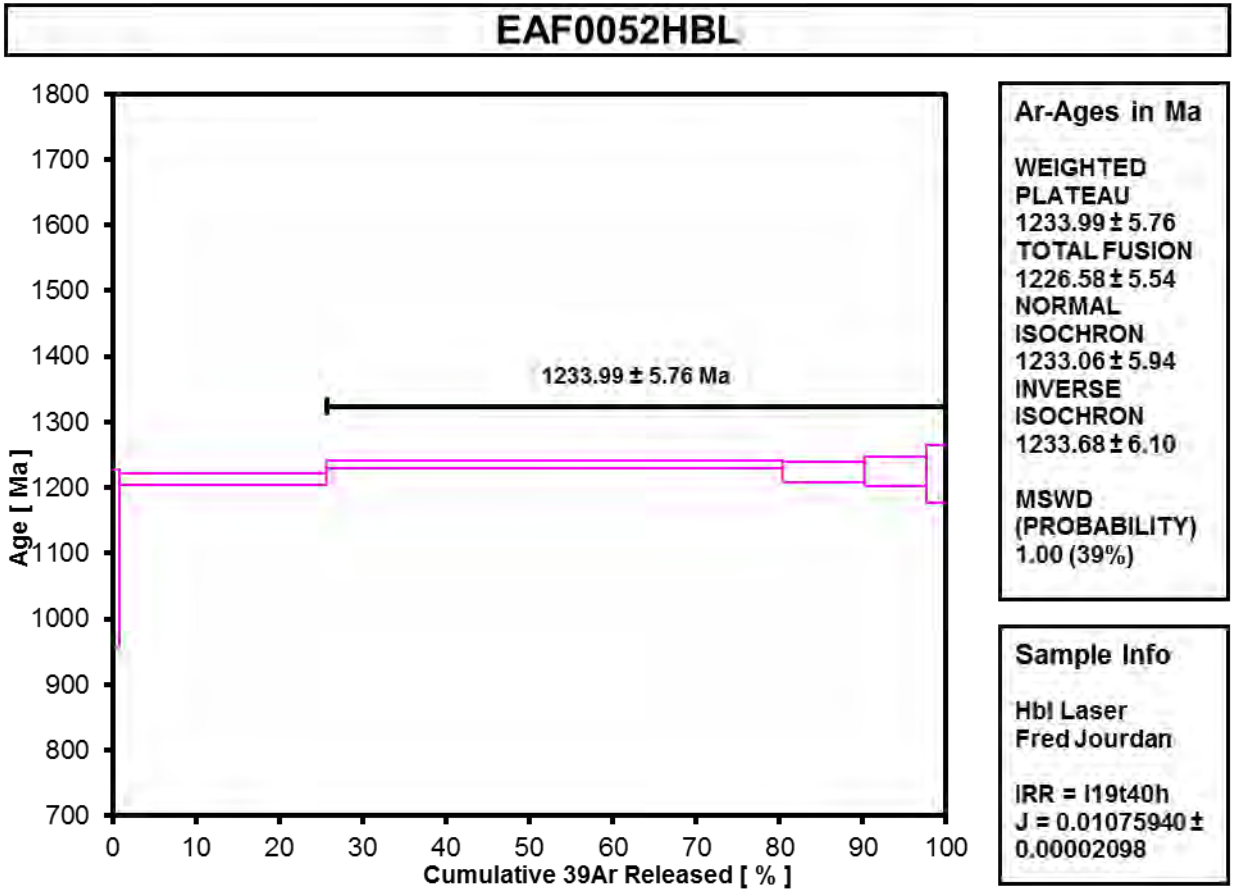

Figure A4.2-9 EAF52 Hornblende

Table A4.2-10 EAF021 Biotite 1

Incremental Heating			36Ar(a) [V]	37Ar(ca) [V]	38Ar(cl) [V]	39Ar(k) [V]	40Ar(r) [V]	Age ± 2σ (Ma)	40Ar(r) (%)	39Ar(k) (%)	K/Ca ± 2σ
5M36483D	58 °C		0.0000838	0.0011716	0.0003612	0.0009561	0.066849	2572.50 ± 371.29	72.77	0.64	0.35 ± 0.05
5M36484D	59 °C		0.0000336	0.0013078	0.0002064	0.0025484	0.401147	1801.76 ± 33.82	97.56	1.70	0.84 ± 0.12
5M36486D	59 °C	4	0.0000244	0.0024950	0.0000000	0.0152523	1.922182	1558.72 ± 8.60	99.62	10.17	2.63 ± 0.20
5M36487D	60 °C	4	0.0001422	0.0162528	0.0000000	0.0833845	10.460283	1553.91 ± 5.98	99.60	55.58	2.21 ± 0.07
5M36488D~	61 °C	4	0.0000475	0.0124812	0.0000000	0.0388460	4.891352	1557.81 ± 5.53	99.71	25.89	1.34 ± 0.07
5M36489D	63 °C		0.0000123	0.0247775	0.0000000	0.0106242	1.354694	1570.98 ± 5.12	99.73	7.08	0.18 ± 0.01
5M36490D	65 °C		0.0000120	0.0080885	0.0000000	0.0003239	0.067735	2142.47 ± 134.72	105.59	0.22	0.02 ± 0.00

Information on Analysis	Results	40(r)/39(k)	± 2σ	Age ± 2σ (Ma)		MSWD	39Ar(k) (%,n)	K/Ca	± 2σ
Sample = EAF021BIO	**Age Plateau**	125.75850	± 0.44255	1556.50	± 5.41	0.62	91.64	1.78	± 0.66
Material = bio			± 0.35%		± 0.35%	54%	3		
Location = Laser			Full External Error		± 13.85	3.00	2σ Confidence Limit		
Analyst = Fred Jourdan			Analytical Error		± 3.67	1.0000	Error Magnification		
Project = ALBANYFRASER_ES12									
Mass Discrimination Law = POW	**Total Fusion Age**	127.74185	± 0.46484	1572.89	± 5.53		7	0.97	± 0.02
Irradiation = I19t40h			± 0.36%		± 0.35%				
J = 0.01085500 ± 0.00002062			Full External Error		± 13.99				
WA1ms = 2613.000 ± 2.352 Ma			Analytical Error		± 3.82				
MDF = 1.00323 ± 0.06									

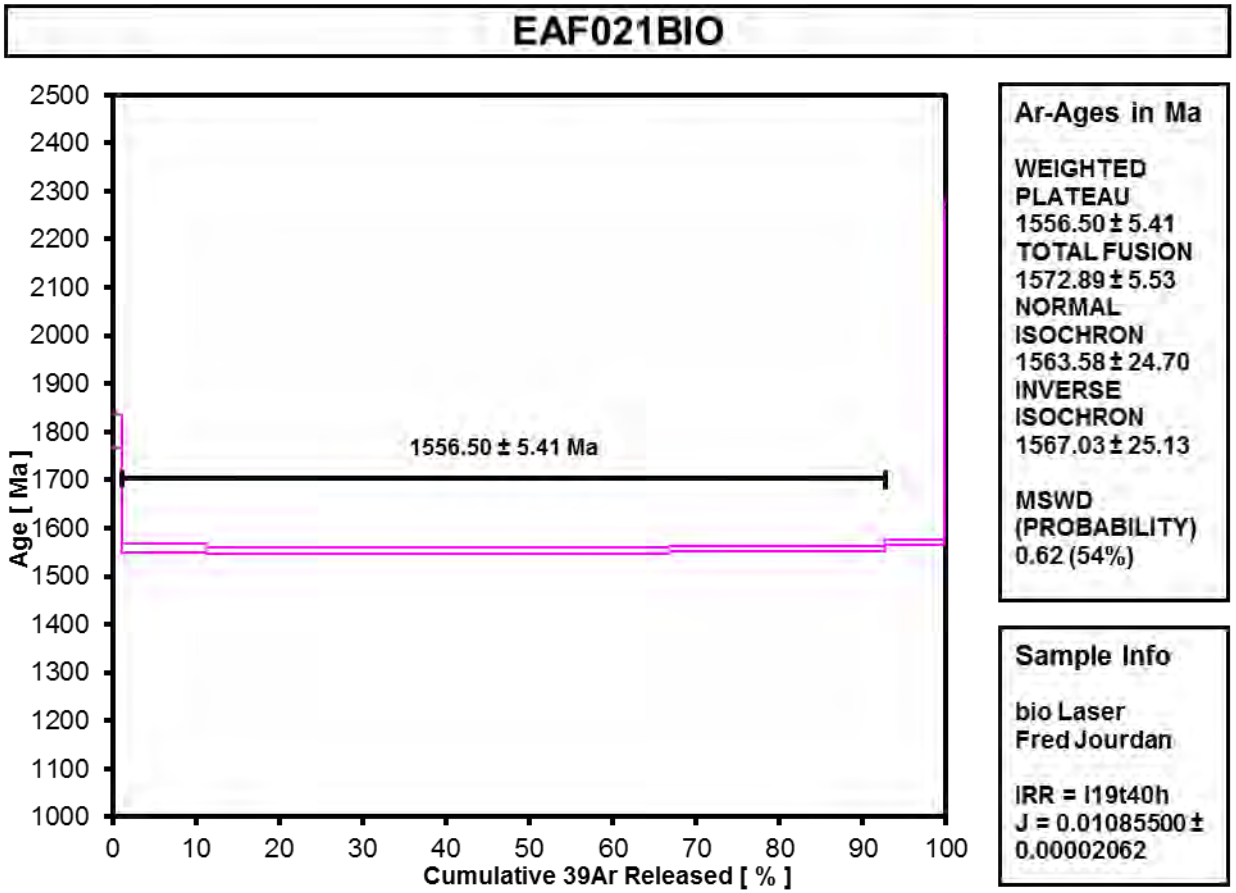

Figure A4.2-10 EAF021 Biotite 1

Table A4.2-11 EAF021 Biotite 2

Incremental Heating			36Ar(a) [V]	37Ar(ca) [V]	38Ar(cl) [V]	39Ar(k) [V]	40Ar(r) [V]	Age (Ma)	± 2σ	40Ar(r) (%)	39Ar(k) (%)	K/Ca	± 2σ
5M38082D	60 °C		0.0000121	0.0010730	0.0000000	0.0001612	0.013165	1147.64	± 559.93	78.47	0.07	0.06	± 0.13
5M38083D	60 °C		0.0000208	0.0017020	0.0000000	0.0005990	0.059509	1322.93	± 135.46	90.55	0.28	0.15	± 0.18
5M38085D	60 °C		0.0000226	0.0004402	0.0000000	0.0003929	0.033572	1186.49	± 263.46	83.24	0.18	0.38	± 1.55
5M38086D	60 °C		0.0000311	0.0011060	0.0000032	0.0010353	0.096724	1266.03	± 88.44	91.25	0.48	0.40	± 0.66
5M38087D	60 °C		0.0000330	0.0016175	0.0000176	0.0033188	0.320525	1296.52	± 29.55	97.02	1.53	0.88	± 1.00
5M38088D	60 °C		0.0000395	0.0010369	0.0000164	0.0057753	0.560061	1300.31	± 17.97	97.94	2.66	2.39	± 4.22
5M38090D	61 °C		0.0000190	0.0008593	0.0000115	0.0202304	1.995859	1316.32	± 5.64	99.72	9.30	10.12	± 21.85
5M38091D	61 °C	4	0.0000269	0.0017038	0.0000000	0.0212344	2.057240	1299.43	± 7.66	99.61	9.77	5.36	± 5.87
5M38092D	61 °C	4	0.0000113	0.0005849	0.0000171	0.0194519	1.910606	1312.20	± 9.10	100.18	8.95	14.30	± 56.14
5M38093D	61 °C	4	0.0000046	0.0028383	0.0000247	0.0220046	2.136969	1301.65	± 8.38	99.94	10.12	3.33	± 2.07
5M38095D	61 °C	4	0.0000181	0.0010464	0.0000087	0.0189441	1.837995	1300.76	± 7.72	99.71	8.71	7.78	± 15.32
5M38096D	62 °C	4	0.0000542	0.0020732	0.0000397	0.1015917	9.890975	1303.99	± 1.69	99.84	46.72	21.07	± 20.40
5M38097D	63 °C	4	0.0000049	0.0016756	0.0000071	0.0024510	0.237304	1298.83	± 36.90	99.39	1.13	0.63	± 0.71
5M38098D	66 °C	4	0.0000041	0.0004112	0.0000002	0.0002406	0.024235	1335.94	± 346.91	95.17	0.11	0.25	± 1.05

Information on Analysis	Results	40(r)/39(k)	± 2σ	Age (Ma)	± 2σ	MSWD	39Ar(k) (%,n)	K/Ca	± 2σ
Sample = EAF0021BIO	**Age Plateau**	97.34189	± 0.16372	1303.82	± 3.86	0.96	85.51	0.79	± 0.88
Material = Bio			± 0.17%		± 0.30%	45%	7		
Location = Laser				Full External Error	± 9.06	2.15	2σ Confidence Limit		
Analyst = Fred Jourdan				Analytical Error	± 1.56	1.0000	Error Magnification		
Project = ALBANYFRASER_ES12									
Mass Discrimination Law = POW	**Total Fusion Age**	97.38590	± 0.22750	1304.24	± 4.14		14	5.15	± 2.05
Irradiation = I19t40h			± 0.23%		± 0.32%				
J = 0.01085500 ± 0.00002062				Full External Error	± 9.18				
FCs = 28.294 ± 0.037 Ma				Analytical Error	± 2.17				
MDF = 1.003286 ± 0.05									

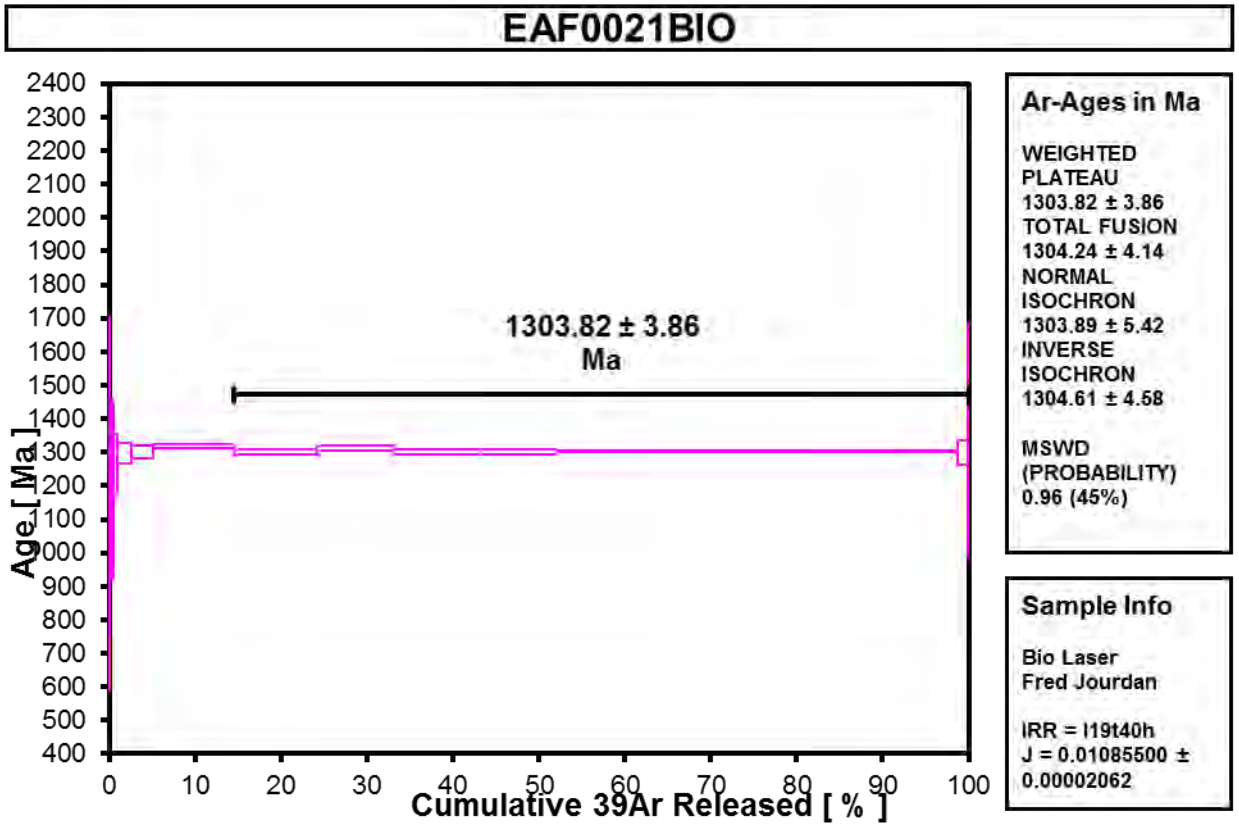

Figure A4.2-11 EAF021 Biotite 2

Table A4.2-12 EAF022 Muscovite

Incremental Heating			36Ar(a) [V]	37Ar(ca) [V]	38Ar(cl) [V]	39Ar(k) [V]	40Ar(r) [V]	Age (Ma)	± 2σ	40Ar(r) (%)	39Ar(k) (%)	K/Ca	± 2σ
5M36125D	58 °C		0.0000025	0.0000617	0.0000000	0.0011903	0.097199	1148.29	± 58.44	100.79	0.32	8	± 66
5M36127D	58 °C		0.0000139	0.0001464	0.0000000	0.0012765	0.098275	1098.99	± 60.51	95.96	0.34	4	± 13
5M36128D	59 °C		0.0000625	0.0002316	0.0000000	0.0015346	0.120751	1117.06	± 49.46	86.61	0.41	3	± 6
5M36129D	59 °C		0.0000169	0.0002448	0.0000039	0.0025829	0.211951	1152.44	± 34.13	97.67	0.69	5	± 9
5M36130D	59 °C		0.0000227	0.0002808	0.0000000	0.0127553	1.046336	1152.17	± 11.72	99.36	3.41	20	± 35
5M36132D	59 °C		0.0000861	0.0003504	0.0000000	0.0113658	0.965828	1182.51	± 12.05	97.41	3.04	14	± 20
5M36133D	59 °C		0.0000290	0.0002577	0.0000200	0.0321331	2.679926	1166.33	± 4.48	99.68	8.59	54	± 104
5M36134D	60 °C	4	0.0000007	0.0003159	0.0000000	0.1217140	10.056930	1158.35	± 2.25	100.00	32.53	166	± 263
5M36135D	61 °C	4	0.0000046	0.0001333	0.0000000	0.1424665	11.836680	1163.07	± 3.28	100.01	38.07	460	± 1767
5M36137D	63 °C	4	0.0000055	0.0001944	0.0000000	0.0103108	0.854913	1161.32	± 11.55	99.81	2.76	23	± 60
5M36138D	66 °C	4	0.0000011	0.0000629	0.0000000	0.0248482	2.053031	1158.30	± 5.20	99.98	6.64	170	± 1386
5M36139D	67 °C	4	0.0000052	0.0000488	0.0000067	0.0120032	0.995526	1161.56	± 10.50	99.84	3.21	106	± 1060

Information on Analysis	Results	40(r)/39(k)	± 2σ	Age (Ma)	± 2σ	MSWD	39Ar(k) (%,n)	K/Ca	± 2σ
Sample = EAF22MSC	**Age Plateau**	82.76441	± 0.20423	1159.76	± 4.62	1.54	83.21	30	± 59
Material = msc			± 0.25%		± 0.40%	19%	5		
Location = Laser			Full External Error		± 9.44	2.41	2σ Confidence Limit		
Analyst = Fred Jourdan			Analytical Error		± 2.11	1.2390	Error Magnification		
Project = ALBANYFRASER_ES12									
Mass Discrimination Law = POW	**Total Fusion Age**	82.89389	± 0.16860	1161.10	± 4.47		12	73	± 58
Irradiation = I19t40h			± 0.20%		± 0.38%				
J = 0.01086400 ± 0.00002607			Full External Error		± 9.38				
Hb3gr = 1081.000 ± 1.081 Ma			Analytical Error		± 1.74				
MDF = 1.003122 ± 0.07									

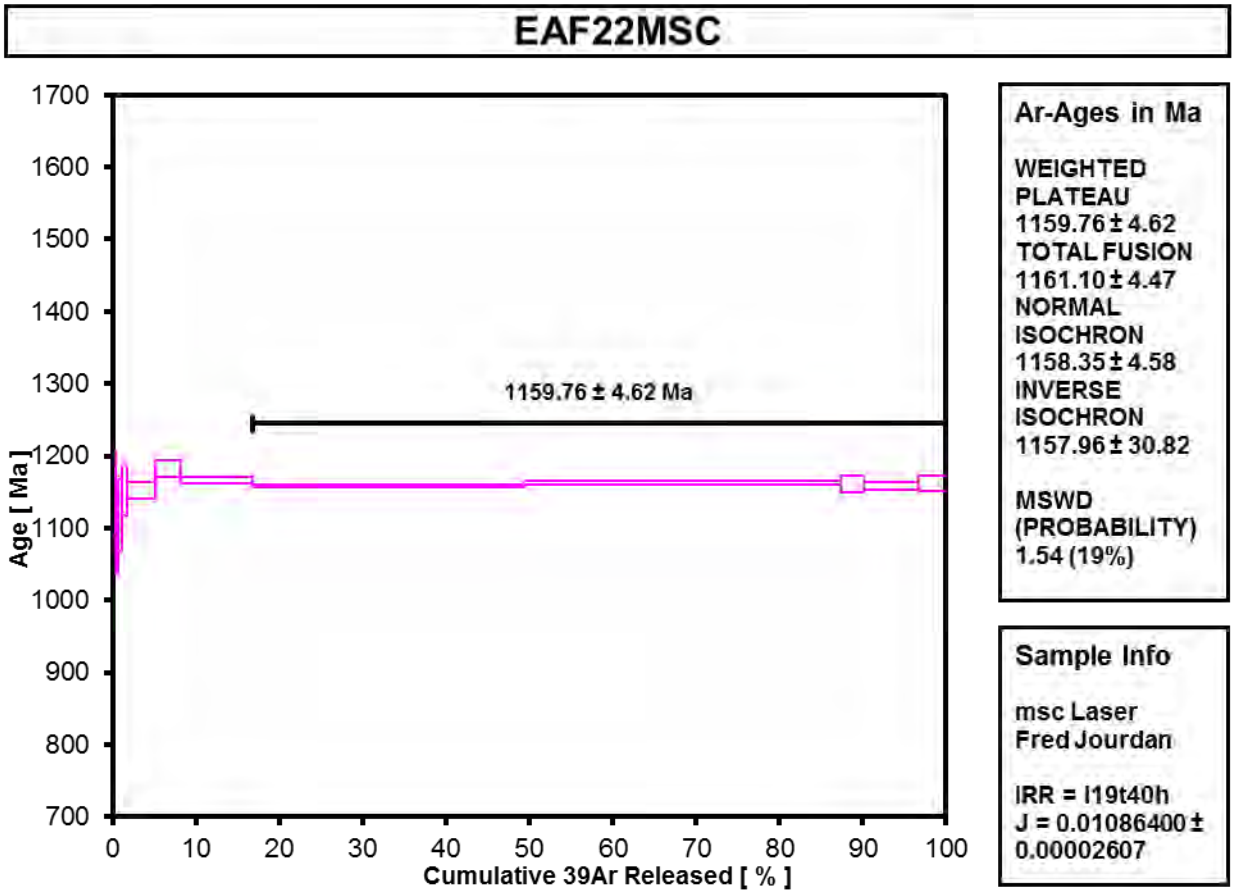

Figure A4.2-12 EAF022 Muscovite

Table A4.2-13 EAF018 Biotite

Incremental Heating			36Ar(a) [V]	37Ar(ca) [V]	38Ar(cl) [V]	39Ar(k) [V]	40Ar(r) [V]	Age (Ma)	± 2σ	40Ar(r) (%)	39Ar(k) (%)	K/Ca	± 2σ
5M36200D	58 °C		0.0000186	0.0001391	0.0000196	0.0071248	0.566172	1124.62	± 12.11	99.03	3.20	22	± 35
5M36201D	58 °C	4	0.0000160	0.0001165	0.0000179	0.0120675	1.002097	1161.91	± 7.74	99.53	5.42	45	± 73
5M36202D	59 °C	4	0.0000269	0.0001552	0.0001876	0.0912802	7.635052	1168.13	± 2.54	99.89	41.00	253	± 343
5M36204D	59 °C	4	0.0000084	0.0000582	0.0001395	0.0732728	6.110718	1165.58	± 2.81	99.96	32.91	541	± 1707
5M36205D	60 °C	4	0.0000145	0.0000848	0.0000571	0.0384102	3.204636	1165.94	± 4.56	99.86	17.25	195	± 545
5M36206D	61 °C	4	0.0000051	0.0000028	0.0000049	0.0004884	0.042180	1195.91	± 126.91	103.77	0.22	74	± 5641

Information on Analysis	Results	40(r)/39(k)	± 2σ	Age (Ma)	± 2σ	MSWD	39Ar(k) (%,n)	K/Ca	± 2σ
Sample = EAF018BIO	**Age Plateau**	83.49514	± 0.16497	1166.59	± 3.68	0.93	96.80	57	± 71
Material = bio			± 0.20%		± 0.32%	44%	5		
Location = Laser			Full External Error		± 10.82	2.41	2σ Confidence Limit		
Analyst = Fred Jourdan			Analytical Error		± 1.70	1.0000	Error Magnification		
Project = ALBANYFRASER_ES12									
Mass Discrimination Law = POW	**Total Fusion Age**	83.36565	± 0.16701	1165.26	± 3.69		6	174	± 163
Irradiation = I19t40h			± 0.20%		± 0.32%				
J = 0.01085500 ± 0.00002062			Full External Error		± 10.82				
WA1ms = 2613.000 ± 2.352 Ma			Analytical Error		± 1.72				
MDF = 1.003122 ± 0.07									

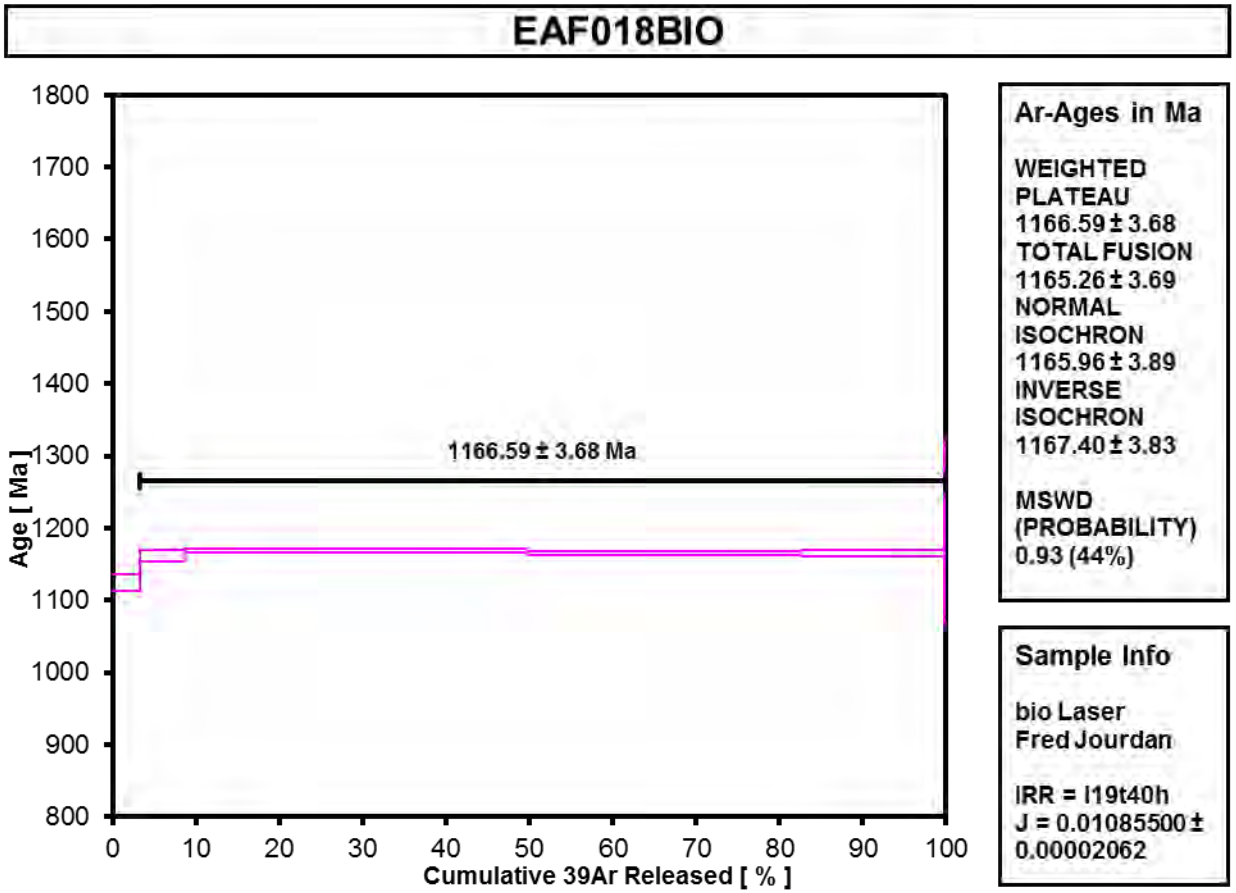

Figure A4.2-13 EAF018 Biotite

Table A4.2-14 EAF020-2 Biotite

Relative Abundances			36Ar [V]	%1σ	37Ar [V]	%1σ	38Ar [V]	%1σ	39Ar [V]	%1σ	40Ar [V]	%1σ	40(r)/ 39(k)	%1σ
5M36189D	58 °C		0.0002306	6.005	0.0000502	204.316	0.0001149	7.831	0.0064336	0.695	0.499459	0.090	66.92850	1.59299
5M36190D	58 °C		0.0001304	8.246	0.0000487	209.185	0.0009073	2.155	0.0652959	0.090	5.428117	0.042	82.53415	0.19171
5M36191D	59 °C	4	0.0000344	35.828	0.0000387	244.970	0.0015107	1.362	0.1068048	0.139	9.083185	0.047	84.94770	0.25931
5M36193D	59 °C	4	0.0000450	28.626	0.0000910	146.609	0.0013420	1.093	0.1005534	0.158	8.581045	0.042	85.20395	0.28963
5M36194D	60 °C	4	0.0000003	3893.556	0.0000796	125.328	0.0012193	2.285	0.0889620	0.128	7.558616	0.024	84.96297	0.23424
5M36195D	61 °C	4	0.0000137	78.627	0.0000423	263.043	0.0000190	49.122	0.0004793	4.257	0.042481	0.603	80.08403	15.08856

Information on Analysis and Constants Used in Calculations

Sample = EAF20-2BIO	Age Equations = Min et al. (2000)
Material = bio	Decay Constant 40K = 5.531 ± 0.013 E-10 1/a
Location = Laser	Decay Constant 39Ar = 2.940 ± 0.029 E-07 1/h
Analyst = Fred Jourdan	Decay Constant 37Ar = 8.230 ± 0.082 E-04 1/h
Project = ALBANYFRASER_ES12	Decay Constant 36Cl = 2.303 ± 0.046 E-06 1/a
Mass Discrimination Law = POW	Decay Constant 40K(EC,β^+) = 0.576 ± 0.002 E-10 1/a
Irradiation = I19t40h	Decay Constant 40K(β^-) = 4.955 ± 0.013 E-10 1/a
J = 0.01085500 ± 0.00002062	Atmospheric Ratio 40/36(a) = 298.56 ± 0.30
WA1ms = 2613.000 ± 2.352 Ma	Atmospheric Ratio 38/36(a) = 0.1869 ± 0.0002
Heating = 60 sec	Production Ratio 39/37(ca) = 0.000760 ± 0.000009
Isolation = 5.00 min	Production Ratio 38/37(ca) = 0.000023 ± 0.000002
Instrument = MAP-215-50	Production Ratio 36/37(ca) = 0.000270 ± 0.000002
Lithology = Undefined	Production Ratio 40/39(k) = 0.000730 ± 0.000091
Lat-Lon = Undefined - Undefined	Production Ratio 38/39(k) = 0.012400 ± 0.003968
Feature = Undefined	Production Ratio 36/38(cl) = 263.00 ± 13.15
MDF = 1.003122 ± 0.07	Scaling Ratio K/Ca = 0.430
	Abundance Ratio 40K/K = 1.1700 ± 0.0100 E-04
	Atomic Weight K = 39.0983 ± 0.0001 g

Relative Abundances		Age (Ma)	± 2σ (%)	40Ar(r) (%)	39Ar(k)	K/Ca	± 2σ
5M36189D	58 °C	987.44	18.11	86.21	1.75	55	± 225
5M36190D	58 °C	1156.67	1.98	99.28	17.72	577	± 2414
5M36191D	59 °C	1181.49	2.65	99.89	28.98	1186	± 5810
5M36193D	59 °C	1184.10	2.95	99.84	27.29	475	± 1394
5M36194D	60 °C	1181.64	2.39	100.00	24.14	481	± 1205
5M36195D	61 °C	1131.13	158.43	90.36	0.13	5	± 26

Table A4.2-14 (continued) EAF020-2 Biotite

Results	40(a)/36(a)	± 2σ	40(r)/39(k)	± 2σ	Age (Ma)	± 2σ	MSWD	39Ar(k) (%,n)	K/Ca	± 2σ
Age Plateau			85.02126	± 0.14904	1182.24	± 3.63	0.86	80.54	5	± 26
				± 0.18%		± 0.31%	46%	4		
				Full External Error		± 10.91	2.63	2σ Confidence Limit		
				Analytical Error		± 1.52	1.0000	Error Magnification		
Total Fusion Age			84.27277	± 0.13175	1174.58	± 3.55		6	17046	± 970023
				± 0.16%		± 0.30%				
				Full External Error		± 10.83				
				Analytical Error		± 1.35				
Normal Isochron	234.28	± 361.36	84.96266	± 0.20332	1181.64	± 3.90	1.39	80.54		
				± 0.24%		± 0.33%	25%	4		
				Full External Error		± 11.00	3.00	2σ Confidence Limit		
				Analytical Error		± 2.08	1.1803	Error Magnification		
							1	Number of Iterations		
							0.0000000001	Convergence		
Inverse Isochron Clustered Points	682.94	± 764.00	84.93325	± 0.24267	1181.34	± 4.12	0.98	80.54		
				± 0.29%		± 0.35%	38%	4		
				Full External Error		± 11.08	3.00	2σ Confidence Limit		
				Analytical Error		± 2.48	1.0000	Error Magnification		
							15	Number of Iterations		
							0.0000403583	Convergence		
							5%	Spreading Factor		

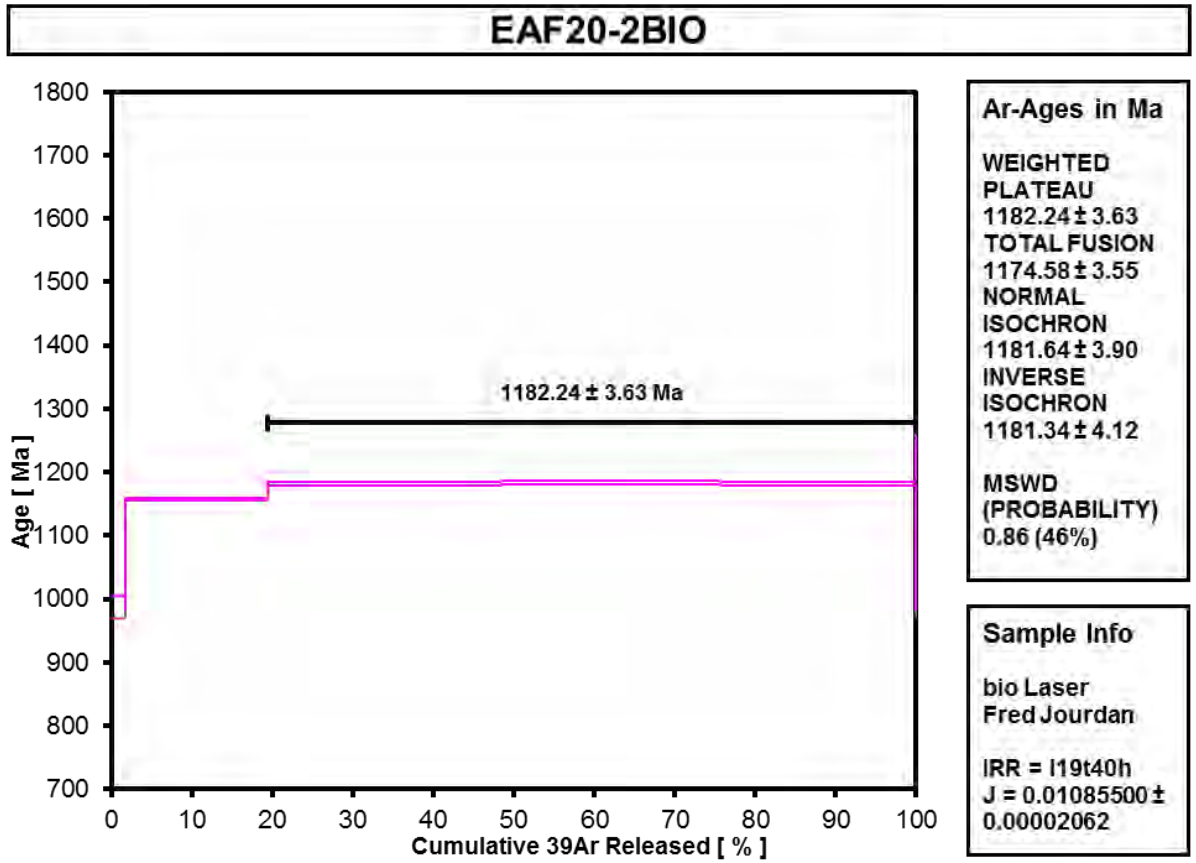

Figure A4.2-14 EAF020-2 Biotite

Table A4.2-15 EAF027 Muscovite

Incremental Heating			36Ar(a) [V]	37Ar(ca) [V]	38Ar(cl) [V]	39Ar(k) [V]	40Ar(r) [V]	Age (Ma)	± 2σ	40Ar(r) (%)	39Ar(k) (%)	K/Ca	± 2σ
5M36090D	58 °C		0.0000037	0.0000442	0.0000071	0.0006357	0.047738	1078.68	± 97.00	97.72	0.23	6	± 32
5M36092D	58 °C		0.0000003	0.0000552	0.0000019	0.0003614	0.027331	1084.38	± 148.96	99.67	0.13	3	± 9
5M36093D	59 °C		0.0000048	0.0000709	0.0000014	0.0006486	0.053128	1150.93	± 94.28	97.38	0.23	4	± 10
5M36094D	59 °C		0.0000172	0.0000567	0.0000000	0.0012962	0.117668	1240.83	± 59.81	104.55	0.46	10	± 38
5M36095D	59 °C	4	0.0000066	0.0001665	0.0000000	0.0013204	0.109768	1163.56	± 46.72	98.24	0.47	3	± 4
5M36097D	59 °C	4	0.0000001	0.0002241	0.0000068	0.0013907	0.118291	1183.37	± 42.66	100.03	0.49	3	± 2
5M36098D	59 °C	4	0.0000042	0.0001498	0.0000074	0.0038333	0.323654	1176.93	± 21.37	99.61	1.36	11	± 16
5M36099D~	60 °C	4	0.0000543	0.0021835	0.0000000	0.1795091	14.744554	1153.28	± 2.44	99.89	63.66	35	± 5
5M36100D	61 °C	4	0.0000098	0.0000815	0.0000000	0.0308837	2.548137	1157.11	± 5.44	99.88	10.95	163	± 412
5M36102D	63 °C	4	0.0000153	0.0000935	0.0000000	0.0519111	4.259996	1152.50	± 8.58	99.89	18.41	239	± 428
5M36103D	66 °C	4	0.0000041	0.0001649	0.0000000	0.0097816	0.813571	1163.99	± 11.50	99.85	3.47	26	± 29
5M36104D	67 °C	4	0.0000084	0.0001227	0.0000041	0.0004088	0.033454	1150.15	± 151.00	93.05	0.14	1	± 2

Information on Analysis	Results	40(r)/39(k)	± 2σ	Age (Ma)	± 2σ	MSWD	39Ar(k) (%,n)	K/Ca	± 2σ
Sample = EAF27MSC	**Age Plateau**	82.25326	± 0.25569	1154.47	± 4.88	1.59	98.96	2	± 8
Material = msc			± 0.31%		± 0.42%	13%	8		
Location = Laser			Full External Error		± 9.54	2.07	2σ Confidence Limit		
Analyst = Fred Jourdan			Analytical Error		± 2.65	1.2628	Error Magnification		
Project = ALBANYFRASER_ES12									
Mass Discrimination Law = POW	**Total Fusion Age**	82.26558	± 0.23316	1154.60	± 4.76		12	65	± 24
Irradiation = I19t40h			± 0.28%		± 0.41%				
J = 0.01086400 ± 0.00002607			Full External Error		± 9.48				
Hb3gr = 1081.000 ± 1.081 Ma			Analytical Error		± 2.42				
MDF = 1.003122 ± 0.07									

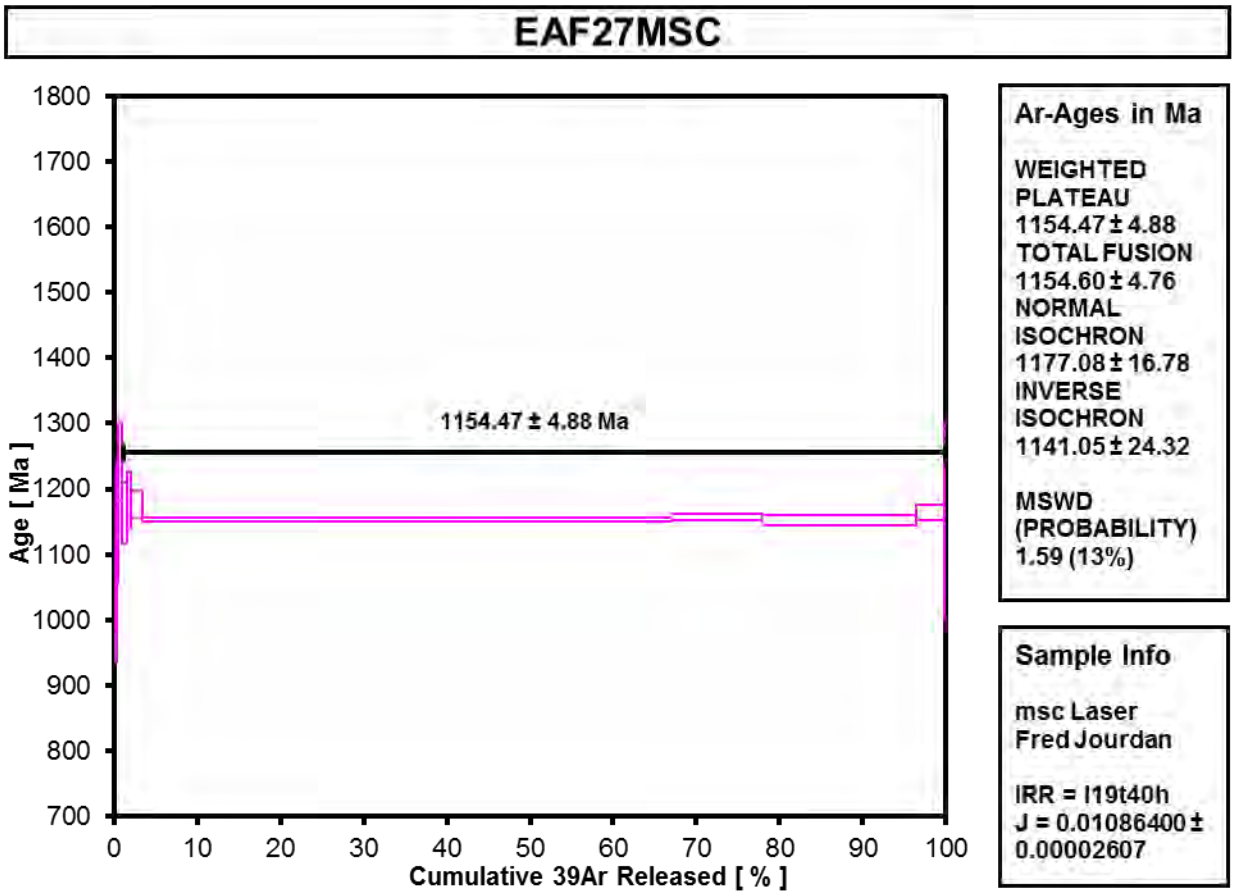

Figure A4.2-15 EAF027 Muscovite

Table A4.2-16 EAF029 Biotite

Incremental Heating			36Ar(a) [V]	37Ar(ca) [V]	38Ar(cl) [V]	39Ar(k) [V]	40Ar(r) [V]	Age ± 2σ (Ma)	40Ar(r) (%)	39Ar(k) (%)	K/Ca ± 2σ
5M36472D	58 °C		0.0000377	0.0001023	0.0000246	0.0103082	0.729392	1030.46 ± 8.61	98.48	4.34	43 ± 110
5M36473D	59 °C		0.0000693	0.0002138	0.0000646	0.0508346	4.037909	1124.27 ± 3.61	99.49	21.43	102 ± 152
5M36475D	59 °C	4	0.0000279	0.0003150	0.0001078	0.0943911	7.782825	1155.83 ± 3.55	99.89	39.78	129 ± 105
5M36476D	60 °C	4	0.0000382	0.0003298	0.0001251	0.0806652	6.673109	1158.66 ± 2.83	99.83	34.00	105 ± 86
5M36477D	61 °C	4	0.0000006	0.0001865	0.0000045	0.0006000	0.048935	1146.50 ± 102.77	99.61	0.25	1 ± 2
5M36478D	63 °C	4	0.0000070	0.0002891	0.0000062	0.0004600	0.035134	1091.87 ± 145.35	94.37	0.19	1 ± 1

Information on Analysis	Results	40(r)/39(k)	± 2σ	Age (Ma)	± 2σ	MSWD	39Ar(k) (%,n)	K/Ca	± 2σ
Sample = EAF029BIO	**Age Plateau**	82.61768	± 0.21356	1157.54	± 3.93	0.82	74.23	1	± 1
Material = bio			± 0.26%		± 0.34%	48%	4		
Location = Laser			Full External Error		± 10.85	2.63	2σ Confidence Limit		
Analyst = Fred Jourdan			Analytical Error		± 2.21	1.0000	Error Magnification		
Project = ALBANYFRASER_ES12									
Mass Discrimination Law = POW	**Total Fusion Age**	81.37642	± 0.18640	1144.65	± 3.76		6	71	± 34
Irradiation = I19t40h			± 0.23%		± 0.33%				
J = 0.01085500 ± 0.00002062			Full External Error		± 10.71				
WA1ms = 2613.000 ± 2.352 Ma			Analytical Error		± 1.94				
MDF = 1.00323 ± 0.06									

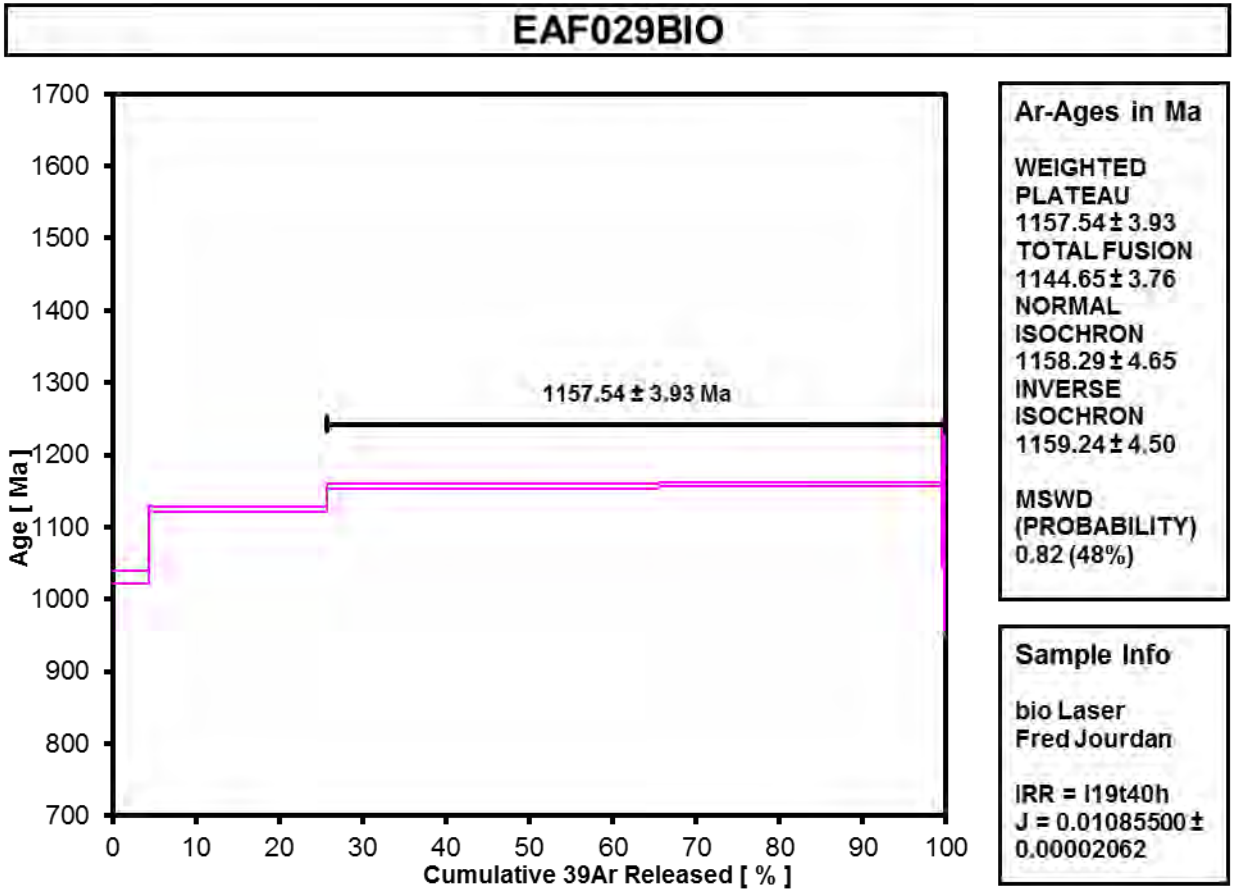

Figure A4.2-16 EAF029 Biotite

Table A4.2-17 EAF030 Hornblende

Incremental Heating			36Ar(a) [V]	37Ar(ca) [V]	38Ar(cl) [V]	39Ar(k) [V]	40Ar(r) [V]	Age (Ma)	± 2σ	40Ar(r) (%)	39Ar(k) (%)	K/Ca	± 2σ
5M37304D	60.0 %		0.0000035	0.0023918	0.0000071	0.0004897	0.0497005	1334.62	± 147.83	97.95	1.08	0.088	± 0.025
5M37305D	60.5 %		0.0000222	0.0356221	0.0000375	0.0075445	0.7424026	1305.67	± 12.28	99.11	16.62	0.091	± 0.005
5M37306D	61.0 %	4	0.0000037	0.0943888	0.0000869	0.0198469	1.8807238	1270.93	± 6.57	99.94	43.73	0.090	± 0.005
5M37308D	61.5 %	4	0.0000050	0.0483220	0.0000526	0.0101037	0.9519855	1265.72	± 13.24	99.84	22.26	0.090	± 0.005
5M37309D	62.0 %	4	0.0000064	0.0226169	0.0000081	0.0045696	0.4324301	1269.68	± 19.19	100.44	10.07	0.087	± 0.006
5M37310D	62.5 %	4	0.0000011	0.0124589	0.0000090	0.0026090	0.2492856	1278.50	± 25.33	100.13	5.75	0.090	± 0.009
5M37311D	63.0 %	4	0.0000009	0.0012343	0.0000028	0.0002258	0.0206962	1240.74	± 345.84	98.74	0.50	0.079	± 0.040

Information on Analysis	Results	40(r)/39(k)	± 2σ	Age (Ma)	± 2σ	MSWD	39Ar(k) (%,n)	K/Ca	± 2σ
Sample = EAF0030HBL	**Age Plateau**	94.69351	± 0.56973	1270.28	± 6.54	0.24	82.30	0.089	± 0.003
Material = Hbl	**Overestimated Error**		± 0.60%		± 0.52%	91%	5		
Location = Laser			Full External Error		± 10.26	2.41	2σ Confidence Limit		
Analyst = Fred Jourdan			Analytical Error		± 5.49	1.0000	Error Magnification		
Project = ALBANYFRASER_ES12									
Mass Discrimination Law = POW	**Total Fusion Age**	95.33599	± 0.59444	1276.46	± 6.73		7	0.090	± 0.003
Irradiation = I19t40h			± 0.62%		± 0.53%				
J = 0.01075940 ± 0.00002098			Full External Error		± 10.41				
FCs = 28.294 ± 0.031 Ma			Analytical Error		± 5.71				
MDF = 1.003135 ± 0.06									

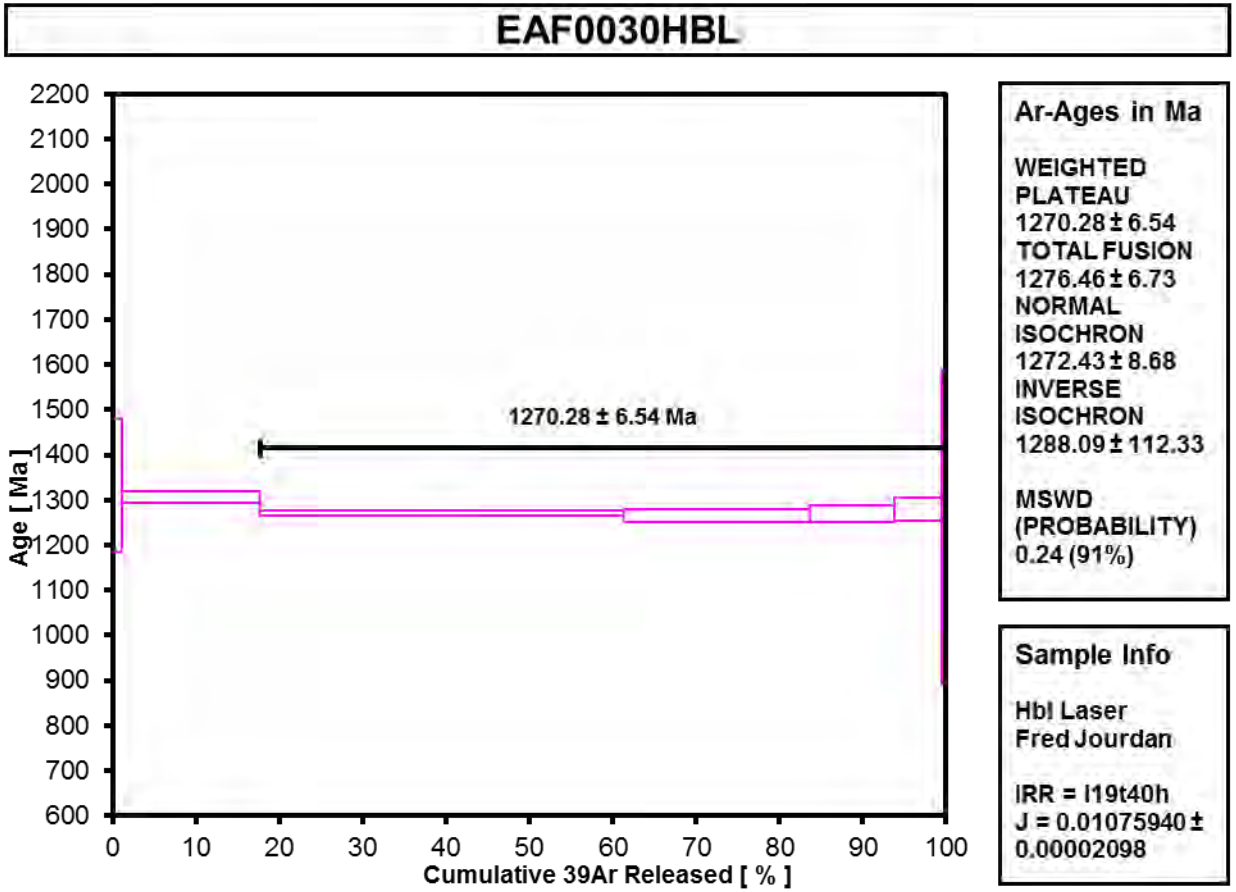

Figure A4.2-17 EAF030 Hornblende

Table A4.2-18 EAF035 Biotite

Incremental Heating			36Ar(a) [V]	37Ar(ca) [V]	38Ar(cl) [V]	39Ar(k) [V]	40Ar(r) [V]	Age (Ma)	± 2σ	40Ar(r) (%)	39Ar(k) (%)	K/Ca	± 2σ
5M36539D	58 °C		0.0000062	0.0000260	0.0000026	0.0011787	0.088125	1074.37	± 49.24	97.94	0.71	20	± 209
5M36541D	58 °C		0.0000236	0.0001772	0.0000052	0.0115327	0.958416	1162.57	± 8.10	99.27	6.96	28	± 55
5M36542D	59 °C	4	0.0000173	0.0002970	0.0000690	0.0504429	4.446499	1213.89	± 5.53	99.88	30.42	73	± 66
5M36544D	59 °C	4	0.0000054	0.0001342	0.0000682	0.0771256	6.740060	1206.26	± 4.65	99.98	46.52	247	± 541
5M36545D	60 °C	4	0.0000147	0.0001645	0.0000267	0.0252184	2.231517	1217.28	± 23.26	100.20	15.21	66	± 156
5M36546D	61 °C	4	0.0000030	0.0001369	0.0000045	0.0003073	0.028541	1260.67	± 169.57	103.26	0.19	1	± 2

Information on Analysis	Results	40(r)/39(k)	± 2σ	Age (Ma)	± 2σ	MSWD	39Ar(k) (%,n)	K/Ca	± 2σ
Sample = EAF035BIO	**Age Plateau**	87.72297	± 0.46269	1209.61	± 5.73	1.75	92.33	1	± 4
Material = bio			± 0.53%		± 0.47%	15%	4		
Location = Laser			Full External Error		± 9.58	2.63	2σ Confidence Limit		
Analyst = Fred Jourdan			Analytical Error		± 4.65	1.3234	Error Magnification		
Project = ALBANYFRASER_ES12									
Mass Discrimination Law = POW	**Total Fusion Age**	87.41052	± 0.44898	1206.46	± 5.62		6	356	± 1410
Irradiation = I19t40h			± 0.51%		± 0.47%				
J = 0.01085500 ± 0.00002062			Full External Error		± 9.50				
FCs = 28.294 ± 0.037 Ma			Analytical Error		± 4.52				
MDF = 1.003231 ± 0.06									

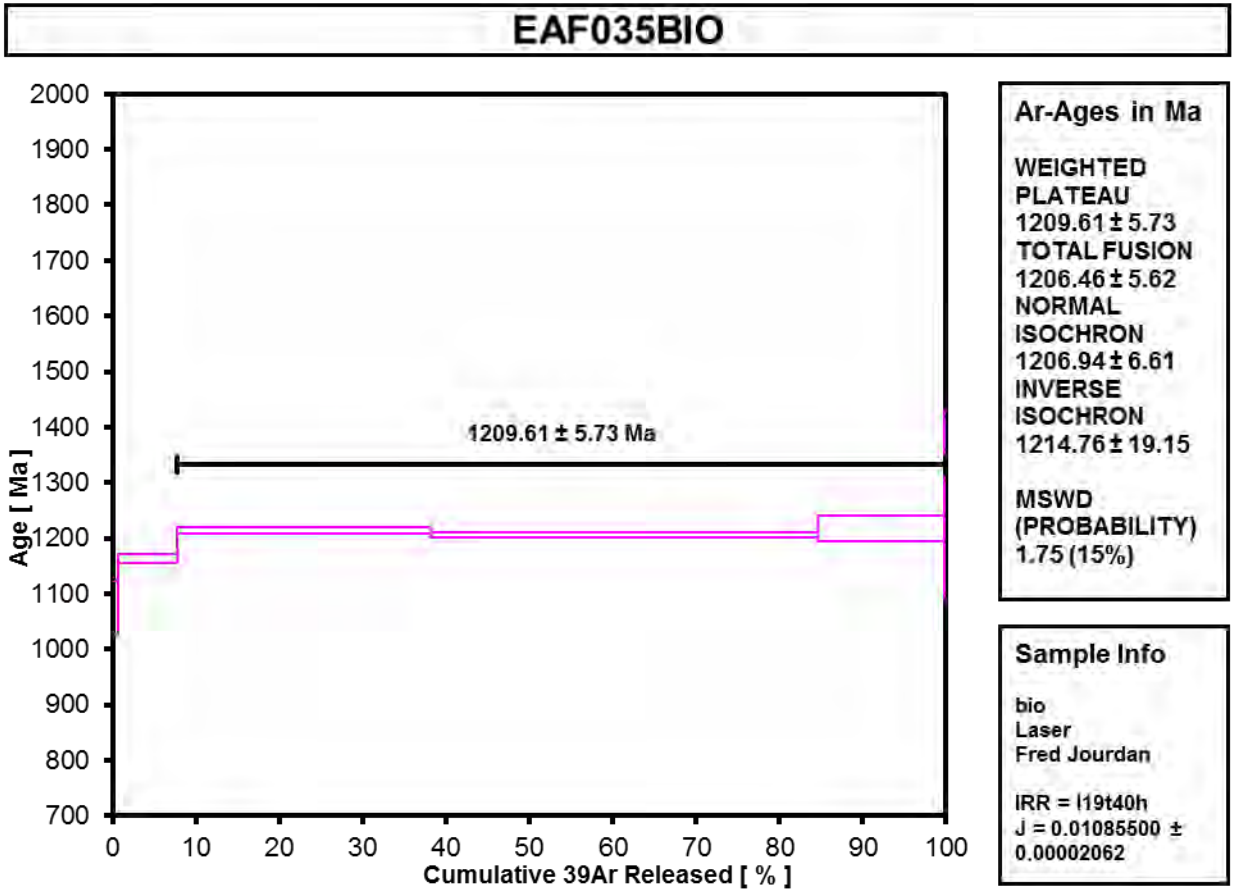

Figure A4.2-18 EAF035 Biotite

Table A4.2-19 EAF035 Hornblende

Incremental Heating			36Ar(a) [V]	37Ar(ca) [V]	38Ar(cl) [V]	39Ar(k) [V]	40Ar(r) [V]	Age (Ma)	± 2σ	40Ar(r) (%)	39Ar(k) (%)	K/Ca	± 2σ
5M37406D	60 °C		0.0000101	0.0179534	0.0000884	0.0082300	0.769350	1266.60	± 8.96	99.61	6.54	0.197	± 0.018
5M37407D	61 °C	4	0.0000229	0.0755178	0.0003436	0.0354484	3.230199	1243.48	± 5.13	99.79	28.19	0.202	± 0.011
5M37408D	61 °C	4	0.0000096	0.0553750	0.0002542	0.0259712	2.363320	1242.24	± 7.18	100.12	20.65	0.202	± 0.012
5M37410D	62 °C	4	0.0000091	0.0550686	0.0002804	0.0259778	2.364641	1242.51	± 5.55	100.11	20.66	0.203	± 0.013
5M37411D	62 °C	4	0.0000109	0.0284018	0.0001087	0.0135383	1.247011	1253.19	± 6.92	100.26	10.77	0.205	± 0.014
5M37412D	63 °C	4	0.0000009	0.0340474	0.0001583	0.0160176	1.467384	1248.28	± 7.07	99.98	12.74	0.202	± 0.014
5M37413D	63 °C	4	0.0000047	0.0006889	0.0000050	0.0005754	0.053313	1258.44	± 85.93	102.68	0.46	0.359	± 0.614

Information on Analysis	Results	40(r)/39(k)	± 2σ	Age (Ma)	± 2σ	MSWD	39Ar(k) (%,n)	K/Ca	± 2σ
Sample = EAF035HBL	**Age Plateau**	91.31227	± 0.35942	1245.34	± 4.92	1.64	93.46	0.203	± 0.006
Material = hbl			± 0.39%		± 0.40%	14%	6		
Location = Laser			Full External Error		± 9.28	2.26	2σ Confidence Limit		
Analyst = Fred Jourdan			Analytical Error		± 3.54	1.2820	Error Magnification		
Project = ALBANYFRASER_ES12									
Mass Discrimination Law = POW	**Total Fusion Age**	91.40697	± 0.27763	1246.27	± 4.38		7	0.202	± 0.005
Irradiation = I19t40h			± 0.30%		± 0.35%				
J = 0.01085500 ± 0.00002062			Full External Error		± 9.01				
FCs = 28.294 ± 0.037 Ma			Analytical Error		± 2.74				
MDF = 1.003236 ± 0.05									

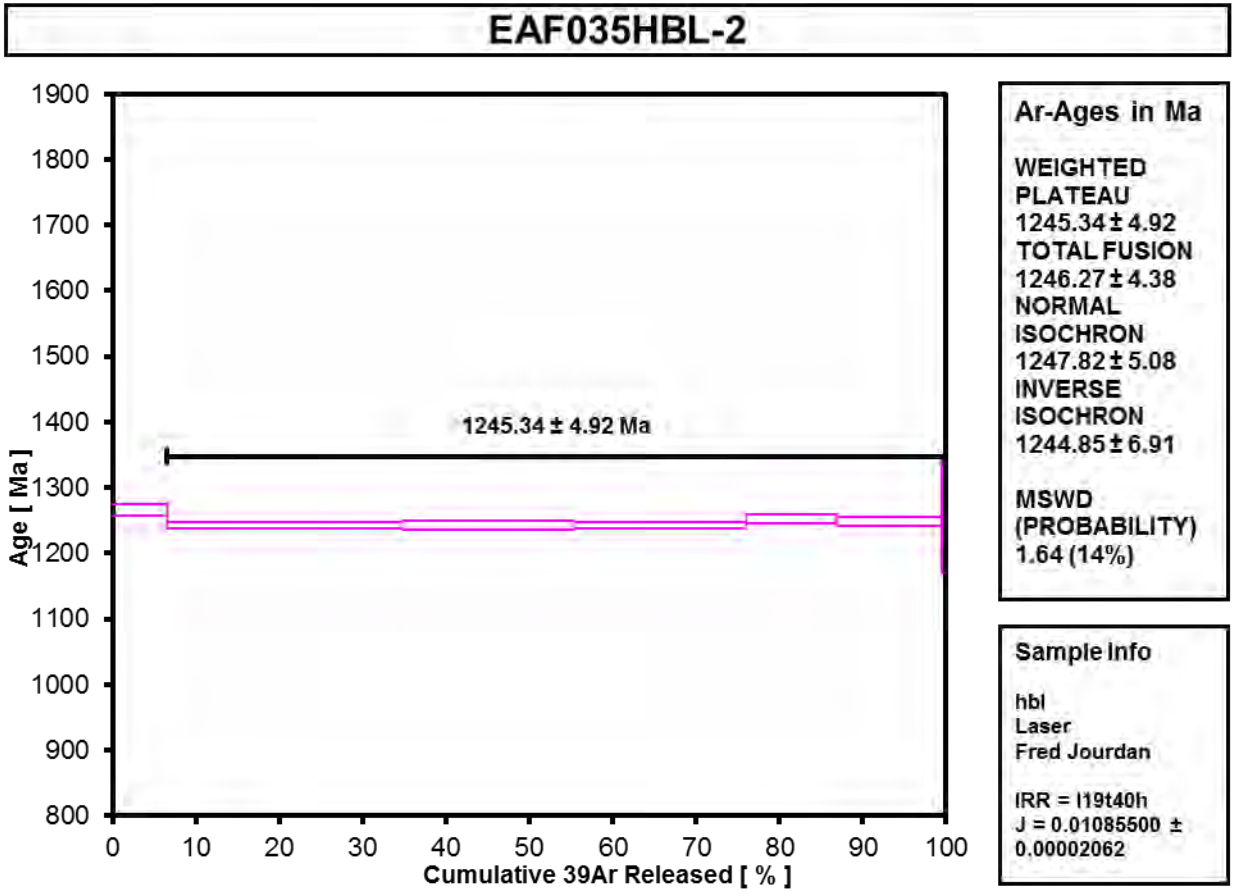

Figure A4.2-19 EAF035 Hornblende

Table A4.2-20 EAF036 Hornblende 1

Incremental Heating			36Ar(a) [V]	37Ar(ca) [V]	38Ar(cl) [V]	39Ar(k) [V]	40Ar(r) [V]	Age (Ma)	± 2σ	40Ar(r) (%)	39Ar(k) (%)	K/Ca	± 2σ
5M37274D	60 °C	4	0.0000143	0.0002054	0.0000000	0.0001966	0.0233356	1488.18	± 482.12	122.47	0.32	0.412	± 1.677
5M37275D	60 °C	4	0.0000082	0.0116939	0.0000337	0.0048310	0.4200862	1194.13	± 23.12	100.59	7.80	0.178	± 0.015
5M37276D	61 °C	4	0.0000256	0.0447600	0.0001497	0.0168545	1.4620735	1192.03	± 6.61	100.52	27.22	0.162	± 0.009
5M37277D	61 °C	4	0.0000220	0.0512399	0.0001687	0.0199140	1.7318977	1194.26	± 7.50	100.38	32.16	0.167	± 0.009
5M37279D	62 °C	4	0.0000069	0.0397087	0.0001137	0.0152300	1.3155562	1188.32	± 7.26	100.16	24.60	0.165	± 0.009
5M37280D	62 °C	4	0.0000026	0.0104098	0.0000286	0.0041029	0.3530751	1185.05	± 27.57	99.78	6.63	0.169	± 0.016
5M37281D	63 °C	4	0.0000001	0.0015128	0.0000000	0.0007836	0.0679909	1192.28	± 123.69	100.04	1.27	0.223	± 0.158

Information on Analysis	Results	40(r)/39(k)	± 2σ	Age (Ma)	± 2σ	MSWD	39Ar(k) (%,n)	K/Ca	± 2σ
Sample = EAF0036HBL	**Age Plateau**	86.69118	± 0.39617	1191.47	± 5.24	0.48	100.00	0.166	± 0.005
Material = Hbl			± 0.46%		± 0.44%	82%	7		
Location = Laser			Full External Error		± 9.13	2.15	2σ Confidence Limit		
Analyst = Fred Jourdan			Analytical Error		± 3.99	1.0000	Error Magnification		
Project = ALBANYFRASER_ES12									
Mass Discrimination Law = POW	**Total Fusion Age**	86.80000	± 0.49128	1192.56	± 6.00		7	0.167	± 0.005
Irradiation = I19t40h			± 0.57%		± 0.50%				
J = 0.01075940 ± 0.00002098			Full External Error		± 9.59				
FCs = 28.294 ± 0.031 Ma			Analytical Error		± 4.94				
MDF = 1.003135 ± 0.06									

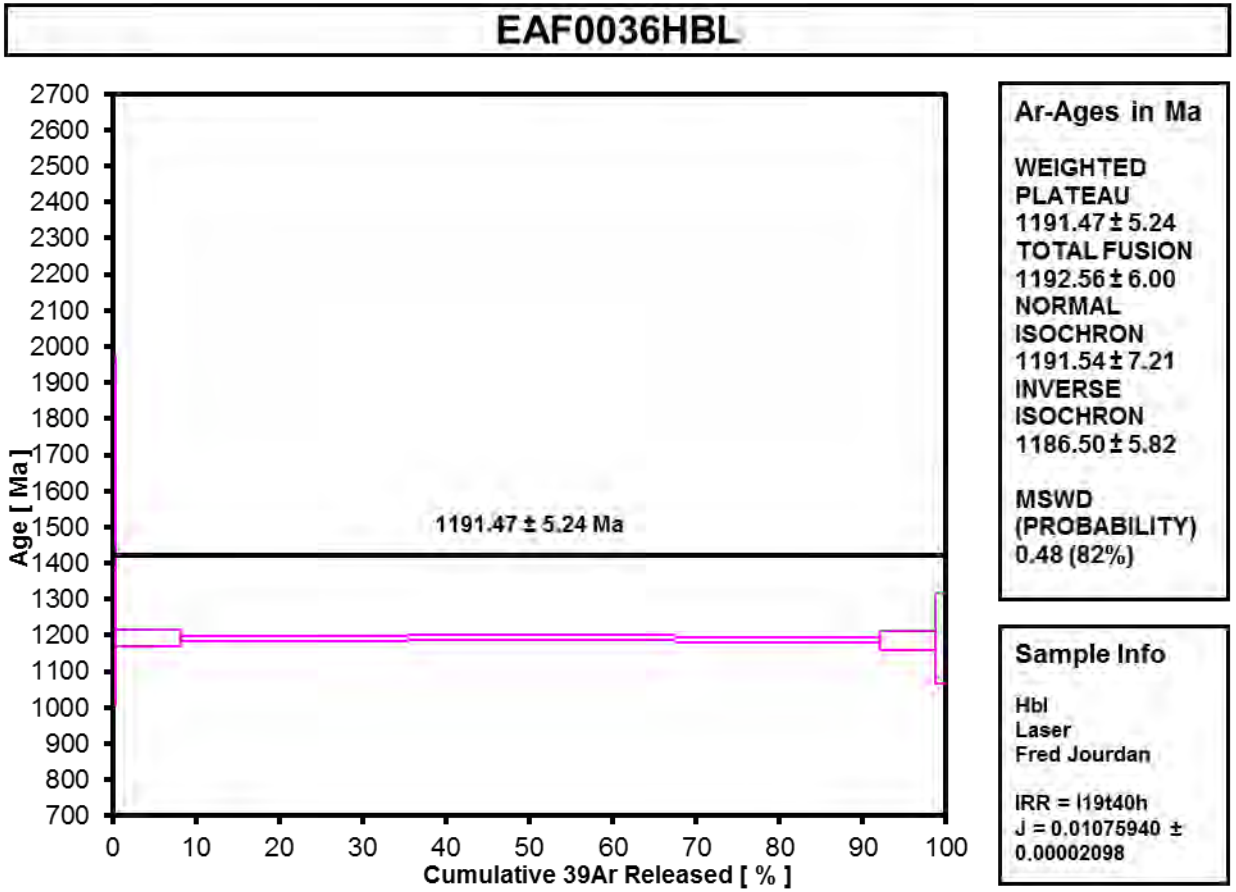

FigureA4.2-20 EAF036 Hornblende 1

Table A4.2-21 EAF036 Hornblende 2

Incremental Heating			36Ar(a) [V]	37Ar(ca) [V]	38Ar(cl) [V]	39Ar(k) [V]	40Ar(r) [V]	Age (Ma)	± 2σ	40Ar(r) (%)	39Ar(k) (%)	K/Ca	± 2σ
5M37981D	61 °C	4	0.0000209	0.0020079	0.0000116	0.0011125	0.0941905	1170.94	± 91.50	93.79	0.99	0.238	± 0.339
5M37982D	61 °C	4	0.0000126	0.0153462	0.0000551	0.0060523	0.5187852	1181.64	± 12.53	99.28	5.40	0.170	± 0.030
5M37984D	62 °C	4	0.0000145	0.0287395	0.0001058	0.0107844	0.9341016	1190.71	± 14.06	99.54	9.62	0.161	± 0.019
5M37985D	62 °C	4	0.0000401	0.0775702	0.0002668	0.0291800	2.5328652	1192.58	± 6.04	99.53	26.03	0.162	± 0.011
5M37986D	63 °C	4	0.0000258	0.0986486	0.0003274	0.0365924	3.1649183	1189.45	± 6.42	99.76	32.65	0.160	± 0.012
5M37987D	63 °C	4	0.0000200	0.0424297	0.0001400	0.0161310	1.3947968	1189.21	± 7.31	99.57	14.39	0.163	± 0.018
5M37989D	64 °C	4	0.0000108	0.0373811	0.0000500	0.0059149	0.5117646	1189.76	± 12.88	99.37	5.28	0.068	± 0.007
5M37990D	64 °C	4	0.0000104	0.0120911	0.0000299	0.0041603	0.3585076	1186.24	± 19.49	99.14	3.71	0.148	± 0.029
5M37991D	65 °C	4	0.0000042	0.0034595	0.0000063	0.0017744	0.1553285	1199.97	± 43.36	99.20	1.58	0.221	± 0.158
5M37992D	65 °C	4	0.0000002	0.0009493	0.0000000	0.0003854	0.0330829	1182.94	± 183.54	100.19	0.34	0.175	± 0.488

Information on Analysis	Results	40(r)/39(k)	± 2σ	Age (Ma)	± 2σ	MSWD	39Ar(k) (%,n)	K/Ca	± 2σ
Sample = EAF0036HBL	**Age Plateau**	86.52788	± 0.32873	1189.82	± 4.75	0.35	100.00		
Material = Hbl			± 0.38%		± 0.40%	96%	10	0.118	± 0.031
Location = Laser			Full External Error		± 8.93	1.94	2σ Confidence Limit		
Analyst = Fred Jourdan			Analytical Error		± 3.31	1.0000	Error Magnification		
Project = ALBANYFRASER_ES12									
Mass Discrimination Law = POW	**Total Fusion Age**	86.52470	± 0.35683	1189.79	± 4.95				
Irradiation = I19t40h			± 0.41%		± 0.42%		10	0.152	± 0.006
J = 0.01075940 ± 0.00002098			Full External Error		± 9.04				
FCs = 28.294 ± 0.037 Ma			Analytical Error		± 3.60				
MDF = 1.003286 ± 0.06									

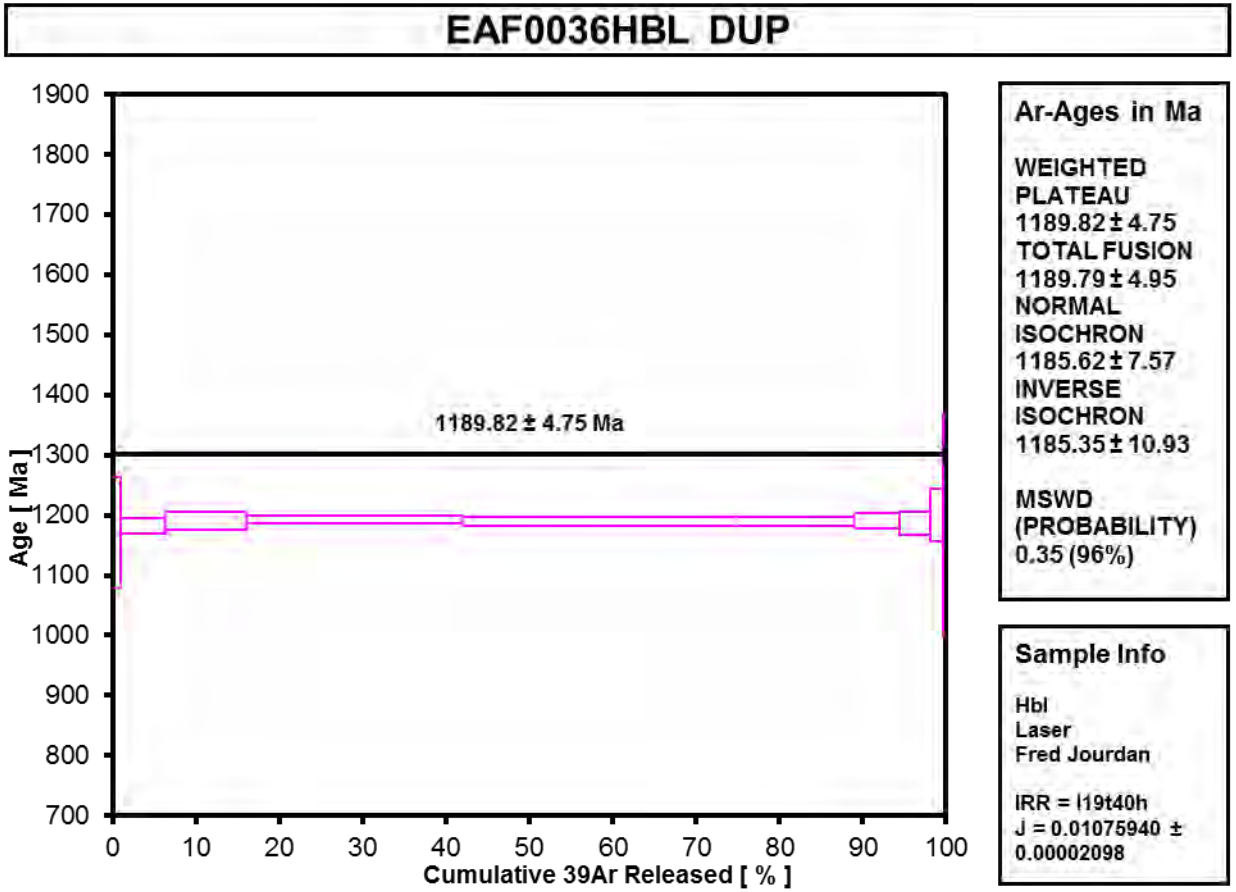

Figure A4.2-21 EAF036 Hornblende 2

Table A4.2-22 EAF036 Biotite 1

Incremental Heating			36Ar(a) [V]	37Ar(ca) [V]	38Ar(cl) [V]	39Ar(k) [V]	40Ar(r) [V]	Age (Ma)	± 2σ	40Ar(r) (%)	39Ar(k) (%)	K/Ca	± 2σ
5M36617D	59 °C		0.0000012	0.0000998	0.0000063	0.0016574	0.132933	1124.97	± 54.21	99.73	0.51	7.1	± 25.3
5M36619D	59 °C		0.0001207	0.0001370	0.0001035	0.0584732	5.184983	1211.31	± 4.39	99.31	17.98	183.5	± 476.3
5M36620D~	60 °C	4	0.0001035	0.0061645	0.0001470	0.2103509	19.020315	1228.64	± 5.83	99.84	64.68	14.7	± 1.8
5M36621D	61 °C	4	0.0000141	0.0000056	0.0000472	0.0503294	4.573316	1233.03	± 5.56	99.91	15.47	3830.5	
5M36622D	63 °C	4	0.0000038	0.0001478	0.0000000	0.0036603	0.330182	1226.50	± 26.93	100.34	1.13	10.7	± 21.8
5M36623D	65 °C	4	0.0000019	0.0000083	0.0000000	0.0007673	0.069344	1228.11	± 98.05	99.20	0.24	39.7	± 1708.0

Information on Analysis	Results	40(r)/39(k)	± 2σ	Age (Ma)	± 2σ	MSWD	39Ar(k) (%,n)	K/Ca	± 2σ
Sample = EAF036	**Age Plateau**	90.64418	± 0.40376	1230.83	± 5.29	0.43	81.51	14.5	± 2.4
Material = bio			± 0.45%		± 0.43%	73%	4		
Location = Laser			Full External Error		± 9.34	2.63	2σ Confidence Limit		
Analyst = Fred Jourdan			Analytical Error		± 3.98	1.0000	Error Magnification		
Project = ALBANYFRASER_ES12									
Mass Discrimination Law = POW	**Total Fusion Age**	90.12177	± 0.40176	1225.67	± 5.27		6	22.4	± 3.8
Irradiation = I19t40h			± 0.45%		± 0.43%				
J = 0.01075940 ± 0.00002098			Full External Error		± 9.31				
GA1550 = 99.738 ± 0.100 Ma			Analytical Error		± 3.97				
MDF = 1.003231 ± 0.06									

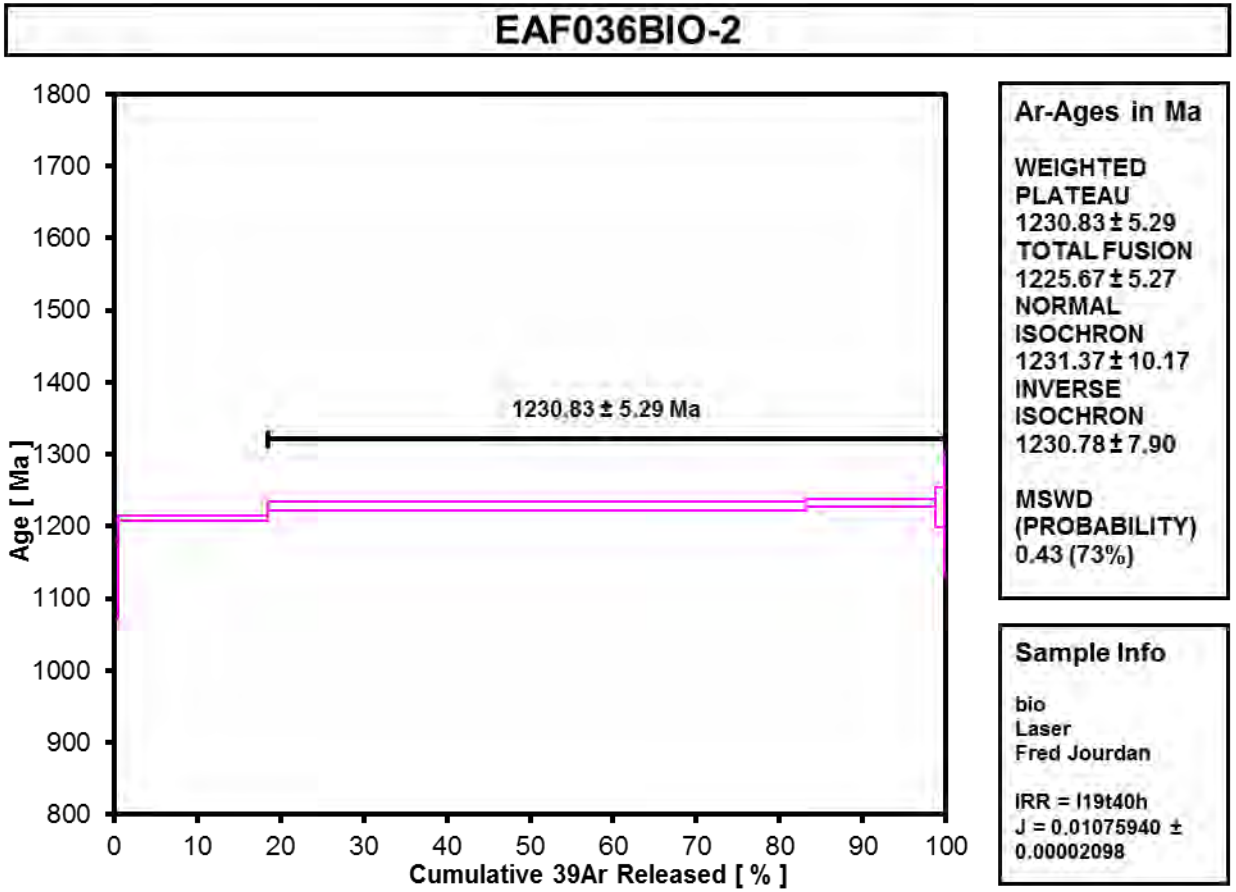

Figure A4.2-22 EAF036 Biotite 1

Table A4.2-23 EAF036 Biotite 2

Incremental Heating		36Ar(a) [V]	37Ar(ca) [V]	38Ar(cl) [V]	39Ar(k) [V]	40Ar(r) [V]	Age (Ma)	± 2σ	40Ar(r) (%)	39Ar(k) (%)	K/Ca	± 2σ
5M37961D	60 °C	0.0006324	0.0001103	0.0000033	0.0073295	0.557740	1081.53	± 15.54	74.71	2.27	28.6	± 459.6
5M37962D~	61 °C	0.0001879	0.0167645	0.0000862	0.1854389	16.650192	1222.37	± 3.57	99.66	57.48	4.8	± 1.0
5M37964D	61 °C	0.0000276	0.0006220	0.0001125	0.1213299	11.040832	1234.31	± 2.93	99.92	37.61	83.9	± 272.0
5M37965D	62 °C	0.0000071	0.0009276	0.0000070	0.0045110	0.411782	1237.12	± 19.61	99.48	1.40	2.1	± 4.8
5M37966D	63 °C	0.0000024	0.0008851	0.0000000	0.0032565	0.299601	1244.14	± 24.67	100.24	1.01	1.6	± 3.3
5M37967D	65 °C	0.0000032	0.0018381	0.0000036	0.0007498	0.071467	1276.20	± 110.60	101.35	0.23	0.2	± 0.2

Information on Analysis	Results	40(r)/39(k)	± 2σ	Age (Ma)	± 2σ	MSWD	39Ar(k) (%,n)	K/Ca	± 2σ
Sample = EAF0036BIO	**Age Plateau Cannot Calculate**								
Material = Bio									
Location = Laser									
Analyst = Fred Jourdan									
Project = ALBANYFRASER_ES12									
Mass Discrimination Law = POW	**Total Fusion Age**	89.98824	± 0.24231	1224.35	± 4.22		6	9.6	± 3.7
Irradiation = I19t40h			± 0.27%		± 0.34%				
J = 0.01075940 ± 0.00002098				Full External Error	± 8.82				
FCs = 28.294 ± 0.037 Ma				Analytical Error	± 2.40				
MDF = 1.003286 ± 0.06									

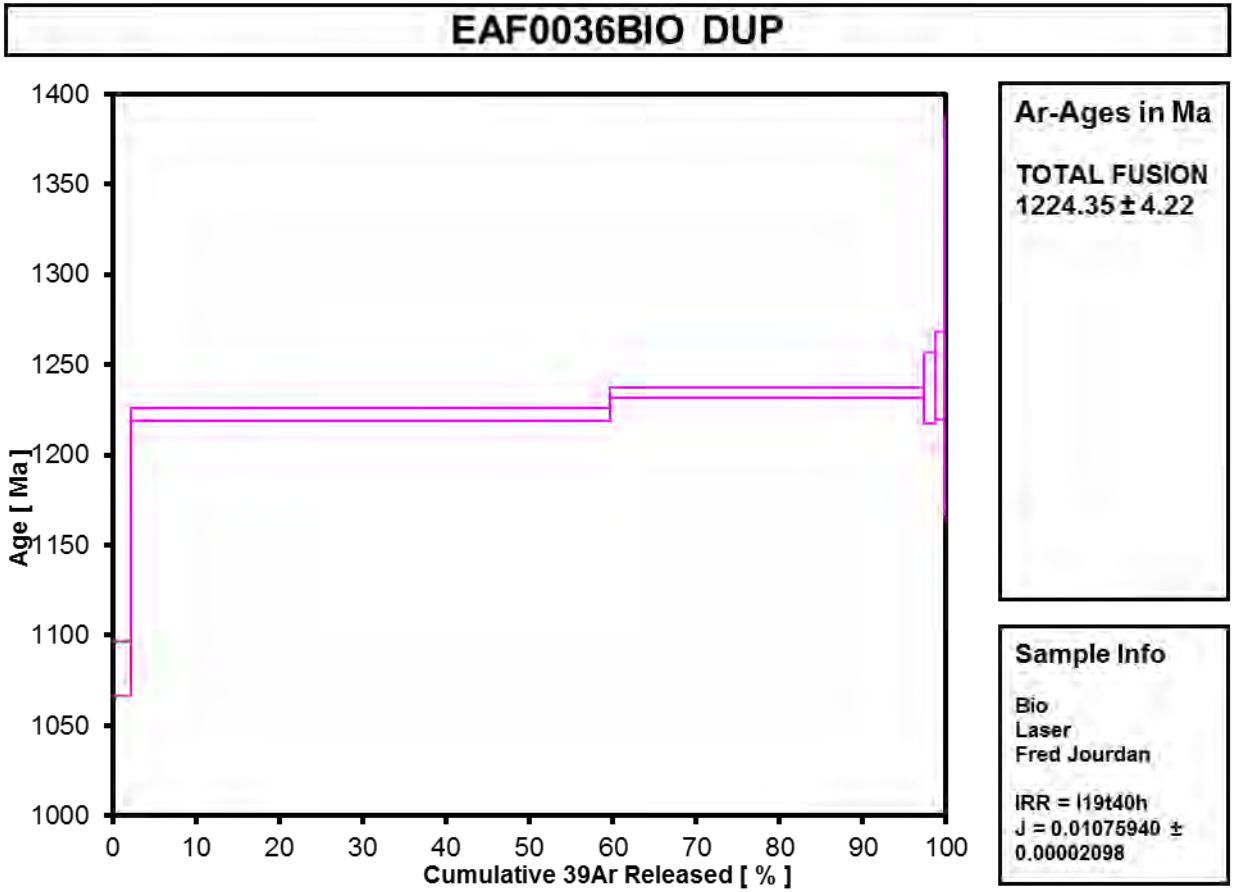

Figure A4.2-23 EAF036 Biotite 2

Table A4.2-24 EAF017 Hornblende 1

Incremental Heating			36Ar(a) [V]	37Ar(ca) [V]	38Ar(cl) [V]	39Ar(k) [V]	40Ar(r) [V]	Age ± 2σ (Ma)	40Ar(r) (%)	39Ar(k) (%)	K/Ca	± 2σ
5M37427D	60 °C		0.0000302	0.0008612	0.0000098	0.0003212	0.4643893	5089.99 ± 139.32	98.09	0.35	0.160	± 0.176
5M37428D	60 °C		0.0000340	0.0065444	0.0000424	0.0027419	0.2422631	1215.96 ± 21.32	95.98	2.97	0.180	± 0.027
5M37429D	61 °C	4	0.0000285	0.0702760	0.0004539	0.0290340	2.5014501	1193.78 ± 5.27	99.66	31.45	0.178	± 0.009
5M37430D	61 °C	4	0.0000041	0.0344296	0.0002356	0.0149175	1.2740685	1186.18 ± 9.75	99.90	16.16	0.186	± 0.011
5M37432D	62 °C	4	0.0000027	0.0743826	0.0004634	0.0319326	2.7439295	1191.48 ± 3.69	99.97	34.59	0.185	± 0.010
5M37433D	62 °C	4	0.0000070	0.0271205	0.0001770	0.0116593	1.0078828	1196.71 ± 9.24	100.21	12.63	0.185	± 0.013
5M37434D	63 °C		0.0000140	0.0039379	0.0000337	0.0016998	0.1529074	1231.90 ± 37.00	102.81	1.84	0.186	± 0.042

Information on Analysis	Results	40(r)/39(k)	± 2σ	Age (Ma)	± 2σ	MSWD	39Ar(k) (%,n)	K/Ca	± 2σ
Sample = EAF017HBL	**Age Plateau**	85.99462	± 0.27145	1192.15	± 4.31	1.00	94.84	0.183	± 0.005
Material = hbl			± 0.32%		± 0.36%	39%	4		
Location = Laser				Full External Error	± 8.71	2.63	2σ Confidence Limit		
Analyst = Fred Jourdan				Analytical Error	± 2.76	1.0000	Error Magnification		
Project = ALBANYFRASER_ES12									
Mass Discrimination Law = POW	**Total Fusion Age**	90.85938	± 0.31489	1240.87	± 4.62		7	0.182	± 0.005
Irradiation = I19t40h			± 0.35%		± 0.37%				
J = 0.01085500 ± 0.00002062				Full External Error	± 9.10				
FCs = 28.294 ± 0.037 Ma				Analytical Error	± 3.11				
MDF = 1.003236 ± 0.05									

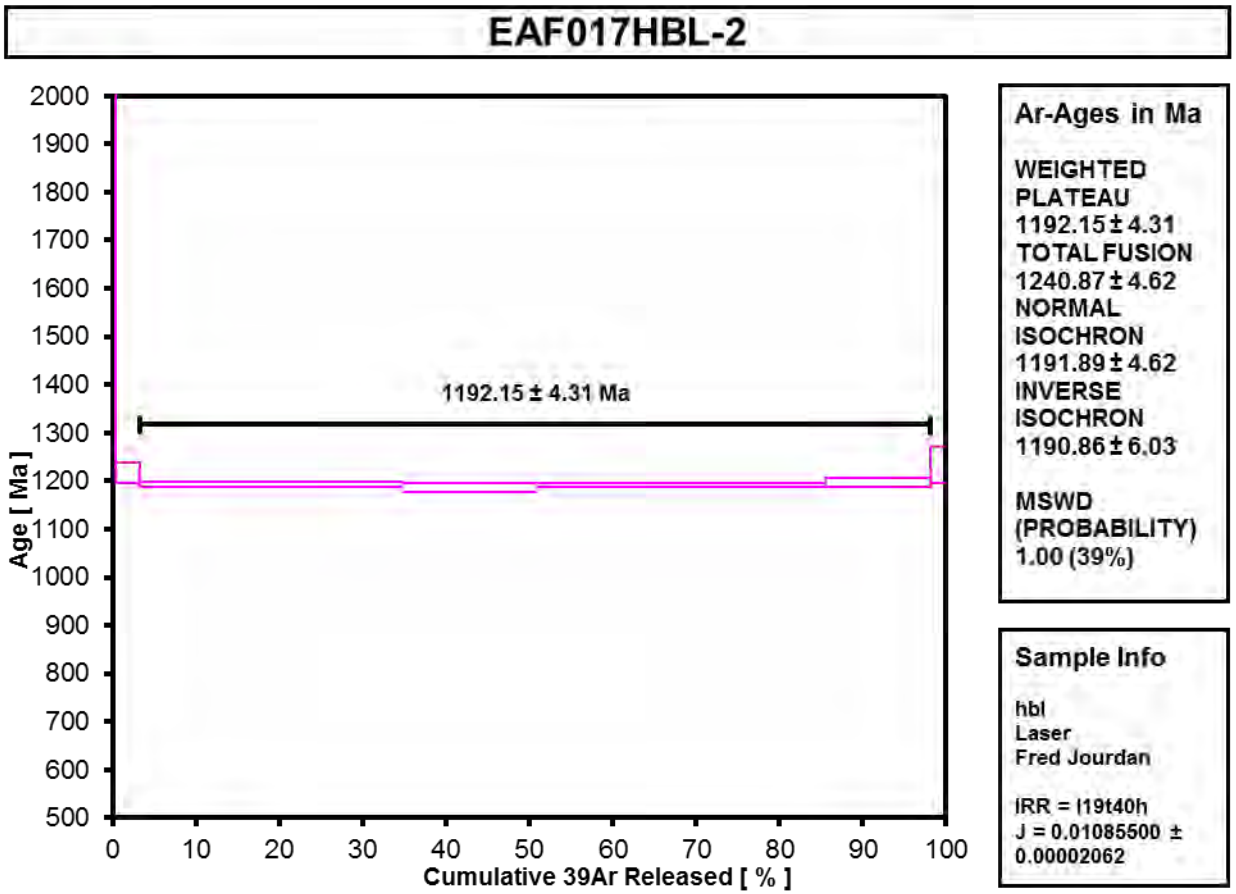

Figure A4.2-24 EAF017 Hornblende 1

Table A4.2-25 EAF017 Hornblende 2

Incremental Heating			36Ar(a) [V]	37Ar(ca) [V]	38Ar(cl) [V]	39Ar(k) [V]	40Ar(r) [V]	Age (Ma)	± 2σ	40Ar(r) (%)	39Ar(k) (%)	K/Ca	± 2σ
5M37972D	62 °C	4	0.0000075	0.0187035	0.0001164	0.0088984	0.7812242	1210.32	± 10.39	99.71	11.66	0.205	± 0.026
5M37973D	62 °C	4	0.0000103	0.0298398	0.0002044	0.0130991	1.1181412	1185.70	± 57.82	99.73	17.16	0.189	± 0.019
5M37975D	64 °C	4	0.0000014	0.0694365	0.0004417	0.0320094	2.7963198	1205.95	± 2.70	100.01	41.93	0.198	± 0.015
5M37976D	64 °C	4	0.0000000	0.0304955	0.0001730	0.0134670	1.1793943	1208.13	± 7.45	100.00	17.64	0.190	± 0.018
5M37977D	65 °C	4	0.0000030	0.0115601	0.0000704	0.0050209	0.4369039	1202.50	± 15.60	100.21	6.58	0.187	± 0.039
5M37978D	65 °C	4	0.0000035	0.0069922	0.0000443	0.0038448	0.3350880	1203.88	± 18.67	99.69	5.04	0.236	± 0.065

Information on Analysis	Results	40(r)/39(k)	± 2σ	Age (Ma)	± 2σ	MSWD	39Ar(k) (%,n)	K/Ca	± 2σ
Sample = EAF0017HBL	**Age Plateau**	87.39029	± 0.23971	1206.26	± 4.13	0.35	100.00	0.195	± 0.009
Material = Hbl			± 0.27%		± 0.34%	89%	6		
Location = Laser			Full External Error		± 8.69	2.26	2σ Confidence Limit		
Analyst = Fred Jourdan			Analytical Error		± 2.41	1.0000	Error Magnification		
Project = ALBANYFRASER_ES12									
Mass Discrimination Law = POW	**Total Fusion Age**	87.07248	± 1.01152	1203.06	± 10.74		6	0.197	± 0.009
Irradiation = I19t40h			± 1.16%		± 0.89%				
J = 0.01085500 ± 0.00002062			Full External Error		± 13.18				
FCs = 28.294 ± 0.037 Ma			Analytical Error		± 10.21				
MDF = 1.003286 ± 0.06									

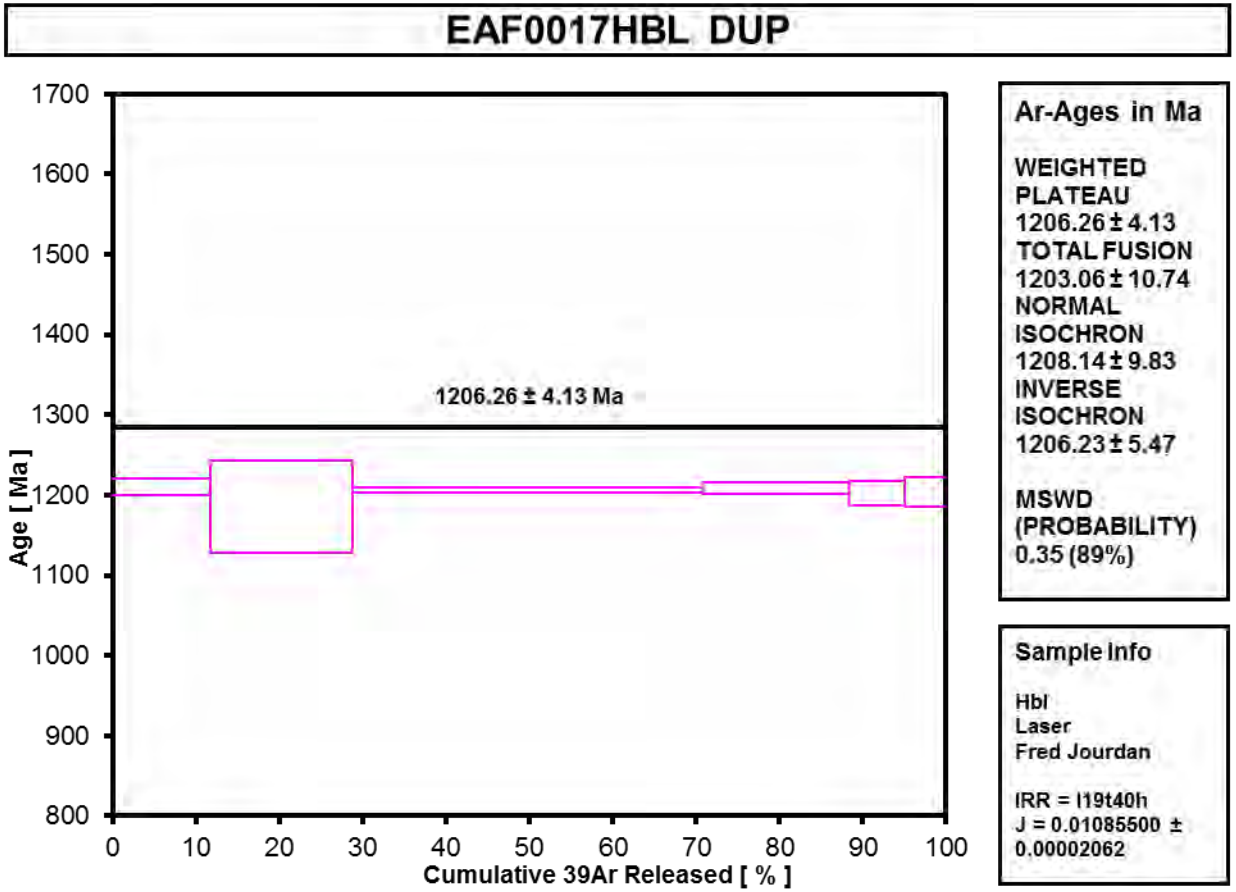

Figure A4.2-25 EAF017 Hornblende 2

Table A4.2-26 EAF017 Biotite 1

Incremental Heating			36Ar(a) [V]	37Ar(ca) [V]	38Ar(cl) [V]	39Ar(k) [V]	40Ar(r) [V]	Age (Ma)	± 2σ	40Ar(r) (%)	39Ar(k) (%)	K/Ca	± 2σ
5M37378D	59 °C		0.0000239	0.0004332	0.0000000	0.0005101	0.032023	939.58	± 122.68	81.79	0.34	0.5	± 0.8
5M37379D	59 °C		0.0000400	0.0009022	0.0000087	0.0047917	0.394417	1154.37	± 17.20	97.06	3.19	2.3	± 1.6
5M37380D	59 °C	4	0.0000316	0.0003900	0.0000365	0.0416661	3.772907	1237.82	± 3.97	99.75	27.74	45.9	± 69.6
5M37382D	60 °C	4	0.0000236	0.0007811	0.0000396	0.0340232	3.105695	1245.04	± 5.45	99.77	22.65	18.7	± 14.3
5M37383D	60 °C	4	0.0000233	0.0006064	0.0000300	0.0322619	2.939055	1243.24	± 5.50	99.76	21.48	22.9	± 21.4
5M37384D	60 °C	4	0.0000198	0.0007687	0.0000302	0.0241597	2.212616	1248.00	± 6.92	99.73	16.08	13.5	± 12.6
5M37385D	61 °C	4	0.0000142	0.0000831	0.0000087	0.0120631	1.106267	1249.22	± 8.78	99.62	8.03	62.4	± 477.8
5M37387D	61 °C	4	0.0000108	0.0003555	0.0000050	0.0004915	0.043842	1224.48	± 129.57	93.16	0.33	0.6	± 0.8
5M37388D	62 °C	4	0.0000082	0.0006920	0.0000008	0.0002570	0.022432	1205.09	± 217.35	90.20	0.17	0.2	± 0.2

Information on Analysis	Results	40(r)/39(k)	± 2σ	Age (Ma)	± 2σ	MSWD	39Ar(k) (%,n)	K/Ca	± 2σ
Sample = EAF017BIO	**Age Plateau**	91.03117	± 0.34723	1242.57	± 4.84	1.93	96.47	0.2	± 0.3
Material = bio			± 0.38%		± 0.39%	7%	7		
Location = Laser			Full External Error		± 9.22	2.15	2σ Confidence Limit		
Analyst = Fred Jourdan			Analytical Error		± 3.43	1.3890	Error Magnification		
Project = ALBANYFRASER_ES12									
Mass Discrimination Law = POW	**Total Fusion Age**	90.72600	± 0.25962	1239.55	± 4.27		9	12.9	± 4.9
Irradiation = I19t40h			± 0.29%		± 0.34%				
J = 0.01085500 ± 0.00002062			Full External Error		± 8.92				
FCs = 28.294 ± 0.037 Ma			Analytical Error		± 2.57				
MDF = 1.003236 ± 0.05									

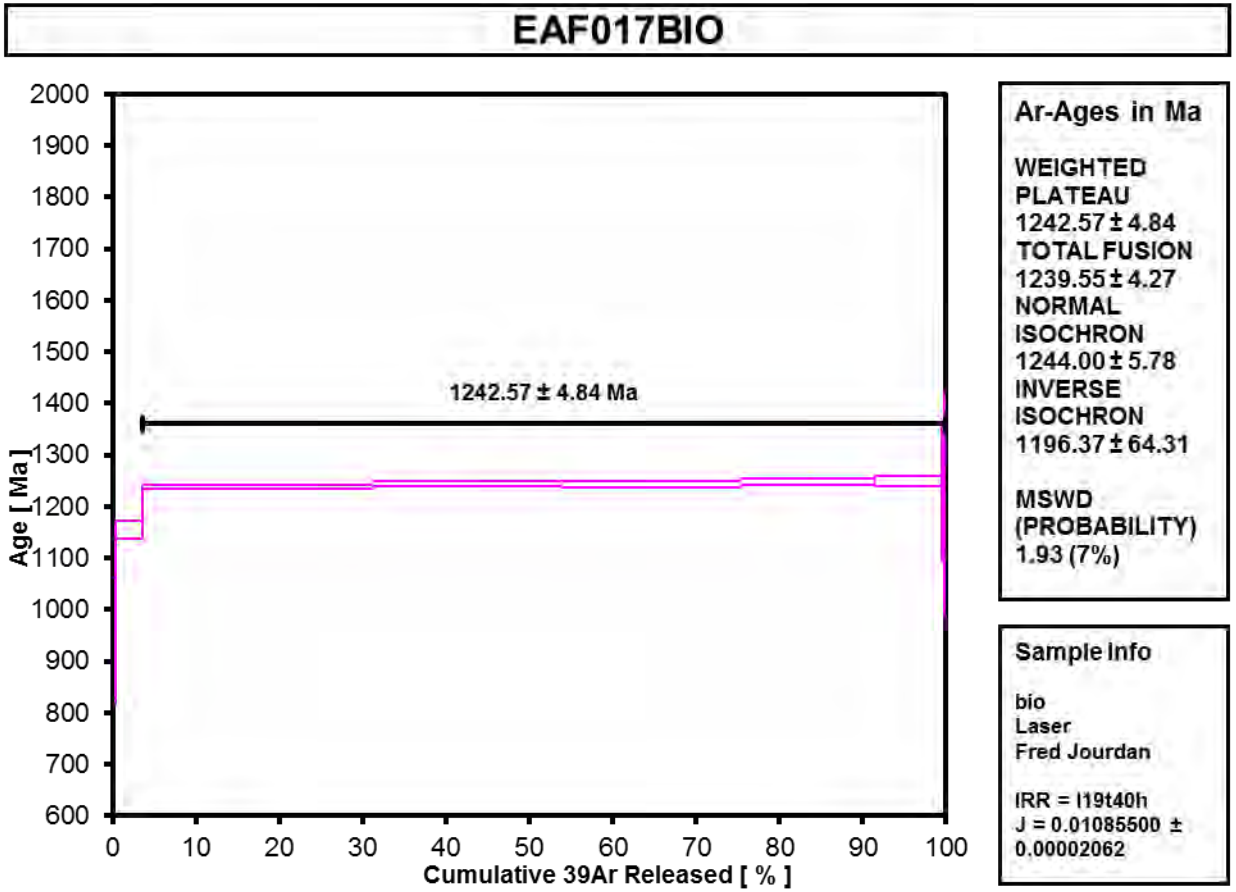

Figure A4.2-26 EAF017 Biotite 1

Table A4.2-27 EAF017 Biotite 2

Incremental Heating			36Ar(a) [V]	37Ar(ca) [V]	38Ar(cl) [V]	39Ar(k) [V]	40Ar(r) [V]	Age ± 2σ (Ma)	40Ar(r) (%)	39Ar(k) (%)	K/Ca ± 2σ
5M36154D	58 °C		0.0000024	0.0001445	0.0000017	0.0004927	0.050617	1354.63 ± 107.48	101.43	0.27	1.5 ± 2.4
5M36156D	58 °C		0.0000353	0.0002987	0.0000061	0.0031227	0.264219	1178.06 ± 22.37	96.17	1.74	4.5 ± 3.4
5M36157D	58 °C		0.0000560	0.0017826	0.0001231	0.0542662	5.610102	1360.55 ± 4.62	99.70	30.16	13.1 ± 1.5
5M36158D	59 °C	4	0.0000228	0.0004550	0.0000939	0.0626881	6.578498	1374.92 ± 4.65	99.90	34.84	59.2 ± 23.5
5M36160D	59 °C	4	0.0000094	0.0002728	0.0000725	0.0517990	5.414317	1371.11 ± 2.63	99.95	28.79	81.6 ± 42.4
5M36161D	60 °C	4	0.0000082	0.0000502	0.0000005	0.0075404	0.785660	1368.05 ± 13.35	99.69	4.19	64.5 ± 261.9

Information on Analysis	Results	40(r)/39(k) ± 2σ	Age ± 2σ (Ma)	MSWD	39Ar(k) (%,n)	K/Ca ± 2σ
Sample = EAF17BIO	**Age Plateau**	104.61310 ± 0.26752	1371.91 ± 4.40	1.19	67.83	64.5 ± 20.5
Material = bio		± 0.26%	± 0.32%	31%	3	
Location = Laser		Full External Error	± 10.46	3.00	2σ Confidence Limit	
Analyst = Fred Jourdan		Analytical Error	± 2.46	1.0894	Error Magnification	
Project = ALBANYFRASER_ES12						
Mass Discrimination Law = POW	**Total Fusion Age**	103.96032 ± 0.25843	1365.90 ± 4.35		6	28.5 ± 5.1
Irradiation = I19t40h		± 0.25%	± 0.32%			
J = 0.01085500 ± 0.00002062		Full External Error	± 10.40			
Hb3gr = 1081.000 ± 1.081 Ma		Analytical Error	± 2.38			
MDF = 1.003122 ± 0.07						

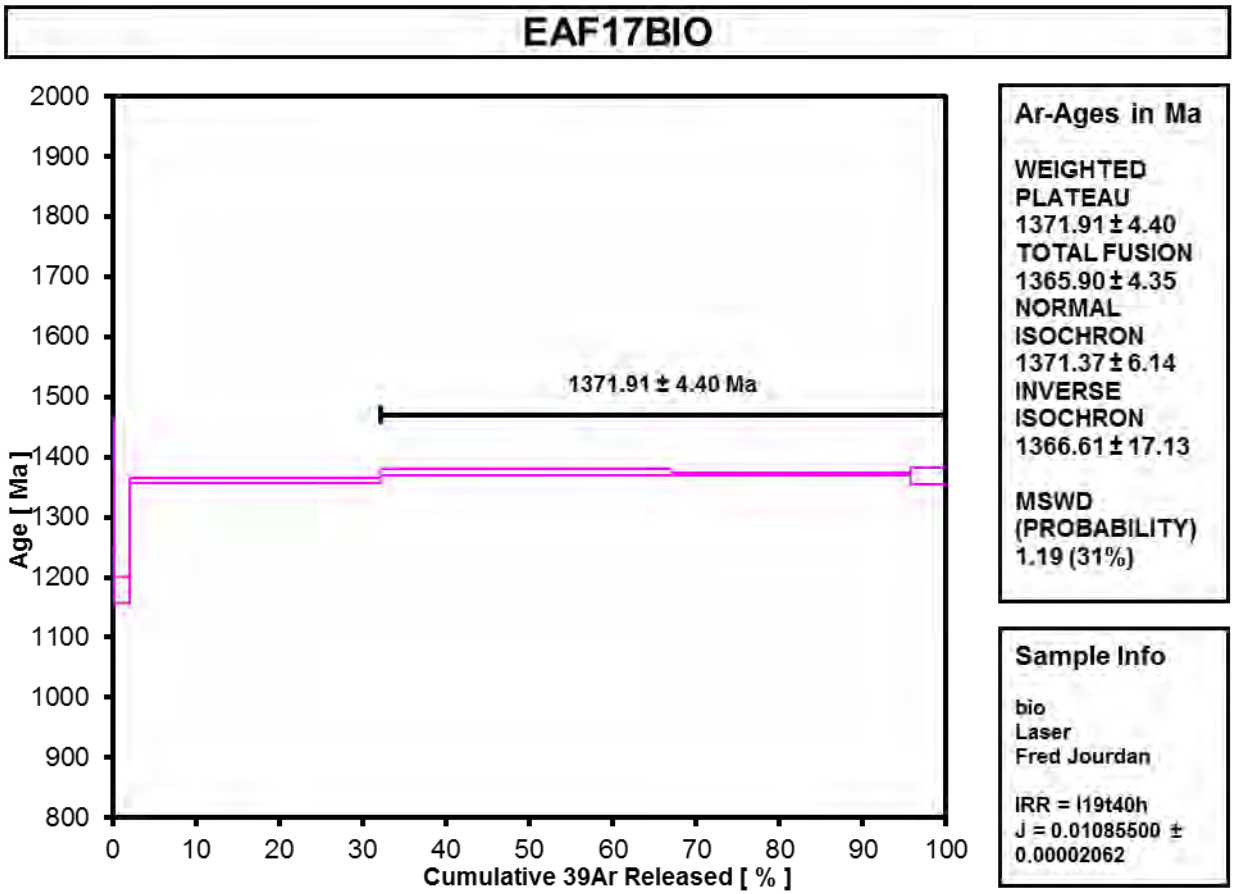

Figure A4.2-27 EAF017 Biotite 2

Table A4.2-28 EAF017 Biotite 3

Incremental Heating			36Ar(a) [V]	37Ar(ca) [V]	38Ar(cl) [V]	39Ar(k) [V]	40Ar(r) [V]	Age (Ma)	± 2σ	40Ar(r) (%)	39Ar(k) (%)	K/Ca	± 2σ
5M37945D	59 °C		0.0000328	0.0008616	0.0000097	0.0030684	0.298017	1301.75	± 26.76	96.82	1.70	1.5	± 2.4
5M37947D	60 °C		0.0000004	0.0014024	0.0000000	0.0007368	0.067728	1251.34	± 103.72	99.84	0.41	0.2	± 0.2
5M37948D	60 °C		0.0000640	0.0017573	0.0000032	0.0068765	0.659087	1289.48	± 13.25	97.18	3.82	1.7	± 1.4
5M37949D	60 °C		0.0000688	0.0019532	0.0000302	0.0317122	3.108159	1310.20	± 6.39	99.34	17.61	7.0	± 4.6
5M37950D~	61 °C	4	0.0001419	0.0195686	0.0002543	0.1190939	11.932334	1330.82	± 4.59	99.65	66.12	2.6	± 0.6
5M37952D	61 °C	4	0.0000134	0.0020487	0.0000332	0.0175571	1.771937	1337.69	± 7.31	100.23	9.75	3.7	± 3.4
5M37953D	62 °C	4	0.0000038	0.0009390	0.0000000	0.0004793	0.046942	1309.52	± 192.17	97.66	0.27	0.2	± 0.4
5M37954D	63 °C	4	0.0000125	0.0017198	0.0000000	0.0005815	0.061861	1388.15	± 129.31	106.43	0.32	0.1	± 0.1

Information on Analysis	Results	40(r)/39(k)	± 2σ	Age (Ma)	± 2σ	MSWD	39Ar(k) (%,n)	K/Ca	± 2σ
Sample = EAF0017BIO	**Age Plateau**	100.40250	± 0.43371	1332.79	± 5.43	1.10	76.46	0.1	± 0.6
Material = Bio			± 0.43%		± 0.41%	35%	4		
Location = Laser				Full External Error	± 9.96	2.63	2σ Confidence Limit		
Analyst = Fred Jourdan				Analytical Error	± 4.07	1.0489	Error Magnification		
Project = ALBANYFRASER_ES12									
Mass Discrimination Law = POW	**Total Fusion Age**	99.64186	± 0.36773	1325.64	± 4.98		8	8.7	± 5.9
Irradiation = I19t40h			± 0.37%		± 0.38%				
J = 0.01085500 ± 0.00002062				Full External Error	± 9.69				
FCs = 28.294 ± 0.037 Ma				Analytical Error	± 3.47				
MDF = 1.003286 ± 0.06									

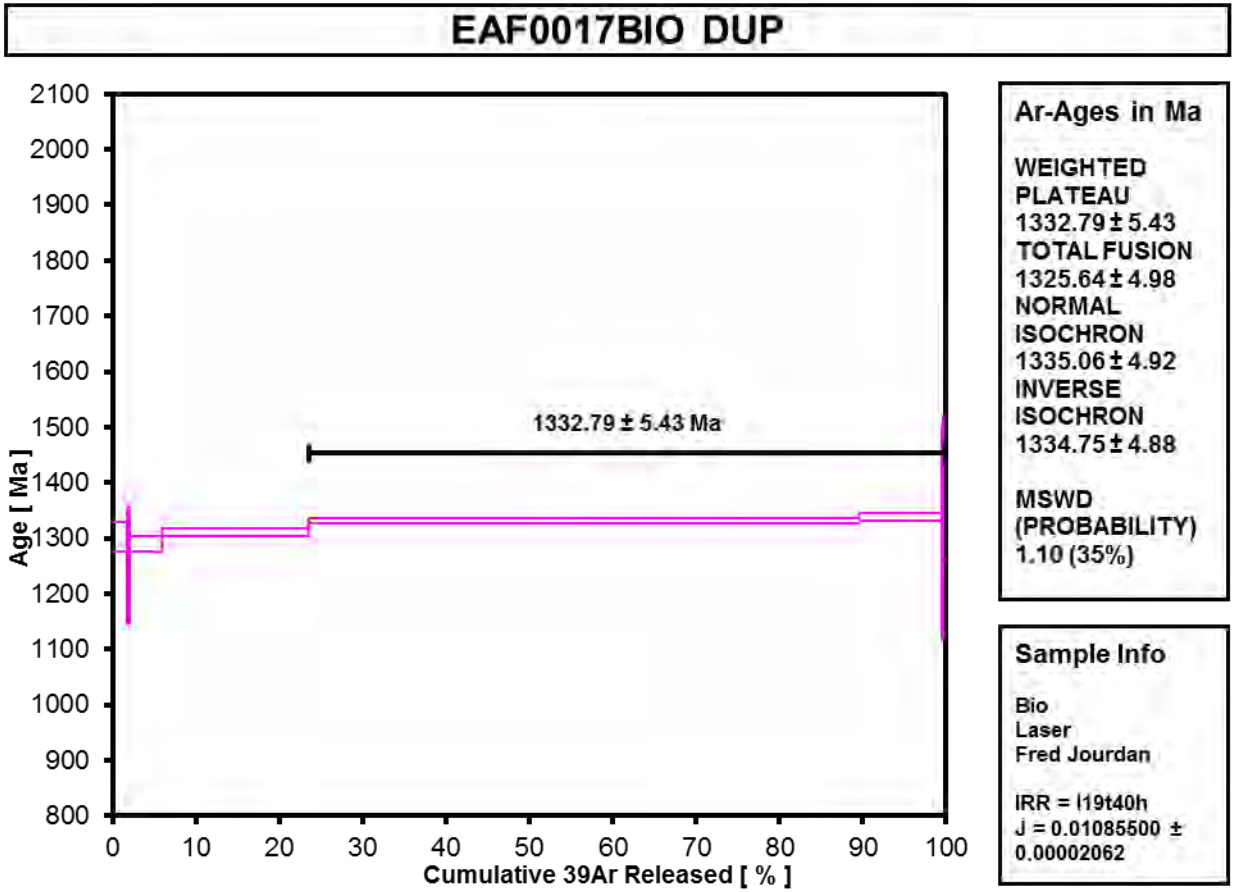

Figure A4.2-28 EAF017 Biotite 3

Table A4.2-29 EAF015 Muscovite

Incremental Heating			36Ar(a) [V]	37Ar(ca) [V]	38Ar(cl) [V]	39Ar(k) [V]	40Ar(r) [V]	Age (Ma)	± 2σ	40Ar(r) (%)	39Ar(k) (%)	K/Ca	± 2σ
5M36106D	58 °C		0.0000018	0.0000477	0.0000004	0.0007367	0.060712	1156.15	± 139.22	99.13	0.33	7	± 64
5M36108D	58 °C		0.0000316	0.0000602	0.0000054	0.0007612	0.049867	971.89	± 139.21	84.07	0.34	5	± 41
5M36109D	58 °C	4	0.0000154	0.0000013	0.0000023	0.0025026	0.201107	1134.70	± 48.47	97.76	1.11	860	± 314810
5M36111D	58 °C	4	0.0000197	0.0000171	0.0000000	0.0247986	2.094166	1177.09	± 5.81	99.72	11.05	624	± 16914
5M36112D	59 °C	4	0.0000086	0.0000004	0.0000000	0.0414363	3.519289	1182.05	± 6.65	99.93	18.46	41197	
5M36113D	59 °C	4	0.0000165	0.0000799	0.0000000	0.0281497	2.374112	1175.98	± 5.00	99.79	12.54	151	± 864
5M36114D	59 °C	4	0.0000122	0.0001084	0.0000000	0.0410316	3.452126	1173.87	± 4.51	99.89	18.28	163	± 682
5M36116D	59 °C	4	0.0000169	0.0000830	0.0000000	0.0364426	3.081256	1178.15	± 3.93	99.84	16.23	189	± 1049
5M36117D	59 °C	4	0.0000062	0.0000032	0.0000057	0.0111361	0.946387	1182.58	± 10.44	99.81	4.96	1494	± 224975
5M36118D	60 °C	4	0.0000160	0.0001065	0.0000007	0.0053506	0.449550	1172.69	± 19.13	98.95	2.38	22	± 95
5M36119D	61 °C	4	0.0000008	0.0002815	0.0000000	0.0239476	2.025219	1178.33	± 7.49	100.01	10.67	37	± 60
5M36121D	63 °C	4	0.0000059	0.0004431	0.0000000	0.0075920	0.644985	1182.30	± 14.88	99.73	3.38	7	± 8
5M36122D	66 °C	4	0.0000047	0.0003055	0.0000000	0.0006101	0.050561	1160.83	± 157.55	97.29	0.27	1	± 1

Information on Analysis	Results	40(r)/39(k)	± 2σ	Age (Ma)	± 2σ	MSWD	39Ar(k) (%,n)	K/Ca	± 2σ
Sample = EAF15MSC	**Age Plateau**	84.46411	± 0.19901	1177.26	± 4.63	0.98	99.33	1	± 1
Material = msc			± 0.24%		± 0.39%	46%	11		
Location = Laser				Full External Error	± 9.54	1.89	2σ Confidence Limit		
Analyst = Fred Jourdan				Analytical Error	± 2.04	1.0000	Error Magnification		
Project = ALBANYFRASER_ES12									
Mass Discrimination Law = POW	**Total Fusion Age**	84.40846	± 0.23140	1176.69	± 4.78		13	108	± 203
Irradiation = I19t40h			± 0.27%		± 0.41%				
J = 0.01086400 ± 0.00002607				Full External Error	± 9.61				
Hb3gr = 1081.000 ± 1.081 Ma				Analytical Error	± 2.37				
MDF = 1.003122 ± 0.07									

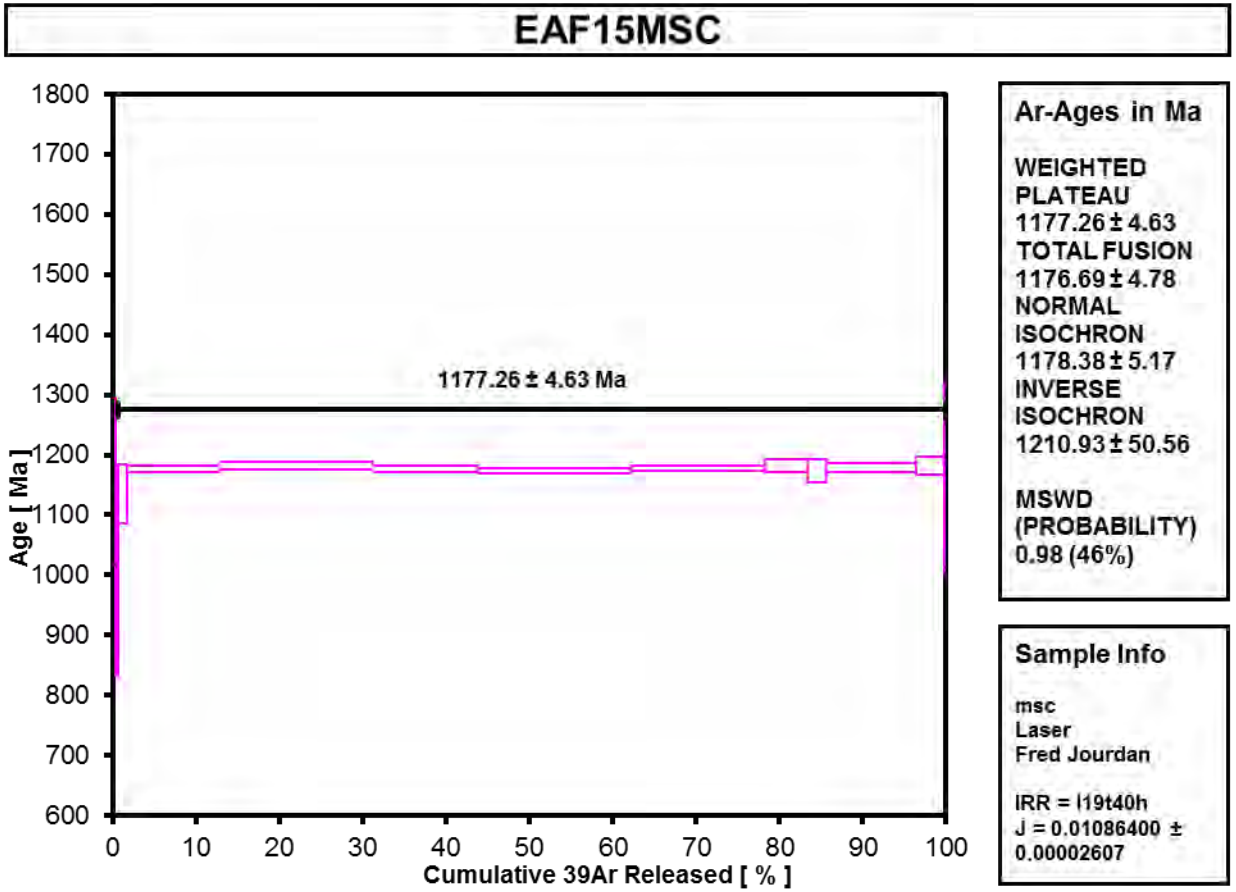

Figure A4.2-29 EAF015 Muscovite

Table A4.2-30 EAF012 Hornblende

Incremental Heating			36Ar(a) [V]	37Ar(ca) [V]	38Ar(cl) [V]	39Ar(k) [V]	40Ar(r) [V]	Age (Ma)	± 2σ	40Ar(r) (%)	39Ar(k) (%)	K/Ca	± 2σ
5M37438D	60 °C	4	0.0000054	0.0027610	0.0000114	0.0009102	0.0761860	1168.72	± 76.45	97.92	1.70	0.142	± 0.062
5M37439D	60 °C	4	0.0000037	0.0461149	0.0001958	0.0187621	1.6169934	1194.07	± 7.38	99.93	35.11	0.175	± 0.010
5M37440D	61 °C	4	0.0000053	0.0562492	0.0002414	0.0238118	2.0570604	1196.14	± 6.67	99.92	44.56	0.182	± 0.010
5M37441D	61 °C	4	0.0000058	0.0139301	0.0000642	0.0059873	0.5161619	1194.33	± 13.42	99.67	11.20	0.185	± 0.018
5M37443D	62 °C	4	0.0000062	0.0090291	0.0000382	0.0039631	0.3376192	1183.96	± 19.61	99.46	7.42	0.189	± 0.027

Information on Analysis	Results	40(r)/39(k)	± 2σ	Age (Ma)	± 2σ	MSWD	39Ar(k) (%,n)	K/Ca	± 2σ
Sample = EAF012HBL	**Age Plateau**	86.21791	± 0.44477	1194.41	± 5.60	0.47	100.00	0.180	± 0.006
Material = hbl			± 0.52%		± 0.47%	76%	5		
Location = Laser			Full External Error		± 9.43	2.41	2σ Confidence Limit		
Analyst = Fred Jourdan			Analytical Error		± 4.51	1.0000	Error Magnification		
Project = ALBANYFRASER_ES12									
Mass Discrimination Law = POW	**Total Fusion Age**	86.16182	± 0.45773	1193.84	± 5.71		5	0.179	± 0.007
Irradiation = I19t40h			± 0.53%		± 0.48%				
J = 0.01085500 ± 0.00002062			Full External Error		± 9.49				
FCs = 28.294 ± 0.037 Ma			Analytical Error		± 4.64				
MDF = 1.003236 ± 0.05									

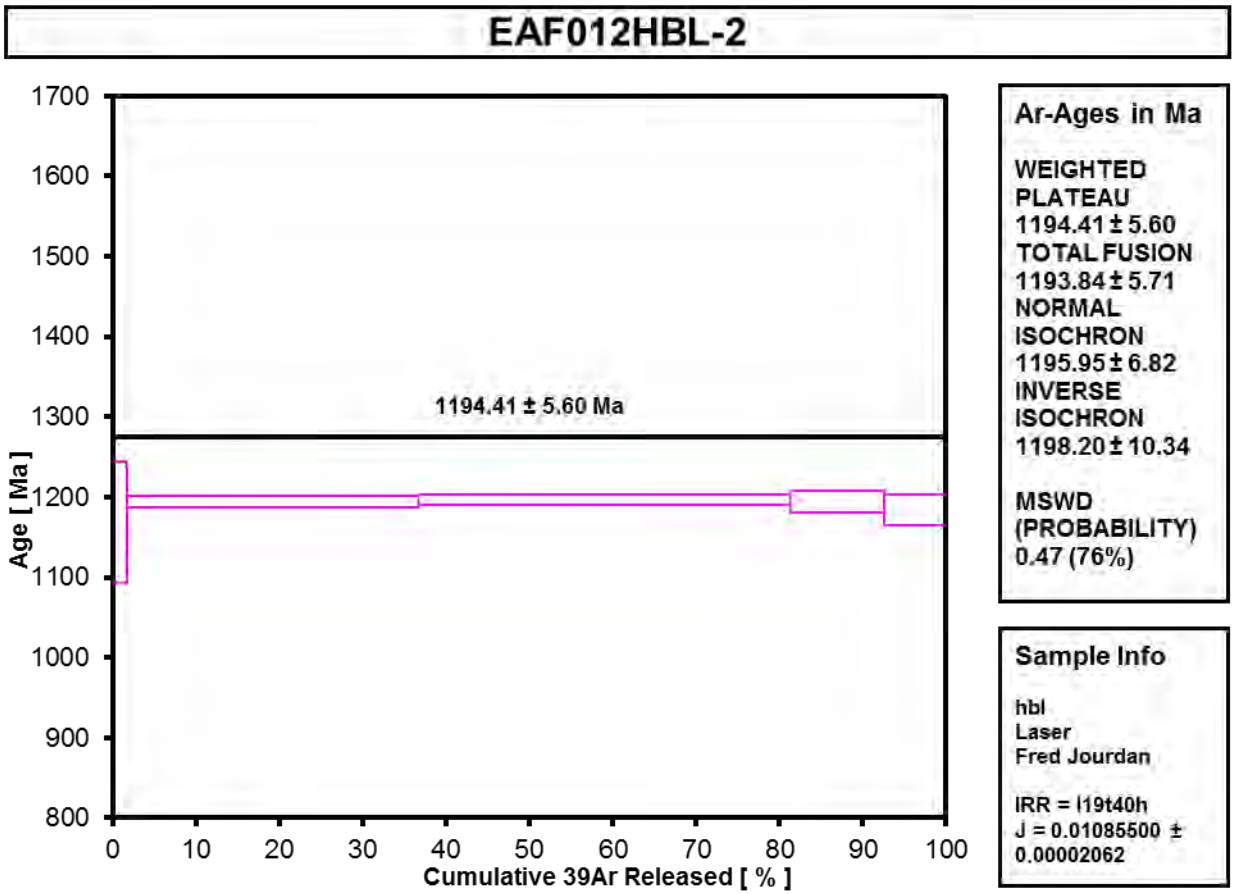

Figure A4.2-30 EAF012 Hornblende

Table A4.2-31 EAF012 Biotite

Incremental Heating			36Ar(a) [V]	37Ar(ca) [V]	38Ar(cl) [V]	39Ar(k) [V]	40Ar(r) [V]	Age (Ma)	± 2σ	40Ar(r) (%)	39Ar(k) (%)	K/Ca	± 2σ
5M36500D	58 °C		0.0000417	0.0000836	0.0000000	0.0030815	0.185902	910.81	± 29.61	93.72	1.25	16	± 53
5M36501D	59 °C		0.0000301	0.0001586	0.0000137	0.0241649	2.055441	1182.62	± 6.33	99.56	9.82	66	± 137
5M36503D	59 °C	4	0.0001063	0.0002175	0.0000807	0.0900213	7.887497	1208.55	± 3.89	99.60	36.57	178	± 230
5M36504D	60 °C	4	0.0001320	0.0003621	0.0001463	0.1267584	11.172077	1213.76	± 2.76	99.65	51.49	151	± 95
5M36505D	61 °C	4	0.0000022	0.0002313	0.0000000	0.0015191	0.133859	1213.57	± 53.71	99.52	0.62	3	± 3
5M36506D	63 °C	4	0.0000001	0.0000777	0.0000004	0.0006237	0.055350	1219.92	± 105.06	100.05	0.25	3	± 11

Information on Analysis	Results	40(r)/39(k)	± 2σ	Age (Ma)	± 2σ	MSWD	39Ar(k) (%,n)	K/Ca	± 2σ
Sample = EAF012BIO	**Age Plateau**	87.96362	± 0.28315	1212.03	± 4.40	1.60	88.93	2	± 7
Material = bio			± 0.32%		± 0.36%	19%	4		
Location = Laser			Full External Error		± 11.38	2.63	2σ Confidence Limit		
Analyst = Fred Jourdan			Analytical Error		± 2.84	1.2649	Error Magnification		
Project = ALBANYFRASER_ES12									
Mass Discrimination Law = POW	**Total Fusion Age**	87.29831	± 0.21561	1205.33	± 3.99		6	158	± 159
Irradiation = I19t40h			± 0.25%		± 0.33%				
J = 0.01085500 ± 0.00002062			Full External Error		± 11.18				
WA1ms = 2613.000 ± 2.352 Ma			Analytical Error		± 2.17				
MDF = 1.00323 ± 0.06									

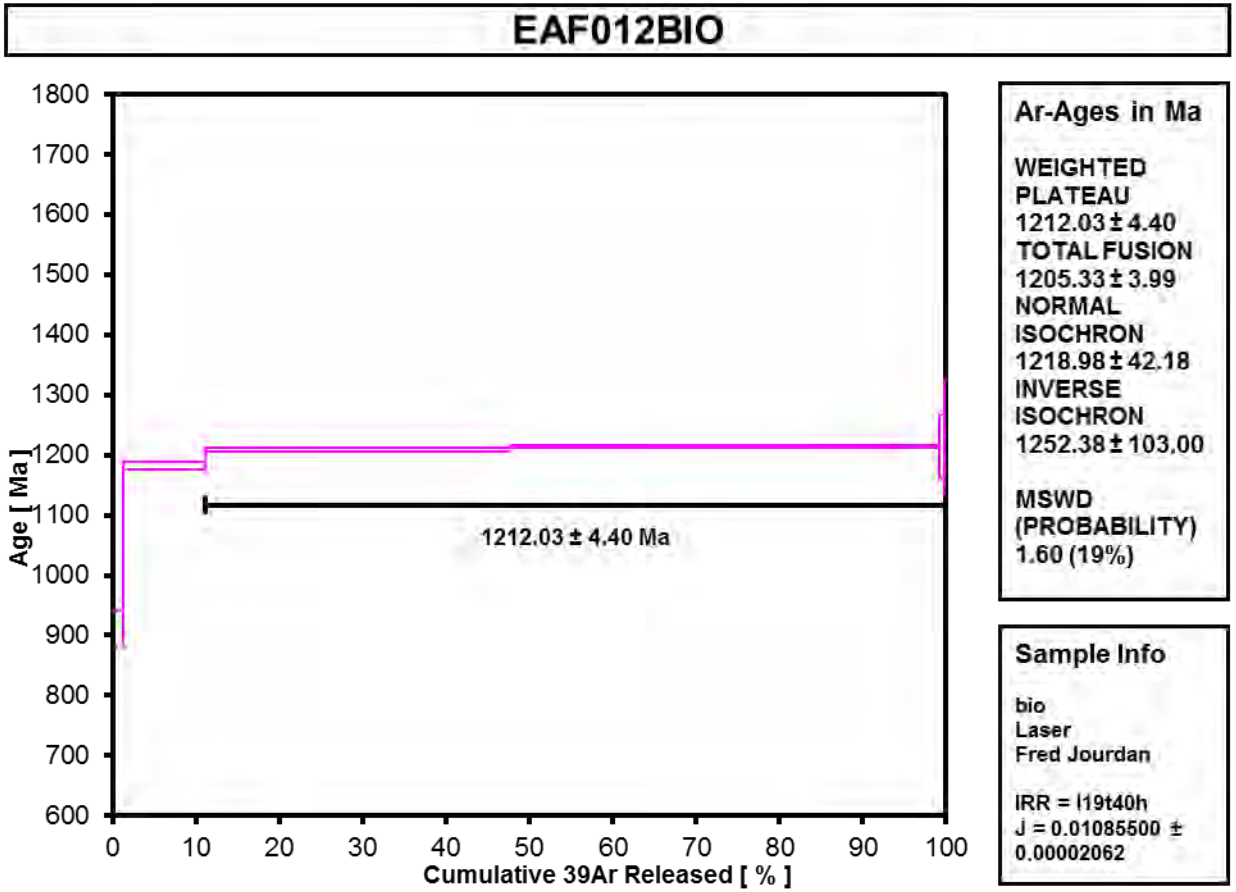

Figure A4.2-31 EAF012 Biotite

Table A4.2-32 EAF038 Hornblende

Incremental Heating			36Ar(a) [V]	37Ar(ca) [V]	38Ar(cl) [V]	39Ar(k) [V]	40Ar(r) [V]	Age ± 2σ (Ma)	40Ar(r) (%)	39Ar(k) (%)	K/Ca	± 2σ
5M37265D	60 °C	4	0.0000061	0.0195540	0.0000057	0.0039489	0.3469042	1203.08 ± 36.78	99.48	16.14	0.087	± 0.006
5M37266D	61 °C	4	0.0000054	0.0233211	0.0000022	0.0049662	0.4283961	1187.14 ± 29.74	99.62	20.29	0.092	± 0.005
5M37267D	61 °C	4	0.0000035	0.0517162	0.0000073	0.0106681	0.9243474	1191.01 ± 16.12	100.11	43.59	0.089	± 0.005
5M37269D	62 °C	4	0.0000037	0.0211390	0.0000187	0.0044000	0.3815607	1191.74 ± 35.75	99.71	17.98	0.090	± 0.006
5M37270D	62 °C	4	0.0000172	0.0022470	0.0000118	0.0004889	0.0385129	1110.03 ± 308.31	88.25	2.00	0.094	± 0.031

Information on Analysis	Results	40(r)/39(k)	± 2σ	Age (Ma)	± 2σ	MSWD	39Ar(k) (%,n)	K/Ca	± 2σ
Sample = EAF0038HBL	**Age Plateau**	86.70867	± 1.23121	1191.64	± 12.85	0.19	100.00	0.089	± 0.003
Material = Hbl	**Overestimated Error**		± 1.42%		± 1.08%	94%	5		
Location = Laser			Full External Error		± 14.86	2.41	2σ Confidence Limit		
Analyst = Fred Jourdan			Analytical Error		± 12.39	1.0000	Error Magnification		
Project = ALBANYFRASER_ES12									
Mass Discrimination Law = POW	**Total Fusion Age**	86.61804	± 1.39563	1190.73	± 14.46		5	0.089	± 0.003
Irradiation = I19t40h			± 1.61%		± 1.21%				
J = 0.01075940 ± 0.00002098			Full External Error		± 16.27				
FCs = 28.294 ± 0.031 Ma			Analytical Error		± 14.05				
MDF = 1.003135 ± 0.06									

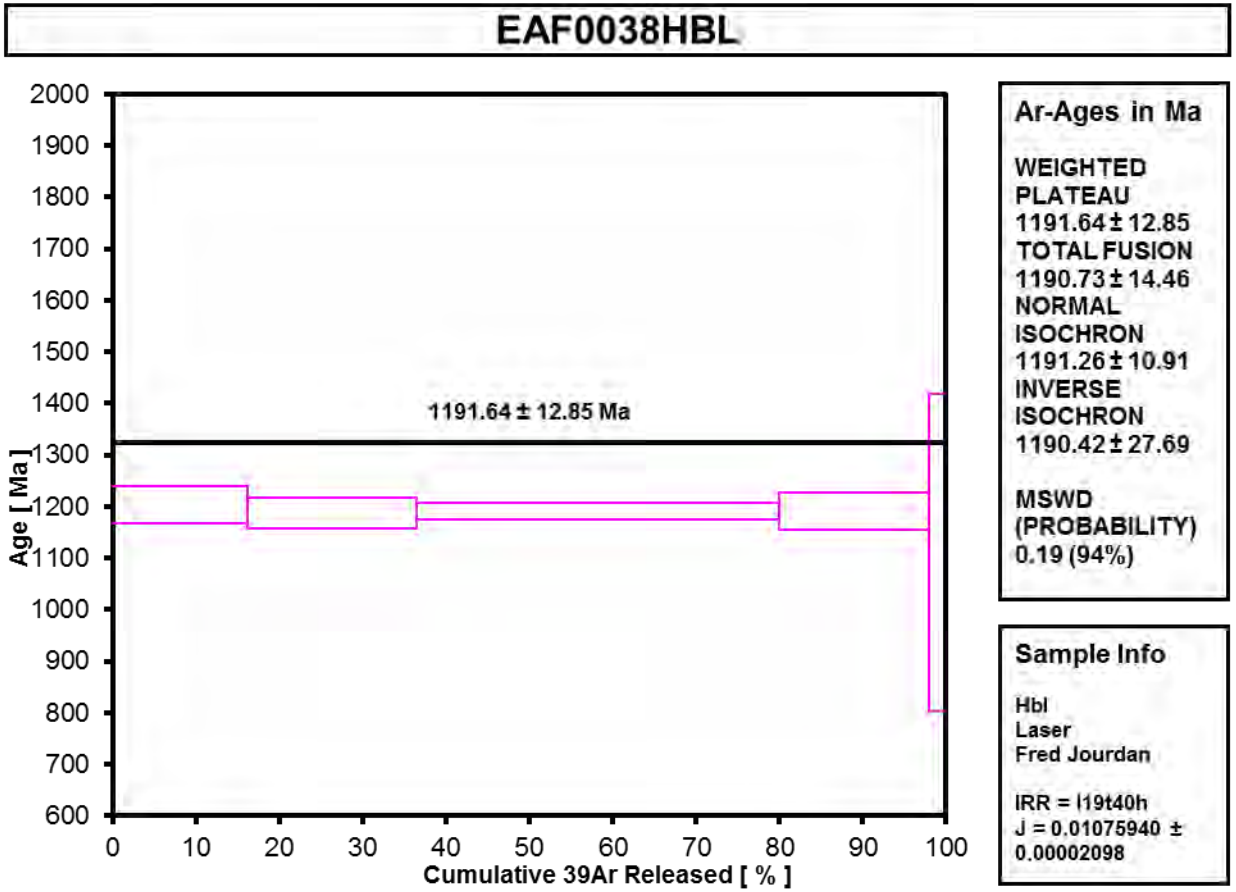

Figure A4.2-32 EAF038 Hornblende

Table A4.2-33 EAF039B Biotite

Incremental Heating			36Ar(a) [V]	37Ar(ca) [V]	38Ar(cl) [V]	39Ar(k) [V]	40Ar(r) [V]	Age (Ma)	± 2σ	40Ar(r) (%)	39Ar(k) (%)	K/Ca	± 2σ
5M36562D	58 °C		0.0000234	0.0002656	0.0000000	0.0116729	0.9580028	1151.87	± 8.68	99.27	10.69	19	± 19
5M36563D	58 °C	4	0.0000057	0.0000213	0.0000173	0.0177719	1.4931347	1171.95	± 10.77	99.89	16.27	359	± 5119
5M36564D	59 °C	4	0.0000051	0.0002380	0.0000017	0.0207769	1.7328251	1165.63	± 5.86	99.91	19.03	38	± 42
5M36566D	59 °C	4	0.0000097	0.0000643	0.0000192	0.0443170	3.7134610	1169.66	± 4.98	99.92	40.58	296	± 1167
5M36567D	60 °C	4	0.0000068	0.0000246	0.0000182	0.0138302	1.1589089	1169.69	± 10.45	99.82	12.66	242	± 2720
5M36568D	61 °C	4	0.0000030	0.0000541	0.0000078	0.0008357	0.0714002	1186.45	± 86.77	98.75	0.77	7	± 38

Information on Analysis	Results	40(r)/39(k)	± 2σ	Age (Ma)	± 2σ	MSWD	39Ar(k) (%,n)	K/Ca	± 2σ
Sample = EAF039BBIO	**Age Plateau**	83.68674	± 0.32917	1168.57	± 4.71	0.45	89.31	13	± 28
Material = bio			± 0.39%		± 0.40%	77%	5		
Location = Laser				Full External Error	± 8.80	2.41	2σ Confidence Limit		
Analyst = Fred Jourdan				Analytical Error	± 3.39	1.0000	Error Magnification		
Project = ALBANYFRASER_ES12									
Mass Discrimination Law = POW	**Total Fusion Age**	83.58373	± 0.32881	1167.51	± 4.70		6	121	± 215
Irradiation = I19t40h			± 0.39%		± 0.40%				
J = 0.01085500 ± 0.00002062				Full External Error	± 8.80				
FCs = 28.294 ± 0.037 Ma				Analytical Error	± 3.38				
MDF = 1.003231 ± 0.06									

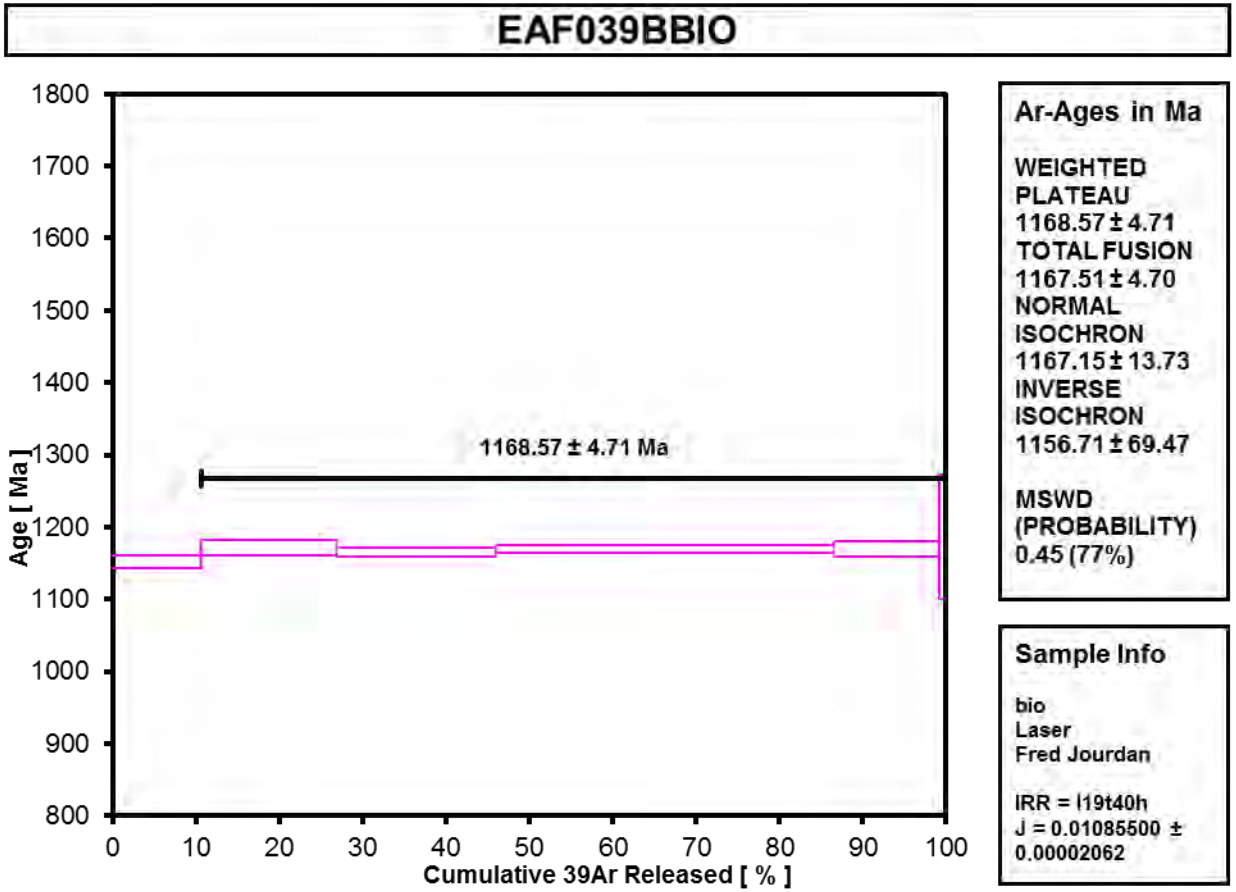

Figure A4.2-33 EAF039B Biotite

Table A4.2-34 EAF041 Biotite

Incremental Heating			36Ar(a) [V]	37Ar(ca) [V]	38Ar(cl) [V]	39Ar(k) [V]	40Ar(r) [V]	Age (Ma)	± 2σ	40Ar(r) (%)	39Ar(k) (%)	K/Ca	± 2σ
5M36249D	58 °C	4	0.0000035	0.0001752	0.0000000	0.0005282	0.048479	1249.91	± 115.65	102.21	0.33	1.3	± 1.3
5M36251D	58 °C	4	0.0001301	0.0000448	0.0000274	0.0264599	2.369016	1227.71	± 5.29	98.39	16.75	253.8	± 1053.3
5M36252D	59 °C	4	0.0000289	0.0000570	0.0000919	0.0611830	5.505910	1232.27	± 6.39	99.84	38.72	461.9	± 1706.3
5M36254D	59 °C	4	0.0000107	0.0023607	0.0001197	0.0698310	6.312546	1236.30	± 4.55	99.95	44.20	12.7	± 1.3

Information on Analysis	Results	40(r)/39(k)	± 2σ	Age (Ma)	± 2σ	MSWD	39Ar(k) (%,n)	K/Ca	± 2σ
Sample = EAF041BIO	**Age Plateau**	90.02029	± 0.43835	1232.56	± 5.52	2.06	100.00	5.4	± 8.1
Material = bio			± 0.49%		± 0.45%	10%	4		
Location = Laser				Full External Error	± 11.98	2.63	2σ Confidence Limit		
Analyst = Fred Jourdan				Analytical Error	± 4.35	1.4345	Error Magnification		
Project = ALBANYFRASER_ES12									
Mass Discrimination Law = POW	**Total Fusion Age**	90.09970	± 0.33577	1233.35	± 4.76		4	32.6	± 6.4
Irradiation = I19t40h			± 0.37%		± 0.39%				
J = 0.01085500 ± 0.00002062				Full External Error	± 11.66				
WA1ms = 2613.000 ± 2.352 Ma				Analytical Error	± 3.33				
MDF = 1.003122 ± 0.07									

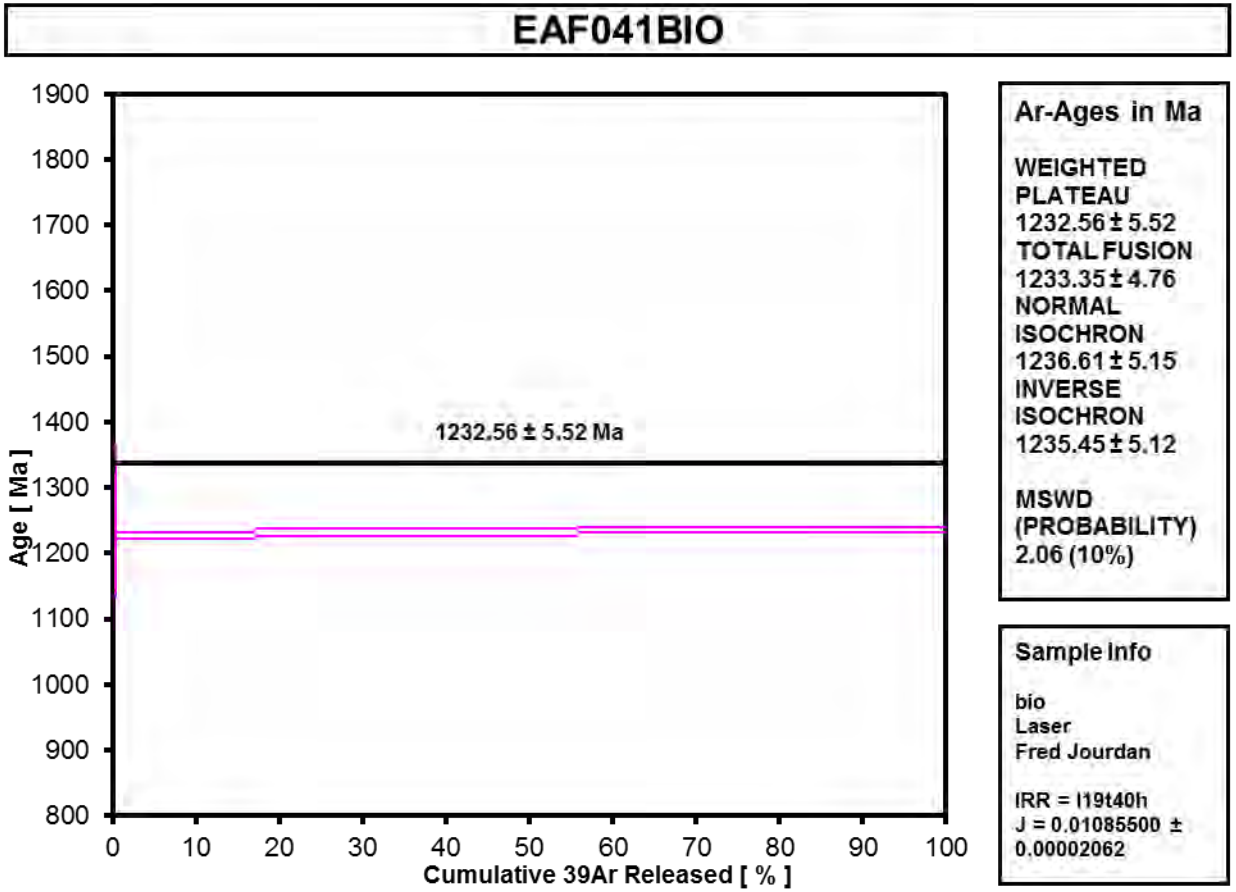

Figure A4.2-34 EAF041 Biotite

Table A4.2-35 EAF042 Biotite 1

Incremental Heating			36Ar(a) [V]	37Ar(ca) [V]	38Ar(cl) [V]	39Ar(k) [V]	40Ar(r) [V]	Age (Ma)	± 2σ	40Ar(r) (%)	39Ar(k) (%)	K/Ca	± 2σ
5M37362D	59 °C		0.0000360	0.0010338	0.0000108	0.0015906	0.116051	1054.74	± 53.62	91.52	0.44	0.7	± 0.5
5M37363D	59 °C		0.0000512	0.0014101	0.0000345	0.0129991	1.258877	1299.05	± 8.26	98.80	3.58	4.0	± 2.1
5M37364D	59 °C		0.0000426	0.0015582	0.0000544	0.0291637	2.920466	1330.33	± 5.38	99.57	8.03	8.0	± 3.6
5M37366D	60 °C		0.0000289	0.0011637	0.0000848	0.0407716	4.063949	1325.96	± 5.30	99.79	11.22	15.1	± 9.4
5M37367D	60 °C	4	0.0000363	0.0007705	0.0000857	0.0437348	4.169808	1284.64	± 4.04	99.74	12.04	24.4	± 24.8
5M37368D	60 °C	4	0.0000203	0.0007684	0.0001131	0.0517857	4.918213	1281.06	± 3.45	99.88	14.25	29.0	± 29.5
5M37369D	61 °C	4	0.0000091	0.0003154	0.0002340	0.1145284	10.842468	1278.14	± 2.63	99.97	31.52	156.1	± 352.4
5M37371D	61 °C	4	0.0000048	0.0000281	0.0001226	0.0573528	5.463927	1283.92	± 6.79	99.97	15.79	877.5	± 28308.3
5M37372D	62 °C	4	0.0000007	0.0000234	0.0000068	0.0069795	0.667115	1286.94	± 12.64	100.03	1.92	128.5	± 4133.3
5M37373D	63 °C	4	0.0000006	0.0002624	0.0000091	0.0043945	0.416188	1278.48	± 17.17	99.96	1.21	7.2	± 21.4

Information on Analysis	Results	40(r)/39(k)	± 2σ	Age (Ma)	± 2σ	MSWD	39Ar(k) (%,n)	K/Ca	± 2σ
Sample = EAF042BIO	**Age Plateau**	94.93514	± 0.25261	1280.70	± 4.26	1.92	76.73	11.8	± 15.8
Material = bio			± 0.27%		± 0.33%	9%	6		
Location = Laser			Full External Error		± 9.12	2.26	2σ Confidence Limit		
Analyst = Fred Jourdan			Analytical Error		± 2.44	1.3845	Error Magnification		
Project = ALBANYFRASER_ES12									
Mass Discrimination Law = POW	**Total Fusion Age**	95.89041	± 0.18283	1289.91	± 3.92		10	23.1	± 8.3
Irradiation = I19t40h			± 0.19%		± 0.30%				
J = 0.01085500 ± 0.00002062			Full External Error		± 9.01				
FCs = 28.294 ± 0.037 Ma			Analytical Error		± 1.76				
MDF = 1.003236 ± 0.05									

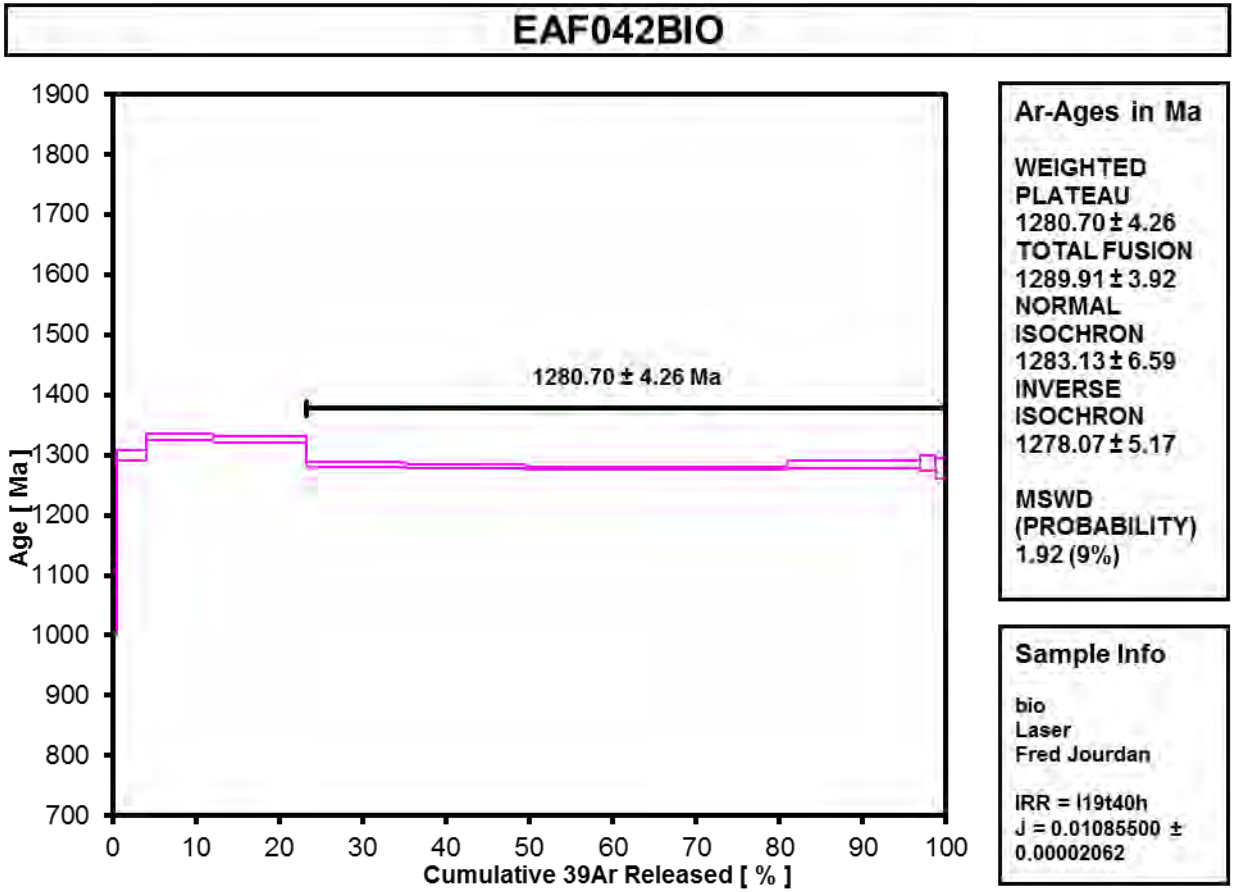

Figure A4.2-35 EAF042 Biotite 1

Table A4.2-36 EAF042 Biotite 2

Incremental Heating		36Ar(a) [V]	37Ar(ca) [V]	38Ar(cl) [V]	39Ar(k) [V]	40Ar(r) [V]	Age ± 2σ (Ma)	40Ar(r) (%)	39Ar(k) (%)	K/Ca ± 2σ
5M36143D	58 °C	0.0000273	0.0000400	0.0000113	0.0004849	0.035588	1060.21 ± 183.66	81.37	0.31	5 ± 29
5M36145D	58 °C	0.0000324	0.0002234	0.0000217	0.0079057	0.735416	1262.88 ± 9.66	98.70	5.09	15 ± 17
5M36146D	58 °C	0.0000245	0.0000431	0.0000914	0.0459557	4.392847	1287.77 ± 6.00	99.83	29.56	458 ± 2368
5M36147D	59 °C	0.0000107	0.0000216	0.0000853	0.0455358	4.378087	1293.13 ± 4.11	99.93	29.29	908 ± 7666
5M36149D	59 °C	0.0000003	0.0000182	0.0000915	0.0450098	4.372528	1302.72 ± 3.90	100.00	28.95	1063 ± 10537
5M36150D	60 °C	0.0000016	0.0000237	0.0000182	0.0105597	1.017370	1295.04 ± 8.82	99.95	6.79	192 ± 1395

Information on Analysis	Results	40(r)/39(k) ± 2σ	Age ± 2σ (Ma)	MSWD	39Ar(k) (%,n)	K/Ca ± 2σ
Sample = EAF042BIO Material = bio Location = Laser Analyst = Fred Jourdan Project = ALBANYFRASER_ES12 Mass Discrimination Law = POW Irradiation = I19t40h J = 0.01086400 ± 0.00002600 Hb3gr = 1081.000 ± 1.081 Ma MDF = 1.003122 ± 0.07	**Age Plateau Cannot Calculate**					
	Total Fusion Age	96.05457 ± 0.26986 ± 0.28%	1292.26 ± 5.12 ± 0.40% Full External Error ± 10.38 Analytical Error ± 2.59		6	416 ± 1308

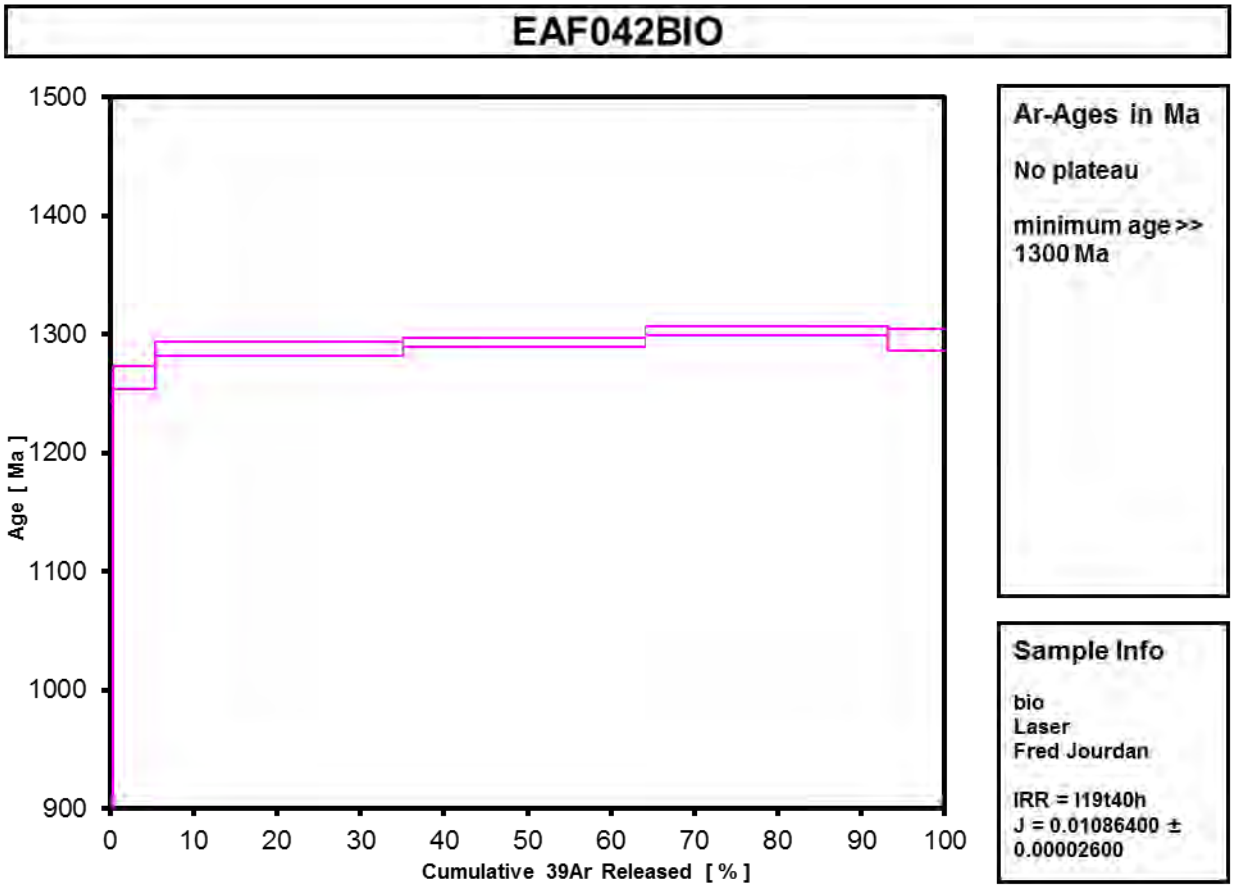

Figure A4.2-36 EAF042 Biotite 2

Table A4.2-37 EAF042 Biotite 3

Incremental Heating			36Ar(a) [V]	37Ar(ca) [V]	38Ar(cl) [V]	39Ar(k) [V]	40Ar(r) [V]	Age (Ma)	± 2σ	40Ar(r) (%)	39Ar(k) (%)	K/Ca	± 2σ
5M38100D	60 °C		0.0000307	0.0007260	0.0000219	0.0008631	0.071457	1159.33	± 79.20	88.65	0.46	0.5	± 1.3
5M38101D	60 °C		0.0000267	0.0002803	0.0000167	0.0009900	0.083339	1173.59	± 79.41	91.26	0.53	1.5	± 10.8
5M38103D	60 °C		0.0000273	0.0001878	0.0000118	0.0025551	0.231559	1238.57	± 32.12	96.60	1.36	5.8	± 58.2
5M38104D	60 °C		0.0000127	0.0002089	0.0000118	0.0042784	0.398207	1262.61	± 16.74	99.06	2.28	8.8	± 70.0
5M38105D	60 °C	4	0.0000078	0.0008509	0.0000165	0.0048217	0.455030	1275.25	± 15.72	99.49	2.56	2.4	± 5.7
5M38106D	60 °C	4	0.0000092	0.0005502	0.0000307	0.0256465	2.417700	1274.26	± 7.53	99.89	13.64	20.0	± 68.9
5M38108D	61 °C	4	0.0000117	0.0001169	0.0000554	0.0372134	3.536359	1281.61	± 5.22	99.90	19.79	136.9	± 2249.4
5M38109D	61 °C	4	0.0000048	0.0001636	0.0000434	0.0218946	2.084003	1283.10	± 6.14	99.93	11.64	57.5	± 766.3
5M38110D	61 °C	4	0.0000098	0.0008052	0.0000529	0.0263749	2.501923	1279.98	± 6.57	99.88	14.03	14.1	± 35.2
5M38111D	61 °C	4	0.0000077	0.0000475	0.0000500	0.0266166	2.517802	1277.41	± 5.15	99.91	14.16	241.2	± 9248.1
5M38113D	61 °C	4	0.0000018	0.0002098	0.0000271	0.0174138	1.659921	1284.44	± 6.30	100.03	9.26	35.7	± 325.8
5M38114D	62 °C	4	0.0000093	0.0012235	0.0000260	0.0184758	1.767450	1287.72	± 6.35	100.16	9.83	6.5	± 10.9
5M38115D	63 °C	4	0.0000060	0.0000553	0.0000000	0.0006967	0.064290	1254.86	± 114.20	102.89	0.37	5.4	± 198.2
5M38116D	66 °C	4	0.0000067	0.0008473	0.0000074	0.0001791	0.015187	1180.07	± 302.87	115.25	0.10	0.1	± 0.2

Information on Analysis
Sample = EAF0042BIO
Material = Bio
Location = Laser
Analyst = Fred Jourdan
Project = ALBANYFRASER_ES12
Mass Discrimination Law = POW
Irradiation = I19t40h
J = 0.01085500 ± 0.00002062
FCs = 28.294 ± 0.037 Ma
MDF = 1.003286 ± 0.05

Results	40(r)/39(k)	± 2σ	Age (Ma)	± 2σ	MSWD	39Ar(k) (%,n)	K/Ca	± 2σ
Age Plateau	94.97908	± 0.27710	1281.13	± 4.40	1.40	95.38	0.1	± 0.2
		± 0.29%		± 0.34%	18%	10		
		Full External Error		± 9.19	1.94	2σ Confidence Limit		
		Analytical Error		± 2.68	1.1848	Error Magnification		
Total Fusion Age	94.69337	± 0.24814	1278.36	± 4.23		14	31.0	± 86.3
		± 0.26%		± 0.33%				
		Full External Error		± 9.09				
		Analytical Error		± 2.40				

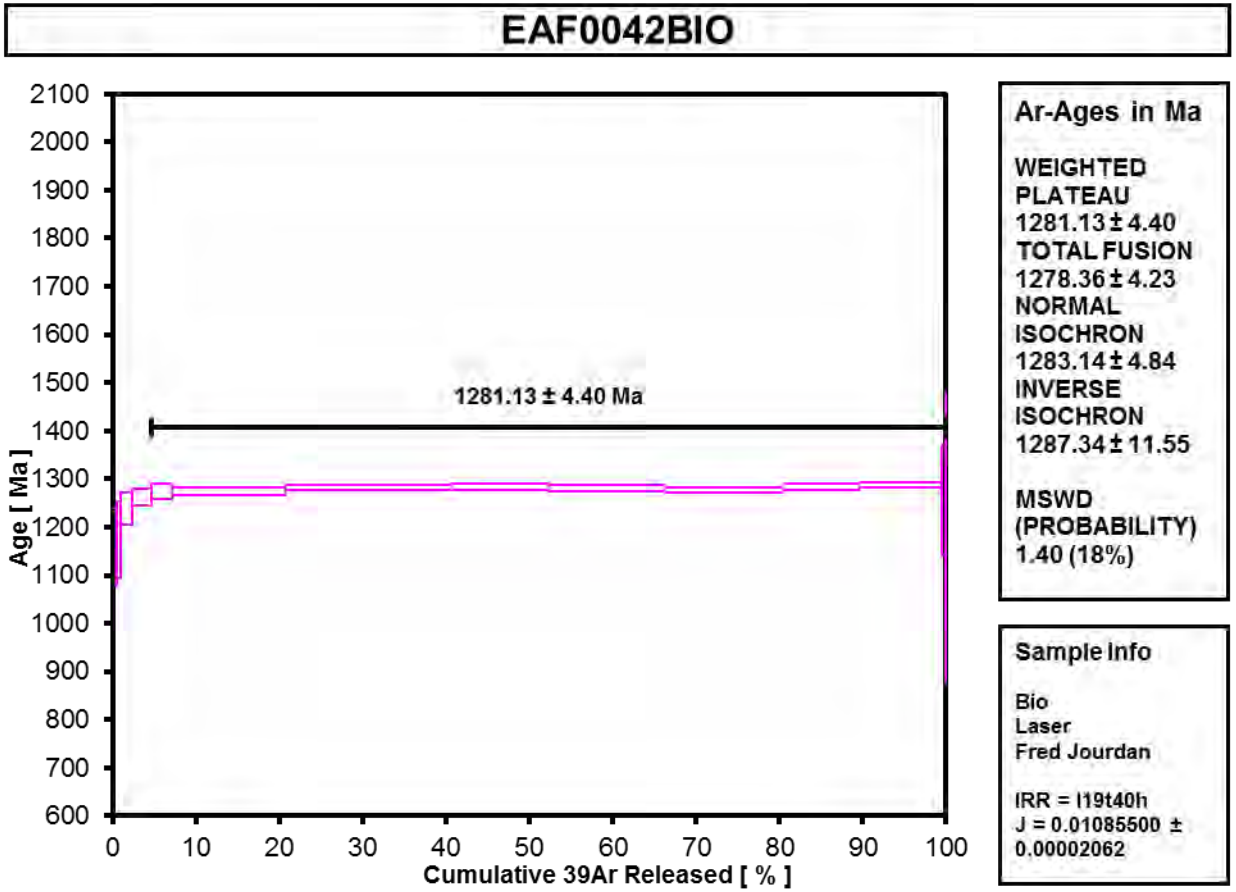

Figure A4.2-37 EAF042 Biotite 3

Table A4.2-38 EAF037 Biotite

Incremental Heating			36Ar(a) [V]	37Ar(ca) [V]	38Ar(cl) [V]	39Ar(k) [V]	40Ar(r) [V]	Age (Ma)	± 2σ	40Ar(r) (%)	39Ar(k) (%)	K/Ca	± 2σ
5M36511D	58 °C		0.0000105	0.0000251	0.0000054	0.0120392	0.9876142	1151.48	± 7.19	99.68	13.82	206	± 2290
5M36512D	59 °C	4	0.0000056	0.0000955	0.0000235	0.0330812	2.7611212	1166.28	± 6.20	100.06	37.98	149	± 406
5M36514D	59 °C	4	0.0000061	0.0001567	0.0000108	0.0295755	2.4853720	1172.14	± 3.96	99.93	33.95	81	± 137
5M36515D	60 °C	4	0.0000010	0.0000331	0.0000147	0.0124137	1.0431135	1172.08	± 8.66	100.03	14.25	161	± 1321

Information on Analysis	Results	40(r)/39(k)	± 2σ	Age (Ma)	± 2σ	MSWD	39Ar(k) (%,n)	K/Ca	± 2σ
Sample = EAF037BIO	**Age Plateau**	83.88991	± 0.34994	1170.65	± 4.86	1.33	86.18	86	± 129
Material = bio			± 0.42%		± 0.42%	26%	3		
Location = Laser				Full External Error	± 11.31	3.00	2σ Confidence Limit		
Analyst = Fred Jourdan				Analytical Error	± 3.59	1.1545	Error Magnification		
Project = ALBANYFRASER_ES12									
Mass Discrimination Law = POW									
Irradiation = I19t40h	**Total Fusion Age**	83.54094	± 0.30522	1167.07	± 4.53		4	153	± 338
J = 0.01085500 ± 0.00002062			± 0.37%		± 0.39%				
WA1ms = 2613.000 ± 2.352 Ma				Full External Error	± 11.14				
MDF = 1.00323 ± 0.06				Analytical Error	± 3.14				

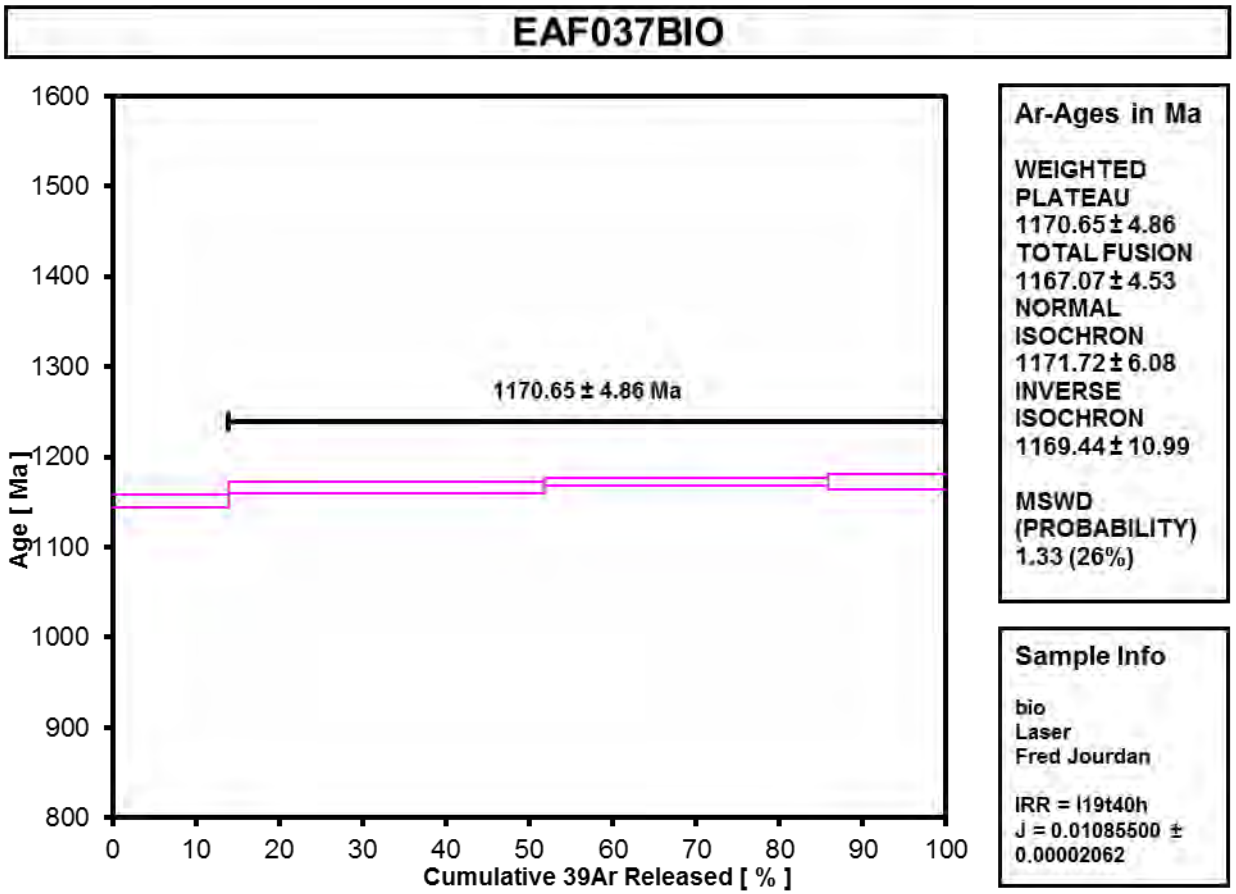

Figure A4.2-38 EAF037 Biotite

Appendix 4.3: Calculation of closure temperatures and cooling rates

$^{40}Ar/^{39}Ar$ closure temperatures and cooling rates were calculated for the three mica grains that also produced hornblende cooling ages at the same locality. The calculations were performed by iterating Equation 1 five times (Dodson, 1973):

$$E / (R \times T_C) = ln (- (A \times R \times T_{C0}^2 \times D_0) / (E \times dT/dt \times a^2). \quad (1)$$

In this equation, E is the activation energy, R is the gas constant, T_C is the closure temperature, A is the volume constant, T_{C0} is the initial estimate of closure temperature, D_0 is the diffusion coefficient, dT/dt is the cooling rate, and a is the grainsize.

Initial cooling rates (dT/dt) were calculated between hornblende closure temperature and biotite closure temperature, using the temperature-time (T-t) pair provided by the hornblende cooling age and closure temperature from the same site. The formula for cooling rates is:

$$dT/dt = (\text{hornblende } T_C - \text{mica } T_C) / (\text{hornblende cooling age} - \text{mica cooling age}). \quad (2)$$

For the calculation of dT/dt, a hornblende T_C of 550 °C was assumed (Harrison, 1981). The values of all inputs to Equation 1 and Equation 2 are in Table A4.3-1 below.

The Monte Carlo simulation was performed in the Python programming language (www.python.org), using the NumPy and Matplotlib packages (www.scipy.org). The probability distribution of each uncertain variable is summarised in Table A4.3-2. The Monte Carlo simulation was performed using 20,000 trials. After each iteration of Equation 1, dT/dt was recalculated using the newly-calculated closure temperature. Further details on the use of the Monte Carlo simulation are available in Scibiorski et al. (2015).

Histograms of the output values for closure temperature and cooling rate are shown in Figures A4.3-1 and A4.3-2 respectively. These histograms represent probability distributions, within which lie the true values of the closure temperature and cooling rate.

Table A4.3-1 Initial inputs to Dodson's equation (Equation 1 above). Values for the activation energy (E), diffusion coefficient (D_0) and volume constant (A) for biotite were taken from Grove and Harrison (1996), as biotites analysed in this study have similar Fe/Mg ratios. The initial closure temperature estimates (T_{C0}) for biotite was 300 °C (Harrison et al., 1985).Values for the activation energy (E), diffusion coefficient (D_0), volume constant (A) and the initial closure temperature estimate (T_{C0}) of 425 °C for muscovite were taken from Harrison et al. (2009). Grainsize (a) was estimated at the time of $^{40}Ar/^{39}Ar$ analysis.

Locality	Hornblende cooling age		Mica cooling age			Mineral Constants				
	Sample	Cooling age (Ma, ± 2σ)	Sample	Mineral	Cooling age (Ma, ± 2σ)	T_{C0} (°C)	a (μm)	E (kcal/mol)	D_0 (cm^2/s)	A
Biranup Zone										
SW of Urayrie Rock	EAF012	1194 ± 6	EAF015	Ms	1177 ± 5	425	350	63 ± 7	$2.3^{+70}_{-2.2}$	55
Ponton Creek	EAF038	1192 ± 13	EAF039B	Bt	1169 ± 5	300	350	50.5 ± 2.2	$0.4^{+0.96}_{-0.28}$	27
Fraser Zone										
Wyralinu Hill	EAF055B	1217 ± 8	EAF054	Bt	1205 ± 4	300	350	50.5 ± 2.2	$0.4^{+0.96}_{-0.28}$	27

Table A4.3-2 Probability distributions and values of variables used in the Monte Carlo simulation. The uncertainty of each random variable was modelled using either a uniform, triangular or normal probability distribution. The values of all other variables in Equation 1 are the same as those in Table A4.3-1 above.

Variable	Input Probability Distribution	Value	Source
Hornblende			
$^{40}Ar/^{39}Ar$ age (Ma)	Normal (mean, σ)	Varies for each mineral	Table 4.3
Biotite			
E	Triangular (min, mode, max)	50.5 ± 2.2 kcal/mol	Grove and Harrison (1996)
D_0	Triangular (min, mode, max)	$0.4\ ^{+0.96}_{-0.28}$ cm²/s	
Muscovite			
E	Triangular (min, mode, max)	63 ± 7 kcal/mol	Harrison et al. (2009)
D_0	Triangular (min, mode, max)	$2.3\ ^{+70}_{-2.2}$ cm²/s	
Mica			
$^{40}Ar/^{39}Ar$ cooling age (Ma)	Normal (mean, σ)	Varies for each mineral	Table 4.3
$^{40}Ar/^{39}Ar$ closure temperature (°C)	n/a	Directly calculated by iterating Equation 1	
Cooling rate (°C/Ma)	n/a	Initially calculated based on hornblende cooling age and closure temperature, and mica cooling age and initial closure temperature (T_{C0}). Cooling rate is recalculated after each iteration of Equation 1, using the newly calculated closure temperature.	

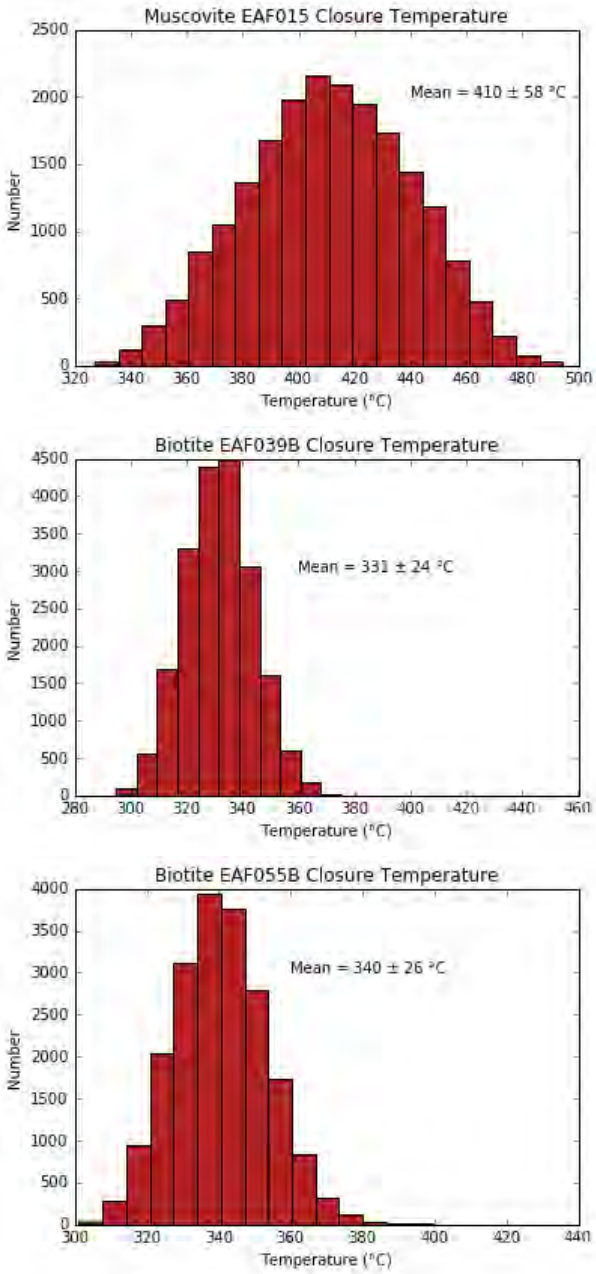

Figure A4.3-1 Histograms showing the results of the Monte Carlo simulation modelling the $^{40}Ar/^{39}Ar$ closure temperature in muscovite and biotite. The mean is reported with ± 2σ.

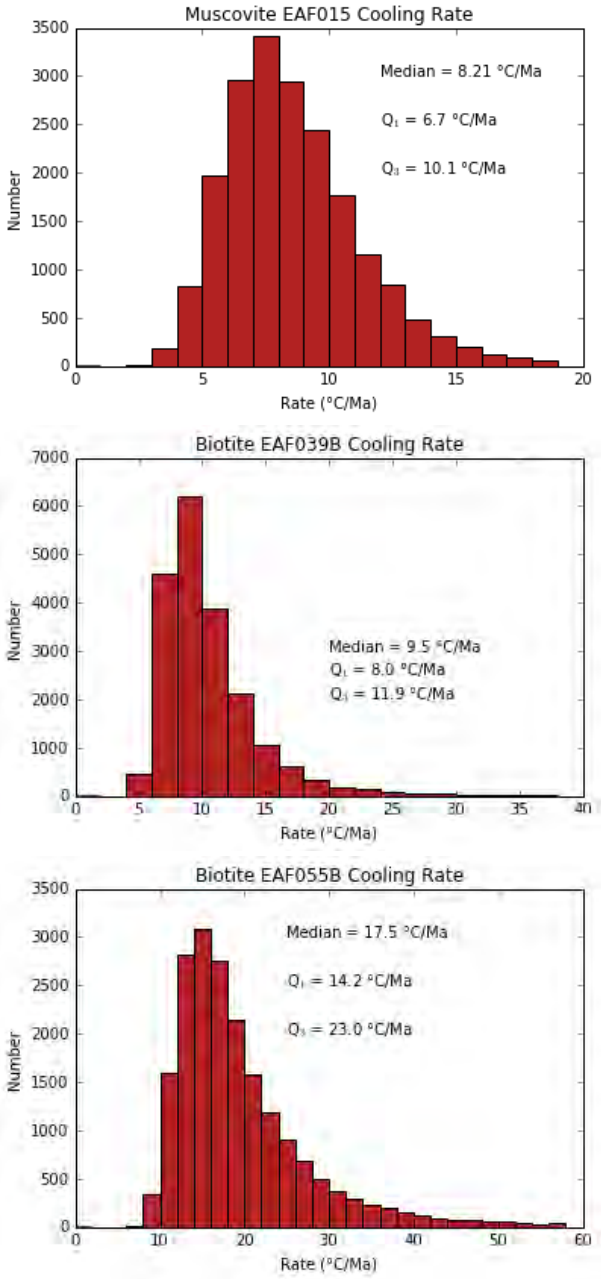

Figure A4.3-2 Histograms showing the results of the Monte Carlo simulation modelling the cooling rate between hornblende and mica closure temperature. The strongly right-tailed skew of the histograms is due to the large range in mathematically calculated cooling rates. This also skews the mean and standard deviation to unrealistically high values. For this reason, the median is a better measure of the central tendency of these populations, and the inter-quartile range is a more robust measure of scale than the standard deviation.

References

Dodson, M. H., 1973, Closure temperature in cooling geochronological and petrological systems: Contributions in Mineralogy and Petrology, v. 40, p. 259-274.

Grove, M., and Harrison, T. M., 1996, ^{40}Ar* diffusion in Fe-rich biotite: American Mineralogist, v. 81, p. 940-951.

Harrison, T. M., 1981, Diffusion of ^{40}Ar in hornblende: Contributions in Mineralogy and Petrology, v. 78, p. 324 - 331.

Harrison, T. M., Célérier, J., Aikman, A. B., Hermann, J., and Heizler, M. T., 2009, Diffusion of ^{40}Ar in muscovite: Geochimica et Cosmochimica Acta, v. 73, p. 1039-1051.

Harrison, T. M., Duncan, I., and McDougall, I., 1985, Diffusion of ^{40}Ar in biotite: Temperature, pressure and compositional effects: Geochimica et Cosmochimica Acta, v. 49, p. 2461 - 2468.

Scibiorski, E., Tohver, E., and Jourdan, F., 2015, Rapid cooling and exhumation in the western part of the Mesoproterozoic Albany-Fraser Orogen, Western Australia: Precambrian Research, v. 265, p. 232-248.

Appendix 5.1: Backscatter electron images of biotite

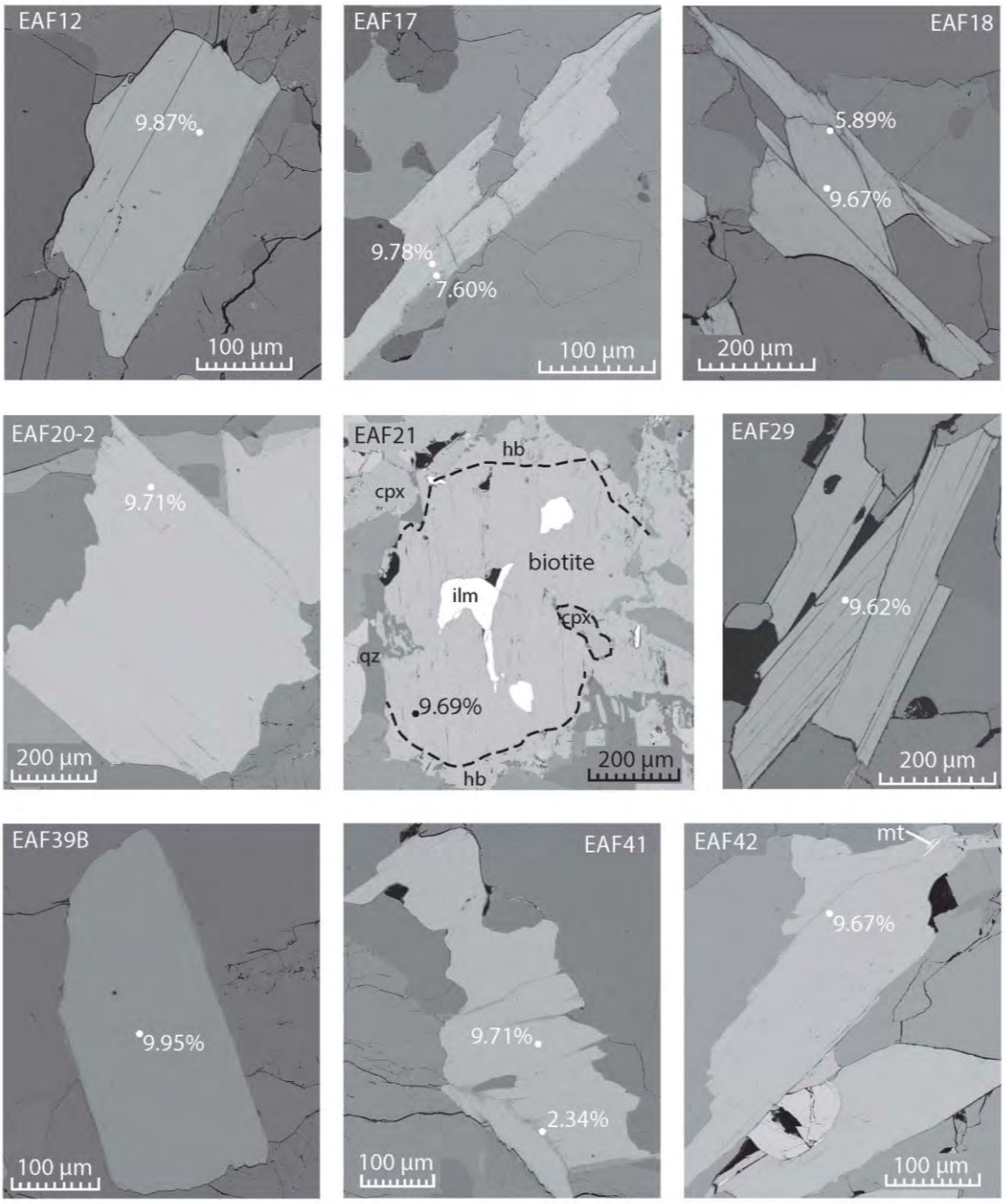

Figure A5.1.1 Backscatter electron (BSE) images of representative biotite from all Biranup Zone samples.

Appendix 6.1: Detailed sample descriptions and existing geochronology

EAF60: Mafic gneiss, Gnamma Hill, Fraser Zone

Site Description

Sample EAF60 is a mafic gneiss collected at Gnamma Hill in the southwestern Fraser Zone (Figure 6.1). This locality is dominated by metapelitic gneisses with a strong northeast trending, steeply dipping foliation. The mafic gneiss outcrops at the southwestern end of the outcrop, and is foliated parallel to the regional trend, although the contact with the metapelitic gneiss is not exposed. The protoliths of the pelitic gneisses were deposited between 1334 – 1293 Ma (Clark et al., 2014). Phase equilibria modelling of the metapelites at Gnamma Hill suggests that peak metamorphic assemblages equilibrated at 850 – 900 °C and > 7.7 GPa (Clark et al., 2014). Metamorphic zircon growth at Gnamma Hill occurred at 1292 ± 5 Ma, followed by leucosome crystallisation at 1285 ± 7 Ma (Clark et al., 2014).

Petrography

Sample EAF60 contains clinopyroxene, orthopyroxene, plagioclase, quartz, garnet, ilmenite, titanite, and minor hornblende, rutile, apatite, and zircon. The fabric is defined by gneissic compositional banding, with large intergrown porphyroclasts of hornblende and clinopyroxene. Quartz and feldspar occur as small, recrystallised grains with polygonal grain boundaries. Primary igneous textures are partially replaced by metamorphic granulitization at 0.1 – 0.2 mm grainsize. Titanite occurs as large anhedral to subhedral grains, locally rimmed by myrmekitic ilmenite and clinopyroxene.

EAF12: Pelitic garnet gneiss, Fly Dam Formation, Biranup Zone

Site Description

Sample EAF12 is a pelitic garnet gneiss from the Fly Dam Formation within the eastern Biranup Zone. The outcrop consists of a migmatitic, coarse-grained garnet-

bearing gneiss. The site is located at the hinge zone of a large synform with a shallowly east-plunging axis (Figure 6.1), approximately 30 m south of a larger outcrop sampled by Kirkland et al. (2016).

Kirkland et al. (2016) analysed U/Pb of zircon and titanite in two samples from this locality. Detrital zircons produced a weighted mean $^{207}Pb/^{206}Pb$ SIMS U/Pb age of 1685 ± 8 Ma, interpreted as the age of crystallisation of an igneous protolith. Metamorphic zircon rims from the same sample gave a concordia age of 1196 ± 11 Ma, interpreted as the age of metamorphism and migmatisation (Kirkland et al., 2016). From the second sample, titanite yielded a median ^{207}Pb-corrected $^{238}U/^{206}Pb$ age of 1203 ± 6 Ma, interpreted as the age of metamorphism, although a large fraction of titanite analyses (the youngest 45% of analyses) yielded a weighted average ^{207}Pb-corrected $^{238}U/^{206}Pb$ age of 1164 ± 5 Ma.

Petrography

In sample EAF12, large porphyroblasts of quartz, garnet (1 – 2 cm), plagioclase and perthitic alkali feldspar are wrapped by bands of finer-grained biotite, hornblende, titanite, ilmenite, and feldspar. Minor zircon, rutile, allanite and apatite are also present. Titanite occurs in two textural positions: as large euhedral to subhedral wedge-shaped grains with rounded ends associated with the bands of biotite and hornblende, and as subhedral to anhedral inclusions in large garnet porphyroblasts.

EAF35: Granitic gneiss, Uraryie Rock, Biranup Zone

Site Description

Sample EAF35 is a garnet-bearing granitic gneiss collected at Uraryie Rock within the eastern Biranup Zone (Figure 6.1). At this locality, the granitic gneiss is foliated ESE-WSW throughout the outcrop, and contains abundant coarse-grained leucosomes parallel to the gneissic foliation. Several mafic enclaves, parallel to the foliation, are also present.

U/Pb zircon geochronology of a different sample from Uraryie Rock yielded a population of detrital zircons with an interpreted magmatic crystallisation age of

1668 ± 11 Ma, and a smaller population of zircon rims interpreted to date metamorphism at 1162 ± 39 Ma (1σ; n = 6) (Kirkland et al., 2012).

Petrography

Sample EAF35 contains larger grains of quartz, microcline feldspar, and plagioclase with recrystallised or sutured grain boundaries, as well as minor hornblende, biotite, titanite, garnet, and ilmenite. Additional accessory minerals present include allanite, zircon, rutile and apatite. Titanite is relatively abundant and occurs as large subhedral grains (0.5 – 1.5 mm), some of which contain inclusions of rutile.

EAF38: Amphibolite, Ponton Creek, Biranup Zone

Site Description

Sample EAF38 is a garnet-bearing amphibolite from Ponton Creek, within the eastern Biranup Zone (Figure 6.1). The outcrop is foliated in a north-south direction, with a well-defined mineral lineation plunging steeply to the south. In addition to the sampled amphibolite, a range of lithologies outcrop at Ponton Creek, many of which have published U/Pb zircon geochronology: c. 1683 Ma migmatitic granitic gneisses, c. 1689 Ma psammitic gneisses, c. 1667 Ma foliated metagranodiorite and c. 1666 Ma porphyritic metamonzogranite (Geological Survey of Western Australia, 2016). Although most of the published zircon geochronology records migmatisation at c. 1680 Ma, one sample of migmatitic granitic gneiss (GSWA sample 194734) also yielded a small population of four zircon rim ages of 1193 ± 9 Ma, interpreted to date zircon growth during high-grade metamorphism (Kirkland et al., 2010).

Petrography

Sample EAF38 contains abundant plagioclase, hornblende, quartz, and garnet, and minor titanite, rutile, ilmenite, apatite, and zircon. Grainsizes are typically small and polygonal (0.2 – 2 mm), and garnet and hornblende are symplectitically intergrown. Titanite occurs as rims around intergrown grains of rutile and ilmenite.

DG02: Tonalitic orthogneiss, Daly Downs farm, Biranup Zone

Site Description

Sample DG02 is a migmatised, tonalitic orthogneiss collected at Daly Downs farm in the central Biranup Zone (Figure 6.1). At the outcrop, gneissic compositional banding defines a strong northeast-southwest striking foliation. Locally, the orientation of leucosomes define a C-C′ fabric suggesting sinistral shearing.

Although no previous U/Pb geochronology exists at this locality, zircon from a hornblende-biotite granodiorite gneiss 4km to the southwest yielded a magmatic crystallisation age of 1692 ± 22 Ma (GSWA sample 83658; Geological Survey of Western Australia, 2016). In addition, a granite pegmatite at Lake Gidong 23 km to the southwest records a crystallisation age of 1187 ± 12 Ma, interpreted as dating Stage II deformation (Nelson et al., 1995). Within the Coramup Gneiss 25 km to the southeast, Bodorkos and Clark (2004a, 2004b) report Stage I granulite facies metamorphism at c. 1300 - 1290 Ma, and Stage II metamorphism at 450 – 800 °C, 5 – 6 GPa; a Stage II syn-kinematic pegmatite dyke yielded a U/Pb zircon age of 1168 ± 12 Ma. Stage II metamorphism was followed by amphibolite facies retrogression.

Petrography

Sample DG02 consists largely of plagioclase, quartz and orthoclase feldspar. The foliation is defined by the gneissic compositional banding, with mafic schlieren composed of biotite, hornblende, magnetite, ilmenite, and titanite. Accessory minerals rutile, apatite and zircon are also present. Titanite is present both as small subhedral grains in the matrix, or as thin rims around large magnetite crystals.

References

Bodorkos, S., and Clark, D., 2004a, Evolution of a crustal-scale transpressive shear zone in the Albany-Fraser Orogen, SW Australia: 1. P-T conditions of Mesoproterozoic metamorphism in the Coramup Gneiss: Journal of Metamorphic Geology, v. 22, p. 691 - 711.

-, 2004b, Evolution of a crustal-scale transpressive shear zone in the Albany-Fraser Orogen, SW Australia: 2. Tectonic history of the Coramup Gneiss and a

kinematic framework for Mesoproterozoic collision of the West Australian and Mawson cratons: Journal of Metamorphic Geology, v. 22, p. 713-731.

Clark, C., Kirkland, C. L., Spaggiari, C. V., Oorschot, C. W., Wingate, M. T. D., and Taylor, B., 2014, Proterozoic granulite formation driven by mafic magmatism: An example from the Fraser Range Metamorphics, Western Australia: Precambrian Research, v. 240, p. 1-21.

Geological Survey of Western Australia, 2016, Compilation of geochronology information 2016: Government of Western Australia, ISBN: 9781741686876.

Kirkland, C. L., Spaggiari, C. V., Johnson, T. E., Smithies, R. H., Danišík, M., Evans, N., Wingate, M. T. D., Clark, C., Spencer, C., Mikucki, E., and McDonald, B. J., 2016, Grain size matters: Implications for element and isotopic mobility in titanite: Precambrian Research, v. 278, p. 283-302.

Kirkland, C. L., Wingate, M. T. D., Spaggiari, C. V., and Pawley, M. J., 2010, 194734: migmatitic granitic gneiss, Ponton Creek: Geological Survey of Western Australia, Geochronology Record 857.

-, 2012, 194726: granodiorite gneiss, Uraryie Rock: Geological Survey of Western Australia, Geochronology Record 1020.

Nelson, D. R., Myers, J. S., and Nutman, A. P., 1995, Chronology and evolution of the Middle Proterozoic Albany-Fraser Orogen, Western Australia: Australian Journal of Earth Sciences, v. 42, no. 5, p. 481 - 495.

Appendix 6.2: Garnet EMP and LA-ICPMS data

Electron microprobe method

Representative garnets from samples EAF60, EAF12 and EAF38 were analysed by wavelength dispersive spectroscopy at the Centre for Microscopy, Characterisation and Analysis (University of Western Australia, Perth, Australia). Compositional analyses of garnet were acquired on a JEOL JXA8530F electron microprobe equipped with 5 tuneable wavelength dispersive spectrometers, and with operating conditions of a 40° take-off angle, and beam energy of 15 keV. The beam current was 15 nA, and the beam diameter was defocussed to 5 μm.

Elements were acquired using analyzing crystals LiF for Ti kα, Fe kα and Mn kα; PETJ for Ca kα and K kα; TAP for Mg kα, Si kα, Al kα and Na kα. The standards were Magnetite for Fe kα, Periclase for Mg kα, Rutile for Ti kα, Wollastonite for Ca kα, Si kα, Jadeite for Na kα, Mn for Mn kα, Orthoclase for K kα, and Kakanui Pyrope for Al kα. Counting time was 20 seconds for all elements: Si kα, Al kα, Na kα, Mg kα, Ti kα, Ca kα, K kα, Fe kα, and Mn kα.

The intensity data was corrected for Time Dependent Intensity (TDI) loss (or gain) using a self-calibrated correction for Si kα, K kα, and Fe kα. MAN background intensity data was used throughout (Donovan and Tingle, 1996). Interference corrections were applied to Fe for interference by Mn (Donovan et al., 1993).

Detection limits were 0.011 wt% for Ca kα, 0.013 wt% for Al kα, 0.038 wt% for Mn kα, and 0.063 wt% for Ti kα. Analytical sensitivity (at the 99% confidence level) ranged from 0.425 % relative for Si kα, to 0.787 % relative for K kα, to 20.111 % relative for Ca kα.

Oxygen was calculated by cation stoichiometry and included in the matrix correction. Element H was calculated by stoichiometry to oxygen, at 0.167 atoms H relative to 1.0 atom of O. The ZAF algorithm utilised was the Armstrong-Love/Scott correction (Armstrong, 1988).

Garnet compositions were calculated on a 24(O) basis, with Fe^{3+} calculated using the method of Droop (1987), and are summarised in Table A6.2-1 below.

Table A6.2-1 Representative garnet compositions from electron microprobe analysis.

	EAF12			EAF60			EAF38		
	Grt1	Grt2	Grt3	Grt1	Grt2	Grt3	Grt1	Grt2	Grt3
SiO_2	36.42	36.59	37.10	38.02	38.20	38.46	36.93	37.69	37.26
TiO_2	0.08	0.11	0.13	0.07	0.19	4.23	0.11	0.03	0.03
Al_2O_3	21.53	21.43	20.75	21.38	21.54	19.43	21.80	22.15	21.77
Cr_2O_3	0.02	0.01	0.02	0.01	0.01	0.02	0.08	0.01	0.03
Fe_2O_3	3.19	3.08	2.25	0.72	0.75	0.00	2.99	2.19	2.73
FeO	20.57	20.93	21.75	24.65	25.19	23.28	23.64	24.02	24.02
MnO	0.79	0.86	0.93	1.13	0.70	0.73	0.70	0.72	0.64
MgO	2.21	2.30	1.43	1.57	2.28	1.66	5.14	5.28	5.26
CaO	14.28	13.97	14.96	13.17	12.39	14.31	8.35	8.50	8.12
Na_2O	0.01	0.02	0.01	0.01	0.00	0.01	0.01	0.01	0.01
K_2O	0.00	0.00	0.01	0.01	0.00	0.01	0.01	0.00	0.04
Total	99.09	99.29	99.34	100.74	101.26	102.15	99.75	100.59	99.91
				Garnet formula based on 24 O					
Si	5.78	5.80	5.90	5.97	5.95	5.93	5.79	5.85	5.83
Ti	0.01	0.01	0.02	0.01	0.02	0.50	0.01	0.00	0.00
Zn	0.00	0.00	0.00	0.00	0.00	0.00	0.00	0.00	0.00
Al	4.03	4.00	3.89	3.96	3.96	3.53	4.03	4.05	4.01
Cr	0.00	0.00	0.00	0.00	0.00	0.00	0.01	0.00	0.00
Fe^{3+}	0.38	0.37	0.27	0.09	0.09	0.00	0.35	0.26	0.32
Fe^{2+}	2.73	2.78	2.89	3.24	3.28	3.00	3.10	3.12	3.14
Mn	0.11	0.12	0.13	0.15	0.09	0.10	0.09	0.09	0.08
Mg	0.52	0.54	0.34	0.37	0.53	0.38	1.20	1.22	1.23
Ca	2.43	2.37	2.55	2.22	2.07	2.37	1.40	1.41	1.36
Na	0.00	0.00	0.00	0.00	0.00	0.00	0.00	0.00	0.00
K	0.00	0.00	0.00	0.00	0.00	0.00	0.00	0.00	0.00
Pyrope	*9.0*	*9.4*	*5.5*	*6.1*	*8.9*	*7.2*	*20.7*	*20.9*	*21.1*
Almandine	*47.2*	*47.8*	*48.9*	*54.2*	*55.0*	*56.4*	*53.5*	*53.3*	*54.0*
Spessartine	*1.8*	*2.0*	*1.9*	*2.5*	*1.5*	*1.8*	*1.6*	*1.6*	*1.5*
Gr-Uv-An	*42.0*	*40.9*	*43.6*	*37.1*	*34.6*	*34.7*	*24.2*	*24.2*	*23.4*

References

Armstrong, J., 1988, Quantitative analysis of silicate and oxide minerals: comparison of Monte Carlo, ZAF and phi-rho-z procedures: Microbeam analysis, v. 23, p. 239-246.

Donovan, J. J., Snyder, D. A., and Rivers, M. L., 1993, An improved interference correction for trace element analysis: Microbeam Analysis, v. 2, p. 23-28.

Donovan, J. J., and Tingle, T. N., 1996, An improved mean atomic number background correction for quantitative microanalysis: Journal of Microscopy and Microanalysis, v. 2, no. 1, p. 1-7.

Droop, G. T. R., 1987, A general equation for estimating Fe3+ concentrations in ferromagnesian silicates and oxides from microprobe analyses, using stoichiometric criteria: Mineralogical Magazine, v. 51, p. 431-435.

Table A6.2-2 LA-ICPMS analyses of garnet in sample EAF60. Concentration, 1s uncertainty and LOD reported in ppm.

Element	Grt1a			Grt2a			Grt3a			Grt3b		
	Conc.	1s	LOD	Conc.	1s	LOD	Conc.	1s	LOD	Conc.	1s	LOD
Si29	181140.7	7678.5	2240.0	181140.7	7873.2	2450.3	181140.7	8005.4	2491.9	181140.7	8083.8	2533.4
Ca44	77784.8	4105.5	44.3	75397.9	4088.0	44.0	78819.0	4317.7	43.7	75577.1	4175.0	42.3
Ca43	77486.4	4380.0	144.9	75362.7	4382.0	140.1	77674.3	4562.7	144.4	78422.5	4646.4	142.9
Ti49	411.75	28.17	0.92	1212.02	84.81	0.96	617.31	43.80	0.92	676.23	48.38	0.96
V51	18.03	0.99	0.08	210.53	11.69	0.10	212.61	11.93	0.09	197.02	11.14	0.09
Cr52	< LOD	2.01	2.70	189.84	26.47	2.76	80.12	11.30	2.84	80.49	11.42	2.73
Rb85	< LOD	0.02	0.04	< LOD	0.02	0.04	0.06	0.02	0.04	< LOD	0.02	0.04
Sr88	< LOD	0.01	0.02	0.02	0.01	0.02	0.06	0.01	0.01	< LOD	0.01	0.02
Y89	34.40	2.44	0.03	24.24	1.78	0.03	20.12	1.50	0.03	11.13	0.84	0.02
Zr91	5.016	0.344	0.111	7.234	0.495	0.142	2.325	0.215	0.151	3.520	0.291	0.128
Nb93	< LOD	0.002	0.006	< LOD	0.004	0.009	0.009	0.005	0.007	< LOD	0.005	0.013
La139	< LOD	0.002	0.004	0.009	0.003	0.006	< LOD	0.003	0.006	< LOD	0.003	0.006
Ce140	0.059	0.006	0.002	0.043	0.006	0.005	0.042	0.006	0.005	0.030	0.005	0.005
Pr141	0.050	0.006	0.004	0.013	0.003	0.005	0.027	0.004	0.003	0.022	0.004	0.006
Nd143	0.718	0.064	0.027	0.231	0.032	0.024	0.341	0.043	0.031	0.352	0.043	0.020
Sm147	1.636	0.118	0.016	0.412	0.043	0.022	0.708	0.064	0.021	0.569	0.056	0.024
Eu151	0.870	0.057	0.005	0.316	0.025	0.006	0.546	0.040	0.004	0.645	0.046	0.006
Gd157	4.166	0.291	0.030	1.247	0.103	0.031	2.067	0.161	0.031	1.787	0.140	0.026
Tb159	0.794	0.052	0.004	0.346	0.025	0.005	0.466	0.033	0.004	0.300	0.023	0.004
Dy163	5.737	0.388	0.013	3.068	0.215	0.015	3.402	0.248	0.023	2.390	0.183	0.014
Ho165	1.155	0.071	0.004	0.820	0.054	0.004	0.701	0.046	0.003	0.364	0.026	0.005
Er167	3.079	0.205	0.018	2.917	0.194	0.012	1.798	0.129	0.016	0.912	0.072	0.016
Tm169	0.437	0.029	0.002	0.459	0.031	0.003	0.255	0.019	0.003	0.105	0.009	0.004

Element	Grt1a			Grt2a			Grt3a			Grt3b		
	Conc.	1s	LOD	Conc.	1s	LOD	Conc.	1s	LOD	Conc.	1s	LOD
Yb171	3.488	0.215	0.016	3.305	0.215	0.017	1.690	0.118	0.025	0.724	0.065	0.026
Lu175	0.506	0.030	0.005	0.568	0.034	0.004	0.280	0.019	0.003	0.119	0.010	0.004
Hf179	0.161	0.025	0.024	0.079	0.018	0.023	0.085	0.022	0.029	0.088	0.022	0.028
Ta181	< LOD	0.002	0.004	< LOD	0.002	0.005	< LOD	0.000	0.006	< LOD	0.002	0.005
Pb208	< LOD	0.009	0.020	< LOD	0.010	0.021	< LOD	0.010	0.022	< LOD	0.009	0.020
Th232	< LOD	0.006	0.014	0.021	0.006	0.011	0.012	0.006	0.012	< LOD	0.005	0.012
U238	< LOD	0.006	0.013	< LOD	0.006	0.014	< LOD	0.006	0.013	< LOD	0.006	0.014

Table A6.2-3 LA-ICPMS analyses of garnet in sample EAF12. Concentration, 1s uncertainty and LOD reported in ppm.

Element	Grt1a			Grt1b			Grt1c			Grt2c			Grt2d			Grt3b			Grt3c		
	Conc.	1s	LOD	Conc.	1s	LOD	Conc.	1s	LOD	Conc.	1s	LOD	Conc.	1s	LOD	Conc.	1s	LOD	Conc.	1s	LOD
Si29	170233.2	7444.5	2444.3	170233.2	7332.7	2018.2	170233.2	7428.9	2034.6	170233.2	7492.8	2466.6	170233.2	7596.3	2438.5	170233.2	7541.4	2220.8	170233.2	7471.2	2237.8
Ca44	83141.94	4930.44	39.85	75078.92	4472.14	37.59	80516.18	4854.21	40.06	82200.28	5101.03	38.61	85862.25	5395.63	38.74	91690.65	5858.97	38.80	85298.62	5490.03	36.68
Ca43	81158.8	5202.1	132.4	74958.1	4832.7	118.6	79578.5	5194.0	129.9	82488.8	5551.9	125.6	84783.4	5780.0	124.2	91792.0	6373.3	131.9	85612.2	5993.9	123.6
Ti49	406.54	32.04	0.87	309.25	24.62	1.02	264.90	21.42	1.18	420.39	34.97	0.96	319.04	26.97	1.00	323.87	27.96	0.87	316.34	27.58	0.83
V51	175.99	10.66	0.08	358.83	21.82	0.08	141.63	8.73	0.08	223.76	14.16	0.10	119.30	7.66	0.10	163.19	10.63	0.09	114.02	7.49	0.07
Cr52	158.26	24.30	2.58	304.93	47.18	2.49	210.10	32.86	2.63	91.79	14.83	2.53	9.69	1.95	2.50	8.24	1.79	2.54	45.98	7.79	2.37
Rb85	< LOD	0.021	0.051	0.038	0.018	0.038	< LOD	0.019	0.044	< LOD	0.017	0.035	< LOD	0.019	0.040	0.063	0.020	0.037	< LOD	0.019	0.048
Sr88	< LOD	0.011	0.022	< LOD	0.011	0.023	< LOD	0.010	0.020	< LOD	0.009	0.019	< LOD	0.008	0.016	0.033	0.011	0.021	0.032	0.011	0.020
Y89	174.24	14.40	0.02	276.70	23.06	0.02	160.72	13.58	0.03	202.42	17.73	0.03	121.86	10.82	0.02	161.97	14.72	0.03	99.72	9.17	0.02
Zr91	1.416	0.152	0.111	1.234	0.142	0.105	1.052	0.132	0.135	1.032	0.132	0.098	1.416	0.162	0.136	1.052	0.121	0.049	< LOD	1.740	1.497
Nb93	< LOD	0.005	0.008	< LOD	0.003	0.009	0.008	0.004	0.005	< LOD	0.004	0.010	< LOD	0.005	0.009	< LOD	0.006	0.014	< LOD	0.003	0.006
La139	< LOD	0.003	0.006	< LOD	0.002	0.005	< LOD	0.003	0.006	< LOD	0.002	0.006	< LOD	0.002	0.005	< LOD	0.002	0.005	< LOD	0.002	0.005
Ce140	0.012	0.003	0.004	0.014	0.004	0.005	0.017	0.004	0.004	0.013	0.003	0.005	0.017	0.004	0.004	0.012	0.003	0.003	< LOD	0.001	0.003
Pr141	0.010	0.003	0.004	0.009	0.003	0.005	0.016	0.003	0.004	0.006	0.003	0.005	0.008	0.003	0.005	0.008	0.003	0.004	< LOD	0.002	0.004
Nd143	0.284	0.037	0.027	0.192	0.030	0.031	0.228	0.034	0.033	0.200	0.031	0.027	0.209	0.033	0.027	0.152	0.029	0.034	0.036	0.015	0.023
Sm147	0.928	0.081	0.022	0.984	0.085	0.025	0.824	0.075	0.023	1.254	0.111	0.014	0.602	0.061	0.014	0.693	0.069	0.020	0.126	0.020	0.000
Eu151	0.520	0.040	0.006	0.288	0.024	0.006	0.534	0.042	0.007	0.391	0.033	0.006	0.354	0.031	0.006	0.330	0.029	0.006	0.134	0.015	0.007
Gd157	5.139	0.415	0.031	8.144	0.658	0.031	5.918	0.486	0.025	10.015	0.850	0.028	2.853	0.253	0.029	4.421	0.395	0.031	1.143	0.111	0.031
Tb159	2.033	0.152	0.003	3.085	0.223	0.003	1.932	0.142	0.003	3.429	0.263	0.003	1.136	0.090	0.003	1.720	0.142	0.004	0.635	0.053	0.003
Dy163	22.731	1.760	0.017	35.144	2.752	0.011	20.809	1.649	0.012	32.817	2.701	0.013	13.697	1.153	0.015	20.435	1.750	0.008	9.125	0.799	0.015
Ho165	6.383	0.445	0.000	10.015	0.698	0.004	5.159	0.364	0.003	7.172	0.526	0.003	4.218	0.314	0.005	5.847	0.445	0.003	3.278	0.253	0.004
Er167	20.293	1.477	0.019	31.643	2.317	0.013	15.700	1.173	0.021	17.703	1.366	0.014	14.638	1.143	0.017	19.797	1.588	0.019	12.686	1.032	0.016
Tm169	2.934	0.212	0.003	4.704	0.334	0.003	2.327	0.172	0.003	2.003	0.152	0.004	2.135	0.162	0.003	2.974	0.233	0.003	2.033	0.162	0.003

Element	Grt1a			Grt1b			Grt1c			Grt2c			Grt2d			Grt3b			Grt3c		
	Conc.	1s	LOD	Conc.	1s	LOD	Conc.	1s	LOD	Conc.	1s	LOD	Conc.	1s	LOD	Conc.	1s	LOD	Conc.	1s	LOD
Yb171	20.698	1.366	0.037	32.260	2.135	0.019	16.995	1.153	0.029	11.512	0.809	0.028	14.881	1.062	0.022	21.922	1.588	0.020	15.093	1.103	0.025
Lu175	3.116	0.192	0.005	4.552	0.283	0.004	2.499	0.162	0.005	1.342	0.090	0.004	2.185	0.152	0.004	3.369	0.233	0.004	2.215	0.152	0.004
Hf179	< LOD	0.014	0.029	< LOD	0.017	0.035	< LOD	0.015	0.028	0.038	0.016	0.029	0.046	0.015	0.020	< LOD	0.015	0.029	0.023	0.012	0.022
Ta181	< LOD	0.002	0.003	0.010	0.002	0.000	0.010	0.002	0.002	< LOD	0.002	0.004	0.008	0.003	0.003	0.003	0.001	0.000	< LOD	0.002	0.005
Pb208	< LOD	0.008	0.018	< LOD	0.008	0.018	< LOD	0.009	0.021	< LOD	0.008	0.020	< LOD	0.008	0.019	< LOD	0.009	0.017	< LOD	0.008	0.017
Th232	< LOD	0.006	0.013	< LOD	0.005	0.012	< LOD	0.006	0.015	< LOD	0.004	0.011	0.013	0.006	0.011	0.017	0.005	0.010	< LOD	0.006	0.013
U238	< LOD	0.006	0.013	< LOD	0.006	0.014	< LOD	0.006	0.014	< LOD	0.005	0.013	< LOD	0.006	0.013	< LOD	0.006	0.013	< LOD	0.006	0.012

Table A6.2-4 LA-ICPMS analyses of garnet in sample EAF38. Concentration, 1s uncertainty and LOD reported in ppm.

Element	Grt1b			Grt1c			Grt2c			Grt3a			Grt3b			Grt3c		
	Conc.	1s	LOD	Conc.	1s	LOD	Conc.	1s	LOD	Conc.	1s	LOD	Conc.	1s	LOD	Conc.	1s	LOD
Si29	174465.2	8546.2	2103.6	174465.2	7620.0	1765.1	174465.2	7703.9	1909.1	174465.2	7773.6	2456.4	174465.2	7684.9	1876.7	174465.2	8574.1	2341.1
Ca44	52735.7	3865.3	36.5	46016.1	3327.2	36.8	48213.0	3597.6	32.9	45870.4	3461.9	38.3	43387.9	3300.2	34.8	52771.5	4134.2	36.8
Ca43	53062.6	4253.8	116.1	45559.9	3616.7	113.5	47939.1	3932.5	113.8	46841.0	3887.8	127.5	44126.0	3694.8	117.0	51827.2	4459.2	126.6
Ti49	231.80	23.36	0.77	129.76	13.09	0.88	195.85	20.34	0.83	221.58	23.25	0.94	132.54	14.14	0.98	173.71	18.96	0.92
V51	474.50	35.27	0.08	169.07	12.41	0.08	88.31	6.69	0.06	131.78	10.08	0.08	143.00	11.02	0.07	84.28	6.70	0.07
Cr52	96.50	18.17	2.26	< LOD	1.04	2.29	3.30	1.16	2.05	< LOD	1.88	2.36	< LOD	1.08	2.16	< LOD	1.53	2.28
Rb85	< LOD	0.02	0.05	0.05	0.02	0.04	0.11	0.02	0.04	0.07	0.02	0.04	< LOD	0.02	0.04	0.04	0.02	0.03
Sr88	0.13	0.02	0.02	< LOD	0.01	0.02	0.09	0.02	0.02	0.03	0.01	0.02	0.03	0.01	0.02	0.05	0.01	0.02
Y89	64.53	6.86	0.03	54.74	5.83	0.03	72.98	8.07	0.03	32.38	3.63	0.03	43.18	4.88	0.03	38.97	4.51	0.03
Zr91	1.607	0.207	0.112	1.306	0.156	0.068	1.814	0.207	0.084	1.690	0.187	0.051	1.006	0.145	0.123	2.353	0.280	0.099
Nb93	< LOD	0.005	0.008	< LOD	0.004	0.009	< LOD	0.005	0.010	< LOD	0.005	0.013	0.016	0.005	0.000	0.011	0.007	0.010
La139	0.090	0.011	0.004	0.016	0.004	0.004	0.046	0.007	0.006	< LOD	0.003	0.006	< LOD	0.003	0.006	0.013	0.004	0.005
Ce140	0.148	0.017	0.004	0.019	0.004	0.005	0.105	0.011	0.004	0.046	0.007	0.005	0.022	0.004	0.004	0.025	0.007	0.009
Pr141	0.027	0.005	0.005	0.007	0.003	0.005	0.055	0.008	0.005	0.021	0.004	0.005	0.006	0.003	0.005	0.031	0.006	0.004
Nd143	0.230	0.044	0.032	0.145	0.028	0.024	0.695	0.081	0.026	0.359	0.049	0.013	0.167	0.031	0.023	0.408	0.063	0.035
Sm147	0.337	0.049	0.016	0.281	0.039	0.027	1.545	0.156	0.012	0.577	0.067	0.018	0.312	0.044	0.025	1.524	0.166	0.029
Eu151	0.179	0.022	0.006	0.205	0.022	0.005	0.822	0.079	0.006	0.350	0.036	0.005	0.301	0.032	0.006	0.830	0.085	0.008
Gd157	1.555	0.176	0.029	2.281	0.249	0.031	6.739	0.726	0.031	2.613	0.290	0.031	2.146	0.249	0.030	5.402	0.622	0.026
Tb159	0.627	0.061	0.003	0.659	0.063	0.003	1.555	0.156	0.004	0.669	0.067	0.005	0.698	0.071	0.003	1.099	0.114	0.003
Dy163	6.977	0.715	0.010	6.915	0.705	0.017	12.431	1.317	0.015	5.609	0.601	0.011	6.760	0.736	0.014	7.434	0.829	0.020
Ho165	2.208	0.197	0.003	1.783	0.166	0.004	2.602	0.238	0.003	1.120	0.104	0.004	1.566	0.156	0.003	1.275	0.124	0.003
Er167	8.419	0.798	0.017	5.474	0.518	0.016	6.780	0.674	0.013	2.550	0.259	0.019	3.971	0.404	0.014	3.017	0.321	0.011
Tm169	1.348	0.124	0.005	0.800	0.076	0.004	0.798	0.078	0.000	0.289	0.030	0.004	0.476	0.049	0.001	0.346	0.037	0.004

Element	Grt1b			Grt1c			Grt2c			Grt3a			Grt3b			Grt3c		
	Conc.	1s	LOD	Conc.	1s	LOD	Conc.	1s	LOD	Conc.	1s	LOD	Conc.	1s	LOD	Conc.	1s	LOD
Yb171	10.534	0.912	0.021	5.339	0.467	0.022	5.132	0.467	0.029	1.493	0.145	0.024	2.519	0.238	0.031	1.783	0.187	0.021
Lu175	1.763	0.145	0.004	0.771	0.062	0.006	0.706	0.059	0.005	0.149	0.015	0.005	0.297	0.027	0.004	0.204	0.021	0.004
Hf179	0.089	0.026	0.027	0.041	0.017	0.025	0.031	0.016	0.025	< LOD	0.017	0.034	< LOD	0.017	0.033	0.033	0.018	0.024
Ta181	< LOD	0.003	0.005	< LOD	0.002	0.005	< LOD	0.001	0.003	< LOD	0.003	0.007	< LOD	0.002	0.005	< LOD	0.002	0.005
Pb208	0.213	0.026	0.015	0.050	0.011	0.018	0.367	0.037	0.018	< LOD	0.009	0.017	< LOD	0.009	0.018	0.027	0.010	0.016
Th232	0.058	0.010	0.012	< LOD	0.006	0.014	< LOD	0.006	0.012	< LOD	0.006	0.013	< LOD	0.006	0.012	0.031	0.008	0.011
U238	0.025	0.008	0.013	< LOD	0.006	0.014	< LOD	0.006	0.013	0.016	0.007	0.013	< LOD	0.006	0.012	< LOD	0.007	0.014

Appendix 6.3: Common lead composition for calculation of ^{207}Pb-corrected $^{238}U/^{206}Pb$ ages

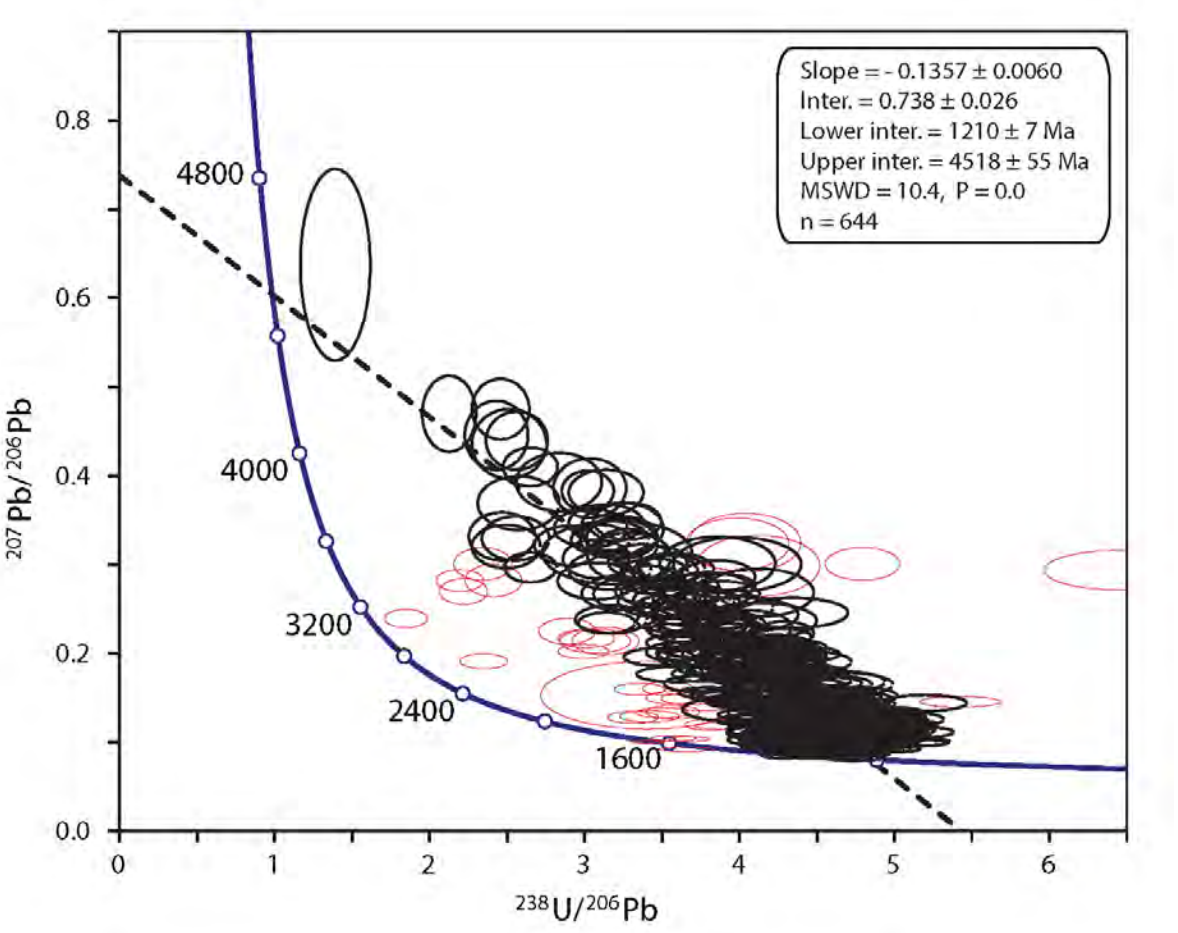

Figure A6.3-1 Tera-Wasserburg concordia plot of all U/Pb analyses. All five samples appear to have a similar common lead (Pb_C) composition, with an average $^{207}Pb/^{206}Pb$ ratio of 0.738 ± 0.026. This average Pb_C composition is used to calculate the ^{207}Pb-corrected $^{238}U/^{206}Pb$ ages. Error ellipses are plotted at 2σ. Black analyses are used for the age calculation (n = 644), and red analyses were excluded (n = 33) due to evidence for Pb mobility (i.e. significantly displaced to the left or right of the Pb_C – Pb* mixing line).

Appendix 6.4: Titanite LA-ICPMS data

Table A6.4-1: LA-ICPMS analytical data for sample EAF60.

Analysis number	Na23 ppm	Na23 ppm 2SE	Na23 ppm LOD	Al27 ppm	Al27 ppm 2SE	Al27 ppm LOD	Si28 ppm	Si28 ppm 2SE	Si28 ppm LOD	Ca44 ppm	Ca44 ppm 2SE	Ca44 ppm LOD
eaf60 - 1.d	86	9.6	27	13550	240	3	149000	2300	8500	214000	3100	250
eaf60 - 2.d	80.9	7.1	29	13400	190	3.4	150100	2500	9200	214100	3600	380
eaf60 - 3.d	81	8.8	38	13830	170	2.9	146400	2300	6100	214400	2300	290
eaf60 - 4.d	117.1	8.3	24	14130	180	2.6	145100	3000	7600	216100	2600	320
eaf60 - 5.d	102.1	7.6	32	13960	240	3.9	148500	2200	5800	214000	3200	290
eaf60 - 6.d	171	16	22	13840	180	3	147100	2300	5800	213700	3400	310
eaf60 - 7.d	104.1	9.5	25	12480	140	2.9	148300	3100	6100	215400	2600	270
eaf60 - 8.d	98.6	7.9	23	12990	170	3.3	149900	1900	7800	213900	2400	330
eaf60 - 9.d	97	10	20	12540	210	3.5	148700	2800	4600	213900	2300	230
eaf60 - 10.d	160	11	32	13180	210	4.5	147700	2100	5400	214500	3200	350
eaf60 - 11.d	141.2	9.3	32	14980	210	2.8	150000	2600	3000	214300	3400	280
eaf60 - 12.d	329	17	27	14650	160	2.4	149800	3300	7100	216000	2500	280
eaf60 - 13.d	324	11	25	15150	170	4.5	149800	2600	7600	214800	2700	300
eaf60 - 14.d	254	11	31	14020	210	4.1	147800	1900	9100	215400	2700	310
eaf60 - 15.d	138	11	24	13320	170	4.5	148700	2700	6900	215400	2900	180
eaf60 - 16.d	100.5	9.3	24	13170	140	2.3	146600	2100	7500	215400	2400	400
eaf60 - 17.d	139	10	27	13530	150	2.9	147800	2400	8400	215800	2800	310
eaf60 - 18.d	108	10	19	13190	160	4.2	146800	2100	4200	215200	2700	380
eaf60 - 19.d	88.7	9.2	27	13390	160	2.8	148200	1700	5200	214300	2600	220
eaf60 - 20.d	91	7.6	25	14980	150	3.9	148900	2200	4300	214500	2500	250
eaf60 - 21.d	747	18	24	15920	230	3.8	147100	2200	9800	213700	3200	330
eaf60 - 22.d	493	12	23	14720	190	3.9	146600	2200	5800	211800	2800	350
eaf60 - 23.d	164	11	24	13870	180	4.9	146900	2400	4600	215400	2700	210
eaf60 - 24.d	77.2	9.7	28	14620	180	3.6	147400	1900	9300	215000	2900	290
eaf60 - 25.d	95.5	8.4	18	11950	140	4.2	147700	2400	4900	216800	2600	260
eaf60 - 26.d	75.5	9.1	24	15320	200	4.1	147200	2500	2200	216000	3000	220

Analysis number	Na23 ppm	Na23 ppm 2SE	Na23 ppm LOD	Al27 ppm	Al27 ppm 2SE	Al27 ppm LOD	Si28 ppm	Si28 ppm 2SE	Si28 ppm LOD	Ca44 ppm	Ca44 ppm 2SE	Ca44 ppm LOD
eaf60 - 27.d	68.3	9.8	24	13500	190	5.4	150000	2700	4400	216800	3100	210
eaf60 - 28.d	55.8	8.6	28	14440	200	4.1	150100	2400	7100	212500	2900	370
eaf60 - 29.d	191	11	22	12880	180	3.8	145300	2200	8600	215700	2800	310
eaf60 - 30.d	54.7	8	17	12690	170	2.7	146700	1800	6400	218300	2800	250
eaf60 - 31.d	79.1	9.3	32	12060	190	3.5	147100	2300	4400	215300	2900	240
eaf60 - 32.d	74.6	8.6	21	11740	200	3.9	147400	3000	7000	215000	3600	370
eaf60 - 33.d	64.8	8.9	23	13920	150	3.4	145800	2700	4900	216800	2700	310
eaf60 - 34.d	74.8	6.2	28	13980	210	3	145300	1900	6000	215600	2900	310
eaf60 - 35.d	77.4	7.8	21	15650	230	3.6	148600	2200	4700	216900	2900	200
eaf60 - 36.d	79.9	8.1	27	15340	210	3.6	146200	2300	7400	216600	3500	240
eaf60 - 37.d	93.8	8.4	22	14350	190	3	145200	2600	5000	215600	2500	360
eaf60 - 38.d	81.3	7	19	14550	190	3.7	147600	2300	5000	213900	2400	300
eaf60 - 39.d	88.4	8.6	28	14830	180	3.2	149400	2600	5200	219200	3400	270
eaf60 - 40.d	249.5	8	28	15230	230	3.3	147200	2300	8400	213800	2800	230
eaf60 - 41.d	104.2	8.2	28	13920	260	3.8	143900	3300	4600	217100	3300	370
eaf60 - 42.d	112.4	8.9	28	13590	180	3.4	144800	2800	7800	216800	3100	350
eaf60 - 43.d	104	7.4	31	14690	190	3.7	149900	2200	5800	213800	3200	260
eaf60 - 44.d	106	10	29	12780	160	4	145500	2500	4100	215700	2600	370
eaf60 - 45.d	201.1	9.3	24	13840	160	3.9	146800	2700	5700	213700	2900	290
eaf60 - 46.d	123.6	8.2	23	13600	130	3.5	146600	1700	6900	213400	2700	310
eaf60 - 47.d	97.5	7.9	24	12650	170	2.6	147900	2600	7700	217900	3100	220
eaf60 - 48.d	97	9.7	21	12970	180	3.1	148200	2600	6400	218000	3100	230
eaf60 - 49.d	98.3	7.6	34	13110	180	3	148100	2800	9900	219100	3200	320
eaf60 - 50.d	98.7	9.4	17	12360	130	2.9	147600	2500	7000	214900	2900	240
eaf60 - 51.d	108.9	9.8	16	12890	200	2.5	148000	2500	7700	212000	3500	290
eaf60 - 52.d	97.7	9.2	20	14150	200	3.7	147300	2400	5700	213600	2900	230
eaf60 - 53.d	96.4	8.2	24	12650	190	3.4	148800	2200	7700	217300	3100	300
eaf60 - 54.d	97.4	8.6	34	12720	180	3.2	148400	2100	12000	214300	3300	230
eaf60 - 55.d	95.5	7.9	21	12830	180	5	148100	2200	5800	213900	2900	270
eaf60 - 56.d	93.1	8.4	30	13570	220	3	144200	2000	7500	215700	3400	270
eaf60 - 57.d	94	8.5	22	13340	200	4.6	144600	2700	6100	215700	3500	270

Analysis number	Na23 ppm	Na23 ppm 2SE	Na23 ppm LOD	Al27 ppm	Al27 ppm 2SE	Al27 ppm LOD	Si28 ppm	Si28 ppm 2SE	Si28 ppm LOD	Ca44 ppm	Ca44 ppm 2SE	Ca44 ppm LOD
eaf60 - 58.d	102	9.9	33	12380	190	4.6	146700	2700	12000	216000	3100	300
eaf60 - 59.d	107.8	7.3	29	12620	140	4.3	147200	2000	11000	217900	2500	370
eaf60 - 60.d	104	9.4	27	13690	200	4.4	143400	2600	6900	219100	3100	360
eaf60 - 61.d	81.1	7.1	25	13160	180	4.3	146400	2200	6100	218100	2800	380
eaf60 - 62.d	116	11	26	12880	190	4.1	144300	2700	5400	218400	3100	300
eaf60 - 63.d	104.6	9.9	23	13620	190	2.7	144300	2700	7800	215500	2600	220
eaf60 - 64.d	91.1	8.8	21	14470	230	3.3	144900	2300	6000	216000	2900	340
eaf60 - 65.d	89	10	26	14120	180	3	147800	2800	7500	217200	2200	280
eaf60 - 66.d	92.2	8.2	31	14000	180	5.1	143500	2000	9300	218100	2900	300
eaf60 - 67.d	103	10	32	14530	210	4.7	144800	2500	7600	219300	3100	310
eaf60 - 68.d	93.8	9.3	25	13760	170	3.8	148400	2200	5300	218200	2600	220
eaf60 - 69.d	86	10	20	13800	190	2.5	147700	2800	6200	215500	3100	330
eaf60 - 70.d	100.8	8.8	28	13750	190	3.7	144700	2300	6700	216200	2800	200
eaf60 - 71.d	111.2	8.7	27	13290	200	3.5	145000	2300	5400	213600	2900	210
eaf60 - 72.d	110.2	7.7	31	13240	180	2.7	142600	3100	8800	214600	2800	290
eaf60 - 73.d	103	9.1	18	13780	230	2.4	146600	2300	8100	215000	3200	320
eaf60 - 74.d	61.7	8	22	13800	240	3.8	147000	3100	7800	213000	3400	300
eaf60 - 75.d	95.9	8.1	24	13500	200	3.8	146500	2200	12000	217500	2600	200
eaf60 - 76.d	94	12	20	12960	200	4.3	149200	2800	6100	217300	2600	210
eaf60 - 77.d	91.7	8.7	31	12940	160	2.9	147000	2400	7700	215300	2600	150
eaf60 - 78.d	100.6	7.4	25	13250	190	4.4	147800	2900	9000	216600	3300	270
eaf60 - 79.d	110.5	8.3	27	12180	170	3.8	147300	2200	6000	214800	3000	300
eaf60 - 80.d	94.6	8.1	18	12890	170	3.6	151100	3000	7500	215600	2300	290
eaf60 - 81.d	103.2	8.9	19	12130	190	2.7	147900	2900	6800	215500	3600	280
eaf60 - 82.d	99	11	29	12120	160	2.8	149200	2800	8000	215800	3300	310
eaf60 - 83.d	82.6	8.2	26	12430	190	4	148000	2300	4700	215300	3500	210
eaf60 - 84.d	103.1	6.6	30	12540	150	4.8	147400	2000	5900	217500	2300	290
eaf60 - 85.d	87.6	8.6	20	13050	180	3.5	148500	2000	2700	213200	3600	250
eaf60 - 86.d	75.5	7.2	19	13830	190	5.9	148700	2500	5900	217200	2900	280
eaf60 - 87.d	73.1	8.5	23	15450	200	4.5	146100	2700	8600	218200	3000	240
eaf60 - 88.d	93.7	8.3	29	13630	180	4	145100	2300	5400	217500	2600	300

Analysis number	Na23 ppm	Na23 ppm 2SE	Na23 ppm LOD	Al27 ppm	Al27 ppm 2SE	Al27 ppm LOD	Si28 ppm	Si28 ppm 2SE	Si28 ppm LOD	Ca44 ppm	Ca44 ppm 2SE	Ca44 ppm LOD
eaf60 - 89.d	83.2	8.4	19	13450	160	4	146500	2100	6100	217200	3300	220
eaf60 - 90.d	84.5	6.8	23	14150	200	3	144000	2600	3100	219500	2800	230
eaf60 - 91.d	78.9	7.3	31	13220	190	3.5	147000	2100	5400	218100	3000	200
eaf60 - 92.d	101.5	6.7	36	13600	190	3.5	145900	2500	8600	211400	3200	260
eaf60 - 93.d	99	11	33	12830	190	3.1	149100	2200	6500	215600	3400	230
eaf60 - 94.d	86.4	9.5	30	14250	200	3.3	147400	1900	4600	215600	2400	290
eaf60 - 95.d	83.5	7.8	22	12780	200	3.3	145400	1900	5200	215900	3500	270
eaf60 - 96.d	79.8	9.5	20	12810	220	3.4	145400	3100	7700	214400	3500	370
eaf60 - 97.d	119	31	32	15080	180	4.8	147900	1900	3300	215300	2700	270
eaf60 - 98.d	90.8	7.7	28	13380	180	3.6	148300	2200	6200	217600	3000	290
eaf60 - 99.d	96.1	9.6	28	13420	170	4.2	145700	1700	4700	216300	2900	300
eaf60 - 100.d	100.4	8.7	22	13520	160	3	147200	2400	8700	217600	2900	320
eaf60 - 101.d	61	10	25	12980	170	3.9	147700	1800	7000	217300	2300	330
eaf60 - 102.d	98	8.7	24	13170	200	3	146200	2500	7700	214500	2900	300
eaf60 - 103.d	102.1	9.2	32	13140	190	3.8	146000	2700	9600	218200	3300	350
eaf60 - 104.d	104.9	7.2	44	13370	200	4.1	144900	1900	13000	218200	2900	380
eaf60 - 105.d	95.1	8.2	30	13200	190	4.6	144700	2900	5700	217900	3200	370
eaf60 - 106.d	109.9	9.5	25	15280	210	4.4	145900	2100	8400	217500	2800	260
eaf60 - 107.d	95.9	8.5	35	14730	220	3.8	143200	2100	5100	219200	3000	260
eaf60 - 108.d	356	10	32	14210	160	3.7	146900	2700	9300	216400	3000	340
eaf60 - 109.d	79.2	8.2	35	13470	190	3.9	144900	3200	6600	219800	3200	310
eaf60 - 110.d	92.1	8.6	24	12880	130	3.9	142700	2400	9600	221500	2700	250
eaf60 - 111.d	80.7	8.7	25	13220	210	3.7	145300	2800	8600	218300	3200	240
eaf60 - 112.d	77.4	8.5	34	14020	180	5.2	146300	2700	8900	218100	2400	270
eaf60 - 114.d	88.5	7.8	26	15010	180	2.8	147600	2300	9500	216600	2500	290
eaf60 - 115.d	93	10	28	14170	170	3.2	146200	3000	8600	220000	2700	380
eaf60 - 116.d	102.2	8.8	26	13340	150	4.6	144100	2600	9700	221700	2600	280
eaf60 - 117.d	97.7	5.7	23	12720	160	3.7	149300	2800	8100	217700	3000	290
eaf60 - 118.d	98	10	30	13430	180	3	148200	2100	10000	219900	3100	380
eaf60 - 119.d	75.7	7.8	30	13400	210	3.7	148900	1900	13000	216300	3700	310
eaf60 - 120.d	89	10	27	13350	190	3	145900	2500	8700	217100	3000	280

Analysis number	Na23 ppm	Na23 ppm 2SE	Na23 ppm LOD	Al27 ppm	Al27 ppm 2SE	Al27 ppm LOD	Si28 ppm	Si28 ppm 2SE	Si28 ppm LOD	Ca44 ppm	Ca44 ppm 2SE	Ca44 ppm LOD
eaf60 - 121.d	85	6.6	24	13710	150	3.8	146800	2200	6800	216700	2600	320
eaf60 - 122.d	95.3	8	22	12780	170	2	145100	2400	4600	217300	3000	220
eaf60 - 123.d	298	10	26	14080	160	3.6	147800	2700	5600	217000	2800	250
eaf60 - 124.d	105.9	9.2	21	12400	200	3.4	145200	2300	5500	218900	3300	390
eaf60 - 126.d	96.4	7.8	21	13060	180	4.7	147100	2500	7200	221600	3800	240
eaf60 - 127.d	108.1	7	25	12140	160	4.5	146000	2200	4200	215900	3300	250
eaf60 - 128.d	118.9	9.2	26	12520	150	3.6	145800	2100	5500	221800	2700	260
eaf60 - 129.d	139.8	7.4	17	12660	190	3.6	150300	2300	5500	221100	3300	280
eaf60 - 130.d	119	11	30	12660	170	2.8	150100	3000	6100	219200	2800	260
eaf60 - 131.d	97.3	8.5	33	12510	150	4.5	146700	2800	8900	222300	3100	350
eaf60 - 132.d	83.2	7.6	27	13370	190	3.3	147100	2500	7800	222100	3100	360
eaf60 - 133.d	372	11	28	13350	160	3.4	146300	2000	5900	219600	2300	310
eaf60 - 134.d	85.5	8.7	19	13360	200	3.3	147100	3000	7200	221900	3300	300
eaf60 - 135.d	83.7	9.2	31	15020	190	3.3	148200	2500	7000	219400	3000	300
eaf60 - 136.d	109.5	9.5	36	15130	180	2.9	147100	2500	8000	217500	2700	230
eaf60 - 137.d	140.1	7.9	22	12840	140	3.4	147600	3200	4900	216000	2500	260
eaf60 - 138.d	107	8.6	21	12640	130	5	149800	1900	6400	221700	2600	180
eaf60 - 139.d	158.4	9	26	13230	150	2.8	147400	3000	6700	222300	2900	140
eaf60 - 140.d	128	11	30	13290	190	4.2	147700	2800	9500	221300	2800	260
eaf60 - 141.d	83.4	8.1	24	14480	210	3.1	144700	2800	7300	221600	2600	330
eaf60 - 142.d	136	8.7	28	13260	190	5	149000	3000	7300	223000	2800	230
eaf60 - 143.d	101	10	21	13050	200	3.8	145600	2500	9100	225100	3100	310
eaf60 - 144.d	77.7	9.2	27	13540	160	4.3	145600	2100	9100	223000	2900	230
eaf60 - 145.d	61.2	7.3	26	14510	210	4.2	149100	2400	7500	220000	2700	210
eaf60 - 146.d	92.1	9.2	29	13680	210	3.5	145200	2600	6000	226100	2900	310
eaf60 - 147.d	106.9	8.3	19	13120	140	3.8	145200	3200	10000	223800	3100	370
eaf60 - 148.d	83.6	9.4	31	12560	190	2.8	147600	2600	6400	224200	2800	300
eaf60 - 149.d	74.6	6.5	27	13120	190	2.5	148500	2900	11000	220700	2900	370
eaf60 - 150.d	105.8	9.1	24	12200	180	4.4	144000	2400	7100	223100	4000	250
eaf60 - 151.d	104.5	8.4	26	12280	170	3.8	145900	2100	7600	223000	2200	260
eaf60 - 152.d	77.7	8.2	23	13920	220	4.2	145600	2500	5500	222900	3700	320

Analysis number	Na23 ppm	Na23 ppm 2SE	Na23 ppm LOD	Al27 ppm	Al27 ppm 2SE	Al27 ppm LOD	Si28 ppm	Si28 ppm 2SE	Si28 ppm LOD	Ca44 ppm	Ca44 ppm 2SE	Ca44 ppm LOD
eaf60 - 153.d	94.1	8	31	13850	240	4.2	147400	2800	3800	221900	3500	260
eaf60 - 154.d	92	9.6	35	13210	220	4.3	146800	3300	9300	227600	3100	250
eaf60 - 155.d	329	33	24	14140	170	3.8	147300	2600	4700	218900	3400	250
eaf60 - 156.d	118	8.1	17	13500	150	3.8	146300	2300	6200	221900	2600	210
eaf60 - 157.d	93.2	5.3	32	12510	150	3.8	146500	1700	7500	225900	2700	260
eaf60 - 158.d	94.7	7.7	29	15210	220	3.2	148700	2100	5600	224900	2700	250
eaf60 - 159.d	85.1	9.6	39	15040	190	3.1	147200	2900	6100	223100	3100	280
eaf60 - 160.d	153.1	8.4	26	14210	160	3.4	148800	2100	11000	223500	2800	340

Analysis number	Ti49 ppm	Ti49 ppm 2SE	Ti49 ppm LOD	V51 ppm	V51 ppm 2SE	V51 ppm LOD	Cr52 ppm	Cr52 ppm 2SE	Cr52 ppm LOD	Mn55 ppm	Mn55 ppm 2SE	Mn55 ppm LOD
eaf60 - 1.d	216600	3100	2.4	282.8	5	0.39	64.2	2.3	4.4	586.7	9.5	9.9
eaf60 - 2.d	221300	2800	2.4	281	5	0.45	62.3	2	4.4	573.5	8.1	11
eaf60 - 3.d	220400	2800	3.6	282.2	4.1	0.34	62.3	2.7	4.5	541.8	8.1	9.1
eaf60 - 4.d	216900	2600	NaN	294.5	3.9	0.42	65.3	2	6.4	516.7	8	8.4
eaf60 - 5.d	219700	3300	2.3	284.3	3.6	0.21	59.7	2.2	3.1	596.9	9.9	10
eaf60 - 6.d	217000	3800	1.2	329.5	5.9	0.3	69.4	1.9	3.5	554.9	9.1	7.6
eaf60 - 7.d	223900	1900	NaN	271.3	4.3	0.34	56.4	2.7	4.5	585.4	7.7	10
eaf60 - 8.d	220200	2700	3.2	272.6	4	0.32	57.4	2.9	4.9	572.6	8.9	11
eaf60 - 9.d	220600	2800	2.5	264.8	3.6	0.2	56.1	2	4.7	547.8	7.7	6.8
eaf60 - 10.d	220600	3000	NaN	278.6	5.6	0.39	58.9	2.4	4.1	565.6	8.2	8.1
eaf60 - 11.d	218600	3300	NaN	291.6	4.6	0.5	78.5	2.8	4.2	634.5	9.3	7.8
eaf60 - 12.d	215600	2600	NaN	290.8	5.1	0.39	76.2	2.5	5	625	10	11
eaf60 - 13.d	218200	2200	NaN	303.1	5.7	0.31	77.2	2.5	4.7	576.2	9	6.9
eaf60 - 14.d	221600	2600	2.3	287.2	4.3	0.54	75.7	2.3	4.8	616	11	7.8
eaf60 - 15.d	222400	2700	NaN	297.7	4.8	0.54	77.3	2.3	4.8	634	11	8.3
eaf60 - 16.d	224700	3000	1.2	301.6	5.6	0.24	72.9	2.6	3.6	605	8.1	9.5
eaf60 - 17.d	222400	3200	2.5	284.6	4.3	0.34	72.4	2.3	6	546	9.3	14
eaf60 - 18.d	221300	2500	NaN	287.1	4.9	0.3	73.7	2	5	584.1	9.5	7.7
eaf60 - 19.d	220900	2700	2.4	295.2	4.9	0.37	72.3	2.4	3.6	607	10	10
eaf60 - 20.d	218200	3200	NaN	304.5	4.5	0.42	75.8	2.4	3.7	563	11	6.9
eaf60 - 21.d	215100	2500	2.9	291.8	5.8	0.43	75.5	2.3	5.7	577.6	9.3	9.1
eaf60 - 22.d	215400	2600	2.7	290	4.3	0.4	71.8	2.4	4.3	460.1	8.2	9.1
eaf60 - 23.d	218700	2800	1.2	293.2	5.3	0.31	70.6	2.3	3.1	394	6.2	8.5
eaf60 - 24.d	215600	2700	1.6	398.9	6.9	0.6	128.7	3.2	3.9	95.5	3.8	12
eaf60 - 25.d	222800	2600	2.5	261.5	4.4	0.34	65.6	2.8	5	98.9	3.2	6.8
eaf60 - 26.d	214500	2500	NaN	464	6.8	0.38	121.5	3.3	3.5	101	3.7	7.2
eaf60 - 27.d	220300	2800	1.2	281.7	4.2	0.41	83	2.7	2.3	107.7	4.9	6.7
eaf60 - 28.d	215400	3100	1.6	304.9	5.9	0.34	81.1	2.3	4.1	131.5	4	8.4
eaf60 - 29.d	223200	2700	3.2	279.4	4.6	0.52	127.3	3.1	5.2	137	3.8	9.3

Analysis number	Ti49 ppm	Ti49 ppm 2SE	Ti49 ppm LOD	V51 ppm	V51 ppm 2SE	V51 ppm LOD	Cr52 ppm	Cr52 ppm 2SE	Cr52 ppm LOD	Mn55 ppm	Mn55 ppm 2SE	Mn55 ppm LOD
eaf60 - 30.d	223500	2900	1.1	463.8	7.7	0.32	124.6	4.3	5.5	114.5	3.3	8.9
eaf60 - 31.d	224000	3000	2.2	362	5.5	0.31	58.1	2.5	5.4	148	4.1	8.2
eaf60 - 32.d	222900	3500	2.4	419.1	6.7	0.35	88.3	2.8	4.3	199.6	4	9.1
eaf60 - 33.d	217900	2700	1.5	352.5	5.8	0.52	116.3	2.7	5.5	184.9	4	8.9
eaf60 - 34.d	220900	2900	2.2	439.4	6.7	0.45	115.5	2.9	5.9	192.2	4.3	10
eaf60 - 35.d	214100	2500	NaN	413.9	7	0.34	198.4	4.7	3.5	237.2	4.9	8.8
eaf60 - 36.d	215800	3700	2.4	309.3	4.6	0.41	159.1	3.2	3.9	200	4.6	10
eaf60 - 37.d	218300	2500	1.1	273.4	4.1	0.43	58	1.9	6.2	590	12	7.6
eaf60 - 38.d	218200	2200	1.5	282.3	3.5	0.39	56.5	2.4	5.7	617.3	9.6	7
eaf60 - 39.d	220200	2500	2.3	286.5	5.2	0.31	57	2.1	3.6	631.6	8.6	8.1
eaf60 - 40.d	219700	2600	2.4	291.2	5.6	0.31	55.7	2.5	4.1	631.1	9	10
eaf60 - 41.d	223700	3700	1.1	281.3	5.7	0.49	54.1	1.8	3.4	632	10	8.6
eaf60 - 42.d	223100	2800	1.5	282.2	4.8	0.28	53.8	2.4	5.2	636.5	9.6	9.9
eaf60 - 43.d	218600	3200	NaN	285	4.6	0.3	55.8	1.6	4.7	633.5	9.9	8.2
eaf60 - 44.d	219300	2500	2.4	258	5.2	0.55	58.7	2.5	3	600.2	8.5	10
eaf60 - 45.d	216500	2900	NaN	265.8	4.8	0.2	60.9	2.4	3.9	589	9.3	7.4
eaf60 - 46.d	213900	2100	2.7	263	4.2	0.42	58.9	1.7	4	613.9	7.6	10
eaf60 - 47.d	218500	2700	NaN	272.1	5.2	0.33	46	1.7	4.6	599.6	8.6	9.5
eaf60 - 48.d	220900	2900	NaN	267.2	4.3	0.37	48.9	1.9	6.1	587	8.2	9.6
eaf60 - 49.d	221700	2700	1.2	273.5	5.6	0.35	50.7	1.9	5.1	602.1	9.7	12
eaf60 - 50.d	219600	3300	1.2	274.2	4.5	0.27	51.3	2.1	4	617.3	7.7	11
eaf60 - 51.d	216200	3500	2.3	268.7	4.9	0.49	49.8	2.3	4.7	582.6	8.6	7.6
eaf60 - 52.d	214900	2100	2.5	277.8	4.3	0.59	64.2	1.8	4.1	603.3	7.3	7.3
eaf60 - 53.d	220700	3100	2.3	254	4.2	0.45	57.3	1.5	4.2	598.4	8.5	9.8
eaf60 - 54.d	221800	3100	3.1	255.9	3.7	0.48	57.4	2.2	6	602.3	8	11
eaf60 - 55.d	217500	3100	NaN	267.6	4.4	0.37	61.7	2.5	6.1	616.9	8.6	7.8
eaf60 - 56.d	219400	3200	NaN	280.5	4.7	0.41	60.3	2.2	5.5	593.5	7.4	11
eaf60 - 57.d	220800	3200	1.2	279.5	4.3	0.24	58.2	2.2	4.7	617	10	7.2
eaf60 - 58.d	223800	2700	NaN	271.4	4.5	0.37	59.5	2.1	4.7	604.9	7.9	13

Analysis number	Ti49 ppm	Ti49 ppm 2SE	Ti49 ppm LOD	V51 ppm	V51 ppm 2SE	V51 ppm LOD	Cr52 ppm	Cr52 ppm 2SE	Cr52 ppm LOD	Mn55 ppm	Mn55 ppm 2SE	Mn55 ppm LOD
eaf60 - 59.d	224000	3000	NaN	281.5	4.6	0.22	59.1	2.6	4	616.8	7.6	12
eaf60 - 60.d	219400	3100	2.5	290.4	6.9	0.27	61.1	2.8	5.4	598.4	7.9	11
eaf60 - 61.d	219800	2500	2.6	290.7	4.8	0.36	61.8	2.2	4.5	557.9	7.7	9.5
eaf60 - 62.d	224800	2600	2.5	289.4	4.5	0.34	60.8	1.9	5.4	610.4	8.4	6.5
eaf60 - 63.d	217300	3100	NaN	294.1	5.7	0.33	61.6	2.7	5.1	597	9.1	11
eaf60 - 64.d	218000	2700	2.3	301.9	4.9	0.38	63.5	2.4	5.6	590.9	7.5	8.1
eaf60 - 65.d	219200	2400	1.1	290	4.7	0.3	62.5	2.2	6.4	566.9	7.5	12
eaf60 - 66.d	222700	3000	1.2	301.1	4.2	0.39	63.5	2.7	3.9	590.4	9.8	8.6
eaf60 - 67.d	221600	3700	3.2	302.9	5.7	0.33	67.6	2.4	4.1	604.7	8.7	10
eaf60 - 68.d	219100	2700	NaN	292.9	5.4	0.34	64.7	2.3	3.1	610.3	9.4	6.9
eaf60 - 69.d	217600	2900	2.4	287.7	6.3	0.32	63.8	2.3	3.6	582	11	6.8
eaf60 - 70.d	221100	3000	NaN	283.8	4	0.52	64.7	2.5	5	611	7.9	8
eaf60 - 71.d	214800	2900	2.3	280.7	5.8	0.47	64.5	2.6	4.9	615.7	8.9	8.9
eaf60 - 72.d	218700	2800	2.4	278.4	4.7	0.32	63.8	2	4.1	595.6	9.7	13
eaf60 - 73.d	217100	3600	2.4	293.9	5.2	0.29	66.1	2.4	4.1	614.1	8	9.5
eaf60 - 74.d	212400	2700	NaN	296.7	4.6	0.38	62.2	2.3	4.6	482	10	7.3
eaf60 - 75.d	218300	2600	1.2	263.3	3.9	0.31	62	2	5.2	594.1	8.2	11
eaf60 - 76.d	219500	3500	NaN	240.8	4.7	0.26	71.7	2.7	3	613.9	8.8	8.4
eaf60 - 77.d	219500	2800	2.7	242.8	4.7	0.37	87.3	2.5	5.5	613	11	9.4
eaf60 - 78.d	217400	3600	NaN	250.4	4.4	0.48	66.4	2.2	5.2	605.7	7.7	10
eaf60 - 79.d	221400	3500	2.3	228.4	3.7	0.38	88.3	2.6	5.4	649	11	11
eaf60 - 80.d	220000	2700	3.7	243.9	4.6	0.35	67.8	2.7	4.9	625	11	10
eaf60 - 81.d	223200	2900	2.3	223.5	4.1	0.36	78.2	2.2	3.6	634.5	9.1	6.7
eaf60 - 82.d	223900	3500	2.3	223.6	4	0.35	100.7	2.7	4.8	656	10	9.5
eaf60 - 83.d	222600	3100	2.3	234.6	4.4	0.52	76.2	2.3	3.8	570.6	8.5	7.6
eaf60 - 84.d	222400	2600	1.1	241	4.2	0.23	91.2	2.6	4.5	638.8	9.5	5.5
eaf60 - 85.d	220200	3400	NaN	252.1	4.3	0.32	75.7	2.6	3.3	604	11	8.3
eaf60 - 86.d	222200	3100	1.9	259.3	5.1	0.43	64.9	2.2	3.3	579.1	9.7	8
eaf60 - 87.d	219900	3000	NaN	306.7	5.5	0.3	66.3	2.6	5.5	540.1	6.7	8.6

Analysis number	Ti49 ppm	Ti49 ppm 2SE	Ti49 ppm LOD	V51 ppm	V51 ppm 2SE	V51 ppm LOD	Cr52 ppm	Cr52 ppm 2SE	Cr52 ppm LOD	Mn55 ppm	Mn55 ppm 2SE	Mn55 ppm LOD
eaf60 - 88.d	222600	3200	NaN	263.1	3.6	0.3	62.9	2.1	4.4	611.7	9.3	9.1
eaf60 - 89.d	225500	3500	NaN	261.7	4.7	0.28	58.3	2	4.9	598.3	8.3	8.3
eaf60 - 90.d	224200	3000	2.5	272.3	4.6	0.41	60.7	2.1	4.8	586.5	8.2	7.4
eaf60 - 91.d	222900	2900	1.1	260.2	4.2	0.27	61	2.3	5.6	580.6	9.7	9
eaf60 - 92.d	226400	3400	2.8	274.2	4.7	0.61	60.9	2.1	6	687	17	10
eaf60 - 93.d	222500	3200	1.1	251	5.8	0.31	59.7	1.8	3.6	598	10	8.9
eaf60 - 94.d	222700	2600	NaN	267	4.6	0.35	57.5	2.3	3.4	586.2	8.2	8.5
eaf60 - 95.d	223000	3500	3.3	239.7	5.1	0.39	51.2	2	4.7	591	10	6.9
eaf60 - 96.d	222200	2500	NaN	247.7	4.3	0.45	54.1	2	5.1	576.7	8.6	9
eaf60 - 97.d	222700	3400	2.6	309.3	4.8	0.38	59.3	2.6	3.5	461.9	7.1	5
eaf60 - 98.d	225000	2700	NaN	267.8	3.9	0.35	55.2	2.1	4.4	558.5	7.8	7
eaf60 - 99.d	226400	3000	2.4	272.7	5	0.47	60.1	2.1	3.3	557.5	7.6	6
eaf60 - 100.d	225500	2700	NaN	290.3	5.7	0.34	62.5	2.8	4.3	589.8	8.5	8.8
eaf60 - 101.d	226000	1800	1.2	285.4	5.5	0.32	60.1	2.2	3.7	462.8	6.4	7.5
eaf60 - 102.d	226600	2600	NaN	285.2	5	0.33	63.9	2.6	4.6	600.6	9.2	10
eaf60 - 103.d	227900	3600	NaN	289	5.4	0.37	60.9	2	3.3	610	10	12
eaf60 - 104.d	226600	3200	2.4	290.8	4.3	0.37	63.2	2.4	5.9	596.8	9.5	14
eaf60 - 105.d	230100	2900	NaN	290.8	5.2	0.49	64.4	2.3	5.4	597	9.4	7.7
eaf60 - 106.d	224000	3000	1.2	307.1	5	0.42	66.6	2.5	6.4	630	11	9.1
eaf60 - 107.d	226000	3100	2.7	307.8	5.6	0.43	69	2.2	4.3	599.3	9.6	7.7
eaf60 - 108.d	225400	3400	2.3	311	5.4	0.3	60	2.2	4	525	6.3	12
eaf60 - 109.d	228400	3000	2.4	280.6	6	0.51	50.1	1.9	4.8	595.2	9.6	7.8
eaf60 - 110.d	232100	2600	2.4	281.3	4.3	0.38	53	1.8	3.7	592.3	7.5	8.2
eaf60 - 111.d	229500	3500	1.6	279	5	0.27	51	1.7	5.3	594.6	7.7	10
eaf60 - 112.d	224700	3200	2.5	277.8	5.1	0.31	52.9	2.1	3.4	595.8	8.4	7.9
eaf60 - 114.d	223600	3300	NaN	299.5	5.5	0.49	51.9	1.8	5.8	630.6	9.3	10
eaf60 - 115.d	230000	3200	1.6	289.5	5.2	0.43	49.8	2.2	5.7	619.4	9.5	9.2
eaf60 - 116.d	234600	2700	NaN	272.6	5.2	0.36	47.6	2	5.5	618	8.9	10
eaf60 - 117.d	231200	3100	3.2	273.6	4	0.32	45	1.9	5.1	623.7	9.7	11

Analysis number	Ti49 ppm	Ti49 ppm 2SE	Ti49 ppm LOD	V51 ppm	V51 ppm 2SE	V51 ppm LOD	Cr52 ppm	Cr52 ppm 2SE	Cr52 ppm LOD	Mn55 ppm	Mn55 ppm 2SE	Mn55 ppm LOD
eaf60 - 118.d	230300	2700	1.2	305.3	4.8	0.44	67.5	2.3	4.8	617.9	9.9	11
eaf60 - 119.d	223900	3500	2.8	285.1	5.1	0.34	65	2.7	6.8	604.2	8	15
eaf60 - 120.d	226900	3200	2.4	282.4	5.1	0.53	64.1	2.1	4.5	607.8	9.8	7.9
eaf60 - 121.d	227500	2600	2.4	281.9	4.7	0.32	63.5	3	4.6	601.9	9.5	4.9
eaf60 - 122.d	225600	2800	NaN	261.7	4.5	0.36	43.1	2.3	5.7	595.6	9.5	8.2
eaf60 - 123.d	225300	2600	1.2	265.6	3.9	0.33	49.4	2	3.6	593.7	9.6	9.1
eaf60 - 124.d	230200	3500	1.2	268.1	5.3	0.33	42.5	1.9	4.3	562.8	8.6	10
eaf60 - 126.d	233000	3300	NaN	279.7	4.5	0.44	61.6	1.9	4.8	594.8	9.8	9.8
eaf60 - 127.d	229800	3200	2.3	278.2	4.5	0.32	58.4	2	3.3	602.6	6.8	7
eaf60 - 128.d	230700	2800	4.1	277.7	4.2	0.37	61	2.2	4.7	631.7	8.5	9.2
eaf60 - 129.d	231500	3500	1.2	283.7	5.7	0.68	63.5	2.5	3	648	11	6.7
eaf60 - 130.d	230500	3300	3.3	287.3	5.5	0.38	65.5	2.1	4.5	626	10	6.7
eaf60 - 131.d	233200	3300	3.2	288.5	4	0.35	64.1	2.2	6	564.8	9.8	11
eaf60 - 132.d	230800	2600	NaN	279.3	5.6	0.34	63.6	2.3	5.6	520.7	6.8	9.3
eaf60 - 133.d	227100	2700	NaN	286	4.4	0.36	62.1	2.5	3.5	500.8	6.7	7.2
eaf60 - 134.d	228800	3600	3.7	282.9	5.9	0.55	63.1	2.6	4.8	542.8	9.2	8.6
eaf60 - 135.d	228000	2300	NaN	293.7	4.8	0.4	66.1	2.2	4	591	9.5	9.3
eaf60 - 136.d	227000	2900	1.2	288.2	4.5	0.41	62.9	2.4	3.7	601.8	7.2	7.5
eaf60 - 137.d	226200	3700	NaN	257.4	4.4	0.45	58.2	2.4	3.7	604.7	9	8.3
eaf60 - 138.d	236700	3200	2.3	252.8	3.5	0.4	57.3	2.2	4	560.3	8.8	9.4
eaf60 - 139.d	234200	2900	2.3	291.9	3.8	0.41	66.5	2.5	4.1	640	10	11
eaf60 - 140.d	234100	2700	2.5	291.8	4.5	0.39	65.2	2.6	7.4	640.7	8.3	8.9
eaf60 - 141.d	231800	3100	3.2	293.8	4	0.33	70.2	2.6	4.2	594.7	9	6.7
eaf60 - 142.d	234600	3200	2.3	285.8	4.6	0.41	65.4	2.3	4.1	648	12	8.5
eaf60 - 143.d	234800	3400	2.3	294	6.4	0.47	63.6	2.1	4.1	579.8	8.4	12
eaf60 - 144.d	233600	3300	10	288.7	4.9	0.43	70.3	2.1	5.5	568.9	6.2	9.5
eaf60 - 145.d	229600	2700	1.1	313.7	3.8	0.31	72.7	2.4	4.4	547.8	7.8	7.4
eaf60 - 146.d	235400	3000	1.2	298	4.8	0.28	66.7	2.2	4.2	587.8	8.4	9.7
eaf60 - 147.d	232900	3000	NaN	285.8	5.5	0.4	66.7	2.1	7.5	624	10	11

Analysis number	Ti49 ppm	Ti49 ppm 2SE	Ti49 ppm LOD	V51 ppm	V51 ppm 2SE	V51 ppm LOD	Cr52 ppm	Cr52 ppm 2SE	Cr52 ppm LOD	Mn55 ppm	Mn55 ppm 2SE	Mn55 ppm LOD
eaf60 - 148.d	234400	3300	3.5	266	4.9	0.37	57.1	1.9	2.9	597	11	9
eaf60 - 149.d	232600	3600	NaN	272.8	4.7	0.45	59.9	2.1	6	600.8	9.9	12
eaf60 - 150.d	233600	3400	1.8	269.6	4.9	0.35	57.3	1.8	5.4	605.2	9.4	8.5
eaf60 - 151.d	236500	2800	2.6	266.6	4.6	0.42	57.8	1.9	4.7	612.8	9.5	9.5
eaf60 - 152.d	230300	3900	3.1	284.4	5.9	0.33	60.8	2.3	3	594	10	6.9
eaf60 - 153.d	233700	3500	1.1	278.8	5.8	0.46	58.7	1.9	2.1	619	10	10
eaf60 - 154.d	236000	3800	NaN	279.4	5.4	0.3	58.4	2.5	4.4	585	10	12
eaf60 - 155.d	226000	2800	2.4	288.2	4.7	0.35	61	2.1	4.3	575.3	8.9	6.5
eaf60 - 156.d	234700	2700	2.3	266.4	4.5	0.35	60	2	4	633.8	9.1	11
eaf60 - 157.d	237300	3200	1.1	266.2	4.3	0.4	60.8	2.1	4.5	612	10	11
eaf60 - 158.d	232500	3400	NaN	280.5	5.3	0.51	61.5	1.9	6	611.9	7.9	7.8
eaf60 - 159.d	229300	3300	1.2	275.4	5.7	0.36	59.9	2.1	3	586.6	7.4	7.8
eaf60 - 160.d	230200	3100	NaN	279.3	4.7	0.35	59.3	2.2	6.3	597	11	13

Analysis number	Fe57 ppm	Fe57 ppm 2SE	Fe57 ppm LOD	Y89 ppm	Y89 ppm 2SE	Y89 ppm LOD	Zr90 ppm	Zr90 ppm 2SE	Zr90 ppm LOD	Nb93 ppm	Nb93 ppm 2SE	Nb93 ppm LOD
eaf60 - 1.d	5080	100	34	712	11	0.079	2137	39	NaN	252.8	3.9	0.042
eaf60 - 2.d	5069	94	31	761	11	NaN	2161	35	0.091	304.2	5.2	NaN
eaf60 - 3.d	4800	120	34	761.5	8.9	0.066	2161	30	0.12	332.2	5.3	NaN
eaf60 - 4.d	4753	90	34	728	13	0.023	2139	26	0.042	291.9	5	NaN
eaf60 - 5.d	5430	120	18	731	11	0.045	2217	43	0.042	267.7	4.3	0.042
eaf60 - 6.d	6130	220	29	888	12	0.062	2340	45	0.083	228.6	3.6	NaN
eaf60 - 7.d	5170	110	37	808	9.8	0.044	2349	36	0.042	273.7	4.2	NaN
eaf60 - 8.d	5110	120	32	759	12	0.051	2298	45	0.082	279.6	4.6	NaN
eaf60 - 9.d	5150	100	28	802	11	0.077	2251	36	0.12	329.5	5	NaN
eaf60 - 10.d	5078	88	29	786	11	0.048	2305	53	NaN	265.3	3.8	NaN
eaf60 - 11.d	6010	120	34	628.9	9.8	0.045	2088	29	NaN	146.3	2.8	0.021
eaf60 - 12.d	6460	130	35	612.3	9.6	0.096	2097	32	0.095	167.9	2.5	NaN
eaf60 - 13.d	5097	95	36	639.7	9.6	0.03	2115	38	0.041	151.2	2.7	NaN
eaf60 - 14.d	5562	92	30	611.3	9.7	NaN	2115	34	NaN	185.8	2.8	NaN
eaf60 - 15.d	5730	96	22	537.7	6.1	NaN	2040	34	NaN	155.7	2.8	NaN
eaf60 - 16.d	5470	110	38	492.2	7.5	0.064	1958	27	NaN	124.4	1.8	NaN
eaf60 - 17.d	5200	120	28	566.6	7.6	0.022	2063	33	0.088	185.9	2.5	0.041
eaf60 - 18.d	5300	120	27	547.4	7.9	0.066	2066	29	NaN	181.1	3.1	NaN
eaf60 - 19.d	5410	110	31	485.2	6.9	0.14	1966	24	0.14	124.8	2	NaN
eaf60 - 20.d	5184	96	28	615	8.3	0.053	2069	30	0.086	136.9	2.2	NaN
eaf60 - 21.d	5290	100	42	622.9	9.6	0.05	2074	28	NaN	146.2	2.7	NaN
eaf60 - 22.d	4581	89	34	717.8	9.6	0.061	1952	29	0.13	188.5	3.1	NaN
eaf60 - 23.d	4390	110	26	886	8.9	0.045	1881	32	NaN	195.7	2.9	NaN
eaf60 - 24.d	4101	80	41	34.71	0.8	0.048	322.2	5.5	0.11	62.5	1.1	NaN
eaf60 - 25.d	3859	87	32	21.11	0.56	0.044	425.5	7.1	0.094	93.2	1.4	NaN
eaf60 - 26.d	4250	100	37	73.8	1.4	0.063	312.8	5.3	0.083	53	1	NaN
eaf60 - 27.d	3993	91	22	28.42	0.65	0.022	368.1	6.6	0.041	93.6	1.6	NaN
eaf60 - 28.d	3730	86	36	22.91	0.53	0.022	318.9	4.3	NaN	74.2	1.5	NaN
eaf60 - 29.d	4178	77	46	64.4	1.5	0.048	381.1	6	NaN	161.7	3	NaN

Analysis number	Fe57 ppm	Fe57 ppm 2SE	Fe57 ppm LOD	Y89 ppm	Y89 ppm 2SE	Y89 ppm LOD	Zr90 ppm	Zr90 ppm 2SE	Zr90 ppm LOD	Nb93 ppm	Nb93 ppm 2SE	Nb93 ppm LOD
eaf60 - 30.d	3435	81	30	144.3	3	0.087	316.8	5.9	0.081	87.7	1.9	NaN
eaf60 - 31.d	3436	78	39	118	1.7	NaN	370.4	5.8	0.086	115.6	1.8	0.04
eaf60 - 32.d	3553	92	28	319.7	5.9	0.029	912	12	0.08	113.7	2.1	NaN
eaf60 - 33.d	4004	85	23	57.1	1.5	0.059	324.6	4.2	0.11	55.6	1.3	NaN
eaf60 - 34.d	4041	86	32	216.8	3.9	0.029	346.5	5.8	0.04	78.1	1.4	NaN
eaf60 - 35.d	4820	100	31	225.7	4.6	0.043	345.5	4.9	NaN	85.3	1.6	NaN
eaf60 - 36.d	4750	100	31	51.3	1.1	NaN	328.1	4.7	0.08	38.98	0.86	NaN
eaf60 - 37.d	5189	94	33	727	9.9	0.066	2198	44	0.092	306.5	3.9	NaN
eaf60 - 38.d	5644	97	31	726	11	NaN	2132	37	0.039	277.4	4.1	0.02
eaf60 - 39.d	6040	130	22	740	9.3	0.063	2164	34	NaN	284.3	4.8	NaN
eaf60 - 40.d	5920	110	25	718.9	8.7	0.07	2083	35	NaN	251	3.9	NaN
eaf60 - 41.d	6550	120	34	752	10	NaN	2322	49	0.11	359.3	5.3	NaN
eaf60 - 42.d	5930	110	33	740	10	0.06	2282	48	0.04	379.3	4.5	NaN
eaf60 - 43.d	5880	140	34	727	11	NaN	2148	37	0.04	270.9	4.8	NaN
eaf60 - 44.d	5610	110	31	772.6	9.2	0.064	2436	49	0.12	173.2	3.2	NaN
eaf60 - 45.d	6230	120	30	755	9.1	0.046	2368	45	NaN	259.3	4.3	NaN
eaf60 - 46.d	6360	110	33	752	10	0.068	2315	46	0.042	357	4.4	NaN
eaf60 - 47.d	5430	100	26	728	10	0.022	2263	40	NaN	223.4	3.6	NaN
eaf60 - 48.d	5400	110	29	719.2	7.8	0.08	2316	39	0.12	328.9	4.1	NaN
eaf60 - 49.d	5530	120	32	747	11	0.062	2326	38	NaN	358.6	5.7	NaN
eaf60 - 50.d	5600	110	22	727.6	9.7	NaN	2256	41	0.041	183.3	3.5	NaN
eaf60 - 51.d	5630	230	23	740	12	0.044	2336	50	0.082	316.8	6.3	NaN
eaf60 - 52.d	5522	95	35	776.2	9.8	0.072	2323	52	0.12	250.4	4.3	NaN
eaf60 - 53.d	5320	110	26	842	14	0.048	2354	58	0.083	320.9	5.7	NaN
eaf60 - 54.d	5440	110	35	847	12	0.044	2394	53	NaN	309.9	4.7	NaN
eaf60 - 55.d	5400	110	31	826	14	0.044	2361	55	0.089	286.8	4.3	NaN
eaf60 - 56.d	5510	100	37	800	12	0.044	2386	66	NaN	290.6	4.2	NaN
eaf60 - 57.d	5590	150	33	829	13	0.048	2406	51	0.09	282.3	5	NaN
eaf60 - 58.d	5320	100	29	811.1	9.6	NaN	2326	46	0.088	294.5	4.2	NaN

Analysis number	Fe57 ppm	Fe57 ppm 2SE	Fe57 ppm LOD	Y89 ppm	Y89 ppm 2SE	Y89 ppm LOD	Zr90 ppm	Zr90 ppm 2SE	Zr90 ppm LOD	Nb93 ppm	Nb93 ppm 2SE	Nb93 ppm LOD
eaf60 - 59.d	5489	91	29	830	11	0.022	2317	47	0.081	293.1	3.3	NaN
eaf60 - 60.d	5530	120	30	769	12	0.044	2282	51	0.057	280.4	4	NaN
eaf60 - 61.d	5053	90	27	782	10	0.03	2323	49	0.088	279.9	4.1	NaN
eaf60 - 62.d	5620	120	27	821	12	0.051	2405	54	0.083	289	3.9	0.021
eaf60 - 63.d	5360	82	32	749	11	0.022	2282	48	NaN	272.8	4.8	0.02
eaf60 - 64.d	5310	120	27	740	12	0.047	2230	47	0.055	213.6	3.3	0.061
eaf60 - 65.d	5728	97	25	779	12	0.022	2291	43	NaN	244	3.2	NaN
eaf60 - 66.d	6590	130	36	736	12	0.044	2173	33	0.082	363.3	5.1	0.021
eaf60 - 67.d	5790	110	29	726	11	0.051	2168	27	NaN	249.1	4	NaN
eaf60 - 68.d	5550	150	28	811	10	0.022	2169	34	NaN	385.4	5.5	NaN
eaf60 - 69.d	5100	110	22	801	12	0.05	2153	30	0.12	356.3	5.8	NaN
eaf60 - 70.d	5570	130	37	715.5	8.5	0.023	2190	40	NaN	253	4	NaN
eaf60 - 71.d	5550	130	21	724	11	0.067	2172	43	NaN	281.2	4.4	NaN
eaf60 - 72.d	5390	110	42	808	13	0.046	2191	40	NaN	294.9	5.4	NaN
eaf60 - 73.d	5478	88	27	694.9	9.7	0.074	2156	30	0.043	226.7	3.2	0.043
eaf60 - 74.d	4158	93	31	1144	19	NaN	1701	53	0.1	394.9	6.1	0.042
eaf60 - 75.d	5507	92	27	837	15	0.031	2350	48	0.042	316	5.2	NaN
eaf60 - 76.d	5450	120	27	864	14	0.072	2391	56	NaN	567.7	7.8	NaN
eaf60 - 77.d	5330	120	35	875	14	0.051	2343	53	NaN	580.6	8.7	0.021
eaf60 - 78.d	5560	130	29	844	14	NaN	2402	58	0.041	391.1	6	0.042
eaf60 - 79.d	5680	92	32	889	13	0.048	2578	62	0.083	612.6	9.2	NaN
eaf60 - 80.d	5550	120	36	855	13	NaN	2446	62	0.056	467.7	5.8	NaN
eaf60 - 81.d	5648	97	33	899	11	0.048	2525	57	0.083	440.5	5.7	0.046
eaf60 - 82.d	5370	120	32	922	13	0.054	2516	59	0.041	879	13	NaN
eaf60 - 83.d	5190	130	44	888	14	0.05	2493	68	NaN	471	8.3	NaN
eaf60 - 84.d	5460	110	23	911	11	0.048	2346	51	NaN	832	10	NaN
eaf60 - 85.d	5090	100	38	863	12	0.022	2295	46	0.04	604	11	NaN
eaf60 - 86.d	5640	100	31	855	13	0.071	2313	54	0.13	545.6	8.5	0.021
eaf60 - 87.d	5000	130	33	837	17	0.022	2122	31	NaN	188.9	3.7	0.063

Analysis number	Fe57 ppm	Fe57 ppm 2SE	Fe57 ppm LOD	Y89 ppm	Y89 ppm 2SE	Y89 ppm LOD	Zr90 ppm	Zr90 ppm 2SE	Zr90 ppm LOD	Nb93 ppm	Nb93 ppm 2SE	Nb93 ppm LOD
eaf60 - 88.d	5679	89	33	806	10	0.062	2338	52	0.056	322.7	4.4	NaN
eaf60 - 89.d	5490	110	42	831	12	0.048	2322	53	0.15	371.8	7	NaN
eaf60 - 90.d	5410	120	29	808	12	0.048	2261	50	0.083	387.8	6.8	NaN
eaf60 - 91.d	5248	89	28	845	12	0.059	2333	57	NaN	404.7	6.9	0.041
eaf60 - 92.d	8480	410	32	839	13	0.054	2170	32	0.044	464.9	7	NaN
eaf60 - 93.d	5450	130	35	866	17	0.022	2325	61	NaN	578.2	9.2	0.021
eaf60 - 94.d	5400	86	26	801.7	9.9	0.055	2286	32	NaN	292.9	3.1	NaN
eaf60 - 95.d	5390	120	30	872	16	NaN	2219	45	0.043	741	12	NaN
eaf60 - 96.d	5425	97	34	853	13	NaN	2294	46	NaN	317.3	5.4	NaN
eaf60 - 97.d	3790	110	29	1127	17	0.11	2019	28	NaN	218	4.7	NaN
eaf60 - 98.d	5018	74	25	803	12	0.031	2358	45	0.086	316.5	4.8	0.043
eaf60 - 99.d	4850	110	23	861	14	0.065	2057	29	NaN	189.5	3.3	NaN
eaf60 - 100.d	5220	110	32	801	12	0.023	2182	31	0.043	294	3.7	NaN
eaf60 - 101.d	3882	93	25	1116	23	0.046	2252	37	NaN	167.7	3.1	NaN
eaf60 - 102.d	5220	120	32	746	12	NaN	2189	40	NaN	302.2	5.6	NaN
eaf60 - 103.d	5530	120	29	816	12	0.046	2210	32	0.043	296.7	5.1	NaN
eaf60 - 104.d	5240	120	33	746	12	0.023	2157	32	0.093	311.4	5.7	NaN
eaf60 - 105.d	5400	110	39	833	15	0.023	2201	42	0.042	313.6	6.2	NaN
eaf60 - 106.d	6240	140	22	731	12	NaN	2198	37	0.043	199.3	3.1	NaN
eaf60 - 107.d	5210	110	26	722	10	0.049	2220	40	0.18	196.7	3.3	NaN
eaf60 - 108.d	4880	110	19	1151	14	0.07	2169	40	NaN	373.6	4.9	NaN
eaf60 - 109.d	5562	97	45	755	11	0.037	2328	48	NaN	218	2.9	0.059
eaf60 - 110.d	5581	90	24	765.2	9.8	0.023	2456	46	NaN	304.7	4.5	NaN
eaf60 - 111.d	5550	110	39	745	11	0.045	2296	42	NaN	268.1	4.8	NaN
eaf60 - 112.d	5480	160	29	733	13	NaN	2207	42	NaN	373.5	6.2	NaN
eaf60 - 114.d	5800	110	34	717	10	0.048	2076	35	NaN	273.1	5.2	0.021
eaf60 - 115.d	6100	120	30	731	11	0.049	2278	41	NaN	394.8	5.6	NaN
eaf60 - 116.d	6050	120	25	722	11	0.067	2420	49	0.042	392.5	5.7	NaN
eaf60 - 117.d	5620	120	27	744.9	9.9	0.022	2355	51	NaN	326.2	4.5	NaN

Analysis number	Fe57 ppm	Fe57 ppm 2SE	Fe57 ppm LOD	Y89 ppm	Y89 ppm 2SE	Y89 ppm LOD	Zr90 ppm	Zr90 ppm 2SE	Zr90 ppm LOD	Nb93 ppm	Nb93 ppm 2SE	Nb93 ppm LOD
eaf60 - 118.d	5730	100	34	729	11	0.022	2362	53	NaN	478.5	5.6	NaN
eaf60 - 119.d	5580	130	25	700	11	0.046	2299	48	0.059	442.2	8.6	0.044
eaf60 - 120.d	5680	110	29	700	10	0.1	2300	36	NaN	465.3	7.4	0.044
eaf60 - 121.d	5540	100	16	692.1	9.3	0.046	2258	42	NaN	453.7	6.7	NaN
eaf60 - 122.d	5420	130	21	734.3	8.8	NaN	2354	50	NaN	336.6	5.7	0.043
eaf60 - 123.d	5440	100	31	760	11	0.023	2261	43	0.043	323.8	4.6	NaN
eaf60 - 124.d	5310	110	54	768.9	9.2	0.064	2375	42	NaN	357.1	5.8	0.022
eaf60 - 126.d	5420	110	26	627	9.2	NaN	2196	34	NaN	216	3.5	NaN
eaf60 - 127.d	5390	120	29	601.7	9.9	0.073	2209	52	NaN	193.7	3.5	NaN
eaf60 - 128.d	5410	120	27	554.2	7.5	0.052	2134	25	0.058	189.2	3.1	NaN
eaf60 - 129.d	5840	150	37	491.6	7.2	0.061	2103	26	0.12	155.3	3.1	NaN
eaf60 - 130.d	5510	110	33	497.8	9	NaN	2103	35	NaN	152	3	NaN
eaf60 - 131.d	5183	92	37	578	10	NaN	2177	34	0.085	167.2	2.8	NaN
eaf60 - 132.d	4930	120	31	687.3	8.7	0.023	2185	39	0.12	219.1	4	NaN
eaf60 - 133.d	4131	85	32	782	12	0.061	2119	31	0.057	198.5	2.9	NaN
eaf60 - 134.d	4728	95	38	653	11	0.048	2179	35	NaN	203	3.5	NaN
eaf60 - 135.d	5360	110	40	685	9.6	NaN	2237	38	0.084	161.8	2.3	NaN
eaf60 - 136.d	6140	110	38	636.4	9.2	0.022	2145	36	0.042	160.9	2.8	NaN
eaf60 - 137.d	6980	320	20	766	11	0.022	2278	54	0.083	346.7	4.5	NaN
eaf60 - 138.d	5190	99	38	996	14	0.061	2460	59	NaN	352.3	5.2	0.021
eaf60 - 139.d	5650	120	38	618.3	8.4	0.044	2189	30	NaN	199.2	2.8	NaN
eaf60 - 140.d	5810	100	36	623.9	8.5	0.044	2211	44	0.042	210.8	3.7	NaN
eaf60 - 141.d	5413	85	33	669	10	0.078	2231	52	0.042	173.7	2.5	0.021
eaf60 - 142.d	6810	230	25	608.7	7.9	0.036	2194	36	NaN	196.5	3.1	NaN
eaf60 - 143.d	6570	200	28	609.2	9.8	0.045	2174	35	0.084	189.3	3.5	0.021
eaf60 - 144.d	5166	95	27	637.4	8.8	0.044	2207	42	0.041	202.1	2.9	0.029
eaf60 - 145.d	4736	92	18	673	9.6	NaN	2231	49	0.056	179.7	2.8	NaN
eaf60 - 146.d	5120	100	49	632.8	8.4	0.063	2183	31	0.083	213.3	3	NaN
eaf60 - 147.d	5390	110	44	657	11	0.022	2250	47	0.042	218.7	3.5	NaN

Analysis number	Fe57 ppm	Fe57 ppm 2SE	Fe57 ppm LOD	Y89 ppm	Y89 ppm 2SE	Y89 ppm LOD	Zr90 ppm	Zr90 ppm 2SE	Zr90 ppm LOD	Nb93 ppm	Nb93 ppm 2SE	Nb93 ppm LOD
eaf60 - 148.d	5290	100	29	847	14	NaN	2102	38	0.041	113.2	2.4	NaN
eaf60 - 149.d	5260	100	31	803	11	0.047	2213	50	0.041	211	3.9	0.041
eaf60 - 150.d	5390	110	32	808	13	0.078	2367	56	NaN	293.9	4.2	0.021
eaf60 - 151.d	5550	110	28	817.7	9.4	NaN	2395	46	NaN	316.7	4	NaN
eaf60 - 152.d	5240	140	41	778	14	0.062	2367	61	NaN	267.3	5	NaN
eaf60 - 153.d	5610	110	37	796	11	0.044	2426	64	NaN	289.2	3.7	NaN
eaf60 - 154.d	5490	130	28	815	13	0.048	2457	64	0.083	323.6	5.3	0.021
eaf60 - 155.d	5120	120	23	858	18	0.043	2147	28	NaN	303.8	3.9	NaN
eaf60 - 156.d	6220	120	32	803	10	0.044	2517	52	0.11	322	4.3	0.042
eaf60 - 157.d	5570	110	31	826	10	0.06	2678	56	0.055	334.8	4.8	NaN
eaf60 - 158.d	5430	110	27	786	13	0.048	2242	45	0.11	230	3.7	0.042
eaf60 - 159.d	5330	110	22	781	12	0.048	2190	37	0.09	223.3	3.5	0.021
eaf60 - 160.d	5470	130	29	773	14	0.022	2332	57	0.082	274.9	4.8	NaN

Analysis number	La139 ppm	La139 ppm 2SE	La139 ppm LOD	Ce140 ppm	Ce140 ppm 2SE	Ce140 ppm LOD	Pr141 ppm	Pr141 ppm 2SE	Pr141 ppm LOD	Nd146 ppm	Nd146 ppm 2SE	Nd146 ppm LOD
eaf60 - 1.d	656	12	NaN	1861	31	0.025	210.5	3.6	NaN	894	16	NaN
eaf60 - 2.d	707	18	0.027	2021	33	0.041	230.1	3.1	NaN	992	17	NaN
eaf60 - 3.d	685	13	NaN	2005	27	NaN	230.9	3.5	NaN	1014	17	NaN
eaf60 - 4.d	634.8	9.9	NaN	1808	26	NaN	203	3	0.022	886	16	NaN
eaf60 - 5.d	636	13	0.025	1800	25	0.025	203.4	3.3	NaN	882	15	NaN
eaf60 - 6.d	668	15	0.025	1984	30	NaN	229.6	3.4	NaN	1012	15	NaN
eaf60 - 7.d	796	23	0.027	2121	32	NaN	238	3.3	0.031	1034	16	0.06
eaf60 - 8.d	739	22	0.012	2005	25	NaN	227.5	3.9	0.011	964	17	NaN
eaf60 - 9.d	805	26	NaN	2173	30	NaN	247.4	3.8	0.021	1070	17	NaN
eaf60 - 10.d	731	23	NaN	1987	33	NaN	222.9	3.7	0.042	958	15	NaN
eaf60 - 11.d	599	10	0.013	1592	25	0.013	173.3	2.8	NaN	716	12	NaN
eaf60 - 12.d	593.4	8.7	0.012	1574	20	NaN	170.9	2.2	0.023	714	11	NaN
eaf60 - 13.d	618.7	9.8	NaN	1634	28	0.025	175	2.3	0.029	720	12	NaN
eaf60 - 14.d	597	10	NaN	1594	20	0.013	171.5	2.5	0.011	710	14	0.06
eaf60 - 15.d	566.1	8.1	NaN	1438	19	0.025	150.7	2.4	NaN	607	11	0.12
eaf60 - 16.d	546.3	7.8	NaN	1338	21	NaN	135.7	1.9	NaN	530.8	8.9	0.12
eaf60 - 17.d	579.2	9.6	0.033	1510	21	NaN	159.9	2.5	NaN	661	11	NaN
eaf60 - 18.d	564.4	7.7	0.012	1474	21	NaN	155.9	2.5	NaN	642.5	8.9	NaN
eaf60 - 19.d	536.9	7.3	NaN	1338	21	NaN	135.6	2.1	NaN	534.3	9.3	NaN
eaf60 - 20.d	606.4	9	NaN	1600	26	NaN	171	2.6	NaN	701	12	0.17
eaf60 - 21.d	605	10	0.013	1605	30	NaN	170.6	2.8	NaN	713	13	0.063
eaf60 - 22.d	574	8.1	0.027	1594	20	NaN	175.6	2.5	0.017	745	13	NaN
eaf60 - 23.d	566.8	9	NaN	1550	26	0.025	171.8	2.5	0.023	743	10	NaN
eaf60 - 24.d	62.6	1.2	0.027	151.4	2.3	NaN	19.97	0.5	0.011	81.1	2.5	NaN
eaf60 - 25.d	55.87	0.76	NaN	123.2	1.9	0.025	15.35	0.39	NaN	62.4	1.3	NaN
eaf60 - 26.d	66.2	1.1	NaN	172.6	2.5	NaN	24.15	0.54	NaN	102.8	2.2	0.06
eaf60 - 27.d	57.59	0.95	NaN	131.4	2.1	NaN	17.72	0.38	NaN	74.2	2.2	0.12
eaf60 - 28.d	52.4	1	NaN	119.4	1.8	NaN	15.36	0.45	0.021	63.9	1.6	NaN
eaf60 - 29.d	61.5	1.2	NaN	130	1.8	NaN	16.76	0.34	NaN	71.8	1.7	0.13

Analysis number	La139 ppm	La139 ppm 2SE	La139 ppm LOD	Ce140 ppm	Ce140 ppm 2SE	Ce140 ppm LOD	Pr141 ppm	Pr141 ppm 2SE	Pr141 ppm LOD	Nd146 ppm	Nd146 ppm 2SE	Nd146 ppm LOD
eaf60 - 30.d	100.3	1.5	NaN	281.5	3.8	0.012	42.95	0.78	NaN	210.3	3.9	NaN
eaf60 - 31.d	241.6	4.2	NaN	717	14	NaN	99.9	2	NaN	433.6	7.8	0.13
eaf60 - 32.d	327.6	5.7	NaN	1425	22	NaN	210.7	3.7	NaN	1039	19	NaN
eaf60 - 33.d	76.2	1.5	0.012	203.2	3.6	0.024	28.28	0.7	NaN	121.7	2	0.13
eaf60 - 34.d	191.9	2.8	NaN	647	10	NaN	103.7	1.9	NaN	481	7.9	0.058
eaf60 - 35.d	148.7	2.8	NaN	447.2	7.6	NaN	64.2	1.2	NaN	279.8	5.5	0.12
eaf60 - 36.d	49.16	0.89	NaN	119.7	2.1	NaN	15.85	0.38	0.014	68.3	1.8	0.13
eaf60 - 37.d	598.6	8.6	NaN	1713	27	0.012	194	3	0.01	848	13	0.058
eaf60 - 38.d	596.6	8.8	0.012	1700	25	NaN	192.7	2.7	0.027	836	11	NaN
eaf60 - 39.d	592.9	8.4	0.025	1698	25	0.025	195.1	2.8	NaN	843	13	0.12
eaf60 - 40.d	592.7	8.8	0.012	1685	26	NaN	190.2	2.8	0.02	817	12	0.12
eaf60 - 41.d	611	10	0.012	1784	34	NaN	203.2	3.4	NaN	880	16	NaN
eaf60 - 42.d	608	11	NaN	1752	27	NaN	200.9	3.4	0.01	876	15	NaN
eaf60 - 43.d	589	11	NaN	1683	25	0.012	191.4	2.8	NaN	821	15	NaN
eaf60 - 44.d	661.1	9	NaN	1906	22	NaN	214.4	2.9	NaN	922	14	NaN
eaf60 - 45.d	653	10	NaN	1884	24	0.028	214.4	2.8	NaN	931.3	9.6	NaN
eaf60 - 46.d	629.1	9.3	0.013	1824	22	NaN	209.9	3	NaN	914	13	0.12
eaf60 - 47.d	645.7	8.2	0.013	1800	25	0.038	199.5	2.9	NaN	843	11	0.061
eaf60 - 48.d	651.8	9	NaN	1864	28	0.028	209.2	2.8	NaN	900	12	NaN
eaf60 - 49.d	635.5	8.8	0.013	1863	28	NaN	208.4	3.1	NaN	907	13	NaN
eaf60 - 50.d	645.7	9.8	0.012	1794	27	NaN	195.6	2.7	NaN	826	11	NaN
eaf60 - 51.d	619.1	9.7	0.017	1805	33	NaN	203.9	4	NaN	880	15	NaN
eaf60 - 52.d	624.2	9.7	0.025	1775	27	0.025	204.2	3.1	NaN	889	13	NaN
eaf60 - 53.d	810	29	NaN	2234	36	NaN	260.5	5	NaN	1129	19	0.083
eaf60 - 54.d	730	22	NaN	2093	32	0.025	241.9	3.6	0.014	1069	19	NaN
eaf60 - 55.d	708	17	NaN	2032	32	0.049	232.9	3.4	0.021	1008	15	0.13
eaf60 - 56.d	652	11	NaN	1903	30	0.025	218.9	3.8	NaN	953	14	0.12
eaf60 - 57.d	677	13	0.025	1961	32	NaN	223.3	3.5	0.043	976	20	NaN
eaf60 - 58.d	783	23	NaN	2107	30	NaN	237	3	0.01	1024	14	NaN

Analysis number	La139 ppm	La139 ppm 2SE	La139 ppm LOD	Ce140 ppm	Ce140 ppm 2SE	Ce140 ppm LOD	Pr141 ppm	Pr141 ppm 2SE	Pr141 ppm LOD	Nd146 ppm	Nd146 ppm 2SE	Nd146 ppm LOD
eaf60 - 59.d	762	25	0.033	2063	31	0.012	232.1	2.6	0.01	1010	15	0.12
eaf60 - 60.d	647	13	0.025	1858	30	0.012	210.9	3.1	NaN	918	15	NaN
eaf60 - 61.d	662	14	0.012	1877	27	NaN	213.3	2.6	0.021	928	14	NaN
eaf60 - 62.d	729	20	0.058	2028	25	NaN	229.5	3.2	0.021	992	15	NaN
eaf60 - 63.d	627	10	NaN	1781	29	0.012	202.1	3.4	NaN	864	15	0.12
eaf60 - 64.d	624.3	9.4	0.026	1750	27	NaN	194.2	3.6	0.01	837	15	0.059
eaf60 - 65.d	623.5	7.9	NaN	1784	26	0.012	201.4	3.1	NaN	867	12	NaN
eaf60 - 66.d	675	13	NaN	1942	28	NaN	224	3.5	0.011	965	16	NaN
eaf60 - 67.d	623	10	0.012	1745	27	NaN	195	2.5	0.011	835	13	0.12
eaf60 - 68.d	708	20	0.024	2011	21	0.024	234.7	3.5	0.01	1042	14	NaN
eaf60 - 69.d	679	12	NaN	1996	31	NaN	233.6	3.8	NaN	1031	17	NaN
eaf60 - 70.d	682	12	0.026	1902	32	NaN	213.5	3.5	NaN	910	13	NaN
eaf60 - 71.d	685	17	NaN	1917	35	NaN	211.7	3.7	0.011	919	18	0.17
eaf60 - 72.d	733	17	0.013	2060	33	NaN	235.6	3.7	0.03	1027	16	0.062
eaf60 - 73.d	606.8	9.1	0.013	1674	26	0.028	184.7	2.8	NaN	795	13	NaN
eaf60 - 74.d	565	11	NaN	1774	29	NaN	219	2.9	0.021	1013	14	0.061
eaf60 - 75.d	678	11	NaN	2008	30	0.026	228	4.7	NaN	998	17	0.12
eaf60 - 76.d	746	26	NaN	2133	41	NaN	245.3	4.2	NaN	1075	20	0.06
eaf60 - 77.d	746	24	NaN	2125	30	NaN	243	3.3	0.021	1053	14	NaN
eaf60 - 78.d	717	23	NaN	2069	36	0.21	237.3	3.8	NaN	1032	17	NaN
eaf60 - 79.d	844	25	0.025	2290	38	NaN	256.8	4.3	NaN	1087	17	NaN
eaf60 - 80.d	724	21	0.025	2094	24	NaN	240.6	3	NaN	1052	17	0.059
eaf60 - 81.d	822	29	0.038	2267	34	0.075	259.3	4.2	NaN	1111	17	NaN
eaf60 - 82.d	808	26	NaN	2278	38	0.034	261.7	3.7	0.021	1110	17	NaN
eaf60 - 83.d	818	28	NaN	2253	34	NaN	256.2	4	NaN	1118	17	0.059
eaf60 - 84.d	789	21	0.017	2221	34	0.027	254.8	4	NaN	1083	13	0.12
eaf60 - 85.d	713	21	NaN	2061	36	0.024	238.5	4.7	NaN	1034	19	0.058
eaf60 - 86.d	695	20	NaN	2018	33	NaN	231.8	4.3	0.011	1013	17	NaN
eaf60 - 87.d	629.2	9.9	0.012	1811	28	0.025	203.5	3.4	NaN	884	14	NaN

Analysis number	La139 ppm	La139 ppm 2SE	La139 ppm LOD	Ce140 ppm	Ce140 ppm 2SE	Ce140 ppm LOD	Pr141 ppm	Pr141 ppm 2SE	Pr141 ppm LOD	Nd146 ppm	Nd146 ppm 2SE	Nd146 ppm LOD
eaf60 - 88.d	686	17	NaN	1987	27	NaN	230.2	3.4	NaN	1010	14	NaN
eaf60 - 89.d	695	18	NaN	2037	36	NaN	234.4	3.6	NaN	1027	13	NaN
eaf60 - 90.d	644.4	9.1	NaN	1894	29	NaN	219.6	3.2	NaN	966	13	0.12
eaf60 - 91.d	726	23	0.012	2065	32	NaN	236.9	3.5	0.01	1048	16	NaN
eaf60 - 92.d	645	11	0.026	1917	37	NaN	221.1	3.5	NaN	971	14	NaN
eaf60 - 93.d	742	28	NaN	2109	38	0.012	241.1	4.8	0.021	1053	20	NaN
eaf60 - 94.d	664.6	9.6	NaN	1922	26	0.029	218.8	2.5	NaN	953	11	NaN
eaf60 - 95.d	795	26	0.013	2207	32	0.052	249.8	3.7	0.022	1064	16	NaN
eaf60 - 96.d	693	16	NaN	2050	26	0.013	232.9	3.7	NaN	1021	17	NaN
eaf60 - 97.d	671	11	NaN	1982	28	0.018	230.4	3.5	0.022	1017	13	0.062
eaf60 - 98.d	690	15	0.028	1987	27	NaN	226.1	3.1	0.011	986	15	NaN
eaf60 - 99.d	714	13	NaN	2149	32	0.013	250.7	4.3	NaN	1124	20	NaN
eaf60 - 100.d	677	11	NaN	1961	28	0.013	221.6	2.7	NaN	962	17	NaN
eaf60 - 101.d	757	23	0.026	2246	33	0.026	266.9	4.2	NaN	1173	18	0.062
eaf60 - 102.d	758	24	NaN	2085	33	NaN	230.5	4.1	NaN	1002	17	NaN
eaf60 - 103.d	765	24	NaN	2116	32	NaN	235.7	3.4	NaN	1010	16	0.062
eaf60 - 104.d	743	22	NaN	2042	37	NaN	230.1	4.1	NaN	978	16	NaN
eaf60 - 105.d	760	26	NaN	2120	35	NaN	240.8	3.6	NaN	1032	19	NaN
eaf60 - 106.d	613.6	9	NaN	1709	28	NaN	191.3	3.2	NaN	817	13	NaN
eaf60 - 107.d	615.8	8.5	NaN	1714	26	0.013	186.2	2.7	0.022	803	14	0.17
eaf60 - 108.d	630	10	0.012	2028	26	NaN	247.2	3	NaN	1118	14	NaN
eaf60 - 109.d	661.6	8.8	0.013	1861	27	0.039	205.7	3.2	NaN	868	14	0.062
eaf60 - 110.d	668	9.8	NaN	1892	22	NaN	211.3	2.5	NaN	898	11	NaN
eaf60 - 111.d	647	12	0.034	1853	27	NaN	205.8	3.7	NaN	880	15	NaN
eaf60 - 112.d	610	10	0.027	1768	27	NaN	200.4	2.9	0.021	865	16	NaN
eaf60 - 114.d	595.8	9.6	0.025	1694	29	NaN	188.4	3.1	0.024	800	15	NaN
eaf60 - 115.d	633.6	8.7	NaN	1812	31	NaN	203	2.9	NaN	868	15	0.083
eaf60 - 116.d	659.4	8.4	NaN	1881	30	NaN	209.7	3.1	0.023	901	16	NaN
eaf60 - 117.d	657	12	0.012	1863	29	NaN	204.7	3.2	NaN	869	14	NaN

Analysis number	La139 ppm	La139 ppm 2SE	La139 ppm LOD	Ce140 ppm	Ce140 ppm 2SE	Ce140 ppm LOD	Pr141 ppm	Pr141 ppm 2SE	Pr141 ppm LOD	Nd146 ppm	Nd146 ppm 2SE	Nd146 ppm LOD
eaf60 - 118.d	608.1	8.9	0.012	1769	23	NaN	195.9	3.3	NaN	844	14	NaN
eaf60 - 119.d	597	11	NaN	1747	31	NaN	193.1	3.3	NaN	831	14	NaN
eaf60 - 120.d	597.8	9.4	0.013	1735	29	NaN	194.8	3.8	NaN	835	14	NaN
eaf60 - 121.d	593.9	8.1	NaN	1725	24	0.013	191.6	3.2	NaN	830	8.8	0.062
eaf60 - 122.d	650.9	8	0.028	1873	28	NaN	210.2	2.7	NaN	892	14	NaN
eaf60 - 123.d	614.3	8.4	0.013	1784	23	NaN	200.8	2.5	NaN	866	14	NaN
eaf60 - 124.d	669	11	0.013	1939	34	0.028	215.2	3.4	NaN	922	14	NaN
eaf60 - 126.d	606	11	0.04	1616	26	NaN	169.6	2.4	0.011	723	13	NaN
eaf60 - 127.d	596.8	8.9	NaN	1545	25	0.017	162.2	2.4	NaN	668	14	NaN
eaf60 - 128.d	581.9	8.3	0.028	1495	21	NaN	153.4	2.9	0.024	617	12	0.13
eaf60 - 129.d	565.5	9.1	0.025	1417	24	NaN	139.5	2.5	NaN	553.8	9.8	NaN
eaf60 - 130.d	562	10	NaN	1412	23	NaN	142.5	2.6	0.011	561	12	0.12
eaf60 - 131.d	591.9	9.1	NaN	1510	24	NaN	156.6	2.8	NaN	626	11	NaN
eaf60 - 132.d	631.6	9.7	0.028	1697	25	NaN	180.3	2.5	NaN	757	12	NaN
eaf60 - 133.d	582.2	8	NaN	1600	22	NaN	173.6	2.7	NaN	744.3	9.7	NaN
eaf60 - 134.d	605	10	NaN	1659	28	NaN	176.4	3	0.011	737	11	NaN
eaf60 - 135.d	641.7	7.3	NaN	1739	18	0.013	182	2.6	NaN	745	9.7	NaN
eaf60 - 136.d	611.8	9.1	0.025	1646	22	0.039	174.2	3.1	NaN	711	12	0.061
eaf60 - 137.d	673	16	NaN	1890	25	0.025	206.4	3.6	NaN	901	16	NaN
eaf60 - 138.d	792	25	NaN	2138	32	0.013	240.5	3.7	0.023	1052	15	NaN
eaf60 - 139.d	591.1	9.1	0.025	1555	22	NaN	165.5	2.7	NaN	686	13	NaN
eaf60 - 140.d	597.2	8.9	NaN	1602	22	NaN	169.1	2.5	NaN	701	13	NaN
eaf60 - 141.d	607.7	8.8	0.025	1657	21	NaN	175.5	2.7	NaN	727	12	NaN
eaf60 - 142.d	575.6	8.7	NaN	1526	29	NaN	160.5	2.8	NaN	679	12	NaN
eaf60 - 143.d	581.9	9.5	NaN	1525	26	NaN	160.7	2.8	NaN	661	14	NaN
eaf60 - 144.d	596	11	0.012	1611	23	0.027	170.1	2.7	NaN	709	12	0.12
eaf60 - 145.d	611.2	8.3	0.012	1697	24	NaN	178.8	2.2	0.01	739	12	0.12
eaf60 - 146.d	601.6	9.8	NaN	1641	23	NaN	172.1	2.7	NaN	709	9.6	NaN
eaf60 - 147.d	631	12	0.035	1714	26	NaN	182.9	3.5	NaN	766	15	0.06

Analysis number	La139 ppm	La139 ppm 2SE	La139 ppm LOD	Ce140 ppm	Ce140 ppm 2SE	Ce140 ppm LOD	Pr141 ppm	Pr141 ppm 2SE	Pr141 ppm LOD	Nd146 ppm	Nd146 ppm 2SE	Nd146 ppm LOD
eaf60 - 148.d	704	19	NaN	2096	37	0.012	237.4	4.3	NaN	1043	17	NaN
eaf60 - 149.d	716	22	0.026	2043	27	NaN	228.9	3.1	0.021	992	16	NaN
eaf60 - 150.d	784	27	0.024	2161	35	0.012	241.8	3.5	0.01	1045	18	0.08
eaf60 - 151.d	843	23	0.025	2230	29	NaN	251.2	2.6	NaN	1080	16	0.059
eaf60 - 152.d	611	12	NaN	1801	35	NaN	199.9	3.5	NaN	866	18	0.12
eaf60 - 153.d	653	11	NaN	1917	31	0.012	213.9	3.7	NaN	915	14	NaN
eaf60 - 154.d	714	20	NaN	2066	32	NaN	231.8	3.8	NaN	1008	17	NaN
eaf60 - 155.d	641.4	8.4	0.012	1923	25	NaN	219.2	2.8	0.022	970	13	0.16
eaf60 - 156.d	666	10	NaN	1940	20	0.025	215.5	2.7	NaN	943	12	0.12
eaf60 - 157.d	763	26	0.012	2095	34	NaN	229.2	3.1	NaN	1005	16	0.058
eaf60 - 158.d	613.9	9.5	NaN	1796	30	0.013	198.3	3.4	NaN	868	14	0.06
eaf60 - 159.d	604.1	7.3	NaN	1776	26	0.012	196.4	3.1	NaN	860	15	0.12
eaf60 - 160.d	624.5	9.9	0.012	1827	31	NaN	206.4	3.8	NaN	892	16	NaN

Analysis number	Sm147 ppm	Sm147 ppm 2SE	Sm147 ppm LOD	Eu153 ppm	Eu153 ppm 2SE	Eu153 ppm LOD	Gd157 ppm	Gd157 ppm 2SE	Gd157 ppm LOD	Tb159 ppm	Tb159 ppm 2SE	Tb159 ppm LOD
eaf60 - 1.d	196.4	3.9	NaN	47	1.3	0.019	184.7	4.8	0.13	26.15	0.66	0.0097
eaf60 - 2.d	213.1	4	0.072	50.2	1.1	NaN	208.9	4.4	NaN	29.34	0.72	NaN
eaf60 - 3.d	219.8	4.5	0.073	49.86	0.79	NaN	212.2	3.8	0.13	29.51	0.59	NaN
eaf60 - 4.d	193.4	4.3	NaN	46.4	1.2	0.039	178	4.2	NaN	26.33	0.55	NaN
eaf60 - 5.d	194.7	4.2	NaN	45.3	1.1	NaN	188.2	3.3	0.15	26.24	0.49	NaN
eaf60 - 6.d	230.8	3.9	0.14	59.3	1	0.019	216.1	3.6	0.065	31.35	0.69	NaN
eaf60 - 7.d	224.1	4.1	0.15	50.41	0.99	NaN	207.8	3.9	0.065	29.56	0.48	NaN
eaf60 - 8.d	208	4.5	0.21	47.91	0.92	NaN	199.3	3.9	NaN	28.55	0.57	0.0095
eaf60 - 9.d	228.4	4.7	0.071	51.7	1.1	0.042	218.4	3.9	NaN	30.62	0.58	0.019
eaf60 - 10.d	208.5	4	NaN	48.3	1	NaN	196.6	3.4	NaN	28.15	0.58	0.0096
eaf60 - 11.d	148.9	3.7	NaN	41.01	0.9	0.039	140.5	3	0.065	21.18	0.44	0.026
eaf60 - 12.d	149.8	2.6	NaN	41.9	1	NaN	142.4	2.5	NaN	20.72	0.45	0.0095
eaf60 - 13.d	148.7	3.4	0.071	43.38	0.97	NaN	141.2	3.2	0.13	20.85	0.44	NaN
eaf60 - 14.d	148.8	3.3	0.071	41.38	0.84	NaN	144.4	3	NaN	20.78	0.44	0.0096
eaf60 - 15.d	127.1	2.8	NaN	38.18	0.91	0.038	117.2	3.1	0.13	17.59	0.45	NaN
eaf60 - 16.d	106.4	1.9	NaN	34.95	0.76	NaN	95.3	1.9	NaN	14.71	0.32	NaN
eaf60 - 17.d	139.7	3.1	NaN	39.36	0.67	NaN	133	3.3	NaN	19.12	0.39	NaN
eaf60 - 18.d	133.6	3.1	NaN	38.65	0.86	0.019	124.7	3.1	0.064	18.46	0.53	NaN
eaf60 - 19.d	106.5	2.3	0.14	35.28	0.77	0.02	99.8	2	NaN	14.71	0.27	0.0098
eaf60 - 20.d	141.2	3.4	NaN	42.63	0.93	0.02	136.1	2.8	0.067	20.3	0.37	NaN
eaf60 - 21.d	146.8	3.6	NaN	42.9	0.82	NaN	138.9	2.5	NaN	20.67	0.44	NaN
eaf60 - 22.d	165.7	4.1	NaN	45.66	0.88	0.039	159.8	2.6	0.13	23.54	0.38	NaN
eaf60 - 23.d	173.9	3.6	0.098	50.14	0.86	NaN	173	3	NaN	27.4	0.52	NaN
eaf60 - 24.d	15.44	0.74	NaN	8.42	0.36	0.084	10.67	0.67	0.13	1.219	0.068	NaN
eaf60 - 25.d	10.77	0.77	0.14	6.92	0.31	NaN	6.41	0.49	NaN	0.767	0.067	0.019
eaf60 - 26.d	22	1.1	NaN	10.65	0.45	NaN	18.75	0.94	NaN	2.576	0.085	NaN
eaf60 - 27.d	14.7	0.69	NaN	7.17	0.27	NaN	9.12	0.68	NaN	1.113	0.09	NaN
eaf60 - 28.d	11.3	0.69	0.14	6.5	0.31	0.038	7.09	0.46	0.13	0.911	0.087	NaN
eaf60 - 29.d	16.91	0.82	NaN	6.88	0.31	0.038	15.98	0.63	0.13	2.201	0.097	NaN

Analysis number	Sm147 ppm	Sm147 ppm 2SE	Sm147 ppm LOD	Eu153 ppm	Eu153 ppm 2SE	Eu153 ppm LOD	Gd157 ppm	Gd157 ppm 2SE	Gd157 ppm LOD	Tb159 ppm	Tb159 ppm 2SE	Tb159 ppm LOD
eaf60 - 30.d	53.5	1.5	0.14	17.28	0.42	0.019	51.8	1.5	NaN	6.78	0.23	NaN
eaf60 - 31.d	86.4	2.2	0.19	36.06	0.85	0.018	60	1.8	NaN	6.88	0.2	NaN
eaf60 - 32.d	239.6	5.1	NaN	71.8	1.3	NaN	158.9	3.8	0.062	18.04	0.41	0.013
eaf60 - 33.d	24.79	0.98	NaN	10	0.37	NaN	17.1	1	0.063	2.33	0.12	0.02
eaf60 - 34.d	113.4	2.5	0.068	37.34	0.82	NaN	78.6	2	NaN	9.93	0.26	NaN
eaf60 - 35.d	61.5	1.7	NaN	26.61	0.74	0.025	49.5	1.8	NaN	7.25	0.22	NaN
eaf60 - 36.d	14	0.82	NaN	5.99	0.28	NaN	11.52	0.54	0.12	1.634	0.093	NaN
eaf60 - 37.d	187	2.6	NaN	42.54	0.92	NaN	177.5	3.2	0.062	25.4	0.5	0.02
eaf60 - 38.d	177	3.6	0.15	44.31	0.91	0.036	167.7	3.6	NaN	24.63	0.47	NaN
eaf60 - 39.d	180.9	2.9	0.07	44.61	0.99	0.038	174.1	2.6	0.13	25.39	0.45	0.0094
eaf60 - 40.d	179.7	4.3	0.14	44.7	0.99	0.018	169.8	3	NaN	24.17	0.47	0.026
eaf60 - 41.d	190.6	3.3	0.21	45.53	0.85	0.019	182.4	3.8	NaN	26.23	0.65	NaN
eaf60 - 42.d	188.2	3.3	NaN	43.24	0.94	0.037	183.4	4	0.12	26.2	0.51	NaN
eaf60 - 43.d	181.2	4.2	NaN	44.36	0.67	0.04	172.2	3.2	0.13	24.41	0.42	NaN
eaf60 - 44.d	204.1	4.8	NaN	47.33	0.88	0.039	193.4	3.6	NaN	28.62	0.62	NaN
eaf60 - 45.d	200.2	4.3	NaN	46.55	0.89	NaN	194.6	3.6	NaN	27.77	0.44	NaN
eaf60 - 46.d	198.8	3.3	NaN	45.65	0.97	NaN	190.6	3.7	0.066	27.57	0.51	NaN
eaf60 - 47.d	183	4	0.072	43.69	0.93	NaN	171.4	3.5	0.066	25.26	0.43	0.019
eaf60 - 48.d	197.8	4.2	NaN	44.4	1	NaN	183.1	3.9	NaN	25.94	0.53	NaN
eaf60 - 49.d	194.9	4.2	NaN	45.3	1.1	0.039	182.4	3.5	0.13	26.57	0.55	NaN
eaf60 - 50.d	171.8	3.7	NaN	43.66	0.72	0.038	162.6	3.3	NaN	24.23	0.42	0.021
eaf60 - 51.d	188.2	3.7	0.14	43.86	0.96	0.038	178.4	3.4	0.13	26.05	0.53	NaN
eaf60 - 52.d	189.7	3.9	NaN	45.5	1	NaN	188.3	3.4	NaN	27.18	0.53	NaN
eaf60 - 53.d	239.2	5.5	NaN	50.7	1.1	0.019	219	3.8	0.089	31.27	0.81	NaN
eaf60 - 54.d	228.9	4.6	NaN	50.26	0.92	NaN	219.3	4.9	0.17	31.17	0.64	0.038
eaf60 - 55.d	215.9	4.2	NaN	50.1	1	NaN	205.1	4.5	0.064	29.53	0.48	NaN
eaf60 - 56.d	208.5	4.1	NaN	49.1	1.2	0.052	197.4	4.4	NaN	28.66	0.73	NaN
eaf60 - 57.d	211.9	3.6	NaN	49.4	1.2	NaN	205.9	4.6	NaN	29.51	0.51	0.019
eaf60 - 58.d	222.4	4.4	NaN	50.1	1	NaN	206.9	3.6	NaN	29.35	0.61	NaN

Analysis number	Sm147 ppm	Sm147 ppm 2SE	Sm147 ppm LOD	Eu153 ppm	Eu153 ppm 2SE	Eu153 ppm LOD	Gd157 ppm	Gd157 ppm 2SE	Gd157 ppm LOD	Tb159 ppm	Tb159 ppm 2SE	Tb159 ppm LOD
eaf60 - 59.d	219.3	4.3	0.14	49.4	1.1	NaN	205.8	3	NaN	30.15	0.5	0.025
eaf60 - 60.d	199.5	3.8	NaN	46.4	1.2	0.038	189.9	4.1	NaN	27.07	0.47	0.019
eaf60 - 61.d	201.2	4.3	NaN	48.07	0.94	NaN	191.9	3.3	0.063	27.31	0.49	0.02
eaf60 - 62.d	216.7	3.8	0.097	50.75	0.93	0.042	206.3	4.4	0.065	29.8	0.63	NaN
eaf60 - 63.d	191.9	3.3	NaN	45.7	1.1	NaN	180	3.3	0.13	26.49	0.58	NaN
eaf60 - 64.d	179.2	3.6	NaN	45.8	1.2	NaN	173.9	3.8	NaN	25.25	0.53	NaN
eaf60 - 65.d	193.7	2.5	NaN	45.9	1.1	NaN	183.6	3.9	NaN	26.87	0.49	NaN
eaf60 - 66.d	210.7	5.1	NaN	48.41	0.96	NaN	197.1	3.9	0.088	27.75	0.57	0.019
eaf60 - 67.d	182.1	3.4	0.14	45.46	0.89	0.038	175.1	3.4	0.065	25.16	0.54	NaN
eaf60 - 68.d	225.8	4.5	0.14	50.79	0.98	NaN	217.7	3.6	NaN	30.28	0.52	NaN
eaf60 - 69.d	226.9	4.3	0.073	50.81	0.98	NaN	216.5	3.8	NaN	30.29	0.62	NaN
eaf60 - 70.d	197.1	3.8	NaN	46.69	0.94	NaN	188	4.2	0.14	25.95	0.65	NaN
eaf60 - 71.d	198.2	4.1	0.14	46.24	0.71	NaN	184.3	3.8	NaN	26.47	0.38	NaN
eaf60 - 72.d	220.9	4.4	NaN	51.08	0.94	NaN	210	4.9	NaN	29.79	0.54	0.0099
eaf60 - 73.d	171	3.2	NaN	43.75	0.93	0.039	161.4	3	NaN	23.66	0.42	NaN
eaf60 - 74.d	247.8	5.2	0.097	60.6	1.2	NaN	249.2	4.6	NaN	37.42	0.76	NaN
eaf60 - 75.d	215.9	4.2	NaN	49.9	1.4	NaN	208.4	4.4	0.13	29.84	0.56	0.0098
eaf60 - 76.d	231	4.5	0.07	51.9	1.1	NaN	218.6	5.1	0.18	31.37	0.6	NaN
eaf60 - 77.d	224.2	4.2	0.14	52.5	1	NaN	212	3.6	0.14	31.4	0.53	NaN
eaf60 - 78.d	225.1	4.2	0.14	50.22	0.91	NaN	212.1	4.4	NaN	30.31	0.51	NaN
eaf60 - 79.d	226.8	4.7	0.14	54.3	1.1	NaN	213.7	3.9	0.13	31.59	0.67	0.0096
eaf60 - 80.d	226.1	4.7	0.069	51.05	0.97	0.053	213.9	3.2	NaN	30.79	0.49	NaN
eaf60 - 81.d	238.5	5.3	NaN	55.8	1.1	NaN	226.6	4.4	NaN	32.79	0.67	0.019
eaf60 - 82.d	240.8	4.8	0.14	54.9	1.1	0.019	222.3	5	NaN	31.98	0.66	NaN
eaf60 - 83.d	240.9	4.7	0.28	53.4	1.1	NaN	229.2	4.7	0.13	32.66	0.52	0.0094
eaf60 - 84.d	233.2	4.8	NaN	53	1.1	NaN	218	4.2	NaN	31.25	0.58	0.021
eaf60 - 85.d	224.5	5.2	NaN	51.1	1.2	NaN	211.4	3.8	0.086	30.86	0.61	NaN
eaf60 - 86.d	218.6	4.5	0.14	50.1	1.3	NaN	208.3	3.8	NaN	29.99	0.57	NaN
eaf60 - 87.d	199.5	5	NaN	52	1.2	NaN	190.2	5	0.15	27.85	0.7	0.019

Analysis number	Sm147 ppm	Sm147 ppm 2SE	Sm147 ppm LOD	Eu153 ppm	Eu153 ppm 2SE	Eu153 ppm LOD	Gd157 ppm	Gd157 ppm 2SE	Gd157 ppm LOD	Tb159 ppm	Tb159 ppm 2SE	Tb159 ppm LOD
eaf60 - 88.d	217.8	4.6	NaN	47.9	0.95	0.019	211.6	4.8	NaN	29.54	0.6	NaN
eaf60 - 89.d	226	4.2	NaN	50.1	1.1	0.019	216.2	4.4	NaN	31.01	0.53	NaN
eaf60 - 90.d	213.8	4.9	NaN	48.79	0.77	0.038	206.1	4.2	NaN	29.23	0.68	NaN
eaf60 - 91.d	228.8	4.1	NaN	50.7	1	NaN	213.7	4.3	NaN	30.75	0.6	NaN
eaf60 - 92.d	217.4	4.4	0.17	49	1.3	NaN	206.9	4.2	NaN	29.85	0.6	NaN
eaf60 - 93.d	229.2	4.7	NaN	51.2	1	0.019	217.2	4.4	0.13	30.77	0.62	NaN
eaf60 - 94.d	210	3.5	NaN	48.2	1	NaN	200.5	3.7	NaN	29.36	0.55	0.01
eaf60 - 95.d	233.7	4.5	NaN	52.1	1.2	NaN	220.7	3.7	NaN	31.2	0.65	0.02
eaf60 - 96.d	225.7	4.8	0.14	50.01	0.95	NaN	218	3.5	NaN	30.73	0.58	0.0098
eaf60 - 97.d	232.2	4	NaN	61.7	1.3	NaN	230.9	4.1	0.13	34.27	0.61	NaN
eaf60 - 98.d	214.7	3.4	NaN	49.68	0.99	NaN	207.6	3.8	NaN	29.25	0.58	NaN
eaf60 - 99.d	249.8	4.6	NaN	56.8	1.3	NaN	238.8	4	NaN	33.61	0.57	NaN
eaf60 - 100.d	210.7	4.1	0.15	49.98	0.92	NaN	205.7	4.6	NaN	28.95	0.61	0.01
eaf60 - 101.d	266.5	6.4	NaN	67.4	1.3	NaN	261.4	4.6	NaN	37.96	0.82	NaN
eaf60 - 102.d	215.5	4.3	0.14	49.5	1.1	NaN	205.5	4	NaN	28.6	0.57	0.02
eaf60 - 103.d	219	4	0.15	49.9	1	NaN	214.6	4.3	0.15	30.24	0.59	NaN
eaf60 - 104.d	208	4.8	NaN	47.99	0.94	NaN	198	3.7	NaN	27.88	0.46	NaN
eaf60 - 105.d	218.2	5	NaN	53.1	1.1	0.02	209.9	4.6	0.13	30.08	0.57	NaN
eaf60 - 106.d	182.4	3.9	NaN	44.5	1.1	NaN	173.8	3.8	NaN	24.79	0.54	NaN
eaf60 - 107.d	170.8	3.4	0.14	44.9	1	NaN	169.8	3.9	NaN	24.26	0.44	0.013
eaf60 - 108.d	262.2	5.4	NaN	64.38	0.93	0.019	265.1	3.5	0.065	38	0.61	0.0096
eaf60 - 109.d	184.6	3.7	NaN	45.81	0.97	NaN	177.1	3	0.13	25.55	0.45	NaN
eaf60 - 110.d	189.2	3.9	0.098	46.09	0.89	NaN	185.8	2.6	0.13	26.35	0.5	NaN
eaf60 - 111.d	192.4	4	NaN	44.48	0.87	0.039	183.3	4	NaN	25.96	0.62	NaN
eaf60 - 112.d	188.5	4.3	0.07	43.9	1.1	NaN	181.7	3.6	NaN	25.59	0.61	0.019
eaf60 - 114.d	175.1	3.8	0.19	46.38	0.99	NaN	168.6	2.6	NaN	24.51	0.59	NaN
eaf60 - 115.d	190.8	3.8	NaN	45.51	0.71	NaN	180	3.3	NaN	26.13	0.55	0.0097
eaf60 - 116.d	193	3.5	0.15	44.92	0.9	NaN	188.9	3.9	0.13	26.32	0.58	NaN
eaf60 - 117.d	190.9	4.8	NaN	44.34	0.85	0.019	180.8	3.8	0.17	26.31	0.48	NaN

Analysis number	Sm147 ppm	Sm147 ppm 2SE	Sm147 ppm LOD	Eu153 ppm	Eu153 ppm 2SE	Eu153 ppm LOD	Gd157 ppm	Gd157 ppm 2SE	Gd157 ppm LOD	Tb159 ppm	Tb159 ppm 2SE	Tb159 ppm LOD
eaf60 - 118.d	185.4	3	0.21	43.58	0.9	0.038	179.1	2.3	NaN	25.46	0.42	0.019
eaf60 - 119.d	179.8	3.9	NaN	43.38	0.83	NaN	174.1	3.4	NaN	25.02	0.52	0.02
eaf60 - 120.d	183.4	3.3	NaN	42.4	1	NaN	174.9	3.7	NaN	24.84	0.58	0.03
eaf60 - 121.d	180.4	3.2	NaN	42.36	0.89	0.04	170.4	2.8	0.13	24.28	0.41	NaN
eaf60 - 122.d	193.8	4.2	0.14	45.64	0.94	0.039	190.3	4	NaN	26.46	0.47	0.0099
eaf60 - 123.d	189.9	3.6	NaN	46.44	0.82	NaN	183.9	3.3	NaN	26.44	0.41	0.035
eaf60 - 124.d	198.9	3.3	NaN	46.6	1.2	NaN	196.3	3.3	NaN	27.4	0.51	NaN
eaf60 - 126.d	155.6	3.1	NaN	44.9	1	0.02	152.2	3	NaN	21.83	0.58	0.0099
eaf60 - 127.d	141.6	3.2	0.14	44.3	1	NaN	139.3	2.8	NaN	19.61	0.41	NaN
eaf60 - 128.d	127.8	2.9	0.14	41.47	0.9	0.02	123.9	3.2	NaN	17.78	0.44	NaN
eaf60 - 129.d	108.4	2.7	NaN	38.96	0.87	0.039	100.3	2.8	NaN	15.46	0.38	0.021
eaf60 - 130.d	116.1	3.3	0.14	38.74	0.85	0.039	104.2	2.6	NaN	15.34	0.43	0.02
eaf60 - 131.d	129.9	3.2	NaN	42.86	0.82	NaN	122.9	3.2	NaN	18.4	0.43	0.02
eaf60 - 132.d	165	3.3	NaN	46.3	1.2	0.039	162.1	4.2	0.13	23.62	0.45	NaN
eaf60 - 133.d	168.5	3.4	0.071	49.11	0.91	NaN	170.3	2.9	NaN	24.79	0.52	NaN
eaf60 - 134.d	155.4	4.4	0.14	42.2	1	0.019	150.8	2.8	NaN	21.89	0.46	0.019
eaf60 - 135.d	156.2	3.2	NaN	45.31	0.89	0.039	148.3	3.3	NaN	21.98	0.48	0.0097
eaf60 - 136.d	150.9	3.6	NaN	43.64	0.93	0.026	144.8	2.7	NaN	21.12	0.59	0.019
eaf60 - 137.d	201.4	4.6	0.07	48.9	1.2	NaN	195.4	4.6	0.064	28.39	0.62	0.026
eaf60 - 138.d	240.8	3.9	0.19	57	1.3	0.044	237.7	4.3	NaN	34.67	0.58	NaN
eaf60 - 139.d	140.1	3.1	0.15	41.7	0.84	0.038	141.8	3.3	NaN	20.7	0.34	0.0096
eaf60 - 140.d	149.9	3	NaN	41.24	0.76	0.038	143.9	3.6	NaN	20.8	0.38	0.0096
eaf60 - 141.d	153.3	2.5	NaN	42.82	0.74	NaN	150.5	3.7	NaN	21.98	0.41	0.0097
eaf60 - 142.d	142.9	4.1	0.071	41.7	1	NaN	139.5	2.8	NaN	20.26	0.42	0.0096
eaf60 - 143.d	142.6	3.6	0.071	43.46	0.98	0.042	135.1	3.2	0.066	20.09	0.5	NaN
eaf60 - 144.d	151.8	3.1	NaN	41.71	0.7	NaN	148.8	3.2	0.13	21.51	0.52	0.013
eaf60 - 145.d	159.7	3	NaN	43.89	0.63	0.019	150.6	3	NaN	22.11	0.47	0.019
eaf60 - 146.d	152.9	2.8	0.07	41.43	0.53	NaN	147	3.4	NaN	21.37	0.35	NaN
eaf60 - 147.d	162.8	3.7	NaN	45.4	1.2	0.042	159.4	2.6	0.065	22.44	0.55	0.0096

Analysis number	Sm147 ppm	Sm147 ppm 2SE	Sm147 ppm LOD	Eu153 ppm	Eu153 ppm 2SE	Eu153 ppm LOD	Gd157 ppm	Gd157 ppm 2SE	Gd157 ppm LOD	Tb159 ppm	Tb159 ppm 2SE	Tb159 ppm LOD
eaf60 - 148.d	232.2	5	NaN	55.7	1.2	NaN	222.8	4.6	0.17	31.33	0.66	NaN
eaf60 - 149.d	224.5	4	0.068	51.2	1.2	NaN	211.5	2.9	NaN	29.75	0.54	NaN
eaf60 - 150.d	227.9	5.4	NaN	52.1	1.3	0.051	218.9	4.5	NaN	30.12	0.59	0.028
eaf60 - 151.d	236.9	4.1	NaN	52.5	1.1	NaN	219.9	4.2	0.064	30.84	0.53	0.0095
eaf60 - 152.d	194.2	4.5	0.069	45.21	0.98	NaN	188.9	4	NaN	26.42	0.49	NaN
eaf60 - 153.d	204.8	3.3	NaN	47.4	1.1	NaN	195.5	4.1	NaN	27.91	0.61	NaN
eaf60 - 154.d	218.7	4.3	NaN	49.2	1.2	0.019	214.3	4.6	NaN	30.05	0.66	NaN
eaf60 - 155.d	219.9	5.4	0.14	50.7	1.5	NaN	209	5.4	NaN	30.21	0.59	0.02
eaf60 - 156.d	205.4	3.8	0.07	47.03	0.94	NaN	204.7	3.6	0.19	28.5	0.55	0.019
eaf60 - 157.d	221.2	3.3	NaN	48.8	1	NaN	213	4	0.13	29.21	0.45	NaN
eaf60 - 158.d	194.8	2.6	NaN	47.4	1.1	NaN	188.3	3.6	0.065	27.02	0.51	0.022
eaf60 - 159.d	190.8	4	0.07	46.15	0.82	NaN	186.3	4.1	0.13	26.52	0.5	NaN
eaf60 - 160.d	198.6	4.3	0.14	45.7	1	0.051	191.8	4.1	NaN	27.27	0.4	NaN

Analysis number	Dy163 ppm	Dy163 ppm 2SE	Dy163 ppm LOD	Ho165 ppm	Ho165 ppm 2SE	Ho165 ppm LOD	Er166 ppm	Er166 ppm 2SE	Er166 ppm LOD	Tm169 ppm	Tm169 ppm 2SE	Tm169 ppm LOD
eaf60 - 1.d	156	2.8	NaN	28.79	0.65	NaN	72.7	1.3	NaN	9.26	0.32	0.0095
eaf60 - 2.d	172.1	2.9	0.08	31.53	0.62	NaN	80.2	1.7	NaN	9.74	0.29	0.019
eaf60 - 3.d	174.1	3.2	NaN	31.36	0.55	0.02	80	1.4	NaN	9.57	0.27	NaN
eaf60 - 4.d	152.4	2.9	0.04	29.07	0.54	0.01	76.7	1.8	NaN	10.04	0.3	NaN
eaf60 - 5.d	160.9	2.8	NaN	29.11	0.5	NaN	77.9	1.8	0.029	9.65	0.27	0.019
eaf60 - 6.d	188.2	3.7	NaN	34.77	0.57	NaN	93.6	1.8	0.058	12.06	0.28	NaN
eaf60 - 7.d	177	3	NaN	32.48	0.59	NaN	83	1.2	0.059	10.15	0.31	0.015
eaf60 - 8.d	165.1	2.7	0.039	30.21	0.53	0.043	79.3	1.7	0.058	10.1	0.28	NaN
eaf60 - 9.d	178	2.8	0.086	33.03	0.64	NaN	84.4	1.5	NaN	9.94	0.29	0.013
eaf60 - 10.d	170.4	3.4	NaN	31.55	0.54	0.02	80.7	1.6	NaN	10.07	0.21	0.019
eaf60 - 11.d	126	2.4	NaN	24	0.49	NaN	65.4	1.6	NaN	8.84	0.28	NaN
eaf60 - 12.d	124	2.4	NaN	23.63	0.51	NaN	65.3	1.4	NaN	8.39	0.25	0.019
eaf60 - 13.d	128.4	2.6	0.039	24.24	0.52	NaN	67.4	1.1	0.029	9.08	0.23	0.0094
eaf60 - 14.d	126.3	2.3	NaN	24.03	0.33	0.0098	65.2	1.3	NaN	8.58	0.22	NaN
eaf60 - 15.d	105.1	1.3	0.11	20.32	0.41	0.02	56.6	1	0.029	7.71	0.22	0.02
eaf60 - 16.d	91.7	1.7	0.04	17.86	0.31	NaN	52	1.1	0.064	7.13	0.25	NaN
eaf60 - 17.d	118.2	2.3	NaN	22.24	0.47	NaN	60.9	1.5	0.057	8.14	0.25	0.028
eaf60 - 18.d	110.3	2.5	NaN	20.94	0.35	NaN	58.4	1	NaN	7.84	0.19	NaN
eaf60 - 19.d	89.7	1.7	0.081	18.08	0.4	0.022	51.05	0.92	NaN	7.22	0.21	NaN
eaf60 - 20.d	123.3	1.8	0.041	23.72	0.38	NaN	65.7	1.3	0.03	8.86	0.21	NaN
eaf60 - 21.d	125.6	2.3	NaN	23.94	0.47	NaN	66.8	1.6	0.061	8.74	0.25	0.021
eaf60 - 22.d	144.8	3	0.04	28.01	0.52	0.02	76.7	1.2	NaN	10.04	0.23	NaN
eaf60 - 23.d	173.5	2.5	0.04	33.51	0.53	0.02	95.3	1.4	NaN	13.07	0.29	NaN
eaf60 - 24.d	7.22	0.44	0.04	1.228	0.087	0.02	3.61	0.25	NaN	0.44	0.047	NaN
eaf60 - 25.d	4.05	0.26	0.039	0.744	0.066	0.0096	1.81	0.15	NaN	0.25	0.039	NaN
eaf60 - 26.d	15.45	0.62	NaN	2.79	0.14	0.043	7.34	0.38	0.059	0.996	0.073	NaN
eaf60 - 27.d	6.43	0.42	NaN	1.134	0.096	NaN	2.67	0.25	NaN	0.381	0.047	NaN
eaf60 - 28.d	4.41	0.33	NaN	0.848	0.074	NaN	2.16	0.19	0.058	0.313	0.044	NaN
eaf60 - 29.d	13.54	0.5	NaN	2.5	0.12	0.0098	6.74	0.31	NaN	0.893	0.058	NaN

Analysis number	Dy163 ppm	Dy163 ppm 2SE	Dy163 ppm LOD	Ho165 ppm	Ho165 ppm 2SE	Ho165 ppm LOD	Er166 ppm	Er166 ppm 2SE	Er166 ppm LOD	Tm169 ppm	Tm169 ppm 2SE	Tm169 ppm LOD
eaf60 - 30.d	36.4	1	NaN	6.21	0.18	NaN	15.05	0.59	0.029	1.631	0.08	NaN
eaf60 - 31.d	33.8	0.86	NaN	4.66	0.17	NaN	9.91	0.38	0.028	0.981	0.087	NaN
eaf60 - 32.d	83.3	1.7	0.038	12.29	0.34	NaN	27.26	0.75	0.056	3.07	0.15	0.009
eaf60 - 33.d	12.16	0.6	NaN	2.23	0.13	NaN	5.73	0.24	0.057	0.79	0.065	NaN
eaf60 - 34.d	51.6	1.5	0.1	8.57	0.22	0.013	21.05	0.6	NaN	2.56	0.13	0.018
eaf60 - 35.d	42	1.3	0.038	8.17	0.3	0.019	22.97	0.71	0.028	3.31	0.16	NaN
eaf60 - 36.d	10.68	0.48	0.076	1.91	0.1	NaN	5.48	0.21	NaN	0.729	0.072	0.0091
eaf60 - 37.d	152.6	2.8	NaN	28.19	0.5	NaN	74.6	1.3	NaN	9.89	0.25	0.012
eaf60 - 38.d	148.6	1.8	NaN	27.32	0.5	NaN	73.9	1.5	0.056	9.68	0.27	0.019
eaf60 - 39.d	150.6	2.7	0.078	28.49	0.47	NaN	73.7	1.5	NaN	9.63	0.32	NaN
eaf60 - 40.d	145.4	3.4	NaN	27.98	0.55	0.013	73.5	1.3	0.028	9.6	0.24	0.025
eaf60 - 41.d	155.1	3.2	NaN	28.51	0.59	0.0096	77.4	1.7	0.086	9.38	0.21	0.018
eaf60 - 42.d	152.9	3.3	NaN	28.42	0.59	NaN	74.2	1.9	0.057	9.37	0.23	NaN
eaf60 - 43.d	146.7	3.2	NaN	27.93	0.55	NaN	73.9	1.6	NaN	9.73	0.22	NaN
eaf60 - 44.d	165.3	3.1	NaN	30.83	0.57	0.02	80.1	1.6	0.06	9.79	0.24	NaN
eaf60 - 45.d	162.1	2	NaN	29.56	0.55	0.028	77.7	1.5	0.083	9.68	0.19	NaN
eaf60 - 46.d	159.7	2.6	NaN	29.58	0.46	NaN	76.4	1.5	NaN	9.67	0.24	NaN
eaf60 - 47.d	152	2.2	NaN	28.46	0.48	NaN	75.2	1.8	NaN	9.37	0.24	NaN
eaf60 - 48.d	153.8	2.8	NaN	28.5	0.56	NaN	74.3	1.6	NaN	9.19	0.26	0.0096
eaf60 - 49.d	159.9	3.4	NaN	29.76	0.5	0.03	76.2	1.5	NaN	9.42	0.24	NaN
eaf60 - 50.d	145.6	3.1	0.039	27.9	0.52	0.0098	73.8	1.2	0.064	9.24	0.22	NaN
eaf60 - 51.d	152.4	2.9	NaN	28.75	0.52	NaN	76.1	1.9	0.058	9.37	0.27	0.013
eaf60 - 52.d	160.3	3.4	NaN	30.09	0.66	0.02	78.8	1.8	NaN	10.25	0.25	0.019
eaf60 - 53.d	183.2	3.2	NaN	33.33	0.65	0.0099	86.2	2	NaN	10.46	0.33	0.0094
eaf60 - 54.d	183.3	3.1	NaN	34.08	0.59	NaN	85.9	1.5	NaN	10.68	0.32	NaN
eaf60 - 55.d	172.4	3.1	NaN	32.26	0.59	0.019	83.9	1.5	NaN	10.51	0.27	0.013
eaf60 - 56.d	169.3	2.8	NaN	31.28	0.6	NaN	82	1.5	NaN	10.46	0.25	NaN
eaf60 - 57.d	174.6	3.1	0.086	32.26	0.78	0.031	85.9	1.7	NaN	10.67	0.28	NaN
eaf60 - 58.d	175.1	2.8	0.077	32.23	0.66	NaN	83.7	1.6	NaN	10.33	0.25	NaN

Analysis number	Dy163 ppm	Dy163 ppm 2SE	Dy163 ppm LOD	Ho165 ppm	Ho165 ppm 2SE	Ho165 ppm LOD	Er166 ppm	Er166 ppm 2SE	Er166 ppm LOD	Tm169 ppm	Tm169 ppm 2SE	Tm169 ppm LOD
eaf60 - 59.d	176.7	3.6	NaN	32.3	0.54	NaN	84.9	1.3	NaN	10.51	0.3	NaN
eaf60 - 60.d	162.7	2.8	NaN	29.89	0.5	0.02	79.2	1.4	NaN	10.15	0.29	0.028
eaf60 - 61.d	164.5	2.4	0.084	30.4	0.47	0.019	79.3	1.5	NaN	10.02	0.24	NaN
eaf60 - 62.d	175.6	2.7	NaN	32.27	0.56	0.0099	85.1	1.4	NaN	10.83	0.26	0.026
eaf60 - 63.d	153.4	2.6	0.039	29.36	0.67	0.021	78.3	1.7	NaN	9.72	0.27	NaN
eaf60 - 64.d	150.7	3.2	NaN	27.81	0.54	NaN	73.8	1.5	NaN	9.78	0.25	NaN
eaf60 - 65.d	159.7	2.8	NaN	30.11	0.54	0.0096	79.1	1.5	NaN	10.15	0.23	0.018
eaf60 - 66.d	159.2	3	0.039	29.35	0.62	NaN	74.5	1.6	NaN	9.37	0.27	0.019
eaf60 - 67.d	150.3	3.1	0.04	28.46	0.47	0.0099	74.9	1.6	0.059	9.63	0.27	0.021
eaf60 - 68.d	176	3.4	NaN	32.34	0.58	NaN	82.9	1.6	NaN	10.17	0.27	NaN
eaf60 - 69.d	178.5	3.3	0.056	32.02	0.49	NaN	81.7	1.4	0.06	10.09	0.23	0.0097
eaf60 - 70.d	154.9	3	0.083	29.14	0.57	NaN	76	1.3	0.031	9.41	0.29	0.02
eaf60 - 71.d	153	2.5	0.04	29.28	0.58	NaN	76.1	1.5	NaN	9.46	0.31	NaN
eaf60 - 72.d	174.1	3.1	0.082	32.15	0.58	NaN	82.6	1.9	NaN	10.33	0.32	NaN
eaf60 - 73.d	141.7	2.7	NaN	26.88	0.57	NaN	70.9	1.8	0.06	9.33	0.24	NaN
eaf60 - 74.d	233.7	3.7	NaN	43.93	0.91	NaN	118.4	2.5	0.081	15.56	0.24	0.019
eaf60 - 75.d	176.6	3.3	NaN	33.56	0.65	NaN	85.8	1.9	NaN	10.83	0.27	NaN
eaf60 - 76.d	184.3	3.6	NaN	34.11	0.61	NaN	88.7	1.9	0.029	10.76	0.25	NaN
eaf60 - 77.d	181.8	3.2	NaN	34.76	0.54	NaN	88.4	1.5	NaN	10.91	0.22	0.019
eaf60 - 78.d	179.5	3.3	0.078	33.53	0.72	NaN	84.8	1.8	0.079	10.62	0.32	0.019
eaf60 - 79.d	187.1	2.7	0.079	35.41	0.59	0.0098	91.9	2.1	NaN	11.28	0.34	0.019
eaf60 - 80.d	180.2	2.6	NaN	33.79	0.7	NaN	86.4	1.6	NaN	10.47	0.28	0.019
eaf60 - 81.d	190.7	3.3	0.079	35.45	0.79	NaN	92.5	2	NaN	10.93	0.3	0.0094
eaf60 - 82.d	192.8	2.8	NaN	35.59	0.71	0.0097	92.2	2.1	NaN	11.26	0.31	NaN
eaf60 - 83.d	189.3	3.8	0.039	35.73	0.62	NaN	89.1	1.8	0.029	10.39	0.29	NaN
eaf60 - 84.d	187.9	2.8	NaN	35.71	0.62	NaN	92	1.7	NaN	11.22	0.31	0.019
eaf60 - 85.d	177.6	3.2	0.038	34.01	0.6	0.0096	89.1	1.2	NaN	10.92	0.26	0.018
eaf60 - 86.d	175.8	3.2	NaN	33.27	0.56	0.02	85.5	1.8	NaN	10.64	0.29	0.029
eaf60 - 87.d	168.5	3.7	0.039	31.39	0.74	0.0098	83.8	2.1	NaN	11.68	0.3	0.019

Analysis number	Dy163 ppm	Dy163 ppm 2SE	Dy163 ppm LOD	Ho165 ppm	Ho165 ppm 2SE	Ho165 ppm LOD	Er166 ppm	Er166 ppm 2SE	Er166 ppm LOD	Tm169 ppm	Tm169 ppm 2SE	Tm169 ppm LOD
eaf60 - 88.d	171.9	3.2	NaN	32.12	0.67	NaN	82.3	1.5	NaN	9.81	0.23	0.037
eaf60 - 89.d	180.8	3.5	NaN	33.09	0.63	NaN	86.5	1.7	NaN	10.27	0.23	NaN
eaf60 - 90.d	173.9	2.6	0.039	31.89	0.64	0.0098	82.7	1.7	0.029	10.48	0.21	NaN
eaf60 - 91.d	179.5	3.2	NaN	33.26	0.63	NaN	85.6	1.5	NaN	10.43	0.24	NaN
eaf60 - 92.d	173.1	2.8	0.083	32.7	0.58	NaN	83.9	1.5	NaN	10.42	0.24	NaN
eaf60 - 93.d	184.8	3.9	NaN	34.36	0.62	NaN	88	2	NaN	10.63	0.3	NaN
eaf60 - 94.d	171.6	3	NaN	31.47	0.54	NaN	85.5	1.5	NaN	10.34	0.29	NaN
eaf60 - 95.d	186.4	2.8	0.082	34.8	0.61	0.01	90.3	1.8	0.061	11.01	0.28	NaN
eaf60 - 96.d	182.6	3.6	NaN	33.76	0.73	0.03	88.1	1.7	0.082	10.76	0.31	NaN
eaf60 - 97.d	218	2.9	NaN	42.1	0.68	NaN	118.3	1.8	0.12	16.76	0.35	0.02
eaf60 - 98.d	172.5	3	0.081	32.25	0.54	0.02	84.3	1.6	NaN	10.15	0.24	0.027
eaf60 - 99.d	195.5	3.4	0.09	34.52	0.7	NaN	89.3	1.8	NaN	10.71	0.28	NaN
eaf60 - 100.d	170.2	3.6	NaN	32.05	0.67	0.01	82.2	1.7	NaN	10.33	0.27	NaN
eaf60 - 101.d	225.4	4.4	0.081	43.53	0.9	0.02	117.5	2.5	NaN	15.21	0.43	0.0097
eaf60 - 102.d	165.9	3	0.041	30.18	0.56	NaN	78.7	1.7	0.06	9.67	0.27	NaN
eaf60 - 103.d	176.9	3.3	0.082	32.64	0.68	NaN	83.6	1.3	0.03	10.36	0.28	NaN
eaf60 - 104.d	159.7	3	NaN	29.48	0.56	NaN	77.7	1.5	NaN	9.85	0.23	NaN
eaf60 - 105.d	175.8	3.3	NaN	32.95	0.52	NaN	84.1	1.9	0.082	10.51	0.23	NaN
eaf60 - 106.d	149.9	2.8	NaN	28.08	0.6	NaN	76.1	1.6	NaN	9.46	0.3	0.019
eaf60 - 107.d	144.8	2.7	NaN	27.19	0.64	NaN	73.5	1.5	NaN	9.73	0.26	NaN
eaf60 - 108.d	230.9	3.2	0.039	43.9	0.51	NaN	117.4	1.5	0.059	15.02	0.37	NaN
eaf60 - 109.d	153.9	2.8	NaN	29.2	0.69	0.01	77.3	1.5	NaN	9.74	0.29	NaN
eaf60 - 110.d	157.5	3.1	NaN	29.32	0.43	NaN	77.8	1.5	NaN	10.1	0.24	NaN
eaf60 - 111.d	152.1	2.7	NaN	28.93	0.65	NaN	76.4	1.8	NaN	9.47	0.25	NaN
eaf60 - 112.d	153.4	2.5	NaN	28.78	0.56	0.02	77.5	1.8	NaN	9.4	0.24	NaN
eaf60 - 114.d	145.9	2.9	NaN	27.54	0.63	NaN	75.1	1.5	NaN	9.56	0.3	NaN
eaf60 - 115.d	152.1	2.8	NaN	28.29	0.51	0.0099	74.3	1.5	0.059	9.45	0.27	0.0095
eaf60 - 116.d	155.3	3	NaN	28.71	0.57	NaN	74.4	1.7	NaN	9.05	0.29	NaN
eaf60 - 117.d	153.5	3	NaN	29.18	0.54	NaN	74.6	1.6	NaN	9.32	0.22	0.0093

Analysis number	Dy163 ppm	Dy163 ppm 2SE	Dy163 ppm LOD	Ho165 ppm	Ho165 ppm 2SE	Ho165 ppm LOD	Er166 ppm	Er166 ppm 2SE	Er166 ppm LOD	Tm169 ppm	Tm169 ppm 2SE	Tm169 ppm LOD
eaf60 - 118.d	149.7	2.6	NaN	28.59	0.52	NaN	74.2	1.4	NaN	9.25	0.23	0.019
eaf60 - 119.d	147.4	2.5	NaN	27.83	0.53	NaN	72.7	1.5	NaN	8.9	0.25	0.02
eaf60 - 120.d	146.2	3.1	NaN	27.41	0.51	NaN	71.7	1.1	0.083	9.27	0.25	NaN
eaf60 - 121.d	147.3	2.7	NaN	27.14	0.53	NaN	71.8	1.2	NaN	9.1	0.27	NaN
eaf60 - 122.d	158.4	3	0.16	29.48	0.56	0.02	75.6	1.6	NaN	9.7	0.29	NaN
eaf60 - 123.d	156	2.8	NaN	29.59	0.52	0.01	79.4	1.8	0.061	10.1	0.29	0.0097
eaf60 - 124.d	162	2.7	NaN	30.12	0.46	0.02	80.3	2.2	NaN	9.69	0.26	NaN
eaf60 - 126.d	128.3	2.3	NaN	24.93	0.47	NaN	66.7	1.4	0.061	8.69	0.21	NaN
eaf60 - 127.d	121.2	2.5	NaN	22.92	0.37	0.02	63.8	1.4	NaN	8.48	0.19	NaN
eaf60 - 128.d	109.2	1.8	0.04	21.35	0.37	0.01	58.9	1.4	0.082	7.81	0.22	NaN
eaf60 - 129.d	93.6	1.6	NaN	18.18	0.39	NaN	51	1.2	NaN	7.18	0.17	NaN
eaf60 - 130.d	93.2	2	0.04	18.85	0.53	NaN	52.5	1.3	0.03	7.12	0.24	NaN
eaf60 - 131.d	113	1.8	0.04	22.23	0.4	NaN	60.5	1.2	NaN	8.21	0.22	NaN
eaf60 - 132.d	138.8	2.2	NaN	27.23	0.66	0.01	73.6	1.8	NaN	9.56	0.23	NaN
eaf60 - 133.d	152.9	2.6	0.11	30.11	0.71	0.0099	84.9	1.5	NaN	11.39	0.28	NaN
eaf60 - 134.d	130.1	3.3	NaN	25.05	0.57	NaN	69.2	1.8	NaN	8.81	0.25	NaN
eaf60 - 135.d	133.4	2.6	0.087	25.46	0.56	NaN	71.6	1.4	0.059	9.48	0.21	NaN
eaf60 - 136.d	127.3	2.3	0.08	24.79	0.56	0.01	67.9	1.2	0.065	8.79	0.23	0.026
eaf60 - 137.d	161.1	3.1	0.039	30.68	0.66	0.0098	80.9	1.8	NaN	10.11	0.29	0.019
eaf60 - 138.d	207.1	3.4	NaN	38.7	0.64	NaN	104.6	1.5	0.029	13.09	0.26	NaN
eaf60 - 139.d	124.4	2.6	NaN	23.96	0.39	0.02	66.5	1.4	0.059	8.22	0.16	NaN
eaf60 - 140.d	123.1	2.5	NaN	23.97	0.36	0.0098	66	1.1	0.059	8.46	0.24	NaN
eaf60 - 141.d	131.5	2.4	0.08	25.19	0.46	NaN	69.1	1.5	0.03	9.25	0.19	0.0095
eaf60 - 142.d	121.5	2.4	0.08	23.78	0.4	NaN	64.1	1.5	NaN	8.63	0.25	NaN
eaf60 - 143.d	121.6	2.4	0.11	23.63	0.53	NaN	64	1.5	NaN	8.28	0.25	NaN
eaf60 - 144.d	128.7	2.2	NaN	24.25	0.53	NaN	66.7	1.3	0.029	8.65	0.33	NaN
eaf60 - 145.d	134.3	2.7	NaN	25.47	0.38	NaN	69.7	1.3	NaN	8.98	0.26	NaN
eaf60 - 146.d	129.3	2.2	0.079	24.2	0.46	NaN	66	1.5	0.029	8.8	0.25	NaN
eaf60 - 147.d	135.7	2.7	NaN	25.62	0.62	0.02	70.3	1.4	NaN	8.94	0.25	0.013

Analysis number	Dy163 ppm	Dy163 ppm 2SE	Dy163 ppm LOD	Ho165 ppm	Ho165 ppm 2SE	Ho165 ppm LOD	Er166 ppm	Er166 ppm 2SE	Er166 ppm LOD	Tm169 ppm	Tm169 ppm 2SE	Tm169 ppm LOD
eaf60 - 148.d	183.4	3.4	0.085	34.55	0.49	NaN	85.9	1.8	0.058	10.03	0.27	NaN
eaf60 - 149.d	174.5	3.5	NaN	31.52	0.55	NaN	81.6	1.4	NaN	9.76	0.21	NaN
eaf60 - 150.d	173.6	2.9	0.078	32.31	0.67	NaN	82.1	2.2	0.063	9.77	0.29	NaN
eaf60 - 151.d	180.6	3	0.078	32.19	0.64	NaN	83.1	1.7	NaN	9.92	0.26	NaN
eaf60 - 152.d	162.1	3.2	NaN	29.93	0.69	NaN	80.3	1.7	NaN	9.76	0.23	NaN
eaf60 - 153.d	167.6	3.2	0.039	30.69	0.69	0.0097	82	1.7	NaN	10.01	0.24	NaN
eaf60 - 154.d	174	3.1	NaN	31.94	0.64	0.0098	83.9	2	NaN	10.13	0.27	0.019
eaf60 - 155.d	177.7	2.5	NaN	33.02	0.71	0.0096	86.6	2.2	NaN	11.21	0.29	NaN
eaf60 - 156.d	167.7	2.8	0.085	31.03	0.57	NaN	81.8	1.6	0.029	9.94	0.24	0.037
eaf60 - 157.d	176.3	2.9	0.038	31.86	0.62	NaN	84	1.6	0.057	10.02	0.27	NaN
eaf60 - 158.d	161.6	2.5	0.079	30.05	0.56	0.02	80.1	1.6	NaN	9.92	0.27	NaN
eaf60 - 159.d	160.3	3	NaN	29.94	0.58	0.021	79.1	1.3	NaN	10.03	0.29	NaN
eaf60 - 160.d	161.6	3	NaN	29.27	0.56	NaN	79.7	1.6	0.058	9.66	0.27	NaN

Analysis number	Yb172 ppm	Yb172 ppm 2SE	Yb172 ppm LOD	Lu175 ppm	Lu175 ppm 2SE	Lu175 ppm LOD	Hf178 ppm	Hf178 ppm 2SE	Hf178 ppm LOD	Ta181 ppm	Ta181 ppm 2SE	Ta181 ppm LOD
eaf60 - 1.d	53.7	1.3	NaN	7.03	0.2	0.0099	55.3	1.3	NaN	14.64	0.37	NaN
eaf60 - 2.d	55.4	1.5	0.089	6.81	0.25	NaN	57.7	1.2	0.033	18.12	0.5	NaN
eaf60 - 3.d	55.9	1.4	0.091	7.12	0.25	NaN	58.4	1.3	NaN	18.82	0.47	0.019
eaf60 - 4.d	60.6	1.5	NaN	8.09	0.29	0.031	57.2	1.2	NaN	16.57	0.45	NaN
eaf60 - 5.d	56.4	1.2	NaN	7.19	0.2	NaN	60.2	1.6	0.066	16.61	0.48	0.018
eaf60 - 6.d	75.1	1.5	0.044	9.44	0.24	0.0097	64.3	1.5	NaN	13.48	0.33	0.018
eaf60 - 7.d	56.9	1.4	NaN	6.98	0.24	NaN	61.6	1.4	0.033	16.02	0.36	NaN
eaf60 - 8.d	55.5	1.2	NaN	6.91	0.21	NaN	60	1.2	0.066	16.16	0.41	NaN
eaf60 - 9.d	57.3	1.6	0.088	7.18	0.27	NaN	62.1	1.4	NaN	17.94	0.43	0.009
eaf60 - 10.d	58.1	1.5	NaN	6.98	0.22	NaN	61	1.2	NaN	15.7	0.37	0.009
eaf60 - 11.d	55	1.3	0.089	7.38	0.23	NaN	53.6	1.5	NaN	4.67	0.17	NaN
eaf60 - 12.d	53.2	1.3	NaN	6.97	0.23	0.019	52.2	1.2	NaN	5.59	0.14	0.039
eaf60 - 13.d	55.5	1.3	NaN	7.78	0.28	NaN	53.9	1.4	NaN	4.94	0.2	0.039
eaf60 - 14.d	51.9	1.5	NaN	6.97	0.21	NaN	53.3	1.1	NaN	6.23	0.21	NaN
eaf60 - 15.d	48.9	1.1	NaN	6.34	0.21	0.0098	48.3	1.4	NaN	3.47	0.16	NaN
eaf60 - 16.d	47.2	1.1	NaN	6.15	0.16	NaN	44.46	0.81	0.033	1.66	0.1	NaN
eaf60 - 17.d	49.7	1.4	0.043	6.73	0.21	NaN	52.1	1.3	0.032	4.79	0.19	NaN
eaf60 - 18.d	48	1	NaN	6.56	0.21	NaN	51.9	1.2	NaN	5.01	0.15	NaN
eaf60 - 19.d	45.7	1.2	0.045	6.32	0.22	NaN	47.8	1.1	NaN	2.06	0.12	NaN
eaf60 - 20.d	56.5	1.4	0.091	7.59	0.24	0.01	53.3	0.95	0.034	4.25	0.15	NaN
eaf60 - 21.d	55.1	1.3	0.1	7.81	0.26	NaN	52.8	1.2	NaN	4.85	0.22	0.02
eaf60 - 22.d	64.3	1.5	0.089	8.44	0.22	NaN	51.9	1.3	NaN	6.57	0.13	0.0091
eaf60 - 23.d	83.8	1.8	0.097	11.15	0.3	NaN	50	1.2	NaN	7.26	0.23	0.0091
eaf60 - 24.d	2.99	0.28	NaN	0.435	0.051	0.02	11.43	0.41	0.033	2.27	0.12	0.018
eaf60 - 25.d	1.68	0.21	NaN	0.224	0.035	0.019	14.39	0.65	NaN	3.53	0.16	NaN
eaf60 - 26.d	6.77	0.39	NaN	0.91	0.05	NaN	11.35	0.51	0.093	2.37	0.12	0.009
eaf60 - 27.d	2.32	0.27	0.095	0.278	0.043	0.013	14.22	0.43	NaN	3.6	0.13	0.018
eaf60 - 28.d	1.7	0.17	0.043	0.218	0.036	0.019	10.23	0.44	0.045	2.46	0.13	0.0089
eaf60 - 29.d	5.41	0.32	0.088	0.729	0.076	NaN	13.3	0.57	NaN	6.71	0.2	0.009

Analysis number	Yb172 ppm	Yb172 ppm 2SE	Yb172 ppm LOD	Lu175 ppm	Lu175 ppm 2SE	Lu175 ppm LOD	Hf178 ppm	Hf178 ppm 2SE	Hf178 ppm LOD	Ta181 ppm	Ta181 ppm 2SE	Ta181 ppm LOD
eaf60 - 30.d	8.35	0.54	NaN	0.899	0.065	NaN	12.27	0.52	NaN	2.71	0.13	0.018
eaf60 - 31.d	5.21	0.34	0.042	0.549	0.05	NaN	16.16	0.52	0.063	3.21	0.15	NaN
eaf60 - 32.d	16.88	0.55	NaN	1.906	0.098	NaN	44.2	1.1	NaN	3.65	0.16	NaN
eaf60 - 33.d	5.03	0.34	NaN	0.725	0.069	0.026	10.55	0.48	0.032	2.41	0.12	NaN
eaf60 - 34.d	14.48	0.63	NaN	1.837	0.096	0.019	17.35	0.66	NaN	2.63	0.12	NaN
eaf60 - 35.d	20.88	0.72	0.086	3.3	0.11	0.019	14.81	0.49	0.088	4.03	0.15	NaN
eaf60 - 36.d	5.08	0.29	NaN	0.86	0.072	0.026	9.94	0.46	NaN	3.07	0.13	0.017
eaf60 - 37.d	55.6	1.1	NaN	7.08	0.21	0.0094	59.6	1.2	0.069	19.14	0.42	NaN
eaf60 - 38.d	56.66	0.98	0.084	7.46	0.26	NaN	57.5	1.3	0.063	16.89	0.38	NaN
eaf60 - 39.d	58.9	1.5	NaN	7.65	0.28	NaN	59.4	1.3	0.033	17.21	0.32	NaN
eaf60 - 40.d	57.2	1.4	NaN	7.52	0.21	0.013	56.1	1.3	NaN	15.16	0.41	NaN
eaf60 - 41.d	57.3	1.3	0.086	7.19	0.2	0.0095	61.1	1.4	NaN	23.54	0.65	0.0088
eaf60 - 42.d	55.9	1.2	NaN	6.91	0.25	NaN	62.8	1.5	0.064	25.71	0.53	NaN
eaf60 - 43.d	57.7	1.7	NaN	7.58	0.26	0.019	58.6	1.4	0.032	16.44	0.45	NaN
eaf60 - 44.d	55.9	1.3	NaN	7.02	0.19	NaN	65.6	1.1	NaN	5.4	0.22	0.019
eaf60 - 45.d	56.5	1.1	NaN	6.94	0.24	NaN	68.8	1.2	NaN	14.38	0.38	0.019
eaf60 - 46.d	55.9	1.7	NaN	6.9	0.2	0.027	67.9	1.4	0.034	23.77	0.41	0.018
eaf60 - 47.d	53.9	1.1	NaN	6.55	0.16	NaN	56.8	1.2	0.067	8.04	0.26	NaN
eaf60 - 48.d	53.8	1.6	0.045	6.59	0.15	NaN	67.7	1.2	NaN	21.62	0.5	0.018
eaf60 - 49.d	54.8	1.2	0.045	6.94	0.23	NaN	69.3	1.7	NaN	23.48	0.44	0.013
eaf60 - 50.d	53.3	1.5	NaN	6.56	0.28	NaN	52.9	1.1	NaN	3.79	0.14	NaN
eaf60 - 51.d	55.8	1.2	NaN	6.81	0.2	0.0097	66.7	1.8	NaN	19.59	0.39	0.018
eaf60 - 52.d	60.4	1.4	0.044	7.38	0.25	NaN	62.8	1.4	NaN	13.57	0.34	0.009
eaf60 - 53.d	58.8	1.4	NaN	7.13	0.22	NaN	62.5	1.6	NaN	14.29	0.4	0.02
eaf60 - 54.d	59.6	1.7	NaN	7.22	0.2	NaN	67.3	1.5	NaN	17.57	0.41	0.0089
eaf60 - 55.d	59.7	1.4	NaN	7.31	0.22	NaN	65.1	1.5	0.065	15.27	0.34	NaN
eaf60 - 56.d	59.5	1.4	0.12	7.54	0.2	0.021	64.9	1.4	NaN	13.3	0.38	0.018
eaf60 - 57.d	61.3	1.4	NaN	7.49	0.21	NaN	66.3	1.4	NaN	13.89	0.35	0.009
eaf60 - 58.d	58.4	1.4	NaN	7.13	0.2	NaN	61.6	1.3	0.065	14.97	0.31	0.0088

Analysis number	Yb172 ppm	Yb172 ppm 2SE	Yb172 ppm LOD	Lu175 ppm	Lu175 ppm 2SE	Lu175 ppm LOD	Hf178 ppm	Hf178 ppm 2SE	Hf178 ppm LOD	Ta181 ppm	Ta181 ppm 2SE	Ta181 ppm LOD
eaf60 - 59.d	60.7	1.6	NaN	7.41	0.21	0.0095	60.2	1.4	0.065	14.67	0.33	NaN
eaf60 - 60.d	58.4	1.3	0.088	7.31	0.27	0.021	60.6	1.2	0.099	17.21	0.36	0.028
eaf60 - 61.d	60.4	1.5	0.12	7.47	0.24	0.0096	61.4	1.2	0.032	16.65	0.33	NaN
eaf60 - 62.d	59.9	1.1	NaN	7.75	0.24	0.0098	63.1	1.1	NaN	16.32	0.26	NaN
eaf60 - 63.d	56.5	1	0.043	7.37	0.23	0.019	61	1.3	0.032	16.75	0.38	NaN
eaf60 - 64.d	58	1.4	NaN	7.55	0.21	0.013	59.3	1.5	NaN	13.58	0.31	0.018
eaf60 - 65.d	59	1.2	0.086	7.48	0.21	NaN	60.4	1.1	NaN	14.28	0.27	0.025
eaf60 - 66.d	55.5	1.4	NaN	7.11	0.21	0.027	57.6	1.3	NaN	29.13	0.57	0.0089
eaf60 - 67.d	57.6	1.6	0.044	7.31	0.21	NaN	58.5	1.4	NaN	14.93	0.4	NaN
eaf60 - 68.d	56.7	1.6	NaN	7.11	0.22	NaN	55.1	1.3	NaN	25.59	0.49	0.019
eaf60 - 69.d	58.3	1.5	0.091	7.17	0.24	NaN	55.9	1.4	0.094	22.32	0.56	NaN
eaf60 - 70.d	54.9	1.7	NaN	7.32	0.24	NaN	57.5	1.2	NaN	13.08	0.29	0.02
eaf60 - 71.d	54.8	1.2	NaN	7.14	0.19	NaN	57.9	1.2	0.033	14.69	0.34	NaN
eaf60 - 72.d	56.5	1.5	0.046	7.15	0.26	NaN	59.9	1.1	NaN	15.74	0.33	NaN
eaf60 - 73.d	55.5	1.4	NaN	7.09	0.23	NaN	57.2	1.4	NaN	11.47	0.31	NaN
eaf60 - 74.d	93.5	1.8	0.089	12.21	0.3	NaN	49.8	1.7	0.067	32.8	1.1	0.018
eaf60 - 75.d	61.6	1.5	NaN	7.43	0.24	0.031	66.8	1.7	0.046	18.49	0.45	NaN
eaf60 - 76.d	61.5	1.7	NaN	7.25	0.21	NaN	62.5	1.3	0.066	51.51	0.8	NaN
eaf60 - 77.d	61.1	1.5	NaN	7.29	0.23	0.021	57.1	1.3	NaN	35.29	0.64	0.019
eaf60 - 78.d	60.4	1.7	NaN	7.01	0.21	NaN	64.7	1.8	NaN	23.79	0.57	NaN
eaf60 - 79.d	62.3	1.4	NaN	7.32	0.21	NaN	60.3	1.6	0.033	30.9	0.68	NaN
eaf60 - 80.d	60	1.4	NaN	7.23	0.2	0.0097	64.8	1.4	NaN	30.06	0.63	0.018
eaf60 - 81.d	60.1	1.7	NaN	7.2	0.21	NaN	66.2	1.2	NaN	32.44	0.59	0.018
eaf60 - 82.d	62.3	1.6	NaN	7.3	0.21	NaN	62.9	1.3	NaN	96.8	1.8	NaN
eaf60 - 83.d	59.8	1.1	NaN	6.99	0.19	0.019	67.3	1.5	0.065	28.68	0.72	NaN
eaf60 - 84.d	60.3	1.2	NaN	7.3	0.23	0.027	54.5	1.1	0.033	66.5	1	NaN
eaf60 - 85.d	61.3	1.6	0.043	7.22	0.18	NaN	55.5	1.4	NaN	22.63	0.58	NaN
eaf60 - 86.d	61.1	1.3	NaN	7.58	0.21	0.019	58.8	1.6	0.033	29.95	0.65	0.018
eaf60 - 87.d	71.6	2.1	0.044	9.92	0.3	NaN	59.5	1.1	NaN	12.32	0.32	NaN

Analysis number	Yb172 ppm	Yb172 ppm 2SE	Yb172 ppm LOD	Lu175 ppm	Lu175 ppm 2SE	Lu175 ppm LOD	Hf178 ppm	Hf178 ppm 2SE	Hf178 ppm LOD	Ta181 ppm	Ta181 ppm 2SE	Ta181 ppm LOD
eaf60 - 88.d	57.9	1.3	NaN	7.11	0.19	0.0097	65.4	1.4	0.066	19.26	0.41	NaN
eaf60 - 89.d	58.4	1.2	NaN	7.29	0.21	NaN	65.4	1.7	0.045	25.92	0.69	0.0089
eaf60 - 90.d	60.1	1.3	0.044	7.35	0.24	NaN	63.5	1.4	NaN	34.64	0.75	NaN
eaf60 - 91.d	59.2	1.1	NaN	7.19	0.22	NaN	64	1.5	NaN	27.16	0.55	NaN
eaf60 - 92.d	61.4	1.8	NaN	7.62	0.24	0.01	61.2	1.4	0.048	30.43	0.6	0.033
eaf60 - 93.d	60.5	1.4	NaN	7	0.23	0.019	58.4	1.4	NaN	43.53	0.89	NaN
eaf60 - 94.d	61.4	1.7	NaN	7.48	0.22	NaN	65.9	1.4	NaN	18.09	0.4	0.019
eaf60 - 95.d	60.9	1.1	NaN	7.47	0.2	NaN	50.8	1.4	NaN	44.65	0.85	0.019
eaf60 - 96.d	61.4	1.7	0.045	7.53	0.26	NaN	64.5	1.5	NaN	26.68	0.57	NaN
eaf60 - 97.d	106.8	2.1	0.092	14.48	0.35	0.01	61.4	1.5	NaN	13.47	0.42	NaN
eaf60 - 98.d	58.8	1.3	NaN	7.4	0.19	0.02	66.8	1.5	0.16	19.65	0.34	0.0093
eaf60 - 99.d	60.1	1.4	NaN	7.65	0.23	0.01	53.4	1.2	0.075	13.84	0.38	NaN
eaf60 - 100.d	58.9	1.7	NaN	7.35	0.21	NaN	59.3	1.5	0.035	18.31	0.41	NaN
eaf60 - 101.d	96.7	2.2	0.14	12.74	0.4	0.02	60.4	1.2	0.068	12.92	0.33	NaN
eaf60 - 102.d	55.9	1.5	NaN	6.95	0.22	NaN	58.6	1.6	NaN	17.02	0.45	NaN
eaf60 - 103.d	59.2	1.7	NaN	7.43	0.23	NaN	57.3	1.5	NaN	17.1	0.43	0.0093
eaf60 - 104.d	56.4	1.1	NaN	7.12	0.24	0.01	57	1.4	NaN	16.52	0.4	NaN
eaf60 - 105.d	59.9	1.8	0.045	7.47	0.25	NaN	54.1	1.2	NaN	11.31	0.34	NaN
eaf60 - 106.d	58.8	1.6	NaN	7.68	0.28	NaN	59	1.3	NaN	11.33	0.28	NaN
eaf60 - 107.d	58.4	1.7	0.045	7.46	0.19	0.014	58.4	1.1	NaN	10.71	0.27	NaN
eaf60 - 108.d	94.8	1.9	0.044	11.9	0.33	0.021	66.2	1.2	0.066	23.85	0.47	0.009
eaf60 - 109.d	59.2	1.7	NaN	7.1	0.23	0.01	59.4	1.9	0.069	8.73	0.26	0.019
eaf60 - 110.d	57.1	1.1	0.12	7	0.21	0.02	67.4	1.5	NaN	16.02	0.35	NaN
eaf60 - 111.d	55.2	1.4	NaN	6.76	0.26	NaN	64.3	1.5	NaN	11.1	0.3	0.025
eaf60 - 112.d	54.6	1.5	NaN	7.25	0.24	NaN	63.2	1.5	NaN	24.05	0.55	0.024
eaf60 - 114.d	59.1	1.3	NaN	7.47	0.27	NaN	56.9	1.4	0.09	18.43	0.44	NaN
eaf60 - 115.d	57.5	1.3	0.09	7.23	0.28	NaN	61.9	1.3	NaN	29.7	0.62	0.018
eaf60 - 116.d	53.4	1.5	0.13	6.77	0.22	NaN	67.9	1.3	NaN	26.64	0.52	NaN
eaf60 - 117.d	53.2	1.5	NaN	6.58	0.23	0.013	63	1.5	NaN	18.89	0.38	0.0088

Analysis number	Yb172 ppm	Yb172 ppm 2SE	Yb172 ppm LOD	Lu175 ppm	Lu175 ppm 2SE	Lu175 ppm LOD	Hf178 ppm	Hf178 ppm 2SE	Hf178 ppm LOD	Ta181 ppm	Ta181 ppm 2SE	Ta181 ppm LOD
eaf60 - 118.d	51.6	1.5	0.089	6.77	0.21	0.0098	61.7	1.2	NaN	40.65	0.87	NaN
eaf60 - 119.d	51.1	1.4	NaN	6.34	0.23	NaN	63.2	1.2	NaN	38.88	0.89	NaN
eaf60 - 120.d	53.1	1.6	NaN	6.53	0.22	0.02	64.4	1.6	NaN	42.26	0.85	NaN
eaf60 - 121.d	52.1	1.5	0.046	6.53	0.21	NaN	63.4	1.3	0.075	39.32	0.58	0.02
eaf60 - 122.d	54.1	1.5	NaN	6.83	0.23	NaN	69.4	1.1	NaN	22.48	0.44	0.0092
eaf60 - 123.d	57.6	1.4	0.092	7.45	0.21	NaN	61.6	1.1	NaN	21.77	0.51	NaN
eaf60 - 124.d	55.1	1.3	0.12	6.82	0.21	NaN	69.3	1.5	NaN	22.27	0.4	NaN
eaf60 - 126.d	51.4	1.3	NaN	6.97	0.25	0.01	57.89	0.99	NaN	9.38	0.26	NaN
eaf60 - 127.d	52.1	1.1	0.098	6.87	0.2	0.02	56	1.2	0.067	6.6	0.27	0.02
eaf60 - 128.d	50.2	1.3	0.045	6.93	0.22	NaN	52.7	1.1	0.034	5.74	0.2	NaN
eaf60 - 129.d	46.8	1.4	0.045	6.15	0.2	0.01	51.39	0.94	0.034	3.46	0.14	0.018
eaf60 - 130.d	45.4	1.3	0.09	6.43	0.21	0.01	50.9	1.3	0.068	3.43	0.16	NaN
eaf60 - 131.d	51.5	1.4	0.091	7.12	0.16	NaN	53.4	1.2	NaN	3.72	0.15	NaN
eaf60 - 132.d	59.1	1.5	NaN	7.97	0.23	0.022	54.4	1.3	NaN	6.7	0.19	NaN
eaf60 - 133.d	75.3	1	NaN	10.33	0.27	0.02	56.4	1.1	0.034	7.46	0.23	NaN
eaf60 - 134.d	54.5	1.4	NaN	7.37	0.21	0.0098	56.5	1.5	NaN	7.79	0.16	NaN
eaf60 - 135.d	60.4	1.7	NaN	8.11	0.23	NaN	56.6	1.5	NaN	7.29	0.16	0.036
eaf60 - 136.d	56.9	1.3	NaN	7.37	0.21	NaN	55.9	1.4	0.034	7.19	0.2	NaN
eaf60 - 137.d	57.4	1.4	NaN	7.64	0.19	NaN	62.3	1.4	NaN	25.1	0.56	NaN
eaf60 - 138.d	77.4	1.7	NaN	9.69	0.31	0.027	65.2	1.5	NaN	24.82	0.56	0.018
eaf60 - 139.d	52.7	1.2	0.089	6.73	0.23	NaN	54.4	1.2	NaN	6.95	0.23	NaN
eaf60 - 140.d	52	1.3	NaN	6.87	0.18	NaN	56.4	1.3	0.095	7.37	0.21	0.018
eaf60 - 141.d	57.1	1.5	NaN	7.7	0.24	NaN	56.2	1.6	NaN	6.23	0.19	NaN
eaf60 - 142.d	52.8	1.4	0.089	7.04	0.26	NaN	54.9	1.3	NaN	7.12	0.23	0.018
eaf60 - 143.d	51	1.1	NaN	7.06	0.21	0.02	53.6	1.2	0.067	5.96	0.19	NaN
eaf60 - 144.d	52.1	1.4	0.044	6.91	0.21	NaN	55.6	1.3	0.066	7.94	0.25	0.019
eaf60 - 145.d	57.1	1.3	NaN	8.21	0.21	0.019	56.8	1.1	0.065	6.99	0.22	0.0088
eaf60 - 146.d	52.1	1.3	NaN	6.91	0.19	0.02	56.9	1.2	NaN	8.52	0.27	0.02
eaf60 - 147.d	54.6	1.3	NaN	7.04	0.21	0.0099	57.7	1.4	NaN	9.16	0.3	0.02

Analysis number	Yb172 ppm	Yb172 ppm 2SE	Yb172 ppm LOD	Lu175 ppm	Lu175 ppm 2SE	Lu175 ppm LOD	Hf178 ppm	Hf178 ppm 2SE	Hf178 ppm LOD	Ta181 ppm	Ta181 ppm 2SE	Ta181 ppm LOD
eaf60 - 148.d	59.5	1.8	0.044	7.23	0.2	0.0097	57.7	1.1	NaN	9.38	0.25	0.0088
eaf60 - 149.d	54.9	1.7	NaN	7.18	0.24	NaN	58.2	1.4	NaN	12.7	0.35	NaN
eaf60 - 150.d	55.1	1.4	0.088	6.89	0.26	NaN	63.1	1.6	NaN	17.73	0.39	NaN
eaf60 - 151.d	56.6	1.4	NaN	6.74	0.23	0.019	62.3	1.1	0.045	20.31	0.35	NaN
eaf60 - 152.d	58	1.4	NaN	7.58	0.2	NaN	62.9	2	NaN	15.91	0.41	NaN
eaf60 - 153.d	58.2	1.8	NaN	7.37	0.21	0.0096	65.3	1.5	NaN	16.97	0.35	0.018
eaf60 - 154.d	56	1.6	NaN	7.08	0.23	NaN	65.4	1.3	0.066	18.75	0.44	NaN
eaf60 - 155.d	63.4	1.7	0.043	8.29	0.27	NaN	58.8	1.3	0.065	19.65	0.44	0.0087
eaf60 - 156.d	56.2	1.4	0.088	7	0.21	NaN	69	1.3	NaN	20.94	0.39	NaN
eaf60 - 157.d	56.5	1.7	0.059	6.95	0.21	0.038	71.3	1.6	NaN	21.48	0.48	NaN
eaf60 - 158.d	60.4	1.5	NaN	7.91	0.22	NaN	61.3	1.4	NaN	14.9	0.38	0.018
eaf60 - 159.d	60.1	2.1	NaN	7.96	0.22	NaN	61.7	1.2	NaN	14.49	0.3	NaN
eaf60 - 160.d	56.9	1.5	NaN	7.34	0.24	NaN	63.4	1.5	NaN	15.56	0.38	NaN

Analysis number	W182 ppm	W182 ppm 2SE	W182 ppm LOD	Pb204 ppm	Pb204 ppm 2SE	Pb204 ppm LOD	Pb206 ppm	Pb206 ppm 2SE	Pb206 ppm LOD	Pb207 ppm	Pb207 ppm 2SE	Pb207 ppm LOD
eaf60 - 1.d	13.98	0.55	0.075	< LOD	< LOD	6.6	20.99	0.96	0.11	2.61	0.12	0.064
eaf60 - 2.d	15.5	0.59	NaN	< LOD	< LOD	5.7	21.46	0.87	0.15	2.636	0.099	0.037
eaf60 - 3.d	15.97	0.56	0.038	< LOD	< LOD	7.6	22.25	0.76	0.12	2.465	0.092	0.036
eaf60 - 4.d	15.1	0.65	0.038	< LOD	< LOD	6.9	22.14	0.78	0.17	2.522	0.086	0.047
eaf60 - 5.d	14.16	0.59	NaN	< LOD	< LOD	6.5	22.6	1	0.2	2.791	0.082	0.055
eaf60 - 6.d	14.51	0.47	NaN	< LOD	< LOD	6.2	26.1	1.3	0.11	3.034	0.098	0.04
eaf60 - 7.d	15.48	0.55	NaN	< LOD	< LOD	5	27.9	1.1	0.17	3.19	0.12	0.059
eaf60 - 8.d	15.58	0.56	0.037	< LOD	< LOD	7.2	24.6	0.86	0.14	2.85	0.11	0.033
eaf60 - 9.d	16.82	0.7	NaN	< LOD	< LOD	7.2	24.46	0.73	0.18	2.869	0.093	0.047
eaf60 - 10.d	15.17	0.63	NaN	< LOD	< LOD	8.3	25.17	0.85	0.1	2.92	0.12	0.043
eaf60 - 11.d	11.54	0.44	NaN	< LOD	< LOD	5.6	18.98	0.69	0.22	2.433	0.085	0.046
eaf60 - 12.d	12.67	0.54	NaN	< LOD	< LOD	7.5	19.31	0.81	0.27	2.49	0.1	0.043
eaf60 - 13.d	11.86	0.57	NaN	< LOD	< LOD	5.3	19.84	0.83	0.15	2.41	0.11	0.041
eaf60 - 14.d	14.21	0.46	0.074	< LOD	< LOD	4.7	20.65	0.66	0.093	2.636	0.084	0.046
eaf60 - 15.d	13.66	0.64	0.075	< LOD	< LOD	6.3	19.42	0.87	0.15	2.437	0.092	0.046
eaf60 - 16.d	12.44	0.62	0.075	< LOD	< LOD	6.3	18.68	0.74	0.28	2.401	0.081	0.061
eaf60 - 17.d	13.03	0.52	0.079	< LOD	< LOD	5.6	18.52	0.84	0.16	2.371	0.084	0.044
eaf60 - 18.d	12.73	0.58	0.037	< LOD	< LOD	4.9	18.59	0.59	0.25	2.298	0.08	0.049
eaf60 - 19.d	12.41	0.68	NaN	< LOD	< LOD	5.3	18.52	0.81	0.13	2.321	0.09	0.07
eaf60 - 20.d	11.02	0.55	NaN	< LOD	< LOD	7.6	20.25	0.8	0.18	2.48	0.11	0.056
eaf60 - 21.d	11.48	0.51	0.039	< LOD	< LOD	5.2	18.8	0.88	0.18	2.357	0.092	0.049
eaf60 - 22.d	13.53	0.57	NaN	< LOD	< LOD	4.7	22.67	0.8	0.053	2.64	0.11	0.048
eaf60 - 23.d	12.73	0.49	NaN	< LOD	< LOD	7.3	26.6	1	0.22	2.77	0.12	0.033
eaf60 - 24.d	3.68	0.25	NaN	< LOD	< LOD	8.1	1.31	0.23	0.2	0.638	0.046	0.042
eaf60 - 25.d	6.11	0.3	0.08	< LOD	< LOD	6.1	1.35	0.22	0.12	0.658	0.041	0.063
eaf60 - 26.d	3.29	0.28	NaN	< LOD	< LOD	4.8	1.33	0.21	0.13	0.611	0.047	0.048
eaf60 - 27.d	5.28	0.38	NaN	< LOD	< LOD	7.1	1.18	0.21	0.18	0.678	0.043	0.057
eaf60 - 28.d	4.64	0.29	0.074	< LOD	< LOD	5.2	1.28	0.15	0.051	0.652	0.042	0.038
eaf60 - 29.d	7.94	0.45	NaN	< LOD	< LOD	7.6	1.69	0.2	0.093	0.772	0.053	0.059

Analysis number	W182 ppm	W182 ppm 2SE	W182 ppm LOD	Pb204 ppm	Pb204 ppm 2SE	Pb204 ppm LOD	Pb206 ppm	Pb206 ppm 2SE	Pb206 ppm LOD	Pb207 ppm	Pb207 ppm 2SE	Pb207 ppm LOD
eaf60 - 30.d	5.2	0.35	NaN	< LOD	< LOD	6	1.49	0.22	0.07	0.643	0.047	0.048
eaf60 - 31.d	11.27	0.47	0.071	< LOD	< LOD	6.3	6.54	0.59	0.21	1.008	0.05	0.042
eaf60 - 32.d	16.62	0.64	0.072	< LOD	< LOD	10	15.19	0.75	0.12	1.744	0.085	0.049
eaf60 - 33.d	4.16	0.31	NaN	< LOD	< LOD	6.7	1.89	0.29	0.082	0.618	0.036	0.047
eaf60 - 34.d	9.95	0.41	0.072	< LOD	< LOD	6.2	6.53	0.38	0.14	0.992	0.06	0.051
eaf60 - 35.d	4.79	0.29	0.072	< LOD	< LOD	6.5	5.93	0.44	0.12	0.97	0.055	0.043
eaf60 - 36.d	2.61	0.21	NaN	< LOD	< LOD	7	1.08	0.16	0.14	0.551	0.042	0.055
eaf60 - 37.d	14.79	0.47	0.036	< LOD	< LOD	6.8	21.26	0.64	0.16	2.67	0.12	0.041
eaf60 - 38.d	13.76	0.54	0.035	< LOD	< LOD	6.2	20.66	0.62	0.16	2.537	0.084	0.051
eaf60 - 39.d	13.87	0.57	NaN	< LOD	< LOD	6.4	22.2	1	0.15	2.665	0.077	0.062
eaf60 - 40.d	12.55	0.54	0.072	< LOD	< LOD	7.5	19.34	0.64	0.18	2.46	0.1	0.06
eaf60 - 41.d	16.74	0.56	NaN	< LOD	< LOD	5.9	23.3	1	0.051	2.84	0.1	0.06
eaf60 - 42.d	16.47	0.64	NaN	< LOD	< LOD	5.9	23.64	0.67	0.14	2.67	0.1	0.084
eaf60 - 43.d	13.27	0.52	0.036	< LOD	< LOD	4.3	19.63	0.79	0.19	2.544	0.083	0.028
eaf60 - 44.d	14.1	0.53	0.039	< LOD	< LOD	5.3	23.49	0.85	0.19	2.87	0.13	0.036
eaf60 - 45.d	14.1	0.52	NaN	< LOD	< LOD	6.8	23.14	0.87	0.16	2.708	0.083	0.052
eaf60 - 46.d	17.21	0.57	NaN	< LOD	< LOD	5	24.9	1	0.23	3.023	0.085	0.033
eaf60 - 47.d	14.7	0.68	NaN	< LOD	< LOD	6.1	22.89	0.75	0.25	2.66	0.12	0.044
eaf60 - 48.d	17.4	0.67	NaN	< LOD	< LOD	4.7	22.69	0.95	0.25	2.701	0.081	0.045
eaf60 - 49.d	18.29	0.66	0.038	< LOD	< LOD	8.7	23.5	1	0.12	2.79	0.12	0.088
eaf60 - 50.d	14.28	0.65	NaN	< LOD	< LOD	4	22.1	0.95	0.052	2.684	0.086	0.058
eaf60 - 51.d	16.54	0.51	NaN	< LOD	< LOD	5.9	22.95	0.68	0.083	2.739	0.098	0.044
eaf60 - 52.d	14.2	0.51	0.037	< LOD	< LOD	7.9	24.6	1	0.36	2.86	0.1	0.068
eaf60 - 53.d	15.76	0.62	NaN	< LOD	< LOD	7.9	24.7	0.98	NaN	2.93	0.1	0.056
eaf60 - 54.d	16.12	0.51	NaN	< LOD	< LOD	5.9	24.13	0.89	0.1	2.91	0.12	0.055
eaf60 - 55.d	15.72	0.64	NaN	< LOD	< LOD	8.8	23.9	1	0.051	2.865	0.098	0.041
eaf60 - 56.d	15.09	0.7	0.075	< LOD	< LOD	5.2	24.05	0.66	0.2	2.831	0.095	0.047
eaf60 - 57.d	15.53	0.67	0.075	< LOD	< LOD	5.7	25.78	0.85	0.25	3.07	0.11	0.055
eaf60 - 58.d	15.95	0.52	NaN	< LOD	< LOD	5.5	24.24	0.97	0.091	2.91	0.11	0.037

Analysis number	W182 ppm	W182 ppm 2SE	W182 ppm LOD	Pb204 ppm	Pb204 ppm 2SE	Pb204 ppm LOD	Pb206 ppm	Pb206 ppm 2SE	Pb206 ppm LOD	Pb207 ppm	Pb207 ppm 2SE	Pb207 ppm LOD
eaf60 - 59.d	15.93	0.55	0.036	< LOD	< LOD	5	24.69	0.86	0.15	2.846	0.085	0.05
eaf60 - 60.d	14.98	0.58	0.081	< LOD	< LOD	4.6	24.08	0.99	0.071	2.85	0.1	0.059
eaf60 - 61.d	14.77	0.57	NaN	< LOD	< LOD	4.6	24.96	0.96	0.051	2.87	0.11	0.059
eaf60 - 62.d	15.13	0.57	0.075	< LOD	< LOD	7.5	24.35	0.78	0.15	3.052	0.089	0.054
eaf60 - 63.d	14.34	0.52	NaN	< LOD	< LOD	4.2	23.06	0.66	0.12	2.73	0.1	0.043
eaf60 - 64.d	12.3	0.5	0.073	< LOD	< LOD	5.7	21.9	0.86	0.26	2.528	0.096	0.047
eaf60 - 65.d	14.54	0.64	0.036	< LOD	< LOD	7.8	23.91	0.86	0.24	2.79	0.098	0.049
eaf60 - 66.d	15.65	0.59	0.074	< LOD	< LOD	4.6	20.45	0.97	0.15	2.607	0.088	0.043
eaf60 - 67.d	13.72	0.4	0.075	< LOD	< LOD	6.2	20.07	0.63	0.17	2.392	0.093	0.029
eaf60 - 68.d	15.18	0.64	NaN	< LOD	< LOD	7.1	20.43	0.74	0.17	2.5	0.095	0.053
eaf60 - 69.d	14.89	0.67	0.11	< LOD	< LOD	6.2	21.63	0.87	0.19	2.51	0.11	0.063
eaf60 - 70.d	15.08	0.61	NaN	< LOD	< LOD	6	20.62	0.93	0.075	2.554	0.099	0.046
eaf60 - 71.d	15.2	0.6	0.082	< LOD	< LOD	7.8	21.61	0.89	0.21	2.623	0.094	0.039
eaf60 - 72.d	15.02	0.58	NaN	< LOD	< LOD	6.2	21.34	0.67	0.19	2.539	0.09	0.047
eaf60 - 73.d	14.41	0.52	NaN	< LOD	< LOD	4.2	20.93	0.75	0.073	2.62	0.1	0.079
eaf60 - 74.d	16.49	0.69	NaN	< LOD	< LOD	5.7	28.91	0.85	0.11	2.944	0.095	0.063
eaf60 - 75.d	15.6	0.74	NaN	< LOD	< LOD	6.9	24.2	1.1	0.15	2.79	0.12	0.051
eaf60 - 76.d	26.64	0.91	NaN	< LOD	< LOD	7.4	23.78	0.92	0.052	2.8	0.12	0.05
eaf60 - 77.d	18.64	0.72	NaN	< LOD	< LOD	6	24.06	0.92	NaN	2.84	0.1	0.031
eaf60 - 78.d	15.32	0.57	0.051	< LOD	< LOD	8.6	22.7	1.1	0.12	2.705	0.07	0.05
eaf60 - 79.d	27.82	0.74	NaN	< LOD	< LOD	6.4	26.31	0.96	0.21	3.11	0.079	0.052
eaf60 - 80.d	15.73	0.69	0.037	< LOD	< LOD	7.8	24.13	0.77	0.12	2.95	0.11	0.036
eaf60 - 81.d	16.9	0.54	NaN	< LOD	< LOD	7	24.79	0.74	0.15	2.96	0.11	0.059
eaf60 - 82.d	15.25	0.6	NaN	< LOD	< LOD	5.7	25.56	0.98	0.15	2.95	0.12	0.046
eaf60 - 83.d	20.86	0.64	NaN	< LOD	< LOD	6.6	23.72	0.86	0.19	2.725	0.074	0.073
eaf60 - 84.d	19.68	0.74	NaN	< LOD	< LOD	3.6	23.99	0.84	0.071	2.81	0.1	0.042
eaf60 - 85.d	15.85	0.62	0.073	< LOD	< LOD	5.7	24.24	0.73	0.15	2.629	0.096	0.044
eaf60 - 86.d	16.59	0.66	NaN	< LOD	< LOD	7.4	23.5	1.1	0.21	2.689	0.088	0.041
eaf60 - 87.d	10.45	0.6	NaN	< LOD	< LOD	3.7	20.03	0.69	0.12	2.415	0.09	0.065

Analysis number	W182 ppm	W182 ppm 2SE	W182 ppm LOD	Pb204 ppm	Pb204 ppm 2SE	Pb204 ppm LOD	Pb206 ppm	Pb206 ppm 2SE	Pb206 ppm LOD	Pb207 ppm	Pb207 ppm 2SE	Pb207 ppm LOD
eaf60 - 88.d	16.25	0.6	NaN	< LOD	< LOD	8.9	21.16	0.88	0.12	2.66	0.1	0.056
eaf60 - 89.d	15.64	0.55	NaN	< LOD	< LOD	6.4	21.4	0.81	0.25	2.566	0.094	0.047
eaf60 - 90.d	14.44	0.63	NaN	< LOD	< LOD	6	21.58	0.84	0.17	2.47	0.1	0.062
eaf60 - 91.d	15.48	0.69	NaN	< LOD	< LOD	4.5	21.82	0.73	0.1	2.496	0.094	0.047
eaf60 - 92.d	15.45	0.64	0.079	< LOD	< LOD	6.4	23	1.1	0.13	2.71	0.11	0.049
eaf60 - 93.d	14.74	0.47	0.1	< LOD	< LOD	8.8	22.93	0.87	0.18	2.565	0.093	0.036
eaf60 - 94.d	15.25	0.61	NaN	< LOD	< LOD	8.3	22.8	1	0.2	2.85	0.14	0.049
eaf60 - 95.d	11.9	0.57	0.078	< LOD	< LOD	8.2	24.28	0.96	0.16	2.799	0.098	0.061
eaf60 - 96.d	14.75	0.53	0.077	< LOD	< LOD	5.9	23.42	0.9	0.15	2.79	0.11	0.056
eaf60 - 97.d	12.7	0.54	NaN	< LOD	< LOD	11	29.6	1.2	0.054	3.2	0.1	0.048
eaf60 - 98.d	16.26	0.75	NaN	< LOD	< LOD	7.1	25.55	0.83	0.11	2.86	0.1	0.05
eaf60 - 99.d	14.44	0.55	0.078	< LOD	< LOD	4.9	23.13	0.77	0.15	2.78	0.11	0.064
eaf60 - 100.d	15.36	0.66	NaN	< LOD	< LOD	6.6	23.7	0.99	0.16	2.79	0.1	0.037
eaf60 - 101.d	13.35	0.53	0.12	< LOD	< LOD	7.4	32.8	1.1	0.16	3.3	0.12	0.046
eaf60 - 102.d	15.39	0.56	NaN	< LOD	< LOD	4.2	23.9	0.73	0.16	2.75	0.13	0.044
eaf60 - 103.d	16.08	0.7	NaN	< LOD	< LOD	7.6	25.45	0.84	0.19	3.008	0.093	0.039
eaf60 - 104.d	16.2	0.6	NaN	< LOD	< LOD	6.2	23.65	0.84	0.13	2.85	0.12	0.047
eaf60 - 105.d	15.2	0.5	NaN	< LOD	< LOD	9.1	25.78	0.86	0.15	2.9	0.1	0.031
eaf60 - 106.d	12.34	0.39	0.077	< LOD	< LOD	9.5	21.98	0.85	0.21	2.74	0.1	0.047
eaf60 - 107.d	12.69	0.53	NaN	< LOD	< LOD	5	21.6	0.74	0.12	2.71	0.11	0.059
eaf60 - 108.d	16.63	0.62	NaN	< LOD	< LOD	4.1	35.28	0.97	0.14	3.636	0.099	0.044
eaf60 - 109.d	14.68	0.55	NaN	< LOD	< LOD	4.8	22.53	0.83	0.18	2.661	0.086	0.051
eaf60 - 110.d	16.69	0.77	0.076	< LOD	< LOD	5.7	23.61	0.83	0.12	2.677	0.094	0.05
eaf60 - 111.d	15.85	0.67	0.11	< LOD	< LOD	5.4	22.56	0.81	0.2	2.59	0.1	0.059
eaf60 - 112.d	16.47	0.64	0.075	< LOD	< LOD	7.7	21.46	0.96	0.2	2.57	0.12	0.07
eaf60 - 114.d	12.38	0.64	NaN	< LOD	< LOD	4.2	19.44	0.85	0.21	2.31	0.11	0.032
eaf60 - 115.d	15.42	0.54	NaN	< LOD	< LOD	5.9	21.9	1	0.072	2.618	0.098	0.044
eaf60 - 116.d	18.48	0.7	0.038	< LOD	< LOD	7	22.7	0.77	0.19	2.746	0.086	0.044
eaf60 - 117.d	17.27	0.64	NaN	< LOD	< LOD	7.4	24.82	0.83	0.15	2.87	0.12	0.049

Analysis number	W182 ppm	W182 ppm 2SE	W182 ppm LOD	Pb204 ppm	Pb204 ppm 2SE	Pb204 ppm LOD	Pb206 ppm	Pb206 ppm 2SE	Pb206 ppm LOD	Pb207 ppm	Pb207 ppm 2SE	Pb207 ppm LOD
eaf60 - 118.d	18.66	0.58	0.037	< LOD	< LOD	8.6	23.26	0.82	0.19	2.7	0.1	0.056
eaf60 - 119.d	17.83	0.74	NaN	< LOD	< LOD	6	21.78	0.8	0.18	2.567	0.082	0.056
eaf60 - 120.d	18.58	0.84	NaN	< LOD	< LOD	6.2	22.9	1	0.21	2.645	0.086	0.04
eaf60 - 121.d	18.9	0.69	0.085	< LOD	< LOD	7.5	22.07	0.97	0.25	2.69	0.1	0.052
eaf60 - 122.d	17.06	0.79	NaN	< LOD	< LOD	7.2	22.71	0.95	0.19	2.82	0.11	0.059
eaf60 - 123.d	15.09	0.5	NaN	< LOD	< LOD	3.7	23.53	0.83	0.18	2.616	0.089	0.046
eaf60 - 124.d	17.82	0.8	NaN	< LOD	< LOD	6.3	24.44	0.97	0.087	2.765	0.092	0.052
eaf60 - 126.d	13.43	0.57	0.084	< LOD	< LOD	5.6	18.29	0.67	0.13	2.383	0.078	0.071
eaf60 - 127.d	12.2	0.47	NaN	< LOD	< LOD	6.5	14.91	0.5	0.15	2.047	0.099	0.04
eaf60 - 128.d	13.15	0.52	0.077	< LOD	< LOD	4.5	16.43	0.68	0.15	2.279	0.088	0.062
eaf60 - 129.d	12.33	0.62	NaN	< LOD	< LOD	9.3	17.24	0.83	0.2	2.367	0.099	0.048
eaf60 - 130.d	12.57	0.52	NaN	< LOD	< LOD	7.8	17.56	0.79	0.23	2.381	0.086	0.039
eaf60 - 131.d	11.71	0.5	NaN	< LOD	< LOD	6.7	15.61	0.59	0.15	2.058	0.089	0.03
eaf60 - 132.d	12.71	0.45	NaN	< LOD	< LOD	6.8	19.38	0.93	0.17	2.36	0.096	0.051
eaf60 - 133.d	13.16	0.45	NaN	< LOD	< LOD	7	25.74	0.81	0.15	2.74	0.1	0.046
eaf60 - 134.d	14.8	0.61	0.1	< LOD	< LOD	6.2	22.6	0.77	0.19	2.707	0.087	0.041
eaf60 - 135.d	12.25	0.59	NaN	< LOD	< LOD	5.3	19.5	0.7	0.14	2.359	0.096	0.07
eaf60 - 136.d	12.59	0.58	NaN	< LOD	< LOD	6.8	19.39	0.85	0.17	2.57	0.1	0.041
eaf60 - 137.d	14.27	0.62	0.037	< LOD	< LOD	6.1	18.88	0.82	0.16	2.49	0.1	0.047
eaf60 - 138.d	14.33	0.59	0.11	< LOD	< LOD	7.5	22.38	0.85	0.12	2.62	0.12	0.055
eaf60 - 139.d	14	0.67	0.037	< LOD	< LOD	8.5	19.98	0.84	0.12	2.604	0.09	0.049
eaf60 - 140.d	14.58	0.68	NaN	< LOD	< LOD	5.6	20.73	0.88	0.1	2.743	0.088	0.062
eaf60 - 141.d	12.95	0.5	NaN	< LOD	< LOD	4.8	21.19	0.88	0.26	2.459	0.086	0.052
eaf60 - 142.d	12.39	0.56	NaN	< LOD	< LOD	6.7	18.33	0.82	NaN	2.553	0.084	0.039
eaf60 - 143.d	12.54	0.59	NaN	< LOD	< LOD	4.9	17.7	0.75	0.2	2.43	0.1	0.036
eaf60 - 144.d	13.13	0.56	0.074	< LOD	< LOD	7.2	20.15	0.82	0.11	2.356	0.082	0.06
eaf60 - 145.d	12.77	0.55	0.12	< LOD	< LOD	5.8	21.56	0.9	NaN	2.487	0.097	0.068
eaf60 - 146.d	13.82	0.46	0.037	< LOD	< LOD	4.8	18.92	0.89	0.11	2.381	0.077	0.05
eaf60 - 147.d	12.12	0.47	0.082	< LOD	< LOD	4.7	19	0.9	0.085	2.437	0.097	0.044

Analysis number	W182 ppm	W182 ppm 2SE	W182 ppm LOD	Pb204 ppm	Pb204 ppm 2SE	Pb204 ppm LOD	Pb206 ppm	Pb206 ppm 2SE	Pb206 ppm LOD	Pb207 ppm	Pb207 ppm 2SE	Pb207 ppm LOD
eaf60 - 148.d	13.24	0.49	NaN	< LOD	< LOD	5.6	22.15	0.81	0.21	2.64	0.1	0.043
eaf60 - 149.d	14.15	0.51	0.079	< LOD	< LOD	5.4	21.53	0.83	0.16	2.6	0.1	0.048
eaf60 - 150.d	16.94	0.72	NaN	< LOD	< LOD	5.5	25.53	0.8	0.07	3.01	0.12	0.039
eaf60 - 151.d	17.55	0.61	0.051	< LOD	< LOD	5.8	24.6	0.81	0.12	2.92	0.1	0.055
eaf60 - 152.d	14.02	0.51	NaN	< LOD	< LOD	5.7	23.07	0.96	0.12	2.68	0.094	0.035
eaf60 - 153.d	15.14	0.56	0.073	< LOD	< LOD	5.8	22.13	0.86	0.051	2.7	0.11	0.032
eaf60 - 154.d	16.63	0.54	NaN	< LOD	< LOD	5.7	23.4	1	0.21	2.85	0.1	0.069
eaf60 - 155.d	14.76	0.64	NaN	< LOD	< LOD	6.2	23.22	0.63	0.18	2.79	0.11	0.045
eaf60 - 156.d	15.73	0.42	NaN	< LOD	< LOD	6.3	24.95	0.81	0.17	2.96	0.12	0.052
eaf60 - 157.d	16.1	0.56	0.072	< LOD	< LOD	5.5	27.02	0.74	0.082	3.135	0.088	0.057
eaf60 - 158.d	12.15	0.51	NaN	< LOD	< LOD	4.7	21.12	0.73	0.23	2.609	0.068	0.067
eaf60 - 159.d	12.85	0.59	0.074	< LOD	< LOD	5.9	20.98	0.76	0.15	2.536	0.096	0.055
eaf60 - 160.d	14.6	0.49	0.08	< LOD	< LOD	6.1	21.93	0.71	0.12	2.688	0.093	0.048

Analysis number	Pb208 ppm	Pb208 ppm 2SE	Pb208 ppm LOD	Th232 ppm	Th232 ppm 2SE	Th232 ppm LOD	U238 ppm	U238 ppm 2SE	U238 ppm LOD	Zr in Tt temp (°C)	grain number	REE group
eaf60 - 1.d	14.21	0.2	0.023	126.8	1.8	0.016	25.69	0.48	0.011	906	1	60A
eaf60 - 2.d	16.55	0.22	0.029	152.1	2.8	NaN	26.41	0.49	0.014	907	1	60A
eaf60 - 3.d	17.58	0.26	0.027	164.3	2.4	NaN	26.88	0.49	0.011	907	1	60A
eaf60 - 4.d	15.07	0.23	0.032	141.3	2.3	NaN	27.42	0.5	0.015	906	1	60A
eaf60 - 5.d	15.1	0.24	0.029	134.9	2.3	0.016	27.79	0.49	0.011	908	2	60A
eaf60 - 6.d	14.54	0.21	0.03	134.6	2.3	NaN	32.65	0.65	0.013	912	2	60A
eaf60 - 7.d	18.85	0.3	0.044	171.1	2.6	0.008	34.9	0.55	NaN	913	2	60A
eaf60 - 8.d	17.96	0.23	0.029	163.4	2.8	0.016	30.23	0.5	NaN	911	2	60A
eaf60 - 9.d	20	0.28	0.045	186.2	3.6	0.016	31.07	0.61	0.017	910	2	60A
eaf60 - 10.d	16.64	0.26	0.034	152.2	2.3	0.011	31.14	0.58	NaN	911	2	60A
eaf60 - 11.d	10.34	0.18	0.021	87.3	1.6	0.008	22.95	0.51	0.0056	904	3	60A
eaf60 - 12.d	10.72	0.21	0.024	93.4	1.2	0.0079	23.58	0.48	0.016	904	3	60A
eaf60 - 13.d	10.15	0.16	0.026	90	1.3	NaN	23.68	0.49	0.0055	905	3	60A
eaf60 - 14.d	11.27	0.2	0.036	97.7	1.4	NaN	23.88	0.45	0.012	905	3	60A
eaf60 - 15.d	10.17	0.16	0.031	87.1	1	0.011	23.38	0.43	NaN	903	3	60A
eaf60 - 16.d	8.98	0.14	0.021	77.9	1.1	0.022	22.09	0.39	NaN	900	3	60A
eaf60 - 17.d	10.2	0.16	0.037	91	1.7	NaN	23.35	0.54	0.015	903	3	60A
eaf60 - 18.d	10.08	0.16	0.027	89.6	1.3	NaN	22.61	0.36	0.019	903	3	60A
eaf60 - 19.d	8.85	0.13	0.021	79.5	1.3	0.0081	23.64	0.32	0.0056	900	3	60A
eaf60 - 20.d	9.75	0.18	0.033	87.4	1.1	0.016	24.74	0.5	0.011	904	3	60A
eaf60 - 21.d	10.06	0.2	0.027	89.7	1.9	0.0083	22.78	0.38	0.013	904	3	60A
eaf60 - 22.d	10.27	0.19	0.032	94.9	1.5	NaN	28.56	0.55	0.013	899	3	60A
eaf60 - 23.d	9.23	0.15	0.031	87.2	1.6	0.017	33.64	0.56	0.017	897	3	60A
eaf60 - 24.d	0.611	0.033	0.029	0.483	0.045	0.017	1.021	0.062	0.011	785	4	60B
eaf60 - 25.d	0.696	0.035	0.028	0.477	0.045	0.016	0.896	0.05	NaN	801	4	60B
eaf60 - 26.d	0.582	0.036	0.023	0.701	0.051	NaN	1.119	0.064	NaN	783	4	60B
eaf60 - 27.d	0.61	0.031	0.023	0.425	0.041	0.017	0.952	0.062	0.011	793	4	60B
eaf60 - 28.d	0.537	0.031	0.039	0.34	0.034	0.0078	0.936	0.052	0.015	784	4	60B
eaf60 - 29.d	0.731	0.037	0.023	0.53	0.047	0.0079	1.332	0.052	0.0055	795	4	60B

Analysis number	Pb208 ppm	Pb208 ppm 2SE	Pb208 ppm LOD	Th232 ppm	Th232 ppm 2SE	Th232 ppm LOD	U238 ppm	U238 ppm 2SE	U238 ppm LOD	Zr in Tt temp (°C)	grain number	REE group
eaf60 - 30.d	0.612	0.029	0.03	0.792	0.065	NaN	1.549	0.052	0.0054	784	4	60B
eaf60 - 31.d	1.014	0.035	0.03	4.78	0.16	0.015	7.87	0.18	0.015	793	4	60B
eaf60 - 32.d	1.53	0.046	0.032	10.12	0.3	0.015	18.5	0.46	NaN	848	5	60B
eaf60 - 33.d	0.571	0.032	0.036	0.89	0.056	NaN	1.636	0.074	0.0053	785	5	60B
eaf60 - 34.d	0.884	0.037	0.035	4.26	0.15	NaN	8.58	0.22	0.0053	789	5	60B
eaf60 - 35.d	0.711	0.032	0.032	2.48	0.12	0.015	6.6	0.21	0.0073	789	5	60B
eaf60 - 36.d	0.531	0.027	0.025	0.424	0.036	0.0076	0.971	0.055	NaN	786	5	60B
eaf60 - 37.d	12.54	0.17	0.026	111.1	1.8	0.015	26.99	0.46	0.011	908	6	60A
eaf60 - 38.d	11.29	0.19	0.02	100.5	1.7	0.016	25.73	0.46	0.012	906	7	60A
eaf60 - 39.d	11.77	0.17	0.037	103.8	1.9	0.0078	26.54	0.58	0.021	907	7	60A
eaf60 - 40.d	10.56	0.17	0.026	93.4	1.6	0.022	23.95	0.38	0.0053	904	7	60A
eaf60 - 41.d	14.17	0.31	0.026	124.4	2.4	0.017	28.48	0.62	0.012	912	7	60A
eaf60 - 42.d	13.51	0.26	0.035	123.2	2.2	0.01	28.03	0.51	0.012	911	7	60A
eaf60 - 43.d	11.03	0.15	0.024	99.1	2.2	NaN	25.6	0.55	0.0072	906	7	60A
eaf60 - 44.d	15.11	0.21	0.028	134.2	2	0.018	29.72	0.53	0.012	915	8	60A
eaf60 - 45.d	15.05	0.28	0.02	136.9	1.6	0.0083	28.24	0.51	0.018	913	8	60A
eaf60 - 46.d	16.45	0.27	0.037	144.9	2.2	NaN	30.25	0.4	0.012	912	8	60A
eaf60 - 47.d	13.83	0.23	0.037	125.1	1.7	0.016	27.5	0.46	0.0056	910	9	60A
eaf60 - 48.d	15.41	0.2	0.033	139.6	2.4	0.022	27.9	0.41	NaN	912	9	60A
eaf60 - 49.d	15.57	0.21	0.029	142	2.3	0.0082	28.82	0.52	0.011	912	9	60A
eaf60 - 50.d	13.34	0.18	0.025	120	1.8	0.0079	26.95	0.58	0.0089	910	9	60A
eaf60 - 51.d	14.54	0.18	0.038	130.8	2.6	0.016	28.5	0.72	0.0055	912	9	60A
eaf60 - 52.d	13.62	0.22	0.025	121.1	1.9	0.0079	28.76	0.52	0.023	912	10	60A
eaf60 - 53.d	25.52	0.37	0.03	229.4	4.2	0.032	29.61	0.59	NaN	913	10	60A
eaf60 - 54.d	18.63	0.28	0.025	167.3	2.7	NaN	29.37	0.49	NaN	914	10	60A
eaf60 - 55.d	18.42	0.26	0.027	169.2	3	0.016	29.16	0.66	NaN	913	10	60A
eaf60 - 56.d	16.48	0.22	0.025	148.8	2.6	0.016	30.3	0.55	0.0055	914	10	60A
eaf60 - 57.d	16.87	0.2	0.033	152.9	2.7	0.017	31.33	0.57	0.019	914	10	60A
eaf60 - 58.d	18.68	0.26	0.037	169.7	2.8	NaN	29.97	0.49	0.0054	912	11	60A

Analysis number	Pb208 ppm	Pb208 ppm 2SE	Pb208 ppm LOD	Th232 ppm	Th232 ppm 2SE	Th232 ppm LOD	U238 ppm	U238 ppm 2SE	U238 ppm LOD	Zr in Tt temp (°C)	grain number	REE group
eaf60 - 59.d	18.41	0.26	0.026	164.4	2	NaN	29.72	0.47	0.011	912	11	60A
eaf60 - 60.d	15.5	0.29	0.03	138.7	2.3	NaN	28.98	0.45	0.012	911	11	60A
eaf60 - 61.d	15.47	0.2	0.039	139.2	2.2	0.016	29.87	0.57	0.012	912	11	60A
eaf60 - 62.d	17.26	0.31	0.041	156	2.3	0.017	31.39	0.59	NaN	914	11	60A
eaf60 - 63.d	14.61	0.25	0.037	127.3	2	NaN	27.49	0.52	NaN	911	11	60A
eaf60 - 64.d	12.12	0.22	0.033	106.5	1.8	NaN	26.54	0.39	NaN	909	11	60A
eaf60 - 65.d	13.67	0.26	0.015	119.6	1.7	0.0078	28.74	0.51	NaN	911	12	60A
eaf60 - 66.d	19.87	0.33	0.031	177.9	3	0.017	25.23	0.38	0.015	907	13	60A
eaf60 - 67.d	12.75	0.17	0.035	115	2.1	NaN	24.81	0.47	0.018	907	13	60A
eaf60 - 68.d	20.37	0.36	0.031	186.9	2.4	NaN	24.98	0.41	0.011	907	13	60A
eaf60 - 69.d	21.09	0.34	0.029	197.1	3.5	0.018	27.12	0.42	0.0057	906	13	60A
eaf60 - 70.d	15.17	0.23	0.032	136.1	2.3	NaN	25.16	0.54	NaN	908	14	60A
eaf60 - 71.d	16.17	0.27	0.038	146.9	2.7	NaN	26.05	0.54	0.0076	907	14	60A
eaf60 - 72.d	17.9	0.28	0.045	161	3.2	0.019	26.04	0.52	0.011	908	14	60A
eaf60 - 73.d	12.78	0.21	0.029	116	2	NaN	25.91	0.5	0.0057	906	14	60A
eaf60 - 74.d	12.44	0.19	0.016	117.1	2.7	0.018	36.07	0.54	0.016	890	15	60A
eaf60 - 75.d	17.28	0.26	0.035	156.4	2.5	NaN	29	0.53	0.0057	913	15	60A
eaf60 - 76.d	21.5	0.26	0.029	195.7	3.5	NaN	29.54	0.69	0.011	914	15	60A
eaf60 - 77.d	20.32	0.3	0.03	187.8	2.9	0.0079	30.01	0.51	NaN	912	15	60A
eaf60 - 78.d	17.69	0.24	0.038	160.8	2.6	0.017	28.25	0.58	0.011	914	15	60A
eaf60 - 79.d	22.2	0.42	0.044	202.6	4.2	0.016	32.01	0.63	0.011	919	15	60A
eaf60 - 80.d	17.17	0.26	0.039	153.4	2.3	0.0079	30.52	0.57	0.011	916	15	60A
eaf60 - 81.d	18.25	0.28	0.024	164.1	2.6	NaN	30.87	0.5	0.011	918	15	60A
eaf60 - 82.d	20.13	0.31	0.032	183.1	3.4	0.011	30.92	0.54	0.012	918	15	60A
eaf60 - 83.d	20.46	0.27	0.027	185.3	3	0.031	29.61	0.56	0.0054	917	15	60A
eaf60 - 84.d	22.37	0.32	0.03	204.8	2.7	NaN	30.35	0.51	0.015	913	15	60A
eaf60 - 85.d	18.02	0.3	0.026	164	2.7	0.011	29.51	0.55	0.013	911	15	60A
eaf60 - 86.d	17.36	0.34	0.031	157.2	3.2	0.017	28.79	0.55	0.011	911	15	60A
eaf60 - 87.d	10.17	0.16	0.03	91.6	1.2	0.022	25.05	0.6	0.0055	905	16	60A

Analysis number	Pb208 ppm	Pb208 ppm 2SE	Pb208 ppm LOD	Th232 ppm	Th232 ppm 2SE	Th232 ppm LOD	U238 ppm	U238 ppm 2SE	U238 ppm LOD	Zr in Tt temp (°C)	grain number	REE group
eaf60 - 88.d	18.54	0.28	0.032	167.4	2.3	NaN	26.61	0.5	0.017	912	17	60A
eaf60 - 89.d	18.58	0.28	0.038	168.1	2.9	0.0079	26.73	0.49	0.013	912	17	60A
eaf60 - 90.d	15.92	0.22	0.031	143.3	2.1	0.0079	26.02	0.5	0.011	910	17	60A
eaf60 - 91.d	18.83	0.28	0.036	170.2	2.7	0.016	27.45	0.55	0.0054	912	17	60A
eaf60 - 92.d	17.18	0.21	0.022	152.1	2.3	NaN	27.76	0.52	NaN	907	17	60A
eaf60 - 93.d	18.15	0.32	0.026	164	3.3	0.016	27.58	0.68	0.0074	912	17	60A
eaf60 - 94.d	16.36	0.28	0.044	148.6	1.4	NaN	28.84	0.41	0.0059	911	17	60A
eaf60 - 95.d	19.32	0.35	0.027	178.2	3	NaN	29.3	0.48	NaN	909	17	60A
eaf60 - 96.d	17.85	0.33	0.035	161.6	2.7	0.016	29.17	0.49	0.027	911	17	60A
eaf60 - 97.d	11.61	0.23	0.032	110.2	2.5	0.017	38.62	0.64	0.011	902	18	60A
eaf60 - 98.d	17.75	0.31	0.026	159.2	2.1	0.0082	30.53	0.57	0.0057	913	19	60A
eaf60 - 99.d	15.73	0.31	0.023	142	2.7	0.0083	29.17	0.49	0.0079	903	20	60A
eaf60 - 100.d	17.34	0.34	0.035	155.3	2.2	NaN	28.13	0.59	0.0058	907	20	60A
eaf60 - 101.d	13.12	0.16	0.03	123.9	1.7	NaN	43.29	0.77	0.011	910	20	60A
eaf60 - 102.d	18.65	0.27	0.024	168.9	3.1	NaN	28.95	0.47	0.012	908	21	60A
eaf60 - 103.d	18.84	0.3	0.026	172.8	3.2	0.018	31.44	0.62	0.012	908	21	60A
eaf60 - 104.d	19.31	0.26	0.028	177	3	0.018	28.52	0.54	0.012	906	21	60A
eaf60 - 105.d	21.46	0.29	0.033	197.3	3.8	0.016	30.87	0.62	NaN	908	21	60A
eaf60 - 106.d	12.4	0.25	0.027	106.8	1.6	0.019	25.45	0.48	0.016	908	22	60A
eaf60 - 107.d	11.84	0.2	0.049	104	2	0.023	25.47	0.56	0.011	909	23	60A
eaf60 - 108.d	11.66	0.22	0.021	110	2.1	0.016	42.21	0.6	0.02	907	24	60A
eaf60 - 109.d	13.74	0.19	0.036	122.4	2.1	NaN	27.48	0.55	0.0057	912	24	60A
eaf60 - 110.d	15.23	0.25	0.037	137.8	1.9	0.016	29.25	0.45	0.015	916	24	60A
eaf60 - 111.d	15.04	0.24	0.024	136.2	2.1	NaN	27.85	0.58	0.0056	911	24	60A
eaf60 - 112.d	13.95	0.24	0.025	126.6	2.4	NaN	26.06	0.45	0.0075	908	24	60A
eaf60 - 114.d	10.14	0.18	0.029	89.3	1.7	0.017	23.17	0.46	0.0055	904	25	60A
eaf60 - 115.d	13.21	0.23	0.031	117.2	2	NaN	27.41	0.56	0.0056	910	25	60A
eaf60 - 116.d	15.57	0.3	0.042	140.7	2.6	NaN	27.8	0.57	0.016	915	26	60A
eaf60 - 117.d	14.72	0.26	0.035	132.7	2.1	NaN	28.97	0.45	NaN	913	26	60A

Analysis number	Pb208 ppm	Pb208 ppm 2SE	Pb208 ppm LOD	Th232 ppm	Th232 ppm 2SE	Th232 ppm LOD	U238 ppm	U238 ppm 2SE	U238 ppm LOD	Zr in Tt temp (°C)	grain number	REE group
eaf60 - 118.d	13.91	0.24	0.03	124.5	1.9	NaN	28.25	0.47	NaN	913	27	60A
eaf60 - 119.d	13.76	0.19	0.031	124.6	2.3	0.013	26.85	0.51	0.0057	911	27	60A
eaf60 - 120.d	14.45	0.28	0.036	130	2.5	0.017	27.83	0.51	NaN	911	27	60A
eaf60 - 121.d	13.55	0.18	0.034	122.9	2	0.0083	27.19	0.55	0.013	910	27	60A
eaf60 - 122.d	15.29	0.3	0.038	137.3	2.4	NaN	28.21	0.53	NaN	913	28	60A
eaf60 - 123.d	13.11	0.26	0.026	117	1.7	NaN	28.68	0.53	0.017	910	28	60A
eaf60 - 124.d	15.67	0.27	0.032	142.6	2.3	NaN	29.05	0.44	NaN	913	28	60A
eaf60 - 126.d	9.6	0.15	0.03	82.2	1.6	0.0083	21	0.45	0.011	908	29	60A
eaf60 - 127.d	7.42	0.13	0.028	62.7	1.2	0.018	17.78	0.36	0.015	908	29	60A
eaf60 - 128.d	9.07	0.16	0.039	77.7	1.3	0.0082	20.55	0.39	0.012	906	29	60A
eaf60 - 129.d	8.72	0.2	0.038	73.2	1.2	NaN	20.53	0.47	0.022	905	29	60A
eaf60 - 130.d	8.53	0.18	0.036	73.2	1.4	0.018	20.5	0.4	0.0056	905	29	60A
eaf60 - 131.d	6.67	0.12	0.03	56.7	1.1	0.023	19.73	0.44	NaN	907	29	60A
eaf60 - 132.d	7.55	0.18	0.03	64.3	1.3	0.0082	23.68	0.38	NaN	907	30	60A
eaf60 - 133.d	9.16	0.16	0.025	83.3	1.1	0.019	31.84	0.62	0.0056	905	31	60A
eaf60 - 134.d	11.26	0.18	0.027	101.8	2	NaN	27.81	0.56	NaN	907	31	60A
eaf60 - 135.d	10.22	0.21	0.032	90.2	1.7	0.017	23.97	0.58	NaN	909	32	60A
eaf60 - 136.d	10.52	0.18	0.041	87.7	1.5	0.0081	22.86	0.4	0.017	906	32	60A
eaf60 - 137.d	10.1	0.18	0.036	88.1	1.5	0.017	23.46	0.5	0.015	910	32	60A
eaf60 - 138.d	10.8	0.21	0.031	96.2	1.8	0.016	26.08	0.44	0.0055	916	32	60A
eaf60 - 139.d	10.98	0.16	0.031	94.6	1.5	NaN	23.69	0.47	0.015	908	33	60A
eaf60 - 140.d	11.66	0.17	0.028	101	1.6	NaN	24.91	0.49	NaN	908	33	60A
eaf60 - 141.d	10.51	0.17	0.027	92.4	1.6	NaN	25.1	0.42	0.011	909	33	60A
eaf60 - 142.d	9.67	0.18	0.032	82.5	1.7	NaN	21.43	0.43	NaN	908	33	60A
eaf60 - 143.d	9.17	0.21	0.032	79.1	1.7	NaN	21.32	0.44	0.011	907	33	60A
eaf60 - 144.d	10.35	0.21	0.037	91.9	1.8	NaN	23.83	0.42	0.016	908	34	60A
eaf60 - 145.d	10.56	0.2	0.043	94.1	1.5	NaN	26.41	0.44	0.013	909	34	60A
eaf60 - 146.d	11.17	0.21	0.032	98.9	1.7	NaN	23.67	0.37	0.022	907	34	60A
eaf60 - 147.d	9.83	0.19	0.035	84.4	1.7	0.016	22.64	0.52	0.0056	910	34	60A

Analysis number	Pb208 ppm	Pb208 ppm 2SE	Pb208 ppm LOD	Th232 ppm	Th232 ppm 2SE	Th232 ppm LOD	U238 ppm	U238 ppm 2SE	U238 ppm LOD	Zr in Tt temp (°C)	grain number	REE group
eaf60 - 148.d	13.12	0.19	0.029	118.6	2.5	0.0079	27.17	0.64	0.0074	905	35	60A
eaf60 - 149.d	15.34	0.21	0.039	140	2.1	0.016	26.06	0.42	0.012	908	35	60A
eaf60 - 150.d	18.92	0.41	0.032	169.1	3	0.022	30.77	0.54	0.0054	913	36	60A
eaf60 - 151.d	21.77	0.41	0.04	197.9	2.6	0.016	28.94	0.51	0.011	914	36	60A
eaf60 - 152.d	12.6	0.25	0.032	115.5	2.4	0.016	28.47	0.63	0.012	913	37	60A
eaf60 - 153.d	15.34	0.26	0.035	138.6	2.2	NaN	27.16	0.56	0.011	915	37	60A
eaf60 - 154.d	18.72	0.29	0.023	168.9	3.2	0.008	28.47	0.57	0.013	916	38	60A
eaf60 - 155.d	14.81	0.4	0.027	131.7	2.3	0.015	28.6	0.62	0.012	906	39	60A
eaf60 - 156.d	15.72	0.24	0.032	138	2.1	0.026	29.52	0.57	0.01	918	40	60A
eaf60 - 157.d	17.79	0.28	0.037	158.8	2.6	0.011	33.14	0.57	0.011	922	40	60A
eaf60 - 158.d	11.47	0.15	0.03	101.4	1.8	0.008	24.71	0.42	0.022	909	40	60A
eaf60 - 159.d	11.3	0.15	0.025	98.7	1.4	0.022	24.61	0.54	0.0055	908	40	60A
eaf60 - 160.d	13.96	0.21	0.033	124.9	2.3	0.027	26.78	0.53	0.011	912	41	60A

Analysis number	$^{238}U/^{206}Pb$	±1s	$^{207}Pb/^{206}Pb$	±1s	$^{238}U/^{206}Pb$ age (Ma)	±1s	$^{207}Pb/^{206}Pb$ age (Ma)	±1s	Disc (%)	f207%	^{207}Pb-corrected $^{238}U/^{206}Pb$ Age (Ma)	±1s
eaf60 - 1.d	4.38117	0.10446	0.09990	0.00265	1325	28	1622	49	18.3	2.4	1296	31
eaf60 - 2.d	4.44697	0.09942	0.09720	0.00230	1308	26	1571	44	16.8	2.1	1283	29
eaf60 - 3.d	4.43688	0.07850	0.09020	0.00240	1310	21	1430	50	8.4	0.9	1300	23
eaf60 - 4.d	4.48371	0.08988	0.09150	0.00220	1298	23	1457	45	10.9	1.2	1284	26
eaf60 - 5.d	4.40090	0.10533	0.09770	0.00280	1320	28	1581	53	16.5	2.1	1295	31
eaf60 - 6.d	4.44091	0.10712	0.09380	0.00275	1309	28	1504	54	13.0	1.5	1291	31
eaf60 - 7.d	4.51062	0.08984	0.09090	0.00220	1291	23	1445	45	10.6	1.2	1277	25
eaf60 - 8.d	4.40686	0.09099	0.09430	0.00230	1318	24	1514	45	12.9	1.5	1300	27
eaf60 - 9.d	4.55266	0.08314	0.09510	0.00180	1280	21	1530	35	16.3	1.9	1258	23
eaf60 - 10.d	4.42883	0.08306	0.09230	0.00200	1312	22	1474	41	10.9	1.2	1298	24
eaf60 - 11.d	4.30207	0.09266	0.10120	0.00255	1347	26	1646	46	18.2	2.5	1317	28
eaf60 - 12.d	4.37920	0.09378	0.10280	0.00235	1326	25	1675	42	20.9	2.9	1291	28
eaf60 - 13.d	4.34609	0.10101	0.09480	0.00240	1335	27	1524	47	12.4	1.5	1317	30
eaf60 - 14.d	4.18595	0.07870	0.10020	0.00235	1381	23	1628	43	15.2	2.1	1355	26
eaf60 - 15.d	4.32301	0.10191	0.10090	0.00245	1341	28	1641	44	18.2	2.5	1312	31
eaf60 - 16.d	4.30776	0.09659	0.10320	0.00225	1346	27	1682	40	20.0	2.8	1311	29
eaf60 - 17.d	4.50230	0.10682	0.10070	0.00235	1293	27	1637	43	21.0	2.8	1261	30
eaf60 - 18.d	4.38313	0.07686	0.09980	0.00200	1325	21	1620	37	18.2	2.4	1296	23
eaf60 - 19.d	4.52734	0.09658	0.10150	0.00280	1287	24	1652	50	22.1	2.9	1252	27
eaf60 - 20.d	4.42081	0.08376	0.09640	0.00260	1315	22	1556	50	15.5	1.9	1292	25
eaf60 - 21.d	4.38117	0.10446	0.09830	0.00235	1325	28	1592	44	16.8	2.1	1300	31
eaf60 - 22.d	4.58901	0.08745	0.09340	0.00230	1271	22	1496	46	15.1	1.7	1251	24
eaf60 - 23.d	4.59765	0.09089	0.08330	0.00200	1269	22	1276	46	0.6	0.1	1268	25
eaf60 - 24.d	NaN	NaN	NaN	NaN	NaN	NaN	NaN	NaN	NaN	NaN	NaN	NaN
eaf60 - 25.d	NaN	NaN	NaN	NaN	NaN	NaN	NaN	NaN	NaN	NaN	NaN	NaN
eaf60 - 26.d	NaN	NaN	NaN	NaN	NaN	NaN	NaN	NaN	NaN	NaN	NaN	NaN
eaf60 - 27.d	NaN	NaN	NaN	NaN	NaN	NaN	NaN	NaN	NaN	NaN	NaN	NaN
eaf60 - 28.d	NaN	NaN	NaN	NaN	NaN	NaN	NaN	NaN	NaN	NaN	NaN	NaN
eaf60 - 29.d	NaN	NaN	NaN	NaN	NaN	NaN	NaN	NaN	NaN	NaN	NaN	NaN

Analysis number	$^{238}U/^{206}Pb$	±1s	$^{207}Pb/^{206}Pb$	±1s	$^{238}U/^{206}Pb$ age (Ma)	±1s	$^{207}Pb/^{206}Pb$ age (Ma)	±1s	Disc (%)	f207%	^{207}Pb-corrected $^{238}U/^{206}Pb$ Age (Ma)	±1s
eaf60 - 30.d	NaN	NaN	NaN	NaN	NaN	NaN	NaN	NaN	NaN	NaN	NaN	NaN
eaf60 - 31.d	4.38117	0.18318	0.13000	0.00650	1325	48	2098	85	36.8	NaN	NaN	NaN
eaf60 - 32.d	4.38117	0.10446	0.09250	0.00280	1325	28	1478	56	10.3	NaN	NaN	NaN
eaf60 - 33.d	NaN	NaN	NaN	NaN	NaN	NaN	NaN	NaN	NaN	NaN	NaN	NaN
eaf60 - 34.d	4.65238	0.17241	0.11900	0.00500	1255	41	1941	73	35.3	NaN	NaN	NaN
eaf60 - 35.d	4.03719	0.16467	0.13300	0.00600	1427	50	2138	77	33.3	NaN	NaN	NaN
eaf60 - 36.d	NaN	NaN	NaN	NaN	NaN	NaN	NaN	NaN	NaN	NaN	NaN	NaN
eaf60 - 37.d	4.49609	0.07247	0.09910	0.00270	1295	19	1607	50	19.5	2.5	1265	21
eaf60 - 38.d	4.43688	0.08917	0.09670	0.00205	1310	23	1561	39	16.1	2.0	1287	26
eaf60 - 39.d	4.28133	0.08911	0.09580	0.00225	1353	25	1544	44	12.3	1.5	1335	28
eaf60 - 40.d	4.42883	0.08306	0.09830	0.00285	1312	22	1592	53	17.6	2.2	1286	24
eaf60 - 41.d	4.43486	0.09695	0.09670	0.00250	1311	25	1561	48	16.1	2.0	1287	28
eaf60 - 42.d	4.29262	0.07148	0.09010	0.00195	1350	20	1428	41	5.4	0.6	1343	22
eaf60 - 43.d	4.58255	0.10086	0.10340	0.00255	1272	25	1686	45	24.5	3.3	1234	27
eaf60 - 44.d	4.49816	0.09950	0.09470	0.00270	1294	25	1522	53	15.0	1.8	1273	28
eaf60 - 45.d	4.36356	0.09698	0.09500	0.00190	1330	26	1528	37	13.0	1.6	1311	29
eaf60 - 46.d	4.35966	0.09113	0.09640	0.00190	1331	25	1556	37	14.4	1.8	1310	27
eaf60 - 47.d	4.33259	0.08453	0.09220	0.00230	1339	23	1472	47	9.0	1.0	1326	26
eaf60 - 48.d	4.38313	0.10068	0.09440	0.00210	1325	27	1516	41	12.6	1.5	1307	30
eaf60 - 49.d	4.46935	0.09734	0.09370	0.00255	1302	25	1502	51	13.3	1.5	1283	28
eaf60 - 50.d	4.39101	0.09714	0.09620	0.00245	1323	26	1552	47	14.8	1.8	1301	29
eaf60 - 51.d	4.48783	0.07615	0.09300	0.00245	1297	20	1488	49	12.8	1.5	1280	22
eaf60 - 52.d	4.26638	0.10864	0.09400	0.00245	1357	30	1508	48	10.0	1.2	1343	34
eaf60 - 53.d	4.27946	0.08723	0.09390	0.00200	1354	24	1506	40	10.1	1.2	1339	27
eaf60 - 54.d	4.44293	0.07009	0.09600	0.00240	1309	18	1548	46	15.4	1.9	1286	20
eaf60 - 55.d	4.34802	0.08600	0.09480	0.00250	1334	23	1524	49	12.4	1.5	1316	26
eaf60 - 56.d	4.48371	0.08291	0.09080	0.00160	1298	21	1442	33	10.0	1.1	1285	24
eaf60 - 57.d	4.37332	0.07010	0.09400	0.00155	1327	19	1508	31	12.0	1.4	1311	21
eaf60 - 58.d	4.39101	0.08467	0.09430	0.00180	1323	23	1514	36	12.6	1.5	1305	25

Analysis number	$^{238}U/^{206}Pb$	±1s	$^{207}Pb/^{206}Pb$	±1s	$^{238}U/^{206}Pb$ age (Ma)	±1s	$^{207}Pb/^{206}Pb$ age (Ma)	±1s	Disc (%)	f207%	^{207}Pb-corrected $^{238}U/^{206}Pb$ Age (Ma)	±1s
eaf60 - 59.d	4.33452	0.08460	0.08850	0.00195	1338	23	1393	42	4.0	0.4	1333	26
eaf60 - 60.d	4.27010	0.09051	0.09520	0.00250	1356	25	1532	49	11.5	1.4	1339	28
eaf60 - 61.d	4.31537	0.07754	0.09160	0.00225	1344	21	1459	46	7.9	0.9	1333	24
eaf60 - 62.d	4.53785	0.08980	0.09920	0.00215	1284	23	1609	40	20.2	2.6	1254	25
eaf60 - 63.d	4.27010	0.05470	0.09350	0.00185	1356	15	1498	37	9.5	1.1	1343	17
eaf60 - 64.d	4.38510	0.08827	0.09110	0.00215	1324	24	1449	44	8.6	1.0	1313	26
eaf60 - 65.d	4.35772	0.08166	0.09220	0.00200	1332	22	1472	41	9.5	1.1	1319	25
eaf60 - 66.d	4.42081	0.11612	0.10050	0.00300	1315	31	1633	54	19.5	2.6	1284	34
eaf60 - 67.d	4.44495	0.07779	0.09400	0.00200	1308	20	1508	40	13.3	1.5	1290	23
eaf60 - 68.d	4.33067	0.08911	0.09790	0.00250	1339	24	1585	47	15.5	2.0	1315	27
eaf60 - 69.d	4.48165	0.09682	0.09280	0.00270	1298	25	1484	54	12.5	1.4	1282	28
eaf60 - 70.d	4.38117	0.10446	0.10060	0.00315	1325	28	1635	57	19.0	2.5	1295	31
eaf60 - 71.d	4.42081	0.08763	0.09640	0.00220	1315	23	1556	42	15.5	1.9	1292	26
eaf60 - 72.d	4.39101	0.08087	0.09310	0.00225	1323	22	1490	45	11.2	1.3	1307	24
eaf60 - 73.d	4.44697	0.08758	0.09930	0.00240	1308	23	1611	44	18.8	2.4	1279	25
eaf60 - 74.d	4.51687	0.08199	0.08030	0.00125	1289	21	1204	30	-7.0	0.6	1296	23
eaf60 - 75.d	4.35383	0.08903	0.09300	0.00235	1333	24	1488	47	10.4	1.2	1318	27
eaf60 - 76.d	4.48577	0.08696	0.09110	0.00245	1297	22	1449	50	10.4	1.1	1284	25
eaf60 - 77.d	4.57183	0.10042	0.09520	0.00270	1275	25	1532	52	16.8	2.0	1252	27
eaf60 - 78.d	4.46119	0.10803	0.09450	0.00245	1304	28	1518	48	14.1	1.7	1284	31
eaf60 - 79.d	4.49816	0.08939	0.09440	0.00200	1294	23	1516	39	14.6	1.7	1274	25
eaf60 - 80.d	4.61939	0.08637	0.09620	0.00215	1263	21	1552	41	18.6	2.2	1238	23
eaf60 - 81.d	4.54630	0.07787	0.09520	0.00210	1282	20	1532	41	16.3	1.9	1259	22
eaf60 - 82.d	4.34802	0.07672	0.09230	0.00225	1334	21	1474	46	9.4	1.1	1321	23
eaf60 - 83.d	4.53154	0.08855	0.09080	0.00210	1285	22	1442	43	10.9	1.2	1272	25
eaf60 - 84.d	4.49816	0.07547	0.09230	0.00220	1294	19	1474	45	12.2	1.4	1278	21
eaf60 - 85.d	4.37724	0.07949	0.08630	0.00165	1326	21	1345	36	1.4	0.1	1325	24
eaf60 - 86.d	4.43688	0.09802	0.09190	0.00260	1310	26	1465	53	10.6	1.2	1296	29
eaf60 - 87.d	4.45103	0.07604	0.09640	0.00285	1306	20	1556	54	16.0	2.0	1283	22

Analysis number	$^{238}U/^{206}Pb$	±1s	$^{207}Pb/^{206}Pb$	±1s	$^{238}U/^{206}Pb$ age (Ma)	±1s	$^{207}Pb/^{206}Pb$ age (Ma)	±1s	Disc (%)	f207%	^{207}Pb-corrected $^{238}U/^{206}Pb$ Age (Ma)	±1s
eaf60 - 88.d	4.53785	0.10009	0.09880	0.00290	1284	25	1602	54	19.8	2.5	1255	28
eaf60 - 89.d	4.56329	0.08554	0.09400	0.00225	1277	21	1508	45	15.3	1.8	1257	24
eaf60 - 90.d	4.35383	0.10039	0.09430	0.00285	1333	27	1514	56	12.0	1.4	1316	30
eaf60 - 91.d	4.45305	0.07997	0.09020	0.00225	1306	21	1430	47	8.7	0.9	1295	23
eaf60 - 92.d	4.39101	0.10198	0.09110	0.00255	1323	27	1449	52	8.7	1.0	1311	30
eaf60 - 93.d	4.38117	0.10446	0.09080	0.00255	1325	28	1442	53	8.1	0.9	1315	31
eaf60 - 94.d	4.54419	0.11181	0.09780	0.00280	1282	28	1583	53	19.0	2.4	1255	31
eaf60 - 95.d	4.30966	0.09203	0.09130	0.00195	1345	25	1453	40	7.4	0.8	1335	28
eaf60 - 96.d	4.48783	0.08404	0.09370	0.00220	1297	22	1502	44	13.7	1.6	1278	24
eaf60 - 97.d	4.72666	0.10005	0.08370	0.00190	1237	23	1286	44	3.8	0.3	1233	26
eaf60 - 98.d	4.35577	0.07145	0.09090	0.00180	1332	19	1445	37	7.8	0.9	1322	22
eaf60 - 99.d	4.51062	0.08883	0.09410	0.00260	1291	23	1510	51	14.5	1.7	1271	25
eaf60 - 100.d	4.26265	0.09657	0.09500	0.00270	1359	27	1528	53	11.1	1.4	1342	30
eaf60 - 101.d	4.73812	0.08483	0.07960	0.00180	1234	20	1187	44	-4.0	0.3	1238	22
eaf60 - 102.d	4.35189	0.07684	0.09090	0.00230	1333	21	1445	47	7.7	0.9	1323	23
eaf60 - 103.d	4.42482	0.07338	0.09390	0.00235	1313	19	1506	47	12.8	1.5	1296	22
eaf60 - 104.d	4.31537	0.08302	0.09470	0.00235	1344	23	1522	46	11.7	1.4	1326	26
eaf60 - 105.d	4.34802	0.06493	0.08940	0.00175	1334	18	1413	37	5.5	0.6	1327	20
eaf60 - 106.d	4.15745	0.09487	0.09880	0.00265	1389	28	1602	49	13.2	1.8	1367	31
eaf60 - 107.d	4.21666	0.08408	0.09830	0.00260	1372	24	1592	49	13.8	1.8	1349	27
eaf60 - 108.d	4.28885	0.06009	0.08200	0.00175	1351	17	1246	41	-8.5	0.8	1360	19
eaf60 - 109.d	4.35966	0.08924	0.09280	0.00215	1331	24	1484	43	10.3	1.2	1317	27
eaf60 - 110.d	4.43889	0.07568	0.09130	0.00195	1310	20	1453	40	9.9	1.1	1297	22
eaf60 - 111.d	4.44091	0.08834	0.08940	0.00220	1309	23	1413	46	7.3	0.8	1300	26
eaf60 - 112.d	4.31347	0.10056	0.09500	0.00295	1344	28	1528	57	12.0	1.5	1326	31
eaf60 - 114.d	4.38904	0.08937	0.09470	0.00280	1323	24	1522	55	13.1	1.6	1305	27
eaf60 - 115.d	4.37332	0.08312	0.09530	0.00225	1327	22	1534	44	13.5	1.6	1308	25
eaf60 - 116.d	4.38707	0.08548	0.09430	0.00210	1324	23	1514	41	12.6	1.5	1306	25
eaf60 - 117.d	4.20215	0.07493	0.09180	0.00235	1376	22	1463	48	6.0	0.7	1368	25

Analysis number	$^{238}U/^{206}Pb$	±1s	$^{207}Pb/^{206}Pb$	±1s	$^{238}U/^{206}Pb$ age (Ma)	±1s	$^{207}Pb/^{206}Pb$ age (Ma)	±1s	Disc (%)	f207%	^{207}Pb-corrected $^{238}U/^{206}Pb$ Age (Ma)	±1s
eaf60 - 118.d	4.37528	0.08036	0.08970	0.00165	1327	22	1419	35	6.5	0.7	1319	24
eaf60 - 119.d	4.39496	0.09247	0.09330	0.00230	1322	25	1494	46	11.5	1.3	1306	27
eaf60 - 120.d	4.40487	0.09867	0.09300	0.00235	1319	26	1488	47	11.4	1.3	1303	29
eaf60 - 121.d	4.40884	0.09689	0.09480	0.00295	1318	26	1524	58	13.5	1.6	1299	29
eaf60 - 122.d	4.48989	0.09412	0.09960	0.00225	1296	24	1617	41	19.8	2.6	1266	26
eaf60 - 123.d	4.35189	0.08614	0.08850	0.00200	1333	23	1393	43	4.3	0.5	1328	26
eaf60 - 124.d	4.32492	0.08611	0.08910	0.00225	1341	24	1406	48	4.7	0.5	1335	27
eaf60 - 126.d	4.17521	0.10436	0.10660	0.00290	1384	30	1742	49	20.5	3.1	1345	34
eaf60 - 127.d	4.34029	0.08946	0.11220	0.00320	1337	24	1835	51	27.2	4.4	1284	27
eaf60 - 128.d	4.47344	0.09850	0.10750	0.00275	1301	25	1757	46	26.0	3.8	1255	28
eaf60 - 129.d	4.28509	0.10027	0.10540	0.00295	1352	28	1721	51	21.4	3.1	1314	31
eaf60 - 130.d	4.36161	0.10360	0.10960	0.00315	1331	28	1793	51	25.8	4.0	1283	31
eaf60 - 131.d	4.52106	0.09327	0.10280	0.00260	1288	24	1675	46	23.1	3.1	1251	26
eaf60 - 132.d	4.38904	0.10286	0.09830	0.00230	1323	27	1592	43	16.9	2.2	1297	30
eaf60 - 133.d	4.49402	0.07339	0.08450	0.00175	1295	19	1304	40	0.7	0.1	1294	21
eaf60 - 134.d	4.51270	0.07589	0.09540	0.00175	1290	19	1536	34	16.0	1.9	1268	21
eaf60 - 135.d	4.41682	0.09039	0.09720	0.00245	1316	24	1571	46	16.3	2.0	1291	26
eaf60 - 136.d	4.31156	0.08748	0.10840	0.00290	1345	24	1773	48	24.1	3.7	1300	27
eaf60 - 137.d	4.49195	0.09723	0.10080	0.00280	1296	25	1639	51	20.9	2.8	1263	27
eaf60 - 138.d	4.20396	0.07670	0.09230	0.00205	1376	22	1474	42	6.6	0.8	1366	25
eaf60 - 139.d	4.23310	0.09088	0.10610	0.00225	1367	26	1733	38	21.1	3.1	1328	28
eaf60 - 140.d	4.25337	0.09528	0.10560	0.00310	1361	27	1725	53	21.1	3.1	1323	30
eaf60 - 141.d	4.28697	0.09574	0.09480	0.00270	1352	27	1524	53	11.3	1.4	1335	30
eaf60 - 142.d	4.17521	0.10436	0.10940	0.00275	1384	30	1789	45	22.6	3.6	1339	33
eaf60 - 143.d	4.34609	0.08780	0.11200	0.00345	1335	24	1832	55	27.1	4.3	1282	26
eaf60 - 144.d	4.26824	0.09771	0.09460	0.00225	1357	27	1520	44	10.7	1.3	1341	31
eaf60 - 145.d	4.35577	0.08628	0.09010	0.00195	1332	23	1428	41	6.7	0.7	1324	26
eaf60 - 146.d	4.52315	0.11085	0.10010	0.00280	1288	28	1626	51	20.8	2.7	1256	31
eaf60 - 147.d	4.25337	0.08897	0.10170	0.00260	1361	25	1655	47	17.8	2.5	1331	28

Analysis number	$^{238}U/^{206}Pb$	±1s	$^{207}Pb/^{206}Pb$	±1s	$^{238}U/^{206}Pb$ age (Ma)	±1s	$^{207}Pb/^{206}Pb$ age (Ma)	±1s	Disc (%)	f207%	^{207}Pb-corrected $^{238}U/^{206}Pb$ Age (Ma)	±1s
eaf60 - 148.d	4.48165	0.08582	0.09400	0.00265	1298	22	1508	52	13.9	1.6	1279	25
eaf60 - 149.d	4.31347	0.08479	0.09520	0.00265	1344	23	1532	52	12.3	1.5	1326	26
eaf60 - 150.d	4.35383	0.05976	0.09210	0.00190	1333	16	1469	39	9.3	1.1	1320	18
eaf60 - 151.d	4.32110	0.06253	0.09610	0.00205	1342	17	1550	40	13.4	1.7	1322	19
eaf60 - 152.d	4.49195	0.09824	0.09150	0.00165	1296	25	1457	34	11.1	1.2	1281	28
eaf60 - 153.d	4.41283	0.08062	0.09740	0.00235	1317	21	1575	45	16.4	2.1	1292	24
eaf60 - 154.d	4.33452	0.08553	0.09630	0.00280	1338	23	1554	54	13.9	1.7	1317	26
eaf60 - 155.d	4.42081	0.07515	0.09400	0.00230	1315	20	1508	46	12.8	1.5	1297	22
eaf60 - 156.d	4.23861	0.07780	0.09550	0.00240	1365	22	1538	47	11.2	1.4	1348	25
eaf60 - 157.d	4.37920	0.07117	0.09140	0.00195	1326	19	1455	40	8.9	1.0	1314	21
eaf60 - 158.d	4.25337	0.09167	0.09760	0.00220	1361	26	1579	42	13.8	1.8	1339	29
eaf60 - 159.d	4.28885	0.07315	0.09770	0.00230	1351	20	1581	43	14.5	1.9	1328	23
eaf60 - 160.d	4.32684	0.07699	0.09620	0.00270	1340	21	1552	52	13.6	1.7	1320	24

Analysis number	Reason for exclusion
eaf60 - 113.d	reanalysis of spot 112
eaf60 - 125.d	did not ablate properly

Table A6.4-2 LA-ICPMS analytical data for sample EAF12.

Analysis number	Na23 ppm	Na23 ppm 2SE	Na23 ppm LOD	Al27 ppm	Al27 ppm 2SE	Al27 ppm LOD	Si28 ppm	Si28 ppm 2SE	Si28 ppm LOD	Ca44 ppm	Ca44 ppm 2SE	Ca44 ppm LOD
eaf12 - 1.d	186	14	44	12020	160	4.3	141100	1700	5800	198800	3800	290
eaf12 - 2.d	129	14	49	12330	200	5.8	138500	2100	6700	209900	3900	310
eaf12 - 3.d	135	12	39	12300	120	4.7	139900	1700	4600	206200	2400	310
eaf12 - 4.d	165	17	49	12630	180	4.3	139600	2300	5200	208300	3100	230
eaf12 - 5.d	135	12	46	12820	160	7	140900	2100	5800	209800	2700	360
eaf12 - 6.d	99	12	30	13240	220	6.6	140300	2000	3600	209200	2900	320
eaf12 - 7.d	130	16	38	12830	160	3.7	144800	1700	4100	204600	2300	350
eaf12 - 8.d	69	13	39	14430	200	5.9	141700	2600	7200	205300	2500	270
eaf12 - 9.d	98	15	35	13330	150	4.2	141000	2000	6500	203900	2900	310
eaf12 - 10.d	96	11	36	12710	130	4.6	141200	1900	3400	206700	2200	250
eaf12 - 11.d	106	14	40	13500	220	7.2	142200	1800	5900	204200	3100	170
eaf12 - 12.d	132	13	38	14270	200	6.1	144200	1800	4400	204600	2700	370
eaf12 - 13.d	143	13	40	15000	190	6.1	145600	1700	8700	201600	2400	280
eaf12 - 14.d	148	12	37	14020	170	5.1	146500	2300	4100	226200	4000	380
eaf12 - 15.d	202	16	35	13070	180	4.7	141800	2100	3300	201900	3000	300
eaf12 - 16.d	165	16	42	12820	170	4.6	143400	2200	6500	201000	2500	280
eaf12 - 17.d	101	13	44	13220	200	4	144000	1700	4200	203100	2500	260
eaf12 - 18.d	111	12	39	11220	160	7.1	140200	1900	3200	200400	3000	270
eaf12 - 19.d	100	12	42	11500	200	4.6	140500	2000	5500	201400	2900	360
eaf12 - 20.d	162	14	27	13610	160	6.2	141700	1700	5100	203900	2300	280
eaf12 - 21.d	205	12	27	12590	200	6.4	141100	1700	6200	201800	2300	360
eaf12 - 22.d	197	12	45	14290	230	6.2	141800	1700	7600	202100	2300	300
eaf12 - 23.d	102	14	31	12770	240	4.2	144600	1700	4500	204200	2800	310
eaf12 - 24.d	166	12	44	13880	170	5.9	142800	1500	7000	200300	2200	370
eaf12 - 25.d	148	12	37	12330	170	3.4	146000	1800	3800	206200	2500	240
eaf12 - 26.d	213	16	22	13420	180	5.6	144500	1700	8200	209100	2700	380

Analysis number	Na23 ppm	Na23 ppm 2SE	Na23 ppm LOD	Al27 ppm	Al27 ppm 2SE	Al27 ppm LOD	Si28 ppm	Si28 ppm 2SE	Si28 ppm LOD	Ca44 ppm	Ca44 ppm 2SE	Ca44 ppm LOD
eaf12 - 27.d	128	12	36	12900	200	6.1	142400	2000	3300	211200	3500	310
eaf12 - 28.d	85	13	35	12910	240	6.7	142600	2700	5200	209100	4100	340
eaf12 - 29.d	83.3	9.5	37	12900	240	4.6	139800	2300	5900	207600	3000	290
eaf12 - 30.d	122	14	34	13100	150	4.4	140400	2000	4400	211600	2400	240
eaf12 - 31.d	184	14	37	11830	140	4.6	139500	1800	6200	206900	2800	390
eaf12 - 32.d	191	17	49	13150	220	5.9	139700	1900	4800	206900	2900	240
eaf12 - 33.d	181	16	64	13020	190	3.5	141500	1900	5100	208200	3100	340
eaf12 - 34.d	235	15	33	13550	170	4.5	139200	2100	5200	207300	2500	290
eaf12 - 35.d	155	14	32	12850	150	5.3	139800	1800	7600	205000	2100	260
eaf12 - 36.d	108	13	41	13180	180	5.2	142500	2600	5800	205900	2900	310
eaf12 - 37.d	197	14	36	12790	170	5.4	144800	2400	3400	206400	3000	260
eaf12 - 38.d	75	14	38	12380	170	6.6	143400	2200	8800	204700	3200	320
eaf12 - 39.d	88	14	38	13160	180	4.8	142100	1800	6700	206000	2400	220
eaf12 - 40.d	66	10	42	10950	200	5.7	142200	1800	6600	205300	2700	330
eaf12 - 41.d	111	13	42	12250	110	4.4	144500	1800	4300	208200	2600	320
eaf12 - 42.d	76	11	40	13270	180	4.8	145500	1300	5100	205500	2500	330
eaf12 - 43.d	63	11	40	11760	140	5.2	144100	1700	4000	204900	2500	270
eaf12 - 44.d	90	14	42	12990	160	3.8	143600	1600	5500	203600	2500	330
eaf12 - 45.d	74	11	27	13900	170	4.7	141600	1900	4500	203400	2400	410
eaf12 - 46.d	73	12	29	12960	120	5.1	141400	2100	5600	198700	2300	400
eaf12 - 47.d	66	13	37	14740	200	6.6	140600	1600	1900	226000	3100	300
eaf12 - 48.d	108	12	38	12680	130	3.5	144300	1600	4300	203000	1900	270
eaf12 - 49.d	84	12	33	14140	160	4.7	145400	1600	7200	199000	2700	360
eaf12 - 50.d	101	13	33	13440	210	5	143600	1600	3500	197000	2500	280
eaf12 - 51.d	92	12	32	12480	210	2.9	140900	1600	7200	213100	2200	390
eaf12 - 52.d	108	12	40	13040	180	5.6	140300	2000	4000	214800	3000	240
eaf12 - 53.d	90	11	36	11880	180	5.4	143100	1400	6400	214000	3100	340
eaf12 - 54.d	141	15	41	12020	140	4.7	144700	1900	9400	212800	2600	340

Analysis number	Na23 ppm	Na23 ppm 2SE	Na23 ppm LOD	Al27 ppm	Al27 ppm 2SE	Al27 ppm LOD	Si28 ppm	Si28 ppm 2SE	Si28 ppm LOD	Ca44 ppm	Ca44 ppm 2SE	Ca44 ppm LOD
eaf12 - 55.d	100.2	9.1	30	12820	180	4.3	144200	1700	2400	210000	3300	230
eaf12 - 56.d	119	12	37	12900	160	4	146700	2200	6900	209600	2500	310
eaf12 - 57.d	104	10	32	12280	170	4.6	145900	2100	5700	212000	2600	250
eaf12 - 58.d	147	13	40	12110	110	4.5	144100	1500	5000	209700	3200	270
eaf12 - 59.d	103	11	41	11920	150	4.9	146400	1300	5300	208300	2100	300
eaf12 - 60.d	95	10	20	13270	200	6.7	145900	2000	4100	208100	2300	320
eaf12 - 61.d	101	12	29	13620	180	5.9	143500	2200	4400	203300	2800	280
eaf12 - 62.d	140	12	30	11690	160	3.4	143000	1500	4700	200600	2400	330
eaf12 - 63.d	91.8	7.9	24	10860	120	4.5	145600	1700	1900	208600	2900	270
eaf12 - 64.d	235	15	25	14140	150	3.6	142800	1700	7400	196800	2800	370
eaf12 - 65.d	166	12	25	13130	200	3.8	142500	1800	3900	203400	3100	410
eaf12 - 66.d	215	11	34	13110	160	4.1	145600	1400	7100	204100	2700	360
eaf12 - 67.d	204	11	33	13180	200	5.4	144600	1500	5500	202500	2800	350
eaf12 - 68.d	157	12	24	13600	200	3.9	143200	2100	5200	202300	3000	290
eaf12 - 69.d	136	10	26	11230	140	4.5	145600	1800	4100	205200	2800	340
eaf12 - 70.d	106	9.4	29	13550	150	4.7	142600	1700	5800	205500	2300	250
eaf12 - 71.d	160	12	31	12790	170	4.1	143400	2200	6500	199200	2400	240
eaf12 - 72.d	117.5	8.4	33	12610	140	3.4	144500	1600	3900	202900	2800	300
eaf12 - 73.d	185	12	28	13050	220	5.8	140700	2100	9400	200300	2400	350
eaf12 - 74.d	112.1	9.2	21	13110	180	3.3	143500	1800	5800	201500	2300	320
eaf12 - 75.d	191.5	9.5	36	13110	170	4.3	146700	1800	6100	200900	1900	280
eaf12 - 76.d	77.3	8.9	28	13790	150	4.8	142700	2300	6800	218500	3100	320
eaf12 - 77.d	203	11	25	12790	200	3.7	142300	1600	4800	221500	2900	280
eaf12 - 78.d	137	12	29	12080	160	6.8	143700	2100	8800	216600	2800	400
eaf12 - 79.d	153	12	38	13250	150	4.5	143000	1600	5700	218000	2400	320
eaf12 - 80.d	192	11	30	13530	180	4	142300	2000	6800	213500	2400	390
eaf12 - 81.d	175	13	17	13690	190	3.4	143600	2100	3600	212000	2500	260
eaf12 - 82.d	165	14	35	13910	220	5.7	144100	2000	6100	214200	2700	290

Analysis number	Na23 ppm	Na23 ppm 2SE	Na23 ppm LOD	Al27 ppm	Al27 ppm 2SE	Al27 ppm LOD	Si28 ppm	Si28 ppm 2SE	Si28 ppm LOD	Ca44 ppm	Ca44 ppm 2SE	Ca44 ppm LOD
eaf12 - 83.d	105	14	31	13750	250	6	145200	2100	2500	209800	2800	340
eaf12 - 84.d	118	12	37	13500	160	3.8	141700	2000	1800	211100	2400	340
eaf12 - 85.d	125	11	24	14510	210	3.7	143300	1700	4700	208600	2800	230
eaf12 - 86.d	169	11	32	14180	190	5.3	143700	2200	6500	208400	2700	340
eaf12 - 87.d	99	11	25	12960	200	4.3	140500	1500	6000	209400	2500	300
eaf12 - 88.d	80.7	9.1	28	13760	150	3.8	144900	1900	5100	204600	3100	280
eaf12 - 89.d	154	13	23	14020	200	4.6	145400	2200	6500	209200	2800	250
eaf12 - 90.d	175.2	9.8	19	13910	190	3.1	143200	1800	5100	202300	2700	350
eaf12 - 92.d	179	11	41	13210	190	3	144200	1600	3500	202900	2400	310
eaf12 - 93.d	116	11	25	14880	180	4.6	145900	1900	4600	201500	2500	310
eaf12 - 94.d	107	12	29	13360	200	3.3	144700	1900	4000	204700	2600	260
eaf12 - 95.d	77.2	9.4	23	13510	140	3.6	146500	2000	4300	199800	2400	280
eaf12 - 96.d	72	10	30	13190	190	4.6	145200	2100	4200	202800	2900	320
eaf12 - 97.d	72.4	7.2	21	13190	180	4.7	147100	1800	3700	201800	2900	200
eaf12 - 98.d	129	10	29	13520	210	2.9	145700	2100	6200	205500	2900	280
eaf12 - 99.d	151.2	9.8	26	13990	210	3.2	143700	2200	3700	204000	2800	250
eaf12 - 100.d	83.3	7.8	32	13610	210	3.9	144800	2200	5400	205300	2700	290
eaf12 - 101.d	90	12	37	13490	190	4.6	144900	2000	5700	218100	3000	290
eaf12 - 102.d	232	13	37	12460	170	4.2	143800	1800	3400	219600	3100	310
eaf12 - 103.d	142	13	35	13410	200	3.5	145900	2200	3100	220100	3200	330
eaf12 - 104.d	82	11	24	15210	180	4.7	143100	2000	3200	217800	2200	290
eaf12 - 105.d	126	8.6	33	12870	170	4.1	146000	1600	7500	216900	3500	350
eaf12 - 106.d	112	12	33	13300	180	4.2	146700	2000	4100	216200	3200	310
eaf12 - 107.d	147	14	31	13570	180	4.2	141300	1900	8300	212100	2800	440
eaf12 - 108.d	125	14	20	13450	160	4.1	146700	1900	7100	214500	2700	340
eaf12 - 109.d	199	11	33	12710	140	4.5	145700	1700	5500	211000	2000	280
eaf12 - 110.d	159.4	8.7	32	12480	190	4.7	143200	2100	7100	207700	2600	320
eaf12 - 111.d	154.7	8.6	31	12500	170	3.4	140600	2100	6800	210200	3600	270

Analysis number	Na23 ppm	Na23 ppm 2SE	Na23 ppm LOD	Al27 ppm	Al27 ppm 2SE	Al27 ppm LOD	Si28 ppm	Si28 ppm 2SE	Si28 ppm LOD	Ca44 ppm	Ca44 ppm 2SE	Ca44 ppm LOD
eaf12 - 112.d	92	10	24	11940	210	2.7	144800	2800	4200	208800	2600	260
eaf12 - 113.d	108	11	27	12010	200	3.2	143600	1500	2800	208600	2800	330
eaf12 - 114.d	96.2	8.7	26	11660	110	3.9	142600	1900	3700	207400	2900	290
eaf12 - 115.d	84.8	8.4	29	13410	200	4.5	149400	1700	8700	204200	2500	360
eaf12 - 116.d	98	6.5	36	12500	200	5	146700	2100	5200	206800	2400	300
eaf12 - 117.d	66	8.9	25	12390	160	3	148900	1900	4400	206800	2700	200
eaf12 - 118.d	59.3	8.7	28	11510	130	4.1	151100	1700	6600	202800	2400	350
eaf12 - 119.d	100.9	8.9	22	11730	190	3.4	148000	2000	5100	204100	2800	200
eaf12 - 120.d	114.3	9.4	31	13080	170	4.6	145200	2400	5300	206900	2400	250
eaf12 - 121.d	72.7	8.7	32	11840	130	3.1	142900	2400	3900	206000	2300	330
eaf12 - 122.d	65.4	9.7	32	10910	150	3.7	146000	1800	5300	207300	1800	300
eaf12 - 123.d	88.7	9.1	43	12370	190	6	144100	2500	8800	205900	2400	320
eaf12 - 124.d	199	11	23	12440	190	4.1	145200	2100	5100	204600	2300	220
eaf12 - 125.d	135	11	35	12300	150	3.3	142800	2500	9900	206800	2900	320
eaf12 - 126.d	105	10	26	12300	200	3.8	148300	2500	5900	221900	3000	330
eaf12 - 127.d	72	12	38	11910	200	4.5	145400	1700	8200	220600	3300	300
eaf12 - 128.d	58.4	9.3	27	12200	150	3.9	144400	2200	4600	221400	2400	270
eaf12 - 129.d	68	10	24	13870	240	4.2	145200	2200	5500	217500	2600	320
eaf12 - 130.d	76.8	9.3	25	12940	160	3	146100	1800	6000	212500	2200	460
eaf12 - 131.d	65.8	9.7	35	12160	130	4	148600	1900	5900	216800	2900	270
eaf12 - 132.d	129.7	8.1	33	13540	160	4.9	148000	2500	8700	216400	2700	380
eaf12 - 133.d	137	11	25	12760	200	4	149000	2200	4300	211200	2600	230
eaf12 - 134.d	153	11	25	12740	170	5	150100	2000	6100	210800	2900	320
eaf12 - 135.d	220	10	21	12040	170	3.2	150100	1800	4300	208800	2700	350
eaf12 - 136.d	74	10	31	12190	150	4.5	146900	2000	9200	210300	2300	320
eaf12 - 137.d	84	12	37	13680	120	3.7	148100	3200	6400	211600	2100	330
eaf12 - 138.d	68.9	9.4	30	13560	170	4.9	150100	2000	6000	212300	2400	350
eaf12 - 139.d	77.9	9.3	21	13940	230	4.4	152100	2300	3500	206800	2700	190

Analysis number	Na23 ppm	Na23 ppm 2SE	Na23 ppm LOD	Al27 ppm	Al27 ppm 2SE	Al27 ppm LOD	Si28 ppm	Si28 ppm 2SE	Si28 ppm LOD	Ca44 ppm	Ca44 ppm 2SE	Ca44 ppm LOD
eaf12 - 140.d	130.1	8.7	28	13550	160	3.5	146400	2600	8800	208600	2500	370
eaf12 - 141.d	104.7	5.9	39	10810	150	4.8	143100	2300	5400	217100	2700	270
eaf12 - 142.d	198.3	9.4	24	13350	160	3.9	142800	2400	6500	207800	3300	310
eaf12 - 143.d	103	10	31	12550	160	4.3	144200	2400	7700	207500	2600	390
eaf12 - 144.d	88.9	8.1	29	13160	180	4	142300	2300	4700	211400	2800	230
eaf12 - 145.d	108.8	8	23	12980	150	2.2	137500	3000	4700	206300	2200	290
eaf12 - 146.d	105.4	9.5	26	12080	140	4.3	140800	2100	5800	208200	2200	300
eaf12 - 147.d	114	10	26	11990	140	4.2	142000	2100	5700	208400	2500	240
eaf12 - 148.d	81.9	9.2	32	12100	160	4.1	144100	1900	5700	207200	2300	180
eaf12 - 149.d	98	11	28	11950	170	4.3	144200	1700	6300	210200	2700	320
eaf12 - 150.d	111.7	9.9	20	11650	180	4.3	145700	2200	5900	209900	2700	280
eaf12 - 151.d	115	10	27	12180	180	4.8	146100	1900	9000	217000	3100	320
eaf12 - 152.d	68.2	9.5	40	13350	140	4.3	144700	2100	6500	217800	2800	320
eaf12 - 153.d	150	13	38	11910	210	3.2	145500	2100	8000	215800	2800	350
eaf12 - 154.d	67	10	29	14180	150	4.4	147000	2100	6000	212700	3100	350
eaf12 - 155.d	105	11	23	12500	160	3.4	147100	2100	8300	215500	3100	370
eaf12 - 156.d	122.5	8.3	31	11930	180	4.9	147100	2200	7500	210400	3300	460
eaf12 - 157.d	122.5	9.7	29	14450	180	3.8	145700	2500	6500	211000	2200	250
eaf12 - 158.d	112.8	9.2	22	13820	170	4.4	147700	2100	6000	213700	2700	400
eaf12 - 159.d	131.1	7.6	31	12710	150	3.8	145100	1800	3500	209300	2400	350
eaf12 - 160.d	102.6	9.2	25	14020	190	3.1	147400	2100	5700	211600	2500	360
eaf12 - 161.d	114	8.7	23	13110	190	3.9	150600	2300	4400	210100	2800	250
eaf12 - 162.d	131.2	8.2	24	12910	160	4.3	147700	2000	4600	211000	2400	370
eaf12 - 163.d	170	11	25	14000	180	4.6	142300	2600	7500	211800	2000	350
eaf12 - 164.d	126	11	29	10840	170	4.4	146700	2500	4800	208100	3100	300

Analysis number	Ti49 ppm	Ti49 ppm 2SE	Ti49 ppm LOD	V51 ppm	V51 ppm 2SE	V51 ppm LOD	Cr52 ppm	Cr52 ppm 2SE	Cr52 ppm LOD	Mn55 ppm	Mn55 ppm 2SE	Mn55 ppm LOD
eaf12 - 1.d	202600	3400	2.9	368.5	7.1	0.34	28.3	1.6	3.5	162.8	3.8	6.1
eaf12 - 2.d	206900	3100	2.1	393.2	7.7	0.31	31.2	1.9	3.8	255	4.9	7
eaf12 - 3.d	207000	2800	2.3	446.6	7	0.34	32.2	1.4	4.3	262.5	4.2	6.2
eaf12 - 4.d	208200	3200	1	351.7	5.3	0.34	35.6	2.1	3.7	194.8	4	6.9
eaf12 - 5.d	207600	3000	1.1	340.7	5.8	0.4	41.3	1.6	3.9	233.7	4.6	7
eaf12 - 6.d	208700	2700	3	374.8	6.1	0.28	35.7	1.4	4.6	266.2	4.5	4.3
eaf12 - 7.d	205200	2300	NaN	420.9	5.9	0.3	33.8	2.1	3.8	259.1	4.9	6.6
eaf12 - 8.d	205400	3000	2.3	344.5	5.2	0.28	44.9	2	2.4	288.3	4.5	8.7
eaf12 - 9.d	203500	2700	2.4	343.6	5.8	0.47	36.6	2	4.2	280.2	4.2	6.7
eaf12 - 10.d	208500	2000	NaN	292.7	4.7	0.33	35.2	1.8	3.9	279.8	3.4	6
eaf12 - 11.d	206500	2700	2.3	208.6	4	0.36	36.1	1.6	3.7	259.8	4.8	6.6
eaf12 - 12.d	201200	2700	2.3	335	6	0.32	36.1	1.8	3.5	217.4	5.6	9.6
eaf12 - 13.d	201900	2900	3.2	199.7	3.1	0.22	33.9	1.7	4.7	226.1	5.6	8.7
eaf12 - 14.d	204800	2600	2.9	351.6	4.5	0.28	47.9	1.9	3.9	242.2	3.7	7.9
eaf12 - 15.d	202200	3200	2	289.4	5.9	0.52	35.2	1.8	3.4	140.1	4.4	4.9
eaf12 - 16.d	205600	2000	NaN	371	5.2	0.37	23	1.7	4.8	238.9	5.2	7
eaf12 - 17.d	206900	3000	1	320.5	5.4	0.38	41.6	2.2	3.5	270	4.5	6
eaf12 - 18.d	207200	3500	NaN	196.4	3.7	0.4	57.4	2.4	3.8	270.5	6	6.2
eaf12 - 19.d	206600	2400	2	168.7	2.6	0.21	56.5	2.4	5.4	277.2	5.1	9.1
eaf12 - 20.d	203100	2500	1.4	301.6	4.7	0.31	55.6	1.8	5.3	84.4	3.5	6.8
eaf12 - 21.d	204100	2700	1.7	422.4	5.8	0.27	29.3	1.9	3.8	161.8	3.6	8.3
eaf12 - 22.d	202500	2500	NaN	431.1	6.5	0.48	47	2	6.2	147.3	2.5	12
eaf12 - 23.d	207900	3100	NaN	356.3	5.6	0.31	35.2	1.7	3.7	271.9	4.4	6.8
eaf12 - 24.d	203600	3300	2.1	415.8	6.1	0.31	40.4	1.9	4.9	196.9	4.5	9.2
eaf12 - 25.d	207700	2200	2.2	393.8	6.2	0.28	32.4	1.6	3.5	195.8	3.9	5.9
eaf12 - 26.d	207400	2900	2.2	444.6	6.4	0.35	39.8	1.5	3.1	149.8	3.8	8
eaf12 - 27.d	212700	3100	1.5	242.6	4.5	0.25	34.6	1.9	4.3	225.4	4	6.6
eaf12 - 28.d	210300	3300	2.1	314.6	6.1	0.43	40.6	1.9	4.1	279.3	5.8	8.2
eaf12 - 29.d	208300	3000	2.5	393.7	6.9	0.33	33.6	2.3	3.8	283	4.6	8.9

Analysis number	Ti49 ppm	Ti49 ppm 2SE	Ti49 ppm LOD	V51 ppm	V51 ppm 2SE	V51 ppm LOD	Cr52 ppm	Cr52 ppm 2SE	Cr52 ppm LOD	Mn55 ppm	Mn55 ppm 2SE	Mn55 ppm LOD
eaf12 - 30.d	209800	1900	2.2	427.5	6.2	0.3	31.6	1.7	5.7	256.3	5	7.8
eaf12 - 31.d	212100	2800	1.5	399.3	5.9	0.31	28.5	1.8	4.2	202	4.8	8.1
eaf12 - 32.d	208000	2600	2.1	342.4	7	0.36	32.8	1.8	4.1	136.5	3.6	6.3
eaf12 - 33.d	211900	2600	2.9	429.3	5.5	0.42	38.4	2	5	195.8	4.9	10
eaf12 - 34.d	209900	2600	NaN	368.9	6.9	0.42	26.8	1.8	4.1	144.2	3.7	4.8
eaf12 - 35.d	210000	2300	2.1	373.2	4.9	0.38	28.7	1.8	3.8	193.5	4.8	11
eaf12 - 36.d	207400	2800	2.1	351.9	6.2	0.31	29.3	1.4	3.8	236.3	3.7	7.4
eaf12 - 37.d	210100	3100	2.9	367	5.4	0.43	26.2	1.8	4.3	174.1	3.9	7
eaf12 - 38.d	207000	3400	NaN	364.8	6.6	0.43	38.9	2.9	6.5	285.5	6.1	11
eaf12 - 39.d	207600	2500	2.1	364.7	4.8	0.35	34	1.7	5.5	267.9	6	7.8
eaf12 - 40.d	211900	2000	1.1	260.7	6.1	0.41	30.1	1.9	3.8	271	5.9	8
eaf12 - 41.d	210200	3100	2.1	389.2	7.3	0.37	41.3	1.6	4.3	256.2	5.4	8.5
eaf12 - 42.d	205400	2500	2.3	326.8	5.5	0.48	51.7	2.7	6	285.1	6.7	9.2
eaf12 - 43.d	208700	2100	2.1	344.6	6.2	0.35	57.9	2.2	4.3	275.1	5.2	7.4
eaf12 - 44.d	206000	2300	NaN	313.6	4.5	0.36	45.5	1.7	5	269	4.5	7.3
eaf12 - 45.d	202400	2900	NaN	322.6	5.5	0.4	82.6	2.6	3.8	275.9	5.2	6
eaf12 - 46.d	203500	2700	1	326.4	5.5	0.28	37.4	2.2	5.3	263.8	6	7.7
eaf12 - 47.d	201500	2800	1.1	343.8	6.4	0.42	91.2	3.3	4.6	287	6.9	5.1
eaf12 - 48.d	208400	2200	1	326.1	5.4	0.35	55.8	2.6	4.2	260.7	5	6.9
eaf12 - 49.d	202000	2600	2.1	342.3	5	0.32	60.4	1.4	4.2	277.2	4.6	9.6
eaf12 - 50.d	202500	2600	NaN	286.3	4.5	0.41	45.3	2	3.9	269.4	6.2	5
eaf12 - 51.d	214200	2700	NaN	488.8	6.7	0.36	77.4	2.4	3.3	245	4.1	11
eaf12 - 52.d	218200	3100	4.6	498.9	9.9	0.25	68.3	2.4	3.4	223.4	4.6	8.5
eaf12 - 53.d	217200	2700	4.6	475.1	6.8	0.31	69.2	2.2	5	235.1	4.5	7.9
eaf12 - 54.d	219000	2900	2.5	344.7	4.5	0.25	24.4	1.9	3.8	318	8.2	12
eaf12 - 55.d	213600	3500	2.2	321.3	5.6	0.25	15.9	1.7	4	327.1	8.9	6
eaf12 - 56.d	213800	3000	2.2	359.8	4.3	0.3	17.7	1.4	5.7	409	12	11
eaf12 - 57.d	215500	2700	1.1	430.3	7.3	0.36	43.7	2.1	4.1	182.2	4	7.6
eaf12 - 58.d	213300	2800	NaN	317.5	5.1	0.27	52.9	2.6	3.9	178.9	3.2	8

Analysis number	Ti49 ppm	Ti49 ppm 2SE	Ti49 ppm LOD	V51 ppm	V51 ppm 2SE	V51 ppm LOD	Cr52 ppm	Cr52 ppm 2SE	Cr52 ppm LOD	Mn55 ppm	Mn55 ppm 2SE	Mn55 ppm LOD
eaf12 - 59.d	213800	2800	NaN	359.7	5.8	0.53	77.9	2	6	200.5	3.6	7.5
eaf12 - 60.d	209300	2600	2.1	347.8	5.5	0.27	72.8	2.6	3.8	260.8	4.4	7.3
eaf12 - 61.d	207400	3000	1.1	382.8	7.3	0.17	91.9	2.9	5.1	262.2	5.4	6.2
eaf12 - 62.d	206100	2600	2.1	390	11	0.37	142.3	4	3.8	249.8	4.7	6.1
eaf12 - 63.d	213800	2700	2.3	779	9.2	0.43	191.2	3.3	3.5	282	4	4.7
eaf12 - 64.d	201500	2500	2.3	385.6	6.8	0.27	37.7	1.7	6	449	14	10
eaf12 - 65.d	207700	2600	3.4	280.9	5.1	0.32	28.4	1.6	4.5	76.5	3.7	8.1
eaf12 - 66.d	209500	2300	3	337.1	6.4	0.32	28.4	1.8	4	96.3	4.2	7.3
eaf12 - 67.d	210100	2900	2.1	357.7	6.8	0.35	29.1	1.8	4.6	115.3	3.7	10
eaf12 - 68.d	207800	2400	2.1	283.6	4.4	0.29	29	2	5.7	148.8	4.5	6.9
eaf12 - 69.d	209800	2200	2	321	6.4	0.34	132.5	3.7	3.8	243.5	4.9	6.9
eaf12 - 70.d	207200	2400	2.3	260.3	4.1	0.45	34.6	2.1	5.7	223.6	5.2	11
eaf12 - 71.d	205000	2400	1	394.8	5.5	0.29	29.8	2	5.5	216.4	4.2	9.3
eaf12 - 72.d	204500	2400	2.7	228.4	3.6	0.38	47.4	1.9	4.5	243.4	5.4	7.6
eaf12 - 73.d	207100	3100	2.1	433.4	6.3	0.28	34	2	6.8	189.3	4.4	12
eaf12 - 74.d	208200	2700	2.8	354	6.4	0.3	39	1.9	4.6	248.8	5.1	8.6
eaf12 - 75.d	204600	2500	NaN	391.7	4.6	0.25	35.2	1.8	4.7	182.3	3.8	9.5
eaf12 - 76.d	220800	3100	3.3	286.7	5.8	0.36	32.7	1.9	5.9	289.1	5.9	8.7
eaf12 - 77.d	225200	3100	1.1	388.2	7.7	0.5	38.5	1.8	4	151.1	3.7	8.4
eaf12 - 78.d	224600	3100	NaN	432.4	6.5	0.31	52.3	2.2	5.1	271.2	5.5	12
eaf12 - 79.d	222000	2400	NaN	239.5	3.6	0.34	33.6	1.8	6.4	93.8	4.6	11
eaf12 - 80.d	218800	2300	2.2	393.2	5.7	0.47	41.7	1.8	4.1	152.2	4.1	10
eaf12 - 81.d	216900	2100	2.4	383.5	5.9	0.27	46.2	2.5	5.5	114.3	4.1	7.5
eaf12 - 82.d	217900	2800	1.1	352.1	5.9	0.49	44.4	2.1	4.8	131.9	4.2	8.5
eaf12 - 83.d	217700	2500	1.1	385.4	5.7	0.44	33.5	2.3	3.5	278.9	5.9	6.2
eaf12 - 84.d	219000	2600	NaN	384.4	5.6	0.3	39.6	1.7	2.4	258.3	4.9	5.3
eaf12 - 85.d	210500	2700	2.4	388.8	5.7	0.27	49.9	2.2	5.5	218.5	4.2	7.2
eaf12 - 86.d	215100	2500	NaN	373.7	5.3	0.36	35.2	1.9	5.3	170.8	4.6	9.4
eaf12 - 87.d	217900	2400	3.1	375.2	6.4	0.31	35.1	1.5	5.5	254.9	5.2	9.2

Analysis number	Ti49 ppm	Ti49 ppm 2SE	Ti49 ppm LOD	V51 ppm	V51 ppm 2SE	V51 ppm LOD	Cr52 ppm	Cr52 ppm 2SE	Cr52 ppm LOD	Mn55 ppm	Mn55 ppm 2SE	Mn55 ppm LOD
eaf12 - 88.d	210100	2700	1.1	372.5	6.7	0.35	52.1	1.9	3.7	270.2	6.1	9.5
eaf12 - 89.d	215900	3000	NaN	333.6	5	0.41	45.1	1.5	6.1	176.5	4	8.8
eaf12 - 90.d	212500	2700	NaN	336.7	4.6	0.52	38.8	1.8	4.6	114.8	2.9	11
eaf12 - 92.d	210700	2700	2.1	354.2	6.3	0.31	87.7	2.7	3.4	136	4.1	5.2
eaf12 - 93.d	209300	2500	NaN	357.8	5.2	0.38	91.5	2.9	3.6	214.8	4.4	7.2
eaf12 - 94.d	212300	2900	4.3	381.6	6	0.41	41.3	2	3.7	257.5	6	5.7
eaf12 - 95.d	209200	2900	NaN	333.3	4.6	0.44	42.9	2.2	4	269	4.9	8.2
eaf12 - 96.d	211600	2700	1	317.6	5	0.51	30.9	1.9	3.2	269.3	6.1	5.8
eaf12 - 97.d	213800	2800	1	323.7	6.3	0.39	41.2	2	4.1	270.9	5.1	8.1
eaf12 - 98.d	215500	2900	NaN	360.5	5.4	0.37	54.4	2.3	5.4	211.7	4.7	8.3
eaf12 - 99.d	210800	2400	2.3	359.6	6.8	0.32	57.9	2.5	3.4	156	3.3	8.2
eaf12 - 100.d	214300	2800	NaN	362.1	6.2	0.33	41.1	2.5	4.4	268.9	5.8	6.6
eaf12 - 101.d	225900	3200	NaN	237.9	5.3	0.33	29.8	1.6	6.3	276.7	4.7	11
eaf12 - 102.d	227100	2600	NaN	430.1	6.4	0.33	30.4	1.9	3.5	148.9	4.1	8.4
eaf12 - 103.d	231500	3600	3.3	423	6.6	0.47	57.1	2.8	5.2	225.9	6.8	6.5
eaf12 - 104.d	224000	2700	1.2	337.2	5.2	0.34	85.2	2.3	4.6	288.9	5.7	6.5
eaf12 - 105.d	227200	3200	1.1	418.8	6.8	0.61	39.5	2.1	5.7	254.9	6.1	10
eaf12 - 106.d	227700	3700	2.2	371.7	6	0.6	75	3.1	3.7	228.6	5	9.2
eaf12 - 107.d	221700	2300	1.1	355	5.4	0.32	50.2	2.1	6.6	213.7	4.9	9.8
eaf12 - 108.d	225900	3100	2.4	377.5	5.6	0.41	49.8	2.5	5.4	232.6	5.2	11
eaf12 - 109.d	224400	2900	1.5	421.6	6.7	0.19	30.2	2	4.4	208.7	4.4	8.2
eaf12 - 110.d	221000	3000	NaN	413.8	7.5	0.62	47.7	2	4.9	226.2	4.1	11
eaf12 - 111.d	223900	3700	3.5	400.2	6.9	0.29	34.8	2.1	4.6	213.1	6	10
eaf12 - 112.d	225100	3000	NaN	415.7	5.6	0.21	40.7	2.4	4	258.8	5.3	11
eaf12 - 113.d	223200	2900	2.3	391.1	6.1	0.46	36.3	2.2	3.9	251.6	4.6	4.8
eaf12 - 114.d	224100	3100	NaN	410.1	6.6	0.37	43.8	1.9	3.7	250.5	5.5	8.1
eaf12 - 115.d	217600	3000	1	376.3	5.9	0.47	69	2.5	3.9	141.7	4.6	10
eaf12 - 116.d	219800	2500	NaN	456.6	6.5	0.46	80	2.5	5.1	127.3	3.4	10
eaf12 - 117.d	219400	2700	3.1	396.3	6.3	0.3	70.4	2.1	4.5	111.1	3.4	6.8

Analysis number	Ti49 ppm	Ti49 ppm 2SE	Ti49 ppm LOD	V51 ppm	V51 ppm 2SE	V51 ppm LOD	Cr52 ppm	Cr52 ppm 2SE	Cr52 ppm LOD	Mn55 ppm	Mn55 ppm 2SE	Mn55 ppm LOD
eaf12 - 118.d	219300	2700	2	415.9	7.2	0.34	138.3	3.2	4.5	128.2	4.5	7.9
eaf12 - 119.d	221900	3100	NaN	465.6	7.7	0.28	161.4	3.5	3.1	136	5	6
eaf12 - 120.d	219800	2600	2.8	375.7	6.5	0.31	80.8	3.6	3	129.9	4.2	5.7
eaf12 - 121.d	222500	3100	2.2	428	6.6	0.35	180.1	3.6	3.2	99.7	3.8	6.1
eaf12 - 122.d	221100	2400	1	406.4	6.3	0.4	81.5	2	4.5	96.7	3.2	8.6
eaf12 - 123.d	220000	2500	2.2	420	4.9	0.36	44.9	2.1	5.9	117.5	3.3	9.3
eaf12 - 124.d	219500	3200	2.3	462.9	7.5	0.35	50.6	1.6	5	136.5	2.7	6.9
eaf12 - 125.d	219700	3000	2.1	443.3	7.2	0.28	44.5	2.1	3.2	121.3	4	11
eaf12 - 126.d	234900	2700	2.5	425.6	6	0.3	38.9	2.4	4.4	142.1	6.1	7
eaf12 - 127.d	235800	3400	NaN	674.5	8.1	0.26	181.8	5.4	5.7	118.9	3.4	12
eaf12 - 128.d	231900	3000	1.2	639.3	8.4	0.3	104.3	2.5	4.8	116.1	3.3	8.4
eaf12 - 129.d	227700	2900	2.3	601.2	8.9	0.39	94.1	3.8	4.7	119.9	4.3	8.9
eaf12 - 130.d	224300	2600	2.4	365	5.8	0.2	74.2	2.2	5.1	274.6	5.6	13
eaf12 - 131.d	229500	3100	1.5	309.4	5.1	0.33	51.1	2.4	3.3	279.4	6.7	9.1
eaf12 - 132.d	227400	3000	NaN	365.9	4.6	0.39	59.1	2.5	6.5	198.2	4.8	14
eaf12 - 133.d	223400	3000	1.1	320.6	5.3	0.35	44.5	1.8	3.5	178.8	4.8	5.4
eaf12 - 134.d	223100	3100	2.4	311.5	5.8	0.4	43.2	1.7	5.2	155.2	4.6	8.5
eaf12 - 135.d	224500	3200	2.1	411.9	6.9	0.28	126	3.1	3.9	142.8	3.8	7.1
eaf12 - 136.d	225600	2500	NaN	371.9	4.6	0.41	49.7	1.8	4.5	268	5.7	11
eaf12 - 137.d	225100	2600	NaN	380.3	6.3	0.45	54.9	3.1	5.7	279.2	6.9	11
eaf12 - 138.d	223400	1900	2.3	370	5.5	0.33	56.4	2.6	4.1	260.9	4.4	9.3
eaf12 - 139.d	217700	3000	NaN	363.3	4.5	0.37	43.7	1.8	3.5	265.6	5.3	5.9
eaf12 - 140.d	218800	3100	2.2	369.8	6	0.31	47.1	2.4	3.6	212.8	5	9.9
eaf12 - 141.d	225200	3000	2.1	304.7	4.2	0.43	65.7	2.9	2.9	249.9	4.1	7.9
eaf12 - 142.d	219200	3300	1.1	371.8	6.7	0.31	42.1	1.8	7.5	121.4	3.9	8.1
eaf12 - 143.d	219500	3200	1	299.7	4.4	0.4	45.2	2.1	3.9	248.9	5.8	9.3
eaf12 - 144.d	221900	3000	3	360.7	5.3	0.34	41.6	1.7	4.3	244.6	3.9	7.2
eaf12 - 145.d	219600	2300	NaN	334.5	4.7	0.3	37.9	1.9	3.3	240.9	5.5	7.3
eaf12 - 146.d	221300	3200	4.2	397.8	6.5	0.41	33.8	1.8	3.9	217.9	4.5	7.1

Analysis number	Ti49 ppm	Ti49 ppm 2SE	Ti49 ppm LOD	V51 ppm	V51 ppm 2SE	V51 ppm LOD	Cr52 ppm	Cr52 ppm 2SE	Cr52 ppm LOD	Mn55 ppm	Mn55 ppm 2SE	Mn55 ppm LOD
eaf12 - 147.d	222400	2700	1.1	327.2	5.1	0.34	28.9	2	5.6	221.8	5.2	8.1
eaf12 - 148.d	218900	2800	2.9	349.6	5	0.45	27.1	1.8	2.9	226.9	4.4	7.1
eaf12 - 149.d	222000	3200	2.3	325.2	6.1	0.33	29.2	2	5.1	221.8	3.3	8.2
eaf12 - 150.d	222900	3000	NaN	297	5.9	0.4	33	1.7	4	217.8	4.6	8.4
eaf12 - 151.d	226300	3100	2.7	336.7	5.1	0.41	34.4	1.9	7.1	220.2	5.1	12
eaf12 - 152.d	224100	2900	1.2	379.1	6.8	0.33	32.9	1.7	5	268.1	5.5	7.2
eaf12 - 153.d	224900	2800	2.4	451.4	6.6	0.4	33.6	1.9	6.2	166.9	5.1	12
eaf12 - 154.d	219400	3400	NaN	406.5	6.5	0.41	38.6	2.1	4.3	193.9	4.1	6
eaf12 - 155.d	223600	2800	1.2	514.1	8.1	0.2	46.1	2.8	6.4	228.3	5.7	12
eaf12 - 156.d	221200	2900	2.4	404.5	6.9	0.33	27.9	2.2	4.9	227.7	4.5	9.7
eaf12 - 157.d	217300	2400	1.1	376.3	5.6	0.35	48.6	1.9	3.9	192.2	4.2	9.4
eaf12 - 158.d	220900	3000	NaN	375.6	6.1	0.32	46.3	2.1	5	246.6	6.3	8.8
eaf12 - 159.d	220000	3300	1.1	388.7	6.4	0.45	42.1	1.7	4.6	224.1	5.2	6.9
eaf12 - 160.d	219200	2900	2.2	341.2	6.6	0.25	45.7	1.9	4.1	251.2	5.1	5.7
eaf12 - 161.d	221500	3000	2.1	492	10	0.28	65.1	2.3	4.9	240.7	4.6	7.4
eaf12 - 162.d	219500	3100	2.9	369.2	6.1	0.32	32.7	1.6	5.1	234.3	5.1	9.1
eaf12 - 163.d	221700	2300	1.7	330.7	5.3	0.55	33	2	5.3	158.9	4.6	9.8
eaf12 - 164.d	222800	3400	2.2	403.1	5.5	0.48	67.4	2.3	4.4	270.2	4.8	6.5

Analysis number	Fe57 ppm	Fe57 ppm 2SE	Fe57 ppm LOD	Y89 ppm	Y89 ppm 2SE	Y89 ppm LOD	Zr90 ppm	Zr90 ppm 2SE	Zr90 ppm LOD	Nb93 ppm	Nb93 ppm 2SE	Nb93 ppm LOD
eaf12 - 1.d	3204	95	53	696	9.6	0.054	157.1	3	0.097	955	18	0.024
eaf12 - 2.d	3427	87	61	790	12	0.038	168.4	3.8	0.049	902	16	0.037
eaf12 - 3.d	3526	69	59	913	17	NaN	194	3.4	0.035	868	12	NaN
eaf12 - 4.d	3090	84	36	550	10	0.052	152	3.5	0.07	933	12	NaN
eaf12 - 5.d	3059	68	38	548.4	8.4	0.093	129.9	2.6	NaN	867	11	NaN
eaf12 - 6.d	3363	78	48	658.8	8.1	0.019	139.2	2.7	NaN	788	12	NaN
eaf12 - 7.d	3717	77	46	739.5	8.4	0.038	175	3.4	0.035	848.5	9.5	NaN
eaf12 - 8.d	2907	69	35	827	12	0.044	136.3	2	0.077	696	11	NaN
eaf12 - 9.d	3077	69	32	614.9	8.4	0.12	141.4	2.5	0.048	813	13	NaN
eaf12 - 10.d	2981	68	49	642	13	0.052	124.3	2.2	0.07	965	17	NaN
eaf12 - 11.d	2690	71	47	458	14	0.052	73.4	1.6	0.035	763.9	9	0.036
eaf12 - 12.d	3661	88	48	467.8	9.2	NaN	137.1	2.5	0.076	772	12	0.036
eaf12 - 13.d	3125	71	36	386.5	4.9	0.053	86.4	1.4	0.048	900	11	NaN
eaf12 - 14.d	3373	65	29	623.3	8.8	0.026	134.1	2.6	0.098	846	12	NaN
eaf12 - 15.d	3258	71	43	342	5.6	0.037	117.9	2.3	0.047	1100	31	NaN
eaf12 - 16.d	3392	76	24	627	18	0.019	158.2	3.1	0.076	989	18	NaN
eaf12 - 17.d	3139	65	26	607.5	9.3	0.053	141.1	2	NaN	941	14	NaN
eaf12 - 18.d	3511	86	42	1082	23	0.04	125.5	2.7	0.14	1296	15	NaN
eaf12 - 19.d	3132	57	47	851	13	0.051	116.3	2	0.069	945	13	NaN
eaf12 - 20.d	2920	59	38	385.5	6	0.037	129.8	2.9	NaN	825	12	NaN
eaf12 - 21.d	3614	83	45	656.5	9.5	0.043	176.9	3.3	0.14	880	15	0.018
eaf12 - 22.d	3663	83	37	678.9	9.4	0.038	177.9	2.8	NaN	595.7	8.3	0.036
eaf12 - 23.d	3388	71	34	513.8	8.1	0.051	139.4	3	0.035	814	13	0.018
eaf12 - 24.d	3825	82	39	669.3	8.2	0.041	174.7	2.5	NaN	692.8	9	0.048
eaf12 - 25.d	3586	79	38	621.7	9.1	0.018	161.3	3.1	NaN	968	16	NaN
eaf12 - 26.d	3944	88	33	763	11	0.039	178.3	3.3	0.036	749	12	NaN
eaf12 - 27.d	3541	82	31	620	13	0.07	129.4	2.3	NaN	1241	25	NaN
eaf12 - 28.d	4270	120	42	1268	23	0.042	143.2	3	0.036	1041	27	0.037
eaf12 - 29.d	3630	91	35	839	17	0.063	158.7	4	NaN	889	15	0.025

Analysis number	Fe57 ppm	Fe57 ppm 2SE	Fe57 ppm LOD	Y89 ppm	Y89 ppm 2SE	Y89 ppm LOD	Zr90 ppm	Zr90 ppm 2SE	Zr90 ppm LOD	Nb93 ppm	Nb93 ppm 2SE	Nb93 ppm LOD
eaf12 - 30.d	4118	97	39	957	21	0.039	185.2	3.7	NaN	866	12	0.019
eaf12 - 31.d	4399	85	34	1589	40	NaN	157.2	3	0.079	1150	29	0.037
eaf12 - 32.d	4890	100	37	447	9.6	0.039	146.7	3.1	0.036	888	14	NaN
eaf12 - 33.d	3917	69	36	1492	21	0.053	186.6	2.8	0.079	880	14	NaN
eaf12 - 34.d	5759	97	33	540.3	7.9	0.043	160.6	2.8	0.081	948	13	NaN
eaf12 - 35.d	3549	78	39	609.2	8	0.042	154.1	3.2	0.036	825	12	0.036
eaf12 - 36.d	3627	79	38	517.6	9	0.019	140.1	2.7	0.072	866	17	NaN
eaf12 - 37.d	3755	74	29	551.8	8.6	0.019	151.5	3.3	0.073	901	13	NaN
eaf12 - 38.d	34200	5000	39	584	12	0.048	132.6	2.8	0.078	817	13	NaN
eaf12 - 39.d	3429	87	35	731	11	0.042	149.4	2.6	NaN	798	12	NaN
eaf12 - 40.d	3208	66	45	909	14	NaN	111	3.6	0.036	482	26	NaN
eaf12 - 41.d	3635	81	38	1034	39	0.052	168	3.3	NaN	919	11	NaN
eaf12 - 42.d	4020	110	31	526.6	7.4	0.019	117.9	2	NaN	766	10	NaN
eaf12 - 43.d	5240	110	34	569	12	0.041	87.8	1.6	0.07	476	6.2	NaN
eaf12 - 44.d	2978	62	26	436.3	7.6	0.046	115.3	2.2	0.036	764	12	NaN
eaf12 - 45.d	2855	65	39	365.4	5.4	0.041	108.5	2	0.035	668.8	7.8	0.048
eaf12 - 46.d	3509	84	42	497.5	8.5	0.066	134.9	2	0.035	822	11	0.018
eaf12 - 47.d	3257	69	42	666	10	0.058	136.2	3	0.091	626.2	9.8	NaN
eaf12 - 48.d	5370	110	31	214.1	3.8	0.073	78.4	1.7	NaN	586.3	8.3	NaN
eaf12 - 49.d	2991	59	34	445.2	4.9	0.019	130.4	2.4	0.076	699.9	9.1	NaN
eaf12 - 50.d	4250	120	33	326.2	4.8	0.039	89.2	2.1	0.078	782	13	0.037
eaf12 - 51.d	3200	82	29	1280	22	0.02	130.3	2.7	NaN	967	11	0.019
eaf12 - 52.d	3420	83	29	1242	22	0.028	149.2	2.7	0.039	1059	34	NaN
eaf12 - 53.d	3216	77	37	1416	26	0.021	122	2.3	NaN	1031	21	NaN
eaf12 - 54.d	3614	71	41	862	12	NaN	166.7	3.1	0.1	938	14	NaN
eaf12 - 55.d	3634	75	30	828	15	0.062	144.3	2.3	NaN	879	12	0.019
eaf12 - 56.d	3948	74	25	848	13	0.041	164.7	2.7	0.076	997	13	0.039
eaf12 - 57.d	3602	70	30	959	14	0.04	186.9	3	0.11	985	12	0.019
eaf12 - 58.d	3211	51	32	684.4	7.2	0.04	134.7	2	NaN	721	16	NaN

Analysis number	Fe57 ppm	Fe57 ppm 2SE	Fe57 ppm LOD	Y89 ppm	Y89 ppm 2SE	Y89 ppm LOD	Zr90 ppm	Zr90 ppm 2SE	Zr90 ppm LOD	Nb93 ppm	Nb93 ppm 2SE	Nb93 ppm LOD
eaf12 - 59.d	3460	83	38	1064	18	0.043	148.7	2	0.1	1460	20	0.019
eaf12 - 60.d	3393	76	35	793	9.2	0.069	129.9	2.4	0.073	907	10	NaN
eaf12 - 61.d	3227	73	28	827	14	0.02	121	1.9	0.05	1329	22	NaN
eaf12 - 62.d	4192	93	38	2202	29	0.046	122.3	2.3	0.097	667.7	7.4	NaN
eaf12 - 63.d	4956	75	35	1009	22	NaN	98.2	1.9	0.036	416	11	0.036
eaf12 - 64.d	4410	100	34	605.3	7.7	0.039	159.2	2.4	0.15	869	11	0.08
eaf12 - 65.d	2975	74	30	295.8	4.2	0.042	120.5	1.8	0.036	840	11	NaN
eaf12 - 66.d	3492	70	29	473.3	6.9	0.042	144.4	2.2	0.036	919	14	0.018
eaf12 - 67.d	3542	78	27	607.8	8.2	0.079	149.2	2.9	NaN	893	12	NaN
eaf12 - 68.d	2935	61	37	319.5	6.4	0.038	125.7	2.6	0.077	853	15	NaN
eaf12 - 69.d	3736	86	30	294.9	3.8	0.052	146.5	2.6	0.035	662	10	0.018
eaf12 - 70.d	2874	65	37	346.4	3.8	0.044	111.6	1.4	NaN	952	12	0.018
eaf12 - 71.d	3894	94	21	654.9	8.7	0.043	171.4	2.9	NaN	878	15	NaN
eaf12 - 72.d	3042	81	29	222.1	3.3	0.052	104.5	1.8	0.069	933	12	NaN
eaf12 - 73.d	4421	87	35	1011	21	0.043	191.1	2.9	NaN	899	15	NaN
eaf12 - 74.d	3090	62	30	617.1	8	0.041	131.1	2.3	0.036	826	11	NaN
eaf12 - 75.d	3681	81	29	564.7	6.8	NaN	161.8	2.8	0.035	827	12	NaN
eaf12 - 76.d	3588	78	31	782	11	0.021	134.6	2.6	0.039	922	12	NaN
eaf12 - 77.d	3710	72	25	564.8	7.1	NaN	153.6	2.7	NaN	917	13	NaN
eaf12 - 78.d	4990	110	28	2323	34	0.092	222.9	4.6	0.11	1078	20	0.04
eaf12 - 79.d	3384	81	32	505.7	7.8	0.042	122.6	2.4	0.11	1131	22	NaN
eaf12 - 80.d	4490	110	37	623	18	0.058	156.4	2.8	NaN	784	13	NaN
eaf12 - 81.d	3882	89	28	472	6.5	0.02	144.6	2.2	0.1	748.2	9.6	NaN
eaf12 - 82.d	3589	87	24	518.4	8.2	0.02	135	2.1	NaN	760	12	0.039
eaf12 - 83.d	5470	110	27	563.1	7.1	0.028	153.5	2.3	0.083	845	11	0.042
eaf12 - 84.d	3909	75	28	622.6	9.5	0.044	151.5	2.5	0.037	851	11	NaN
eaf12 - 85.d	4392	97	28	650	11	0.043	149.8	2.6	0.1	725	11	NaN
eaf12 - 86.d	4680	130	35	456.8	7.1	0.054	142.3	2.5	NaN	866.8	9.7	NaN
eaf12 - 87.d	3631	71	32	779	12	0.02	149	3.1	NaN	983	13	0.019

Analysis number	Fe57 ppm	Fe57 ppm 2SE	Fe57 ppm LOD	Y89 ppm	Y89 ppm 2SE	Y89 ppm LOD	Zr90 ppm	Zr90 ppm 2SE	Zr90 ppm LOD	Nb93 ppm	Nb93 ppm 2SE	Nb93 ppm LOD
eaf12 - 88.d	4140	140	36	1012	12	0.019	149.7	2.4	NaN	827.9	7.8	NaN
eaf12 - 89.d	3453	68	36	329	6.6	0.043	137.5	2.9	0.15	747	13	0.019
eaf12 - 90.d	3567	75	35	368.1	5.7	0.055	135.7	2.6	0.084	735	10	NaN
eaf12 - 92.d	3378	66	20	380	4.9	0.063	128.9	2.5	NaN	778	11	NaN
eaf12 - 93.d	3283	85	25	425.6	4.6	0.038	122.3	2.5	0.17	657.9	8.2	NaN
eaf12 - 94.d	3696	85	39	560.5	7.7	0.038	155	2.3	NaN	788	13	NaN
eaf12 - 95.d	3409	88	30	349.3	4.7	NaN	107.4	1.7	NaN	706	10	NaN
eaf12 - 96.d	3364	76	18	534	10	0.043	128.5	2.3	0.07	900	12	NaN
eaf12 - 97.d	3428	87	32	487.5	6.5	0.04	136.5	2.1	NaN	843	12	NaN
eaf12 - 98.d	3560	69	30	415.8	6.9	0.026	133.4	2.5	0.071	751	11	NaN
eaf12 - 99.d	3498	81	35	414.7	5.3	0.038	130.5	2.6	0.036	715	11	NaN
eaf12 - 100.d	3582	87	21	626.3	9.7	0.044	142.1	2	0.071	818	13	0.049
eaf12 - 101.d	3620	100	34	425.1	6.8	NaN	90.8	2.4	0.039	1054	33	NaN
eaf12 - 102.d	4431	77	39	632	10	0.034	172	3.1	0.039	998	15	NaN
eaf12 - 103.d	4019	84	32	700	11	0.047	159.2	2.8	0.11	839	10	NaN
eaf12 - 104.d	3436	78	25	527.5	7.9	0.067	109	2	NaN	709	10	0.041
eaf12 - 105.d	3944	95	33	605.4	9.9	0.021	162.8	3.7	NaN	929	15	NaN
eaf12 - 106.d	3436	69	37	417.5	7	0.045	137.9	2.6	NaN	876	12	NaN
eaf12 - 107.d	3237	93	34	441.2	6.8	0.08	128.8	2.8	0.084	797	13	NaN
eaf12 - 108.d	4147	90	23	527	12	0.087	148.7	3.1	NaN	865	11	NaN
eaf12 - 109.d	5458	87	31	594.7	7.8	0.057	177.6	3.1	0.038	1021	14	NaN
eaf12 - 110.d	4493	92	36	1501	21	NaN	199.2	3	0.074	875	13	NaN
eaf12 - 111.d	3814	87	38	986	13	0.04	166.8	2.6	0.06	955	13	0.056
eaf12 - 112.d	3537	87	30	1042	17	NaN	139.9	2	0.078	913	10	NaN
eaf12 - 113.d	3687	72	21	1100	16	0.019	160.3	3.2	0.079	905	11	0.037
eaf12 - 114.d	4372	91	35	1467	32	NaN	136	2.3	0.036	813	15	NaN
eaf12 - 115.d	4590	110	41	2548	31	0.041	264.5	3.6	NaN	1530	21	NaN
eaf12 - 116.d	3965	93	36	1314	32	0.027	172.9	2.9	NaN	999	14	0.037
eaf12 - 117.d	3419	99	26	844	18	0.019	144.1	3.3	0.098	1734	25	NaN

Analysis number	Fe57 ppm	Fe57 ppm 2SE	Fe57 ppm LOD	Y89 ppm	Y89 ppm 2SE	Y89 ppm LOD	Zr90 ppm	Zr90 ppm 2SE	Zr90 ppm LOD	Nb93 ppm	Nb93 ppm 2SE	Nb93 ppm LOD
eaf12 - 118.d	4455	90	33	981	22	0.019	189.5	3.4	NaN	692	16	NaN
eaf12 - 119.d	4709	79	33	1797	25	0.054	136.2	2.1	0.071	549.9	7.9	0.018
eaf12 - 120.d	3661	77	17	1538	21	0.069	152.4	3.1	NaN	1562	21	NaN
eaf12 - 121.d	3930	89	30	1448	21	0.062	139.8	2.6	NaN	600	12	NaN
eaf12 - 122.d	3920	75	27	1407	49	0.067	159	4.2	NaN	1355	37	0.018
eaf12 - 123.d	3754	91	31	788	14	0.053	160.7	3	0.12	967	15	NaN
eaf12 - 124.d	4256	79	22	869	13	0.054	191.7	2.6	0.078	915	19	0.018
eaf12 - 125.d	3935	72	34	766	10	0.019	177.4	2.8	NaN	1042	19	NaN
eaf12 - 126.d	3730	88	35	709	11	0.046	161.8	2.7	0.04	1033	14	NaN
eaf12 - 127.d	3951	92	23	1520	20	0.043	183.8	2.7	NaN	1074	17	NaN
eaf12 - 128.d	3741	97	36	1732	20	0.067	125.1	2.6	0.088	1642	22	NaN
eaf12 - 129.d	3508	84	29	1776	24	NaN	125.1	2.7	0.054	1514	20	NaN
eaf12 - 130.d	3772	95	22	487.8	7.3	0.021	146	2.9	NaN	860	12	NaN
eaf12 - 131.d	3780	100	36	704.4	8.4	0.028	123.6	1.9	0.077	988	13	NaN
eaf12 - 132.d	3489	62	42	404.4	6.2	0.042	131	3.1	0.079	857	12	0.02
eaf12 - 133.d	3193	80	44	346.6	6.6	0.047	121.7	2.4	0.076	1068	17	NaN
eaf12 - 134.d	3043	66	33	368.9	4.8	0.02	121.2	2.4	NaN	1253	23	NaN
eaf12 - 135.d	4278	83	28	521.9	8.8	0.08	157.3	3.4	NaN	817	16	0.019
eaf12 - 136.d	3925	72	25	706.5	8.8	0.02	160.4	2.9	NaN	882.9	9.9	NaN
eaf12 - 137.d	3859	99	31	475.8	6.9	0.021	150.7	3	0.039	828	13	NaN
eaf12 - 138.d	3559	78	25	517.7	8.1	0.02	148.8	2.5	0.15	798.9	9.3	NaN
eaf12 - 139.d	3498	70	26	475.4	7.8	0.02	141.1	2.8	0.08	774	13	NaN
eaf12 - 140.d	3592	73	30	462	7.1	0.02	144.8	2.8	NaN	836	15	0.057
eaf12 - 141.d	4254	92	33	348.8	4.3	0.057	50.1	1.5	0.081	604	11	0.043
eaf12 - 142.d	3800	89	29	512.2	8.7	0.02	147.4	2.8	NaN	832	14	NaN
eaf12 - 143.d	3314	81	21	451.2	7	0.074	121.5	2.5	0.083	897	13	0.036
eaf12 - 144.d	3508	66	31	836	13	0.039	154.1	2.5	0.037	885	14	NaN
eaf12 - 145.d	3597	78	31	689.9	7.3	0.048	142.5	2.1	0.1	928	14	NaN
eaf12 - 146.d	3807	83	21	1026	33	0.019	180.4	3.4	NaN	911	11	NaN

Analysis number	Fe57 ppm	Fe57 ppm 2SE	Fe57 ppm LOD	Y89 ppm	Y89 ppm 2SE	Y89 ppm LOD	Zr90 ppm	Zr90 ppm 2SE	Zr90 ppm LOD	Nb93 ppm	Nb93 ppm 2SE	Nb93 ppm LOD
eaf12 - 147.d	3782	80	21	648	11	0.027	138.8	2.2	NaN	792	12	0.019
eaf12 - 148.d	3719	71	22	704	7.7	0.053	149.9	2.2	0.079	874	11	NaN
eaf12 - 149.d	3515	89	33	578	11	0.039	131.9	2.5	0.073	793	11	NaN
eaf12 - 150.d	3420	70	31	605	11	0.027	125.4	2.8	NaN	685.8	9.1	NaN
eaf12 - 151.d	3610	100	33	497.5	9.7	0.047	136.9	2.9	NaN	898	13	0.021
eaf12 - 152.d	3521	84	33	726	14	0.06	136.6	2.5	0.089	1033	20	0.041
eaf12 - 153.d	3230	61	39	1267	23	NaN	119.7	2.8	0.056	1027	18	0.021
eaf12 - 154.d	3400	87	37	675	20	NaN	120	2.9	NaN	1038	25	NaN
eaf12 - 155.d	3730	99	31	1379	49	NaN	137.8	2.6	NaN	1169	27	NaN
eaf12 - 156.d	3879	85	27	901	19	0.091	156.4	2.9	NaN	938	18	NaN
eaf12 - 157.d	3616	74	43	491.2	9.6	0.043	138.4	2.8	0.087	706	10	NaN
eaf12 - 158.d	3724	99	30	518.1	9.9	0.021	146.2	2.7	NaN	814	13	NaN
eaf12 - 159.d	3852	75	22	527.3	9.1	0.071	148.1	2.9	0.1	866	11	NaN
eaf12 - 160.d	3323	68	29	444.3	9.7	0.056	127.8	2.4	0.089	848	16	0.039
eaf12 - 161.d	3192	61	43	647	19	0.04	101.8	1.7	0.082	1281	23	NaN
eaf12 - 162.d	3720	100	32	575	7.8	0.02	150.3	2.6	0.051	911	12	NaN
eaf12 - 163.d	3333	80	36	397.7	6.3	0.04	132.8	2.5	NaN	841	11	NaN
eaf12 - 164.d	4236	82	20	1838	32	0.088	181.1	2.9	0.036	952	18	NaN

Analysis number	La139 ppm	La139 ppm 2SE	La139 ppm LOD	Ce140 ppm	Ce140 ppm 2SE	Ce140 ppm LOD	Pr141 ppm	Pr141 ppm 2SE	Pr141 ppm LOD	Nd146 ppm	Nd146 ppm 2SE	Nd146 ppm LOD
eaf12 - 1.d	42.5	1	NaN	262.1	4.2	0.022	67.1	1.3	NaN	471.9	7.8	NaN
eaf12 - 2.d	47.9	1	NaN	296.1	5.1	NaN	73.8	1.4	NaN	520.6	8.7	NaN
eaf12 - 3.d	65.2	1	0.011	393.4	4.3	0.015	96	1.2	0.02	651	7.8	NaN
eaf12 - 4.d	20.09	0.69	NaN	124.8	3.1	NaN	33	0.82	NaN	233.5	5.2	NaN
eaf12 - 5.d	24.65	0.73	0.024	150.3	3.2	NaN	37.85	0.97	NaN	255.4	6.1	0.054
eaf12 - 6.d	28.93	0.92	NaN	176.7	4.5	0.023	43.8	1.2	NaN	293.2	6.9	NaN
eaf12 - 7.d	64.68	0.91	0.011	396.2	4.3	0.044	97.6	1.3	NaN	677	9.9	NaN
eaf12 - 8.d	12.39	0.35	NaN	81.4	1.6	NaN	20.98	0.44	NaN	149.9	2.7	0.054
eaf12 - 9.d	10.45	0.32	NaN	68.9	1.1	0.011	17.73	0.4	NaN	129.1	2.7	NaN
eaf12 - 10.d	10.3	0.48	NaN	64.7	2.8	NaN	15.45	0.73	NaN	106	4.9	NaN
eaf12 - 11.d	69.9	1.4	NaN	260.3	4.9	NaN	38.14	0.77	NaN	185.3	6.6	NaN
eaf12 - 12.d	10.54	0.32	NaN	65.8	1.5	NaN	17.21	0.55	NaN	128.9	3.2	NaN
eaf12 - 13.d	32	0.92	NaN	144.4	2.9	NaN	25.48	0.56	NaN	139.7	3.4	NaN
eaf12 - 14.d	8.33	0.27	0.022	51.5	1.2	NaN	13.1	0.27	NaN	92.5	1.9	NaN
eaf12 - 15.d	8.01	0.34	0.021	56	1.7	NaN	15.35	0.56	NaN	111.9	3.5	NaN
eaf12 - 16.d	41.69	0.95	0.022	242.6	5.1	0.03	59.1	1.1	NaN	403.8	8.5	NaN
eaf12 - 17.d	10.17	0.34	NaN	69.4	1.5	NaN	18.03	0.48	NaN	125.9	2.9	0.053
eaf12 - 18.d	32.6	2.2	NaN	200	11	NaN	46.5	2.1	NaN	288	11	NaN
eaf12 - 19.d	27.3	3.5	NaN	140	12	NaN	30.2	1.7	NaN	187.9	6.8	NaN
eaf12 - 20.d	2.91	0.16	0.022	20.9	0.42	0.011	5.74	0.17	NaN	41.9	1.2	NaN
eaf12 - 21.d	68.7	1.3	NaN	410.5	6.3	NaN	99.2	1.5	NaN	668	13	0.052
eaf12 - 22.d	67.5	1.1	0.011	401.9	5.7	NaN	96.9	1.5	NaN	636	10	0.072
eaf12 - 23.d	18.18	0.44	0.017	116.3	2.4	NaN	29.7	0.72	NaN	209.6	4.6	0.052
eaf12 - 24.d	61.42	0.94	0.021	364.6	5.7	0.011	89.5	1.3	0.02	595.9	7.2	0.052
eaf12 - 25.d	49.98	0.86	0.01	302.7	5.2	0.011	75	1.3	0.009	513	10	0.051
eaf12 - 26.d	69.6	1.2	NaN	415.1	6.2	NaN	100.2	1.7	0.0096	664	11	NaN
eaf12 - 27.d	15.01	0.4	NaN	95.3	1.8	NaN	23.77	0.49	0.0096	165.7	3.7	NaN
eaf12 - 28.d	30.25	0.9	NaN	193.2	5.3	NaN	47.3	1.3	0.0096	314.9	6.5	NaN
eaf12 - 29.d	36.8	1.2	0.022	224.9	7.3	0.023	56.4	1.8	NaN	382	12	NaN

Analysis number	La139 ppm	La139 ppm 2SE	La139 ppm LOD	Ce140 ppm	Ce140 ppm 2SE	Ce140 ppm LOD	Pr141 ppm	Pr141 ppm 2SE	Pr141 ppm LOD	Nd146 ppm	Nd146 ppm 2SE	Nd146 ppm LOD
eaf12 - 30.d	62.62	0.97	NaN	376.6	6.6	NaN	91.6	1.6	NaN	627.4	9.9	NaN
eaf12 - 31.d	50.7	1.3	0.011	312.3	4.8	0.023	80.8	1.7	NaN	563	10	NaN
eaf12 - 32.d	11.75	0.49	0.022	59.7	2.7	NaN	14.81	0.65	NaN	102.9	4.8	NaN
eaf12 - 33.d	65.3	1	NaN	398.7	6.7	0.023	98.8	1.4	NaN	677.6	9.7	NaN
eaf12 - 34.d	35.64	0.89	NaN	203.4	4.6	NaN	50.6	1.3	NaN	352.9	8.3	NaN
eaf12 - 35.d	35.02	0.77	NaN	211.8	3.3	0.011	52.38	0.9	0.019	361.7	5.5	NaN
eaf12 - 36.d	15.04	0.38	0.011	89.2	2.1	NaN	22.6	0.69	NaN	161	4.3	NaN
eaf12 - 37.d	30.66	0.65	NaN	182.6	2.7	NaN	45.71	0.91	0.026	308.8	5.8	0.11
eaf12 - 38.d	37.37	0.93	0.012	156.9	3.9	NaN	29.22	0.8	0.021	175.7	4.5	NaN
eaf12 - 39.d	33.46	0.78	NaN	185.9	4.3	NaN	43.9	0.94	NaN	294.2	8	NaN
eaf12 - 40.d	27.27	0.69	0.011	151.7	5.3	0.015	34.8	1.7	NaN	219	11	NaN
eaf12 - 41.d	55.9	1.5	0.011	318.9	4.7	NaN	75.5	1.1	NaN	496.7	7	0.054
eaf12 - 42.d	17.75	0.51	0.015	87.3	1.6	NaN	18.44	0.41	NaN	114.4	2.5	NaN
eaf12 - 43.d	41.24	0.61	0.015	149.4	2.1	NaN	25.22	0.51	0.0093	134.6	2.5	0.072
eaf12 - 44.d	12.91	0.33	NaN	68.5	1.1	0.011	15.67	0.35	NaN	100	2.6	NaN
eaf12 - 45.d	12.32	0.36	NaN	68.6	1.6	NaN	15.37	0.4	NaN	96.3	1.9	NaN
eaf12 - 46.d	19.97	0.69	NaN	115.9	2.8	NaN	28.3	0.88	0.0093	191.7	6	NaN
eaf12 - 47.d	18.26	0.36	NaN	108.6	1.9	NaN	26.61	0.54	0.01	180.3	3.6	NaN
eaf12 - 48.d	35.53	0.67	NaN	135.5	1.9	0.022	24.23	0.47	NaN	125.7	2.9	0.053
eaf12 - 49.d	18.68	0.3	NaN	114.2	1.3	0.011	27.85	0.59	NaN	193.1	3.6	0.15
eaf12 - 50.d	25.75	0.55	0.011	125.2	2	0.023	25.29	0.37	0.021	143.4	3.5	0.11
eaf12 - 51.d	21.32	0.62	0.016	157.6	3.2	NaN	42.39	0.92	NaN	294.2	5.8	NaN
eaf12 - 52.d	20.97	0.55	NaN	153.5	3.2	NaN	42.36	0.86	NaN	287.7	6.3	NaN
eaf12 - 53.d	17.77	0.4	NaN	143.6	2.6	NaN	39.97	0.81	NaN	281.3	4.8	NaN
eaf12 - 54.d	46.82	0.84	0.024	289.8	4.5	0.012	72	1.1	NaN	479.8	8.4	NaN
eaf12 - 55.d	26.69	0.65	0.012	175.7	2.6	0.033	43.85	0.89	NaN	299.3	4.9	NaN
eaf12 - 56.d	39.34	0.53	0.012	250.6	2.9	NaN	62.25	0.85	NaN	425.5	7	0.12
eaf12 - 57.d	45.91	0.89	NaN	298.3	3.2	0.023	74.4	1.1	NaN	497.2	7.3	0.076
eaf12 - 58.d	29.39	0.69	0.025	191.2	3.7	NaN	47.06	0.75	NaN	296	5.2	0.056

Analysis number	La139 ppm	La139 ppm 2SE	La139 ppm LOD	Ce140 ppm	Ce140 ppm 2SE	Ce140 ppm LOD	Pr141 ppm	Pr141 ppm 2SE	Pr141 ppm LOD	Nd146 ppm	Nd146 ppm 2SE	Nd146 ppm LOD
eaf12 - 59.d	41	0.8	NaN	276	4.2	0.012	67.5	1.2	0.021	422.1	7.4	NaN
eaf12 - 60.d	13.05	0.44	NaN	93.6	1.9	0.023	26.38	0.55	0.019	190.7	3.6	0.13
eaf12 - 61.d	17.88	0.44	0.011	123	2	0.031	32.87	0.53	NaN	231.5	4.4	NaN
eaf12 - 62.d	67.4	1.8	NaN	423.8	7.8	NaN	103.9	1.6	NaN	659	10	NaN
eaf12 - 63.d	110.3	2.3	NaN	515.9	9.2	NaN	98.6	2.1	NaN	535	11	NaN
eaf12 - 64.d	138	6.9	NaN	523	16	NaN	101	2.8	0.0096	573	11	NaN
eaf12 - 65.d	4.01	0.18	0.045	27.19	0.84	0.023	7.31	0.28	NaN	52.2	1.9	NaN
eaf12 - 66.d	14.53	0.32	NaN	89.7	2	0.011	22.96	0.51	0.019	164.9	4.4	NaN
eaf12 - 67.d	30.79	0.55	NaN	194.8	2.7	NaN	50.04	0.79	0.0095	356.2	4.6	NaN
eaf12 - 68.d	6.01	0.25	0.011	40.8	1.1	NaN	10.78	0.33	NaN	76.8	1.7	0.11
eaf12 - 69.d	110.4	2.9	0.011	334.5	8.4	0.022	41.45	0.94	NaN	152.7	3.3	0.1
eaf12 - 70.d	10.5	0.45	0.011	63.6	1.4	NaN	16.08	0.39	0.0094	113.2	1.9	NaN
eaf12 - 71.d	71	1.5	0.011	410.3	5.9	NaN	99.9	1.6	0.018	657	10	NaN
eaf12 - 72.d	27.53	0.84	NaN	141.5	2.6	NaN	28.42	0.59	0.009	157.4	2.7	0.051
eaf12 - 73.d	59.7	1.1	NaN	356.4	5.1	NaN	89.2	1.5	NaN	598	10	NaN
eaf12 - 74.d	4.9	0.22	0.022	35.5	0.67	NaN	10.85	0.27	NaN	81.9	2	NaN
eaf12 - 75.d	39.99	0.74	0.011	251.8	4	NaN	62.9	1.1	NaN	426.8	7.8	NaN
eaf12 - 76.d	26.45	0.64	0.024	160.1	2.6	NaN	38.59	0.9	NaN	250.2	6.4	NaN
eaf12 - 77.d	19.29	0.51	NaN	128.1	2.7	0.025	34.63	0.94	NaN	242.8	4.2	NaN
eaf12 - 78.d	99.5	1.9	0.012	598.2	9.6	NaN	145.4	2.4	NaN	941	15	NaN
eaf12 - 79.d	7.29	0.3	NaN	49.31	0.82	NaN	13.74	0.27	0.021	95.1	2.2	0.13
eaf12 - 80.d	32.28	0.8	0.024	195	5.6	0.024	50.6	1.2	NaN	345.4	9.2	NaN
eaf12 - 81.d	12.31	0.27	NaN	81.3	1.3	0.033	21.77	0.54	NaN	156.1	3	0.11
eaf12 - 82.d	15.69	0.4	0.024	102.7	1.7	0.012	26.88	0.53	NaN	187.2	3.9	0.078
eaf12 - 83.d	19.92	0.38	NaN	112	1.8	0.024	28.27	0.56	NaN	192.1	3.5	NaN
eaf12 - 84.d	26.15	0.53	0.011	167.6	2.7	NaN	43.58	0.79	NaN	307.4	4.6	NaN
eaf12 - 85.d	29.27	0.65	NaN	182.7	3.8	NaN	47.25	0.95	NaN	324	7.1	NaN
eaf12 - 86.d	20.57	0.63	0.011	115.1	2.6	NaN	29.85	0.71	NaN	203.9	4.5	NaN
eaf12 - 87.d	23.42	0.7	0.011	142.8	2.1	NaN	36.57	0.7	0.02	250.4	4.1	0.055

Analysis number	La139 ppm	La139 ppm 2SE	La139 ppm LOD	Ce140 ppm	Ce140 ppm 2SE	Ce140 ppm LOD	Pr141 ppm	Pr141 ppm 2SE	Pr141 ppm LOD	Nd146 ppm	Nd146 ppm 2SE	Nd146 ppm LOD
eaf12 - 88.d	49.1	7.8	0.024	132.3	4.7	0.023	37	1.7	NaN	227.7	6.5	NaN
eaf12 - 89.d	4.71	0.17	0.011	29.21	0.66	NaN	7.45	0.26	NaN	51.1	1.5	0.11
eaf12 - 90.d	12.21	0.41	0.011	75	2.1	NaN	18.76	0.59	NaN	126.8	4.2	NaN
eaf12 - 92.d	4.43	0.19	0.03	31.79	0.77	NaN	8.29	0.29	0.019	59.1	1.8	NaN
eaf12 - 93.d	5.38	0.21	NaN	36.72	0.73	NaN	9.94	0.29	0.0094	70.9	1.7	0.16
eaf12 - 94.d	33.22	0.62	NaN	202.1	3.1	NaN	49.55	0.94	NaN	326.8	5.3	NaN
eaf12 - 95.d	19.08	0.57	NaN	62.4	1.5	0.03	10.67	0.29	0.0093	60.7	1.4	0.11
eaf12 - 96.d	10.51	0.27	0.011	69.3	1.1	NaN	18.13	0.39	NaN	125.4	2.6	NaN
eaf12 - 97.d	7.07	0.18	0.011	43.38	0.84	NaN	11.02	0.33	0.018	75	1.6	NaN
eaf12 - 98.d	10.12	0.28	NaN	63.4	1.5	0.022	16.13	0.33	0.02	112.9	2.6	NaN
eaf12 - 99.d	9.12	0.27	NaN	59.2	1.2	0.011	15.38	0.37	NaN	105.9	2.2	0.053
eaf12 - 100.d	12.64	0.37	NaN	84.5	1.6	NaN	21.15	0.5	NaN	142.9	3.1	NaN
eaf12 - 101.d	46.8	1.1	NaN	134.6	2.5	0.012	21.37	0.53	NaN	106.7	2.4	NaN
eaf12 - 102.d	59.94	0.93	0.016	359.8	4.6	0.033	88.3	1.4	NaN	582.3	8.9	NaN
eaf12 - 103.d	41.52	0.99	NaN	248.3	4.6	NaN	60.26	0.9	0.011	397.9	7.6	NaN
eaf12 - 104.d	26.45	0.71	NaN	115.3	2.4	0.025	21.92	0.55	NaN	116.5	3.3	0.12
eaf12 - 105.d	45.11	0.87	NaN	271.2	4.1	NaN	67.2	1.2	NaN	444.5	8.8	0.057
eaf12 - 106.d	5.71	0.25	NaN	36.2	0.85	NaN	9.14	0.26	NaN	64.7	2.4	NaN
eaf12 - 107.d	10.31	0.4	NaN	66.8	2.7	0.012	17.07	0.71	NaN	117.8	4.5	0.057
eaf12 - 108.d	19.18	0.74	NaN	113.8	3.6	0.032	29.37	0.83	NaN	189.3	5.5	0.11
eaf12 - 109.d	71	1.2	NaN	403.1	6.1	NaN	96.3	1.4	NaN	616	9.5	NaN
eaf12 - 110.d	84.9	1.4	NaN	504.7	7.2	NaN	119.2	1.9	0.019	755	13	0.054
eaf12 - 111.d	50.7	1	0.011	307.1	5	0.023	75.1	1.4	0.0098	498.3	6.8	0.11
eaf12 - 112.d	32.35	0.79	0.031	216.6	3.1	NaN	57.09	0.95	NaN	398	5.8	NaN
eaf12 - 113.d	50.19	0.64	NaN	310.8	4.6	0.034	76.3	1.3	0.028	504.6	7.2	NaN
eaf12 - 114.d	32.6	1.1	0.011	228	4.6	NaN	61.71	0.94	NaN	433.5	5.4	NaN
eaf12 - 115.d	1072	16	NaN	3885	55	NaN	491.8	7	NaN	2053	24	NaN
eaf12 - 116.d	210.3	4.9	0.022	1010	22	NaN	156	3.2	0.0095	796	17	NaN
eaf12 - 117.d	96.5	6.3	0.011	444	25	NaN	87.3	4.5	NaN	508	20	NaN

Analysis number	La139 ppm	La139 ppm 2SE	La139 ppm LOD	Ce140 ppm	Ce140 ppm 2SE	Ce140 ppm LOD	Pr141 ppm	Pr141 ppm 2SE	Pr141 ppm LOD	Nd146 ppm	Nd146 ppm 2SE	Nd146 ppm LOD
eaf12 - 118.d	322.8	6.5	NaN	1343	31	NaN	181.7	4	NaN	828	19	0.051
eaf12 - 119.d	550.2	6.4	NaN	2304	27	NaN	306.8	4.7	NaN	1354	17	NaN
eaf12 - 120.d	424.5	5.9	NaN	1737	25	NaN	230.9	2.9	NaN	1049	17	0.053
eaf12 - 121.d	418.3	6.2	0.022	1854	24	NaN	260.4	3.6	NaN	1183	16	NaN
eaf12 - 122.d	403	21	0.011	1853	89	NaN	261	11	NaN	1173	44	NaN
eaf12 - 123.d	44.59	0.95	NaN	277.3	5.2	0.022	69.1	1.3	NaN	460.9	9.9	0.052
eaf12 - 124.d	66.8	1.2	NaN	413.2	7	NaN	101.2	2.1	0.019	676	14	0.053
eaf12 - 125.d	59.15	0.99	0.022	359.6	5.4	NaN	88.5	1.4	NaN	584	10	0.053
eaf12 - 126.d	34.94	0.72	NaN	224	2.8	0.012	55.45	0.88	0.01	381.4	6.3	0.058
eaf12 - 127.d	111.9	1.9	NaN	512.4	5.7	NaN	97.3	1.4	0.021	556.7	7.2	0.13
eaf12 - 128.d	54.23	0.75	0.017	302.6	4	0.013	72.8	1.2	NaN	477.6	6.4	NaN
eaf12 - 129.d	19.45	0.64	0.024	160.7	3	0.012	48.85	0.96	NaN	375.2	5.4	NaN
eaf12 - 130.d	6.45	0.25	0.032	41.9	1.3	0.016	10.73	0.3	0.02	76.4	2.3	NaN
eaf12 - 131.d	31.01	0.9	NaN	160.6	3.4	0.026	32.52	0.77	NaN	188.9	3.3	NaN
eaf12 - 132.d	3.91	0.19	0.026	27.46	0.58	NaN	7.46	0.24	0.01	51	1.4	NaN
eaf12 - 133.d	8.48	0.33	NaN	56.73	0.97	0.012	14.85	0.4	NaN	104.2	1.9	NaN
eaf12 - 134.d	9.32	0.34	0.025	62.4	1	0.023	16.33	0.3	NaN	117.3	2.2	NaN
eaf12 - 135.d	48.88	0.96	0.023	287.3	4.9	0.023	67.3	1.3	NaN	428	6.7	0.054
eaf12 - 136.d	43.7	1.1	0.023	258.6	3.5	NaN	61.6	1	0.019	400.1	5.9	0.054
eaf12 - 137.d	18.15	0.49	NaN	110.2	1.7	NaN	26.55	0.52	NaN	179.6	2.9	NaN
eaf12 - 138.d	12.51	0.32	0.025	76.1	1.4	0.012	18.45	0.38	0.019	119.1	2.7	0.054
eaf12 - 139.d	11.24	0.43	0.022	71.8	1.6	NaN	18.05	0.45	NaN	125	2.5	NaN
eaf12 - 140.d	8.95	0.3	NaN	55.9	1	NaN	14.13	0.47	NaN	96.5	2.7	NaN
eaf12 - 141.d	33.95	0.51	0.023	115.3	1.8	NaN	18.99	0.43	NaN	99.5	1.9	NaN
eaf12 - 142.d	20.09	0.46	0.024	126.5	2	NaN	31.96	0.48	0.019	221.8	4.3	NaN
eaf12 - 143.d	8.83	0.61	NaN	57.7	3.7	NaN	13.67	0.74	0.019	84.1	4.2	NaN
eaf12 - 144.d	19.54	0.51	0.045	124.1	2.3	NaN	31.6	0.69	NaN	207	4.4	NaN
eaf12 - 145.d	25.79	0.98	NaN	156.7	5.6	0.023	38.4	1.4	NaN	251.4	9.4	0.11
eaf12 - 146.d	55.6	1.7	NaN	343.9	8.7	NaN	82.6	2	NaN	541	15	0.053

Analysis number	La139 ppm	La139 ppm 2SE	La139 ppm LOD	Ce140 ppm	Ce140 ppm 2SE	Ce140 ppm LOD	Pr141 ppm	Pr141 ppm 2SE	Pr141 ppm LOD	Nd146 ppm	Nd146 ppm 2SE	Nd146 ppm LOD
eaf12 - 147.d	31.31	0.7	0.034	194.9	3.9	0.023	46.77	0.88	NaN	313.1	7.5	0.074
eaf12 - 148.d	34.93	0.9	0.024	217.4	4.1	NaN	53.6	1.1	NaN	357.7	7.4	NaN
eaf12 - 149.d	27.97	0.71	NaN	172.5	3.5	NaN	41.93	0.89	NaN	274.6	6.1	NaN
eaf12 - 150.d	30.82	0.59	0.022	188.6	2.3	NaN	44.28	0.97	0.0095	275.7	4.7	NaN
eaf12 - 151.d	21.78	0.62	NaN	132.4	3.3	0.025	32.28	0.93	NaN	215.7	6	NaN
eaf12 - 152.d	17.85	0.48	NaN	125.3	2.2	0.025	34.6	0.79	NaN	252.8	5.2	0.06
eaf12 - 153.d	12.84	0.44	NaN	104.2	2.1	0.025	32.79	0.57	NaN	260.2	4.8	0.082
eaf12 - 154.d	12.74	0.41	NaN	104	2.6	NaN	32.6	0.74	0.021	248.9	5.5	NaN
eaf12 - 155.d	50.2	1.7	0.025	335.7	9.6	0.025	77.9	1.9	0.011	485	11	0.24
eaf12 - 156.d	38.53	0.86	NaN	248.7	4.9	0.012	63.1	1.3	NaN	439.9	8.7	NaN
eaf12 - 157.d	12.26	0.59	NaN	81.1	3.6	NaN	21.24	0.9	NaN	151.7	6.1	0.058
eaf12 - 158.d	18.17	0.87	0.012	116.8	4.6	NaN	29.9	1.3	0.01	211.7	8	NaN
eaf12 - 159.d	25.68	0.61	0.023	163.3	2.9	NaN	41.27	0.87	NaN	288.6	4.4	NaN
eaf12 - 160.d	3.87	0.2	0.012	27	1.1	0.012	7.47	0.3	0.014	52.8	1.8	0.11
eaf12 - 161.d	9.53	0.36	NaN	83.4	1.4	0.012	26.26	0.55	NaN	208.6	4.2	0.055
eaf12 - 162.d	23.02	0.48	NaN	151.4	2.5	0.025	39.39	0.82	0.021	276.3	4.6	NaN
eaf12 - 163.d	3.07	0.15	0.015	24.84	0.57	0.012	7.35	0.23	NaN	60.4	1.8	NaN
eaf12 - 164.d	89.7	1.7	0.022	538.9	8.8	NaN	127.9	2.2	0.02	799	16	NaN

Analysis number	Sm147 ppm	Sm147 ppm 2SE	Sm147 ppm LOD	Eu153 ppm	Eu153 ppm 2SE	Eu153 ppm LOD	Gd157 ppm	Gd157 ppm 2SE	Gd157 ppm LOD	Tb159 ppm	Tb159 ppm 2SE	Tb159 ppm LOD
eaf12 - 1.d	253	5.4	NaN	82.8	1.8	0.017	341	5.9	NaN	53.04	0.92	0.0083
eaf12 - 2.d	270.2	6.1	NaN	87.9	1.8	NaN	365.8	4.9	0.13	55.5	1	NaN
eaf12 - 3.d	320.7	5.2	0.17	96.6	1.4	0.034	409.2	5.6	0.11	58.16	0.77	NaN
eaf12 - 4.d	131.8	3.1	0.12	50.1	1.3	0.017	203	4.5	NaN	34.54	0.78	NaN
eaf12 - 5.d	123.3	3.1	0.063	47.8	1.2	NaN	168.1	4.2	NaN	27.87	0.59	0.0086
eaf12 - 6.d	151.1	4.3	0.13	55.9	1.3	NaN	212.1	4.8	0.08	33.94	0.71	NaN
eaf12 - 7.d	338	4.3	0.12	100.3	1.4	0.034	422.4	6.2	0.078	58.02	0.89	NaN
eaf12 - 8.d	90.4	2.3	NaN	31.67	0.71	NaN	142.8	2.8	NaN	28.26	0.59	NaN
eaf12 - 9.d	80.4	2.1	NaN	31.13	0.68	0.017	127.5	2.1	NaN	25.67	0.47	NaN
eaf12 - 10.d	62.5	2.9	NaN	20.84	0.69	0.017	100.8	3.5	NaN	20.11	0.71	NaN
eaf12 - 11.d	63.4	3.3	NaN	22.22	0.86	NaN	84.9	4.9	NaN	15.33	0.76	0.017
eaf12 - 12.d	75.2	1.9	NaN	28.07	0.67	NaN	118.6	2.8	NaN	21.87	0.49	0.018
eaf12 - 13.d	55.9	1.5	0.062	13.58	0.46	NaN	79.8	1.6	0.057	14.18	0.29	NaN
eaf12 - 14.d	54.9	1.9	NaN	23.04	0.53	NaN	93.6	1.9	0.058	18.88	0.42	NaN
eaf12 - 15.d	72	2.8	NaN	12.71	0.46	0.017	107.7	3.2	NaN	17.97	0.46	NaN
eaf12 - 16.d	215	5.2	NaN	74.8	1.6	NaN	294.9	5.3	0.11	44.7	1	NaN
eaf12 - 17.d	76.2	2	NaN	29.47	0.66	0.017	121.4	2	0.078	23.61	0.41	NaN
eaf12 - 18.d	127	3.5	0.061	30.6	1.1	NaN	172.8	4.1	NaN	32.78	0.65	NaN
eaf12 - 19.d	87.9	1.9	NaN	19.19	0.59	NaN	126.2	2.2	NaN	24.31	0.44	0.0083
eaf12 - 20.d	25.51	0.97	NaN	11.33	0.36	0.034	44.6	1.4	0.057	9.99	0.27	NaN
eaf12 - 21.d	309	4.9	0.12	98.4	1.6	NaN	375.8	6	NaN	51.53	0.87	NaN
eaf12 - 22.d	294.3	4.6	NaN	94.1	1.7	NaN	360.2	6.1	NaN	49.86	0.94	0.0084
eaf12 - 23.d	117.8	2.7	NaN	47.1	1.1	0.033	181.2	3.9	NaN	31.53	0.53	NaN
eaf12 - 24.d	291.1	4.6	NaN	93.2	1.2	0.017	359.3	4.8	NaN	50.97	0.73	NaN
eaf12 - 25.d	254.9	5.3	NaN	84.1	1.4	NaN	330.7	5.2	NaN	48.39	0.81	0.018
eaf12 - 26.d	322.7	6.4	0.064	98.3	2.2	0.035	393.2	5.5	NaN	54.45	0.81	NaN
eaf12 - 27.d	94.3	1.8	NaN	22.06	0.46	0.035	142.5	2.7	NaN	25.33	0.37	NaN
eaf12 - 28.d	166.6	3.3	0.13	53.9	1.2	NaN	234.9	5	NaN	42.03	0.78	0.019
eaf12 - 29.d	201.1	6.5	NaN	71.5	1.8	0.035	274.9	8.7	NaN	43.5	1.1	0.017

Analysis number	Sm147 ppm	Sm147 ppm 2SE	Sm147 ppm LOD	Eu153 ppm	Eu153 ppm 2SE	Eu153 ppm LOD	Gd157 ppm	Gd157 ppm 2SE	Gd157 ppm LOD	Tb159 ppm	Tb159 ppm 2SE	Tb159 ppm LOD
eaf12 - 30.d	307.4	5.8	NaN	95.9	1.5	NaN	393.4	6	NaN	57.35	0.93	NaN
eaf12 - 31.d	299.2	6.5	NaN	95.8	1.7	0.018	425.7	9.3	0.12	68.9	1.5	NaN
eaf12 - 32.d	61.7	2.5	0.064	27.9	1.1	NaN	109.1	3.9	NaN	21.22	0.7	NaN
eaf12 - 33.d	336.1	6.3	0.13	99.4	1.8	NaN	455.9	7.7	0.059	70.3	1.3	0.0087
eaf12 - 34.d	181.8	4.3	0.13	69.2	1.6	NaN	252.8	5.4	NaN	39.55	0.63	0.0089
eaf12 - 35.d	186.5	4.1	NaN	66.6	1.3	NaN	255.7	4	NaN	39.56	0.66	0.0086
eaf12 - 36.d	94.6	2.6	NaN	40.89	0.91	NaN	153	3.5	NaN	28.14	0.65	NaN
eaf12 - 37.d	167.9	3.5	NaN	65.7	1.4	0.038	240.4	3.8	NaN	38.74	0.46	NaN
eaf12 - 38.d	85.8	2.5	NaN	40.73	0.98	NaN	126.5	3.5	NaN	22.85	0.5	NaN
eaf12 - 39.d	155.3	3.4	NaN	60.1	1.3	NaN	221.2	4.8	NaN	36.91	0.83	0.0086
eaf12 - 40.d	109.6	5.4	0.13	37.3	1.1	NaN	149.2	6.3	NaN	28.18	0.8	NaN
eaf12 - 41.d	240.6	4	NaN	70.6	1.4	NaN	311.3	5.4	0.16	48.6	1.1	NaN
eaf12 - 42.d	53.4	1.7	NaN	23.85	0.7	0.024	77	2	NaN	15.34	0.35	NaN
eaf12 - 43.d	57.4	2	NaN	29.48	0.68	NaN	79.6	2.5	0.057	15.51	0.4	0.0084
eaf12 - 44.d	51.4	1.7	NaN	19.83	0.52	NaN	71.4	2	NaN	14.27	0.32	NaN
eaf12 - 45.d	46.5	1	0.061	17.2	0.42	0.05	67.6	1.5	NaN	12.64	0.25	0.0083
eaf12 - 46.d	102.2	2.8	NaN	36.7	1	NaN	142.1	3.5	NaN	23.48	0.56	0.018
eaf12 - 47.d	95.9	2.6	0.18	37.24	0.85	NaN	141.4	2.8	0.12	25.5	0.43	0.009
eaf12 - 48.d	36.2	1.1	NaN	18.41	0.43	NaN	37.25	0.94	NaN	5.9	0.16	0.0085
eaf12 - 49.d	104.9	2.1	NaN	40.74	0.68	NaN	150.6	3.2	NaN	24.61	0.38	NaN
eaf12 - 50.d	50.2	1.3	0.063	19.38	0.47	NaN	57.4	1.8	NaN	9.81	0.24	0.017
eaf12 - 51.d	152.9	3	NaN	27.08	0.72	NaN	221.7	2.7	0.12	41.45	0.59	NaN
eaf12 - 52.d	156.4	3.1	NaN	27.51	0.71	0.019	226.9	4	NaN	42.28	0.65	NaN
eaf12 - 53.d	156.7	3.5	0.13	20.64	0.57	NaN	228.6	4.5	NaN	44.42	0.97	NaN
eaf12 - 54.d	237.3	4.5	NaN	74	1	0.018	314.8	5.1	0.14	47.71	0.96	NaN
eaf12 - 55.d	157.8	3.6	NaN	52.69	0.91	0.036	218	3.6	NaN	37.3	0.69	NaN
eaf12 - 56.d	222.6	3.1	NaN	73.9	1.3	NaN	305.5	5	NaN	48.34	0.71	0.009
eaf12 - 57.d	244	3.7	NaN	71.91	0.97	NaN	333.6	5.7	0.17	52.21	0.84	NaN
eaf12 - 58.d	139.5	2.3	NaN	37.46	0.7	NaN	188.6	2.9	NaN	30.36	0.51	0.018

Analysis number	Sm147 ppm	Sm147 ppm 2SE	Sm147 ppm LOD	Eu153 ppm	Eu153 ppm 2SE	Eu153 ppm LOD	Gd157 ppm	Gd157 ppm 2SE	Gd157 ppm LOD	Tb159 ppm	Tb159 ppm 2SE	Tb159 ppm LOD
eaf12 - 59.d	194.5	4.3	NaN	48.79	0.99	0.018	257.9	5.1	NaN	44.49	0.76	NaN
eaf12 - 60.d	108.3	2	NaN	27.56	0.87	0.018	162.5	3.3	NaN	30.29	0.53	NaN
eaf12 - 61.d	136.8	2.8	NaN	21.77	0.47	0.035	200.9	3.7	NaN	35.96	0.56	NaN
eaf12 - 62.d	287.5	5	NaN	122.9	1.7	NaN	353.3	5.3	NaN	61.42	0.8	NaN
eaf12 - 63.d	165.5	4	NaN	23.65	0.72	NaN	194.2	4.3	NaN	31.8	0.65	0.0085
eaf12 - 64.d	258.3	5.1	0.064	81.6	1.1	NaN	322	4.9	0.059	47.35	0.71	0.017
eaf12 - 65.d	33.8	1.3	0.063	13.18	0.42	NaN	60.6	2.1	NaN	12.34	0.38	NaN
eaf12 - 66.d	98.4	2.3	NaN	38.59	0.75	NaN	156.4	2.9	NaN	27.27	0.5	0.0087
eaf12 - 67.d	196.4	2.8	NaN	70.6	1.2	NaN	283.1	4.5	NaN	44.48	0.64	0.026
eaf12 - 68.d	48.9	1.7	NaN	16.18	0.4	NaN	82	2.5	NaN	15.27	0.38	0.018
eaf12 - 69.d	36.5	1.6	NaN	45.1	1	NaN	41.3	1	NaN	7.46	0.24	NaN
eaf12 - 70.d	67.8	1.4	NaN	14.03	0.34	NaN	103.9	1.8	NaN	18.01	0.37	NaN
eaf12 - 71.d	299.2	4.6	0.12	95.9	1.7	NaN	362.2	6.1	0.11	50.68	0.53	NaN
eaf12 - 72.d	53	1.5	NaN	17.59	0.64	0.033	58.6	1.5	0.055	8.85	0.24	0.0081
eaf12 - 73.d	298.2	4.7	0.14	87.6	1.3	NaN	387.5	5.8	NaN	58.6	1.1	NaN
eaf12 - 74.d	57	1.9	NaN	14.76	0.47	0.017	106.8	2	NaN	21.76	0.45	NaN
eaf12 - 75.d	214.2	4.2	NaN	69.1	1	0.017	277.8	3.4	0.11	40.71	0.66	NaN
eaf12 - 76.d	127.7	4.7	0.14	41.3	1.1	0.025	175.1	3.6	NaN	29.91	0.66	NaN
eaf12 - 77.d	138.7	3.4	NaN	48.21	0.89	NaN	209	4	NaN	35.25	0.63	NaN
eaf12 - 78.d	437.3	6.4	0.14	114.1	2.1	NaN	564.3	9.2	0.063	90.6	1.4	NaN
eaf12 - 79.d	55.7	1.5	NaN	12.13	0.43	NaN	90	2	NaN	17.74	0.35	NaN
eaf12 - 80.d	182.4	4.8	0.15	61.9	1.5	NaN	257.3	5.3	NaN	40.45	0.88	0.018
eaf12 - 81.d	89.8	2.3	NaN	35.35	0.65	0.018	143.8	2.6	NaN	25.27	0.54	NaN
eaf12 - 82.d	102.8	2.4	NaN	35.92	0.77	NaN	151.2	3.5	0.13	25.7	0.63	NaN
eaf12 - 83.d	106.1	2.2	0.066	35.63	0.89	NaN	152.6	2.4	0.061	25.93	0.44	NaN
eaf12 - 84.d	165.1	3.3	0.18	56.4	1.1	NaN	231	3.5	NaN	36.68	0.69	NaN
eaf12 - 85.d	170.1	4.7	NaN	58	1.5	NaN	232.1	4.8	NaN	36.81	0.82	NaN
eaf12 - 86.d	112.7	3	NaN	44.97	0.76	NaN	170.5	3.4	NaN	28.19	0.55	NaN
eaf12 - 87.d	145.5	3.2	NaN	55.5	1.2	NaN	215.1	3.8	0.24	36.85	0.76	NaN

Analysis number	Sm147 ppm	Sm147 ppm 2SE	Sm147 ppm LOD	Eu153 ppm	Eu153 ppm 2SE	Eu153 ppm LOD	Gd157 ppm	Gd157 ppm 2SE	Gd157 ppm LOD	Tb159 ppm	Tb159 ppm 2SE	Tb159 ppm LOD
eaf12 - 88.d	123.4	2.2	NaN	47.44	0.86	NaN	181.8	3.1	NaN	35.56	0.54	NaN
eaf12 - 89.d	29.25	0.84	NaN	16.08	0.36	0.038	51.6	1.5	NaN	10.67	0.31	NaN
eaf12 - 90.d	68.5	1.6	NaN	26.87	0.82	NaN	99.3	2.9	0.059	16.73	0.42	NaN
eaf12 - 92.d	34.1	1.3	0.13	12.65	0.47	NaN	58.4	1.9	NaN	11.97	0.33	NaN
eaf12 - 93.d	43.4	1.4	NaN	15.71	0.39	NaN	71.3	1.4	0.11	14.51	0.25	0.017
eaf12 - 94.d	161.6	2.5	NaN	57.87	0.77	NaN	215.5	3.1	NaN	34.32	0.48	0.0085
eaf12 - 95.d	28.5	1	0.061	25.47	0.67	0.017	49.1	1.6	NaN	9.83	0.21	NaN
eaf12 - 96.d	76.3	2.3	NaN	23.76	0.69	0.033	117.7	2.2	NaN	21.34	0.41	NaN
eaf12 - 97.d	45.3	1.2	0.06	18.92	0.54	0.016	80.1	1.8	NaN	16.55	0.4	NaN
eaf12 - 98.d	63.9	2	0.12	28.6	0.66	NaN	103.2	2.1	NaN	19.64	0.47	NaN
eaf12 - 99.d	62.5	1.7	NaN	27.35	0.64	NaN	100.6	2.3	NaN	18.7	0.41	0.018
eaf12 - 100.d	84.7	2.4	0.061	34.15	0.76	0.034	129.4	2	NaN	25.22	0.47	NaN
eaf12 - 101.d	35.6	1.3	NaN	33.8	1.2	NaN	48.4	1.9	NaN	9.51	0.35	NaN
eaf12 - 102.d	282.6	4.5	NaN	92.5	1.3	0.019	354.4	5.9	0.14	50.78	0.9	NaN
eaf12 - 103.d	199.5	3.9	0.16	67.3	1	NaN	263	5	0.064	41.28	0.7	0.019
eaf12 - 104.d	48.8	1.5	NaN	21.3	0.46	NaN	69.7	1.8	NaN	14.2	0.35	NaN
eaf12 - 105.d	220.8	4.5	NaN	77.9	1.5	NaN	291.5	4.7	0.14	43.68	0.58	NaN
eaf12 - 106.d	38.7	1.3	NaN	16.34	0.58	0.036	64.6	1.6	NaN	13.19	0.3	NaN
eaf12 - 107.d	69.2	2.7	NaN	25.83	0.73	0.037	108.3	3.8	0.062	19.92	0.55	NaN
eaf12 - 108.d	100.9	3.4	0.13	38.9	1.1	NaN	144.2	4.5	NaN	25.3	0.65	0.018
eaf12 - 109.d	286.7	5.4	NaN	88.3	1.4	0.039	343.3	4.1	NaN	48.46	0.77	NaN
eaf12 - 110.d	328.4	6.6	NaN	98.9	2	NaN	407.7	7.2	0.16	62.2	1	NaN
eaf12 - 111.d	240.6	3.1	NaN	71.2	1.2	NaN	321.3	4.7	0.059	50.92	0.62	0.012
eaf12 - 112.d	214.8	5	NaN	47.51	0.83	NaN	306	5	NaN	49.94	0.81	0.018
eaf12 - 113.d	247.2	3.5	NaN	68.7	1.3	NaN	320.9	6	NaN	51.9	0.77	NaN
eaf12 - 114.d	234.5	3.7	NaN	46.7	1.3	0.034	336.3	5.5	0.13	56.47	0.71	NaN
eaf12 - 115.d	437.9	6.8	0.13	126.9	1.4	NaN	406.5	6.2	0.11	65.74	0.98	0.017
eaf12 - 116.d	283.5	4.8	NaN	70.8	1.7	NaN	337	6.4	0.079	52.79	0.88	0.017
eaf12 - 117.d	228.4	6.1	NaN	33.04	0.88	NaN	303.2	5.7	NaN	48.45	0.95	NaN

Analysis number	Sm147 ppm	Sm147 ppm 2SE	Sm147 ppm LOD	Eu153 ppm	Eu153 ppm 2SE	Eu153 ppm LOD	Gd157 ppm	Gd157 ppm 2SE	Gd157 ppm LOD	Tb159 ppm	Tb159 ppm 2SE	Tb159 ppm LOD
eaf12 - 118.d	200.3	5.4	NaN	53.2	1.4	0.036	212.8	7.2	NaN	34.3	1	NaN
eaf12 - 119.d	312.1	6	NaN	77	1.4	NaN	300.9	4.9	0.11	47.16	0.77	NaN
eaf12 - 120.d	287.3	4.8	NaN	66.1	1.3	NaN	313.1	5.5	0.057	50.77	0.76	NaN
eaf12 - 121.d	287.7	4.2	NaN	81.9	1.6	0.034	292	5.7	0.11	47.69	0.75	0.0084
eaf12 - 122.d	301.8	8.7	NaN	86.3	2.9	0.033	315.7	6.8	NaN	49.7	1.2	NaN
eaf12 - 123.d	236.2	5.3	NaN	70.3	1.4	0.017	316.4	6.7	NaN	48.5	1	NaN
eaf12 - 124.d	327.1	5.7	NaN	96.1	1.9	NaN	405	7.4	NaN	57.75	0.91	0.017
eaf12 - 125.d	284.6	5.2	NaN	88.3	1.5	NaN	362.5	5.6	NaN	54.05	0.86	NaN
eaf12 - 126.d	201.5	4.2	NaN	65.2	1.2	NaN	280.9	4.2	NaN	44.21	0.73	NaN
eaf12 - 127.d	234.3	3.4	0.14	32	1.1	NaN	319.5	5.3	NaN	57.51	0.86	0.019
eaf12 - 128.d	259.4	4.7	NaN	27.61	0.8	NaN	398.5	5.5	NaN	71.17	0.83	NaN
eaf12 - 129.d	245.6	4	NaN	26.93	0.66	0.037	399.2	5.1	0.13	73.73	0.96	0.0093
eaf12 - 130.d	45.4	1.7	0.066	19.97	0.64	NaN	76.2	1.7	0.12	16.02	0.4	NaN
eaf12 - 131.d	86.8	1.8	NaN	32.5	0.62	0.049	124.1	2.4	0.14	23.4	0.46	NaN
eaf12 - 132.d	31.7	1.2	NaN	10.6	0.32	NaN	53.2	1.3	NaN	11.27	0.23	0.018
eaf12 - 133.d	62.2	2.1	NaN	16.7	0.37	NaN	101.1	2	NaN	17.41	0.37	NaN
eaf12 - 134.d	72.5	1.9	NaN	17.3	0.58	0.039	115.6	2.2	NaN	19.96	0.38	NaN
eaf12 - 135.d	197.8	3.6	NaN	72.6	1.2	NaN	252.9	4.8	0.058	37.32	0.59	NaN
eaf12 - 136.d	197.4	3.6	NaN	71.7	1.2	NaN	265.9	4.4	0.058	41.21	0.67	NaN
eaf12 - 137.d	96.1	2.9	NaN	39.22	0.92	NaN	144.5	2.8	NaN	25.14	0.44	0.018
eaf12 - 138.d	63	2	NaN	27.91	0.65	NaN	98.4	2.2	0.059	19.19	0.33	NaN
eaf12 - 139.d	73.4	2.3	NaN	29.88	0.67	0.035	115.8	2.5	NaN	21.65	0.45	0.019
eaf12 - 140.d	53.6	1.6	0.18	23.52	0.56	0.035	92.2	2.2	NaN	18.13	0.4	NaN
eaf12 - 141.d	37.6	1.3	NaN	18.09	0.48	0.017	46.9	1.5	NaN	9.38	0.27	NaN
eaf12 - 142.d	128.3	2.8	0.13	48.9	1	NaN	189.9	3.4	NaN	32.19	0.55	NaN
eaf12 - 143.d	40.8	2	NaN	13.39	0.3	NaN	56.3	1.7	0.11	11.7	0.3	NaN
eaf12 - 144.d	116.8	3.6	NaN	46.1	1.1	NaN	169.8	2.5	0.16	31.61	0.78	0.017
eaf12 - 145.d	126.3	4.3	NaN	42.2	1.2	NaN	174.4	3.7	NaN	29.36	0.55	NaN
eaf12 - 146.d	259.8	7.2	NaN	79.4	2	NaN	338.7	7.8	NaN	51.5	1.1	NaN

Analysis number	Sm147 ppm	Sm147 ppm 2SE	Sm147 ppm LOD	Eu153 ppm	Eu153 ppm 2SE	Eu153 ppm LOD	Gd157 ppm	Gd157 ppm 2SE	Gd157 ppm LOD	Tb159 ppm	Tb159 ppm 2SE	Tb159 ppm LOD
eaf12 - 147.d	153.6	3.2	NaN	48.4	1.1	NaN	204.7	3.9	NaN	32.61	0.57	0.024
eaf12 - 148.d	183.5	4.8	0.25	58.2	1.3	NaN	241.3	4.4	NaN	37.13	0.66	0.018
eaf12 - 149.d	135.2	3.8	NaN	42.7	1	NaN	181	3.6	NaN	28.98	0.77	NaN
eaf12 - 150.d	132.1	2.7	NaN	40.4	1.1	NaN	170.3	4.6	NaN	26.5	0.46	NaN
eaf12 - 151.d	108.9	3.8	NaN	35.4	1.3	NaN	153.6	4.1	NaN	25.05	0.78	NaN
eaf12 - 152.d	153.4	3.8	NaN	30.49	0.76	NaN	224.9	5.7	NaN	37.49	0.82	NaN
eaf12 - 153.d	184.8	3	NaN	23.35	0.91	NaN	321.2	5.3	0.13	62.69	0.82	NaN
eaf12 - 154.d	175.2	4.5	NaN	23.75	0.84	0.019	255.8	5.9	0.064	40.4	1	NaN
eaf12 - 155.d	228.5	5.1	0.07	33.62	0.87	NaN	318.8	5.5	NaN	54.7	1	NaN
eaf12 - 156.d	232.7	4.4	NaN	60.8	1.4	0.018	319.4	6.4	NaN	52.5	0.84	0.0092
eaf12 - 157.d	90.5	3.9	NaN	31.7	1.1	NaN	139.9	4.5	0.063	24.56	0.46	NaN
eaf12 - 158.d	116.2	4.4	NaN	38.9	1	0.018	167.2	4.3	NaN	27.96	0.65	NaN
eaf12 - 159.d	151.2	3.8	0.066	51.06	0.96	0.018	213.1	3.8	NaN	34.15	0.7	0.018
eaf12 - 160.d	34.7	1.6	NaN	12.41	0.53	NaN	59.5	2.2	NaN	13.15	0.39	NaN
eaf12 - 161.d	152.6	3.5	0.064	16.1	0.49	0.035	242.4	4	NaN	40.87	0.79	0.017
eaf12 - 162.d	154.9	2.5	NaN	49.76	0.97	0.052	220.9	3.5	0.12	35.74	0.5	0.0086
eaf12 - 163.d	42.2	1.5	NaN	10.58	0.33	0.017	74.7	2	NaN	14.85	0.34	NaN
eaf12 - 164.d	322.4	5.9	NaN	106.4	2.1	NaN	377.7	6.7	NaN	59.9	1.1	0.017

Analysis number	Dy163 ppm	Dy163 ppm 2SE	Dy163 ppm LOD	Ho165 ppm	Ho165 ppm 2SE	Ho165 ppm LOD	Er166 ppm	Er166 ppm 2SE	Er166 ppm LOD	Tm169 ppm	Tm169 ppm 2SE	Tm169 ppm LOD
eaf12 - 1.d	249.8	5.2	NaN	28.57	0.67	NaN	44.05	0.95	NaN	3.64	0.13	NaN
eaf12 - 2.d	263.8	4.2	0.072	31.62	0.54	NaN	53.5	1.2	0.053	4.84	0.17	NaN
eaf12 - 3.d	283	4.9	NaN	38.25	0.67	0.0087	72.3	1.7	NaN	6.73	0.26	NaN
eaf12 - 4.d	177.9	4	NaN	22.22	0.49	NaN	35.78	0.93	0.026	2.8	0.14	NaN
eaf12 - 5.d	145	2.8	0.036	20.79	0.45	NaN	43.89	0.98	0.036	5.04	0.15	NaN
eaf12 - 6.d	177	3.1	NaN	24.07	0.47	NaN	48.77	0.92	NaN	5.61	0.19	NaN
eaf12 - 7.d	262.9	3.4	NaN	30.34	0.4	NaN	49.28	0.88	NaN	4.51	0.12	NaN
eaf12 - 8.d	178	2.8	0.036	28.87	0.54	NaN	69	1.3	NaN	8.86	0.25	NaN
eaf12 - 9.d	151.8	2.7	NaN	22.91	0.42	NaN	47.3	1.1	NaN	5.09	0.17	0.017
eaf12 - 10.d	136	3.6	0.035	22.64	0.69	NaN	55.4	1.8	NaN	6.74	0.25	0.023
eaf12 - 11.d	94.7	4.4	NaN	16.36	0.57	NaN	42	1.4	0.057	5.61	0.2	NaN
eaf12 - 12.d	125.5	2.4	NaN	18.01	0.46	NaN	34.6	1.1	0.052	3.49	0.15	0.017
eaf12 - 13.d	83.9	1.5	NaN	14.6	0.3	NaN	38.32	0.79	NaN	5.08	0.14	NaN
eaf12 - 14.d	128	1.9	NaN	22.85	0.32	0.018	58.54	0.91	NaN	7.08	0.2	NaN
eaf12 - 15.d	93.8	2.2	0.035	13.71	0.34	NaN	30.55	0.58	NaN	3.33	0.13	0.0082
eaf12 - 16.d	209.9	4.6	NaN	25.11	0.94	NaN	41.4	1.8	0.026	3.69	0.28	0.0084
eaf12 - 17.d	145.4	2.5	0.077	23.38	0.43	NaN	51.64	0.99	NaN	5.93	0.17	NaN
eaf12 - 18.d	218.4	5.3	0.035	42.71	0.95	0.017	119.3	2.8	NaN	14.65	0.52	NaN
eaf12 - 19.d	165.3	2.7	0.035	32.6	0.51	NaN	91.2	1.7	0.077	11.82	0.33	NaN
eaf12 - 20.d	73.6	1.3	NaN	14.32	0.32	NaN	37.61	0.92	NaN	4.57	0.15	NaN
eaf12 - 21.d	232.3	3.9	NaN	27.43	0.5	NaN	43.6	1	0.026	3.55	0.11	NaN
eaf12 - 22.d	223.1	3.4	NaN	27.19	0.43	NaN	44.8	1.1	0.052	3.76	0.14	0.0083
eaf12 - 23.d	163.6	3.2	0.035	20.63	0.39	NaN	34.08	0.98	0.026	2.88	0.12	NaN
eaf12 - 24.d	227.9	3.1	0.07	26.75	0.52	NaN	43.11	0.87	NaN	3.67	0.15	NaN
eaf12 - 25.d	221.7	4	NaN	26.11	0.59	0.018	39.23	0.83	NaN	3.03	0.15	0.013
eaf12 - 26.d	252.8	3.5	NaN	31.79	0.65	0.024	53.9	1.1	0.027	4.65	0.15	0.019
eaf12 - 27.d	152.1	3.2	NaN	25.06	0.54	NaN	58	1.3	NaN	6.88	0.2	NaN
eaf12 - 28.d	263.1	3.8	NaN	44.73	0.74	NaN	115.4	1.8	0.027	14.56	0.41	NaN
eaf12 - 29.d	227.2	4.9	0.072	31.62	0.76	NaN	66.4	1.9	NaN	7.85	0.32	0.019

Analysis number	Dy163 ppm	Dy163 ppm 2SE	Dy163 ppm LOD	Ho165 ppm	Ho165 ppm 2SE	Ho165 ppm LOD	Er166 ppm	Er166 ppm 2SE	Er166 ppm LOD	Tm169 ppm	Tm169 ppm 2SE	Tm169 ppm LOD
eaf12 - 30.d	282.3	5.1	NaN	37.52	0.92	0.018	75	2.1	NaN	8.05	0.29	0.0087
eaf12 - 31.d	378.2	7.6	NaN	59.4	1.6	NaN	134.7	3.8	NaN	14.86	0.49	NaN
eaf12 - 32.d	125.4	3.3	NaN	17.87	0.44	NaN	32.27	0.73	NaN	2.72	0.11	NaN
eaf12 - 33.d	374.1	6.4	0.072	57.53	0.97	NaN	123.3	2.2	NaN	12.77	0.29	0.017
eaf12 - 34.d	188	3.5	NaN	22.36	0.49	NaN	33.58	0.66	0.028	2.72	0.11	0.018
eaf12 - 35.d	196.3	2.4	NaN	24.63	0.49	NaN	41.58	0.85	NaN	3.61	0.13	NaN
eaf12 - 36.d	154.8	2	0.036	20.59	0.46	NaN	35.37	0.95	0.053	2.93	0.14	NaN
eaf12 - 37.d	186.2	2.8	0.072	22.19	0.36	NaN	33.79	0.94	NaN	2.71	0.12	NaN
eaf12 - 38.d	137.3	2.3	NaN	21.3	0.48	0.0096	48.1	1.2	NaN	5.35	0.21	0.0092
eaf12 - 39.d	195.9	3.7	0.036	27.23	0.64	NaN	56	1.2	0.054	6.22	0.22	NaN
eaf12 - 40.d	176.3	3.7	NaN	30.63	0.76	NaN	79.4	1.5	0.027	11.01	0.26	NaN
eaf12 - 41.d	265.6	6.5	NaN	41.2	1.5	NaN	91	4.1	NaN	9.94	0.48	NaN
eaf12 - 42.d	99.7	1.9	NaN	17.55	0.38	0.018	46.1	1.5	NaN	6.12	0.18	NaN
eaf12 - 43.d	99.5	2.1	NaN	17.73	0.44	0.012	50.2	1.4	0.079	7.27	0.2	NaN
eaf12 - 44.d	87.6	2.3	NaN	14.7	0.37	NaN	37.07	0.74	NaN	4.8	0.19	0.0084
eaf12 - 45.d	75.5	1.3	NaN	12.47	0.25	NaN	31.22	0.74	0.06	4.09	0.16	NaN
eaf12 - 46.d	128.5	2.7	NaN	17.95	0.45	0.0086	38.15	0.98	0.052	4.19	0.15	NaN
eaf12 - 47.d	145.7	2.5	NaN	23.14	0.44	NaN	55	1.1	NaN	7.18	0.19	NaN
eaf12 - 48.d	36.4	0.94	NaN	7.01	0.23	NaN	19.48	0.66	NaN	2.86	0.14	NaN
eaf12 - 49.d	126.3	2.3	0.069	16.47	0.38	NaN	31.7	0.62	NaN	3.25	0.13	0.0082
eaf12 - 50.d	58.3	1.5	NaN	11.17	0.32	0.019	30.76	0.78	NaN	4.19	0.1	NaN
eaf12 - 51.d	267.4	4.1	NaN	48.71	0.72	0.0093	124.7	2	0.028	15.38	0.26	NaN
eaf12 - 52.d	270.1	4.3	NaN	48.09	0.86	0.021	123.3	2.1	NaN	14.91	0.49	NaN
eaf12 - 53.d	292.6	5.7	0.076	53.97	0.95	NaN	143.8	2.8	0.028	17.59	0.35	0.018
eaf12 - 54.d	253.2	4.1	NaN	35.29	0.6	NaN	71	1.5	NaN	6.97	0.2	NaN
eaf12 - 55.d	211.3	4	0.081	31.74	0.61	NaN	68.7	1.5	0.028	7.55	0.26	NaN
eaf12 - 56.d	247.9	3.5	0.082	34.26	0.66	0.028	67.1	1.8	NaN	7.04	0.21	NaN
eaf12 - 57.d	274.5	4.4	NaN	39.34	0.66	NaN	78.7	1.5	0.028	7.79	0.19	NaN
eaf12 - 58.d	172.2	2.5	NaN	26.47	0.61	0.0091	57.9	1	0.028	6.49	0.2	NaN

Analysis number	Dy163 ppm	Dy163 ppm 2SE	Dy163 ppm LOD	Ho165 ppm	Ho165 ppm 2SE	Ho165 ppm LOD	Er166 ppm	Er166 ppm 2SE	Er166 ppm LOD	Tm169 ppm	Tm169 ppm 2SE	Tm169 ppm LOD
eaf12 - 59.d	260.7	3.6	NaN	43.04	0.91	0.0091	100.9	2.4	NaN	11.2	0.34	NaN
eaf12 - 60.d	188.5	2.7	NaN	31.71	0.49	0.018	79.2	1.6	NaN	9.35	0.22	NaN
eaf12 - 61.d	215.1	3.6	NaN	35.56	0.61	0.0089	85.6	1.7	0.037	9.86	0.27	NaN
eaf12 - 62.d	403.6	5.1	0.07	78.24	0.99	0.019	225.3	3.2	NaN	31.6	0.43	0.0083
eaf12 - 63.d	205.6	3.8	0.035	39.5	0.88	NaN	109.6	2.1	NaN	14.52	0.33	0.0084
eaf12 - 64.d	217.4	3.4	NaN	25.39	0.52	NaN	39.1	1	NaN	3.2	0.14	NaN
eaf12 - 65.d	74.2	2	NaN	11.11	0.25	0.012	22.94	0.67	NaN	2.2	0.11	NaN
eaf12 - 66.d	147	1.9	0.078	18.98	0.43	NaN	32.15	0.81	0.054	2.58	0.11	NaN
eaf12 - 67.d	216.7	2.8	NaN	25.19	0.51	NaN	37.67	0.79	NaN	2.93	0.11	NaN
eaf12 - 68.d	84.2	1.8	NaN	12.2	0.25	NaN	23.51	0.66	NaN	2.28	0.11	NaN
eaf12 - 69.d	47.6	1.2	NaN	9.08	0.23	0.0085	27.62	0.66	0.026	4.59	0.17	0.018
eaf12 - 70.d	97.7	1.7	0.12	13.69	0.33	NaN	27.13	0.71	0.053	2.58	0.11	0.0084
eaf12 - 71.d	226.3	3.9	NaN	26.21	0.47	0.018	44.6	1	NaN	3.75	0.14	NaN
eaf12 - 72.d	47.2	1.1	NaN	8	0.24	0.017	19.96	0.57	NaN	2.58	0.11	NaN
eaf12 - 73.d	298.3	4.2	0.069	41.38	0.68	NaN	81.6	1.7	0.052	7.99	0.26	0.0082
eaf12 - 74.d	150.9	2.6	NaN	25.65	0.54	NaN	59.7	1.2	0.036	6.44	0.17	NaN
eaf12 - 75.d	192.5	2.8	0.069	23.67	0.3	0.017	38.45	0.97	NaN	3.39	0.13	0.016
eaf12 - 76.d	173.4	3.4	NaN	28	0.52	NaN	65.9	1.2	NaN	8.53	0.22	NaN
eaf12 - 77.d	183.3	3.6	0.039	23.12	0.46	0.0096	38.06	0.85	0.029	3.14	0.16	0.0092
eaf12 - 78.d	519.5	8.5	NaN	85.6	1.2	NaN	200.4	3.4	NaN	22.92	0.5	NaN
eaf12 - 79.d	112.1	2	NaN	19.77	0.46	NaN	51.38	0.98	0.029	6.64	0.21	0.018
eaf12 - 80.d	198.7	5.1	NaN	25.42	0.73	NaN	43.5	1.8	0.028	3.65	0.21	NaN
eaf12 - 81.d	139.6	2.3	NaN	18.73	0.41	NaN	31.56	0.7	0.028	2.55	0.11	NaN
eaf12 - 82.d	142.2	2.9	NaN	20.81	0.54	0.019	43	1.2	NaN	4.6	0.15	NaN
eaf12 - 83.d	149.5	2.6	NaN	22.92	0.38	NaN	48.6	1	NaN	5.2	0.15	NaN
eaf12 - 84.d	182.3	2.7	NaN	24.84	0.51	0.018	45.3	1	NaN	4.66	0.16	NaN
eaf12 - 85.d	188.8	3.9	NaN	24.91	0.49	NaN	48.6	1.2	NaN	5.09	0.19	NaN
eaf12 - 86.d	143.6	2.5	NaN	17.44	0.35	0.018	28.28	0.75	NaN	2.47	0.14	NaN
eaf12 - 87.d	197.8	2.7	NaN	28.53	0.48	NaN	58.6	1	NaN	6.68	0.22	0.017

Analysis number	Dy163 ppm	Dy163 ppm 2SE	Dy163 ppm LOD	Ho165 ppm	Ho165 ppm 2SE	Ho165 ppm LOD	Er166 ppm	Er166 ppm 2SE	Er166 ppm LOD	Tm169 ppm	Tm169 ppm 2SE	Tm169 ppm LOD
eaf12 - 88.d	217.7	2.7	NaN	35.04	0.51	NaN	82.6	1.3	NaN	10.45	0.27	0.017
eaf12 - 89.d	70.5	1.8	NaN	11.82	0.28	NaN	26.59	0.65	NaN	2.81	0.11	NaN
eaf12 - 90.d	95.5	2.2	NaN	14.01	0.36	0.0089	28.99	0.65	NaN	3.01	0.13	NaN
eaf12 - 92.d	81.6	2.1	NaN	14.9	0.32	0.0088	36.65	0.91	NaN	4.2	0.15	0.017
eaf12 - 93.d	95.3	1.4	NaN	16.2	0.3	0.012	38.63	0.82	0.026	4.39	0.12	NaN
eaf12 - 94.d	174.5	2.5	NaN	22.09	0.43	NaN	40.45	0.86	NaN	3.52	0.13	0.017
eaf12 - 95.d	70.2	1.5	NaN	13.31	0.3	NaN	34.2	0.71	NaN	4.03	0.14	NaN
eaf12 - 96.d	129.7	2.9	0.068	20.03	0.54	NaN	44.4	1.6	NaN	5.16	0.19	0.0081
eaf12 - 97.d	110.8	1.9	NaN	19.08	0.34	NaN	45.14	0.87	0.025	4.81	0.15	0.017
eaf12 - 98.d	117.2	2.4	NaN	16.02	0.32	0.0087	29.02	0.72	NaN	2.67	0.11	0.017
eaf12 - 99.d	111.9	1.8	NaN	15.64	0.31	0.0087	29.62	0.65	NaN	2.62	0.11	NaN
eaf12 - 100.d	151.5	2.7	NaN	23.35	0.47	NaN	47.89	0.92	0.051	5.64	0.18	NaN
eaf12 - 101.d	70.4	1.6	0.038	15.09	0.33	NaN	46.9	1.1	NaN	7.15	0.21	0.018
eaf12 - 102.d	226.6	3.9	NaN	26.66	0.44	0.013	39.5	1.1	NaN	3.32	0.13	0.012
eaf12 - 103.d	209	3.8	NaN	28.15	0.64	0.02	53.7	1.5	NaN	5.28	0.18	NaN
eaf12 - 104.d	98.7	1.9	NaN	18.75	0.35	0.02	51.87	0.95	NaN	6.93	0.23	NaN
eaf12 - 105.d	204.2	3.5	0.038	24.05	0.44	NaN	40.4	1.1	0.028	3.45	0.11	0.012
eaf12 - 106.d	90.2	1.9	0.038	15.81	0.29	0.0094	37.82	0.97	NaN	4.36	0.16	NaN
eaf12 - 107.d	117.2	2.2	NaN	17.57	0.29	0.019	37.48	0.88	NaN	3.81	0.14	NaN
eaf12 - 108.d	140.6	2.6	NaN	20.97	0.51	0.012	40.9	1.2	NaN	4.15	0.17	NaN
eaf12 - 109.d	216.3	3.1	NaN	25.05	0.41	NaN	39.23	0.83	0.058	3.1	0.11	0.017
eaf12 - 110.d	345.9	5	NaN	56.2	0.96	0.009	127.6	2.2	NaN	14.24	0.34	NaN
eaf12 - 111.d	279.5	3.8	NaN	41.42	0.64	NaN	86.4	1.5	0.053	8.36	0.22	0.017
eaf12 - 112.d	283.8	4	NaN	42.66	0.74	NaN	93.8	1.9	NaN	9.78	0.29	0.0083
eaf12 - 113.d	289.1	4.5	NaN	44.92	0.65	0.018	97.2	1.6	NaN	10.44	0.27	0.0084
eaf12 - 114.d	336.7	5.5	0.071	56.1	1	NaN	132.1	2.8	0.026	15.51	0.44	NaN
eaf12 - 115.d	432.3	6.3	0.035	86.35	0.99	0.019	265.1	3.6	0.076	39.78	0.46	NaN
eaf12 - 116.d	298.8	4.8	NaN	49.41	0.86	NaN	120.6	2.5	NaN	15.89	0.42	NaN
eaf12 - 117.d	247	5.3	0.035	34.45	0.86	NaN	68	2.1	0.076	6.91	0.2	0.013

Analysis number	Dy163 ppm	Dy163 ppm 2SE	Dy163 ppm LOD	Ho165 ppm	Ho165 ppm 2SE	Ho165 ppm LOD	Er166 ppm	Er166 ppm 2SE	Er166 ppm LOD	Tm169 ppm	Tm169 ppm 2SE	Tm169 ppm LOD
eaf12 - 118.d	212.5	5.3	0.034	39.22	0.86	0.017	101.1	2.2	NaN	12.31	0.28	0.016
eaf12 - 119.d	310.3	3.7	0.069	62.92	0.95	NaN	189	3.2	0.025	27.32	0.5	0.018
eaf12 - 120.d	297	4.3	NaN	53.41	0.89	NaN	149.5	2.7	NaN	21.48	0.43	NaN
eaf12 - 121.d	300.2	4.9	NaN	54.76	0.79	NaN	139.4	2.6	NaN	15.68	0.34	NaN
eaf12 - 122.d	299.6	6.4	NaN	52.8	1.4	NaN	131.2	3.5	NaN	14.83	0.51	0.0081
eaf12 - 123.d	247	4.8	0.069	32.85	0.74	0.0086	59.7	1.4	NaN	5.58	0.2	NaN
eaf12 - 124.d	284.3	4	NaN	37.83	0.65	0.0087	68.1	1.2	NaN	5.85	0.16	NaN
eaf12 - 125.d	259.8	3	0.095	33.2	0.58	NaN	56.4	1	NaN	5.06	0.14	NaN
eaf12 - 126.d	225	3.2	0.038	29.3	0.46	NaN	51.3	1.1	NaN	4.51	0.19	0.0091
eaf12 - 127.d	358.5	5.9	0.053	59.87	0.85	NaN	138.3	2.2	NaN	14.97	0.4	0.0093
eaf12 - 128.d	432.7	5.7	NaN	69.52	0.8	NaN	145.9	1.7	NaN	14.66	0.27	NaN
eaf12 - 129.d	438.6	4.4	NaN	69.09	0.92	0.021	144.1	2.2	NaN	14.22	0.38	0.0092
eaf12 - 130.d	107.5	2.3	0.074	18.98	0.46	NaN	43.92	0.83	NaN	4.87	0.2	NaN
eaf12 - 131.d	151.8	2.1	NaN	26.99	0.41	0.0093	69.2	1.1	NaN	8.2	0.2	NaN
eaf12 - 132.d	81.3	1.3	NaN	16.02	0.41	NaN	44	1.1	NaN	5.39	0.19	NaN
eaf12 - 133.d	95.9	1.7	0.037	13.81	0.32	0.018	28.63	0.83	0.037	2.92	0.13	NaN
eaf12 - 134.d	109.9	1.9	NaN	15.17	0.28	0.0092	30.07	0.7	NaN	2.89	0.11	NaN
eaf12 - 135.d	177.5	3.5	0.072	21.29	0.42	NaN	33.47	0.82	NaN	2.73	0.12	NaN
eaf12 - 136.d	208.7	2.8	NaN	27.95	0.54	NaN	53.77	0.97	NaN	5.48	0.22	NaN
eaf12 - 137.d	137	2.3	NaN	18.99	0.42	0.029	33.15	0.98	NaN	3.05	0.13	NaN
eaf12 - 138.d	120.8	2.1	NaN	19.91	0.43	NaN	44.9	1	NaN	4.92	0.18	NaN
eaf12 - 139.d	127.9	2.3	0.036	18.44	0.37	NaN	34.43	0.93	NaN	3.29	0.15	0.0085
eaf12 - 140.d	112.1	2.5	0.073	17.75	0.37	NaN	37.61	0.95	NaN	3.73	0.14	NaN
eaf12 - 141.d	63.1	1.4	0.036	11.28	0.23	NaN	29.41	0.76	0.052	4.31	0.16	NaN
eaf12 - 142.d	166.6	3	NaN	20.83	0.44	NaN	32.66	0.93	NaN	2.597	0.095	NaN
eaf12 - 143.d	83.2	1.8	0.07	16.5	0.39	0.017	46.9	1.1	0.025	6.07	0.16	0.0083
eaf12 - 144.d	193.1	3.6	0.036	30.71	0.54	NaN	69.7	1.2	NaN	8.69	0.26	0.018
eaf12 - 145.d	167.3	2.9	NaN	26.38	0.56	0.019	61.4	1.2	0.052	7.35	0.18	0.023
eaf12 - 146.d	278.9	6.5	NaN	41.9	1.4	0.0088	87.5	3.1	0.026	9.35	0.43	NaN

Analysis number	Dy163 ppm	Dy163 ppm 2SE	Dy163 ppm LOD	Ho165 ppm	Ho165 ppm 2SE	Ho165 ppm LOD	Er166 ppm	Er166 ppm 2SE	Er166 ppm LOD	Tm169 ppm	Tm169 ppm 2SE	Tm169 ppm LOD
eaf12 - 147.d	173	3.6	0.071	24.91	0.45	NaN	52.5	1.5	NaN	5.74	0.23	0.017
eaf12 - 148.d	192.3	4	NaN	27.52	0.46	0.0087	55.7	1.3	NaN	6.18	0.19	NaN
eaf12 - 149.d	150.5	3.4	0.071	21.71	0.47	0.0088	46.86	0.94	NaN	5.38	0.18	0.017
eaf12 - 150.d	148.1	2.9	NaN	23.46	0.5	NaN	53.08	0.78	0.026	6.01	0.18	0.017
eaf12 - 151.d	133.9	3.2	NaN	19.36	0.52	0.02	38.4	1.1	NaN	4.01	0.16	NaN
eaf12 - 152.d	205.6	3.3	NaN	28.18	0.54	0.02	57	1.1	NaN	6.07	0.18	NaN
eaf12 - 153.d	380.8	6.6	NaN	56.5	1.3	NaN	106.3	2.5	NaN	9.23	0.26	NaN
eaf12 - 154.d	200	4.9	0.053	25.82	0.77	0.0097	51.3	1.5	NaN	5.5	0.23	0.018
eaf12 - 155.d	327.2	6.9	NaN	54.2	1.3	NaN	126.8	3.6	NaN	15.39	0.49	NaN
eaf12 - 156.d	279.1	5.5	NaN	38.33	0.81	NaN	73.7	1.8	NaN	6.93	0.23	0.009
eaf12 - 157.d	142.2	2.5	0.077	19.21	0.45	0.019	35.8	1.1	NaN	3.28	0.13	NaN
eaf12 - 158.d	152.1	3	0.038	20.55	0.57	0.013	37.8	1.3	NaN	3.54	0.13	NaN
eaf12 - 159.d	171.1	3.8	NaN	21.28	0.42	NaN	35.53	0.92	0.054	3.16	0.12	NaN
eaf12 - 160.d	91.5	2.3	NaN	16.98	0.36	NaN	41.8	1.2	NaN	4.93	0.18	NaN
eaf12 - 161.d	208.3	4	NaN	26.87	0.81	NaN	52.3	2	0.026	5.51	0.26	NaN
eaf12 - 162.d	182.4	2.5	NaN	22.96	0.49	NaN	38.96	0.84	0.052	3.63	0.13	NaN
eaf12 - 163.d	98.7	1.8	NaN	16.19	0.53	NaN	34.37	0.81	0.053	3.45	0.11	0.027
eaf12 - 164.d	360.7	5.6	NaN	64.3	1.3	NaN	164.7	2.5	NaN	20.41	0.5	NaN

Analysis number	Yb172 ppm	Yb172 ppm 2SE	Yb172 ppm LOD	Lu175 ppm	Lu175 ppm 2SE	Lu175 ppm LOD	Hf178 ppm	Hf178 ppm 2SE	Hf178 ppm LOD	Ta181 ppm	Ta181 ppm 2SE	Ta181 ppm LOD
eaf12 - 1.d	15.7	0.76	NaN	1.355	0.096	NaN	9.59	0.36	0.058	77.7	1.3	NaN
eaf12 - 2.d	25.35	0.86	NaN	2.79	0.12	0.012	10.24	0.45	0.06	64.1	1.1	0.016
eaf12 - 3.d	33.1	1.2	0.054	3.5	0.15	NaN	12.51	0.5	NaN	61.2	1.2	NaN
eaf12 - 4.d	11.19	0.52	0.079	0.967	0.081	NaN	10.42	0.49	0.064	74.4	1.5	NaN
eaf12 - 5.d	28.3	0.88	NaN	3.44	0.13	0.025	8.48	0.42	NaN	45.22	0.79	NaN
eaf12 - 6.d	32.11	0.94	0.081	3.93	0.15	NaN	8.1	0.32	NaN	54.45	0.98	NaN
eaf12 - 7.d	22.44	0.66	0.039	2.37	0.12	0.018	9.88	0.3	NaN	69	1.1	0.0081
eaf12 - 8.d	55.5	1.4	0.04	6.88	0.24	NaN	9.02	0.31	0.03	52.4	1.2	NaN
eaf12 - 9.d	27.59	0.91	0.078	3.03	0.12	0.018	9.72	0.49	0.059	68.2	1.1	0.016
eaf12 - 10.d	40.3	1.5	NaN	4.89	0.25	NaN	9.48	0.43	NaN	79.6	1.1	NaN
eaf12 - 11.d	38.6	1.4	NaN	5.66	0.2	NaN	4.82	0.27	0.03	58.4	1.1	NaN
eaf12 - 12.d	17.08	0.68	NaN	1.62	0.11	0.019	9.9	0.39	0.059	61.7	1.1	NaN
eaf12 - 13.d	35.5	1.1	NaN	4.98	0.14	NaN	8.29	0.41	NaN	68.36	0.96	NaN
eaf12 - 14.d	39.1	1.1	NaN	4.42	0.16	0.018	8.5	0.53	0.03	57.28	0.89	0.017
eaf12 - 15.d	17.84	0.62	NaN	1.883	0.093	NaN	11.42	0.54	NaN	60.2	1.1	NaN
eaf12 - 16.d	16.9	1.2	0.079	1.8	0.16	0.018	10.69	0.39	NaN	98.3	1.8	0.0081
eaf12 - 17.d	32.6	1	NaN	3.74	0.14	0.0088	9.84	0.37	0.059	69.7	1	NaN
eaf12 - 18.d	82.7	2.3	NaN	9.71	0.36	0.0086	10.93	0.39	NaN	127.3	2.9	0.011
eaf12 - 19.d	69.3	1.6	NaN	8.43	0.27	NaN	10.71	0.49	0.087	61.7	1.3	NaN
eaf12 - 20.d	23.6	0.8	NaN	2.36	0.12	0.0087	8.73	0.33	NaN	64.4	1	0.022
eaf12 - 21.d	15.03	0.58	NaN	1.373	0.088	NaN	10.55	0.4	0.029	61.3	1.2	0.024
eaf12 - 22.d	16.64	0.62	NaN	1.563	0.077	NaN	9.77	0.4	NaN	32.28	0.63	NaN
eaf12 - 23.d	12.03	0.54	0.039	1.221	0.081	NaN	7.78	0.33	0.04	46.1	0.8	NaN
eaf12 - 24.d	16.39	0.66	NaN	1.467	0.084	0.017	10.45	0.37	0.058	44.46	0.67	NaN
eaf12 - 25.d	12.01	0.72	0.038	1.053	0.057	NaN	10.36	0.47	NaN	74.4	1.3	NaN
eaf12 - 26.d	20.76	0.62	0.081	2.07	0.1	0.018	10.69	0.51	0.042	44.85	0.89	0.033
eaf12 - 27.d	37	1.1	0.088	4.19	0.17	NaN	11.96	0.43	NaN	92.9	1.9	NaN
eaf12 - 28.d	85.6	1.7	NaN	10.43	0.23	NaN	11.21	0.54	NaN	101.2	2.4	NaN
eaf12 - 29.d	48.3	1.2	NaN	6.36	0.24	NaN	9.68	0.39	NaN	63.1	1.6	0.017

Analysis number	Yb172 ppm	Yb172 ppm 2SE	Yb172 ppm LOD	Lu175 ppm	Lu175 ppm 2SE	Lu175 ppm LOD	Hf178 ppm	Hf178 ppm 2SE	Hf178 ppm LOD	Ta181 ppm	Ta181 ppm 2SE	Ta181 ppm LOD
eaf12 - 30.d	47.8	1.8	NaN	5.39	0.22	NaN	11.26	0.47	NaN	67	1.4	0.025
eaf12 - 31.d	78.1	2.9	NaN	9.34	0.39	NaN	10.62	0.45	0.067	98.9	1.5	NaN
eaf12 - 32.d	11.24	0.39	0.088	0.952	0.073	NaN	9.35	0.39	0.031	74	1.3	0.017
eaf12 - 33.d	64.4	1.5	0.081	7.01	0.17	NaN	12.21	0.45	NaN	78.6	1.2	NaN
eaf12 - 34.d	10.04	0.42	0.041	0.856	0.055	0.0093	9.98	0.45	NaN	73.45	0.98	NaN
eaf12 - 35.d	15.44	0.7	NaN	1.46	0.11	0.021	9.39	0.42	0.03	65.4	1.1	0.016
eaf12 - 36.d	13.15	0.59	NaN	1.218	0.079	0.018	8.89	0.39	NaN	72.8	1.4	0.023
eaf12 - 37.d	11.8	0.53	NaN	1.13	0.084	NaN	9.17	0.34	NaN	68.14	0.96	NaN
eaf12 - 38.d	31.9	1.2	NaN	4.29	0.19	NaN	8.93	0.46	NaN	53.5	1	NaN
eaf12 - 39.d	38.83	0.95	NaN	4.87	0.19	0.009	9	0.39	NaN	60.19	0.92	NaN
eaf12 - 40.d	71.3	1.3	NaN	9.04	0.28	0.009	6.97	0.52	NaN	32.12	0.97	0.011
eaf12 - 41.d	56.4	3	NaN	6.39	0.4	0.018	11.19	0.53	NaN	64.11	0.99	NaN
eaf12 - 42.d	39.9	1.2	NaN	5.22	0.15	NaN	7.45	0.32	0.061	39.96	0.64	NaN
eaf12 - 43.d	48.9	1.4	NaN	6.51	0.2	NaN	5.11	0.29	0.03	20.89	0.46	NaN
eaf12 - 44.d	30.08	0.77	NaN	3.82	0.12	0.019	8.31	0.37	NaN	37.01	0.71	0.018
eaf12 - 45.d	25.55	0.87	NaN	3.26	0.12	NaN	7.81	0.39	NaN	27.88	0.36	0.008
eaf12 - 46.d	25.62	0.92	NaN	3.07	0.13	NaN	9.92	0.45	NaN	44.78	0.86	0.023
eaf12 - 47.d	45.11	0.99	NaN	5.74	0.17	0.013	8.68	0.44	NaN	34.59	0.79	NaN
eaf12 - 48.d	19.8	0.65	NaN	2.8	0.13	NaN	4.84	0.26	NaN	24.18	0.58	NaN
eaf12 - 49.d	17.44	0.66	NaN	1.95	0.11	0.017	8.04	0.38	NaN	43.77	0.86	0.016
eaf12 - 50.d	27.46	0.8	NaN	3.91	0.12	NaN	5.92	0.37	NaN	42.55	0.82	0.018
eaf12 - 51.d	90.9	1.8	NaN	10.26	0.26	NaN	13.16	0.44	NaN	79	1.4	NaN
eaf12 - 52.d	84.2	2	0.086	9.89	0.29	NaN	15.86	0.56	0.075	87.4	3.6	NaN
eaf12 - 53.d	94.1	2.3	NaN	10.29	0.26	NaN	14.5	0.52	NaN	96.8	3.3	0.036
eaf12 - 54.d	34.49	0.97	NaN	3.47	0.16	NaN	12.29	0.48	NaN	91.8	1.4	NaN
eaf12 - 55.d	40.2	1.1	NaN	4.35	0.18	0.019	11.59	0.58	NaN	90.2	1.7	0.024
eaf12 - 56.d	34.8	1	NaN	3.68	0.16	NaN	12.08	0.62	NaN	100.1	1.8	NaN
eaf12 - 57.d	35.35	0.9	0.083	3.39	0.14	0.02	14.23	0.6	NaN	82	1.3	NaN
eaf12 - 58.d	32.09	0.88	0.11	3.25	0.11	0.0092	11.43	0.55	NaN	53.3	1.7	0.0085

Analysis number	Yb172 ppm	Yb172 ppm 2SE	Yb172 ppm LOD	Lu175 ppm	Lu175 ppm 2SE	Lu175 ppm LOD	Hf178 ppm	Hf178 ppm 2SE	Hf178 ppm LOD	Ta181 ppm	Ta181 ppm 2SE	Ta181 ppm LOD
eaf12 - 59.d	54.5	1.6	NaN	5.71	0.24	NaN	14.72	0.52	NaN	134	2	NaN
eaf12 - 60.d	48.2	1.4	0.081	5.67	0.21	0.018	10.47	0.44	NaN	65.4	1.6	NaN
eaf12 - 61.d	52.4	1.2	NaN	5.85	0.18	0.009	14.39	0.45	NaN	165.9	2.7	0.017
eaf12 - 62.d	206.4	3	0.039	27.02	0.41	NaN	13.36	0.51	0.041	48.17	0.67	NaN
eaf12 - 63.d	94.2	2	0.04	12.63	0.3	NaN	9.01	0.36	NaN	27.71	0.61	NaN
eaf12 - 64.d	12.52	0.55	NaN	1.059	0.079	0.009	9.52	0.38	NaN	63.8	1	NaN
eaf12 - 65.d	10.69	0.45	NaN	0.936	0.07	0.018	9.28	0.44	NaN	55.44	0.69	NaN
eaf12 - 66.d	10.47	0.5	NaN	0.837	0.063	0.009	10.84	0.52	0.061	74.1	1.3	0.018
eaf12 - 67.d	10.99	0.41	NaN	0.883	0.069	NaN	9.68	0.43	NaN	77.9	1.1	0.018
eaf12 - 68.d	9.82	0.4	NaN	0.961	0.07	0.0087	9.17	0.34	0.059	48.49	0.8	0.016
eaf12 - 69.d	35.84	0.99	NaN	5.6	0.2	NaN	9.85	0.4	NaN	37.66	0.74	0.016
eaf12 - 70.d	13.24	0.61	0.079	1.261	0.093	0.019	10.41	0.34	NaN	63.78	0.71	0.016
eaf12 - 71.d	17.52	0.67	0.077	1.7	0.1	0.017	9.8	0.46	0.058	67.18	0.98	0.017
eaf12 - 72.d	16.32	0.7	NaN	2.1	0.12	NaN	9.43	0.38	NaN	55.57	0.87	0.0078
eaf12 - 73.d	37.14	0.9	NaN	3.94	0.16	0.0086	12.16	0.41	NaN	65.9	1.2	NaN
eaf12 - 74.d	31.28	0.93	NaN	3.12	0.13	NaN	9.36	0.4	NaN	59.4	1	NaN
eaf12 - 75.d	13.87	0.61	NaN	1.195	0.096	NaN	9.25	0.42	NaN	54.87	0.84	NaN
eaf12 - 76.d	52.19	0.96	0.086	6.43	0.18	NaN	9.53	0.47	NaN	53.02	0.94	NaN
eaf12 - 77.d	12.94	0.43	0.086	1.129	0.078	NaN	9.86	0.49	NaN	61.87	0.93	NaN
eaf12 - 78.d	123.3	2.7	NaN	14.56	0.39	0.0096	14.64	0.53	0.033	55.7	1.2	NaN
eaf12 - 79.d	38	1.1	0.086	4.71	0.19	NaN	11.49	0.5	NaN	72.2	1.4	0.019
eaf12 - 80.d	16.1	1.4	NaN	1.67	0.17	0.013	9.91	0.45	0.07	55.3	1.1	0.017
eaf12 - 81.d	10.46	0.38	NaN	0.847	0.073	NaN	9.74	0.39	NaN	45.16	0.59	0.024
eaf12 - 82.d	22.46	0.75	NaN	2.24	0.12	0.019	8.9	0.37	NaN	55.6	1	NaN
eaf12 - 83.d	25.74	0.8	0.042	2.798	0.092	NaN	9.92	0.49	0.086	53.87	0.86	NaN
eaf12 - 84.d	24.46	0.84	NaN	2.72	0.11	NaN	9.88	0.47	NaN	53.97	0.72	NaN
eaf12 - 85.d	28.89	0.77	NaN	3.36	0.12	NaN	9.18	0.38	NaN	47.55	0.89	NaN
eaf12 - 86.d	9.44	0.48	0.081	0.805	0.067	NaN	9.38	0.44	NaN	70.8	1	NaN
eaf12 - 87.d	36.6	1.2	0.081	4.3	0.16	NaN	10.91	0.45	NaN	100.2	1.5	NaN

Analysis number	Yb172 ppm	Yb172 ppm 2SE	Yb172 ppm LOD	Lu175 ppm	Lu175 ppm 2SE	Lu175 ppm LOD	Hf178 ppm	Hf178 ppm 2SE	Hf178 ppm LOD	Ta181 ppm	Ta181 ppm 2SE	Ta181 ppm LOD
eaf12 - 88.d	62.3	1.3	0.087	7.31	0.21	0.012	9.74	0.37	0.03	62.31	0.92	NaN
eaf12 - 89.d	13.6	0.47	0.081	1.355	0.097	NaN	8.67	0.44	0.061	38.85	0.88	NaN
eaf12 - 90.d	13.31	0.51	NaN	1.232	0.059	0.0089	8.34	0.33	NaN	45.49	0.8	NaN
eaf12 - 92.d	21.11	0.63	0.079	2.099	0.092	NaN	8.41	0.38	NaN	33.59	0.64	NaN
eaf12 - 93.d	21.12	0.8	NaN	2.35	0.11	0.017	8.88	0.38	NaN	34.62	0.66	0.0081
eaf12 - 94.d	17.91	0.75	NaN	1.75	0.12	NaN	10.42	0.45	NaN	50.87	0.83	0.016
eaf12 - 95.d	22.12	0.82	NaN	2.51	0.11	NaN	6.56	0.32	NaN	41.04	0.81	NaN
eaf12 - 96.d	26.8	0.96	0.038	3.15	0.14	NaN	9.91	0.41	NaN	51.94	0.75	0.016
eaf12 - 97.d	25.07	0.64	NaN	2.68	0.14	0.0084	9.26	0.34	0.057	56.25	0.81	NaN
eaf12 - 98.d	11.13	0.45	NaN	0.957	0.069	NaN	8.47	0.41	0.029	24.76	0.61	NaN
eaf12 - 99.d	11.28	0.37	NaN	0.972	0.06	NaN	8.39	0.44	NaN	23.85	0.61	0.016
eaf12 - 100.d	32.5	1.1	NaN	3.66	0.14	NaN	8.93	0.34	NaN	42.32	0.76	0.008
eaf12 - 101.d	46.6	1.4	0.093	6.51	0.2	0.019	7.04	0.33	NaN	64.8	2.9	NaN
eaf12 - 102.d	11.63	0.59	NaN	0.949	0.07	NaN	12.46	0.45	0.064	84.5	1.2	0.0088
eaf12 - 103.d	24.2	1.1	NaN	2.61	0.14	NaN	11.24	0.53	0.033	68.5	1.1	0.018
eaf12 - 104.d	42.3	1.2	NaN	5.25	0.21	NaN	8.41	0.4	0.033	48.33	0.85	0.018
eaf12 - 105.d	16.52	0.62	0.042	1.624	0.095	0.019	11.2	0.4	NaN	68.7	1.2	NaN
eaf12 - 106.d	21.94	0.64	0.084	2.34	0.13	NaN	9.3	0.4	0.032	47.86	0.77	0.017
eaf12 - 107.d	19.95	0.87	NaN	2.01	0.091	0.013	10.28	0.38	0.043	48.99	0.99	0.0087
eaf12 - 108.d	18.57	0.71	NaN	1.95	0.1	NaN	10.34	0.36	0.084	63	0.94	0.017
eaf12 - 109.d	12.48	0.6	NaN	1.081	0.081	0.018	12	0.48	0.031	85.9	1.1	NaN
eaf12 - 110.d	72.8	1.3	NaN	7.88	0.21	NaN	12.58	0.44	NaN	72.3	1.3	0.017
eaf12 - 111.d	41.4	1.5	0.088	4.55	0.21	0.018	11.59	0.41	NaN	84.4	1.4	0.018
eaf12 - 112.d	49	1.7	NaN	5.23	0.27	NaN	12.74	0.51	NaN	65.85	0.96	NaN
eaf12 - 113.d	52.4	1.1	NaN	5.62	0.17	NaN	12.41	0.38	0.03	79.7	1.3	0.016
eaf12 - 114.d	84.6	2.7	NaN	9.8	0.27	NaN	12.95	0.63	NaN	61.8	2.1	NaN
eaf12 - 115.d	268.6	5.1	0.077	36.99	0.76	NaN	24.39	0.61	NaN	62.7	1.1	NaN
eaf12 - 116.d	96.9	2.3	NaN	11.68	0.32	NaN	17.14	0.53	0.06	72.5	1.1	0.016
eaf12 - 117.d	33.1	0.8	NaN	3.34	0.16	NaN	21.16	0.66	0.064	144.6	2	NaN

Analysis number	Yb172 ppm	Yb172 ppm 2SE	Yb172 ppm LOD	Lu175 ppm	Lu175 ppm 2SE	Lu175 ppm LOD	Hf178 ppm	Hf178 ppm 2SE	Hf178 ppm LOD	Ta181 ppm	Ta181 ppm 2SE	Ta181 ppm LOD
eaf12 - 118.d	67	1.5	NaN	8.01	0.29	0.0084	22.49	0.7	NaN	47.2	1	NaN
eaf12 - 119.d	184.6	3.1	0.076	25.92	0.53	NaN	14.07	0.56	NaN	24.95	0.54	0.016
eaf12 - 120.d	140.8	3	NaN	19.51	0.45	0.0087	18.68	0.73	0.029	108.7	1.6	0.0081
eaf12 - 121.d	78.8	1.9	0.077	8.51	0.22	NaN	12.64	0.49	NaN	27.86	0.78	NaN
eaf12 - 122.d	69.8	2.4	NaN	7.38	0.3	0.0085	15.2	0.44	NaN	72.1	2.1	0.0079
eaf12 - 123.d	24.67	0.83	0.088	2.4	0.1	NaN	12.33	0.39	NaN	84.7	1.1	0.016
eaf12 - 124.d	25.26	0.79	NaN	2.35	0.12	0.0087	13.04	0.51	NaN	84.8	3.6	NaN
eaf12 - 125.d	21.75	0.54	NaN	1.969	0.098	NaN	13.35	0.62	0.08	96.8	1.3	0.016
eaf12 - 126.d	19.52	0.65	NaN	1.67	0.11	NaN	11.78	0.51	NaN	94.2	1.6	0.018
eaf12 - 127.d	74.2	2	NaN	7.95	0.3	NaN	19.76	0.62	NaN	82.5	1.8	0.018
eaf12 - 128.d	66.9	1.3	0.12	6.5	0.18	0.019	18.19	0.52	NaN	118.9	1.3	0.018
eaf12 - 129.d	61.3	1.4	NaN	5.71	0.2	0.021	19.12	0.53	0.07	113.4	2.1	0.018
eaf12 - 130.d	24.58	0.65	NaN	2.88	0.12	NaN	9.53	0.44	NaN	48.91	0.92	NaN
eaf12 - 131.d	45.3	1.2	NaN	5.47	0.17	NaN	10.29	0.37	0.031	49.82	0.84	NaN
eaf12 - 132.d	29.9	1.1	NaN	3.24	0.12	0.019	9.66	0.45	NaN	44.26	0.93	NaN
eaf12 - 133.d	15.22	0.61	NaN	1.525	0.096	NaN	10.6	0.56	NaN	61.3	1.1	NaN
eaf12 - 134.d	13.29	0.62	NaN	1.361	0.081	NaN	10.38	0.35	NaN	72.55	0.95	NaN
eaf12 - 135.d	10.39	0.5	NaN	0.82	0.066	NaN	10.76	0.51	NaN	57.6	0.9	NaN
eaf12 - 136.d	30.6	1.1	0.04	3.76	0.18	0.0089	11.07	0.47	NaN	81.4	1.4	0.017
eaf12 - 137.d	13.49	0.54	0.083	1.232	0.098	NaN	9.56	0.49	NaN	52.17	0.87	NaN
eaf12 - 138.d	24.57	0.72	NaN	2.54	0.12	0.014	9.19	0.43	NaN	42.89	0.64	0.017
eaf12 - 139.d	15.06	0.56	NaN	1.494	0.079	NaN	9.1	0.34	NaN	45.15	0.91	NaN
eaf12 - 140.d	17.42	0.58	0.041	1.66	0.11	0.0091	9.6	0.43	NaN	43.39	0.94	NaN
eaf12 - 141.d	26.4	0.82	NaN	3.46	0.16	NaN	1.89	0.18	0.03	32.82	0.72	NaN
eaf12 - 142.d	10.23	0.5	NaN	0.794	0.063	0.0089	10.25	0.39	NaN	63.5	1.1	NaN
eaf12 - 143.d	35.1	1.1	0.077	4.2	0.16	NaN	9.38	0.53	NaN	48.2	1	NaN
eaf12 - 144.d	50.7	1.5	0.11	5.9	0.18	0.019	9.44	0.52	0.03	61.1	1.2	0.016
eaf12 - 145.d	42.52	0.89	NaN	5.04	0.2	NaN	10.65	0.36	NaN	53.42	0.68	NaN
eaf12 - 146.d	48.3	2.1	NaN	5.04	0.31	0.0088	11.86	0.44	0.059	63.1	1.9	0.023

Analysis number	Yb172 ppm	Yb172 ppm 2SE	Yb172 ppm LOD	Lu175 ppm	Lu175 ppm 2SE	Lu175 ppm LOD	Hf178 ppm	Hf178 ppm 2SE	Hf178 ppm LOD	Ta181 ppm	Ta181 ppm 2SE	Ta181 ppm LOD
eaf12 - 147.d	29.92	0.94	NaN	3.43	0.17	NaN	9.86	0.41	NaN	60.36	0.86	NaN
eaf12 - 148.d	33.15	0.8	NaN	3.66	0.14	NaN	10.8	0.45	NaN	77.3	1.2	NaN
eaf12 - 149.d	29.4	1.2	NaN	3.58	0.14	0.0088	9.6	0.49	NaN	64.2	1.3	NaN
eaf12 - 150.d	33.39	0.92	0.079	4.02	0.12	NaN	8.72	0.35	NaN	54.29	0.73	NaN
eaf12 - 151.d	20.21	0.72	0.088	2.27	0.13	NaN	10.3	0.52	0.066	70.1	1.1	0.02
eaf12 - 152.d	32.9	1.1	NaN	3.65	0.15	NaN	13.24	0.5	0.045	76.5	2.3	NaN
eaf12 - 153.d	34.8	1	NaN	2.87	0.12	NaN	15.12	0.51	NaN	72.2	2.4	NaN
eaf12 - 154.d	29	1	NaN	2.82	0.16	0.0097	13.8	0.5	NaN	79.1	2.3	0.009
eaf12 - 155.d	85.4	2.8	0.088	10.79	0.34	NaN	17.18	0.64	0.066	71.8	1	0.0091
eaf12 - 156.d	30.33	0.82	NaN	3.01	0.12	NaN	12.43	0.6	0.064	70.9	1.4	NaN
eaf12 - 157.d	15.45	0.68	0.086	1.55	0.12	0.019	8.63	0.39	0.032	44.76	0.66	0.018
eaf12 - 158.d	16.03	0.63	0.091	1.54	0.1	0.019	9.25	0.37	NaN	56.21	0.98	0.0087
eaf12 - 159.d	12.88	0.7	NaN	1.216	0.086	NaN	9.67	0.39	0.062	44.9	0.82	0.0085
eaf12 - 160.d	26.52	0.9	0.056	2.52	0.11	NaN	9.11	0.44	0.062	63.4	1.5	0.0085
eaf12 - 161.d	27.4	1.7	0.088	3.14	0.22	NaN	13.87	0.55	0.061	107.7	1.5	NaN
eaf12 - 162.d	16.5	0.64	0.04	1.53	0.11	NaN	10.59	0.48	NaN	76.4	1.2	0.011
eaf12 - 163.d	15.97	0.61	0.088	1.48	0.079	0.009	10.77	0.39	0.061	53.61	0.94	0.033
eaf12 - 164.d	119.5	2.3	0.039	15.01	0.35	0.024	11.81	0.43	NaN	26.45	0.69	NaN

Analysis number	W182 ppm	W182 ppm 2SE	W182 ppm LOD	Pb204 ppm	Pb204 ppm 2SE	Pb204 ppm LOD	Pb206 ppm	Pb206 ppm 2SE	Pb206 ppm LOD	Pb207 ppm	Pb207 ppm 2SE	Pb207 ppm LOD
eaf12 - 1.d	37.54	0.93	0.066	< LOD	< LOD	4.9	61.6	1.6	0.14	10.77	0.34	0.063
eaf12 - 2.d	37.2	1	NaN	< LOD	< LOD	4.9	67	1.7	0.066	10.85	0.24	0.048
eaf12 - 3.d	35.2	1.1	NaN	< LOD	< LOD	6.7	96.1	1.8	0.076	12.92	0.22	0.064
eaf12 - 4.d	42.4	1	NaN	< LOD	< LOD	6.4	36.9	1.1	0.18	8.52	0.19	0.04
eaf12 - 5.d	50.4	1.2	0.068	< LOD	< LOD	6.5	35.4	1.5	0.17	7.92	0.21	0.063
eaf12 - 6.d	43.3	1.3	0.069	< LOD	< LOD	6.3	47.3	1.3	0.097	8.4	0.21	0.054
eaf12 - 7.d	29.27	0.94	NaN	6.4	2.5	5.2	84.7	1.7	0.094	12.15	0.25	0.04
eaf12 - 8.d	47.9	1.2	NaN	4	2.3	3.1	30.5	1.2	0.065	6.13	0.16	0.041
eaf12 - 9.d	46.3	1.2	0.054	< LOD	< LOD	5.2	23.23	0.84	0.25	6.04	0.16	0.037
eaf12 - 10.d	54.8	1.2	NaN	< LOD	< LOD	4.8	21.21	0.86	NaN	5.64	0.12	0.051
eaf12 - 11.d	28.02	0.81	NaN	< LOD	< LOD	7.4	22.6	0.79	0.15	5.38	0.14	0.048
eaf12 - 12.d	44.1	1.1	NaN	< LOD	< LOD	5.4	22.78	0.78	0.11	6.51	0.17	0.061
eaf12 - 13.d	52.2	1.4	NaN	< LOD	< LOD	6.7	11.28	0.52	0.11	4.2	0.12	0.054
eaf12 - 14.d	58	1.2	0.047	< LOD	< LOD	5	19.04	0.78	0.12	5.73	0.12	0.062
eaf12 - 15.d	73.5	1.9	0.065	< LOD	< LOD	5.3	11.82	0.56	0.16	4.96	0.16	0.054
eaf12 - 16.d	39.5	1.2	NaN	< LOD	< LOD	3.8	67.4	1.5	0.12	10.88	0.26	0.055
eaf12 - 17.d	56	1.4	NaN	< LOD	< LOD	7.8	26.17	0.75	0.12	6.11	0.14	0.051
eaf12 - 18.d	43.9	1.3	NaN	< LOD	< LOD	5.5	23.07	0.98	0.11	5.75	0.16	0.034
eaf12 - 19.d	62.4	1.2	NaN	< LOD	< LOD	5.7	18.85	0.81	0.15	5.42	0.14	0.045
eaf12 - 20.d	55.4	1.4	0.033	< LOD	< LOD	7.6	8.34	0.49	0.16	4.89	0.13	0.036
eaf12 - 21.d	27.8	0.87	NaN	< LOD	< LOD	6	86.5	2.2	0.13	12.86	0.29	0.035
eaf12 - 22.d	21.92	0.63	NaN	< LOD	< LOD	5.2	88.1	2.1	0.25	12.97	0.23	0.038
eaf12 - 23.d	41.3	1	0.095	7.4	2.4	6.8	33.1	1	0.15	7.4	0.2	0.043
eaf12 - 24.d	27.6	0.72	NaN	< LOD	< LOD	6.6	85.6	2	0.22	12.51	0.26	0.039
eaf12 - 25.d	36.2	1	NaN	< LOD	< LOD	5.5	74.2	1.6	0.17	11.65	0.22	0.032
eaf12 - 26.d	27.05	0.87	NaN	< LOD	< LOD	7.8	94.6	2.3	0.15	13.33	0.3	0.04
eaf12 - 27.d	75.1	1.6	NaN	< LOD	< LOD	6.5	25.11	0.89	0.14	6.28	0.15	0.036
eaf12 - 28.d	59.1	1.9	NaN	< LOD	< LOD	8.6	47.1	1.3	0.096	7.34	0.15	0.041
eaf12 - 29.d	44.9	1	NaN	< LOD	< LOD	10	59.8	1.7	0.14	9.21	0.22	0.044

Analysis number	W182 ppm	W182 ppm 2SE	W182 ppm LOD	Pb204 ppm	Pb204 ppm 2SE	Pb204 ppm LOD	Pb206 ppm	Pb206 ppm 2SE	Pb206 ppm LOD	Pb207 ppm	Pb207 ppm 2SE	Pb207 ppm LOD
eaf12 - 30.d	35.41	0.78	NaN	< LOD	< LOD	4.5	91.8	2.1	0.11	12.68	0.28	0.053
eaf12 - 31.d	52.5	1.4	0.035	< LOD	< LOD	6.8	72.8	2	0.12	10.87	0.23	0.046
eaf12 - 32.d	47	1.2	NaN	< LOD	< LOD	6.4	18.35	0.82	0.22	6.82	0.14	0.035
eaf12 - 33.d	44.6	1.2	NaN	< LOD	< LOD	5.6	94.4	2.4	0.16	12.45	0.29	0.075
eaf12 - 34.d	47.4	1.2	0.035	9.8	2.8	6.2	60.5	1.5	0.068	12.17	0.18	0.044
eaf12 - 35.d	36.33	0.84	NaN	< LOD	< LOD	5.9	54.6	1.4	0.27	9.77	0.2	0.033
eaf12 - 36.d	46.2	1.1	NaN	6.1	2.7	5.4	29.8	1.2	0.18	7.55	0.18	0.054
eaf12 - 37.d	40.67	0.9	0.034	< LOD	< LOD	7	52.1	1.7	0.11	10.31	0.2	0.049
eaf12 - 38.d	45.3	1	NaN	< LOD	< LOD	7.5	36.6	1.2	0.19	7.46	0.19	0.076
eaf12 - 39.d	39.9	1.1	NaN	< LOD	< LOD	5.7	48.7	1.3	0.12	7.87	0.17	0.048
eaf12 - 40.d	46.6	2.7	NaN	< LOD	< LOD	4.6	37.7	1	0.096	6.67	0.16	0.032
eaf12 - 41.d	55.7	2	NaN	4.4	2.2	4.3	64.5	1.4	0.13	9.46	0.17	0.052
eaf12 - 42.d	51.9	1.3	NaN	< LOD	< LOD	4.9	22.31	0.89	0.086	5.52	0.12	0.052
eaf12 - 43.d	30.4	0.82	NaN	< LOD	< LOD	8.7	28.88	0.88	0.19	5.96	0.16	0.04
eaf12 - 44.d	56.9	0.72	0.034	6.2	2.6	6.1	18.4	0.72	0.11	5.16	0.14	0.044
eaf12 - 45.d	56.5	1.2	0.065	< LOD	< LOD	6	18.34	0.75	0.13	5.18	0.14	0.039
eaf12 - 46.d	53.9	1.5	0.033	< LOD	< LOD	7.7	30.9	1	0.2	6.68	0.13	0.043
eaf12 - 47.d	45.3	1.4	NaN	< LOD	< LOD	7.7	39.7	1.1	0.11	7.2	0.18	0.062
eaf12 - 48.d	40.37	0.9	NaN	< LOD	< LOD	7	14.02	0.74	0.19	5.1	0.17	0.043
eaf12 - 49.d	42.9	1.1	NaN	< LOD	< LOD	5.9	34.1	1.2	0.16	7.05	0.19	0.064
eaf12 - 50.d	51.5	1.2	NaN	< LOD	< LOD	6.9	17.19	0.76	0.1	5.62	0.14	0.044
eaf12 - 51.d	61.9	1.4	NaN	< LOD	< LOD	7	21.11	0.86	0.15	5.26	0.12	0.049
eaf12 - 52.d	62.7	1.6	0.072	< LOD	< LOD	6.3	22.36	0.72	0.18	5.59	0.18	0.045
eaf12 - 53.d	67.9	1.4	NaN	< LOD	< LOD	8.9	13.81	0.61	0.1	4.94	0.12	0.034
eaf12 - 54.d	48.2	1.3	NaN	< LOD	< LOD	7	70.5	1.5	0.14	10.36	0.19	0.037
eaf12 - 55.d	49.3	1.2	0.035	< LOD	< LOD	4.4	50.1	1.7	0.14	7.98	0.21	0.042
eaf12 - 56.d	50.9	1.4	NaN	< LOD	< LOD	6.7	68.4	1.9	0.15	10.4	0.2	0.047
eaf12 - 57.d	56.7	1.3	NaN	< LOD	< LOD	4.9	68.7	1.7	0.11	9.55	0.17	0.058
eaf12 - 58.d	55	1.5	NaN	< LOD	< LOD	4.9	34.09	0.94	NaN	7.1	0.18	0.046

Analysis number	W182 ppm	W182 ppm 2SE	W182 ppm LOD	Pb204 ppm	Pb204 ppm 2SE	Pb204 ppm LOD	Pb206 ppm	Pb206 ppm 2SE	Pb206 ppm LOD	Pb207 ppm	Pb207 ppm 2SE	Pb207 ppm LOD
eaf12 - 59.d	56.7	1.4	NaN	< LOD	< LOD	6	38.7	1.2	0.27	6.68	0.15	0.066
eaf12 - 60.d	57.4	1.1	NaN	< LOD	< LOD	5.7	22.17	0.7	0.11	5.69	0.14	0.055
eaf12 - 61.d	73.1	1.5	NaN	4.3	2.4	4.3	22.64	0.89	0.22	5.64	0.13	0.047
eaf12 - 62.d	28.12	0.71	0.066	4.5	2.6	3.6	83.6	2.5	0.18	11.3	0.23	0.043
eaf12 - 63.d	28.59	0.9	0.1	< LOD	< LOD	7	12.68	0.56	0.094	4.11	0.11	0.064
eaf12 - 64.d	36.59	0.78	NaN	9.1	2.6	7.4	79	2.1	0.1	14.48	0.27	0.059
eaf12 - 65.d	61.4	1.3	0.068	< LOD	< LOD	8.4	9.74	0.4	0.14	4.82	0.12	0.05
eaf12 - 66.d	46	1.2	NaN	< LOD	< LOD	6	29.69	0.85	0.21	7.82	0.16	0.051
eaf12 - 67.d	37.98	0.91	NaN	< LOD	< LOD	5.9	60.7	1.7	0.29	10.84	0.17	0.039
eaf12 - 68.d	59.2	1.4	NaN	< LOD	< LOD	6.6	12.13	0.66	0.15	5.02	0.1	0.022
eaf12 - 69.d	43	1.2	0.065	< LOD	< LOD	6	19.41	0.75	0.27	4.62	0.12	0.056
eaf12 - 70.d	69.7	1.3	0.046	< LOD	< LOD	5.7	14.48	0.87	0.064	4.89	0.13	0.068
eaf12 - 71.d	26.63	0.81	0.044	< LOD	< LOD	5.6	85.3	1.8	0.11	12.55	0.22	0.066
eaf12 - 72.d	75.4	1.4	0.13	< LOD	< LOD	7.3	15.12	0.52	0.12	4.84	0.12	0.052
eaf12 - 73.d	40.34	0.99	0.033	< LOD	< LOD	5.9	80.5	1.7	0.092	11.42	0.21	0.054
eaf12 - 74.d	55.3	1.3	0.033	< LOD	< LOD	5.4	12.12	0.57	0.11	5.18	0.12	0.045
eaf12 - 75.d	38.39	0.95	NaN	8.3	2.7	7.5	55.7	1.4	0.11	10.03	0.22	0.056
eaf12 - 76.d	61.3	1.3	NaN	< LOD	< LOD	4.9	44	1.3	0.11	7.62	0.13	0.06
eaf12 - 77.d	46.6	1.2	0.037	< LOD	< LOD	5.3	35.95	0.87	0.15	8.51	0.18	0.035
eaf12 - 78.d	71	1.6	NaN	< LOD	< LOD	8.2	137.4	2.5	0.26	15.75	0.26	0.064
eaf12 - 79.d	74.9	1.7	NaN	< LOD	< LOD	7.5	10.78	0.66	0.11	5.18	0.14	0.063
eaf12 - 80.d	38.1	1.1	NaN	< LOD	< LOD	6.8	49.7	1	0.069	9.7	0.19	0.057
eaf12 - 81.d	42.41	0.9	NaN	8	2	6.6	22.79	0.95	0.14	7.22	0.16	0.054
eaf12 - 82.d	49.3	1.1	NaN	< LOD	< LOD	4.5	29.17	0.87	0.14	7.04	0.19	0.041
eaf12 - 83.d	52.6	1.1	0.035	6.4	2.1	3.8	30.4	1.2	0.14	7.43	0.18	0.045
eaf12 - 84.d	45.4	1.1	NaN	< LOD	< LOD	9.5	44.6	1.1	0.14	8.52	0.13	0.042
eaf12 - 85.d	40.37	0.83	0.035	< LOD	< LOD	8.1	45.9	1.1	0.16	8.16	0.17	0.068
eaf12 - 86.d	48.3	1.1	NaN	< LOD	< LOD	8	36.96	0.99	0.26	8.14	0.18	0.049
eaf12 - 87.d	46.6	1.1	NaN	4.5	2.6	3.9	46	1.4	0.17	7.85	0.19	0.047

Analysis number	W182 ppm	W182 ppm 2SE	W182 ppm LOD	Pb204 ppm	Pb204 ppm 2SE	Pb204 ppm LOD	Pb206 ppm	Pb206 ppm 2SE	Pb206 ppm LOD	Pb207 ppm	Pb207 ppm 2SE	Pb207 ppm LOD
eaf12 - 88.d	48.6	1.2	0.034	< LOD	< LOD	7.3	43.1	1	0.15	6.87	0.15	0.041
eaf12 - 89.d	53.9	1.4	0.068	< LOD	< LOD	6.4	11.09	0.53	0.21	5.13	0.12	0.037
eaf12 - 90.d	46.7	1.2	NaN	< LOD	< LOD	5	20.87	0.68	0.21	6.17	0.11	0.032
eaf12 - 92.d	56	1.3	NaN	< LOD	< LOD	5.7	9.2	0.49	0.22	4.98	0.14	0.064
eaf12 - 93.d	48.1	1	0.066	< LOD	< LOD	5.9	12.05	0.61	0.18	4.88	0.12	0.046
eaf12 - 94.d	39.7	1.1	NaN	< LOD	< LOD	7.2	50.2	1.1	0.11	8.56	0.2	0.052
eaf12 - 95.d	44.93	0.99	NaN	< LOD	< LOD	7.1	11.93	0.64	0.15	4.82	0.12	0.032
eaf12 - 96.d	60.5	1.2	NaN	< LOD	< LOD	5.2	22.1	1	0.073	5.32	0.16	0.044
eaf12 - 97.d	56.5	1.1	NaN	5.9	2.7	5.1	13.77	0.64	0.2	5.07	0.1	0.055
eaf12 - 98.d	46.35	0.94	NaN	6.2	2.4	3.8	17.85	0.71	0.11	6.16	0.15	0.037
eaf12 - 99.d	43.99	0.97	NaN	< LOD	< LOD	7.8	16.35	0.86	0.17	5.83	0.16	0.035
eaf12 - 100.d	47.9	1.1	0.066	< LOD	< LOD	8.3	26.6	1	0.16	5.53	0.15	0.042
eaf12 - 101.d	93	3.5	NaN	< LOD	< LOD	5.4	13.94	0.75	0.17	5	0.11	0.069
eaf12 - 102.d	37.4	1.1	NaN	< LOD	< LOD	7	89.9	1.8	0.22	13.08	0.2	0.047
eaf12 - 103.d	42.5	1.3	0.074	< LOD	< LOD	7.3	62.2	1.2	0.13	10.38	0.22	0.047
eaf12 - 104.d	53.9	1.1	NaN	< LOD	< LOD	6.7	19.94	0.78	0.11	5.44	0.16	0.039
eaf12 - 105.d	39.2	1	0.072	< LOD	< LOD	5.3	68.7	1.2	0.16	10.94	0.21	0.049
eaf12 - 106.d	58.9	1.5	NaN	< LOD	< LOD	6.2	11.53	0.64	0.12	5.39	0.13	0.042
eaf12 - 107.d	54.3	1.2	0.036	< LOD	< LOD	5.7	19.23	0.92	0.17	6.32	0.19	0.032
eaf12 - 108.d	51.2	1.1	NaN	< LOD	< LOD	9.4	33.8	1.2	0.14	7.65	0.2	0.044
eaf12 - 109.d	36.35	0.9	NaN	< LOD	< LOD	7.7	88.5	1.9	0.13	13.34	0.21	0.041
eaf12 - 110.d	56.1	1.2	NaN	< LOD	< LOD	6.6	95.2	1.8	0.24	12	0.23	0.044
eaf12 - 111.d	53.7	1.4	NaN	5.9	2.8	5.7	62.9	2	0.066	9.59	0.18	0.041
eaf12 - 112.d	53	1.4	0.066	< LOD	< LOD	5.5	42.3	1.4	0.11	7.76	0.19	0.029
eaf12 - 113.d	53.9	1.1	0.033	< LOD	< LOD	5.9	61.7	1.9	0.12	9.23	0.21	0.062
eaf12 - 114.d	50.8	0.95	0.033	< LOD	< LOD	5.1	40	1.6	0.23	6.78	0.21	0.05
eaf12 - 115.d	97.1	1.6	NaN	< LOD	< LOD	8.3	90.8	1.6	0.15	12.3	0.24	0.036
eaf12 - 116.d	55.1	1.2	0.067	< LOD	< LOD	5.2	55.4	1.3	0.18	8.75	0.16	0.043
eaf12 - 117.d	84.5	1.3	0.053	< LOD	< LOD	7.5	27.2	1.1	0.16	5.72	0.14	0.044

Analysis number	W182 ppm	W182 ppm 2SE	W182 ppm LOD	Pb204 ppm	Pb204 ppm 2SE	Pb204 ppm LOD	Pb206 ppm	Pb206 ppm 2SE	Pb206 ppm LOD	Pb207 ppm	Pb207 ppm 2SE	Pb207 ppm LOD
eaf12 - 118.d	34.59	0.9	NaN	< LOD	< LOD	5.4	25.58	0.65	0.13	5.62	0.12	0.046
eaf12 - 119.d	41.36	0.99	NaN	< LOD	< LOD	7.3	34.7	0.98	0.11	6.43	0.16	0.035
eaf12 - 120.d	76.8	1.8	NaN	< LOD	< LOD	6	43.3	1.5	0.2	7.7	0.16	0.052
eaf12 - 121.d	30.83	0.92	NaN	< LOD	< LOD	5.7	36.3	1.1	0.28	6.48	0.19	0.034
eaf12 - 122.d	54.8	1.4	0.032	< LOD	< LOD	6.1	40.1	1.6	0.13	6.98	0.17	0.045
eaf12 - 123.d	44.9	1.1	0.033	< LOD	< LOD	6.2	62.6	1.4	0.14	9.54	0.18	0.037
eaf12 - 124.d	30.26	0.88	0.045	6.2	1.6	5.1	88.1	2	0.15	12.41	0.21	0.04
eaf12 - 125.d	37.93	0.92	NaN	< LOD	< LOD	6.1	81.7	2	0.13	11.62	0.22	0.052
eaf12 - 126.d	46	1.2	0.036	6.4	2.4	5.3	54.3	1.9	0.18	9.86	0.2	0.046
eaf12 - 127.d	55.8	1.3	0.037	< LOD	< LOD	9	25.95	0.97	0.15	6.02	0.16	0.053
eaf12 - 128.d	71.4	1.4	NaN	< LOD	< LOD	9.7	22.26	0.66	0.17	5.41	0.16	0.041
eaf12 - 129.d	80.8	2.3	NaN	< LOD	< LOD	5.1	24.65	0.93	0.15	5.49	0.15	0.052
eaf12 - 130.d	57.4	1.4	0.035	< LOD	< LOD	4.9	15.45	0.69	0.14	5.5	0.16	0.05
eaf12 - 131.d	68.1	1.5	0.035	< LOD	< LOD	6.3	30.8	1.1	0.12	6.23	0.16	0.053
eaf12 - 132.d	62.7	1.3	0.1	< LOD	< LOD	6.7	9.29	0.59	0.069	4.904	0.098	0.054
eaf12 - 133.d	73.7	1.7	NaN	< LOD	< LOD	5.8	12.47	0.68	0.11	5.31	0.12	0.049
eaf12 - 134.d	77.8	1.5	NaN	< LOD	< LOD	6.9	13.47	0.63	0.11	5.34	0.12	0.044
eaf12 - 135.d	30.8	0.71	0.034	8.3	2.4	6.7	64.4	1.6	0.15	11.03	0.2	0.042
eaf12 - 136.d	38.05	0.95	0.034	5	2.5	4.2	62.7	1.6	0.15	9.24	0.16	0.039
eaf12 - 137.d	45.4	1.2	NaN	8.1	3.2	6.8	29.06	0.8	0.14	6.96	0.17	0.053
eaf12 - 138.d	53.5	1	NaN	< LOD	< LOD	8.6	25.18	0.86	0.11	5.92	0.15	0.046
eaf12 - 139.d	45.9	1.3	0.067	< LOD	< LOD	7.2	21.67	0.77	0.13	5.94	0.16	0.041
eaf12 - 140.d	54.5	1.3	NaN	< LOD	< LOD	7	16.58	0.74	0.14	5.63	0.12	0.054
eaf12 - 141.d	13.59	0.56	NaN	< LOD	< LOD	5	18.18	0.65	0.077	5.35	0.15	0.061
eaf12 - 142.d	40.6	1.4	0.067	< LOD	< LOD	11	36.5	1.1	0.18	8.52	0.16	0.046
eaf12 - 143.d	78.3	2.7	0.072	< LOD	< LOD	6	13.92	0.64	0.11	5.02	0.15	0.029
eaf12 - 144.d	50.9	1.1	0.068	< LOD	< LOD	6.2	39.5	1	0.047	6.43	0.22	0.071
eaf12 - 145.d	62.6	1.5	NaN	< LOD	< LOD	8.8	36.1	1.7	0.11	6.76	0.2	0.041
eaf12 - 146.d	53.9	2.2	NaN	< LOD	< LOD	7.7	73.6	2.4	0.21	9.87	0.31	0.038

Analysis number	W182 ppm	W182 ppm 2SE	W182 ppm LOD	Pb204 ppm	Pb204 ppm 2SE	Pb204 ppm LOD	Pb206 ppm	Pb206 ppm 2SE	Pb206 ppm LOD	Pb207 ppm	Pb207 ppm 2SE	Pb207 ppm LOD
eaf12 - 147.d	48.6	1.5	NaN	< LOD	< LOD	7.4	40.7	1.3	0.094	7.35	0.17	0.061
eaf12 - 148.d	47.6	1.4	NaN	< LOD	< LOD	7.6	49.1	1.6	0.092	7.96	0.22	0.034
eaf12 - 149.d	50.3	1	NaN	< LOD	< LOD	10	38.3	1.4	NaN	6.86	0.17	0.063
eaf12 - 150.d	44.6	0.87	NaN	< LOD	< LOD	6.4	34.94	0.89	0.093	6.79	0.15	0.033
eaf12 - 151.d	54.7	1.9	0.037	< LOD	< LOD	7.5	30.2	1.6	0.24	6.87	0.23	0.041
eaf12 - 152.d	69.4	1.5	0.037	< LOD	< LOD	8.7	25.36	0.89	0.11	5.83	0.15	0.046
eaf12 - 153.d	65.8	1.3	0.075	< LOD	< LOD	7	16.67	0.85	0.072	5.77	0.19	0.066
eaf12 - 154.d	78	2	0.074	< LOD	< LOD	7.3	21	0.8	0.11	5.54	0.18	0.042
eaf12 - 155.d	63.49	0.94	NaN	< LOD	< LOD	5	16.2	0.65	0.21	5.11	0.15	0.035
eaf12 - 156.d	51.5	1.6	NaN	< LOD	< LOD	4.1	48.6	2	0.12	8.54	0.17	0.052
eaf12 - 157.d	42.4	1.2	NaN	< LOD	< LOD	7.7	22.86	0.96	0.12	6.61	0.17	0.052
eaf12 - 158.d	46.2	1.1	0.071	< LOD	< LOD	6.2	32.1	1.1	0.11	7.02	0.18	0.034
eaf12 - 159.d	42.7	1.2	0.035	< LOD	< LOD	7.5	38.3	1.1	0.14	8.42	0.19	0.044
eaf12 - 160.d	57.5	1.4	NaN	6	2.8	5.2	11.78	0.46	0.17	4.77	0.12	0.065
eaf12 - 161.d	77.1	1.5	NaN	< LOD	< LOD	6.4	11.45	0.72	0.15	4.66	0.14	0.042
eaf12 - 162.d	41.8	0.91	NaN	< LOD	< LOD	5.2	38.3	1.1	0.047	7.67	0.17	0.053
eaf12 - 163.d	56.7	1.1	0.093	< LOD	< LOD	8.1	8.34	0.52	0.17	4.77	0.12	0.035
eaf12 - 164.d	77.1	1.8	0.033	< LOD	< LOD	7	87.8	2.4	0.13	10.39	0.24	0.043

Analysis number	Pb208 ppm	Pb208 ppm 2SE	Pb208 ppm LOD	Th232 ppm	Th232 ppm 2SE	Th232 ppm LOD	U238 ppm	U238 ppm 2SE	U238 ppm LOD	Zr in Tt temp (°C)	grain number	REE group
eaf12 - 1.d	6.03	0.16	0.033	5.08	0.2	0.014	78.3	1.5	0.018	734	1	12C
eaf12 - 2.d	5.88	0.11	0.028	6.08	0.19	NaN	86.1	1.8	0.01	737	1	12C
eaf12 - 3.d	5.579	0.099	0.025	11.53	0.35	NaN	130	3.1	0.011	745	1	12C
eaf12 - 4.d	5.86	0.12	0.034	2.45	0.12	NaN	44	1	0.007	732	2	12C
eaf12 - 5.d	5.463	0.095	0.025	3.26	0.15	0.015	42.08	0.94	0.014	724	3	12C
eaf12 - 6.d	4.88	0.12	0.028	4.12	0.17	0.021	58.1	1.3	0.01	727	3	12C
eaf12 - 7.d	6.75	0.15	0.022	9.12	0.27	0.016	108.4	1.5	0.012	739	4	12C
eaf12 - 8.d	3.877	0.068	0.025	1.597	0.083	0.015	36.11	0.66	NaN	726	5	12C
eaf12 - 9.d	4.604	0.083	0.025	1.617	0.095	0.015	27.15	0.54	NaN	728	5	12C
eaf12 - 10.d	3.952	0.093	0.025	1.582	0.077	NaN	25.3	0.98	0.014	722	5	12C
eaf12 - 11.d	4.443	0.076	0.044	7.84	0.27	NaN	23.6	1.3	NaN	695	5	12B
eaf12 - 12.d	5.04	0.11	0.026	1.28	0.064	NaN	24.57	0.52	0.01	727	5	12C
eaf12 - 13.d	3.852	0.086	0.021	4.05	0.18	0.0074	10.48	0.22	0.0051	703	5	12B
eaf12 - 14.d	5.04	0.12	0.036	0.916	0.067	NaN	17.95	0.4	0.0052	726	6	12C
eaf12 - 15.d	4.62	0.11	0.03	0.441	0.049	NaN	10.09	0.24	0.011	719	6	12C
eaf12 - 16.d	6.79	0.13	0.035	5.69	0.24	NaN	82.6	1.7	0.0051	734	7	12C
eaf12 - 17.d	4.46	0.1	0.026	1.142	0.075	NaN	27.38	0.6	0.0051	728	7	12C
eaf12 - 18.d	4.78	0.1	0.031	2.48	0.18	NaN	26.69	0.64	0.0068	722	7	12B
eaf12 - 19.d	4.98	0.19	0.026	1.07	0.16	0.012	19.76	0.32	0.0068	718	7	12B
eaf12 - 20.d	4.257	0.086	0.037	0.276	0.029	NaN	5.67	0.13	0.005	724	7	12C
eaf12 - 21.d	6.64	0.13	0.032	12.31	0.34	NaN	113.1	1.9	0.005	740	8	12C
eaf12 - 22.d	7.19	0.15	0.026	12.38	0.25	0.02	115.7	1.8	0.01	740	8	12C
eaf12 - 23.d	5.294	0.084	0.025	2.54	0.1	NaN	38.6	0.85	0.01	728	8	12C
eaf12 - 24.d	6.68	0.1	0.026	10.92	0.24	0.0072	110.2	1.4	0.011	739	8	12C
eaf12 - 25.d	6.221	0.091	0.029	7.92	0.24	NaN	95.3	1.3	NaN	735	8	12C
eaf12 - 26.d	7.34	0.15	0.036	13.12	0.37	0.033	124.1	2.1	0.01	740	8	12C
eaf12 - 27.d	5.24	0.12	0.02	2.36	0.1	NaN	25.34	0.46	0.01	724	9	12C
eaf12 - 28.d	4.243	0.092	0.027	3.81	0.17	0.0075	61.5	1.1	NaN	729	9	12C
eaf12 - 29.d	4.67	0.11	0.037	5.67	0.24	0.015	78.2	2.1	0.01	734	10	12C

Analysis number	Pb208 ppm	Pb208 ppm 2SE	Pb208 ppm LOD	Th232 ppm	Th232 ppm 2SE	Th232 ppm LOD	U238 ppm	U238 ppm 2SE	U238 ppm LOD	Zr in Tt temp (°C)	grain number	REE group
eaf12 - 30.d	6.72	0.17	0.027	10.96	0.23	0.015	120.9	2.2	NaN	742	10	12C
eaf12 - 31.d	5.93	0.13	0.025	7.7	0.23	0.016	99.3	1.6	0.018	734	10	12C
eaf12 - 32.d	6.3	0.12	0.021	2.11	0.2	0.015	24.03	0.89	0.0052	730	10	12C
eaf12 - 33.d	5.32	0.12	0.028	10.97	0.25	NaN	127.1	2.1	0.014	743	11	12C
eaf12 - 34.d	10.07	0.17	0.036	9.29	0.22	NaN	69.2	1.4	0.011	735	11	12C
eaf12 - 35.d	5.93	0.1	0.028	6.71	0.17	0.015	67.03	0.99	0.014	733	11	12C
eaf12 - 36.d	5.493	0.072	0.022	2.392	0.09	NaN	33.8	0.8	0.01	728	11	12C
eaf12 - 37.d	6.38	0.12	0.019	5.04	0.15	0.0075	64.67	0.96	0.01	732	11	12C
eaf12 - 38.d	4.86	0.14	0.034	3.08	0.15	NaN	41.3	1.1	0.011	725	12	12C
eaf12 - 39.d	4.578	0.061	0.019	4.98	0.17	0.02	61.4	1.2	NaN	731	12	12C
eaf12 - 40.d	3.82	0.1	0.025	2.72	0.23	0.016	47.8	1.3	0.0052	716	12	12B
eaf12 - 41.d	5.087	0.092	0.032	8.31	0.19	NaN	86.1	1.2	NaN	737	12	12C
eaf12 - 42.d	4.025	0.072	0.02	1.5	0.08	NaN	25.96	0.6	0.01	719	12	12B
eaf12 - 43.d	4.296	0.09	0.025	3.14	0.12	0.016	36	0.72	NaN	704	12	12B
eaf12 - 44.d	3.898	0.072	0.034	1.186	0.069	0.0073	20.26	0.38	0.022	718	12	12B
eaf12 - 45.d	4.018	0.068	0.032	1.2	0.072	0.0072	19.44	0.36	0.005	715	12	12B
eaf12 - 46.d	4.844	0.086	0.023	2.65	0.11	0.014	37.84	0.88	0.011	726	12	12C
eaf12 - 47.d	4.371	0.099	0.028	2.68	0.12	0.017	44.33	0.7	0.012	726	12	12C
eaf12 - 48.d	4.967	0.097	0.03	2.247	0.086	0.015	24.37	0.52	NaN	699	12	12B
eaf12 - 49.d	4.63	0.097	0.022	2.766	0.096	0.022	40.62	0.69	NaN	724	12	12C
eaf12 - 50.d	5.036	0.087	0.029	1.81	0.1	NaN	18.7	0.36	0.014	705	12	12B
eaf12 - 51.d	3.879	0.065	0.023	1.324	0.07	0.018	25.32	0.58	0.0054	724	13	12C
eaf12 - 52.d	4.294	0.099	0.037	1.77	0.093	0.026	27.07	0.47	0.011	731	13	12C
eaf12 - 53.d	4.078	0.093	0.031	0.549	0.056	0.0079	12.9	0.32	0.011	721	13	12C
eaf12 - 54.d	5.56	0.1	0.038	7.63	0.23	NaN	92.9	1.6	0.0075	737	14	12C
eaf12 - 55.d	4.54	0.1	0.04	3.93	0.13	0.0077	61.51	0.77	0.011	729	14	12C
eaf12 - 56.d	5.328	0.082	0.029	6.05	0.18	NaN	86.3	1.1	0.019	736	14	12C
eaf12 - 57.d	4.68	0.1	0.032	5.99	0.21	NaN	91.5	1.5	NaN	743	15	12C
eaf12 - 58.d	4.895	0.097	0.038	3.1	0.11	0.021	41.82	0.55	0.011	726	15	12C

Analysis number	Pb208 ppm	Pb208 ppm 2SE	Pb208 ppm LOD	Th232 ppm	Th232 ppm 2SE	Th232 ppm LOD	U238 ppm	U238 ppm 2SE	U238 ppm LOD	Zr in Tt temp (°C)	grain number	REE group
eaf12 - 59.d	3.98	0.086	0.032	2.76	0.12	NaN	50.16	0.98	0.023	731	15	12C
eaf12 - 60.d	4.276	0.065	0.026	0.76	0.046	0.017	23.71	0.57	NaN	724	16	12C
eaf12 - 61.d	4.31	0.088	0.027	1.028	0.063	0.016	22.37	0.5	NaN	720	16	12C
eaf12 - 62.d	3.716	0.066	0.038	2.52	0.11	NaN	96.4	1.3	0.005	721	16	12B
eaf12 - 63.d	3.274	0.066	0.024	1.79	0.1	0.015	11.26	0.38	0.012	710	16	12B
eaf12 - 64.d	14.36	0.42	0.03	11.84	0.51	0.0075	87.2	1.2	0.011	734	16	12C
eaf12 - 65.d	4.248	0.066	0.045	0.382	0.038	NaN	7.09	0.23	0.014	720	17	12C
eaf12 - 66.d	5.699	0.094	0.024	1.786	0.09	NaN	34.95	0.71	0.01	729	17	12C
eaf12 - 67.d	5.942	0.093	0.034	4.57	0.15	0.01	77.96	0.9	0.0051	731	17	12C
eaf12 - 68.d	4.34	0.1	0.026	0.688	0.054	NaN	10.83	0.31	0.011	722	17	12C
eaf12 - 69.d	3.852	0.075	0.031	9.03	0.25	NaN	21.46	0.46	0.0049	730	17	12B
eaf12 - 70.d	3.894	0.078	0.026	0.79	0.066	0.032	14.86	0.23	0.014	716	17	12C
eaf12 - 71.d	6.32	0.12	0.029	10.46	0.26	NaN	111	1.7	0.013	738	17	12C
eaf12 - 72.d	3.954	0.088	0.032	1.878	0.082	0.007	15.89	0.32	0.0078	713	17	12B
eaf12 - 73.d	5.631	0.092	0.032	9	0.18	NaN	106	1.7	0.0068	744	18	12C
eaf12 - 74.d	4.397	0.073	0.032	0.239	0.03	0.0072	10.23	0.3	0.012	724	18	12C
eaf12 - 75.d	6.04	0.11	0.029	6.16	0.17	0.014	71.5	1.2	NaN	735	19	12C
eaf12 - 76.d	4.242	0.094	0.028	2.68	0.12	0.017	54.49	0.96	0.0088	726	19	12C
eaf12 - 77.d	5.85	0.095	0.03	1.57	0.11	NaN	42.78	0.92	0.011	733	19	12C
eaf12 - 78.d	5.77	0.12	0.038	16.73	0.44	NaN	187.3	2.8	0.019	752	19	12C
eaf12 - 79.d	4.539	0.074	0.028	0.868	0.075	0.0079	9.16	0.18	0.012	721	19	12B
eaf12 - 80.d	6.12	0.14	0.032	3.94	0.18	0.0078	63.2	1.5	0.0054	734	19	12C
eaf12 - 81.d	5.7	0.1	0.028	1.287	0.063	0.0077	24.03	0.31	NaN	729	19	12C
eaf12 - 82.d	4.98	0.11	0.025	1.664	0.086	0.0078	32.43	0.64	0.0054	726	19	12C
eaf12 - 83.d	5.72	0.11	0.024	2.37	0.11	0.018	36.38	0.61	0.011	733	19	12C
eaf12 - 84.d	5.23	0.087	0.032	2.6	0.11	NaN	54.15	0.72	NaN	732	19	12C
eaf12 - 85.d	4.867	0.093	0.019	3.53	0.13	0.016	60.6	1.3	NaN	731	19	12C
eaf12 - 86.d	5.52	0.1	0.028	1.99	0.13	NaN	42.88	0.84	NaN	729	20	12C
eaf12 - 87.d	4.149	0.066	0.026	2.6	0.11	0.01	60.19	0.86	0.01	731	21	12C

Analysis number	Pb208 ppm	Pb208 ppm 2SE	Pb208 ppm LOD	Th232 ppm	Th232 ppm 2SE	Th232 ppm LOD	U238 ppm	U238 ppm 2SE	U238 ppm LOD	Zr in Tt temp (°C)	grain number	REE group
eaf12 - 88.d	3.945	0.085	0.032	2.141	0.091	NaN	55.99	0.7	0.01	731	21	12C
eaf12 - 89.d	4.569	0.099	0.029	0.644	0.048	NaN	9.16	0.22	0.01	727	22	12C
eaf12 - 90.d	4.779	0.083	0.035	1.72	0.11	0.0074	21.81	0.57	0.01	726	22	12C
eaf12 - 92.d	4.597	0.092	0.024	0.348	0.036	0.024	6.44	0.21	0.01	723	24	12C
eaf12 - 93.d	4.191	0.075	0.025	0.359	0.032	0.014	10.56	0.19	0.005	721	24	12C
eaf12 - 94.d	5	0.1	0.013	3.62	0.13	0.016	63.42	0.9	0.011	733	24	12C
eaf12 - 95.d	4.053	0.083	0.033	0.943	0.07	0.0071	10.77	0.2	0.016	714	24	12C
eaf12 - 96.d	3.823	0.074	0.033	0.849	0.062	0.014	24.56	0.49	NaN	723	24	12C
eaf12 - 97.d	4.173	0.06	0.021	0.53	0.037	NaN	13.59	0.33	0.011	726	24	12C
eaf12 - 98.d	4.89	0.11	0.032	0.822	0.063	0.014	16.82	0.36	0.01	725	24	12C
eaf12 - 99.d	4.823	0.095	0.034	0.682	0.047	NaN	15.79	0.31	0.0068	724	24	12C
eaf12 - 100.d	3.693	0.084	0.036	1.227	0.092	NaN	31.94	0.68	0.0068	729	24	12C
eaf12 - 101.d	4.484	0.067	0.029	3.81	0.14	0.025	13.86	0.4	0.011	706	24	12B
eaf12 - 102.d	6.64	0.11	0.033	7.6	0.23	NaN	116.8	1.8	NaN	739	24	12C
eaf12 - 103.d	5.71	0.11	0.025	5.72	0.26	NaN	81.2	1.4	0.011	734	25	12C
eaf12 - 104.d	4.154	0.086	0.031	2.174	0.088	0.019	21.79	0.37	0.011	715	25	12B
eaf12 - 105.d	5.96	0.1	0.027	5.05	0.2	0.016	89.7	1.4	NaN	736	26	12C
eaf12 - 106.d	4.75	0.11	0.021	0.561	0.04	NaN	9.94	0.27	0.012	727	26	12C
eaf12 - 107.d	4.873	0.097	0.028	0.977	0.089	NaN	19.88	0.94	0.016	723	26	12C
eaf12 - 108.d	5.4	0.12	0.018	2.34	0.11	0.016	37.89	0.98	0.01	731	26	12C
eaf12 - 109.d	7.55	0.14	0.036	8.86	0.26	NaN	118.2	1.5	NaN	740	26	12C
eaf12 - 110.d	5.152	0.092	0.024	13.28	0.32	0.015	129.6	2	0.01	746	26	12C
eaf12 - 111.d	5.065	0.098	0.028	6.15	0.25	0.0075	81.8	1.7	0.018	737	27	12C
eaf12 - 112.d	4.502	0.092	0.026	3.75	0.14	NaN	53.59	0.81	NaN	728	27	12C
eaf12 - 113.d	4.422	0.085	0.033	6.09	0.18	0.0073	80	1	0.014	735	27	12C
eaf12 - 114.d	3.871	0.083	0.037	2.9	0.17	0.016	54.1	1.6	0.016	726	27	12C
eaf12 - 115.d	9.64	0.16	0.03	54.94	0.89	NaN	108	1.5	0.0049	762	28	12A
eaf12 - 116.d	5.54	0.11	0.027	12.23	0.35	NaN	65.1	1.6	NaN	739	28	12A
eaf12 - 117.d	3.969	0.083	0.022	3.61	0.27	0.0071	32.02	0.86	NaN	729	28	12C

Analysis number	Pb208 ppm	Pb208 ppm 2SE	Pb208 ppm LOD	Th232 ppm	Th232 ppm 2SE	Th232 ppm LOD	U238 ppm	U238 ppm 2SE	U238 ppm LOD	Zr in Tt temp (°C)	grain number	REE group
eaf12 - 118.d	4.752	0.083	0.021	9.81	0.28	0.015	29.08	0.63	NaN	744	28	12A
eaf12 - 119.d	5.613	0.091	0.037	19.76	0.41	0.014	37.14	0.67	0.0049	726	28	12A
eaf12 - 120.d	6.33	0.13	0.038	21.99	0.37	0.016	47.58	0.71	0.0099	732	28	12A
eaf12 - 121.d	4.892	0.095	0.032	15.41	0.34	NaN	46.87	0.77	0.0049	728	28	12A
eaf12 - 122.d	5.5	0.11	0.022	19.1	1.4	NaN	50.1	1.9	0.011	734	28	12A
eaf12 - 123.d	4.93	0.083	0.037	6.21	0.17	0.014	83.1	1.2	NaN	735	29	12C
eaf12 - 124.d	5.91	0.13	0.025	10.87	0.22	0.016	115.8	2	0.022	744	29	12C
eaf12 - 125.d	5.67	0.12	0.031	9.07	0.18	0.014	108	1.5	0.0099	740	29	12C
eaf12 - 126.d	5.73	0.12	0.027	4.78	0.18	0.028	69.9	1.1	0.011	735	29	12C
eaf12 - 127.d	4.251	0.099	0.026	1.97	0.12	0.016	30.5	1.4	0.015	742	29	12C
eaf12 - 128.d	3.704	0.086	0.025	0.967	0.081	0.011	27.16	0.75	0.011	722	30	12C
eaf12 - 129.d	3.745	0.085	0.031	0.512	0.046	0.017	27.63	0.68	0.0055	722	30	12C
eaf12 - 130.d	4.616	0.082	0.027	0.606	0.044	0.015	16.7	0.5	NaN	730	31	12C
eaf12 - 131.d	4.1	0.076	0.028	3.05	0.13	0.027	38.29	0.7	0.022	721	31	12C
eaf12 - 132.d	4.61	0.069	0.032	0.687	0.057	NaN	6.1	0.2	0.0054	724	31	12B
eaf12 - 133.d	4.531	0.075	0.026	0.867	0.059	NaN	11.17	0.2	0.011	721	31	12C
eaf12 - 134.d	4.43	0.079	0.025	0.96	0.065	0.02	12.05	0.24	NaN	720	31	12C
eaf12 - 135.d	6.94	0.13	0.028	5.85	0.16	0.016	78.8	1.5	0.011	734	31	12C
eaf12 - 136.d	4.502	0.088	0.024	4.81	0.16	0.016	81.7	1.1	0.0051	735	32	12C
eaf12 - 137.d	4.838	0.078	0.03	1.946	0.09	0.015	35.23	0.5	0.015	732	32	12C
eaf12 - 138.d	4.237	0.093	0.026	1.438	0.088	0.016	29.67	0.49	0.022	731	32	12C
eaf12 - 139.d	4.546	0.091	0.015	0.974	0.066	0.0073	23.59	0.51	0.011	728	32	12C
eaf12 - 140.d	4.521	0.087	0.02	0.89	0.048	NaN	17.42	0.39	0.0051	729	32	12C
eaf12 - 141.d	4.457	0.097	0.026	4.41	0.16	0.015	19.41	0.4	0.0069	677	33	12B
eaf12 - 142.d	5.76	0.1	0.021	1.7	0.084	0.014	43.13	0.78	NaN	730	33	12C
eaf12 - 143.d	4.172	0.096	0.026	0.582	0.051	NaN	13.51	0.52	0.0049	720	33	12B
eaf12 - 144.d	3.42	0.094	0.025	1.944	0.099	0.0073	50.42	0.99	0.011	733	33	12C
eaf12 - 145.d	4.135	0.091	0.032	2.35	0.14	0.016	47.6	1.5	0.0051	729	33	12C
eaf12 - 146.d	4.39	0.1	0.03	9.11	0.33	0.0072	98.9	2.7	0.016	741	34	12C

Analysis number	Pb208 ppm	Pb208 ppm 2SE	Pb208 ppm LOD	Th232 ppm	Th232 ppm 2SE	Th232 ppm LOD	U238 ppm	U238 ppm 2SE	U238 ppm LOD	Zr in Tt temp (°C)	grain number	REE group
eaf12 - 147.d	4.426	0.079	0.027	3.85	0.15	NaN	51.7	1.1	0.012	727	34	12C
eaf12 - 148.d	4.375	0.095	0.024	4.78	0.15	0.02	63	1.2	NaN	731	34	12C
eaf12 - 149.d	4.293	0.084	0.035	3.57	0.14	NaN	45.2	1.1	0.012	725	34	12C
eaf12 - 150.d	4.42	0.11	0.021	4.03	0.13	0.021	44.51	0.95	0.011	722	34	12C
eaf12 - 151.d	4.84	0.11	0.036	2.75	0.13	0.008	34.5	1.4	0.012	727	34	12C
eaf12 - 152.d	4.067	0.084	0.038	0.786	0.065	0.008	31.24	0.57	0.016	726	35	12C
eaf12 - 153.d	4.619	0.095	0.025	0.553	0.077	NaN	14.4	1	0.016	720	36	12C
eaf12 - 154.d	3.88	0.1	0.028	0.437	0.049	NaN	25.14	0.95	0.0075	720	37	12C
eaf12 - 155.d	4.038	0.065	0.023	1.372	0.084	0.0079	17.62	0.36	0.011	727	38	12C
eaf12 - 156.d	4.78	0.11	0.036	4.58	0.17	0.017	63.3	1.6	0.013	734	38	12C
eaf12 - 157.d	4.88	0.12	0.032	1.49	0.12	0.018	25	1.1	0.015	727	39	12C
eaf12 - 158.d	4.87	0.1	0.033	2.48	0.14	0.015	36.3	1.3	0.0085	730	39	12C
eaf12 - 159.d	5.589	0.096	0.027	3.67	0.15	0.015	44.13	0.74	0.015	731	39	12C
eaf12 - 160.d	4.04	0.1	0.026	0.455	0.046	0.015	9.89	0.44	NaN	723	39	12C
eaf12 - 161.d	4.036	0.087	0.026	0.265	0.033	0.015	10.25	0.42	NaN	711	40	12C
eaf12 - 162.d	4.905	0.07	0.023	2.66	0.12	0.0072	47.24	0.75	NaN	731	41	12C
eaf12 - 163.d	4.313	0.096	0.028	0.113	0.023	NaN	5	0.17	0.0051	725	41	12C
eaf12 - 164.d	4.233	0.093	0.03	13.55	0.39	0.028	117.9	2.4	0.0048	741	41	12C

Analysis number	$^{238}U/^{206}Pb$	±1s	$^{207}Pb/^{206}Pb$	±1s	$^{238}U/^{206}Pb$ age (Ma)	±1s	$^{207}Pb/^{206}Pb$ age (Ma)	±1s	Disc (%)	f207%	^{207}Pb-corrected $^{238}U/^{206}Pb$ Age (Ma)	±1s
eaf12 - 1.d	4.6128423	0.0635	0.1386	0.0023	1265	16	2210	29	43	9	1159	16
eaf12 - 2.d	4.710704	0.0525	0.1289	0.0015	1241	12	2083	20	40	8	1154	13
eaf12 - 3.d	4.9644309	0.048	0.109	0.0011	1183	10	1783	18	34	5	1131	11
eaf12 - 4.d	4.3949618	0.0643	0.1894	0.0032	1322	17	2737	28	52	17	1115	18
eaf12 - 5.d	4.3635552	0.0866	0.1811	0.0041	1330	23	2663	37	50	16	1139	24
eaf12 - 6.d	4.4775435	0.0758	0.1407	0.0022	1299	20	2236	26	42	9	1189	20
eaf12 - 7.d	4.6858513	0.0455	0.1167	0.0014	1247	11	1906	21	35	6	1182	12
eaf12 - 8.d	4.3058616	0.08	0.1617	0.0029	1346	22	2474	29	46	12	1193	23
eaf12 - 9.d	4.2645133	0.0786	0.2075	0.004	1358	22	2886	31	53	20	1111	23
eaf12 - 10.d	4.2813322	0.0774	0.214	0.0045	1353	22	2936	33	54	21	1093	23
eaf12 - 11.d	3.7204874	0.0758	0.1924	0.0036	1535	27	2763	30	44	17	1305	28
eaf12 - 12.d	3.9538648	0.0805	0.2256	0.0042	1454	26	3021	29	52	22	1156	26
eaf12 - 13.d	3.3689655	0.0879	0.301	0.008	1676	38	3475	41	52	34	1157	39
eaf12 - 14.d	3.5270758	0.0771	0.249	0.0055	1609	31	3178	35	49	26	1235	32
eaf12 - 15.d	3.1414791	0.0973	0.344	0.0085	1782	47	3681	37	52	40	1120	45
eaf12 - 16.d	4.5357474	0.0647	0.1316	0.002	1284	16	2119	26	39	8	1192	17
eaf12 - 17.d	3.863187	0.0623	0.1904	0.0034	1484	21	2746	29	46	16	1262	22
eaf12 - 18.d	4.2093925	0.0847	0.2056	0.0048	1374	24	2871	37	52	19	1129	25
eaf12 - 19.d	3.8893312	0.0812	0.228	0.0055	1475	27	3038	38	51	23	1170	28
eaf12 - 20.d	2.4609572	0.0753	0.474	0.014	2198	56	4162	43	47	60	962	68
eaf12 - 21.d	4.7798434	0.0546	0.1198	0.0014	1225	13	1953	21	37	6	1154	13
eaf12 - 22.d	4.796269	0.058	0.1172	0.0016	1221	13	1914	24	36	6	1155	14
eaf12 - 23.d	4.2478261	0.072	0.1818	0.0033	1363	20	2669	30	49	16	1168	21
eaf12 - 24.d	4.7312349	0.0589	0.1184	0.0013	1236	14	1932	20	36	6	1168	15
eaf12 - 25.d	4.7038999	0.0553	0.1275	0.0018	1243	13	2064	24	40	7	1158	14
eaf12 - 26.d	4.8057059	0.054	0.1125	0.0013	1219	12	1840	21	34	5	1161	13
eaf12 - 27.d	3.675696	0.071	0.2013	0.0037	1551	26	2837	29	45	18	1300	27
eaf12 - 28.d	4.7289448	0.064	0.1259	0.002	1237	15	2041	28	39	7	1155	16
eaf12 - 29.d	4.7868692	0.0599	0.1232	0.0014	1223	14	2003	19	39	7	1146	14

Analysis number	$^{238}U/^{206}Pb$	±1s	$^{207}Pb/^{206}Pb$	±1s	$^{238}U/^{206}Pb$ age (Ma)	±1s	$^{207}Pb/^{206}Pb$ age (Ma)	±1s	Disc (%)	f207%	^{207}Pb-corrected $^{238}U/^{206}Pb$ Age (Ma)	±1s
eaf12 - 30.d	4.7915645	0.0497	0.1101	0.0012	1222	11	1801	19	32	5	1169	12
eaf12 - 31.d	4.9770759	0.0614	0.1219	0.0014	1180	13	1984	20	41	7	1106	14
eaf12 - 32.d	4.7939156	0.0981	0.301	0.0075	1221	22	3475	38	65	35	821	24
eaf12 - 33.d	4.9070819	0.0557	0.1055	0.0014	1196	12	1723	24	31	4	1150	13
eaf12 - 34.d	4.2112069	0.0625	0.1634	0.0025	1373	18	2491	25	45	13	1216	19
eaf12 - 35.d	4.4530538	0.0638	0.1431	0.0021	1306	17	2265	25	42	10	1191	17
eaf12 - 36.d	4.1415854	0.0831	0.2057	0.0042	1394	25	2872	33	51	19	1147	25
eaf12 - 37.d	4.5085371	0.0738	0.1594	0.003	1291	19	2449	31	47	12	1145	20
eaf12 - 38.d	4.0640599	0.0716	0.1643	0.0029	1418	22	2500	29	43	12	1257	23
eaf12 - 39.d	4.6172023	0.0616	0.1306	0.0019	1264	15	2106	25	40	8	1173	16
eaf12 - 40.d	4.6063178	0.0644	0.143	0.0025	1266	16	2264	29	44	10	1153	17
eaf12 - 41.d	4.8438275	0.0677	0.1202	0.0015	1210	15	1959	22	38	6	1138	16
eaf12 - 42.d	4.2148404	0.0779	0.1991	0.0043	1372	22	2819	35	51	18	1141	23
eaf12 - 43.d	4.5315399	0.0774	0.1657	0.0033	1285	20	2515	33	49	13	1128	20
eaf12 - 44.d	3.8924303	0.0918	0.2207	0.0046	1474	30	2986	33	51	21	1185	30
eaf12 - 45.d	3.8464567	0.0825	0.2289	0.0048	1490	28	3044	33	51	23	1180	28
eaf12 - 46.d	4.5043799	0.0786	0.1753	0.0029	1292	20	2609	27	50	15	1116	20
eaf12 - 47.d	4.0776294	0.061	0.1493	0.0024	1414	19	2338	27	40	10	1285	20
eaf12 - 48.d	6.4318631	0.1885	0.294	0.009	932	25	3439	47	73	34	626	23
eaf12 - 49.d	4.3480196	0.0694	0.1671	0.0031	1334	19	2529	30	47	13	1171	20
eaf12 - 50.d	3.8924303	0.0994	0.263	0.0065	1474	33	3265	38	55	28	1090	33
eaf12 - 51.d	4.3077601	0.0837	0.2027	0.0047	1346	23	2848	37	53	19	1110	14
eaf12 - 52.d	4.3811659	0.0759	0.203	0.0032	1325	20	2850	25	54	19	1091	24
eaf12 - 53.d	3.4522968	0.086	0.289	0.006	1640	35	3412	32	52	32	1160	35
eaf12 - 54.d	4.7915645	0.059	0.1176	0.0013	1222	14	1920	20	36	6	1155	26
eaf12 - 55.d	4.4429286	0.0608	0.1282	0.0023	1309	16	2073	31	37	7	1223	15
eaf12 - 56.d	4.6193853	0.0597	0.1202	0.0014	1263	15	1959	20	36	6	1192	27
eaf12 - 57.d	4.863116	0.0726	0.1146	0.0013	1205	16	1874	20	36	6	1144	17
eaf12 - 58.d	4.3674564	0.0709	0.1703	0.0029	1329	19	2561	28	48	14	1160	35

Analysis number	$^{238}U/^{206}Pb$	±1s	$^{207}Pb/^{206}Pb$	±1s	$^{238}U/^{206}Pb$ age (Ma)	±1s	$^{207}Pb/^{206}Pb$ age (Ma)	±1s	Disc (%)	f207%	^{207}Pb-corrected $^{238}U/^{206}Pb$ Age (Ma)	±1s
eaf12 - 59.d	4.7038999	0.074	0.1383	0.0024	1243	18	2206	30	44	9	1138	17
eaf12 - 60.d	3.8769841	0.0599	0.2065	0.0049	1479	20	2878	38	49	19	1222	23
eaf12 - 61.d	3.5787546	0.0728	0.1986	0.0042	1588	28	2815	34	44	17	1341	30
eaf12 - 62.d	4.2166595	0.0553	0.1098	0.0015	1372	16	1796	25	24	4	1326	17
eaf12 - 63.d	3.2785235	0.0891	0.264	0.0075	1716	40	3271	44	48	28	1287	42
eaf12 - 64.d	4.0040984	0.0439	0.1448	0.0018	1437	14	2285	21	37	9	1318	15
eaf12 - 65.d	2.6548913	0.0722	0.408	0.009	2061	47	3939	33	48	50	1110	50
eaf12 - 66.d	4.2331023	0.0664	0.2099	0.0036	1367	19	2905	27	53	20	1114	20
eaf12 - 67.d	4.6971154	0.0602	0.1426	0.0019	1244	14	2259	22	45	10	1132	15
eaf12 - 68.d	3.2458472	0.0927	0.328	0.0095	1731	42	3608	44	52	38	1128	44
eaf12 - 69.d	3.9650974	0.0679	0.1916	0.0045	1450	22	2756	38	47	17	1228	24
eaf12 - 70.d	3.8015564	0.117	0.268	0.0085	1505	40	3294	49	54	29	1104	40
eaf12 - 71.d	4.7427184	0.051	0.119	0.0015	1233	12	1941	22	36	6	1164	13
eaf12 - 72.d	3.7765752	0.0792	0.257	0.005	1514	28	3228	30	53	27	1137	28
eaf12 - 73.d	4.796269	0.058	0.1127	0.0012	1221	13	1843	19	34	5	1163	14
eaf12 - 74.d	3.0436137	0.0964	0.339	0.009	1831	49	3658	40	50	39	1169	48
eaf12 - 75.d	4.6791188	0.0609	0.1451	0.0016	1249	15	2289	18	45	10	1131	15
eaf12 - 76.d	4.4857668	0.0674	0.1411	0.0023	1297	17	2241	28	42	9	1187	18
eaf12 - 77.d	4.315371	0.049	0.189	0.0029	1344	14	2733	25	51	17	1136	15
eaf12 - 78.d	4.9974425	0.0527	0.0917	0.0009	1176	11	1461	19	20	2	1154	12
eaf12 - 79.d	3.0341615	0.0959	0.384	0.0135	1836	49	3848	52	52	47	1044	55
eaf12 - 80.d	4.5547786	0.0528	0.1544	0.002	1279	13	2395	22	47	12	1144	14
eaf12 - 81.d	3.7722008	0.0938	0.254	0.0065	1516	33	3210	40	53	27	1145	33
eaf12 - 82.d	4.0589946	0.0628	0.1936	0.0036	1420	19	2773	30	49	17	1196	21
eaf12 - 83.d	4.3096603	0.0865	0.1984	0.0049	1345	24	2813	39	52	18	1118	25
eaf12 - 84.d	4.4409091	0.0544	0.1537	0.0022	1309	14	2388	24	45	11	1174	15
eaf12 - 85.d	4.7542579	0.0562	0.1433	0.0015	1231	13	2267	18	46	10	1117	14
eaf12 - 86.d	4.2422927	0.0624	0.1787	0.0033	1364	18	2641	30	48	15	1176	19
eaf12 - 87.d	4.7061657	0.0646	0.1337	0.0026	1242	15	2147	33	42	8	1146	16

Analysis number	$^{238}U/^{206}Pb$	±1s	$^{207}Pb/^{206}Pb$	±1s	$^{238}U/^{206}Pb$ age (Ma)	±1s	$^{207}Pb/^{206}Pb$ age (Ma)	±1s	Disc (%)	f207%	^{207}Pb-corrected $^{238}U/^{206}Pb$ Age (Ma)	±1s
eaf12 - 88.d	4.7084337	0.0774	0.1286	0.0019	1242	18	2079	25	40	8	1155	19
eaf12 - 89.d	3.0247678	0.0684	0.381	0.0095	1841	36	3836	37	52	46	1055	42
eaf12 - 90.d	3.7941748	0.0728	0.2387	0.0044	1508	25	3111	29	52	24	1174	26
eaf12 - 92.d	2.5643045	0.0809	0.438	0.0135	2123	56	4045	45	48	55	1046	64
eaf12 - 93.d	3.1928105	0.09	0.326	0.0085	1756	42	3598	39	51	38	1151	43
eaf12 - 94.d	4.5696913	0.0549	0.1372	0.0016	1276	14	2192	20	42	9	1173	14
eaf12 - 95.d	3.2350993	0.0922	0.326	0.009	1736	42	3598	42	52	38	1137	43
eaf12 - 96.d	4.0371901	0.0981	0.1951	0.0042	1427	30	2786	34	49	17	1199	31
eaf12 - 97.d	3.5656934	0.0848	0.293	0.006	1594	33	3434	31	54	33	1115	33
eaf12 - 98.d	3.4160839	0.073	0.28	0.0065	1655	31	3363	36	51	30	1195	33
eaf12 - 99.d	3.5270758	0.0832	0.289	0.0085	1609	33	3412	45	53	32	1136	36
eaf12 - 100.d	4.3460854	0.0878	0.1699	0.0032	1335	24	2557	31	48	14	1166	24
eaf12 - 101.d	3.5919118	0.0988	0.292	0.0075	1583	38	3428	39	54	33	1109	37
eaf12 - 102.d	4.7312349	0.0558	0.1187	0.0012	1236	13	1937	17	36	6	1168	14
eaf12 - 103.d	4.6880998	0.0601	0.1334	0.0018	1246	14	2143	23	42	8	1151	15
eaf12 - 104.d	3.9747762	0.082	0.221	0.0055	1447	26	2988	39	52	22	1160	28
eaf12 - 105.d	4.7038999	0.0543	0.1293	0.0013	1243	13	2088	18	41	8	1155	13
eaf12 - 106.d	3.1414791	0.0973	0.379	0.0105	1782	47	3828	41	53	46	1023	48
eaf12 - 107.d	3.6923658	0.0729	0.269	0.007	1545	27	3300	40	53	29	1134	30
eaf12 - 108.d	4.0539419	0.0793	0.1834	0.0038	1421	25	2684	33	47	16	1219	25
eaf12 - 109.d	4.8825587	0.0553	0.122	0.0014	1201	12	1986	20	40	7	1126	13
eaf12 - 110.d	4.9293643	0.0486	0.1005	0.0011	1191	11	1633	19	27	3	1154	11
eaf12 - 111.d	4.7198068	0.0702	0.125	0.0017	1239	17	2029	23	39	7	1159	17
eaf12 - 112.d	4.5378542	0.0628	0.1467	0.0024	1284	16	2308	28	44	10	1162	15
eaf12 - 113.d	4.6724055	0.0828	0.1203	0.0017	1250	20	1961	25	36	6	1179	21
eaf12 - 114.d	4.8246914	0.0728	0.139	0.0029	1214	16	2215	36	45	9	1109	16
eaf12 - 115.d	4.2757112	0.0469	0.1085	0.0012	1355	13	1774	20	24	4	1310	52
eaf12 - 116.d	4.3364403	0.0577	0.1311	0.002	1338	16	2113	26	37	7	1247	16
eaf12 - 117.d	4.3134658	0.0931	0.1714	0.0038	1344	26	2571	36	48	14	1172	15

Analysis number	$^{238}U/^{206}Pb$	±1s	$^{207}Pb/^{206}Pb$	±1s	$^{238}U/^{206}Pb$ age (Ma)	±1s	$^{207}Pb/^{206}Pb$ age (Ma)	±1s	Disc (%)	f207%	^{207}Pb-corrected $^{238}U/^{206}Pb$ Age (Ma)	±1s
eaf12 - 118.d	4.1171513	0.0683	0.1793	0.0027	1402	21	2646	24	47	15	1210	26
eaf12 - 119.d	3.8816051	0.0538	0.1503	0.0023	1478	18	2349	25	37	10	1347	19
eaf12 - 120.d	3.9828781	0.0685	0.1441	0.0026	1444	22	2277	30	37	9	1327	25
eaf12 - 121.d	4.6858513	0.06	0.1424	0.0021	1247	14	2257	25	45	10	1135	17
eaf12 - 122.d	4.4632252	0.0774	0.1401	0.0028	1303	20	2228	34	42	9	1194	20
eaf12 - 123.d	4.8009828	0.0602	0.1212	0.0015	1220	14	1974	22	38	7	1147	21
eaf12 - 124.d	4.6813608	0.0682	0.1127	0.0014	1248	16	1843	22	32	5	1191	19
eaf12 - 125.d	4.7939156	0.0611	0.1138	0.0015	1221	14	1861	23	34	5	1162	23
eaf12 - 126.d	4.6435361	0.0622	0.1481	0.0021	1257	15	2324	24	46	11	1134	15
eaf12 - 127.d	4.3306738	0.0966	0.1913	0.005	1339	26	2753	42	51	17	1127	23
eaf12 - 128.d	4.4693504	0.0727	0.1962	0.003	1302	19	2795	25	53	18	1083	23
eaf12 - 129.d	4.0623701	0.0723	0.1794	0.0036	1419	22	2647	33	46	15	1225	18
eaf12 - 130.d	3.8616601	0.0979	0.284	0.0075	1484	33	3385	41	56	32	1051	33
eaf12 - 131.d	4.5696913	0.0899	0.1629	0.003	1276	22	2486	30	49	13	1124	23
eaf12 - 132.d	2.436409	0.0827	0.444	0.016	2217	62	4065	53	45	56	1078	76
eaf12 - 133.d	3.2785235	0.0891	0.346	0.0085	1716	40	3689	37	53	41	1069	41
eaf12 - 134.d	3.2785235	0.0785	0.319	0.0075	1716	35	3565	36	52	37	1141	37
eaf12 - 135.d	4.529439	0.0655	0.1389	0.0021	1286	17	2214	25	42	9	1180	17
eaf12 - 136.d	4.7705078	0.0607	0.1198	0.0017	1227	14	1953	24	37	6	1156	15
eaf12 - 137.d	4.2982842	0.0611	0.1886	0.0034	1348	17	2730	29	51	17	1141	18
eaf12 - 138.d	4.2552265	0.0801	0.1918	0.0046	1361	23	2758	38	51	17	1146	24
eaf12 - 139.d	3.9861281	0.0716	0.222	0.0055	1443	23	2995	39	52	22	1155	25
eaf12 - 140.d	3.8769841	0.0911	0.273	0.0055	1479	30	3323	31	55	30	1072	30
eaf12 - 141.d	3.9095638	0.0774	0.2358	0.0044	1468	26	3092	29	53	24	1146	26
eaf12 - 142.d	4.2257785	0.0645	0.1852	0.003	1369	19	2700	26	49	16	1167	19
eaf12 - 143.d	3.4768683	0.0752	0.3	0.0075	1630	31	3470	38	53	34	1125	34
eaf12 - 144.d	4.6768789	0.0786	0.1308	0.0024	1249	19	2109	32	41	8	1158	20
eaf12 - 145.d	4.7312349	0.063	0.1521	0.0027	1236	15	2370	29	48	11	1106	16
eaf12 - 146.d	4.9745418	0.066	0.1101	0.0016	1181	14	1801	26	34	5	1127	14

Analysis number	$^{238}U/^{206}Pb$	±1s	$^{207}Pb/^{206}Pb$	±1s	$^{238}U/^{206}Pb$ age (Ma)	±1s	$^{207}Pb/^{206}Pb$ age (Ma)	±1s	Disc (%)	f207%	^{207}Pb-corrected $^{238}U/^{206}Pb$ Age (Ma)	±1s
eaf12 - 147.d	4.5933239	0.0793	0.1453	0.003	1270	20	2291	35	45	10	1151	19
eaf12 - 148.d	4.6391263	0.0661	0.1297	0.0018	1258	16	2094	24	40	8	1170	14
eaf12 - 149.d	4.3831314	0.0685	0.1451	0.0021	1325	18	2289	24	42	10	1206	17
eaf12 - 150.d	4.5976471	0.0622	0.1553	0.0019	1269	15	2405	20	47	12	1131	17
eaf12 - 151.d	4.2331023	0.0864	0.1881	0.0043	1367	25	2726	37	50	17	1159	20
eaf12 - 152.d	4.5043799	0.0916	0.1869	0.0043	1292	23	2715	37	52	17	1093	24
eaf12 - 153.d	3.0820189	0.1035	0.279	0.0085	1811	51	3357	47	46	30	1325	21
eaf12 - 154.d	4.2888499	0.0776	0.219	0.0055	1351	22	2973	40	55	22	1081	22
eaf12 - 155.d	4.0205761	0.0813	0.249	0.0055	1432	25	3178	35	55	26	1087	21
eaf12 - 156.d	4.710704	0.0774	0.14	0.0024	1241	18	2227	29	44	9	1133	17
eaf12 - 157.d	3.9554656	0.0867	0.229	0.0055	1453	28	3045	38	52	23	1148	29
eaf12 - 158.d	4.1258446	0.0792	0.1766	0.0036	1399	24	2621	33	47	15	1213	25
eaf12 - 159.d	4.2003439	0.0664	0.1771	0.0027	1377	19	2626	25	48	15	1191	20
eaf12 - 160.d	3.111465	0.0764	0.326	0.007	1797	38	3598	33	50	37	1181	39
eaf12 - 161.d	3.2458472	0.1086	0.338	0.012	1731	49	3654	53	53	40	1101	52
eaf12 - 162.d	4.4611872	0.0696	0.1627	0.0028	1304	18	2484	29	48	13	1151	19
eaf12 - 163.d	2.1285403	0.0701	0.468	0.0175	2483	66	4143	54	40	59	1132	90
eaf12 - 164.d	4.8462302	0.0547	0.0961	0.0012	1209	12	1550	23	22	3	1181	13

Analysis number	Reason for exclusion
eaf12 - 91.d	Zr inclusion

Table A6.4-3 LA-ICPMS analytical data for sample EAF35.

Analysis number	Na23 ppm	Na23 ppm 2SE	Na23 ppm LOD	Al27 ppm	Al27 ppm 2SE	Al27 ppm LOD	Si28 ppm	Si28 ppm 2SE	Si28 ppm LOD	Ca44 ppm	Ca44 ppm 2SE	Ca44 ppm LOD
eaf35 - 1.d	318	15	34	24240	260	5.5	1.38E+05	1.80E+03	4700	1.97E+05	3.50E+03	910
eaf35 - 2.d	348	14	47	20900	190	7	1.35E+05	2.20E+03	11000	2.03E+05	2.70E+03	640
eaf35 - 3.d	278	16	33	23470	300	5.7	1.41E+05	2.00E+03	5600	2.04E+05	3.40E+03	920
eaf35 - 4.d	328	13	47	27380	310	7.5	1.40E+05	2.00E+03	3600	2.01E+05	3.70E+03	980
eaf35 - 5.d	305	15	34	26670	300	8.2	1.37E+05	2.10E+03	4800	1.97E+05	3.40E+03	990
eaf35 - 6.d	317	14	40	23330	300	5.4	1.42E+05	2.00E+03	8600	1.97E+05	3.00E+03	900
eaf35 - 7.d	352	18	36	26200	250	5.9	1.42E+05	2.30E+03	4600	2.01E+05	3.10E+03	1100
eaf35 - 8.d	327	15	39	25770	390	4.5	1.40E+05	2.60E+03	8100	2.01E+05	3.30E+03	1100
eaf35 - 9.d	316	16	28	24910	360	6	1.37E+05	2.70E+03	5400	2.00E+05	4.20E+03	1100
eaf35 - 10.d	296	11	40	21630	260	7.2	1.39E+05	1.70E+03	7600	2.04E+05	2.70E+03	950
eaf35 - 11.d	315	12	20	23110	370	5.9	1.40E+05	1.70E+03	3900	2.05E+05	4.20E+03	1300
eaf35 - 12.d	390	15	39	25850	310	7.3	1.38E+05	2.20E+03	5000	2.00E+05	3.90E+03	720
eaf35 - 13.d	349	16	33	25710	290	6.5	1.36E+05	1.80E+03	6600	2.01E+05	3.30E+03	1100
eaf35 - 14.d	354	15	49	27250	280	6.7	1.41E+05	2.10E+03	3500	2.03E+05	3.10E+03	1100
eaf35 - 15.d	337	15	65	26390	390	9.2	1.36E+05	2.90E+03	10000	2.02E+05	2.90E+03	870
eaf35 - 16.d	335	18	39	24360	290	5.5	1.38E+05	2.00E+03	4200	1.98E+05	3.70E+03	870
eaf35 - 17.d	383	19	38	29030	430	8.9	1.40E+05	2.50E+03	6100	1.94E+05	4.00E+03	1100
eaf35 - 18.d	214	12	41	20630	230	6.9	1.39E+05	2.60E+03	5000	2.01E+05	2.80E+03	870
eaf35 - 19.d	356	15	56	24300	250	8	1.37E+05	2.70E+03	14000	2.01E+05	3.30E+03	1000
eaf35 - 20.d	332	12	38	23310	260	5	1.37E+05	1.80E+03	4500	2.05E+05	3.30E+03	960
eaf35 - 22.d	295	15	29	29640	350	5.2	1.42E+05	2.20E+03	10000	1.94E+05	3.60E+03	1200
eaf35 - 23.d	314	18	40	25250	290	4.1	1.43E+05	1.50E+03	5200	2.01E+05	3.30E+03	810
eaf35 - 24.d	352	14	53	28250	410	5.8	1.38E+05	1.90E+03	5100	2.03E+05	2.20E+03	870
eaf35 - 25.d	350	13	39	23720	270	6	1.42E+05	2.00E+03	12000	2.02E+05	3.30E+03	1200
eaf35 - 26.d	327	12	31	24980	320	5.5	1.39E+05	2.50E+03	7100	2.03E+05	3.40E+03	980
eaf35 - 27.d	247	13	42	26940	380	5.2	1.39E+05	2.40E+03	7000	2.03E+05	3.80E+03	660
eaf35 - 28.d	323	15	48	23070	310	7.4	1.37E+05	2.50E+03	7000	2.06E+05	3.60E+03	1000
eaf35 - 29.d	283	15	23	23290	390	5.5	1.40E+05	2.60E+03	6300	2.00E+05	4.50E+03	990

Analysis number	Na23 ppm	Na23 ppm 2SE	Na23 ppm LOD	Al27 ppm	Al27 ppm 2SE	Al27 ppm LOD	Si28 ppm	Si28 ppm 2SE	Si28 ppm LOD	Ca44 ppm	Ca44 ppm 2SE	Ca44 ppm LOD
eaf35 - 30.d	303	17	41	22200	210	6.4	1.37E+05	2.50E+03	9200	2.02E+05	2.90E+03	790
eaf35 - 31.d	303	14	35	23950	320	6.4	1.39E+05	2.60E+03	6000	2.04E+05	3.50E+03	900
eaf35 - 32.d	269	15	33	27190	360	5	1.40E+05	2.50E+03	3600	2.01E+05	3.70E+03	1100
eaf35 - 33.d	240	16	45	26050	300	5.6	1.45E+05	3.00E+03	6700	1.99E+05	3.20E+03	1200
eaf35 - 34.d	294	14	35	25070	260	6.2	1.40E+05	2.20E+03	7000	1.98E+05	3.30E+03	870
eaf35 - 35.d	338	14	62	23950	330	4.8	1.35E+05	1.90E+03	9500	2.02E+05	3.50E+03	1200
eaf35 - 36.d	315	17	53	22690	300	6.8	1.43E+05	3.70E+03	11000	2.04E+05	3.70E+03	990
eaf35 - 37.d	272	14	35	22380	320	6.1	1.45E+05	2.10E+03	3500	2.02E+05	3.10E+03	1000
eaf35 - 38.d	321	17	29	24550	350	6.1	1.40E+05	3.40E+03	6500	2.05E+05	3.30E+03	690
eaf35 - 39.d	249	14	54	24880	280	5.4	1.43E+05	2.50E+03	11000	2.02E+05	4.20E+03	820
eaf35 - 40.d	219	15	36	22840	260	5.3	1.38E+05	2.30E+03	7000	1.96E+05	3.10E+03	980
eaf35 - 41.d	342	17	52	23720	210	5.4	1.39E+05	2.40E+03	12000	2.01E+05	3.20E+03	830
eaf35 - 42.d	212	14	40	24370	310	4.7	1.38E+05	2.40E+03	8800	2.01E+05	2.60E+03	460
eaf35 - 43.d	258	18	45	24470	240	4.7	1.36E+05	2.70E+03	10000	2.01E+05	3.40E+03	910
eaf35 - 44.d	251	15	35	24230	330	8.3	1.43E+05	2.40E+03	6200	2.03E+05	3.50E+03	950
eaf35 - 45.d	240	16	57	24430	340	5.9	1.39E+05	2.80E+03	13000	2.02E+05	3.70E+03	830
eaf35 - 48.d	226	15	35	25870	370	5.4	1.37E+05	2.60E+03	5200	2.05E+05	4.70E+03	610
eaf35 - 49.d	375	19	34	25060	260	5.5	1.37E+05	2.00E+03	6700	2.01E+05	3.60E+03	650
eaf35 - 50.d	345	11	28	23130	260	5.8	1.38E+05	1.90E+03	5800	2.06E+05	2.70E+03	630
eaf35 - 51.d	265	12	44	27340	300	4.7	1.41E+05	2.20E+03	14000	2.03E+05	3.70E+03	740
eaf35 - 52.d	346	16	39	28550	470	3.4	1.36E+05	2.60E+03	4600	2.07E+05	4.20E+03	990
eaf35 - 53.d	305	14	51	28160	400	5	1.36E+05	2.50E+03	7800	2.03E+05	3.70E+03	750
eaf35 - 54.d	333	14	34	24010	300	3.6	1.41E+05	2.40E+03	7100	2.06E+05	3.70E+03	1100
eaf35 - 55.d	316	20	47	22330	350	6.5	1.38E+05	3.20E+03	8200	2.10E+05	3.80E+03	1200
eaf35 - 56.d	293	13	36	28050	380	5	1.41E+05	2.20E+03	5800	2.02E+05	3.50E+03	730
eaf35 - 57.d	286	18	47	22130	330	6.8	1.41E+05	2.20E+03	6900	2.07E+05	3.10E+03	750
eaf35 - 58.d	310	12	22	23190	320	6.3	1.42E+05	2.00E+03	4100	2.07E+05	3.70E+03	980
eaf35 - 59.d	346	14	36	23080	310	3.9	1.41E+05	2.40E+03	7300	2.07E+05	3.60E+03	810
eaf35 - 60.d	292	13	34	23610	420	6.5	1.45E+05	2.70E+03	3700	2.05E+05	3.70E+03	870

Analysis number	Na23 ppm	Na23 ppm 2SE	Na23 ppm LOD	Al27 ppm	Al27 ppm 2SE	Al27 ppm LOD	Si28 ppm	Si28 ppm 2SE	Si28 ppm LOD	Ca44 ppm	Ca44 ppm 2SE	Ca44 ppm LOD
eaf35 - 61.d	293	15	29	23240	360	6	1.46E+05	3.10E+03	6800	1.99E+05	4.30E+03	700
eaf35 - 62.d	281	12	42	27570	320	4.5	1.38E+05	2.00E+03	5100	2.08E+05	3.60E+03	650
eaf35 - 63.d	298	15	43	22910	300	5.3	1.40E+05	2.10E+03	11000	2.07E+05	3.30E+03	650
eaf35 - 64.d	348	20	36	22770	300	3.1	1.36E+05	3.00E+03	7100	2.09E+05	3.30E+03	690
eaf35 - 65.d	300	15	33	21840	220	4.7	1.38E+05	1.90E+03	5200	2.05E+05	3.80E+03	720
eaf35 - 66.d	290	14	31	24340	320	5.5	1.42E+05	2.40E+03	6800	1.97E+05	3.10E+03	530
eaf35 - 67.d	303	14	36	23040	300	5.8	1.47E+05	2.20E+03	6900	2.07E+05	3.60E+03	740
eaf35 - 68.d	236	13	42	23460	290	5.4	1.39E+05	2.20E+03	8300	2.08E+05	3.40E+03	660
eaf35 - 69.d	258	13	40	21510	280	5.4	1.41E+05	3.00E+03	8300	2.08E+05	3.40E+03	880
eaf35 - 70.d	252	16	34	22400	340	5.6	1.37E+05	3.80E+03	6100	2.06E+05	3.90E+03	800
eaf35 - 71.d	187	15	39	22140	290	5.7	1.34E+05	3.30E+03	5400	2.10E+05	2.60E+03	760
eaf35 - 72.d	318	14	36	26890	310	5.3	1.37E+05	2.00E+03	9800	2.01E+05	3.20E+03	690
eaf35 - 73.d	279	15	32	27660	360	4.1	1.40E+05	2.00E+03	6400	2.07E+05	3.20E+03	770
eaf35 - 74.d	296	14	29	22970	440	3.1	1.35E+05	2.70E+03	6700	2.07E+05	3.40E+03	720
eaf35 - 75.d	273	15	34	24330	340	5.4	1.37E+05	2.00E+03	6800	2.06E+05	3.40E+03	970
eaf35 - 76.d	266	11	42	23340	290	4.4	1.43E+05	2.00E+03	7600	2.03E+05	3.00E+03	740
eaf35 - 77.d	299	18	50	24930	200	4.1	1.39E+05	2.10E+03	9300	1.97E+05	3.00E+03	680
eaf35 - 78.d	233	13	46	21810	250	5.1	1.41E+05	1.90E+03	10000	2.01E+05	3.50E+03	740
eaf35 - 79.d	360	17	49	22710	320	5.2	1.40E+05	2.40E+03	11000	2.04E+05	4.20E+03	880
eaf35 - 80.d	330	12	30	28820	390	3.4	1.40E+05	2.00E+03	5200	2.07E+05	4.10E+03	910
eaf35 - 81.d	353	17	31	28650	440	5.2	1.42E+05	2.90E+03	8000	2.02E+05	3.40E+03	1000
eaf35 - 82.d	204	14	33	31420	470	5.6	1.43E+05	1.80E+03	6100	2.02E+05	3.50E+03	520
eaf35 - 83.d	173	13	20	23780	290	6	1.39E+05	2.10E+03	7300	2.07E+05	3.40E+03	810
eaf35 - 84.d	263	14	30	20790	300	6.2	1.37E+05	2.60E+03	9800	2.10E+05	4.90E+03	860
eaf35 - 85.d	303	17	26	20920	330	3	1.38E+05	3.30E+03	5600	2.06E+05	3.50E+03	810
eaf35 - 86.d	298	11	42	22270	280	5.7	1.37E+05	2.80E+03	8100	2.01E+05	4.00E+03	800
eaf35 - 88.d	292	15	38	22940	330	5	1.41E+05	3.00E+03	5900	2.11E+05	3.00E+03	430
eaf35 - 89.d	332	16	26	27260	300	6.1	1.39E+05	2.30E+03	4300	2.04E+05	4.00E+03	640
eaf35 - 90.d	322	12	43	22660	320	5.8	1.41E+05	2.30E+03	6200	2.03E+05	3.60E+03	700

Analysis number	Na23 ppm	Na23 ppm 2SE	Na23 ppm LOD	Al27 ppm	Al27 ppm 2SE	Al27 ppm LOD	Si28 ppm	Si28 ppm 2SE	Si28 ppm LOD	Ca44 ppm	Ca44 ppm 2SE	Ca44 ppm LOD
eaf35 - 91.d	261	12	25	21510	240	4.6	1.40E+05	2.20E+03	3900	2.06E+05	3.10E+03	520
eaf35 - 92.d	313	11	41	24450	280	5.5	1.40E+05	1.80E+03	4800	2.08E+05	3.70E+03	1100
eaf35 - 93.d	322	19	48	26540	300	5.9	1.38E+05	3.40E+03	8400	2.08E+05	3.20E+03	760
eaf35 - 94.d	293	14	46	27220	310	4.7	1.40E+05	2.30E+03	5600	2.01E+05	3.40E+03	680
eaf35 - 96.d	328	15	38	23080	370	6.2	1.40E+05	1.80E+03	4500	2.05E+05	3.40E+03	900
eaf35 - 97.d	321	11	36	27510	330	5.9	1.43E+05	2.40E+03	4200	2.02E+05	3.40E+03	670
eaf35 - 98.d	358	17	35	25180	300	6	1.38E+05	3.00E+03	5800	2.04E+05	4.30E+03	650
eaf35 - 99.d	312	11	33	23790	310	7.1	1.42E+05	2.10E+03	5200	2.01E+05	3.50E+03	600
eaf35 - 100.d	224	14	37	25130	320	4.7	1.42E+05	2.30E+03	3800	2.04E+05	3.60E+03	720
eaf35 - 101.d	323	12	25	23480	270	3.8	1.39E+05	2.60E+03	3700	2.06E+05	4.30E+03	550
eaf35 - 102.d	256	14	28	26170	270	4.2	1.43E+05	2.60E+03	3400	2.03E+05	3.70E+03	460
eaf35 - 103.d	311	17	56	24280	300	4.6	1.40E+05	2.40E+03	9600	2.04E+05	3.10E+03	1000
eaf35 - 104.d	329	11	40	23680	260	4.4	1.42E+05	1.70E+03	4600	2.01E+05	3.30E+03	730
eaf35 - 106.d	305	13	36	23720	290	4.1	1.40E+05	2.20E+03	5400	1.99E+05	3.60E+03	500
eaf35 - 107.d	281	10	41	17570	250	4.8	1.40E+05	2.00E+03	7500	2.08E+05	3.60E+03	590
eaf35 - 108.d	301	12	31	23430	320	6.7	1.41E+05	2.40E+03	3200	2.04E+05	3.20E+03	680
eaf35 - 109.d	239	13	31	19900	200	5	1.46E+05	2.10E+03	6200	2.04E+05	3.40E+03	840
eaf35 - 110.d	245	15	47	19920	240	5.6	1.43E+05	2.00E+03	6800	2.05E+05	3.70E+03	560
eaf35 - 111.d	253	14	34	27460	390	4.8	1.44E+05	2.50E+03	4000	2.06E+05	3.50E+03	790
eaf35 - 112.d	258	13	51	21900	240	4.7	1.45E+05	2.00E+03	10000	2.04E+05	3.30E+03	610
eaf35 - 113.d	288	13	27	23100	360	4	1.46E+05	1.60E+03	7100	2.03E+05	3.10E+03	620
eaf35 - 114.d	235	14	33	19780	240	6.3	1.47E+05	2.80E+03	6200	2.06E+05	3.60E+03	590
eaf35 - 115.d	256	16	54	27070	360	4.3	1.43E+05	2.70E+03	12000	2.05E+05	3.50E+03	610
eaf35 - 116.d	328	15	24	27790	340	4.2	1.42E+05	1.90E+03	3500	2.02E+05	3.70E+03	700
eaf35 - 117.d	268	12	27	26220	310	4.9	1.38E+05	2.50E+03	5500	2.01E+05	3.70E+03	590
eaf35 - 118.d	208	14	40	25460	290	4	1.45E+05	2.10E+03	5400	2.01E+05	4.00E+03	660
eaf35 - 119.d	344	16	33	24810	400	5.5	1.38E+05	2.40E+03	4800	1.97E+05	3.50E+03	630
eaf35 - 120.d	325	16	38	22390	360	4.2	1.44E+05	2.20E+03	4600	2.04E+05	3.10E+03	660

Analysis number	Ti47 ppm	Ti47 ppm 2SE	Ti47 ppm LOD	Ti49 ppm	Ti49 ppm 2SE	Ti49 ppm LOD	V51 ppm	V51 ppm 2SE	V51 ppm LOD	Cr52 ppm	Cr52 ppm 2SE	Cr52 ppm LOD
eaf35 - 1.d	170200	2.00E+03	5.8	172100	2.00E+03	1	204.2	3.9	0.33	39.1	2.1	3.7
eaf35 - 2.d	177300	1.90E+03	5.3	178400	1.90E+03	NaN	229.6	3	0.59	68.5	2	6.3
eaf35 - 3.d	167600	1.80E+03	3.8	170200	2.10E+03	3.7	247.1	5.1	0.36	25	1.2	5.5
eaf35 - 4.d	164200	1.70E+03	5.7	167400	1.80E+03	3.1	267.8	4.9	0.31	30.2	1.5	3
eaf35 - 5.d	164000	1.70E+03	7.2	166700	2.00E+03	3.1	269.1	4	0.24	30.8	1.7	2.7
eaf35 - 6.d	167300	2.30E+03	5.2	171100	1.90E+03	3.2	219	3.4	0.32	28	1.6	5.2
eaf35 - 7.d	168300	1.80E+03	6.7	170800	2.20E+03	4	360.1	5.4	0.32	35.5	1.6	3.5
eaf35 - 8.d	167300	2.40E+03	6.3	169700	2.50E+03	3.1	348.6	6	0.45	32.1	1.7	3.1
eaf35 - 9.d	171900	2.10E+03	7.1	175500	2.20E+03	NaN	203.9	3.4	0.28	16.4	1.7	4.3
eaf35 - 10.d	176300	1.80E+03	5.2	179200	2.30E+03	2.6	227.2	3.9	0.42	43.7	2.1	5.8
eaf35 - 11.d	173200	2.50E+03	4	176700	2.50E+03	1.1	177	3.7	0.54	14.1	1.4	4.5
eaf35 - 12.d	168000	2.20E+03	4	170700	2.00E+03	3.1	297.6	4.6	0.55	50.4	2	4.9
eaf35 - 13.d	169400	1.90E+03	7.8	171500	1.90E+03	2.4	293.9	3.6	0.37	51.5	1.9	5.1
eaf35 - 14.d	168300	2.00E+03	7.2	170400	2.10E+03	6.6	309.3	4.4	0.36	37.5	1.9	3.9
eaf35 - 15.d	169500	2.20E+03	6.8	172800	2.20E+03	5	223.3	4.3	0.45	14.7	1.6	6
eaf35 - 16.d	173000	2.40E+03	6.6	175600	2.20E+03	2.6	190	3.4	0.48	13.3	1.9	3.9
eaf35 - 17.d	180400	2.40E+03	3.7	183900	2.50E+03	4.8	283.3	5.4	0.49	26.1	1.9	5
eaf35 - 18.d	175800	1.70E+03	10	179800	1.70E+03	3.8	241.4	4.2	0.38	51.7	1.9	3.1
eaf35 - 19.d	173400	2.20E+03	3.8	177200	2.30E+03	1.1	186.2	2.9	0.51	15.2	1.3	5.5
eaf35 - 20.d	176200	1.90E+03	5.1	178800	2.00E+03	2.5	203.1	3.2	0.57	20.7	1.3	3.8
eaf35 - 22.d	165800	2.00E+03	4.3	170000	2.20E+03	1.5	309	4.3	0.42	30.9	1.5	5.7
eaf35 - 23.d	168800	1.70E+03	10	173800	1.90E+03	1.4	224.8	3.5	0.29	20.9	1.4	3.1
eaf35 - 24.d	167200	2.50E+03	5.8	171400	2.50E+03	5.3	286	5	0.35	22.7	1.4	3.9
eaf35 - 25.d	178500	1.90E+03	6.1	183700	2.30E+03	2.4	165.4	3	0.36	16.7	1.6	7.3
eaf35 - 26.d	173000	1.90E+03	5.3	177100	1.60E+03	3.2	203.8	3.4	0.41	23.3	1.5	4.8
eaf35 - 27.d	169000	2.10E+03	4.9	174600	2.10E+03	4.4	282.4	4.4	0.23	36.3	1.8	4.3
eaf35 - 28.d	179600	2.50E+03	5.6	185100	2.50E+03	3.8	156.9	2.6	0.38	8.2	1.3	4.7
eaf35 - 29.d	176500	2.50E+03	5.6	180800	2.50E+03	3.1	158.3	3.3	0.41	13.4	1.4	5.3
eaf35 - 30.d	176300	1.80E+03	3.6	181300	1.70E+03	NaN	218.7	4.4	0.36	42.7	1.5	6.8

Analysis number	Ti47 ppm	Ti47 ppm 2SE	Ti47 ppm LOD	Ti49 ppm	Ti49 ppm 2SE	Ti49 ppm LOD	V51 ppm	V51 ppm 2SE	V51 ppm LOD	Cr52 ppm	Cr52 ppm 2SE	Cr52 ppm LOD
eaf35 - 31.d	172800	2.10E+03	3.6	178700	2.30E+03	2.1	228.6	4.2	0.39	22	1.9	4.2
eaf35 - 32.d	167300	2.00E+03	5	171800	2.00E+03	2.5	286.8	4.5	0.36	30.2	1.5	2.8
eaf35 - 33.d	168300	2.30E+03	6.2	171200	1.80E+03	3.4	330.3	5.6	0.29	36.9	1.5	4.4
eaf35 - 34.d	170000	2.20E+03	3.3	175800	2.00E+03	3.7	198.4	3.3	0.39	23.3	1.4	4
eaf35 - 35.d	174900	1.70E+03	6.2	179400	2.30E+03	3.6	177.8	2.7	0.51	21.4	1.5	3.7
eaf35 - 36.d	181000	2.60E+03	7	184900	1.90E+03	1.4	164.8	3.5	0.26	19.5	1.7	5.3
eaf35 - 37.d	175400	2.20E+03	6.4	180700	2.20E+03	3.6	159	2.7	0.3	19.5	1.2	4
eaf35 - 38.d	174700	2.20E+03	5.2	178900	2.40E+03	2.1	218.8	4.8	0.57	23.6	1.7	4.3
eaf35 - 39.d	173000	1.90E+03	5.1	176400	1.90E+03	2.3	356.1	5.8	0.38	28.1	1.6	5
eaf35 - 40.d	175300	2.50E+03	4.9	178600	1.80E+03	4.2	411.7	4.3	0.25	45.5	2	5.6
eaf35 - 41.d	175100	1.90E+03	5.6	178800	1.90E+03	2.5	161.6	3.1	0.25	17.9	1.7	5.6
eaf35 - 42.d	172400	2.20E+03	5.5	174600	2.20E+03	NaN	248.4	3.9	0.28	52.6	1.2	5.7
eaf35 - 43.d	175000	1.80E+03	5.7	179300	1.80E+03	1.7	243.9	3.5	0.32	46.3	1.6	4.5
eaf35 - 44.d	172600	2.60E+03	4.2	177600	2.70E+03	23	240.9	4.2	0.33	47.3	2.1	4.5
eaf35 - 45.d	172800	2.40E+03	2.6	176100	2.00E+03	2.1	254.2	4.9	0.54	76.2	2.7	4.9
eaf35 - 48.d	171300	2.70E+03	5.1	175800	2.60E+03	3.4	253.2	4.7	0.31	58.5	2	3.8
eaf35 - 49.d	172500	1.90E+03	3.8	177400	2.20E+03	2.1	230.9	3.5	0.37	26.6	1.9	4
eaf35 - 50.d	178800	1.90E+03	3.9	181700	2.00E+03	3.2	195.5	3.4	0.42	27.2	1.5	4
eaf35 - 51.d	169500	1.90E+03	5.9	172600	2.10E+03	NaN	268.8	3.9	0.49	29.1	1.5	6.8
eaf35 - 52.d	169000	2.50E+03	3.7	172200	3.20E+03	1.5	297.8	6	0.46	28.5	2.1	4.4
eaf35 - 53.d	170300	2.40E+03	9	174000	2.50E+03	3.5	304.8	5.8	0.28	30.8	1.8	4.5
eaf35 - 54.d	175300	2.30E+03	4.2	180200	2.40E+03	3.6	196.3	3.3	0.55	26.8	1.7	3.7
eaf35 - 55.d	183500	2.60E+03	5	188100	2.60E+03	3.2	278.5	5.1	0.24	52.6	1.9	5.1
eaf35 - 56.d	169600	2.10E+03	4.1	173200	2.10E+03	2.3	273.4	4.4	0.54	31.4	1.7	3.6
eaf35 - 57.d	180500	2.50E+03	7	183400	2.80E+03	1	217.3	5.2	0.39	39.5	2.3	4.4
eaf35 - 58.d	179400	2.10E+03	5.1	183400	2.30E+03	2.4	178.9	3.5	0.37	24.8	1.8	4
eaf35 - 59.d	177600	2.30E+03	2.9	181200	2.00E+03	2.6	202.6	3.2	0.45	24.4	1.5	5.7
eaf35 - 60.d	175900	2.50E+03	3.2	179100	2.60E+03	7.4	212.1	3.1	0.4	30	1.7	4.6
eaf35 - 61.d	171900	2.70E+03	5	176900	2.40E+03	0.99	183.7	2.9	0.25	32.5	1.9	5.2

Analysis number	Ti47 ppm	Ti47 ppm 2SE	Ti47 ppm LOD	Ti49 ppm	Ti49 ppm 2SE	Ti49 ppm LOD	V51 ppm	V51 ppm 2SE	V51 ppm LOD	Cr52 ppm	Cr52 ppm 2SE	Cr52 ppm LOD
eaf35 - 62.d	174100	1.80E+03	5.7	178200	2.20E+03	1.5	351.4	5.1	0.36	27.5	1.6	4
eaf35 - 63.d	180000	2.10E+03	3.9	184800	2.60E+03	2.4	143.8	2.4	0.43	14	1.5	4.8
eaf35 - 64.d	184300	2.40E+03	3.9	187800	2.40E+03	3.1	162.9	2.4	0.66	11.1	1.7	3.9
eaf35 - 65.d	181700	1.90E+03	5.6	185300	1.80E+03	5	194	3.5	0.33	25.3	1.6	5.1
eaf35 - 66.d	175400	2.10E+03	5.8	177700	2.10E+03	2.2	193.7	3.4	0.44	31.6	1.3	4.1
eaf35 - 67.d	179800	2.20E+03	7.3	184000	2.40E+03	2.8	178.5	2.6	0.24	25.4	1.6	5.1
eaf35 - 68.d	177800	2.30E+03	6.8	179800	2.60E+03	3.7	305.6	4.5	0.36	54.6	1.6	4.8
eaf35 - 69.d	181700	2.10E+03	4.9	183500	1.70E+03	2.9	501	8.2	0.35	97.1	2.6	4.8
eaf35 - 70.d	177400	2.60E+03	6.1	179300	2.40E+03	2.9	286.2	5.9	0.4	57.5	2.2	4.5
eaf35 - 71.d	179000	2.20E+03	4.9	183500	2.10E+03	3	307	4.3	0.25	76.5	2.7	4.4
eaf35 - 72.d	169800	1.70E+03	2.6	171600	1.50E+03	3.6	353.1	5.5	0.32	37.6	1.5	5.1
eaf35 - 73.d	172200	1.60E+03	5.5	174600	1.90E+03	2.6	298.6	6.1	0.25	29.5	1.6	4.2
eaf35 - 74.d	181400	2.10E+03	4.8	181400	2.40E+03	3.3	323.9	7.1	0.61	49.6	2.3	4
eaf35 - 75.d	180000	2.40E+03	3.5	181500	2.40E+03	3.8	317.7	6.4	0.57	95.6	3	5.9
eaf35 - 76.d	182000	2.20E+03	6.1	182000	2.10E+03	2.3	154.6	2.5	0.21	24.3	1.8	4.5
eaf35 - 77.d	190500	2.40E+03	5.4	191200	2.60E+03	2.9	309.8	4.9	0.65	82.3	2.1	5.2
eaf35 - 78.d	181300	2.00E+03	3.7	181900	1.90E+03	3.7	356.9	4.5	0.3	221.2	4.5	4.3
eaf35 - 79.d	180200	2.70E+03	2.3	182900	2.40E+03	2.3	167.4	3.1	0.36	10.1	1.7	5.7
eaf35 - 80.d	173000	2.60E+03	4.1	173300	2.20E+03	1.1	266.4	4.7	0.43	27.5	1.8	4.7
eaf35 - 81.d	177500	2.50E+03	3.7	178300	2.20E+03	3	264.6	4.4	0.29	29.8	2	4.3
eaf35 - 82.d	167300	2.30E+03	22	167700	2.40E+03	2.6	282.9	4.5	0.37	79.1	2.7	4.7
eaf35 - 83.d	179400	2.50E+03	3.7	179500	2.30E+03	2.9	916	12	0.37	381.9	6.2	3.3
eaf35 - 84.d	184200	2.70E+03	4.7	184800	2.30E+03	2.5	901	13	0.38	310.5	6.5	5.5
eaf35 - 85.d	183700	2.30E+03	4.5	184300	2.70E+03	2.3	854	14	0.32	204.9	3	3.9
eaf35 - 86.d	183800	2.10E+03	6.2	183800	2.40E+03	3.4	831	11	0.4	215.7	4.7	5.9
eaf35 - 88.d	179700	2.10E+03	6.1	181400	3.00E+03	2.5	189.4	2.5	0.29	24.9	1.8	3.9
eaf35 - 89.d	173600	2.80E+03	7.2	174900	2.20E+03	1.1	329.7	6.5	0.34	28.8	1.5	4.4
eaf35 - 90.d	179100	2.10E+03	4.8	179700	2.60E+03	2.9	185	2.9	0.46	33.2	1.3	4.2
eaf35 - 91.d	181200	2.90E+03	3.2	180400	2.60E+03	2.9	274.5	6.2	0.49	45.8	1.4	3.3

Analysis number	Ti47 ppm	Ti47 ppm 2SE	Ti47 ppm LOD	Ti49 ppm	Ti49 ppm 2SE	Ti49 ppm LOD	V51 ppm	V51 ppm 2SE	V51 ppm LOD	Cr52 ppm	Cr52 ppm 2SE	Cr52 ppm LOD
eaf35 - 92.d	180900	2.10E+03	7.3	180000	2.00E+03	2.9	214.8	3.8	0.35	24.2	1.3	4.1
eaf35 - 93.d	176000	1.80E+03	4.1	175800	2.00E+03	2.8	350.1	5.4	0.74	32	2.3	5.6
eaf35 - 94.d	171900	1.80E+03	4.6	170900	1.60E+03	1	264	4.1	0.35	30.2	1.6	4.5
eaf35 - 96.d	180600	2.30E+03	5.3	180900	2.50E+03	2.2	198.8	2.8	0.35	26	1.7	3
eaf35 - 97.d	172400	2.30E+03	8.7	172800	1.90E+03	2.9	307.8	5.1	0.31	31.6	1.8	4.8
eaf35 - 98.d	178000	2.20E+03	5	178500	2.30E+03	2.3	227.5	3.7	0.34	31.6	1.7	3.8
eaf35 - 99.d	177900	2.40E+03	3.5	179400	2.40E+03	2.2	206	4	0.32	29.3	1.9	4.1
eaf35 - 100.d	174300	2.20E+03	5	174200	2.70E+03	1.8	248.4	3.8	0.43	37.7	1.9	4.1
eaf35 - 101.d	182000	2.60E+03	4.6	183100	2.50E+03	3	189.6	3.1	0.43	23.4	1.9	3.3
eaf35 - 102.d	175300	2.30E+03	2.3	175200	2.30E+03	3.2	225.3	3.8	0.26	26.3	1.6	3.6
eaf35 - 103.d	179000	1.90E+03	5.5	179600	2.10E+03	NaN	197.3	2.8	0.26	37.4	1.9	5.8
eaf35 - 104.d	177100	2.30E+03	2.6	177800	2.10E+03	2.3	194.5	3.3	0.21	35.9	1.6	4
eaf35 - 106.d	174800	1.80E+03	3.7	174500	2.10E+03	2.9	190.6	3.4	0.3	45.5	1.7	3.2
eaf35 - 107.d	186700	2.40E+03	4.9	185800	2.20E+03	1.4	466.8	6.8	0.5	197.8	4.2	4.6
eaf35 - 108.d	178200	2.40E+03	5.2	178900	2.10E+03	3.7	187.9	3.1	0.42	29.8	1.6	3.2
eaf35 - 109.d	180200	1.90E+03	3.8	180700	1.80E+03	2.1	305.9	7.3	0.19	69.7	2.4	3.9
eaf35 - 110.d	183600	1.90E+03	4.1	183900	2.40E+03	2.8	383.4	7.3	0.24	195.9	4.2	4.7
eaf35 - 111.d	173500	2.70E+03	6.8	172000	2.60E+03	2.3	249.2	4	0.25	27.6	1.5	3.8
eaf35 - 112.d	180100	2.10E+03	2.8	179000	2.00E+03	3	174.2	2.9	0.21	35.1	1.7	3.7
eaf35 - 113.d	177600	2.60E+03	3.3	177800	2.30E+03	0.99	181.2	3.1	0.28	23.3	1.5	3.9
eaf35 - 114.d	181200	2.20E+03	4.4	181200	2.20E+03	3.5	546.9	8	0.47	135.3	3.8	3.3
eaf35 - 115.d	173200	2.10E+03	3.2	173900	2.40E+03	4.5	231.8	3.9	0.19	28	1.6	5.6
eaf35 - 116.d	172900	2.70E+03	3.6	172900	2.70E+03	5.2	209.4	3.8	0.37	25.8	1.6	4.3
eaf35 - 117.d	177400	2.30E+03	5.9	178500	2.00E+03	4.1	262.9	4	0.36	43.1	1.9	4.2
eaf35 - 118.d	177500	1.90E+03	3.9	176800	1.90E+03	2.5	267.8	4.4	0.35	48.4	2	5.1
eaf35 - 119.d	176800	2.20E+03	3	175900	1.70E+03	3.7	184.3	2.8	0.31	30.3	1.7	3.9
eaf35 - 120.d	182400	2.80E+03	4.3	180500	2.80E+03	2	188.1	3.5	0.21	27.4	1.6	3.8

Analysis number	Mn55 ppm	Mn55 ppm 2SE	Mn55 ppm LOD	Fe56 ppm	Fe56 ppm 2SE	Fe56 ppm LOD	Y89 ppm	Y89 ppm 2SE	Y89 ppm LOD	Zr90 ppm	Zr90 ppm 2SE	Zr90 ppm LOD
eaf35 - 1.d	241.8	4.1	4.3	8810	95	41	1002	14	0.043	90.7	1.5	0.034
eaf35 - 2.d	540.2	6.7	12	9008	97	63	650.6	6.7	0.05	97.9	2.1	0.068
eaf35 - 3.d	527.1	6.9	5.5	9570	140	43	678.4	8.1	NaN	206.3	5.2	0.091
eaf35 - 4.d	208.8	4.3	3.8	9760	100	39	1303	16	NaN	98.2	1.7	0.069
eaf35 - 5.d	298.3	4.5	7.2	9640	100	45	1228	14	0.03	105.4	2	0.034
eaf35 - 6.d	292.4	5.6	6.4	8892	96	56	1246	15	0.051	92.9	1.8	0.033
eaf35 - 7.d	138.8	3.4	4.6	11340	100	29	1297	17	0.041	140.6	2.6	0.035
eaf35 - 8.d	158.7	4	8.1	10770	140	57	1218	19	0.066	134	2.3	0.034
eaf35 - 9.d	666.5	8.6	4.3	9320	150	43	1254	19	0.026	93.9	1.8	0.098
eaf35 - 10.d	648.6	7.3	7.6	8740	100	54	1390	15	0.06	96.3	1.7	0.034
eaf35 - 11.d	624.9	6.7	5.1	8400	110	35	987	13	0.08	88.8	2.1	NaN
eaf35 - 12.d	528.9	7.4	6.1	12050	150	35	3787	54	0.067	162.6	3.2	0.076
eaf35 - 13.d	624.9	6.4	7.3	11330	110	61	3602	37	0.053	161.5	2.9	0.071
eaf35 - 14.d	259.6	4	5.4	11150	130	26	2623	32	0.026	135.1	1.7	NaN
eaf35 - 15.d	639	10	9.4	11590	450	66	1356	17	0.055	112.7	3.6	NaN
eaf35 - 16.d	581.6	7.4	7.3	11700	140	29	1020	11	0.038	110.8	1.9	0.049
eaf35 - 17.d	658	10	5.5	11310	160	35	1724	27	0.042	122.7	2	0.086
eaf35 - 18.d	611.1	6.4	6.6	11840	100	42	1133	14	NaN	87.5	1.4	NaN
eaf35 - 19.d	471.4	5.9	12	10330	130	60	913	11	0.034	96.9	1.6	NaN
eaf35 - 20.d	604.2	7.5	4.8	9027	62	40	1418	18	0.025	106.6	2.3	0.035
eaf35 - 22.d	579.2	7.4	8.4	11220	130	50	1515	19	0.067	121.2	2.3	0.077
eaf35 - 23.d	589	10	6.4	8575	88	35	1537	22	0.049	93.3	1.6	0.034
eaf35 - 24.d	359.8	5.4	4.8	9980	130	36	1611	23	0.054	102.1	1.9	NaN
eaf35 - 25.d	534.8	7.3	12	9060	95	53	742	10	0.019	103.7	1.4	0.076
eaf35 - 26.d	296.9	5.8	7.7	10000	110	39	1229	15	0.037	103.7	2.3	0.056
eaf35 - 27.d	525.4	7	6.3	9360	130	41	1338	19	0.029	108.4	2	0.14
eaf35 - 28.d	527.9	7.2	6.4	8307	80	41	711	12	NaN	82.4	1.4	0.097
eaf35 - 29.d	571.5	8.1	5.6	9500	120	39	594	11	0.036	63.6	1.3	0.074
eaf35 - 30.d	594.9	7.4	8	7907	71	49	552.7	6.9	0.051	56	1.2	NaN

Analysis number	Mn55 ppm	Mn55 ppm 2SE	Mn55 ppm LOD	Fe56 ppm	Fe56 ppm 2SE	Fe56 ppm LOD	Y89 ppm	Y89 ppm 2SE	Y89 ppm LOD	Zr90 ppm	Zr90 ppm 2SE	Zr90 ppm LOD
eaf35 - 31.d	590.6	9.1	5.2	8760	110	37	1028	12	0.036	103.4	1.7	0.034
eaf35 - 32.d	475.7	6.6	6.5	9492	97	28	1216	16	0.036	110.4	1.7	0.074
eaf35 - 33.d	562.3	7.2	7.5	9825	92	32	1298	17	0.039	125.7	1.9	0.072
eaf35 - 34.d	604.1	8.1	8.4	9740	100	36	1096	16	0.039	97.4	2.1	0.15
eaf35 - 35.d	595.1	7.4	7	10520	170	48	590.9	6.9	0.051	86.9	1.9	0.096
eaf35 - 36.d	638.7	9	10	7909	88	47	611.6	9.5	0.043	76.2	1.5	NaN
eaf35 - 37.d	357.6	3.2	5.2	8110	93	21	566	8.1	0.092	70.1	1.5	0.033
eaf35 - 38.d	547.7	8.1	7.4	8360	120	33	1201	18	0.042	93.1	1.5	0.034
eaf35 - 39.d	636.3	6.7	9	10290	110	46	656.8	9.2	0.025	57.2	1.2	0.092
eaf35 - 40.d	584.9	7.4	8.3	18080	310	38	462.9	5.8	0.037	88.9	2.2	NaN
eaf35 - 41.d	509.5	9.8	8.6	10060	120	50	664.9	9.8	0.041	77.4	1.3	0.081
eaf35 - 42.d	654	10	7.7	9440	110	42	2113	33	0.039	91.7	2	0.034
eaf35 - 43.d	710.9	7.7	8.1	10081	87	58	2364	27	0.059	112.6	1.5	0.11
eaf35 - 44.d	712.4	8.3	6.2	10150	140	21	2671	42	0.057	127	2.4	NaN
eaf35 - 45.d	683	10	9.4	10540	120	68	2292	29	0.048	104.4	1.6	NaN
eaf35 - 48.d	675.7	8.9	7.3	9650	110	34	2103	34	0.074	85.8	2	NaN
eaf35 - 49.d	235.8	4.9	6.4	10080	110	41	1274	18	0.042	102.6	2.2	0.034
eaf35 - 50.d	567.9	7.1	6.5	8856	88	31	683	11	0.05	96.4	2.1	NaN
eaf35 - 51.d	561.4	7.6	9.7	9141	90	74	1122	13	0.018	104	1.9	0.067
eaf35 - 52.d	182.8	3.9	5.1	10520	150	21	1189	19	NaN	111.3	2.1	0.081
eaf35 - 53.d	455.8	5.9	8.2	10600	140	40	1236	19	0.06	124.4	2	0.14
eaf35 - 54.d	258.4	4.2	7.8	8290	100	37	957	20	0.035	85.7	1.7	0.099
eaf35 - 55.d	668.6	8.3	12	9510	100	36	1173	21	0.037	100.8	1.7	0.069
eaf35 - 56.d	539.3	7.1	5.2	9870	130	33	1364	31	0.075	113.8	2.4	0.074
eaf35 - 57.d	488.7	8	7.3	9600	140	32	584.7	8.4	0.048	81.6	1.9	NaN
eaf35 - 58.d	452.3	7	5.9	8270	130	22	708	10	0.036	93.1	1.6	0.046
eaf35 - 59.d	347.6	6.7	5.9	8094	95	34	823	11	0.018	89.5	1.8	0.11
eaf35 - 60.d	491.1	5.7	7.1	8177	92	24	970	18	0.058	85.8	2.2	NaN
eaf35 - 61.d	382.4	5.6	7.8	9400	160	29	813	13	0.017	83.7	1.7	NaN

Analysis number	Mn55 ppm	Mn55 ppm 2SE	Mn55 ppm LOD	Fe56 ppm	Fe56 ppm 2SE	Fe56 ppm LOD	Y89 ppm	Y89 ppm 2SE	Y89 ppm LOD	Zr90 ppm	Zr90 ppm 2SE	Zr90 ppm LOD
eaf35 - 62.d	643.3	6.9	5.4	9310	110	26	1720	19	0.037	119.4	2.1	0.076
eaf35 - 63.d	666.4	8.4	12	7761	81	54	825	11	0.035	86.7	1.8	0.072
eaf35 - 64.d	541.5	8	7.9	7863	95	39	742	11	0.071	86.2	1.7	NaN
eaf35 - 65.d	643.9	9.2	8	8450	110	34	677.1	8	0.039	73.4	1.5	NaN
eaf35 - 66.d	649.1	7.5	7.5	9541	93	31	922	12	0.041	97.2	1.8	0.072
eaf35 - 67.d	477.7	5.5	9.3	7761	87	44	667	8.6	0.043	81.8	1.4	0.13
eaf35 - 68.d	691.5	9.5	9.5	10290	140	38	1449	17	0.044	85	1.7	0.046
eaf35 - 69.d	653.7	8.1	12	11670	170	36	1178	23	0.05	125.4	3.3	0.066
eaf35 - 70.d	621.3	8.9	6.8	10950	100	22	1088	14	0.072	94	1.8	0.09
eaf35 - 71.d	558.2	6.1	7.5	13490	130	24	848	10	0.055	83.7	1.5	0.034
eaf35 - 72.d	222.5	5.4	11	10700	140	42	1448	31	0.039	133.3	2.8	NaN
eaf35 - 73.d	465.9	6.6	6.2	9530	120	42	1346	17	0.039	113	1.7	0.046
eaf35 - 74.d	638.3	8.3	7.3	9860	110	30	976	38	0.079	79.3	3.2	0.068
eaf35 - 75.d	443.2	5.9	4.8	10360	160	34	377.3	6.4	0.038	66.7	1.5	NaN
eaf35 - 76.d	344.7	5.1	5.7	8275	89	35	532.5	5.8	NaN	81.2	1.5	0.1
eaf35 - 77.d	569.7	8.8	10	11400	160	34	458	11	NaN	72.6	1.6	NaN
eaf35 - 78.d	642.9	8.4	9.8	10370	110	31	818	9.7	0.051	81.9	1.7	0.055
eaf35 - 79.d	456.4	5.3	12	8820	160	42	899	14	0.057	94.3	2.1	0.08
eaf35 - 80.d	203	5.1	4.5	9290	110	31	1522	20	0.037	99.5	2	NaN
eaf35 - 81.d	249.7	3.5	9.5	9700	130	31	1446	21	0.056	112.7	2.7	0.078
eaf35 - 82.d	657.6	9.5	6.7	13380	270	35	2292	37	0.038	83.6	1.9	0.079
eaf35 - 83.d	728.8	8.3	7.8	7756	98	32	910	11	0.039	63.1	1.3	0.18
eaf35 - 84.d	623.5	8.8	9.7	9600	130	37	2043	35	0.058	105.9	2.3	0.097
eaf35 - 85.d	745.4	8.5	7.2	9940	120	26	2093	27	0.049	146.5	2.9	0.073
eaf35 - 86.d	688.7	9.1	9.9	10460	120	29	2357	27	0.071	139.8	2.7	0.047
eaf35 - 88.d	629.1	8.3	7.8	7749	84	25	952	10	0.035	89.5	1.8	0.1
eaf35 - 89.d	369.7	4.4	5	11350	180	27	1104	18	NaN	129.9	2.7	0.075
eaf35 - 90.d	424	5.9	5.4	7907	87	35	922	14	NaN	83.8	1.8	NaN
eaf35 - 91.d	656.1	7.8	5.9	8924	93	20	1875	39	0.048	88.7	1.5	0.088

Analysis number	Mn55 ppm	Mn55 ppm 2SE	Mn55 ppm LOD	Fe56 ppm	Fe56 ppm 2SE	Fe56 ppm LOD	Y89 ppm	Y89 ppm 2SE	Y89 ppm LOD	Zr90 ppm	Zr90 ppm 2SE	Zr90 ppm LOD
eaf35 - 92.d	572.6	8.8	7.2	8340	110	22	1305	16	0.039	94.6	1.6	0.091
eaf35 - 93.d	281.7	5.3	8.5	10490	110	38	1251	19	0.078	133	2	0.073
eaf35 - 94.d	374.1	6.5	7.2	9910	120	24	1204	14	0.039	107.2	1.9	NaN
eaf35 - 96.d	407.7	7	5.5	8830	100	19	984	16	0.028	96.3	2	0.033
eaf35 - 97.d	176.6	4.3	5.7	11580	290	17	1023	12	0.041	125.3	2.3	0.067
eaf35 - 98.d	213.4	4.1	5.7	10330	110	25	1190	16	0.018	99.5	1.7	NaN
eaf35 - 99.d	203.5	2.8	6.3	8633	85	27	899	12	0.038	86.5	1.8	0.066
eaf35 - 100.d	697.3	9.6	4.9	9810	110	21	2125	24	0.024	89.5	1.6	0.09
eaf35 - 101.d	665.7	8.9	7.3	9050	120	25	757	11	0.025	89.5	2	0.035
eaf35 - 102.d	682.7	8.4	5.1	9200	110	33	1223	20	0.042	674	30	0.047
eaf35 - 103.d	178.6	4.1	9.3	9410	100	42	592.7	7.8	0.054	86.9	1.4	0.068
eaf35 - 104.d	427.6	5.4	5.8	9230	100	28	641.6	7.6	0.051	89	1.4	0.1
eaf35 - 106.d	393.7	5.7	5.6	10130	110	25	644.9	8.4	0.058	95.6	1.9	NaN
eaf35 - 107.d	655.1	9.8	7	11550	130	30	926	12	0.028	157.5	2.7	NaN
eaf35 - 108.d	561.3	8.3	6	9140	100	18	875	13	0.057	88	1.8	0.067
eaf35 - 109.d	701.8	8.1	8	9790	120	29	963	12	0.049	126.2	1.8	0.086
eaf35 - 110.d	630.5	9.5	7.1	10340	200	36	703	17	0.038	77.9	1.8	0.11
eaf35 - 111.d	709.8	9.1	4.8	10390	150	25	1506	17	0.059	112.9	1.9	NaN
eaf35 - 112.d	689	10	8.5	9160	130	43	934	14	0.017	94.2	2	0.091
eaf35 - 113.d	440.7	5	9.4	8080	86	28	992	15	0.037	87.5	1.9	NaN
eaf35 - 114.d	633	11	8.6	10610	120	25	858	10	0.048	98.6	1.7	NaN
eaf35 - 115.d	602.3	7.7	12	9397	79	45	1281	21	0.094	102.3	1.4	NaN
eaf35 - 116.d	372.6	5.7	6.8	11430	160	24	1319	21	0.043	101.2	2.1	0.068
eaf35 - 117.d	683.2	9	7.8	11680	160	23	1880	19	0.019	134.5	2.9	NaN
eaf35 - 118.d	686.7	7	6.3	10630	110	31	1632	18	0.036	86.7	1.2	0.067
eaf35 - 119.d	266.1	7.2	7	11490	280	27	874	16	0.036	97.8	2.3	NaN
eaf35 - 120.d	394	11	7.2	7969	91	21	666	15	0.024	83.9	1.7	NaN

Analysis number	Nb93 ppm	Nb93 ppm 2SE	Nb93 ppm LOD	La139 ppm	La139 ppm 2SE	La139 ppm LOD	Ce140 ppm	Ce140 ppm 2SE	Ce140 ppm LOD	Pr141 ppm	Pr141 ppm 2SE	Pr141 ppm LOD
eaf35 - 1.d	1137	15	NaN	5.1	0.19	0.023	28.96	0.73	NaN	7.86	0.25	0.018
eaf35 - 2.d	1536	15	NaN	30.21	0.78	0.021	340	32	NaN	14.8	0.47	NaN
eaf35 - 3.d	1634	28	NaN	26.4	1.1	0.029	98	11	NaN	11.9	0.6	NaN
eaf35 - 4.d	1113	13	NaN	12.9	0.31	NaN	78	1.3	0.011	20.11	0.42	NaN
eaf35 - 5.d	1074	14	0.018	14.86	0.29	0.011	88.2	1.5	0.011	22.05	0.42	NaN
eaf35 - 6.d	1251	16	NaN	3.5	0.13	NaN	22.33	0.55	0.021	5.97	0.16	NaN
eaf35 - 7.d	1026	14	0.018	34.91	0.59	0.023	199.2	2	0.011	46.91	0.71	NaN
eaf35 - 8.d	1003	15	NaN	29.98	0.69	0.023	172.9	3.5	0.022	41.89	0.77	NaN
eaf35 - 9.d	1237	15	NaN	16.53	0.57	NaN	71.2	1.9	NaN	15.05	0.49	NaN
eaf35 - 10.d	1149	11	NaN	36.6	0.81	0.01	152.7	2.7	NaN	28.08	0.5	NaN
eaf35 - 11.d	1174	14	0.024	6.84	0.33	0.034	29.9	1.1	NaN	6.56	0.27	NaN
eaf35 - 12.d	1430	21	NaN	97.7	1.8	0.011	539.7	8.3	0.022	121.1	2.1	0.0094
eaf35 - 13.d	1328	12	NaN	96.6	1.3	0.011	529.1	5.9	NaN	120.8	1.4	NaN
eaf35 - 14.d	1074	13	NaN	45.06	0.82	0.022	254.2	4.1	NaN	60.37	0.91	0.0094
eaf35 - 15.d	1286	19	NaN	138.9	6.4	NaN	226.4	9.9	NaN	25.5	1.1	0.027
eaf35 - 16.d	1174	16	NaN	20.94	0.56	0.024	71.5	1.7	0.011	13.68	0.35	NaN
eaf35 - 17.d	1274	15	NaN	48.1	1.2	0.012	235.6	8.6	NaN	44.4	1.2	0.015
eaf35 - 18.d	957.7	9.3	0.035	58.2	1.1	NaN	184.6	2.7	NaN	34.15	0.72	NaN
eaf35 - 19.d	1152	15	NaN	71	7.5	NaN	107.2	6.2	0.011	13.01	0.48	NaN
eaf35 - 20.d	1283	13	0.018	32.9	1.1	0.011	205	6.4	0.011	48.4	1.7	0.0094
eaf35 - 22.d	1156	15	0.036	95.8	5.1	0.03	254.7	8.6	0.015	38.9	1	NaN
eaf35 - 23.d	1343	17	NaN	8.18	0.39	0.01	73.5	6.2	0.021	10.46	0.32	NaN
eaf35 - 24.d	1209	19	NaN	19.76	0.49	NaN	113.3	1.7	NaN	23.87	0.53	NaN
eaf35 - 25.d	1170	12	NaN	10.7	0.26	NaN	67.2	1.9	NaN	7.54	0.26	NaN
eaf35 - 26.d	1069	13	0.018	21.65	0.72	NaN	107.7	3	NaN	18.35	0.45	NaN
eaf35 - 27.d	1021	14	0.017	18.01	0.43	NaN	105.3	1.7	NaN	26.11	0.41	0.015
eaf35 - 28.d	1274	16	0.017	9.14	0.31	NaN	48	1.8	0.022	7.53	0.3	NaN
eaf35 - 29.d	1228	16	0.017	4.82	0.19	0.021	16.96	0.45	NaN	3.18	0.16	NaN
eaf35 - 30.d	980.2	9.5	NaN	13.72	0.44	0.01	48.9	1.8	0.011	9.15	0.33	NaN

Analysis number	Nb93 ppm	Nb93 ppm 2SE	Nb93 ppm LOD	La139 ppm	La139 ppm 2SE	La139 ppm LOD	Ce140 ppm	Ce140 ppm 2SE	Ce140 ppm LOD	Pr141 ppm	Pr141 ppm 2SE	Pr141 ppm LOD
eaf35 - 31.d	1136	17	0.034	15.01	0.82	0.014	80.7	4.4	NaN	18.7	1.1	0.018
eaf35 - 32.d	1066	15	NaN	17.53	0.35	NaN	104	1.9	NaN	26.77	0.55	NaN
eaf35 - 33.d	968	14	NaN	27.76	0.54	NaN	164.4	2.7	0.021	40.25	0.76	NaN
eaf35 - 34.d	1143	15	NaN	24.2	1.8	0.023	78.4	3.1	0.032	14.46	0.43	NaN
eaf35 - 35.d	1183	10	0.018	19.57	0.91	0.03	38.3	1	0.022	7.9	0.28	0.0095
eaf35 - 36.d	1289	21	0.059	10.33	0.48	0.042	52.8	1.8	NaN	6.74	0.27	NaN
eaf35 - 37.d	1271	19	NaN	5.86	0.19	0.01	60.5	3.6	NaN	3.76	0.15	NaN
eaf35 - 38.d	1197	18	NaN	5.03	0.23	0.021	31.19	0.9	NaN	8.22	0.27	0.019
eaf35 - 39.d	802	11	0.034	31.1	0.65	0.021	129.3	2.4	0.011	21.94	0.44	NaN
eaf35 - 40.d	737.3	8.5	NaN	199	16	0.029	446	21	NaN	59	1.7	0.0094
eaf35 - 41.d	1245	14	NaN	13.39	0.38	NaN	53.4	1.6	0.022	7.18	0.24	0.0095
eaf35 - 42.d	746	12	NaN	33.03	0.82	0.014	208.6	3.9	NaN	52.2	1	0.0091
eaf35 - 43.d	855	12	0.054	61.8	1.8	NaN	397	15	NaN	80.5	1.5	NaN
eaf35 - 44.d	906	14	NaN	63	1.2	NaN	369.4	6.6	0.021	85.4	1.5	NaN
eaf35 - 45.d	833.6	9.6	0.017	50.14	0.92	0.014	289.2	5	0.023	67.5	1.3	NaN
eaf35 - 48.d	672	14	NaN	30.31	0.85	NaN	197.4	4.8	0.011	48.6	1.3	0.0093
eaf35 - 49.d	1253	15	NaN	24.5	1.3	NaN	277	59	NaN	16.01	0.71	NaN
eaf35 - 50.d	1112	14	NaN	18.39	0.38	0.01	77.7	1.6	0.015	9.67	0.28	NaN
eaf35 - 51.d	1062	14	NaN	16.01	0.38	NaN	104.1	2.6	0.021	19.96	0.47	0.0091
eaf35 - 52.d	1037	14	NaN	20.91	0.62	0.011	131	8.1	0.022	26.88	0.9	0.0095
eaf35 - 53.d	1015	16	NaN	65.5	5.6	NaN	229.2	6.7	NaN	38.74	0.91	NaN
eaf35 - 54.d	1125	12	0.017	2.61	0.14	0.021	15.9	0.5	NaN	4.18	0.15	0.018
eaf35 - 55.d	901	14	0.035	45.9	1.3	0.011	173.1	7.5	NaN	29.5	1.1	0.0093
eaf35 - 56.d	1114	15	NaN	29.4	1	NaN	160.6	5	0.011	30.8	1	0.0092
eaf35 - 57.d	1142	13	0.023	30.8	1.5	0.01	90	3.1	NaN	12.99	0.57	0.009
eaf35 - 58.d	1044	15	NaN	8.94	0.44	NaN	37.1	1.4	NaN	6.86	0.23	0.0091
eaf35 - 59.d	1117	15	NaN	3.13	0.13	0.022	19	0.44	NaN	5.04	0.19	0.018
eaf35 - 60.d	1090	14	NaN	2.32	0.12	NaN	15.99	0.46	NaN	4.9	0.19	NaN
eaf35 - 61.d	1185	18	NaN	11.31	0.82	0.02	27.9	1.6	NaN	6.58	0.32	NaN

Analysis number	Nb93 ppm	Nb93 ppm 2SE	Nb93 ppm LOD	La139 ppm	La139 ppm 2SE	La139 ppm LOD	Ce140 ppm	Ce140 ppm 2SE	Ce140 ppm LOD	Pr141 ppm	Pr141 ppm 2SE	Pr141 ppm LOD
eaf35 - 62.d	1021	13	NaN	23.43	0.49	0.022	134.5	2.1	0.022	32.23	0.48	0.0094
eaf35 - 63.d	1087	15	0.017	2.21	0.11	NaN	14.15	0.41	NaN	3.56	0.15	NaN
eaf35 - 64.d	1169	15	NaN	2.14	0.14	0.021	14.04	0.43	0.022	3.55	0.16	NaN
eaf35 - 65.d	984	12	0.037	17.8	1.2	NaN	79	5.1	0.011	14.16	0.78	0.012
eaf35 - 66.d	1088	13	NaN	32.6	1	NaN	114.1	2.8	0.011	18.64	0.46	NaN
eaf35 - 67.d	1129	15	NaN	1.32	0.11	NaN	9.26	0.51	NaN	2.57	0.16	NaN
eaf35 - 68.d	859	10	NaN	29.54	0.7	0.014	137.8	2.4	NaN	27.63	0.55	NaN
eaf35 - 69.d	782	14	0.034	73	1.6	0.01	308	6	0.021	54.12	0.94	NaN
eaf35 - 70.d	1050	15	0.017	51.87	0.91	0.01	217.1	3.6	NaN	36.33	0.63	0.018
eaf35 - 71.d	627.5	7.8	NaN	52.62	0.97	NaN	235.7	3.7	0.024	40.22	0.61	NaN
eaf35 - 72.d	903	10	NaN	32.41	0.92	0.021	187.9	5.5	NaN	46	1.2	NaN
eaf35 - 73.d	1071	11	NaN	19.07	0.69	NaN	114.6	3.7	NaN	28.27	0.92	NaN
eaf35 - 74.d	877	29	NaN	37.9	1.3	NaN	155	3.5	NaN	26.19	0.63	NaN
eaf35 - 75.d	637.1	7.9	NaN	78.8	5.5	0.025	135.4	7.7	0.011	14.77	0.89	NaN
eaf35 - 76.d	1085	13	NaN	4.69	0.32	NaN	18.2	1	NaN	3.66	0.22	0.0092
eaf35 - 77.d	723	13	0.021	26.52	0.8	0.013	114.6	3.1	NaN	15.4	0.45	0.022
eaf35 - 78.d	834.8	9	0.017	49.9	1.2	0.021	150.3	2.8	NaN	22.64	0.45	NaN
eaf35 - 79.d	1364	22	NaN	6.69	0.42	0.011	30	1.8	NaN	5.72	0.38	NaN
eaf35 - 80.d	1233	17	NaN	7.59	0.24	NaN	45.4	1.1	0.022	11.51	0.32	NaN
eaf35 - 81.d	1474	24	0.018	702	43	0.046	581	33	NaN	128.2	9.3	NaN
eaf35 - 82.d	684.3	9.6	0.037	45.1	1.2	NaN	170.1	3.1	0.023	43.59	0.93	NaN
eaf35 - 83.d	405.2	4.9	0.017	15.05	0.36	0.011	82.7	1.2	0.011	18.78	0.41	NaN
eaf35 - 84.d	473.9	7.8	NaN	102	13	0.011	315	12	NaN	69.6	3.1	NaN
eaf35 - 85.d	492.8	8	0.039	94.4	2.1	NaN	537	10	NaN	97.1	1.9	0.018
eaf35 - 86.d	500.4	7.5	NaN	129.8	5	0.011	554	11	NaN	108.4	1.9	0.028
eaf35 - 88.d	1134	12	NaN	4.4	0.21	NaN	27.37	0.53	NaN	7.43	0.22	NaN
eaf35 - 89.d	990	15	NaN	36.4	1.5	NaN	173.7	3.3	0.032	45.19	0.9	NaN
eaf35 - 90.d	1221	18	NaN	1.483	0.099	0.02	11.05	0.33	NaN	3.4	0.13	0.0089
eaf35 - 91.d	1216	17	NaN	28.79	0.92	NaN	218.2	6.5	NaN	63.6	1.9	0.018

Analysis number	Nb93 ppm	Nb93 ppm 2SE	Nb93 ppm LOD	La139 ppm	La139 ppm 2SE	La139 ppm LOD	Ce140 ppm	Ce140 ppm 2SE	Ce140 ppm LOD	Pr141 ppm	Pr141 ppm 2SE	Pr141 ppm LOD
eaf35 - 92.d	1175	14	0.017	4.15	0.17	0.01	27.36	0.5	NaN	8.24	0.2	NaN
eaf35 - 93.d	928	11	0.051	30.42	0.64	NaN	183	2.9	0.022	45.71	0.8	NaN
eaf35 - 94.d	1027	10	NaN	26.31	0.58	0.062	118.5	2.1	NaN	27.81	0.6	0.018
eaf35 - 96.d	1191	14	NaN	18.98	0.87	NaN	77	4.2	0.011	14.76	0.57	NaN
eaf35 - 97.d	944	11	NaN	36	2.1	0.01	186.1	7.2	0.021	39.2	1.2	0.018
eaf35 - 98.d	1197	17	0.017	31.15	0.89	0.021	143.7	4.1	NaN	21.07	0.51	NaN
eaf35 - 99.d	1038	15	0.017	2.35	0.12	0.017	15.71	0.32	0.021	4.11	0.17	0.009
eaf35 - 100.d	697	10	0.034	39.66	0.56	NaN	240	3.3	0.011	53.9	1.1	NaN
eaf35 - 101.d	1138	18	0.035	14.33	0.78	0.022	39.8	1.5	NaN	8.6	0.29	NaN
eaf35 - 102.d	1098	14	0.017	28.79	0.92	0.015	116.2	3.7	NaN	22.22	0.64	0.041
eaf35 - 103.d	992	10	0.017	39.7	5.2	0.023	61.4	5.9	NaN	9.82	0.64	0.019
eaf35 - 104.d	1043	14	NaN	17.49	0.55	0.014	47.1	1.1	NaN	9.82	0.3	NaN
eaf35 - 106.d	999	12	NaN	18.85	0.6	NaN	51.9	2.1	NaN	9.73	0.36	NaN
eaf35 - 107.d	654.4	8.6	NaN	82.6	1.3	NaN	261.1	3.6	NaN	40.58	0.62	NaN
eaf35 - 108.d	1089	11	0.017	11.17	0.37	NaN	40.6	1	0.023	7.42	0.27	0.0091
eaf35 - 109.d	998.3	9.5	NaN	53	1.5	0.0098	188.6	5.3	NaN	31.81	0.89	NaN
eaf35 - 110.d	714.9	8.4	NaN	52.2	1.6	0.01	175.5	6.5	NaN	26.49	0.82	0.018
eaf35 - 111.d	1089	15	NaN	34.29	0.98	NaN	129.9	3	NaN	29.61	0.73	NaN
eaf35 - 112.d	1098	14	0.016	26.17	0.71	NaN	127.5	3	NaN	20.02	0.44	NaN
eaf35 - 113.d	1193	17	NaN	2.85	0.12	0.01	17.55	0.44	NaN	5.11	0.16	NaN
eaf35 - 114.d	680	11	NaN	65.02	0.95	0.01	246.9	3.4	NaN	43.36	0.68	0.0088
eaf35 - 115.d	1042	12	NaN	21.07	0.71	0.023	105	4.4	NaN	22.89	0.47	NaN
eaf35 - 116.d	1139	15	0.034	22.12	0.69	0.03	79.6	1.6	0.011	16.81	0.49	0.0093
eaf35 - 117.d	733.7	9.7	0.018	75.7	4.6	0.011	444	39	0.011	77.8	2.7	NaN
eaf35 - 118.d	675.3	8.7	NaN	43.5	5.4	NaN	218.5	9.8	NaN	48.6	1.3	0.0092
eaf35 - 119.d	1151	16	NaN	20.5	1.1	0.029	164.8	5	0.044	9.65	0.39	NaN
eaf35 - 120.d	1055	13	NaN	2.04	0.14	NaN	12.56	0.55	NaN	3.67	0.21	NaN

Analysis number	Nd146 ppm	Nd146 ppm 2SE	Nd146 ppm LOD	Sm147 ppm	Sm147 ppm 2SE	Sm147 ppm LOD	Eu153 ppm	Eu153 ppm 2SE	Eu153 ppm LOD	Gd157 ppm	Gd157 ppm 2SE	Gd157 ppm LOD
eaf35 - 1.d	54.3	1.4	NaN	43.7	1.5	NaN	14.35	0.42	0.032	100.9	2.2	NaN
eaf35 - 2.d	72.2	2.2	0.07	32.3	1.3	NaN	15.28	0.38	NaN	54.7	1.7	0.11
eaf35 - 3.d	64.3	2.6	NaN	31.5	1.3	0.081	16.25	0.55	NaN	56.9	2	NaN
eaf35 - 4.d	140.3	2.4	0.052	107.5	2.5	NaN	28.48	0.56	NaN	215.3	4.3	NaN
eaf35 - 5.d	152.7	3.4	NaN	109.1	2	NaN	28.91	0.74	NaN	213.9	4	0.057
eaf35 - 6.d	44.8	1.2	0.05	38.42	0.87	NaN	12.06	0.39	0.032	95.1	2.1	NaN
eaf35 - 7.d	304.6	4.4	NaN	193.9	3.4	0.062	48.27	0.89	0.034	327.3	4.8	NaN
eaf35 - 8.d	280.5	4.8	0.14	181.9	3.6	NaN	44.52	0.97	NaN	302.4	6.2	NaN
eaf35 - 9.d	87.8	2.4	NaN	57.7	1.4	NaN	17.07	0.49	NaN	118.5	3	NaN
eaf35 - 10.d	152.2	3.1	NaN	79	1.9	NaN	26.05	0.58	NaN	125.3	1.9	NaN
eaf35 - 11.d	41	1.4	0.1	31.1	1.1	NaN	9.32	0.34	NaN	69.8	1.7	NaN
eaf35 - 12.d	723	11	NaN	353.4	6.1	NaN	79.3	1.3	NaN	506.4	7.2	0.058
eaf35 - 13.d	737.8	9.1	NaN	363.1	5.2	0.13	79.48	0.99	0.034	505.8	6.7	0.12
eaf35 - 14.d	385.2	6.6	NaN	223.1	3.8	NaN	50.2	0.94	NaN	360.4	6.3	0.12
eaf35 - 15.d	121.4	5.5	NaN	61.5	1.5	NaN	18.59	0.44	NaN	126.8	2.6	NaN
eaf35 - 16.d	70.3	1.8	NaN	44.6	1.3	NaN	12.97	0.42	NaN	93.9	2.2	NaN
eaf35 - 17.d	239.7	5.3	NaN	137.3	2.7	NaN	34.06	0.7	0.038	239	5.7	NaN
eaf35 - 18.d	221.8	4.2	NaN	123.3	3	NaN	62.9	1.1	NaN	199.4	3.8	NaN
eaf35 - 19.d	60	1.4	NaN	35.9	1	NaN	10.86	0.29	0.034	80.9	1.8	NaN
eaf35 - 20.d	297.1	9.1	0.12	125.6	3.9	NaN	28.01	0.73	NaN	171.5	3.3	NaN
eaf35 - 22.d	238.7	6.2	0.21	132.3	3.1	0.14	33.09	0.76	NaN	222	4.7	NaN
eaf35 - 23.d	70.7	1.9	0.051	54.8	1.2	0.06	16.83	0.48	NaN	120	2.6	NaN
eaf35 - 24.d	160.2	3	NaN	115.3	2.5	0.17	32.82	0.79	NaN	231.2	3.9	NaN
eaf35 - 25.d	38.8	1.2	NaN	22.8	1	0.063	6.97	0.26	0.039	46.1	1.3	NaN
eaf35 - 26.d	104.4	2.7	0.053	59.9	1.7	NaN	15.94	0.33	NaN	110	2.2	NaN
eaf35 - 27.d	179	3.7	NaN	121.9	2.4	0.12	30.42	0.7	0.016	223.1	4.4	0.11
eaf35 - 28.d	40.4	1.5	NaN	24.3	1.4	NaN	6.73	0.32	0.033	46	1.1	0.057
eaf35 - 29.d	17.18	0.87	NaN	11.42	0.68	NaN	3.19	0.19	NaN	25.4	1	0.1
eaf35 - 30.d	47.7	2.1	NaN	23.21	0.63	0.18	10.4	0.42	NaN	39	1.3	NaN

Analysis number	Nd146 ppm	Nd146 ppm 2SE	Nd146 ppm LOD	Sm147 ppm	Sm147 ppm 2SE	Sm147 ppm LOD	Eu153 ppm	Eu153 ppm 2SE	Eu153 ppm LOD	Gd157 ppm	Gd157 ppm 2SE	Gd157 ppm LOD
eaf35 - 31.d	119	7.2	0.052	81.6	3.8	0.061	19.49	0.89	NaN	144.5	6.3	NaN
eaf35 - 32.d	187.8	3.6	NaN	129.8	2.9	NaN	32.9	0.85	NaN	244.4	5.2	0.056
eaf35 - 33.d	276.3	4.9	NaN	181.1	3	NaN	42.32	0.95	NaN	307.6	5.9	NaN
eaf35 - 34.d	83.5	1.9	NaN	57.8	2	0.12	15.66	0.46	0.033	117.5	2.9	0.11
eaf35 - 35.d	42.5	1.6	0.053	21.13	0.83	NaN	6.03	0.2	0.023	45.2	1.4	NaN
eaf35 - 36.d	30.1	1.3	0.1	15.7	0.84	NaN	3.74	0.2	NaN	30.56	0.97	NaN
eaf35 - 37.d	17.89	0.73	0.05	10.74	0.7	NaN	3.17	0.15	NaN	28.1	1.2	0.054
eaf35 - 38.d	61.8	1.9	NaN	52	1.7	NaN	14.74	0.46	0.05	118	2.9	NaN
eaf35 - 39.d	111	2.6	NaN	45	1.6	NaN	21.97	0.53	NaN	64.9	1.5	NaN
eaf35 - 40.d	247.2	5.3	0.11	69.7	1.5	NaN	26.65	0.59	NaN	73.7	1.6	NaN
eaf35 - 41.d	34.6	1.2	NaN	19.9	1	NaN	4.79	0.24	0.034	42.3	1.1	0.12
eaf35 - 42.d	339.1	7.6	NaN	171.8	3.3	NaN	45.35	0.95	NaN	235.9	4.2	0.055
eaf35 - 43.d	490.2	9.1	0.1	217.8	3.9	NaN	55.08	0.97	NaN	279.4	4.4	NaN
eaf35 - 44.d	534	10	NaN	250	4.3	0.059	57.6	1.4	0.032	323	5.9	0.054
eaf35 - 45.d	420.7	7.1	0.05	208.3	4.5	NaN	48.6	1.2	NaN	276.8	4.5	NaN
eaf35 - 48.d	324.2	8.5	0.11	163.8	4.4	NaN	43.58	0.97	0.046	232.6	5.3	0.11
eaf35 - 49.d	83.9	3	0.052	52.2	1.9	NaN	14.52	0.51	0.038	111.3	2.7	NaN
eaf35 - 50.d	51.7	1.4	NaN	31.8	1.1	NaN	8.51	0.26	0.032	66.5	1.7	NaN
eaf35 - 51.d	129.7	2.3	0.051	82.7	1.8	NaN	21.24	0.5	NaN	157.8	3.2	0.055
eaf35 - 52.d	178.1	5.1	0.054	124.8	3.2	NaN	31.03	0.82	NaN	236.5	7.1	NaN
eaf35 - 53.d	239.9	6	NaN	149.9	4.5	0.085	36	1.1	0.017	275.4	6.7	NaN
eaf35 - 54.d	33.8	1	NaN	29.5	1.1	NaN	9.66	0.34	0.016	75	1.7	0.12
eaf35 - 55.d	157.2	5.3	NaN	77.1	2.8	NaN	29.21	0.72	NaN	114.5	2.9	0.11
eaf35 - 56.d	186.3	4.2	0.052	121.8	3.4	NaN	32.46	0.86	0.033	233	5.1	NaN
eaf35 - 57.d	63.6	3	NaN	25.8	1.1	NaN	14.69	0.73	NaN	43.5	1.8	0.054
eaf35 - 58.d	39	1.3	NaN	27.4	1	NaN	8.97	0.4	NaN	64.2	1.7	0.11
eaf35 - 59.d	40.7	1.1	NaN	35.8	1.3	NaN	10.99	0.36	NaN	88.4	2.1	0.055
eaf35 - 60.d	38	1	0.1	34.6	1.5	NaN	7.99	0.26	NaN	80	2.4	NaN
eaf35 - 61.d	36.5	1.4	NaN	26.2	1.1	NaN	6.11	0.25	0.043	64	1.8	0.052

Analysis number	Nd146 ppm	Nd146 ppm 2SE	Nd146 ppm LOD	Sm147 ppm	Sm147 ppm 2SE	Sm147 ppm LOD	Eu153 ppm	Eu153 ppm 2SE	Eu153 ppm LOD	Gd157 ppm	Gd157 ppm 2SE	Gd157 ppm LOD
eaf35 - 62.d	224.3	4	NaN	154	3	NaN	43.15	0.8	NaN	292.7	5.1	0.057
eaf35 - 63.d	25.58	0.96	NaN	19.7	1	NaN	7.76	0.29	0.022	44.5	1.2	NaN
eaf35 - 64.d	24.3	1.2	NaN	19.19	0.96	0.062	7.44	0.26	NaN	44.2	1.3	0.11
eaf35 - 65.d	76.2	3.7	NaN	33.1	1.2	NaN	20.28	0.98	NaN	53.6	1.6	NaN
eaf35 - 66.d	89.1	2.2	NaN	46.5	1.2	NaN	9.47	0.29	NaN	81.4	1.6	NaN
eaf35 - 67.d	22.3	0.91	0.1	20.35	0.82	0.12	4.51	0.23	NaN	50.6	1.3	0.11
eaf35 - 68.d	156.4	3.2	0.1	79.1	2.1	0.13	17.94	0.48	NaN	123.1	2.6	0.055
eaf35 - 69.d	269.1	5	NaN	104.1	2.2	NaN	21.64	0.53	0.035	135.1	2.9	0.055
eaf35 - 70.d	172.1	3.3	NaN	70.2	1.6	NaN	37.59	0.8	0.016	108.8	2.5	0.054
eaf35 - 71.d	186.1	3.4	NaN	66.2	2.1	0.061	38.58	0.81	NaN	89.7	2.4	NaN
eaf35 - 72.d	318	9.3	NaN	204	4.6	NaN	46.98	0.87	0.048	350.3	7.1	NaN
eaf35 - 73.d	199.6	6.6	NaN	142.7	4.3	NaN	35.25	0.65	NaN	260.2	6.1	NaN
eaf35 - 74.d	136.6	3.9	0.1	63.7	2.5	NaN	25.23	0.73	0.016	99	3.3	0.15
eaf35 - 75.d	57.6	2.5	0.054	18.04	0.88	NaN	28.53	0.6	0.034	28.2	1.2	NaN
eaf35 - 76.d	19.69	0.96	0.052	11.99	0.74	NaN	4.89	0.22	NaN	26.6	1.1	NaN
eaf35 - 77.d	63.8	2	NaN	23.5	1	NaN	23.49	0.6	NaN	30.7	1.1	NaN
eaf35 - 78.d	109.8	2.3	NaN	48.5	1.3	NaN	41.52	0.8	NaN	74.2	1.7	0.056
eaf35 - 79.d	33.2	1.6	0.085	26.3	1	NaN	7.74	0.32	NaN	62.1	2.2	NaN
eaf35 - 80.d	85.4	2	NaN	65.5	1.4	NaN	29.64	0.66	NaN	143.9	2.2	NaN
eaf35 - 81.d	485	19	NaN	123.9	5.3	NaN	32.87	0.73	NaN	184.7	5.5	NaN
eaf35 - 82.d	271.9	5.4	NaN	153.2	3.3	0.13	50.8	1.1	NaN	230.5	4.5	0.13
eaf35 - 83.d	119.8	2.3	NaN	60.7	1.8	NaN	15.41	0.44	NaN	86.8	2	0.11
eaf35 - 84.d	399	12	0.052	185.1	3.3	NaN	40.1	0.79	NaN	247.2	5.2	NaN
eaf35 - 85.d	522.8	8.5	NaN	210.1	4.9	0.12	48.3	1.2	0.036	254	4.8	NaN
eaf35 - 86.d	590	11	NaN	237	5.1	0.12	52.8	1.2	0.017	289.2	5	NaN
eaf35 - 88.d	54.2	1.6	NaN	45.1	1.7	NaN	11.68	0.34	0.032	97.9	2.4	0.055
eaf35 - 89.d	307.3	6	0.11	198.5	4.7	0.12	42.74	0.9	0.017	326	5.6	NaN
eaf35 - 90.d	28.5	1	NaN	26.5	1.1	0.059	5.88	0.26	NaN	63.2	1.8	0.054
eaf35 - 91.d	446	14	NaN	212.1	7.4	NaN	18.29	0.54	0.016	277.5	7.9	0.11

Analysis number	Nd146 ppm	Nd146 ppm 2SE	Nd146 ppm LOD	Sm147 ppm	Sm147 ppm 2SE	Sm147 ppm LOD	Eu153 ppm	Eu153 ppm 2SE	Eu153 ppm LOD	Gd157 ppm	Gd157 ppm 2SE	Gd157 ppm LOD
eaf35 - 92.d	62.6	1.8	NaN	55.7	1.8	0.13	13.63	0.32	0.016	122.4	2.4	0.12
eaf35 - 93.d	329.2	5.8	NaN	209.6	3.8	NaN	47.1	1	0.016	353.5	6.7	0.15
eaf35 - 94.d	183.4	3.9	NaN	129.2	2.8	0.12	29.94	0.75	0.032	234.5	3.9	NaN
eaf35 - 96.d	74.3	2.4	NaN	45.2	1.4	NaN	9.33	0.39	0.016	84.7	2.6	NaN
eaf35 - 97.d	248	5	NaN	160.7	3.4	NaN	37.92	0.91	0.033	275	4.3	NaN
eaf35 - 98.d	99.9	2.5	NaN	50.7	1.4	NaN	12.75	0.42	NaN	98.4	2.3	NaN
eaf35 - 99.d	34.6	1	0.1	30	1	NaN	8.41	0.25	NaN	70.6	1.6	NaN
eaf35 - 100.d	346.4	5.7	NaN	166	3.6	0.12	41.81	0.76	0.016	229.4	4.2	NaN
eaf35 - 101.d	48.7	1.8	0.11	31.7	1	NaN	7.63	0.26	0.034	67.2	1.9	NaN
eaf35 - 102.d	122.6	3.2	NaN	77.2	2.3	NaN	19.5	0.61	NaN	142.7	3.4	0.057
eaf35 - 103.d	50.7	2.2	NaN	30.7	1.3	NaN	6.21	0.25	NaN	64.5	1.8	NaN
eaf35 - 104.d	55.1	1.7	NaN	33.5	1.2	0.061	6.88	0.25	NaN	70.1	1.6	0.056
eaf35 - 106.d	50.2	1.8	NaN	27.8	1.2	NaN	7.76	0.25	NaN	55.9	1.7	NaN
eaf35 - 107.d	190.7	3.3	NaN	75	1.7	NaN	41.72	0.92	NaN	96	2.3	NaN
eaf35 - 108.d	44.8	1.5	NaN	32.9	1.4	NaN	9.33	0.35	NaN	72.5	1.6	NaN
eaf35 - 109.d	159	3.5	NaN	69.8	1.5	NaN	25.56	0.88	NaN	100.2	2.1	NaN
eaf35 - 110.d	129.8	3.8	NaN	52.8	1.8	0.12	27.94	0.88	NaN	68	2.2	0.11
eaf35 - 111.d	187.3	4	NaN	126	2.9	NaN	33.87	0.9	0.017	236.6	4.1	0.11
eaf35 - 112.d	110.3	2.9	NaN	52.6	1.5	NaN	12.36	0.29	NaN	81.8	1.8	NaN
eaf35 - 113.d	38.2	1.2	0.049	35.6	1.6	NaN	10.3	0.41	NaN	82.3	1.9	NaN
eaf35 - 114.d	222.9	3.8	NaN	83.2	2	0.12	31.55	0.72	NaN	105.7	2.1	NaN
eaf35 - 115.d	157.7	2.8	0.11	115.4	3.1	0.12	30.49	0.76	NaN	213.7	4.4	NaN
eaf35 - 116.d	109.1	2.4	NaN	82.2	2.2	NaN	22.99	0.65	NaN	174.7	4.2	0.11
eaf35 - 117.d	439.6	9.7	NaN	199.8	4.2	NaN	44.1	0.79	NaN	247.4	5	0.058
eaf35 - 118.d	311.1	5.8	NaN	155.6	3.2	0.12	37.59	0.81	0.016	202.8	2.6	0.11
eaf35 - 119.d	50	1.8	NaN	31.2	1.6	NaN	7.89	0.37	0.033	65.9	2.9	NaN
eaf35 - 120.d	29.5	1.5	0.1	27	1.1	0.19	6.77	0.36	0.032	59.3	1.9	0.15

Analysis number	Tb159 ppm	Tb159 ppm 2SE	Tb159 ppm LOD	Dy163 ppm	Dy163 ppm 2SE	Dy163 ppm LOD	Ho165 ppm	Ho165 ppm 2SE	Ho165 ppm LOD	Er166 ppm	Er166 ppm 2SE	Er166 ppm LOD
eaf35 - 1.d	25.17	0.48	NaN	199.9	3.1	NaN	38.8	0.75	NaN	87.2	1.7	NaN
eaf35 - 2.d	11.92	0.3	0.017	97.1	1.3	NaN	22.42	0.35	NaN	69.4	1.1	0.051
eaf35 - 3.d	12.41	0.3	NaN	104.7	1.9	NaN	23.59	0.39	NaN	70	1.4	NaN
eaf35 - 4.d	45.99	0.74	NaN	321.6	5.1	NaN	51	0.81	NaN	96.8	1.7	NaN
eaf35 - 5.d	45.04	0.81	0.017	302.6	4.5	NaN	48.96	0.76	0.012	91	1.7	NaN
eaf35 - 6.d	26.03	0.45	NaN	229.5	3.7	NaN	48.57	0.81	NaN	120.3	1.7	NaN
eaf35 - 7.d	62.84	0.99	0.025	374.2	5.8	NaN	53.58	0.88	NaN	90.2	1.2	NaN
eaf35 - 8.d	58.13	0.96	NaN	346.9	6.2	0.07	49.37	0.96	0.026	80.9	1.7	NaN
eaf35 - 9.d	29.21	0.61	NaN	234.4	4.1	NaN	46.92	0.87	NaN	117.7	2.4	NaN
eaf35 - 10.d	29.07	0.48	NaN	235.5	3.3	NaN	51.37	0.89	NaN	150.3	2.6	NaN
eaf35 - 11.d	20.13	0.53	0.0083	172.9	3.9	0.035	36.19	0.82	NaN	89.3	1.9	NaN
eaf35 - 12.d	95.6	1.2	NaN	675	10	NaN	141.6	2.1	NaN	426	5.5	0.057
eaf35 - 13.d	93.1	1.1	0.023	646.7	7.5	0.071	136.3	2	0.0088	401.5	5	NaN
eaf35 - 14.d	73	1.2	NaN	518.9	7.2	0.071	103	1.5	NaN	271	4.4	0.052
eaf35 - 15.d	32.51	0.55	0.0088	264.3	3.9	NaN	52.24	0.84	NaN	132.3	2.5	0.059
eaf35 - 16.d	24.89	0.42	0.017	204.8	3.3	NaN	38.14	0.64	0.0089	88.3	1.8	0.027
eaf35 - 17.d	53.3	1.1	0.021	376.9	7.8	NaN	69.2	1.4	0.02	158.7	2.8	NaN
eaf35 - 18.d	34.47	0.8	NaN	225.8	4.5	0.035	44.99	0.71	0.019	117.5	2	NaN
eaf35 - 19.d	22.19	0.37	NaN	186	3	NaN	34.66	0.51	0.0087	77	1.5	NaN
eaf35 - 20.d	34.37	0.63	0.017	259.1	4.5	0.07	52.16	0.82	NaN	140.1	2.3	NaN
eaf35 - 22.d	47.34	0.87	NaN	337.3	5.7	0.071	58.6	1.2	0.018	128	2.7	NaN
eaf35 - 23.d	32.23	0.44	0.016	275.3	4.3	NaN	58.34	0.98	NaN	153.4	2.8	NaN
eaf35 - 24.d	51.73	0.74	NaN	371.3	5.7	NaN	63.7	1.2	0.0086	131.5	2.2	NaN
eaf35 - 25.d	12.86	0.25	NaN	117.9	2.2	NaN	27.16	0.49	NaN	79	1.5	NaN
eaf35 - 26.d	26.16	0.55	0.017	218.7	3.3	0.07	47.08	0.68	0.024	128.1	2.1	NaN
eaf35 - 27.d	45.87	0.73	0.0083	305.3	4.4	NaN	50.05	0.96	0.0085	107	2.1	0.055
eaf35 - 28.d	12.37	0.34	NaN	112	2.4	NaN	25.13	0.47	NaN	71.6	1.5	0.051
eaf35 - 29.d	7.78	0.31	NaN	78.2	2	NaN	20.35	0.49	0.017	68.4	1.6	NaN
eaf35 - 30.d	8.98	0.22	0.022	80	1.6	0.073	18.71	0.4	NaN	58.6	1	NaN

Analysis number	Tb159 ppm	Tb159 ppm 2SE	Tb159 ppm LOD	Dy163 ppm	Dy163 ppm 2SE	Dy163 ppm LOD	Ho165 ppm	Ho165 ppm 2SE	Ho165 ppm LOD	Er166 ppm	Er166 ppm 2SE	Er166 ppm LOD
eaf35 - 31.d	31.4	1.1	NaN	220.3	4.6	NaN	38.74	0.58	NaN	86.2	1.5	0.025
eaf35 - 32.d	50.16	0.81	NaN	317.8	5.6	NaN	48.43	0.9	NaN	87.6	1.9	NaN
eaf35 - 33.d	59.14	0.8	NaN	349.3	6	NaN	51.2	1	NaN	92.7	2	NaN
eaf35 - 34.d	27.98	0.65	NaN	219.9	4	0.14	41.09	0.78	0.0084	96.5	1.9	0.055
eaf35 - 35.d	12.08	0.34	NaN	103.8	1.6	0.035	22.04	0.38	NaN	54.1	1.1	0.052
eaf35 - 36.d	8.75	0.3	NaN	85.1	2.1	NaN	21.13	0.46	NaN	68	1.5	NaN
eaf35 - 37.d	8.55	0.27	NaN	84.4	2.2	NaN	20.73	0.5	0.022	61.9	1.3	0.049
eaf35 - 38.d	29.72	0.57	0.019	238.3	5.1	NaN	46.6	1	NaN	110.4	2.4	0.026
eaf35 - 39.d	13.52	0.33	NaN	102.3	2	NaN	22.43	0.54	0.017	68.3	1.5	NaN
eaf35 - 40.d	12.04	0.31	0.02	80.3	1.7	NaN	16.36	0.35	0.017	47.9	1.1	NaN
eaf35 - 41.d	11.97	0.23	NaN	109.9	2.1	NaN	24.9	0.43	0.017	67.9	1.6	NaN
eaf35 - 42.d	43.36	0.81	0.0082	316.3	5.4	NaN	74.5	1.2	NaN	250.9	4.6	0.05
eaf35 - 43.d	50.01	0.74	NaN	358.5	5.3	0.075	82.1	1.2	NaN	274.3	3.7	0.076
eaf35 - 44.d	58	1.2	NaN	413.4	7.8	0.067	93.4	1.8	NaN	302.3	5.2	NaN
eaf35 - 45.d	50.38	0.86	NaN	357.4	5.5	NaN	81.7	1.3	0.0082	267	3.8	NaN
eaf35 - 48.d	42.61	0.78	NaN	310.4	6.2	NaN	73.1	1.6	0.0086	246.6	4.3	NaN
eaf35 - 49.d	28.19	0.66	0.0083	239.9	3.8	0.047	49.92	0.63	NaN	124.2	2.2	0.051
eaf35 - 50.d	16.92	0.37	NaN	136	2.3	NaN	25.4	0.48	NaN	57.7	1.3	NaN
eaf35 - 51.d	36.26	0.61	0.0082	250	3.6	NaN	41.86	0.65	NaN	84.3	1.6	0.05
eaf35 - 52.d	49.9	1.4	NaN	317	7.2	NaN	47.2	1.2	NaN	81.4	1.8	NaN
eaf35 - 53.d	54.4	1.4	NaN	338.8	7.6	NaN	49.3	1	NaN	86.3	2	NaN
eaf35 - 54.d	20.8	0.46	0.0081	177.6	3.8	NaN	35.89	0.72	NaN	86.5	2.2	0.068
eaf35 - 55.d	25.89	0.72	NaN	200.9	6	NaN	41.2	1	NaN	117.4	3.1	NaN
eaf35 - 56.d	49.1	1	0.0083	333.5	7.5	NaN	53.4	1.3	0.017	105.9	3.2	NaN
eaf35 - 57.d	10.43	0.3	NaN	85.2	2.3	0.067	20.37	0.4	NaN	63	1.5	NaN
eaf35 - 58.d	17.17	0.43	NaN	142.7	2.8	0.046	27.01	0.53	0.0084	58	1.2	NaN
eaf35 - 59.d	23.59	0.53	0.016	184.2	4.1	NaN	31.54	0.64	0.0083	60.6	1.5	NaN
eaf35 - 60.d	21.2	0.55	NaN	176	3.7	0.033	36.59	0.81	NaN	91	2.2	0.025
eaf35 - 61.d	17.4	0.4	0.0078	155	4.1	NaN	31.69	0.72	NaN	75.5	1.9	NaN

Analysis number	Tb159 ppm	Tb159 ppm 2SE	Tb159 ppm LOD	Dy163 ppm	Dy163 ppm 2SE	Dy163 ppm LOD	Ho165 ppm	Ho165 ppm 2SE	Ho165 ppm LOD	Er166 ppm	Er166 ppm 2SE	Er166 ppm LOD
eaf35 - 62.d	62.3	0.88	NaN	417.9	6.5	NaN	67.27	0.98	NaN	135.7	2.1	NaN
eaf35 - 63.d	12.31	0.25	NaN	118.3	3.3	0.034	28.29	0.52	NaN	89.2	2	0.077
eaf35 - 64.d	11.87	0.28	NaN	112	2.2	0.07	26.63	0.57	NaN	79.7	1.5	0.035
eaf35 - 65.d	12.31	0.29	0.0082	100.8	2.2	0.068	23.89	0.46	0.017	71.8	1.5	0.025
eaf35 - 66.d	20.71	0.48	NaN	169.4	2.7	NaN	33.38	0.54	NaN	83	1.7	NaN
eaf35 - 67.d	13.75	0.26	0.016	117	2	NaN	25.04	0.45	NaN	59.4	1.3	NaN
eaf35 - 68.d	27.61	0.54	0.0082	218.6	3.9	0.046	48.68	0.85	NaN	156.6	2.4	NaN
eaf35 - 69.d	26.12	0.56	NaN	190.2	4.7	NaN	40.1	0.86	0.017	122	2.9	NaN
eaf35 - 70.d	23.61	0.62	NaN	180.2	3.6	0.033	37	0.69	0.011	108.3	2.1	0.025
eaf35 - 71.d	17.16	0.3	0.017	124.3	2.3	0.069	27.72	0.62	NaN	88.2	1.4	0.035
eaf35 - 72.d	67.4	1.2	NaN	404.6	7.9	NaN	58.7	1.3	0.017	104.3	2.5	0.025
eaf35 - 73.d	53.2	1.1	NaN	342.6	6.4	NaN	53.3	1	NaN	98.8	1.9	0.025
eaf35 - 74.d	21.09	0.83	NaN	162.8	7.4	NaN	34.7	1.6	0.0085	98.8	4	NaN
eaf35 - 75.d	6.09	0.2	0.0087	52.4	1.4	NaN	12.78	0.31	NaN	41.4	1.1	NaN
eaf35 - 76.d	7.98	0.21	0.0083	75.4	1.6	NaN	19.33	0.37	NaN	61.5	1.3	0.055
eaf35 - 77.d	7.35	0.23	NaN	63.2	2.1	NaN	15.36	0.47	NaN	50.6	1.3	NaN
eaf35 - 78.d	15.63	0.38	NaN	118.7	1.6	NaN	26.53	0.47	NaN	82.2	1.2	NaN
eaf35 - 79.d	18.38	0.4	NaN	167.3	3.2	NaN	33.62	0.63	0.0087	77.9	1.4	NaN
eaf35 - 80.d	35.84	0.77	NaN	280.1	4.7	NaN	56	1.1	NaN	144.1	2.9	0.026
eaf35 - 81.d	37.3	0.92	NaN	274.6	6	NaN	53.1	1.2	0.009	132.7	3.3	0.027
eaf35 - 82.d	46.98	0.77	0.0088	348	5.7	NaN	78.9	1.7	NaN	264	4.3	NaN
eaf35 - 83.d	16.81	0.36	0.0083	128.3	2.1	0.034	31.45	0.59	NaN	113.2	1.9	NaN
eaf35 - 84.d	44.7	0.87	NaN	325.6	6.9	NaN	75.1	1.5	NaN	246.9	4.1	NaN
eaf35 - 85.d	45.57	0.91	0.0082	323.1	5.7	NaN	73.4	1.5	0.0084	244.6	4.5	NaN
eaf35 - 86.d	51.9	0.96	0.017	375.5	6.4	NaN	82.4	1.4	NaN	279.2	4.9	NaN
eaf35 - 88.d	24.81	0.61	NaN	192	3.4	0.067	35.15	0.7	NaN	77.4	1.7	0.054
eaf35 - 89.d	58.7	1.2	NaN	327.1	5.8	NaN	43.82	0.79	NaN	73.2	1.5	NaN
eaf35 - 90.d	16.99	0.34	NaN	150.5	3.4	NaN	34.08	0.73	NaN	93.2	1.9	NaN
eaf35 - 91.d	51.5	1.2	0.017	358.9	9.5	NaN	74.7	1.7	NaN	204.6	4.2	NaN

Analysis number	Tb159 ppm	Tb159 ppm 2SE	Tb159 ppm LOD	Dy163 ppm	Dy163 ppm 2SE	Dy163 ppm LOD	Ho165 ppm	Ho165 ppm 2SE	Ho165 ppm LOD	Er166 ppm	Er166 ppm 2SE	Er166 ppm LOD
eaf35 - 92.d	31.56	0.55	NaN	258.3	4.4	NaN	50.95	0.95	0.017	120.1	1.9	NaN
eaf35 - 93.d	64.4	1.3	NaN	366.1	7	NaN	51.25	0.87	NaN	83.3	2.1	0.055
eaf35 - 94.d	48.72	0.91	NaN	305.8	4	0.067	47.39	0.66	0.0083	87	1.1	0.05
eaf35 - 96.d	21.74	0.57	0.0081	182	3.9	NaN	37.5	0.77	NaN	92.2	1.8	NaN
eaf35 - 97.d	51.14	0.81	NaN	293.5	5.1	NaN	39.15	0.69	NaN	63	1.3	0.05
eaf35 - 98.d	25.61	0.52	0.0084	213.3	4.3	NaN	45.58	0.93	NaN	118.7	2	0.051
eaf35 - 99.d	18.94	0.41	NaN	160.1	2.9	NaN	32.87	0.67	NaN	82.6	2	0.054
eaf35 - 100.d	42.87	0.77	NaN	315.3	4.6	0.067	74.7	1.2	NaN	258.4	4.9	NaN
eaf35 - 101.d	17.4	0.4	NaN	144.7	2.5	NaN	27.74	0.55	NaN	66.6	1.3	0.026
eaf35 - 102.d	34.15	0.66	NaN	247.3	3.7	NaN	45.02	0.98	NaN	105	2.3	0.052
eaf35 - 103.d	15.86	0.37	0.0083	124.9	2.5	0.069	22.36	0.38	0.0085	46.6	1.2	NaN
eaf35 - 104.d	17.55	0.41	NaN	133.9	2.7	NaN	24.86	0.44	0.0085	52.1	1.1	0.025
eaf35 - 106.d	14.54	0.29	0.016	120.4	2.6	NaN	24.56	0.47	0.011	58.1	1.4	0.05
eaf35 - 107.d	18.64	0.42	NaN	134.1	2.5	NaN	29.44	0.49	NaN	91.7	1.8	0.049
eaf35 - 108.d	19.2	0.39	0.016	160.5	2.7	NaN	32.71	0.62	NaN	78.6	1.4	0.05
eaf35 - 109.d	20.75	0.39	0.011	155.9	2.6	0.032	32.25	0.57	0.011	92.1	1.5	NaN
eaf35 - 110.d	13.91	0.51	NaN	103.2	2.5	NaN	22.65	0.59	0.0082	70.3	1.7	NaN
eaf35 - 111.d	50.62	0.8	0.0084	341.1	5.4	0.075	57.3	1	NaN	123	2	0.035
eaf35 - 112.d	18.57	0.33	NaN	149.4	3.1	NaN	32.73	0.55	0.018	93.3	1.8	0.024
eaf35 - 113.d	21.57	0.54	NaN	183.6	3.6	NaN	37.23	0.7	NaN	88.5	1.4	0.053
eaf35 - 114.d	19.49	0.28	NaN	137.8	2.6	NaN	29.61	0.47	NaN	86.8	1.3	NaN
eaf35 - 115.d	44.85	0.91	NaN	300.1	4.4	NaN	50.06	0.87	NaN	99.3	2.1	NaN
eaf35 - 116.d	39.88	0.65	NaN	289.1	4.4	0.034	53.46	0.98	NaN	116.8	2.3	NaN
eaf35 - 117.d	42.18	0.74	0.0086	298.2	5.2	0.071	68.6	1.1	NaN	234.2	2.8	0.026
eaf35 - 118.d	35.69	0.64	NaN	255	3.9	NaN	58.81	0.84	NaN	203.9	2.9	0.025
eaf35 - 119.d	18.15	0.66	NaN	157.2	4	NaN	32.97	0.81	NaN	78.9	1.7	NaN
eaf35 - 120.d	15.03	0.29	NaN	126.5	2.6	NaN	25.29	0.55	0.017	57.8	1.3	NaN

Analysis number	Tm169 ppm	Tm169 ppm 2SE	Tm169 ppm LOD	Yb172 ppm	Yb172 ppm 2SE	Yb172 ppm LOD	Lu175 ppm	Lu175 ppm 2SE	Lu175 ppm LOD	Hf178 ppm	Hf178 ppm 2SE	Hf178 ppm LOD
eaf35 - 1.d	8.71	0.2	0.016	38.91	0.83	NaN	3.36	0.13	0.02	6.35	0.34	NaN
eaf35 - 2.d	9.5	0.23	NaN	57.2	1.4	0.083	7.38	0.2	NaN	8.83	0.42	NaN
eaf35 - 3.d	9.03	0.25	NaN	54.8	1.2	NaN	7.85	0.27	NaN	17.81	0.67	0.029
eaf35 - 4.d	7.85	0.19	0.016	31.6	1	NaN	2.78	0.12	0.019	7.01	0.28	NaN
eaf35 - 5.d	7.89	0.23	NaN	33.3	1.3	NaN	3.24	0.15	0.0086	7.9	0.35	NaN
eaf35 - 6.d	13.4	0.33	0.016	64.6	1.1	NaN	6.33	0.16	NaN	6.89	0.42	NaN
eaf35 - 7.d	6.87	0.18	NaN	25.68	0.78	NaN	2.17	0.11	0.0087	9.81	0.45	NaN
eaf35 - 8.d	6.01	0.15	NaN	22.88	0.85	0.039	1.83	0.11	NaN	9.2	0.38	0.059
eaf35 - 9.d	13.71	0.37	NaN	76.8	1.8	NaN	9.65	0.25	NaN	6.84	0.38	0.031
eaf35 - 10.d	20.08	0.35	0.016	122	2.2	NaN	15.88	0.4	NaN	6.83	0.27	0.029
eaf35 - 11.d	10.49	0.29	NaN	60.8	1.6	NaN	7.22	0.24	NaN	6.97	0.39	NaN
eaf35 - 12.d	58.33	0.83	NaN	360	6.6	0.11	45.21	0.69	0.0087	11.91	0.48	0.03
eaf35 - 13.d	54.98	0.9	NaN	342.4	3.7	0.086	44.08	0.71	NaN	11.52	0.43	0.03
eaf35 - 14.d	32.76	0.56	NaN	183.1	3	NaN	22.65	0.42	0.017	8.6	0.36	NaN
eaf35 - 15.d	15.04	0.34	0.0087	82.1	2	NaN	9.18	0.25	0.02	8.21	0.4	NaN
eaf35 - 16.d	10.48	0.26	NaN	61.7	1.3	NaN	8.04	0.24	NaN	7.48	0.32	NaN
eaf35 - 17.d	19.27	0.54	0.019	115.2	2.5	NaN	14.8	0.44	0.0098	8.85	0.4	0.074
eaf35 - 18.d	13.7	0.28	0.016	73.4	1.8	NaN	9.49	0.21	0.017	6.8	0.35	NaN
eaf35 - 19.d	7.66	0.19	NaN	36.8	1	0.039	3.87	0.14	NaN	7.41	0.28	0.065
eaf35 - 20.d	17.14	0.44	NaN	102	2.3	NaN	13.25	0.31	0.0086	10.31	0.45	0.06
eaf35 - 22.d	13.6	0.29	0.0084	74.3	1.7	0.054	8.88	0.21	NaN	9.57	0.44	NaN
eaf35 - 23.d	17.98	0.44	0.008	97	3.1	NaN	10.98	0.38	NaN	6.95	0.29	NaN
eaf35 - 24.d	11.71	0.32	0.023	51.5	1.2	NaN	4.89	0.18	NaN	7.24	0.35	0.03
eaf35 - 25.d	10.4	0.26	NaN	61.3	1.6	0.039	7.27	0.26	NaN	7.64	0.38	NaN
eaf35 - 26.d	15.31	0.3	NaN	87	1.9	0.078	10.36	0.3	0.0086	7.84	0.35	NaN
eaf35 - 27.d	12.36	0.25	NaN	73.8	1.9	0.076	9.78	0.24	NaN	7.52	0.34	0.058
eaf35 - 28.d	9	0.28	NaN	53.4	1.8	0.077	6.59	0.32	NaN	6.24	0.31	NaN
eaf35 - 29.d	9.29	0.29	0.016	54.5	1.8	NaN	5.68	0.18	NaN	5.25	0.26	NaN
eaf35 - 30.d	7.89	0.18	NaN	48.3	1.5	NaN	5.99	0.18	NaN	5.04	0.32	NaN

Analysis number	Tm169 ppm	Tm169 ppm 2SE	Tm169 ppm LOD	Yb172 ppm	Yb172 ppm 2SE	Yb172 ppm LOD	Lu175 ppm	Lu175 ppm 2SE	Lu175 ppm LOD	Hf178 ppm	Hf178 ppm 2SE	Hf178 ppm LOD
eaf35 - 31.d	9.46	0.27	NaN	49.2	1.3	NaN	5.46	0.17	NaN	7.07	0.35	NaN
eaf35 - 32.d	6.91	0.22	NaN	29.64	0.76	0.052	2.842	0.095	0.0084	7.49	0.41	NaN
eaf35 - 33.d	8.78	0.24	NaN	45.8	1.1	NaN	5.47	0.18	0.0082	8.51	0.37	NaN
eaf35 - 34.d	10.27	0.29	NaN	54.8	1.3	0.076	6.48	0.23	0.0083	7.22	0.45	NaN
eaf35 - 35.d	5.84	0.19	0.017	28.44	0.82	NaN	3.17	0.14	NaN	6.58	0.38	0.03
eaf35 - 36.d	8.87	0.25	NaN	48.4	1.2	NaN	5.01	0.18	0.016	5.47	0.3	NaN
eaf35 - 37.d	7.56	0.24	NaN	38.28	0.92	NaN	3.59	0.13	NaN	5.42	0.26	NaN
eaf35 - 38.d	11.52	0.33	0.0082	56.6	1.5	NaN	5.78	0.19	NaN	6.67	0.41	NaN
eaf35 - 39.d	9.72	0.22	0.008	63.7	1.7	NaN	8.86	0.23	NaN	4.03	0.24	NaN
eaf35 - 40.d	6.3	0.18	0.0083	42.1	1.2	NaN	5.66	0.17	0.017	6.14	0.35	NaN
eaf35 - 41.d	7.85	0.22	NaN	39.1	1	NaN	3.86	0.16	NaN	6.02	0.28	NaN
eaf35 - 42.d	37.85	0.74	NaN	268.2	4.2	NaN	40.01	0.71	NaN	7.46	0.35	0.029
eaf35 - 43.d	42.49	0.89	NaN	294.9	4.4	0.038	43.49	0.89	NaN	8.52	0.39	0.029
eaf35 - 44.d	46.65	0.87	0.016	311.3	5	NaN	45.77	0.79	NaN	9.49	0.36	NaN
eaf35 - 45.d	40.53	0.66	NaN	276	4.5	NaN	40.38	0.75	NaN	8.18	0.35	NaN
eaf35 - 48.d	38.14	0.84	NaN	274.3	5.4	NaN	40.9	0.79	0.0085	6.93	0.39	0.059
eaf35 - 49.d	13.38	0.3	NaN	64.9	1.5	NaN	6.67	0.2	NaN	7.15	0.31	NaN
eaf35 - 50.d	5.97	0.19	NaN	30.2	1.2	NaN	3.43	0.14	0.0083	7.14	0.29	NaN
eaf35 - 51.d	8.21	0.24	NaN	39.6	1.1	0.038	4.5	0.17	NaN	7.44	0.33	0.029
eaf35 - 52.d	5.74	0.23	NaN	21.06	0.65	NaN	1.7	0.093	NaN	7.69	0.39	NaN
eaf35 - 53.d	6.99	0.2	0.0083	31.22	0.78	0.039	3.09	0.14	0.017	8.41	0.41	NaN
eaf35 - 54.d	8.64	0.36	NaN	39.3	1.3	0.037	3.62	0.2	0.0082	6.5	0.28	NaN
eaf35 - 55.d	15.75	0.45	NaN	100.6	2.6	0.077	13.37	0.35	0.0085	6.94	0.27	0.059
eaf35 - 56.d	10	0.43	NaN	46.9	2.5	0.038	4.95	0.28	NaN	7.69	0.39	NaN
eaf35 - 57.d	8.3	0.2	NaN	47.1	1.6	NaN	5.55	0.21	0.0082	6.15	0.32	0.028
eaf35 - 58.d	5.4	0.18	NaN	24.21	0.78	0.082	2.225	0.097	NaN	6.69	0.42	NaN
eaf35 - 59.d	4.77	0.13	0.008	19.77	0.84	NaN	1.506	0.091	NaN	6.81	0.34	NaN
eaf35 - 60.d	9.67	0.29	0.024	48.3	1.9	0.074	4.84	0.2	NaN	6.26	0.34	NaN
eaf35 - 61.d	7.15	0.25	NaN	31.9	1.2	NaN	2.76	0.11	NaN	5.66	0.33	NaN

Analysis number	Tm169 ppm	Tm169 ppm 2SE	Tm169 ppm LOD	Yb172 ppm	Yb172 ppm 2SE	Yb172 ppm LOD	Lu175 ppm	Lu175 ppm 2SE	Lu175 ppm LOD	Hf178 ppm	Hf178 ppm 2SE	Hf178 ppm LOD
eaf35 - 62.d	13.8	0.36	NaN	76.5	1.5	NaN	9.38	0.27	NaN	8.5	0.42	0.03
eaf35 - 63.d	11.81	0.28	NaN	73.2	1.8	NaN	9.27	0.27	NaN	6.62	0.28	NaN
eaf35 - 64.d	9.96	0.27	NaN	56.9	1.5	NaN	7	0.21	NaN	6.74	0.33	NaN
eaf35 - 65.d	9.32	0.21	0.008	55.9	1.4	0.037	7.03	0.2	0.0083	6.34	0.32	NaN
eaf35 - 66.d	10.48	0.29	NaN	64	1.6	NaN	8.66	0.23	NaN	6.63	0.37	NaN
eaf35 - 67.d	5.69	0.18	NaN	25.68	0.85	NaN	2.46	0.11	NaN	5.99	0.42	0.028
eaf35 - 68.d	23.27	0.44	0.008	164	2.7	0.037	22.46	0.46	NaN	6.02	0.39	NaN
eaf35 - 69.d	17.77	0.53	NaN	119.3	3.1	NaN	16.54	0.45	0.016	10.95	0.41	0.066
eaf35 - 70.d	15.27	0.32	NaN	100.7	1.8	NaN	14.17	0.26	0.0082	6.8	0.37	0.057
eaf35 - 71.d	13.19	0.28	NaN	86.8	1.8	NaN	12.2	0.32	NaN	6.24	0.33	0.058
eaf35 - 72.d	8.39	0.34	0.008	31.8	1.5	NaN	2.72	0.14	0.017	9.11	0.42	NaN
eaf35 - 73.d	8.52	0.21	NaN	36.92	0.97	0.076	3.96	0.15	NaN	8.14	0.39	NaN
eaf35 - 74.d	13.12	0.42	0.011	78.5	2.2	0.038	10.26	0.23	0.0084	5.91	0.38	NaN
eaf35 - 75.d	6.02	0.16	0.023	38.5	1	0.086	5.4	0.16	NaN	4.79	0.28	NaN
eaf35 - 76.d	7.87	0.21	NaN	40.9	1.1	NaN	4.26	0.14	NaN	5.76	0.33	NaN
eaf35 - 77.d	7.7	0.32	NaN	52.3	1.3	0.091	7.29	0.25	NaN	5.35	0.37	NaN
eaf35 - 78.d	12.27	0.24	NaN	84.2	1.7	0.038	12.37	0.25	NaN	6.29	0.37	NaN
eaf35 - 79.d	7.47	0.23	NaN	34.28	0.74	NaN	3.26	0.14	0.012	8.01	0.42	0.059
eaf35 - 80.d	16.19	0.36	NaN	80.2	1.9	NaN	7.71	0.21	NaN	8.75	0.39	0.059
eaf35 - 81.d	14.74	0.42	0.0087	72.4	1.7	0.081	7.39	0.26	0.039	7.94	0.28	NaN
eaf35 - 82.d	39.46	0.77	NaN	273.3	5	0.11	41.98	0.78	NaN	7.1	0.36	NaN
eaf35 - 83.d	17.61	0.4	NaN	135.5	2.5	0.038	22.65	0.45	NaN	5	0.24	0.058
eaf35 - 84.d	37.39	0.73	0.024	249.2	4.2	NaN	35.7	0.65	NaN	7.95	0.33	0.079
eaf35 - 85.d	36.31	0.77	0.0081	257.2	4.1	NaN	37.63	0.88	0.017	10.58	0.47	NaN
eaf35 - 86.d	42.1	0.73	NaN	284.4	6.4	NaN	40.39	0.8	NaN	9.94	0.42	NaN
eaf35 - 88.d	8.54	0.24	NaN	48.4	1.4	NaN	6.3	0.18	NaN	6.77	0.28	NaN
eaf35 - 89.d	5.9	0.19	NaN	26.97	0.87	NaN	2.746	0.087	0.017	8.71	0.44	NaN
eaf35 - 90.d	10.12	0.24	NaN	50.3	1.4	0.037	4.86	0.2	0.026	6.53	0.3	0.038
eaf35 - 91.d	26.54	0.51	0.0078	153.8	3.7	NaN	18.84	0.41	NaN	8.33	0.4	NaN

Analysis number	Tm169 ppm	Tm169 ppm 2SE	Tm169 ppm LOD	Yb172 ppm	Yb172 ppm 2SE	Yb172 ppm LOD	Lu175 ppm	Lu175 ppm 2SE	Lu175 ppm LOD	Hf178 ppm	Hf178 ppm 2SE	Hf178 ppm LOD
eaf35 - 92.d	12.97	0.24	NaN	63	1.1	NaN	6.56	0.19	0.017	6.7	0.28	0.057
eaf35 - 93.d	6.67	0.22	0.016	25.59	0.72	NaN	2.39	0.11	0.0084	9.34	0.41	NaN
eaf35 - 94.d	7.34	0.2	NaN	31.28	0.73	0.075	2.85	0.11	NaN	7.24	0.36	NaN
eaf35 - 96.d	9.93	0.26	NaN	52.2	1.3	0.11	5.56	0.19	0.016	6.6	0.37	NaN
eaf35 - 97.d	4.53	0.14	NaN	16.62	0.78	NaN	1.35	0.075	0.0083	8.52	0.32	0.057
eaf35 - 98.d	12.39	0.39	NaN	60.8	1.7	NaN	6.05	0.19	0.012	6.5	0.31	0.09
eaf35 - 99.d	8.54	0.22	0.008	39.1	1.1	NaN	3.47	0.14	NaN	6.04	0.32	NaN
eaf35 - 100.d	39.11	0.65	0.008	275.6	4.9	0.037	41.38	0.67	NaN	7.63	0.32	0.039
eaf35 - 101.d	7.34	0.18	NaN	40.6	1.3	0.085	4.88	0.18	0.017	6.2	0.38	NaN
eaf35 - 102.d	12.42	0.3	NaN	72.2	2	0.053	8.99	0.28	NaN	22.4	1.1	NaN
eaf35 - 103.d	4.09	0.13	NaN	15.86	0.61	NaN	1.393	0.082	NaN	6.29	0.31	NaN
eaf35 - 104.d	4.91	0.15	NaN	23.78	0.96	0.038	2.47	0.1	NaN	6.57	0.31	0.058
eaf35 - 106.d	5.55	0.16	NaN	26.8	0.85	NaN	2.76	0.13	0.017	6.6	0.33	0.029
eaf35 - 107.d	14.61	0.33	NaN	102.2	1.7	NaN	15.63	0.36	NaN	10.6	0.39	NaN
eaf35 - 108.d	7.96	0.21	0.016	37.7	1.2	NaN	3.92	0.15	NaN	6.7	0.38	0.029
eaf35 - 109.d	12.57	0.26	NaN	80.4	2.1	0.071	11.9	0.35	0.022	9.16	0.35	0.12
eaf35 - 110.d	10.32	0.28	0.0079	67.8	1.8	NaN	9.65	0.33	NaN	5.35	0.28	NaN
eaf35 - 111.d	12.05	0.26	NaN	59.8	1.4	0.083	7.63	0.16	NaN	7.71	0.39	0.058
eaf35 - 112.d	11.94	0.32	NaN	71.2	1.6	NaN	9.36	0.23	0.016	6.56	0.32	0.056
eaf35 - 113.d	8.83	0.24	NaN	39.5	1.1	0.072	3.79	0.11	NaN	6.82	0.39	NaN
eaf35 - 114.d	11.65	0.29	0.0078	71.4	1.3	0.036	8.76	0.18	NaN	6.86	0.34	NaN
eaf35 - 115.d	9.57	0.33	0.0081	48.1	1.4	0.1	5.37	0.17	0.017	6.98	0.33	NaN
eaf35 - 116.d	11.41	0.31	NaN	53.1	1.3	0.076	5.46	0.16	0.018	6.72	0.36	0.058
eaf35 - 117.d	36.35	0.6	NaN	247.1	3.9	NaN	37.98	0.56	NaN	9.14	0.41	0.03
eaf35 - 118.d	31.7	0.6	NaN	220.8	3.3	NaN	34.42	0.51	NaN	6.66	0.36	NaN
eaf35 - 119.d	7.72	0.22	0.0082	33.9	1	NaN	3.12	0.14	NaN	7.29	0.33	NaN
eaf35 - 120.d	5.94	0.22	NaN	26.6	1.5	NaN	2.85	0.2	0.011	5.78	0.36	NaN

Analysis number	Ta181 ppm	Ta181 ppm 2SE	Ta181 ppm LOD	Pb204 ppm	Pb204 ppm 2SE	Pb204 ppm LOD	Pb206 ppm	Pb206 ppm 2SE	Pb206 ppm LOD	Pb207 ppm	Pb207 ppm 2SE	Pb207 ppm LOD
eaf35 - 1.d	82.5	1.4	0.016	< LOD	< LOD	5.4	19.27	0.71	0.22	4.21	0.12	0.072
eaf35 - 2.d	130.8	1.5	NaN	< LOD	< LOD	8.6	19.37	0.57	0.12	4.88	0.13	0.078
eaf35 - 3.d	115.6	2.1	0.016	< LOD	< LOD	6.5	25.62	0.87	0.2	4.78	0.13	0.068
eaf35 - 4.d	56.55	0.85	0.0081	< LOD	< LOD	7.9	35.8	1	0.25	5.24	0.14	0.097
eaf35 - 5.d	68.7	1.2	0.016	< LOD	< LOD	8.6	35.5	1.1	0.18	5.16	0.13	0.093
eaf35 - 6.d	102.2	1.2	0.0077	< LOD	< LOD	6.6	14.85	0.59	0.22	3.84	0.12	0.071
eaf35 - 7.d	37.43	0.65	NaN	< LOD	< LOD	11	59.2	1.3	0.32	7.86	0.2	0.064
eaf35 - 8.d	35.2	0.76	NaN	< LOD	< LOD	8.4	56	1.2	0.17	7.18	0.17	0.064
eaf35 - 9.d	101.9	1.9	NaN	< LOD	< LOD	9.6	32.1	1.1	0.13	5.96	0.14	0.045
eaf35 - 10.d	98.5	1.4	NaN	< LOD	< LOD	6.6	30.4	1.1	0.22	5.16	0.12	0.072
eaf35 - 11.d	102.9	1.7	NaN	< LOD	< LOD	7.7	16.68	0.7	0.1	4.359	0.095	0.055
eaf35 - 12.d	106.1	1.6	NaN	6.5	2.6	5.4	184.7	4.9	0.28	20.75	0.7	0.084
eaf35 - 13.d	82.1	1.4	NaN	< LOD	< LOD	6.3	159.2	3.6	0.13	16.36	0.35	0.055
eaf35 - 14.d	50.27	0.94	0.0082	< LOD	< LOD	11	69.1	2	0.19	8.2	0.17	0.055
eaf35 - 15.d	120.2	1.7	NaN	< LOD	< LOD	9.1	33.7	1.6	0.17	7.16	0.37	0.11
eaf35 - 16.d	110.3	1.5	NaN	< LOD	< LOD	7.6	28.48	0.93	0.22	6.76	0.13	0.09
eaf35 - 17.d	94.2	1.5	0.0093	14.1	3.6	9.7	127	4.5	0.2	22.99	0.93	0.095
eaf35 - 18.d	80.8	1.1	NaN	< LOD	< LOD	9.5	20.2	0.66	0.14	3.28	0.12	0.068
eaf35 - 19.d	104.4	1.6	NaN	< LOD	< LOD	6.8	18.95	0.93	0.16	5.42	0.11	0.058
eaf35 - 20.d	117.3	1.6	NaN	< LOD	< LOD	6.9	38.49	0.99	0.13	6.06	0.14	0.089
eaf35 - 22.d	90.7	1.6	NaN	< LOD	< LOD	6.9	57.6	2.2	0.23	8.41	0.29	0.082
eaf35 - 23.d	125.9	1.9	NaN	< LOD	< LOD	8.7	24.09	0.61	0.25	4.64	0.1	0.089
eaf35 - 24.d	65.2	1.2	0.0082	< LOD	< LOD	8.9	41.8	1.2	0.17	5.95	0.15	0.068
eaf35 - 25.d	105.7	1.6	NaN	< LOD	< LOD	7.2	15.02	0.7	0.25	4.45	0.11	0.056
eaf35 - 26.d	75.3	1.2	NaN	< LOD	< LOD	9.3	25.86	0.97	0.19	5.44	0.15	0.054
eaf35 - 27.d	53.3	1.2	NaN	< LOD	< LOD	4.5	43	1.2	0.2	5.69	0.14	0.064
eaf35 - 28.d	121	1.9	NaN	< LOD	< LOD	8.6	14.15	0.83	0.25	4.01	0.13	0.044
eaf35 - 29.d	147.7	2.9	0.008	< LOD	< LOD	8.8	9.07	0.58	0.24	3.649	0.098	0.047
eaf35 - 30.d	95.5	1.1	0.016	< LOD	< LOD	7.5	13.8	0.69	0.15	3.6	0.1	0.08

Analysis number	Ta181 ppm	Ta181 ppm 2SE	Ta181 ppm LOD	Pb204 ppm	Pb204 ppm 2SE	Pb204 ppm LOD	Pb206 ppm	Pb206 ppm 2SE	Pb206 ppm LOD	Pb207 ppm	Pb207 ppm 2SE	Pb207 ppm LOD
eaf35 - 31.d	79.8	2.1	0.011	< LOD	< LOD	6.9	29.1	1.5	0.2	5.24	0.16	0.073
eaf35 - 32.d	44.94	0.86	0.017	< LOD	< LOD	8	40.9	1	0.24	5.93	0.16	0.053
eaf35 - 33.d	39.61	0.78	NaN	< LOD	< LOD	8.6	56.4	1.6	0.15	6.98	0.16	0.067
eaf35 - 34.d	88	1.8	0.032	< LOD	< LOD	5.5	22.6	0.62	0.16	5.32	0.11	0.085
eaf35 - 35.d	92	1.4	0.016	< LOD	< LOD	6.7	13.8	0.68	0.28	5.03	0.16	0.076
eaf35 - 36.d	157.6	3.4	NaN	< LOD	< LOD	9.4	9.62	0.4	0.21	3.583	0.091	0.081
eaf35 - 37.d	149.2	2.1	NaN	< LOD	< LOD	5.9	5.99	0.41	0.19	3.18	0.1	0.081
eaf35 - 38.d	87.9	1.5	NaN	< LOD	< LOD	7.2	19.95	0.78	0.22	4.32	0.13	0.056
eaf35 - 39.d	60.4	1.2	NaN	< LOD	< LOD	7.5	26.45	0.97	0.13	5.17	0.13	0.073
eaf35 - 40.d	24.15	0.55	NaN	< LOD	< LOD	5.8	35.5	1.2	0.17	8.53	0.46	0.072
eaf35 - 41.d	126.2	1.5	NaN	< LOD	< LOD	8.1	11.26	0.69	0.22	4.414	0.099	0.054
eaf35 - 42.d	6.77	0.19	NaN	< LOD	< LOD	9.5	41.9	1.2	0.13	4.97	0.14	0.082
eaf35 - 43.d	9.66	0.31	NaN	< LOD	< LOD	6.1	71.6	2.4	0.25	8.47	0.3	0.062
eaf35 - 44.d	16.03	0.36	0.0077	< LOD	< LOD	8	75.1	1.9	0.17	8.23	0.18	0.082
eaf35 - 45.d	29.34	0.61	NaN	< LOD	< LOD	10	52.7	1.9	0.12	6.61	0.18	0.071
eaf35 - 48.d	6.19	0.29	NaN	< LOD	< LOD	10	41	1.2	0.22	5.1	0.12	0.091
eaf35 - 49.d	89.1	1.4	NaN	< LOD	< LOD	9.7	20.59	0.87	0.2	4.86	0.14	0.051
eaf35 - 50.d	76.11	0.96	NaN	< LOD	< LOD	7.5	13.36	0.59	0.25	4.36	0.12	0.051
eaf35 - 51.d	62.8	1.1	0.0078	< LOD	< LOD	6.6	29.9	0.93	0.22	4.7	0.11	0.059
eaf35 - 52.d	49.29	0.84	NaN	< LOD	< LOD	9.1	41.1	1.4	0.16	5.92	0.19	0.061
eaf35 - 53.d	43.63	0.68	NaN	< LOD	< LOD	8.4	50.3	1.6	0.18	7.3	0.15	0.042
eaf35 - 54.d	85.7	1.1	0.0077	< LOD	< LOD	6.5	12.26	0.57	0.25	3.78	0.13	0.067
eaf35 - 55.d	55.2	1.4	NaN	< LOD	< LOD	5.4	29.1	1.3	0.21	5.5	0.21	0.075
eaf35 - 56.d	58.8	1.1	NaN	< LOD	< LOD	8.9	47.3	1	0.2	7.3	0.19	0.072
eaf35 - 57.d	100.3	1.4	0.011	< LOD	< LOD	6.6	13.68	0.6	0.22	3.81	0.12	0.077
eaf35 - 58.d	72.8	1.3	NaN	< LOD	< LOD	7.8	12.74	0.67	0.17	4.12	0.12	0.072
eaf35 - 59.d	78.8	1.5	NaN	< LOD	< LOD	6.3	13.79	0.59	0.15	4.03	0.11	0.055
eaf35 - 60.d	80.4	1.7	NaN	< LOD	< LOD	6.7	10.98	0.51	0.19	3.44	0.1	0.067
eaf35 - 61.d	118.2	2.4	NaN	< LOD	< LOD	7.1	14.32	0.74	0.18	5	0.16	0.054

Analysis number	Ta181 ppm	Ta181 ppm 2SE	Ta181 ppm LOD	Pb204 ppm	Pb204 ppm 2SE	Pb204 ppm LOD	Pb206 ppm	Pb206 ppm 2SE	Pb206 ppm LOD	Pb207 ppm	Pb207 ppm 2SE	Pb207 ppm LOD
eaf35 - 62.d	44.16	0.76	NaN	< LOD	< LOD	9.3	54.5	1.6	0.16	6.95	0.16	0.053
eaf35 - 63.d	100.7	1.8	0.023	< LOD	< LOD	8.2	12.56	0.59	0.12	3.55	0.12	0.056
eaf35 - 64.d	103.1	1.9	NaN	< LOD	< LOD	8.4	11.51	0.57	0.18	3.59	0.13	0.087
eaf35 - 65.d	70.85	0.95	NaN	< LOD	< LOD	8.2	16.11	0.68	0.19	3.54	0.11	0.08
eaf35 - 66.d	88.7	1.1	NaN	< LOD	< LOD	9	34.4	1.1	0.14	9.76	0.25	0.054
eaf35 - 67.d	75.7	1.3	NaN	< LOD	< LOD	9	6.94	0.44	0.12	3.253	0.089	0.058
eaf35 - 68.d	71.01	0.93	NaN	< LOD	< LOD	7.8	33.3	1.3	0.2	5.38	0.16	0.065
eaf35 - 69.d	37.61	0.91	0.0077	< LOD	< LOD	7	34.5	1.3	0.13	6.93	0.32	0.067
eaf35 - 70.d	47.3	1.2	NaN	< LOD	< LOD	9.4	35.8	1.2	0.21	5.39	0.17	0.048
eaf35 - 71.d	42.66	0.79	0.016	< LOD	< LOD	9.7	25.62	0.77	0.096	4.01	0.13	0.062
eaf35 - 72.d	40.84	0.65	0.016	< LOD	< LOD	8.1	62.5	1.3	0.043	7.7	0.14	0.054
eaf35 - 73.d	47.26	0.8	NaN	< LOD	< LOD	5.9	46	1.5	0.24	6.06	0.14	0.068
eaf35 - 74.d	42.4	1.7	0.0079	< LOD	< LOD	4.9	27.75	0.87	0.2	5.55	0.15	0.078
eaf35 - 75.d	24.5	0.6	0.0082	< LOD	< LOD	7.8	15.5	1.1	0.16	4.1	0.25	0.058
eaf35 - 76.d	62.5	1.2	NaN	< LOD	< LOD	5.8	14.28	0.73	0.16	4.9	0.19	0.063
eaf35 - 77.d	40.07	0.8	NaN	10.1	3.4	9.9	38.3	1.6	0.25	9.35	0.34	0.083
eaf35 - 78.d	29.84	0.46	0.024	< LOD	< LOD	5.1	32.5	1.2	0.17	5.99	0.18	0.061
eaf35 - 79.d	143.4	2.4	0.016	6.8	2.8	5	25	1.1	0.21	7.34	0.29	0.075
eaf35 - 80.d	105.9	1.8	NaN	< LOD	< LOD	7.4	36.88	0.99	0.13	5.46	0.16	0.057
eaf35 - 81.d	134.1	2.4	0.0084	6.9	2.5	5.9	42.1	1.7	0.17	9.65	0.56	0.066
eaf35 - 82.d	19.21	0.48	NaN	< LOD	< LOD	7.3	55.6	1.4	0.25	9.7	0.22	0.063
eaf35 - 83.d	2.75	0.14	0.0079	< LOD	< LOD	7.8	22.49	0.74	0.13	3.41	0.12	0.051
eaf35 - 84.d	5.22	0.18	NaN	< LOD	< LOD	8.4	35.3	1.1	0.21	6.18	0.32	0.06
eaf35 - 85.d	4.78	0.15	NaN	< LOD	< LOD	7.5	67.1	1.6	0.11	8.32	0.2	0.072
eaf35 - 86.d	5.77	0.12	0.016	< LOD	< LOD	8.8	68.7	1.2	0.21	8.84	0.15	0.065
eaf35 - 88.d	79.2	1.4	NaN	< LOD	< LOD	8.1	16.01	0.64	0.12	4.1	0.14	0.066
eaf35 - 89.d	46.2	0.97	NaN	< LOD	< LOD	7.4	55.3	1.3	0.17	7.43	0.18	0.048
eaf35 - 90.d	98.9	2.1	0.015	< LOD	< LOD	7.6	9.09	0.56	0.12	3.41	0.11	0.059
eaf35 - 91.d	108.1	1.7	NaN	< LOD	< LOD	6.8	26.88	0.61	0.18	4.55	0.13	0.063

Analysis number	Ta181 ppm	Ta181 ppm 2SE	Ta181 ppm LOD	Pb204 ppm	Pb204 ppm 2SE	Pb204 ppm LOD	Pb206 ppm	Pb206 ppm 2SE	Pb206 ppm LOD	Pb207 ppm	Pb207 ppm 2SE	Pb207 ppm LOD
eaf35 - 92.d	100.1	1.8	0.021	< LOD	< LOD	7	17.99	0.64	0.15	3.96	0.13	0.064
eaf35 - 93.d	38.68	0.67	NaN	< LOD	< LOD	6.8	60.5	2	0.18	7.66	0.29	0.068
eaf35 - 94.d	49.52	0.84	NaN	< LOD	< LOD	6.5	38.6	1	0.18	6.45	0.12	0.071
eaf35 - 96.d	97.2	1.9	NaN	< LOD	< LOD	5.6	16.04	0.63	0.14	4.8	0.17	0.071
eaf35 - 97.d	31.65	0.57	0.016	< LOD	< LOD	8	48.6	1.3	0.1	7.56	0.2	0.04
eaf35 - 98.d	59	1.2	NaN	< LOD	< LOD	6.6	21.81	0.89	0.11	6.4	0.13	0.05
eaf35 - 99.d	54.52	0.99	NaN	< LOD	< LOD	8	11.37	0.59	0.14	3.53	0.1	0.076
eaf35 - 100.d	5.52	0.16	NaN	< LOD	< LOD	6.5	38.8	1.1	0.14	5.57	0.13	0.069
eaf35 - 101.d	84.6	2.3	NaN	< LOD	< LOD	6.8	12.8	0.66	0.098	4.22	0.12	0.045
eaf35 - 102.d	66.91	0.92	0.008	< LOD	< LOD	7.8	33.5	1.6	0.14	7.19	0.24	0.056
eaf35 - 103.d	59.1	1.1	0.011	< LOD	< LOD	10	9.87	0.55	0.27	4.05	0.11	0.042
eaf35 - 104.d	71.4	1.4	0.0079	< LOD	< LOD	10	11.31	0.53	0.14	4.44	0.12	0.058
eaf35 - 106.d	43.99	0.86	0.0078	6.6	2.6	5.6	14.18	0.56	0.15	5.22	0.14	0.074
eaf35 - 107.d	22.33	0.39	NaN	< LOD	< LOD	7.9	59.9	1.7	0.22	7.77	0.13	0.04
eaf35 - 108.d	76.1	1.3	NaN	< LOD	< LOD	7.2	16.13	0.55	0.22	4.36	0.14	0.042
eaf35 - 109.d	50.74	0.87	NaN	< LOD	< LOD	6.4	44.7	1.5	0.21	6.55	0.26	0.066
eaf35 - 110.d	45	1.7	0.017	< LOD	< LOD	5.7	39.1	1.1	0.26	6.53	0.22	0.038
eaf35 - 111.d	44.12	0.73	0.0079	< LOD	< LOD	7.8	48.6	1.2	0.14	7.11	0.16	0.048
eaf35 - 112.d	88	1.3	NaN	< LOD	< LOD	5.2	19.31	0.7	0.23	4.46	0.12	0.045
eaf35 - 113.d	102.9	1.5	NaN	< LOD	< LOD	6.7	13.98	0.47	0.25	3.79	0.11	0.056
eaf35 - 114.d	56.1	1.6	NaN	< LOD	< LOD	6.2	18.85	0.75	0.15	3.54	0.1	0.05
eaf35 - 115.d	53.89	0.91	0.016	< LOD	< LOD	6	39.2	1.3	0.24	5.93	0.19	0.071
eaf35 - 116.d	74.6	1.5	NaN	< LOD	< LOD	7.9	28.42	0.94	0.22	5.26	0.13	0.068
eaf35 - 117.d	14.51	0.35	NaN	8.3	2.7	4.8	63.7	4.3	0.13	13.6	1.2	0.06
eaf35 - 118.d	10.48	0.3	0.016	< LOD	< LOD	7.2	35.95	0.95	0.18	6.01	0.18	0.06
eaf35 - 119.d	77.4	1.4	0.008	< LOD	< LOD	8.8	19.16	0.78	0.17	6.56	0.25	0.056
eaf35 - 120.d	60.35	0.86	0.017	< LOD	< LOD	6.3	9.82	0.65	0.15	3.52	0.12	0.057

Analysis number	Pb208 ppm	Pb208 ppm 2SE	Pb208 ppm LOD	Th232 ppm	Th232 ppm 2SE	Th232 ppm LOD	U238 ppm	U238 ppm 2SE	U238 ppm LOD	Zr in Tt temp (°C)	grain number	REE group
eaf35 - 1.d	4.01	0.1	0.045	1.632	0.09	NaN	20.64	0.41	NaN	706	1	35B
eaf35 - 2.d	10.7	0.25	0.046	8.21	0.32	0.0068	16.54	0.26	0.014	710	1	35C
eaf35 - 3.d	5.01	0.26	0.046	11.24	0.53	NaN	25.81	0.89	0.01	748	1	35C
eaf35 - 4.d	2.763	0.076	0.051	4.71	0.15	NaN	46.04	0.64	NaN	710	1	35B
eaf35 - 5.d	3.162	0.063	0.059	5.4	0.17	NaN	46.36	0.79	NaN	713	1	35B
eaf35 - 6.d	2.817	0.058	0.043	1.175	0.073	NaN	17.86	0.34	0.012	707	1	35B
eaf35 - 7.d	6.79	0.17	0.052	13.69	0.24	0.014	76.7	1.1	0.0066	728	2	35B
eaf35 - 8.d	3.713	0.075	0.047	12.33	0.27	NaN	72.1	1.3	0.0048	725	2	35B
eaf35 - 9.d	12.58	0.45	0.051	2.84	0.1	NaN	34.41	0.7	0.026	707	2	35A
eaf35 - 10.d	3.862	0.076	0.049	13.42	0.32	0.018	38.37	0.6	0.011	709	2	35A
eaf35 - 11.d	5.94	0.19	0.038	1.053	0.068	0.014	16.76	0.35	0.009	705	2	35A
eaf35 - 12.d	32.9	3.9	0.064	58.8	2.3	0.015	231.1	3.5	0.0097	736	3	35A
eaf35 - 13.d	7.72	0.15	0.034	50.7	0.75	0.024	215.5	2.6	NaN	735	3	35A
eaf35 - 14.d	4.376	0.087	0.061	19.65	0.37	NaN	92.8	1.5	NaN	726	4	35A
eaf35 - 15.d	18.5	2.2	0.047	4.72	0.35	NaN	33.99	0.58	0.0068	717	5	35E
eaf35 - 16.d	16.8	0.3	0.03	8.45	0.26	0.0071	27.64	0.75	0.011	716	5	35B
eaf35 - 17.d	94.5	4.4	0.04	28.5	1.2	NaN	84.8	2	0.012	721	5	35B
eaf35 - 18.d	4.13	0.12	0.042	23.19	0.48	NaN	19.66	0.38	NaN	704	6	35B
eaf35 - 19.d	11.52	0.23	0.044	15.24	0.33	0.016	17.07	0.28	NaN	709	7	35E
eaf35 - 20.d	5.11	0.28	0.039	19.56	0.69	NaN	43.8	0.99	0.013	714	7	35A
eaf35 - 22.d	16.6	1.1	0.037	11.92	0.33	0.0069	62.3	1	0.017	720	7	35B
eaf35 - 23.d	5.01	0.16	0.033	2.91	0.17	0.013	30.25	0.5	NaN	707	8	35C
eaf35 - 24.d	6.05	0.11	0.046	7.58	0.15	NaN	53.16	0.96	0.01	712	8	35B
eaf35 - 25.d	9.8	0.2	0.039	0.722	0.063	0.0069	17.78	0.68	0.0048	712	9	35C
eaf35 - 26.d	12.31	0.33	0.044	5.31	0.2	0.015	29.31	0.78	0.0047	712	9	35A
eaf35 - 27.d	2.785	0.075	0.046	5.68	0.15	0.0066	56.9	1	0.0075	715	10	35B
eaf35 - 28.d	6.63	0.3	0.049	1.24	0.13	0.015	14.15	0.6	0.015	701	10	35A
eaf35 - 29.d	6.95	0.22	0.04	0.312	0.031	0.0066	6.42	0.27	0.01	688	10	35A
eaf35 - 30.d	3.72	0.068	0.031	4.18	0.18	0.0065	12.45	0.37	NaN	682	10	35A

Analysis number	Pb208 ppm	Pb208 ppm 2SE	Pb208 ppm LOD	Th232 ppm	Th232 ppm 2SE	Th232 ppm LOD	U238 ppm	U238 ppm 2SE	U238 ppm LOD	Zr in Tt temp (°C)	grain number	REE group
eaf35 - 31.d	6.33	0.16	0.036	8.74	0.47	NaN	34.7	1.4	0.0063	712	10	35B
eaf35 - 32.d	2.957	0.052	0.041	6.33	0.17	NaN	53.06	0.83	0.0046	716	10	35B
eaf35 - 33.d	3.378	0.081	0.04	10.23	0.27	0.0065	71.9	1.2	0.009	722	10	35B
eaf35 - 34.d	8.78	0.23	0.037	5.05	0.17	0.014	26.15	0.47	0.018	709	11	35B
eaf35 - 35.d	12.26	0.35	0.039	0.577	0.047	NaN	9.01	0.18	NaN	704	11	35B
eaf35 - 36.d	6.61	0.18	0.062	0.517	0.048	0.0065	8.35	0.2	0.016	697	11	35C
eaf35 - 37.d	4.52	0.12	0.038	0.422	0.038	0.0064	4.36	0.14	0.0097	693	11	35C
eaf35 - 38.d	3.36	0.25	0.041	1.511	0.076	0.013	22.06	0.52	0.02	707	11	35B
eaf35 - 39.d	9.17	0.5	0.049	6.02	0.16	NaN	27.18	0.48	0.0074	683	11	35A
eaf35 - 40.d	31.3	2.3	0.049	14.37	0.3	0.011	23.49	0.57	0.0047	705	11	35D
eaf35 - 41.d	10.43	0.17	0.04	0.652	0.047	0.014	8.03	0.21	0.01	698	11	35C
eaf35 - 42.d	2.654	0.066	0.036	9.64	0.27	NaN	53.8	1	0.014	706	12	35A
eaf35 - 43.d	7.9	0.82	0.055	19.32	0.44	NaN	95.7	1.8	0.015	717	12	35A
eaf35 - 44.d	4.85	0.1	0.04	21.38	0.37	NaN	101.7	2	NaN	723	12	35A
eaf35 - 45.d	5.8	0.13	0.039	13.63	0.29	0.013	65.5	1.3	NaN	713	12	35A
eaf35 - 48.d	2.66	0.12	0.047	9.31	0.33	NaN	54.5	1.2	NaN	703	12	35A
eaf35 - 49.d	8.87	0.5	0.038	1.304	0.089	NaN	21.13	0.66	0.013	712	13	35C
eaf35 - 50.d	8.61	0.18	0.03	0.83	0.052	0.013	12.86	0.18	0.0099	709	13	35C
eaf35 - 51.d	3.457	0.071	0.049	5.06	0.16	0.021	40.87	0.55	NaN	713	13	35B
eaf35 - 52.d	5.41	0.36	0.041	6.46	0.21	0.0068	50.7	1.4	NaN	716	13	35B
eaf35 - 53.d	10.72	0.41	0.046	8.51	0.32	NaN	62.3	1.5	NaN	722	13	35B
eaf35 - 54.d	2.909	0.073	0.026	0.76	0.044	0.013	12.67	0.36	0.009	703	14	35B
eaf35 - 55.d	9.78	0.97	0.029	8.51	0.24	NaN	37.5	1.4	0.015	711	14	35A
eaf35 - 56.d	18.17	0.93	0.045	6.01	0.28	NaN	55.1	1.3	0.01	717	14	35B
eaf35 - 57.d	7.63	0.21	0.05	5.41	0.34	0.0064	10.89	0.4	0.0089	700	14	35C
eaf35 - 58.d	6.18	0.25	0.036	0.715	0.061	0.0065	12.31	0.28	0.0062	707	14	35B
eaf35 - 59.d	3.152	0.067	0.033	0.838	0.044	NaN	14.45	0.29	0.009	705	14	35B
eaf35 - 60.d	2.881	0.064	0.052	0.67	0.055	NaN	11.21	0.3	0.0097	703	15	35B
eaf35 - 61.d	18.24	0.77	0.03	13.01	0.91	NaN	9.98	0.34	NaN	702	15	35B

Analysis number	Pb208 ppm	Pb208 ppm 2SE	Pb208 ppm LOD	Th232 ppm	Th232 ppm 2SE	Th232 ppm LOD	U238 ppm	U238 ppm 2SE	U238 ppm LOD	Zr in Tt temp (°C)	grain number	REE group
eaf35 - 62.d	3.428	0.065	0.051	10.71	0.22	NaN	73.6	0.92	NaN	720	16	35B
eaf35 - 63.d	2.845	0.06	0.036	0.707	0.061	NaN	13.35	0.29	NaN	703	16	35A
eaf35 - 64.d	2.882	0.069	0.039	0.75	0.067	0.0067	11.33	0.36	0.01	703	17	35A
eaf35 - 65.d	2.92	0.073	0.052	5.15	0.36	0.02	17.69	0.37	0.0045	695	17	35A
eaf35 - 66.d	58.4	1.5	0.038	128.2	3	0.017	34.58	0.75	NaN	709	18	35A
eaf35 - 67.d	3.32	0.12	0.041	1.42	0.19	0.023	5.51	0.17	0.0044	701	18	35B
eaf35 - 68.d	9.85	0.46	0.049	14.99	0.43	0.014	39.28	0.69	NaN	702	18	35A
eaf35 - 69.d	28.3	1.9	0.041	115.3	3.6	0.017	32.94	0.93	0.0045	722	18	35A
eaf35 - 70.d	8.55	0.49	0.05	21.28	0.51	NaN	38.93	0.67	0.014	707	19	35A
eaf35 - 71.d	5.39	0.52	0.037	20.1	1.1	0.009	23.71	0.37	0.015	702	19	35A
eaf35 - 72.d	3.9	0.11	0.04	12.98	0.49	NaN	80.6	1.7	0.0098	725	20	35B
eaf35 - 73.d	2.974	0.077	0.046	6.72	0.3	0.013	58.5	1.2	0.014	717	20	35B
eaf35 - 74.d	12.57	0.31	0.044	10.59	0.7	NaN	27.51	0.44	0.019	699	20	35A
eaf35 - 75.d	10.9	1.3	0.046	3.99	0.13	NaN	13.48	0.5	0.0048	691	21	35D
eaf35 - 76.d	14.4	1	0.04	1.076	0.079	NaN	8.53	0.29	NaN	700	21	35A
eaf35 - 77.d	43.1	1.5	0.05	5.53	0.2	0.0078	40.5	1.4	0.024	695	21	35D
eaf35 - 78.d	14.67	0.74	0.029	14.96	0.44	0.013	35.24	0.46	NaN	701	21	35D
eaf35 - 79.d	21.1	1	0.041	3.98	0.46	0.0067	12.85	0.52	0.0047	708	22	35B
eaf35 - 80.d	2.698	0.076	0.025	3.21	0.12	0.0067	45.4	0.87	0.0076	710	23	35B
eaf35 - 81.d	11.19	0.93	0.039	4.55	0.17	NaN	50.7	1.3	0.014	717	23	35E
eaf35 - 82.d	24.9	0.63	0.032	226.9	8.5	0.007	59.1	1.2	0.017	702	24	35A
eaf35 - 83.d	2.065	0.058	0.041	4.61	0.12	0.013	30.68	0.66	0.0091	688	25	35A
eaf35 - 84.d	13.17	0.81	0.036	8.81	0.25	0.0065	39.37	0.87	0.016	713	25	35A
eaf35 - 85.d	8.73	0.42	0.044	23.46	0.63	0.0065	92.6	2.4	0.0046	730	25	35A
eaf35 - 86.d	12.88	0.36	0.041	21.72	0.42	NaN	82.8	1.4	NaN	728	25	35A
eaf35 - 88.d	3.149	0.076	0.028	1.376	0.087	0.0064	18.44	0.32	0.0045	705	26	35B
eaf35 - 89.d	5.29	0.35	0.037	15.06	0.65	NaN	69.7	1.2	0.0094	724	26	35B
eaf35 - 90.d	2.916	0.079	0.031	0.435	0.042	0.013	8.36	0.18	0.012	702	27	35B
eaf35 - 91.d	3.436	0.065	0.043	5.42	0.21	0.01	32.88	0.69	NaN	705	27	35A

Analysis number	Pb208 ppm	Pb208 ppm 2SE	Pb208 ppm LOD	Th232 ppm	Th232 ppm 2SE	Th232 ppm LOD	U238 ppm	U238 ppm 2SE	U238 ppm LOD	Zr in Tt temp (°C)	grain number	REE group
eaf35 - 92.d	2.693	0.052	0.042	1.278	0.058	0.0088	20.5	0.42	0.013	708	27	35B
eaf35 - 93.d	3.6	0.11	0.037	11.43	0.31	0.014	81	1.5	0.0099	725	28	35B
eaf35 - 94.d	8.16	0.2	0.039	4.24	0.18	NaN	46.89	0.87	NaN	714	29	35B
eaf35 - 96.d	9.16	0.24	0.039	2.59	0.15	0.013	16.05	0.43	0.0098	709	29	35B
eaf35 - 97.d	10.16	0.5	0.043	9.45	0.29	0.0064	61.6	1.1	0.0091	722	30	35B
eaf35 - 98.d	17.99	0.28	0.028	6.01	0.22	0.013	19.19	0.43	0.0046	710	30	35C
eaf35 - 99.d	2.886	0.078	0.042	0.923	0.064	0.014	11.03	0.27	NaN	703	30	35B
eaf35 - 100.d	7.95	0.24	0.038	11.03	0.23	0.015	48.48	0.86	NaN	705	30	35A
eaf35 - 101.d	6.82	0.3	0.034	0.693	0.051	0.027	11.42	0.23	NaN	705	31	35B
eaf35 - 102.d	17.32	0.79	0.029	4.34	0.13	0.0066	35.46	0.73	0.012	817	31	35B
eaf35 - 103.d	5.95	0.18	0.041	0.884	0.044	0.013	7.07	0.18	NaN	704	32	35E
eaf35 - 104.d	8.69	0.28	0.035	2.47	0.12	0.013	9.33	0.17	0.013	705	31	35B
eaf35 - 106.d	12.45	0.25	0.035	0.776	0.06	NaN	10.5	0.26	0.0045	708	33	35B
eaf35 - 107.d	4.34	0.093	0.037	21.98	0.48	0.014	60.52	0.97	0.0044	734	33	35D
eaf35 - 108.d	6.23	0.13	0.047	0.786	0.063	0.0064	14.07	0.31	NaN	704	33	35B
eaf35 - 109.d	6.71	0.96	0.034	24.92	0.62	0.0083	50.8	1	0.0085	722	33	35A
eaf35 - 110.d	11.9	1.8	0.044	11.06	0.33	0.014	37.96	0.94	0.0097	698	33	35A
eaf35 - 111.d	13.35	0.47	0.049	7.55	0.44	0.013	58.72	0.97	NaN	717	34	35B
eaf35 - 112.d	8.57	0.24	0.028	7.98	0.25	NaN	22.13	0.41	NaN	708	34	35A
eaf35 - 113.d	2.832	0.057	0.041	0.842	0.059	0.012	14.85	0.39	0.0095	704	35	35B
eaf35 - 114.d	4.211	0.091	0.038	19.75	0.36	0.0062	19.39	0.32	0.0044	710	35	35A
eaf35 - 115.d	6.02	0.39	0.044	3.95	0.14	0.018	52.7	1.1	0.018	712	35	35B
eaf35 - 116.d	9.26	0.19	0.045	2.004	0.068	0.018	32.06	0.58	0.0063	711	35	35B
eaf35 - 117.d	87	10	0.04	41.1	1.1	0.0067	69.6	2.3	0.011	726	36	35A
eaf35 - 118.d	23.05	0.87	0.033	37.6	1.1	0.021	46.48	0.64	0.0046	703	36	35A
eaf35 - 119.d	27.4	1.4	0.042	7.42	0.26	NaN	11.96	0.39	NaN	709	36	35C
eaf35 - 120.d	2.942	0.079	0.038	0.594	0.047	NaN	8.48	0.33	0.0089	702	37	35B

Analysis number	$^{238}U/^{206}Pb$	±1s	$^{207}Pb/^{206}Pb$	±1s	$^{238}U/^{206}Pb$ age (Ma)	±1s	$^{207}Pb/^{206}Pb$ age (Ma)	±1s	Disc (%)	f207%	^{207}Pb-corrected $^{238}U/^{206}Pb$ age (Ma)	±1s
eaf35 - 1.d	3.80620	0.08674	0.18100	0.00415	1504	30	2662	37	44	14.8	1302	31
eaf35 - 2.d	2.99390	0.06705	0.20220	0.00330	1858	35	2844	26	35	16.3	1590	38
eaf35 - 3.d	3.57872	0.07601	0.15030	0.00295	1588	29	2349	33	32	9.1	1459	32
eaf35 - 4.d	4.58664	0.08219	0.11820	0.00235	1271	20	1929	35	34	5.8	1205	22
eaf35 - 5.d	4.63208	0.08528	0.11690	0.00225	1260	21	1909	34	34	5.6	1195	22
eaf35 - 6.d	4.19658	0.10109	0.20500	0.00490	1378	29	2866	38	52	19.3	1134	29
eaf35 - 7.d	4.64962	0.06999	0.10690	0.00150	1256	17	1747	25	28	4.0	1210	18
eaf35 - 8.d	4.65624	0.06579	0.10440	0.00145	1254	16	1704	25	26	3.6	1213	17
eaf35 - 9.d	3.80768	0.08037	0.15230	0.00250	1503	28	2372	28	37	10.0	1368	29
eaf35 - 10.d	4.49840	0.08802	0.13440	0.00255	1294	23	2156	33	40	8.3	1196	24
eaf35 - 11.d	3.61029	0.08607	0.20890	0.00380	1576	33	2897	29	46	19.0	1304	33
eaf35 - 12.d	4.43942	0.05891	0.08960	0.00105	1310	16	1417	22	8	0.8	1300	17
eaf35 - 13.d	4.81373	0.05877	0.08230	0.00085	1217	13	1253	20	3	0.2	1214	15
eaf35 - 14.d	4.71889	0.06336	0.09620	0.00130	1239	15	1552	25	20	2.4	1212	16
eaf35 - 15.d	3.59707	0.10346	0.17300	0.00350	1581	39	2587	33	39	13.0	1397	41
eaf35 - 16.d	3.48227	0.09253	0.19240	0.00400	1627	37	2763	34	41	16.0	1393	39
eaf35 - 17.d	2.39279	0.05223	0.14460	0.00130	2251	41	2283	15	1	0.6	2240	56
eaf35 - 18.d	3.42160	0.07963	0.12910	0.00265	1653	33	2086	36	21	4.9	1581	38
eaf35 - 19.d	3.17799	0.09435	0.23500	0.00650	1764	45	3086	43	43	22.5	1407	46
eaf35 - 20.d	4.03120	0.07053	0.12740	0.00205	1428	22	2062	28	31	6.3	1347	24
eaf35 - 22.d	3.88603	0.07176	0.11900	0.00160	1476	24	1941	24	24	4.5	1416	26
eaf35 - 23.d	4.42941	0.07242	0.15570	0.00275	1312	19	2409	30	46	11.6	1173	20
eaf35 - 24.d	4.55684	0.07603	0.11690	0.00180	1279	19	1909	27	33	5.5	1215	20
eaf35 - 25.d	4.34513	0.14375	0.24300	0.00700	1335	39	3140	45	57	25.5	1020	37
eaf35 - 26.d	4.01472	0.09121	0.16970	0.00320	1434	29	2555	31	44	13.3	1261	29
eaf35 - 27.d	4.70757	0.07571	0.10740	0.00150	1242	18	1756	25	29	4.2	1194	19
eaf35 - 28.d	3.59707	0.10346	0.23400	0.00550	1581	39	3080	37	49	23.2	1248	39
eaf35 - 29.d	2.47355	0.08763	0.32900	0.01100	2189	64	3612	50	39	36.7	1469	69
eaf35 - 30.d	3.13738	0.08799	0.21400	0.00650	1784	43	2936	48	39	18.8	1484	46

Analysis number	$^{238}U/^{206}Pb$	±1s	$^{207}Pb/^{206}Pb$	±1s	$^{238}U/^{206}Pb$ age (Ma)	±1s	$^{207}Pb/^{206}Pb$ age (Ma)	±1s	Disc (%)	f207%	^{207}Pb-corrected $^{238}U/^{206}Pb$ age (Ma)	±1s
eaf35 - 31.d	4.24190	0.07685	0.14750	0.00295	1365	22	2317	34	41	10.0	1240	23
eaf35 - 32.d	4.61249	0.07458	0.11600	0.00185	1265	18	1895	28	33	5.4	1202	19
eaf35 - 33.d	4.48402	0.05875	0.09910	0.00125	1298	15	1607	23	19	2.5	1269	17
eaf35 - 34.d	4.05953	0.07183	0.18710	0.00305	1420	22	2717	27	48	16.2	1210	23
eaf35 - 35.d	2.34368	0.07621	0.30100	0.00750	2291	61	3475	38	34	31.3	1657	65
eaf35 - 36.d	3.07837	0.08979	0.30400	0.00900	1813	45	3491	45	48	33.8	1256	47
eaf35 - 37.d	2.51795	0.09879	0.43400	0.01600	2156	70	4031	54	47	54.1	1079	76
eaf35 - 38.d	3.96928	0.08678	0.17690	0.00450	1448	28	2624	42	45	14.4	1259	29
eaf35 - 39.d	3.71407	0.08001	0.16200	0.00340	1537	29	2477	35	38	11.4	1379	31
eaf35 - 40.d	2.34928	0.06307	0.19130	0.00350	2286	51	2753	30	17	10.2	2087	63
eaf35 - 41.d	2.49873	0.08899	0.31800	0.01000	2170	64	3560	48	39	34.9	1493	67
eaf35 - 42.d	4.57382	0.06861	0.09760	0.00180	1275	17	1579	34	19	2.4	1247	19
eaf35 - 43.d	4.80666	0.05869	0.09650	0.00095	1218	13	1558	18	22	2.5	1190	14
eaf35 - 44.d	4.84699	0.06895	0.08920	0.00110	1209	15	1408	23	14	1.4	1193	17
eaf35 - 45.d	4.41944	0.06668	0.10020	0.00175	1315	18	1628	32	19	2.5	1285	19
eaf35 - 48.d	4.75315	0.08662	0.10220	0.00160	1231	20	1664	29	26	3.4	1193	21
eaf35 - 49.d	3.64514	0.07232	0.19280	0.00475	1563	27	2766	40	44	16.4	1331	29
eaf35 - 50.d	3.43357	0.09595	0.26700	0.00600	1648	40	3288	35	50	28.3	1222	39
eaf35 - 51.d	4.81845	0.09052	0.12740	0.00195	1216	20	2062	27	41	7.6	1131	21
eaf35 - 52.d	4.40556	0.07765	0.11470	0.00180	1319	21	1875	28	30	4.9	1260	22
eaf35 - 53.d	4.43942	0.06248	0.11900	0.00195	1310	16	1941	29	33	5.7	1242	18
eaf35 - 54.d	3.67790	0.10097	0.24900	0.00600	1550	37	3178	38	51	25.7	1186	36
eaf35 - 55.d	4.47380	0.10017	0.14960	0.00365	1300	26	2341	41	44	10.7	1173	27
eaf35 - 56.d	4.12778	0.06128	0.12560	0.00185	1398	18	2037	26	31	6.2	1320	20
eaf35 - 57.d	2.88824	0.07449	0.22500	0.00600	1917	42	3017	42	36	19.9	1578	46
eaf35 - 58.d	3.48227	0.09813	0.26500	0.00700	1627	40	3277	41	50	28.1	1211	40
eaf35 - 59.d	3.67790	0.09469	0.23700	0.00650	1550	35	3100	43	50	23.8	1214	36
eaf35 - 60.d	3.69173	0.10159	0.25700	0.00750	1545	37	3228	45	52	27.1	1162	38
eaf35 - 61.d	2.41278	0.07434	0.28200	0.00750	2235	57	3374	41	34	28.2	1680	62

Analysis number	$^{238}U/^{206}Pb$	±1s	$^{207}Pb/^{206}Pb$	±1s	$^{238}U/^{206}Pb$ age (Ma)	±1s	$^{207}Pb/^{206}Pb$ age (Ma)	±1s	Disc (%)	f207%	^{207}Pb-corrected $^{238}U/^{206}Pb$ age (Ma)	±1s
eaf35 - 62.d	4.76237	0.07788	0.10250	0.00160	1229	18	1670	29	26	3.5	1190	19
eaf35 - 63.d	3.71970	0.10286	0.22800	0.00550	1535	37	3038	38	49	22.4	1222	37
eaf35 - 64.d	3.53237	0.08893	0.25600	0.00700	1607	35	3222	43	50	26.7	1216	36
eaf35 - 65.d	3.89683	0.09686	0.17850	0.00375	1473	32	2639	34	44	14.5	1278	33
eaf35 - 66.d	3.58394	0.07027	0.22270	0.00305	1586	27	3000	22	47	21.3	1280	27
eaf35 - 67.d	2.83815	0.11307	0.39100	0.01350	1946	65	3875	51	50	47.6	1092	64
eaf35 - 68.d	4.26400	0.08055	0.13310	0.00250	1358	23	2139	32	37	7.7	1263	24
eaf35 - 69.d	3.35612	0.06770	0.15960	0.00270	1681	29	2451	28	31	10.0	1531	32
eaf35 - 70.d	3.82250	0.07270	0.11980	0.00250	1498	25	1953	37	23	4.5	1437	28
eaf35 - 71.d	3.31421	0.06758	0.12810	0.00265	1700	30	2072	36	18	4.3	1635	34
eaf35 - 72.d	4.57169	0.06690	0.09820	0.00100	1275	17	1590	19	20	2.5	1247	18
eaf35 - 73.d	4.51079	0.07161	0.10640	0.00200	1291	18	1739	34	26	3.7	1247	20
eaf35 - 74.d	3.54001	0.06721	0.16090	0.00310	1604	27	2465	32	35	10.8	1449	29
eaf35 - 75.d	3.06875	0.09366	0.21400	0.00550	1818	47	2936	41	38	18.6	1517	50
eaf35 - 76.d	2.19687	0.06254	0.28200	0.00500	2418	56	3374	27	28	27.0	1849	62
eaf35 - 77.d	3.65736	0.07889	0.19680	0.00330	1558	29	2800	27	44	17.1	1317	30
eaf35 - 78.d	3.86462	0.07626	0.14760	0.00235	1483	26	2318	27	36	9.3	1359	27
eaf35 - 79.d	1.84934	0.05603	0.23970	0.00420	2787	67	3118	28	11	13.6	2472	99
eaf35 - 80.d	4.35477	0.06557	0.12000	0.00205	1333	18	1956	30	32	5.7	1264	19
eaf35 - 81.d	4.26030	0.09684	0.18770	0.00330	1359	27	2722	29	50	16.6	1153	27
eaf35 - 82.d	3.76967	0.06300	0.14090	0.00205	1517	22	2238	25	32	8.0	1408	24
eaf35 - 83.d	4.77162	0.08306	0.11940	0.00225	1227	19	1947	33	37	6.2	1157	20
eaf35 - 84.d	3.97893	0.07870	0.14230	0.00305	1445	25	2255	37	36	8.7	1332	27
eaf35 - 85.d	4.91246	0.06814	0.09940	0.00110	1194	15	1613	20	26	3.2	1160	16
eaf35 - 86.d	4.30324	0.05668	0.10280	0.00105	1347	16	1675	19	20	2.7	1314	17
eaf35 - 88.d	4.06121	0.08246	0.20470	0.00450	1419	25	2864	35	50	19.1	1171	26
eaf35 - 89.d	4.55262	0.06740	0.10860	0.00140	1280	17	1776	23	28	4.1	1232	18
eaf35 - 90.d	3.29530	0.11024	0.30600	0.01150	1708	49	3501	57	51	34.5	1169	51
eaf35 - 91.d	4.34129	0.06534	0.13360	0.00215	1336	18	2146	28	38	7.9	1240	19

Analysis number	$^{238}U/^{206}Pb$	±1s	$^{207}Pb/^{206}Pb$	±1s	$^{238}U/^{206}Pb$ age (Ma)	±1s	$^{207}Pb/^{206}Pb$ age (Ma)	±1s	Disc (%)	f207%	^{207}Pb-corrected $^{238}U/^{206}Pb$ age (Ma)	±1s
eaf35 - 92.d	4.02294	0.07993	0.17550	0.00465	1431	25	2611	43	45	14.3	1246	27
eaf35 - 93.d	4.75545	0.06389	0.10150	0.00150	1230	15	1652	27	26	3.3	1193	16
eaf35 - 94.d	4.31269	0.06852	0.13290	0.00195	1344	19	2137	25	37	7.7	1250	20
eaf35 - 96.d	3.66418	0.08801	0.24300	0.00600	1556	32	3140	39	50	24.7	1204	33
eaf35 - 97.d	4.49017	0.07799	0.12440	0.00175	1296	20	2020	25	36	6.6	1218	21
eaf35 - 98.d	3.14744	0.07537	0.23090	0.00485	1779	36	3058	33	42	21.7	1432	38
eaf35 - 99.d	3.46996	0.10321	0.25500	0.00700	1632	42	3216	43	49	26.4	1240	42
eaf35 - 100.d	4.45554	0.07051	0.11400	0.00170	1305	18	1864	27	30	4.9	1248	20
eaf35 - 101.d	3.19870	0.08601	0.26500	0.00750	1754	40	3277	44	46	27.6	1316	42
eaf35 - 102.d	3.75239	0.07452	0.17330	0.00330	1523	26	2590	31	41	13.4	1339	28
eaf35 - 103.d	2.55729	0.08924	0.32700	0.01000	2128	61	3603	46	41	36.6	1429	64
eaf35 - 104.d	2.89676	0.08953	0.31900	0.00900	1912	50	3565	43	46	36.0	1288	51
eaf35 - 106.d	2.65405	0.06988	0.29400	0.00700	2061	45	3439	36	40	31.2	1486	49
eaf35 - 107.d	3.57872	0.05935	0.10450	0.00130	1588	23	1706	23	7	1.1	1573	26
eaf35 - 108.d	3.01227	0.07498	0.21650	0.00420	1848	39	2955	31	37	18.8	1538	41
eaf35 - 109.d	4.05116	0.08072	0.12040	0.00235	1422	25	1962	34	28	5.2	1356	27
eaf35 - 110.d	3.50589	0.07040	0.13330	0.00230	1618	28	2142	30	24	5.9	1532	31
eaf35 - 111.d	4.26215	0.06613	0.11870	0.00150	1359	19	1937	22	30	5.3	1293	20
eaf35 - 112.d	4.10879	0.07507	0.18610	0.00360	1404	23	2708	32	48	16.1	1198	23
eaf35 - 113.d	3.77112	0.08302	0.21550	0.00445	1516	29	2947	33	49	20.4	1234	30
eaf35 - 114.d	3.67515	0.07422	0.14940	0.00285	1551	27	2339	32	34	9.2	1424	29
eaf35 - 115.d	4.84221	0.07767	0.12370	0.00200	1210	17	2010	28	40	7.0	1132	18
eaf35 - 116.d	3.94695	0.08815	0.14680	0.00295	1456	29	2309	34	37	9.4	1333	30
eaf35 - 117.d	3.92329	0.07328	0.17010	0.00255	1464	24	2559	25	43	13.2	1289	25
eaf35 - 118.d	4.59093	0.07681	0.13330	0.00215	1270	19	2142	28	41	8.2	1175	20
eaf35 - 119.d	2.22172	0.06328	0.27000	0.00600	2396	56	3306	34	28	24.9	1877	64
eaf35 - 120.d	3.16774	0.10795	0.29100	0.00900	1769	51	3423	47	48	31.8	1257	51

Analysis number	Reason for exclusion
eaf35 - 21.d	Outlier
eaf35 - 46.d	Not titanite
eaf35 - 47.d	Not titanite
eaf35 - 87.d	Not titanite
eaf35 - 95.d	Not titanite
eaf35 - 105.d	Outlier

Table A6.4-4 LA-ICPMS analytical data for sample EAF38.

Analysis number	Na23 ppm	Na23 ppm 2SE	Na23 ppm LOD	Al27 ppm	Al27 ppm 2SE	Al27 ppm LOD	Si28 ppm	Si28 ppm 2SE	Si28 ppm LOD	Ca44 ppm	Ca44 ppm 2SE	Ca44 ppm LOD
eaf38 - 2.d	37.5	8.8	24	6943	95	3	1.49E+05	2.50E+03	6500	2.23E+05	3.00E+03	270
eaf38 - 6.d	42.3	6.7	23	7060	100	3.2	1.48E+05	2.20E+03	4600	2.24E+05	3.20E+03	180
eaf38 - 7.d	63.7	9.3	29	6554	83	3.7	1.44E+05	1.70E+03	9200	2.25E+05	2.80E+03	190
eaf38 - 8.d	147	21	32	6820	160	3.1	1.46E+05	2.00E+03	8600	2.21E+05	2.30E+03	200
eaf38 - 9.d	68.8	9.9	23	6860	100	3.7	1.47E+05	1.60E+03	6000	2.19E+05	2.70E+03	270
eaf38 - 10.d	40.2	7.2	23	6636	99	4.4	1.47E+05	2.10E+03	7400	2.20E+05	2.50E+03	320
eaf38 - 11.d	35.9	5.7	24	6505	78	3	1.47E+05	2.50E+03	4100	2.18E+05	2.70E+03	160
eaf38 - 12.d	36.8	8.9	23	6800	120	2.8	1.46E+05	2.90E+03	5300	2.18E+05	3.30E+03	310
eaf38 - 13.d	42.1	9.1	23	6104	76	3.7	1.49E+05	2.30E+03	8800	2.18E+05	2.70E+03	330
eaf38 - 14.d	28.4	6.6	27	6748	97	3.1	1.51E+05	3.00E+03	5200	2.18E+05	2.60E+03	280
eaf38 - 15.d	41	8.3	18	7083	87	3.1	1.50E+05	2.70E+03	6100	2.17E+05	2.70E+03	190
eaf38 - 16.d	32.8	9.6	21	6402	78	2.3	1.49E+05	2.00E+03	5600	2.19E+05	2.90E+03	280
eaf38 - 17.d	25.1	7.4	24	19590	210	2.5	1.52E+05	2.10E+03	7000	1.86E+05	2.50E+03	290
eaf38 - 18.d	33.5	7.3	22	7284	95	3.7	1.52E+05	2.20E+03	5600	2.18E+05	3.00E+03	370
eaf38 - 19.d	35.5	6.1	21	6561	80	3.7	1.48E+05	3.10E+03	8400	2.19E+05	2.80E+03	230
eaf38 - 20.d	33.1	9.3	23	6062	73	3.6	1.52E+05	2.00E+03	6900	2.21E+05	2.50E+03	310
eaf38 - 21.d	38.5	8.3	21	6405	79	3.5	1.49E+05	1.90E+03	9400	2.18E+05	2.60E+03	260
eaf38 - 23.d	42.3	7.4	22	5790	85	2.7	1.48E+05	1.90E+03	3400	2.25E+05	2.40E+03	260
eaf38 - 24.d	28.1	7.8	20	6140	63	3.3	1.48E+05	2.30E+03	7300	2.20E+05	2.70E+03	220
eaf38 - 25.d	558	25	20	9040	110	2.9	1.49E+05	2.50E+03	6300	2.14E+05	2.90E+03	300
eaf38 - 26.d	37.7	9.6	30	6788	83	3.4	1.47E+05	2.10E+03	8400	2.24E+05	2.50E+03	230
eaf38 - 27.d	57	11	28	6663	98	4.4	1.47E+05	2.50E+03	11000	2.24E+05	2.50E+03	360
eaf38 - 28.d	50.2	9.5	20	6680	100	4.1	1.47E+05	2.50E+03	5300	2.26E+05	3.30E+03	300
eaf38 - 29.d	84	16	37	6997	97	4.3	1.46E+05	2.30E+03	10000	2.18E+05	4.20E+03	300
eaf38 - 30.d	< LOD	< LOD	30	6424	55	2.8	1.46E+05	3.20E+03	8000	2.24E+05	3.10E+03	250
eaf38 - 31.d	33.7	7	23	5906	60	3.2	1.44E+05	1.90E+03	6200	2.29E+05	3.80E+03	240
eaf38 - 32.d	45.1	8.6	32	6765	85	3.7	1.46E+05	2.50E+03	5100	2.27E+05	2.80E+03	340
eaf38 - 33.d	76	16	41	6050	92	4.7	1.48E+05	2.30E+03	10000	2.26E+05	3.20E+03	290

Analysis number	Na23 ppm	Na23 ppm 2SE	Na23 ppm LOD	Al27 ppm	Al27 ppm 2SE	Al27 ppm LOD	Si28 ppm	Si28 ppm 2SE	Si28 ppm LOD	Ca44 ppm	Ca44 ppm 2SE	Ca44 ppm LOD
eaf38 - 34.d	144	12	34	8200	110	3.3	1.45E+05	2.30E+03	8700	2.01E+05	3.20E+03	350
eaf38 - 35.d	53.9	7.6	21	7437	87	5.5	1.42E+05	2.20E+03	5000	2.20E+05	2.60E+03	230
eaf38 - 36.d	60.2	7.1	21	6529	87	3.4	1.43E+05	2.70E+03	4700	2.21E+05	2.90E+03	270
eaf38 - 37.d	50.2	8.3	21	7163	90	3.2	1.46E+05	2.50E+03	8000	2.22E+05	3.20E+03	300
eaf38 - 38.d	36.7	6.4	28	7033	96	3.3	1.44E+05	1.80E+03	6400	2.20E+05	2.60E+03	260
eaf38 - 39.d	51.4	8	31	7128	80	2.5	1.45E+05	1.80E+03	5800	2.21E+05	2.70E+03	270
eaf38 - 40.d	38.4	9.8	27	6616	92	3.2	1.48E+05	2.70E+03	6000	2.20E+05	2.70E+03	240
eaf38 - 41.d	55	8.1	21	6734	85	3.1	1.47E+05	2.10E+03	8200	2.21E+05	2.60E+03	300
eaf38 - 42.d	38.9	6.2	28	6579	82	3.5	1.47E+05	2.10E+03	7100	2.22E+05	2.80E+03	250
eaf38 - 43.d	44.4	9.3	26	6190	74	3.3	1.49E+05	2.40E+03	12000	2.19E+05	3.40E+03	240
eaf38 - 44.d	40.8	8.3	25	5908	90	3.3	1.49E+05	2.20E+03	5100	2.20E+05	2.80E+03	300
eaf38 - 45.d	39.3	7.8	21	6698	93	3.2	1.47E+05	2.40E+03	7900	2.18E+05	2.90E+03	380
eaf38 - 46.d	35.8	9.2	23	6533	93	3.5	1.47E+05	2.90E+03	5700	2.19E+05	3.10E+03	390
eaf38 - 47.d	60	8.9	21	7090	90	4	1.47E+05	2.30E+03	6000	2.20E+05	2.70E+03	310
eaf38 - 48.d	< LOD	< LOD	32	7019	85	2.6	1.47E+05	2.30E+03	9300	2.20E+05	2.70E+03	270
eaf38 - 49.d	83	27	28	7870	110	3.4	1.48E+05	2.80E+03	4900	2.24E+05	2.80E+03	230
eaf38 - 50.d	46.4	8.3	23	6623	98	3.1	1.48E+05	2.20E+03	11000	2.21E+05	3.00E+03	230
eaf38 - 51.d	34.2	7.1	23	5904	68	4.1	1.47E+05	2.10E+03	6700	2.21E+05	3.00E+03	340
eaf38 - 52.d	38.5	9.3	20	6200	100	2.9	1.48E+05	2.20E+03	7000	2.23E+05	3.30E+03	220
eaf38 - 53.d	42.1	9.9	23	6130	100	4.2	1.44E+05	2.90E+03	3600	2.28E+05	3.70E+03	210
eaf38 - 54.d	47.3	8.2	33	6442	78	3.1	1.47E+05	2.80E+03	10000	2.25E+05	3.70E+03	240
eaf38 - 55.d	31.6	8.2	21	6303	86	4	1.50E+05	2.00E+03	8700	2.24E+05	2.50E+03	230
eaf38 - 56.d	37.8	9.3	27	6223	78	3.3	1.44E+05	2.50E+03	4900	2.27E+05	2.50E+03	280
eaf38 - 57.d	91	12	35	7140	130	3.8	1.48E+05	2.50E+03	6200	2.28E+05	2.60E+03	250
eaf38 - 58.d	90	17	29	6610	140	3.5	1.46E+05	2.40E+03	6000	2.23E+05	3.00E+03	310
eaf38 - 59.d	65	10	25	6769	72	4.4	1.45E+05	2.60E+03	4800	2.20E+05	2.50E+03	290
eaf38 - 60.d	92.9	9.5	26	6541	85	1.7	1.48E+05	2.50E+03	9100	2.19E+05	2.90E+03	320
eaf38 - 61.d	48.3	9.5	31	6414	96	3.9	1.49E+05	2.00E+03	7000	2.21E+05	2.90E+03	280
eaf38 - 62.d	36	10	24	6308	79	3	1.47E+05	3.70E+03	4800	2.21E+05	3.20E+03	220

Analysis number	Na23 ppm	Na23 ppm 2SE	Na23 ppm LOD	Al27 ppm	Al27 ppm 2SE	Al27 ppm LOD	Si28 ppm	Si28 ppm 2SE	Si28 ppm LOD	Ca44 ppm	Ca44 ppm 2SE	Ca44 ppm LOD
eaf38 - 63.d	41.7	9.1	22	6700	110	4	1.45E+05	1.90E+03	4900	2.21E+05	3.00E+03	260
eaf38 - 64.d	32	10	16	7090	110	4.7	1.49E+05	2.80E+03	8400	2.19E+05	3.00E+03	230
eaf38 - 65.d	42.4	8.3	27	6311	90	3.7	1.47E+05	2.00E+03	11000	2.22E+05	3.00E+03	390
eaf38 - 68.d	39	7.1	19	6221	88	3.7	1.51E+05	1.90E+03	5800	2.20E+05	3.00E+03	210
eaf38 - 69.d	43.3	5.7	15	6446	76	3.9	1.48E+05	1.60E+03	8600	2.18E+05	2.80E+03	240
eaf38 - 70.d	46.3	6.6	25	6557	89	3.9	1.47E+05	2.20E+03	6700	2.23E+05	2.80E+03	280
eaf38 - 71.d	44.6	7.9	27	6610	83	3.8	1.45E+05	2.90E+03	5600	2.18E+05	2.60E+03	310
eaf38 - 72.d	50.1	7.2	22	6320	81	3.5	1.47E+05	2.10E+03	5000	2.19E+05	2.70E+03	300
eaf38 - 73.d	432	22	18	8150	190	3.2	1.45E+05	2.20E+03	6600	2.15E+05	2.10E+03	160
eaf38 - 74.d	416	24	19	6661	83	4.7	1.43E+05	2.60E+03	8400	2.16E+05	3.00E+03	300
eaf38 - 75.d	46	6.8	33	6351	93	3.7	1.46E+05	2.50E+03	8600	2.23E+05	3.10E+03	260
eaf38 - 76.d	32	7.9	26	6586	99	4.6	1.48E+05	3.20E+03	12000	2.23E+05	3.60E+03	350
eaf38 - 77.d	80	15	23	7250	150	3.4	1.46E+05	2.40E+03	7000	2.18E+05	3.10E+03	260
eaf38 - 78.d	26.4	5.4	19	6160	81	4	1.49E+05	1.80E+03	5300	2.23E+05	2.90E+03	230
eaf38 - 79.d	39.9	7.7	26	6182	74	3.6	1.44E+05	2.50E+03	7100	2.26E+05	2.80E+03	240
eaf38 - 80.d	< LOD	< LOD	33	6044	66	3.4	1.48E+05	3.20E+03	6600	2.24E+05	3.00E+03	290
eaf38 - 81.d	39.7	8.8	22	6163	82	3.6	1.50E+05	3.00E+03	8700	2.26E+05	2.50E+03	300
eaf38 - 82.d	45.3	8.1	23	6329	66	3.3	1.49E+05	2.20E+03	4200	2.26E+05	3.20E+03	270
eaf38 - 83.d	48.6	9.3	30	6017	75	3.1	1.47E+05	2.70E+03	9900	2.23E+05	2.90E+03	350
eaf38 - 84.d	39.3	7.9	30	6210	100	4.3	1.48E+05	2.20E+03	5700	2.18E+05	2.90E+03	260
eaf38 - 85.d	28.2	8.2	20	6442	89	2.4	1.51E+05	2.40E+03	6200	2.20E+05	2.50E+03	280
eaf38 - 86.d	< LOD	< LOD	32	5828	81	4.3	1.49E+05	2.10E+03	11000	2.20E+05	2.90E+03	330
eaf38 - 87.d	75	9.7	27	6126	94	2.8	1.48E+05	2.00E+03	4700	2.20E+05	2.50E+03	330
eaf38 - 88.d	39.7	9.5	23	6076	66	3.1	1.46E+05	2.50E+03	4300	2.20E+05	2.60E+03	420
eaf38 - 89.d	32.8	9.2	27	7180	110	2.4	1.47E+05	2.20E+03	7900	2.24E+05	2.60E+03	310
eaf38 - 90.d	45.3	6.5	27	6010	68	2.7	1.47E+05	2.10E+03	7200	2.23E+05	2.70E+03	210
eaf38 - 91.d	43.7	8	26	6352	70	5.4	1.46E+05	2.00E+03	8100	2.24E+05	2.70E+03	390
eaf38 - 92.d	91	11	23	8040	190	3.3	1.48E+05	2.70E+03	7900	2.16E+05	3.50E+03	280
eaf38 - 93.d	38.8	7.8	26	6412	96	3.7	1.48E+05	2.70E+03	6100	2.24E+05	2.70E+03	290

Analysis number	Na23 ppm	Na23 ppm 2SE	Na23 ppm LOD	Al27 ppm	Al27 ppm 2SE	Al27 ppm LOD	Si28 ppm	Si28 ppm 2SE	Si28 ppm LOD	Ca44 ppm	Ca44 ppm 2SE	Ca44 ppm LOD
eaf38 - 94.d	43.6	8.9	25	6370	100	4	1.51E+05	2.40E+03	7700	2.23E+05	3.10E+03	270
eaf38 - 95.d	1033	64	30	8090	160	3.2	1.49E+05	2.60E+03	9200	2.05E+05	3.90E+03	350
eaf38 - 96.d	50.7	7.2	22	5923	84	3.2	1.48E+05	2.40E+03	4800	2.23E+05	3.60E+03	230
eaf38 - 97.d	37.3	6.8	17	6179	85	3.4	1.50E+05	2.30E+03	3600	2.24E+05	2.60E+03	260
eaf38 - 98.d	73	7.7	25	6830	140	2.6	1.49E+05	1.90E+03	8700	2.19E+05	2.90E+03	190
eaf38 - 99.d	30	7.7	16	7184	73	3.6	1.51E+05	1.80E+03	9800	2.24E+05	2.90E+03	340
eaf38 - 100.d	43.2	8.3	24	6519	90	3.8	1.51E+05	2.90E+03	6000	2.25E+05	2.90E+03	400
eaf38 - 101.d	37.3	8.1	32	5992	92	4.3	1.50E+05	2.70E+03	6100	2.22E+05	3.30E+03	220
eaf38 - 102.d	32.9	6.5	24	6580	100	2.4	1.51E+05	2.70E+03	7700	2.21E+05	2.90E+03	300
eaf38 - 103.d	< LOD	< LOD	41	6377	96	3.8	1.49E+05	2.50E+03	6300	2.22E+05	3.80E+03	350
eaf38 - 104.d	34.5	7.5	27	6138	69	3.6	1.46E+05	2.90E+03	9700	2.25E+05	3.50E+03	190
eaf38 - 105.d	400	110	21	8510	540	3.3	1.50E+05	3.00E+03	6300	2.14E+05	5.30E+03	250
eaf38 - 106.d	93	19	25	6754	88	3.2	1.51E+05	2.60E+03	8400	2.28E+05	3.10E+03	220
eaf38 - 107.d	41.9	7.8	20	6890	89	3.6	1.50E+05	2.30E+03	5100	2.27E+05	3.40E+03	290
eaf38 - 108.d	101	14	25	8820	260	4.9	1.52E+05	2.80E+03	4600	2.23E+05	3.50E+03	200
eaf38 - 109.d	< LOD	< LOD	35	6957	81	5.3	1.52E+05	2.00E+03	10000	2.17E+05	2.60E+03	300
eaf38 - 110.d	32.4	7.4	22	6511	77	4.6	1.48E+05	2.40E+03	5000	2.21E+05	2.50E+03	260
eaf38 - 111.d	45	8.6	23	7190	100	3.7	1.52E+05	2.20E+03	5000	2.19E+05	2.70E+03	250
eaf38 - 112.d	42.6	9.1	25	6863	98	4.1	1.51E+05	2.90E+03	4100	2.21E+05	3.00E+03	240
eaf38 - 113.d	26.8	7.8	19	6363	96	2.5	1.51E+05	2.60E+03	7100	2.21E+05	2.90E+03	180
eaf38 - 114.d	34	8.4	29	5687	70	3.8	1.53E+05	2.30E+03	5400	2.24E+05	2.70E+03	430
eaf38 - 115.d	36.2	8.1	27	6032	71	3.6	1.51E+05	2.40E+03	11000	2.22E+05	2.90E+03	290
eaf38 - 116.d	43.9	8.4	25	6270	100	3.4	1.48E+05	2.40E+03	8300	2.22E+05	3.70E+03	250
eaf38 - 117.d	61	10	19	6630	120	3.8	1.49E+05	3.10E+03	5700	2.25E+05	3.20E+03	280
eaf38 - 118.d	76	6.5	27	6622	88	3.6	1.49E+05	2.00E+03	6700	2.22E+05	3.20E+03	340
eaf38 - 119.d	105.8	8.5	23	6660	87	2.7	1.50E+05	2.00E+03	4000	2.25E+05	2.60E+03	240
eaf38 - 120.d	86.8	9.2	21	6651	82	3.3	1.51E+05	3.40E+03	5200	2.26E+05	3.90E+03	330
eaf38 - 121.d	45.1	9	25	6290	110	3.9	1.53E+05	2.40E+03	4000	2.27E+05	3.80E+03	300
eaf38 - 125.d	53.2	8.6	23	7737	92	3.7	1.50E+05	2.70E+03	4900	2.25E+05	2.80E+03	280

Analysis number	Na23 ppm	Na23 ppm 2SE	Na23 ppm LOD	Al27 ppm	Al27 ppm 2SE	Al27 ppm LOD	Si28 ppm	Si28 ppm 2SE	Si28 ppm LOD	Ca44 ppm	Ca44 ppm 2SE	Ca44 ppm LOD
eaf38 - 126.d	55	10	37	6940	110	2.7	1.51E+05	2.20E+03	4200	2.28E+05	2.70E+03	300
eaf38 - 127.d	71.6	7.6	22	8100	110	5	1.48E+05	2.30E+03	5100	2.28E+05	2.50E+03	320
eaf38 - 128.d	71.4	8.8	26	7104	98	2.6	1.48E+05	2.30E+03	8800	2.30E+05	2.60E+03	380
eaf38 - 129.d	47	10	23	6770	83	4	1.49E+05	3.20E+03	5600	2.31E+05	3.30E+03	260
eaf38 - 130.d	43.7	9.1	33	6765	88	4.4	1.50E+05	2.00E+03	9800	2.33E+05	3.20E+03	280
eaf38 - 131.d	41	8.1	27	6791	95	3.3	1.50E+05	2.00E+03	5800	2.29E+05	3.40E+03	270
eaf38 - 132.d	48.1	7	24	7001	97	3.4	1.50E+05	2.60E+03	5700	2.34E+05	2.50E+03	340
eaf38 - 133.d	57	7.9	33	6477	96	4.9	1.51E+05	1.80E+03	7800	2.30E+05	2.70E+03	240
eaf38 - 134.d	36.8	9.9	27	6793	96	3.2	1.51E+05	2.60E+03	5100	2.30E+05	3.20E+03	280
eaf38 - 135.d	39	10	30	7460	110	3.3	1.50E+05	2.20E+03	6100	2.34E+05	2.70E+03	160
eaf38 - 136.d	59.7	9.5	31	6880	120	5.4	1.47E+05	2.20E+03	5400	2.36E+05	3.80E+03	230
eaf38 - 137.d	39	10	37	6314	81	4.1	1.48E+05	2.60E+03	12000	2.37E+05	3.40E+03	280
eaf38 - 138.d	< LOD	< LOD	35	7950	110	2.4	1.48E+05	3.10E+03	7400	2.34E+05	4.20E+03	240
eaf38 - 139.d	43	13	33	7812	92	3.8	1.45E+05	3.50E+03	4300	2.38E+05	3.70E+03	280
eaf38 - 140.d	28	9.5	21	6502	84	4.5	1.49E+05	2.00E+03	3600	2.40E+05	3.70E+03	310
eaf38 - 141.d	39.3	9.2	24	6486	85	2.7	1.49E+05	2.60E+03	6700	2.40E+05	3.40E+03	430
eaf38 - 142.d	< LOD	< LOD	31	6731	93	3	1.48E+05	2.30E+03	11000	2.39E+05	3.40E+03	260
eaf38 - 143.d	51	10	29	6130	110	3.7	1.48E+05	2.50E+03	8600	2.42E+05	4.20E+03	280

Analysis number	Ti49 ppm	Ti49 ppm 2SE	Ti49 ppm LOD	V51 ppm	V51 ppm 2SE	V51 ppm LOD	Cr52 ppm	Cr52 ppm 2SE	Cr52 ppm LOD	Mn55 ppm	Mn55 ppm 2SE	Mn55 ppm LOD
eaf38 - 2.d	2.50E+05	3.50E+03	2.3	434.1	7	0.23	20.9	2.2	4.3	189.6	4.1	10
eaf38 - 6.d	2.50E+05	3.00E+03	1.5	450.4	7.3	0.3	23.6	1.9	3.4	175.4	3.5	9.7
eaf38 - 7.d	2.49E+05	2.80E+03	1.1	439	6.5	0.49	22.7	1.7	5.4	178.4	3.8	10
eaf38 - 8.d	2.46E+05	3.30E+03	7.4	434.4	6.3	0.49	20.9	1.1	4.7	168.6	3.3	10
eaf38 - 9.d	2.39E+05	2.90E+03	2.3	472.5	7.4	0.47	27.7	1.8	5.1	162.5	4.1	8.1
eaf38 - 10.d	2.40E+05	3.80E+03	NaN	994	18	0.42	33.3	1.5	5.7	148.5	3.6	8.9
eaf38 - 11.d	2.38E+05	3.10E+03	NaN	1056	12	0.3	30.6	2	4.6	160.7	4.9	5.1
eaf38 - 12.d	2.38E+05	3.30E+03	2.3	1062	20	0.28	31	2	4.4	137.1	3	7.8
eaf38 - 13.d	2.47E+05	2.70E+03	2.3	1003	14	0.29	31.9	1.9	4.1	189	19	7.3
eaf38 - 14.d	2.39E+05	2.50E+03	3.1	1043	13	0.46	31.7	1.6	4.5	158.4	3.4	5.4
eaf38 - 15.d	2.39E+05	3.50E+03	1.1	1023	15	0.12	33.6	1.4	4.3	133.8	3.9	6.7
eaf38 - 16.d	2.42E+05	2.90E+03	1.5	382.7	5.8	0.27	5.5	1.1	3.6	126.3	4.1	10
eaf38 - 17.d	2.00E+05	2.80E+03	NaN	334.5	6.2	0.32	9.2	1.6	4.8	934	11	7.2
eaf38 - 18.d	2.40E+05	3.90E+03	1.1	1029	14	0.27	62.6	2.4	2.6	117.7	3	8.4
eaf38 - 19.d	2.41E+05	3.50E+03	2.2	861	12	0.41	48.9	2.2	4	116.6	3.9	9.9
eaf38 - 20.d	2.45E+05	2.80E+03	2.1	978	14	0.35	48.6	2	4.6	116.4	3.1	8.3
eaf38 - 21.d	2.41E+05	3.20E+03	2.2	973	14	0.52	55.9	1.7	5.7	126	3.5	11
eaf38 - 23.d	2.54E+05	2.60E+03	NaN	970	10	0.28	62.7	2.4	3.1	107	3.1	5
eaf38 - 24.d	2.43E+05	3.20E+03	2.2	999	15	0.36	60.7	2.2	5.2	106.9	2.6	8.1
eaf38 - 25.d	2.29E+05	2.80E+03	2.4	1015	17	0.25	79.5	2.6	4.1	124.3	4.4	8.9
eaf38 - 26.d	2.46E+05	3.20E+03	NaN	1067	16	0.34	51.7	2.5	5.1	107.8	3.1	11
eaf38 - 27.d	2.50E+05	3.50E+03	1.1	1148	16	0.43	55	2	5.2	136.3	4.2	11
eaf38 - 28.d	2.53E+05	2.30E+03	3.1	1103	15	0.43	60.6	2	4.6	99.5	3.4	8.8
eaf38 - 29.d	2.49E+05	4.10E+03	3.3	1156	19	0.35	73.4	2.4	4.5	106.8	3.9	8.5
eaf38 - 30.d	2.47E+05	3.60E+03	NaN	1083	13	0.33	64.5	2.1	3.6	101.4	3.5	11
eaf38 - 31.d	2.52E+05	3.20E+03	6.8	985	15	0.36	50.3	1.9	4.8	122.1	2.9	8.7
eaf38 - 32.d	2.52E+05	3.70E+03	NaN	1007	15	0.29	51.8	2	4.6	117.5	2.2	6.6
eaf38 - 33.d	2.52E+05	3.40E+03	1.8	1032	21	0.52	66.9	3	7.2	105.4	4.1	12
eaf38 - 34.d	2.23E+05	2.60E+03	1.2	909	14	0.32	47.9	1.9	2.6	117.7	3.8	8.8

Analysis number	Ti49 ppm	Ti49 ppm 2SE	Ti49 ppm LOD	V51 ppm	V51 ppm 2SE	V51 ppm LOD	Cr52 ppm	Cr52 ppm 2SE	Cr52 ppm LOD	Mn55 ppm	Mn55 ppm 2SE	Mn55 ppm LOD
eaf38 - 35.d	2.41E+05	2.70E+03	NaN	1151	13	0.42	58.6	2.1	5.5	110.6	2.6	7
eaf38 - 36.d	2.44E+05	3.10E+03	2.7	627.5	9	0.42	37.6	2	5	129.6	3.5	6.5
eaf38 - 37.d	2.45E+05	3.10E+03	2.4	641.7	9.5	0.35	47.4	1.7	5	117.5	3.5	9.7
eaf38 - 38.d	2.43E+05	3.00E+03	2.3	616.6	7.4	0.26	45.2	1.6	3.7	112.4	3.1	8.5
eaf38 - 39.d	2.42E+05	3.20E+03	2.3	661	11	0.27	51.6	1.8	4.3	111.3	3.8	5.5
eaf38 - 40.d	2.44E+05	3.20E+03	1.1	576.3	6.5	0.42	40.6	2.2	4.1	109.9	3.3	7
eaf38 - 41.d	2.47E+05	4.20E+03	2.3	569	11	0.32	36.8	1.7	3.7	123.5	4.3	8.6
eaf38 - 42.d	2.47E+05	2.70E+03	3.6	605.9	8.1	0.3	46.3	1.6	4.4	101.4	3.4	7.5
eaf38 - 43.d	2.46E+05	3.20E+03	NaN	623.5	8.7	0.36	44.5	2	6.9	98.7	3.8	13
eaf38 - 44.d	2.49E+05	3.20E+03	NaN	599.9	7.9	0.52	51.9	1.8	5.6	103.6	3	6.4
eaf38 - 45.d	2.42E+05	3.00E+03	2.4	626.1	9.3	0.32	46.5	1.9	4.3	105.6	3.4	11
eaf38 - 46.d	2.44E+05	3.80E+03	1.1	666.4	9.8	0.45	45	2.2	5.4	108.4	3.3	7.4
eaf38 - 47.d	2.49E+05	3.10E+03	NaN	566.5	9.3	0.29	38.2	1.7	4.1	126.2	3.8	8.8
eaf38 - 48.d	2.44E+05	3.00E+03	1.1	565.2	9	0.32	41.8	1.9	4.9	115.7	3.3	13
eaf38 - 49.d	2.47E+05	3.20E+03	1.1	553	8	0.4	40.4	2.2	3.9	123.5	3.1	8.7
eaf38 - 50.d	2.49E+05	3.00E+03	2.2	588.1	7.8	0.34	45.7	1.3	6.2	118.7	3	11
eaf38 - 51.d	2.47E+05	3.40E+03	3.3	497.3	8.3	0.41	44.8	1.7	6.2	110.1	3.2	11
eaf38 - 52.d	2.51E+05	3.50E+03	2.4	537.3	8.7	0.32	45.5	2	4.7	116.3	3.6	6.8
eaf38 - 53.d	2.56E+05	4.00E+03	2.5	596	10	0.42	47.2	1.9	4.2	106.8	4	8.3
eaf38 - 54.d	2.49E+05	3.60E+03	3.1	573.9	9.7	0.37	47.8	2.1	4.7	109.4	3.7	11
eaf38 - 55.d	2.51E+05	3.50E+03	2.2	574	10	0.19	48.3	2	4.7	106.7	3.9	11
eaf38 - 56.d	2.57E+05	2.80E+03	NaN	582.7	7.8	0.25	47.5	2.2	4.1	105.8	4.2	6.4
eaf38 - 57.d	2.52E+05	3.00E+03	NaN	599.8	8.5	0.31	53	2.2	4.7	118.8	3.8	8.5
eaf38 - 58.d	2.50E+05	3.20E+03	3.1	562.6	9	0.36	49	2.4	3.9	104	2.7	10
eaf38 - 59.d	2.44E+05	2.20E+03	NaN	725.6	8.6	0.34	3.3	1.2	3.1	118.5	4.3	7.8
eaf38 - 60.d	2.44E+05	3.20E+03	2.6	723	11	0.32	4.3	1.2	4.3	131.5	4.1	12
eaf38 - 61.d	2.43E+05	3.10E+03	2.4	734	12	0.29	4.8	1.5	4.5	100.2	2.9	6.6
eaf38 - 62.d	2.62E+05	4.50E+03	3.6	784	12	0.31	6.5	2	5.2	278	53	11
eaf38 - 63.d	2.46E+05	3.10E+03	2.6	747	11	0.28	5.6	1.2	3.3	105.3	3.2	6.8

Analysis number	Ti49 ppm	Ti49 ppm 2SE	Ti49 ppm LOD	V51 ppm	V51 ppm 2SE	V51 ppm LOD	Cr52 ppm	Cr52 ppm 2SE	Cr52 ppm LOD	Mn55 ppm	Mn55 ppm 2SE	Mn55 ppm LOD
eaf38 - 64.d	2.44E+05	4.30E+03	1.2	767	16	0.39	7	1.9	4.9	106.2	3.8	11
eaf38 - 65.d	2.46E+05	3.00E+03	NaN	747.1	9.9	0.31	6.2	1.3	3.2	95.3	3.1	13
eaf38 - 68.d	2.48E+05	3.80E+03	NaN	1078	15	0.41	46.3	1.8	4.3	103	3.2	7.4
eaf38 - 69.d	2.42E+05	3.10E+03	2.4	1147	16	0.35	48.9	1.3	6.3	95.3	3.2	9.2
eaf38 - 70.d	2.47E+05	3.40E+03	NaN	1129	18	0.41	42.5	2.1	4.4	97.4	3.6	9.9
eaf38 - 71.d	2.74E+05	6.00E+03	NaN	1288	28	0.35	80.7	4.9	4	96.5	3.6	7.8
eaf38 - 72.d	2.47E+05	2.50E+03	NaN	1116	15	0.22	44.7	1.9	4.8	100.3	3.3	9.1
eaf38 - 73.d	2.39E+05	2.60E+03	1.5	1125	14	0.46	51.2	2	3	105.3	3.4	9.6
eaf38 - 74.d	2.44E+05	3.80E+03	1.1	1052	16	0.1	46.2	1.7	3.6	93.6	2.9	11
eaf38 - 75.d	2.48E+05	2.80E+03	1.1	1160	16	0.34	43.2	2.4	4.5	101.4	3.6	8.5
eaf38 - 76.d	2.54E+05	3.70E+03	NaN	1159	19	0.26	42.4	1.8	4.3	106.2	3.7	12
eaf38 - 77.d	2.42E+05	3.40E+03	NaN	1082	18	0.44	47.2	2	4	107.4	3.5	8
eaf38 - 78.d	2.51E+05	2.80E+03	1.5	1181	17	0.4	45.9	1.9	4.8	104.7	3.6	7.6
eaf38 - 79.d	2.54E+05	2.70E+03	2.2	1122	16	0.58	48	2	3.9	100.3	3.6	11
eaf38 - 80.d	2.53E+05	2.80E+03	1.1	1170	13	0.5	45.2	2.2	3.9	97.9	3.9	7
eaf38 - 81.d	2.54E+05	3.70E+03	3.1	1043	15	0.44	46.1	1.9	5.3	93.6	3.6	8.6
eaf38 - 82.d	2.50E+05	3.30E+03	1.1	1061	15	0.41	45.8	1.9	4	103.3	3	7.7
eaf38 - 83.d	2.55E+05	3.70E+03	2.2	1061	16	0.4	48	1.6	4.9	97.8	3.4	12
eaf38 - 84.d	2.46E+05	3.00E+03	NaN	1107	13	0.3	46.1	2.1	4.5	96.5	3.3	6.5
eaf38 - 85.d	2.45E+05	3.70E+03	NaN	1146	16	0.26	49.1	2	4.2	95.4	3.1	7.3
eaf38 - 86.d	2.45E+05	3.00E+03	2.5	995	16	0.34	49.9	2.1	5.1	100.2	2.8	11
eaf38 - 87.d	2.46E+05	3.10E+03	NaN	1016	15	0.29	55.6	1.9	3.7	99.9	2.9	7.2
eaf38 - 88.d	2.49E+05	3.30E+03	4.1	1085	14	0.36	47.5	2	3	95.5	2.7	6.6
eaf38 - 89.d	2.48E+05	3.00E+03	NaN	1207	15	0.35	57.5	1.6	4.5	105	3.4	9.2
eaf38 - 90.d	2.50E+05	3.60E+03	NaN	1112	14	0.43	50.1	2.3	5.4	96.6	3.3	9.2
eaf38 - 91.d	2.52E+05	3.10E+03	1.2	1163	13	0.3	49.7	1.8	4.1	106.8	3.3	8
eaf38 - 92.d	2.46E+05	2.80E+03	NaN	1150	14	0.47	51.9	2.3	4.2	94.2	3.5	8.8
eaf38 - 93.d	2.52E+05	3.70E+03	NaN	1158	18	0.42	47.2	2.2	3.6	104.4	3.8	9.6
eaf38 - 94.d	2.51E+05	3.60E+03	2.5	1107	17	0.46	47.7	2.4	3.7	104.5	3.5	12

Analysis number	Ti49 ppm	Ti49 ppm 2SE	Ti49 ppm LOD	V51 ppm	V51 ppm 2SE	V51 ppm LOD	Cr52 ppm	Cr52 ppm 2SE	Cr52 ppm LOD	Mn55 ppm	Mn55 ppm 2SE	Mn55 ppm LOD
eaf38 - 95.d	2.40E+05	3.70E+03	NaN	1001	14	0.3	44.2	2	4.2	84.1	3.3	9.3
eaf38 - 96.d	2.71E+05	5.10E+03	2.4	1227	28	0.41	71.2	6.2	4	95.5	4.1	9.1
eaf38 - 97.d	2.51E+05	3.30E+03	4.4	1109	17	0.37	48.7	1.5	4.1	97.3	3.8	6.8
eaf38 - 98.d	2.50E+05	3.30E+03	2.4	1126	13	0.66	46.2	2.3	4	116.6	3.8	9.2
eaf38 - 99.d	2.50E+05	3.40E+03	2.2	1232	15	0.31	63.7	2.5	6.2	102.9	3.3	11
eaf38 - 100.d	2.57E+05	3.10E+03	3	737.5	6.8	0.49	18.3	1.5	4	110.7	4	6.6
eaf38 - 101.d	2.57E+05	4.00E+03	1.1	661	11	0.48	16.1	2	4.5	92.8	2.7	8
eaf38 - 102.d	2.53E+05	4.00E+03	1.1	581	11	0.33	15.8	1.6	4.7	98.1	3.2	9.2
eaf38 - 103.d	3.16E+05	1.30E+04	NaN	827	35	0.42	30.5	4.3	3.9	94.2	4.1	9.2
eaf38 - 104.d	2.57E+05	3.80E+03	1.8	697.8	9.5	0.3	13.7	1.8	4.5	93.5	3.3	9.3
eaf38 - 105.d	2.44E+05	6.40E+03	NaN	593	11	0.53	16.8	1.7	5.6	110.1	5.1	9.8
eaf38 - 106.d	2.60E+05	2.80E+03	2.2	658.4	7.9	0.3	15.6	2	4	95	3.4	8.9
eaf38 - 107.d	2.61E+05	4.00E+03	NaN	661	13	0.32	16.2	1.5	4.3	105.3	3.9	7
eaf38 - 108.d	2.52E+05	3.20E+03	3.1	906.5	9.9	0.32	69.2	2.7	3.6	137.3	4.8	6.4
eaf38 - 109.d	2.48E+05	2.50E+03	1.2	1168	15	0.33	73.2	2.7	3.4	113.8	3.5	9.6
eaf38 - 110.d	2.50E+05	3.10E+03	NaN	1224	17	0.45	33.3	1.8	3.8	95.5	3.4	8.2
eaf38 - 111.d	2.48E+05	3.00E+03	2.8	1263	16	0.42	40	2	4.6	124	3	6.9
eaf38 - 112.d	2.48E+05	2.90E+03	NaN	1219	18	0.44	36.8	1.6	5.6	119.7	4.1	6.7
eaf38 - 113.d	2.51E+05	3.40E+03	NaN	1210	15	0.41	32	1.8	5.1	101.3	3.1	6.4
eaf38 - 114.d	2.53E+05	3.10E+03	NaN	1170	14	0.56	30.9	1.6	2.9	108	2.8	8.1
eaf38 - 115.d	2.54E+05	3.10E+03	2.4	1155	19	0.43	34.7	1.8	4.8	103.7	4.2	13
eaf38 - 116.d	2.52E+05	3.90E+03	3.5	1117	15	0.39	33.5	1.9	4.4	101.7	3.8	7.9
eaf38 - 117.d	2.56E+05	3.40E+03	1.2	1161	16	0.39	38.9	1.9	3.7	123.3	3.5	9.4
eaf38 - 118.d	2.54E+05	3.20E+03	3.1	1221	16	0.37	40.9	1.7	4.5	141.3	3.9	7.3
eaf38 - 119.d	2.58E+05	3.30E+03	2.5	1135	17	0.35	44	2	4.4	142	3.1	6.6
eaf38 - 120.d	2.60E+05	3.80E+03	2.3	1128	18	0.37	44	1.8	5.6	143.9	4	9.1
eaf38 - 121.d	2.59E+05	4.70E+03	1.6	1190	19	0.31	60.8	2.3	3.7	117.7	3.1	7.7
eaf38 - 125.d	2.57E+05	3.40E+03	NaN	1604	21	0.34	70.3	2.1	4.6	125	3.5	7.8
eaf38 - 126.d	2.59E+05	3.60E+03	2.5	1313	18	0.23	50	2.1	2.7	129.6	3.5	8.4

Analysis number	Ti49 ppm	Ti49 ppm 2SE	Ti49 ppm LOD	V51 ppm	V51 ppm 2SE	V51 ppm LOD	Cr52 ppm	Cr52 ppm 2SE	Cr52 ppm LOD	Mn55 ppm	Mn55 ppm 2SE	Mn55 ppm LOD
eaf38 - 127.d	2.60E+05	3.30E+03	2.5	1641	27	0.4	73.6	2.1	4.8	137.4	3	6.3
eaf38 - 128.d	2.61E+05	3.20E+03	2.3	1230	14	0.33	45.9	1.8	5.9	135.3	3.8	9.8
eaf38 - 129.d	2.63E+05	3.10E+03	2.3	1401	22	0.3	53	2.2	4.5	113.1	3.8	9.6
eaf38 - 130.d	2.65E+05	3.60E+03	NaN	1317	23	0.31	48.9	2.3	3.7	121.4	3.3	12
eaf38 - 131.d	2.65E+05	3.40E+03	NaN	1555	21	0.36	60.4	1.9	3.8	104.5	3	10
eaf38 - 132.d	2.65E+05	3.70E+03	2.3	1489	21	0.33	62.4	2.3	4	100	3.5	7.2
eaf38 - 133.d	2.61E+05	4.00E+03	1.1	532	8.2	0.33	35.6	1.5	5.6	179.2	4.1	13
eaf38 - 134.d	2.64E+05	3.90E+03	2.3	665	11	0.17	38.5	1.9	2.5	120.3	3.4	8
eaf38 - 135.d	2.65E+05	2.80E+03	NaN	718.8	9.1	0.42	44.7	1.9	5.1	132	3.8	7.8
eaf38 - 136.d	2.69E+05	3.20E+03	3.4	557.2	8.4	0.22	39.3	2.2	4.2	194.6	4	8.8
eaf38 - 137.d	2.71E+05	3.70E+03	2.3	1310	18	0.35	111.6	3	5.4	122.8	3.2	11
eaf38 - 138.d	2.62E+05	4.40E+03	1.8	1427	25	0.31	167	3.7	2.7	134.6	3.6	7.6
eaf38 - 139.d	2.67E+05	4.50E+03	1.2	1430	22	0.37	148.7	2.9	2.9	124.2	4	11
eaf38 - 140.d	2.75E+05	4.10E+03	3.2	1101	16	0.39	96.5	2.3	3.7	119.9	2.8	8.6
eaf38 - 141.d	2.74E+05	5.20E+03	NaN	1174	18	0.43	100.7	3.1	3.1	120	3.1	7.7
eaf38 - 142.d	2.74E+05	3.80E+03	3.3	1089	18	0.39	90.9	2.6	5.4	126.5	3.6	12
eaf38 - 143.d	2.78E+05	4.40E+03	NaN	1303	22	0.42	96.4	2.3	4.7	125.2	3.2	9.6

Analysis number	Fe57 ppm	Fe57 ppm 2SE	Fe57 ppm LOD	Y89 ppm	Y89 ppm 2SE	Y89 ppm LOD	Zr90 ppm	Zr90 ppm 2SE	Zr90 ppm LOD	Nb93 ppm	Nb93 ppm 2SE	Nb93 ppm LOD
eaf38 - 2.d	2016	55	32	939	16	0.05	308.8	5.6	0.039	109.7	1.8	NaN
eaf38 - 6.d	2130	60	20	1695	23	NaN	282.9	5.1	NaN	60.85	0.96	NaN
eaf38 - 7.d	2200	62	32	1689	25	0.056	270.9	4.1	0.053	69.4	1.7	0.039
eaf38 - 8.d	2730	180	29	1327	41	NaN	268.6	3.9	0.038	101.4	1.5	0.019
eaf38 - 9.d	1951	69	26	1621	36	0.022	231.4	4.4	0.082	72.9	1.3	NaN
eaf38 - 10.d	1725	56	26	503.7	6.3	0.06	243.5	3.7	NaN	33.97	0.69	NaN
eaf38 - 11.d	1769	53	27	427.5	5.7	0.059	232.8	3.3	NaN	33.59	0.68	NaN
eaf38 - 12.d	1709	53	21	392.6	5.4	NaN	247	4.4	0.041	40.27	0.76	NaN
eaf38 - 13.d	5.10E+03	1.20E+03	34	508	5.8	0.063	270.8	5.1	0.083	49.7	1.1	0.021
eaf38 - 14.d	1899	62	36	326.9	7.6	0.058	250	4.3	NaN	64.4	1.2	0.04
eaf38 - 15.d	1991	56	25	433	9.7	0.021	269.4	4.3	0.085	57.3	1.4	0.04
eaf38 - 16.d	1758	49	25	419.9	4.7	NaN	245.5	3.8	0.04	78.5	1.6	NaN
eaf38 - 17.d	23760	300	26	472.6	5.9	0.043	237.4	4.1	0.08	63.4	1.5	NaN
eaf38 - 18.d	1741	49	27	311.7	4.2	0.057	221.4	4.1	NaN	58.74	0.94	NaN
eaf38 - 19.d	1929	59	28	363.3	6.7	0.021	226	3.6	NaN	65.4	1.2	NaN
eaf38 - 20.d	1870	59	36	257	3.5	0.021	225.5	3.8	0.077	78.3	1.2	NaN
eaf38 - 21.d	1850	46	16	203.5	3.6	0.029	235.2	4.1	NaN	86.3	1.8	0.02
eaf38 - 23.d	1694	71	40	398.4	6.6	0.063	307.3	5.1	NaN	91.6	1.2	NaN
eaf38 - 24.d	1588	41	29	200.7	2.9	0.042	265.5	4.3	NaN	72.2	1.3	NaN
eaf38 - 25.d	5500	170	23	231.9	4.1	0.074	256.6	6	0.079	77.1	1.7	NaN
eaf38 - 26.d	2121	68	36	618.5	8.1	0.044	240.8	4.4	0.041	72.2	1.4	NaN
eaf38 - 27.d	2280	60	25	551.4	7	0.047	220.6	3.9	0.081	61.2	1.2	NaN
eaf38 - 28.d	1703	62	29	530.2	8	0.066	296.1	4.2	0.083	62.1	1.4	0.042
eaf38 - 29.d	2312	88	34	557	11	0.032	333.2	6.1	NaN	104.6	3.7	0.022
eaf38 - 30.d	1701	56	32	555.3	7.7	0.029	327.5	5.1	NaN	56.2	1.2	NaN
eaf38 - 31.d	1970	69	34	362.1	6.5	0.05	229.8	4.3	0.082	77.4	1.4	0.021
eaf38 - 32.d	2152	68	36	572.8	6.8	NaN	244.9	3.6	NaN	80.7	2.4	NaN
eaf38 - 33.d	1677	59	38	510	9.5	0.076	276.5	5.1	0.13	65.3	1.7	NaN
eaf38 - 34.d	7740	260	27	501.3	8.2	0.023	253.1	3.2	0.095	79.3	1.5	NaN

Analysis number	Fe57 ppm	Fe57 ppm 2SE	Fe57 ppm LOD	Y89 ppm	Y89 ppm 2SE	Y89 ppm LOD	Zr90 ppm	Zr90 ppm 2SE	Zr90 ppm LOD	Nb93 ppm	Nb93 ppm 2SE	Nb93 ppm LOD
eaf38 - 35.d	2000	65	37	569.8	6	0.053	219.2	3.9	NaN	51.42	0.85	NaN
eaf38 - 36.d	2147	57	36	564	10	0.088	237.4	4.5	0.093	63.6	1.5	NaN
eaf38 - 37.d	1858	55	24	613.2	8.8	0.07	241	4.6	NaN	59.2	1.2	NaN
eaf38 - 38.d	1947	61	31	604.2	9.3	0.091	257.5	3.8	0.12	54.8	1.2	NaN
eaf38 - 39.d	1870	50	21	683	10	0.022	253.6	3.6	0.041	60.1	1.4	NaN
eaf38 - 40.d	1858	40	29	668	9.2	0.061	270.5	3.8	0.19	67.9	1.4	0.041
eaf38 - 41.d	2155	57	30	548.7	8.8	0.06	267.4	4.3	0.1	69.08	0.87	0.042
eaf38 - 42.d	1701	49	29	730	10	0.046	300.6	4.6	NaN	53.1	1	NaN
eaf38 - 43.d	1768	64	36	655.1	9.5	0.049	267.1	5	0.12	55.1	1.1	0.04
eaf38 - 44.d	1687	47	49	654	11	NaN	288.4	4.5	NaN	70.2	1.4	NaN
eaf38 - 45.d	2238	70	33	639.9	9.4	NaN	253.5	3.6	0.079	76.5	1.3	NaN
eaf38 - 46.d	1744	54	30	511	11	0.068	231.3	4.1	0.04	73.4	1.3	0.04
eaf38 - 47.d	2429	67	36	465.6	6.4	NaN	290.5	4.2	NaN	93.3	1.8	0.04
eaf38 - 48.d	1985	68	36	431.9	7.7	0.059	279.2	3.9	NaN	72.3	1.4	0.02
eaf38 - 49.d	2200	170	27	838	11	0.043	263	4.4	0.088	66.1	1.5	NaN
eaf38 - 50.d	2035	72	28	730.6	8.6	NaN	254.1	3.8	NaN	92.3	1.5	NaN
eaf38 - 51.d	1503	59	38	531.2	8.5	0.046	314.5	5.7	0.11	128.7	2	NaN
eaf38 - 52.d	1772	55	35	470.7	8.5	0.021	282.4	5.2	0.04	142.4	2.1	NaN
eaf38 - 53.d	1715	57	33	562.1	9.5	0.071	289	5.6	0.083	102.6	1.8	NaN
eaf38 - 54.d	2480	110	28	581	9.4	0.044	277.9	4.8	0.12	93	1.9	NaN
eaf38 - 55.d	1618	54	29	665	11	0.043	338	7	0.11	111.2	2	NaN
eaf38 - 56.d	1657	65	21	644.9	9.7	0.071	301.6	5.6	NaN	88.4	1.5	NaN
eaf38 - 57.d	4060	220	31	671	13	0.049	254.9	4.2	0.13	82.2	1	NaN
eaf38 - 58.d	2280	150	27	710	11	0.059	305	5.9	0.082	97.2	2.1	NaN
eaf38 - 59.d	2137	74	27	293	5.3	0.064	207.6	4.2	0.086	85.8	1.7	NaN
eaf38 - 60.d	2263	63	36	311.5	4.6	0.037	189.7	3.1	0.059	77	1.4	NaN
eaf38 - 61.d	2049	72	34	362.9	4.3	0.046	240.4	4	0.093	115.6	2.4	NaN
eaf38 - 62.d	1.35E+04	3.50E+03	38	432.1	7.3	0.044	291.7	5.2	0.15	137.1	2.1	NaN
eaf38 - 63.d	2020	36	32	308.1	5	NaN	233.2	3.9	0.042	118.4	2.4	NaN

Analysis number	Fe57 ppm	Fe57 ppm 2SE	Fe57 ppm LOD	Y89 ppm	Y89 ppm 2SE	Y89 ppm LOD	Zr90 ppm	Zr90 ppm 2SE	Zr90 ppm LOD	Nb93 ppm	Nb93 ppm 2SE	Nb93 ppm LOD
eaf38 - 64.d	1953	58	41	486.7	8.4	NaN	241	5.3	NaN	125.2	2.3	NaN
eaf38 - 65.d	1812	53	32	462	5.8	0.061	247.1	3.1	NaN	134.6	1.9	NaN
eaf38 - 68.d	1801	55	25	369.6	5	NaN	235.3	4.1	NaN	79.3	1.4	NaN
eaf38 - 69.d	1798	55	30	385.9	4.5	0.042	236.7	3.1	NaN	63.7	0.96	0.039
eaf38 - 70.d	1991	54	27	434.5	7.4	0.067	228.6	3.6	0.081	72.8	1.4	0.02
eaf38 - 71.d	2163	72	33	389.4	5.5	0.065	212.2	3	NaN	89.4	5.5	NaN
eaf38 - 72.d	2252	82	39	368.3	4.5	0.048	235.6	3.5	0.054	78.6	1.5	NaN
eaf38 - 73.d	5140	240	30	297.5	4.4	0.029	201.4	3.7	0.14	80.2	1.5	NaN
eaf38 - 74.d	2065	97	41	423.4	6	0.042	249.5	3.8	0.079	84	1.3	NaN
eaf38 - 75.d	1976	57	17	368.4	5	NaN	208.5	3.8	NaN	100	1.5	NaN
eaf38 - 76.d	2073	64	34	368.6	6.2	NaN	203.7	4	NaN	101.4	1.9	NaN
eaf38 - 77.d	5030	520	31	343.9	5.1	NaN	231.4	3.2	NaN	88.8	1.9	NaN
eaf38 - 78.d	1843	56	30	341.5	5.6	0.042	224.9	4.5	NaN	96.5	1.8	NaN
eaf38 - 79.d	1891	46	33	406	7.7	0.049	229.3	3.1	NaN	72.4	1.6	NaN
eaf38 - 80.d	1694	47	36	399.9	4.7	0.029	276.8	3.8	NaN	94.1	1.5	NaN
eaf38 - 81.d	1910	100	31	565	8.2	NaN	267.7	4.2	0.089	100	2.2	NaN
eaf38 - 82.d	2511	71	32	502	8.5	NaN	231.9	3.9	0.081	73.3	1.3	NaN
eaf38 - 83.d	1886	61	41	486.7	7.4	NaN	252.5	5.6	0.088	70.5	1.3	NaN
eaf38 - 84.d	1755	57	21	416.5	6.6	0.023	255.9	3.7	0.085	63.49	0.92	NaN
eaf38 - 85.d	1567	54	31	412.3	5.9	0.044	299.2	5.3	NaN	60.1	1.2	NaN
eaf38 - 86.d	1664	57	27	316.6	6.7	0.022	251.5	4.8	NaN	63	1.5	NaN
eaf38 - 87.d	2006	64	19	362	10	0.022	251.9	4.4	NaN	51.9	1.6	NaN
eaf38 - 88.d	1734	45	28	403.8	6.1	0.079	266.7	4.4	0.092	55.4	1.1	NaN
eaf38 - 89.d	1878	53	28	414.4	5.7	0.023	267.1	3.8	NaN	59.57	0.89	NaN
eaf38 - 90.d	1759	61	23	420.1	7.4	0.045	309.1	4.5	0.042	63.6	1	NaN
eaf38 - 91.d	1950	56	32	434.3	5.8	0.062	259.3	4.3	0.043	70	1.2	0.021
eaf38 - 92.d	4450	290	38	439.4	5.7	0.023	293.6	5.4	0.085	72.8	1.8	NaN
eaf38 - 93.d	1886	67	27	404.6	5.8	NaN	257.9	3.9	0.042	67.5	1.5	NaN
eaf38 - 94.d	2198	62	29	479.9	8.2	0.044	258.4	4.4	0.041	57.4	1.1	NaN

Analysis number	Fe57 ppm	Fe57 ppm 2SE	Fe57 ppm LOD	Y89 ppm	Y89 ppm 2SE	Y89 ppm LOD	Zr90 ppm	Zr90 ppm 2SE	Zr90 ppm LOD	Nb93 ppm	Nb93 ppm 2SE	Nb93 ppm LOD
eaf38 - 95.d	4870	340	31	506.4	8.6	0.071	272.5	6.8	NaN	57.1	1.4	NaN
eaf38 - 96.d	2311	75	24	454.2	7.5	NaN	326	5.7	0.044	78.8	5.5	NaN
eaf38 - 97.d	1696	62	29	442.4	7.3	0.058	263.3	6	NaN	65.7	1.5	0.02
eaf38 - 98.d	3570	210	28	374.5	5.5	NaN	234.5	4.5	0.039	77	1.3	NaN
eaf38 - 99.d	1654	52	27	397.6	5.7	0.076	265.5	4	0.054	51.55	0.97	NaN
eaf38 - 100.d	2630	140	26	494	15	0.049	274.4	3.9	0.04	143	2.6	0.04
eaf38 - 101.d	1686	42	26	436.4	7.9	0.042	280.6	4.9	0.085	109.8	2.2	0.054
eaf38 - 102.d	1999	60	45	639	8.9	0.021	278.6	4.8	0.039	140.1	2.4	NaN
eaf38 - 103.d	2420	140	25	546.1	6.7	0.051	351	13	NaN	238	26	NaN
eaf38 - 104.d	1825	58	33	426.5	5.3	0.042	279.5	4.6	NaN	141.4	2.7	NaN
eaf38 - 105.d	5.30E+03	1.10E+03	30	630	16	NaN	294.6	6.8	NaN	116.1	4.8	NaN
eaf38 - 106.d	2048	56	34	582	12	0.021	294.2	5.6	NaN	130.4	2.6	NaN
eaf38 - 107.d	2157	69	29	650	10	0.047	262.9	4.6	0.041	154.1	2.7	NaN
eaf38 - 108.d	4590	410	47	803	12	NaN	241.5	4.1	0.089	102	1.8	NaN
eaf38 - 109.d	1756	55	30	479.9	6.9	0.037	244.1	3.5	0.085	60.6	1.4	NaN
eaf38 - 110.d	1798	46	34	351.9	5.3	NaN	253.3	4.3	NaN	80.6	1.9	0.043
eaf38 - 111.d	2106	54	28	334.2	4.9	0.045	247.4	4.4	0.12	91.5	1.4	0.043
eaf38 - 112.d	2223	48	36	264.5	5.3	0.071	253.7	3.9	NaN	96.2	1.6	NaN
eaf38 - 113.d	1719	53	33	415.4	7	0.031	270.2	4.5	0.15	82.8	1.6	NaN
eaf38 - 114.d	1866	51	28	252.7	3.2	0.045	260.1	4	0.12	101.5	1.6	NaN
eaf38 - 115.d	1658	65	30	301.6	3.8	0.023	284.4	4.5	NaN	109.1	2	0.043
eaf38 - 116.d	1752	61	20	406.2	6.4	0.061	289.1	5.6	NaN	95.5	1.6	NaN
eaf38 - 117.d	4270	350	35	400.3	5.5	0.092	264.2	4.9	NaN	151.8	3.2	NaN
eaf38 - 118.d	2610	300	23	245.9	6.6	0.03	276.9	4.8	0.13	152.5	3.8	NaN
eaf38 - 119.d	2334	72	29	529	8.6	0.066	272.8	2.9	NaN	131	1.9	0.021
eaf38 - 120.d	2346	75	31	516	6.5	0.052	276.3	4.5	0.091	125	2.2	0.021
eaf38 - 121.d	2067	70	29	411	10	0.036	261.5	5.7	0.083	123.6	2.5	0.021
eaf38 - 125.d	2153	59	47	585.6	8.3	0.064	219.8	4.2	NaN	255.9	4	NaN
eaf38 - 126.d	2339	88	34	611	11	0.022	256.1	4.6	NaN	121.9	1.9	NaN

Analysis number	Fe57 ppm	Fe57 ppm 2SE	Fe57 ppm LOD	Y89 ppm	Y89 ppm 2SE	Y89 ppm LOD	Zr90 ppm	Zr90 ppm 2SE	Zr90 ppm LOD	Nb93 ppm	Nb93 ppm 2SE	Nb93 ppm LOD
eaf38 - 127.d	2608	54	31	681.5	9	0.022	224.8	3.8	NaN	275.5	4	NaN
eaf38 - 128.d	3298	76	31	590	9.2	0.022	262.2	4.2	0.084	117.5	2.1	NaN
eaf38 - 129.d	2097	46	37	607	11	0.073	238.8	4	NaN	200.2	3.3	0.021
eaf38 - 130.d	2157	73	30	612	11	0.045	253.8	4.9	0.042	144	2.1	NaN
eaf38 - 131.d	2191	66	32	566.8	7.1	0.051	228.5	3.5	NaN	274.3	3.5	NaN
eaf38 - 132.d	2345	54	27	581.4	7.6	0.045	244.2	4.6	0.084	185.2	3.1	NaN
eaf38 - 133.d	1979	55	20	446.3	7.6	0.059	249.9	4.7	NaN	83.2	1.6	NaN
eaf38 - 134.d	1717	44	29	591.6	9.7	0.03	214.8	3.1	NaN	82.6	1.2	NaN
eaf38 - 135.d	1799	52	35	664.8	9.3	NaN	218	4.1	0.084	82.5	1.5	NaN
eaf38 - 136.d	2071	58	30	501.5	8.3	0.056	278.3	5.4	0.084	95.9	1.6	NaN
eaf38 - 137.d	1983	65	39	380	10	0.061	240.1	3.5	0.14	55	2.3	0.021
eaf38 - 138.d	1701	64	30	277	6	0.022	175.8	3.1	0.056	32.3	1	0.021
eaf38 - 139.d	1940	53	25	327.2	6.5	0.052	175.5	3.2	NaN	34.96	0.92	0.043
eaf38 - 140.d	1915	58	28	481.5	7.5	0.023	236.5	3.7	NaN	73.8	1.5	NaN
eaf38 - 141.d	2022	62	33	397	12	NaN	215.4	5.7	0.085	59.9	2.5	NaN
eaf38 - 142.d	1919	34	49	698	10	0.088	237.2	3.8	0.042	91.4	1.6	0.043
eaf38 - 143.d	2036	71	39	429	22	0.063	196.8	4.7	0.086	73.8	2.9	NaN

Analysis number	La139 ppm	La139 ppm 2SE	La139 ppm LOD	Ce140 ppm	Ce140 ppm 2SE	Ce140 ppm LOD	Pr141 ppm	Pr141 ppm 2SE	Pr141 ppm LOD	Nd146 ppm	Nd146 ppm 2SE	Nd146 ppm LOD
eaf38 - 2.d	725	24	NaN	2267	39	NaN	240.4	4	0.02	926	17	NaN
eaf38 - 6.d	973	13	0.012	3569	40	NaN	470.9	5.3	NaN	2114	27	0.057
eaf38 - 7.d	983	16	NaN	3753	52	0.023	504.1	8.6	NaN	2271	35	NaN
eaf38 - 8.d	899	16	NaN	3250	53	NaN	403.9	6.3	0.013	1748	29	0.074
eaf38 - 9.d	739	25	0.012	3344	41	NaN	456.8	8.6	NaN	2081	32	0.059
eaf38 - 10.d	1038	15	0.02	3386	45	NaN	410.7	6.4	NaN	1742	29	NaN
eaf38 - 11.d	983	12	NaN	3226	32	NaN	393.4	5	0.023	1687	17	0.12
eaf38 - 12.d	949	14	NaN	2992	33	NaN	353.3	4.8	NaN	1489	20	NaN
eaf38 - 13.d	1025	25	NaN	3481	52	NaN	426.6	5.6	NaN	1869	30	NaN
eaf38 - 14.d	692	24	NaN	2345	38	NaN	272.3	6.2	NaN	1143	23	0.057
eaf38 - 15.d	865	28	0.016	2785	59	0.012	331.3	8	0.01	1402	35	NaN
eaf38 - 16.d	843	20	NaN	2671	30	0.033	314.7	4.5	0.01	1329	17	0.11
eaf38 - 17.d	694	20	NaN	2439	34	0.024	292.7	3.9	0.01	1275	19	NaN
eaf38 - 18.d	663	21	0.025	1769	31	NaN	179.8	3.4	0.022	700	14	NaN
eaf38 - 19.d	1046	20	NaN	2670	52	NaN	281.5	4.8	0.02	1141	23	NaN
eaf38 - 20.d	837	23	NaN	1979	27	0.016	194	2.3	NaN	732	10	0.22
eaf38 - 21.d	790	26	NaN	1832	27	NaN	171.8	3	0.01	624	10	NaN
eaf38 - 23.d	1100	21	0.024	2832	47	NaN	298.6	5.5	0.028	1216	25	NaN
eaf38 - 24.d	812	25	NaN	1752	23	NaN	155.6	2.4	NaN	546.3	9.8	NaN
eaf38 - 25.d	761	23	0.026	1809	25	NaN	170.9	3	0.02	626	11	NaN
eaf38 - 26.d	909	27	NaN	2531	40	NaN	293	4.9	0.021	1290	17	0.059
eaf38 - 27.d	732	21	NaN	2240	26	NaN	261.2	2.7	NaN	1141	13	0.16
eaf38 - 28.d	976	13	NaN	2552	29	0.012	281.5	4.5	NaN	1181	20	NaN
eaf38 - 29.d	825	29	0.046	2337	43	NaN	261.8	4.7	NaN	1150	19	NaN
eaf38 - 30.d	938	20	NaN	2450	31	0.024	273.5	4.6	NaN	1171	20	NaN
eaf38 - 31.d	937	13	0.043	2183	28	NaN	221.3	3.3	NaN	886	13	NaN
eaf38 - 32.d	1006	20	NaN	2660	45	0.012	300	5.9	0.01	1289	21	NaN
eaf38 - 33.d	860	34	0.019	2414	36	NaN	258.4	4.1	NaN	1073	18	NaN
eaf38 - 34.d	849	28	NaN	2381	33	0.013	271.5	4.4	0.034	1166	17	NaN

Analysis number	La139 ppm	La139 ppm 2SE	La139 ppm LOD	Ce140 ppm	Ce140 ppm 2SE	Ce140 ppm LOD	Pr141 ppm	Pr141 ppm 2SE	Pr141 ppm LOD	Nd146 ppm	Nd146 ppm 2SE	Nd146 ppm LOD
eaf38 - 35.d	674.8	8.4	NaN	2204	22	NaN	257.7	3.1	NaN	1166	16	NaN
eaf38 - 36.d	895	27	0.025	2687	45	NaN	312.6	5.2	0.022	1333	21	NaN
eaf38 - 37.d	837	26	0.027	2567	42	NaN	301.7	5.1	NaN	1287	13	NaN
eaf38 - 38.d	974	24	NaN	2708	48	NaN	309.4	6	0.021	1313	27	NaN
eaf38 - 39.d	830	29	0.012	2505	39	0.025	295.9	4.6	NaN	1305	21	0.06
eaf38 - 40.d	1079	17	NaN	3045	47	0.025	352.1	5.6	NaN	1512	29	NaN
eaf38 - 41.d	1094	19	NaN	3020	52	NaN	339.3	6.8	NaN	1431	28	NaN
eaf38 - 42.d	1113	13	0.032	3092	41	NaN	359	4.2	NaN	1563	18	NaN
eaf38 - 43.d	1027	17	0.024	2894	49	0.024	335.9	6.6	NaN	1465	28	NaN
eaf38 - 44.d	959	19	0.012	2800	40	NaN	336.9	5.5	0.02	1453	20	NaN
eaf38 - 45.d	915	11	0.012	2649	38	NaN	311.6	4.2	NaN	1370	17	0.11
eaf38 - 46.d	706	27	0.016	2187	43	NaN	251.8	5.4	0.01	1096	24	NaN
eaf38 - 47.d	976	15	NaN	2542	40	NaN	279.9	3.9	0.02	1170	21	NaN
eaf38 - 48.d	877	23	NaN	2331	33	NaN	253.5	4	0.01	1054	17	0.11
eaf38 - 49.d	1019	14	NaN	3062	43	NaN	379	4.5	0.01	1771	24	NaN
eaf38 - 50.d	1010	13	0.035	3013	44	NaN	371.9	4.8	0.01	1697	23	NaN
eaf38 - 51.d	961	13	NaN	2681	39	NaN	301.9	4.6	NaN	1256	17	NaN
eaf38 - 52.d	1097	16	0.024	2719	49	NaN	304.8	4.8	NaN	1234	22	NaN
eaf38 - 53.d	1014	20	NaN	2819	48	NaN	321.3	6	NaN	1356	22	NaN
eaf38 - 54.d	999	17	NaN	2773	52	NaN	329.4	6.4	NaN	1429	25	NaN
eaf38 - 55.d	1157	24	NaN	3304	68	0.033	383	6.7	NaN	1656	31	0.058
eaf38 - 56.d	1017	15	0.024	2838	41	0.025	323.2	5.5	0.014	1376	23	NaN
eaf38 - 57.d	909	31	NaN	2803	43	0.013	334.6	6.6	NaN	1503	28	0.061
eaf38 - 58.d	1028	15	NaN	3115	48	NaN	378.4	5.1	0.028	1678	32	NaN
eaf38 - 59.d	1017	24	0.013	2210	43	NaN	211.1	4.1	0.022	816	19	0.062
eaf38 - 60.d	981	21	0.026	2192	33	0.026	213.6	2.8	NaN	846	14	NaN
eaf38 - 61.d	1208	18	NaN	2761	41	0.018	272.3	3.8	0.022	1065	16	NaN
eaf38 - 62.d	1280	22	NaN	3045	59	NaN	304.6	5.8	0.012	1201	20	NaN
eaf38 - 63.d	1041	19	NaN	2159	38	0.077	196.7	3.6	NaN	739	16	0.17

Analysis number	La139 ppm	La139 ppm 2SE	La139 ppm LOD	Ce140 ppm	Ce140 ppm 2SE	Ce140 ppm LOD	Pr141 ppm	Pr141 ppm 2SE	Pr141 ppm LOD	Nd146 ppm	Nd146 ppm 2SE	Nd146 ppm LOD
eaf38 - 64.d	1210	24	0.013	2878	50	0.013	293.9	5.5	NaN	1211	24	NaN
eaf38 - 65.d	1247	16	0.025	2935	41	NaN	299.5	4.1	NaN	1212	19	0.12
eaf38 - 68.d	1123	19	0.023	2799	42	NaN	298	4	NaN	1231	21	NaN
eaf38 - 69.d	1041	16	NaN	2581	40	0.032	274	4.4	NaN	1137	18	0.056
eaf38 - 70.d	1196	19	NaN	3114	43	NaN	349.6	5.7	NaN	1500	27	NaN
eaf38 - 71.d	878	24	NaN	2440	32	NaN	266.3	3.3	NaN	1119	16	NaN
eaf38 - 72.d	1044	14	NaN	2523	40	NaN	264.7	6.7	0.02	1095	28	0.057
eaf38 - 73.d	890	19	0.012	2218	27	NaN	226.9	3.4	NaN	938	14	0.13
eaf38 - 74.d	1035	16	0.016	2545	34	NaN	274.9	4.2	0.02	1150	18	NaN
eaf38 - 75.d	1002	13	NaN	2530	37	NaN	269.7	3.7	NaN	1109	18	NaN
eaf38 - 76.d	1059	17	0.033	2665	39	NaN	282.7	3.9	0.021	1181	20	NaN
eaf38 - 77.d	1051	16	0.048	2591	36	0.017	274.3	4.6	NaN	1121	19	NaN
eaf38 - 78.d	754	26	0.024	1958	29	0.012	201.5	3.5	NaN	826	15	NaN
eaf38 - 79.d	1029	14	0.036	2643	39	0.024	289.1	4.3	NaN	1248	25	0.12
eaf38 - 80.d	1024	12	0.024	2488	27	NaN	262	3	0.02	1063	13	NaN
eaf38 - 81.d	1083	17	0.024	2900	35	0.025	326.5	4.8	NaN	1404	19	0.12
eaf38 - 82.d	1082	18	0.026	2893	40	0.024	322.9	4.3	NaN	1387	18	NaN
eaf38 - 83.d	1130	20	0.036	2978	49	NaN	333.1	5.8	NaN	1406	19	NaN
eaf38 - 84.d	939	28	NaN	2394	39	NaN	253.3	4.5	NaN	1053	21	NaN
eaf38 - 85.d	999	15	NaN	2470	34	NaN	263.4	5.1	NaN	1069	19	NaN
eaf38 - 86.d	982	26	NaN	2179	36	NaN	214	4.1	0.011	818	19	NaN
eaf38 - 87.d	1117	15	NaN	2586	46	NaN	262.8	5.7	NaN	1057	25	0.06
eaf38 - 88.d	977	26	0.013	2402	42	0.026	254.1	4.3	NaN	1062	22	NaN
eaf38 - 89.d	691	12	0.013	2119	37	0.026	237.3	3.4	NaN	1035	18	NaN
eaf38 - 90.d	1043	18	NaN	2588	40	0.035	274.8	4.7	NaN	1165	18	NaN
eaf38 - 91.d	842	27	0.013	2223	31	0.013	234.7	3.2	NaN	988	17	0.062
eaf38 - 92.d	959	22	0.013	2490	34	0.013	267.5	3.7	NaN	1135	17	NaN
eaf38 - 93.d	792	28	0.025	2176	30	0.028	235.1	3.6	NaN	976	15	NaN
eaf38 - 94.d	1055	18	0.012	2679	35	NaN	297.8	4.8	NaN	1255	18	NaN

Analysis number	La139 ppm	La139 ppm 2SE	La139 ppm LOD	Ce140 ppm	Ce140 ppm 2SE	Ce140 ppm LOD	Pr141 ppm	Pr141 ppm 2SE	Pr141 ppm LOD	Nd146 ppm	Nd146 ppm 2SE	Nd146 ppm LOD
eaf38 - 95.d	1024	52	NaN	2555	95	NaN	296.9	9.2	0.021	1263	33	NaN
eaf38 - 96.d	990	28	NaN	2546	37	NaN	271.2	3.8	0.015	1116	12	NaN
eaf38 - 97.d	1042	14	NaN	2635	42	NaN	278.6	4.5	0.01	1173	20	NaN
eaf38 - 98.d	886	28	NaN	2292	32	NaN	239.9	3.9	NaN	970	15	NaN
eaf38 - 99.d	603	12	0.024	1812	26	NaN	202.2	3.6	0.02	881	15	NaN
eaf38 - 100.d	1043	18	NaN	3176	68	NaN	389.1	9.2	NaN	1825	47	NaN
eaf38 - 101.d	1123	19	NaN	3062	48	NaN	341.8	6.1	NaN	1426	23	0.11
eaf38 - 102.d	1316	20	NaN	3852	50	NaN	457.6	6.4	NaN	2039	28	NaN
eaf38 - 103.d	1081	31	0.014	3293	50	NaN	381.6	5.2	NaN	1682	23	0.069
eaf38 - 104.d	1105	19	NaN	3076	45	NaN	347.3	5.7	0.02	1500	21	NaN
eaf38 - 105.d	1250	38	NaN	3690	100	NaN	434	12	NaN	1935	54	NaN
eaf38 - 106.d	1205	23	NaN	3515	68	NaN	412.3	7.6	NaN	1851	35	0.13
eaf38 - 107.d	1212	14	0.033	3742	48	NaN	454.1	6.2	NaN	2089	30	NaN
eaf38 - 108.d	1115	14	NaN	3715	52	0.012	473.9	5.6	NaN	2198	28	NaN
eaf38 - 109.d	1056	18	NaN	3368	48	NaN	404.2	5.6	NaN	1789	23	NaN
eaf38 - 110.d	764	24	0.035	2069	27	NaN	219.9	3.6	NaN	940	15	NaN
eaf38 - 111.d	635.8	9	0.013	1861	27	0.013	198.6	2.9	NaN	842	11	NaN
eaf38 - 112.d	628	9.9	0.013	1669	29	0.026	163.1	2.9	NaN	653	12	NaN
eaf38 - 113.d	1040	19	NaN	2486	41	NaN	250.5	4.7	NaN	997	18	NaN
eaf38 - 114.d	669	11	0.012	1644	22	NaN	152.7	2	NaN	566	8.3	0.12
eaf38 - 115.d	896	30	0.013	2006	30	0.013	186.8	3.1	NaN	684	10	0.061
eaf38 - 116.d	1159	19	0.012	2666	43	NaN	264.1	4.5	NaN	1034	18	NaN
eaf38 - 117.d	1010	13	0.013	2449	31	NaN	253.4	3.3	NaN	1006	13	0.12
eaf38 - 118.d	657	21	NaN	1694	39	NaN	161.2	4.6	0.011	593	15	0.12
eaf38 - 119.d	1245	16	NaN	3323	44	0.025	370.8	6.1	0.01	1573	23	NaN
eaf38 - 120.d	1272	20	0.012	3397	53	0.025	370.9	5.2	0.015	1565	16	0.12
eaf38 - 121.d	1052	25	0.027	2774	74	NaN	298.5	8.6	0.021	1256	39	NaN
eaf38 - 125.d	1166	16	0.034	4391	53	0.025	682	21	NaN	3200	71	NaN
eaf38 - 126.d	1071	17	NaN	3047	53	NaN	365.1	5.9	NaN	1674	27	NaN

Analysis number	La139 ppm	La139 ppm 2SE	La139 ppm LOD	Ce140 ppm	Ce140 ppm 2SE	Ce140 ppm LOD	Pr141 ppm	Pr141 ppm 2SE	Pr141 ppm LOD	Nd146 ppm	Nd146 ppm 2SE	Nd146 ppm LOD
eaf38 - 127.d	1169	16	0.025	4501	75	NaN	713	23	0.011	3376	74	0.12
eaf38 - 128.d	1138	17	0.025	3174	42	0.013	364.6	5	0.023	1617	21	NaN
eaf38 - 129.d	1193	19	0.012	3978	60	0.013	529.5	7.8	NaN	2587	43	0.13
eaf38 - 130.d	1073	15	0.025	3082	50	0.013	372.2	6.2	NaN	1701	25	NaN
eaf38 - 131.d	1251	18	0.012	4634	53	NaN	728	23	0.021	3177	61	0.13
eaf38 - 132.d	1161	17	0.025	3929	48	NaN	516.4	6.9	NaN	2494	33	NaN
eaf38 - 133.d	1059	15	0.026	2984	47	NaN	314.9	5	NaN	1228	17	NaN
eaf38 - 134.d	915	21	NaN	3287	45	NaN	426.3	6.1	0.011	1984	26	NaN
eaf38 - 135.d	782	21	NaN	2913	31	0.013	376.4	4.7	NaN	1767	24	NaN
eaf38 - 136.d	1109	18	NaN	3130	39	0.02	336.6	4.8	0.011	1319	18	0.083
eaf38 - 137.d	807	27	NaN	2299	38	NaN	239.5	4.9	0.011	961	27	NaN
eaf38 - 138.d	470.4	9	0.012	1447	27	NaN	150	2.8	NaN	588	11	NaN
eaf38 - 139.d	558	10	0.025	1832	34	NaN	198.6	4.1	NaN	798	15	0.12
eaf38 - 140.d	1054	16	NaN	2949	44	0.013	330.5	4.8	NaN	1368	18	NaN
eaf38 - 141.d	887	47	0.025	2445	93	0.013	254	10	0.022	1017	46	0.061
eaf38 - 142.d	1144	19	NaN	3388	66	NaN	404.5	7.4	0.011	1801	33	NaN
eaf38 - 143.d	740	35	0.013	2224	80	0.026	243	11	NaN	1008	57	0.085

Analysis number	Sm147 ppm	Sm147 ppm 2SE	Sm147 ppm LOD	Eu153 ppm	Eu153 ppm 2SE	Eu153 ppm LOD	Gd157 ppm	Gd157 ppm 2SE	Gd157 ppm LOD	Tb159 ppm	Tb159 ppm 2SE	Tb159 ppm LOD
eaf38 - 2.d	184.4	4.3	0.13	94.7	1.7	0.049	159.2	3	NaN	25.31	0.54	NaN
eaf38 - 6.d	451	6.6	NaN	160.1	2.2	NaN	379.6	5.8	NaN	54.71	0.74	0.018
eaf38 - 7.d	492.3	8.8	0.065	168.4	2.6	NaN	402.6	5.7	0.06	58.1	0.83	0.0089
eaf38 - 8.d	362.7	7.1	0.19	135.1	3	0.035	298.5	6.5	NaN	42.69	0.89	NaN
eaf38 - 9.d	451.6	7.8	NaN	168.2	2.6	NaN	373.1	5.7	NaN	54	1	NaN
eaf38 - 10.d	354.1	6.4	NaN	122.4	2.2	0.019	252.3	3.7	NaN	30.6	0.52	0.019
eaf38 - 11.d	338.9	5	0.15	122.9	1.9	NaN	243.5	3.9	NaN	28.53	0.49	0.019
eaf38 - 12.d	285.1	5.7	NaN	105.9	1.8	NaN	198.8	3.1	0.13	23.55	0.41	NaN
eaf38 - 13.d	375.7	5.9	0.14	129	1.7	NaN	270.3	4.8	NaN	31.78	0.57	NaN
eaf38 - 14.d	225.8	6	0.068	102.8	2.1	NaN	164.4	4.4	NaN	19.44	0.52	0.0092
eaf38 - 15.d	288.6	7.9	NaN	114.7	2.5	NaN	213.5	6.4	NaN	25.83	0.77	NaN
eaf38 - 16.d	285.9	4.9	NaN	111.4	1.8	NaN	220.3	4	0.12	26.84	0.57	NaN
eaf38 - 17.d	283.4	4.5	NaN	103.6	2.2	0.018	225.5	3.3	NaN	29.27	0.4	NaN
eaf38 - 18.d	133.4	2.7	0.067	55.9	1	0.036	108.5	2.6	NaN	13.35	0.33	NaN
eaf38 - 19.d	204.4	3.9	0.066	80.5	1.7	0.018	156.6	4	NaN	18.9	0.38	NaN
eaf38 - 20.d	129.1	2.6	NaN	54.8	1	0.035	101.2	2.1	0.12	11.88	0.26	NaN
eaf38 - 21.d	101.3	2.6	0.067	49.39	0.88	NaN	77.3	2	NaN	9.2	0.26	NaN
eaf38 - 23.d	223.2	5.3	NaN	82.6	1.6	NaN	179.7	4.2	0.063	21.38	0.44	0.019
eaf38 - 24.d	85.5	2.2	NaN	43.14	0.91	NaN	66.6	1.7	NaN	8.16	0.2	NaN
eaf38 - 25.d	103.3	3.1	0.067	47.8	1	0.04	79.8	2.1	NaN	9.69	0.22	0.0091
eaf38 - 26.d	275.4	5	NaN	78.4	1.2	NaN	249.6	4.6	NaN	31.56	0.5	NaN
eaf38 - 27.d	251.2	4.4	0.14	79	1.5	0.019	222	4.1	NaN	27.33	0.49	0.013
eaf38 - 28.d	249.8	4.9	NaN	85.5	1.6	NaN	206.3	5.5	NaN	25.96	0.59	0.019
eaf38 - 29.d	252.4	4.9	NaN	74.5	1.2	0.02	218.3	4.4	NaN	26.96	0.68	0.03
eaf38 - 30.d	244.2	4.7	NaN	75.5	1.2	NaN	213.6	3.1	0.13	26.99	0.51	0.02
eaf38 - 31.d	166.8	3.9	0.15	54.5	1.1	NaN	137.1	2.4	0.064	17.25	0.37	NaN
eaf38 - 32.d	270.5	5.3	NaN	82.3	1.6	NaN	233	4	0.13	29.96	0.57	0.0094
eaf38 - 33.d	212.2	4.6	0.16	70.4	1.1	NaN	185.6	3.5	0.15	23.64	0.36	NaN
eaf38 - 34.d	242.8	4.5	0.16	75	1.2	NaN	208.1	3.3	NaN	26.36	0.45	0.02

Analysis number	Sm147 ppm	Sm147 ppm 2SE	Sm147 ppm LOD	Eu153 ppm	Eu153 ppm 2SE	Eu153 ppm LOD	Gd157 ppm	Gd157 ppm 2SE	Gd157 ppm LOD	Tb159 ppm	Tb159 ppm 2SE	Tb159 ppm LOD
eaf38 - 35.d	263.8	3.7	NaN	81.5	1.4	NaN	232.1	4.2	NaN	28.2	0.52	NaN
eaf38 - 36.d	271.1	5.5	NaN	96.8	1.7	0.039	211.9	4.9	NaN	26.37	0.55	NaN
eaf38 - 37.d	278.3	4.4	0.072	92.8	1.8	NaN	221.4	4.3	0.066	28.38	0.49	NaN
eaf38 - 38.d	267.9	7.2	NaN	100	2	NaN	210.5	5	0.13	26.34	0.65	NaN
eaf38 - 39.d	279.8	5.9	NaN	98.6	1.6	0.019	231.2	4.3	NaN	28.86	0.61	NaN
eaf38 - 40.d	315.6	4.6	0.069	105.6	2	0.019	252.7	4.7	NaN	32.44	0.75	NaN
eaf38 - 41.d	279.1	6.4	NaN	90.8	1.9	NaN	219.2	5.8	0.064	27.14	0.54	NaN
eaf38 - 42.d	323.5	4.5	NaN	102.4	1.5	NaN	269.8	4.8	NaN	33.52	0.64	NaN
eaf38 - 43.d	306.5	3.9	0.067	98.2	1.7	0.036	252.2	3.9	0.062	30.86	0.71	NaN
eaf38 - 44.d	307.8	5.3	0.2	96.4	1.6	NaN	257.2	4.3	NaN	33.11	0.6	NaN
eaf38 - 45.d	303.1	4.6	NaN	96.6	1.4	0.018	244.6	3.9	NaN	30.99	0.63	NaN
eaf38 - 46.d	238.8	5.3	NaN	80.2	1.7	0.056	190.4	5.1	NaN	23.08	0.71	NaN
eaf38 - 47.d	235.6	4.4	NaN	84	1.5	NaN	189.1	3.6	0.062	23.23	0.45	NaN
eaf38 - 48.d	214.3	4.7	NaN	73.8	1.5	NaN	172.3	4.1	NaN	20.94	0.46	0.025
eaf38 - 49.d	412.2	5.5	0.069	118.5	1.7	0.025	341.3	4.6	NaN	43.16	0.66	NaN
eaf38 - 50.d	376	6.4	NaN	115.5	2.1	0.018	302.3	5	NaN	36.8	0.81	NaN
eaf38 - 51.d	257.5	4.1	0.18	82.4	1.5	NaN	206.2	4	NaN	25.74	0.52	NaN
eaf38 - 52.d	241.8	5.2	NaN	78.5	1.2	NaN	181.2	4	0.13	22.26	0.49	NaN
eaf38 - 53.d	276.4	5.7	NaN	99.7	2.1	0.038	208.8	4.4	NaN	25.29	0.53	NaN
eaf38 - 54.d	301.5	7.1	0.07	98.9	1.6	0.019	226	4.7	NaN	27.64	0.77	NaN
eaf38 - 55.d	348.1	6.7	NaN	106.7	1.8	0.037	271.1	4.8	0.14	33.26	0.6	0.0093
eaf38 - 56.d	284.8	5.6	NaN	98.6	1.7	NaN	222.2	4.6	NaN	28.12	0.55	NaN
eaf38 - 57.d	335	7.8	0.071	111.6	1.8	0.019	258.1	6.5	NaN	31.01	0.79	NaN
eaf38 - 58.d	370.3	6.2	0.14	109.1	1.8	NaN	293	5.6	NaN	35.47	0.71	NaN
eaf38 - 59.d	139	4.9	NaN	35.94	0.94	NaN	117	4.2	NaN	14.11	0.46	0.02
eaf38 - 60.d	151	3.4	NaN	36.9	0.9	0.02	126.3	2.6	NaN	15.22	0.27	0.02
eaf38 - 61.d	176.7	3.5	0.073	49.8	1.2	NaN	151.3	3	NaN	18.26	0.37	NaN
eaf38 - 62.d	202	4.6	0.079	56	1.2	NaN	173.1	5	NaN	21.1	0.5	NaN
eaf38 - 63.d	118.4	2.7	NaN	38.28	0.89	0.019	103.6	2.8	NaN	12.89	0.31	0.019

Analysis number	Sm147 ppm	Sm147 ppm 2SE	Sm147 ppm LOD	Eu153 ppm	Eu153 ppm 2SE	Eu153 ppm LOD	Gd157 ppm	Gd157 ppm 2SE	Gd157 ppm LOD	Tb159 ppm	Tb159 ppm 2SE	Tb159 ppm LOD
eaf38 - 64.d	222.2	4.5	0.073	58.8	1.3	0.042	197.2	4.1	NaN	24.57	0.57	NaN
eaf38 - 65.d	218.3	4.2	NaN	56.9	1	NaN	189.3	3.1	0.065	23.37	0.46	NaN
eaf38 - 68.d	238.5	5.4	0.067	66.8	1.4	NaN	194.6	3.9	NaN	21.91	0.5	NaN
eaf38 - 69.d	219.1	4.7	NaN	60.4	1.2	NaN	183.9	4.3	0.12	21.86	0.5	NaN
eaf38 - 70.d	301.3	6	NaN	77.4	1.3	NaN	252.3	5.3	0.063	28.66	0.5	NaN
eaf38 - 71.d	219.2	5.9	0.1	61.1	1.1	0.083	180.8	3.2	0.069	21.63	0.37	0.02
eaf38 - 72.d	215.6	7.4	NaN	63.4	1.4	0.018	177.4	5.4	0.13	20.61	0.65	NaN
eaf38 - 73.d	177.8	4.3	0.14	57.7	1.1	NaN	141.5	3	NaN	15.99	0.51	0.018
eaf38 - 74.d	230.9	4.3	NaN	66.6	1.3	0.036	189.8	3	NaN	22.25	0.51	NaN
eaf38 - 75.d	211.1	3.4	NaN	61.1	1.2	NaN	171	2.8	0.13	19.64	0.45	0.018
eaf38 - 76.d	227.1	4.8	0.14	65	1.2	NaN	185.5	4.6	0.13	21.41	0.48	NaN
eaf38 - 77.d	210.9	3.7	0.14	60.5	1.1	NaN	172.9	3.1	NaN	19.71	0.35	NaN
eaf38 - 78.d	160.1	3.7	NaN	47.5	1.1	NaN	132.8	3.4	NaN	15.94	0.36	NaN
eaf38 - 79.d	249.6	5.7	NaN	65.4	1.2	NaN	202.4	4	NaN	23.9	0.43	NaN
eaf38 - 80.d	209.6	3.6	NaN	58.5	1.1	NaN	174.5	3.1	NaN	20.6	0.4	NaN
eaf38 - 81.d	300.7	4.8	0.14	86	1.5	NaN	256.6	5.1	0.063	31.54	0.61	0.026
eaf38 - 82.d	286.5	3.6	NaN	81.5	1.2	0.04	233.4	4.3	0.063	28.65	0.5	0.019
eaf38 - 83.d	291.8	5.9	0.14	80	1.6	NaN	240.1	4.7	0.19	28.81	0.63	0.0093
eaf38 - 84.d	213.7	4.5	NaN	65.2	1.3	0.02	169	3.6	0.14	21.74	0.45	NaN
eaf38 - 85.d	207	4	NaN	64.8	1.4	NaN	164.4	3.6	0.14	20.59	0.47	NaN
eaf38 - 86.d	149.5	4.1	0.071	47.9	1.2	NaN	124.9	3.2	NaN	15.43	0.4	NaN
eaf38 - 87.d	196.5	6	0.14	61.3	1.9	0.019	158.5	5.3	NaN	19.27	0.67	0.0096
eaf38 - 88.d	211.7	5.6	0.14	62.4	1.5	0.019	169.2	4.2	NaN	21.1	0.55	NaN
eaf38 - 89.d	223.8	4.7	NaN	61	1.1	NaN	183	3.7	0.18	21.55	0.42	0.02
eaf38 - 90.d	235.4	4.2	0.097	65.6	1.2	0.019	193.4	3.3	0.13	23	0.41	NaN
eaf38 - 91.d	206.8	3.4	0.15	61.1	1.2	NaN	173.2	3.1	NaN	21.9	0.46	NaN
eaf38 - 92.d	234.1	4.2	0.072	66.9	1.2	NaN	187.9	3.6	NaN	23.31	0.47	NaN
eaf38 - 93.d	198.8	4.2	NaN	62.5	1.3	NaN	157.3	2.5	0.13	19.78	0.4	NaN
eaf38 - 94.d	259.6	5.1	NaN	75.5	1	0.038	206	4.7	NaN	25.47	0.4	0.0095

Analysis number	Sm147 ppm	Sm147 ppm 2SE	Sm147 ppm LOD	Eu153 ppm	Eu153 ppm 2SE	Eu153 ppm LOD	Gd157 ppm	Gd157 ppm 2SE	Gd157 ppm LOD	Tb159 ppm	Tb159 ppm 2SE	Tb159 ppm LOD
eaf38 - 95.d	257.3	6.6	NaN	73.8	2.2	0.038	212.9	4.5	0.14	26.92	0.69	NaN
eaf38 - 96.d	226.2	4.8	NaN	67.9	1.1	NaN	186.2	4.5	0.14	23.5	0.45	0.02
eaf38 - 97.d	230.3	4.3	0.14	69.6	1.3	0.055	185.4	3.8	NaN	23.03	0.46	NaN
eaf38 - 98.d	189.1	3.8	NaN	58.89	0.87	0.018	150.2	2.4	0.084	18.76	0.36	NaN
eaf38 - 99.d	195.5	4.3	NaN	52.06	0.95	0.018	165.1	3.5	0.12	19.29	0.36	0.018
eaf38 - 100.d	416	14	NaN	124	2	NaN	318.3	9.5	0.17	34	1.2	NaN
eaf38 - 101.d	291.2	6.1	NaN	103.4	1.8	0.036	221.6	5.1	NaN	24.84	0.52	NaN
eaf38 - 102.d	428.8	8.5	0.13	101.7	2	NaN	354.6	6.3	NaN	42	0.9	0.018
eaf38 - 103.d	356.3	7.2	NaN	105.3	2.6	NaN	290.8	5.5	0.16	33.38	0.61	0.022
eaf38 - 104.d	313.1	5.7	NaN	106.3	1.7	0.036	244.1	4.1	NaN	26.49	0.37	NaN
eaf38 - 105.d	408	11	NaN	99.6	3	0.036	337.8	9.5	NaN	40.2	1.1	NaN
eaf38 - 106.d	393.8	7.9	NaN	105.9	1.7	NaN	327.7	8	NaN	37.05	0.92	0.018
eaf38 - 107.d	464.9	8.3	0.15	113.5	1.8	NaN	387.1	5.6	0.13	43.2	0.78	NaN
eaf38 - 108.d	494.4	6.6	NaN	144.4	2.2	0.019	396.6	5.6	0.19	47.91	0.81	NaN
eaf38 - 109.d	390	5.8	NaN	132.6	2.5	NaN	277	4.7	NaN	30.44	0.54	NaN
eaf38 - 110.d	188.1	4.3	0.22	45.31	0.99	NaN	165.5	3.3	NaN	19.66	0.43	0.0098
eaf38 - 111.d	170.8	3	NaN	50.7	0.81	NaN	144	3.3	NaN	17.25	0.35	NaN
eaf38 - 112.d	115.5	2.9	NaN	39.36	0.87	NaN	98	2.5	NaN	11.85	0.31	NaN
eaf38 - 113.d	191.6	4.3	0.14	59.7	1.2	0.019	165.5	3.6	NaN	21.16	0.53	0.019
eaf38 - 114.d	92.2	2.4	NaN	35.89	0.87	0.042	81.3	2	0.065	10.35	0.3	NaN
eaf38 - 115.d	115	3.1	0.16	42.76	0.86	0.039	99.1	2.5	NaN	12.96	0.25	NaN
eaf38 - 116.d	183.7	3.3	0.14	62.5	1.5	0.039	167.7	4	0.13	21.53	0.43	0.021
eaf38 - 117.d	189.5	3.9	NaN	62.96	0.87	NaN	167.8	3.2	0.13	21.19	0.5	0.0098
eaf38 - 118.d	100.4	3.1	0.14	45.63	0.94	0.038	86.5	3	NaN	10.53	0.42	0.0095
eaf38 - 119.d	313.8	4.4	0.07	86	1.5	NaN	280.4	4.6	NaN	35.17	0.62	0.019
eaf38 - 120.d	306.5	5.4	NaN	86.8	1.6	NaN	273	4.4	0.065	34.62	0.69	NaN
eaf38 - 121.d	245.9	8.8	NaN	74.7	2.3	0.038	213.3	6.7	NaN	26.49	0.87	NaN
eaf38 - 125.d	780	14	NaN	231.4	3.2	NaN	510.7	6.9	0.18	47.09	0.65	0.013
eaf38 - 126.d	370.3	6.6	0.14	95.1	1.6	NaN	320.5	6.1	NaN	37.02	0.82	0.0095

Analysis number	Sm147 ppm	Sm147 ppm 2SE	Sm147 ppm LOD	Eu153 ppm	Eu153 ppm 2SE	Eu153 ppm LOD	Gd157 ppm	Gd157 ppm 2SE	Gd157 ppm LOD	Tb159 ppm	Tb159 ppm 2SE	Tb159 ppm LOD
eaf38 - 127.d	869	12	0.071	251.6	3.2	NaN	580.5	9.5	NaN	55.33	0.86	0.0096
eaf38 - 128.d	347.3	5.7	0.098	93.3	1.7	0.019	299.3	6.1	NaN	35.42	0.55	0.0097
eaf38 - 129.d	635	12	NaN	181	3	0.038	459	8.2	NaN	45.81	0.78	NaN
eaf38 - 130.d	379	5.9	NaN	97.2	2.1	0.052	327	5.9	NaN	37.9	0.82	NaN
eaf38 - 131.d	791	11	NaN	249.5	2.9	NaN	521.2	7.8	0.13	49.53	0.79	NaN
eaf38 - 132.d	590.2	9.1	0.14	173.4	2.4	NaN	424.4	7.2	NaN	43.76	0.86	0.021
eaf38 - 133.d	210.7	4.3	0.069	90.6	1.6	0.043	161.2	2.8	0.086	20.39	0.51	NaN
eaf38 - 134.d	468.5	6.6	NaN	180.5	2.8	NaN	347.5	5.4	0.088	37.48	0.73	NaN
eaf38 - 135.d	427.5	8.2	NaN	161.7	2.9	0.045	344.5	4.7	NaN	38.45	0.67	NaN
eaf38 - 136.d	232.8	3.8	0.29	99.6	1.7	0.019	181.2	3.2	NaN	23.07	0.45	NaN
eaf38 - 137.d	179.7	6.7	NaN	80.9	1.5	NaN	139.5	5.1	0.13	17.32	0.66	0.0096
eaf38 - 138.d	114.5	3.1	0.14	61.1	1.4	0.019	87	1.8	NaN	11.51	0.33	NaN
eaf38 - 139.d	156.8	4	NaN	72.6	1.5	NaN	119.5	3	NaN	14.8	0.38	NaN
eaf38 - 140.d	265.6	5.1	NaN	99	1.5	0.055	204.7	3.9	0.13	25.18	0.52	0.019
eaf38 - 141.d	188.3	9.5	NaN	82.5	2.6	0.02	143.1	6.5	NaN	17.65	0.87	0.0098
eaf38 - 142.d	380.9	6.9	NaN	119.6	1.7	NaN	312.7	6.3	NaN	38.89	0.76	0.02
eaf38 - 143.d	200	13	NaN	84.1	2.9	NaN	153	11	NaN	19.4	1.4	NaN

Analysis number	Dy163 ppm	Dy163 ppm 2SE	Dy163 ppm LOD	Ho165 ppm	Ho165 ppm 2SE	Ho165 ppm LOD	Er166 ppm	Er166 ppm 2SE	Er166 ppm LOD	Tm169 ppm	Tm169 ppm 2SE	Tm169 ppm LOD
eaf38 - 2.d	161.7	3.2	NaN	32.74	0.54	NaN	99.4	2.1	NaN	13.63	0.35	NaN
eaf38 - 6.d	316.8	4.4	0.075	58.7	0.77	NaN	155	2.5	NaN	19.25	0.37	NaN
eaf38 - 7.d	336.5	5.7	NaN	59.2	0.79	0.018	156.4	2.2	NaN	18.8	0.44	0.017
eaf38 - 8.d	252.2	5	0.036	46.8	0.92	NaN	124.6	2.4	0.027	16.19	0.28	NaN
eaf38 - 9.d	318.2	6.1	NaN	58.11	0.82	0.0097	150.1	2.3	NaN	18.89	0.47	NaN
eaf38 - 10.d	143.4	2.8	NaN	20.33	0.36	NaN	42.54	0.96	0.029	4.58	0.13	NaN
eaf38 - 11.d	127.1	2.1	NaN	17.49	0.31	NaN	35.9	0.73	NaN	3.55	0.14	NaN
eaf38 - 12.d	109.8	2.1	0.039	15.44	0.26	0.019	34.13	0.72	0.057	3.58	0.15	0.018
eaf38 - 13.d	145.9	2.9	NaN	20.57	0.4	0.021	42.4	1	NaN	4.45	0.19	NaN
eaf38 - 14.d	87.6	2.7	NaN	12.54	0.37	0.019	26	1	NaN	2.87	0.13	NaN
eaf38 - 15.d	121.7	3.4	NaN	16.73	0.49	0.019	34.7	1.1	NaN	3.64	0.14	NaN
eaf38 - 16.d	126.7	1.9	NaN	17.29	0.4	0.019	33.33	0.8	NaN	3.21	0.1	NaN
eaf38 - 17.d	137.6	2.1	0.11	19.52	0.51	0.019	37.28	0.79	0.057	3.74	0.16	0.02
eaf38 - 18.d	68.7	1.7	NaN	11.16	0.32	0.019	27.31	0.74	0.056	3.2	0.17	0.0089
eaf38 - 19.d	93.4	2	NaN	13.79	0.3	0.0092	29.83	0.69	NaN	3.04	0.16	NaN
eaf38 - 20.d	60.5	1.4	NaN	9.71	0.25	NaN	22.1	0.56	NaN	2.42	0.12	NaN
eaf38 - 21.d	45.6	1.1	0.075	7.41	0.2	0.022	17.13	0.43	0.028	1.999	0.091	0.0089
eaf38 - 23.d	104.5	2	0.039	15.5	0.4	NaN	32.8	0.97	NaN	3.17	0.13	NaN
eaf38 - 24.d	43.62	0.94	0.037	7.12	0.2	NaN	17.21	0.6	NaN	2.024	0.07	NaN
eaf38 - 25.d	51.9	1.3	0.038	8.46	0.2	NaN	18.71	0.47	NaN	2.3	0.11	NaN
eaf38 - 26.d	160.7	2.9	NaN	24.29	0.43	0.0097	50.9	1.1	0.058	5.21	0.15	NaN
eaf38 - 27.d	136.7	2.3	NaN	20.81	0.44	0.019	47.09	0.78	NaN	5.31	0.14	NaN
eaf38 - 28.d	130	3.3	NaN	19.95	0.58	0.0097	44.24	0.81	NaN	4.78	0.17	0.0093
eaf38 - 29.d	135.2	3.2	NaN	20.96	0.45	0.021	45.2	1.1	0.043	4.79	0.19	NaN
eaf38 - 30.d	137.1	2.7	NaN	21.04	0.44	NaN	45.8	1.1	0.028	4.6	0.17	NaN
eaf38 - 31.d	88.5	1.9	NaN	13.77	0.25	NaN	30.23	0.88	0.058	3.3	0.17	NaN
eaf38 - 32.d	145.6	2.6	0.039	22.09	0.46	0.0097	47.5	1.2	NaN	4.8	0.16	0.019
eaf38 - 33.d	123.5	2.1	NaN	18.97	0.45	NaN	42.2	1.1	0.046	4.34	0.21	NaN
eaf38 - 34.d	130.3	2.8	0.091	19.7	0.51	NaN	42.9	1.1	0.062	4.38	0.16	NaN

Analysis number	Dy163 ppm	Dy163 ppm 2SE	Dy163 ppm LOD	Ho165 ppm	Ho165 ppm 2SE	Ho165 ppm LOD	Er166 ppm	Er166 ppm 2SE	Er166 ppm LOD	Tm169 ppm	Tm169 ppm 2SE	Tm169 ppm LOD
eaf38 - 35.d	138.6	1.9	0.082	21.34	0.43	0.02	49.06	0.95	NaN	5.38	0.15	NaN
eaf38 - 36.d	133.4	2.2	NaN	21.55	0.5	NaN	52.9	1.4	NaN	6.09	0.23	NaN
eaf38 - 37.d	148	2.7	NaN	23.34	0.56	NaN	55.6	1.2	0.048	6.56	0.2	NaN
eaf38 - 38.d	137.8	3.1	NaN	22.85	0.6	NaN	56.8	1.1	NaN	6.55	0.2	NaN
eaf38 - 39.d	153.9	2.7	NaN	25.99	0.54	NaN	63.8	1.2	NaN	7.79	0.29	NaN
eaf38 - 40.d	161	2.7	0.077	25.7	0.51	NaN	59.6	1.4	0.087	6.6	0.24	0.0092
eaf38 - 41.d	137.1	2.8	0.039	21.12	0.47	NaN	48.6	1.3	NaN	5.31	0.19	0.0093
eaf38 - 42.d	170.5	2.5	0.038	27.57	0.43	NaN	64.1	1.2	0.028	7	0.18	NaN
eaf38 - 43.d	158.8	2.6	0.038	24.82	0.53	NaN	54.6	1.2	0.061	6.02	0.19	NaN
eaf38 - 44.d	165.7	2.8	NaN	25.25	0.54	0.0094	55.4	1.2	0.056	5.77	0.17	NaN
eaf38 - 45.d	156.6	3	NaN	24.28	0.44	NaN	54.3	1.2	NaN	6.02	0.19	0.0089
eaf38 - 46.d	119	2.8	NaN	19.28	0.52	0.02	46.2	1.2	0.028	5.31	0.2	0.0089
eaf38 - 47.d	116	1.9	0.038	17.92	0.49	0.0095	39.37	0.62	NaN	4.42	0.15	NaN
eaf38 - 48.d	106.5	2.5	0.075	15.9	0.34	0.0093	37.76	0.98	NaN	4.06	0.16	NaN
eaf38 - 49.d	215.2	3.1	NaN	32.51	0.69	0.019	72	1.4	NaN	7.85	0.22	NaN
eaf38 - 50.d	183.3	2.9	NaN	28.63	0.55	0.019	66.5	1.6	NaN	7.45	0.21	0.018
eaf38 - 51.d	130.5	2.4	NaN	20.39	0.46	0.02	46.99	0.87	NaN	5.24	0.21	NaN
eaf38 - 52.d	112.1	2.8	NaN	18.52	0.5	0.0095	43.4	0.95	0.057	5.02	0.14	NaN
eaf38 - 53.d	129.8	2.5	0.079	21.05	0.45	0.0098	51.3	1.1	0.029	6.37	0.21	NaN
eaf38 - 54.d	142.3	2.8	NaN	22.43	0.65	NaN	53.6	1.5	0.029	6.22	0.16	0.0092
eaf38 - 55.d	168.1	3	NaN	25.86	0.51	NaN	60	1.4	0.057	6.8	0.18	NaN
eaf38 - 56.d	148.6	3	NaN	24.36	0.36	NaN	60.3	1.1	NaN	6.94	0.22	NaN
eaf38 - 57.d	160.6	4.4	NaN	25.71	0.75	0.0099	62.3	1.6	NaN	7.33	0.25	NaN
eaf38 - 58.d	178.9	3.1	0.14	27.59	0.55	0.021	62.9	1.3	NaN	7.05	0.17	NaN
eaf38 - 59.d	69.6	1.8	NaN	10.74	0.29	0.02	23.38	0.73	NaN	2.42	0.13	NaN
eaf38 - 60.d	73.6	1.4	0.041	11.77	0.27	NaN	25.47	0.74	NaN	2.69	0.11	NaN
eaf38 - 61.d	94.5	1.6	0.041	13.93	0.4	0.014	29.66	0.67	NaN	3.08	0.15	NaN
eaf38 - 62.d	106.3	2.3	NaN	16.23	0.39	NaN	33.5	1.1	0.033	3.38	0.14	NaN
eaf38 - 63.d	66.3	1.8	NaN	11.2	0.33	0.02	25.33	0.69	NaN	2.87	0.14	0.0096

Analysis number	Dy163 ppm	Dy163 ppm 2SE	Dy163 ppm LOD	Ho165 ppm	Ho165 ppm 2SE	Ho165 ppm LOD	Er166 ppm	Er166 ppm 2SE	Er166 ppm LOD	Tm169 ppm	Tm169 ppm 2SE	Tm169 ppm LOD
eaf38 - 64.d	125.9	2.5	NaN	18.6	0.42	NaN	36.68	0.96	NaN	3.71	0.15	NaN
eaf38 - 65.d	116.9	1.9	0.079	17.39	0.38	NaN	36.36	0.91	0.059	3.54	0.17	NaN
eaf38 - 68.d	101.5	2.3	NaN	13.97	0.41	NaN	27.67	0.64	NaN	2.62	0.12	NaN
eaf38 - 69.d	100.2	2.1	NaN	14.65	0.35	NaN	29.96	0.92	NaN	2.9	0.11	0.0088
eaf38 - 70.d	128.8	3	NaN	16.84	0.36	NaN	31.71	0.68	0.029	2.84	0.12	NaN
eaf38 - 71.d	101.2	2	0.092	14.22	0.3	NaN	28.92	0.91	0.063	3.01	0.12	NaN
eaf38 - 72.d	97.1	2.5	0.037	13.83	0.33	NaN	28.03	0.76	NaN	2.77	0.12	NaN
eaf38 - 73.d	75.9	1.5	NaN	11.27	0.26	0.019	23.83	0.7	0.056	2.51	0.12	NaN
eaf38 - 74.d	106.1	2.3	NaN	16.01	0.34	NaN	35.14	0.97	NaN	3.85	0.14	0.0089
eaf38 - 75.d	96.5	1.5	NaN	14.08	0.31	0.0094	29.19	0.56	NaN	2.96	0.15	NaN
eaf38 - 76.d	97.5	2.5	NaN	14.1	0.32	0.019	28.6	0.55	NaN	2.83	0.12	NaN
eaf38 - 77.d	94.3	1.7	0.11	13.35	0.32	NaN	26.9	0.65	NaN	2.77	0.11	NaN
eaf38 - 78.d	79.6	1.8	0.082	12.23	0.35	NaN	26.27	0.74	NaN	3.01	0.14	NaN
eaf38 - 79.d	108.4	2.5	NaN	15.32	0.36	NaN	30.75	0.81	NaN	2.95	0.12	NaN
eaf38 - 80.d	101.4	1.6	0.076	14.9	0.27	NaN	30.58	0.82	0.028	3.17	0.14	NaN
eaf38 - 81.d	155.4	2.8	0.12	22.5	0.47	NaN	45.49	0.91	NaN	4.44	0.15	NaN
eaf38 - 82.d	137.4	2.3	0.038	19.6	0.33	NaN	41.08	0.75	NaN	4.1	0.12	0.018
eaf38 - 83.d	137.4	3.2	NaN	19.28	0.51	0.019	39.23	0.97	NaN	3.89	0.17	0.018
eaf38 - 84.d	106.1	2.4	0.088	16.25	0.33	NaN	36.35	0.72	NaN	3.84	0.19	0.019
eaf38 - 85.d	104	1.8	NaN	16.1	0.3	NaN	35.03	0.98	0.059	3.71	0.14	NaN
eaf38 - 86.d	77	1.9	0.079	12.06	0.31	NaN	26.72	0.74	0.04	2.93	0.15	NaN
eaf38 - 87.d	95.1	3	NaN	14.31	0.43	0.02	30.31	0.75	0.059	3.33	0.17	0.013
eaf38 - 88.d	100.8	2.4	NaN	15.49	0.37	0.02	34.08	0.89	NaN	3.58	0.16	0.019
eaf38 - 89.d	104.5	2.1	NaN	16.36	0.29	0.01	34.35	0.8	NaN	3.83	0.14	NaN
eaf38 - 90.d	109.9	2.4	0.086	16.91	0.3	0.02	35.3	0.71	0.059	3.75	0.15	0.019
eaf38 - 91.d	109.3	1.7	NaN	16.97	0.39	0.02	37.03	0.93	NaN	4.01	0.15	NaN
eaf38 - 92.d	114	2.7	NaN	17.05	0.35	NaN	37.82	0.95	NaN	3.98	0.14	NaN
eaf38 - 93.d	100.3	2.2	NaN	15.68	0.36	NaN	34.99	0.79	0.059	3.96	0.1	0.0094
eaf38 - 94.d	123.4	2.7	0.13	18.74	0.52	NaN	41.2	1	0.063	4.24	0.14	NaN

Analysis number	Dy163 ppm	Dy163 ppm 2SE	Dy163 ppm LOD	Ho165 ppm	Ho165 ppm 2SE	Ho165 ppm LOD	Er166 ppm	Er166 ppm 2SE	Er166 ppm LOD	Tm169 ppm	Tm169 ppm 2SE	Tm169 ppm LOD
eaf38 - 95.d	132	2.7	NaN	19.85	0.43	NaN	40	1	NaN	4.27	0.12	0.0093
eaf38 - 96.d	114.6	2.5	0.042	17.4	0.45	NaN	37.93	0.88	NaN	3.98	0.16	NaN
eaf38 - 97.d	113.6	2.3	NaN	17.17	0.41	0.0093	37	0.79	NaN	3.87	0.16	0.018
eaf38 - 98.d	92.1	2	NaN	14.42	0.34	0.019	30.95	0.87	NaN	3.44	0.1	NaN
eaf38 - 99.d	93.6	1.8	NaN	14.68	0.33	0.019	32.61	0.94	NaN	3.64	0.15	NaN
eaf38 - 100.d	141.6	5.2	0.11	19.26	0.54	NaN	36.7	1	0.028	3.71	0.12	NaN
eaf38 - 101.d	112.4	2.8	NaN	16.05	0.42	0.021	32.35	0.97	NaN	3.42	0.16	0.018
eaf38 - 102.d	186.6	3.5	0.081	25.5	0.44	0.0092	47.2	1.1	NaN	4.33	0.14	0.025
eaf38 - 103.d	149.3	3.1	0.091	20.68	0.52	0.011	41.8	1	NaN	3.97	0.15	NaN
eaf38 - 104.d	116.4	2	NaN	15.83	0.24	NaN	31.91	0.68	0.028	3.27	0.14	0.0089
eaf38 - 105.d	179.7	4.8	0.037	24.89	0.74	NaN	47.7	1.2	0.055	4.06	0.18	0.0088
eaf38 - 106.d	166	3.2	NaN	22.8	0.71	0.0095	42.8	1.1	NaN	4.1	0.17	0.018
eaf38 - 107.d	192	3.4	NaN	26.05	0.5	NaN	49.3	1.2	NaN	4.48	0.13	0.02
eaf38 - 108.d	229.7	3.4	0.078	32.11	0.64	0.028	62.1	1.3	NaN	6.01	0.21	0.0093
eaf38 - 109.d	132.2	2.2	0.04	18.09	0.32	NaN	36.27	0.98	0.06	3.67	0.13	0.0096
eaf38 - 110.d	93.4	1.9	0.08	13.46	0.31	NaN	28.61	0.8	0.03	2.97	0.14	NaN
eaf38 - 111.d	80	1.6	NaN	12.49	0.29	0.023	27.82	0.82	0.065	3.15	0.14	NaN
eaf38 - 112.d	59.2	1.4	0.081	9.38	0.26	0.014	23.31	0.57	NaN	2.67	0.14	0.019
eaf38 - 113.d	105.8	2.1	NaN	15.86	0.44	NaN	33.44	0.89	NaN	3.39	0.13	NaN
eaf38 - 114.d	55.1	1.2	0.039	9.29	0.26	0.0098	22.14	0.8	NaN	2.56	0.14	NaN
eaf38 - 115.d	68.1	1.5	NaN	11.16	0.28	NaN	25.53	0.82	0.03	2.83	0.12	NaN
eaf38 - 116.d	104.8	2	0.04	15.82	0.44	0.03	33.29	0.8	NaN	3.4	0.12	NaN
eaf38 - 117.d	104.9	2.3	0.04	15.72	0.38	0.022	31.77	0.98	NaN	3.07	0.16	NaN
eaf38 - 118.d	54.1	1.9	NaN	9.13	0.25	NaN	19.99	0.67	0.029	2.31	0.14	0.013
eaf38 - 119.d	161.6	2.9	0.053	21.55	0.39	0.019	38.93	0.9	0.029	3.17	0.14	NaN
eaf38 - 120.d	161.9	3.2	NaN	21.44	0.47	NaN	37.2	1	NaN	3.45	0.18	NaN
eaf38 - 121.d	122.4	3.7	0.079	16.4	0.46	NaN	30.56	0.78	NaN	2.8	0.14	0.019
eaf38 - 125.d	185.2	2.6	NaN	22.2	0.45	0.027	39.34	0.98	0.058	3.35	0.15	0.019
eaf38 - 126.d	171.7	3.7	0.14	23.72	0.53	0.021	46	1.2	NaN	3.92	0.17	0.0093

Analysis number	Dy163 ppm	Dy163 ppm 2SE	Dy163 ppm LOD	Ho165 ppm	Ho165 ppm 2SE	Ho165 ppm LOD	Er166 ppm	Er166 ppm 2SE	Er166 ppm LOD	Tm169 ppm	Tm169 ppm 2SE	Tm169 ppm LOD
eaf38 - 127.d	214.9	3.3	NaN	25.93	0.47	NaN	44.78	0.94	0.029	3.88	0.14	0.026
eaf38 - 128.d	165.1	3.5	0.079	23.23	0.43	NaN	43	1.2	0.03	3.85	0.14	NaN
eaf38 - 129.d	189.5	3.1	NaN	23.63	0.48	NaN	41.78	0.97	NaN	3.63	0.15	NaN
eaf38 - 130.d	172	2.9	NaN	23.96	0.47	0.021	43.52	0.85	0.059	3.84	0.12	NaN
eaf38 - 131.d	187.3	3.6	NaN	21.96	0.61	0.013	36.87	0.91	NaN	3.22	0.13	NaN
eaf38 - 132.d	178.9	3	NaN	22.1	0.39	NaN	39.72	0.95	NaN	3.57	0.13	0.0094
eaf38 - 133.d	102.9	1.8	0.038	16.4	0.42	0.0095	38.4	1.1	NaN	4.17	0.16	NaN
eaf38 - 134.d	162.7	2.5	0.078	21.86	0.41	NaN	42.94	0.99	NaN	4.29	0.13	0.019
eaf38 - 135.d	171.1	3	NaN	23.87	0.63	NaN	47.8	1.2	0.059	4.95	0.21	0.019
eaf38 - 136.d	118.7	2	0.079	18.69	0.31	0.022	41.78	0.89	0.059	4.68	0.17	0.0095
eaf38 - 137.d	85.6	3.3	0.086	13.92	0.41	NaN	31.8	1.1	NaN	3.57	0.15	0.0094
eaf38 - 138.d	58	1.4	NaN	9.89	0.28	0.019	23.94	0.79	0.039	3.03	0.13	NaN
eaf38 - 139.d	75.7	2.2	NaN	11.53	0.37	NaN	26.87	0.77	NaN	3.1	0.15	NaN
eaf38 - 140.d	121.8	2.3	NaN	17.83	0.43	NaN	39.3	0.92	NaN	3.94	0.15	NaN
eaf38 - 141.d	90.2	4	NaN	13.97	0.54	0.027	31.9	1.2	NaN	3.55	0.15	0.0096
eaf38 - 142.d	183.4	3.2	NaN	26.51	0.56	NaN	53.9	1.1	0.041	5.26	0.21	NaN
eaf38 - 143.d	98.4	6.7	0.081	15.05	0.99	0.02	34.6	1.9	NaN	3.71	0.21	0.0097

Analysis number	Yb172 ppm	Yb172 ppm 2SE	Yb172 ppm LOD	Lu175 ppm	Lu175 ppm 2SE	Lu175 ppm LOD	Hf178 ppm	Hf178 ppm 2SE	Hf178 ppm LOD	Ta181 ppm	Ta181 ppm 2SE	Ta181 ppm LOD
eaf38 - 2.d	89.1	2	NaN	12.59	0.36	NaN	15.38	0.52	NaN	7.04	0.18	NaN
eaf38 - 6.d	111.6	1.9	0.084	12.94	0.31	0.0093	14.28	0.44	0.063	4.39	0.12	0.017
eaf38 - 7.d	102	2.1	NaN	12.12	0.25	NaN	14.29	0.55	NaN	4.15	0.15	0.018
eaf38 - 8.d	95.4	2.1	NaN	11.96	0.28	NaN	12.55	0.58	0.03	11.14	0.34	NaN
eaf38 - 9.d	107.4	2.1	NaN	12.58	0.31	NaN	13.05	0.62	NaN	11.63	0.27	NaN
eaf38 - 10.d	22.34	0.78	NaN	2.46	0.1	0.019	10.46	0.46	0.065	0.411	0.046	NaN
eaf38 - 11.d	18.23	0.73	NaN	1.97	0.11	NaN	9.87	0.45	0.032	0.612	0.054	NaN
eaf38 - 12.d	19.34	0.69	NaN	2.21	0.13	NaN	10.88	0.5	0.065	0.972	0.068	NaN
eaf38 - 13.d	20.55	0.78	NaN	2.376	0.085	0.0098	13.28	0.65	NaN	1.44	0.12	NaN
eaf38 - 14.d	15.36	0.58	NaN	1.677	0.079	NaN	13.15	0.44	NaN	12.23	0.28	NaN
eaf38 - 15.d	18.17	0.63	NaN	2.09	0.12	NaN	13.05	0.57	NaN	7.05	0.29	NaN
eaf38 - 16.d	14.75	0.45	NaN	1.47	0.083	0.0093	13.44	0.59	NaN	9.36	0.23	NaN
eaf38 - 17.d	16.06	0.6	NaN	1.749	0.09	NaN	12.26	0.52	NaN	5.29	0.15	NaN
eaf38 - 18.d	16.55	0.61	0.091	2.07	0.11	0.0093	12.2	0.46	NaN	5.91	0.22	NaN
eaf38 - 19.d	14.85	0.51	NaN	1.616	0.093	0.026	11.23	0.51	0.062	2.65	0.12	NaN
eaf38 - 20.d	14.34	0.72	0.041	1.584	0.073	0.02	13.3	0.5	NaN	4.1	0.11	NaN
eaf38 - 21.d	10.9	0.44	0.042	1.427	0.09	0.02	13.06	0.5	0.094	7.56	0.2	0.017
eaf38 - 23.d	15.43	0.76	0.043	1.73	0.1	NaN	15.18	0.59	0.065	8.29	0.26	0.0088
eaf38 - 24.d	11.16	0.58	NaN	1.502	0.084	0.0093	13.7	0.56	0.031	3.53	0.15	NaN
eaf38 - 25.d	12.14	0.51	0.092	1.467	0.066	NaN	13.03	0.53	NaN	4.37	0.16	0.019
eaf38 - 26.d	24.71	0.74	NaN	2.61	0.13	NaN	13.91	0.55	0.033	4.73	0.18	NaN
eaf38 - 27.d	26.78	0.9	0.12	3.11	0.12	NaN	14.01	0.44	NaN	4.32	0.14	0.0088
eaf38 - 28.d	24.38	0.91	0.044	2.58	0.13	NaN	14.82	0.38	NaN	3.65	0.16	NaN
eaf38 - 29.d	23.8	0.96	0.11	2.55	0.14	NaN	16.25	0.76	0.035	3.93	0.19	NaN
eaf38 - 30.d	22.4	0.67	NaN	2.44	0.13	NaN	15.57	0.55	0.064	4.04	0.13	0.03
eaf38 - 31.d	17.14	0.7	0.044	1.939	0.086	NaN	13.81	0.46	0.033	10.12	0.26	0.0088
eaf38 - 32.d	23.23	0.9	NaN	2.46	0.14	0.0096	13.98	0.42	0.033	7.3	0.27	NaN
eaf38 - 33.d	23.09	0.83	0.12	2.55	0.14	0.011	16.01	0.81	0.052	15.61	0.34	0.022
eaf38 - 34.d	22.45	0.85	0.094	2.45	0.14	0.022	13.26	0.5	NaN	8.84	0.35	0.019

Analysis number	Yb172 ppm	Yb172 ppm 2SE	Yb172 ppm LOD	Lu175 ppm	Lu175 ppm 2SE	Lu175 ppm LOD	Hf178 ppm	Hf178 ppm 2SE	Hf178 ppm LOD	Ta181 ppm	Ta181 ppm 2SE	Ta181 ppm LOD
eaf38 - 35.d	27.56	0.95	0.092	3.3	0.1	0.01	13.17	0.56	0.034	3.4	0.12	0.022
eaf38 - 36.d	33.69	0.67	0.046	4.01	0.14	NaN	14.02	0.47	0.034	2.18	0.11	0.0092
eaf38 - 37.d	35.62	0.87	NaN	4.15	0.14	0.02	13.94	0.53	NaN	3.26	0.14	0.018
eaf38 - 38.d	37.6	1	0.096	4.58	0.14	NaN	14.18	0.45	NaN	2.12	0.11	0.018
eaf38 - 39.d	43.9	1.3	NaN	5.17	0.2	0.0097	14.52	0.53	NaN	6.47	0.27	NaN
eaf38 - 40.d	34.63	0.84	0.095	4.04	0.13	NaN	15.15	0.59	0.065	3.16	0.17	NaN
eaf38 - 41.d	27.96	0.74	0.044	3.25	0.13	0.019	14.54	0.5	NaN	2.067	0.081	0.0089
eaf38 - 42.d	37.3	0.82	NaN	4.33	0.19	NaN	15.59	0.5	NaN	1.61	0.11	0.0086
eaf38 - 43.d	30.24	0.98	NaN	3.57	0.13	0.0093	14.99	0.5	0.032	3.03	0.1	0.017
eaf38 - 44.d	28.3	1	NaN	3.06	0.14	NaN	16.08	0.53	0.032	6.59	0.23	NaN
eaf38 - 45.d	29.82	0.93	NaN	3.41	0.14	0.021	14.5	0.53	NaN	6.11	0.19	NaN
eaf38 - 46.d	29.77	0.94	NaN	3.52	0.15	NaN	13.85	0.48	NaN	6.07	0.2	NaN
eaf38 - 47.d	23.45	0.86	NaN	2.68	0.13	0.0094	17.34	0.62	0.064	10.55	0.29	NaN
eaf38 - 48.d	22.02	0.66	NaN	2.646	0.099	0.0093	15.84	0.62	NaN	3.1	0.17	NaN
eaf38 - 49.d	39.3	1.1	0.094	4.18	0.16	NaN	12.79	0.51	NaN	3.42	0.11	0.017
eaf38 - 50.d	38.3	1.3	0.084	4.65	0.17	0.0093	13.3	0.41	0.086	6.15	0.25	0.017
eaf38 - 51.d	27.92	0.99	NaN	3.15	0.12	NaN	14.3	0.5	NaN	10.41	0.26	NaN
eaf38 - 52.d	27.4	1.1	NaN	3.15	0.11	0.0095	13.11	0.49	NaN	10.89	0.26	0.019
eaf38 - 53.d	34.1	1	NaN	4.05	0.13	0.013	14.51	0.56	0.072	4.68	0.15	0.0089
eaf38 - 54.d	33.1	1.4	0.044	3.92	0.16	NaN	14.03	0.56	0.044	4.53	0.18	0.018
eaf38 - 55.d	35.9	1	NaN	4.08	0.16	NaN	15.2	0.59	NaN	7.06	0.18	0.017
eaf38 - 56.d	37.1	1.3	NaN	4.15	0.14	0.019	15.04	0.63	0.033	3.36	0.14	0.018
eaf38 - 57.d	37.7	1.1	0.089	4.73	0.18	0.0099	13.12	0.41	0.067	5.1	0.19	NaN
eaf38 - 58.d	37.1	1	NaN	3.85	0.16	0.021	14.88	0.5	NaN	8.36	0.25	NaN
eaf38 - 59.d	12.49	0.58	NaN	1.267	0.084	NaN	12.65	0.55	0.034	8.18	0.24	NaN
eaf38 - 60.d	13.45	0.63	0.046	1.46	0.096	0.01	12.59	0.53	NaN	6.6	0.25	NaN
eaf38 - 61.d	14.63	0.55	0.046	1.579	0.098	NaN	13.9	0.57	0.034	12.08	0.42	0.018
eaf38 - 62.d	15.87	0.61	NaN	1.751	0.095	NaN	16.37	0.7	NaN	20.12	0.47	0.01
eaf38 - 63.d	14.84	0.66	NaN	1.73	0.11	NaN	13.44	0.52	0.067	12.86	0.43	NaN

Analysis number	Yb172 ppm	Yb172 ppm 2SE	Yb172 ppm LOD	Lu175 ppm	Lu175 ppm 2SE	Lu175 ppm LOD	Hf178 ppm	Hf178 ppm 2SE	Hf178 ppm LOD	Ta181 ppm	Ta181 ppm 2SE	Ta181 ppm LOD
eaf38 - 64.d	17.22	0.67	0.091	1.74	0.1	0.027	13.3	0.5	NaN	18.1	0.45	0.025
eaf38 - 65.d	16.18	0.77	NaN	1.62	0.12	0.0098	14.49	0.48	0.099	20	0.46	NaN
eaf38 - 68.d	12.86	0.52	0.042	1.431	0.097	NaN	10.43	0.5	0.031	7.37	0.2	0.023
eaf38 - 69.d	14.67	0.46	0.041	1.609	0.097	NaN	9.37	0.42	NaN	4.04	0.19	NaN
eaf38 - 70.d	13.18	0.36	NaN	1.3	0.075	0.0095	10.21	0.42	0.032	5.47	0.18	NaN
eaf38 - 71.d	14.9	0.71	NaN	1.555	0.087	NaN	9.08	0.43	0.035	5.02	0.29	NaN
eaf38 - 72.d	13.09	0.51	0.11	1.356	0.084	0.019	10.02	0.42	0.062	5.98	0.21	NaN
eaf38 - 73.d	13.12	0.55	0.042	1.478	0.057	0.0094	9.34	0.43	NaN	7.93	0.19	NaN
eaf38 - 74.d	20.89	0.69	0.042	2.59	0.12	NaN	10.82	0.46	NaN	9.13	0.3	0.012
eaf38 - 75.d	14.19	0.53	0.093	1.527	0.086	0.0094	9.45	0.45	0.064	15.83	0.37	0.0086
eaf38 - 76.d	13.52	0.67	NaN	1.445	0.089	NaN	9.74	0.53	NaN	17.95	0.4	0.019
eaf38 - 77.d	12.9	0.64	NaN	1.362	0.088	NaN	10.17	0.43	NaN	14.75	0.43	0.017
eaf38 - 78.d	14.22	0.67	NaN	1.534	0.078	NaN	10.87	0.48	NaN	11.93	0.32	0.017
eaf38 - 79.d	13.23	0.59	0.085	1.483	0.081	0.019	10.41	0.4	0.064	6.3	0.24	NaN
eaf38 - 80.d	14.82	0.63	0.042	1.55	0.099	NaN	11.33	0.43	0.032	15.74	0.39	0.0086
eaf38 - 81.d	21.22	0.86	0.094	2.27	0.12	0.019	12.85	0.56	0.032	10.45	0.39	NaN
eaf38 - 82.d	19.02	0.8	NaN	2.07	0.11	0.0095	10.91	0.5	NaN	4.55	0.19	0.019
eaf38 - 83.d	17.97	0.69	NaN	1.89	0.1	NaN	12.21	0.4	NaN	7.77	0.4	NaN
eaf38 - 84.d	18.48	0.65	NaN	2.054	0.098	NaN	11.81	0.61	NaN	6.25	0.19	NaN
eaf38 - 85.d	18.79	0.64	NaN	2.114	0.071	0.02	12.37	0.45	0.076	3.38	0.16	0.036
eaf38 - 86.d	15.84	0.67	0.044	1.94	0.081	NaN	12.25	0.58	NaN	3.26	0.12	NaN
eaf38 - 87.d	17.47	0.74	NaN	1.924	0.092	NaN	12.36	0.59	0.14	2.05	0.12	0.0089
eaf38 - 88.d	19.13	0.81	NaN	2.16	0.11	0.01	11.99	0.52	NaN	3.42	0.13	NaN
eaf38 - 89.d	19.4	0.78	NaN	2.21	0.1	NaN	13.7	0.55	NaN	5.17	0.16	0.02
eaf38 - 90.d	18.09	0.79	NaN	2.06	0.1	NaN	14.18	0.59	NaN	5.34	0.19	0.018
eaf38 - 91.d	19.47	0.74	NaN	2.36	0.14	NaN	12.23	0.4	0.034	7.06	0.22	NaN
eaf38 - 92.d	19.82	0.8	0.13	2.06	0.14	NaN	13.38	0.44	NaN	7.68	0.26	NaN
eaf38 - 93.d	20.33	0.71	NaN	2.42	0.11	NaN	13.45	0.51	NaN	6.03	0.15	NaN
eaf38 - 94.d	21.19	0.7	NaN	2.3	0.14	NaN	11.95	0.5	NaN	3.9	0.13	0.018

Analysis number	Yb172 ppm	Yb172 ppm 2SE	Yb172 ppm LOD	Lu175 ppm	Lu175 ppm 2SE	Lu175 ppm LOD	Hf178 ppm	Hf178 ppm 2SE	Hf178 ppm LOD	Ta181 ppm	Ta181 ppm 2SE	Ta181 ppm LOD
eaf38 - 95.d	20.41	0.77	NaN	2.15	0.11	0.019	12.8	0.54	NaN	4.77	0.22	NaN
eaf38 - 96.d	19.76	0.71	0.047	2.2	0.11	0.024	13.93	0.48	0.035	4.86	0.22	0.0094
eaf38 - 97.d	17.87	0.7	NaN	2.15	0.13	0.026	11.46	0.45	0.1	3.99	0.17	NaN
eaf38 - 98.d	16.91	0.92	0.042	1.89	0.1	NaN	10.52	0.46	NaN	6.71	0.2	NaN
eaf38 - 99.d	19.71	0.82	0.042	2.35	0.11	NaN	12.53	0.57	0.068	4.18	0.15	NaN
eaf38 - 100.d	18.04	0.82	0.042	1.81	0.09	0.026	18.17	0.72	0.069	11.4	0.33	NaN
eaf38 - 101.d	16.75	0.79	0.083	1.626	0.086	NaN	18.21	0.65	0.062	7.31	0.23	0.0084
eaf38 - 102.d	19.07	0.75	0.041	1.79	0.11	0.018	15.81	0.52	NaN	11.15	0.31	0.0084
eaf38 - 103.d	18.27	0.76	NaN	1.87	0.1	NaN	20.51	0.79	NaN	19.7	1.3	NaN
eaf38 - 104.d	16.19	0.77	0.084	1.78	0.12	0.0093	19.46	0.62	NaN	16.62	0.49	NaN
eaf38 - 105.d	18.8	0.84	0.041	1.817	0.099	0.0092	15.11	0.58	0.062	7.94	0.48	NaN
eaf38 - 106.d	17.7	0.69	NaN	1.93	0.11	NaN	17.32	0.7	NaN	11.28	0.36	NaN
eaf38 - 107.d	19.54	0.83	0.094	1.95	0.1	NaN	16.15	0.51	NaN	15.64	0.38	0.0087
eaf38 - 108.d	25.4	1.1	0.044	2.52	0.12	0.0097	12.69	0.49	0.033	5.14	0.18	NaN
eaf38 - 109.d	18.32	0.9	0.045	1.905	0.093	NaN	17.22	0.65	0.034	5.36	0.16	NaN
eaf38 - 110.d	14.87	0.53	NaN	1.65	0.11	NaN	13.48	0.55	NaN	3.78	0.17	0.0091
eaf38 - 111.d	15.92	0.77	0.073	1.921	0.095	0.01	12.78	0.56	NaN	12.93	0.35	0.018
eaf38 - 112.d	14.55	0.63	0.045	1.689	0.091	0.02	13.33	0.4	0.034	12.38	0.31	0.0092
eaf38 - 113.d	15.75	0.57	0.09	1.73	0.081	0.01	13.58	0.6	0.034	5.01	0.17	NaN
eaf38 - 114.d	13.41	0.62	0.088	1.586	0.08	NaN	13.05	0.44	NaN	3.03	0.18	NaN
eaf38 - 115.d	14.8	0.59	NaN	1.76	0.11	NaN	15.09	0.6	0.073	6.1	0.21	NaN
eaf38 - 116.d	16.27	0.67	0.089	1.69	0.12	0.02	14.99	0.5	NaN	6.24	0.2	0.018
eaf38 - 117.d	14.27	0.65	NaN	1.42	0.091	NaN	14.49	0.57	NaN	21.02	0.82	0.0092
eaf38 - 118.d	10.98	0.55	0.044	1.378	0.086	NaN	15.13	0.61	NaN	23.52	0.45	0.0088
eaf38 - 119.d	14.07	0.54	NaN	1.207	0.094	0.0097	14.03	0.59	0.045	10.27	0.24	NaN
eaf38 - 120.d	13.46	0.62	NaN	1.264	0.083	NaN	14.53	0.62	NaN	8.52	0.22	0.018
eaf38 - 121.d	13.19	0.65	0.044	1.33	0.1	NaN	15.75	0.68	NaN	7.79	0.22	NaN
eaf38 - 125.d	14.84	0.69	NaN	1.415	0.096	NaN	14.71	0.53	0.033	14.53	0.38	NaN
eaf38 - 126.d	17.13	0.73	0.044	1.499	0.094	NaN	14.48	0.64	NaN	8.2	0.23	NaN

Analysis number	Yb172 ppm	Yb172 ppm 2SE	Yb172 ppm LOD	Lu175 ppm	Lu175 ppm 2SE	Lu175 ppm LOD	Hf178 ppm	Hf178 ppm 2SE	Hf178 ppm LOD	Ta181 ppm	Ta181 ppm 2SE	Ta181 ppm LOD
eaf38 - 127.d	16.82	0.53	NaN	1.551	0.093	0.0098	15.66	0.47	0.072	18.41	0.42	NaN
eaf38 - 128.d	16.2	0.65	0.044	1.547	0.096	NaN	13.76	0.62	0.033	7.52	0.19	NaN
eaf38 - 129.d	14.61	0.72	0.088	1.336	0.084	NaN	15.36	0.48	NaN	10.03	0.23	NaN
eaf38 - 130.d	15.94	0.59	0.088	1.474	0.083	0.02	15.13	0.47	0.033	8.94	0.24	0.024
eaf38 - 131.d	12.86	0.76	0.044	1.165	0.095	0.027	15.5	0.49	NaN	11.65	0.34	NaN
eaf38 - 132.d	15.19	0.66	NaN	1.377	0.09	0.0099	15.5	0.62	NaN	6.79	0.22	NaN
eaf38 - 133.d	23.36	0.79	0.043	2.81	0.13	NaN	13.89	0.68	0.032	4.74	0.16	0.017
eaf38 - 134.d	22.01	0.82	NaN	2.289	0.096	0.0097	14.19	0.54	NaN	11.33	0.27	0.018
eaf38 - 135.d	24.5	0.63	0.1	2.57	0.11	NaN	14.34	0.55	NaN	12.38	0.32	NaN
eaf38 - 136.d	23.21	0.82	0.044	2.86	0.13	NaN	13.94	0.5	NaN	8.17	0.3	NaN
eaf38 - 137.d	20.18	0.66	NaN	2.32	0.12	NaN	9.8	0.5	0.067	2.03	0.23	NaN
eaf38 - 138.d	17.33	0.81	NaN	2.109	0.083	NaN	9.64	0.31	0.066	2.317	0.096	NaN
eaf38 - 139.d	17.26	0.59	0.045	2.23	0.13	0.01	8.92	0.35	0.068	2.05	0.12	0.012
eaf38 - 140.d	21.14	0.82	0.12	2.25	0.13	NaN	10.08	0.41	0.068	2.92	0.14	0.0091
eaf38 - 141.d	20.21	0.74	NaN	2.24	0.13	NaN	10.11	0.44	NaN	2.39	0.18	NaN
eaf38 - 142.d	23.58	0.71	NaN	2.48	0.14	NaN	11.32	0.52	NaN	7.12	0.24	NaN
eaf38 - 143.d	20.19	0.86	NaN	2.25	0.13	0.031	9.83	0.5	NaN	6.06	0.37	0.018

Analysis number	W182 ppm	W182 ppm 2SE	W182 ppm LOD	Pb204 ppm	Pb204 ppm 2SE	Pb204 ppm LOD	Pb206 ppm	Pb206 ppm 2SE	Pb206 ppm LOD	Pb207 ppm	Pb207 ppm 2SE	Pb207 ppm LOD
eaf38 - 2.d	0.428	0.076	0.076	< LOD	< LOD	5.1	70.1	1.8	0.049	7.87	0.17	0.042
eaf38 - 6.d	0.51	0.11	NaN	< LOD	< LOD	3.9	85.9	1.8	0.18	9.23	0.22	0.055
eaf38 - 7.d	0.69	0.11	0.069	< LOD	< LOD	5.3	81.4	1.7	0.11	9.24	0.2	0.043
eaf38 - 8.d	0.47	0.092	NaN	< LOD	< LOD	5	75.6	1.6	0.091	8.35	0.2	0.051
eaf38 - 9.d	0.53	0.11	NaN	< LOD	< LOD	8.5	86.9	2	0.2	10	0.24	0.059
eaf38 - 10.d	0.394	0.095	NaN	< LOD	< LOD	7	86	1.3	0.11	9.33	0.21	0.069
eaf38 - 11.d	0.345	0.085	0.1	< LOD	< LOD	5.4	79.8	2	0.051	8.73	0.21	0.051
eaf38 - 12.d	0.42	0.1	NaN	< LOD	< LOD	7	72.1	1.7	0.17	8.18	0.17	0.046
eaf38 - 13.d	1.04	0.17	0.037	< LOD	< LOD	6	82.4	2.2	0.12	11.67	0.79	0.038
eaf38 - 14.d	1.09	0.14	NaN	< LOD	< LOD	8.7	55.6	1.3	0.12	6.64	0.14	0.036
eaf38 - 15.d	0.94	0.12	0.11	< LOD	< LOD	8.6	69.5	1.6	0.18	8.02	0.16	0.064
eaf38 - 16.d	1.11	0.16	NaN	< LOD	< LOD	6.5	48	1.5	0.14	6.04	0.15	0.051
eaf38 - 17.d	1.32	0.16	NaN	< LOD	< LOD	8.2	49.1	1.3	0.14	5.84	0.14	0.034
eaf38 - 18.d	0.89	0.13	0.035	< LOD	< LOD	9.3	28.3	1.1	0.16	4.13	0.13	0.048
eaf38 - 19.d	1.17	0.15	NaN	< LOD	< LOD	7.3	33.02	0.93	0.16	4.59	0.091	0.048
eaf38 - 20.d	0.98	0.16	0.035	< LOD	< LOD	4.5	29.3	1.1	0.078	4.327	0.097	0.045
eaf38 - 21.d	1.07	0.14	0.07	< LOD	< LOD	5.9	25.6	0.93	0.3	4.15	0.13	0.055
eaf38 - 23.d	2.64	0.51	0.036	< LOD	< LOD	7.7	32.5	1.4	0.051	5.12	0.19	0.07
eaf38 - 24.d	1.03	0.16	NaN	< LOD	< LOD	5	27.95	0.92	0.17	4.19	0.1	0.045
eaf38 - 25.d	1.22	0.15	NaN	< LOD	< LOD	5.8	26.96	0.8	0.18	4.12	0.13	0.033
eaf38 - 26.d	0.77	0.13	0.073	< LOD	< LOD	7	37.8	1.2	0.051	5.35	0.14	0.051
eaf38 - 27.d	0.72	0.14	0.036	< LOD	< LOD	6.5	44.6	1.2	0.18	5.96	0.14	0.055
eaf38 - 28.d	0.682	0.089	NaN	< LOD	< LOD	6	42.8	1	0.23	5.36	0.11	0.042
eaf38 - 29.d	10.53	0.7	NaN	< LOD	< LOD	6.5	39.9	1.4	0.16	6.05	0.18	0.043
eaf38 - 30.d	1.39	0.19	NaN	< LOD	< LOD	7.1	37.2	1.1	0.16	4.83	0.13	0.042
eaf38 - 31.d	0.62	0.11	NaN	< LOD	< LOD	12	29.65	0.94	0.24	4.7	0.12	0.064
eaf38 - 32.d	0.9	0.14	0.11	< LOD	< LOD	4.8	37	1.1	0.22	5.06	0.14	0.052
eaf38 - 33.d	1.99	0.3	NaN	< LOD	< LOD	8.8	32.7	1.1	0.06	4.51	0.14	0.084
eaf38 - 34.d	0.95	0.13	0.078	< LOD	< LOD	4.7	32.2	1.1	0.11	5.03	0.22	0.027

Analysis number	W182 ppm	W182 ppm 2SE	W182 ppm LOD	Pb204 ppm	Pb204 ppm 2SE	Pb204 ppm LOD	Pb206 ppm	Pb206 ppm 2SE	Pb206 ppm LOD	Pb207 ppm	Pb207 ppm 2SE	Pb207 ppm LOD
eaf38 - 35.d	0.65	0.12	NaN	< LOD	< LOD	9.1	44.7	1.6	0.16	5.89	0.13	0.042
eaf38 - 36.d	1.06	0.17	0.083	< LOD	< LOD	6.2	44.3	1.7	0.17	5.84	0.17	0.055
eaf38 - 37.d	0.82	0.12	0.038	< LOD	< LOD	7.2	44.5	1.3	0.13	5.75	0.16	0.034
eaf38 - 38.d	1.06	0.14	NaN	< LOD	< LOD	8.6	48.8	1.1	0.19	6.1	0.15	0.054
eaf38 - 39.d	0.96	0.13	0.037	< LOD	< LOD	8.9	48.7	1.5	0.1	6.04	0.17	0.045
eaf38 - 40.d	1.13	0.14	NaN	< LOD	< LOD	6.9	44.25	0.98	0.22	5.67	0.16	0.054
eaf38 - 41.d	1.44	0.19	NaN	< LOD	< LOD	9.6	39.8	1.1	NaN	5.49	0.14	0.053
eaf38 - 42.d	1.11	0.14	NaN	< LOD	< LOD	7.5	45.4	1.3	0.12	5.63	0.13	0.04
eaf38 - 43.d	0.7	0.14	NaN	< LOD	< LOD	7.7	42.6	1.4	0.068	5.32	0.16	0.037
eaf38 - 44.d	0.94	0.19	0.071	< LOD	< LOD	7	36.93	0.94	0.099	5.17	0.16	0.055
eaf38 - 45.d	1.15	0.13	NaN	< LOD	< LOD	6.9	40.8	1.6	0.16	5.5	0.16	0.058
eaf38 - 46.d	0.82	0.16	0.099	< LOD	< LOD	5.1	38.71	0.96	0.099	5.1	0.12	0.067
eaf38 - 47.d	1.49	0.18	NaN	< LOD	< LOD	5	34.7	1.2	0.18	4.89	0.14	0.05
eaf38 - 48.d	1.47	0.19	0.035	< LOD	< LOD	7.7	31.8	0.97	0.22	4.69	0.12	0.036
eaf38 - 49.d	1.23	0.13	0.036	< LOD	< LOD	5	43.1	1.1	0.15	5.77	0.16	0.04
eaf38 - 50.d	0.86	0.16	0.077	< LOD	< LOD	6.4	47.5	1.2	0.16	5.88	0.17	0.054
eaf38 - 51.d	1.2	0.15	0.035	< LOD	< LOD	7.4	39.5	1	0.099	5.17	0.11	0.037
eaf38 - 52.d	1.55	0.16	NaN	< LOD	< LOD	6.5	41.9	1.2	0.14	5.6	0.17	0.069
eaf38 - 53.d	1.16	0.13	0.074	< LOD	< LOD	3.5	48	1.8	0.15	5.73	0.14	0.051
eaf38 - 54.d	2.46	0.41	0.1	< LOD	< LOD	7	42.5	1.2	0.07	5.77	0.22	0.059
eaf38 - 55.d	1.18	0.17	0.036	< LOD	< LOD	7.6	52.9	1.6	0.16	6.15	0.19	0.047
eaf38 - 56.d	1.22	0.16	NaN	< LOD	< LOD	7.8	49.4	1.4	0.17	5.8	0.15	0.035
eaf38 - 57.d	1.39	0.16	0.11	< LOD	< LOD	5.2	42.4	1.1	0.12	5.81	0.15	0.036
eaf38 - 58.d	1.12	0.18	NaN	< LOD	< LOD	7.7	44.8	1.5	0.11	5.54	0.15	0.044
eaf38 - 59.d	0.66	0.11	0.1	< LOD	< LOD	6	23.37	0.98	0.16	4.15	0.12	0.025
eaf38 - 60.d	0.57	0.12	NaN	< LOD	< LOD	6.3	24.4	0.92	0.15	4.52	0.12	0.051
eaf38 - 61.d	1.12	0.18	NaN	< LOD	< LOD	7.3	29.93	0.97	0.19	4.73	0.17	0.043
eaf38 - 62.d	1.99	0.26	0.11	14.3	4.3	8.2	40.4	2.4	0.33	11.2	1.8	0.06
eaf38 - 63.d	1.04	0.16	0.038	< LOD	< LOD	7.7	25.48	0.91	0.26	4.22	0.15	0.044

Analysis number	W182 ppm	W182 ppm 2SE	W182 ppm LOD	Pb204 ppm	Pb204 ppm 2SE	Pb204 ppm LOD	Pb206 ppm	Pb206 ppm 2SE	Pb206 ppm LOD	Pb207 ppm	Pb207 ppm 2SE	Pb207 ppm LOD
eaf38 - 64.d	1.27	0.19	NaN	< LOD	< LOD	5.4	37.9	0.96	0.17	5.45	0.16	0.042
eaf38 - 65.d	1.17	0.15	NaN	< LOD	< LOD	5.6	35.8	1.2	0.071	4.89	0.12	0.037
eaf38 - 68.d	0.77	0.12	0.035	< LOD	< LOD	6.4	32.4	1.1	0.16	4.68	0.11	0.052
eaf38 - 69.d	0.58	0.11	NaN	< LOD	< LOD	5.9	32	1.2	0.16	4.4	0.12	0.039
eaf38 - 70.d	0.72	0.13	0.072	< LOD	< LOD	5.9	33.98	0.95	0.13	4.89	0.14	0.042
eaf38 - 71.d	14.6	1.8	NaN	< LOD	< LOD	5.2	30.1	1.2	0.24	5.2	0.14	0.048
eaf38 - 72.d	0.81	0.12	0.14	< LOD	< LOD	4.8	31.69	0.99	0.067	4.66	0.14	0.044
eaf38 - 73.d	0.69	0.11	0.071	< LOD	< LOD	5.9	28.4	1	0.21	4.27	0.12	0.066
eaf38 - 74.d	2.63	0.37	NaN	< LOD	< LOD	7.3	31.2	1	0.16	4.75	0.15	0.038
eaf38 - 75.d	0.59	0.12	0.071	< LOD	< LOD	6	29.7	0.95	0.22	4.49	0.14	0.052
eaf38 - 76.d	0.79	0.11	NaN	< LOD	< LOD	5.2	31.8	1.1	0.14	4.76	0.13	0.06
eaf38 - 77.d	0.69	0.13	NaN	< LOD	< LOD	6.2	28.7	1.1	0.14	4.27	0.13	0.049
eaf38 - 78.d	0.67	0.11	NaN	< LOD	< LOD	6.8	26.3	1.1	0.12	4.14	0.13	0.038
eaf38 - 79.d	0.44	0.1	NaN	< LOD	< LOD	4.8	30.37	0.92	0.14	4.5	0.11	0.05
eaf38 - 80.d	1.29	0.16	0.071	< LOD	< LOD	6	31	1	0.14	4.38	0.16	0.07
eaf38 - 81.d	0.6	0.1	NaN	< LOD	< LOD	5.9	33.5	1	0.16	4.67	0.12	0.044
eaf38 - 82.d	1.09	0.13	0.072	< LOD	< LOD	6.3	36	1.1	0.12	6.12	0.12	0.058
eaf38 - 83.d	0.501	0.099	0.072	< LOD	< LOD	7.8	34.4	1.3	0.15	4.77	0.15	0.06
eaf38 - 84.d	0.4	0.09	0.076	< LOD	< LOD	8	35.2	1.5	0.17	4.7	0.15	0.071
eaf38 - 85.d	0.437	0.098	NaN	< LOD	< LOD	7.3	33.79	0.99	0.12	4.6	0.12	0.063
eaf38 - 86.d	0.57	0.12	NaN	< LOD	< LOD	10	30.2	1.1	0.12	4.53	0.14	0.034
eaf38 - 87.d	0.55	0.1	NaN	< LOD	< LOD	6.3	34.9	1.1	0.071	4.7	0.12	0.059
eaf38 - 88.d	0.37	0.083	0.075	< LOD	< LOD	5.4	32.7	1.3	0.13	4.64	0.14	0.052
eaf38 - 89.d	0.411	0.097	NaN	< LOD	< LOD	11	32.4	1.3	0.19	4.65	0.14	0.044
eaf38 - 90.d	0.55	0.11	0.037	< LOD	< LOD	8.3	33.4	1.4	0.094	4.95	0.17	0.042
eaf38 - 91.d	0.359	0.092	NaN	< LOD	< LOD	9	31.58	0.97	0.16	4.38	0.14	0.062
eaf38 - 92.d	0.406	0.093	NaN	< LOD	< LOD	5.6	34.5	1.3	0.16	4.96	0.13	0.04
eaf38 - 93.d	0.378	0.095	NaN	< LOD	< LOD	4.5	31.5	1.1	0.1	4.65	0.14	0.052
eaf38 - 94.d	0.387	0.085	NaN	< LOD	< LOD	5.9	34.1	1.2	0.11	4.91	0.13	0.055

Analysis number	W182 ppm	W182 ppm 2SE	W182 ppm LOD	Pb204 ppm	Pb204 ppm 2SE	Pb204 ppm LOD	Pb206 ppm	Pb206 ppm 2SE	Pb206 ppm LOD	Pb207 ppm	Pb207 ppm 2SE	Pb207 ppm LOD
eaf38 - 95.d	1.14	0.15	NaN	< LOD	< LOD	8.2	34.8	1.1	0.22	6.77	0.3	0.04
eaf38 - 96.d	3.5	0.63	NaN	22.15	< LOD	< LOD	6.5	34.2	1	0.12	5.64	0.2
eaf38 - 97.d	0.436	0.09	0.071	22.24	< LOD	< LOD	6.6	33.1	1	0.12	4.61	0.16
eaf38 - 98.d	0.406	0.09	NaN	21.61	< LOD	< LOD	8.1	30.12	0.95	NaN	4.63	0.12
eaf38 - 99.d	0.287	0.071	0.035	13.84	< LOD	< LOD	5.2	27.53	0.85	0.14	4.07	0.12
eaf38 - 100.d	12.1	2.5	NaN	22.51	< LOD	< LOD	9.3	50.2	1.7	0.16	8.25	0.43
eaf38 - 101.d	2.09	0.22	NaN	18.5	< LOD	< LOD	6.5	45.3	1.1	0.098	5.68	0.13
eaf38 - 102.d	1.72	0.18	0.035	28.02	< LOD	< LOD	4.5	43.6	1.2	0.11	5.49	0.17
eaf38 - 103.d	23.1	5.5	NaN	22.94	< LOD	< LOD	9.3	46.5	1.4	0.13	7.43	0.23
eaf38 - 104.d	2.23	0.17	0.11	19.59	< LOD	< LOD	4.4	43.7	1.2	0.11	5.67	0.13
eaf38 - 105.d	1.7	0.2	NaN	26.13	< LOD	< LOD	4.2	43.5	1.4	0.17	5.44	0.16
eaf38 - 106.d	1.49	0.15	0.072	23.51	< LOD	< LOD	5.8	47	1.3	0.22	5.7	0.16
eaf38 - 107.d	2.02	0.18	NaN	27.52	< LOD	< LOD	4.4	47.5	1.3	0.15	5.85	0.15
eaf38 - 108.d	1.61	0.21	0.1	24.97	< LOD	< LOD	4.9	64	2.1	0.14	7.65	0.24
eaf38 - 109.d	4.71	0.67	0.076	21.68	< LOD	< LOD	5.1	57	1.7	0.15	7.28	0.2
eaf38 - 110.d	0.63	0.15	NaN	12.03	< LOD	< LOD	5.1	23.8	0.89	0.17	3.8	0.11
eaf38 - 111.d	0.492	0.088	NaN	10.41	< LOD	< LOD	7.8	24.31	0.94	0.25	4.25	0.13
eaf38 - 112.d	0.74	0.14	NaN	9.95	< LOD	< LOD	6.5	18.57	0.67	0.11	3.63	0.12
eaf38 - 113.d	0.82	0.13	NaN	17.32	< LOD	< LOD	6.8	27.92	0.95	0.073	4.21	0.1
eaf38 - 114.d	0.67	0.12	NaN	10.58	< LOD	< LOD	9.5	18.67	0.88	0.11	3.567	0.083
eaf38 - 115.d	1.37	0.2	NaN	12.71	< LOD	< LOD	5.1	22.27	0.91	0.13	3.85	0.16
eaf38 - 116.d	2.14	0.23	NaN	18.73	< LOD	< LOD	7.7	28.29	0.93	0.15	4.23	0.11
eaf38 - 117.d	1.08	0.14	0.052	15.81	< LOD	< LOD	5.7	23.91	0.89	0.16	4.16	0.13
eaf38 - 118.d	1.38	0.18	NaN	9.97	< LOD	< LOD	6.7	16.5	0.9	0.15	3.59	0.12
eaf38 - 119.d	0.9	0.12	NaN	23.29	< LOD	< LOD	5.3	33.2	1.2	0.092	5.09	0.19
eaf38 - 120.d	0.94	0.14	NaN	23.8	< LOD	< LOD	6.7	35.6	1.2	0.12	5.45	0.13
eaf38 - 121.d	1.17	0.16	0.037	17.2	< LOD	< LOD	5.3	30	1.1	0.15	4.8	0.16
eaf38 - 125.d	1.22	0.14	NaN	16.22	< LOD	< LOD	7.6	69.6	2	0.15	8.47	0.2
eaf38 - 126.d	0.67	0.11	0.05	15.78	< LOD	< LOD	9.1	32.8	1	0.19	5	0.12

Analysis number	W182 ppm	W182 ppm 2SE	W182 ppm LOD	Pb204 ppm	Pb204 ppm 2SE	Pb204 ppm LOD	Pb206 ppm	Pb206 ppm 2SE	Pb206 ppm LOD	Pb207 ppm	Pb207 ppm 2SE	Pb207 ppm LOD
eaf38 - 127.d	1.51	0.19	NaN	16.61	< LOD	< LOD	5.7	75.5	2.1	NaN	9.4	0.21
eaf38 - 128.d	0.74	0.11	NaN	18.88	< LOD	< LOD	5.2	35.7	1	0.12	6.16	0.16
eaf38 - 129.d	0.85	0.14	0.081	15.76	< LOD	< LOD	5.7	52.4	1.8	0.19	6.58	0.19
eaf38 - 130.d	0.69	0.11	NaN	16.39	< LOD	< LOD	7.9	31.9	1	0.11	5.06	0.14
eaf38 - 131.d	1.35	0.17	NaN	16.77	< LOD	< LOD	5.1	71.6	1.8	0.15	8.24	0.21
eaf38 - 132.d	0.87	0.14	0.081	15.46	< LOD	< LOD	6.1	55.6	1.4	0.11	6.7	0.18
eaf38 - 133.d	1	0.15	NaN	17.77	< LOD	< LOD	8.9	53.9	1.3	0.21	6.71	0.19
eaf38 - 134.d	1.14	0.17	NaN	14.17	< LOD	< LOD	5	44.9	1.7	0.34	5.69	0.17
eaf38 - 135.d	1.43	0.21	NaN	13.13	< LOD	< LOD	7.2	40.9	1.4	0.13	6.12	0.18
eaf38 - 136.d	1.33	0.15	0.075	19.85	< LOD	< LOD	7	54.6	1.6	0.11	6.85	0.22
eaf38 - 137.d	0.55	0.12	NaN	15.14	< LOD	< LOD	6.9	43.6	1.2	0.14	5.63	0.16
eaf38 - 138.d	0.362	0.09	NaN	9.16	< LOD	< LOD	7	29.7	1.1	0.052	4.19	0.11
eaf38 - 139.d	0.332	0.071	0.038	11.06	< LOD	< LOD	6.4	37	1.2	0.12	4.8	0.12
eaf38 - 140.d	0.7	0.11	0.038	20.97	< LOD	< LOD	5.9	42.4	1.1	0.17	5.32	0.16
eaf38 - 141.d	0.67	0.12	0.052	17.72	< LOD	< LOD	5.7	41	1.2	0.054	5.19	0.11
eaf38 - 142.d	0.93	0.15	NaN	24.73	< LOD	< LOD	6.4	48.5	1.4	0.15	5.83	0.16
eaf38 - 143.d	0.74	0.14	NaN	16.31	< LOD	< LOD	8.8	36.4	1.3	0.054	5.09	0.11

Analysis number	Pb208 ppm	Pb208 ppm 2SE	Pb208 ppm LOD	Th232 ppm	Th232 ppm 2SE	Th232 ppm LOD	U238 ppm	U238 ppm 2SE	U238 ppm LOD	Zr in Tt temp (°C)	grain number	REE group
eaf38 - 2.d	12.74	0.25	0.024	110	2.4	NaN	89.7	1.7	0.0052	771	1	38B
eaf38 - 6.d	17.55	0.31	0.03	158.2	2.2	NaN	112.3	1.7	0.014	766	1	38B
eaf38 - 7.d	17.91	0.32	0.029	159.9	2.6	NaN	108.7	1.7	0.012	763	1	38B
eaf38 - 8.d	14.13	0.18	0.025	128.4	2.9	0.016	101.7	1.8	0.014	763	1	38B
eaf38 - 9.d	14.71	0.26	0.034	127.9	2.7	0.021	118.6	2	0.0054	755	1	38B
eaf38 - 10.d	17.75	0.24	0.043	165.4	2.3	0.021	114.9	1.8	0.0054	757	2	38A
eaf38 - 11.d	17.64	0.31	0.027	157.8	2.1	0.0078	103.2	1.5	0.011	755	2	38A
eaf38 - 12.d	15.65	0.27	0.038	143.3	2.4	0.011	99.8	1.9	0.0074	758	2	38A
eaf38 - 13.d	21.66	0.87	0.034	167.8	3.4	0.008	106.5	1.8	0.0055	763	2	38A
eaf38 - 14.d	10.83	0.18	0.033	92	1.7	0.01	73.4	1.4	0.011	759	3	38A
eaf38 - 15.d	12.99	0.25	0.028	111.8	2.9	0.015	92	2	0.01	763	3	38A
eaf38 - 16.d	13.67	0.27	0.041	119.4	1.9	0.015	63.21	0.93	0.011	758	4	38A
eaf38 - 17.d	12.06	0.15	0.028	107.1	1.8	0.024	64.9	1.1	0.0053	756	4	38A
eaf38 - 18.d	15.88	0.32	0.021	143.4	2.8	NaN	35.76	0.61	0.01	752	5	38A
eaf38 - 19.d	23.06	0.35	0.024	213.3	4.1	NaN	41.92	0.88	0.0052	753	5	38A
eaf38 - 20.d	19.37	0.36	0.027	178.5	2.2	0.0074	37.19	0.63	0.014	753	5	38A
eaf38 - 21.d	17.84	0.28	0.031	161	2.4	0.0075	32.32	0.64	0.01	755	5	38A
eaf38 - 23.d	18.12	0.3	0.033	164	4.5	NaN	42.6	1	0.015	770	5	38A
eaf38 - 24.d	16.44	0.26	0.032	148.7	3	0.021	36.37	0.68	0.014	762	5	38A
eaf38 - 25.d	15.96	0.2	0.024	145.9	2.4	0.0076	33.67	0.56	0.011	760	5	38A
eaf38 - 26.d	23.33	0.33	0.021	213	3.1	0.027	49.6	0.75	0.011	757	6	38A
eaf38 - 27.d	24.55	0.45	0.029	223.1	3.5	0.017	55.25	0.92	0.0074	752	6	38A
eaf38 - 28.d	22.26	0.32	0.025	210.2	3.4	NaN	56.9	1.1	0.011	768	6	38A
eaf38 - 29.d	22.98	0.4	0.028	220.9	5.4	0.012	54.7	1	NaN	775	6	38A
eaf38 - 30.d	20.11	0.36	0.028	201	3.2	0.027	51.34	0.83	0.011	774	6	38A
eaf38 - 31.d	20.47	0.34	0.028	185.2	3.3	0.0078	38.7	0.8	0.011	754	7	38A
eaf38 - 32.d	23.6	0.35	0.027	221.3	3	0.018	47.48	0.85	0.015	758	7	38A
eaf38 - 33.d	17.25	0.38	0.039	167.3	4.1	0.02	44.59	0.98	0.01	764	8	38A
eaf38 - 34.d	20.49	0.4	0.033	198.8	4	0.017	43.08	0.99	0.013	759	7	38A

Analysis number	Pb208 ppm	Pb208 ppm 2SE	Pb208 ppm LOD	Th232 ppm	Th232 ppm 2SE	Th232 ppm LOD	U238 ppm	U238 ppm 2SE	U238 ppm LOD	Zr in Tt temp (°C)	grain number	REE group
eaf38 - 35.d	23.42	0.37	0.035	218.5	2.9	NaN	58.47	0.8	0.0078	752	6	38A
eaf38 - 36.d	22.64	0.31	0.034	212.8	3.7	NaN	56.88	0.96	0.026	756	9	38A
eaf38 - 37.d	21.09	0.34	0.037	192.8	3.1	0.016	58.6	1	NaN	757	9	38A
eaf38 - 38.d	21.04	0.3	0.02	198.3	3.5	0.008	64.3	1.2	0.0089	760	9	38A
eaf38 - 39.d	19.03	0.27	0.029	175.1	3.7	0.022	66.2	1.2	0.011	760	9	38A
eaf38 - 40.d	21.72	0.29	0.029	203	3.1	NaN	59.73	0.96	0.0054	763	9	38A
eaf38 - 41.d	24.86	0.44	0.034	230.3	3.6	NaN	50.65	0.92	0.018	762	9	38A
eaf38 - 42.d	21.83	0.3	0.044	212.8	3.1	NaN	62.87	0.8	NaN	769	9	38A
eaf38 - 43.d	22.03	0.41	0.04	210.7	3.6	NaN	56.66	0.91	NaN	762	9	38A
eaf38 - 44.d	16.86	0.23	0.021	148.1	3.3	0.015	47.92	0.79	0.011	767	9	38A
eaf38 - 45.d	20.04	0.38	0.031	185.3	2.8	0.015	53.53	0.94	NaN	760	9	38A
eaf38 - 46.d	17.78	0.27	0.033	160.4	3.1	NaN	50.5	1.1	0.021	754	9	38A
eaf38 - 47.d	20.86	0.35	0.028	187.7	3.4	0.015	42.54	0.81	NaN	767	10	38A
eaf38 - 48.d	18.1	0.27	0.024	159.6	3.1	NaN	38.88	0.72	0.0072	765	10	38A
eaf38 - 49.d	23.02	0.31	0.018	209.8	3.4	0.015	57.11	0.96	NaN	762	11	38A
eaf38 - 50.d	19.9	0.27	0.027	181.3	2.6	NaN	62.8	1.1	0.011	760	12	38A
eaf38 - 51.d	12.71	0.17	0.035	111.9	1.7	0.012	51.57	0.71	NaN	772	12	38A
eaf38 - 52.d	19.26	0.28	0.027	173.9	3.4	0.018	53.9	1.1	0.011	766	12	38A
eaf38 - 53.d	17.96	0.34	0.035	166.9	3.5	0.017	62.1	1.1	NaN	767	12	38A
eaf38 - 54.d	17.44	0.28	0.025	159.8	3.4	NaN	56.6	1	0.022	765	12	38A
eaf38 - 55.d	22.34	0.47	0.029	217.1	5.3	0.015	69.4	1.2	0.0053	776	12	38A
eaf38 - 56.d	19.01	0.41	0.028	175.5	3.2	0.017	64.8	1.1	0.0054	769	12	38A
eaf38 - 57.d	18.8	0.28	0.025	170.7	3.5	0.011	57.05	0.96	0.0056	760	12	38A
eaf38 - 58.d	18.43	0.33	0.026	174.9	2.9	0.0078	60.28	0.88	0.0054	770	12	38A
eaf38 - 59.d	21.79	0.3	0.033	199.8	4	0.018	28.9	0.54	0.012	749	13	38A
eaf38 - 60.d	22.61	0.43	0.029	207.5	3.9	0.0083	30.28	0.58	0.012	744	13	38A
eaf38 - 61.d	23.8	0.33	0.03	222	3.9	0.018	38.08	0.64	0.011	757	13	38A
eaf38 - 62.d	32.6	2.4	0.027	235.1	4.3	NaN	43.25	0.88	NaN	767	13	38A
eaf38 - 63.d	21.64	0.33	0.024	195.3	3.6	0.016	31.98	0.55	0.012	755	13	38A

Analysis number	Pb208 ppm	Pb208 ppm 2SE	Pb208 ppm LOD	Th232 ppm	Th232 ppm 2SE	Th232 ppm LOD	U238 ppm	U238 ppm 2SE	U238 ppm LOD	Zr in Tt temp (°C)	grain number	REE group
eaf38 - 64.d	26.58	0.44	0.028	248.8	4.5	0.022	48.57	0.82	0.011	757	13	38A
eaf38 - 65.d	25.36	0.39	0.029	243	3.6	NaN	47.54	0.7	0.0055	758	13	38A
eaf38 - 68.d	25.27	0.37	0.03	241	3.9	0.0075	42.6	0.74	0.015	755	15	38A
eaf38 - 69.d	24.41	0.34	0.03	226.7	3.4	NaN	40.68	0.69	0.0071	756	15	38A
eaf38 - 70.d	27.07	0.37	0.032	258.7	3.9	0.022	44.73	0.76	NaN	754	15	38A
eaf38 - 71.d	22.61	0.46	0.024	201.8	3.2	0.024	36.87	0.58	NaN	750	15	38A
eaf38 - 72.d	24.57	0.78	0.03	228.5	4.7	NaN	41.4	0.68	0.0052	755	15	38A
eaf38 - 73.d	21.68	0.45	0.034	205.3	2.9	0.018	36.45	0.58	0.015	747	15	38A
eaf38 - 74.d	22.77	0.37	0.024	215.9	3.4	0.0076	40.79	0.58	0.011	759	15	38A
eaf38 - 75.d	24.97	0.35	0.029	233.9	3.5	NaN	37.97	0.73	0.012	749	15	38A
eaf38 - 76.d	26.35	0.43	0.029	249.7	4.2	NaN	42.07	0.87	0.011	748	15	38A
eaf38 - 77.d	22.11	0.2	0.028	224	3.9	0.0077	40.03	0.62	0.011	755	15	38A
eaf38 - 78.d	19.08	0.27	0.032	171.5	3	0.016	33.99	0.51	0.013	753	15	38A
eaf38 - 79.d	22.44	0.27	0.03	210.6	3.9	0.0077	40.19	0.88	NaN	754	15	38A
eaf38 - 80.d	22.23	0.39	0.028	212.3	2.9	0.0076	41.27	0.59	0.012	764	15	38A
eaf38 - 81.d	22.45	0.42	0.028	213.2	3.7	NaN	43.51	0.78	0.019	763	16	38A
eaf38 - 82.d	25.99	0.43	0.029	226.9	3.6	NaN	43.58	0.81	0.0054	755	16	38A
eaf38 - 83.d	23.03	0.6	0.03	214.5	4.8	0.022	43.9	0.66	0.011	759	16	38A
eaf38 - 84.d	20.86	0.3	0.027	197.1	3.2	0.018	44.79	0.86	0.0056	760	16	38A
eaf38 - 85.d	22.28	0.38	0.025	215.7	3.4	0.008	45.6	0.87	0.011	769	16	38A
eaf38 - 86.d	17.72	0.28	0.037	159	3.2	NaN	39.2	0.69	0.0076	759	16	38A
eaf38 - 87.d	21.59	0.26	0.028	199.8	3.8	NaN	44.42	0.8	0.0055	759	16	38A
eaf38 - 88.d	20.21	0.33	0.029	185.9	2.8	0.018	42.41	0.7	NaN	762	16	38A
eaf38 - 89.d	17.53	0.31	0.03	157.9	2.7	0.016	41.97	0.67	0.012	762	16	38A
eaf38 - 90.d	20.5	0.37	0.027	191.7	3	0.026	44.46	0.76	0.013	771	16	38A
eaf38 - 91.d	17.06	0.25	0.025	164.7	2.3	0.016	43.07	0.62	0.0057	761	16	38A
eaf38 - 92.d	20.8	0.32	0.029	195.2	2.8	0.016	44.02	0.77	NaN	768	16	38A
eaf38 - 93.d	19.36	0.3	0.031	171.8	3.1	NaN	40.24	0.6	0.0056	760	16	38A
eaf38 - 94.d	23.25	0.42	0.026	217.3	3.1	0.0079	44.15	0.79	0.011	761	16	38A

Analysis number	Pb208 ppm	Pb208 ppm 2SE	Pb208 ppm LOD	Th232 ppm	Th232 ppm 2SE	Th232 ppm LOD	U238 ppm	U238 ppm 2SE	U238 ppm LOD	Zr in Tt temp (°C)	grain number	REE group
eaf38 - 95.d	21.13	0.54	0.037	179.4	5	NaN	44.29	0.81	0.015	764	16	38A
eaf38 - 96.d	0.032	0.39	0.045	194.2	3.3	0.017	42.23	0.75	0.013	774	16	38A
eaf38 - 97.d	0.06	0.4	0.027	213.9	3.3	NaN	44.81	0.78	NaN	762	16	38A
eaf38 - 98.d	0.045	0.3	0.027	199.4	3.1	0.0075	39.11	0.59	0.0084	755	16	38A
eaf38 - 99.d	0.076	0.2	0.027	123.6	2.1	0.015	34.66	0.57	0.0053	762	16	38A
eaf38 - 100.d	0.043	0.55	0.031	182.9	4.7	0.0076	62.3	1.4	0.011	764	17	38A
eaf38 - 101.d	0.037	0.29	0.022	168.6	3.1	0.016	58.7	1	0.01	765	17	38A
eaf38 - 102.d	0.037	0.41	0.03	269.2	4.3	0.016	56.8	1.1	0.011	765	17	38A
eaf38 - 103.d	0.047	0.62	0.029	192	2.9	0.02	55.7	1.1	0.018	778	17	38A
eaf38 - 104.d	0.032	0.35	0.026	182.6	3.2	0.0076	57.61	0.92	NaN	765	17	38A
eaf38 - 105.d	0.057	0.52	0.025	253.7	6.9	NaN	58.5	1.7	0.0052	768	17	38A
eaf38 - 106.d	0.054	0.49	0.034	225.1	5.2	NaN	61.2	1.1	0.0053	768	17	38A
eaf38 - 107.d	0.062	0.55	0.029	256.3	4	0.016	61.4	1	NaN	762	17	38A
eaf38 - 108.d	0.069	0.53	0.03	230.9	4.2	0.016	84.3	1.4	0.017	757	18	38A
eaf38 - 109.d	0.06	0.34	0.025	200.3	3.6	NaN	76.6	1.2	0.0056	757	18	38A
eaf38 - 110.d	0.051	0.22	0.028	104.3	1.7	NaN	29.91	0.55	0.0077	759	19	38A
eaf38 - 111.d	0.05	0.16	0.033	82	1.6	0.0082	29.86	0.43	0.016	758	19	38A
eaf38 - 112.d	0.058	0.17	0.037	79.6	1.4	NaN	22.39	0.43	0.0057	760	19	38A
eaf38 - 113.d	0.049	0.25	0.022	159.7	2.3	0.0081	36.87	0.74	0.0056	763	19	38A
eaf38 - 114.d	0.055	0.17	0.037	86.4	1.2	0.008	21.09	0.43	0.011	761	19	38A
eaf38 - 115.d	0.051	0.21	0.035	111.8	2	0.0081	28.71	0.53	0.018	766	19	38A
eaf38 - 116.d	0.05	0.31	0.037	176.2	3.3	0.017	37	0.62	0.0076	767	19	38A
eaf38 - 117.d	0.046	0.33	0.028	131.8	2.4	NaN	28.59	0.52	NaN	762	20	38A
eaf38 - 118.d	0.063	0.14	0.029	74.6	2	NaN	18.94	0.51	0.018	764	20	38A
eaf38 - 119.d	0.049	0.44	0.039	213.2	3.3	0.0079	41.95	0.68	0.011	764	21	38A
eaf38 - 120.d	0.056	0.35	0.038	218	3.6	0.016	44.13	0.62	0.011	764	21	38A
eaf38 - 121.d	0.054	0.39	0.035	151.4	4.5	NaN	37.2	1.1	NaN	761	21	38A
eaf38 - 125.d	0.038	0.33	0.024	139.2	2.7	NaN	89.4	1.5	0.024	752	22	38A
eaf38 - 126.d	0.047	0.26	0.032	135.9	2.9	0.022	39.8	0.79	0.013	760	22	38A

Analysis number	Pb208 ppm	Pb208 ppm 2SE	Pb208 ppm LOD	Th232 ppm	Th232 ppm 2SE	Th232 ppm LOD	U238 ppm	U238 ppm 2SE	U238 ppm LOD	Zr in Tt temp (°C)	grain number	REE group
eaf38 - 127.d	0.041	0.25	0.028	139.9	2.2	0.016	99.2	1.7	0.011	753	22	38A
eaf38 - 128.d	0.041	0.31	0.035	155.4	3.3	NaN	42.02	0.83	0.015	761	22	38A
eaf38 - 129.d	0.054	0.23	0.034	140.6	2.6	0.024	67.7	1.4	0.0076	756	22	38A
eaf38 - 130.d	0.038	0.31	0.032	139	2.2	0.022	41.18	0.87	0.018	760	22	38A
eaf38 - 131.d	0.052	0.27	0.032	148.8	2.7	0.0079	92.5	1.5	0.011	754	22	38A
eaf38 - 132.d	0.047	0.25	0.032	137.6	2.7	0.008	71.9	1.2	0.0056	757	22	38A
eaf38 - 133.d	0.034	0.31	0.034	158.9	2.6	0.017	70.4	1.3	0.015	759	23	38A
eaf38 - 134.d	0.049	0.29	0.039	123.6	2.1	0.017	58.3	1.3	0.0055	750	23	38A
eaf38 - 135.d	0.042	0.3	0.033	105.2	1.5	0.019	52.3	1	0.014	751	23	38A
eaf38 - 136.d	0.054	0.52	0.039	176.9	3.5	0.016	71.4	1.3	0.017	765	23	38A
eaf38 - 137.d	0.057	0.27	0.032	135.3	3.3	NaN	56.2	1	0.024	757	24	38A
eaf38 - 138.d	0.078	0.15	0.018	76.1	1.7	0.0079	38.58	0.93	0.018	740	24	38A
eaf38 - 139.d	0.043	0.21	0.038	97.2	2.1	0.016	49.49	0.97	0.016	740	24	38A
eaf38 - 140.d	0.071	0.4	0.029	200.4	3.1	0.029	53.44	0.85	NaN	756	24	38A
eaf38 - 141.d	0.055	0.6	0.021	163.6	7.8	0.0081	51.9	1.5	0.015	751	24	38A
eaf38 - 142.d	0.035	0.36	0.034	240.2	4.3	0.0082	64.7	1.2	0.0057	756	24	38A
eaf38 - 143.d	0.047	0.55	0.018	148.6	6.6	0.016	49.1	1.3	0.012	746	24	38A

Analysis number	$^{238}U/^{206}Pb$	±1s	$^{207}Pb/^{206}Pb$	±1s	$^{238}U/^{206}Pb$ age (Ma)	±1s	$^{207}Pb/^{206}Pb$ age (Ma)	±1s	Disc (%)	f207%	^{207}Pb-corrected $^{238}U/^{206}Pb$ age (Ma)	±1s
eaf38 - 2.d	4.63033	0.06089	0.09010	0.00130	1261	15	1428	27	11.71	1.23	1246.445256	16.258641
eaf38 - 6.d	4.67912	0.05294	0.08480	0.00125	1249	13	1311	28	4.76	0.44	1243.59668	13.98699
eaf38 - 7.d	4.81755	0.04618	0.09080	0.00085	1216	11	1442	18	15.70	1.64	1197.716954	11.350463
eaf38 - 8.d	4.84383	0.05462	0.08900	0.00085	1210	12	1404	18	13.84	1.38	1194.601781	13.275846
eaf38 - 9.d	4.88500	0.04699	0.09010	0.00125	1201	10	1428	26	15.91	1.62	1182.786335	11.361745
eaf38 - 10.d	4.78687	0.04967	0.08600	0.00090	1223	11	1338	20	8.61	0.81	1213.980249	12.445489
eaf38 - 11.d	4.70390	0.06243	0.08770	0.00155	1243	15	1376	34	9.69	0.96	1231.794024	16.274798
eaf38 - 12.d	4.92191	0.05483	0.09010	0.00100	1192	12	1428	21	16.48	1.67	1174.109864	12.922809
eaf38 - 13.d	4.59548	0.05536	0.11050	0.00310	1269	14	1808	50	29.79	4.52	1216.957307	15.583828
eaf38 - 14.d	4.71525	0.05753	0.09500	0.00130	1240	14	1528	26	18.86	2.17	1215.377206	14.733793
eaf38 - 15.d	4.80334	0.06239	0.09110	0.00125	1219	14	1449	26	15.84	1.66	1200.63972	15.439255
eaf38 - 16.d	4.74272	0.07725	0.09920	0.00170	1233	18	1609	32	23.35	2.90	1200.758848	19.416217
eaf38 - 17.d	4.75657	0.06039	0.09310	0.00140	1230	14	1490	28	17.44	1.92	1208.525438	15.248532
eaf38 - 18.d	4.54630	0.08498	0.11500	0.00225	1282	21	1880	35	31.82	5.18	1221.21101	22.830211
eaf38 - 19.d	4.58470	0.06785	0.11050	0.00185	1272	17	1808	30	29.64	4.50	1219.759876	18.08399
eaf38 - 20.d	4.59981	0.08782	0.12070	0.00195	1268	22	1967	29	35.52	6.19	1196.487872	22.74359
eaf38 - 21.d	4.54842	0.08097	0.12860	0.00245	1281	20	2079	33	38.38	7.40	1194.564456	21.468288
eaf38 - 23.d	4.71753	0.09524	0.12570	0.00365	1239	22	2039	50	39.21	7.17	1158.034266	23.932897
eaf38 - 24.d	4.72437	0.08001	0.11980	0.00275	1238	19	1953	40	36.63	6.22	1167.286041	20.07749
eaf38 - 25.d	4.53154	0.07643	0.11970	0.00260	1285	19	1952	38	34.14	5.92	1216.054974	20.789113
eaf38 - 26.d	4.81993	0.07605	0.11160	0.00200	1215	17	1826	32	33.43	5.02	1159.497738	18.311041
eaf38 - 27.d	4.50646	0.06405	0.10800	0.00180	1292	16	1766	30	26.84	3.96	1245.346879	17.743424
eaf38 - 28.d	4.85345	0.08739	0.09870	0.00160	1208	20	1600	30	24.51	2.97	1174.850306	20.904847
eaf38 - 29.d	4.92688	0.06960	0.12000	0.00200	1191	15	1956	29	39.10	6.51	1120.030046	15.9719
eaf38 - 30.d	4.91449	0.08937	0.10500	0.00185	1194	19	1714	32	30.35	4.08	1149.403398	20.724717
eaf38 - 31.d	4.68585	0.08426	0.12370	0.00255	1247	20	2010	36	37.97	6.80	1169.408785	21.211078
eaf38 - 32.d	4.67688	0.07329	0.10890	0.00170	1249	18	1781	28	29.87	4.38	1199.20672	18.714335
eaf38 - 33.d	4.90462	0.08310	0.10970	0.00245	1196	18	1794	40	33.34	4.82	1143.306786	19.476533
eaf38 - 34.d	4.85586	0.07703	0.12680	0.00280	1207	17	2054	38	41.23	7.52	1123.814643	18.267774
eaf38 - 35.d	4.77051	0.07142	0.10530	0.00190	1227	16	1720	33	28.66	3.93	1182.759194	17.707264
eaf38 - 36.d	4.69712	0.09119	0.10640	0.00245	1244	22	1739	42	28.44	4.00	1198.794247	23.259253

Analysis number	$^{238}U/^{206}Pb$	±1s	$^{207}Pb/^{206}Pb$	±1s	$^{238}U/^{206}Pb$ age (Ma)	±1s	$^{207}Pb/^{206}Pb$ age (Ma)	±1s	Disc (%)	f207%	^{207}Pb-corrected $^{238}U/^{206}Pb$ age (Ma)	±1s
eaf38 - 37.d	4.77051	0.06815	0.10210	0.00180	1227	16	1663	32	26.21	3.41	1188.610551	16.968242
eaf38 - 38.d	4.72666	0.07032	0.09850	0.00140	1237	17	1596	26	22.48	2.76	1206.044333	17.773295
eaf38 - 39.d	4.89234	0.07223	0.09750	0.00165	1199	16	1577	31	23.97	2.83	1167.858167	17.134746
eaf38 - 40.d	4.88989	0.06420	0.09960	0.00135	1199	14	1617	25	25.80	3.17	1164.684414	15.172276
eaf38 - 41.d	4.59765	0.07019	0.11280	0.00215	1269	17	1845	34	31.24	4.90	1212.031348	18.63613
eaf38 - 42.d	4.96443	0.08005	0.09710	0.00150	1183	17	1569	29	24.61	2.86	1151.980483	18.364704
eaf38 - 43.d	4.71298	0.06786	0.10010	0.00155	1240	16	1626	29	23.71	3.00	1206.508913	17.270475
eaf38 - 44.d	4.64795	0.07566	0.11090	0.00220	1256	18	1814	36	30.76	4.66	1202.755828	19.658912
eaf38 - 45.d	4.69260	0.09763	0.10710	0.00195	1245	23	1751	33	28.87	4.11	1198.620829	24.705654
eaf38 - 46.d	4.76818	0.07027	0.10430	0.00165	1227	16	1702	29	27.89	3.76	1185.153494	17.389238
eaf38 - 47.d	4.42081	0.07610	0.11170	0.00200	1315	20	1827	32	28.06	4.43	1261.689465	21.717095
eaf38 - 48.d	4.43889	0.07568	0.11630	0.00235	1310	20	1900	36	31.07	5.22	1247.60059	21.429096
eaf38 - 49.d	4.78687	0.05369	0.10430	0.00160	1223	12	1702	28	28.14	3.79	1180.627258	13.327171
eaf38 - 50.d	4.77284	0.06497	0.09720	0.00165	1226	15	1571	31	21.95	2.61	1196.999005	16.247128
eaf38 - 51.d	4.78218	0.07172	0.10340	0.00205	1224	16	1686	36	27.40	3.64	1183.400418	17.792884
eaf38 - 52.d	4.60198	0.07030	0.10440	0.00180	1268	17	1704	31	25.60	3.53	1226.844205	18.706854
eaf38 - 53.d	4.65904	0.08234	0.09570	0.00155	1253	20	1542	30	18.71	2.19	1228.425779	21.475998
eaf38 - 54.d	4.88744	0.07558	0.10820	0.00210	1200	17	1769	35	32.18	4.56	1149.908779	17.830137
eaf38 - 55.d	4.77517	0.06395	0.09130	0.00165	1226	15	1453	34	15.64	1.66	1207.206862	16.117457
eaf38 - 56.d	4.78218	0.07062	0.09410	0.00145	1224	16	1510	29	18.94	2.12	1200.365656	17.559884
eaf38 - 57.d	4.93434	0.07565	0.11000	0.00170	1190	16	1799	28	33.89	4.91	1136.047178	17.340446
eaf38 - 58.d	4.84383	0.07442	0.09810	0.00200	1210	17	1588	38	23.83	2.86	1178.213697	18.088531
eaf38 - 59.d	4.43285	0.08320	0.14190	0.00300	1311	22	2251	36	41.73	9.40	1198.862472	23.01284
eaf38 - 60.d	4.55054	0.08206	0.14470	0.00285	1281	21	2284	34	43.94	10.02	1163.159652	21.468705
eaf38 - 61.d	4.67241	0.08061	0.12410	0.00275	1250	19	2016	39	37.99	6.84	1171.952485	20.542276
eaf38 - 62.d	3.87698	0.09864	0.19500	0.01050	1479	33	2785	86	46.88	17.21	1247.599071	39.633108
eaf38 - 63.d	4.55690	0.08226	0.12860	0.00280	1279	21	2079	38	38.48	7.41	1192.387856	21.864436
eaf38 - 64.d	4.55690	0.07616	0.11180	0.00210	1279	19	1829	34	30.07	4.67	1224.557199	20.502398
eaf38 - 65.d	4.83185	0.09951	0.10630	0.00220	1213	22	1737	37	30.19	4.18	1166.268201	23.849217
eaf38 - 68.d	4.74272	0.07506	0.11430	0.00170	1233	18	1869	27	34.01	5.35	1172.985461	18.497028
eaf38 - 69.d	4.73123	0.10249	0.11070	0.00225	1236	24	1811	36	31.74	4.75	1182.406442	25.436751

Analysis number	$^{238}U/^{206}Pb$	±1s	$^{207}Pb/^{206}Pb$	±1s	$^{238}U/^{206}Pb$ age (Ma)	±1s	$^{207}Pb/^{206}Pb$ age (Ma)	±1s	Disc (%)	f207%	^{207}Pb-corrected $^{238}U/^{206}Pb$ age (Ma)	±1s
eaf38 - 70.d	4.75889	0.06896	0.11140	0.00195	1230	16	1822	31	32.53	4.90	1174.402951	17.08915
eaf38 - 71.d	4.43084	0.08896	0.13530	0.00290	1312	23	2168	37	39.49	8.32	1212.391738	24.662889
eaf38 - 72.d	4.71070	0.07099	0.11460	0.00220	1241	17	1874	34	33.77	5.36	1180.22541	17.945169
eaf38 - 73.d	4.59332	0.08342	0.11660	0.00250	1270	21	1905	38	33.34	5.51	1205.929394	22.029757
eaf38 - 74.d	4.71753	0.07654	0.11800	0.00205	1239	18	1926	31	35.66	5.92	1172.269492	19.072039
eaf38 - 75.d	4.58685	0.07193	0.12020	0.00210	1271	18	1959	31	35.11	6.09	1200.746345	18.959631
eaf38 - 76.d	4.79156	0.08314	0.11750	0.00260	1222	19	1919	39	36.31	5.94	1155.469051	20.243189
eaf38 - 77.d	5.04649	0.09376	0.11590	0.00260	1165	19	1894	40	38.47	5.99	1101.190566	20.54599
eaf38 - 78.d	4.79156	0.10608	0.12600	0.00285	1222	24	2043	39	40.19	7.31	1139.999345	25.297711
eaf38 - 79.d	4.76818	0.07355	0.11560	0.00185	1227	17	1889	29	35.04	5.60	1164.483028	17.968882
eaf38 - 80.d	4.78922	0.08761	0.10960	0.00255	1222	20	1793	42	31.81	4.65	1170.409065	21.490848
eaf38 - 81.d	4.67241	0.08491	0.10990	0.00210	1250	20	1798	34	30.46	4.54	1198.463039	21.719078
eaf38 - 82.d	4.38510	0.05603	0.13480	0.00210	1324	15	2161	27	38.73	8.16	1225.769301	16.138926
eaf38 - 83.d	4.64133	0.08498	0.11220	0.00220	1258	21	1835	35	31.47	4.86	1201.992108	21.986422
eaf38 - 84.d	4.68136	0.08089	0.10710	0.00240	1248	19	1751	40	28.71	4.09	1201.437808	20.843192
eaf38 - 85.d	5.02572	0.07318	0.10990	0.00140	1170	15	1798	23	34.93	5.01	1116.04268	16.120626
eaf38 - 86.d	4.71298	0.07858	0.11950	0.00245	1240	19	1949	36	36.35	6.15	1170.600552	19.711081
eaf38 - 87.d	4.65682	0.06860	0.10690	0.00175	1254	17	1747	30	28.23	4.02	1208.010294	17.771136
eaf38 - 88.d	4.76585	0.07791	0.11230	0.00230	1228	18	1837	37	33.16	5.06	1171.077708	19.250162
eaf38 - 89.d	4.68136	0.08955	0.11560	0.00260	1248	21	1889	40	33.94	5.48	1185.597683	22.773076
eaf38 - 90.d	4.82708	0.09699	0.11910	0.00310	1214	22	1943	46	37.53	6.24	1144.27075	23.23154
eaf38 - 91.d	5.01026	0.08506	0.10950	0.00230	1173	18	1791	38	34.50	4.92	1120.102339	19.053323
eaf38 - 92.d	4.61720	0.07584	0.11310	0.00220	1264	19	1850	35	31.68	4.97	1206.438985	19.901798
eaf38 - 93.d	4.63253	0.09001	0.11890	0.00285	1260	22	1940	42	35.04	5.94	1191.609505	23.35629
eaf38 - 94.d	4.68810	0.07359	0.11320	0.00205	1246	18	1851	32	32.68	5.10	1188.396261	18.714084
eaf38 - 95.d	4.56542	0.08975	0.15090	0.00320	1277	22	2356	36	45.81	11.04	1147.609313	23.155803
eaf38 - 96.d	4.42081	0.06486	0.12570	0.00245	1315	17	2039	34	35.52	6.73	1234.036572	18.525708
eaf38 - 97.d	4.81755	0.07599	0.10790	0.00210	1216	17	1764	35	31.08	4.42	1166.755071	18.43987
eaf38 - 98.d	4.70843	0.07629	0.12070	0.00225	1242	18	1967	33	36.87	6.34	1169.481987	19.095022
eaf38 - 99.d	4.58040	0.07480	0.11850	0.00250	1273	19	1934	37	34.17	5.80	1205.639769	19.941043
eaf38 - 100.d	4.52315	0.07420	0.12800	0.00355	1288	19	2071	48	37.82	7.26	1202.251979	20.620356

Analysis number	$^{238}U/^{206}Pb$	±1s	$^{207}Pb/^{206}Pb$	±1s	$^{238}U/^{206}Pb$ age (Ma)	±1s	$^{207}Pb/^{206}Pb$ age (Ma)	±1s	Disc (%)	f207%	^{207}Pb-corrected $^{238}U/^{206}Pb$ age (Ma)	±1s
eaf38 - 101.d	4.63472	0.05413	0.09890	0.00135	1259	13	1603	25	21.46	2.68	1228.711402	14.312025
eaf38 - 102.d	4.65017	0.07783	0.10030	0.00185	1256	19	1630	34	22.95	2.93	1222.087068	20.351924
eaf38 - 103.d	4.40288	0.07276	0.12820	0.00215	1319	19	2073	29	36.37	7.11	1234.003691	20.569181
eaf38 - 104.d	4.81518	0.06481	0.10210	0.00165	1216	15	1663	30	26.84	3.47	1177.823376	15.826201
eaf38 - 105.d	4.88256	0.07661	0.10090	0.00200	1201	17	1641	36	26.79	3.37	1164.071954	18.237731
eaf38 - 106.d	4.69937	0.06859	0.09700	0.00190	1244	16	1567	36	20.64	2.47	1215.683577	17.74483
eaf38 - 107.d	4.66794	0.07200	0.09760	0.00145	1251	17	1579	28	20.74	2.52	1222.577941	18.684665
eaf38 - 108.d	4.74733	0.06335	0.09370	0.00125	1232	15	1502	25	17.96	2.00	1209.726504	15.981447
eaf38 - 109.d	4.90955	0.07383	0.10070	0.00160	1195	16	1637	29	27.00	3.37	1158.171463	17.289283
eaf38 - 110.d	4.46731	0.09227	0.12700	0.00280	1302	24	2057	38	36.69	7.02	1218.915295	25.35941
eaf38 - 111.d	4.47140	0.09742	0.13830	0.00355	1301	25	2206	44	41.02	8.87	1195.772881	26.579511
eaf38 - 112.d	4.32301	0.10191	0.15430	0.00385	1341	28	2394	42	43.97	11.26	1203.646906	29.095252
eaf38 - 113.d	4.77517	0.09395	0.11960	0.00235	1226	22	1950	35	37.15	6.25	1155.510914	22.714538
eaf38 - 114.d	4.12236	0.09341	0.15190	0.00415	1400	28	2367	46	40.86	10.54	1266.100885	29.729527
eaf38 - 115.d	4.60632	0.09863	0.13730	0.00390	1266	24	2193	49	42.26	8.89	1163.400314	25.607038
eaf38 - 116.d	4.80098	0.08004	0.11930	0.00210	1220	18	1946	31	37.31	6.24	1149.984024	19.216019
eaf38 - 117.d	4.29073	0.08491	0.14150	0.00340	1351	24	2246	41	39.86	9.11	1238.546713	25.191011
eaf38 - 118.d	4.15745	0.11228	0.17600	0.00500	1389	33	2616	47	46.88	14.55	1205.020426	33.936344
eaf38 - 119.d	4.56755	0.07953	0.12150	0.00240	1276	20	1978	35	35.49	6.27	1203.228514	21.108845
eaf38 - 120.d	4.45508	0.06946	0.11870	0.00210	1305	18	1937	31	32.60	5.64	1238.452351	19.453488
eaf38 - 121.d	4.43688	0.07276	0.12700	0.00295	1310	19	2057	40	36.30	6.97	1227.102572	20.680735
eaf38 - 125.d	4.76585	0.05848	0.09700	0.00135	1228	14	1567	26	21.65	2.57	1199.08179	14.630365
eaf38 - 126.d	4.47140	0.08350	0.12210	0.00220	1301	22	1987	32	34.52	6.22	1227.388009	22.950769
eaf38 - 127.d	4.73123	0.06829	0.09900	0.00130	1236	16	1605	24	23.00	2.85	1203.980013	17.201433
eaf38 - 128.d	4.26265	0.06374	0.13410	0.00240	1359	18	2152	31	36.88	7.85	1261.703591	19.341904
eaf38 - 129.d	4.74964	0.08520	0.10060	0.00165	1232	20	1635	30	24.68	3.13	1196.475906	21.241928
eaf38 - 130.d	4.69712	0.07705	0.12630	0.00205	1244	18	2047	28	39.22	7.24	1161.839324	19.151431
eaf38 - 131.d	4.78452	0.05570	0.09070	0.00115	1224	13	1440	24	15.05	1.57	1205.990837	13.91068
eaf38 - 132.d	4.74502	0.06120	0.09590	0.00125	1233	14	1546	24	20.25	2.36	1206.25635	15.418815
eaf38 - 133.d	4.73812	0.06315	0.09890	0.00140	1234	15	1603	26	23.02	2.84	1202.452196	15.921304
eaf38 - 134.d	4.72209	0.07994	0.10030	0.00195	1238	19	1630	36	24.02	3.04	1203.860612	20.292211

Analysis number	$^{238}U/^{206}Pb$	±1s	$^{207}Pb/^{206}Pb$	±1s	$^{238}U/^{206}Pb$ age (Ma)	±1s	$^{207}Pb/^{206}Pb$ age (Ma)	±1s	Disc (%)	f207%	^{207}Pb-corrected $^{238}U/^{206}Pb$ age (Ma)	±1s
eaf38 - 135.d	4.64795	0.07148	0.11880	0.00195	1256	17	1938	29	35.19	5.95	1187.927683	18.342485
eaf38 - 136.d	4.73353	0.06942	0.10090	0.00160	1236	16	1641	29	24.70	3.16	1199.907276	17.499924
eaf38 - 137.d	4.81044	0.05826	0.10240	0.00160	1218	13	1668	29	27.01	3.51	1178.41484	14.296808
eaf38 - 138.d	4.79156	0.07976	0.11410	0.00250	1222	18	1866	39	34.51	5.39	1161.657312	19.514194
eaf38 - 139.d	4.89234	0.08273	0.10230	0.00190	1199	18	1666	34	28.05	3.61	1159.301447	19.490642
eaf38 - 140.d	4.73123	0.05885	0.09950	0.00160	1236	14	1615	30	23.45	2.93	1203.057943	14.969733
eaf38 - 141.d	4.76818	0.06810	0.10080	0.00150	1227	16	1639	27	25.11	3.19	1191.556734	16.903399
eaf38 - 142.d	4.88989	0.07333	0.09540	0.00155	1199	16	1536	30	21.91	2.49	1172.175577	17.424744
eaf38 - 143.d	5.02572	0.09558	0.11320	0.00235	1170	20	1851	37	36.81	5.54	1110.317065	21.080008

Analysis number	Reason for exclusion
eaf38 - 1.d	zircon inclusion
eaf38 - 3.d	zircon inclusion
eaf38 - 4.d	re-analysis of spot 3
eaf38 - 5.d	zircon inclusion
eaf38 - 22.d	re-analysis of spot 21
eaf38 - 66.d	not titanite
eaf38 - 67.d	not titanite
eaf38 - 122.d	not titanite
eaf38 - 123.d	not titanite
eaf38 - 124.d	not titanite

Table A6.4-5 LA-ICPMS analytical data for sample DG02.

Analysis number	Na23 ppm	Na23 ppm 2SE	Na23 ppm LOD	Al27 ppm	Al27 ppm 2SE	Al27 ppm LOD	Si28 ppm	Si28 ppm 2SE	Si28 ppm LOD	Ca44 ppm	Ca44 ppm 2SE	Ca44 ppm LOD
dg02 - 1.d	177	36	23	7169	98	2	141400	1900	3100	203700	2800	310
dg02 - 2.d	111.3	9.7	39	7724	86	3.2	145100	2200	8500	201400	2700	260
dg02 - 3.d	113	10	28	7311	93	3.8	146600	2100	4100	204800	2500	260
dg02 - 4.d	213	14	31	7459	73	2.8	143600	1900	6600	196600	3100	340
dg02 - 5.d	163.5	8.8	24	7423	85	3.7	144300	2100	3900	204800	2600	250
dg02 - 6.d	161.7	7.7	21	7365	91	5.1	146400	1800	5000	206300	2500	290
dg02 - 7.d	141.3	9.5	30	7248	81	4	143100	2400	7500	211100	2700	280
dg02 - 8.d	116.4	8.8	21	7730	110	3.9	145400	2600	7900	208700	2600	290
dg02 - 9.d	98.4	6.8	24	6856	92	2.9	148000	1700	8900	209500	2200	350
dg02 - 10.d	193	16	26	7436	82	3.2	144700	2000	4900	206800	2300	230
dg02 - 11.d	112	12	23	6950	100	3.6	149800	2200	3900	208500	2700	290
dg02 - 12.d	244	17	21	7295	74	3	147500	2500	6700	198500	2900	310
dg02 - 13.d	149	11	20	7140	99	2.3	146600	1700	5600	202500	2600	230
dg02 - 14.d	105.5	8.9	22	7140	110	3.5	144100	2200	7600	210100	3200	280
dg02 - 15.d	145	16	32	9180	120	3	140800	2200	5200	206300	2300	360
dg02 - 16.d	150	20	19	8950	110	3.6	142200	1600	6600	205500	2700	300
dg02 - 17.d	1620	300	21	10120	410	3.5	140200	2300	5000	199500	4000	340
dg02 - 18.d	78.9	8.1	23	8880	120	2.6	141900	2500	6300	209600	2600	260
dg02 - 19.d	2320	110	16	11430	150	3.2	141300	2400	4200	192500	3000	320
dg02 - 20.d	101.7	9	21	8400	120	3.5	140200	2300	5100	207000	2500	310
dg02 - 21.d	129.4	8.4	24	8396	99	3.9	143800	2700	6900	209200	3200	400
dg02 - 22.d	149	11	35	8120	110	4.5	142800	2400	6800	205700	2800	350
dg02 - 23.d	118.7	8.3	26	7920	120	4	145500	2800	9900	208800	2800	200
dg02 - 24.d	201.2	9.2	22	8020	76	5.1	143100	1700	8100	204800	1800	390
dg02 - 25.d	363	67	23	8640	110	3.6	142700	2300	3200	203500	3100	250
dg02 - 26.d	730	120	32	8840	130	3.9	146600	2400	6500	191200	3400	210
dg02 - 27.d	372	22	20	8910	100	4.9	143800	2400	3300	190800	2900	270
dg02 - 28.d	103.1	7.7	29	7930	110	4.4	147800	2400	7500	204600	2100	320

Analysis number	Na23 ppm	Na23 ppm 2SE	Na23 ppm LOD	Al27 ppm	Al27 ppm 2SE	Al27 ppm LOD	Si28 ppm	Si28 ppm 2SE	Si28 ppm LOD	Ca44 ppm	Ca44 ppm 2SE	Ca44 ppm LOD
dg02 - 29.d	2691	62	22	12710	200	3.4	144600	1800	6200	186700	2200	340
dg02 - 30.d	680	110	23	9450	170	3.6	144200	2100	5700	197200	3100	220
dg02 - 31.d	165	10	18	7750	100	4	144600	2200	7600	210000	3700	400
dg02 - 32.d	137.5	7	26	8393	84	3.6	144900	2500	5400	211200	3100	370
dg02 - 33.d	480	90	43	12610	330	3.9	147700	2800	8900	182000	2600	300
dg02 - 34.d	82.9	8.5	20	7609	99	3.7	146200	2100	8000	209100	3400	380
dg02 - 35.d	320	58	28	7662	88	5.3	145000	2400	7200	206300	2600	300
dg02 - 36.d	5570	140	23	18870	270	5.2	146000	1800	5200	170500	2700	280
dg02 - 37.d	130.8	9.4	30	7520	100	3.1	145500	2500	6200	205800	2800	260
dg02 - 38.d	93.6	6.9	24	7027	99	2.8	146600	2100	8300	209900	2300	250
dg02 - 39.d	106.1	7.7	19	7580	100	2.6	144300	2700	4400	208800	3000	240
dg02 - 40.d	111	11	27	7467	81	3.6	146500	2200	4100	209000	2700	230
dg02 - 41.d	131.2	8.4	23	7308	82	3.7	146100	2000	5100	205800	3000	300
dg02 - 42.d	108.8	7.9	34	7043	97	2.6	141500	2200	8700	207600	3100	230
dg02 - 43.d	134.1	9.5	30	7518	87	2.8	144800	2500	4800	207600	2500	260
dg02 - 44.d	176.1	9.9	24	7499	71	2.8	144300	2600	8200	210800	2800	300
dg02 - 45.d	98.8	7.5	37	7160	110	3	144500	2300	6900	212800	2800	220
dg02 - 46.d	90.8	9.6	29	6923	85	2.9	147400	2400	6200	208400	2600	280
dg02 - 47.d	116.3	9.4	19	7231	91	3.7	144300	2200	7900	206000	2700	270
dg02 - 48.d	119	11	23	7110	88	3.7	145000	2500	9100	206600	3000	280
dg02 - 49.d	98.2	7.4	20	7247	90	3.4	148100	2300	4000	210200	2600	320
dg02 - 50.d	102.1	5.9	25	7466	73	4.8	145900	2500	9000	207000	2500	310
dg02 - 51.d	129	10	15	7235	93	4.8	146400	2400	5700	206500	2400	220
dg02 - 52.d	102.6	6.9	25	7232	92	4.2	145000	2100	10000	213400	2800	310
dg02 - 53.d	195	15	25	7760	110	3.4	145200	2500	7200	204300	2600	390
dg02 - 54.d	126.1	9.5	18	7420	110	3	146000	2300	8900	210200	2600	350
dg02 - 55.d	116.1	9.1	29	7520	110	4.4	142700	2000	3300	213100	3100	250
dg02 - 56.d	125.5	8.4	25	7411	81	3.6	146200	2400	5600	212600	2700	250
dg02 - 57.d	102	10	20	7300	120	3.5	145300	2100	7700	210900	2600	250

Analysis number	Na23 ppm	Na23 ppm 2SE	Na23 ppm LOD	Al27 ppm	Al27 ppm 2SE	Al27 ppm LOD	Si28 ppm	Si28 ppm 2SE	Si28 ppm LOD	Ca44 ppm	Ca44 ppm 2SE	Ca44 ppm LOD
dg02 - 58.d	103.4	7.2	20	7410	110	2.2	145800	1900	6000	213100	3000	280
dg02 - 59.d	600	130	27	7920	180	3	144700	2200	6200	205900	3300	340
dg02 - 60.d	101.4	6.8	34	7199	87	4	147300	1900	11000	208500	2600	270
dg02 - 62.d	499	22	25	8790	180	4.4	149100	2600	8700	205100	2800	230
dg02 - 63.d	127	11	31	7525	87	4	145500	2200	4300	209000	2800	160
dg02 - 64.d	155	18	24	7374	80	2.9	146100	2400	5200	210500	3000	290
dg02 - 65.d	109	12	21	7423	88	4	148100	2800	6200	208800	2500	330
dg02 - 66.d	113.1	6.7	22	7265	90	4.1	147000	1900	3500	208800	2100	270
dg02 - 67.d	204	58	26	7099	89	3.3	146400	2500	5000	208200	2600	350
dg02 - 68.d	164	21	26	7237	77	3	149200	2300	5800	211500	2700	230
dg02 - 69.d	122.2	9.7	17	7457	96	4.4	146700	2300	7400	209900	3100	330
dg02 - 70.d	117.3	8.2	29	7300	77	3.5	145900	2800	7700	211400	2000	240
dg02 - 71.d	95.2	9.7	34	7450	110	1.7	143300	2300	5700	212300	3200	310
dg02 - 72.d	154	11	25	7690	95	5.1	146700	2600	5500	207600	2200	230
dg02 - 73.d	128	9.8	20	8219	94	3.7	149100	1900	6900	211300	1700	290
dg02 - 74.d	175.7	9.8	29	9220	130	4.5	143300	2300	8800	205800	2200	280
dg02 - 75.d	1537	41	23	12580	300	3.2	142800	2700	8100	190100	3200	200
dg02 - 76.d	208	13	37	8953	95	2.9	144200	2400	14000	204500	2600	270
dg02 - 77.d	132	10	34	8570	150	3	145600	3000	7900	209200	3100	310
dg02 - 78.d	215.6	9.7	26	8740	100	3.9	149800	2100	6600	202700	2800	260
dg02 - 79.d	91.5	6.9	22	9160	110	4.8	142900	2300	7700	211500	2400	250
dg02 - 80.d	398	11	28	8040	110	2.9	145900	1700	7700	209100	3100	400
dg02 - 82.d	103	11	27	8500	100	3.5	146500	2500	5800	209900	2000	340
dg02 - 83.d	126	11	20	8360	120	4.4	145600	2100	2600	207700	3000	290
dg02 - 84.d	131.1	8.6	21	8060	100	3.8	149100	2000	2800	206600	3000	270
dg02 - 85.d	2090	200	24	11700	260	3.6	150000	2200	9300	196600	3100	350
dg02 - 86.d	124.9	9.4	23	8670	140	4.2	147200	2600	4900	207500	2900	270
dg02 - 87.d	331	11	27	8524	99	3.7	149700	2000	7500	199700	2200	330
dg02 - 88.d	47.2	7.3	25	9890	110	3.4	149100	2200	7500	212800	2700	390

Analysis number	Na23 ppm	Na23 ppm 2SE	Na23 ppm LOD	Al27 ppm	Al27 ppm 2SE	Al27 ppm LOD	Si28 ppm	Si28 ppm 2SE	Si28 ppm LOD	Ca44 ppm	Ca44 ppm 2SE	Ca44 ppm LOD
dg02 - 89.d	157	12	33	7509	95	3.7	146500	2000	8900	207400	3100	300
dg02 - 90.d	137.5	9.7	21	7860	110	4.8	148200	2300	4800	209100	3000	210
dg02 - 91.d	61.6	8.2	27	8926	97	3	143400	2400	12000	217400	2800	320
dg02 - 92.d	75.4	7.1	24	8142	91	4.1	146400	2200	5000	215200	2300	300
dg02 - 95.d	88.3	9.6	21	7118	99	3.3	147700	2500	8600	214900	3200	320
dg02 - 96.d	99.4	7.4	26	7193	90	2.6	145600	2100	7900	214300	2300	280
dg02 - 97.d	85.4	8.3	24	6705	85	3.7	149500	2600	4800	213600	2500	260
dg02 - 98.d	80.8	7.8	25	7360	100	2.2	148300	2400	6400	217400	3200	220
dg02 - 99.d	67.5	6.8	24	6920	110	3.2	149100	2000	4700	215300	2900	350
dg02 - 100.d	81.1	6.5	25	7346	91	2.6	149200	2100	4300	215600	3100	150
dg02 - 101.d	1530	150	38	9540	170	2.5	150800	2500	6300	208600	4200	240
dg02 - 103.d	2820	190	25	11760	370	4.7	150100	2200	8500	192500	3500	280
dg02 - 104.d	91.7	9	32	8320	110	3.1	148700	2500	9700	214700	3400	340
dg02 - 105.d	100	10	34	8860	100	3.6	147000	2400	7300	213800	2500	320
dg02 - 106.d	2100	260	20	11060	440	4.2	147500	2800	5600	199400	3700	240
dg02 - 107.d	3190	570	28	13100	1000	2	147700	1800	6300	189000	6300	250
dg02 - 110.d	49	8	26	9000	130	3.6	148100	1900	8500	216400	2600	320
dg02 - 111.d	67.1	6.4	31	7150	130	3	148600	2800	8200	213800	3600	330

Analysis number	Ti49 ppm	Ti49 ppm 2SE	Ti49 ppm LOD	V51 ppm	V51 ppm 2SE	V51 ppm LOD	Cr52 ppm	Cr52 ppm 2SE	Cr52 ppm LOD	Mn55 ppm	Mn55 ppm 2SE	Mn55 ppm LOD
dg02 - 1.d	226500	3700	2.1	533.3	8	0.29	16	1.3	3.3	1185	16	6
dg02 - 2.d	222700	2700	2.1	523.9	7	0.33	22.4	1.7	4.6	1141	16	10
dg02 - 3.d	228000	2900	4.2	522	7	0.44	16.6	1.4	4.6	1244	18	6.2
dg02 - 4.d	228900	2500	NaN	526.1	8.5	0.31	17.6	1.6	5.1	1199	14	7.9
dg02 - 5.d	232700	2900	1.1	532.1	6.8	0.32	16.2	1.7	3	1264	18	6.9
dg02 - 6.d	233600	3000	2.2	548.7	8.2	0.32	16.3	1.6	4.9	1236	19	8.9
dg02 - 7.d	233000	3100	3	517.2	9.6	0.37	15.8	1.6	4.6	1127	16	10
dg02 - 8.d	231100	2800	NaN	480.4	7.9	0.27	16.6	1.8	4.9	1256	16	9
dg02 - 9.d	231800	2300	2.2	539.1	7.6	0.42	20.3	1.1	4.6	1079	14	11
dg02 - 10.d	232100	3000	NaN	513.5	7.9	0.19	15.9	1.4	3.4	1153	11	5.9
dg02 - 11.d	233500	3200	NaN	547.3	8	0.25	17.9	1.5	3.9	1091	13	4.6
dg02 - 12.d	225000	3300	3	471.4	7.7	0.38	15.1	1.7	5.1	1076	12	9.9
dg02 - 13.d	228900	3200	NaN	480.8	5.3	0.3	15	1.3	4.3	1103	15	5.1
dg02 - 14.d	235600	3000	2.2	477.4	8.3	0.33	15.2	1.2	4.3	1154	18	8.5
dg02 - 15.d	225500	2200	2.5	472.9	6.2	0.39	18.4	1.5	4.6	1066	14	9.7
dg02 - 16.d	222400	2400	NaN	460	5.9	0.36	19.2	1.7	4.2	1086	13	7.4
dg02 - 17.d	217700	4400	NaN	435	10	0.36	14.4	1.7	3.1	1080	23	7.4
dg02 - 18.d	229900	2700	3	467.1	7.7	0.32	23.4	1.5	5.2	1168	17	9.8
dg02 - 19.d	212300	2800	1.1	408.4	5.5	0.36	12.8	1.4	3.9	1081	14	6.3
dg02 - 20.d	228000	2700	NaN	451.5	5.4	0.4	20.2	1.7	5.1	1236	15	8.3
dg02 - 21.d	232800	2700	3	456.4	6.7	0.27	19.9	1.6	3	1263	20	8.6
dg02 - 22.d	230800	3800	1.1	439	7.2	0.48	17	1.5	3.3	1111	18	8.3
dg02 - 23.d	231700	3200	NaN	446.5	6.2	0.46	31.1	1.6	4.2	1190	19	9.9
dg02 - 24.d	230400	2800	1.1	432	6.1	0.25	19.5	1.4	5.6	1258	14	9.1
dg02 - 25.d	223800	3700	NaN	437.8	7.3	0.53	20.6	1.6	3.4	944	18	5.2
dg02 - 26.d	225500	4000	NaN	446	12	0.37	17.6	1.4	5.8	954	18	9.5
dg02 - 27.d	221400	3100	NaN	435.1	6.2	0.46	22.9	1.5	3.3	1252	22	7.1
dg02 - 28.d	227700	2800	1	433.2	5.9	0.57	18.8	1.3	5.3	1280	17	5.6
dg02 - 29.d	205900	2700	2.1	393	6.1	0.48	15.7	1.5	4.6	1045	13	8.4

Analysis number	Ti49 ppm	Ti49 ppm 2SE	Ti49 ppm LOD	V51 ppm	V51 ppm 2SE	V51 ppm LOD	Cr52 ppm	Cr52 ppm 2SE	Cr52 ppm LOD	Mn55 ppm	Mn55 ppm 2SE	Mn55 ppm LOD
dg02 - 30.d	224500	3400	2.5	445.4	7.3	0.39	19.1	2.1	4.4	994	15	8.6
dg02 - 31.d	232300	3500	NaN	450.7	9	0.25	11.7	1.7	3.6	1141	19	8.6
dg02 - 32.d	231900	3000	NaN	451.9	5.4	0.4	12.2	1.5	4.4	1233	12	7.5
dg02 - 33.d	201700	2900	2.5	427.1	6.5	0.51	22.1	1.9	4	1227	16	9.8
dg02 - 34.d	229600	2800	NaN	546.7	7.8	0.33	18.2	1.7	3.7	1091	17	8.2
dg02 - 35.d	227200	3100	NaN	485.8	9.2	0.38	14.4	1.4	4.2	964	13	5.2
dg02 - 36.d	181900	2300	1.1	396.7	9	0.46	11.7	1.5	4.7	798	13	6.9
dg02 - 37.d	226200	3100	2.2	450.3	7.5	0.46	11.7	1.4	2.9	1172	18	8
dg02 - 38.d	231100	2700	1.1	465.4	7.6	0.39	10	1.2	5.5	1191	15	8.6
dg02 - 39.d	229400	3300	NaN	448.2	7.9	0.49	12.4	1.6	4.4	1258	20	6.2
dg02 - 40.d	229800	2600	4.4	861	11	0.25	342.6	7.2	4.4	1072	12	7.2
dg02 - 41.d	228800	3100	1.1	484	8.9	0.35	17	1.5	3.9	1149	16	5.7
dg02 - 42.d	229800	3000	2.2	492.5	7.4	0.35	14.8	1.5	4.7	1176	19	9.4
dg02 - 43.d	229200	2500	2.2	535.2	7.2	0.55	15.8	1.2	4.7	1074	13	6.4
dg02 - 44.d	234400	2500	3.2	503.1	6.5	0.21	11.2	1.6	3.9	1209	15	9
dg02 - 45.d	231900	3300	2.4	530.1	8.2	0.37	13.5	1.4	3.9	1142	17	9.5
dg02 - 46.d	232100	3000	NaN	558	5.2	0.28	17.7	1.4	3.6	1000	15	12
dg02 - 47.d	229600	3600	1.1	500.5	7.8	0.31	13.3	1.5	3.5	1089	17	6.4
dg02 - 48.d	228500	2600	NaN	489.1	6.6	0.35	12.5	1.5	6.8	1124	14	10
dg02 - 49.d	230000	2900	2.3	516.3	8.7	0.33	14.7	1.5	5.6	1108	16	5.8
dg02 - 50.d	230900	2600	2.1	530.6	6.2	0.32	14.4	1.6	2.9	1092	14	10
dg02 - 51.d	229100	3100	2.1	494.8	8.5	0.31	11.4	1.4	4.9	1073	10	7.5
dg02 - 52.d	235800	3200	3.1	535.1	8.9	0.35	12.9	1.3	5.3	1157	14	13
dg02 - 53.d	231200	2900	3	503.3	8.4	0.35	13.2	1.6	3.4	1101	14	9.1
dg02 - 54.d	229000	3100	2.1	538.5	8.8	0.33	15.6	1.7	4.5	1148	16	9.9
dg02 - 55.d	232600	3100	2.5	482	7.1	0.38	9.1	1.4	5.4	1240	17	5.6
dg02 - 56.d	232900	2700	2.7	540.5	7.7	0.31	11.1	1.3	4.2	1140	18	9.6
dg02 - 57.d	230300	3000	2.6	518.5	9.1	0.25	12.8	1.5	4.2	1129	15	8.9
dg02 - 58.d	230900	3400	1.1	458.6	7.8	0.41	10.8	1.4	3.9	1198	17	9.8

Analysis number	Ti49 ppm	Ti49 ppm 2SE	Ti49 ppm LOD	V51 ppm	V51 ppm 2SE	V51 ppm LOD	Cr52 ppm	Cr52 ppm 2SE	Cr52 ppm LOD	Mn55 ppm	Mn55 ppm 2SE	Mn55 ppm LOD
dg02 - 59.d	228300	2800	2.5	494.1	6.8	0.38	10.1	1.2	4	1173	14	7
dg02 - 60.d	228900	2600	1.5	565.5	8.6	0.22	16.6	1.4	4.2	1070	14	12
dg02 - 62.d	222600	3200	1.1	454.6	6.7	0.2	14.4	1.3	4.9	1292	17	7.9
dg02 - 63.d	229400	2700	12	494.3	7.3	0.4	12.9	1.8	3.6	1153	14	6.5
dg02 - 64.d	228100	2600	NaN	508.4	8.2	0.34	15.9	1.3	4.7	1051	13	9.6
dg02 - 65.d	229500	3200	2.4	501.2	8.1	0.38	13.9	1.7	2.8	1163	14	7.2
dg02 - 66.d	229500	2400	NaN	540.6	6.1	0.47	16.4	1.6	3.6	1126	16	6.1
dg02 - 67.d	226600	2900	2.2	553.9	7.2	0.3	18.2	1.5	4.7	1080	13	5.6
dg02 - 68.d	229600	3000	4.4	442.7	7.6	0.64	10.9	1.3	2.9	1149	16	7.2
dg02 - 69.d	227900	2700	NaN	444.8	6.5	0.47	10.7	1.2	3.6	1113	15	8.5
dg02 - 70.d	229100	2100	2.2	451.4	6.8	0.35	8.8	1.5	4.7	1074	16	9
dg02 - 71.d	233400	3400	NaN	465.7	6.3	0.32	11.5	1.5	3.4	1138	15	9.2
dg02 - 72.d	229100	2100	1.1	505.7	7.2	0.25	24.3	1.9	4.7	1051	13	8
dg02 - 73.d	228300	2400	1.1	449.3	7.4	0.36	19.1	1.4	3.3	1187.9	9.8	11
dg02 - 74.d	223500	2600	1.1	446.4	5.8	0.37	22.2	1.9	5.9	1091	15	11
dg02 - 75.d	204100	3300	4.3	535.5	9	0.38	22.4	1.3	5.2	857	13	7.7
dg02 - 76.d	227000	2500	2.4	517.2	6.3	0.41	21.8	1.3	5.1	1267	21	15
dg02 - 77.d	228300	3200	NaN	514.6	7.3	0.26	15.1	1.9	4.2	1314	21	10
dg02 - 78.d	223700	3200	NaN	512	7.2	0.41	19.5	1.6	3.9	1221	14	7.5
dg02 - 79.d	227300	2800	2.4	514.9	6.3	0.36	17.7	1.4	4.2	1239	14	9.4
dg02 - 80.d	227100	2600	2.3	490.1	6.3	0.36	14	1.4	4.8	1121	15	7.6
dg02 - 82.d	226100	2500	NaN	472.7	6.2	0.34	15.4	2	5.3	1302	12	9.1
dg02 - 83.d	223300	3900	NaN	498	7.8	0.39	22.3	1.7	3.5	1242	18	8.9
dg02 - 84.d	226200	2700	2.6	474.9	7.1	0.34	10.6	1.5	4	1267	15	4.3
dg02 - 85.d	210700	3600	1.6	461.3	7.5	0.38	30.5	1.6	5	1152	19	8.8
dg02 - 86.d	226200	3200	2.3	521.7	7.5	0.42	19	1.5	3.4	1333	17	6.9
dg02 - 87.d	226600	2000	2.4	515.4	7.7	0.25	22.9	1.6	4.4	1350	17	7.7
dg02 - 88.d	220000	2500	NaN	585.7	7.1	0.28	23.2	1.6	5.1	898	11	8
dg02 - 89.d	229700	2900	NaN	529.9	8	0.31	42.6	1.9	4.1	1185	17	11

Analysis number	Ti49 ppm	Ti49 ppm 2SE	Ti49 ppm LOD	V51 ppm	V51 ppm 2SE	V51 ppm LOD	Cr52 ppm	Cr52 ppm 2SE	Cr52 ppm LOD	Mn55 ppm	Mn55 ppm 2SE	Mn55 ppm LOD
dg02 - 90.d	224500	2900	4.5	506	8.4	0.38	24.6	1.3	3.1	1288	17	6
dg02 - 91.d	226100	3400	2.3	567.2	9.5	0.58	26.8	1.9	3.6	1007	11	10
dg02 - 92.d	227400	2800	2.6	523.3	6.8	0.28	19	1.7	4.4	1082	13	8.1
dg02 - 95.d	228200	2900	2.2	428.6	6.4	0.29	< LOD	< LOD	4.5	1113	16	8.2
dg02 - 96.d	227800	2600	1.1	408.4	5.7	0.27	< LOD	< LOD	4.3	1140	13	9.3
dg02 - 97.d	228600	3200	2.4	402.5	5.3	0.25	3.6	1.4	3.3	1225	16	6.8
dg02 - 98.d	227400	3200	2.2	419.4	5.4	0.35	< LOD	< LOD	4.2	1173	20	7.1
dg02 - 99.d	227300	3000	NaN	417.2	6.6	0.29	< LOD	< LOD	4.2	1108	13	7
dg02 - 100.d	229300	3000	3.1	418.4	6.6	0.29	< LOD	< LOD	3.4	1187	15	5.3
dg02 - 101.d	218700	3400	NaN	395.5	8.8	0.34	< LOD	< LOD	4.2	1332	65	8.4
dg02 - 103.d	205200	3700	3.3	341.7	6.3	0.34	< LOD	< LOD	5.7	1119	16	11
dg02 - 104.d	223300	3300	NaN	457.6	5.9	0.32	< LOD	< LOD	6	1129	13	12
dg02 - 105.d	220600	2600	NaN	466.3	6.2	0.32	< LOD	< LOD	5.2	1134	17	9.1
dg02 - 106.d	210300	4500	2.5	446.5	8	0.37	4.6	1.7	4.5	1088	15	6.9
dg02 - 107.d	195000	6300	2.2	419	15	0.59	5.7	1.3	3.2	923	24	9.5
dg02 - 110.d	221200	2600	2.3	468.5	7	0.32	13.5	1.5	5.1	1074	12	12
dg02 - 111.d	226700	3400	1.1	464.1	7.1	0.24	9.6	1.7	4.6	1013	15	8.9

Analysis number	Fe57 ppm	Fe57 ppm 2SE	Fe57 ppm LOD	Y89 ppm	Y89 ppm 2SE	Y89 ppm LOD	Zr90 ppm	Zr90 ppm 2SE	Zr90 ppm LOD	Nb93 ppm	Nb93 ppm 2SE	Nb93 ppm LOD
dg02 - 1.d	7650	160	24	1333	31	0.072	309.2	5.1	NaN	938	14	NaN
dg02 - 2.d	7810	130	28	1173	19	0.028	308	4.1	0.052	776.8	9.3	NaN
dg02 - 3.d	7670	170	20	1932	20	0.044	347.1	4.1	0.038	1074	20	NaN
dg02 - 4.d	11080	470	38	2132	30	NaN	348.4	5.1	0.077	1021	17	NaN
dg02 - 5.d	10400	180	30	1749	18	NaN	359.3	5.5	0.04	1001	11	0.04
dg02 - 6.d	9390	160	26	1479	26	0.047	372.2	4.5	NaN	963	16	0.04
dg02 - 7.d	6640	120	37	780	9.9	0.046	282.8	4.6	NaN	521.8	7.1	NaN
dg02 - 8.d	7580	170	31	915	15	0.058	316.6	5.1	0.086	552.7	7.1	NaN
dg02 - 9.d	6530	170	25	627.2	7.8	0.041	240.7	3.9	NaN	416	5.5	0.019
dg02 - 10.d	7290	140	32	767	11	0.059	314.9	4.4	0.039	504.7	7.4	NaN
dg02 - 11.d	7220	110	30	585.2	8.5	0.041	281.6	5	0.077	433.2	7.3	NaN
dg02 - 12.d	10210	210	28	875	12	0.042	378.3	5.1	0.16	709	11	NaN
dg02 - 13.d	7810	140	27	812	10	0.055	324.6	5	0.038	611.6	9.5	NaN
dg02 - 14.d	7120	140	23	994	14	0.095	352.4	5.1	0.077	764	13	NaN
dg02 - 15.d	7850	120	37	539.9	7.6	0.041	221.3	3.1	0.13	217.8	4.2	NaN
dg02 - 16.d	7680	130	25	599.9	8.6	0.028	231.7	3.8	NaN	264.5	3.9	NaN
dg02 - 17.d	7230	200	22	686	13	0.044	261.7	5.1	0.076	421.1	7.9	NaN
dg02 - 18.d	7410	110	25	850.8	9.9	0.048	268.6	3.3	0.077	325.3	4.6	0.019
dg02 - 19.d	7570	110	47	1145	18	0.044	290.4	4.3	0.076	678.8	8.2	NaN
dg02 - 20.d	7760	120	35	1665	24	0.066	334.7	4	0.082	637.5	7.4	NaN
dg02 - 21.d	8030	130	36	1975	29	0.045	348.5	4.7	NaN	772.4	9.4	NaN
dg02 - 22.d	8670	230	22	764	13	0.078	307.8	6.5	0.082	626	9.9	NaN
dg02 - 23.d	8140	160	29	1202	37	0.02	311.8	5.2	0.076	806	15	NaN
dg02 - 24.d	9220	180	28	1713	17	NaN	366.6	6.1	NaN	961.9	9.9	NaN
dg02 - 25.d	9920	180	29	1749	26	0.021	381.1	6.5	0.077	860	15	NaN
dg02 - 26.d	12280	390	23	2273	43	0.022	401.9	6	NaN	944	18	0.021
dg02 - 27.d	13000	430	25	2173	32	0.041	363.6	5.2	0.089	820	15	NaN
dg02 - 28.d	8000	160	19	1920	27	NaN	368.2	4.3	0.12	973	18	NaN
dg02 – 29.d	8010	130	36	1489	16	0.055	321.1	4	0.082	802.8	8.9	NaN

Analysis number	Fe57 ppm	Fe57 ppm 2SE	Fe57 ppm LOD	Y89 ppm	Y89 ppm 2SE	Y89 ppm LOD	Zr90 ppm	Zr90 ppm 2SE	Zr90 ppm LOD	Nb93 ppm	Nb93 ppm 2SE	Nb93 ppm LOD
dg02 - 30.d	11330	300	19	1462	31	0.051	319.1	4.3	0.056	579.4	9	NaN
dg02 - 31.d	7890	160	30	1764	29	0.044	319.9	5.2	NaN	773	13	0.041
dg02 - 32.d	8070	170	34	1944	24	0.061	322.1	4.2	NaN	715	8.9	NaN
dg02 - 33.d	17610	320	29	1497	41	0.053	274.8	5.3	NaN	465	10	NaN
dg02 - 34.d	6870	130	45	1199	25	0.021	286.4	4.3	0.08	391.1	5.4	0.04
dg02 - 35.d	7800	130	47	1286	23	0.044	307.4	4.2	NaN	508.1	5.7	NaN
dg02 - 36.d	5720	120	19	1094	15	0.063	260.6	4.8	0.08	444.8	6.2	NaN
dg02 - 37.d	8190	150	36	1578	27	0.059	346.7	6.6	0.078	688.6	8.6	NaN
dg02 - 38.d	7199	86	27	1634	24	0.021	322.6	4.8	0.039	705.4	9	NaN
dg02 - 39.d	7350	160	29	1768	21	NaN	366.8	6.3	NaN	750	13	NaN
dg02 - 40.d	6820	110	36	723	21	NaN	221.4	5.9	NaN	283.7	9.3	NaN
dg02 - 41.d	7430	150	32	1266	29	0.045	297.4	4.6	0.14	502.5	6.9	NaN
dg02 - 42.d	6890	120	19	1582	24	0.042	311.7	3.9	0.039	595.9	7.5	NaN
dg02 - 43.d	7320	170	29	1104	16	0.045	280.9	4.1	0.11	398.1	5	NaN
dg02 - 44.d	8210	130	37	1527	22	0.029	333.2	4.8	NaN	544.1	6.8	0.02
dg02 - 45.d	6660	110	36	1283	26	0.056	291.5	4.6	NaN	425.3	5.9	0.039
dg02 - 46.d	6530	130	21	929	13	0.056	263.2	4.2	NaN	339.9	4.2	0.026
dg02 - 47.d	7080	190	37	1400	31	0.02	320.9	4	0.076	514.4	7.6	NaN
dg02 - 48.d	7070	130	35	1426	17	0.055	320.1	5.2	0.082	536.7	7	0.019
dg02 - 49.d	6850	130	30	1197	28	0.041	301.8	4.8	NaN	427.2	7.9	0.019
dg02 - 50.d	6968	91	17	1150	18	0.065	296.5	3.6	0.038	414.2	5.4	NaN
dg02 - 51.d	7300	130	24	1461	21	0.045	322.6	4.3	NaN	582.8	9.2	NaN
dg02 - 52.d	6980	140	28	1125	22	0.028	303.2	5	0.11	448.4	6.8	NaN
dg02 - 53.d	8650	250	28	1459	22	NaN	326.8	4.7	NaN	560.3	8.7	0.026
dg02 - 54.d	7300	190	21	1079	15	0.028	303.1	4	NaN	415.3	5.6	NaN
dg02 - 55.d	7700	150	25	1640	30	NaN	332	5.7	NaN	629	11	0.02
dg02 - 56.d	7510	140	29	1206	21	0.053	312	4.4	0.041	512.4	6.7	NaN
dg02 - 57.d	6820	180	28	1276	26	NaN	299.4	3.9	NaN	438	5.5	NaN
dg02 - 58.d	7310	140	32	2116	32	0.07	362.7	5.5	NaN	872	13	NaN

Analysis number	Fe57 ppm	Fe57 ppm 2SE	Fe57 ppm LOD	Y89 ppm	Y89 ppm 2SE	Y89 ppm LOD	Zr90 ppm	Zr90 ppm 2SE	Zr90 ppm LOD	Nb93 ppm	Nb93 ppm 2SE	Nb93 ppm LOD
dg02 - 59.d	8050	170	35	1355	40	0.061	330	5.6	0.081	543.8	8.5	NaN
dg02 - 60.d	7250	140	26	856.7	9.2	0.058	242.7	3.7	NaN	334	3.8	NaN
dg02 - 62.d	8400	170	22	2112	29	0.021	362	4.8	NaN	658	10	NaN
dg02 - 63.d	7040	130	32	1835	21	0.073	332.1	5	0.078	607.2	8.3	NaN
dg02 - 64.d	7440	150	23	1659	21	0.029	321.4	5.2	0.079	552.4	8	NaN
dg02 - 65.d	7080	120	38	1721	22	0.048	325.2	5.9	NaN	549.8	9.4	NaN
dg02 - 66.d	7230	140	32	1488	27	0.045	304.1	5.1	0.077	450.1	5.5	NaN
dg02 - 67.d	6830	110	26	1082	20	NaN	258.1	4.2	0.085	360.2	4.5	0.039
dg02 - 68.d	7810	150	25	1561	36	0.021	341.7	5.1	0.11	760	11	NaN
dg02 - 69.d	7840	130	21	1449	40	0.056	346.1	5.6	NaN	795	13	0.044
dg02 - 70.d	7580	110	32	1677	22	0.06	336.5	4.6	NaN	683.7	9.4	NaN
dg02 - 71.d	7160	120	31	494.6	6.4	0.045	264.5	4.5	NaN	473.8	8.1	NaN
dg02 - 72.d	8140	150	46	975	11	0.028	335.8	4.6	0.038	790	12	NaN
dg02 - 73.d	7880	170	25	1455	35	0.056	357.3	5.8	0.038	1016	18	NaN
dg02 - 74.d	8520	370	34	1291	30	0.042	341.6	6	NaN	912	12	0.02
dg02 - 75.d	13670	240	39	68.7	1.8	0.082	108.1	3	0.039	138.7	3.1	NaN
dg02 - 76.d	9990	190	41	3252	39	0.042	366.8	6.4	0.054	697.8	8.3	NaN
dg02 - 77.d	8590	170	25	3773	70	0.045	365.2	5.4	0.078	876	14	NaN
dg02 - 78.d	10000	120	27	2828	41	0.041	330.2	5.2	0.1	679.5	9.9	NaN
dg02 - 79.d	7730	130	34	3145	40	0.042	331.4	4.7	0.091	594.3	8.4	NaN
dg02 - 80.d	7767	95	27	3129	38	0.044	379.3	5.7	0.041	960	10	0.1
dg02 - 82.d	8420	160	29	3101	35	0.078	371.1	4.8	NaN	836	10	NaN
dg02 - 83.d	8420	170	31	2992	41	0.043	341.1	5.5	NaN	807	16	NaN
dg02 - 84.d	8600	140	24	2904	43	0.047	331.2	5.6	0.093	837	14	NaN
dg02 - 85.d	8090	140	27	2626	51	0.03	309	4.7	NaN	682	11	NaN
dg02 - 86.d	8730	180	30	3866	55	0.048	394	6.8	0.041	906	13	NaN
dg02 - 87.d	11150	240	30	3821	36	0.023	394.1	5.8	0.043	891	12	NaN
dg02 - 88.d	9010	140	23	349.3	5.1	0.046	128.9	2.1	0.11	174.9	2.4	NaN
dg02 - 89.d	8760	160	26	2417	30	NaN	308.8	4.8	0.087	789	11	NaN

Analysis number	Fe57 ppm	Fe57 ppm 2SE	Fe57 ppm LOD	Y89 ppm	Y89 ppm 2SE	Y89 ppm LOD	Zr90 ppm	Zr90 ppm 2SE	Zr90 ppm LOD	Nb93 ppm	Nb93 ppm 2SE	Nb93 ppm LOD
dg02 - 90.d	8250	160	35	3013	35	0.043	339.9	6.1	0.088	850	11	NaN
dg02 - 91.d	8180	130	29	561.1	8.3	0.047	175.1	2.9	0.04	231.1	3.3	NaN
dg02 - 92.d	7500	150	28	700	10	0.029	211.6	3.7	0.04	342.1	5.2	NaN
dg02 - 95.d	6690	130	35	124.4	1.5	0.028	254.6	3.6	0.039	167.8	3.4	0.039
dg02 - 96.d	6870	120	34	106.3	1.9	0.066	255.9	3.9	0.039	142.4	2	NaN
dg02 - 97.d	6190	130	33	50.8	0.92	0.029	292.7	4.5	0.04	70.5	1.2	NaN
dg02 - 98.d	6830	140	27	50.04	0.9	0.057	274.8	4.8	0.078	69	1	NaN
dg02 - 99.d	6280	110	34	43.73	0.75	0.045	270.6	3.7	0.078	72.11	0.94	NaN
dg02 - 100.d	6854	94	43	46	1	NaN	272.6	4.9	0.089	71.1	1.3	NaN
dg02 - 101.d	6240	140	39	53.7	1.3	0.048	244.6	5	0.053	58	1.3	NaN
dg02 - 103.d	6060	130	32	116.3	2.1	NaN	234.4	4.2	0.078	66.2	1.2	NaN
dg02 - 104.d	7720	140	33	271.6	3.6	0.041	223.4	3.3	NaN	129.7	2.2	0.039
dg02 - 105.d	8790	120	32	295.3	4.6	0.072	229.6	3.7	0.082	123.5	1.7	NaN
dg02 - 106.d	13250	310	33	587	11	0.044	233.8	4.2	0.041	295.4	6.4	NaN
dg02 - 107.d	13200	380	23	464	12	0.069	191.6	5.9	0.079	231.9	4.9	NaN
dg02 - 110.d	8280	160	18	400	5.8	0.07	157.1	2.7	0.11	466.4	6.8	0.041
dg02 - 111.d	6630	130	28	494.5	7.3	0.021	163.1	3.3	0.11	708	10	NaN

Analysis number	La139 ppm	La139 ppm 2SE	La139 ppm LOD	Ce140 ppm	Ce140 ppm 2SE	Ce140 ppm LOD	Pr141 ppm	Pr141 ppm 2SE	Pr141 ppm LOD	Nd146 ppm	Nd146 ppm 2SE	Nd146 ppm LOD
dg02 - 1.d	910	14	0.011	3449	51	NaN	467.9	6.4	0.019	2120	28	NaN
dg02 - 2.d	751	17	NaN	3041	38	NaN	415.8	4.8	0.0098	1892	21	0.11
dg02 - 3.d	1042	13	NaN	4172	48	0.023	615	18	NaN	2694	33	NaN
dg02 - 4.d	2608	66	0.023	6743	99	0.025	942	13	0.0098	3870	120	NaN
dg02 - 5.d	998	12	NaN	3894	49	NaN	538.3	6.6	NaN	2472	32	NaN
dg02 - 6.d	937	24	NaN	3646	57	NaN	484.9	7.3	0.01	2164	30	NaN
dg02 - 7.d	768	22	0.024	2589	34	0.024	298.8	4	NaN	1174	16	NaN
dg02 - 8.d	945	17	NaN	2945	47	NaN	333.6	4.9	0.02	1313	18	0.11
dg02 - 9.d	546.9	6.5	0.023	1986	23	0.023	231.1	3.2	NaN	955	13	NaN
dg02 - 10.d	824	22	NaN	2670	32	NaN	299.9	4.4	0.01	1185	15	NaN
dg02 - 11.d	653	18	NaN	2255	37	NaN	247.9	4.8	NaN	964	20	NaN
dg02 - 12.d	984	16	NaN	3079	45	NaN	350.7	5.4	NaN	1355	17	NaN
dg02 - 13.d	942	13	NaN	2907	38	NaN	325.8	4.6	NaN	1269	18	0.11
dg02 - 14.d	1052	14	0.023	3374	51	0.023	384.2	7.1	NaN	1520	28	0.056
dg02 - 15.d	397.8	5.1	0.012	1453	18	0.012	171.5	2.4	NaN	727	11	0.056
dg02 - 16.d	458.4	5.9	0.023	1708	23	NaN	203.2	3.1	0.019	853	11	0.12
dg02 - 17.d	581	11	0.011	2168	35	0.012	255.2	4.8	NaN	1063	19	NaN
dg02 - 18.d	569.8	9	NaN	2127	29	NaN	261.3	3.7	NaN	1096	17	NaN
dg02 - 19.d	823	18	NaN	2863	32	0.023	354.3	5.2	NaN	1558	20	0.055
dg02 - 20.d	963	13	0.011	3339	46	0.023	417.5	6	NaN	1858	33	0.055
dg02 - 21.d	1059	15	0.012	3629	58	NaN	463.7	6.8	NaN	2103	38	0.056
dg02 - 22.d	601	14	NaN	2148	37	NaN	253	4.7	NaN	1096	23	NaN
dg02 - 23.d	899	28	NaN	2920	69	0.016	361.4	8.9	0.0097	1584	39	0.055
dg02 - 24.d	1144	14	NaN	3819	41	0.023	476.6	5.6	NaN	2119	27	NaN
dg02 - 25.d	1075	20	0.023	3719	76	0.032	476.5	8.8	0.02	2107	38	0.056
dg02 - 26.d	1077	21	NaN	3956	78	0.025	524	11	NaN	2374	46	NaN
dg02 - 27.d	1031	16	NaN	3703	65	NaN	487.1	8.7	NaN	2244	39	NaN
dg02 - 28.d	1121	17	NaN	3885	61	NaN	493.7	6.5	NaN	2199	30	0.11
dg02 - 29.d	946	11	0.023	3129	29	0.011	387.7	4.1	0.019	1728	24	NaN

Analysis number	La139 ppm	La139 ppm 2SE	La139 ppm LOD	Ce140 ppm	Ce140 ppm 2SE	Ce140 ppm LOD	Pr141 ppm	Pr141 ppm 2SE	Pr141 ppm LOD	Nd146 ppm	Nd146 ppm 2SE	Nd146 ppm LOD
dg02 - 30.d	713	22	NaN	2489	41	NaN	303.6	5.6	NaN	1346	19	NaN
dg02 - 31.d	978	17	NaN	3103	57	NaN	377	7.3	NaN	1697	31	NaN
dg02 - 32.d	1027	26	NaN	3158	49	0.013	391.2	5.5	NaN	1754	26	NaN
dg02 - 33.d	643	12	NaN	2351	48	NaN	287.4	5.9	NaN	1304	28	0.13
dg02 - 34.d	708	19	NaN	2361	39	NaN	277	4.4	NaN	1192	19	0.078
dg02 - 35.d	883	17	NaN	2702	36	NaN	308.8	4.4	0.031	1318	19	NaN
dg02 - 36.d	647	8.8	0.024	2223	24	NaN	261.8	3.5	0.01	1115	15	0.058
dg02 - 37.d	1031	19	0.012	3122	57	NaN	360.6	6.5	0.01	1510	27	NaN
dg02 - 38.d	967	13	0.012	3004	37	NaN	358.1	5.3	NaN	1534	21	NaN
dg02 - 39.d	1077	20	0.032	3291	53	NaN	381	6.3	NaN	1574	32	NaN
dg02 - 40.d	533.4	9.8	NaN	1712	43	0.036	188.2	4.7	NaN	766	22	0.11
dg02 - 41.d	825	20	NaN	2541	44	0.012	294.8	4	NaN	1268	21	NaN
dg02 - 42.d	939	13	0.012	2901	39	0.012	346	5.1	0.02	1486	21	NaN
dg02 - 43.d	691	19	NaN	2256	34	NaN	264	3.7	0.021	1112	17	NaN
dg02 - 44.d	986	13	NaN	2938	35	0.024	339.4	4.5	0.02	1429	19	0.16
dg02 - 45.d	787	19	0.012	2476	30	NaN	286.8	3.6	0.0098	1240	19	0.055
dg02 - 46.d	563	11	0.016	1921	38	NaN	224.4	3.9	NaN	944	20	NaN
dg02 - 47.d	928	15	NaN	2772	36	NaN	323.4	5.1	0.0097	1352	24	0.055
dg02 - 48.d	934	9.9	NaN	2803	36	NaN	323.3	3.8	NaN	1353	15	NaN
dg02 - 49.d	826	26	0.031	2497	42	0.012	287.3	5.5	0.0097	1188	25	NaN
dg02 - 50.d	755	19	NaN	2367	30	0.011	268.7	3.5	NaN	1119	13	0.054
dg02 - 51.d	953	15	NaN	2843	37	0.012	330.6	5.2	NaN	1373	20	NaN
dg02 - 52.d	831	21	0.032	2526	36	0.023	285.3	4	NaN	1196	20	NaN
dg02 - 53.d	946	12	NaN	2834	38	0.012	329.5	5.5	NaN	1359	16	0.11
dg02 - 54.d	783	21	0.023	2381	34	NaN	272.5	4.3	NaN	1117	18	NaN
dg02 - 55.d	995	23	0.012	3004	59	NaN	357.5	7.1	NaN	1532	29	NaN
dg02 - 56.d	785	24	NaN	2536	36	NaN	296.9	3.9	0.011	1262	17	NaN
dg02 - 57.d	828	32	NaN	2592	52	NaN	297.8	4.9	NaN	1284	19	0.12
dg02 - 58.d	1119	16	NaN	3643	54	0.012	447.8	5.6	0.02	1963	28	NaN

Analysis number	La139 ppm	La139 ppm 2SE	La139 ppm LOD	Ce140 ppm	Ce140 ppm 2SE	Ce140 ppm LOD	Pr141 ppm	Pr141 ppm 2SE	Pr141 ppm LOD	Nd146 ppm	Nd146 ppm 2SE	Nd146 ppm LOD
dg02 - 59.d	933	26	NaN	2796	48	0.024	325.4	5.6	NaN	1366	25	0.12
dg02 - 60.d	515.2	5.5	0.012	1762	18	0.024	206.2	2.1	0.02	876.6	9.9	NaN
dg02 - 62.d	1047	17	0.026	3438	51	NaN	417.1	5.9	NaN	1792	26	NaN
dg02 - 63.d	963	16	NaN	3010	46	0.033	361.5	5.6	0.02	1580	25	NaN
dg02 - 64.d	978	18	NaN	2950	46	NaN	351.6	5.2	NaN	1522	24	NaN
dg02 - 65.d	1008	13	0.012	3082	39	NaN	359.9	4.4	0.01	1536	22	NaN
dg02 - 66.d	902	18	NaN	2688	36	NaN	316.8	4.4	NaN	1342	19	NaN
dg02 - 67.d	620	12	NaN	2105	32	NaN	247.6	4.6	0.01	1066	15	0.11
dg02 - 68.d	1035	17	0.012	3069	39	NaN	362.1	4.7	0.022	1554	23	NaN
dg02 - 69.d	1064	18	NaN	3109	55	NaN	355.4	7.2	0.019	1505	32	0.12
dg02 - 70.d	975	13	NaN	2974	34	NaN	361.7	4.6	NaN	1579	26	NaN
dg02 - 71.d	595	10	NaN	1928	33	NaN	207.4	3.3	NaN	789	12	NaN
dg02 - 72.d	1012	17	0.012	3142	45	0.023	362.3	6.8	NaN	1485	21	NaN
dg02 - 73.d	1063	14	NaN	3552	40	0.036	431.2	5.4	NaN	1807	26	NaN
dg02 - 74.d	993	16	0.012	3296	43	NaN	397.9	5.6	0.02	1663	24	NaN
dg02 - 75.d	161.8	4.1	0.012	373	10	0.026	38.1	1	0.03	128	4	NaN
dg02 - 76.d	773	22	NaN	3237	52	NaN	466.6	7.4	0.02	2293	33	NaN
dg02 - 77.d	1013	19	0.023	4021	79	NaN	624	23	NaN	2868	59	NaN
dg02 - 78.d	726	23	NaN	3066	52	0.012	436.9	7.6	0.0098	2118	29	0.055
dg02 - 79.d	761	23	0.024	3194	38	NaN	470.7	7.4	NaN	2301	30	0.057
dg02 - 80.d	1056	12	NaN	4134	55	0.025	586	11	NaN	2837	41	NaN
dg02 - 82.d	1035	14	NaN	3867	56	NaN	535.2	6.3	NaN	2556	34	NaN
dg02 - 83.d	836	29	NaN	3296	58	NaN	466.2	7.8	NaN	2311	39	NaN
dg02 - 84.d	860	24	NaN	3400	48	NaN	477.6	7.4	NaN	2348	33	0.058
dg02 - 85.d	644	14	NaN	2789	48	NaN	396	6.2	NaN	1992	41	NaN
dg02 - 86.d	1082	15	NaN	4389	62	0.025	686	21	0.021	3146	50	0.13
dg02 - 87.d	1022	17	NaN	4198	58	NaN	612	12	0.022	2973	44	0.084
dg02 - 88.d	144.9	2.3	NaN	509.8	7.2	NaN	72.5	1	NaN	315.6	5.9	0.17
dg02 - 89.d	651	11	0.024	2875	42	NaN	404.1	6.3	NaN	2005	31	NaN

Analysis number	La139 ppm	La139 ppm 2SE	La139 ppm LOD	Ce140 ppm	Ce140 ppm 2SE	Ce140 ppm LOD	Pr141 ppm	Pr141 ppm 2SE	Pr141 ppm LOD	Nd146 ppm	Nd146 ppm 2SE	Nd146 ppm LOD
dg02 - 90.d	931	18	0.024	3647	54	NaN	513.1	6.7	0.01	2498	35	0.058
dg02 - 91.d	258.6	3.1	NaN	1062	13	NaN	134.7	1.8	NaN	571.7	7.3	0.13
dg02 - 92.d	329.3	4.8	0.039	1265	20	NaN	151.8	2.5	NaN	634	11	0.058
dg02 - 95.d	495.8	7.3	0.025	1433	19	NaN	148.5	2.2	NaN	576.7	9.5	0.11
dg02 - 96.d	443.9	6.1	NaN	1168	16	0.012	112.7	1.7	NaN	407	6.9	0.056
dg02 - 97.d	372.7	5.5	NaN	667	11	0.036	55.18	0.97	NaN	155.2	3.6	0.11
dg02 - 98.d	384.3	6.6	0.012	741	22	NaN	60.7	1	NaN	164.5	3.9	0.11
dg02 - 99.d	338.8	4.6	0.012	558.3	7.9	NaN	45.38	0.74	NaN	120.9	2.7	0.11
dg02 - 100.d	334.2	5.4	NaN	553	10	NaN	44.7	1.1	0.02	119.5	3.1	NaN
dg02 - 101.d	273.9	6.2	NaN	499	11	NaN	45.8	1.1	NaN	140.2	3.9	0.11
dg02 - 103.d	233.7	5	NaN	494	11	0.024	51.2	1.3	NaN	182.7	5.3	NaN
dg02 - 104.d	348.6	5.2	NaN	1179	15	NaN	123.7	2	0.0099	443.9	6.1	NaN
dg02 - 105.d	347.2	4.8	NaN	1192	19	0.012	129.3	1.5	NaN	477.4	7.8	NaN
dg02 - 106.d	443	8.2	0.012	1708	32	0.027	204.9	4.2	NaN	868	19	NaN
dg02 - 107.d	341	10	0.012	1323	39	NaN	160.4	4.8	NaN	693	19	NaN
dg02 - 110.d	287.9	4.1	NaN	1083	14	NaN	129.4	1.9	NaN	545	7.3	NaN
dg02 - 111.d	324.1	5.9	0.036	1324	20	NaN	167.5	2.7	NaN	728	12	NaN

Analysis number	Sm147 ppm	Sm147 ppm 2SE	Sm147 ppm LOD	Eu153 ppm	Eu153 ppm 2SE	Eu153 ppm LOD	Gd157 ppm	Gd157 ppm 2SE	Gd157 ppm LOD	Tb159 ppm	Tb159 ppm 2SE	Tb159 ppm LOD
dg02 - 1.d	437.5	8.4	NaN	293	4.5	NaN	353.9	5.7	NaN	41.81	0.79	NaN
dg02 - 2.d	388.8	5.8	NaN	264	3.5	0.017	322.2	5.3	0.12	37.79	0.67	NaN
dg02 - 3.d	559.6	6.3	NaN	332.3	3.9	NaN	465.3	5.4	NaN	54.83	0.67	NaN
dg02 - 4.d	733	11	0.09	359	4.6	NaN	576	10	NaN	69.97	0.84	NaN
dg02 - 5.d	518	7.4	NaN	315.8	4.4	NaN	418.5	5.9	0.13	50.4	0.79	NaN
dg02 - 6.d	455.4	5.7	NaN	296.9	3.9	NaN	373.5	5.2	NaN	45.07	0.79	0.018
dg02 - 7.d	209.3	3.9	NaN	140.8	2.6	0.018	173.9	2.6	NaN	21.95	0.38	NaN
dg02 - 8.d	229.4	5.2	NaN	155	3	NaN	185.6	3.8	NaN	23.3	0.46	NaN
dg02 - 9.d	176.6	3.5	NaN	114.2	1.6	NaN	144.5	2.9	0.12	18.06	0.37	0.0089
dg02 - 10.d	201.5	3.2	NaN	146.2	2	NaN	166.5	2.4	NaN	20.22	0.42	NaN
dg02 - 11.d	161.2	3.4	0.066	124.3	2.3	0.018	129.7	3	0.061	16.11	0.35	0.0089
dg02 - 12.d	228.3	4.3	NaN	159.2	2.6	NaN	187.7	3.3	0.12	23.77	0.58	NaN
dg02 - 13.d	217.3	4.8	NaN	151.6	2.2	NaN	172.1	3.6	NaN	21.66	0.46	0.0087
dg02 - 14.d	262	5.2	NaN	174.2	2.6	NaN	210.5	4.4	NaN	26.09	0.5	NaN
dg02 - 15.d	138.2	2.8	NaN	93	1.4	0.018	118.9	2.7	0.061	15.16	0.38	0.018
dg02 - 16.d	160.9	3.4	NaN	104.6	1.5	NaN	134.9	2	NaN	16.5	0.44	NaN
dg02 - 17.d	202.2	4.6	NaN	121.3	2.3	NaN	172.7	4.1	NaN	20.73	0.47	0.012
dg02 - 18.d	214.3	4.5	NaN	125.7	2.1	NaN	188.6	3.9	NaN	23.32	0.42	0.0089
dg02 - 19.d	327.9	6.1	NaN	149.1	2.2	0.035	287.7	5	NaN	36.23	0.63	NaN
dg02 - 20.d	386.8	8.5	NaN	175.5	3	0.017	348.2	5	0.06	44.78	0.98	0.018
dg02 - 21.d	453	10	NaN	195.5	3.1	NaN	401.2	6.2	0.13	51.94	0.81	NaN
dg02 - 22.d	220.3	5.1	0.13	126	2.3	NaN	187.7	4.5	NaN	22.77	0.48	0.017
dg02 - 23.d	331	8.6	NaN	164.6	3.4	0.017	289.7	6.7	0.12	35.47	0.68	NaN
dg02 - 24.d	439.6	6.8	0.21	204.2	2.2	NaN	378.8	6.1	NaN	46.52	0.67	NaN
dg02 - 25.d	440	10	0.066	204.8	4.2	NaN	380.2	8.7	NaN	46.42	0.79	NaN
dg02 - 26.d	526	12	NaN	219.9	4.6	NaN	465.3	9.9	NaN	59.6	1.4	NaN
dg02 - 27.d	499	10	NaN	207.5	3.1	NaN	441.1	6.6	0.083	57.03	0.8	NaN
dg02 - 28.d	474.3	7.1	NaN	208.3	2.9	0.053	419.2	7.3	NaN	51.6	1.1	0.012
dg02 - 29.d	366.3	5.8	NaN	169.5	2.3	NaN	319.2	5.5	NaN	39.94	0.71	NaN

Analysis number	Sm147 ppm	Sm147 ppm 2SE	Sm147 ppm LOD	Eu153 ppm	Eu153 ppm 2SE	Eu153 ppm LOD	Gd157 ppm	Gd157 ppm 2SE	Gd157 ppm LOD	Tb159 ppm	Tb159 ppm 2SE	Tb159 ppm LOD
dg02 - 30.d	313.8	5.7	0.07	135.9	2.7	NaN	299.9	5.9	NaN	40.33	0.75	NaN
dg02 - 31.d	385.3	7.1	NaN	161.3	2.6	NaN	375.9	6.3	NaN	49.94	0.84	0.0094
dg02 - 32.d	413	6.3	NaN	166.6	2.4	NaN	397.6	5.3	NaN	52.57	0.72	0.0096
dg02 - 33.d	315.6	6.6	0.15	133.2	2.9	NaN	311.3	7	0.14	43.2	0.96	0.01
dg02 - 34.d	273.5	4.7	0.068	125.4	2.4	NaN	264.8	5.2	NaN	34.99	0.67	NaN
dg02 - 35.d	296.9	3.7	NaN	140.3	2.2	0.019	281.8	4.6	NaN	38	0.7	NaN
dg02 - 36.d	254.1	4.7	0.14	118.2	1.8	NaN	242.1	4.1	NaN	32.09	0.43	0.013
dg02 - 37.d	326.6	6.1	0.13	156.6	2.4	NaN	310	5.5	NaN	40.38	0.55	0.0091
dg02 - 38.d	343.8	4.9	NaN	160.8	2.5	0.018	323.9	6.2	0.12	42.79	0.8	NaN
dg02 - 39.d	327.4	6.8	0.27	171.5	2.5	NaN	307.3	4.3	NaN	41.39	0.8	NaN
dg02 - 40.d	159.5	4.8	0.13	99.4	2.1	NaN	148.3	5	0.061	19.55	0.62	0.009
dg02 - 41.d	287.3	4.7	NaN	133.4	2.3	0.018	273.4	4.6	NaN	36.38	0.69	0.027
dg02 - 42.d	332.7	5.9	0.13	155.7	2.3	NaN	310.8	5.8	NaN	41.72	0.81	NaN
dg02 - 43.d	241.5	3.9	NaN	122.7	1.7	0.036	234.5	3.8	NaN	31.22	0.5	NaN
dg02 - 44.d	317.2	5	0.14	152.1	2.3	NaN	296.6	5.8	0.13	40.09	0.6	0.0092
dg02 - 45.d	279.2	5.4	NaN	134	2.2	0.039	264.1	4.5	NaN	35.87	0.62	NaN
dg02 - 46.d	216.6	5.1	NaN	105.4	2.1	NaN	202.5	4.5	0.12	26.86	0.51	0.018
dg02 - 47.d	291.6	5.5	NaN	143.4	2	NaN	276.3	4.8	0.12	37.19	0.56	0.0088
dg02 - 48.d	298.8	4.7	NaN	145.3	2.1	NaN	272.2	4	NaN	36.41	0.53	NaN
dg02 - 49.d	257.8	5	NaN	130.5	2.3	NaN	236.2	5.7	0.06	32.11	0.63	0.018
dg02 - 50.d	247.6	4.8	NaN	124.5	1.8	0.017	226.8	2.9	0.059	31.06	0.56	NaN
dg02 - 51.d	303.1	5.3	0.065	146.3	2	NaN	279	4.7	0.082	37.82	0.63	0.0088
dg02 - 52.d	254.6	4.6	NaN	131	2.3	NaN	235.4	3.8	0.12	31.5	0.67	NaN
dg02 - 53.d	295.8	4.9	NaN	145.1	2.4	NaN	277.5	4.5	0.06	37.26	0.7	0.0089
dg02 - 54.d	238.2	3.5	NaN	121	1.8	0.018	220.5	3.5	NaN	29.69	0.45	NaN
dg02 - 55.d	349	7.1	NaN	160.1	2.9	0.019	327.9	6.5	0.064	44.04	0.92	NaN
dg02 - 56.d	283.5	5	NaN	132.6	2.1	NaN	264.1	5.3	NaN	35.36	0.56	0.021
dg02 - 57.d	278.5	4.1	NaN	131.5	2.1	NaN	261.9	4.9	0.13	35.55	0.65	NaN
dg02 - 58.d	453.9	7.4	NaN	193.4	3.3	NaN	428.3	7	NaN	57.4	1.1	NaN

Analysis number	Sm147 ppm	Sm147 ppm 2SE	Sm147 ppm LOD	Eu153 ppm	Eu153 ppm 2SE	Eu153 ppm LOD	Gd157 ppm	Gd157 ppm 2SE	Gd157 ppm LOD	Tb159 ppm	Tb159 ppm 2SE	Tb159 ppm LOD
dg02 - 59.d	295.6	5.8	0.14	145.2	3	NaN	274.9	6	NaN	37.22	0.71	NaN
dg02 - 60.d	194.4	3.5	NaN	96.4	1.3	NaN	178.5	3.2	NaN	24.44	0.44	NaN
dg02 - 62.d	400	6.7	NaN	182.8	2.5	0.018	371.6	6.7	NaN	50.86	0.99	NaN
dg02 - 63.d	371.2	5.4	0.067	157.2	2.4	0.036	360.9	6.5	NaN	49.5	0.74	0.0091
dg02 - 64.d	349.9	6	0.067	153.7	2.1	NaN	335.2	4.8	NaN	44.93	0.76	NaN
dg02 - 65.d	345.1	4.6	NaN	155.8	2.1	NaN	327.9	4.6	NaN	43.95	0.74	NaN
dg02 - 66.d	306.6	4.5	NaN	137.9	1.5	0.018	292.9	4.4	NaN	39.36	0.63	NaN
dg02 - 67.d	248.4	5	NaN	112	2.1	0.042	235.7	4.3	NaN	31.29	0.69	NaN
dg02 - 68.d	343.5	5.5	NaN	159.6	1.9	NaN	326.8	6.1	NaN	42.55	0.76	NaN
dg02 - 69.d	321.2	9.9	NaN	155.7	3.4	NaN	296.7	6.5	0.06	38	1	NaN
dg02 - 70.d	367.3	5.9	0.066	159.3	2.2	0.036	353.9	5.6	NaN	46.74	0.81	NaN
dg02 - 71.d	129.1	3	0.065	115.5	2.3	NaN	102	1.8	NaN	12.62	0.31	NaN
dg02 - 72.d	274.9	5.2	NaN	176.5	2.8	NaN	227.8	4.9	0.12	28.26	0.51	0.019
dg02 - 73.d	360.1	5.9	NaN	210.2	3.5	NaN	302.4	5.3	NaN	37.2	0.5	NaN
dg02 - 74.d	331.1	6.1	NaN	194	2.9	0.039	276.6	5.1	0.083	34.98	0.61	NaN
dg02 - 75.d	17.9	1.2	0.15	40.4	1.2	0.073	13.86	0.73	0.13	1.665	0.091	0.0091
dg02 - 76.d	593	11	NaN	210.5	3.1	0.036	561.8	8.3	0.13	79.4	1	NaN
dg02 - 77.d	738	15	0.14	241.4	4.9	NaN	689	14	0.061	94.3	2	NaN
dg02 - 78.d	531.3	7.7	NaN	191	2.9	0.024	494.2	8.2	NaN	68.8	1	NaN
dg02 - 79.d	600	12	NaN	209.2	3.1	NaN	565.5	8.5	0.061	77.9	1.5	0.0091
dg02 - 80.d	690.1	9.3	NaN	244	3.6	NaN	628.9	9	0.064	84.1	1.3	0.0095
dg02 - 82.d	648	9.2	NaN	221.5	3.5	0.042	612.1	9.5	NaN	82.9	1.1	0.0096
dg02 - 83.d	615	10	NaN	186.6	3.1	NaN	610	11	0.063	84	1.4	0.019
dg02 - 84.d	627.7	9.5	NaN	190.3	2.7	0.037	617.8	8.6	NaN	82.1	1	NaN
dg02 - 85.d	547	11	0.15	160.7	3.3	NaN	548	12	NaN	74.6	1.3	NaN
dg02 - 86.d	822	14	0.14	266	4.3	0.059	758	15	NaN	105.4	1.4	NaN
dg02 - 87.d	773	12	NaN	253.5	4	NaN	717.7	8.8	NaN	99.8	1.3	NaN
dg02 - 88.d	65.7	1.7	NaN	62.4	1.3	0.018	62.7	1.4	NaN	8.14	0.17	NaN
dg02 - 89.d	531	11	NaN	183.9	3.5	NaN	500.6	7.8	NaN	67.99	0.83	NaN

Analysis number	Sm147 ppm	Sm147 ppm 2SE	Sm147 ppm LOD	Eu153 ppm	Eu153 ppm 2SE	Eu153 ppm LOD	Gd157 ppm	Gd157 ppm 2SE	Gd157 ppm LOD	Tb159 ppm	Tb159 ppm 2SE	Tb159 ppm LOD
dg02 - 90.d	631.4	8.8	NaN	224	3.6	NaN	588	8.6	NaN	78.7	1.1	NaN
dg02 - 91.d	115.3	2.9	NaN	95	1.5	0.019	104.8	2.1	NaN	13.08	0.31	NaN
dg02 - 92.d	122.3	2.3	0.068	89.8	1.6	0.018	109.2	2.3	NaN	15.03	0.36	0.013
dg02 - 95.d	77.9	1.7	0.066	74.8	1.4	NaN	46.8	1.4	NaN	4.61	0.16	NaN
dg02 - 96.d	52.2	1.5	0.15	67.7	1.1	0.049	33.9	1.1	NaN	3.48	0.14	0.009
dg02 - 97.d	13.74	0.77	NaN	49.4	1.2	NaN	9.06	0.62	NaN	1.041	0.065	0.012
dg02 - 98.d	14.72	0.79	0.15	57.8	1.2	0.018	9.98	0.65	0.17	1.098	0.064	NaN
dg02 - 99.d	12.25	0.71	0.14	76	1.4	NaN	8.63	0.38	NaN	0.974	0.072	0.009
dg02 - 100.d	12.51	0.72	NaN	72.1	1.5	0.036	8.94	0.55	0.18	1	0.074	NaN
dg02 - 101.d	17.4	1	NaN	75.5	2	NaN	12.79	0.75	0.061	1.406	0.087	NaN
dg02 - 103.d	28.2	1.3	NaN	44	1.1	NaN	25.9	1	NaN	3.13	0.14	0.018
dg02 - 104.d	67.5	1.5	NaN	103.9	2.1	NaN	51.5	1.6	NaN	6.5	0.18	0.019
dg02 - 105.d	73	2	NaN	107.2	1.8	NaN	56.9	1.5	0.088	6.82	0.25	NaN
dg02 - 106.d	165.1	4	NaN	132.8	2.6	NaN	138	2.9	NaN	17.11	0.47	0.019
dg02 - 107.d	131.9	4.3	0.068	109.3	3.6	NaN	109.1	3.3	NaN	13.48	0.34	NaN
dg02 - 110.d	99.9	1.8	NaN	138.5	2.1	0.054	87.3	2.1	0.063	10.25	0.24	0.02
dg02 - 111.d	139.2	3.7	NaN	169.6	2.4	0.018	118.5	2.4	NaN	13.73	0.36	NaN

Analysis number	Dy163 ppm	Dy163 ppm 2SE	Dy163 ppm LOD	Ho165 ppm	Ho165 ppm 2SE	Ho165 ppm LOD	Er166 ppm	Er166 ppm 2SE	Er166 ppm LOD	Tm169 ppm	Tm169 ppm 2SE	Tm169 ppm LOD
dg02 - 1.d	229.7	3.7	0.073	43.09	0.73	0.012	121.3	2.3	NaN	16.16	0.39	0.0086
dg02 - 2.d	207.2	2.9	NaN	39.28	0.53	NaN	110.3	1.5	NaN	14.77	0.33	NaN
dg02 - 3.d	299.6	4.7	NaN	58.83	0.79	NaN	165.4	2.4	NaN	22.83	0.44	NaN
dg02 - 4.d	370.1	5.3	0.074	68.22	0.94	NaN	182.3	2.8	NaN	24.48	0.46	NaN
dg02 - 5.d	280.7	4.2	NaN	53.87	0.82	0.019	151.9	2.6	NaN	21.07	0.34	0.018
dg02 - 6.d	254.3	3.7	0.062	48.03	0.74	0.019	134.6	2.1	NaN	18.18	0.34	NaN
dg02 - 7.d	126.4	1.9	0.038	26.19	0.52	NaN	79.7	1.4	NaN	11.62	0.29	NaN
dg02 - 8.d	137.5	2.4	NaN	29.29	0.49	0.037	92.3	1.6	NaN	14.07	0.33	0.018
dg02 - 9.d	104.4	1.8	NaN	21.35	0.4	0.0091	63.1	1.4	NaN	8.75	0.18	0.017
dg02 - 10.d	121	1.8	NaN	25.58	0.52	0.02	79.5	1.4	0.055	11.57	0.28	NaN
dg02 - 11.d	94	2.2	NaN	19.62	0.46	NaN	59.6	1.2	0.081	9.33	0.23	0.024
dg02 - 12.d	141.5	2.5	NaN	29.18	0.47	NaN	92.2	1.7	0.037	14.06	0.34	0.0088
dg02 - 13.d	128.2	2.6	NaN	26.87	0.54	0.019	84	1.7	NaN	12.96	0.31	0.017
dg02 - 14.d	157.5	2.6	0.074	33.07	0.54	NaN	103.9	1.6	NaN	15.56	0.33	NaN
dg02 - 15.d	86	1.9	0.15	17.66	0.41	NaN	53.6	1.2	NaN	7.92	0.23	0.018
dg02 - 16.d	98.4	1.8	NaN	20.05	0.38	0.012	59.6	1.1	0.053	8.86	0.21	NaN
dg02 - 17.d	118.6	2.6	NaN	24.35	0.47	NaN	69.5	1.7	NaN	9.7	0.3	0.0086
dg02 - 18.d	139	2.9	NaN	28.78	0.46	NaN	84.8	1.7	0.027	12.58	0.24	0.017
dg02 - 19.d	207.4	3.2	0.036	41.45	0.6	NaN	115.5	1.8	NaN	15.78	0.42	NaN
dg02 - 20.d	262	5.5	NaN	52.9	1.1	NaN	156.7	3.1	0.027	21.99	0.45	0.024
dg02 - 21.d	308.1	5.2	0.037	61.91	0.88	NaN	184.1	2.5	NaN	25.98	0.46	NaN
dg02 - 22.d	131.3	3.3	NaN	26.36	0.67	NaN	76.5	1.9	0.027	10.85	0.21	NaN
dg02 - 23.d	203.7	4.6	NaN	40.9	1.1	NaN	118.1	2.8	NaN	16.68	0.52	0.017
dg02 - 24.d	269.7	3.9	0.037	54.4	0.8	NaN	156.2	2.3	NaN	22.28	0.38	0.012
dg02 - 25.d	269.5	4.9	0.037	54.45	0.97	0.0092	163.7	2.5	0.059	22.82	0.45	NaN
dg02 - 26.d	348.7	7.5	NaN	71.5	1.3	0.0098	211.8	4.5	0.079	30.9	0.76	0.0094
dg02 - 27.d	334.8	6	NaN	67.3	1.1	NaN	195.1	2.5	NaN	28.37	0.54	0.018
dg02 - 28.d	300.3	3.7	NaN	60.27	0.8	NaN	175.3	2.8	0.057	25.21	0.46	NaN
dg02 - 29.d	235.5	4	NaN	46.87	0.67	NaN	136.4	1.9	0.043	19.81	0.46	NaN

Analysis number	Dy163 ppm	Dy163 ppm 2SE	Dy163 ppm LOD	Ho165 ppm	Ho165 ppm 2SE	Ho165 ppm LOD	Er166 ppm	Er166 ppm 2SE	Er166 ppm LOD	Tm169 ppm	Tm169 ppm 2SE	Tm169 ppm LOD
dg02 - 30.d	243	3.7	NaN	49.03	0.72	0.02	143.3	2.5	NaN	20.23	0.48	NaN
dg02 - 31.d	297.6	3.6	NaN	58	1.1	NaN	164.3	3.4	NaN	23	0.48	0.019
dg02 - 32.d	311.7	4.1	NaN	62.97	0.74	0.0098	180.5	2.4	0.067	24.9	0.5	0.0094
dg02 - 33.d	258.5	4.9	NaN	51.7	1	0.021	149.5	3.6	NaN	20.23	0.45	0.014
dg02 - 34.d	209.5	3.4	0.038	42.21	0.76	0.019	124.1	2.1	NaN	17.4	0.35	NaN
dg02 - 35.d	225.1	3.8	NaN	44.88	0.61	0.019	128.1	2.2	NaN	17.86	0.35	NaN
dg02 - 36.d	196.5	2.2	NaN	39.06	0.63	0.0096	113.7	1.4	0.056	15.92	0.28	NaN
dg02 - 37.d	247.4	3.5	NaN	50	0.63	NaN	149.7	2.6	NaN	21.48	0.42	NaN
dg02 - 38.d	256.1	3.7	NaN	52.03	0.7	0.0092	153.7	2.4	NaN	21.97	0.39	0.018
dg02 - 39.d	256.4	4.2	0.038	54.74	0.87	NaN	173.5	2.5	NaN	26.28	0.57	NaN
dg02 - 40.d	118.5	4.4	0.11	24.34	0.75	0.02	73	2.2	NaN	11.4	0.45	NaN
dg02 - 41.d	216.6	3.2	NaN	43.18	0.81	0.0092	124.6	2.1	0.027	17.35	0.34	NaN
dg02 - 42.d	251.8	4.6	NaN	51.23	0.64	NaN	148.4	2.4	0.054	21.19	0.36	NaN
dg02 - 43.d	191.5	3.2	NaN	38.43	0.63	NaN	113.3	2.3	NaN	16.38	0.36	NaN
dg02 - 44.d	238.4	3.5	NaN	49.26	0.85	0.0095	144.9	2.7	NaN	21.02	0.42	0.0091
dg02 - 45.d	213	3.6	NaN	43.08	0.78	0.018	128.1	2.1	NaN	17.84	0.42	0.017
dg02 - 46.d	163.4	2.9	0.073	32.85	0.73	NaN	97	1.8	NaN	13.55	0.29	0.017
dg02 - 47.d	222.6	3.4	0.036	45.68	0.73	NaN	136	2.1	NaN	19.89	0.43	NaN
dg02 - 48.d	219.9	3	0.036	46.03	0.64	NaN	133.7	2.2	NaN	19.48	0.32	NaN
dg02 - 49.d	194.6	3.8	NaN	40.41	0.72	0.018	120.4	2.2	0.027	17.06	0.35	NaN
dg02 - 50.d	189.7	2.6	0.079	38.77	0.66	0.018	117.9	2.5	0.053	17.22	0.33	NaN
dg02 - 51.d	228.9	4.1	NaN	47.13	0.69	NaN	140.7	2.3	NaN	20.18	0.35	NaN
dg02 - 52.d	192.8	2.9	0.074	39.57	0.76	0.013	116.9	2.2	NaN	17.11	0.31	NaN
dg02 - 53.d	229	3.4	0.1	46.62	0.66	NaN	142.1	3	NaN	20.73	0.5	NaN
dg02 - 54.d	179.8	3.2	NaN	37.52	0.62	NaN	113.8	2.1	0.027	17.06	0.38	0.026
dg02 - 55.d	258.1	4.8	NaN	53.38	0.84	NaN	153.7	2.5	0.057	21.8	0.5	NaN
dg02 - 56.d	212.2	3.5	NaN	43.09	0.73	NaN	127.2	2.5	0.029	18.08	0.41	0.0093
dg02 - 57.d	213.3	3.1	NaN	43.48	0.74	NaN	128.4	1.8	NaN	18.22	0.28	NaN
dg02 - 58.d	343.2	6	NaN	69.13	0.86	NaN	201.8	2.9	NaN	28.51	0.46	NaN

Analysis number	Dy163 ppm	Dy163 ppm 2SE	Dy163 ppm LOD	Ho165 ppm	Ho165 ppm 2SE	Ho165 ppm LOD	Er166 ppm	Er166 ppm 2SE	Er166 ppm LOD	Tm169 ppm	Tm169 ppm 2SE	Tm169 ppm LOD
dg02 - 59.d	225.4	3.6	0.077	47	0.91	0.019	139.1	2.8	0.028	19.85	0.43	NaN
dg02 - 60.d	148.8	1.8	NaN	29.96	0.53	NaN	90.4	1.3	NaN	13.25	0.3	NaN
dg02 - 62.d	318.7	4.6	NaN	66.09	0.93	NaN	203.5	2.8	NaN	30.71	0.5	NaN
dg02 - 63.d	297.8	5.1	NaN	61.04	0.85	NaN	176.9	3.4	NaN	25.08	0.48	NaN
dg02 - 64.d	271.6	4.7	NaN	54.26	0.85	NaN	159.8	2.4	NaN	21.89	0.47	NaN
dg02 - 65.d	268.5	3.1	NaN	55.98	0.97	NaN	165.4	2.7	NaN	23.81	0.52	NaN
dg02 - 66.d	239.5	3.2	NaN	48.53	0.85	0.025	143.5	2.2	0.073	20.01	0.36	0.0087
dg02 - 67.d	187.2	3.1	NaN	38.08	0.69	0.021	112.8	1.9	NaN	15.61	0.35	NaN
dg02 - 68.d	252.7	4	NaN	51.81	0.82	NaN	149.7	2.7	NaN	21.13	0.53	NaN
dg02 - 69.d	230.8	6	0.073	47.2	1.3	0.018	140.1	3.2	0.053	20.04	0.41	NaN
dg02 - 70.d	276.2	3.7	NaN	55.13	0.94	NaN	158.3	1.7	0.054	22.23	0.44	0.018
dg02 - 71.d	73.4	1.5	NaN	15.32	0.34	0.018	48.2	1	0.027	7.17	0.24	0.017
dg02 - 72.d	162.8	2.9	NaN	32.79	0.48	0.018	97.7	1.6	NaN	14.28	0.31	NaN
dg02 - 73.d	216.9	3.3	NaN	44.33	0.76	NaN	133.4	1.9	NaN	19.27	0.41	0.017
dg02 - 74.d	202.3	3.3	0.075	41.22	0.6	0.019	123.4	2.1	NaN	18	0.35	NaN
dg02 - 75.d	9.18	0.47	0.075	2.05	0.12	0.028	6.65	0.37	0.028	1.008	0.077	NaN
dg02 - 76.d	495.2	7.6	0.075	101.4	1.2	NaN	302.2	3.3	0.028	43.87	0.57	0.018
dg02 - 77.d	580.6	9.8	0.074	118.8	1.9	NaN	349.8	5.9	0.027	51.46	0.86	NaN
dg02 - 78.d	422.7	6.9	NaN	88.4	1.5	NaN	261.2	4.2	0.054	37.77	0.57	NaN
dg02 - 79.d	481	5.2	0.075	97.5	1.6	NaN	295.2	3.6	NaN	43	0.8	NaN
dg02 - 80.d	508.8	8.6	NaN	101.7	1.3	NaN	296.3	4.8	NaN	42.06	0.69	NaN
dg02 - 82.d	499.5	6.9	NaN	101.9	1.5	NaN	294.3	4.4	NaN	41.49	0.68	0.0094
dg02 - 83.d	505.1	8.5	NaN	100.6	1.5	0.0096	282.4	4.7	0.057	38.68	0.77	NaN
dg02 - 84.d	499.4	6.5	NaN	98.2	1.6	NaN	280.9	4.9	NaN	37.72	0.58	NaN
dg02 - 85.d	446.2	8.3	NaN	89.5	1.8	NaN	247.4	4.6	NaN	33.59	0.73	NaN
dg02 - 86.d	630.7	9.4	NaN	125.9	1.8	NaN	365.5	5	NaN	52.09	0.89	0.019
dg02 - 87.d	612	10	NaN	122.8	1.9	NaN	364.8	5.1	NaN	52.16	0.72	0.019
dg02 - 88.d	48.53	0.99	NaN	11.02	0.27	0.013	36.86	0.74	NaN	5.55	0.19	0.009
dg02 - 89.d	404.4	6.7	0.15	79.8	1.3	NaN	229.3	3.3	NaN	31.79	0.48	NaN

Analysis number	Dy163 ppm	Dy163 ppm 2SE	Dy163 ppm LOD	Ho165 ppm	Ho165 ppm 2SE	Ho165 ppm LOD	Er166 ppm	Er166 ppm 2SE	Er166 ppm LOD	Tm169 ppm	Tm169 ppm 2SE	Tm169 ppm LOD
dg02 - 90.d	479.1	5.5	0.077	97.1	1.3	NaN	281.9	3.7	NaN	40.81	0.61	NaN
dg02 - 91.d	81.4	1.8	NaN	17.51	0.37	0.019	58.6	1.2	NaN	9.34	0.26	0.0092
dg02 - 92.d	96.7	1.7	0.1	22.04	0.44	0.019	77.1	1.1	0.056	12.83	0.26	0.018
dg02 - 95.d	22.09	0.78	NaN	4.22	0.13	NaN	10.84	0.34	0.055	1.346	0.091	NaN
dg02 - 96.d	17.2	0.77	NaN	3.42	0.13	NaN	9.57	0.45	NaN	1.385	0.081	0.012
dg02 - 97.d	6.42	0.35	NaN	1.572	0.096	NaN	5.23	0.3	NaN	0.803	0.067	0.009
dg02 - 98.d	6.91	0.39	0.037	1.56	0.1	0.0093	5.23	0.34	0.06	0.961	0.067	NaN
dg02 - 99.d	5.49	0.39	NaN	1.187	0.092	0.0092	4.57	0.3	NaN	0.703	0.065	NaN
dg02 - 100.d	6.1	0.4	NaN	1.326	0.076	NaN	4.78	0.26	NaN	0.782	0.058	NaN
dg02 - 101.d	7.49	0.4	NaN	1.651	0.092	NaN	5.2	0.29	NaN	0.794	0.084	0.0088
dg02 - 103.d	18.9	0.74	NaN	3.69	0.13	0.0093	10.09	0.44	0.028	1.194	0.068	NaN
dg02 - 104.d	37.99	0.99	0.051	8.75	0.24	NaN	29.72	0.8	NaN	4.84	0.16	0.018
dg02 - 105.d	42.73	0.97	NaN	9.38	0.16	NaN	30.98	0.76	NaN	5.42	0.14	NaN
dg02 - 106.d	98.9	2.4	0.11	20.09	0.45	NaN	58.5	1.2	NaN	8.51	0.26	0.0093
dg02 - 107.d	77.5	2.4	NaN	15.87	0.46	0.0094	45.8	1.3	NaN	6.36	0.26	NaN
dg02 - 110.d	59.6	1.4	NaN	12.52	0.31	NaN	37.32	0.79	NaN	5.76	0.2	0.0092
dg02 - 111.d	78.3	1.9	NaN	15.87	0.39	NaN	47.2	1.2	NaN	6.93	0.2	0.018

Analysis number	Yb172 ppm	Yb172 ppm 2SE	Yb172 ppm LOD	Lu175 ppm	Lu175 ppm 2SE	Lu175 ppm LOD	Hf178 ppm	Hf178 ppm 2SE	Hf178 ppm LOD	Ta181 ppm	Ta181 ppm 2SE	Ta181 ppm LOD
dg02 - 1.d	109.1	2	NaN	18.34	0.38	NaN	19.63	0.61	NaN	32.88	0.62	0.016
dg02 - 2.d	103.5	1.9	0.082	16.86	0.34	NaN	20.17	0.66	0.031	27.4	0.63	NaN
dg02 - 3.d	156.5	3	NaN	25.73	0.45	NaN	22.1	0.69	0.03	38.47	0.75	NaN
dg02 - 4.d	158.4	2.8	0.082	25.95	0.49	NaN	21.05	0.54	NaN	38.58	0.68	NaN
dg02 - 5.d	145.5	2.5	NaN	23.67	0.44	NaN	21.86	0.68	NaN	38.5	0.62	NaN
dg02 - 6.d	122.6	2.7	NaN	19.96	0.34	NaN	22.3	0.7	NaN	39.18	0.59	0.0087
dg02 - 7.d	86	2	NaN	15.45	0.35	NaN	14.02	0.45	0.032	25.45	0.6	NaN
dg02 - 8.d	108.2	2.4	NaN	19.13	0.41	NaN	15.32	0.56	NaN	14.68	0.33	NaN
dg02 - 9.d	61.9	1.8	0.041	10.99	0.24	NaN	11.65	0.49	NaN	18.14	0.79	NaN
dg02 - 10.d	89.5	2.2	0.042	16	0.37	NaN	14.66	0.52	0.043	14.89	0.32	0.023
dg02 - 11.d	66.7	1.9	0.041	11.99	0.28	NaN	13.59	0.5	NaN	12.03	0.49	0.0083
dg02 - 12.d	101.7	2.4	NaN	17.48	0.37	0.018	18.22	0.54	NaN	23.73	0.43	NaN
dg02 - 13.d	94.9	2.2	NaN	16.82	0.4	NaN	15.76	0.43	NaN	18.18	0.4	0.016
dg02 - 14.d	116.5	2.5	0.041	20.66	0.47	NaN	17.19	0.54	0.087	29.12	0.68	NaN
dg02 - 15.d	59.5	1.4	NaN	11.15	0.31	NaN	10.93	0.39	0.031	3.32	0.16	NaN
dg02 - 16.d	66.4	1.7	NaN	12.03	0.24	NaN	12.59	0.58	NaN	3.44	0.12	0.0082
dg02 - 17.d	70.4	2	NaN	12.43	0.32	NaN	13.65	0.44	NaN	5.8	0.2	NaN
dg02 - 18.d	92	1.7	NaN	16.45	0.38	NaN	14.44	0.45	0.062	5.88	0.17	NaN
dg02 - 19.d	109.2	1.8	NaN	17.87	0.35	0.025	16.86	0.54	0.03	24.18	0.67	0.0082
dg02 - 20.d	159.4	3.3	0.04	26.26	0.51	NaN	19.18	0.53	0.041	19.31	0.39	NaN
dg02 - 21.d	178.4	3.2	0.11	28.74	0.6	NaN	20.77	0.52	0.062	28.86	0.53	NaN
dg02 - 22.d	77.2	1.9	NaN	13.71	0.36	NaN	15.66	0.61	NaN	17.98	0.57	0.022
dg02 - 23.d	118.9	3	0.081	19.29	0.57	0.009	17.44	0.61	0.03	29.71	0.71	NaN
dg02 - 24.d	160.3	2.7	NaN	25.67	0.46	0.0091	21.38	0.5	NaN	34.73	0.63	0.017
dg02 - 25.d	162.6	2.4	0.041	26.12	0.56	0.018	20.71	0.58	0.031	28.19	0.62	NaN
dg02 - 26.d	221.7	5.1	NaN	34.95	0.83	NaN	22.01	0.8	0.066	34	0.79	0.0089
dg02 - 27.d	205.2	3.6	NaN	32.61	0.58	NaN	20.08	0.6	0.062	44.75	0.84	NaN
dg02 - 28.d	179.7	2.9	NaN	28.82	0.58	0.018	20.04	0.63	NaN	44.55	0.87	NaN
dg02 - 29.d	136.4	2.6	NaN	22.49	0.45	0.009	17.92	0.64	0.03	35.89	0.57	NaN

Analysis number	Yb172 ppm	Yb172 ppm 2SE	Yb172 ppm LOD	Lu175 ppm	Lu175 ppm 2SE	Lu175 ppm LOD	Hf178 ppm	Hf178 ppm 2SE	Hf178 ppm LOD	Ta181 ppm	Ta181 ppm 2SE	Ta181 ppm LOD
dg02 - 30.d	138.9	2.6	NaN	22	0.41	0.02	18.23	0.68	NaN	17.61	0.39	NaN
dg02 - 31.d	152.4	3.4	NaN	24.17	0.47	NaN	18.74	0.68	0.033	26.63	0.55	NaN
dg02 - 32.d	171.1	3.1	0.088	26.59	0.52	0.0098	18.5	0.5	0.09	30.83	0.57	NaN
dg02 - 33.d	138.8	2.7	0.066	21.98	0.49	0.011	15.42	0.59	0.072	14.19	0.4	NaN
dg02 - 34.d	120.1	2.1	NaN	19.29	0.35	0.028	15.34	0.53	0.073	5.64	0.17	0.034
dg02 - 35.d	124.8	2.2	NaN	20.54	0.46	0.013	16.09	0.53	NaN	10.34	0.28	NaN
dg02 - 36.d	108.5	2.2	NaN	17.74	0.34	0.019	13.93	0.61	0.032	11.67	0.35	NaN
dg02 - 37.d	152.3	2.6	0.13	25.2	0.39	0.028	18.43	0.66	0.062	11.98	0.3	0.0085
dg02 - 38.d	154.7	2.8	NaN	24.9	0.48	NaN	17.35	0.48	0.031	16.64	0.33	0.018
dg02 - 39.d	189.4	3.9	0.042	31.82	0.63	0.0093	20.71	0.57	0.063	14.96	0.34	NaN
dg02 - 40.d	82.4	2.8	NaN	14.3	0.46	NaN	9.31	0.56	NaN	7.68	0.27	NaN
dg02 - 41.d	121.2	2.3	0.082	20.16	0.43	NaN	15.71	0.53	NaN	18.24	0.37	NaN
dg02 - 42.d	148.2	2.6	NaN	23.97	0.5	NaN	15.91	0.57	NaN	18.25	0.44	NaN
dg02 - 43.d	116.4	2.5	NaN	19.05	0.45	0.0091	13.75	0.43	NaN	11.47	0.25	NaN
dg02 - 44.d	149.2	3	0.042	23.95	0.42	NaN	16.08	0.45	NaN	15.45	0.28	NaN
dg02 - 45.d	123.6	2.3	0.041	20.53	0.39	NaN	14.67	0.55	0.061	8.64	0.23	NaN
dg02 - 46.d	94.3	2.5	NaN	15.31	0.34	NaN	12.83	0.48	NaN	6.04	0.14	NaN
dg02 - 47.d	137.7	3	0.081	22.57	0.47	0.025	16	0.58	NaN	12	0.28	NaN
dg02 - 48.d	139.4	2.3	0.08	22.99	0.47	NaN	16.02	0.5	NaN	12.94	0.34	NaN
dg02 - 49.d	124	1.9	0.081	20.66	0.37	NaN	14.56	0.54	NaN	9.48	0.25	0.016
dg02 - 50.d	123.3	2.1	NaN	20.32	0.45	NaN	14	0.4	0.06	9.58	0.23	0.016
dg02 - 51.d	144.5	3	NaN	23.37	0.48	0.018	16.04	0.58	0.066	19.26	0.52	0.0082
dg02 - 52.d	120	2.6	NaN	19.87	0.33	NaN	14.7	0.64	NaN	10.87	0.27	NaN
dg02 - 53.d	145.3	2.4	0.041	23.68	0.55	0.0091	17.09	0.44	0.031	16.5	0.43	NaN
dg02 - 54.d	122.9	2.1	NaN	20.06	0.41	NaN	14.26	0.54	NaN	10.67	0.28	0.011
dg02 - 55.d	154	3.1	NaN	24.63	0.46	NaN	17.52	0.52	NaN	40.14	0.79	0.024
dg02 - 56.d	122.7	2	0.044	20.53	0.43	NaN	15.37	0.63	NaN	25.65	0.36	0.0089
dg02 - 57.d	128.6	2.7	NaN	20.38	0.44	0.019	15.05	0.56	0.032	15.01	0.31	NaN
dg02 - 58.d	193	3.6	NaN	30.72	0.57	NaN	19.8	0.66	NaN	52.1	1	NaN

Analysis number	Yb172 ppm	Yb172 ppm 2SE	Yb172 ppm LOD	Lu175 ppm	Lu175 ppm 2SE	Lu175 ppm LOD	Hf178 ppm	Hf178 ppm 2SE	Hf178 ppm LOD	Ta181 ppm	Ta181 ppm 2SE	Ta181 ppm LOD
dg02 - 59.d	139.3	2.6	0.043	23.07	0.57	NaN	16.43	0.54	NaN	18.17	0.28	NaN
dg02 - 60.d	94.3	1.6	0.042	15.05	0.31	0.019	12.31	0.46	0.063	9.31	0.26	0.017
dg02 - 62.d	227.5	4.1	NaN	36.85	0.81	0.018	19.5	0.73	0.031	21.45	0.5	NaN
dg02 - 63.d	173.5	3.3	NaN	27.61	0.51	NaN	17.49	0.58	NaN	20.68	0.46	NaN
dg02 - 64.d	150.2	2.8	NaN	23.75	0.51	NaN	16.48	0.55	0.031	15.06	0.4	NaN
dg02 - 65.d	167.7	3.4	0.096	27.18	0.52	NaN	16.35	0.6	0.031	10.22	0.28	NaN
dg02 - 66.d	140.5	1.7	NaN	22.74	0.33	0.009	15.89	0.49	NaN	8.44	0.22	NaN
dg02 - 67.d	105.6	2.2	NaN	17.69	0.4	0.0092	12.87	0.57	NaN	6.52	0.2	NaN
dg02 - 68.d	144.6	3.4	NaN	23.11	0.48	NaN	18.62	0.58	NaN	16.58	0.37	NaN
dg02 - 69.d	139.3	2.9	0.081	23.1	0.55	0.018	17.9	0.57	0.06	24.82	0.65	NaN
dg02 - 70.d	147.7	2.3	NaN	23.46	0.42	NaN	18.51	0.6	NaN	14.81	0.3	0.0084
dg02 - 71.d	59.6	1.3	NaN	11.13	0.24	0.02	13.02	0.42	NaN	8.66	0.21	0.0083
dg02 - 72.d	101.4	1.9	NaN	17.5	0.35	0.0091	16.91	0.43	NaN	44.1	1.3	0.017
dg02 - 73.d	143.7	2.4	NaN	23.81	0.54	0.009	19.61	0.66	NaN	63.61	0.88	0.0083
dg02 - 74.d	132.1	2.4	NaN	22.22	0.37	NaN	19.08	0.5	NaN	55.88	0.91	0.018
dg02 - 75.d	8.77	0.57	NaN	2.015	0.099	NaN	3.72	0.27	NaN	0.634	0.062	0.0085
dg02 - 76.d	309	5.4	NaN	47.25	0.77	NaN	20.21	0.63	NaN	13.92	0.24	0.023
dg02 - 77.d	355.6	6.1	NaN	52.8	1.2	NaN	21.74	0.7	NaN	24.19	0.6	0.017
dg02 - 78.d	266.7	4.9	0.056	42.27	0.94	0.018	18.44	0.62	NaN	9.61	0.24	NaN
dg02 - 79.d	302.5	5.3	NaN	47.35	0.78	NaN	20.47	0.7	0.068	13.01	0.29	0.0085
dg02 - 80.d	291.9	5.1	NaN	43.62	0.77	NaN	22.36	0.6	NaN	19.06	0.47	0.018
dg02 - 82.d	291.1	4.6	0.088	44.33	0.78	0.0097	23.68	0.67	0.071	21.31	0.35	NaN
dg02 - 83.d	254.8	5.7	NaN	38.91	0.74	NaN	21.45	0.8	NaN	24.82	0.52	NaN
dg02 - 84.d	248.6	3.6	0.12	37.15	0.71	0.019	20.78	0.8	NaN	22.74	0.63	NaN
dg02 - 85.d	219.5	4.7	NaN	33.06	0.7	NaN	20.14	0.65	NaN	21.34	0.49	NaN
dg02 - 86.d	356.7	4.5	NaN	52.99	0.99	NaN	24.66	0.69	0.065	32.43	0.59	NaN
dg02 - 87.d	354	6	0.045	52.99	0.83	NaN	23.55	0.81	NaN	31.77	0.47	0.0093
dg02 - 88.d	45.08	0.93	NaN	9.47	0.25	NaN	6.01	0.27	NaN	1.111	0.083	NaN
dg02 - 89.d	216.7	4.1	NaN	32.96	0.62	NaN	18.96	0.67	0.032	19.86	0.54	NaN

Analysis number	Yb172 ppm	Yb172 ppm 2SE	Yb172 ppm LOD	Lu175 ppm	Lu175 ppm 2SE	Lu175 ppm LOD	Hf178 ppm	Hf178 ppm 2SE	Hf178 ppm LOD	Ta181 ppm	Ta181 ppm 2SE	Ta181 ppm LOD
dg02 - 90.d	279.1	3.8	NaN	42.4	0.58	NaN	20.64	0.54	0.064	18.52	0.46	0.019
dg02 - 91.d	74.7	1.8	0.043	14.78	0.35	NaN	10.19	0.46	0.032	1.407	0.067	0.012
dg02 - 92.d	107.6	2	0.092	21	0.4	NaN	11.9	0.52	NaN	1.81	0.1	NaN
dg02 - 95.d	9.67	0.51	NaN	1.87	0.11	NaN	8.96	0.4	NaN	8.8	0.23	NaN
dg02 - 96.d	9.31	0.4	0.083	1.96	0.1	0.0092	9.05	0.48	NaN	6.07	0.19	0.012
dg02 - 97.d	6.99	0.5	0.13	1.56	0.11	0.038	10	0.46	0.063	0.768	0.062	0.026
dg02 - 98.d	7.99	0.43	NaN	1.74	0.1	NaN	10.21	0.39	NaN	0.676	0.064	0.0085
dg02 - 99.d	6.54	0.39	0.083	1.611	0.098	NaN	10.28	0.42	0.031	0.653	0.048	NaN
dg02 - 100.d	7.32	0.55	NaN	1.565	0.096	NaN	9.83	0.5	0.061	0.583	0.06	0.018
dg02 - 101.d	6.55	0.4	NaN	1.44	0.1	0.032	8.73	0.33	NaN	1.066	0.074	NaN
dg02 - 103.d	8.57	0.49	NaN	1.529	0.074	0.018	7.72	0.36	0.062	1.432	0.097	NaN
dg02 - 104.d	43.7	1.2	NaN	8.57	0.29	NaN	9.99	0.45	0.061	0.997	0.061	NaN
dg02 - 105.d	44.8	1.4	0.044	9.2	0.24	NaN	9.99	0.51	NaN	0.999	0.073	NaN
dg02 - 106.d	64.1	1.7	0.087	11.31	0.26	NaN	10.95	0.51	NaN	4.41	0.11	NaN
dg02 - 107.d	47.4	1.8	0.084	8.68	0.26	NaN	9.51	0.51	NaN	3.35	0.14	0.017
dg02 - 110.d	43.3	1.1	NaN	8.5	0.25	NaN	7.43	0.39	0.044	8.45	0.32	NaN
dg02 - 111.d	50.1	1.5	NaN	9.41	0.26	0.019	8.08	0.44	0.032	9.34	0.24	NaN

Analysis number	W182 ppm	W182 ppm 2SE	W182 ppm LOD	Pb204 ppm	Pb204 ppm 2SE	Pb204 ppm LOD	Pb206 ppm	Pb206 ppm 2SE	Pb206 ppm LOD	Pb207 ppm	Pb207 ppm 2SE	Pb207 ppm LOD
dg02 - 1.d	2.7	0.22	0.034	< LOD	< LOD	6.9	45.2	1.3	0.15	5.39	0.14	0.033
dg02 - 2.d	2.39	0.2	0.069	< LOD	< LOD	6.7	47.7	1.3	0.14	5.82	0.13	0.047
dg02 - 3.d	2.95	0.26	NaN	< LOD	< LOD	6.9	62.2	1.6	0.17	6.8	0.2	0.028
dg02 - 4.d	2.78	0.22	NaN	< LOD	< LOD	8.8	78.7	3.3	0.2	14.2	1.1	0.051
dg02 - 5.d	2.72	0.26	NaN	8.6	2.5	5.6	76.5	2.1	0.14	12.93	0.39	0.036
dg02 - 6.d	2.72	0.17	0.036	< LOD	< LOD	6.2	65.2	1.5	0.05	10.93	0.3	0.044
dg02 - 7.d	2.26	0.21	NaN	< LOD	< LOD	6.4	29.9	1	0.11	4.01	0.15	0.055
dg02 - 8.d	2.6	0.19	NaN	< LOD	< LOD	6.6	35.1	1.1	0.2	4.58	0.12	0.038
dg02 - 9.d	2.38	0.22	NaN	< LOD	< LOD	5.2	21.18	0.72	0.11	3.73	0.2	0.043
dg02 - 10.d	2.37	0.19	NaN	< LOD	< LOD	5.1	29.8	0.95	0.14	4.34	0.12	0.053
dg02 - 11.d	2.46	0.23	0.069	< LOD	< LOD	7.1	26.2	0.97	0.22	4.36	0.13	0.051
dg02 - 12.d	2.63	0.21	0.035	< LOD	< LOD	6.2	41.1	1.1	0.2	6.78	0.21	0.049
dg02 - 13.d	2.57	0.25	0.068	< LOD	< LOD	7.7	34.7	1.2	0.15	5.01	0.14	0.046
dg02 - 14.d	2.76	0.2	NaN	< LOD	< LOD	5.3	38.5	1.1	0.12	4.75	0.15	0.035
dg02 - 15.d	1.57	0.17	NaN	5.3	2.3	4.7	13.17	0.72	0.19	2.637	0.096	0.048
dg02 - 16.d	1.85	0.19	0.034	< LOD	< LOD	7.8	15.92	0.74	0.12	2.89	0.1	0.047
dg02 - 17.d	1.88	0.17	0.068	6.4	2.2	4.8	19.68	0.74	0.16	3.25	0.11	0.037
dg02 - 18.d	2.04	0.16	NaN	< LOD	< LOD	5.5	20.7	0.87	0.14	3.02	0.1	0.037
dg02 - 19.d	2.29	0.2	0.074	< LOD	< LOD	4.7	28.4	1	0.1	4.59	0.17	0.046
dg02 - 20.d	2.37	0.2	NaN	< LOD	< LOD	6.8	35.9	1.1	0.16	4.77	0.12	0.041
dg02 - 21.d	2.27	0.23	NaN	< LOD	< LOD	6.5	39.8	1.4	0.13	4.98	0.17	0.045
dg02 - 22.d	2.12	0.23	0.034	< LOD	< LOD	7.9	22.27	0.76	0.11	4.18	0.15	0.039
dg02 - 23.d	2.39	0.23	0.034	< LOD	< LOD	5.7	29.6	1.1	0.16	4.56	0.13	0.038
dg02 - 24.d	2.5	0.25	NaN	< LOD	< LOD	5.6	43.1	1.2	0.17	6.13	0.15	0.051
dg02 - 25.d	2.42	0.24	NaN	< LOD	< LOD	6.4	43.4	1.1	0.12	6.9	0.21	0.056
dg02 - 26.d	2.57	0.23	NaN	11.6	3.7	8.4	77.6	3.1	0.15	13.83	0.67	0.056
dg02 - 27.d	2.35	0.22	0.08	5.7	2.8	5.3	66.6	3	0.11	11.38	0.61	0.052
dg02 - 28.d	2.43	0.22	NaN	< LOD	< LOD	6.5	43.5	1.3	0.11	5.01	0.11	0.036
dg02 - 29.d	2.28	0.21	NaN	< LOD	< LOD	4.4	31.87	0.86	0.095	4.84	0.13	0.051

Analysis number	W182 ppm	W182 ppm 2SE	W182 ppm LOD	Pb204 ppm	Pb204 ppm 2SE	Pb204 ppm LOD	Pb206 ppm	Pb206 ppm 2SE	Pb206 ppm LOD	Pb207 ppm	Pb207 ppm 2SE	Pb207 ppm LOD
dg02 - 30.d	2.39	0.2	NaN	< LOD	< LOD	7	37.6	1.3	0.13	7.19	0.3	0.029
dg02 - 31.d	2.7	0.24	0.037	< LOD	< LOD	5.8	33.6	1	0.15	4.82	0.13	0.056
dg02 - 32.d	2.62	0.25	NaN	< LOD	< LOD	4.9	34.54	0.98	0.25	5.03	0.11	0.045
dg02 - 33.d	1.96	0.18	NaN	< LOD	< LOD	6.4	25.6	0.94	0.077	3.89	0.17	0.062
dg02 - 34.d	2.13	0.17	0.036	< LOD	< LOD	6.5	23.5	1.1	0.31	3.41	0.11	0.048
dg02 - 35.d	2.44	0.24	0.073	< LOD	< LOD	5.6	27.02	0.93	0.18	3.92	0.12	0.032
dg02 - 36.d	1.87	0.2	NaN	< LOD	< LOD	7.1	25.87	0.84	0.16	4.56	0.15	0.062
dg02 - 37.d	2.64	0.24	NaN	< LOD	< LOD	6.7	35.3	1.1	0.18	4.97	0.16	0.043
dg02 - 38.d	2.94	0.18	NaN	< LOD	< LOD	6.4	29.08	0.87	0.078	3.95	0.15	0.043
dg02 - 39.d	2.84	0.26	NaN	< LOD	< LOD	7.3	38.93	0.96	0.2	4.81	0.11	0.043
dg02 - 40.d	2.6	0.23	NaN	< LOD	< LOD	4	20.72	0.68	0.21	3.27	0.11	0.067
dg02 - 41.d	2.61	0.19	NaN	< LOD	< LOD	7.1	25.67	0.91	0.11	3.85	0.13	0.034
dg02 - 42.d	2.67	0.21	NaN	< LOD	< LOD	7.3	28.77	0.85	0.11	3.97	0.12	0.048
dg02 - 43.d	2.36	0.19	0.035	< LOD	< LOD	6.9	24.03	0.77	0.13	3.84	0.17	0.027
dg02 - 44.d	2.79	0.23	NaN	< LOD	< LOD	8.2	35.6	1.2	0.14	5.27	0.16	0.045
dg02 - 45.d	2.19	0.22	0.047	< LOD	< LOD	4.9	25.1	1.2	0.11	3.75	0.11	0.037
dg02 - 46.d	2.28	0.17	NaN	< LOD	< LOD	6.6	18.88	0.8	0.16	3.46	0.13	0.037
dg02 - 47.d	2.45	0.23	NaN	< LOD	< LOD	4.9	29.74	0.84	0.11	4.56	0.12	0.044
dg02 - 48.d	2.53	0.24	0.034	< LOD	< LOD	5.9	29.5	1.2	0.12	4.03	0.13	0.027
dg02 - 49.d	2.49	0.22	NaN	< LOD	< LOD	5.4	26.98	0.74	0.15	3.9	0.13	0.044
dg02 - 50.d	2.1	0.25	0.074	< LOD	< LOD	5.3	26.08	0.85	0.13	4.12	0.13	0.036
dg02 - 51.d	2.5	0.21	0.047	< LOD	< LOD	4.7	37	1.4	0.086	5.71	0.17	0.054
dg02 - 52.d	2.44	0.21	NaN	< LOD	< LOD	5.9	26.3	0.92	0.12	3.85	0.11	0.043
dg02 - 53.d	2.37	0.19	0.069	< LOD	< LOD	4.6	38.6	1.5	0.11	6.25	0.38	0.046
dg02 - 54.d	2.39	0.18	0.034	< LOD	< LOD	5.4	28	1	0.14	4.11	0.17	0.035
dg02 - 55.d	2.75	0.27	NaN	< LOD	< LOD	6.3	33.49	0.91	0.23	4.41	0.11	0.049
dg02 - 56.d	2.72	0.25	0.074	< LOD	< LOD	6.5	29.6	1.1	0.21	4.76	0.15	0.058
dg02 - 57.d	2.12	0.2	NaN	< LOD	< LOD	9.3	28.36	0.72	0.069	4.11	0.12	0.055
dg02 - 58.d	3.02	0.18	NaN	< LOD	< LOD	7.3	44.3	1.1	0.23	5.32	0.15	0.035

Analysis number	W182 ppm	W182 ppm 2SE	W182 ppm LOD	Pb204 ppm	Pb204 ppm 2SE	Pb204 ppm LOD	Pb206 ppm	Pb206 ppm 2SE	Pb206 ppm LOD	Pb207 ppm	Pb207 ppm 2SE	Pb207 ppm LOD
dg02 - 59.d	2.5	0.24	NaN	< LOD	< LOD	5.9	37.2	1.4	0.17	6.47	0.34	0.067
dg02 - 60.d	1.95	0.19	NaN	< LOD	< LOD	7.2	18.25	0.71	0.18	3.48	0.11	0.05
dg02 - 62.d	2.65	0.21	NaN	< LOD	< LOD	8.3	52.4	1.6	0.14	6.43	0.19	0.063
dg02 - 63.d	2.7	0.2	0.07	< LOD	< LOD	6.5	31.7	1	0.23	4.43	0.16	0.034
dg02 - 64.d	2.57	0.2	NaN	< LOD	< LOD	8.4	31.5	1.1	0.21	4.59	0.21	0.034
dg02 - 65.d	2.37	0.22	0.07	< LOD	< LOD	7.3	31.2	1.1	0.19	4.17	0.15	0.035
dg02 - 66.d	2.42	0.23	0.034	< LOD	< LOD	6.7	28.3	0.91	0.14	4.07	0.12	0.045
dg02 - 67.d	2.05	0.2	0.048	< LOD	< LOD	7	17.73	0.65	0.16	3.05	0.11	0.048
dg02 - 68.d	2.74	0.24	0.11	< LOD	< LOD	7.4	30.6	1.4	0.12	4.21	0.1	0.036
dg02 - 69.d	3.04	0.2	0.034	< LOD	< LOD	5.2	31.34	0.94	0.14	4.59	0.14	0.054
dg02 - 70.d	2.49	0.23	0.07	< LOD	< LOD	8.8	28.6	1.1	0.049	4.19	0.13	0.043
dg02 - 71.d	2.55	0.21	0.069	< LOD	< LOD	6.2	18.75	0.7	0.2	2.913	0.099	0.039
dg02 - 72.d	2.79	0.26	NaN	< LOD	< LOD	7.2	44.7	1.2	0.16	7.33	0.21	0.053
dg02 - 73.d	2.83	0.21	NaN	< LOD	< LOD	9.5	45.6	1.1	0.048	5.74	0.13	0.057
dg02 - 74.d	2.46	0.21	NaN	< LOD	< LOD	6.8	42.3	1.3	0.27	5.9	0.14	0.049
dg02 - 75.d	1.46	0.16	NaN	< LOD	< LOD	5.6	3.41	0.36	0.16	1.33	0.084	0.064
dg02 - 76.d	2.27	0.17	NaN	< LOD	< LOD	8	49.7	1.7	0.049	7.58	0.3	0.034
dg02 - 77.d	2.5	0.2	NaN	< LOD	< LOD	4.1	54.8	1.7	0.17	6.85	0.21	0.047
dg02 - 78.d	2.26	0.24	NaN	< LOD	< LOD	8.3	39.8	1.3	0.096	5.41	0.14	0.055
dg02 - 79.d	1.96	0.21	NaN	< LOD	< LOD	4.8	38	1	0.18	4.72	0.13	0.06
dg02 - 80.d	2.75	0.2	NaN	< LOD	< LOD	6.5	45.1	1.3	0.07	5.71	0.15	0.048
dg02 - 82.d	2.32	0.17	NaN	< LOD	< LOD	9.1	44.4	1.3	0.11	5.38	0.12	0.072
dg02 - 83.d	2.57	0.21	NaN	< LOD	< LOD	7.6	35.4	1	0.18	4.51	0.14	0.066
dg02 - 84.d	2.46	0.2	NaN	< LOD	< LOD	5.9	35.4	1	0.12	4.68	0.16	0.048
dg02 - 85.d	2.15	0.19	0.074	< LOD	< LOD	8	30.9	1	0.18	4.51	0.12	0.048
dg02 - 86.d	2.61	0.24	NaN	11.9	2.8	10	64.6	1.8	0.17	7.21	0.16	0.034
dg02 - 87.d	2.56	0.19	0.1	17.6	3.4	11	88.7	1.8	0.17	16.15	0.52	0.036
dg02 - 88.d	1.05	0.15	0.071	< LOD	< LOD	6.9	3.75	0.3	0.11	1.315	0.062	0.063
dg02 - 89.d	2.55	0.18	0.072	8.5	2.8	6.5	35.4	1.2	0.11	6.05	0.23	0.047

Analysis number	W182 ppm	W182 ppm 2SE	W182 ppm LOD	Pb204 ppm	Pb204 ppm 2SE	Pb204 ppm LOD	Pb206 ppm	Pb206 ppm 2SE	Pb206 ppm LOD	Pb207 ppm	Pb207 ppm 2SE	Pb207 ppm LOD
dg02 - 90.d	2.7	0.29	NaN	6.7	2.6	5.6	40.9	1.1	NaN	5.24	0.11	0.043
dg02 - 91.d	1.51	0.19	0.099	7.2	2.7	5.2	9.62	0.55	0.069	1.988	0.073	0.056
dg02 - 92.d	1.98	0.2	0.072	8.3	2.8	6.5	11.87	0.55	0.24	2.189	0.088	0.06
dg02 - 95.d	1.98	0.16	NaN	< LOD	< LOD	5.9	5.65	0.43	0.11	2.091	0.067	0.05
dg02 - 96.d	1.88	0.16	NaN	< LOD	< LOD	8.4	4.68	0.29	0.16	1.833	0.082	0.061
dg02 - 97.d	2.01	0.22	0.077	< LOD	< LOD	7.8	5.37	0.41	0.14	1.946	0.09	0.047
dg02 - 98.d	2.32	0.19	0.07	< LOD	< LOD	7	6.02	0.41	0.16	2.023	0.086	0.053
dg02 - 99.d	2.19	0.2	0.07	< LOD	< LOD	6.7	6.19	0.43	0.26	1.804	0.072	0.04
dg02 - 100.d	2.24	0.17	NaN	< LOD	< LOD	4.4	6.39	0.4	0.19	1.984	0.067	0.039
dg02 - 101.d	1.98	0.19	0.069	< LOD	< LOD	5.4	4.88	0.34	0.18	1.88	0.11	0.039
dg02 - 103.d	1.56	0.16	0.07	< LOD	< LOD	6.7	4.52	0.38	0.049	2.187	0.073	0.06
dg02 - 104.d	1.81	0.18	NaN	< LOD	< LOD	5.8	10.59	0.67	0.18	2.197	0.074	0.063
dg02 - 105.d	1.64	0.19	NaN	< LOD	< LOD	7.2	11.03	0.63	0.29	2.293	0.083	0.043
dg02 - 106.d	2.07	0.24	0.037	< LOD	< LOD	7.3	14.36	0.67	0.21	3.34	0.13	0.059
dg02 - 107.d	1.71	0.19	NaN	< LOD	< LOD	4.8	10.38	0.53	0.18	3.02	0.18	0.052
dg02 - 110.d	1.84	0.2	NaN	< LOD	< LOD	6.4	10.99	0.69	0.11	3.04	0.13	0.058
dg02 - 111.d	2.36	0.21	NaN	< LOD	< LOD	5.2	11.06	0.54	0.08	2.034	0.095	0.058

Analysis number	Pb208 ppm	Pb208 ppm 2SE	Pb208 ppm LOD	Th232 ppm	Th232 ppm 2SE	Th232 ppm LOD	U238 ppm	U238 ppm 2SE	U238 ppm LOD	Zr in Tt temp (°C)	grain number	REE group
dg02 - 1.d	16.58	0.24	0.027	161.6	2.8	NaN	64.2	1	NaN	753	1	2B
dg02 - 2.d	15.92	0.25	0.032	133.4	2	NaN	61.6	0.86	0.01	752	1	2B
dg02 - 3.d	20.27	0.33	0.027	194.4	2	NaN	85.9	1	0.011	759	1	2B
dg02 - 4.d	41.4	3.1	0.031	229.6	3.2	0.016	93.6	1.4	0.01	759	1	2B
dg02 - 5.d	38.5	1	0.034	226.6	3.2	NaN	90.2	1.4	0.0085	761	1	2B
dg02 - 6.d	33.93	0.62	0.032	210.9	3.2	0.0076	80.3	1.4	0.021	763	1	2B
dg02 - 7.d	14.21	0.18	0.029	137.7	2.4	NaN	39.64	0.59	NaN	748	2	2A
dg02 - 8.d	18.8	0.25	0.03	174.8	2.3	0.012	46.77	0.86	0.01	754	2	2C
dg02 - 9.d	12.09	0.56	0.024	91.1	1.7	NaN	25.42	0.45	NaN	739	2	2A
dg02 - 10.d	16.61	0.23	0.036	150.5	1.7	0.021	39.55	0.56	0.0051	754	2	2A
dg02 - 11.d	15.77	0.43	0.018	116.7	2.2	0.0073	32.55	0.49	0.012	748	2	2A
dg02 - 12.d	27.08	0.6	0.029	211.7	3.4	NaN	53.3	0.94	0.012	764	2	2A
dg02 - 13.d	21.21	0.24	0.024	179.3	2.2	0.019	45.18	0.73	0.0099	755	2	2A
dg02 - 14.d	21.26	0.28	0.024	201.4	2.8	NaN	52.8	1	0.0051	760	2	2A
dg02 - 15.d	7.13	0.18	0.025	53.66	0.86	NaN	16.58	0.33	NaN	734	3	2A
dg02 - 16.d	8.36	0.16	0.025	67.2	1	NaN	20.96	0.31	0.0068	737	3	2A
dg02 - 17.d	11	0.2	0.023	96.9	1.6	0.0072	24.92	0.6	NaN	744	3	2A
dg02 - 18.d	10.24	0.19	0.028	96	1.5	NaN	28.36	0.46	0.01	745	3	2A
dg02 - 19.d	18.08	0.36	0.024	161.8	1.9	0.025	36.74	0.53	0.02	749	3	2A
dg02 - 20.d	20.78	0.48	0.036	195.1	3.1	0.014	47.18	0.73	NaN	757	3	2A
dg02 - 21.d	22.78	0.43	0.035	218.2	3.5	0.0073	53.01	0.95	NaN	759	3	2A
dg02 - 22.d	12.79	0.37	0.042	87.4	1.9	0.016	29.03	0.7	NaN	752	4	2A
dg02 - 23.d	17.8	0.33	0.024	148.7	3.9	NaN	39.68	0.85	0.01	753	4	2A
dg02 - 24.d	27.33	0.5	0.033	234	2.7	NaN	55.77	0.81	0.014	762	4	2A
dg02 - 25.d	28.14	0.43	0.029	233.1	4.1	NaN	59.7	1.1	0.01	764	4	2A
dg02 - 26.d	47.7	2	0.025	281.7	5.7	0.021	90.1	2.9	NaN	767	4	2A
dg02 - 27.d	39.4	1.7	0.025	247	3.5	0.053	75.6	1.2	NaN	762	5	2A
dg02 - 28.d	23.34	0.27	0.023	228.3	3.6	0.0071	58.8	1	0.0098	762	6	2A
dg02 - 29.d	19.2	0.21	0.021	177.4	2.2	NaN	43.77	0.65	0.005	755	6	2A

Analysis number	Pb208 ppm	Pb208 ppm 2SE	Pb208 ppm LOD	Th232 ppm	Th232 ppm 2SE	Th232 ppm LOD	U238 ppm	U238 ppm 2SE	U238 ppm LOD	Zr in Tt temp (°C)	grain number	REE group
dg02 - 30.d	23.19	0.75	0.031	145.8	1.9	NaN	48.25	0.83	NaN	754	7	2A
dg02 - 31.d	18.38	0.32	0.026	169.1	3.1	0.011	45.01	0.95	NaN	755	7	2A
dg02 - 32.d	18.24	0.31	0.038	169.9	2.1	0.016	46.71	0.63	0.013	755	7	2A
dg02 - 33.d	12.63	0.26	0.039	115.1	2.8	NaN	35.42	0.77	0.012	746	8	2A
dg02 - 34.d	11.66	0.16	0.031	107.5	1.7	0.021	32.05	0.59	NaN	748	9	2A
dg02 - 35.d	14.56	0.36	0.041	135.2	2.4	NaN	36.93	0.54	NaN	752	9	2A
dg02 - 36.d	13.49	0.21	0.04	114.5	1.7	NaN	31.91	0.48	NaN	743	9	2A
dg02 - 37.d	19.03	0.26	0.034	167.2	2.9	0.015	46.41	0.82	0.011	759	10	2A
dg02 - 38.d	16.47	0.29	0.021	160.2	2.4	0.0074	40.26	0.73	0.007	755	10	2A
dg02 - 39.d	18.41	0.3	0.03	178.7	3.1	0.015	52.5	1	0.01	762	10	2A
dg02 - 40.d	9.56	0.22	0.021	74.8	2.3	0.0074	26.28	0.62	0.0052	734	10	2A
dg02 - 41.d	14.01	0.33	0.03	126.2	2	0.024	35.13	0.61	0.014	751	10	2A
dg02 - 42.d	15.52	0.29	0.03	150	2.1	0.015	39.84	0.66	0.0051	753	10	2A
dg02 - 43.d	13.13	0.31	0.02	111.9	2	NaN	32.62	0.61	NaN	747	10	2A
dg02 - 44.d	19.83	0.43	0.027	163.3	2.4	0.015	45.3	0.74	0.011	757	10	2A
dg02 - 45.d	13.07	0.24	0.024	116.6	2.1	0.0073	32.95	0.75	0.0051	749	10	2A
dg02 - 46.d	10.11	0.29	0.034	77.8	1.3	NaN	24.67	0.57	NaN	744	10	2A
dg02 - 47.d	16.92	0.29	0.027	147.6	2.3	NaN	40.7	0.71	0.01	755	10	2A
dg02 - 48.d	15.71	0.28	0.031	147.3	2.2	NaN	39.58	0.65	NaN	755	10	2A
dg02 - 49.d	14.16	0.26	0.024	124.6	2.4	0.014	35.41	0.58	NaN	751	10	2A
dg02 - 50.d	13.96	0.2	0.022	118.3	1.3	0.0072	36.49	0.58	0.016	750	10	2A
dg02 - 51.d	20.96	0.53	0.034	156.1	2.2	0.02	45.09	0.78	NaN	755	10	2A
dg02 - 52.d	13.4	0.2	0.029	124.1	1.7	0.024	35.22	0.57	0.015	752	10	2A
dg02 - 53.d	22.1	1	0.027	163.2	2.6	0.0073	48.5	1.1	0.0051	756	10	2A
dg02 - 54.d	14.46	0.37	0.029	121.2	2.5	NaN	36.01	0.85	NaN	752	10	2A
dg02 - 55.d	18.03	0.23	0.034	170.5	3.2	0.016	44.8	1.1	0.011	757	10	2A
dg02 - 56.d	17.38	0.3	0.04	140	1.7	0.0078	39.62	0.58	0.012	753	10	2A
dg02 - 57.d	14.82	0.24	0.027	136	2.9	NaN	37.44	0.85	0.0053	751	10	2A
dg02 - 58.d	20.69	0.32	0.021	204.7	3.4	NaN	60.4	0.92	0.011	762	10	2A

Analysis number	Pb208 ppm	Pb208 ppm 2SE	Pb208 ppm LOD	Th232 ppm	Th232 ppm 2SE	Th232 ppm LOD	U238 ppm	U238 ppm 2SE	U238 ppm LOD	Zr in Tt temp (°C)	grain number	REE group
dg02 - 59.d	23.36	0.81	0.02	171	2.6	0.0077	47.43	0.86	0.0054	756	10	2A
dg02 - 60.d	10.82	0.27	0.031	75.7	1.1	NaN	23.37	0.36	NaN	739	10	2A
dg02 - 62.d	22.29	0.33	0.034	201.3	2.7	NaN	71.53	0.85	0.015	762	11	2A
dg02 - 63.d	16.48	0.23	0.036	160.1	2.3	0.0075	44.36	0.7	NaN	757	11	2A
dg02 - 64.d	17.73	0.59	0.025	162.5	2.9	NaN	42.64	0.84	0.014	755	12	2A
dg02 - 65.d	17.14	0.36	0.03	166.4	2.3	0.015	44.11	0.67	0.011	755	12	2A
dg02 - 66.d	14.56	0.23	0.026	133.8	2	NaN	37.44	0.67	NaN	752	12	2A
dg02 - 67.d	9.12	0.14	0.018	80.3	1.5	0.015	25.36	0.53	0.012	743	13	2A
dg02 - 68.d	17.35	0.29	0.039	162.2	2.3	0.0075	40.57	0.62	0.013	758	13	2A
dg02 - 69.d	19.08	0.33	0.037	174.3	2.8	0.0073	42.43	0.89	NaN	759	13	2A
dg02 - 70.d	16.8	0.23	0.036	150.8	2.2	NaN	38.73	0.53	NaN	757	13	2A
dg02 - 71.d	8.42	0.18	0.024	72.5	1.5	0.015	23.34	0.38	0.01	744	14	2A
dg02 - 72.d	26.91	0.5	0.024	191.2	3.1	0.015	54.54	0.86	NaN	757	15	2A
dg02 - 73.d	21.86	0.28	0.035	204.9	2.9	0.021	61.89	0.98	0.0069	761	15	2A
dg02 - 74.d	21.49	0.25	0.034	182.3	3.5	NaN	54.1	1	0.016	758	15	2A
dg02 - 75.d	1.896	0.066	0.037	6.09	0.26	NaN	2.67	0.12	0.0052	698	16	2D
dg02 - 76.d	23.2	1	0.037	151	2.3	NaN	62.71	0.85	0.012	762	17	2C
dg02 - 77.d	22.66	0.49	0.026	200.3	4.2	0.015	74.4	1.6	0.015	762	17	2C
dg02 - 78.d	16.22	0.25	0.038	135	2.1	0.016	51.81	0.87	0.022	756	17	2C
dg02 - 79.d	14.42	0.21	0.037	134.9	2.1	NaN	51.69	0.89	0.018	757	18	2C
dg02 - 80.d	21.46	0.32	0.025	205	3	0.017	61.98	0.97	0.018	764	18	2C
dg02 - 82.d	20.2	0.25	0.022	192.8	2.9	0.016	62.36	0.95	NaN	763	19	2C
dg02 - 83.d	15.87	0.31	0.026	153.1	2.6	NaN	49.31	0.81	0.011	758	20	2C
dg02 - 84.d	16.16	0.2	0.034	155.5	2.3	0.0077	49.17	0.58	0.011	757	20	2C
dg02 - 85.d	13.64	0.29	0.023	122.5	2	NaN	41.77	0.95	0.015	753	20	2C
dg02 - 86.d	22.92	0.38	0.03	220.3	3.1	NaN	87.7	1.5	NaN	766	21	2C
dg02 - 87.d	50.5	1.2	0.025	278.4	5.2	0.016	102.6	1.8	0.012	766	21	2C
dg02 - 88.d	1.755	0.064	0.027	6.3	0.22	NaN	4.16	0.12	0.0053	706	22	2A
dg02 - 89.d	18.8	0.66	0.036	132.6	2	0.017	45.89	0.66	0.011	753	23	2C

Analysis number	Pb208 ppm	Pb208 ppm 2SE	Pb208 ppm LOD	Th232 ppm	Th232 ppm 2SE	Th232 ppm LOD	U238 ppm	U238 ppm 2SE	U238 ppm LOD	Zr in Tt temp (°C)	grain number	REE group
dg02 - 90.d	17.84	0.26	0.021	161.6	2.1	0.018	55.87	0.84	0.026	758	24	2C
dg02 - 91.d	3.52	0.11	0.022	22.57	0.42	NaN	11.68	0.25	0.0074	722	25	2A
dg02 - 92.d	4.716	0.098	0.04	35.78	0.65	0.0077	14.92	0.28	0.012	732	25	2A
dg02 - 95.d	12.63	0.23	0.022	115.6	2.2	0.01	6.04	0.18	0.01	742	26	2D
dg02 - 96.d	10.12	0.19	0.026	90.6	1.4	0.016	5.03	0.12	0.015	742	26	2D
dg02 - 97.d	6.15	0.16	0.033	50.2	1.1	0.021	5.99	0.14	NaN	750	27	2D
dg02 - 98.d	6.36	0.11	0.025	49.27	0.98	0.01	6.96	0.18	0.0052	746	27	2D
dg02 - 99.d	4.036	0.091	0.03	27.72	0.61	0.02	7.05	0.2	0.0052	745	28	2D
dg02 - 100.d	4.459	0.084	0.046	30.07	0.68	0.026	7.23	0.19	NaN	746	28	2D
dg02 - 101.d	4.038	0.084	0.02	23.98	0.5	0.015	5.32	0.15	0.01	740	28	2D
dg02 - 103.d	4.884	0.088	0.022	29.89	0.75	0.016	3.33	0.13	0.01	738	30	2D
dg02 - 104.d	5.65	0.12	0.03	43.99	0.58	NaN	13.57	0.27	NaN	735	31	2A
dg02 - 105.d	6.06	0.12	0.032	46.17	0.65	NaN	13.65	0.34	0.0055	736	31	2A
dg02 - 106.d	10.67	0.2	0.025	81.5	1.6	0.0078	16.19	0.35	0.0054	737	31	2A
dg02 - 107.d	8.38	0.11	0.028	59.6	2.1	0.015	11.61	0.39	0.0052	727	31	2A
dg02 - 110.d	6.54	0.17	0.024	37.34	0.56	0.021	11.21	0.24	0.019	716	32	2A
dg02 - 111.d	5.49	0.11	0.025	43.89	0.81	0.015	14.41	0.3	0.011	718	32	2A

Analysis number	$^{238}U/^{206}Pb$	±1s	$^{207}Pb/^{206}Pb$	±1s	$^{238}U/^{206}Pb$ age (Ma)	±1s	$^{207}Pb/^{206}Pb$ age (Ma)	±1s	Disc (%)	f207%	^{207}Pb-corrected $^{238}U/^{206}Pb$ Age (Ma)	±1s
dg02 - 1.d	5.161119915	0.0778877	0.0971	0.0018	1142	16	1569	34	27.2	3.1	1109	17
dg02 - 2.d	4.690350456	0.0736529	0.0985	0.0013	1246	18	1596	24	21.9	2.7	1215	19
dg02 - 3.d	5.007688365	0.0679245	0.0885	0.0014	1174	14	1393	30	15.8	1.5	1157	16
dg02 - 4.d	4.270104895	0.0665047	0.1403	0.00305	1356	19	2231	37	39.2	8.9	1247	20
dg02 - 5.d	4.223951578	0.0499314	0.1358	0.00195	1370	14	2174	25	37.0	8.1	1270	16
dg02 - 6.d	4.430839002	0.0533815	0.1338	0.0019	1312	14	2148	25	38.9	8.1	1215	15
dg02 - 7.d	4.853452558	0.0897268	0.109	0.00225	1208	20	1783	37	32.3	4.6	1156	21
dg02 - 8.d	4.872817955	0.0809841	0.1074	0.0018	1203	18	1756	30	31.5	4.4	1155	19
dg02 - 9.d	4.262652705	0.0866152	0.1474	0.00465	1359	24	2316	53	41.3	10.0	1234	27
dg02 - 10.d	4.843827467	0.0836008	0.1182	0.00235	1210	19	1929	35	37.3	6.1	1142	20
dg02 - 11.d	4.498158379	0.0784234	0.135	0.00275	1294	20	2164	35	40.2	8.4	1195	21
dg02 - 12.d	4.656816015	0.0822731	0.1334	0.0028	1254	20	2143	36	41.5	8.3	1158	21
dg02 - 13.d	4.740417273	0.0882428	0.1156	0.0023	1234	21	1889	35	34.7	5.6	1171	22
dg02 - 14.d	4.974541752	0.0707303	0.1002	0.00165	1181	15	1628	30	27.5	3.4	1144	16
dg02 - 15.d	4.589008924	0.1085552	0.1608	0.00435	1271	27	2464	45	48.4	12.7	1123	28
dg02 - 16.d	4.731234867	0.1172102	0.1487	0.0042	1236	27	2331	48	47.0	10.9	1112	28
dg02 - 17.d	4.652380952	0.1015357	0.1376	0.0041	1255	24	2197	51	42.9	9.0	1152	26
dg02 - 18.d	4.934343434	0.0997584	0.1173	0.003	1190	22	1915	45	37.9	6.1	1123	23
dg02 - 19.d	4.791564492	0.092248	0.1311	0.00315	1222	21	2113	42	42.2	8.1	1131	22
dg02 - 20.d	4.851042701	0.0734755	0.1078	0.0017	1208	16	1763	29	31.5	4.4	1159	17
dg02 - 21.d	4.824691358	0.086465	0.0991	0.0016	1214	20	1607	30	24.5	3.0	1181	21
dg02 - 22.d	4.674641148	0.0753498	0.1513	0.00325	1250	18	2361	36	47.1	11.2	1121	19
dg02 - 23.d	4.765853659	0.0958902	0.1213	0.0024	1228	22	1975	35	37.8	6.5	1155	23
dg02 - 24.d	4.665711557	0.0677771	0.1131	0.00205	1252	16	1850	32	32.3	5.0	1194	17
dg02 - 25.d	5.007688365	0.0739449	0.1298	0.00245	1174	16	2095	33	44.0	8.2	1085	16
dg02 - 26.d	4.21484038	0.062606	0.142	0.0023	1372	18	2252	28	39.1	9.1	1259	19
dg02 - 27.d	4.098154362	0.0677829	0.1351	0.0016	1408	21	2165	21	35.0	7.7	1309	22
dg02 - 28.d	4.88011988	0.075383	0.0926	0.0015	1202	17	1480	30	18.8	2.0	1179	18
dg02 - 29.d	4.959390863	0.0763103	0.1231	0.00245	1184	16	2002	35	40.8	7.0	1107	17

Analysis number	$^{238}U/^{206}Pb$	±1s	$^{207}Pb/^{206}Pb$	±1s	$^{238}U/^{206}Pb$ age (Ma)	±1s	$^{207}Pb/^{206}Pb$ age (Ma)	±1s	Disc (%)	f207%	^{207}Pb-corrected $^{238}U/^{206}Pb$ Age (Ma)	±1s
dg02 - 30.d	4.665711557	0.0606171	0.1458	0.0027	1252	15	2297	31	45.5	10.3	1133	16
dg02 - 31.d	4.808070866	0.0802427	0.1156	0.002	1218	18	1889	31	35.5	5.7	1155	19
dg02 - 32.d	4.848635236	0.076835	0.1188	0.002	1209	17	1938	30	37.6	6.2	1140	18
dg02 - 33.d	5.064800415	0.1033894	0.1221	0.00325	1162	21	1987	47	41.5	7.0	1087	22
dg02 - 34.d	4.956874683	0.1043089	0.1207	0.0022	1185	22	1967	32	39.8	6.7	1112	23
dg02 - 35.d	4.855864811	0.0898071	0.118	0.00195	1207	20	1926	29	37.3	6.1	1140	21
dg02 - 36.d	4.491954023	0.0921848	0.1431	0.0038	1296	24	2265	45	42.8	9.7	1181	25
dg02 - 37.d	4.692603266	0.0823091	0.1115	0.00215	1245	20	1824	35	31.7	4.8	1190	21
dg02 - 38.d	4.997442455	0.0700802	0.108	0.0023	1176	15	1766	38	33.4	4.7	1126	16
dg02 - 39.d	4.860696517	0.0725837	0.0982	0.0018	1206	16	1590	34	24.2	2.9	1174	17
dg02 - 40.d	4.578256795	0.0788262	0.1268	0.00265	1274	20	2054	36	38.0	7.2	1190	21
dg02 - 41.d	4.88988989	0.0993143	0.1211	0.00305	1199	22	1972	44	39.2	6.6	1126	23
dg02 - 42.d	4.984693878	0.0879818	0.1091	0.00245	1179	19	1784	40	34.0	4.8	1126	20
dg02 - 43.d	4.939332659	0.092616	0.1291	0.00265	1189	20	2086	36	43.0	8.0	1101	21
dg02 - 44.d	4.606317775	0.066365	0.1192	0.00225	1266	16	1944	33	34.9	6.0	1198	18
dg02 - 45.d	4.848635236	0.1155864	0.1213	0.00355	1209	26	1975	51	38.8	6.6	1135	27
dg02 - 46.d	4.681360805	0.0950081	0.1468	0.0035	1248	23	2309	40	45.9	10.5	1127	24
dg02 - 47.d	4.949341439	0.0666271	0.1231	0.0023	1186	14	2002	33	40.7	7.0	1110	15
dg02 - 48.d	4.855864811	0.0968679	0.1095	0.0028	1207	22	1791	46	32.6	4.7	1155	23
dg02 - 49.d	4.712976363	0.0764166	0.1141	0.00265	1240	18	1866	41	33.5	5.3	1181	19
dg02 - 50.d	4.984693878	0.0867506	0.1244	0.003	1179	18	2020	42	41.7	7.3	1100	20
dg02 - 51.d	4.448998179	0.0683532	0.1258	0.002	1307	18	2040	28	35.9	6.8	1226	19
dg02 - 52.d	4.834240475	0.0902502	0.1153	0.00245	1212	20	1885	38	35.7	5.6	1149	22
dg02 - 53.d	4.589008924	0.0884911	0.1296	0.00345	1271	22	2093	46	39.3	7.6	1182	23
dg02 - 54.d	4.679118774	0.0776047	0.1201	0.003	1249	19	1958	44	36.2	6.2	1178	20
dg02 - 55.d	4.803343166	0.0623924	0.1056	0.002	1219	14	1725	34	29.3	4.0	1174	15
dg02 - 56.d	4.819930932	0.0794516	0.1267	0.00225	1215	18	2053	31	40.8	7.5	1132	19
dg02 - 57.d	4.751945525	0.0645087	0.1147	0.002	1231	15	1875	31	34.3	5.4	1170	16
dg02 - 58.d	4.936836786	0.0792785	0.0947	0.00175	1189	17	1522	34	21.9	2.4	1163	19

Analysis number	$^{238}U/^{206}Pb$	±1s	$^{207}Pb/^{206}Pb$	±1s	$^{238}U/^{206}Pb$ age (Ma)	±1s	$^{207}Pb/^{206}Pb$ age (Ma)	±1s	Disc (%)	f207%	^{207}Pb-corrected $^{238}U/^{206}Pb$ Age (Ma)	±1s
dg02 - 59.d	4.576112412	0.0880454	0.1357	0.00305	1274	22	2173	39	41.4	8.6	1174	23
dg02 - 60.d	4.544186047	0.0993108	0.1489	0.0037	1282	25	2333	42	45.0	10.7	1157	26
dg02 - 62.d	4.964430894	0.0657931	0.0982	0.0016	1183	14	1590	30	25.6	3.0	1150	15
dg02 - 63.d	5.077962578	0.0757319	0.1097	0.0024	1159	16	1794	39	35.4	5.0	1105	17
dg02 - 64.d	4.867962133	0.0878571	0.114	0.00195	1204	20	1864	31	35.4	5.5	1144	21
dg02 - 65.d	5.117862755	0.1067275	0.1073	0.0025	1151	22	1754	42	34.4	4.7	1101	23
dg02 - 66.d	4.853452558	0.0838952	0.1137	0.0021	1208	19	1859	33	35.0	5.4	1148	20
dg02 - 67.d	5.19404572	0.1097062	0.1399	0.0036	1135	22	2226	44	49.0	10.0	1030	22
dg02 - 68.d	4.7681796	0.0993949	0.1124	0.00325	1227	23	1839	51	33.2	5.1	1170	25
dg02 - 69.d	4.926878467	0.0778141	0.1161	0.00245	1191	17	1897	37	37.2	5.9	1127	18
dg02 - 70.d	4.941831057	0.0890544	0.1148	0.00235	1188	19	1877	36	36.7	5.7	1126	20
dg02 - 71.d	4.546300605	0.0880454	0.1237	0.00245	1282	22	2010	35	36.2	6.6	1205	23
dg02 - 72.d	4.389038634	0.0705177	0.1313	0.00195	1323	19	2115	26	37.5	7.6	1232	20
dg02 - 73.d	4.97961264	0.0696628	0.102	0.0017	1180	15	1661	31	29.0	3.7	1140	16
dg02 - 74.d	4.636924537	0.0660703	0.1106	0.00145	1259	16	1809	24	30.4	4.6	1206	17
dg02 - 75.d	3.213815789	0.1968199	0.311	0.015	1746	89	3526	72	50.5	35.2	1185	83
dg02 - 76.d	4.604147031	0.0683286	0.1187	0.00205	1267	17	1937	31	34.6	5.9	1199	18
dg02 - 77.d	4.96948118	0.0717964	0.1003	0.0021	1182	15	1630	38	27.5	3.4	1145	17
dg02 - 78.d	4.7681796	0.0779724	0.1095	0.0022	1227	18	1791	36	31.5	4.6	1176	19
dg02 - 79.d	4.966954753	0.0646834	0.0977	0.00195	1182	14	1581	37	25.2	3.0	1150	15
dg02 - 80.d	4.977075904	0.0672413	0.1025	0.0017	1180	14	1670	30	29.3	3.8	1140	15
dg02 - 82.d	5.139400316	0.0811968	0.0956	0.00155	1146	16	1540	30	25.6	2.8	1116	17
dg02 - 83.d	5.033487893	0.0758267	0.1008	0.00195	1168	16	1639	35	28.7	3.6	1130	17
dg02 - 84.d	5.049095607	0.0737592	0.1021	0.00175	1165	15	1663	31	29.9	3.8	1124	16
dg02 - 85.d	4.96948118	0.0777818	0.1163	0.00215	1182	17	1900	33	37.8	6.0	1117	18
dg02 - 86.d	4.929364279	0.0719912	0.0885	0.0016	1191	16	1393	34	14.5	1.4	1175	17
dg02 - 87.d	4.242292662	0.0533831	0.1447	0.0018	1364	15	2284	21	40.3	9.6	1246	16
dg02 - 88.d	4.122362869	0.1627146	0.299	0.014	1400	48	3465	71	59.6	34.2	955	49
dg02 - 89.d	4.652380952	0.067458	0.134	0.0024	1255	16	2151	31	41.7	8.4	1158	17

Analysis number	$^{238}U/^{206}Pb$	±1s	$^{207}Pb/^{206}Pb$	±1s	$^{238}U/^{206}Pb$ age (Ma)	±1s	$^{207}Pb/^{206}Pb$ age (Ma)	±1s	Disc (%)	f207%	^{207}Pb-corrected $^{238}U/^{206}Pb$ Age (Ma)	±1s
dg02 - 90.d	4.977075904	0.0684203	0.1028	0.0018	1180	15	1675	32	29.5	3.8	1139	16
dg02 - 91.d	4.440909091	0.1171126	0.167	0.005	1309	31	2528	49	48.2	13.5	1147	31
dg02 - 92.d	4.544186047	0.1223076	0.1436	0.0044	1282	31	2271	52	43.5	9.8	1167	32
dg02 - 95.d	3.861660079	0.1510948	0.299	0.0125	1484	50	3465	63	57.2	34.0	1018	50
dg02 - 96.d	3.987755102	0.1362539	0.323	0.012	1442	43	3584	56	59.8	37.9	934	43
dg02 - 97.d	3.987755102	0.1689875	0.298	0.0125	1442	53	3460	64	58.3	33.9	988	51
dg02 - 98.d	4.122362869	0.145216	0.265	0.011	1400	43	3277	64	57.3	28.8	1027	44
dg02 - 99.d	4.122362869	0.1539565	0.234	0.008	1400	45	3080	54	54.5	23.9	1092	44
dg02 - 100.d	4.020576132	0.146708	0.241	0.008	1432	45	3127	52	54.2	24.9	1104	44
dg02 - 101.d	4.037190083	0.1478779	0.325	0.0135	1427	45	3594	62	60.3	38.2	918	46
dg02 - 103.d	2.577836412	0.1081996	0.367	0.0125	2113	73	3779	51	44.1	43.3	1281	72
dg02 - 104.d	4.652380952	0.138971	0.162	0.0055	1255	33	2477	56	49.3	12.9	1106	34
dg02 - 105.d	4.630331754	0.1267422	0.1646	0.0048	1261	31	2503	48	49.6	13.3	1106	31
dg02 - 106.d	4.105042017	0.101144	0.1862	0.0049	1405	30	2709	43	48.1	16.1	1198	31
dg02 - 107.d	4.053941909	0.1154409	0.226	0.008	1421	35	3024	56	53.0	22.5	1128	37
dg02 - 110.d	3.757692308	0.1433581	0.225	0.007	1521	50	3017	49	49.6	21.9	1217	49
dg02 - 111.d	4.674641148	0.1290589	0.1441	0.00435	1250	31	2277	51	45.1	10.1	1134	32

Analysis number	Reason for exclusion
dg02 - 61.d	analysed inclusion
dg02 - 81.d	not titanite
dg02 - 93.d	not titanite
dg02 - 94.d	not titanite
dg02 - 102.d	analysis on grain boundary
dg02 - 108.d	not titanite
dg02 - 109.d	not titanite

Appendix 7.1: Summary and storage of all samples used in thesis

Table A7.1 Summary of all samples and available sample material used in the preparation of this thesis. The samples listed below are stored at the UWA museum under the sample reference number "UWA #". Available sample material is recorded as a number (PTS, polished thin sections; PS, polished sections) or yes/no (HS, hand specimen; RP, rock powder; RC, rock chips). Mineral abbreviations: Ap, apatite; Bt, biotite; Chl, chlorite; Cpx, clinopyroxene; Ep, epidote; Grt, garnet; Hb, hornblende; Ilm, ilmenite; Kfs, alkali feldspar; Ky, kyanite; Mc, microcline feldspar; Mnz, monazite; Ms, muscovite; Mt, magnetite; Opx, orthopyroxene; Or, orthoclase feldspar; Pl, plagioclase; Py, pyrite; Qz, quartz; Rt, rutile; Sp, spinel; St, staurolite; Tt, titanite; Tur, tourmaline; Zrc, zircon.

UWA #	Sample	Locality	Lithology	HS	PTS	PS	RP	RC
173000	2MB-01	Name: Two Mile Beach East Latitude: -33.94343611 Longitude: 120.1525556	Qz orthogneiss. Mineralogy: Qz+Pl+Mc+Bt+Ms; minor Ap, Zrc. Foliation defined by biotite and elongate grain shapes of Qz and Fsp; sutured grain boundaries. Generally equigranular grainsizes.	Y	1	1	Y	Y
173001	2MB-02	Name: Two Mile Beach West Latitude: -33.94388056 Longitude: 120.1521528	Pl orthogneiss. Mineralogy: Pl+Qz+Or+Bt+Ms; minor Ap. Foliation defined by biotite. Generally polygonal and equigranular grainshapes; some sutured boundaries. Half of the TS is more altered: this half has more sutured grain boundaries, less polygonal recrystallisation, more sericitised feldspar.		1	1	Y	Y
173002	AF01	Name: Ledge Point Latitude: -35.02002778 Longitude: 118.0041722	Porphyritic Bt metagranite. Mineralogy: Pl+Or+Qz+Bt+Mc+oxide+Chl+Ep; no foliation and relict igneous feldspar grain shapes, although deformation is visible as sutured grain boundaries, misoriented subgrains and undulose extinction		1	1	Y	Y
173003	AF01-SCH	Name: West Beach Latitude: -33.95288889 Longitude: 119.9754083	Grt St schist. Mineralogy: Qz+Ms+Bt+Grt+Chl+St; minor Tur, Zrc. Strongly foliated; anastomosing shear bands of micas. Qz is polygonally recrystallised; snowball garnets; foliation bends around garnet porphyroblasts.		1	1	Y	Y
173004	AF02-1	Name: Ledge Point Latitude: -35.02002778 Longitude: 118.0041722	Bt-Cpx orthogneiss cut by Qz-Pl vein. Wallrock mineralogy: Pl + Bt+ Cpx + Mc + Hb + oxide + Opx + Chl; vein mineralogy: Pl+Qz+Mc. Wallrock is weakly foliated with strongly sutured grain boundaries and some polygonal recrystallisation.	Y	1	1	Y	Y
173005	AF02-2	Name: Whalehead Rock Latitude: -35.03176667 Longitude: 117.9204111	Enderbitic orthogneiss. Mineralogy: Pl+Qz+Hb+Opx+oxide+Bt; minor Zrc. Gneiss is weakly foliated with compositional banding; generally sutured to recrystallised grain boundaries		1	1	Y	Y

UWA #	Sample	Locality	Lithology	HS	PTS	PS	RP	RC
173006	AF03	Name: Whalehead Rock Latitude: -35.03176667 Longitude: 117.9204111	Bt orthogneiss. Mineralogy: Pl+Bt+Qz+Or+Hb; minor Chl. No foliation visible in TS; grain boundaries straight with some polygonal recrystallisation of Qz, feldspar and Hb.		1	2	Y	Y
173007	AF04-1	Name: Shannon Latitude: -34.67203889 Longitude: 116.3862194	Granitic gneiss (no hand specimen or thin section available).				Y	Y
173008	AF04-2	Name: Shannon Latitude: -34.67203889 Longitude: 116.3862194	Bt orthogneiss. Mineralogy: Qz+Mc+Bt+Pl+Or; minor Chl, Ep. Strongly foliated; large feldspar porphyroclasts surrounded by bands of polygonally recrystallised quartz.		1	1	Y	Y
173009	AF05	Name: Elephant Rocks Latitude: -35.02600833 Longitude: 117.2384417	Bt metagranite. Mineralogy: Mc+Qz+Pl+Bt; minor Cpx, Chl. No foliation visible in TS; Qz has been recrystallised or displays strong undulose extinction. Generally sutured grain boundaries, some myrmekite present.		1	1	Y	Y
173010	AF06	Name: Shelley Beach Latitude: -35.11069722 Longitude: 117.6294528	Bt-Hb metagranite. Mineralogy: Pl+Or+Qz+Bt+Hb; minor Cpx, Zrc. No foliation visible in TS; some polygonal recrystallisation of Qz. Some symplectitic intergrowths of feldspar, Bt ± Hb.		1	1	Y	Y
173011	AF08A	Name: Peaceful Bay Latitude: -35.06114167 Longitude: 116.9266	Bt orthogneiss. Mineralogy: Qz+Pl+Bt+Or+Mc; minor Chl, oxide, Ap. Large feldspar porphyroclasts with some sutured boundaries, some recrystallisation of quartz, and weak foliation.		1	1	Y	Y
173012	AF08B	Name: Peaceful Bay Latitude: -35.06114167 Longitude: 116.9266	Grt paragneiss. Mineralogy: Qz+Grt+Py+Bt+Chl. Strong foliation; strongly sutured grain boundaries; quartz has small grainsize and polygonal grain shapes. Some compositional banding. Garnet is rounded to slightly elongate; chlorite mostly occurs as inclusions in garnet (not in equilibrium with main assemblage anymore).		1	1	Y	Y
173013	AF08C	Name: Peaceful Bay Latitude: -35.06114167 Longitude: 116.9266	Qz-monzodiorite orthogneiss. Mineralogy: Pl+Hb+Qz+Or+Bt+Mc; minor Cpx, oxide. Granoblastic textures with larger plagioclase porphyroclasts. No foliation visible; some recrystallisation of Qz grains and sutured grain boundaries.		1	1	Y	Y
173014	AF08D	Name: Peaceful Bay Latitude: -35.06114167 Longitude: 116.9266	Bt-Grt orthogneiss. Mineralogy: Qz+Pl+Bt+Grt+Mc; minor Chl. Strong foliation, sutured grain boundaries and some recrystallisation of quartz. Generally equigranular grainsize.		1	1	Y	Y

UWA #	Sample	Locality	Lithology	HS	PTS	PS	RP	RC
173015	BREM-2A	Name: Black Point Latitude: -34.45791667 Longitude: 119.4068167	Intermediate granulite. Mineralogy: Pl+Or+Qz+Hb+Cpx+Mt+Mc+Opx; minor Ap, Bt, Chl, Tur. Little grainsize variation. Sutured grain boundaries; compositional banding and slight foliation.	Y	1	1	Y	Y
173017	BREM-6A	Name: Fishery Beach Latitude: -34.4258 Longitude: 119.4003333	Intermediate granulite. Mineralogy: Pl+Qz+Or+Opx+Il+Cpx+Bt; minor Zrc. Foliation defined by elongation of minerals; sutured grain boundaries.	Y	1	1	Y	Y
173019	BREM10	Name: Fishery Beach Latitude: -34.42673333 Longitude: 119.4024	Retrograde altered granulite. Mineralogy: Or+Pl+Bt+Grt+Mt; minor Chl, Ms, Sp, Opx, Zrc. Weak foliation and compositional banding; sutured to polygonal grain boundaries. Ms crosscuts foliation; felspars strongly sericitised.		1	1	Y	Y
173023	BREM-SA	Name: Barrens Beach Latitude: -33.92605 Longitude: 120.0320417	Bt+St+Ky schist. Mineralogy: Qz+Ms+Bt+St+Ky; minor Chl, Ep, Ap, Tur. Anastomosing shear bands of mica interspersed with bands of polygonal granoblastic quartz grains. Asymmetrical crenulation cleavage defined by folding of shear bands (and some minerals).		1	1	Y	Y
173028	EAF011	Latitude: -31.248134 Longitude: 123.259641	Amphibolite. Major mineralogy: Grt+Hb+Qz+Pl. Grain shapes are ~ polygonal; Grt locally enclosing/rimming (corona texture) epidote.		1	1	Y	Y
173029	EAF012	Latitude: -31.28334001 Longitude: 123.360023	Metasedimentary rock. Mineralogy: Grt+Qz+Bt+Hb+Tt+perthitic Kfs + minor plag; minor Cpx? Tt occurs as inclusions in garnet as well as in the matrix.	Y	1	1	Y	Y
173030	EAF015	Latitude: -31.27957201 Longitude: 123.369269	Ms schist. Mineralogy: Qz, minor Pl, Mc, oxide mineral (Ilm?), Ms. Polygonal recrystallisation of grains very common; small grainsize; patches of brown alteration mineral - clay?	Y	1	1	Y	Y
173031	EAF017	Latitude: -31.25792398 Longitude: 123.431605	Gneiss. Mineralogy: Grt+Bt+Qz+Hb+Tt+minor Pl+minor Mcl; Tt occurs as inclusions in Grt; myrmekite reaction textures between feldspars.	Y	1	1	Y	Y
173032	EAF018	Latitude: -31.30901302 Longitude: 123.483607	Metagranite. Mineralogy: Qz+Mc+Bt; 1 small garnet. Sutured grain boundaries, rounded grainshapes, some small blobby qz grains, some qz grains with polygonal boundaries. Bt defines a foliation.		1	1	Y	Y
173033	EAF020-2	Latitude: -31.30959196 Longitude: 123.483091	Augen gneiss. Mineralogy: Qz+Mc+Bt+Grt; minor Tt; minor amounts of a high relief, colourless, high birefringence mineral. Large grains with lots of recrystallisation; distinct foliation; sutured grain boundaries.		1	1	Y	Y

UWA #	Sample	Locality	Lithology	HS	PTS	PS	RP	RC
173034	EAF021	Latitude: -31.31733198 Longitude: 123.484967	Metanorite. Mineralogy: Pl+Opx+Cpx+Bt+oxide, some chlorite alteration. Relict igneous textures with Pl phenocrysts at all orientations (i.e. unfoliated); Bt spatially associated with Chl.	Y	1	1	Y	Y
173035	EAF022	Latitude: -31.31624803 Longitude: 123.482687	Ms schist. Mineralogy: Qz+Ms; some large grains of Kfs (Or?). Strong foliation; Qz is sutured to polygonal and slightly elongate.		1	1	Y	Y
173036	EAF027	Latitude: -31.35488701 Longitude: 123.433094	Ms mylonite. Mineralogy: Qz+Pl+Ms+minor Bt. Some very large Ms grains. Patchwork texture with patches of large Qz+Pl grains with sericitisation and sutured boundaries, and patches of small 'honeycomb' polygonal qz+pl grains.		1	1	Y	Y
173037	EAF029	Latitude: -31.35488701 Longitude: 123.433094	Augen gneiss. Mineralogy: Qz+Mc+Bt; one large Grt seen in the TS. Mostly large grains with sutured boundaries and some smaller blobby Qz grains; foliated.	Y	1	1	Y	Y
173038	EAF030	Latitude: -31.35273898 Longitude: 123.434121	Metagabbro. Mineralogy: Hb+Qz+Pl. Mostly granulite textures with polygonal grain boundaries (all minerals); some domains with larger grains, some domains of much smaller (still polygonal) recrystallised Qz+Fsp	Y	1	1	Y	Y
173039	EAF035A	Latitude: -31.18497301 Longitude: 123.421842	Metagranite with melanosomes. Metagranite: Mc+Qz+Pl+Grt; large grains with sutured boundaries and some recrystallisation, lots of sericitisation. Grt contains inclusions of Hb and Qz. Melanosome: Hb+Bt+Tt+allanite; some zoisite? (melanosome in 35A; grt in 35B)	Y	1	1	Y	Y
173040	EAF036	Latitude: -31.17295001 Longitude: 123.413636	Gneiss. Mineralogy: Grt+Bt+Hb+Tt+Qz+Pl; myrmekite reaction texture common; Tt occurs as inclusions in Hb and Grt	Y	1	1	Y	Y
173041	EAF037	Latitude: -31.04851998 Longitude: 123.454971	Gneiss with leucosome. Mineralogy: Grt+Bt+Tt+Qz+Pl+Microcline; myrmekite common; sutured grain boundaries	Y	1	1	Y	Y
173042	EAF038	Name: Ponton Creek Latitude: -30.9096 Longitude: 123.642918	Amphibolite. Mineralogy: Hb+Grt+Pl+Tt+Qz+minor Bt; Tt rims rutile. Small grainsize, recrystallised to polygonal grainshapes. Plag strongly sericitised. Garnet and Hb locally myrmekitic with Qz inclusions.	Y	1	1	Y	Y
173043	EAF039B	Name: Ponton Creek Latitude: -30.91110203 Longitude: 123.644351	Bt schist. Mineralogy: Grt+Bt+oxide (Ilm?) +Qz+Mc; minor plag. Medium grainsize with sutured boundaries and lots of small recrystallised domains; some myrmekite in feldspar; lots of sericitisation; strong foliation defined by orientation of Bt and opaque mineral.	Y	1	1	Y	Y

UWA #	Sample	Locality	Lithology	HS	PTS	PS	RP	RC
173044	EAF041	Name: Ponton Creek Latitude: -30.91160696 Longitude: 123.645413	Melanosome in migmatitic gneiss. Mineralogy: Grt+Bt+Qz+Pl+perthitic Or; minor Tt associated with Grt+Bt; foliation defined by Bt; medium grainsize with sutured boundaries and some recrystallisation along grain boundaries and in some domains.	Y	1	1	Y	Y
173045	EAF042	Name: Ponton Creek Latitude: -30.91338602 Longitude: 123.643762	Metagranodiorite. Mineralogy: Grt+Bt+Tt; 1 relict Hb grain seen; Qz+Plag+perthitic Or. Sutured grain boundaries, symplectite common, also lots of recrystallisation of grains; foliation defined by Bt		1	1	Y	Y
173046	EAF046	Latitude: -31.43926403 Longitude: 123.538424	Metagranite. Mineralogy: Qz+Or+minor Pl+Grt+Bt; med grainsize with polygonal to sutured boundaries; lots of perthite in feldspar and some sericitisation; foliation defined by elongate grainshapes		1	1	Y	Y
173048	EAF051	Name: Fraser Fault Zone Latitude: -31.58328398 Longitude: 123.267036	Mylonitic metagranite. Grt+oxide+minor Hb+Qz+minor Pl. Grt has a strong orange colour; strongly recrystallised and sutured Qz of med to small grainsize; Hb associated with oxide; foliation defined by mineral elongation		1	1	Y	Y
173049	EAF052	Name: Fraser Fault Zone Latitude: -31.58328398 Longitude: 123.267036	Mylonitic granulite. Mineralogy: Grt+oxide+Cpx+Hb+Qz+minor Pl. Garnet has strong orange colour with sigma and delta clast shapes and tails; strongly recrystallised and sutured Qz of med to small grainsize; Hb associated with oxide and Cpx; foliation defined by mineral elongation.		1	1	Y	Y
173050	EAF054	Name: Wyralinu Hill Latitude: -32.046793 Longitude: 122.795057	Intermediate metadolerite. Mineralogy: Opx+Cpx+oxide+Bt+Pl+Qz; elongate grainshapes, some polygonal boundaries; Qz grains often sutured and recrystallised.		1	1	Y	Y
173051	EAF055B	Name: Wyralinu Hill Latitude: -32.046793 Longitude: 122.795057	Metagranite. Mineralogy: Grt+Cpx+tiny minor Hb+oxide+Opx+Pl+Qz+Or. Compositional banding evident; colourless minerals (qz, fsp) are in some places large grains with sutured boundaries, and sometimes small grains with polygonal textures.	Y	1	1	Y	
173054	EAF060	Name: Gnamma Hill Latitude: -32.18092198 Longitude: 122.697752	Mafic granulite. Mineralogy: Hb intergrown with Cpx? + Tt + Qz + oxide + Grt + Plag. Compositional banding, strongly sutured boundaries, granulitic texture, colourless minerals (qz, fsp) have small grainsize and polygonal shapes.		1	1	Y	Y
173055	EAF061	Name: Gnamma Hill Latitude: -32.18092198 Longitude: 122.697752	Grt metasediment. Mineralogy: Grt+Bt+oxide+sillimanite+Qz+minor Or. Qz has some large grains and some small recrystallised grains; sutured grain boundaries; foliation defined by mineral elongation.		1	1	Y	Y

UWA #	Sample	Locality	Lithology	HS	PTS	PS	RP	RC
173056	DG02	Name: Daly Downs Latitude: -33.68963102 Longitude: 121.609178	Tonalitic gneiss; mineraology Bt+Hb+oxide+Pl+Qz+Or? Minor Zr, Mnz?; minor Tt. Lots of myrmekite	Y	1	1	Y	

This Report is a PhD thesis that describes the cooling history of the Albany–Fraser Orogen, with temperature-time (T-t) pairs derived from $^{40}Ar/^{39}Ar$, Rb/Sr and U/Pb (titanite and zircon) thermochronology. In the west Albany–Fraser Orogen, rapid exhumation during transpressional tectonics is indicated by $^{40}Ar/^{39}Ar$ thermochronology of hornblende, muscovite and biotite that reveals cooling rates of 22–33°C/Ma between 1169–1159 Ma, following c. 1180 Ma amphibolite to granulite facies metamorphism. In the Biranup Zone of the east Albany–Fraser Orogen, Rb/Sr biotite thermochronology yields consistent c. 1133 Ma cooling ages. In the Fraser Zone, hornblende and biotite $^{40}Ar/^{39}Ar$ thermochronology demonstrates heterogeneous cooling between the southwest and northeast. Differences in cooling rates throughout the orogen reflect differences in tectonic processes during Stage II of the Albany–Fraser Orogeny.

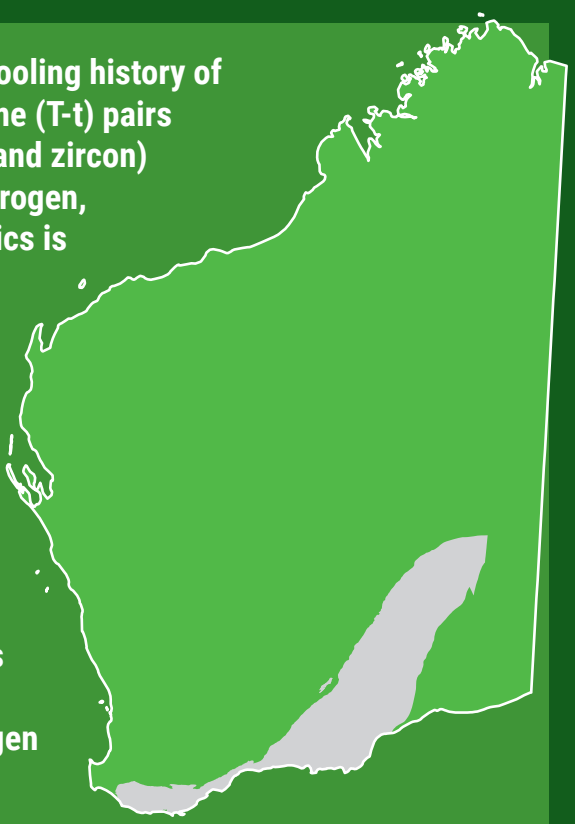

SCIBIORSKI

THE COOLING AND EXHUMATION OF THE ALBANY–FRASER OROGEN, WESTERN AUSTRALIA, CONSTRAINED BY $^{40}Ar/^{39}Ar$, Rb/Sr AND U/Pb THERMOCHRONOLOGY

REPORT 195

Further details of geoscience products are available from:

Information Centre
Department of Mines, Industry Regulation and Safety
100 Plain Street
EAST PERTH WA 6004
Phone: (08) 9222 3459 Fax: (08) 9222 3444

www.dmp.wa.gov.au/GSWApublications